68758

WSRC-RP-94-21

RADIOLOGICAL PERFORMANCE ASSESSMENT FOR THE E-AREA VAULTS DISPOSAL FACILITY

by

James R. Cook

Westinghouse Savannah River Company
Savannah River Site
Aiken, South Carolina 29808

Paul D. Hunt

DOE Contract No. DE-AC09-89SR18035

This paper was prepared in connection with work done under the above contract number with the U. S. Department of Energy. By acceptance of this paper, the publisher and/or recipient acknowledges the U. S. Government's right to retain a nonexclusive, royalty-free license in and to any copyright covering this paper, along with the right to reproduce and to authorize others to reproduce all or part of the copyrighted paper.

DISCLAIMER

This report was prepared as an account of work sponsored by an agency of the United States Government. Neither the United States Government nor any agency thereof, nor any of their employees, makes any warranty, express or implied, or assumes any legal liability or responsibility for the accuracy, completeness, or usefulness of any information, apparatus, product, or process disclosed, or represents that its use would not infringe privately owned rights. Reference herein to any specific commercial product, process, or service by trade name, trademark, manufacturer, or otherwise does not necessarily constitute or imply its endorsement, recommendation, or favoring by the United States Government or any agency thereof. The views and opinions of authors expressed herein do not necessarily state or reflect those of the United States Government or any agency thereof.

This report has been reproduced directly from the best available copy.

Available to DOE and DOE contractors from the Office of Scientific and Technical Information, P. O. Box 62, Oak Ridge, TN 37831; prices available from (615) 576-8401.

Available to the public from the National Technical Information Service, U. S. Department of Commerce, 5285 Port Royal Rd., Springfield, VA 22161

WSRC-RP-94-218

RADIOLOGICAL PERFORMANCE ASSESSMENT FOR THE E-AREA VAULTS DISPOSAL FACILITY (U)

Prepared for the
WESTINGHOUSE SAVANNAH RIVER COMPANY
Aiken, South Carolina

by

MARTIN MARIETTA ENERGY SYSTEMS, INC.
EG&G IDAHO, INC.
WESTINGHOUSE SAVANNAH RIVER COMPANY

April 15, 1994

Authenticated
Mary Mullis
5/16/94

Rev. 0

CONTENTS

FIGURES xi
TABLES xix
ACRONYMS AND ABBREVIATIONS xxv
EXECUTIVE SUMMARY xxix

1. INTRODUCTION 1-1
   1.1 PURPOSE AND SCOPE 1-3
   1.2 PERFORMANCE OBJECTIVES 1-5
      1.2.1 Time for Compliance with Performance Objectives 1-6
      1.2.2 Performance Objective for Groundwater Protection 1-7
      1.2.3 Radon 1-11
2. DISPOSAL FACILITY DESCRIPTION 2-1
   2.1 REGIONAL CHARACTERISTICS 2-1
      2.1.1 Geography of the Region 2-2
      2.1.2 Demography 2-5
      2.1.3 Meteorology 2-7
      2.1.4 Hydrogeology 2-7
      2.1.5 Seismicity 2-13
      2.1.6 Surface Water Hydrology 2-16
      2.1.7 Water Quality and Usage 2-17
      2.1.8 Soils 2-18
      2.1.9 Ecology 2-20
      2.1.10 Existing Radiological Environment 2-21
   2.2 E-AREA SITE DESCRIPTION 2-26
      2.2.1 E-Area Location, Description, and Land Use 2-26
      2.2.2 Hydrogeology of E-Area 2-28
      2.2.3 Surface Water in the Vicinity of E-Area 2-34

2.2.4 Water Quality and Usage in the E-Area Vicinity 2-35
2.2.5 Existing Radiation and Chemical Environment at E-Area 2-38
2.3 DESCRIPTION OF E-AREA OPERATIONS, FACILITIES, AND FEED STREAMS 2-44
2.3.1 Description of the Waste Types at E-Area 2-44
2.4 E-AREA VAULTS WASTE COMPOSITION 2-44
2.4.1 Physical Characteristics of Waste Types 2-44
2.4.2 Waste Packaging 2-46
2.4.3 Radioactive Inventory of Waste Types 2-48
2.5 DESCRIPTION OF THE E-AREA VAULTS DISPOSAL SITE 2-49
2.5.1 Site Layout and Capacity 2-49
2.5.2 Vault Descriptions 2-51
2.6 PROPOSED TRENCHES FOR DISPOSAL OF SUSPECT SOIL 2-56
2.7 PROPOSED NAVAL REACTOR COMPONENT DISPOSAL 2-56
2.8 HAZARDOUS WASTE/MIXED WASTE DISPOSAL FACILITY 2-58
2.9 E-AREA CLOSURE CONCEPT 2-64
2.9.1 Physical Description of the EAVs Closure Concept 2-64
2.9.2 Functional Description of the E-Area Closure Concept 2-67
2.9.3 Post Closure Groundwater Monitoring 2-68
3. ANALYSIS OF PERFORMANCE 3-1
3.1 SOURCE TERM 3-3
3.1.1 Radionuclides of Interest 3-3
3.1.2 Release Mechanisms 3-4
3.1.3 Engineered Barriers Degradation and Failure 3-5
3.2 PATHWAYS AND SCENARIOS 3-10
3.2.1 Time Periods of Concern 3-10
3.2.2 Transport Pathways 3-11
3.2.3 Exposures of Off-Site Members of the Public and Protection of Groundwater 3-19
3.2.4 Exposure Scenarios for Inadvertent Intruders 3-39

3.3 MODELS AND ASSUMPTIONS 3-51
3.3.1 Near-Field Model 3-53
3.3.2 Groundwater Transport Model 3-74
3.3.3 Models for Dose Estimation 3-80
3.4 PERFORMANCE ANALYSIS METHODOLOGY 3-83
3.4.1 Near-Field Model Analysis 3-83
3.4.2 Groundwater Flow and Mass Transport 3-89
3.4.3 Methods for Dose Analysis 3-98
3.5 QUALITY ASSURANCE 3-99
4. RESULTS OF ANALYSIS 4-1
4.1 ANALYSIS RESULTS 4-1
4.1.1 Screening Results for the Groundwater Pathway 4-2
4.1.2 Near-Field Model Results 4-2
4.1.3 Groundwater Concentrations 4-17
4.1.4 Dose Analysis for Off-Site Releases of Radionuclides 4-28
4.1.5 Dose Analysis for Inadvertent Intruders 4-34
4.2 SENSITIVITY AND UNCERTAINTY ANALYSES 4-81
4.2.1 Analysis of Near-Field and Groundwater Transport 4-81
4.2.2 Analysis of Dose Model from Off-Site Releases 4-85
4.2.3 Analysis of Dose Models for Inadvertent Intruders 4-86
4.3 INTERPRETATION OF RESULTS 4-90
4.3.1 Off-Site Doses and Groundwater Protection 4-91
4.3.2 Inadvertent Intruders 4-92
4.3.3 Disposal Limits for Waste at E-Area 4-93
5. PERFORMANCE EVALUATION 5-1
5.1 COMPARISON TO PERFORMANCE OBJECTIVES 5-1
5.2 DESIGN CHANGES REQUIRED TO MEET PERFORMANCE OBJECTIVES 5-2
5.3 DATA AND RESEARCH NEEDS 5-2
6. PREPARERS 6-1
7. REFERENCES 7-1

APPENDIX A DETAILS OF MODELS AND ASSUMPTIONS

A.1 NEAR-FIELD MODEL A-1

A.1.1 Introduction A-1

A.1.2 Flow and Mass Transport Through Vaults A-5

A.2 GROUNDWATER FLOW AND MASS TRANSPORT MODEL AND SIMULATIONS A-14

A.2.1 Conceptual Saturated Flow and Transport Model A-14

A.2.2 Saturated Flow and Transport Simulations A-22

A.3 ANALYSIS OF ATMOSPHERIC EFFLUENT A-22

A.3.1 Dose Analysis of Tritium Crucibles in the ILT Vaults A-23

A.3.2 Dose Analysis of ^{3}H in JCW in the ILT Vaults A-26

A.3.3 Dose Analysis of ^{3}H in JCW in the ILNT Vaults A-29

A.3.4 Dose Analysis of ^{14}C in the ILNT Vaults A-30

A.3.5 Dose Analysis of ^{3}H in JCW in the LAW Vaults A-32

A.3.6 Dose Analysis of ^{14}C in the LAW Vaults A-33

A.3.7 Analysis of Radon Flux A-34

A.4 DOSE ANALYSIS FOR OFF-SITE INDIVIDUALS AND INADVERTENT INTRUDERS A-39

A.4.1 Introduction A-39

A.4.2 Radionuclides of Importance for Dose Analyses A-40

A.4.3 Assumed Exposure Scenarios and Exposure Pathways A-45

A.4.4 Dose Conversion Factors for Internal and External Exposure A-50

A.4.5 Models and Parameter Values for Exposure Pathways A-62

A.4.6 Summary A-97

APPENDIX A REFERENCES A-100

APPENDIX B COMPUTER CODES

B.1 CODE SELECTION CRITERIA AND CONSIDERATIONS B-1

B.2 GEOCHEMICAL COMPUTER CODE B-3

B.3 VAULT DEGRADATION COMPUTER CODE B-7
B.4 SATURATED/UNSATURATED FLOW AND TRANSPORT CODE B-15
APPENDIX B REFERENCES ..... B-[illegible]

APPENDIX C DATA TABULATION
C.1 RADIONUCLIDE SCREENING AND TRIGGER LEVEL RESULTS C-1
C.2 E-AREA STREAM FLOW DATA C-71
C.3 RADIONUCLIDE SCREENING RESULTS FOR SUSPECT SOIL C-74
C.4 NEAR-FIELD RESULTS C-97
C.5 GROUNDWATER RESULTS C-110
C.6 ATMOSPHERIC TRANSPORT C-142

APPENDIX D GEOCHEMICAL INTERACTIONS
D.1 INTRODUCTION D-1
D.2 RADIONUCLIDES CONSIDERED D-2
D.3 VAULT WATER COMPOSITION D-2
D.4 RADIONUCLIDE SORPTION BEHAVIOR D-2
D.5 TRITIUM RELEASE MECHANISMS D-30
D.6 SORPTION IN SOILS D-36
APPENDIX D REFERENCES D-38

APPENDIX E HYDROGEOLOGY OF THE SRS
E.1 GEOLOGY E-1
E.1.1 Late Cretaceous Lumbee Group E-1
E.1.2 Paleocene-Eocene Black Mingo Group E-3
E.1.3 Middle Eocene Orangeburg Group E-4
E.1.4 Late Eocene Barnwell Group E-6
E.1.5 "Upland Unit" E-7
E.1.6 Quaternary Deposits E-7

E.2 GROUNDWATER HYDROLOGY E-7
E.2.1 Aquifer System I E-3
E.2.2 Confining System I-II E-3
E.2.3 Aquifer System II E-8
E.2.4 Hydrologic Characteristics of the Unsaturated Zone E-17
APPENDIX E REFERENCES E-23

APPENDIX F SOFTWARE QA PLANS

APPENDIX G COMPLETENESS REVIEW GUIDE

APPENDIX H PERFORMANCE ASSESSMENT PEER REVIEW PANEL RECOMMENDATIONS

APPENDIX I SUSPECT SOIL PERFORMANCE ANALYSIS
I.1 DESCRIPTION OF SUSPECT SOIL TRENCHES I-1
I.1.1 Physical Characteristics of Suspect Soil I-1
I.1.2 Layout and Capacity of the Trenches I-1
I.1.3 Radioactive Inventory of Suspect Soil I-3
I.1.4 Closure Concept I-3
I.2 ANALYSIS OF PERFORMANCE OF SUSPECT SOIL I-3
I.2.1 Source Term I-4
I.2.2 Pathways and Scenarios I-4
I.2.3 Models and Assumptions I-8
I.2.4 Performance Analysis Methodology I-17
I.2.5 Quality Assurance I-19
I.3 RESULTS OF SUSPECT SOIL ANALYSIS I-19
I.3.1 Analysis Results I-20
I.3.2 Interpretation of Results I-39

I.4 PERFORMANCE EVALUATION I-39
I.4.1 Comparison to Performance Objectives I-39
I.4.2 Design Required to Meet Performance Objectives I-42
I.4.3 Data and Research Needs I-42
I.5 PORFLOW INPUT FILES I-43
APPENDIX I REFERENCES I-60

APPENDIX J SENSITIVITY/UNCERTAINTY ANALYSIS
J.1 INTRODUCTION J-1
J.2 PRELIMINARY SAMPLE J-2
J.3 SENSITIVITY ANALYSIS J-3
J.4 UNCERTAINTY ANALYSIS J-5
J.5 SUMMARY J-6
J.6 RESPONSE PLOTS AND CUMULATIVE PROBABILITY DISTRIBUTION J-6
APPENDIX J REFERENCES J-18

APPENDIX K E-AREA VAULTS VAULT DEGRADATION STUDY

APPENDIX L DESCRIPTION OF NAVAL REACTOR WASTE DISPOSAL
L.1 DESCRIPTION OF NAVAL REACTOR (NR) WASTE DISPOSAL L-1
L.1.1 Description of NR Waste Forms L-1
L.1.2 Layout and Capacity of NR Waste Disposal Site L-1
L.1.3 Radioactive Inventory of NR Waste L-4
L.1.4 Closure Concept L-4
L.2 ANALYSIS OF PERFORMANCE OF NR WASTE L-4
L.2.1 Source Term L-6
L.2.2 Pathways and Scenarios L-7
L.2.3 Models and Assumptions L-10
L.2.4 Performance Analysis Methodology L-20
L.2.5 Quality Assurance L-22

L.3 RESULTS OF NR WASTE ANALYSIS L-22
L.3.1 Analysis Results L-22
L.3.2 Interpretation of Results L-39
L.4 PERFORMANCE EVALUATION L-41
L.4.1 Comparison to Performance Objectives L-41
L.4.2 Design Changes Required to Meet Performance Objectives L-41
L.4.3 Data and Research Needs L-42
L.5 PORFLOW INPUT FILES L-43
APPENDIX L REFERENCES L-51

APPENDIX M PORFLOW INPUT FILES
M.1 PORFLOW INPUT FILES - NEARFIELD M-1
M.2 PORFLOW INPUT FILES - GROUNDWATER M-18

FIGURES

1.1-1. Location map of the Savannah River Site 1-2
2.1-1. SRS regional location map 2-3
2.1-2. Facility location map of the SRS, showing surface drainage 2-4
2.1-3. Population distribution within an 80-km radius of the central SRS 2-6
2.1-4. Average rainfall at SRS: 1952 - 1992 2-8
2.1-5. Hydrologic and stratigraphic units underlying the SRS. 2-10
2.1-6. Location of the Bowman and Charleston-Summerville seismic zones, and the Dunbarton Basin on the SRS 2-14
2.1-7. The total average effective dose equivalent from various sources in the Central Savannah River Area. 2-23
2.2-1. Topographic map in the vicinity of E-Area 2-27
2.2-2. Location of groundwater wells at E-Area. 2-29
2.2-3. Lithologic cross section, D-D[1], in the vicinity of E-Area 2-30
2.2-4. Lithologic cross section, E-E[1], in the vicinity of E-Area 2-31
2.2-5. Location of E-Area monitoring wells used to assess the groundwater quality and radionuclide activities 2-43
2.5-1. Projected vault layout in the EAVDF 2-50
2.5-2. General arrangement of the ILNT and ILT vaults 2-53
2.5-3. Typical section through LAWV cell 2-55
2.6-1. Conceptual drawing of proposed suspect soil trenches 2-57
2.7-1. Conceptual layout of 100 NR waste disposal containers 2-59
2.7-2. Typical NR waste disposal container 2-60
2.8-1. Location map for HW/MWDF 2-63
2.9.1. Vault closure concept (2 cm/year infiltration) 2-65
2.9.2. Vault closure concept (40 cm/year infiltration) 2-66
3.0-1. Overall conceptual model for the Radiological Performance Assessment of the E-Area Vaults Disposal Facility 3-2

3.2-1. Potential pathways to human exposure for undisturbed buried LLW 3-13

3.3-1. Flow path through near-field vadose zone. 3-56

3.3-2. Conceptual model for the cover 3-58

3.3-3. Conceptual model for the ILNT and ILT vaults 3-59

3.3-4. Conceptual model for the LAW vault 3-60

3.3-5. Fitted moisture characteristic curve for the backfill soil 3-65

3.3-6. Fitted moisture characteristic curve for the gravel soil 3-66

3.4-1. Integration of computational methods for the Radiological Performance Assessment of EAVs 3-84

3.4-2. Model domain for PORFLOW simulations of groundwater at E-Area. 3-91

3.4-3. Actual potentiometric surface for Aquifer Unit IIB, Zone 2 (water table), and simulated surface for Aquifer Unit IIB, Zone 2. 3-92

3.4-4. Actual potentiometric surface for Aquifer Unit IIB, Zone 1 (Barnwell/McBean), and simulated surface for Aquifer Unit IIB, Zone 1.. 3-94

3.4-5. Actual potentiometric surface for Aquifer Unit IIA (Congaree) and simulated surface for Aquifer Unit IIA 3-95

3.4-6. Locations of stream-gaging stations in creeks near E-Area.. 3-96

3.4-7. Illustration of EAV source area in PORFLOW grid.. 3-97

3.4-8. Locations of stream-gauging stations in creeks near E-Area. 3-94

4.1-1. Engineered barrier steady-state saturation 4-6

4.1-2. Vertical fluxes beneath the engineered barrier 4-7

4.1-3. Steady state saturation for the Intact period for the ILNT (a), and LAW (b) vaults 4-11

4.1-4. Steady-state saturation for the Cracked period for the ILNT (a), and LAW (b) vaults 4-12

4.1-5. Steady state saturation for the Failed period for the ILNT (a), and LAW (b) vaults 4-13

4.1-6. Contaminant plume overlap for the LAW and ILNT vaults at E-Area 4-18

4.1-7. Illustrated results of preliminary numerical simulations of Tc-99 transport in groundwater in E-Area vicinity 4-34

4.2-1. Cumulative distribution function for peak groundwater concentration of ^{99}Tc, based on ranges of parameters specified in Appendix J 4-83

6.0-1. E-Area PA organizational chart 6-14

A.1-1. Idealized cross-section for the SRS vadose zone. A-2

A.1-2. Domain of the cover simulation A-4

A.2-1. Model domain for PORFLOW simulation of groundwater in E-Area vicinity A-15

A.2-2. Location of E-Area groundwater wells A-16

A.3-1. PORFLOW input file for radon calculations A-37

C.2-1. Locations of stream-gaging stations in creeks near E-Area C-73

C.4-1. Fractional flux to the water table from the ILNT vaults C-98

C.4-2. Fractional flux to the water table from the ILNT vaults C-99

C.4-3. Fractional flux to the water table from the ILNT vaults C-100

C.4-4. Fractional flux to the water table from the ILNT vaults C-101

C.4-5. Fractional flux to the water table from the ILNT vaults C-102

C.4-6. Fractional flux to the water table from the ILNT vaults C-103

C.4-7. Fractional flux to the water table from the LAW vaults C-104

C.4-8. Fractional flux to the water table from the LAW vaults C-105

C.4-9. Fractional flux to the water table from the LAW vaults C-106

C.4-10 Fractional flux to the water table from the LAW vaults C-107

C.4-11 Fractional flux to the water table from the LAW vaults C-108

C.4-12 Fractional flux to the water table from the LAW vaults C-109

C.5-1. Predicted groundwater concentration of H-3 as a function of time C-111

C.5-2. Predicted groundwater concentration of C-14 as a function of time C-112

C.5-3. Predicted groundwater concentration of Ni-59 as a function of time C-113

C.5-4. Predicted groundwater concentration of Se-79 as a function of time C-114

C.5-5. Predicted groundwater concentration of Sr-90 as a function of time C-115

C.5-6. Predicted groundwater concentration of Tc-99 as a function of time C-116
C.5-7. Predicted groundwater concentration of Sn-126 as a function of time C-117
C.5-8. Predicted groundwater concentration of I-129 as a function of time C-118
C.5-9. Predicted groundwater concentration of Cs-135 as a function of time C-119
C.5-10. Predicted groundwater concentration of Th-232 as a function of time C-120
C.5-11. Predicted groundwater concentration of U-233 as a function of time C-121
C.5-12. Predicted groundwater concentration of U-234 as a function of time C-122
C.5-13. Predicted groundwater concentration of U-235 as a function of time C-123
C.5-14. Predicted groundwater concentration of U-236 as a function of time C-124
C.5-15. Predicted groundwater concentration of U-238 as a function of time C-125
C.5-16. Predicted groundwater concentration of Np-237 as a function of time C-126
C.5-17. Predicted groundwater concentration of Am-241 as a function of time C-127
C.5-18. Predicted groundwater concentration of Am-243 as a function of time C-128
C.5-19. Predicted groundwater concentration of Pu-238 as a function of time C-129
C.5-20. Predicted groundwater concentration of Pu-239 as a function of time C-130
C.5-21. Predicted groundwater concentration of Pu-240 as a function of time C-131
C.5-22. Predicted groundwater concentration of Pu-242 as a function of time C-132
C.5-23. Predicted groundwater concentration of Pu-244 as a function of time C-133
C.5-24. Predicted groundwater concentration of Cm-244 as a function of time C-134
C.5-25. Predicted groundwater concentration of Cm-245 as a function of time C-135
C.5-26. Predicted groundwater concentration of Cm-246 as a function of time C-136
C.5-27. Predicted groundwater concentration of Cm-247 as a function of time C-137
C.5-28. Predicted groundwater concentration of Cm-248 as a function of time C-138
C.5-29. Predicted groundwater concentration of Bk-247 as a function of time C-139
C.5-30. Predicted groundwater concentration of Cf-249 as a function of time C-140
C.5-31. Predicted groundwater concentration of Cf-251 as a function of time C-141
D.4-1. Adsorption of Pu on goethite as a function of pH at two plutonium concentrations (from Sanchez et al. 1985) D-6

D.4-2. The effect of carbonate alkalinity on the adsorption of Pu(IV) on goethite (from Sanchez et al. 1985). Alkalinity in the vault will be approximately 60 meq/L D-8

D.4-3. Adsorption of uranyl on a 1 g/L goethite suspension as a function of pH in a 0.1 M $NaNO_3$ solution (from Hsi and Langmuir 1985). a) uranyl at 10^{-5} M, b) dissolved uranium at 10^{-5} M and varying total carbonate, c) effect of changes in total carbonate on the adsorption of uranyl D-10

D.4-4. Adsorption of Sr^{2+} on goethite as a function of pH in a 1.0 M $NaNO_3$ solution (from Dzombak and Morel 1990). a) 6.9 g goethite/L, b) 8.9 g goethite/L, c) 8.9 g goethite/L, d) 8.9 g goethite/L, e) 8.9 g goethite/L, f) 8.9 g goethite/L, g) 8.9 g goethite/L, h) 1.8 g goethite/L, i) 4.4 g goethite/L, j) 8.9 g goethite/L, k) 17.8 g goethite/L D-12

D.4-5. Adsorption of nickel on goethite as a function of pH in a 0.1 M $NaNO_3$ solution (from Dzombak and Morel 1990) D-19

D.4-6. Adsorption of selenite on goethite as a function of pH in a 0.5 M NH_4NO_3 solution (from Dzombak and Morel 1990) D-21

D.4-7. Adsorption of barium on goethite as a function of pH as an analog for radium (from Dzombak and Morel 1990). a) 0.05 g goethite/L, b) 0.05 g goethite/L, c) 0.01 g goethite/L, d) 0.06 g goethite/L, e) 0.2 g goethite/L D-22

D.4-8. Adsorption of thorium on goethite as function of pH in 0.422 mol/Kg NaCl electrolyte at different thorium/oxide ratios (Hunter et al. 1988). Triangles: 9 micromol/L Th, 8.6 g/L goethite; Circles: 9 micromol/L Th, 0.54 g/L goethite; Squares: 45 micromol/L Th, 0.54 g/L goethite D-27

D.4-9. Adsorption of neptunium on goethite as function of pH (Girvin et al. 1988). Triangles: 0.3 g/L goethite; Circles: 0.9 g/L goethite; Squares: 0.09 g/L goethite . D-28

D.4-10. Adsorption of mercury on goethite as function of pH as an analog for tin (from Dzombak and Morel 1990). a) 0.05 g/L goethite, b) 0.05 g/L goethite D-29

D.4-11. Adsorption of chromium III on goethite as function of pH as an analog for americium (from Dzombak and Morel 1990) D-31

D.5-1. Estimated Pu(IV) solubility under E-Area conditions D-33
D.5-2. Estimated total uranium solubility under E-Area conditions D-35
D.5-3. Comparison of uranium solubilities under E-Area conditions D-37
E.1-1. Hydrologic and stratigraphic units underlying the SRS E-2
E.2-1. Surface drainage map of the SRS E-11
E.2-2. Potentiometric surface of Aquifer Unit IIA at E-Area E-12
E.2-3. Regional potentiometric surface of Aquifer Unit IIA (Christensen and Gordon 1983) E-13
E.2-4. Potentiometric surface of Aquifer Unit IIB, Zone 1, at E-Area E-15
E.2-5. Potentiometric surface for Aquifer Unit IIB, Zone 2, at E-Area E-18
E.2-6. Soil water content-pressure relationships for undisturbed soils at SRS burial grounds (Gruber 1980) E-19
E.2-7. Unsaturated hydraulic conductivity as a function of moisture content at SRS burial grounds (Gruber 1980) E-20
E.2-8. Soil water content-pressure relationships for undisturbed soils in Z-Area (Quisenberry 1985) E-21
E.2-9. Unsaturated hydraulic conductivity as a function of moisture content at Z-Area (Quisenberry 1985) E-22
I.1-1. Conceptual drawing of proposed suspect soil trenches I-2
I.2-1. Simulation domain for the suspect soil trenches in the vadose zone I-10
I.5-1. PORFLOW input file - flow in the vadose zone I-43
I.5-2. Example PORFLOW input file - mass transport in vadose zone I-52
I.5-3. Example PORFLOW input file - mass transport in groundwater I-55
L.1.1. Naval reactor waste disposal container L-2
L.1.2. Proposed layout of Naval Reactor Waste Disposal Area in the EAV facility L-3
L.2-1. Near-field simulation domain for NR waste L-11
L.5-1. PORFLOW input file - flow in the vadose zone for NR waste analysis L-43
L.5-2. Example PORFLOW input file - mass transport of NR waste radionuclides in vadose zone L-45

L.5-3. Example PORFLOW input file - mass transport of NR waste radionuclides in groundwater L-43
M.1-1. PORFLOW Input File - File simulation through intact ILNT vault M-1
M.1-2. PORFLOW Input File - File simulation through cracked ILNT vault M-4
M.1-3. PORFLOW Input File - Flow simulation through failed ILNT vault M-7
M.1-4. PORFLOW Input File - Mass transport simulation for intact ILNT vault M-10
M.1-5. PORFLOW Input File - Mass transport simulation for intact ILNT vault, solubility-limited source M-14
M.2-1. PORFLOW-3D input files for the groundwater flow field M-18
M.2-2. PORFLOW-3D input file for the groundwater mass transport of C-14 and Tc-99 . M-23

TABLES

2.1-1. Water quality of the Savannah River above SRS (Cummins et al. 1990) 2-19
2.1-2. Comparison of natural radiation doses near SRS with U.S. averages 2-24
2.2.1. Summary of hydraulic conductivities reported for Aquifer System II 2-33
2.2-2. Concentration of dissolved elements in groundwater in Aquifer Unit IIA and Units IIB1 and IIB2 near E-Area (Cummins et al. 1990) 2-36
2.2-3. Water quality of UTR Creek at Road A (Cummins et al. 1990) 2-37
2.2-4. Maximum constituent results exceeding applicable standards for wells at the EAVDF (Arnett et al. 1991) 2-39
2.2-5. Groundwater monitoring results for the EAVDF (Cummins et al. 1990) 2-40
2.2-6. Monitoring well results of radionuclides in groundwater for the EAVDF (Cummins et al. 1990) 2-42
2.7-1. NR waste radioactive inventory 2-61
2.9.1 Values for hydraulic properties of vault closure design 2-67
3.2-1. Maximum contaminant limits for radionuclides in groundwater corresponding to different options for groundwater protection requirement 3-24
3.3-1. Summary of hydraulic and van Genuchten fitting parameters 3-62
3.3-2. Partition coefficients used in PORFLOW near-field simulations, mL/g 3-69
3.3-3. LAW vault parameters 3-71
3.3-4. ILNT vault parameters 3-72
3.3-5. Degradation times for vaults, years 3-73
3.3-6. Hydraulic conductivities for saturated zone simulations 3-79
3.3-7. Aquifer matrix-specific mass transport parameters 3-80
3.5-1. Implementation of NQA-1 by ORNL for the EAVDF RPA 3-100
3.5-2. Implementation of NQA-1 by INEL for the EAVDF RPA 3-102
4.1-1. Trigger values for radionuclides selected for detailed groundwater analyses 4-3
4.1-2. Simulation time for each state of the vault 4-10

4.1-3. Peak fractional flux release to the aquifer for EAV radionuclides except isotopes of U and Pu 4-15

4.1-4. Solubility limit and peak flux to the aquifer for isotopes of U and Pu 4-16

4.1-5. Predicted groundwater compliance concentration for the ILNT vaults 4-19

4.1-6. Predicted groundwater compliance concentration for the LAW vaults 4-21

4.1-7. Annual EDFs from drinking water pathway per unit concentration of radionuclides in groundwater 4-30

4.1-8. Comparison of MCLs and allowable groundwater concentrations based on the 25 mrem per year performance objective for off-site individuals 4-31

4.1-9. Calculated allowable inventories based on the groundwater pathway (for off-site doses up to 10,000 years after disposal) 4-33

4.1-10. SDCFs for agriculture scenario for inadvertent intruders 4-36

4.1-11. SDCFs for resident scenario for inadvertent intruders 4-37

4.1-12. SDCFs for post-drilling scenario for inadvertent intruders 4-38

4.1-13. Geometrical reduction factors (*G*) used in dose analyses for inadvertent intruders 4-39

4.1-14. Results of dose analysis for intruder agriculture scenario for ILNT vaults 4-46

4.1-15. Results of dose analysis for intruder agriculture scenario for LAW vaults 4-52

4.1-16. Results of dose analysis for intruder agriculture scenario for ILT vaults 4-56

4.1-17. Results of worst-case dose analysis for resident scenario for ILNT vaults at 100 years after disposal 4-60

4.1-18. Results of dose analysis for resident scenario for ILNT vaults at 10,000 years after disposal 4-62

4.1-19. Results of dose analysis for resident scenario for LAW vaults at 100 years after disposal 4-64

4.1-20. Results of worst-case dose analysis for resident scenario for ILT vaults at 100 years after disposal 4-66

4.1-21. Results of dose analysis for resident scenario for ILT vaults at 10,000 years after disposal 4-67

4.1-22. Results of dose analysis for post-drilling scenario for LAW vaults 4-70

4.1-23. Disposal limits of radionuclides for ILNT and ILT vaults based on analyses of exposure scenarios for inadvertent intruders 4-74
4.1-24. Concentration limits of radionuclides for Class-C waste specified in NRC's 10 CFR Part 61 4-76
4.1-25. Disposal limits of radionuclides for LAW vaults based on analyses of exposure scenarios for inadvertent intruders 4-77
4.1-26. Disposal limits of radionuclides for ILT vaults based on analyses of exposure scenarios for inadvertent intruders 4-80
4.3-1. E-Area Vault Disposal Facility performance-based inventory limits (Ci/vault) and limiting performance objectives 4-94
4.3-2. Comparison of LAW vault calculated disposal limits with estimated inventory 4-95
4.3-3. Comparison of ILNT and ILT vault calculated disposal limits with estimated inventory 4-96
6.0-1. E-Area PA organizational chart 6-14
A.1-1. Longitudinal and transverse dispersivities used in the PORFLOW near-field model A-7
A.2-1. Measured and assumed hydraulic conductivities for saturated hydraulic units A-20
A.2-2. Total porosities - E-Area A-21
A.4-1. Radionuclides considered in dose analyses for off-site individuals or inadvertent intruders A-41
A.4-2. Internal dose conversion factors for ingestion of radionuclides A-51
A.4-3. Internal dose conversion factors for inhalation of radionuclides A-53
A.4-4. External dose-rate conversion factors for radionuclides uniformly distributed in 15 cm of surface soil A-57
A.4-5. External dose-rate conversion factors for radionuclides uniformly distributed in infinite thickness of soil-equivalent material A-58
A.4-6. Annual EDEs from drinking water pathway per unit concentration of radionuclides in water A-65
A.4-7. Elemental plant-to-soil concentration ratios in vegetables A-69

A.4-8. Annual EDEs from vegetable pathway per unit concentration of radionuclides in exhumed waste for agriculture scenario A-71
A.4-9. Annual EDEs from soil ingestion pathway per unit concentration of radionuclides in exhumed waste for agriculture scenario A-74
A.4-10. Annual EDEs from external exposure in vegetable garden per unit concentration of radionuclides in exhumed waste for agriculture scenario A-77
A.4-11. Annual EDEs from external exposure in home per unit concentration of radionuclides in disposal units for agriculture scenario A-79
A.4-12. Annual EDEs from inhalation exposure in vegetable garden per unit concentration of radionuclides in exhumed waste for agriculture scenario A-82
A.4-13. Annual EDEs from inhalation exposure in home per unit concentration of radionuclides in disposal units for agriculture scenario A-84
A.4-14. Annual EDEs per unit concentration of radionuclides in disposal units from all exposure pathways for agriculture scenario A-89
A.4-15. Annual EDEs per unit concentration of radionuclides in disposal units for resident scenario A-93
A.4-16. Annual EDEs per unit concentration of radionuclides in exhumed waste for post-drilling scenario A-95
A.4-17. Summary of radionuclide-independent parameter values used in dose analyses for off-site individuals and inadvertent intruders A-99
B.4-1. Evaluation of identified alternative subsurface flow and transport codes B-20
C.1-1. Screening calculations and trigger levels for the ILT vaults C-2
C.1-2. Screening calculations and trigger levels for the ILNT vaults C-24
C.1-3. Screening calculations and trigger levels for the LAW vaults C-46
C.1-4. Weighted dose conversion factors for radionuclides with multiple daughters C-68
C.2-1. Steam gaging results for SRS creeks in the vicinity of E-Area C-72
C.3-1. Screening calculations and trigger values for the suspect soil trenches C-75
C.6-1. AIRDOS-PC data for the volatile radionuclide pathway C-145

D.4-1. Summary of distribution coefficients for selected radionuclides on goethite ..... D
D.4-2. Adsorption of Pu(IV) on goethite as a function of ionic strength D-7
D.4-3. Adsorption data for strontium used to estimate K_d D-13
D.4-4. Adsorption data for barium used to estimate radium K_d D-25
D.5-1. Plutonium reactions considered D-34
D.5-2. Uranium reactions considered D-36
I.2-1. Radionuclides considered in the detailed groundwater analysis for suspect soil trenches I-6
I.2-2. Distribution coefficients assumed for elements in suspect soil trenches I-12
I.3-1. Peak flux to the water table from suspect soil trenches I-21
I.3-2. Predicted groundwater compliance concentration for the suspect soil trenches I-24
I.3-3. Comparison of MCLs and allowable groundwater concentrations based on the 25 mrem per year performance objective for off-site individuals I-28
I.3-4. Groundwater-based disposal limits for the suspect soil trenches I-30
I.3-5. Suspect soil disposal limits based on the air pathway I-33
I.3-6. Results of dose analysis for intruder agriculture scenario for suspect soil trenches .. I-34
I.3-7. Summary of disposal limits for the suspect soil trenches I-40
J.1-1. Factor specification for Latin Hypercube Sample generation J-2
J.3-1. Variable definitions for multiple regression model J-4
J.3-2. Important variable combinations J-4
J.4-1. Confidence intervals for mean J-5
J.4-2. Tolerance limits on response distribution J-5
L.1-1. Radioactive inventory for 41 NR diposal casks to be shipped to E-Area L-5
L.2-2. Distribution coefficients assumed for subsurface transport simulations for radionuclides in NR waste L-14
L.3-1. Peak flux to the water table from NR waste L-23
L.3-2. Predicted groundwater compliance concentration for the NR waste L-25
L.3-3. Groundwater-based disposal limits for the NR waste L-26
L.3-4. Disposal limits for NR waste based on the air pathway L-28
L.3-5. Groundwater-based disposal limits versus expected inventory for the NR waste .. L-40

ACRONYMS AND ABBREVIATIONS

ACRI	Analytic and Computational Research, Inc.
ALARA	as low as reasonably achievable
ANSI	American National Standards Institute
ARARs	applicable or relevant and appropriate requirements
ASL	above sea level
ASME	American Society of Mechanical Engineers
CCF	concentration/consumption factor
CERCLA	Comprehensive Environmental Resource, Compensation, and Liability Act
cm	centimeters
cpu	central processor unit
CRDMS	control rod drive mechanisms
CSRA	Central Savannah River Area
CTT	contaminant travel time
D&D	decommissioning and decontamination
DCF	dose conversion factor
DOE	Department of Energy
DWPF	Defense Waste Processing Facility
DWS	drinking water standards
EAVs	E-Area vaults
EAVDF	E-Area Vault Disposal Facility
EDE	effective dose equivalent
EH	Environment, Safety, and Health
EM	Environmental Restoration and Waste Management
EPA	Environmental Protection Agency
ER	environmental restoration

FM	Facilities Management
GSA	General Separations Area
h	hour(s)
HAD	Hazard Assessment Document
HFO	hydrous ferric oxide
HLW	high-level waste
HW/MWDF	Hazardous Waste/Mixed Waste Disposal Facility
IAW	Intermediate Activity Waste
ILTV	Intermediate Level Tritium Vaults
ILNTV	Intermediate Level Non-Tritium Vaults
in.	inches
INEL	Idaho National Engineering Laboratory
kg	kilograms
L	liter(s)
LAW	Low Activity Waste
LAWV	Low Activity Waste Vault
LLW	low-level waste
LLWSB	long-lived waste storage building
m	meters
MCLs	maximum contaminant levels
mg	milligrams
mm	millimeters
MMI	Modified Mercalli Intensity
mol	mole(s)
MPC	maximum permissible concentration
MSL	mean sea level
MW	mixed waste
NCRP	National Council on Radiation Protection and Measurements

NESHAPs	National Emissions Standards for Hazardous Air Pollutants
NPL	National Priority List
NQA	Nuclear Quality Assurance
NR	naval reactor
NRC	Nuclear Regulatory Commission
ORNL	Oak Ridge National Laboratory
OSRs	Operational Safety Requirements
PA	performance assessment
PC	personal computer
PDWS	primary drinking water standards
ppm	parts per million
QA	Quality Assurance
RCRA	Resource Conservation and Recovery Act
RPA	Radiological Performance Assessment
s	second(s)
SAR	Safety Analysis Report
SCDHEC	South Carolina Department of Health and Environmental Control
SDCFs	scenario dose conversion factors
SDF	Saltstone Disposal Facility
Sect.	Section
SMSA	Standard Metropolitan Statistical Area
SRS	Savannah River Site
SWDF	Solid Waste Disposal Facility
TRU	transuranic waste
TV	trigger value
UTR	Upper Three Runs (Creek)

WAC	waste acceptance criteria
WCR	water to cement ratio
WITS	Waste Information Tracking System
WSRC	Westinghouse Savannah River Company

EXECUTIVE SUMMARY

This radiological performance assessment (RPA) for the Savannah River Site (SRS) E-Area Vaults (EAVs) Disposal Facility was prepared to meet the requirements of Chapter III of the U.S. Department of Energy Order 5820.2A. The Order specifies that an RPA should provide reasonable assurance that a low-level waste (LLW) disposal facility will comply with the performance objectives of the Order. The performance objectives require that: 1) exposures of the general public to radioactivity in the waste or released from the waste will not result in an effective dose equivalent of 25 mrem per year; 2) releases to the atmosphere will meet the requirements of 40 CFR 61; 3) inadvertent intruders will not be committed to an excess of an effective dose equivalent of 100 mrem per year from chronic exposures, or 500 mrem from a single acute exposure; and 4) groundwater resources will be protected in accordance with Federal, State, and local requirements.

The EAVs, located on a 200-acre site immediately north of the current LLW burial site, will provide a new disposal and storage site for solid, low-level, non-hazardous radioactive waste. As presently planned, the EAV Disposal Facility will contain several large concrete vaults divided into cells. The EAVs consist of three types of structures to house four designated waste types. One type of structure is partitioned into two segments [the Intermediate Level Tritium Vaults (ILTV) and Intermediate Level Non-Tritium Vaults (ILNTV)] and receives two categories of waste. The ILNTV receives waste radiating ≥200 mR/h at 5 cm from the exterior of the outer disposal container. The ILTV receives waste which is contaminated with more than incidental quantities of tritium. Administratively, the lower limit for the ILTV is 10 Ci of tritium per package. These two vaults share a similar design, are adjacently located, share waste handling equipment, and will be closed as one facility. The second type of structure is designated as the Low Activity Waste Vaults (LAWV). The LAWV is designed to receive waste radiating <200 mR/h at 5 cm from the exterior of the outer disposal container and containing <10 Ci of tritium per package. The third facility is the Long Lived Waste Storage Building (LLWSB). The LLWSB is designed to provide covered, long term storage for waste containing long lived isotopes which exceeds

performance criteria for disposal. This waste would eventually be removed to a suitable disposal facility. In addition to the disposal activities described previously, two additional types of disposal are proposed: 1) trench disposal of suspect soil, and 2) naval reactor component disposal. Five below grade trenches will be constructed to contain suspect soil, which is soil from regulated areas and designated as potentially contaminated. An area of approximately 1700 m^2 is planned to receive several containers of naval reactor (NR) components. These components can include control rods, control rod drive mechanisms, resin vessels, adapter flanges, and similar equipment.

The long-term performance of the vaults is key to the prediction of the transport of radionuclides into the environment at E-Area. A special study was conducted by an independent engineering firm to study the degradation mechanisms and their effects on the integrity of the vault systems. The results of this study predicted the time required for cracking of the vaults and collapse of the roof structures.

To evaluate the long-term performance of the EAVs, site-specific conceptual models were developed to consider: 1) exposure pathways and scenarios of potential importance; 2) potential releases from the facility to the environment; 3) effects of degradation of engineered features; 4) transport in the environment; and 5) doses potentially received from releases determined from unit concentrations of the radionuclides of interest in each vault type. Initial radionuclide inventories were not assumed in this performance assessment. The EAV performance assessment was used as a means to determine the allowable radionuclide concentrations and inventories in each type of disposal unit. This methodology provides reasonable assurance that the performance objectives will be met if these inventories are used to establish limits in the waste acceptance criteria.

When compared to a reasonable estimate of the amount of waste that could be received at the E-Area Vault Disposal Facility, the performance-based maximum radionuclide inventory limits in this report will allow disposal of all waste types expected at SRS, with the exception of the NR components. These components will be received as planned, but will be stored. It is expected that additional wasteform information will be received to enable revision of the performance assessment for this type of waste, to show acceptable performance.

1. INTRODUCTION

The Savannah River Site (SRS) was acquired by the U.S. Government in 1950. Since that time, the U. S. Government has contracted for the design, development, construction, and operation of various facilities at the SRS to support national defense and space exploration. Because of these activities at the site, low-level, solid, non-hazardous radioactive wastes will continue to be generated. In addition, environmental restoration (ER) and decommissioning and decontamination (D & D) activities will generate increasing quantities of low-level radioactive wastes.

The policies and guidelines of the Department of Energy (DOE) and other regulatory agencies require that radioactive waste be managed, treated, stored, and disposed in a manner that protects public health and safety, the environment, and groundwater resources. These practices must be done in accordance with standards specified in federal, state, and local regulations. The level of radioactivity in any effluent released to the environment should be maintained "as low as reasonably achievable (ALARA)", known as the "ALARA" principle within the DOE complex.

DOE Order 5820.2A, issued in 1988 (U.S.DOE 1988a), established policies, guidelines, and minimum requirements for the management of radioactive waste, mixed waste (MW), and contaminated facilities at the DOE sites. This Order addresses the storage, treatment, and disposal of high-level waste (HLW), MW, low-level waste (LLW), transuranic waste (TRU), and naturally occurring and accelerator-produced radioactive materials that are generated by the DOE operations. Chapter III of the Order requires the DOE field sites to prepare and maintain a site-specific radiological performance assessment (RPA) for any LLW disposal facility located at DOE field sites. An RPA must provide reasonable assurance that the facility design and method of disposal will comply with the performance objectives of the Order (Dodge et al. 1991).

The E-Area Vaults Disposal Facility (EAVDF) (Fig. 1.1-1) is one of several new facilities at SRS that will incorporate radioactive solid waste generated at the SRS for near-surface disposal.

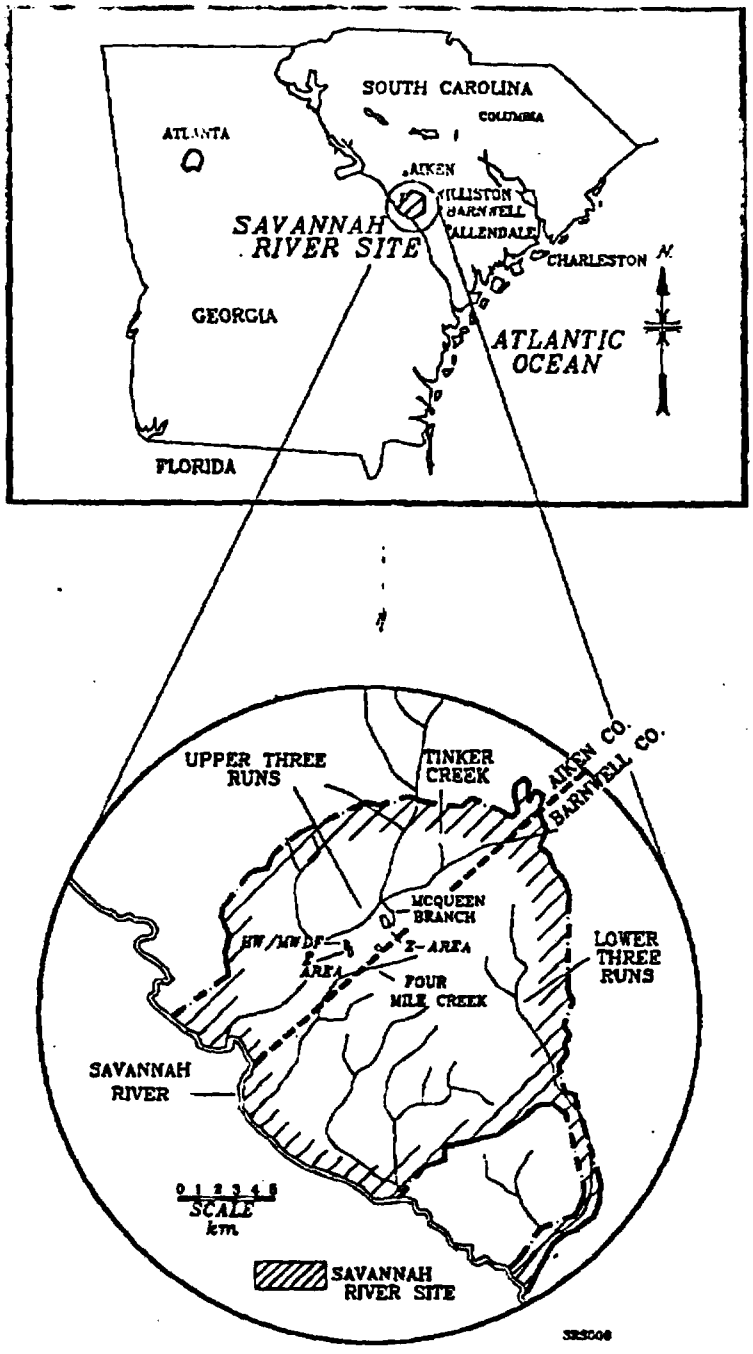

Fig. 1.1-1. Location map of the Savannah River Site.

The E-Area Vaults (EAVs) are only one part of an integrated radioactive waste management system that is being put in place at the SRS. As principal contractor and operator at SRS, the Westinghouse Savannah River Company (WSRC) will complete the design, construct and operate several facilities to manage and dispose of radioactive waste generated at the SRS. Assuming adequate funding is maintained at the SRS, all facilities that are a part of this integrated waste management system are projected to be in operation by the year 2000.

Before the SRS will comply completely with DOE Order 5820.2A, a separate RPA must be completed for at least three operating or planned disposal facilities at the SRS: 1) the EAVs solid waste disposal facility (SWDF), 2) the Saltstone Disposal Facility (SDF) (located in Z-Area), and 3) the Hazardous Waste/Mixed Waste Disposal Facility (HW/MWDF). To fulfill the RPA requirement of DOE Order 5820.2A for the EAV, the long-term radiological impacts on the environment and on the public due to solid waste disposal in E-Area have been assessed. Results of this assessment are documented in this report. An RPA has been completed for the SDF. An RPA has not been completed for the HW/MWDF since the construction and operation of this facility has been postponed. A description of the HW/MWDF is given in Sect. 2.8 along with a description of its integration with this RPA.

1.1 PURPOSE AND SCOPE

E-Area is the location of a new LLW disposal facility located at SRS. The objective of the EAV is to provide a new disposal and storage site for low-level, solid, non-hazardous radioactive waste to support continuing SRS operations. DOE Order 5820.2A defines low-level radioactive waste as waste that contains radioactivity and is not classified as high-level waste (HLW) (waste material that results from the reprocessing of spent nuclear fuel), transuranic waste, or spent nuclear fuel or 11e(2) by product material.

SRS operations further classify the LLW handled by EAV as low-activity waste (LAW), intermediate-activity waste (IAW) and tritiated waste. LAW consists of waste material that radiates greater than 200 mR/hr from an unshielded container at 5 cm. LAW consists of waste material that radiates less than 200 mR/hr from an unshielded container at 5 cm. Tritiated waste is waste that contains greater than 10 Ci of tritium per container regardless of the radiation rate. EAV will not dispose of or store liquid wastes, waste containing greater than 100 nCi/g of TRU isotopes, hazardous waste, or mixed (hazardous and radioactive) wastes.

Monitoring systems and procedures are in place to establish both the impact to the environment and the risks to operating personnel and off-site populations during normal operations and subsequent closure operations at the disposal site. Groundwater monitoring procedures are in place to provide baseline monitoring data and to confirm that disposal and closure operations do not adversely affect water quality. This RPA concentrates on establishing, with reasonable assurance, that LLW disposal in E-Area will meet the performance objectives of DOE Order 5820.2A after the disposal facility is closed. The objectives of the Order are described in Sect. 1.2.

Radiological and other hazards prior to closure have been analyzed in the Safety Analysis Report (SAR) for the operational period of the EAV (WSRC 1991a). In particular, the SAR for the EAV addresses the issues and hazards related to safety and radiological doses to on-site and off-site populations during active disposal operations and interim closure. The location of E-Area is well within the confines of the secured boundary of the SRS, thus precluding inadvertent access to the E-Area site by unauthorized personnel during active disposal operations. Furthermore, the distance to the present SRS site boundary obviates the need for extensive analysis of performance prior to closure and/or loss of institutional control.

1.2 PERFORMANCE OBJECTIVES

The specific performance objectives for solid waste disposal in E-Area are contained in DOE Order 5820.2A (U.S.DOE 1988a):

1. Protect public health and safety in accordance with standards specified in applicable EH Orders and other DOE Orders.

2. Assure that external exposure to the waste and concentrations of radioactive material which may be released to surface water, groundwater, soil, plants, and animals results in an effective dose equivalent (EDE) that does not exceed 25 mrem per year to a member of the general public. Releases to the atmosphere shall meet the requirements of 40 CFR 61 which limits the EDE to 10 mrem per year. Reasonable effort should be made to maintain releases of radioactivity in effluent to the general environment ALARA.

3. Assure that the EDE from all exposure pathways received by individuals who inadvertently may intrude into the facility after the loss of active institutional control (100 years) will not exceed 100 mrem per year for continuous exposure or 500 mrem for a single acute exposure.

4. Protect groundwater resources, consistent with Federal, State, and local requirements.

Compliance with the performance objective to protect groundwater resources is interpreted at SRS as meaning that concentrations of chemical and radioactive contaminants at any points of compliance should not exceed standards for public drinking water supplies established by the Environmental Protection Agency (EPA).

In this analysis, the point of compliance for groundwater protection requirements is taken to be that location more than 100 m from any disposed waste at which the predicted concentrations of contaminants in groundwater are the highest (Dodge et al. 1991). Requirements for protection of groundwater do not apply inside a 100-m buffer zone around the disposal units.

The performance objectives for disposal of LLW in the EAV given above require further interpretation with respect to three issues. The first is the time period over which the performance objectives for protection of off-site members of the public, inadvertent intruders, and groundwater resources should be applied. The second issue is the particular standards (i.e., numerical limits) for radionuclides that should be applied to protection of groundwater resources. The third issue is the inclusion of doses from radon and its decay products in the doses calculated in the intrusion scenarios.

1.2.1 Time for Compliance with Performance Objectives

The various performance objectives for LLW disposal in DOE Order 5820.2A do not specify a time period over which they are to be applied. Therefore, the implication is that all performance objectives apply at any time after disposal.

The DOE is actively considering a change in policy regarding the time for compliance with the performance objectives. In the near future, the DOE is expected to adopt a policy that compliance with the performance objectives would be required only for 10,000 years after disposal but would not be required thereafter. In addition, however, if the predicted doses to off-site individuals or inadvertent intruders or the predicted levels of contaminants in groundwater outside the 100-m buffer zone have not attained their maximum values within the 10,000-year compliance period, the DOE is expected to require that the analysis be continued beyond 10,000 years until such time as the peak doses or contaminant levels are attained. Any calculations beyond the 10,000-year compliance period would be used primarily to provide additional information and perspective on the performance of disposal facilities.

Although strict compliance with the performance objectives beyond 10,000 years would not be required, the results of any analyses beyond 10,000 years could be used by the DOE in rendering judgments on the overall acceptability of disposal facilities.

In accordance with the expected change in DOE policy, the following approach to the time period for compliance with the performance objectives has been taken in this RPA.

1) The performance objectives for protection of off-site members of the public, inadvertent intruders, and groundwater resources are applied for 10,000 years after disposal.

2) If calculated doses to off-site members of the public or inadvertent intruders or calculated contaminant levels in groundwater do not attain their maximum values during the 10,000-year compliance period, the calculations are continued in time until the peak values are obtained.

1.2.2 Performance Objective for Groundwater Protection

DOE Order 5820.2A does not specify either dose or concentration limits for radionuclides in groundwater. Therefore, there is some ambiguity in applying the performance objective even though, as described previously, the performance objective is interpreted as requiring that concentrations of contaminants in groundwater should not exceed values specified in EPA standards for public drinking water supplies (40 CFR Part 141).

In the RPA for the EAV, three different options for specifying maximum contaminant levels (MCLs) of radionuclides in groundwater are considered. The three options, each of which is consistent with EPA standards for radioactivity in drinking water, are described below.

Option 1

In the first option, the MCLs for radionuclides in groundwater are those specified in current EPA standards for radioactivity in drinking water, which were promulgated in 1976. The current standards include: 1) a limit on concentration of 5 pCi/L for Ra-226 and Ra-228 combined; 2) a limit on concentration of 15 pCi/L for gross alpha-particle activity, including Ra-226 but excluding radon and uranium; and 3) a limit on dose equivalent to whole body or any organ of 4 mrem per year from all beta/gamma-emitting radionuclides. The current standards also specify that the concentration of any beta/gamma-emitting radionuclide causing a dose equivalent of 4 mrem to whole body or any organ shall be calculated on the basis of a drinking water intake of 2 L/day and data for converting activity intakes of radionuclides to dose published by the U.S. Department of Commerce (1963), except the MCLs are given as 20,000 pCi/L for tritium (H-3) and 8 pCi/L for Sr-90.

A possible drawback of the approach specified by the EPA for calculating MCLs for beta/gamma-emitting radionuclides is that the concentration limits in water corresponding to a dose equivalent to whole body or any organ of 4 mrem are based on internal dosimetry data (U.S. Department of Commerce 1963) which are now outdated. The dosimetric and metabolic models for radionuclides used to obtain the data in the Department of Commerce report essentially are those recommended in Publication 2 of the International Commission on Radiological Protection (ICRP 1959), but these data have been superseded by data based on the models in ICRP Publication 30 (1979). Although the more recent internal dosimetry data developed by the ICRP have been adopted for use by the EPA (Eckerman et al. 1988) and DOE (1988b), these data have not yet been incorporated in the EPA standards for radioactivity in drinking water. Because these standards use outdated internal dosimetry data for beta/gamma-emitting radionuclides, the MCLs for most radionuclides calculated as specified by the EPA would not correspond to the specified limit on dose equivalent of 4 mrem to whole body or any organ. This consideration leads to the second option for the performance objective adopted for use in this analysis.

Option 2

In the second option, the EPA's current MCLs of 5 pCi/L for Ra-226 and Ra-228 combined and 15 pCi/L for gross alpha-particle activity, including Ra-226 but excluding radon and uranium, and the limit on dose equivalent of 4 mrem per year to whole body or any organ from all beta/gamma-emitting radionuclides are retained. However, the dose limit for any beta/gamma-emitting radionuclide is converted to a concentration limit using the internal dosimetry data from ICRP Publication 30 (1979) that has been adopted for use by the DOE (1988b). Thus, for beta/gamma-emitting radionuclides, the second option uses the same primary standard (i.e., dose limit) as the current EPA standards, but the secondary standards (i.e., concentration limits) are based on up-to-date internal dosimetry data; and, in this option, the MCLs for all beta/gamma-emitting radionuclides correspond, based on the best available information, to the dose limit of 4 mrem per year to whole body or any organ.

Option 3

In the third option, the MCLs for radionuclides in groundwater are those specified in the EPA's proposed revisions of the drinking water standards (DWS) for radionuclides (EPA 1991). The proposed standards include: 1) separate limits on concentration of 20 pCi/L for Ra-226 and Ra-228; 2) a limit on concentration of 20 µg/L for uranium, 3) a limit on concentration of 15 pCi/L for gross alpha-particle activity, excluding Ra-226, uranium, and Rn-222; and 4) a limit on EDE of 4 mrem per year for all beta/gamma-emitting radionuclides. The proposed concentration limit for uranium is based on prevention of chemical toxicity in the kidney, rather than limitation of radiation dose, and corresponds to an activity concentration of 14 pCi/L for naturally occurring uranium with its normal isotopic abundances. The proposed standards also include a concentration limit of 300 pCi/L for Rn-222, but the Energy Policy Act of 1992 directs the EPA not to issue a standard for radon in drinking water at the present time. Final revisions of the DWS for radionuclides have not yet been promulgated.

The proposed revisions of the DWS for radionuclides described above differ from the current standards in two respects that are potentially important for this RPA. First, the proposed revisions include an MCL for uranium, whereas uranium is unregulated in current standards. Second, the proposed revisions include a limit on EDE for beta/gamma-emitting radionuclides, whereas the dose limit in current standards applies to whole body or any organ. For radionuclides that preferentially irradiate only one or a few body organs (e.g., I-129, Pu-239) a limit on EDE of 4 mrem corresponds to a considerably different MCL than a limit on dose equivalent of 4 mrem to whole body or any organ, even when the same dosimetric and metabolic model is used. Internal dosimetry data based on ICRP Publication 30 (1979) presumably would be used to convert the dose limit of 4 mrem EDE to radionuclide-specific MCLs.

Summary

Three different options for specifying the performance objective for protection of groundwater resources have been used in this analysis. These options are summarized as follows:

1) Current EPA standards for radionuclides in drinking water, including the method prescribed by the EPA for calculating MCLs for beta/gamma-emitting radionuclides based on internal dosimetry data from ICRP Publication 2 (1959) and the specified MCLs for H-3 and Sr-90;

2) Current EPA standards for radionuclides in drinking water, except all MCLs for beta/gamma-emitting radionuclides are calculated from the prescribed dose limit using updated internal dosimetry data based on ICRP Publication 30 (1979); and

3) Proposed revisions of the EPA standards for radionuclides in drinking water, with MCLs for beta/gamma-emitting radionuclides calculated using internal dosimetry data based on ICRP Publication 30 (1979), except no standard for radon is assumed.

Option 1 will be used in this RPA to assess compliance with the groundwater protection performance objective; for uranium, a compliance limit of 20 µg/L from Option 3 will be used. The SRS is one of the DOE sites designated as being on the National Priority List (NPL) by the Comprehensive Environmental Response, Compensation, and Liability Act (CERCLA) (40 CFR 300). As a result, all groundwater at SRS is regulated by CERCLA. Under CERCLA, the MCLs promulgated under the Safe Drinking Water Act (40 CFR 141) are used as applicable or relevant and appropriate requirements (ARARs). Thus, even though they use out-dated dose methodology, the current MCLs (Option 1) should be used for compliance. Where the current MCLs do not specify a limit (as in the case of uranium), a proposed MCL can be used as an ARAR. Thus the compliance limit for uranium is 20 µg/L. In most, but not all, cases Option 1 produces the most restrictive MCLs (see Table 3.2-1).

1.2.3 Radon

Radon-222 is produced by the decay of uranium-234 and -238. Radon can be a potentially significant contributor to doses in intruder scenarios. The current DOE Waste Management Order, 5820.2A, does not provide guidance as to whether doses from radon are to be included in assessing compliance with the performance objectives. However, the DOE Waste Management Order is now being revised. As a result of guidance provided by the Performance Assessment Task Team, the draft DOE Order, 5820.2B (U.S.DOE 1994), excludes dose from radon and its decay products in assessing compliance with the general population and intruder protection requirements. A separate exhalation objective is set for radon: "the limit for radon exhalation rate from the ground surface to air will be 20 pCi/m^{2}s

(0.7 Bq/m^2/s)". This performance objective is taken from Subpart Q of 40 CFR 61 [National Emission Standards for Hazardous Air Pollutants (NESHAPs)], which addresses radon emissions from DOE storage and disposal facilities that contain radium (except uranium mill tailings, which are covered under a separate regulation). In this performance assessment (PA), results from intrusion scenarios will be presented to include doses from radon and its decay products. However, compliance will be assessed by excluding the dose from radon and its decay products. Compliance for radon will be assessed versus the radon exhalation rate stated above.

2. DISPOSAL FACILITY DESCRIPTION

In this chapter of the EAV RPA, characteristics which may either govern the impact of the EAVDF or be impacted by the EAV are described. In Sect. 2.1, regional characteristics of the SRS and vicinity are described that focus on geography, demography, meteorology, seismicity, hydrogeology, quality of surface waters and groundwaters, soils, ecology, and the existing radiological environment. Sect. 2.2, organized similarly to Sect. 2.1, concentrates on characteristics specific to E-Area.

In Sect. 2.3, the classification of solid waste sent to E-Area for disposal, the projected composition of the solid waste, and the physical facilities that are used to dispose of solid waste are described. The solid waste properties are described in Sect. 2.4. The disposal vaults and the projected site layout that are used as a basis for this assessment of long-term performance at the EAV are described in Sect. 2.5. The radionuclide contaminants that are pertinent to assessing long-term performance are described in Sect. 2.6. In Sect. 2.9, the site closure concept used to complete this assessment is described.

2.1 REGIONAL CHARACTERISTICS

The EAVDF is located within the SRS in an area designated as E-Area. Before describing the physical facility, the geography, demography, meteorology, seismicity, hydrogeology, surface water hydrology, water quality, soils, and ecology of the SRS relevant to assessing the facility's performance are described.

2.1.1 Geography of the Region

The SRS occupies about 780 km^2 in Aiken, Barnwell, and Allendale counties on the Upper Atlantic Coastal Plain of southwestern South Carolina (Fig. 2.1-1). The center of the SRS is approximately 40 km southeast of Augusta, GA; 32 km south of Aiken, SC; 160 km from the Atlantic Coast; and is bounded on the southwest by the Savannah River, for about 28 km. The Fall Line, which separates the Atlantic Coastal Plain physiographic province from the Piedmont physiographic province, is approximately 50 km northwest of the central SRS.

In addition to the Savannah River, other prominent geographical features within 80 km of the SRS are Thurmond Lake, Par Pond and L-Lake. Thurmond Lake is the largest nearby public recreational area. This reservoir is on the Savannah River and is about 64 km upstream of the center of the SRS. Par Pond is a 11 km^2 reactor cooling water impoundment that lies in the eastern sector of the SRS. L-Lake is a 4 km^2 reactor cooling water impoundment that lies in the southern sector of the SRS (Fig. 2.1-2).

The elevation of the SRS ranges from 24 m above sea level (ASL) at the Savannah River to about 122 m ASL in the upper northwest portion of the site. The Pleistocene Coastal terraces and the Aiken Plateau form two distinct physiographic subregions at the SRS (WSRC 1992a). The Pleistocene Coastal terraces are below 82 m in elevation, with the lowest terrace constituting the present flood plain of the Savannah River and the higher terraces characterized by gently rolling topography. The relatively flat Aiken Plateau occurs above 82 m.

The Aiken Plateau is dissected by numerous streams. Because of the large number of tributaries to small streams on the SRS site, no location on the site is far from a flowing stream, most of which drain to the Savannah River.

The dominant vegetation on the SRS is forest, with types ranging from scrub oak communities on the driest areas to bald cypress and black gum in the swamps. Pine forests cover more area than any other forest type. Land utilization presently is about 56% in pine forests, 35% in hardwoods, 7% in SRS facilities and open fields, and 2% in water (WSRC 1992a).

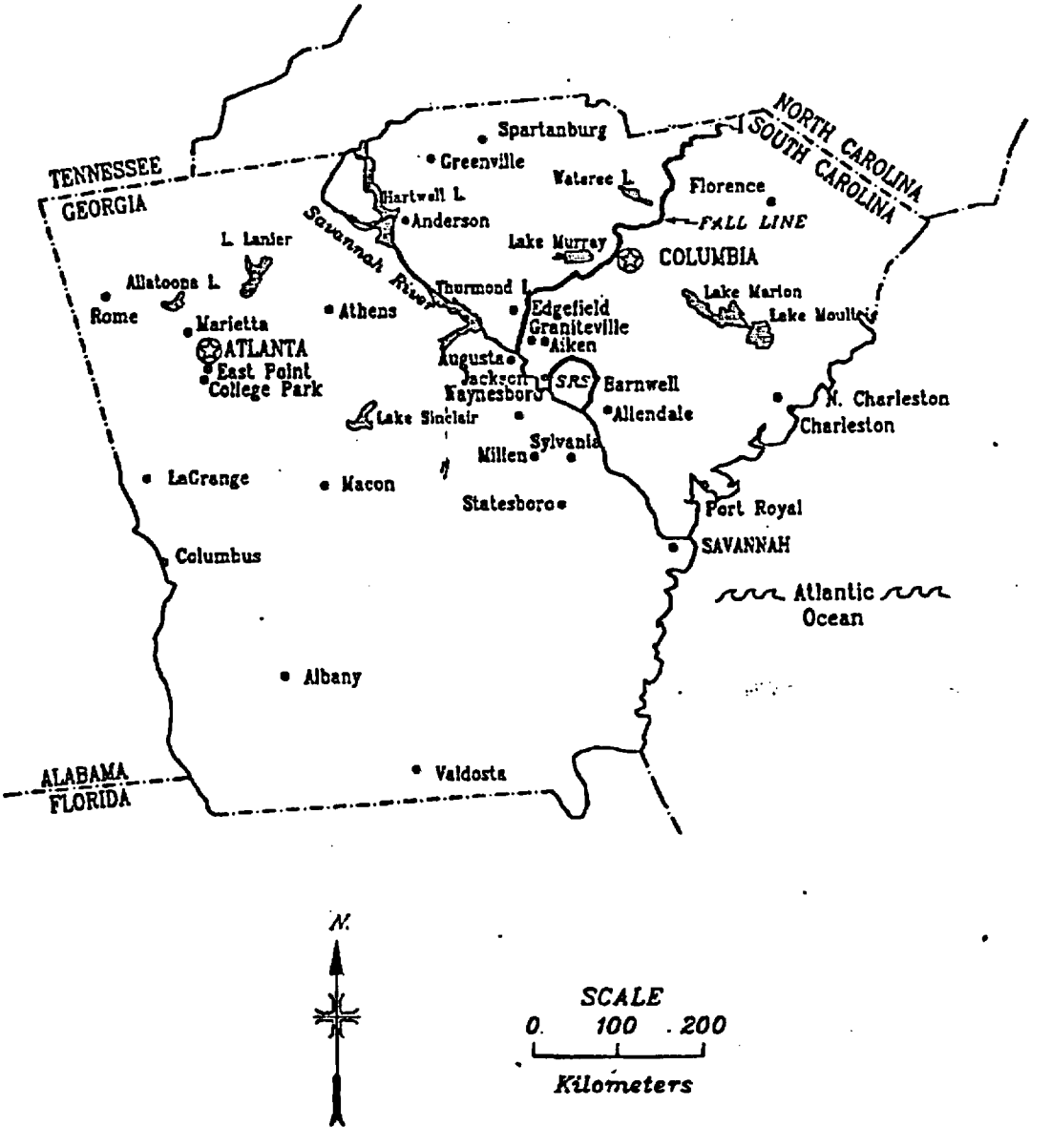

Fig. 2.1-1. SRS regional location map.

SRS081

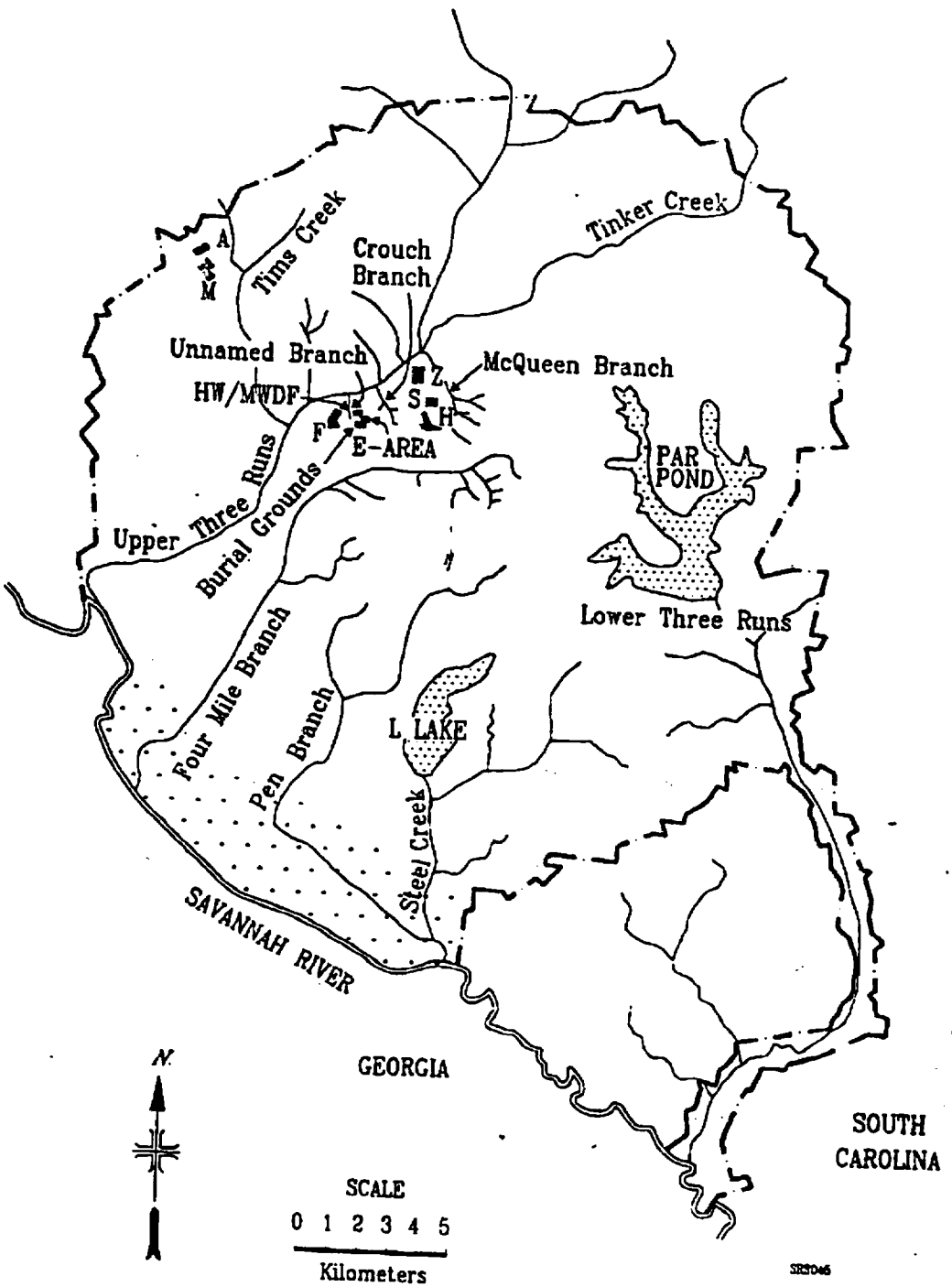

Fig. 2.1-2. Facility location map of the SRS, showing surface drainage.

Except for three roadways and a railway that are near the edge of the SRS, public access to the SRS is restricted to guided tours, controlled deer hunts, and authorized environmental studies. Figure 2.1-2 shows the major areas at the SRS and their location within the site boundary. The major production areas located at the site include: Raw Materials (M Area), Separations (F and H Areas), Waste Management Operations (E, F, and H Areas), and Defense Waste Processing (S and Z Areas) (WSRC 1992). Administrative and support services, the Savannah River Technology Center and the Savannah River Ecology Laboratory, are located in A-Area.

2.1.2 Demography

The population within 80 km of the SRS consists of a permanent (resident) and transient population, the latter of which includes industrial, recreational, and casual components. The distribution of the permanent populations within a 80 km radius of the SRS, based on 1980 U. S. Census data, is illustrated in Fig. 2.1-3. The data were assembled by geographical division formed by subdividing the study area into 16 radial segments centered on the north overlain by concentric circles with radii of 16, 32, 48, 64, and 80 km. The area within the 16 km radii are DOE-owned properties within the SRS. There are no permanent population groups within this area.

The major residential population centers 80 km from the approximate SRS plant center point are Augusta, Georgia, about 40 km to the northwest; Aiken, South Carolina, about 32 km to the north; and Orangeburg, South Carolina, about 79 km to the east northeast (Fig. 2.1-1). In 1980, the estimated population within the 80 km radius around the SRS was approximately 553,000 (Cook et al. 1987). More than 50% of the population is in the Augusta, Georgia - South Carolina Standard Metropolitan Statistical Area (SMSA) which includes Richmond and Columbia Counties in Georgia, Aiken County in South Carolina, and the Fort Gordon Military Reservation. Between 1980 and 2030, the residential population within the 80 km radius of the SRS is projected to increase from 553,000 to 845,000, or 53% (Cook et al. 1987).

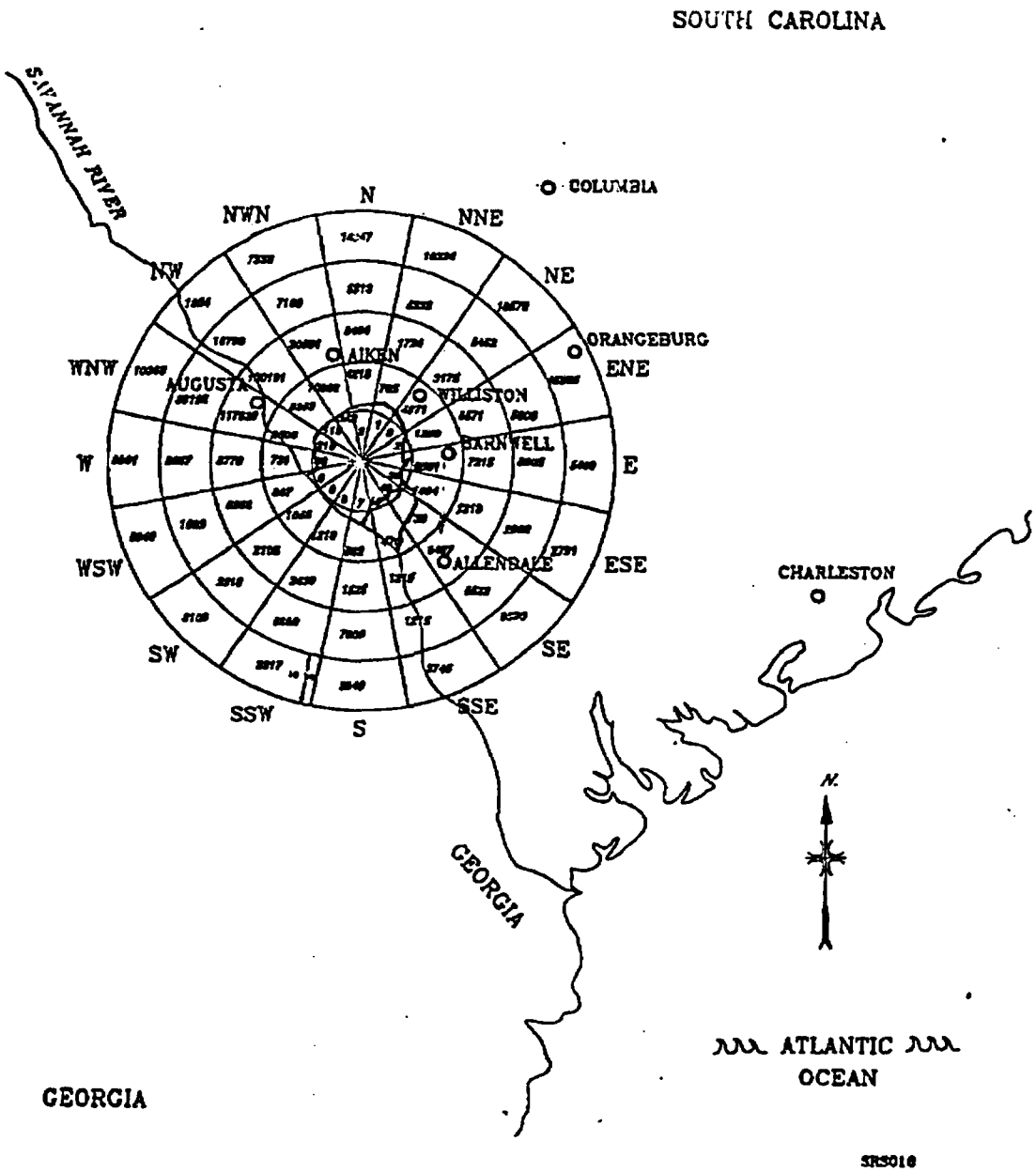

Fig. 2.1-3 Population distribution within an 80-km radius of the central SRS.

The growth characteristics of the cities and towns around the SRS are similar to those of the rest of the state. There is a distinct pattern of population increase in the areas just outside cities. Cities of Aiken and North Augusta, South Carolina are major urban centers with populations over 25,000. No other major urban centers are expected to develop in this area.

The transient population consists almost entirely of the SRS work force. The Fort Gordon Military Reservation, Alvin W. Vogtle Nuclear Power Plant, and Chem-Nuclear Systems employ approximately 4500, 3400, and 300, respectively.

2.1.3 Meteorology

The regional climate of the SRS is classified as humid subtropical, characterized by short, mild winters and long, warm and humid summers. Summer usually lasts from May through September, at which time daytime temperatures are frequently above 90°F. Winter conditions alternate between warm, moist subtropical air from the Gulf of Mexico and cool, dry polar air. Less than one-third of all winter days have a minimum temperature below freezing. Annual average precipitation, computed from daily meteorological data collected at a SRS meteorological tower from 1952 to 1992, is 124 cm yr^{-1} (Fig. 2.1-4). Extreme conditions, such as sustained winds, tornadoes, and maximum 24-h rainfall are not expected to impact the post-closure integrity of the disposal facility.

2.1.4 Hydrogeology

The surface of the Upper Atlantic Plain Province on which SRS is located slopes gently seaward. This province is underlain by a seaward dipping wedge of unconsolidated and semi-consolidated sediments that extends and progressively thickens from the Fall Line southeastward to the edge of the continental shelf. The sediments increase in thickness to more than 1.2 km near the coast of South Carolina and were deposited on the seaward sloping basement rock surface. Basement rocks consist of Late Precambrian and Paleozoic metamorphic and

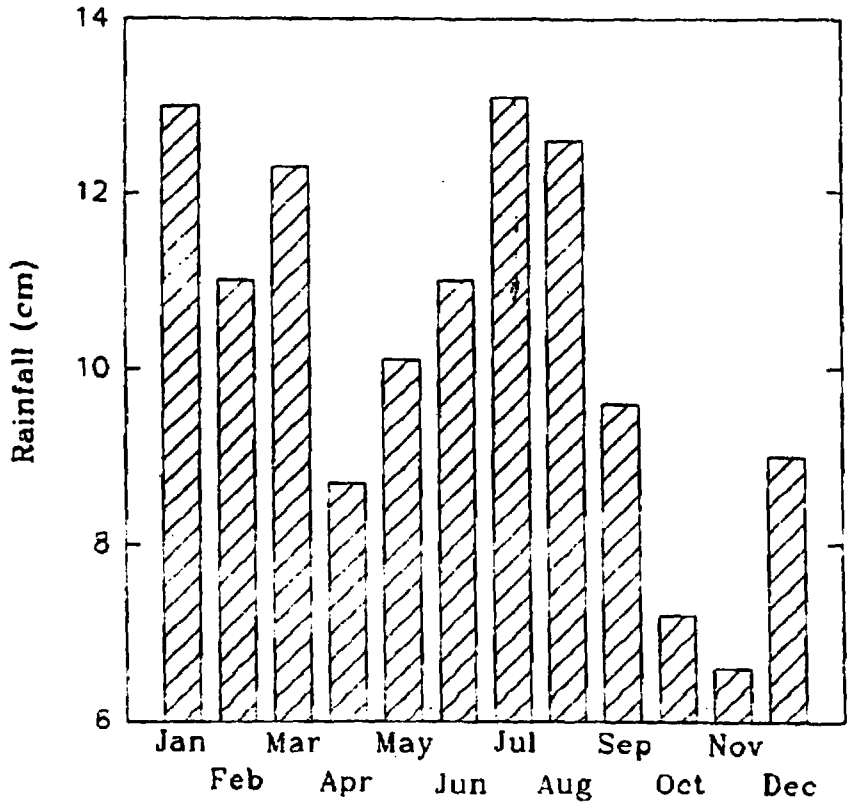

Fig. 2.1-4. Average rainfall at SRS: 1952 - 1992.

igneous rocks and locally of Triassic siltstones and claystones. The Triassic rocks were deposited in fault-bound basins trending NE-SW within the igneous and metamorphic rocks.

SRS is underlain by a sequence of sediments that ranges in thickness from 180 to 370 m and in age from Cretaceous to Recent (WSRC 1992a). The sediments consist primarily of interbedded and unconsolidated gravels, sands, silts, clays, and limestones which were deposited in near-shore marine environments. Locally, the system can be highly heterogeneous and exhibit significant variability in texture both horizontally and vertically. Layers that are regionally extensive tend to thin in the direction of the Fall Line and can pinch out in the subsurface, adding to the complexity of the groundwater system. Vertical leakage is known to occur between layers. Deep dissection of the Aiken Plateau throughout SRS by streams has cut into the upper units which form the groundwater flow system. Consequently, portions of the uppermost aquifers can be isolated, horizontally, from the same units in other areas at SRS.

Numerous investigators have described the coastal plain sediments based upon lithologic and age criteria (WSRC 1991b). More recently, attempts have been made to define hydrostratigraphic units based upon features that relate to their ability to store and transmit water. The most recent classification system proposed for SRS (Aadland 1990) is presented in Fig. 2.1-5 along with correlating stratigraphic nomenclature of earlier investigators. The nomenclature of Aadland 1990 will be utilized throughout this report. The reader is referred to Appendix E for an in-depth discussion of the hydrostratigraphy of SRS.

Following is an overview of the groundwater hydrology associated with the hydrologic units identified in Fig. 2.1-5. Appendix E documents the hydrology of the bedrock formations and the Coastal Plain sediments. In this section, the hydrology of the upper Coastal Plain sediments, specifically Aquifer System II (Fig. 2.1-5) is summarized. Aquifer System I underlies Aquifer System II and is separated by confining System I - II. This confining system is comprised of the Ellenton Clays, which are greater than 30 m thick and act to retard groundwater flow between the units. Also, vertical hydraulic gradients are in the upward direction across the confining unit in the vicinity of the EAVDF. Thus, Aquifer System I is hydraulically isolated from surface disposal activities, and is not of interest for contaminant studies.

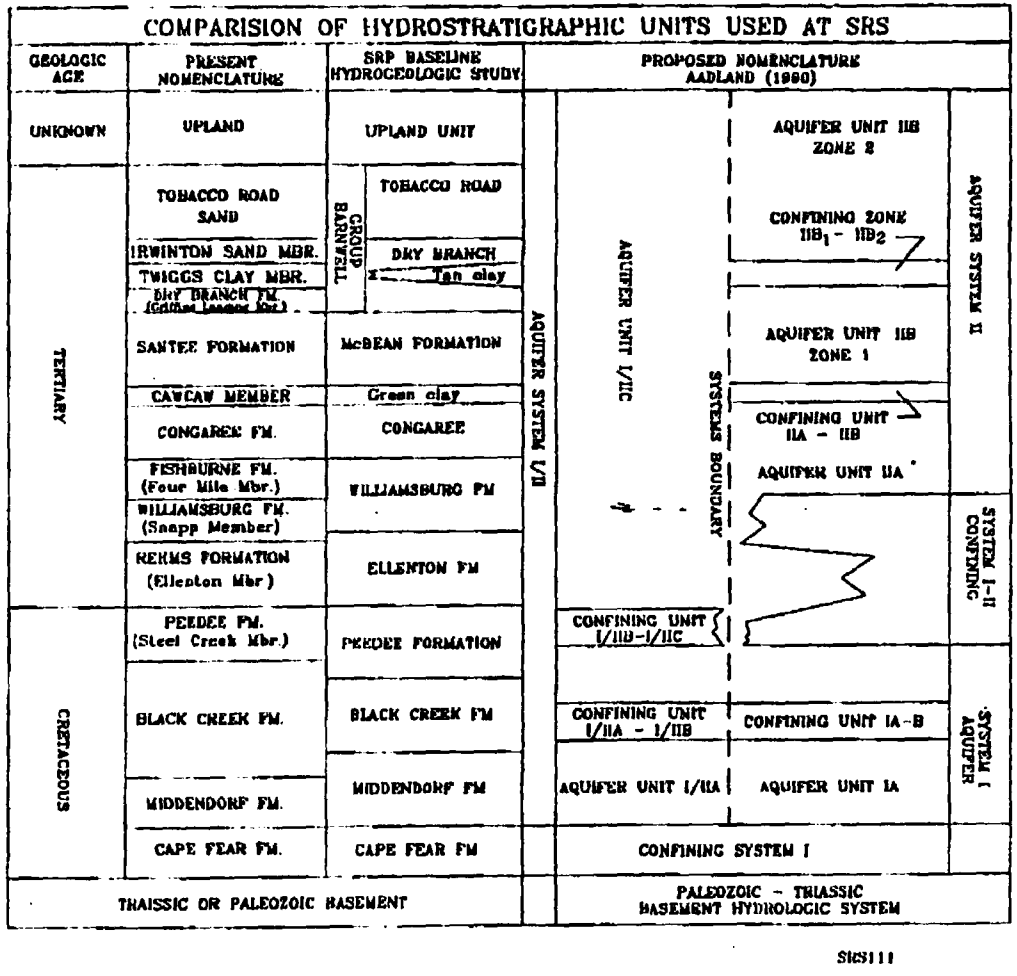

Fig. 2.1-5. Hydrologic and stratigraphic units underlying the SRS.

Aquifer System II is divided into individual units that are further subdivided into zones. These units and zones primarily relate to hydrogeological characteristics. The units and zones which comprise the aquifer system are as follows (GeoTrans 1992):

Nomenclature of Aadland (1990)	Common Nomenclature
Aquifer System II	
Aquifer Unit IIB, Zone 2	Water Table
Confining Unit IIB1-IIB2	Tan Clay
Aquifer Unit IIB, Zone 1	Barnwell/McBean Aquifer
Confining Unit IIA-IIB	Green Clay
Aquifer Unit IIA	Congaree Aquifer
Confining System I-II	Ellenton Clays

2.1.4.1 Hydrogeology of Aquifer Unit IIA (Congaree Aquifer)

Aquifer Unit IIA consists of the clastic sediments of the Congaree Formation and the glauconite-bearing sands and clays of the lowermost Santee Limestone Formation. Aquifer Unit IIA is an aquifer that consists predominantly of fine-to-coarse quartz sand. Clay laminae occur throughout the formation, but they are too thin and discontinuous to be effective seals except locally. Confining Unit IIA - IIB, identified as the "green clay" layer, or Caw Caw member of the Santee Formation, is characterized by rapid facies changes. The permeability of this layer varies greatly from place to place but in most parts of SRS is low enough to form a competent layer between overlying and underlying aquifer units.

The potentiometric surface map for Aquifer IIA, illustrated in Appendix E, shows that flow directions for this unit are convergent toward Upper Three Runs (UTR) Creek. These flow directions reflect that UTR Creek has completely incised Confining Unit IIA-IIB and is a discharge area for Aquifer Unit IIA. Four Mile Creek does not incise Confining Unit IIA-IIB (Parizek and Root 1986), and thus, does not influence the groundwater flow

directions of Aquifer Unit IIA. Elsewhere on the SRS, Aquifer Unit IIA behaves as a confined to semi-confined aquifer (WSRC 1992a). Hydraulic gradients in this unit increase with proximity to UTR Creek. Near UTR Creek, groundwater flow velocities are likely to be proportionately higher, reflecting the increase in hydraulic gradient.

2.1.4.2 Hydrogeology of Aquifer Unit IIB, Zone 1 (Barnwell/McBean)

Aquifer Unit IIB, Zone 1 consists of clastic and carbonate sediments of the Santee Formation and the Dry Branch Formation of the Barnwell Group that lie above the Confining Unit IIA-IIB (Green Clay). Porosity and permeability of Aquifer Unit IIB, Zone 1 strata vary greatly, depending on the dominant lithology and amount of clay present at any particular location. Nowhere on the SRS, however, do the clays in this zone form effective aquitards.

Aquifer Unit IIB, Zone 1 is incised by many of the streams on the SRS, including UTR, McQueen and Crouch Branches. Thus, horizontal flow directions in this zone are affected to a large degree by the incision of drainage ways into the zone.

2.1.4.3 Hydrogeology of Aquifer Unit IIB, Zone 2 (Water Table)

Aquifer Unit IIB, Zone 2 is comprised of the Irwinton Sand Member and the Tobacco Road Formation of the Barnwell Group and the Upland Unit. The Irwinton Sand Member consists of moderately-to-poorly sorted quartz sand with interlaminated clays abundant in places. The Tobacco Road Sand consists of gravels, sands, and appreciable clay layers, but these are discontinuous and do not form an effective regional aquitard. Due to its stratigraphic position, the Tobacco Road Formation is frequently the formation in which the water table occurs in inter-stream areas. Thickness of this formation is extremely variable, but can be as much as 15 m in places. The Upland Unit consists of a mixture of gravel and sand with some finer textured sediments and occurs in thicknesses up to 21 m in some parts of SRS. This unit forms the surficial deposits in the inter-stream upland areas and is part of the vadose zone.

Aquifer Unit IIB, Zone 2 overlies Confining Zone IIB_1-IIB_2, which consists of the Twiggs Clay Member commonly known as the "Tan Clay". Confining Zone IIB_1-IIB_2 varies from 0.6 to 3 m in thickness where present. Like Aquifer Unit IIB, horizontal flow directions in Aquifer Unit IIB, Zone 2, are strongly influenced by incision of the unit by surface water drainage ways.

2.1.5 Seismicity

The susceptibility of the SRS, and particularly E-Area, to seismic motion is of interest to establish if E-Area is suitable for waste disposal. Seismic events could result in cracking of the vaults. Cracking could be fairly severe if liquefaction of supporting soils were to take place. However, liquefaction of supporting soils is not considered to be a potential problem at the SRS based on a review of previous studies at the SRS (URS/Blume 1982). Below is a discussion of seismic zones that are known to exist in the vicinity of the SRS, and the expected intensity associated with seismic activity in these zones at the SRS.

2.1.5.1 Location of Nearby Seismic Zones

The SRS is located in the interior of the North American plate. In the past 200 years the nearest zones of concentrated seismic activity in the region are centered in the Charleston-Summerville area of South Carolina and near Bowman, SC, which is 60 km northwest of Summerville, SC (Fig. 2.1-6). Recent seismic activity in the Charleston area, probably including the earthquake of 1886, has originated largely or entirely in the basement beneath the Coastal Plain sediments. The seismicity in the Charleston area is believed to occur at the intersection of the Ashley River fault and the Woodstock fault, at minimum depths of 4 km and 8 km, respectively. Seismicity associated with the Bowman seismic zone occurs along a border fault of a buried Triassic basin, extending to a depth of about 6 km (WSRC 1992a).

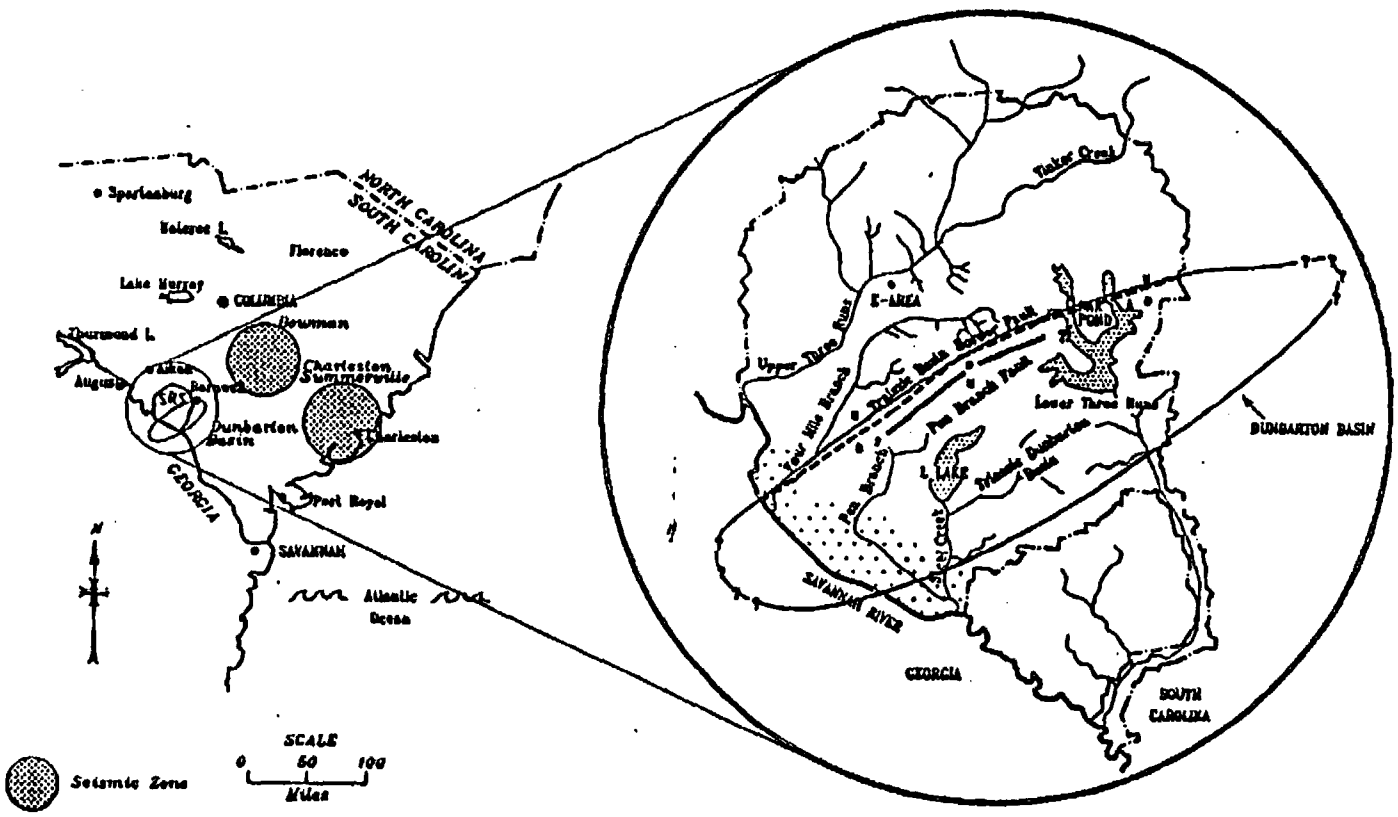

Fig. 2.1-6. Location of the Bowman and Charleston-Summerville seismic zones, and the Dunbarton Basin on the SRS.

Underlying the Coastal Plain sediments of the central and southern portions of the SRS is a Triassic-Jurassic rift basin within the crystalline basement. This basin, called the Dunbarton Triassic basin, is located in the Aiken Plateau, about 50 km southeast of the Fall Line (Fig. 2.1-6). Associated with this basin on the SRS are at least two faults; the northern border fault and a parallel fault, the Pen Branch fault, which may coincide with the border fault. These faults do not extend upward into post-Oligocene sediments at SRS.

Faulting has also been recognized in sediments as young as Oligocene in the Atlantic Coastal Plain sediments of South Carolina. Faulting has been postulated to occur in these sediments based on structure-contour mapping of the Eocene-Oligocene unconformity, which lies between 30 and 61 m below the surface, in the vicinity of Charleston, and about 100 km from the SRS, faulting has been postulated to occur in these sediments. A shallow fault, associated with a 16-km wide graben of Oligocene and Miocene rocks which crosses beneath the Savannah River from Georgia into South Carolina, is postulated about 56 km southeast of the SRS. It is not currently possible to relate these shallow faults to modern earthquakes that occur at depths greater than about 2 km.

2.1.5.2 Intensities of Historical Earthquakes

The largest known earthquake to affect the site region was the Charleston earthquake of 1886. This Modified Mercalli Intensity (MMI) X earthquake struck Charleston SC, on August 31, 1886. The greatest intensity felt at the SRS has been estimated at MMI VI-VII (felt by all; everyone runs outdoors; damage negligible in buildings of good structure, but considerable in poorly built structures) as a result of the Charleston earthquake (WSRC 1992a). Minor tremors from aftershocks of the 1886 Charleston event were also felt in the area where the SRS is now located. Intensities of these tremors were estimated to be equal to or less than MMI IV.

Seismic activity, producing earthquakes of estimated MMI up to V to VII, has been present in the Bowman area (about 95 km northeast of SRS) over the last 200 years (WSRC 1992a). These earthquakes produced motion at the SRS of less than 0.1 g (Stephenson

1993). An earthquake (MMI VII) that struck Union County, SC (about 160 km north-northeast of the SRS) in 1913 was felt at Aiken (6 km north-northwest of SRS) with a MMI of II-III (vibration indoors like a passing truck).

Two earthquakes of MMI III or less have occurred with epicentral locations within the boundaries of the SRS (Stephenson et al., 1985; Stephenson 1988). A MMI III earthquake occurred in June 1985 at the SRS, as did a MMI I-II earthquake in August 1988. Neither of the earthquakes triggered the seismic alarms at the SRS facilities, which are triggered when ground accelerations equal or exceed .002 g. The epicenters of these earthquakes appear to be located within about six miles of the intersection of a northwest-trending fault and the northeast-trending border fault at the northern edge of the Dunbarton Triassic basin, and are relatively shallow (1 to 3 km below the earth's surface).

2.1.5.3 Projected Recurrence of Earthquakes

According to Bollinger et al. (1989), the recurrence interval for a Charleston size shock (MMI X) for the Charleston area and for the Coastal Plain is on the order of 1000 years, at the 95% confidence level. A recurrence of the 1886 Charleston earthquake would result in an intensity of MMI VII at the SRS (URS/Blume 1982). Recurrence of earthquakes associated with other known seismic zones in the region are not expected to be of greater intensity, nor cause greater shaking at the SRS (WSRC 1992a).

2.1.6 Surface Water Hydrology

The Savannah River cuts a broad valley approximately 76 m deep through the Aiken Plateau, on which most of the SRS sits. The Savannah River Swamp lies in the floodplain along the Savannah River and averages about 2.4 km wide. Upper Three Runs Creek, Fourmile Branch, Tinker Creek, Pen Branch, Steel Creek, and Lower Three Runs Creek (Fig. 2.1-2) are the major tributaries of the Savannah River that occur on the SRS. Three breaches of the natural levee occur at the confluences of the Savannah River with Beaver Dam Creek, Fourmile Branch, and Steel Creek, allowing discharge of these streams to the

river. During swamp flooding, water from Beaver Dam Creek and Fourmile Branch flows through the swamp that parallels the river and combines with the Pen Branch flow. Pen Branch joins Steel Creek about 0.8 km above its mouth.

Surface water is held in artificial impoundments and natural wetlands on the Aiken Plateau. Par Pond, the largest impoundment on the SRS, is located in the eastern part of the SRS, covering about 11 km^2. A second impoundment, L Lake, lies in the southern portion of SRS and covers approximately 4 km^2. The waters drain from Par Pond and L Lake to the south, via Lower Three Runs Creek and Steel Creek, respectively, into the Savannah River. Lowland and upland marshes, and natural and man-made basins on the SRS retain water intermittently.

Near the SRS, the flow of the Savannah River has been stabilized by the construction of upstream reservoirs. The yearly average flow is approximately 290 $m^3 s^{-1}$. From the SRS, river water usually reaches the coast in five to six days, but may take as few as three days. At low flow, which usually occurs in autumn months, the Savannah River is about 100 m wide and 3 to 5 m deep, with an average flow of approximately 160 $m^3 s^{-1}$.

2.1.7 Water Quality and Usage

2.1.7.1 Groundwater

INFORMATION ONLY

The sand beds that comprise Aquifer System I are an important source of water for wells in localities neighboring the SRS. Most municipal and industrial water supplies in Aiken County, SC are developed in Aquifer System I. In Barnwell and Allendale counties, some municipal users are supplied from the shallower Aquifer Zones IIA and IIB. Private domestic supplies in all of these counties are primarily obtained from Aquifer System I.

Municipal and industrial groundwater use in the vicinity of the SRS indicated total pumpage from Aquifer System I on the order of 1 $m^3 s^{-1}$; 0.2 $m^3 s^{-1}$ from Aquifer Unit IIA; and up to 0.04 $m^3 s^{-1}$ from Aquifer Zone IIB_1. The SRS uses up to 0.4 $m^3 s^{-1}$ on site, from Aquifer System I (Cook et al. 1987).

Water quality parameters for groundwater at the SRS are likely to be quite variable. Parameters specific to E-Area are presented in Sect. 2.2 below.

2.1.7.2 Surface Water

Water from the Savannah River is used for drinking water at two locations below the SRS. About 160 km downstream of SRS, The Beaufort-Jasper Water Treatment Plant at Hardeeville, SC, withdraws about 0.3 $m^3 s^{-1}$ for a consumer population of approximately 51,000. The Cherokee Hill Water Plant at Port Wentworth, GA, about 160 km downstream of the SRS, presently withdraws about 2 $m^3 s^{-1}$ for a consumer population of about 20,000. The Savannah River is also used for commercial and sport fishing and for recreational boating. Surface water quality is presently monitored by the Environmental Monitoring Section and the Savannah River Technology Center at the SRS (Cummins et al. 1990). Surface water is characterized with respect to radiological and non-radiological aspects, both on site and downstream of the SRS. Some water quality characteristics of the Savannah River upstream of the SRS, classified as a Class B water by the South Carolina Department of Health and Environmental Control (SCDHEC), are listed in Table 2.1-1. The temperature, dissolved oxygen, and pH values reflected in this table are within the standards required for Class B waters (Cummins et al. 1990). Other water quality parameters listed in this table are within the ranges observed in previous years (Cummins et al. 1990), indicating that the quality of the Savannah River is not being degraded at the point of measurement.

2.1.8 Soils

Most of the soils at the SRS are sandy over a loamy or clayey subsoil. The distribution of soil types is very much influenced by the creeks on the site, with colluvial deposits on hill-tops and hillsides giving way to alluvium in valley bottoms (Dennehy et al. 1989). Road cuts and excavations on interstream areas near the SRS commonly expose a deeply developed soil profile. Two horizons are apparent; the A horizon may be up to 3 m thick, and typically consist of structureless fine- to medium-grained quartz sand, and the lower B horizon, which may be from 0.6 to 3 m in thickness, contains iron and aluminum compounds leached from the overlying material.

Table 2.1-1. Water quality of the Savannah River above SRS (Cummins et al. 1990)

Parameter	Units	No. of Analyses	Arithmetic Mean	Max	Min
Temperature	°C	12	18	27	10
pH	pH	12		7.4	6.2
Dissolved oxygen	mg/L	12	8.0	9.6	6.4
Alkalinity	mg/L	12	21	24	17
Conductivity	umhos/cm	12	84	104	61
Turbidity	NTU	12	6.9	18	2.3
Suspended solids	mg/L	12	13	22	6.0
Volatile solids	mg/L	12	2.3	4.0	1.0
Total dissolved solids	mg/L	12	62	76	46
Total solids	mg/L	12	74	86	58
Fixed residue	mg/L	12	10	19	5.0
Chemical oxygen demand	mg/L	12	9.7	17	7.0
Chloride	mg/L	12	7.8	11	4.6
Nitrogen (as NO_2/NO_3)	mg/L	12	0.32	0.99	0.15
Sulfate	mg/L	12	7.8	11	6.0
Phosphorus (as PO_4)	mg/L	12	0.09	0.16	0.05
Nitrogen (as NH_3)	mg/L	12	0.13	0.34	<0.02
Cadmium	mg/L	4	<0.01	<0.01	<0.01
Mercury	µg/L	4	<0.20	0.20	<0.20
Chromium	mg/L	4	<0.02	<0.02	<0.02

Weathering effects are evident. In some areas, intense weathering has produced tensional soil fractures as a result of volume reduction. These fractures are dominant features in shallow exposures such as drainage ditches or roadside embankments. Average soil erosion rates for the area surrounding the SRS, much of which is cropland, range from 1.5 to 2.0 kg m^{-2} yr^{-1}. (U.S. Department of Agriculture 1985) Employing the Universal Soil Loss Equation to predict erosion at the SRS under different vegetative conditions, Horton and Wilhite (1978) estimate that the presence of natural successional forests would reduce erosion by a factor of 400 to 500 over cropland erosion.

2.1.9 Ecology

2.1.9.1 Aquatic Ecology

Flora in the Savannah River basin and in creeks on the SRS site is diverse and seasonally variable. Several species of diatoms, green algae, yellow-green algae, and blue-green algae are present. In seasonally flooded areas, bald cypress and tupelo gum thrive. In less severely flooded areas, oak, maple, ash, sweet gum, ironwood, and other species, less tolerant of flooding, are found. In the river swamp formed by the Savannah River in the vicinity of the SRS, herbaceous growth is sparse. A number of macrophytes, such as cattail and milfoil, are found in areas receiving sufficient sunlight.

The fish communities in the Savannah River and in creeks on the SRS are very diverse. Redbreast sunfish, spotted sucker, channel catfish, and flat bullhead are the dominant species. Sunfish, crappies, darters, minnows, American shad, and striped bass are also abundant.

Macroinvertebrate communities are largely comprised of true flies, mayflies, caddisflies, stoneflies, and beetles. Leaf litter input is high, but is rapidly broken down by macroinvertebrate shredders. The Asiatic clam is found in the Savannah River and its larger tributary streams.

2.1.9.2 Terrestrial Ecology

Prior to its acquisition by the U. S. Government in 1951, approximately one-third of the SRS was cropland, about half was forested, and the remainder was floodplain and swamp. Since that time, the U. S. Forest Service has reclaimed many previously disturbed areas through natural plant succession or by planting pine trees. As was noted in Sect. 2.1.1, 91% is now pine or hardwood forests, with the remaining 9% divided between SRS facilities and water bodies.

A variety of vascular plants exist on the site. Scrub oak communities cover the drier sandy areas, which includes predominantly longleaf pine, turkey oak, bluejack oak, blackjack oak, dwarf post oak, three awn grass, and huckleberry (U.S.DOE 1987). On the more fertile, dry uplands, white oak, post oak, southern red oak, mockernut hickory, pignut hickory, and loblolly pine predominate, with an understory of sparkleberry, holly, greenbriar, and poison ivy. Pine trees cover more area than any other tree genus.

The heterogeneity of the vegetation on the SRS supports a diverse wildlife population. Several species of reptiles and amphibians are present due to the variety of aquatic and terrestrial habitats. These include snakes, frogs, toads, salamanders, turtles, lizards, and alligators. More than 213 species of birds have been identified on the SRS. Burrowing animals at the SRS include: Peromyscus polionotus, known commonly as the Old Field Mouse; Blarine brevicauda, known as the Short Tail Shrew; Scalopus aquiticus, known as the Eastern Mole; Pogonomyrmex badius, known as the Harvester Ant; Dorymyrmex pyramicus, known as the Pyramid Ant; and earthworms (Briese and Smith 1974; Davenport 1964; Golley and Gentry 1964; Smith 1971; Van Pelt 1966).

2.1.10 Existing Radiological Environment

All human beings are exposed to sources of ionizing radiation which include naturally occurring and man-made sources. The average dose contribution estimates from various sources to individuals were obtained from recent reports of the National Council on Radiation Protection and Measurements (NCRP) and the EPA. On average, a person living in the

Central Savannah River Area (CSRA) receives an annual radiation dose of 379 mrem (Cummins et al. 1990). The average dose contributions from the various radiation sources to an individual in the CSRA are given in Fig. 2.1-7.

The major source of radiation exposure to an average member of the public in the CSRA is attributed to naturally-occurring radiation. This naturally-occurring radiation is often referred to as natural background radiation. Natural sources of radiation include cosmic radiation from outer space, cosmogenic radionuclides formed by interaction of cosmic radiation with elements in the earth's atmosphere, terrestrial radiation from natural radioactive materials in the ground, radiation from radionuclides occurring naturally in the body, and inhaled or ingested radionuclides of natural origin. The amount of exposure an individual receives depends on their location. Table 2.1-2 compares national averages for exposure to natural background radiation to average exposures in the vicinity of the SRS.

The average annual dose to people in the U.S. from cosmic radiation is about 27 mrem, which is lower than estimated for the vicinity of the SRS because a large fraction of the U.S. population lives near sea level, where cosmic radiation is lower. A report published by the EPA gives a specific outdoor cosmic radiation dose for Augusta, GA of about 41 mrem (Oakly 1972). When shielding and the time spent indoors are considered, the annual average cosmic radiation dose for the CSRA population is about 33 mrem, about 22% higher than the national average. The average annual EDE from terrestrial gamma radiation is about 28 mrem in the U.S. This annual EDE varies geographically across the U.S. Values from the SRS vicinity include 43 mrem for Augusta, GA, 23 mrem for Charleston, SC, and 68 mrem for Columbia, SC (Oakly 1972).

The major contributors to the annual EDE for internal radionuclides are the short-lived decay products of radon (mostly ^{222}Rn), which contribute an average EDE of about 200 mrem per year. This dose estimate is based on an average radon concentration of about 1 pCi/L (NCRP 1987). The results of long term measurements in living areas of about 30,000 homes in the U.S. suggest that the mean radon concentration levels are about 3.6 pCi/L for the U.S. population and about 1 pCi/L for South Carolina (Alter and Oswald 1988). The average EDE from other internal radionuclides is about 39 mrem per year, which is predominantly

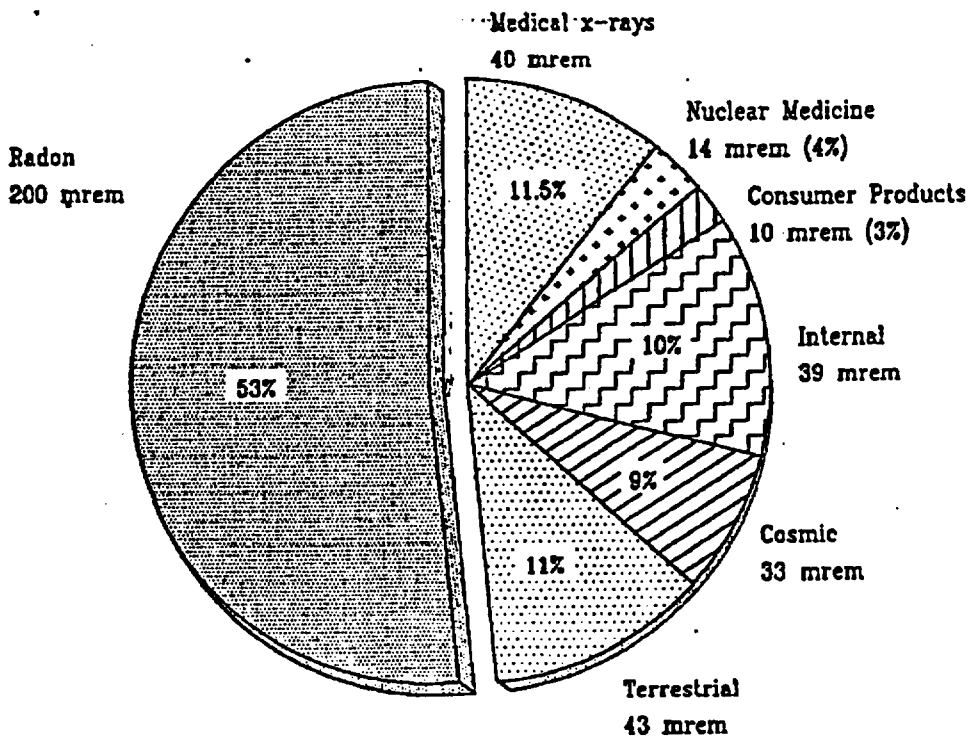

Fig. 2.1-7 The total average effective dose equivalent from various sources in the Central Savannah River Area. SRS072

Table 2.1-2. Comparison of natural radiation doses near SRS with U.S. averages[a]

Natural Radioactivity	Annual Average EDE (mrem)	
	50-mile radius of SRS	U.S. Average
Cosmic radiation	33	27
Terrestrial radiation	43	28
Internal radiation[b]	239	240
Total	315	295

[a] Cummins et al. 1990.

[b] Approximately 200 mrem of the dose from internal radiation is attributed to radon exposure. An EPA study, which was scheduled to be published in 1991, will update the information on the U.S. distribution of doses from radon. Preliminary information suggests that the U.S. average dose from radon may be higher than 200 mrem.

attributed to the naturally occurring radioactive isotope of potassium, ^{40}K. The concentration of ^{40}K in human tissues is similar in all parts of the world (NCRP 1987).

A wide range of consumer products also contain sources of ionizing radiation. The U.S. average annual EDE to an individual is about 10 mrem (NCRP 1987).

Radiation is an important tool of diagnostic medicine and cancer treatment. The average annual EDE to all individuals from all medical examinations is 54 mrem (about 40 mrem for diagnostic x-rays and 14 mrem for nuclear medicine procedures). The actual EDEs to individuals who receive such medical exams is much higher than these values, because not everyone receives such exams each year (NCRP 1989).

There are a few additional minor sources of radiation that contribute to the average EDEs to individuals in the U.S. About 1,320,000 people performed radiation work in 1980 and received an average dose of 110 mrem per year (Cummins et al. 1990). This exposed population represents only about one half of 1% of the U.S. population. The dose to the general public from nuclear fuel cycle facilities, such as uranium mines, mills, fuel processing plants, nuclear power plants, and transportation routes, has been estimated at less than 1 mrem per year.

Small doses to individuals occur as a result of radioactive fallout from atmospheric atomic bomb tests emissions of radioactive materials from other nuclear facilities, such as DOE facilities; emissions from mineral extraction facilities; and transportation of radioactive materials. The combination of these sources contributes less than 1 mrem per year to the average dose to an individual (Cummins et al. 1990).

Environmental monitoring is performed at the SRS to demonstrate that releases of radionuclides from the site do not exceed the radiation protection guidelines for the general public. Thousands of samples are collected and analyzed each year. Materials monitored include: air, groundwater, drinking water, milk, food stuffs, SRS streams and basins, vegetation, rainwater, Savannah River water, soil and sediments, fish, and wildlife. These samples are collected in defined ways from on site, at the site perimeter, and at locations up to 160 km from SRS. The samples are analyzed for specific radionuclides. Measurements of environmental gamma radiation are also made at numerous on-site and off-site locations (Cummins et al. 1990).

The non-radiological environment is also monitored at SRS. The materials sampled in the non-radiological program include: air, groundwater, Savannah River sediment, SRS streams and outfalls, and fish. In addition to laboratory analyses, water and air quality measurements are routinely made in the field. Non-radiological compounds monitored include nitrate, some heavy metals, and some chlorinated organics.

An environmental monitoring program has been maintained continuously in the SRS region since 1951. Public reports have been published since 1959 dealing with various aspects of the environmental program at SRS. In 1985, the on-site and off-site environmental monitoring reports were merged into a single publication. Recent monitoring results specific to E-Area, that provide information on the existing radiological environment at the EAV disposal site, are provided in Sect. 2.2.5.

2.2 E-AREA SITE DESCRIPTION

The following is a discussion of site characteristics specific to E-Area, that were not covered explicitly in the above discussion on regional characteristics..

2.2.1 E-Area Location, Description, and Land Use

The E-Area at the SRS, where the EAVDF is located, consists of approximately 200 acres, and is situated immediately north of the current LLW burial grounds (Fig. 2.1-2). Construction on the EAVDF began in October of 1989. The site is an elbow-shaped, cleared area of 100 acres, curving to the northwest on an interfluvial plateau in the center of SRS. The site slopes from an elevation of 290 feet in the southernmost corner to an elevation of 250 ft in the northernmost corner. Runoff is to the north and east toward UTR Creek and two of its ephemeral tributaries, Crouch Branch to the east of the EAVDF and an unnamed branch to the west. UTR Creek is approximately 2500 feet north of the facility boundary. The nearest perennial stream is approximately 1200 feet northeast of the boundary. A topographic map showing elevations and the local streams in the vicinity of E-Area is provided in Fig. 2.2-1.

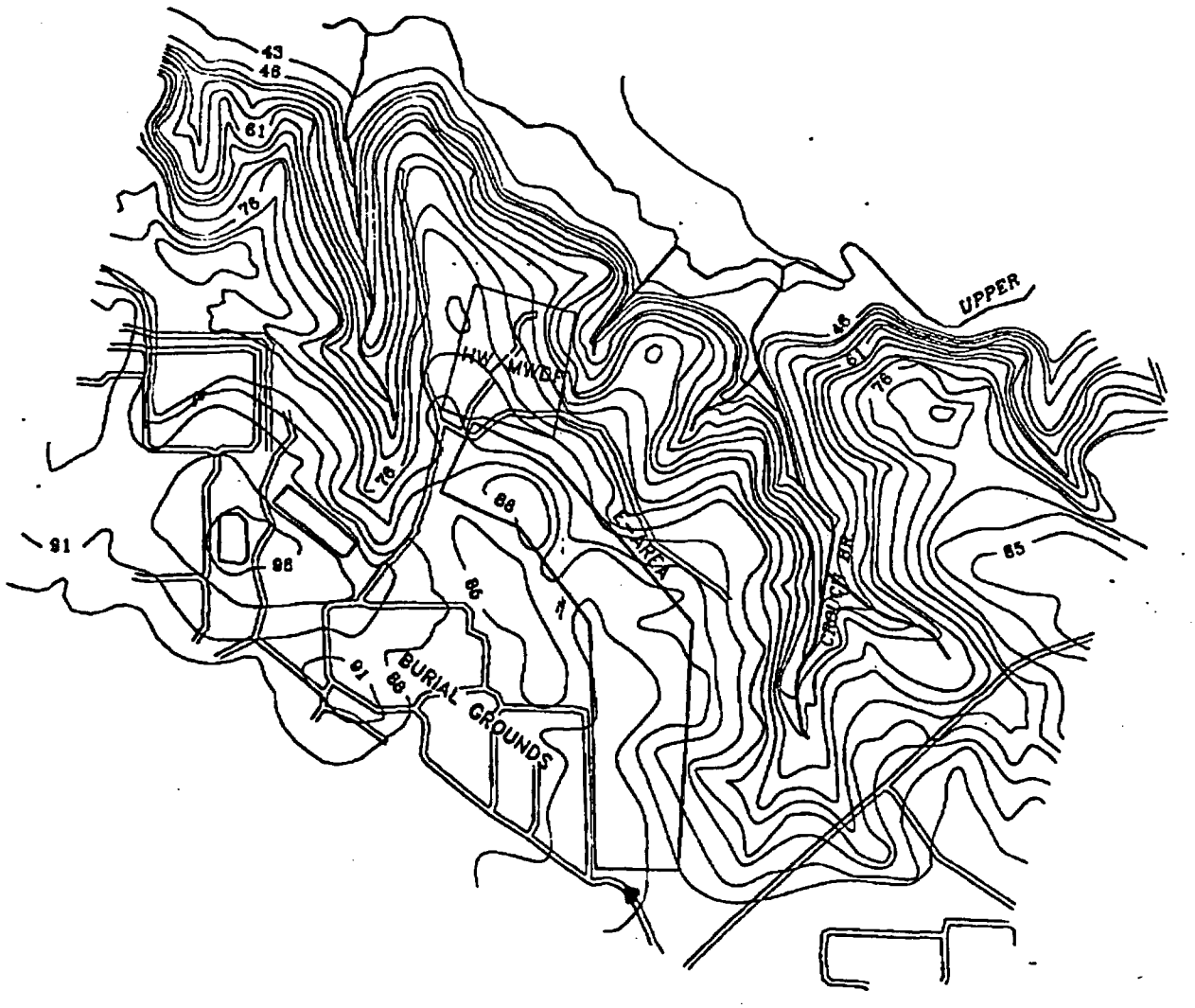

SAVANNAH RIVER PLANT
E-AREA

Scale
0 200 400
Meters

Road
Stream
46 Topographic Contour (masl)

Plant
True
North

Fig. 2.2-1. Topographic map of the vicinity of E-Area.

2.2.2 Hydrogeology of E-Area

The hydrogeology of the upper coastal plains sediments comprising Aquifer System II are discussed in this section. As previously mentioned, this is the only aquifer system that can be impacted by shallow waste disposal activities. The groundwater flow system beneath the EAVDF is relatively constrained and acts to force the groundwater to flow toward nearby surface water discharge zones.

Groundwater flow directions in Aquifer Units IIB, Zones 1 and 2, are northward toward discharge areas along Crouch Branch, UTR Creek, and the unnamed branch. Groundwater flow in these units cannot move southward because natural hydraulic gradients prevent such an occurrence. Vertical-flow directions are downward and some groundwater flows from these units across Confining Unit IIA - IIB into Aquifer IIA.

Horizontal-flow directions in Aquifer Unit IIA are directly toward UTR Creek, which is the regional discharge zone for this unit in the vicinity of the EAVDF. Aquifer Unit IIA is a zone of vertical-flow convergence. Groundwater flow is into the unit from both overlying and underlying aquifers. Natural groundwater gradients prevent the possibility of any contaminants migrating any deeper than Aquifer Unit IIA.

Much of the hydrogeologic information specific to E-Area comes from well boring logs and water level data from a series of wells placed in E-Area. A location map of these wells is provided in Fig. 2.2-2. Two lithologic cross-sections developed from this information are shown in Fig. 2.2-3 and 2.2-4.

Aquifer Unit IIA (Congaree) unconformably overlies Confining System I-II (Ellenton Clays) and ranges from 16 to 33 m thick within the GSA, which includes E-Area. The Unit dips 1.5 to 1.7 m per km to the south and southeast. The hydraulic head distribution for Aquifer Unit IIA declines, in general, from the southeast to the northwest following the trend of UTR Creek, the potentiometric map of this unit is presented in Fig. E.2-2. The horizontal gradient in this unit, beneath the EAVDF, is approximately 0.005. At E-Area, the aquifer unit is under confined conditions except along the fringe of UTR Creek. In this area, Aquifer Unit IIA converts to water-table conditions because Confining Unit IIA-IIB (Green Clay) is completely stripped away by UTR Creek.

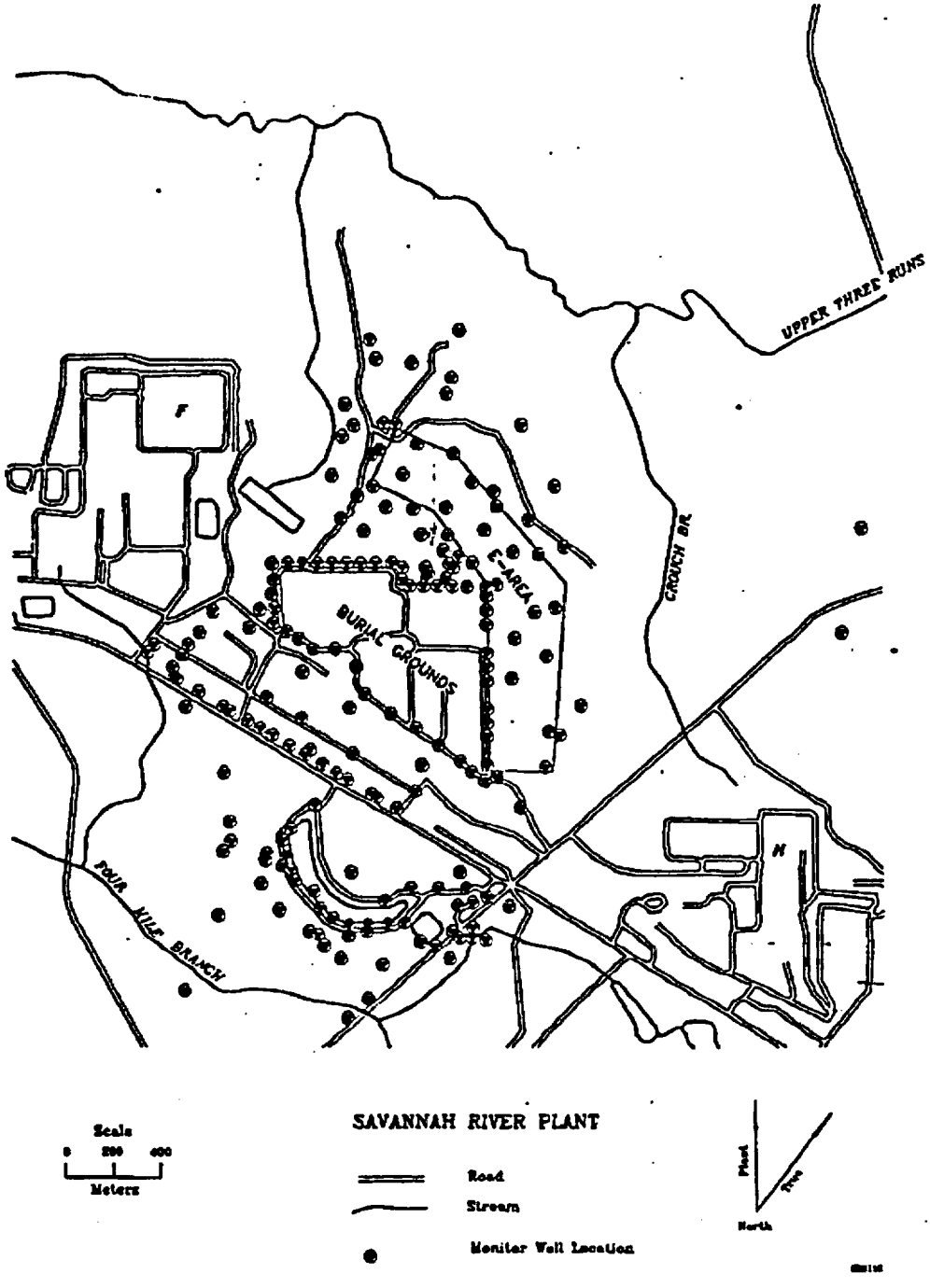

Fig. 2.2-2. Location of groundwater wells at E-Area.

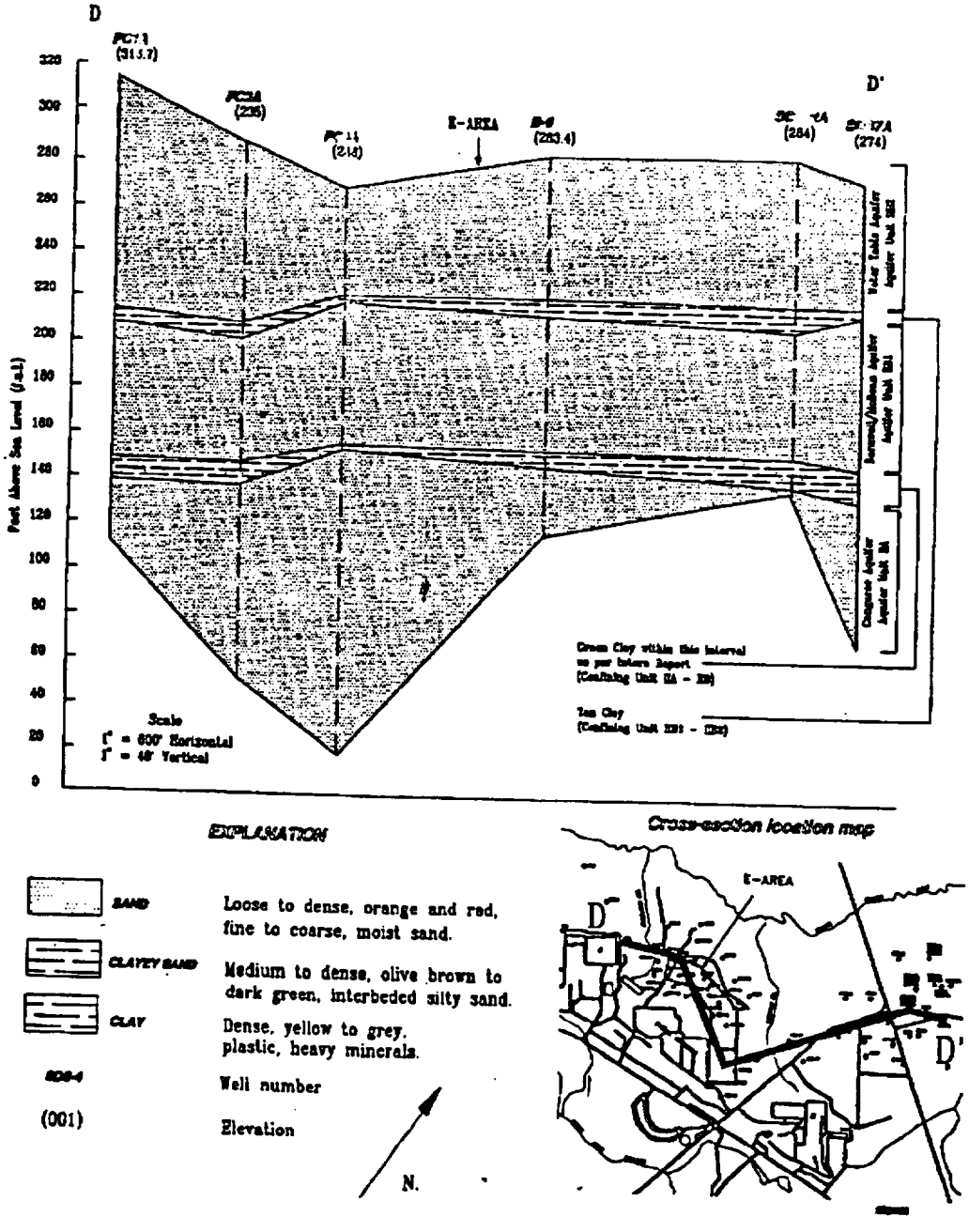

Fig. 2.2-3. Lithologic cross-section, D-D', in the vicinity of E-Area.

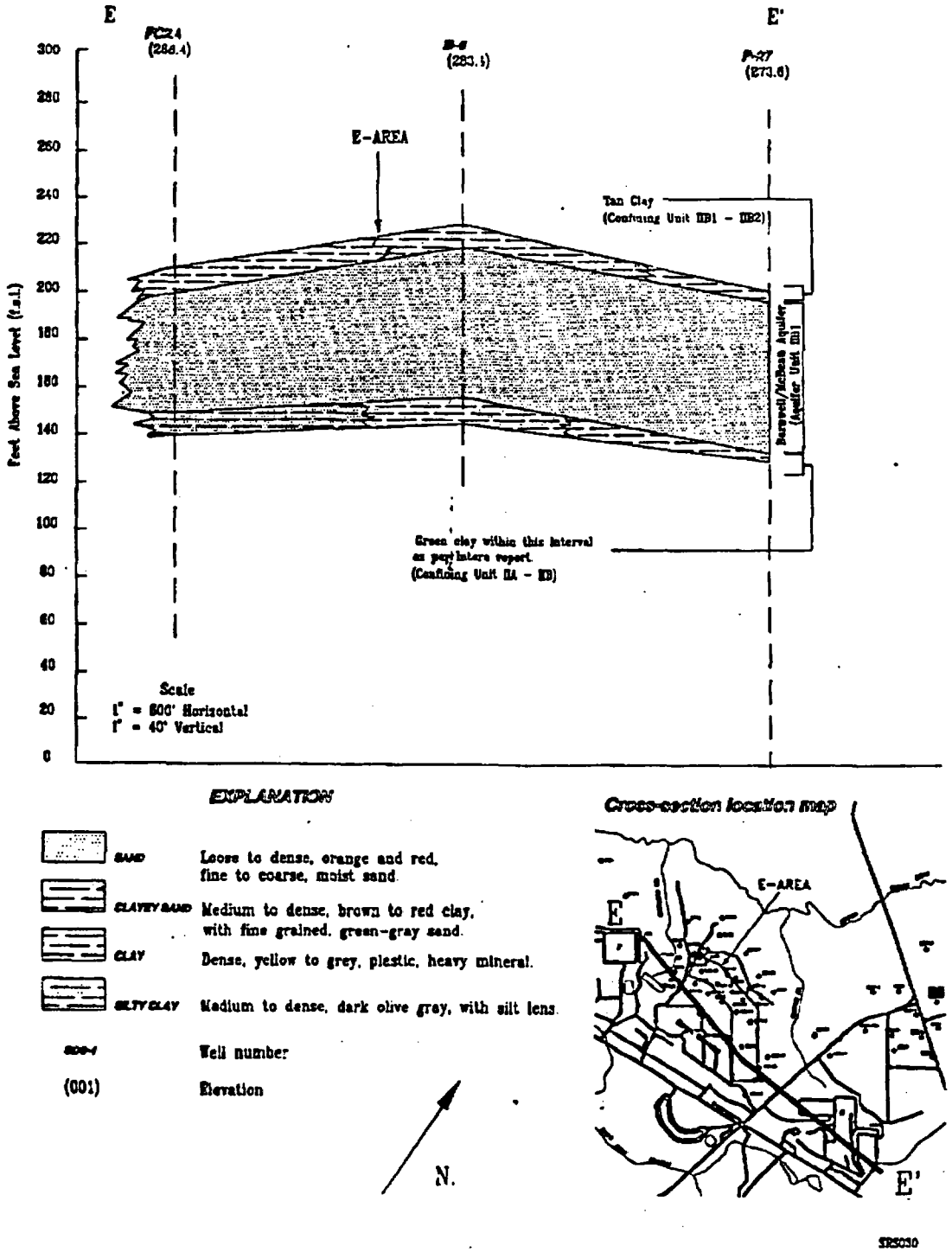

Fig. 2.2-4. Lithologic cross-section, E-E', in the vicinity of E-Area.

Confining Unit IIA-IIB (Green Clay) at E-Area separates Aquifer Unit IIA and Aquifer Unit IIB. The vertical component of flow in Aquifer Unit IIB, Zone 1 (Barnwell/McBean), is downward across the Confining Unit IIA-IIB (Green Clay) into Aquifer Unit IIA (Congaree). Confining Unit IIA-IIB (Green Clay) is more competent than Confining Zone IIB1-IIB2 (Tan Clay), but there is evidence of some leakage near E-Area.

Aquifer Unit IIB, Zone 1 (Barnwell/McBean) overlies Confining Unit IIA-IIB (Green Clay) and underlies Confining Zone IIB1-IIB2 (Tan Clay). This zone ranges in thickness from 12 to 28 m. It thins toward the western portion of the GSA, in the vicinity of the H-Area seepage basins. Aquifer Unit IIB, Zone 1 (Barnwell/McBean) dips approximately 1.5 to 1.7 m per km to the southeast. UTR Creek has eroded through Confining Zone IIB1-IIB2 (Tan Clay), and Aquifer Unit IIB, Zone 1 (Barnwell/McBean). Heads decline toward the bounding streams of UTR Creek, McQueen Branch, and Four Mile Branch as shown in Fig. E.2-4. A groundwater divide exists within this unit and acts to separate groundwater flow in the aquifer to the north and south. The divide follows the east-west trend of the topographic upland between UTR Creek and Four Mile Branch and is situated to the south of the EAVDF. The divide is not located symmetrically between these two lateral boundaries because of the deep incisement of UTR Creek, and instead is shifted slightly to the south.

Confining Zone IIB1-IIB2 (Tan Clay) separates underlying Aquifer Unit IIB, Zone 1 (Barnwell/McBean) from overlying Aquifer Unit IIB, Zone 2 (water table) and consists of multiple-discontinuous clay layers. The vertical component for the flow of water in the water table is downward across Confining Zone IIB1-IIB2 (Tan Clay) into Aquifer Unit IIB, Zone 1 (Barnwell/McBean). Confining Zone IIB1-IIB2 (Tan Clay) is a leaky aquitard with the degree of leakage across the confining zone being variable. Leakage depends on the magnitude of the head difference across the confining zone and the local permeability of the confining zone.

Aquifer Unit IIB, Zone 2 (water table), is the uppermost aquifer and is under unconfined conditions. Aquifer Unit IIB, Zone 2, has a downward hydraulic flow direction toward lower units. The hydraulic head distribution and flow directions are very similar to the Aquifer Unit IIB, Zone 1 (Barnwell/McBean), thus, flow directions are sub-parallel to flow directions in that unit. A groundwater divide exists in the interstream upland with hydraulic heads decreasing toward the bounding streams. Configuration of the water table is shown in Fig. E.2-5.

The water table occurs in Aquifer Zone IIB (water table) at E-Area. The historic high water level under the EAV is estimated to range between 71.6 and 74.8 m above mean sea level (MSL) (Amidon 1990). A review of well data available for E-Area suggests average water table elevations on the order of 69 m to 71 m above MSL. In the northeast section of the facility, where disposal of the intermediate-activity LLW is planned, the average water table elevation is estimated to be 69 m, with a historic high water level of approximately 71.7 m above MSL. The direction of flow is effected by the creeks in all aquifer units.

Measured hydraulic conductivities of the hydrologic zones described above are listed in Table 2.2-1.

Table 2.2-1 Summary of hydraulic conductivities reported for Aquifer System II

Hydrologic Units	Horizontal Hydraulic Conductivity (cm yr^{-1}) [1]	Vertical Hydraulic Conductivity (cm yr^{-1}) [1]
Aquifer Unit IIB, Zone 2	4.1×10^3 to 1.8×10^4	—
Confining Zone IIB_1-IIB_2	0.19 to 3.8	0.04 to 13
Aquifer Unit IIB, Zone 1	2.3×10^3 to 2.3×10^5	—
Confining Unit IIA-IIB	0.44 to 5	0.2 to 1.4
Aquifer Unit IIA	2.0×10^4	—

[1] *Source:* WSRC 1991b.

Hydraulic characteristics of unsaturated soil near E-Area are reported in Appendix E. Soil water content - soil water pressure relationships for soil samples taken from two locations in the General Separations Areas (GSA) are provided, as are relationships between hydraulic conductivity and water content. The disparity between the relationships at the two areas are indicative of the heterogeneous nature of soils at the SRS.

2.2.3 Surface Water in the Vicinity of E-Area

The watershed of UTR Creek drains about 500 km^2 of the Upper Coastal Plain northeast of the Savannah River. Significant tributaries to this creek are Tinker Creek, which is a headwaters branch that comes in northeast of E-Area, and Tims Branch, which connects up west of E-Area (Fig. 2.1-2). There are no lakes or flow control structures on UTR Creek or its tributaries. The stream channel has a low gradient and is meandering. Its floodplain ranges in width from 0.4 to 1.6 km and is heavily forested with hardwoods.

UTR Creek is gauged at three points within SRS: 1) near the northern SRS boundary; 2) just upstream of the Tinker Creek confluence; and 3) about 5 km above the confluence with the Savannah River. The average discharge at the two northernmost gauges normalized to drainage area is 0.013 $m^3\ s^{-1}\ km^{-2}$, ranging from 0.006 $m^3\ s^{-1}\ km^{-2}$ to 0.06 $m^3\ s^{-1}\ km^{-2}$ (Dennehy et al. 1989). Maximum flows are attributed to excess precipitation runoff.

Two smaller tributaries of UTR Creek, Crouch Branch and an unnamed branch, are located northeast and west, respectively, of the E-Area. Both Crouch Branch and the unnamed tributary receive runoff from E-Area. Crouch Branch has a drainage area of about 2.8 km^2 and the drainage area of the unnamed tributary has not been determined. One set of data from gauging stations on Crouch Branch reflects less than a full year's gauging results (Dennehy et al. 1989). At that time, the southeastern United States was in a drought condition. These data thus represent a low-flow condition, in which all streamflow is from groundwater discharge. Discharge rates as a function of gauge height could not be developed due to the low flow. Seepage investigations on one particular day indicated that Crouch Branch gained groundwater at an average rate of 0.010 $m^3\ s^{-1}\ km^{-1}$ of stream length. The average number for UTR Creek at Z-Area, which is on the east side of Crouch Branch, was 0.16 $m^3\ s^{-1}\ km^{-1}$. Stream-flow measurements for Crouch Branch and the unnamed branch were also conducted as part of this investigation. Flow rates were 1.78 and 0.68 cfs for Crouch and unnamed branch, respectively. This information is presented in Appendix C.

2.2 Water Quality and Usage in the E-Area Vicinity

Currently, groundwater in Aquifer Unit IIA (Congaree), Aquifer Units IIB1 (Barnwell/McBean), and IIB2 (water table) is monitored in E-Area. Results of chemical analyses of water samples from five wells upgradient from EAV are presented in Table 2.2-2 (Cummins et al. 1990, Aadland 1990). In general, water from the lower Aquifer Unit IIA (Congaree) tends to be higher in dissolved calcium and magnesium concentrations, higher in dissolved sulfate, and higher in dissolved silica concentrations than water from Aquifer Units IIB1 (Barnwell/McBean) and IIB2 (water table). Dissolved nitrate concentrations in water from Aquifer Unit IIA (Congaree) were significantly lower than in water from Aquifer Units IIB1 (Barnwell/McBean) and IIB2 (water table). The different chemistry of the zones has partially been attributed to the dissolution reactions that occur as water from the upper Aquifer Unit IIB2 (water table) moves downward through the lower calcite-bearing portion of Aquifer Unit IIB1 (Barnwell/McBean), and through the silica-bearing illite/smectite minerals in the Confining Unit IIA-IIB (Green Clay). (Aadland 1990, Dennehy et al. 1989). Differences in nitrate concentrations may be due to the activity of nitrate-reducing bacteria (Dennehy et al. 1989). Elevated pH levels are attributed to well construction problems rather than groundwater contamination (Cummins et al. 1990).

Water from the creeks local to E-Area are not currently used for human consumption. Some water quality characteristics of UTR Creek downstream of E-Area, classified as a Class B water by the SCDHEC, are listed in Table 2.2-3. The temperature, dissolved oxygen, and pH values reflected in this table are within the standards required for Class B waters (Cummins et al. 1990). Other water quality parameters listed in this table are within the ranges observed in previous years (Cummins et al., 1990), indicating that the quality of UTR Creek is not being degraded at the point of measurement.

Table 2.2-2. Concentration of dissolved elements in groundwater in Aquifer Unit IIA and Units IIB1 and IIB2 near E-Area (Cummins et al. 1990)

Parameter	Aquifer Unit IIA (Congaree) (BGO 6A)		Aquifer Unit IIA (Congaree) (BGO 10A)		Aquifer Zone IIB_1 (Barnwell/McBean) (BGO 6C)		Aquifer Zone IIB_1 (Barnwell/McBean) (BGO 10C)		Aquifer Zone IIB_2 (Water Table) (BGO 6D)	
	Min	Max	Min	Max	Min	Max	Min	Max	Min	Max
Ca (mg/L)	36.9	57	32	61	19.9	23	5.97	26.4	20.1	21.2
Mg (mg/L)	1.32	1.42	1.25	1.6	0.464	0.516	0.307	0.95	0.818	1.1
Na (mg/L)	2.19	2.35	2.04	2.66	2.21	3.75	5.45	6.59	2.39	2.93
K (mg/L)	0.73	1.07	<0.5	5.2	<0.5	0.679	0.762	4.49	0.783	1.07
Cl (mg/L)	2.7	3	2.7	3.1	2	2.2	2.1	2.6	1.5	1.8
SO_4 (mg/L)	8.5	9.2	8.9	10.6	<1	<5	1.8	5	1.6	<5
pH	7.1	7.6	6.6	7.6	6.9	7.2	7.6	10.5	6	6.7
Cd (µg/L)	<0.002	<0.004	<0.002	<0.004	<0.002	<0.002	<0.002	<0.004	<0.002	<0.002
NO_3 as N (mg/L)	<0.05	<0.1	<0.05	<0.1	0.68	1.01	0.19	0.48	<0.1	0.2
Total PO_4 (mg/L as P)	0.05	0.114	<0.05	0.106	0.12	0.155	<0.05	0.24	<0.05	0.108
SiO_2 (mg/L)	39.2	44.3	38	46.1	9.53	10.4	14.4	22.1	8.09	10.5

Table 2.2-3. Water quality of UTR Creek at Road A (Cummins et al. 19[illegible])

Parameter	Units	No. of Analyses	Mean	Max	Min
Temperature	°C	12	18	32	8.7
pH	pH	12		7.7	6.4
Dissolved oxygen	mg/L	12	8.9	11	7.3
Alkalinity	mg/L	12	4.3	6.0	1.0
Conductivity	umhos/cm	12	28	40	23
Turbidity	NTU	12	2.5	4.2	1.6
Suspended solids	mg/L	12	8.1	15	2.0
Volatile solids	mg/L	12	3.7	7.0	1.0
Total dissolved solids	mg/L	12	27	32	20
Total solids	mg/L	12	35	41	26
Fixed residue	mg/L	12	4.6	8.0	1.0
Chemical oxygen demand	mg/L	12	8.7	18	3.0
Chloride	mg/L	12	1.8	2.6	0.31
Nitrogen (as NO_2/NO_3)	mg/L	12	0.11	0.14	0.08
Sulfate	mg/L	12	3.2	4.0	2.0
Phosphorus (as PO_4)	mg/L	12	0.03	0.12	<0.02
Nitrogen (as NH_3)	mg/L	12	0.05	0.14	<0.02
Cadmium	mg/L	4	<0.01	<0.01	<0.01
Mercury	μg/L	4	<0.20	<0.20	<0.20
Chromium	mg/L	4	<0.02	0.02	<0.02

2.2.5 Existing Radiation and Chemical Environment at E-Area

The environmental monitoring program at the SRS includes the assessment of radionuclides in the groundwater and in stream sediments. Additional monitoring is performed for the air pathway and river water. The background level of interest at the E-Area site location for this RPA is predominantly the long term concentrations related to the groundwater pathway.

Several wells were installed to obtain background data for the EAVDF and to monitor the EAV Disposal Facility after startup. Wells in the region of the EAV were monitored at the water table, Barnwell/McBean and Congaree aquifer zones. Because the flow of water in Aquifer Unit IIA (Congaree) is toward the UTR Creek, wells were monitored in that unit in the Burial Grounds and Mixed Waste Management Facility regions upgradient of EAVs.

During 1991, results from several wells monitored at EAVs and upgradient to EAVDF contained contaminants above DWS (Table 2.2-4). Tritium concentrations exceeded the applicable standard in Aquifer Units IIB1-IIB2 (Barnwell/McBean; water table) and in Aquifer Unit IIA (Congaree). In the upgradient wells (located at the Burial Grounds and MWMF), 3 of the 15 wells observed exceeded the DWS for tritium concentration. In Aquifer Unit IIA (Congaree), 1 of 2 wells monitored at EAVs exhibited elevated levels of tritium. Total radium concentration was above the PDWS in 1 of 15 EAV wells. Tritium concentration levels have also exceeded PDWS in downgradient wells of the EAVDF (Table 2.2-5 and Table 2.2-6). Tetrachloroethylene exceeded primary drinking water standards (PDWS) in 2 of 15 upgradient wells and trichloroethylene concentrations were exceeded in 5 of the 15 wells sampled. In the region of EAVs, tetrachloroethylene and trichloroethylene exceeded PDWS in 1 of 15 and 2 of 15 wells sampled, respectively. The migration of tritium and solvents toward UTR Creek is partly due to the plume associated with the Burial Grounds facility (643-7E, 643-7E, 643-28E) (WSRC 1992a). The migration of contaminants from the Burial Grounds to EAV contributes to the elevated levels of tritium prior to startup of the vaults. The wells used in this assessment of the existing groundwater-water quality and radionuclide content are shown in Fig. 2.2-5.

Table 2.2-4. Maximum constituent results exceeding applicable standards for wells at the EAVDF (Arnett et al. 1991).

Constituent	Unit	Standard	Maximum Result
Aquifer Unit IIA (Burial Grounds, Mixed Waste Management Facility)			
Alkalinity (as $CaCO_3$)	mg/l	100	385
Americium-241	µCi/ml	6.3×10^{-9}	3.9×10^{-8}
Specific conductance	µS/cm	100	1,840
Lead	mg/l	0.015	0.020
pH	pH	≥8.5	13
Tetrachloroethylene	mg/l	0.0050	0.0055
Total dissolved solids	mg/l	200	435
Trichloroethylene	mg/l	0.0050	0.023
Tritium	µCi/ml	2.0×10^{-5}	1.5×10^{-4}
Aquifer Units IIB1-IIB2 (E-Area Vaults)			
Alkalinity (as $CaCO_3$)	mg/l	100	109
Gross alpha	µCi/ml	1.5×10^{-8}	2.6×10^{-8}
Specific conductance	µS/cm	100	470
pH	pH	≥8.5	11
Tetrachloroethylene	mg/l	0.0050	0.0065
Total radium	µCi/ml	5.0×10^{-9}	1.7×10^{-8}
Trichloroethylene	mg/l	0.0050	0.0090
Tritium	µCi/ml	2.0×10^{-5}	9.8×10^{-3}
Aquifer Unit IIA (E-Area Vaults)			
Alkalinity (as $CaCO_3$)	mg/l	100	1,300
Gross alpha	µCi/ml	1.5×10^{-8}	1.5×10^{-6}
Nonvolatile beta	µCi/ml	5.0×10^{-6}	9.2×10^{-8}
Specific conductance	µS/cm	100	5,030
Lead	mg/l	0.015	0.052
pH	pH	≥8.5	13
Total dissolved solids	mg/l	200	1,490
Total radium	µCi/ml	5.0×10^{-9}	8.1×10^{-9}
Tritium	µCi/ml	2.0×10^{-5}	1.8×10^{-4}

Table 2.2-5. Groundwater monitoring results for the EAVDF (Cummins et al. 1990)

Constituent	Unit	March 1990	May 1990	August 1990	November 1990
WELL: BG 96					
pH	pH	5.5	5.7	4.3	5.6
Specific conductance	µS/cm	48	34	35	29
Alkalinity	meq/L	6	6	6	4
TDS	mg/L	43	35	27	29
Cadmium	mg/L	<0.002	<0.002	<0.002	<0.002
Tritium	µCi/mL	1.3×10^{-5}	1.0×10^{-5}	9.9×10^{-6}	7.0×10^{-7}
Chloride	mg/L	3.5	2.3	2.4	2.8
Chromium	mg/L	<0.004	<0.004	0.01	<0.004
Iron	mg/L	0.034	0.033	0.028	0.38
Lead	mg/L	<0.006	0.018	<0.003	0.004
Manganese	mg/L	0.013	<0.002	0.003	<0.002
Silver	mg/L	<0.002	<0.002	<0.002	<0.002
Sodium	mg/L	2.09	1.83	2.4	1.6
Total phosphates (as P)	mg/L	0.06	0.21	0.2	0.07
Zinc	mg/L	0.025	0.011	0.023	0.007
Nitrate (as N)	mg/L	1.1	1.04	1.15	0.78
Sulfate	mg/L	<5	<1	<1	<1
Phenols	mg/L	<0.005	<0.005	<0.005	<0.005
Total organic carbon	mg/L	2	2	<1	<1
WELL: BG 101					
pH	pH	5	5.1	3.9	5.1
Specific conductance	µS/cm	24	21	20	21
Alkalinity	meq/L	1	1	1	1
TDS	mg/L	54	27	34	36
Tritium	µCi/mL	3.3×10^{-4}	3.0×10^{-4}	3.3×10^{-4}	3.2×10^{-4}
Cadmium	mg/L	<0.002	<0.002	<0.002	<0.002
Chloride	mg/L	1.9	1.9	2	2.2
Chromium	mg/L	<0.004	<0.004	<0.004	<0.004
Iron	mg/L	<0.004	0.03	0.031	0.017
Lead	mg/L	<0.006	0.011	0.004	0.004
Manganese	mg/L	0.007	0.008	0.009	0.008
Silver	mg/L	<0.002	<0.002	<0.002	<0.002
Sodium	mg/L	1.55	1.61	2	1.5
Total phosphates (as P)	mg/L	0.65	0.14	0.13	0.11
Zinc	mg/L	0.091	0.081	0.092	0.11
Nitrate (as N)	mg/L	0.66	0.62	0.71	0.57
Sulfate	mg/L	<5	<1	<1	<1
Phenols	mg/L	<0.005	<0.005	<0.005	<0.005
Total organic carbon	mg/L	<1	2	<1	<1

Table 2.2-5. (cont.)

Constituent	Unit	March 1990	May 1990	August 1990	November 1990
OTHER ANALYSES					
WELL: BG 96					
Aluminum	mg/L	<0.02	<0.02	<0.02	0.047
Beryllium	mg/L	<0.005	<0.003	<0.003	<0.003
Calcium	mg/L	3.89	3.39	4.3	2.28
Cobalt	mg/L	<0.004	<0.004	<0.004	<0.004
Carbonate	mg/L	<1	<1	-	-
Iodine	mg/L	<0.1	<0.1	<0.1	<0.1
Potassium	mg/L	<0.5	<0.5	<0.5	<0.5
Magnesium	mg/L	0.499	0.35	0.43	0.322
Nitrite (as N)	mg/L	<0.01	<0.01	<0.01	<0.4
Antimony	mg/L	<0.003	<0.003	<0.003	<0.003
Silica	mg/L	7.18	13	7.4	6.4
Total carbon	mg/L	8	6	10	7.04
Total inorganic carbon	mg/L	6	4	10	6.04
Uranium	mg/L	<1	<1	<1	<1
Vanadium	mg/L	<0.02	<0.01	<0.01	<0.01
WELL: BG 101					
Aluminum	mg/L	<0.02	0.067	0.028	<0.02
Beryllium	mg/L	<0.005	<0.003	<0.003	<0.003
Calcium	mg/L	1.26	1.27	1.5	0.93
Cobalt	mg/L	<0.004	<0.004	<0.004	<0.004
Carbonate	mg/L	<1	<1	-	-
Iodine	mg/L	<0.1	<0.1	<0.1	<0.1
Potassium	mg/L	<0.5	<0.5	<0.5	<0.5
Magnesium	mg/L	0.324	0.332	0.38	0.32
Nitrite (as N)	mg/L	<0.01	<0.01	<0.01	<0.01
Antimony	mg/L	<0.003	<0.003	<0.003	<0.003
Silica	mg/L	5.39	7.4	7.1	6.8
Total carbon	mg/L	6	6	10	6
Total inorganic carbon	mg/L	6	4	10	6
Uranium	mg/L	<1	<1	<1	<1
Vanadium	mg/L	<0.02	<0.01	<0.01	<0.01

Table 2.2-6. Monitoring well results of radionuclides in groundwater for the EAVDF (Cummins et al. 1990)

		Aquifer Unit IIA		Aquifer Unit IIB, Zone IIB1		Aquifer Unit IIB, Zone IIB2	
		Well: BGO 6A		Well: BGO 6C		Well: BGO 6D	
Constituent	Unit	Min	Max	Min	Max	Min	Max
Americium-241	PCL	<0.2000	<0.3000	0.7400	0.7400	ND	ND
Cobalt-60	PCL	<2.000	<3.000	<4.000	<4.000	ND	ND
Cesium-137	PCL	<2.000	<3.000	<3.000	<3.000	ND	ND
Gross alpha	PCL	<3.000	<6.000	<3.000	<5.000	<3.000	<4.000
Nonvolatile beta	PCL	<2.000	<6.000	3.200	<5.000	2.600	5.300
Tritium	PCML	<0.7000	<1.000	990.0	1750.0	1700	1.18×10^4
Nickel-59	PCL	<90.00	<100.0	<90.00	<90.00	ND	ND
Nickel-63	PCL	<9.000	<10.00	<10.00	<10.00	ND	ND
Neptunium-237	PCL	<3.000	<6.000	<7.000	<7.000	ND	ND
Plutonium-239/240	PCL	<0.2000	<0.2000	<0.0400	<0.0400	ND	ND
Strontium-90	PCL	<0.9000	<1.000	<1.000	<1.000	ND	ND
Technetium-99	PCL	<4.000	<4.000	11.00	11.00	ND	ND
Total Radium	PCL	<1.000	1.000	<1.000	1.500	1.200	3.400
Uranium-234	PCL	0.2800	4.200	0.3000	<0.3000	ND	ND
Uranium-238	PCL	<0.0300	0.8700	<0.2000	<0.2000	ND	ND
Total Activity	PCL	ND	ND	1.00×10^4	2.5×10^3	1150	9.40×10^3
		Well: HSB 85A		Well: HSB 85B		Well: HSB 85C	
Americium-241	PCL	<0.2000	0.6100	<0.2000	0.7500	<0.1000	<0.2000
Cobalt-60	PCL	<3.000	<4.000	<3.000	<6.000	<2.000	<6.000
Cesium-137	PCL	<2.000	<5.000	<4.000	<3.000	<2.000	<6.000
Gross alpha	PCL	<2.000	<4.000	<2.000	<5.000	<2.000	<3.000
Nonvolatile beta	PCL	<4.000	<5.000	<5.000	8.100	<4.000	9.800
Tritium	PCML	<1.000	<1.000	<0.700	1.300	1.400	3.200
Nickel-59	PCL	<100.0	<100.0	<90.00	<100.0	<90.00	<100.0
Nickel-63	PCL	<8.000	<10.00	<9.000	<10.00	<8.000	<10.00
Neptunium-237	PCL	<4.000	<10.00	<9.000	<10.00	<3.000	<10.00
Plutonium-239/240	PCL	<0.0500	<0.2000	<0.0900	<0.2000	<0.0600	<1.000
Strontium-90	PCL	<0.7000	<1.000	<0.7000	<1.000	3.100	<0.7000
Technetium-99	PCL	<3.000	<5.000	<3.000	<8.000	3.400	<10.00
Total Radium	PCL	<1.000	1.200	<1.000	<1.000	<1.000	1.400
Uranium-234	PCL	<0.0400	<2.000	<0.0400	<0.9700	<0.0500	6.300
Uranium-238	PCL	<0.0300	<2.000	0.2300	<0.0200	<0.0200	<2.000
Total Activity	PCL	ND	ND	ND	ND	ND	ND
		Well: BGX 4A		Well: BGX 8D		Well: BGX 6D	
Gross alpha	PCL	<2.000	2.000	<2.000	<2.000	<2.000	<2.000
Nonvolatile beta	PCL	2.000	4.000	0.3000	4.300	<2.000	<2.000
Tritium	PCML	<0.700	<0.700	1.026	1034	3.500	4.100
Total Radium	PCL	0.600	4.800	1.50	5.30	1.700	4.300
Total Activity	PCL	ND	ND	1013	1027	4.450	5.950

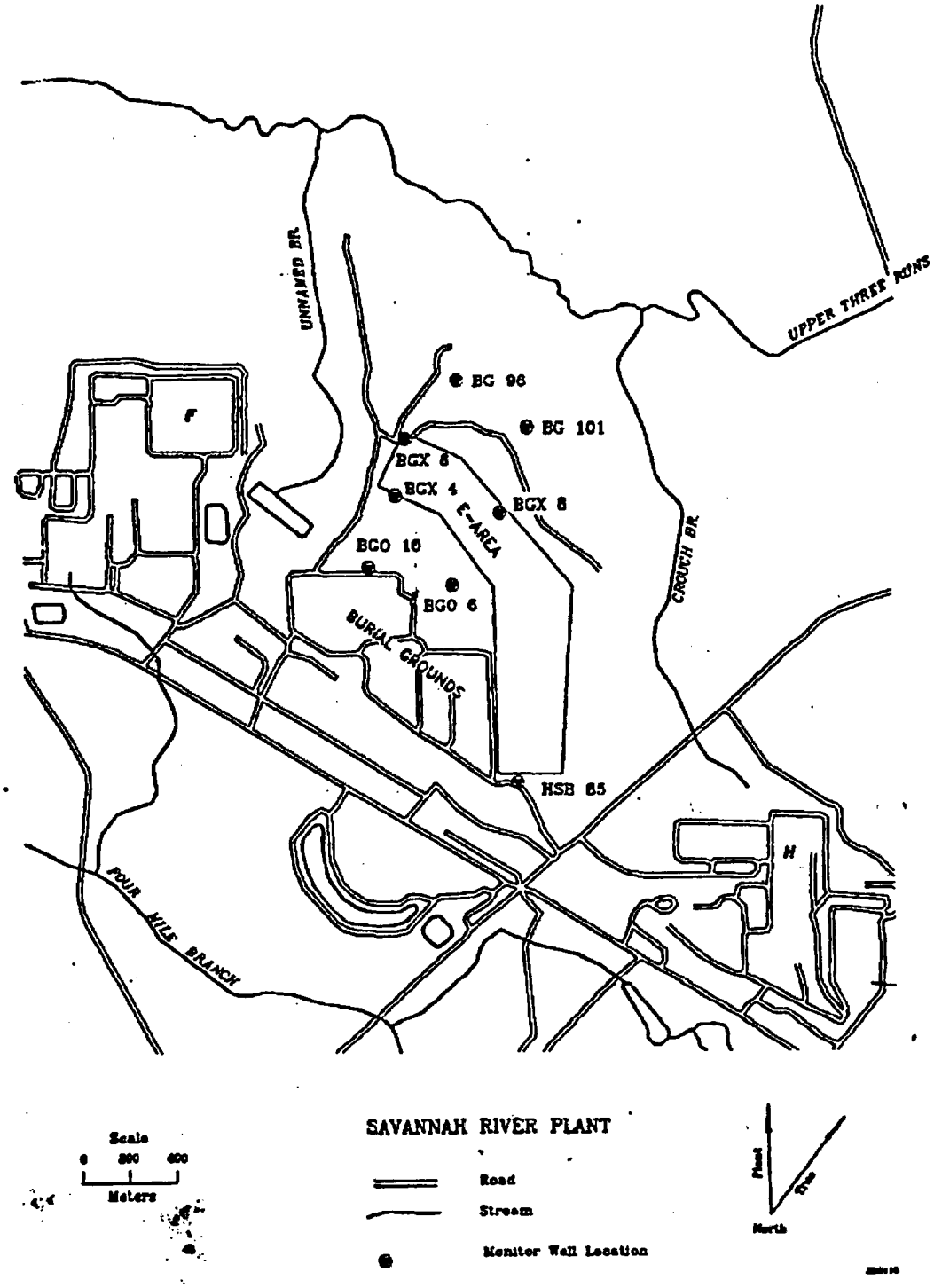

Fig. 2.2-5. Location of E-Area monitoring wells used to assess the groundwater quality and radionuclide activities.

2.3 DESCRIPTION OF E-AREA OPERATIONS, FACILITIES, AND FEED STREAMS

The EAVDF is part of an integrated waste disposal system being installed at the SRS. The EAVDF is regulated by DOE Orders and other Federal regulations that are applicable to disposal of low-level radioactive solid waste.

2.3.1 Description of the Waste Types at E-Area

The EAVs are to provide a new disposal and storage site for solid, low-level, non-hazardous radioactive waste. The U.S. DOE Order 5820.2A defines low-level radioactive waste as waste that contains radioactivity and is not classified as HLW (waste material that results from the reprocessing of spent nuclear fuel), TRU, spent nuclear fuel or 11e(2) byproduct material.

SRS operations further classify LLW into three categories to assist in the reduction of radiological risks to workers at the site. LAW, IAW, and Tritiated Waste. IAW consists of waste material that radiates ≥200 mR/h at 5 cm from the unshielded outer disposal container. LAW is defined as waste material that radiates <200 mR/h at 5 cm from the unshielded outer disposal container. Tritiated Waste is waste material that contains greater than trace quantities of tritium regardless of the radiation rate. For waste acceptance purposes, trace quantities of tritium has been defined as 10 curies of tritium per waste container. The EAV will not dispose of or store liquid wastes, TRU waste, hazardous wastes, or mixed (both hazardous and radioactive) wastes.

2.4 E-AREA VAULTS WASTE COMPOSITION

2.4.1 Physical Characteristics of Waste Types

2.4.1.1 Low Activity Waste (LAW)

LAW will be disposed of in the Low Activity Waste Vault (LAWV). Most of the LAW

will be received in standard 1.2 x 1.2 x 1.8 m metal containers (B25 boxes), but some waste will also be received in standard 0.6 x 1.2 x 1.8 m containers (B12 boxes) or 210-L drums. The LAW may also be received in non-standard engineered concrete or metal containers. These containers shall be preapproved by Solid Waste Management prior to their receipt at the EAV.

The LAW will include job control waste, scrap metal, and contaminated soil and rubble. Job control waste will consist of potentially contaminated protective clothing including plastic suits, shoe covers, lab coats, and plastic sheeting. Scrap metal will be contaminated tools, process equipment, and laboratory equipment. Soil and rubble will be generated from demolition and cleanup activities. Historically, the majority of this waste has been generated by the HLW tank farms. Larger volumes of waste disposed at EAV are anticipated from environmental restoration activities as facilities are decommissioned and old waste sites are remediated.

2.4.1.2 Intermediate Activity Waste (IAW)

The Intermediate Level Non-Tritium Vault (ILNTV) will be used for disposal of IAW. IAW consists of job control waste, scrap hardware, and contaminated soil and rubble. Job control waste is primarily highly contaminated lab coats, plastic suits, shoe covers, plastic sheeting, etc. This material is assumed to be combustible and is contaminated primarily with fission products. Scrap hardware waste will consist of reactor hardware, reactor fuel and target fittings, jumpers, and used canyon and tank farm equipment contaminated with fission products and/or induced activity.

All of the IAW will be packaged in engineered metal or concrete containers that have been approved by Solid Waste Management. The containers will be remotely placed into the vault in layers. IAW containers will be grouted in place to provide better waste isolation, reduce dose to operators, and improve stacking of additional containers.

2.4.1.3 Tritiated Waste

Tritiated waste will be disposed in the Intermediate Level Tritium Vault (ILTV). This facility consists of two cells, one for each of the two subcategories of tritiated waste. Tritium crucibles will be disposed in the first cell. This waste form is generated by the tritium facilities in the process used to recover tritium from target assemblies. The crucibles will be overpacked into a stainless-steel container that is about 0.5 m in diameter and 6.1 m in length. The crucible cell is specially designed with vertical silos to receive waste. All other tritiated waste will be disposed of in the bulk tritiated waste cell. This waste will consist of job control waste and used process equipment that is contaminated with tritium. Bulk tritiated waste will be disposed in engineered metal or concrete containers.

2.4.2 Waste Packaging

Many different containers will be received at the EAV. However, all containers are required by the Operational Safety Requirements (OSRs) to be engineered concrete or metal containers that have been approved by Waste Management. A procedure has been written that defines this approval process and requires Solid Waste Management Engineering, Solid Waste Management Operations, and Solid Waste Management Maintenance to concur that the container can be safely handled, will not impair vault space utilization, and will satisfactorily contain the waste contents.

Standardized B25 and B12 containers will be used for a majority of the waste. These standardized containers have already received approval for acceptance at the EAV. Other containers are specific to the generator or the waste form. These containers will be approved for either one time use or unlimited use, depending on the circumstances.

2.4.2.1 Container Descriptions

Standard Containers

The B25 and B12 are carbon steel boxes that have been used in the past for waste disposal in the SWDF. The boxes are similar in construction with the exception of size. The B25 is a 2.5 m^3 container that is approximately 1.2 m high, 1.2 m wide, and 1.8 m long. It is typically constructed of 14-gauge carbon steel (1.9 mm) but some B25s are constructed of 12-gauge carbon steel (2.6 mm) to allow use in the compactor. The B12 is a 1.3 m^3 container that is approximately 0.6 m high, 1.2 m wide, and 1.8 m long and is typically constructed of 12-gauge carbon steel.

The B12 and B25 containers are constructed with a rubber-gasket seal between the lid and the container conforming to ASTM-D-1056 with a gasket compression of 20 to 30%. The interior and exterior of each container is coated with a zinc chromate primer. The exteriors are given an additional coating of alkyd enamel and a finish coat of paint conforming to ASTM-D-16-75.

DOT 210-L drums will also be received as a standard container. Use of these containers is restricted to situations where use of a B25 is not practical. Drums will be banded together and banded to a fire-resistant pallet prior to shipment to the EAV.

Non-Standard Containers

For waste that cannot be placed in a standard container, specific size and weight limits have been specified. Maximum dimensions for containers to be emplaced in the LAWV are 4.3 m high × 7.3 m wide × 15.2 m long. The maximum dimensions for containers to be emplaced in the Intermediate Vaults are 7.3 m high × 10.7 m long × 6.1 m wide. The maximum uniform load on the vault floor cannot exceed 4.9×10^6 kg m^{-2} for the Intermediate Level Vaults and 2.8×10^6 kg m^{-2} for the LAWV.

Tritium Crucibles

Tritium crucibles will be packaged in a stainless steel overpack container. The overpack will be an 0.46-m diameter pipe which is approximately 6.1 m long. The lid will be sealed to the overpack with a compression O-ring. The O-ring will not prevent off-gassing of tritium in the ILTV crucible silos. The ILTV is designed to receive 142 of these tritium crucible overpacks.

2.4.3 Radioactive Inventory of Waste Types

2.4.3.1 Low Activity Waste (LAW)

The radioactive content of LAW is primarily fission products from the tank farms and Separations. Waste contaminated with uranium will be received from M-Area. Waste will also be received from off-site facilities, which will have a variety of radionuclides.

2.4.3.2 Intermediate Activity Waste (IAW)

Depending on the origin of this waste, it can contain either fission products or induced activity contamination. The induced activity waste will be mostly metal reactor hardware and fittings that have been exposed to a high neutron field. This waste generates a high radiation field but the activity is fairly immobile due to the metal matrix. Job control waste and process piping from Separations and High Level Waste Management will be contaminated with fission products. These fission products will be both loose and fixed surface contamination.

2.4.3.3 Tritiated Waste

The large majority of activity in this waste will be tritium. However, Cobalt-60 and Zinc-65 will also be present due to the activation of impurities during tritium production.

2.5 DESCRIPTION OF THE E-AREA VAULTS DISPOSAL SITE

As presently planned, the EAVDF will contain several large concrete vaults divided into cells. Each of the cells will be filled with LAW, IAW, and tritium waste, as appropriate. The EAV provides primary containment of the waste.

The bottom of the vaults will be approximately 8 m above the average water table height (Sect. 2.2.2) beneath the E-Area site, thus avoiding disposal of waste in a zone of water table fluctuation. Design requirements mandate that the bottom of the vault structures be at least 3 m above the historical maximum water table height. Run-on and runoff controls are installed to minimize site erosion during the operational period.

2.5.1 Site Layout and Capacity

The EAV site will be located on a 200-acre site (Fig. 2.5-1) immediately north of the current LLW burial site; of the 200 acres, only 100 acres have been developed at this time. The neatest SRS boundary to the EAVs is about 11 km to the west. The EAVDF is in a relatively level highland region of SRS at about 90 m ASL.

For the purposes of this RPA, it was assumed that 100 acres would provide disposal capacity for 20 years of SRS operations, which would include 10 ILNTVs, 10 ILTVs, and 21 LAWVs.

2.5.1.1 Intermediate-Level Nontritium Vaults

There are ten ILNTVs designated for use by the EAV project. Three vaults are oriented in a general north-south direction, and the remaining seven vaults are oriented in a general east-west direction (Fig. 2.5-1). Each vault consists of seven cells or subdivided sections within the vault structure and provide approximately 5.7×10^3 m^3 of waste disposal capacity. The base of the ILNTVs are at elevations ranging between approximately 76.4 m and 79.1 m above MSL.

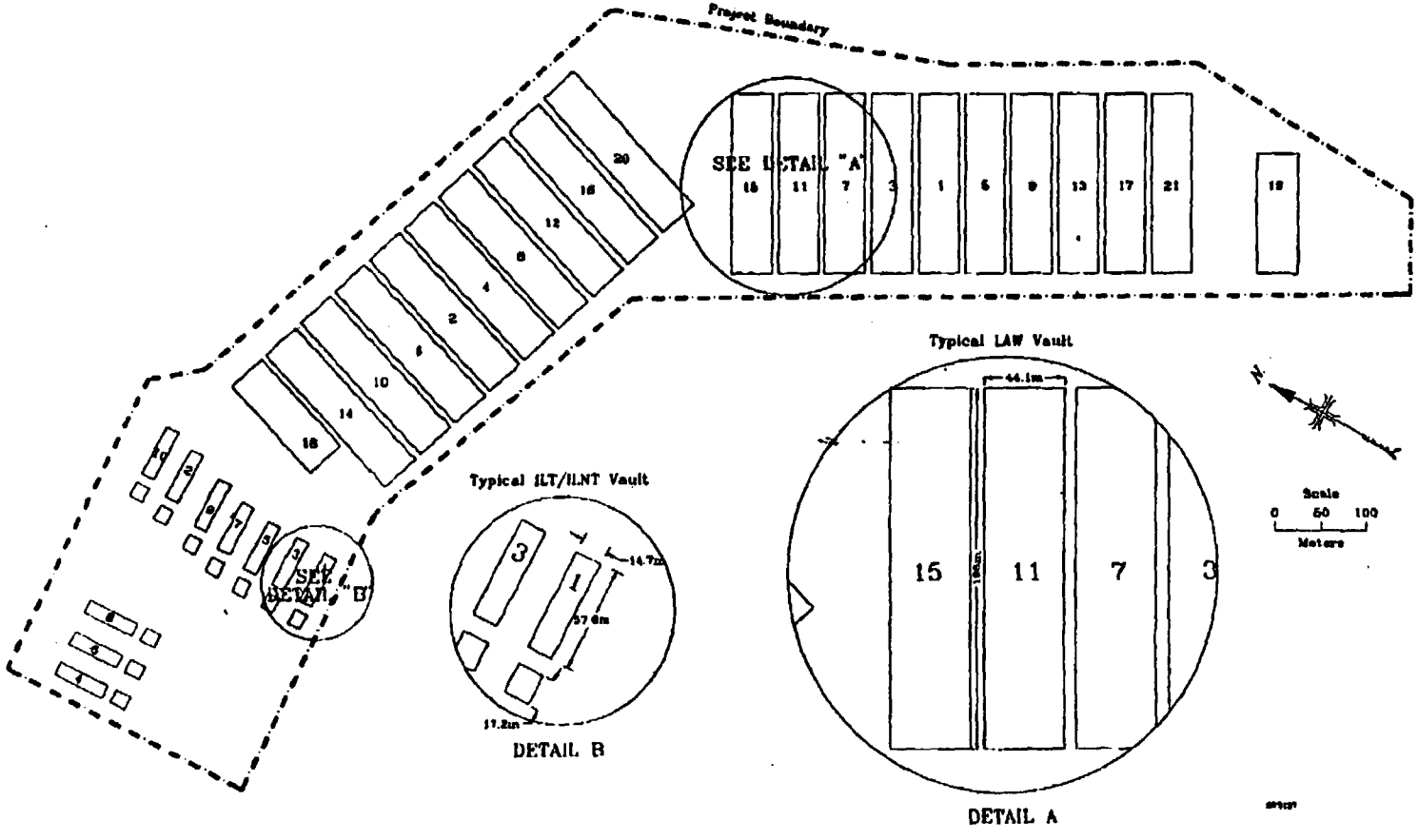

Fig. 2.5-1. Projected vault layout in the EAVDF.

2.5.1.2 Intermediate-Level Tritium Vaults

Ten ILTVs are designated for use by the EAV project. Three vaults are oriented in a general north-south direction and the remaining seven vaults are oriented in a general east-west direction (Fig. 2.5-1). Each vault consists of two cells or subdivided sections within the vault structure and provides approximately 1.6×10^3 m^3 of waste disposal capacity. As originally conceived one cell in each vault would be fitted with a silo system to permit the disposal of tritium crucibles. As operations change at SRS, the need for additional or fewer silo cells will be evaluated. The base of the ILTVs are, like the ILNTVs, at elevations ranging between approximately 76.4 m and 79.1 m above MSL.

2.5.1.3 Low-Activity Waste Vaults

There are 21 LAWVs designated for use by the EAV project. Ten vaults are oriented in a general northeast-southwest direction, and eleven vaults are oriented in a general east-west direction (Fig. 2.5-1). Nineteen vaults consist of three major subdivisions (modules) with each module containing four cells. The remaining two vaults consist of two modules with each module containing four cells. Each three-module vault provides approximately 4.8×10^4 m^3 of waste disposal capacity that will accommodate more than 12,000 B-25 boxes (waste containers). Each two-module vault provides approximately 3.2×10^4 m^3 of waste disposal capacity that will accommodate more than 8,000 B-25 boxes. The base of the LAWs are at elevations ranging between approximately 84.0 m to 84.7 m above MSL.

2.5.2 Vault Descriptions

The EAV consists of three types of structures to house four designated waste types and the necessary roadways to allow waste container delivery.

One type of structure is partitioned into two segments (the ILTV and ILNTV) and receives two categories of waste. The ILNTV receives waste radiating ≥200 mR/h at 5 cm from the exterior of the outer disposal container. The ILTV receives waste which is

contaminated with more than trace quantities of tritium. Administratively, the lower limit for the ILTV is 10 Ci of tritium per waste package. These two vaults share a similar design, are adjacently located, share waste handling equipment, and will be closed as one facility.

The second type of structure is designated as the LAWV. The LAWV is designed to receive waste radiating <200 mR/h at 5 cm from the exterior of the outer disposal container. The third facility is the long-lived waste storage building (LLWSB). The LLWSB is designed to provide covered, long term storage for waste containing long lived isotopes which exceed performance criteria for disposal. This waste would eventually be removed to a suitable disposal facility.

2.5.2.1 Intermediate-Level Non-tritium Vaults

There are currently ten ILNT vaults planned for the EAV. These vaults are subsurface concrete structures approximately 58 m long, 15 m wide, and 8.8 m high (Fig. 2.5-2). The end exterior walls are 0.8 m thick, the side exterior walls are 0.6 m thick, and interior walls are 0.5 m thick. All walls are structurally mated to a base slab, which is 0.8 m thick and extends past the outside of the exterior walls approximately 0.6 m. The 0.8 m base slab rests on two layers of crushed stone placed on the compacted subsurface. Each ILNTV consists of seven cells and provides approximately 5.7×10^3 m^3 of waste disposal capacity.

The floor of each cell slopes to a drain which runs to a sump in the base slab for each cell. Any water accumulating in the sump can be monitored and removed through a 0.15-m - diameter riser pipe at the top of the wall. Any water that collects under the vault will flow to dry wells between the ILNTVs and the ILTVs. Access to the dry well can be obtained through a man hole at grade level.

The operating cell can be covered with reinforced concrete slabs, known as shielding tees, to reduce the radiation level at the edge of the vault. The profile of these tees are in the shape of the letter "T" so that they can be interlocked to provide 0.5 m of shielding. Each cell is also provided with a metal rain cover that is installed over each cell when not operating to minimize the infiltration of rain water.

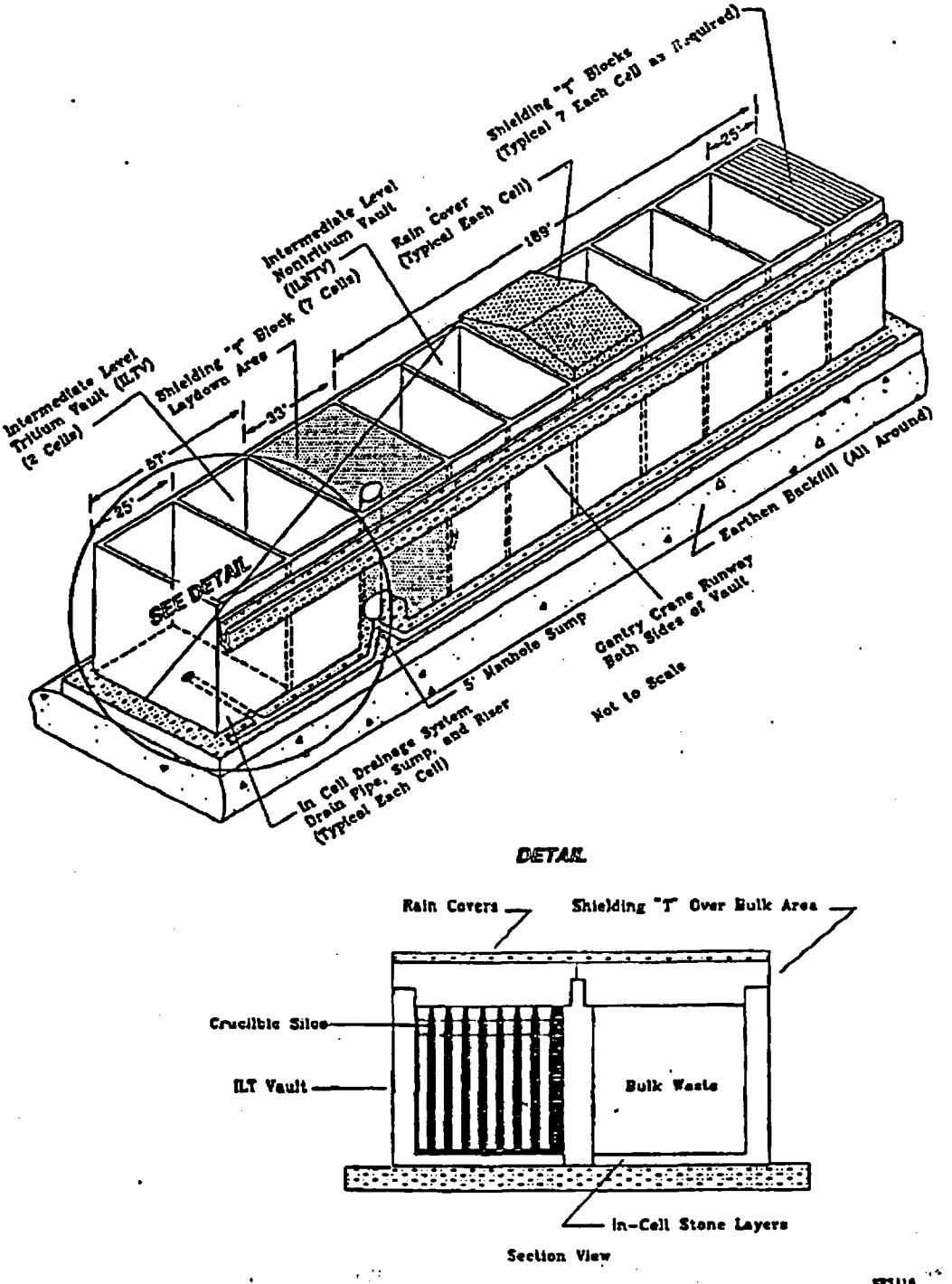

Fig. 2.5-2. General arrangement of the ILNT and ILT vaults.

2.5.2.2 Intermediate-level Tritium Vaults

There are currently ten ILTVs planned for the EAV. Similar to the ILNTV, these vaults are subsurface concrete structures approximately 17 m long, 15 m wide, and 8.8 m high (Fig. 2.5-2). The wall and slab thicknesses are identical to ILNTV. Each ILNTV is composed of 2 cells.

One of the two cells is equipped with 142 silos, for tritium crucible overpacks. A 1-m - thick shielding plug will be used to reduce radiation exposure from the disposed crucibles. A plug will be installed in each silo after a crucible has been placed into it.

Both cells on the ILTV will be covered with metal raincovers when the vault is not operating.

2.5.2.3 Low Activity Waste Vaults

Twenty-one LAWVs are designated for construction in the EAV. These subsurface concrete structures consist of two or three modules depending on the vault location. Each module contains four cells. There are to be nineteen three-module vaults. Each will be approximately 200 m long, 44 m wide, and 8.2 m high (Fig. 2.5-3). There are plans for two vaults consisting of two modules. These vaults are approximately 130 m long, 44 m wide, and 8.2 m high. All exterior walls in the LAWVs will be 0.6 m thick and structurally mated to a 0.8-m thick footer. Interior cell walls are 0.3 m thick. The floor slab is 0.3 m thick and is not mated to the footer or walls.

2.5.2.4 Seismic Qualification

As documented on the Structural Design Criteria (S2889-306-25-0) the EAVs were designed and constructed to be maximum resistance structures after closure. In accordance with Site Specification 7096, a maximum resistance structure shall be designed to withstand a 0.2 g earthquake event.

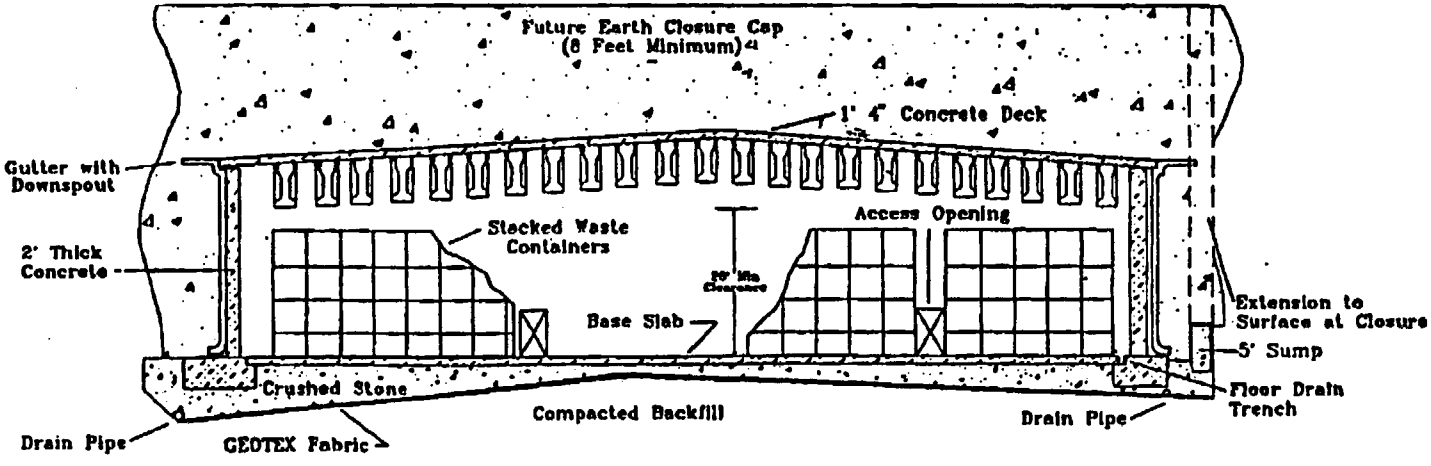

Fig. 2.5-3. Typical section through LAWV cell.

2.6 PROPOSED TRENCHES FOR DISPOSAL OF SUSPECT SOIL

Between 2800 and 5600 m^3 of soil from regulated areas is designated as potentially contaminated soil (i.e., "suspect soil") at the SRS annually (Cook 1991). Non-vault disposal of a portion of this soil is being considered for the EAVDF.

Five below-grade trenches containing suspect soil are considered in this RPA for the EAVDF. The dimensions of each trench are 6 m wide by 200 m long by 6 m deep. The conceptual layout of the trenches is shown in Fig. 2.6-1. The location of these trenches is assumed to be near the LAW vaults, but not close enough to the LAW vaults to receive enhanced infiltration resulting from diversion of water from the vault roofs. The suspect soil is assumed to be placed in the trenches to a depth of 4.8 m, allowing for 1.2 m of a clean soil cover in the trenches. This clean soil is in addition to the final soil and clay cover that will overlay the trenches when final closure of the EAVDF occurs. No engineered barriers are assumed to exist beneath the trenches, and the base of the trenches are assumed to be at an elevation of approximately 84 m ASL, like the LAW vaults. The potential source of radionuclides to the E-Area environment and to inadvertent intruder posed by these trenches is evaluated in this RPA of the EAVDF in Appendix I, and radionuclide limits for disposal of suspect soil in such trenches are provided.

2.7 PROPOSED NAVAL REACTOR COMPONENT DISPOSAL

Within E-Area, disposal of up to 100 stainless steel casks containing naval reactor (NR) components is proposed. The NR waste is composed of activated metals and can include control rods, control rod drive mechanisms (CRDM's), resin vessels, adapter flanges, and similar equipment. The high shielding shipping/disposal containers reduce the safety risks involved in the disposal of NR wastes.

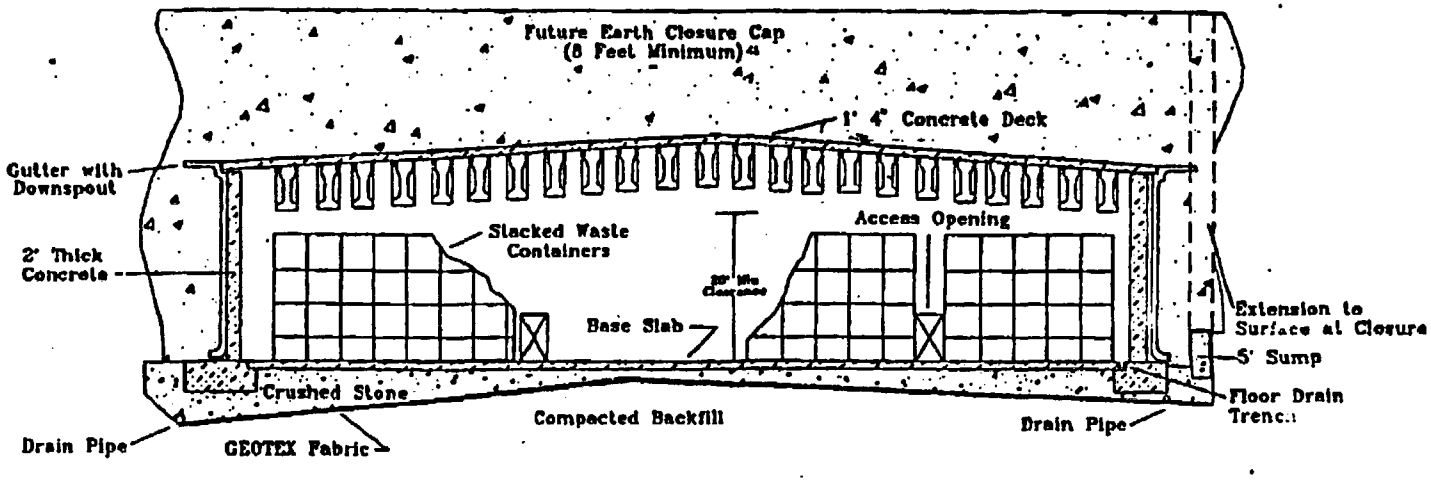

Fig. 2.5-3. Typical section through LAWV cell.

2.6 PROPOSED TRENCHES FOR DISPOSAL OF SUSPECT SOIL

Between 2800 and 5600 m^3 of soil from regulated areas is designated as potentially contaminated soil (i.e., "suspect soil") at the SRS annually (Cook 1991). Non-vault disposal of a portion of this soil is being considered for the EAVDF.

Five below-grade trenches containing suspect soil are considered in this RPA for the EAVDF. The dimensions of each trench are 6 m wide by 200 m long by 6 m deep. The conceptual layout of the trenches is shown in Fig. 2.6-1. The location of these trenches is assumed to be near the LAW vaults, but not close enough to the LAW vaults to receive enhanced infiltration resulting from diversion of water from the vault roofs. The suspect soil is assumed to be placed in the trenches to a depth of 4.8 m, allowing for 1.2 m of a clean soil cover in the trenches. This clean soil is in addition to the final soil and clay cover that will overlay the trenches when final closure of the EAVDF occurs. No engineered barriers are assumed to exist beneath the trenches, and the base of the trenches are assumed to be at an elevation of approximately 84 m ASL, like the LAW vaults. The potential source of radionuclides to the E-Area environment and to inadvertent intruder posed by these trenches is evaluated in this RPA of the EAVDF in Appendix I, and radionuclide limits for disposal of suspect soil in such trenches are provided.

2.7 PROPOSED NAVAL REACTOR COMPONENT DISPOSAL

Within E-Area, disposal of up to 100 stainless steel casks containing naval reactor (NR) components is proposed. The NR waste is composed of activated metals and can include control rods, control rod drive mechanisms (CRDM's), resin vessels, adapter flanges, and similar equipment. The high shielding shipping/disposal containers reduce the safety risks involved in the disposal of NR wastes.

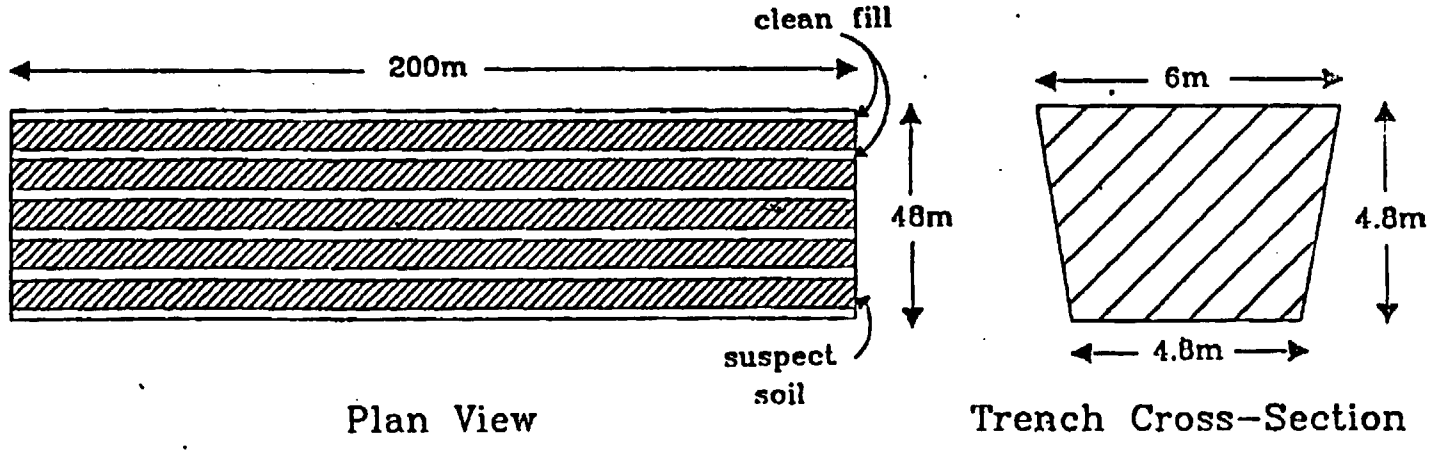

Fig. 2.6-1. Conceptual drawing of proposed suspect soil trenches.

At least 41 containers are planned to be accepted for disposal at E-Area initially, although up to 100 containers may be delivered. The proposed layout of the containers is shown in Fig. 2.7-1. The life expectancy and shielding capacity of the shipping/disposal casks are determined by the specifications of the containers. A detail of the proposed NR waste package is shown in Fig. 2.7-2. Each cylindrical disposal container will have outside dimensions of 3.2 m in diameter and 5.4 m high. The container outer wall is 10-cm-thick carbon steel with a 15 cm base. The stainless steel inner layer is 14 cm thick with a 10 cm base and a 34 cm top plate. The disposal container is expected to be sealed with a 15 cm steel closure cap. The interior volume of the shipping/disposal cask is approximately 27 m^3. The metal volume of the waste is approximately 3.5 m^3. Approximately 3.8×10^{-3} m^3 (1 gal) of water will be present initially in each cask.

The expected inventory of radionuclides for the first 41 NR waste shipments is listed in Table 2.7-1. A separate analysis of the performance of these waste packages is provided in Appendix L.

2.8 HAZARDOUS WASTE/MIXED WASTE DISPOSAL FACILITY

The HW/MWDF will be located in E-Area, Fig. 2.8-1, near the northeast corner of the 200 acre EAVDF. The facility will provide a Resource Conservation and Recovery Act (RCRA) permitted disposal facility for treated hazardous and MW that cannot be disposed in existing or planned facilities at SRS. The site of the HW/MWDF (Fig. 2.8-1) is a square shaped, wooded area of 0.15 km^2 (36 acres).

A separate RPA will be prepared at a later date to determine the performance of the HW/MWDF. The results from the HW/MWDF RPA will be evaluated to determine if it impacts the results determined in this RPA for the EAVs.

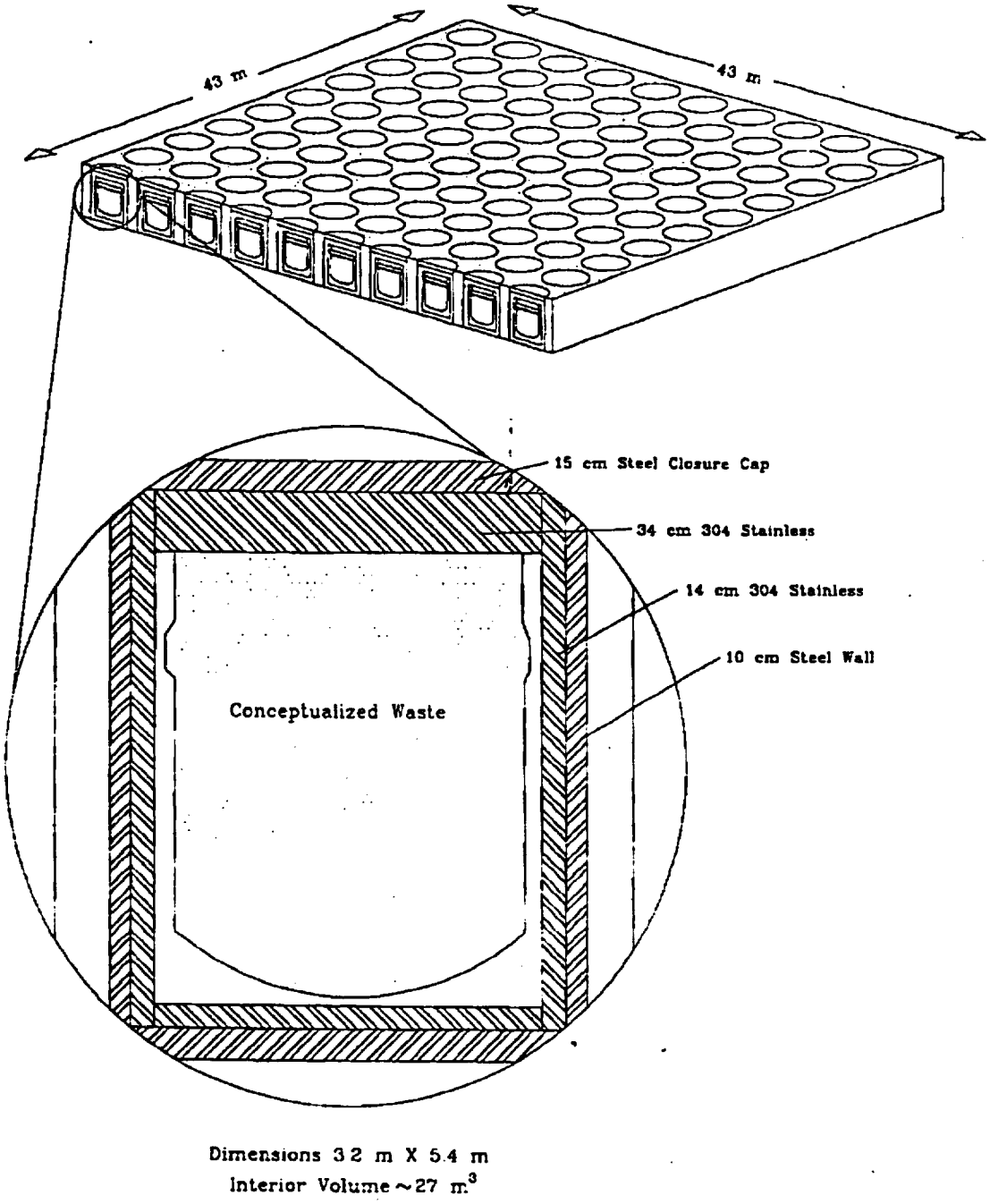

Fig. 2.7-1. Conceptual layout of 100 NR waste disposal containers.

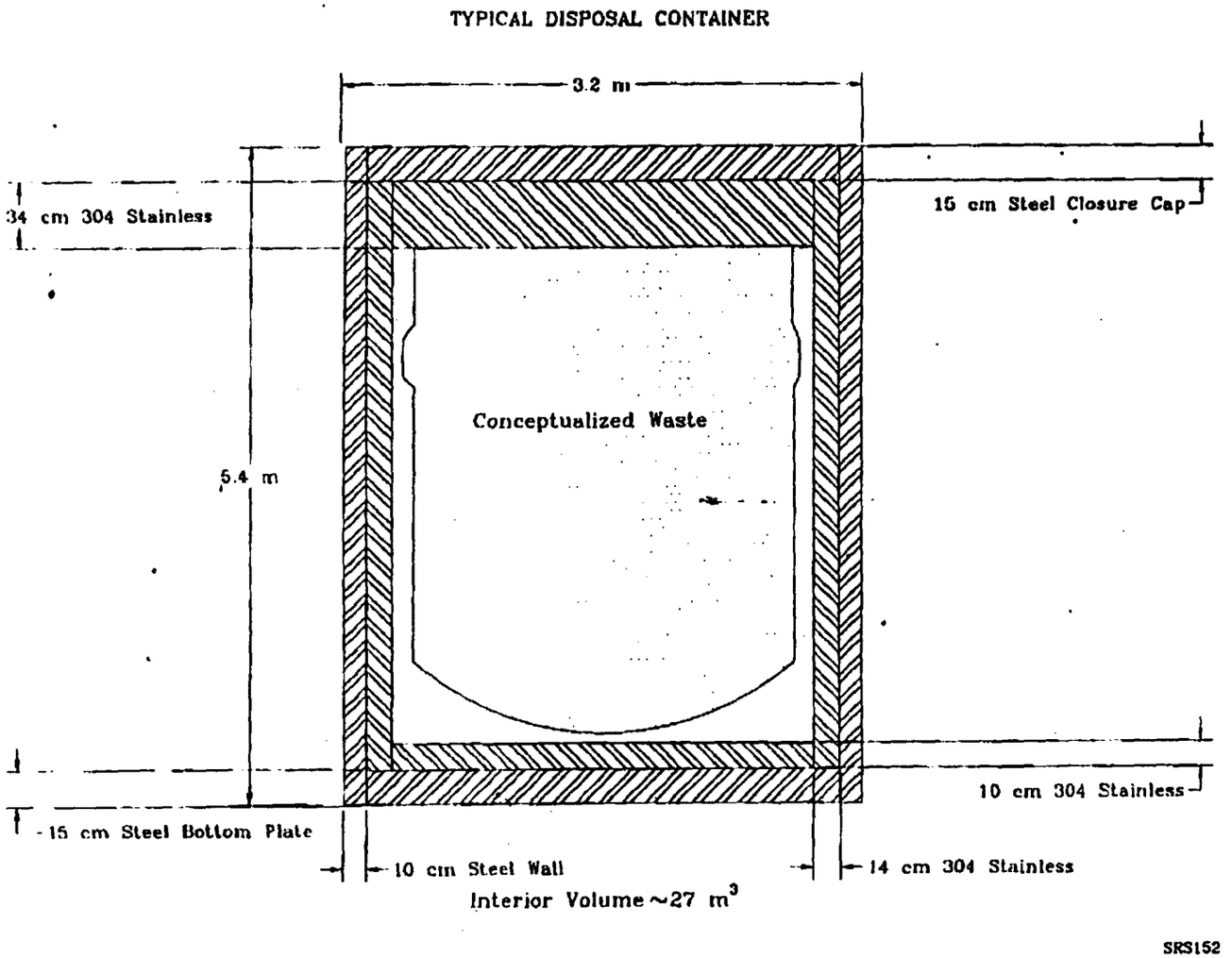

Fig. 2.7-2. Typical NR waste disposal container.

Table 2.7-1. NR waste radioactive inventory

No. of units	1	8	8	16	8	Total all casks, Ci
Description	CBDC Hardware	Core Barrel	Holddown Barrels	CB/TS/CH Hardware	Adapter Flanges	
Isotopes:						
C14	3.12×10^{-1}	3.09×10^{-1}	---	1.10×10^{1}	1.61×10^{-3}	1.79×10^{2}
Co58	1.49×10^{1}	1.40×10^{2}	1.79×10	2.10×10^{4}	3.78×10^{-2}	3.37×10^{5}
Co60.	2.96×10^{2}	5.92×10^{3}	5.79×10^{1}	4.50×10^{4}	1.45×10^{-1}	7.68×10^{5}
Cr51	1.82×10^{-1}	1.53×10^{1}	1.63×10^{-1}	8.10×10^{3}	2.84×10^{-5}	1.30×10^{5}
Cs137	1.22×10^{-2}	3.20×10^{-4}	2.80×10^{-4}	6.30×10^{-3}	6.32×10^{-5}	1.18×10^{-1}
Fe55	2.14×10^{2}	3.69×10^{3}	2.17×10^{1}	2.10×10^{4}	2.62×10^{-1}	3.66×10^{5}
Fe59	5.08×10^{-2}	7.80×10^{-1}	1.09×10^{-2}	1.50×10^{2}	4.40×10^{-4}	2.41×10^{3}
H3	9.55×10^{-3}	1.62×10	---	5.80×10^{-1}	---	2.22×10^{1}
Hf181	4.51×10^{-3}	7.00×10^{-4}	6.30×10^{-4}	2.61×10^{3}	1.41×10^{-4}	4.18×10^{4}
I129	1.25×10^{-6}	---	---	---	---	1.25×10^{-6}
In113	---	---	---	4.40×10^{3}	---	7.04×10^{4}
In114	---	---	---	5.50×10^{2}	---	8.80×10^{3}
Mn54	3.10×10	2.32×10^{1}	1.80×10^{-1}	5.70×10^{2}	8.46×10^{-3}	9.31×10^{3}
Nb94	6.41×10^{-3}	1.60×10^{-4}	1.40×10^{-1}	3.20×10^{-1}	3.22×10^{-5}	6.25×10
Nb95	4.11×10^{-2}	2.40×10^{-3}	2.20×10^{-3}	1.50×10^{5}	4.66×10^{-4}	2.40×10^{6}
Ni59	2.83×10	6.32×10^{1}	7.83×10^{-1}	2.10×10^{2}	4.83×10^{-4}	3.87×10^{3}
Ni63	3.82×10^{2}	6.32×10^{3}	7.83×10^{1}	2.90×10^{4}	4.80×10^{-2}	5.16×10^{5}
Pu239	2.49×10^{-5}	---	---	---	1.00×10^{-7}	2.57×10^{-5}
Pu241	8.86×10^{-4}	2.30×10^{-5}	2.10×10^{-5}	4.73×10^{-4}	4.70×10^{-6}	8.84×10^{-3}
Sb125	---	---	---	1.20×10^{4}	---	1.92×10^{5}
Sc46	3.26×10^{-3}	---	---	---	---	3.26×10^{-3}
Sn113	---	---	---	4.40×10^{3}	---	7.04×10^{4}
Sn119m	---	---	---	5.50×10^{4}	---	8.80×10^{5}

Table 2.7-1. (continued)

No. of units	1	8	8	16	8	Total all casks, Ci
Description	CBDC Hardware	Core Barrel	Holddown Barrels	CB/TS/CH Hardware	Adapter Flanges	
Isotopes:						
Sn123	---	---	---	1.50×10^{3}	---	2.40×10^{4}
Sr90	1.21×10^{-2}	3.20×10^{-4}	2.80×10^{-4}	2.90×10^{1}	6.32×10^{-5}	4.64×10^{2}
Ta182	2.86×10	---	---	1.10×10^{3}	---	1.76×10^{4}
Tc99	3.32×10^{-4}	3.69×10	---	---	---	2.95×10^{1}
Y90	1.21×10^{-2}	3.20×10^{-4}	2.80×10^{-4}	---	6.32×10^{-5}	1.74×10^{-2}
Zr95	---	1.00×10^{-3}	9.40×10^{-4}	---	2.33×10^{-4}	1.74×10^{-2}
Zn65	1.29×10^{-1}	---	---	---	---	1.29×10^{-1}
Totals, Ci	916.47	16,178.10	160.97	3.57×10^{5}	0.50	5.84×10^{6}

Total Curies: 5.84×10^{6} (total curie content for all 41 casks)

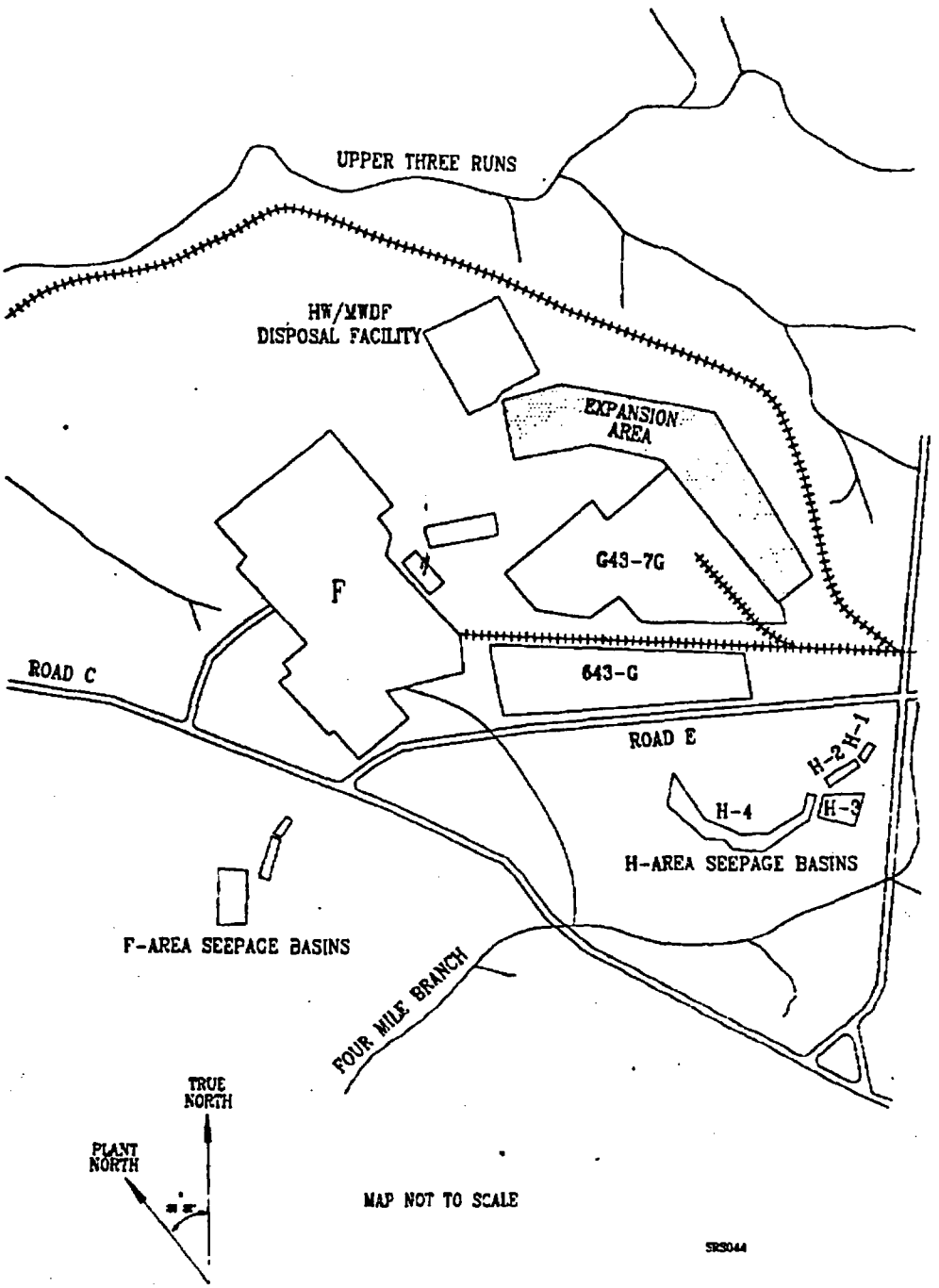

Fig. 2.8-1. Location map for HW/MWDF.

2.9 E-AREA CLOSURE CONCEPT

One of the key objectives of any closure of a waste disposal site is to limit moisture flux through the waste, thus minimizing contamination of the underlying groundwater. Because the EAVs are designed as a controlled release facility, proper closure to meet the objective of limiting moisture through the waste will be an integral part of long-term acceptability of the disposal site. Because backfilling and final closure of the EAVs will be delayed for several years, a detailed closure design has not been fully developed for the EAVs. Thus an integral part of the EAV RPA required that a closure concept be described and subsequently tested in models that simulate the performance characteristics of the proposed closure concept.

2.9.1 Physical Description of the EAVs Closure Concept

Closure concepts developed for this assessment are illustrated in Fig. 2.9-1 and Fig. 2.9-2. Figure 2.9-1 represents the closure concept with an intact cover (moisture barrier) (see Sect. 3.1.3.1 for a discussion of cover degradation), while Fig. 2.9-2 represents the degraded cover system, in which the properties of the moisture barrier have reverted to that of the surrounding soil (see Sect. 3.1.3.1). Closure operations will begin near the end of the active disposal period in the EAVs, i.e., after most or all of the vaults have been constructed and filled. Backfill of Burma Road sand will be placed around the vaults and above a clay cap, which will be emplaced on top of each vault. Above this layer of backfill, a laterally extensive moisture barrier will be installed. This moisture barrier will consist of 0.76 m of clay and an overlying layer of 0.3 m of gravel. A geotextile fabric will be placed on the gravel layer, and a second backfill layer, approximately 0.76 m thick, will be placed over the moisture barrier. Finally, 0.15 m layer of topsoil will be placed on the top layer of backfill to complete disposal operations at E-Area. This sequence of layers along with a minimum backfill of 0.43 m will provide a minimum of 2.9 m of cover for each vault.

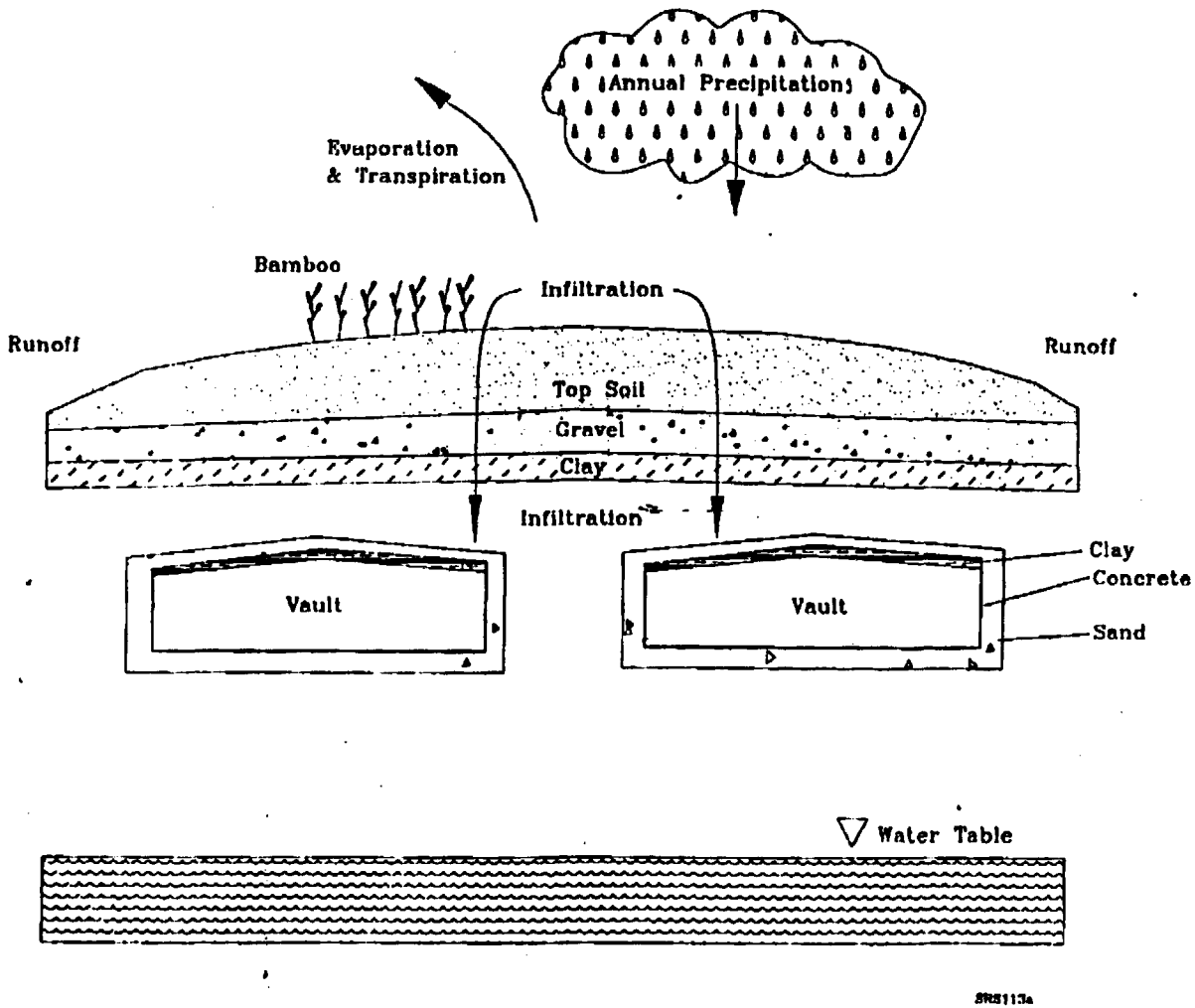

Fig. 2.9-1. Vault closure concept (2 cm/year infiltration).

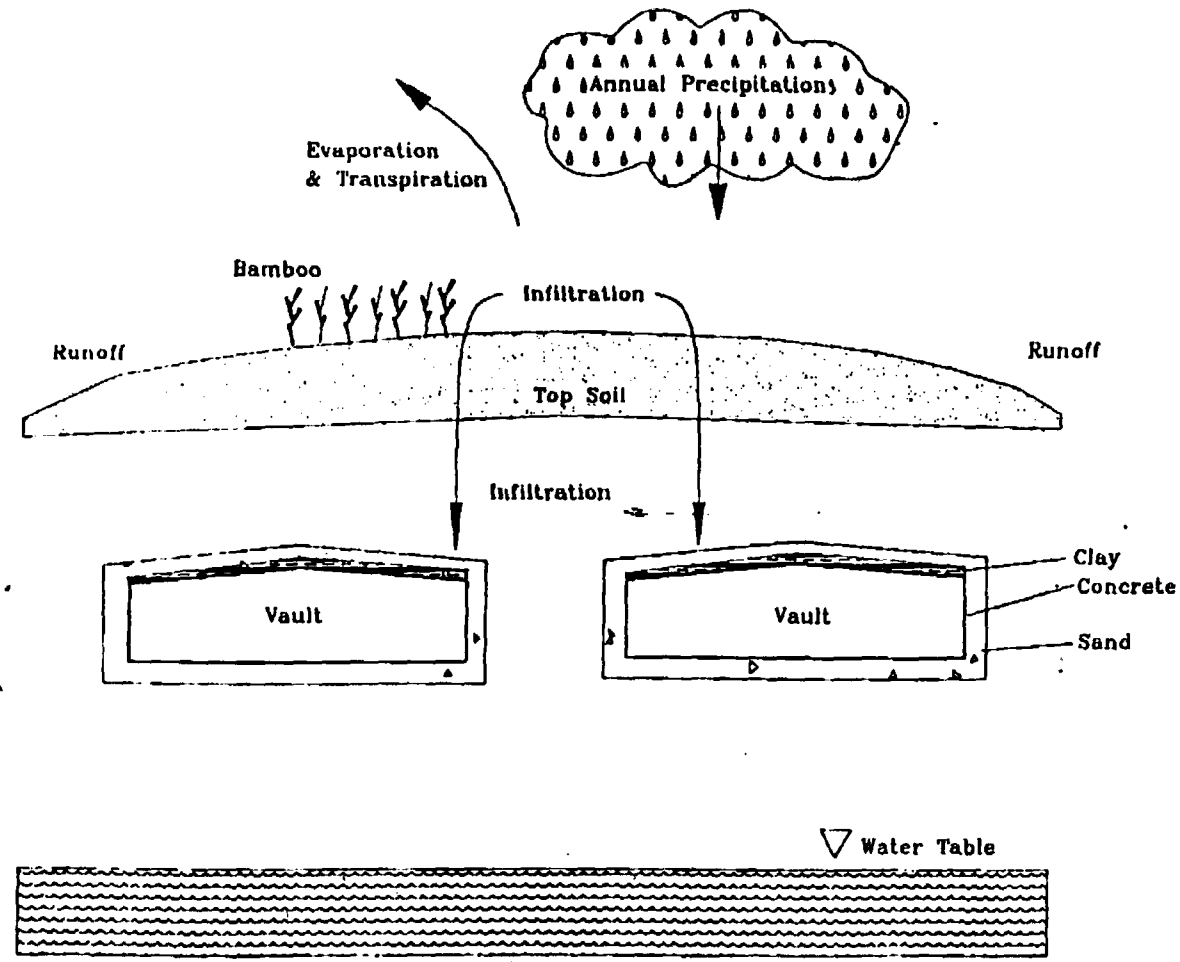

Fig. 2.9-2. Vault closure concept (40 cm/year infiltration).

Final closure of the EAVs will be accomplished by constructing a drainage system and revegetating the site. The drainage system will consist of a system of rip-rap lined ditches that intercept the gravel layer of the moisture barrier. These ditches will divert surface runoff and water intercepted by the moisture barrier away from the disposal site. The drainage ditches will be constructed between rows of vaults and around the perimeter of the EAVDF.

The topsoil will be revegetated with bamboo. A study conducted by the USDA Soil Conservation Service (Salvo and Cook 1993) has shown that the two species of bamboo (Phyllostachys bissetii and Phyllostachys rubromarginata) will quickly establish a dense ground cover which will prevent the growth of pine trees, the most deeply rooted naturally occurring plant type at SRS. Bamboo is a shallow-rooted climax species which evapotranspirates year-round in the SRS climate, thus, removing a large amount of moisture from the soil and decreasing the infiltration into the underlying disposal system.

2.9.2 Functional Description of the E-Area Closure Concept

Performance requirements for the closure concept are expressed in terms of hydraulic properties for the various soil layers (Thompson 1991). These properties are listed in Table 2.9-1. The topsoil and upper backfill layer serve to store and distribute infiltrating water. These layers intercept incoming water and redirect a significant portion in the horizontal direction to drainage ditches installed at the EAVDF. Computer simulations of flow through the cover show that the gravel drainage layer will carry away a major portion of the water that would normally infiltrate at the EAVDF (40 cm/year). The vertical moisture flux through the cover will be limited to less than 2 cm/year, based on the hydraulic properties of the closure system.

Table 2.9-1 Values for hydraulic properties of vault closure design

Layer Description	Hydraulic Conductivity (cm/s)
Clay	1.0×10^{-7}
Gravel	0.5
Backfill	1.0×10^{-5}

2.9.3 Post Closure Groundwater Monitoring

Post-closure monitoring of groundwater quality will serve to verify that the EAVDF is performing according to expectations and to allow differentiation of future EAVDF contaminant plumes from previously existing contaminant plumes.

Numerous groundwater monitoring wells have already been installed in the vicinity of the EAVDF to permit monitoring of contaminant plumes emanating from existing facilities. These wells are currently being sampled on a routine basis to define the current extent of contaminant plumes and to establish groundwater quality trends. Additional wells may be installed immediately surrounding the EAVDF at a later date to supplement this network if it is determined that it does not provide adequate monitoring of the EAVDF.

Continued monitoring in the post-closure period will allow establishment of future trends such that deviations due to EAVDF operation will be apparent. Statistical evaluation methodology will form the basis for making such a determination. An adequate methodology has not yet been developed but is expected to be developed for application at the Z-Area. The methodology will be described in the "Statistical Evaluation Plan" which is required in order to obtain the Industrial Waste Permit from SCDHEC for operation of the Saltstone Facility. When the methodology is developed it will serve as a guide for similar applications at the EAVDF.

3. ANALYSIS OF PERFORMANCE

The methods used to analyze the long-term performance of the EAVDF are described in this chapter. Source term development is discussed first, in Sect. 3.1. This section includes a list of radionuclides considered, potential mechanisms of contaminant release from the facility, and of potential mechanisms responsible for loss of integrity of the engineered barriers of the EAVs.

Following the source term discussion, potential receptors are identified in Sect. 3.2 by recognizing the time periods of concern in this RPA, the potentially significant pathways to human exposure, and exposure scenarios that should be evaluated for both off-site members of the public and inadvertent intruders. In this section, the EAV radionuclides of interest in the analysis have been determined by a screening process which eliminates radionuclides that, under unrealistically conservative conditions, are insignificant with respect to potential human exposures.

The conceptual models developed and the computational approach used to assess the performance of the EAVs are also described in this chapter. The conceptual models are derived from technical information presented in Chapter 2. These models embody a number of simplifying assumptions to facilitate the computational analysis required to assess long-term performance of the EAVs.

An overall conceptual model was used to prepare the RPA for E-Area and is illustrated schematically in Fig. 3.0-1. This overall conceptual model indicates the linkage of 1) a source term submodel (Sect. 3.1), which considers mechanisms of release of radionuclides from ILT, ILNT, and LAW vaults, 2) a near-field submodel (Sect. 3.3.1), which addresses movement of released constituents within the EAVs and through the unsaturated zone around the facility, 3) an environmental transport submodel, which addresses potential transport pathways including groundwater (Sect. 3.2.2 and 3.3.2), and 4) a dose submodel (Sect. 3.3.3) which relies on the exposure/intruder scenarios developed in Sect. 3.2.3 and 3.2.4. The computational methods used to implement the conceptual models are described in Sect. 3.4.

Conceptual Model

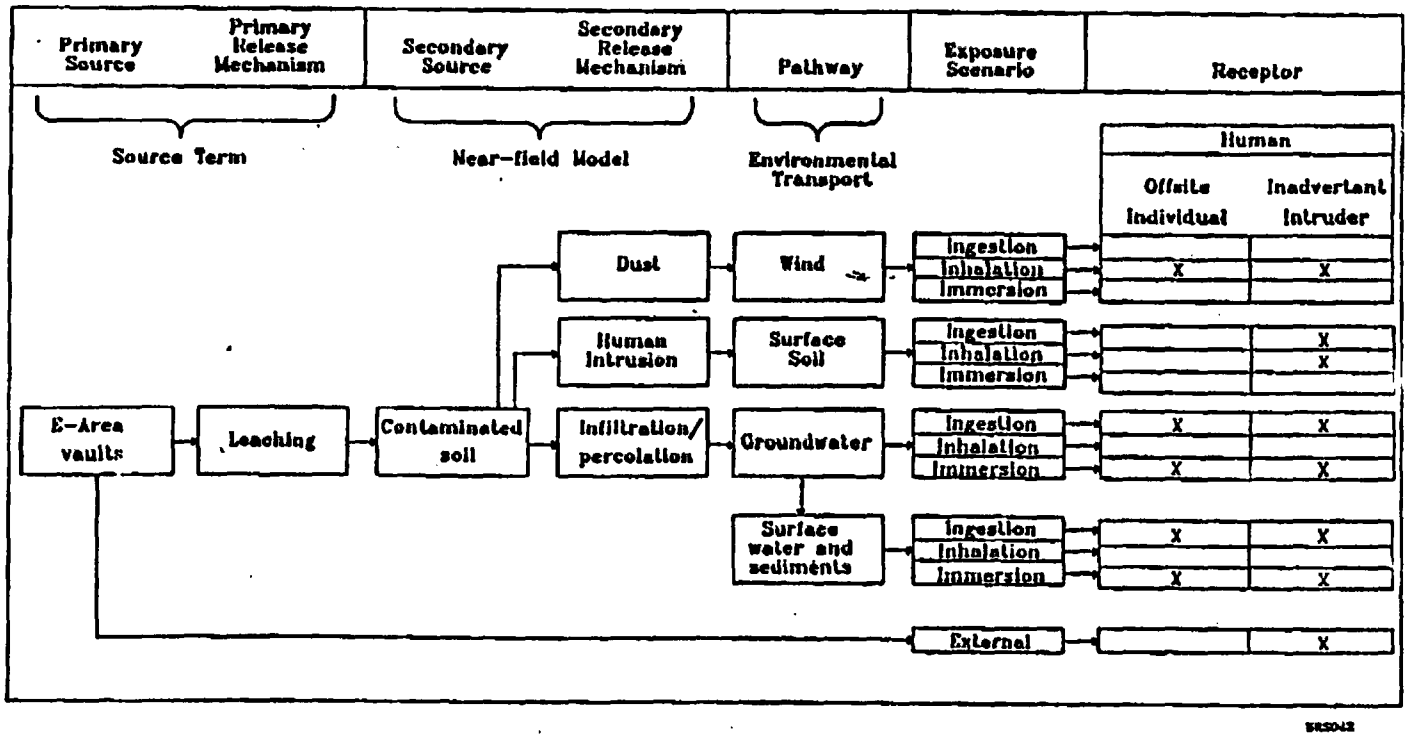

Fig. 3.0-1. Overall conceptual model for the Radiological Performance Assessment of the E-Area Vaults Disposal Facility.

3.1 SOURCE TERM

This section includes discussions of factors affecting the rate at which radionuclides are released from the disposal facility. Source term considerations are typically a large source of uncertainty. The uncertainty starts with trying to project future disposal practices and is compounded by uncertainties related to release mechanisms from the waste form. Once the contaminant is released from the waste forms, then the effectiveness and longevity of the concrete vault must be considered. The source term is also affected by the rate at which water percolates through the engineered cover. Thus, degradation of the cover is also addressed in this section. Each of these topics are discussed in the following paragraphs.

3.1.1 Radionuclides of Interest

The purpose of the PA for the EAVs was to determine the allowable inventory of radionuclides in a given vault type based upon the performance objectives for dose. Since the specific radionuclides that may be encountered in the waste during disposal operations is not known, a conservative screening method was used to determine the allowable inventories of a large suite of radionuclides which may be encountered during disposal operations. These limits are called "trigger values " and indicate the inventory at which the performance objectives may be exceeded. A detailed, site-specific analysis is recommended for a given radionuclide before additional inventories above the trigger value (TV) are placed in E-Area for disposal. The TVs for all radionuclides of interest in the EAVDF are provided in Appendix C. Radionuclides which have relatively small TVs, such that an allowable inventory above the TV is desirable, are included in the detailed site-specific analyses. The screening analysis for determining the TVs is described in detail in Sect. 3.2.3.4 and 3.2.4.4.

3.1.2 Release Mechanisms

Estimating the release of radionuclides from the E-Area disposal facility is difficult because of the variety of contaminated material that will be disposed in the vaults. Conceptually, waste within boxes (B-25 steel) or activated metals disposed in vaults will remain immobile until contacted by water that has leaked into the vaults. Defensible prediction of water movement in the vaults and of the effectiveness of boxes and activated metals in retarding waste release is not possible without developing a conservative simplified conceptual model. The key features of the conceptual model are:

- Waste is immobile until contacted by water.
- The water entering the vault will have a composition that can be represented as a mixture of concrete pore fluid and local groundwater equilibrated with soil levels of carbon dioxide gas.
- The presence of steel and activated metals in the vaults will result in the formation of corrosion products (i.e., hydrous Fe[III] oxides) and lead to reducing conditions inside the vaults.
- The entire inventory of the vault is available to react with the reducing water inside the vault (i.e., continuously stirred tank reactor source term model).
- The aqueous concentrations of radionuclides are controlled by sorption (represented with a K_d or isotherm) onto corrosion products (LAW/ILNT/ILT vaults) or grout (ILNT/ILT) with a solubility limited (oxide and hydroxide phases) upper concentration.
- Contaminated water exiting the vault will interact with the concrete vault and radionuclides will be chemically retarded by the vault wall.

The contaminant release rate will be a function of several physical and chemical factors. The most important factors are:

- water flux into the vault,
- water composition (pH and redox) in the vault,

- physical state (e.g., integrity) and properties (e.g., hydraulic conductivity) of the vault, and
- physical, chemical, and transport properties of the contaminants.

A detailed discussion of geochemical calculations is provided in Appendix D.

3.1.3 Engineered Barriers Degradation and Failure

The following two sections address degradation of the engineered cover and the concrete vaults. Degradation of the cover is addressed first. In general, cover degradation is considered in a binary fashion (i.e., it is assumed to be functional or it is assumed to be non-functional). Vault degradation is addressed in the second section. The primary mode of vault degradation is expected to be cracking and eventual failure of the roof. Subsequent flow and transport conceptual models are based on the conclusions of these two sections, and the detailed discussion in Appendix K.

3.1.3.1 Cover Degradation

Degradation of the cover is expected to occur by a number of processes. Potential processes are erosion; penetration by plants and animals; external events such as settling or slumping, or a seismic event; and human intrusion. These processes will reduce the effectiveness of the cover to limit the vertical moisture flux. Over the period of analysis, the net flux through the cover is expected to approach the background levels for the site, i.e., 40 cm/year.

As presently conceived in the closure concept (Sect. 2.8), shallow-rooted bamboo will be planted on the disposal site and a system of drainage ditches will be constructed to handle surface runoff and diverted infiltration. As specified in DOE Order 5820.2A, active institutional control is assumed for only 100 years. During this time, periodic site inspection would reveal any degradation of the overlying cover and drainage system and corrective actions would be taken. Cover degradation during this first 100 years is likely to be minimal. Sheet erosion will occur, but the bamboo vegetative cover would minimize the effects of this

disturbance. Return of the SRS land to unrestricted use after 100 years may result in a usage conversion to agricultural practices, consistent with past and current land use in the SRS vicinity. Row crop farming, which is consistent with historical practices in the vicinity, would increase the erosive effects of precipitation. Soil erosion rates for cropland in the vicinity of the SRS are on the order of 1.7 kg m^{-2} yr^{-1} (Sect. 2.1.8). Erosion is reduced several hundred fold if a dense vegetative cover is present (Sect. 2.1.8). This suggests that there will be little erosion as long as the bamboo vegetative layer has not been cleared; however, the cover may be eroded down to the gravel layer in as little as 800 years after the bamboo vegetative layer is cleared. However, erosion of the gravel layer is difficult to predict. In this analysis, it is assumed that the cover remains functional until the roof of the vault fails and thus, no longer provides support for the cover.

3.1.3.2 Vault Degradation

The concrete vaults are expected to degrade slowly through a combination of physical, chemical, and mechanical processes (Walton et al. 1990). Physical and mechanical degradation processes that produce cracking are of primary concern, because of the concomitant increase in permeability. Shrinkage cracks occur as a result of the temperature cycling during curing of concrete structures, and thus are present before the facility closure cover is constructed. This allows for filling of the outer portion of the cracks, in the vault walls or roof, with epoxy prior to closure. Cracking might occur after the vaults have been covered as a result of degradation of the epoxy used to fill shrinkage cracks, foundation settling, or rebar expansion due to corrosion.

The principal chemical processes that disrupt the integrity of concrete structures are: sulfate attack, carbonation, calcium hydroxide leaching, and rebar corrosion. The effects of these processes on EAV degradation have been analyzed using the methodology described in Walton, et al. (1990). The methodology quantifies the extent of concrete degradation in terms of the penetration depth. This depth is the amount of wall thickness that has degraded. The analysis of chemical degradation effects and structural considerations are discussed in detail in Appendix K. A brief discussion of the mechanisms affecting vault durability are provided in the following sections.

Sulfate attack

Concrete degrades by sulfate and/or magnesium attack when sulfate or magnesium ions in the pore-fluid migrate into the concrete and react with the cement paste. Sulfate reacts with tri-calcium aluminate in the cement paste to form calcium aluminum sulfates. Magnesium reacts with hydroxide ions to form magnesium hydroxide. The products of these reactions have considerably greater volume than the compounds they replace. The expansive reactions can result in disruption of the concrete.

The major sources of sulfate and magnesium at the site are from soil water. Concentrations of sulfate and magnesium in groundwater at the SRS (Sect. 2.2.4) are very low. Sulfate concentrations range from 0.27 to 15 ppm (2.81×10^{-6} to 1.56×10^{-4} mol/L) with a mean and median of 3.66 and 2 ppm (3.81×10^{-5} and 2.08×10^{-5} mol/L), respectively. Magnesium concentrations range from 0.14 to 8 ppm (5.76×10^{-6} to 3.29×10^{-4} mol/L) with a mean and median of 2.28 and 1.5 ppm (9.37×10^{-5} and 6.17×10^{-5} mol/L), respectively. The sum of Mg and SO_4 range from 0.57 to 18.5 ppm (1.51×10^{-5} to 3.77×10^{-4} mol/L) with a mean and median of 5.94 and 4.95 ppm (1.32×10^{-4} and 1.08×10^{-4} mol/L), respectively (Marine 1976).

The methodology developed by Atkinson and Hearne (1984) (and summarized in Walton et al. 1990) was used to assess the impact of sulfate and magnesium attack associated with the ingress of the soil-moisture.

Carbonation

Carbonation occurs when calcium in concrete reacts with carbon dioxide (CO_2) to form calcium carbonate. At the E-Area disposal site, carbon dioxide will be present in soil-air and dissolved in soil-water. Carbon dioxide will slowly migrate into the concrete, potentially leading to a carbonated zone. Concrete degradation, in this case, is associated with concrete expansion due to corrosion of the reinforcement bars (i.e., rebar). Typically, the pH of concrete is very high which is favorable to very low rebar corrosion. However, the carbonation reaction can reduce the pore-fluid pH which, in turn, makes the rebar susceptible to corrosion.

Carbonation may also result in potentially beneficial effects. For example, carbonate carried by the pore-fluid into cracks and pores of the vault structure may precipitate and reduce the effective porosity of the vaults. At the bottom of the vault, water which has percolated through the vault roof will be saturated with portlandite $Ca(OH)_2$. The $Ca(OH)_2$ can react with soil-air containing CO_2, forming a calcium carbonate mass that then seals cracks and reduces effective pore sizes at any exposed surfaces of the vault structure.

The extent of carbonation was estimated using a shrinking core model (Walton et al. 1990). Carbonation was modeled as a uniform coating which forms on the surface of the concrete.

Calcium hydroxide leaching

Ingress of water into the vaults and flow of water around the vaults will provide a pathway for leaching of soluble components from the concrete. In particular, leaching of calcium hydroxide from the concrete can lead to loss of strength and increases in concrete permeability (Walton et al. 1990). Leaching is typically important in humid sites, such as the SRS, because high infiltration rates promote higher leaching rates.

The rate of leaching can be estimated using simple screening models or more complex numerical models. For this application, conservative screening calculations were performed. Two different simplifying assumptions were used in the calculations (Atkinson and Hearne 1984), namely: 1) concrete controlled leaching, and 2) geology controlled leaching. Concrete controlled leaching assumes that the leaching rate is limited by diffusion through the concrete into the surrounding soil. Once the calcium reaches the soil it is rapidly removed leading to a zero concentration boundary condition. If water is flowing around the vault, then a low concentration of calcium can conservatively be assumed in the soil moisture.

For the case of geology controlled leaching, diffusion of calcium into surrounding soils is assumed to limit the process. For this condition, the degradation effects are insignificant. This particular type of process, however, is only valid in diffusion dominated systems where water flow around the vault is low, such as beneath the vault or when infiltration is low.

Rebar corrosion

Corrosion of the reinforcing bars (rebar) is another possible mechanism of vault degradation. Corrosion occurs when iron in the rebar reacts with oxygen to form iron oxides. Corrosion of the rebar has two major effects on concrete structures: 1) corrosion lowers the strength of the rebar and 2) corrosion disrupts the integrity of the surrounding concrete.

Rebar is used in concrete structures to increase tensile strength. As the rebar corrodes, the tensile strength of the structure declines. For the EAVs, the structural role of the vault is essential to long-term isolation performance.

Iron oxides have a molar volume which is over twice that of steel. As rebar corrosion occurs, the volume occupied by the rebar will expand. The expansion leads to stress development around the reinforcement and eventually to disruption of the integrity of the concrete. This process is easily visible in old concrete structures where fractures and spalling of the concrete occur adjacent to corroded reinforcement.

Reinforcement corrosion is typically modeled in two stages: 1) initiation, and 2) active corrosion (Walton et al 1990). Initially the steel is protected from corrosion by a "passivating layer" of iron oxides on the metal surface. The stability of the passive layer is supported by the high pH of the concrete. Before significant corrosion can begin, the passive layer must be disrupted. This occurs when the pH of the concrete is lowered by carbonation or when aggressive anions (such as chloride) penetrate into the concrete to the depth of the steel.

As discussed previously, carbonation of the structure will occur too slowly to be a factor in concrete corrosion of the vaults. Accordingly, carbonation is even less of a factor in rebar corrosion. Concentrations of chloride ions in the soil moisture at the SRS are also too low to initiate active corrosion. Migration of chloride in the waste out to the rebar would control the time of the initiation stage noted above. To establish if rebar corrosion would significantly affect the rate of vault degradation, active corrosion was assumed to begin immediately after closure and no credit for the initiation lag time was taken in the corrosion calculations.

Once active corrosion begins, the corrosion rate may be limited by availability of oxygen. However, at very low oxygen concentrations, water can be used as a source of oxygen for corrosion (hydrogen evolution reaction). Because the thickness of concrete over the rebar

limits the availability of oxygen for rebar corrosion, hydrogen evolution was considered as an additional process for rebar corrosion. By combining the oxygen diffusion and hydrogen evolution reactions an estimate of the total rebar corrosion can be made.

3.2 PATHWAYS AND SCENARIOS

This section of the RPA addresses the time periods of concern and pathways to human exposure for EAV constituents potentially released in the manner described in Sect. 3.1 above. The information provided in this section is subsequently used in the development of models to evaluate doses potentially received as a result of releases of radionuclides from the EAVDF.

3.2.1 Time Periods of Concern

To assess the performance of the E-Area Disposal Facility, three time periods of concern are addressed: 1) the operational period; 2) the institutional control period; and 3) the post-institutional control period.

3.2.1.1 Operational Period

The operational period is defined as the period during which waste is actively emplaced. During this period, some vaults are sealed as an interim closure, prior to placement of the final closure cap. The facility is fenced and patrolled, preventing unauthorized access during this period.

The operational period for the E-Area Disposal Facility is expected to be at least 20 years. Doses to maximally exposed off-site individuals during this time period are addressed in the SAR for the E-Area Disposal Facility (WSRC 1991a), and are not considered part of this RPA.

3.2.1.2 Institutional Control Period

The institutional control period is the 100-year time interval specified in the DOE Order 5820.2A (U.S.DOE 1988a) following closure of a disposal site. Periodic maintenance and monitoring activities are conducted during this period. The disposal site is assumed to be stabilized and no longer operational during this period, but it will remain part of the SRS, and will therefore, be fenced and patrolled to eliminate the possibility of inadvertent intruders. During this period, doses to operational on-site personnel will be addressed in the SAR. While unlikely, doses to off-site individuals are addressed in this RPA. Realistically, this period is expected to continue for at least 100 years after closure of the EAVs, and possibly longer.

3.2.1.3 Post-Institutional Control Period

The final time period of concern is when the facility is no longer maintained by the SRS, and could be accessed by the public. The total duration of this period for the purpose of performance assessment depends on the time of predicted maximum impact with respect to potentially exposed individuals. Projections of conditions and activities during this period are uncertain and difficult to assess. However, because of the presence of long-lived radionuclides in the waste, the maximum off-site impact will occur many thousands of years after closure.

3.2.2 Transport Pathways

The purpose of this section is to identify potential pathways to human exposure to radionuclides potentially released from the EAV (Sect. 3.2.2.1), and to justify eliminating some of these pathways from further consideration (Sect. 3.2.2.2). The results of this section are used to develop exposure scenarios for off-site members of the public, which are discussed in Sect. 3.2.3.

3.2.2.1 Pathway Identification

Radionuclides released from the EAV to the geosphere have the potential of reaching humans through numerous pathways. Most conceivable pathways for a buried LLW source are indicated in Fig. 3.2-1. The pathways identified in this figure are for facilities undisturbed, from the standpoint of human intrusion. Pathways pertinent to intruder exposures are addressed separately in Sect. 3.2.4. In the list below, each pathway is briefly defined.

(1) Leaching - migration of radionuclides from the wasteform by a combination of dissolution, diffusion, and advection.

(2) Gaseous Diffusion - upward migration of gaseous radionuclides from the wasteform by diffusion through the caps and cover soils to the atmosphere.

(3) Irrigation - contamination of cover soil by radionuclides which have reached groundwater which is subsequently used for irrigation.

(4) Deposition - contamination of surface water by radionuclides which have reached the atmosphere; represents deposition of particulate associated radionuclides or gaseous species partitioning at the air-water interface.

(5) Volatilization - partitioning of volatile radionuclide species present in surface water into air above the water body.

(6) Discharge - discharge of radionuclides present in groundwater into surface water.

(7) Recharge - movement of radionuclides into the groundwater from contaminated surface water.

(8) Irrigation - contamination of cover soil by radionuclides which have reached surface water which is being subsequently used for irrigation.

(9) Washload - contamination of surface water by soil containing radionuclides as a result of erosion by rain or irrigation water.

(10) Deposition - contamination of cover soil by radionuclides which have reached the atmosphere and have become associated with airborne particulate matter.

(11) Resuspension - Resuspension of soil-associated radionuclides as a result of wind erosion.

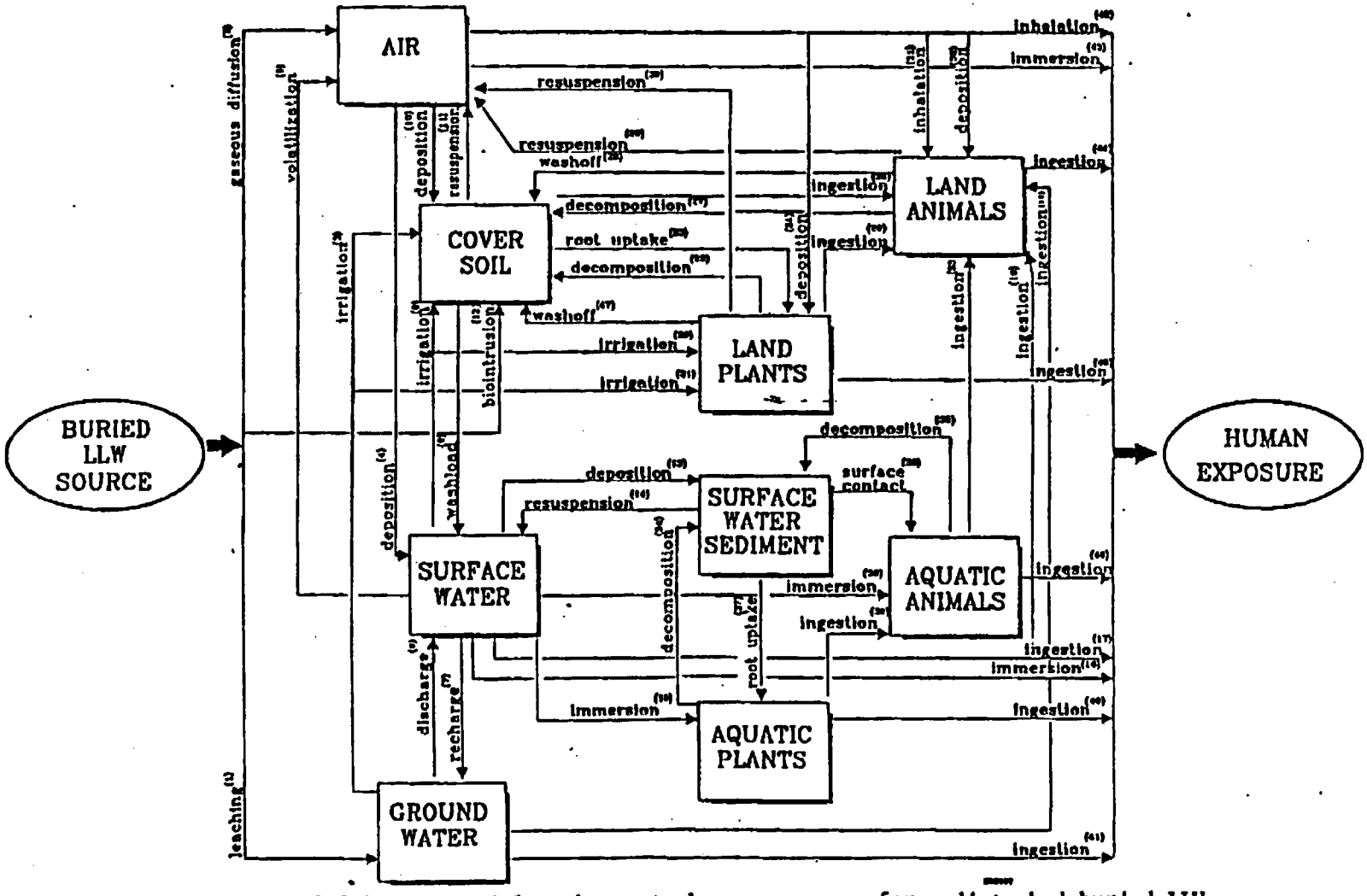

Fig. 3.2-1. Potential pathways to human exposure for undisturbed buried LLW.

(12) Biointrusion - contamination of cover soil by soil-associated radionuclides that are brought to the surface from the vicinity of the wasteform by burrowing animals, such as rodents or ants, or by intruding plant roots.

(13) Deposition - deposition of radionuclides in surface water that have partitioned onto suspended sediment.

(14) Resuspension - resuspension of particulate-borne radionuclides in the sediment of surface water as a result of hydrodynamic forces at the sediment-water interface.

(15) Immersion - contamination of aquatic plants by radionuclides in surface water attributable to the immersion of the plants in the contaminated water.

(16) Immersion - human exposure to radionuclides as a result of immersion in contaminated surface water.

(17) Ingestion - human exposure to radionuclides as a result of ingestion of radionuclides present in surface water.

(18) Ingestion - contamination of terrestrial animals from their ingestion of radionuclides in surface water.

(19) Ingestion - contamination of terrestrial animals from their ingestion of radionuclides in groundwater.

(20) Irrigation - contamination of terrestrial plants as a result of irrigation with surface water containing radionuclides.

(21) Irrigation - contamination of terrestrial plants as a result of irrigation with groundwater.

(22) Decomposition - contamination of cover soil as a result of decomposition of terrestrial plants in the soil.

(23) Root uptake - contamination of terrestrial plants by uptake through roots of soil water containing radionuclides.

(24) Deposition - deposition of airborne radionuclides onto terrestrial plant surfaces.

(25) Ingestion - ingestion of radionuclides by grazing animals as a result of contaminated soil ingestion.

(26) Ingestion - ingestion of radionuclide-containing vegetation by terrestrial animals.

(27) Decomposition - contamination of cover soil as a result of decomposition of terrestrial animals in the soil.

(28) Washoff - contamination of surface soil as a result of washoff of externally contaminated terrestrial animals.

(29) Resuspension - resuspension of surficial radionuclides on terrestrial animals to the atmosphere.

(30) Resuspension - resuspension of surficial radionuclides on terrestrial plants to the atmosphere.

(31) Inhalation - contamination of terrestrial animals as a result of inhalation of radionuclides in the atmosphere.

(32) Deposition - surface contamination of terrestrial animals via deposition of particulate-borne radionuclides in the atmosphere.

(33) Ingestion - contamination of terrestrial animals as a result of their ingestion of aquatic animals.

(34) Decomposition - contamination of surface water sediment as a result of decomposition of aquatic plants in the sediment.

(35) Decomposition - contamination of surface water sediment as a result of decomposition of aquatic animals in the sediment.

(36) Surface contact - surface contamination of aquatic animals as a result of contact with contaminated sediment.

(37) Root uptake - contamination of aquatic flora via radionuclide uptake through roots.

(38) Immersion - contamination of aquatic animals as a result of immersion in surface water containing radionuclides.

(39) Ingestion - contamination of aquatic animals as a result of their ingestion of aquatic plants containing radionuclides.

(40) Ingestion - human exposure to radionuclides as a result of ingestion of contaminated aquatic flora.

(41) Ingestion - human exposure to radionuclides as a result of ingestion of contaminated groundwater.

(42) Inhalation - human exposure to radionuclides as a result of inhalation of airborne radionuclides.

(43) Immersion - human exposure to radionuclides as a result of immersion in contaminated air.

(44) Ingestion - human exposure to radionuclides as a result of ingestion of contaminated terrestrial animals.

(45) Ingestion - human exposure to radionuclides as a result of ingestion of contaminated terrestrial plants.

(46) Ingestion - human exposure to radionuclides as a result of ingestion of contaminated aquatic animals containing radionuclides.

(47) Washoff - contamination of surface soil below vegetation due to rain-induced surface washoff.

3.2.2.2 Pathway Screening

The list in Sect. 3.2.2.1 above is generic in nature, and the significance of each pathway must be evaluated on a site-specific basis to develop an exposure model. Many pathways may be removed from consideration for particular sites because of a negligible contribution to human exposure.

For the EAVs, leaching and transport of radionuclides to the saturated zone (pathway (1)) is the predominant means that radionuclides may be subsequently transported in the environment. Thus, this pathway must be addressed in developing an exposure model, and is addressed in this RPA in the near-field model (Sect. 3.3.1). Other pathways which may contribute to human exposure are those tied to groundwater concentrations of contaminants. Irrigation with contaminated groundwater may lead to contamination of agricultural crops and animals (pathways (3), (21), (23), (25) and (26)). Discharge of contaminated groundwater to surface water (pathway (6)) may result in contamination of the aquatic ecosystem including the water body itself, sediment, and aquatic plants and animals (pathways (13), (14), (15), (34), (35), (36), (37), (38), and (39)). Ingestion of contaminated surface water, aquatic animals or groundwater by terrestrial animals (pathways (18), (33), and (19)) may lead to human exposure, and can be tied to groundwater contamination. Human exposure may occur as a result of direct human ingestion of contaminated surface water or groundwater (pathways (17) and (41)), as a result of consumption of contaminated food supplies (pathways (44), (45),

and (46)), and as a result of immersion in contaminated surface water during recreational activities such as swimming (pathway (16)). Consumption of contaminated aquatic plants (pathway (40)) was not considered in the EAV RPA because there is no indication that aquatic plants present in potentially contaminated surface water in the vicinity of the SRS are consumed by humans.

Of the 47 pathways listed above, only 26 are accounted for in the above discussion. This leaves 21 pathways that are not considered significant for developing exposure scenarios discussed in the next section. The justification for neglecting these pathways is given below. Pathways that result in human exposure directly or indirectly as a result of atmospheric dispersion and deposition (pathways (2), (4), (5), (10), (11), (24), (28), (29), (30), (31), (32), (42), (43), and (47)) are not included in exposure scenarios for the following reason. The only potentially volatile radioactive components of the EAVs are H-3, C-14, and Rn-222. Atmospheric release of these compounds at the time of the operations is addressed in the EAV SAR (WSRC 1991a). Calculations providing an upper bound on doses received from volatilization of these radionuclides from the EAVDF after disposal (pathway (2)) are described in Sect. A.3. Pathways leading to exposure to resuspended contaminated soil (pathways (11), (42), and (43)) are addressed in the intruder exposure analysis (Sect. A.4). Other atmospheric pathways are indirect in nature; e.g., the contaminants must first be suspended or volatilized from one medium, then redeposited in another. These indirect pathways are not believed to be more significant than the direct pathways (2, 11, 42, and 43), and thus are not addressed in this RPA. Therefore, pathways 2, 11, 42, and 43 are included in the dose analysis.

Pathway (7) considers contamination of groundwater due to recharge by surface water. This pathway is not considered significant in the EAV RPA because some dilution of radionuclides in surface water can be expected for all streams, and thus concentrations in groundwater as a result of this pathway will always be lower than the concentrations which led to contamination of the surface water. Pathways (8) and (20), representing contamination of cover soil and terrestrial plants as a result of irrigation with contaminated surface water, respectively, are not considered important because of the relatively dilute concentration of radionuclides expected in surface water with respect to groundwater. Irrigation by groundwater is expected be a more important pathway for radionuclides potentially reaching crops.

Contamination of surface water from erosion of contaminated soil (pathway (9)) was not considered significant, because buildup of radionuclides in surface soil would only result from radionuclides with high sorption potential. These radionuclides would not partition readily into the surface water if introduced as a result of erosive events. Pathways (22) and (27), representing the pathways of radionuclides to surface soil via decomposition of terrestrial plants and animals, were not considered significant relative to the exposure resulting from direct consumption of these potentially contaminated products.

Although surface-water may receive contaminated groundwater, dilution is considerable in the nearby creeks. Because groundwater is expected to exceed surface water concentrations by orders of magnitudes, and direct ingestion of groundwater results in exposures exceeding less direct routes of exposure through aquatic food chains, surface-water pathways were dropped from further consideration.

Finally, contamination of cover soil over the EAVs as a result of biointrusion of burrowing animals or plant roots (pathway (12)) must be addressed. It is acknowledged that biointrusion is a potentially significant pathway of contamination of cover soil over a LLW facility, as is concluded in a study by McKenzie et al. (1983). For the humid southeast, where ground cover and soil moisture limit resuspension of soil, biointrusion is likely to result in contamination of soils over the facility, but probably not significant contamination off-site. Therefore, the relative significance of biointrusion to the inadvertent intruder is the issue of concern in addressing this pathway for this RPA.

Most of the burrowing animals identified as likely residents at the SRS (Sect. 2.1.9) do not burrow below 0.5 m (McKenzie et al. 1986). Only one burrower, the Florida Harvester Ant, is expected to burrow below 2 m, and then, only 5% of its burrows are expected to be that deep, resulting in very little potentially contaminated soil being moved. As the cover soil erodes, however, the significance of burrowers' activities may increase. Furthermore, if E-Area reverts to a hardwood, pine forest sometime after loss of institutional control, it is possible that deeper roots may contact contaminated soil above, or adjacent to, the vaults and translocate radionuclides to other plant organs. Radionuclides may subsequently be released back to the soil as roots and leaves wither and degrade. It is, therefore, likely that biointrusion may cause some mixing of the waste components with the soil column.

The significance of biointrusion is evaluated here by considering the effect of the mixed soil column on an inadvertent intruder. An inadvertent intruder, who is assumed to dig next to, into, or above the vaults, mixes the contaminated soil near the vaults with soil near the surface (Sect. 3.2.4). While it is not known how effective biointruders might be in causing mixing in the soil, the McKenzie et al. (1983) study of a reference humid site estimated that soil concentrations resulting from biointrusion are significantly lower than those resulting from intruder excavation activities, except for more biologically available compounds, where concentrations are of the same order of magnitude. The effect of burrowing animals or intrusive roots, then, is not expected to enhance the inadvertent intruder's contact with contaminated soil by more than a factor of two for any radionuclide. Doses that are calculated in this RPA are uncertain to the extent that a factor of two is inconsequential, and thus, the biointrusion pathway was neglected.

In summary, of the original 47 pathways identified in Fig. 3.2-1, only two are considered to be of possible consequence to exposures of off-site members of the public and to groundwater protection, and are considered further in this RPA. These pathways, related to contaminated groundwater, include: 1) leaching of the wasteform resulting in contamination of groundwater local to E-Area (pathway 1); and 2) contamination of agricultural crops and animals as a result of irrigation with contaminated groundwater (pathways 3, 21, 23, 25, 26). In the following section, the relative importance of these pathways is further addressed.

3.2.3 Exposures of Off-Site Members of the Public and Protection of Groundwater

As described in Sect. 1.2, disposal of low-level radioactive waste in the EAV must meet certain performance objectives for protection of off-site members of the public and sources of groundwater. In this section, the different exposure scenarios and pathways for off-site members of the public, which have been considered in the PA for the EAV are described. Requirements for groundwater protection assumed in this analysis also are described, and an analysis is presented which demonstrates the relative importance of the requirements for protection of off-site members of the public and sources of groundwater in determining the acceptability of waste disposals in the EAV. The greater importance of the assumed groundwater protection requirements is established, and a simple screening analysis to select those

radionuclides in the different disposal units that are considered for the groundwater pathway is presented.

3.2.3.1 Off-Site Members of the Public

This section discusses the requirements for protection of off-site members of the public and the exposure pathways assumed in the dose analysis for such individuals.

The performance objectives for LLW disposal specify that the EDE to off-site members of the public from all exposure pathways should not exceed 25 mrem per year (U.S.DOE 1988a). As described in Sect. 1.2.1, this performance objective is assumed to apply for 10,000 years after disposal. The nearest location from the disposal site for off-site members of the public depends on the time after disposal. During the period of active institutional control, i.e., for the first 100 years after facility closure, off-site members of the public are assumed to be located no closer to the disposal site than the present boundary of the SRS. However, after active institutional control ceases, off-site members of the public could be located as close as 100 m from any of the EAV.

As discussed in Sect. 3.1 and 3.2.2, the primary mechanism for mobilization and release of radionuclides from the EAV is expected to be infiltration of precipitation, and the primary pathway for subsequent exposures of off-site members of the public is expected to be transport of radionuclides in groundwater. Because of such factors as 1) the design and closure concept for the disposal units that are intended to inhibit infiltration of precipitation, 2) the considerable distance from the disposal site to the present boundary of the SRS, and 3) the expected discharge of contaminated groundwater to surface streams within the SRS and the considerable dilution in radionuclide concentrations provided by such discharge, it is reasonable to conclude that the dose analysis for off-site members of the public can focus on exposure pathways resulting from use of contaminated groundwater at distances from the disposal units as close as 100 m for the time period after active institutional control ceases.

Thus, in the dose analysis for the groundwater pathway, an off-site member of the public is assumed to use water from a well for domestic purposes, and the well is assumed to be at the location at least 100 m from the disposal units where the maximum concentrations of radionuclides in groundwater are predicted to occur after loss of active institutional control.

The following exposure pathways involving use of contaminated well water are assumed to occur:

- direct ingestion of contaminated water;
- ingestion of milk and meat from dairy and beef cattle that drink contaminated water;
- ingestion of vegetables grown in garden soil irrigated with contaminated water;
- direct ingestion of contaminated soil in conjunction with intakes of vegetables from the garden;
- external exposure to contaminated soil while working in the garden; and
- inhalation of radionuclides suspended into air from contaminated soil while working in the garden.

Rainfall normally is abundant at the SRS (see Sect. 2.1.3). Therefore, irrigation of a vegetable garden is assumed to occur only occasionally during the summer and only in small amounts relative to the annual rainfall (Murphy 1990). Irrigation of pasture grass ingested by dairy and beef cattle is neglected because agricultural land is not extensively irrigated near the SRS (U.S. Department of Commerce 1977; Baes and Sharp 1983).

Additional exposure pathways for off-site members of the public could involve release of radionuclides into the air and airborne transport to off-site locations. Radionuclides could be attached to particulates suspended into air from the ground surface, and volatile radionuclides (e.g., H-3, C-14, and isotopes of radon) could be released from the waste or contaminated soil. Exposures of off-site members of the public resulting from the air pathway are considered in this analysis.

3.2.3.2 Protection of Groundwater

This section discusses the assumed requirements for protection of groundwater that are applied to the PA for the EAV.

The performance objectives for LLW disposal specify that contamination of groundwater is to be limited in accordance with federal, state, and local standards (U.S.DOE 1988a). The State of South Carolina requires that concentrations of hazardous chemicals in groundwater be limited in accordance with federal DWS at any time after disposal. Presently, no federal, state, or local standards exist that limit radionuclides released to groundwater from the EAV. However, the SRS has established the objective of protecting groundwater for Site operations in accordance with EPA standards for contaminants in public drinking water supplies (40 CFR Part 141).

The performance objective for protection of groundwater resources assumed in this analysis is described in Sect. 1.2.2. Briefly, because there is some ambiguity in selecting particular numerical standards for radioactivity in drinking water to be applied to groundwater protection, three different options for specifying the performance objective are used in this analysis:

1) Current EPA standards for radionuclides in drinking water (40 CFR Part 141), including (a) the method prescribed in the standards for calculating MCLs for beta/gamma-emitting radionuclides from the specified dose limit based on internal dosimetry data from ICRP Publication 2 (1959), as tabulated by the Department of Commerce (1963), and (b) the specified MCLs for H-3 and Sr-90;

2) Current EPA standards for radionuclides in drinking water, except all MCLs for beta/gamma-emitting radionuclides are calculated from the specified dose limit using internal dosimetry data based on ICRP Publication 30 (1979); and

3) Proposed revisions of the EPA standards for radionuclides in drinking water (EPA 1991), with all MCLs for beta/gamma-emitting radionuclides calculated using internal dosimetry data based on ICRP Publication 30 (1979), except no standard for radon is assumed.

For all options, the performance objective is assumed to apply for 10,000 years after disposal (see Sect. 1.2.1). Some of the differences among the three options are summarized as follows.

All options specify concentration limits, rather than dose limits, for alpha-emitting radionuclides. The concentration limits for radium in the third option are higher than the first two options, and the third option is the only one that contains a limit for uranium.

In all options, a limit on dose equivalent is used to define limits on concentrations of beta/gamma-emitting radionuclides in water, but the resulting MCLs are different for all three options. The first two options use the same dose limit for whole body or any organ, but the internal dosimetry data used to obtain the MCLs from the dose limit differ substantially for most radionuclides. The third option differs from the first two in that a limit on EDE, rather than dose equivalent to whole body or any organ, is used. Thus, for most radionuclides, the resulting MCLs for the third option differ substantially from the values for the first two options.

The MCLs for the three options for specifying the performance objective for groundwater protection are given in Table 3.2-1. For all radionuclides except uranium in the third option, the MCLs are given in units of pCi/L to facilitate comparisons of the different options, even though the primary standard for beta/gamma-emitting radionuclides in all options is a dose limit rather than a limit on concentration. For naturally occurring uranium with its normal isotopic abundances, the MCL of 20 μg/L corresponds to an activity concentration of 14 pCi/L.

For all alpha-emitting radionuclides, the MCLs in Table 3.2-1 are obtained directly from current EPA standards for radioactivity in drinking water (40 CFR Part 141) or the proposed revisions of the standards (EPA 1991). The MCLs for beta/gamma-emitting radionuclides for the different options are obtained as described below.

For the first option, the MCLs for H-3 and Sr-90 are the values specified in the current EPA standards. For any other beta/gamma-emitting radionuclide, the MCL is obtained, as specified in the current EPA standards, from the limit on dose equivalent of 4 mrem per year to whole body or any organ using the maximum permissible concentration (MPC) in water for an exposure time of 168 h obtained from a Department of Commerce (1963) tabulation. These MPCs apply to occupational exposure and are based on limits on dose equivalent of

Table 3.2-1. Maximum contaminant limits for radionuclides in groundwater corresponding to different options for groundwater protection requirement[a]

Radionuclide	Option 1[b]	Option 2[b]	Option 3[b,c]
H-3	20,000	90,000	60,900
C-14	6,400	2,600	3,200
Al-26	—	50	420[d]
Co-60	130	110	220
Ni-59	530	5,500	27,000
Ni-63	80	1,600	9,900
Se-79	—	110	660[d]
Rb-87	270	390	501
Sr-90	8	3	42
Zr-93	2,100	160	5,100
Nb-93m	1,100	1,000	10,500
Tc-99	800	420	3,800
Pd-107	—	3,200	37,000
Cd-113m	—	3	40[d]
Sn-121m	—	320	2,260
Sn-126	—	30	290
I-129	0.5	0.6	21
Cs-135	800	800	790
Cs-137	160	110	120
Sm-151	1,100	1,500	14,000
Pb-210	0.3	0.07	1
Ra-226	5	5	20
Uranium	—	—	20[e]
Am-242m	—	0.074	1.27
Other Alpha[f]	15	15	15

[a] Different options are described in Sect. 1.2.2 and 3.2.3.2.
[b] Values are in units of pCi/L, unless otherwise noted.
[c] Value calculated by EPA (1991), unless otherwise noted.
[d] Value calculated using ingestion dose conversion factor (DCF) from DOE compilation (U.S. DOE 1988b).
[e] Value is in units of μg/L.
[f] Adjusted gross alpha emitters (excluding Ra-226, U, and Rn-222).

5 rem per year to whole body or gonads, 30 rem per year to thyroid, or 15 rem per year to any other organ, whichever is more restrictive. Thus, the MCL in groundwater is obtained from the MPC in water by multiplying by the ratio of the applicable dose limit in the DWS to the dose limit used to obtain the MPC. For example, for Tc-99, which has the lower large intestine as the organ receiving the highest dose, the MPC in water for 168 h exposure in the Department of Commerce (1963) tabulation is multiplied by the factor 0.004/15 to obtain the MCL in groundwater.

For the second option, the MCL in groundwater for any beta/gamma-emitting radionuclide is obtained from (1) the dose limit of 4 mrem per year to whole body or any organ specified in the current EPA standards, (2) an assumed intake of contaminated water of 2 L/d (730 L/year), as also specified in the EPA standards, and (3) the dose per unit intake to whole body or the organ receiving the highest dose obtained from the DOE (1988b) compilation of internal DCFs, which are based on the dosimetric and metabolic models of ICRP Publication 30 (1979).

For the third option, the MCL in groundwater for most beta/gamma-emitting radionuclides is the value given by the EPA (1991). In a few cases, a value was not estimated by the EPA but is obtained from the limit on EDE of 4 mrem per year (EPA 1991), a water intake of 2 L/d, and the EDE per unit intake obtained from the DOE (1988b) compilation.

In comparing the second and third options for calculating MCLs for beta/gamma-emitting radionuclides, the change from a limit on dose equivalent to whole body or any organ to the same numerical limit on EDE results in substantial increases in the MCL in most cases. Again, essentially the same internal dosimetry models are used for both options.

3.2.3.3 Comparison of Performance Objectives for Protection of Off-Site Members of the Public and Groundwater

As described in Sect. 3.2.3.1 and 3.2.3.2, concentrations of radionuclides in groundwater at any location more than 100 m from the location of disposal units are limited by two performance objectives: 1) a maximum EDE of 25 mrem per year from all exposure pathways involving use of contaminated water and 2) various options for limiting dose from consumption of drinking water only or concentrations of radionuclides in groundwater. The first

performance objective assumes that use of contaminated groundwater is the only significant source of exposure for off-site members of the public. The question then arises as to which of the two performance objectives would be the more restrictive, i.e., would result in lower limits on acceptable concentrations of radionuclides in groundwater and, thus, in waste in the EAV. A similar question concerns whether exposure pathways other than ingestion of drinking water would contribute significantly to the dose from all exposure pathways.

In order to address the relative importance of the two performance objectives given above and the various exposure pathways listed in Sect. 3.2.3.1 that apply to use of contaminated groundwater, the doses from the pathways involving ingestion of milk and meat from dairy and beef cattle that drink contaminated water, ingestion of vegetables grown in garden soil irrigated with contaminated water, direct ingestion of contaminated soil from the vegetable garden in conjunction with vegetable intakes, external exposure to contaminated soil while working in the garden, and inhalation of radionuclides suspended into air while working in the garden must be investigated in relation to the dose from direct ingestion of contaminated water. For purposes of this analysis, the dose limit from drinking water only for beta/gamma-emitting radionuclides is assumed to be 4 mrem per year EDE, as in the third option for the performance objective for groundwater protection. With this choice, the same dosimetric quantity is used in the performance objectives for all exposure pathways and for drinking water only, but the results do not depend greatly on the choice of dose limits. The relative importance of the pathway involving ingestion of contaminated vegetables is considered first.

For direct consumption of radionuclides in drinking water, the dose to an exposed individual is given by

$$H_w = C_w U_w DCF_{ing}$$

where

H_w = EDE from drinking water pathway (rem/year),

C_w = radionuclide concentration in groundwater (μCi/L),

U_w = consumption of drinking water (L/year), and

DCF_{ing} = EDE per unit activity of a radionuclide ingested, i.e., the ingestion dose conversion factor (rem/μCi).

In determining compliance with the assumed groundwater protection requirement, a consumption rate of drinking water of 730 L/year (i.e., 2 L/d) is used. Therefore, the dose from direct consumption of contaminated groundwater is given by

$$H_w(\text{rem/year}) = (730\ \text{L/y})C_w(\mu\text{Ci/L})DCF_{ing}(\text{rem}/\mu\text{Ci}).$$

In order to estimate the dose per unit concentration of radionuclides in groundwater resulting from consumption of vegetables irrigated with contaminated water, a simple model developed by Baes and Sharp (1983) for estimating radionuclide concentrations in surface soil is used. In this model, the top layer of soil is treated as a well-mixed compartment, and radionuclides deposited in surface soil by irrigation are assumed to be removed from the soil compartment by infiltrating water according to a first-order leaching process as well as by radioactive decay. The removal rate constant describing the leaching process is given by

$$\lambda_1 = (V_w / \theta) / [d(1 + \rho K_d / \theta)],$$

where

λ_1 = fraction of activity in soil compartment removed by leaching per year,
V_w = infiltration rate of water in soil (m/year),
θ = volumetric water content of soil (dimensionless),
d = depth of soil compartment (m),
ρ = bulk density of soil, and
K_d = equilibrium solid/solution distribution coefficient for a radionuclide.

The density of soil and the distribution coefficient must be expressed in compatible units; e.g., if K_d is given in units of mL/g (or L/kg), then ρ must be expressed in g/cm^3. Since radioactive decay also removes activity from soil, the total removal rate constant for a radionuclide in the

surface soil compartment is given by

$$\lambda = \lambda_l + \lambda_r$$

where λ_r is the radiological decay constant (y^{-1}).

In the linear-compartment model described above, the equilibrium activity of a radionuclide in the surface soil compartment is simply the ratio of the input rate of activity to the total removal rate constant. The input rate of activity by irrigation used in this analysis is estimated as follows. At the SRS, the growing of vegetables normally requires irrigation only occasionally during the summer months. On the basis of experience with crop management at the site (Murphy 1990), an amount of irrigation equal to 0.2 m/year is considered to be applied to a vegetable garden. This amount corresponds to application of 2.5 cm once a week during the two hottest summer months. This amount of irrigation probably is more than would occur in most years, since one reported experiment required watering only on one or two occasions during the summer (Murphy 1990). Over a unit area of 1 m^2, the assumed irrigation rate corresponds to 0.2 m^3, or 200 L/year. The unit area is arbitrary and is used only to obtain radionuclide concentrations in soil in the desired units of $\mu Ci/m^3$. Therefore, the average concentration of radionuclides input to surface soil per year from use of contaminated irrigation water, which is denoted by I_s, is given by

$$I_s\ (\mu Ci/m^3 \text{ per year}) = [(200 \text{ L/y per } m^2) / d(m)]\ C_w(\mu Ci/L),$$

where

d = depth of surface soil layer, and

C_w = concentration of a radionuclide in groundwater.

From the equations derived above, the equilibrium concentration of radionuclides in surface soil from use of contaminated groundwater for irrigation then is given by

$$C_s(\mu Ci/m^3) = I_s / \lambda = [(200 \text{ L/y per } m^2) / d(m)]\ C_w(\mu Ci/L) / \lambda(y^{-1}).$$

Given this concentration of a radionuclide in surface soil, the dose from ingestion of contaminated vegetables (see Eqs. A.4-2 and A.4-3) is given by

$$H_v = B_v(C_s/\rho)U_v DCF_{ing}$$

where

H_v = EDE from vegetable intakes (rem/year),
B_v = plant-to-soil concentration ratio for a radionuclide (dimensionless),
ρ = bulk density of soil,
U_v = consumption rate of vegetables (kg/year), and
DCF_{ing} = ingestion dose conversion factor (rem/μCi).

If C_s is expressed in units of $\mu Ci/m^3$ and U_v in units of kg/year, then the density of soil in this equation must be expressed in units of kg/m^3.

Given the equation for the dose from consumption of contaminated vegetables, as derived using the model of Baes and Sharp (1983) for retention of radionuclides in surface soil, and the equation for the dose from direct consumption of drinking water, a direct comparison of the relative importance of the two exposure pathways can be obtained. Using the equations for H_w, H_v, and C_s derived above, the ratio of the doses from the drinking water and vegetable pathways is given by

$$H_w/H_v = [(3.65\ m^2)\ d(m)\ \rho(kg/m^3)\ \lambda(y^{-1})]\ /\ [B_v U_v(kg/y)].$$

This ratio does not depend on the radionuclide concentration in groundwater or the ingestion DCF.

In this analysis, the following radionuclide-independent parameter values are used: 1) a depth of the soil compartment (d) of 0.3 m, which is a typical depth of the root zone for vegetation; 2) a water infiltration rate through soil of 0.4 m/year, which is the average infiltration rate of precipitation at the SRS (see Appendix A.1.1.2) and is appropriate when irrigation is considerably less than the total precipitation; 3) a volumetric water content of soil

(θ) of 0.3 (Baes and Sharp 1983); 4) a bulk density of soil (ρ) of 1,400 kg/m^3, or 1.4 g/cm^3 (Baes and Sharp 1983); and 5) a consumption of contaminated vegetables of 90 kg fresh weight per year, which is half of the estimated total consumption of vegetables by an average adult (Rupp 1980; Hamby 1992). It should be noted that if the removal rate constant, λ, is dominated by the contribution from leaching, λ_1, then the ratio of the doses from the drinking water and vegetable pathways does not depend on the depth of the soil compartment, d.

The equation for H_w/H_v given above has been evaluated for the radionuclides Tc-99, Sn-126, Pu-239, and Cs-137. Tc-99 represents radionuclides with a high plant-to-soil concentration ratio (B_v) but a low distribution coefficient (K_d); Sn-126 has intermediate values of B_v and K_d; Pu-239 has a low value of B_v but a high K_d; and Cs-137 has an intermediate value of B_v and a high K_d, but its half-life is sufficiently short that the equilibrium concentration in soil is determined primarily by the half-life rather than the leaching constant, λ_1. In implementing the model, it is important to recognize that B_v and K_d are correlated; i.e., radionuclides with high plant-to-soil concentration ratios have low distribution coefficients resulting in relatively low equilibrium concentrations in soil, and vice versa (Baes et al. 1984; Sheppard 1985). Thus, evaluating the model for these four radionuclides should give results that are representative of any other important radionuclides in the EAV.

The radionuclide-specific parameter values used for the example calculations are listed as follows:

Tc-99 —	B_v = 0.65,	K_d = 1.5 mL/g;
Sn-126 —	B_v = 0.0026,	K_d = 250 mL/g;
Pu-239 —	B_v = 0.000019,	K_d = 4,500 mL/g;
Cs-137 —	B_v = 0.013,	K_d = 1,000 mL/g.

The values of B_v for each radionuclide are given in Table A.4-7 and were obtained from the compilation of Baes et al. (1984). The values of K_d also were obtained from Baes et al. (1984). These data do not necessarily apply to soils at the SRS but are expected to be reasonably representative.

For the model and parameters described above, the following comparisons of the dose from direct consumption of drinking water and the dose from consumption of vegetables

irrigated with contaminated water are obtained. The dose from the drinking water pathway exceeds the dose from the vegetable pathway by about a factor of 15 for Tc-99, a factor of 25 for Sn-126, a factor of 190 for Pu-239, and a factor of 30 for Cs-137. If removal by radioactive decay were not taken into account for Cs-137 (e.g., if the analyses were performed for Cs-135 instead), the dose from the vegetable pathway would be about the same as the dose from the drinking water pathway. Isotopes of Cs represent an extreme case where the plant-to-soil concentration ratio relative to the distribution coefficient is higher than for almost all other elements (Sheppard 1985), and a similar result would not be expected for most long-lived radionuclides that reasonably could be present in significant quantities in the EAV.

The analysis presented above illustrates that the dose from direct consumption of drinking water is expected to be equal to or greater than the dose from ingestion of vegetables contaminated with irrigation water from the same source; and, for most radionuclides, the dose from drinking water is expected to be substantially greater. This conclusion is expected to apply to all radionuclides that could be present in the EAV.

The next pathways considered in this comparison are consumption of milk and meat from dairy and beef cattle that drink contaminated water. The doses from ingestion of contaminated milk (m) and meat (f) are given by

$$H_m = C_m U_m DCF_{ing},$$
$$H_f = C_f U_f DCF_{ing},$$

respectively, where

H_m, H_f = EDE from milk or meat intakes (rem/year),
C_m, C_f = radionuclide concentration in milk (μCi/L) or meat (μCi/kg),
U_m, U_f = consumption rate of milk (L/year) or meat (kg/year), and
DCF_{ing} = ingestion dose conversion factor (rem/μCi).

Dairy and beef cattle are assumed to drink only contaminated groundwater, and the radionuclide concentrations in milk and meat are given by

$$C_m = C_w Q_m F_m ,$$
$$C_f = C_w Q_f F_f ,$$

respectively, where

C_w = radionuclide concentration in groundwater (μCi/L),
Q_m , Q_f = consumption rate of water by dairy or beef cattle (L/d), and
F_m , F_f = ratio of equilibrium radionuclide concentration in milk (μCi/L) or meat (μCi/kg) to daily intake by dairy or beef cattle (μCi/d).

In implementing the model for the milk and meat pathways, a consumption rate of water by dairy and beef cattle of 60 L/d and 50 L/d, respectively, and a consumption rate of milk and meat by an exposed individual of 110 L/year and 90 kg/year, respectively, are used (NRC 1977). If the transfer coefficients for the milk and meat pathways (F_m and F_f) recommended by Baes et al. (1984) are used, the following comparison of the dose from the drinking water pathway and the doses from the milk and meat pathways is obtained. The dose from the drinking water pathway exceeds the dose from the milk and meat pathways by about a factor of 10 for Tc-99, a factor of 3 for Sn-126, a factor of 5 for Cs-137, and 5 orders of magnitude for Pu-239.

The analysis presented above illustrates that the dose from direct ingestion of drinking water is expected to be considerably greater than the dose from ingestion of milk and meat obtained from dairy and beef cattle that drink contaminated water from the same source. This conclusion is expected to apply to all radionuclides that could be present in the EAV.

The next pathway considered in this comparison is direct ingestion of contaminated soil in conjunction with vegetable intakes. For a given concentration of a radionuclide in garden soil, a direct comparison of the doses from the vegetable and soil ingestion pathways can be obtained from the results given in Tables A.4-8 and A.4-9, respectively, of Appendix A.4.

The dose from the drinking water pathway relative to the dose from the soil ingestion pathway then is the product of two factors: 1) the ratio of the doses from the vegetable and soil ingestion pathways obtained from the tables listed above and 2) the ratio of the doses from the drinking water and vegetable pathways obtained previously in this section. Using this procedure, the dose from the drinking water pathway is found to exceed the dose from the soil ingestion pathway by about 4 orders of magnitude for Tc-99, a factor of 200 for Sn-126, 3 orders of magnitude for Cs-137, and an order of magnitude for Pu-239.

The analysis presented above illustrates that the dose from direct ingestion of drinking water is expected to be considerably greater than the dose from direct ingestion of contaminated soil from a vegetable garden that is contaminated with irrigation water from the same source. This conclusion should apply to all radionuclides that could be present in the EAV.

The next pathway considered in this comparison is external exposure to contaminated soil while working in the vegetable garden. For a given concentration of a radionuclide in garden soil, a direct comparison of the doses from the vegetable and external exposure pathways can be obtained from the results given in Tables A.4-8 and A.4-10, respectively, of Appendix A.4. The dose from the drinking water pathway relative to the dose from the external exposure pathway then is the product of two factors: 1) the ratio of the doses from the vegetable and external exposure pathways obtained from the tables listed above and 2) the ratio of the doses from the drinking water and vegetable pathways obtained previously in this section. Using this procedure, the dose from the drinking water pathway is found to exceed the dose from the external exposure by about 50% for Sn-126 and a factor of 70 for Cs-137. The dose from the external exposure pathway is essentially zero for Tc-99 and Pu-239.

The analysis presented above illustrates that the dose from direct ingestion of drinking water is expected to be greater than the dose from external exposure to contaminated soil while working in a vegetable garden that is contaminated with irrigation water from the same source. This conclusion is expected to apply to all photon-emitting radionuclides that could be present in the EAV.

The final pathway considered in this comparison is inhalation exposure to radionuclides suspended into air from contaminated soil while working in the vegetable garden. For a given concentration of a radionuclide in garden soil, a direct comparison of the doses from the vegetable and inhalation pathways can be obtained from the results given in Tables A.4-8 and A.4-12, respectively, of Appendix A.4. The dose from the drinking water pathway relative to the dose from the inhalation pathway then is the product of two factors: 1) the ratio of the doses from the vegetable and inhalation pathways obtained from the tables listed above and 2) the ratio of the doses from the drinking water and vegetable pathways obtained previously in this section. Using this procedure, the dose from the drinking water pathway is found to exceed the dose from inhalation exposure by about 8 orders of magnitude for Tc-99, 5 orders of magnitude for Sn-126, 7 orders of magnitude for Cs-137, and a factor of 350 for Pu-239.

The analysis presented above illustrates that the dose from direct ingestion of drinking water is expected to be much greater than the dose from inhalation exposure while working in a vegetable garden that is contaminated with irrigation water from the same source. This conclusion should apply to all radionuclides that could be present in the EAV.

The comparison of the doses from the drinking water pathway and the vegetable, milk and meat, soil ingestion, external exposure, and inhalation pathways for the same concentration of particular radionuclides in water may be summarized as follows: for Tc-99, the dose from the drinking water pathway exceeds the dose from all other pathways by about a factor of 6; for Sn-126, the dose from all other pathways is about the same as the dose from the drinking water pathway; for Cs-137, the dose from the drinking water pathway exceeds the dose from all other pathways by about a factor of 4; and, for Pu-239, the dose from the drinking water pathway exceeds the dose from all other pathways by about a factor of 8. These results should be representative of those that would be obtained for any other radionuclides that could be present in the EAV.

Given the doses for the drinking water pathway relative to the doses for the other exposure pathways involving use of contaminated groundwater from the same source, as obtained above, the following conclusions are obtained.'

First, for all beta/gamma-emitting radionuclides, the performance objective for protection of groundwater resources — i.e., a dose limit of either 4 mrem per year to whole body or any organ or 4 mrem per year EDE from the drinking water pathway only — should be more restrictive than the performance objective for protection of off-site members of the public — i.e., a dose limit of 25 mrem per year EDE from all exposure pathways — because the dose from the drinking water pathway only is expected to be greater than the dose from all other exposure pathways combined. Thus, if the performance objective for groundwater protection is met, then the performance objective for protection of off-site individuals also will be met without the need for analysis of the dose from exposure pathways other than drinking water.

Second, for alpha-emitting radionuclides, the performance objective for protection of groundwater resources, which is expressed in terms of concentration limits rather than limits on dose equivalent, may result in doses from the drinking water pathway only that exceed the performance objective for protection of off-site members of the public. For example, the current MCL for Pu-239 in groundwater of 15 pCi/L (see Table 3.2-1) corresponds to an EDE of nearly 50 mrem per year, assuming consumption of 2 L/d of water and the ingestion DCF for Pu-239 given in Table A.4-2. In these cases, the dose limit in the performance objective for off-site individuals would be more restrictive and, in principle, the contributions to the dose from the exposure pathways other than drinking water would need to be considered in demonstrating compliance with the performance objective. However, the contribution from the other exposure pathways is expected to be no more than a few tens of percent, and should be much less for many radionuclides, in which case the other pathways essentially can be neglected in estimating dose. That is, in cases where the performance objective for off-site individuals from all exposure pathways applies, demonstrations of compliance with the performance objective reasonably need to take into account only the dose from the drinking water pathway. In other cases where the MCL for an alpha-emitting radionuclide corresponds to a dose less than the performance objective for off-site individuals, compliance with the MCL would ensure that the dose limit for all exposure pathways would be met without need for further analysis.

Therefore, the general conclusion from this analysis is that only the drinking water pathway needs to be considered for off-site releases of radionuclides in groundwater. In cases where the MCL in groundwater corresponds to a dose equivalent less than the performance objective for off-site individuals of 25 mrem per year from all exposure pathways, compliance with the MCL would ensure that the dose to off-site individuals would be substantially less than the performance objective. In cases where the MCL in groundwater corresponds to a dose equivalent greater than the performance objective for off-site individuals, the dose from all exposure pathways other than drinking water would be insignificant compared with the dose from the drinking water pathway, particularly when the uncertainties in estimating maximum concentrations of radionuclides in groundwater at locations more than 100 m from any disposal units are taken into account.

3.2.3.4 Screening of Radionuclides for Groundwater Pathway

As demonstrated in the previous section, limitation of concentrations of radionuclides in groundwater at any location beyond the boundary of the 100-m buffer zone around the disposal facility is the only concern in the dose analysis for off-site individuals. Although a large number of radionuclides are present in waste placed in the EAV, only a few radionuclides are of interest in estimating the allowable inventories at E-Area. This section presents the results of a simple screening analysis for determining TVs for radionuclides in groundwater. A more detailed analysis of releases from the disposal facility and transport in groundwater is required for those radionuclides for which an allowable inventory above the TV is desirable.

Screening calculations have been made on a large suite of 730 radionuclides (Appendix C) which may be encountered during disposal operations (Appendix C). These radionuclides were selected because they represent all radionuclides having published DCFs (U.S.DOE 1988b). Initial screening utilized spreadsheet calculations that take no credit for the engineered barriers. The travel time to the compliance point was estimated based on the conservative assumption of a five year flow period and retardation due to sorption on the soil.

The waste concentrations (Wc) in Ci/L for a unit inventory can be calculated as follows:

ILTV Wc = Unit inventory (Ci/Vault) / 803,310 (L/Vault)
ILNTV Wc = Unit inventory (Ci/Vault) / 5,880,450 (L/Vault)
LAWV Wc = Unit inventory (Ci/Vault) / 48,138,500 (L/Vault).

The screening doses were calculated based on a contaminant travel time (CTT), which is used for the decay time:

CTT = 5 years * Rf.

Values for the radionuclide-specific retardation factors (Rf) in soils are provided in Appendix C, Table C.1-3. Values on the conservative end of available ranges of values were selected in most cases.

For the majority of the radionuclides, no special calculations were required to account for daughter products. For these radionuclides, the concentration at the receptor (Cr) for a unit inventory of the radionuclides of interest is obtained using:

Cr (Ci/L) = Wc * EXP(-(decay constant)*CTT)/(Rf * Porosity).

Values for the decay constant are provided in Appendix C, Table C.1-3. The porosity is assumed to be 0.5.

The screening dose (D) for a unit inventory of a given radionuclide is obtained using the ingestion DCF and consumption rate (I) (assumed to be 730 L/year):

D (mrem/year per Ci/vault) = Cr * DCF * I.

Ingrowth of daughters for actinides requires a slightly more complicated method for computing the dose. A weighted DCF that accounts for progeny contributions must be calculated. The waste concentrations are calculated in the same manner as previously and the

CTT is computed using the Rf for the parent. This CTT is used as the time for decay and ingrowth in the RADDECAY computer code. The results of RADDECAY are used to determine the fraction of the parent remaining and the fraction of the progeny at time = CTT. These daughter fractions (DFi) are used in the calculation of the weighted DCFs. The radionuclide-specific weighted dose conversion factor (WDCFi) including retardation effects for the ith progeny is calculated using:

$$WDCFi = DCFi * DFi / Rfi$$

where DCFi, DFi, and Rfi are the ingestion DCF, Fraction of the progeny remaining at time CTT, and retardation factor for the ith progeny, respectively. Table C.1-4. in Appendix C is a tabulation of these values.

A concentration/consumption factor (CCF) is necessary to obtain the dose. The CCF is obtained using:

$$CCF(Ci/year) = (Wc(Ci/L) / Porosity) * I(L/year)$$

where Wc represents the concentration of the parent.

The dose for a given parent is then calculated with:

$$D(mrem/year) = CCF(Ci/year) * Sum(WDCFi)(mrem/Ci)$$

where Sum(WDCFi) represents the summation of WDCFi for the parent and each progeny to be considered.

The TV, based on the groundwater pathway, is then determined from the performance objective dose of interest and the dose per unit inventory of the radionuclide.

$$TV\ (Ci/vault) = \frac{Performance\ Objective\ Dose\ of\ Interest\ (4\ mrem/year)}{D\ (mrem/year\ per\ Ci/vault)}$$

The algorithm used in the screening spreadsheet for radionuclides without significant progeny was:

TV = 4 mrem/yr*Rf*porosity*vault volume(L) / EXP(-decay constant(1/yr)*5 yr*Rf) *DCF(mrem/pCi)*730L/yr*1E+12(pCi/Ci)

In thirty-five years of operations SRS has disposed of a total of about 10 million curies, so any radionuclide with a TV over 1E+15 was immediately eliminated from further consideration. A greatly reduced list of radionuclides was then examined in light of SRS operations. Radionuclides not produced by either fission or neutron activation were removed from the list. The only naturally occurring radionuclides retained were U and Th, the only radioactive raw materials used at SRS. This process resulted in the following radionuclides being considered in detailed groundwater analysis:

H-3, C-14, Ni-59, Se-79, Sr-90, Tc-99, Sn-126, I-129, Cs-135, Th-232, U-233, U-234, U-235, U-236, U-238, Np-237, Pu-238, Pu-239, Pu-240, Pu-242, Pu-244, Am-241, Am-243, Cm-244, Cm-248, and Cf-252.

3.2.4 Exposure Scenarios for Inadvertent Intruders

As described in Sect. 1.2, disposal of low-level radioactive waste in the EAV must meet a performance objective for protection of inadvertent intruders onto the disposal site. In particular, after loss of active institutional control at 100 years after facility closure, the EDE to an intruder should not exceed 100 mrem per year for scenarios involving continuous exposure or 500 mrem for scenarios involving a single acute exposure (U.S.DOE 1988a). These dose limits apply to the sum of dose equivalents from all exposure pathways that are assumed to occur in a given exposure scenario for an inadvertent intruder. As described in Sect. 1.2.1, this performance objective is assumed to apply for 10,000 years after disposal.

As described in Sect. 1.2.3, this performance objective is interpreted in this RPA to exclude doses from radon and its daughter products. A separate performance objective of 20 pCi/m^2-s for the radon exhalation rate is used to assess compliance for radon. The analysis of radon exhalation is presented in Appendix A.3.7.

In this section, the different exposure scenarios for an inadvertent intruder which have been considered in the PA for the EAV are described. An important assumption in all scenarios is that an intruder has no prior knowledge of the existence of a waste disposal facility at the site. Therefore, after active institutional control ceases, certain exposure scenarios are assumed to be precluded only by the physical state of the disposal facility, i.e., the integrity of the engineered barriers used in facility construction. Passive institutional controls, such as permanent marker systems at the disposal site and public records of prior land use, also could prevent inadvertent intrusion after active institutional control ceases, but the use of passive institutional controls is not assumed in this analysis.

3.2.4.1 Chronic Exposure Scenarios for Inadvertent Intruders

Three distinct scenarios resulting in chronic exposure of inadvertent intruders are considered in the dose analysis for the EAV. Two of these scenarios, which usually are referred to as the agriculture (or homesteader) and post-drilling scenarios, have often been applied in other intruder dose analyses for LLW disposal (NRC 1981; Oztunali and Roles 1986; Kennedy and Peloquin 1988; ORNL 1990). The third scenario considered in this analysis is referred to as the resident scenario. As noted previously, all chronic exposure scenarios for inadvertent intruders are subject to a limit on EDE of 100 mrem per year.

In previous intruder dose analyses, such as those referred to above, the agriculture scenario usually was found to be more important than the post-drilling scenario; i.e., the agriculture scenario usually results in higher doses per unit concentration of radionuclides in the disposal facility than the post-drilling scenario. Thus, the agriculture scenario usually results in lower concentrations of radionuclides that would be acceptable for disposal. However, as discussed later in this section, the agriculture scenario possibly could be less important than the post-drilling scenario under certain circumstances.

The following sections describe the assumptions for the agriculture, resident, and post-drilling scenarios.

Agriculture scenario

The agriculture scenario assumes that an intruder comes onto the site after active institutional control ceases and establishes a permanent homestead, including on-site sources of water and foodstuffs. Waste in disposed units is assumed to be accessed when an intruder constructs a home directly on top of a disposal facility and the foundation of the home extends into the facility itself. All waste in the disposal facility at the time the foundation is dug is assumed to be physically indistinguishable from native soil.

In the agriculture scenario, some of the waste exhumed from the disposal facility is assumed to be mixed with native soil in the intruder's vegetable garden. The following exposure pathways involving exhumed waste or waste remaining in the exposed disposal facility on which the intruder's home is located then are assumed to occur:

- ingestion of vegetables grown in contaminated garden soil;
- direct ingestion of contaminated soil, primarily in conjunction with intakes of vegetables from the garden;
- external exposure to contaminated soil while working in the garden or residing in the home on top of the disposal facility;
- inhalation of radionuclides attached to soil particles that are suspended into air from contaminated soil while working in the garden or residing in the home; and
- inhalation of volatile radionuclides released into air from contaminated soil while working in the garden or residing in the home.

For the last exposure pathway listed above, the only radionuclides of concern would be H-3, C-14, and isotopes of radon.

The agriculture scenario also assumes that the intruder's entire supply of water for domestic use is obtained from a well on the disposal site. The well is assumed to be placed at the location beyond the 100-m buffer zone around disposal units where the maximum

concentrations of radionuclides in groundwater are predicted to occur. The following exposure pathways involving use of contaminated well water then are assumed to occur:

- direct ingestion of contaminated water;
- ingestion of milk and meat from dairy and beef cattle that drink contaminated water;
- ingestion of vegetables grown in garden soil irrigated with contaminated water;
- direct ingestion of contaminated soil in conjunction with intakes of vegetables from the garden;
- external exposure to contaminated soil while working in the garden; and
- inhalation of radionuclides suspended into air from contaminated soil while working in the garden.

These pathways are the same as those assumed in Sect. 3.2.3 for off-site members of the public who use contaminated groundwater or surface water for domestic purposes. Again, since rainfall normally is abundant at the SRS (see Sect. 2.1.3), irrigation of a vegetable garden is assumed to occur only occasionally during the summer and only in small amounts relative to the annual rainfall (Murphy 1990), and irrigation of pasture grass ingested by dairy and beef cattle is neglected because extensive irrigation of agricultural land is not practiced near the SRS (U.S. Department of Commerce 1977; Baes and Sharp 1983). In the performance assessment for the agriculture scenario, the potential importance of the exposure pathways resulting from use of contaminated well water at the disposal site compared with the exposure pathways resulting from direct intrusion into the disposal facility is described below.

In accordance with the performance objectives for off-site releases of radionuclides described in Sect. 1.2, concentrations of radionuclides in groundwater beyond the 100-m buffer zone around disposal units would be limited either by the MCLs for radionuclides in drinking water or by a limit on EDE of 25 mrem per year from all exposure pathways, whichever is more restrictive. Thus, as shown by the analysis in Sect. 3.2.3.3, the maximum EDE in any year that could result from use of contaminated groundwater on the disposal site, taking into account all of the exposure pathways listed above, is only a small fraction (i.e., about 25% or less) of the maximum EDE to an intruder from all exposure pathways of 100 mrem per year. Therefore, for purposes of demonstrating compliance with the dose limit for inadvertent intruders, only the exposure pathways involving direct intrusion into the

disposal facility need to be considered, and the exposure pathways involving use of contaminated well water can be neglected.

In this analysis, direct intrusion into disposal units is assumed to be precluded for the period of time after loss of active institutional control when the concrete roof on the vaults and other engineered barriers, such as the top layer of uncontaminated grout in the ILNT and ILT vaults, maintain their structural and physical integrity. That is, intact engineered barriers used in constructing disposal units are assumed to preclude direct access to waste in the disposal facility by the types of equipment that normally would be used in digging a foundation for a home at the SRS.

Resident scenario

As in the agriculture scenario described above, the resident scenario assumes that an intruder excavates a foundation for a home on top of a disposal facility. During excavation, however, the intruder is assumed to encounter an intact concrete roof or other engineered barrier above the waste that cannot easily be penetrated by the types of excavation equipment normally used at the SRS. That is, the presence of intact engineered barriers is assumed to preclude direct intrusion into the waste during excavation. But instead of abandoning the site, the intruder constructs a home directly on top of the intact barrier and, thus, establishes a permanent residence at that location.

From the definition of the resident scenario, the primary exposure pathway of concern is external exposure to photon-emitting radionuclides during the time the intruder resides in the home on the disposal site. The presence of intact barriers would preclude any ingestion exposures and most inhalation exposures. Some exposures to radon could occur during indoor residence on top of intact engineered barriers, e.g., as a result of crack formation in concrete. However, such exposures should be much less than exposures to radon in the agriculture scenario when excavation into waste is assumed to occur and residence in a home on top of exposed waste becomes credible. Therefore, potential exposures to radon are ignored in the resident scenario, but such exposures essentially are captured in the agriculture scenario.

The resident scenario is assumed to occur at any time after loss of active institutional control over the disposal facility. However, even though the concentrations of most radionuclides in the disposal facility will decrease monotonically with time, due to radioactive decay and migration from the disposal facility, the dose in the resident scenario is not necessarily the highest at 100 years after facility closure. At this time, the concrete roof on top of the vaults is assumed to be intact. Therefore, at the earliest time the resident scenario could occur, the concrete roof provides a substantial amount of shielding that greatly reduces the external dose compared with the dose from unshielded waste. For the ILNT and ILT vaults, the layer of uncontaminated grout on top of the waste provides a considerable amount of additional shielding. At some later time, however, the concrete roof is assumed to have lost its integrity and most of the layer of uncontaminated grout is assumed to have weathered to soil-equivalent material. These processes presumably take hundreds to thousands of years or more. Therefore, for long-lived radionuclides that are retained in the waste for long periods of time, the external dose in the resident scenario would be considerably higher long after active institutional control ceases, when excavation essentially to the depth of the waste could occur, than at 100 years after disposal, when excavation only to the depth of the top of the concrete roof is credible.

Thus, for the resident scenario, the maximum dose to an inadvertent intruder and the time at which the maximum dose occurs depend on 1) the half-lives and concentrations of the important photon-emitting radionuclides in the waste, 2) the time period over which the engineered barriers above the waste lose their integrity and can easily be excavated, and 3) the rate at which the important radionuclides migrate from the disposal facility. However, the maximum dose for this scenario can be estimated by considering two bounding cases:
1) intrusion at 100 years after disposal in the presence of an intact concrete roof, but with no reduction in radionuclide inventories at disposal except by radioactive decay; and 2) intrusion at a much later time after disposal when exposure to essentially unshielded waste is credible, but again with no reduction in radionuclide inventories except by radioactive decay. The first bounding case takes into account radionuclides of both shorter and longer half-lives and the shielding provided by the concrete roof and any other barriers between the waste and the roof, whereas the second bounding case applies to time periods when only long-lived

radionuclides presumably are present, but the waste is assumed to be unshielded. In both cases, self-shielding provided by the waste and any encapsulating materials is taken into account in estimating external dose.

In this analysis, the two bounding cases for the resident scenario described above are evaluated. The analyses of the bounding cases take into account differences in the design of the engineered barriers for the three types of disposal units in E-Area, i.e., the types and thicknesses of the different barriers in each unit.

Comparison of agriculture and resident scenarios

From the definition of the resident scenario, this scenario can be regarded as a variation of the agriculture scenario in which only one of the exposure pathways is potentially important — namely, external exposure while residing in the home located on top of the disposal facility. Therefore, since this exposure pathway is essentially the same in the two scenarios and the agriculture scenario includes other exposure pathways that are not relevant for the resident scenario, the agriculture scenario probably will be more important than the resident scenario. That is, the dose per unit concentration of radionuclides in disposed waste probably will be higher in the agriculture scenario than in the resident scenario. Thus, the agriculture scenario is expected to be more restrictive in regard to determining acceptable disposals.

However, the tentative conclusion about the relative importance of the agriculture and resident scenarios could be incorrect if the removal rate of radionuclides from the waste by infiltrating water were comparable to or greater than the degradation rate of the engineered barriers above the waste. If such an occurrence were possible, then the external dose that would result at the time the engineered barriers have degraded to soil-equivalent material, but not any of the encapsulated waste itself, could be greater than the total dose from all exposure pathways that would result at a later time when a significant layer of waste also has weathered to soil. This could particularly be the case for the ILNT vaults in which the waste is grouted. In addition, shorter-lived radionuclides could be important in the resident scenario at 100 years after disposal, when all engineered barriers are presumed to be intact, but would be unimportant in the agricultural scenario at much later times. Therefore, the resident scenario, as well as the agriculture scenario, is considered in the intruder dose analysis.

Post-Drilling scenario

The post-drilling scenario assumes that an intruder who resides permanently on the disposal site drills through a disposal unit in constructing a well for a domestic water supply. Following construction of the well, the contaminated material brought to the surface during drilling operations, which is assumed to be indistinguishable from native soil, is assumed to be mixed with native soil in the intruder's vegetable garden. The exposure pathways involving ingestion of contaminated vegetables, ingestion of contaminated soil, and external and inhalation exposures while working in the garden then are the same as the pathways described previously for the agriculture scenario. In the post-drilling scenario, however, external and inhalation exposures while residing in the home on the disposal site, which are important in the agriculture scenario, are not relevant, because all drilling waste is assumed to be mixed with native soil in the garden and the intruder's home is assumed not to be located directly on top of exposed waste.

As in the agriculture scenario, the post-drilling scenario assumes that the intruder's entire supply of water is obtained from the on-site well, and the exposure pathways from use of contaminated well water are the same as those described previously for the agriculture scenario. Again, however, because of the stringent requirement on allowable contamination of groundwater at the disposal site in comparison with the maximum allowable dose to an intruder from all exposure pathways, demonstrations of compliance with the dose limit for inadvertent intruders for the post-drilling scenario can be based only on the exposure pathways involving direct intrusion into solid waste; i.e., the exposure pathways involving use of contaminated well water can be neglected.

In this analysis, as in the agriculture scenario, drilling through a disposal unit is assumed to be precluded during the time when the concrete vaults and any other engineered barriers maintain their integrity. Thus, in most cases, the post-drilling scenario involving drilling through a disposal facility is assumed not to be credible until the same time as the agriculture scenario involving direct excavation into a disposal facility. The basis for this assumption is that the types of drill bits normally used in constructing wells in the soft sand and clay soils at the SRS could not easily penetrate an intact concrete vault or other engineered barrier.

Therefore, in attempting to drill directly through a disposal facility, it seems reasonable to assume that an intruder would encounter considerable resistance and, instead of taking extraordinary measures to obtain a drill bit designed to penetrate through hard rock, would move the drilling operation to a different location away from the disposal facility.

For the LAW vaults, however, the post-drilling scenario conceivably could occur before the agricultural scenario. Because of the void space above the waste, the concrete roof could collapse but still consist primarily of large, intact pieces that would not be removed by normal excavation procedures. Thus, after collapse of the roof, drilling between intact sections of the roof could occur.

Comparison of agriculture and post-drilling scenarios

Previous analyses of the agriculture and post-drilling scenarios (Oztunali and Roles 1986; Kennedy and Peloquin 1988; ORNL 1990) have shown that the dose to an intruder per unit concentration of radionuclides in excavated material should be considerably greater for the agriculture scenario than for the post-drilling scenario, provided the assumptions for the exposure pathways in the two scenarios are reasonably consistent. The principal reasons for the greater doses in the agriculture scenario are 1) the greater volume of waste exhumed during construction of a foundation for a home compared with the volume of waste exhumed during drilling of a well, which results in greater concentrations of radionuclides in contaminated soil in the intruder's vegetable garden, and 2) the doses from external and inhalation exposure while residing in a home on the disposal site, which contribute to the dose for the agriculture scenario but are not relevant for the post-drilling scenario.

However, if the post-drilling scenario could occur before the agriculture scenario (e.g., if the use of drill bits that could easily penetrate intact concrete vaults and waste forms were assumed), then previous analyses have shown that the dose from the post-drilling scenario could exceed the dose from the agriculture scenario (ORNL 1990). Whether or not this is the case depends on the concentrations of the particular radionuclides in the waste and the assumed difference in time between the first credible occurrences of the post-drilling and

agriculture scenarios. Therefore, the post drilling scenario is included in the intruder dose analysis for the EAV. As noted previously, this scenario could be particularly important for the LAW vaults if the roof should collapse long before it loses its physical integrity and resembles soil.

3.2.4.2 Acute Exposure Scenarios for Intruders

Three distinct scenarios resulting in acute exposure of inadvertent intruders have commonly been applied to LLW disposal facilities. These scenarios usually are referred to as the construction, discovery, and drilling scenarios (NRC 1981; Oztunali and Roles 1986; Kennedy and Peloquin 1988). As noted previously, all acute exposure scenarios for inadvertent intruders are subject to a limit on EDE of 500 mrem. The following sections describe the three acute exposure scenarios and their potential importance in the intruder dose analysis for the EAV.

Construction scenario

The chronic agriculture scenario described in Sect. 3.2.4.1 is based on the assumption that an intruder builds a home on the disposal site, with the foundation extending into a disposal unit. The construction scenario considers exposures during the short period of time for digging a foundation and building a home.

During construction, the relevant exposure pathways are assumed to be inhalation of radionuclides suspended into air from an uncovered disposal unit and external exposure to photon-emitting radionuclides in the disposal unit. Ingestion exposure is assumed to be unimportant during normal work activities. The potential importance of the construction scenario arises primarily from the assumption that construction activities result in airborne concentrations of radionuclides that are substantially higher than those during normal activities while inhabiting the site, as in the agriculture scenario. The construction scenario also assumes external exposure to unshielded waste, whereas in the agriculture scenario shielding during indoor residence on the disposal site usually is taken into account.

From its definition, the construction scenario would occur at the same time as the agriculture scenario. Therefore, the dose analysis for the two scenarios would be based on the same concentrations of radionuclides. Previous calculations (Kennedy and Peloquin 1988) provide a direct comparison of doses for the two scenarios. For a few radionuclides, the dose per unit concentration could be slightly higher for the construction scenario but, for most radionuclides, the dose per unit concentration is expected to be much greater for the agriculture scenario. This result assumes a reasonable exposure time for the construction scenario and the use of a reasonably consistent set of assumptions for the exposure pathways in the two scenarios. Therefore, since the dose limit for the acute construction scenario is a factor of 5 higher than the dose limit for the chronic agriculture scenario, the agriculture scenario always will be more restrictive and the construction scenario generally can be neglected in demonstrating compliance of the EAV with the performance objective for protection of inadvertent intruders.

Discovery scenario

As in the resident scenario described in Sect. 3.2.4.1, the discovery scenario assumes that an intruder attempts to dig into a disposal facility while excavating a foundation for a home on the disposal site, but encounters an intact concrete roof or other engineered barrier which cannot easily be penetrated by the types of excavating equipment that normally would be used at the SRS. However, in distinction from the resident scenario, the intruder soon decides to abandon digging at that location and moves elsewhere. Since intact engineered barriers are assumed not to be breached during excavation, the primary exposure pathway for this scenario is external exposure to photon-emitting radionuclides in the disposal facility during the time the intruder digs at the site and the barriers are uncovered. The presence of intact barriers is assumed to preclude any significant inhalation or ingestion exposures.

From its definition, the discovery scenario would occur at the same time as the resident scenario. Furthermore, the relevant exposure pathway — namely, external exposure to photon-emitting radionuclides in the waste — is essentially the same in the discovery and resident scenarios. Other than the exposure time, the only difference is the shielding factor

during indoor residence, which is relevant only for the resident scenario. Therefore, since the exposure time for the discovery scenario presumably would be no more than 100 h (ORNL 1990), which is considerably less than a reasonable exposure time for indoor residence in the resident scenario, and the dose limit for the discovery scenario is a factor of 5 greater than the dose limit for the resident scenario, the resident scenario always will be more restrictive and the discovery scenario generally can be neglected in demonstrating compliance of the EAV with the performance objective for protection of inadvertent intruders.

Drilling scenario

The chronic post-drilling scenario described in Sect. 3.2.4.1 is based on the assumption that an intruder drills a well directly through a disposal unit. The drilling scenario considers exposures during the short period of time for drilling and construction of the well.

During well drilling and construction, the most important exposure pathway is assumed to be external exposure to uncovered drilling wastes confined to a pile near the well. Although some radionuclides in the drilling waste could be suspended into the air and inhaled during well drilling and construction, inhalation exposures are expected to be relatively unimportant due to such factors as the initial water content of the drilling wastes, the small volume of the waste produced, and the absence of direct mechanical disturbance of the waste pile. Ingestion exposure also is assumed to be unimportant during normal drilling activities. The potential importance of the drilling scenario arises primarily from the assumption that an intruder could be located near an unshielded waste pile for a substantial period of time.

From its definition, the drilling scenario would occur at the same time as the post-drilling scenario. Therefore, the dose analyses for the two scenarios would be based on the same concentrations of radionuclides. Previous calculations (Kennedy and Peloquin 1988) provide a direct comparison of doses for the two scenarios. For all radionuclides, the dose per unit concentration for the drilling scenario is expected to be at least an order of magnitude less than the dose per unit concentration for the post-drilling scenario, provided a reasonable exposure time for the drilling scenario and a reasonably consistent set of assumptions for the exposure pathways in the two scenarios are used. Therefore, the post-drilling scenario always will be more restrictive and the drilling scenario generally can be neglected in demonstrating

compliance of the EAV with the performance objective for protection of inadvertent intruders.

Summary of Acute Exposure Scenarios

In this section, three scenarios for acute exposure of inadvertent intruders were discussed, i.e., the construction, discovery, and drilling scenarios. However, an evaluation of these scenarios has shown that all three scenarios can be neglected for purposes of demonstrating compliance of the EAV with the performance objective for protection of intruders because the chronic agriculture, resident, and post-drilling scenarios will always be more restrictive.

3.2.4.3 Summary of Exposure Scenarios for Inadvertent Intruders

Several chronic and acute exposure scenarios for inadvertent intruders have been considered for use in the PA for the EAV. However, on the basis of previous analyses and considerations of how these scenarios would apply to the EAV, it is evident that only the following three chronic exposure scenarios need to be included in the PA:

- an agriculture scenario involving direct intrusion into disposal units at times after the engineered barriers above the waste have lost their structural and physical integrity and can be penetrated by the types of excavation procedures normally used at the SRS;
- a resident scenario involving permanent residence in a home located either on top of an intact concrete roof or other engineered barrier, which first could occur upon loss of active institutional control at 100 years after facility closure, or on top of intact but essentially exposed waste at times after the engineered barriers have lost their integrity; and
- a post-drilling scenario involving exhumation of waste from a disposal unit at times after drilling through a disposal unit becomes credible.

Estimates of dose for all of these scenarios are considered in this analysis. All acute exposure scenarios would be less restrictive in regard to demonstrating compliance with the performance objective for protection of inadvertent intruders and, thus, are not considered further in this analysis.

As described in Sect. 1.2.1, compliance with the performance objective for protection of inadvertent intruders is assumed to be required for 10,000 years after disposal. However, in cases where the maximum dose to an inadvertent intruder is predicted to occur beyond 10,000 years after disposal, the calculations are carried out until the time the maximum dose occurs to provide additional information and perspective on the performance of disposal units. Consideration of potential doses beyond 10,000 years is particularly important for disposal of uranium, due to the very long time required for ingrowth of its radiologically significant decay products.

A comparison of the relative importance of the chronic exposure scenarios for inadvertent intruders considered in this analysis requires a detailed analysis of each scenario based on the expected long-term performance of the engineered barriers in the different types of disposal units. Therefore, all three scenarios are evaluated in this analysis. An important purpose of the analysis of the different scenarios is to determine minimal requirements for the performance of the engineered barriers in order for the performance objective for inadvertent intruders to be met.

3.2.4.4 Screening of Radionuclides for Intruder Dose Analyses

Screening calculations have been made on a suite of 730 radionuclides (Appendix C). These radionuclides were selected because they represent all radionuclides having published DCFs (U.S. DOE 1988b). However, only a few radionuclides are potentially important in estimating doses to inadvertent intruders according to the different scenarios considered in this analysis. This section presents the results of a simple screening analysis for selecting the radionuclides that are potentially of concern for protection of inadvertent intruders.

The commitment that active institutional control will be maintained over the disposal site for 100 years after facility closure is an important factor in eliminating many radionuclides from consideration in the intruder dose analysis. In particular, any radionuclide with a half-life substantially less than 5 years can be neglected, because the inventory at 100 years after disposal will be reduced to innocuous levels by radioactive decay for any reasonable inventory at the time of disposal. Then, dose analyses for the agriculture, resident, and post-drilling scenarios can be used for further screening of radionuclides in each case. In particular, the dose analysis presented in Appendix A.4 can be used in screening of radionuclides for these scenarios.

The intruder dose analysis in Appendix A.4 shows that the agricultural scenario is the most restrictive, and that the EDE per unit concentration of any radionuclide in the waste at the time this scenario could occur would be less than 10 mrem per year per $\mu Ci/m^3$, unless the radionuclide decays to radon. Therefore, for any radionuclide except those which produce radon, the limit on EDE of 100 mrem per year possibly could be exceeded only if the concentration at the time this scenario occurs is greater than 10 $\mu Ci/m^3$. The screening analysis for selecting radionuclides for the intruder scenarios then assumes that the scenarios occur at 100 years after disposal, which is the earliest possible time, and that a safety factor of 10 should be applied in reducing the minimum concentration of concern estimated above.

From the assumptions described above, a radionuclide would be of potential concern only if the concentration in the waste 100 years after disposal, taking into account only the concentration at disposal and the reduction in concentration due to radioactive decay over 100 years, could be greater than 1 $\mu Ci/m^3$. A spreadsheet was created to calculate the vault inventory for each radionuclide which, after 100 years of radioactive decay, would produce a concentration of 1 $\mu Ci/m^3$. This inventory was then used as the TV to decide if more detailed calculations were required.

The algorithm used in the spreadsheet was derived in the following manner:

If X is the concentration, in Ci/m^3, in the vault at the time of disposal, and the target concentration is 1 $\mu Ci/m^3$, then for 100 years of decay:

$$1\ \mu Ci/m^3 = X(Ci/Vault)*EXP(-decay\ constant(1/yr)*100\ yr)$$
$$*1E+06\ \mu Ci/Ci\ /\ Vault\ Volume(L/Vault)*1E-03(m^3/L)$$

Solving for X

$$X = 1\mu Ci/m^3 * 1E\text{-}06 Ci/\mu Ci * \text{Vault Volume (L/vault)} * 1E\text{-}03\ m^3/L\ /\ EXP(-\text{decay constant}(1/yr) * 100\ yr)$$

The equation above is what was implemented in the spreadsheet. The spreadsheets for each of the vault types and the suspect soil disposal trenches are included as Tables C.1-1 through C.1-4 in Appendix C.

In thirty-five years of operations SRS has disposed of a total of about 10 million curies, so any radionuclide with a TV over 1E+15 was immediately eliminated from further consideration. A greatly reduced list of radionuclides was then examined in light of SRS operations. Radionuclides not produced by either fission or neutron activation were removed from the list. The only naturally occurring radionuclides retained were U and Th, the only radioactive raw materials used at SRS. This process resulted in the following radionuclides, including radiologically significant long-lived decay products, being considered in the detailed intruder analysis:

H-3, C-14, Co-60, Ni-59, Ni-63, Se-79, Sr-90, Zr-93, Nb-93m, Tc-99, Pd-107, Cd-113m, Sn-126, I-129, Cs-135, Cs-137, Sm-151, Pb-210, Ra-226, Th-229, Th-230, Th-232, Pa-231, U-232, U-233, U-234, U-235, U-236, U-238, Np-237, Pu-238, Pu-239, Pu-240, Pu-241, Pu-242, Pu-244, Am-241, Am-243, Cm-243, Cm-244, Cm-245, Cm-246, Cm-247, Cm-248, Cf-249, Cf-250, and Cf-251.

3.3 MODELS AND ASSUMPTIONS

Having defined potential mechanisms of release of radionuclides and other contaminants from the EAVDF (Sect. 3.1) and the human exposure scenarios and radionuclides believed to be most significant to this RPA (Sect. 3.2), this section describes the models adopted and assumptions made to carry out the computations necessary to estimate doses.

3.3.1 Near-Field Model

The current conceptual models for screening, and intact and degraded vault analyses are discussed in the following sections. Screening analyses were conducted first to identify radionuclides that must be considered in the detailed analysis. Three sets of conditions for the vaults were considered for the detailed analysis: intact, cracked, and completely failed. Concrete degradation calculations were combined with structural calculations to determine the timing and extent of cracking and the timing of failure. Further details are provided in the following paragraphs.

Screening calculations were used to reduce the list of contaminants that need to be considered in detailed analyses. The screening calculations assumed no credit for performance of the engineered features at the site. The basis for the calculations were conservative groundwater travel time and distribution coefficients appropriate for conditions at the site. Release from the waste form and container degradation were not considered. In essence, the calculations assume that the receptor consumes 2 L/d of the pore fluid that would be present if the radionuclides were deposited directly in the groundwater. Details for the screening calculations are documented in Sect. 3.2.3.4 and the results are summarized in Sect. 4.1.1. More detail regarding the conceptual models for the vault calculations are provided below.

3.3.1.1 Conceptual Model for Vaults

In the conceptual model for water movement, water infiltrates at the surface and either undergoes evapotranspiration back through the surface and out of the domain or it infiltrates. The majority of this infiltrating water is diverted around the engineered barrier; however, some water penetrates the barrier and perches above the concrete vault. Most of this perched water flows through the sand layer surrounding the vault and down to the water table, but some water penetrates the lower barrier and concrete roof and flows through the waste form. So a minute portion of the water that infiltrates from the surface flows through the vault. The process is illustrated in Fig. 3.3-1.

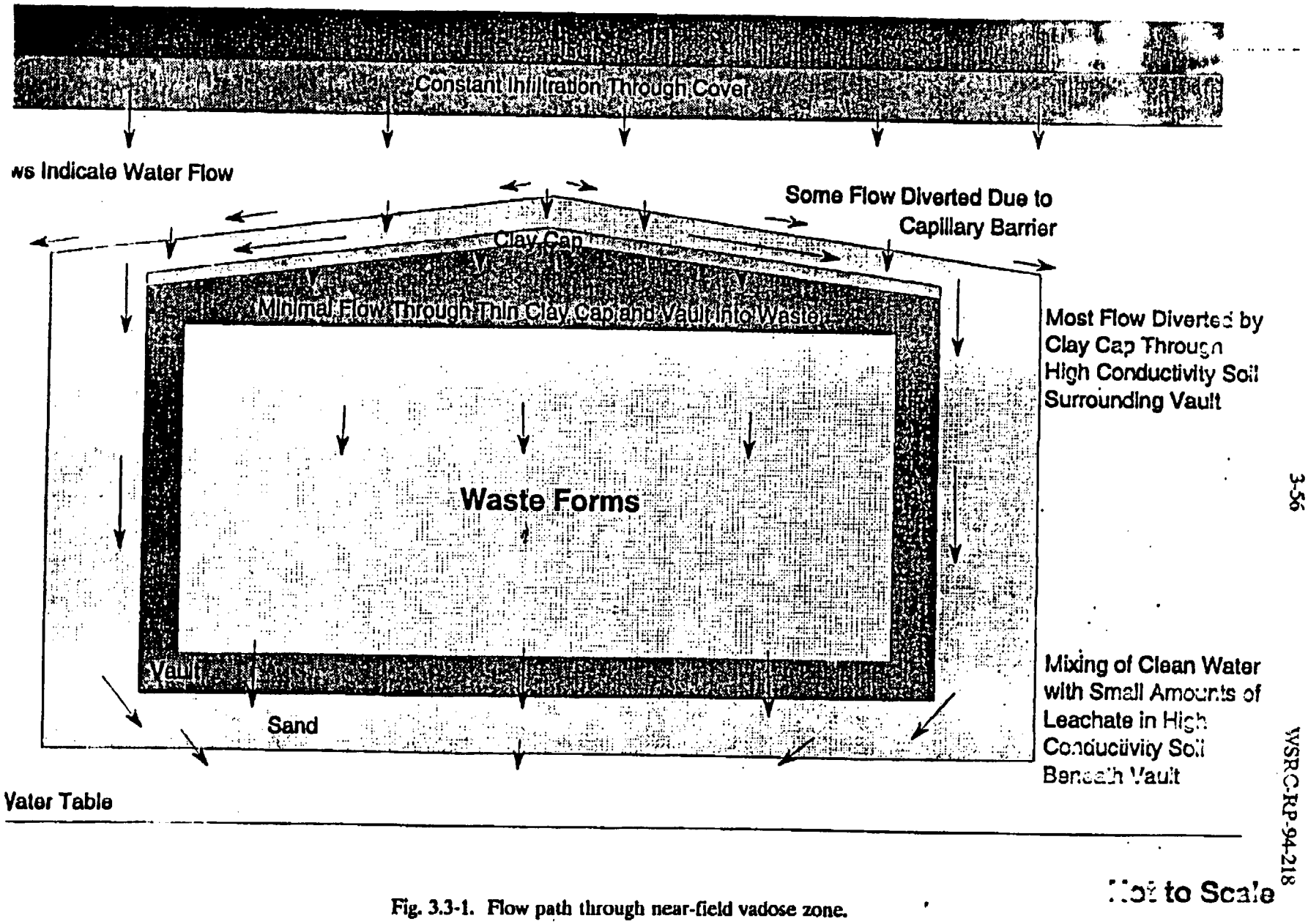

Fig. 3.3-1. Flow path through near-field vadose zone.

The flow regime in the subsurface was separated into four regions for purposes of analysis. The first region is the soil and sediments near the surface where evaporation and transpiration have a dynamic role in reversing the downward movement of water due to gravity. Below this region, but above the concrete vault, is the region that includes the engineered barrier which has the purpose of diverting the majority of the infiltrating water around the concrete vault, and thus, reducing the amount of water contacting the vault (see Fig. 3.3-2). The last region extends down to the water table and consists of backfill, the concrete vault, the waste form, and high permeability sand surrounding the vault (see Fig. 3.3-3 and Fig. 3.3-4).

An assumption inherent in dividing the flow regime in this manner is that contaminants escaping the vault cannot diffuse upwards through the top engineered barrier (cover). Rather, advection dominates transport outside the vault in the conductive soils and these contaminants are swept horizontally past the vault and down to the water table. Results show that the amount of diffusion upwards is minimal in the humid environment at SRS.

The conceptual model for transport involves several processes. These processes are diffusion, advection, adsorption, and radioactive decay. Each of these processes occurs within each of the five material types.

Assumptions involving degradation of both the engineered barrier and the vault are included in the conceptual model. As previously mentioned (Sect. 3.1.3.1, Cover Degradation), the degradation of the engineered barrier is difficult to quantify at this point. For the purposes of this analysis, it is assumed that the cover continues to function as designed until the roof of the vault collapses, which results in subsidence and failure of the cover.

Figure 3.3-4 illustrates the assumptions regarding waste form degradation for the LAW vault. Due to uncertainties in predicting degradation of the containers, it is assumed that the containers have completely degraded and collapsed (voids inside and between boxes are compacted) at the start of the simulation yielding a large void above the waste. Given that minimal flow is predicted in the vault during the time frame that the container could be intact (e.g., the first few hundred years at most), this assumption has minimal impact on the results. In general, the assumption of complete package failure results in more concentrated waste and the waste is closer to the release point. Since the ILNT/ILT vaults are backfilled with grout and voids are minimized, subsidence of the waste form is not expected, and thus, a significant void at the top of the vault is not expected.

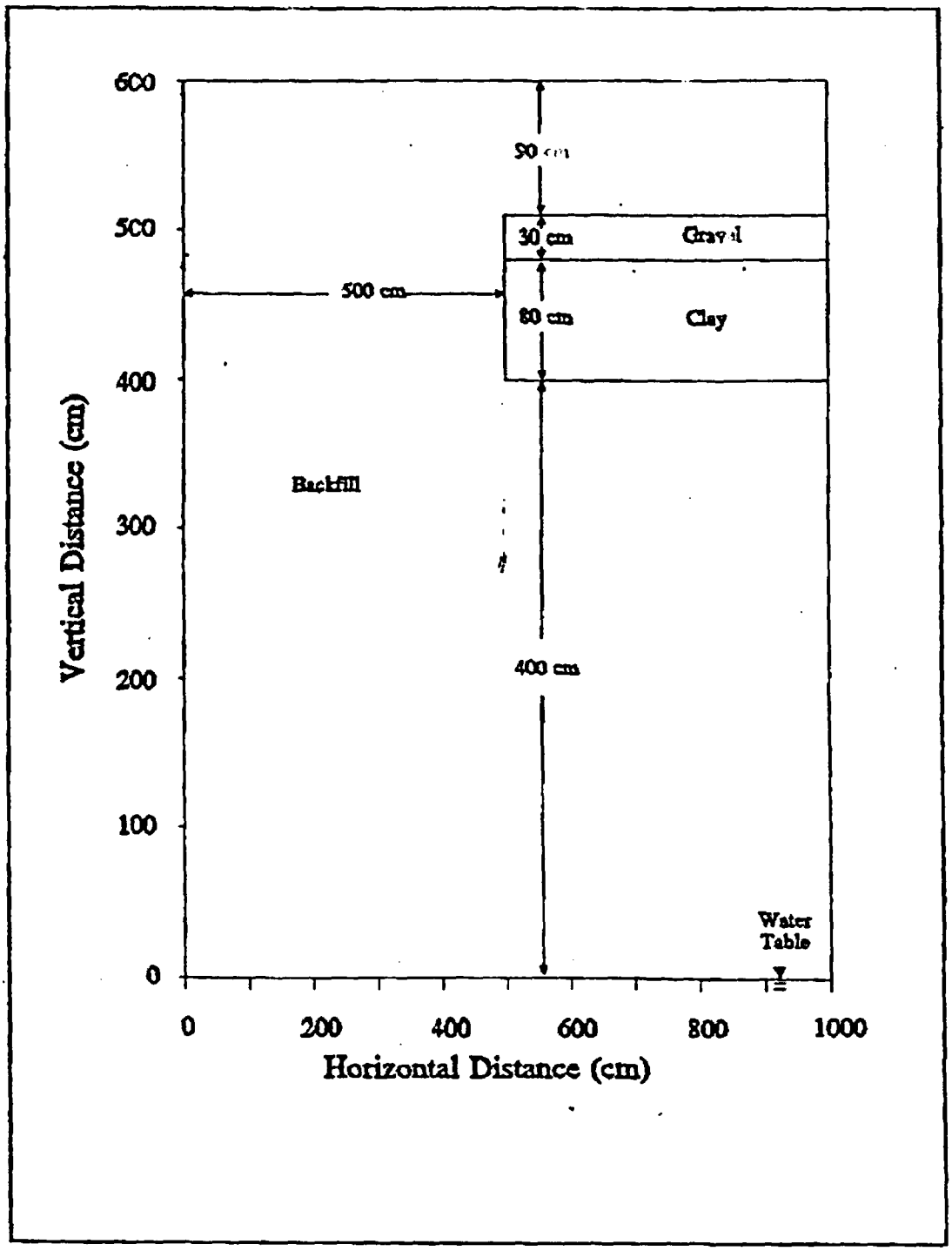

Fig. 3.3-2. Conceptual model for the cover.

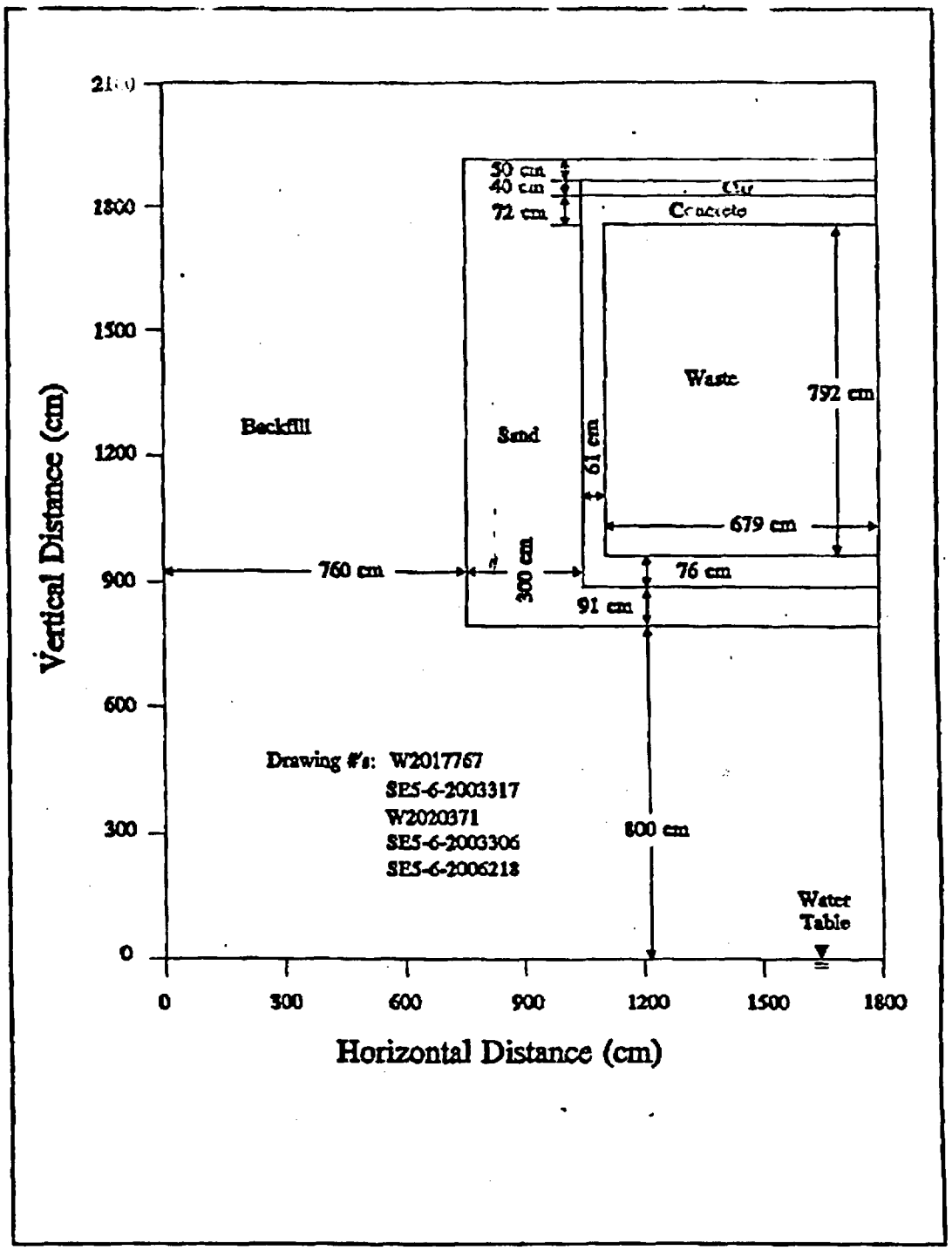

Fig. 3.3-3. Conceptual model for the ILNT and ILT vaults.

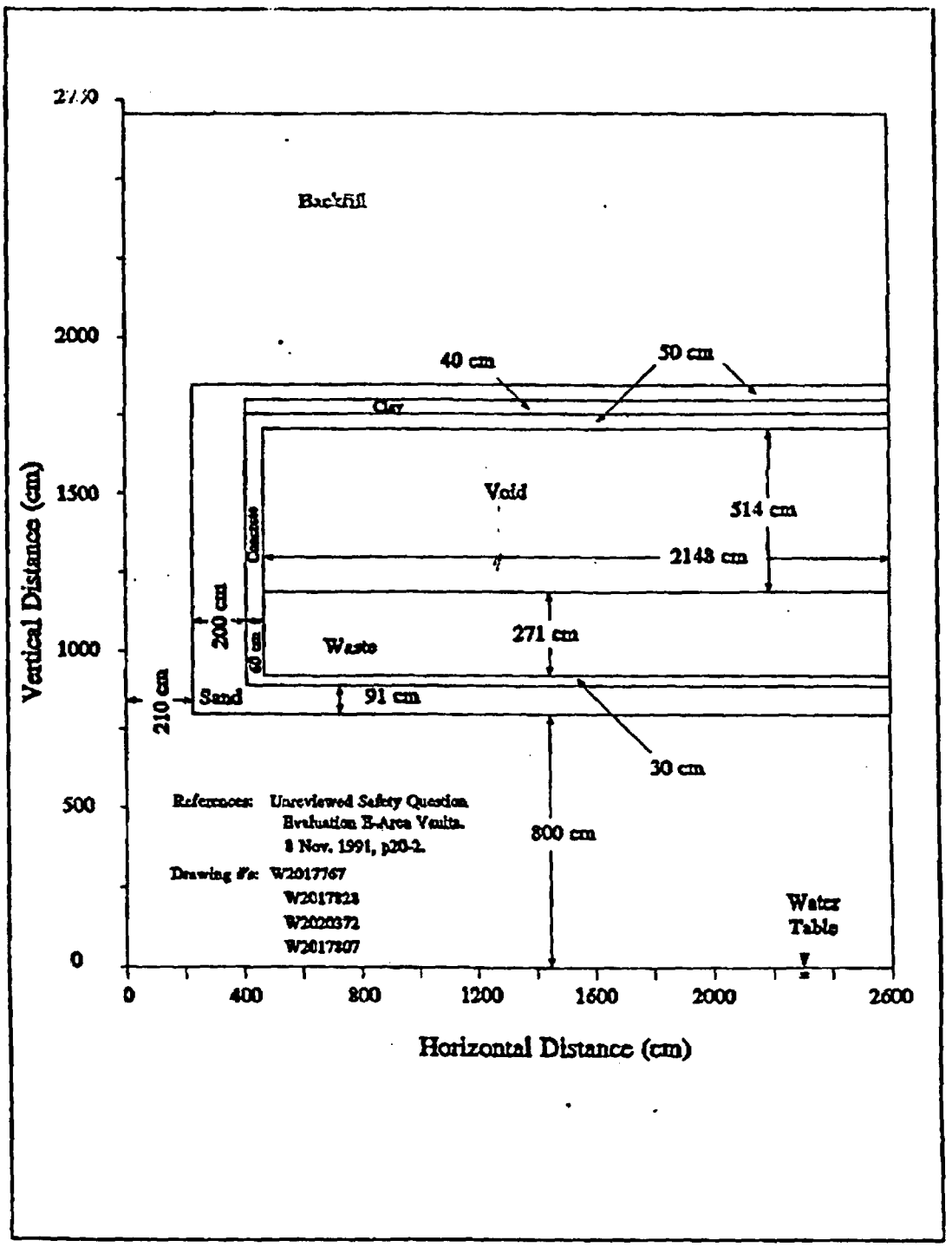

Fig. 3.3-4. Conceptual model for the LAW vault.

The time required for the construction of the barrier and the vault is minimal compared to the period considered in this study. Therefore, the vault and engineered cover are assumed to be emplaced instantaneously.

For the intact barrier scenario, a constant amount of water passes through the barrier. No consideration is given to the time required for water to begin passing through the barrier. Thus, the upper flux in the vault domain is kept constant during the entire simulation while the vault is intact. It is also assumed that flow around the vault is at steady state for the entire time the vault is assumed to remain intact. This assumption is discussed further in Appendix A.1.2.

Numerical simulation has, at its heart, averaging of spatial properties on the field scale in order to fit the problem into a numerical model. The conceptual model used to provide a framework for the numerical simulation of the near-field movement of water and contaminants from the EAV relies heavily on this averaging. The subsurface is treated as if it consists of six material types: 1) the backfill or native soil; 2) clay; 3) gravel; 4) concrete; 5) waste form; and 6) sand. Each of these materials are treated as if they are homogeneous and isotropic. No spatial variation is accounted for within any of the materials.

Flow through each of these mediums is assumed to behave as flow through porous media. Correspondingly, the hydraulic properties for each material type are assumed to be adequately described by the following hydraulic parameters: saturated hydraulic conductivity, effective porosity, and moisture characteristic curves. The moisture characteristic curves describe the nonlinear relationship between the matrix potential or pressure head, the moisture content, and the hydraulic conductivity.

Two different analytic expressions are used for describing the moisture characteristic curve. The van Genuchten (1978) and Mualem (1976) equations were used to describe this nonlinear relationship for every material type except the backfill and waste form, and void zone of the LAW vault. The equations are given as follows:

$$\theta(\psi) = \theta_r + \frac{(\theta_s - \theta_r)}{[1 + (\alpha\psi)^n]^m}$$

and

$$K(\psi) = K_s \frac{[1-(\alpha\psi)^{n-1}[1+(\alpha\psi)^{-m}]]}{[1+(\alpha\psi)^{n}]^{m/2}}$$

where

θ	= the volumetric moisture content (cm^3/cm^3),
θ_r	= the residual moisture content (cm^3/cm^3),
θ_s	= the effective porosity (cm^3/cm^3),
ψ	= the suction pressure head (cm),
K_s	= the saturated hydraulic conductivity (cm/s),
α and n	= fitting parameters, and
m	= $1 - 1/n$.

The α parameter has units of inverse length and is indicative of the air entry pressure. The n parameter is dimensionless and controls the degree of nonlinearity in the moisture characteristic curve. Table 3.3-1 gives a summary of the hydraulic and van Genuchten parameters used for all the materials.

Table 3.3-1. Summary of hydraulic and van Genuchten fitting parameters

Material	K_s (cm/s)	θ_s	θ_r	α (1/cm)	n
Backfill	1.0×10^{-5}	0.439	0.088	7.50×10^{-2}	1.70
Clay	1.0×10^{-7}	0.386	0.340	1.75×10^{-3}	1.51
Gravel	0.5	0.380	0.010	8.19×10^{-2}	3.70
Concrete	1.0×10^{-10}	0.150	0.147	5.98×10^{-4}	3.43
Sand	1.0×10^{-3}	0.375	0.074	5.51×10^{-2}	2.50
Waste Form (ILNT & ILT)	1.0×10^{-10}	0.150	0.147	5.98×10^{-4}	3.43

The backfill, void and waste form, within the LAW vault were described using the Stone correlation curve (Stone 1973). The equation for this curve is given as:

$$\psi = P_1 + P_2(1-S_w) + P_3(1-S_w)^3$$

and

$$K(S_w) = K_s\, K_{ro} \left(\frac{S_w - S_{wi}}{1 - S_{wi}}\right)$$

where

$$S_w = \frac{\theta - \theta_r}{\theta_s - \theta_r}$$

The fitted Stone parameters for the backfill moisture characteristic curve were:

P_1 = fitting parameter, = 0 cm,
P_2 = fitting parameter, = 120 cm,
P_3 = fitting parameter, = 600 cm,
K_{ro} = relative permeability at 100% saturation, = 1.0,
S_{wi} = residual moisture saturation, = 0.22, and
K_s = saturated hydraulic conductivity, = 1.0×10^{-5} cm/s.

The development of these moisture characteristic curves and data sources, for each of the material types, will be discussed in turn.

Backfill

Backfill soils were taken to have the same moisture characteristic curve as the native soil. Gruber's (1980) study of soil near the E-Area was determined to be the most complete because it included analyses of hydraulic conductivity. Sampled data for the soil from Gruber's study was analyzed with the RETC (van Genuchten 1988) code. The code uses a

least square curve fit to generate the van Genuchten parameters, as well as the saturated hydraulic conductivity. This fitting can occur on either moisture content versus hydraulic conductivity data or pressure head versus moisture content data. Analysis of the pressure versus moisture content data showed the backfill soil to be highly drainable. This was not expected for a silt sand soil. Previous studies (INTERA 1989) have used both the pressure versus moisture content and the hydraulic conductivity versus moisture content data sets to estimate a moisture characteristic curve. However, based on professional judgement, only the K versus θ data was used to determine the moisture characteristic curve parameters. As a comparison, Stone's curve was then graphically fitted to the resulting θ versus ψ van Genuchten fitted curve. Both curves are shown in Fig. 3.3-5. As can be seen, the Stone curve does not mimic known behavior at the dry end of the curve; however, this is not a problem in the simulation study because the soils remain wet and in that portion of the Stone curve, that shows a good match with the van Genuchten curve. In order to be consistent in our implementation of moisture characteristic curves, the van Genuchten curve was used for the backfill soil. The van Genuchten fitting parameters used were $\alpha = 0.075$ cm^{-1}, and $n = 1.7$. The saturated hydraulic conductivity used was 1.0×10^{-5} cm/s. Porosity and residual moisture content were 0.439 and 0.088 respectively.

Gravel

The gravel to be used in constructing the engineered barrier was previously analyzed by the University of Texas (INTERA 1989). Coarse sand, glacial outwash, and stony soil were studied to determine the best representation of gravel. A hydraulic conductivity of 0.5 cm/s, and porosity of $\phi = 0.38$ were suggested. Data from the University of Texas report was analyzed with the RETC code to obtain van Genuchten parameters for the gravel. The resulting parameters were $\alpha = 0.0819$ cm^{-1}, and $n = 3.70$, and $\theta_r = 0.01$ cm^3/cm^3. Figure 3.3-6 shows data from several soils and the University of Texas recommended curve, which represents the more drainable end of the spectrum. This is essentially the same curve used by INTERA (1989) in their study of the saltstone vault to represent the gravel moisture characteristic curve.

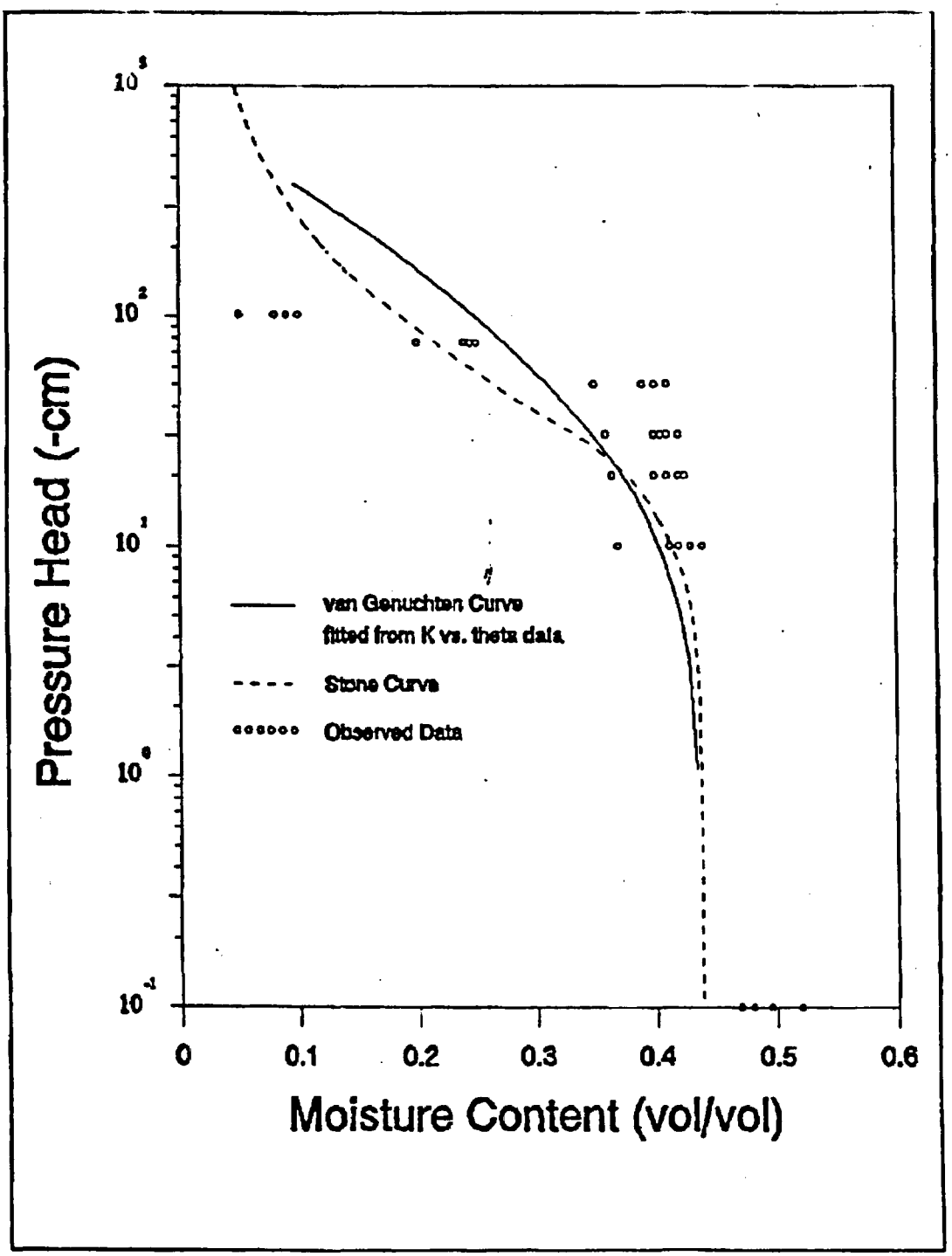

Fig. 3.3-5. Fitted moisture characteristic curve for the backfill soil.

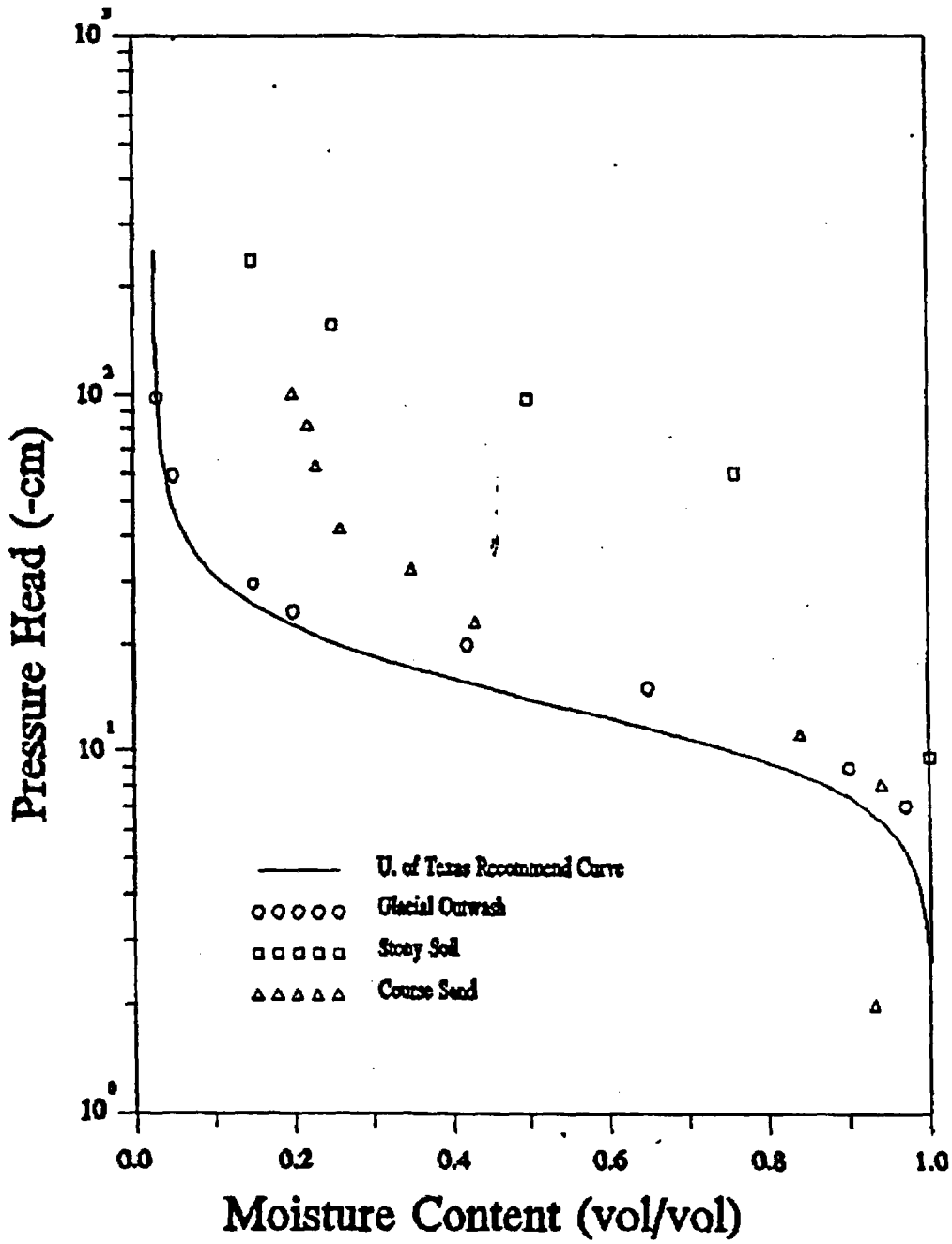

Fig. 3.3-6. Fitted moisture characteristic curve for the gravel soil.

Clay

A clay cap was not considered in the INTERA (1989) study so there is no previous example to follow. The clay soil used in the engineered moisture barrier cover will be taken from the vicinity of SRS. A contracted study on Dixie clay and Grace clay (Yu et al. 1993) was the source of information for the clay data. Hydraulic parameters given for the Dixie clay were used. The hydraulic parameters were: saturated hydraulic conductivity $k_{sat} = 1.0 \times 10^{-7}$ cm/s, porosity of $\phi = 0.386$, Van Genuchten parameters $\alpha = 1.75 \times 10^{-3}$ cm^{-1}, and n = 1.51, and $\theta_r = 0.34$ cm^3/cm^3. Based on considerations of *in-situ* hydraulic conductivity versus laboratory measured values, it was decided to use a k_{sat} of 1.0×10^{-7} cm/s. In general, it is assumed that *in-situ* values would be larger than laboratory values.

Sand

Sand was also tested for its hydraulic performance (Yu et al. 1993). The saturated hydraulic conductivity was reported as $k_{sat} = 1.0 \times 10^{-3}$ cm/s. Porosity and residual moisture content were, $\phi = 0.375$ and $\theta_r = 0.074$. The van Genuchten fitting parameters used in describing the moisture characteristic curve were, $\alpha = 0.051$ and n = 2.43.

Waste Form

Since the waste in the ILNT and ILT vaults is to be grouted in place or enclosed in concrete, it was assumed that the moisture characteristics of grout are similar to that of concrete. The moisture characteristic curve used was the same as that for the concrete. Water flow through the LAW vault waste was assumed to be controlled by the surrounding concrete. Thus, during the intact period of the simulation, the hydraulic parameters were the same as the concrete. From the end of the intact period to the end of the simulations, the LAW vault waste was assumed to have the same hydraulic properties as sand.

Concrete

Samples of concrete to be used for the EAVs were tested to determine their hydraulic parameters by Core Labs (Yu et al. 1993). Results from this analysis gave the following parameters for the E-Area concrete. Saturated hydraulic conductivity, k_{sat} was 1.0×10^{-10} cm/s, $\alpha = 5.98 \times 10^{-4}$ cm^{-1}, n = 3.43, and $\theta_r = 0.147$ cm^3/cm^3. An effective porosity of $\phi = 0.15$ was used in the model.

The molecular diffusivities assumed for each soil type are:

- 158 cm^2/year for the soil and sand,
- 0.315 cm^2/year for the concrete,
- 0.158 cm^2/year for the ILNT and LAW vault wastes, and
- 47 cm^2/year for the clay.

The longitudinal dispersivities for each soil type were:

- 10 cm - for soil and sand,
- 5 cm - for the concrete, ILNT waste, LAW waste, and clay.

The transverse dispersivity was 2 cm for all material types. The transport partition coefficients used in the simulations are given in Table 3.3-2. All transport simulations were conducted assuming a unit concentration as the initial mass in the waste forms.

3.3.1.2 Conceptual Model for Degraded Vault

Two steps of degradation are considered in the detailed flow and transport models: cracking and collapse. The cover is assumed to fail at vault collapse due to the loss of support from the roof of the vault. When the cover fails, the flow field is assumed to be at equilibrium with the background infiltration rate (40 cm/year). Variations in the failed cover

Table 3.3-2. Partition coefficients used in PORFLOW near-field simulations, mL/g

	Soil	Concrete[a]	ILNT Waste[a]	LAW Waste[a]	Sand[b]	Clay[b]
H	0	0	0	0	0	0
C	2[c]	5000	5000	0	5	1
Ni	300[d]	1000	1000	1200	400	650
Se	5[e]	0	200	170	150	740
Sr	10[f]	10	10	3	15	110
Tc	0.36[f]	700	1	0	0.1	1
Sn	130[d]	200	200	50	130	670
I	0.6[f]	30	30	0	1	1
Cs	100[f]	20	2	0	280	1900
Ra	500	10	10	60	500	9100
Th	3000[d]	5000	5000	2200	3200	5800
U	50[g]	5000	200	6000	35	1600
Np	10[g]	5000	2000	750	5	55
Pu	100[f]	5000	5000	2000	550	5100
Am	150[f]	5000	5000	3700	1900	8400
Cm	150[h]	5000	5000	3700	4000	6000
Bk	150[h]	5000	5000	3700	1900	8400
Cf	150[h]	5000	5000	3700	1900	8400

[a] All values from NAGRA (Allard 1985) except Cs-135 from Oblath (1985).
[b] All values from Sheppard and Thibault (1990). Berkelium and californium were assumed to be the same as americium.
[c] *Source:* McIntyre (1988).
[d] *Source:* Sheppard and Thibault (1990).
[e] NEA data base (Ticknor and Ruegger 1989).
[f] *Source:* Hoeffner (1985).
[g] *Source:* Looney et al. (1987).
[h] Assumed to be the same as americium.

infiltration rate are considered in the sensitivity analysis. In all cases, the flow field is maintained at steady state while the transport processes are occurring. At the time of cracking and the time of collapse, new flow fields are obtained for use during the respective time frame.

Parameter values from Sect. 3.3.1.1 will be used for all soils. Parameters for the engineered features are obtained from concrete degradation and structural calculations. The approach for degradation modeling in introduced in Sect. 3.1.3 and discussed in detail in Appendix K. The results of the degradation modeling identify estimates of the times that cracking and collapse occur and the changes in concrete permeability when cracking occurs. Changes in other parameters are based on engineering judgement.

The parameters used for the degraded cases are identified in Tables 3.3-3 and 3.3-4. Tables 3.3-3 and 3.3-4 identify the times for the step changes as t_1 and t_2. Table 3.3-5 provides the times considered best estimates for the step changes in the LAW and ILNT/ILT vaults. Details regarding the degradation calculations are provided in Appendix K.

The material properties used for the backfill, clay, and sand do not change over time for all types of vaults as shown in Tables 3.3-3 and 3.3-4. Also, the material properties for the waste are assumed to be degraded initially for the LAW vault, and thus, do not change with time. The grouted waste forms for the ILNT/ILT vaults are assumed to increase in permeability at the first step change and remain at the larger permeability for the duration of the simulation. Geochemical properties for the waste form are assumed to persist for the duration of the simulations.

The concrete properties for the vault also vary with time based on the degradation calculations in Appendix K. The roof, walls, and floor were treated separately as shown in Tables 3.3-3 and 3.3-4. Note that the times of the step changes are different for the different vaults. The floor actually fails at roughly the same time for all vaults. However, the time of failure for the roof is different. The hydraulic conductivity for the cracked concrete was estimated using an analytic solution as part of the degradation calculations discussed in Appendix K.

Table 3.3-3. LAW vault parameters

	TIME	k_{sat}	Infiltration, cm/year	Porosity
Placement of vaults; all systems work as designed				
Backfill	$t_0 - t_1$	1×10^{-5}	4	0.44
Clay	$t_0 - t_1$	1×10^{-7}	4	0.39
Concrete (roof)	$t_0 - t_1$	1×10^{-10}	4	0.15
Concrete (floor)	$t_0 - t_1$	1×10^{-10}	4	0.15
Concrete (walls)	$t_0 - t_1$	1×10^{-10}	4	0.15
Sand	$t_0 - t_1$	1×10^{-3}	4	0.38
Void	$t_0 - t_1$	1×10^{-3}	4	0.99
Waste	$t_0 - t_1$	1×10^{-3}	4	0.33
Cracks penetrate the floor and walls, and the roof				
Backfill	$t_1 - t_2$	1×10^{-5}	4	0.44
Clay	$t_1 - t_2$	1×10^{-7}	4	0.39
Concrete (roof)	$t_1 - t_2$	1×10^{-7}	4	0.15
Concrete (floor)	$t_1 - t_2$	1×10^{-3}	4	0.15
Concrete (walls)	$t_1 - t_2$	1×10^{-3}	4	0.15
Sand	$t_1 - t_2$	1×10^{-3}	4	0.38
Void	$t_1 - t_2$	1×10^{-3}	4	0.99
Waste	$t_1 - t_2$	1×10^{-3}	4	0.33
Roof collapses, but moisture flux out the vault prevents filling of vault, evapotranspiration yields lower infiltration				
Backfill	$t_2 - t_3$	1×10^{-5}	40	0.44
Clay	$t_2 - t_3$	N/A		
Concrete (roof)	$t_2 - t_3$	N/A		
Concrete (floor)	$t_2 - t_3$	1×10^{-3}	40	0.15
Concrete (walls)	$t_2 - t_3$	1×10^{-3}	40	0.15
Sand	$t_2 - t_3$	1×10^{-3}	40	0.38
Void	$t_2 - t_3$	N/A		
Waste	$t_2 - t_3$	1×10^{-3}	40	0.33

t_0 = beginning of simulation, 0 years
t_1 = cracks penetrate roof
t_2 = roof collapse
t_3 = beyond peak release of each nuclide

Table 3.3-1. ILNT vault parameters

	TIME	k_{sat}	Infiltration, cm/year	Porosity
Placement of vaults; all systems work as designed				
Backfill	$t_0 - t_1$	1×10^{-5}	4	0.44
Clay	$t_0 - t_1$	1×10^{-7}	4	0.39
Concrete (roof)	$t_0 - t_1$	1×10^{-10}	4	0.15
Concrete (floor)	$t_0 - t_1$	1×10^{-10}	4	0.15
Concrete (walls)	$t_0 - t_1$	1×10^{-10}	4	0.15
Sand	$t_0 - t_1$	1×10^{-3}	4	0.38
Waste	$t_0 - t_1$	1×10^{-10}	4	0.50
Cracks penetrate the roof, while the floor and walls remain intact				
Backfill	$t_1 - t_2$	1×10^{-5}	4	0.44
Clay	$t_1 - t_2$	1×10^{-7}	4	0.39
Concrete (roof)	$t_1 - t_2$	1×10^{-7}	4	0.15
Concrete (floor)	$t_1 - t_2$	1×10^{-10}	4	0.15
Concrete (walls)	$t_1 - t_2$	1×10^{-3}	4	0.15
Sand	$t_1 - t_2$	1×10^{-3}	4	0.38
Waste	$t_1 - t_2$	1×10^{-3}	4	0.50
Roof collapses, but moisture flux out the vault prevents filling of vault, evapotranspiration yields lower infiltration				
Backfill	$t_2 - t_3$	1×10^{-5}	40	0.44
Clay	$t_2 - t_3$	N/A		
Concrete (roof)	$t_2 - t_3$	N/A		
Concrete (floor)	$t_2 - t_3$	1×10^{-3}	40	0.15
Concrete (walls)	$t_2 - t_3$	1×10^{-3}	40	0.15
Sand	$t_2 - t_3$	1×10^{-3}	40	0.38
Waste	$t_2 - t_3$	1×10^{-5}	40	0.50

t_0 = beginning of simulation, 0 years
t_1 = cracks penetrate roof
t_2 = roof collapse
t_3 = beyond peak release of each nuclide

Table 3.3-5. Degradation times for vaults, years

Vault State	ILNT/ILT	LAW
Intact, t_0 - t_1	0 to 575	0 to 1400
Cracked, t_1 - t_2	575 to 1050	1400 to 3100
Failed, t_2 - t_3	1050 to end	3100 to end

The conceptual model for the analytic solution assumes, as discussed in Sect. 3.1.3.5, that: 1) fractures occur at regular intervals as determined by the structural calculations; 2) that all frac-tures open simultaneously at the time specified in Table 3.3-5; 3) the fractures are assumed to be continuous and open and filling or plugging by soils or precipitates is not considered; 4) the fracture is saturated with water; and 5) water drains freely at the base of the fracture. These assumptions should yield a conservative estimate of the hydraulic conductivity and flow rates through out the fractures.

The PORFLOW (ACRI 1993) computer code is used to conduct the flow and transport calculations using the assumptions discussed in the previous paragraphs. The analyses are conducted in an iterative fashion. The first set of analyses address intact conditions for the vault and cover for the first time frame (Sect. 3.3.1.1). The second and third time frames are addressed using the parameters in Tables 3.3-3 and 3.3-4. Fractures are modeled as an increase in the effective hydraulic conductivity of the concrete. The material properties and assumptions discussed previously represent the base case values for the input parameters. Sensitivity analyses are conducted to address the impacts of changes in the base case on performance.

3.3.2 Groundwater Transport Model

A brief summary of the conceptual model of the subsurface transport of radionuclides in the saturated zone is provided here, while a more detailed description is given in Appendix A.2. Radionuclides that leach from the EAVs will eventually reach the water table unless their half-lives are sufficiently short relative to the transport time in the unsaturated zone. Radionuclides that reach the water table, as determined in the near-field models for both intact and degraded vaults (Sect. 3.3.1), would be transported in the saturated zone beneath the facility to discharge points along nearby streams; specifically, UTR Creek, unnamed, and Crouch Branches (Fig. 2.1-2). The five hydrologic units (Appendix A.2) of interest, are Aquifer Unit IIA (Congaree Aquifer), Confining Unit IIA-IIB (Green Clay), Aquifer Unit IIB, Zone 1 (Barnwell/McBean Aquifer), Confining Zone IIB_1-IIB_2 (Tan Clay), and Aquifer Unit IIB, Zone 2 (water table). All units are dissected by the three creeks to some degree, except for Aquifer Unit IIA and Confining Unit IIA-IIB, which are incised only by UTR Creek.

The computer code PORFLOW (ACRI 1994) was used to simulate groundwater flow under the EAVDF. PORFLOW is a three dimensional code capable of simulating multi-phase fluid flow in variably saturated porous or fractured media. The PORFLOW computer code is described in detail in Appendix B.5. The purpose of this section is to briefly describe the system simulated with this computer code with respect to the physical boundaries of the model domain, the assumptions made regarding the hydrologic characteristics within that domain, and the assumptions made regarding physical characteristics of the porous media and chemical characteristics of the radionuclides that affect mass transport in groundwater. A more in-depth treatment of the conceptual saturated flow and transport model is provided in Appendix A.2. A description of the method by which the conceptual model described below is represented by PORFLOW simulations is provided in Sect. 3.4.2.

3.3.2.1 Model Domain

The hydrologic setting at E-Area is conceptualized as a three-dimensional domain, due to the divergent nature of the flow in the aquifers of interest. The model domain in the saturated zone beneath the EAVs is defined by the lateral and vertical extent of interest; i.e., that volume which could potentially be impacted by contamination due to waste disposal in the EAVDF. The lateral extent of the model domain was selected not only to assure simulation of the zone of interest but also to permit a reasonable representation of naturally occurring flow boundaries within the model domain. For example, the domain extent on the west, south, and east sides coincide approximately with groundwater divides in Aquifer Units IIB, Zones 1 and 2.

Vertically, the domain is divided into five layers corresponding to the three aquifer units and the two confining units that separate them. All five units potentially will be impacted by the release of radionuclides from the EAVs and will be the units through which the radionuclides will be transported. The upper unit, Aquifer Unit IIB, Zone 2, is the water table and is the unit within which the upper surface of the zone of saturation occurs. Beneath this unit is Confining Unit IIB_1-IIB_2 (or the Tan Clay), which separates it from the Aquifer Unit IIB,

Zone 1 (Barnwell/McBean). Beneath Aquifer IIA, Zone 1, is Confining Unit IIA-IIB (the Green Clay), which separates it from Aquifer Unit IIA (the Congaree Aquifer). The two confining layers both have relatively low hydraulic conductivities and, thus, act to confine the aquifer units which underlie each.

The lower unit, Aquifer IIA, is the lowermost unit of interest because units below this will not be impacted by any long-term releases from the EAVs. Beneath Aquifer IIA is Confining Unit I-II (Ellenton Clays), which separates it from the underlying Aquifer Unit I. Piezometric levels measured near the EAVDF indicate that there is an upward gradient across Confining Unit I-II, which means that the vertical component of flow is upward in this low-permeability unit. Consequently, Aquifer Unit IIA is a zone of groundwater convergence, vertically, and flow within the unit is horizontal in the direction of the discharge zone at UTR Creek. Within the saturated zone model, the base of the Aquifer Unit IIA is the base of the flow field. All of the above mentioned units are described in greater detail within Appendix E.

3.3.2.2 Model Assumptions

Use of the groundwater model described above involves several key assumptions relating to how the model is used to make projections of contaminant migration into the future and how the hydrologic system beneath the EAVDF is represented within the model. One of the primary assumptions is that recharge will remain constant during the future time period that is simulated, and therefore, a steady-state flow will prevail. Since there is no way to project long-term trends in this component of the hydrologic budget, an assumption of steady recharge at a rate close to what occurs today is reasonable. This assumption is embodied in the basic simulation strategy to create a steady-state flow field and then allow contaminants to migrate through that flow field in a transient mode. Other assumptions relate to how the flow field is represented within the model, how certain processes of contaminant migration are simulated, and the validity of these representations. These assumptions are identified below.

Boundary Conditions

Assumptions of boundary conditions are important because they constrain the simulation solution. Boundary types consist of constant head, constant flux, and the special case of constant flux where the flux = 0 (or no flow). In all cases, an effort was made to match natural flow boundaries as closely as possible. Boundaries used in the saturated zone model are described on an unit by unit basis.

Aquifer Unit IIA - The lower boundary of the model domain is the base of Aquifer Unit IIA. This plane is set as a constant flux boundary with the flux being set equal to the calculated inflow from below. The calculation utilized measured hydraulic gradients and estimates of the Ellenton Confining Unit vertical hydraulic conductivity. The western and eastern edges of the domain for this unit are set as no-flow boundaries, while the southern edge of the domain is set as a constant-flux boundary. The southern boundary is an area of inflow and the flux was set based upon known gradients and hydraulic conductivities. The eastern and western edges of the domain are sub-parallel to flow directions in this unit, and therefore, no-flow boundaries are the most valid representations of natural conditions. The area of primary interest within this model is that area south of UTR Creek, hence, the constant-head nodes used to represent this stream from the northern boundary of the area of interest. Although flow enters the steam nodes from the north, the trace of UTR Creek acts as an internal no-flow boundary in this unit since flow converges from both the north and south to these nodes.

Aquifer Unit IIB1 - Three sides of this aquifer unit are represented as no-flow boundaries. The extent of the model domain on the eastern, southern, and western edges was selected to allow a general conformance with sub-regional groundwater divides, which occur within this unit. In theory, these divides delineate vertical planes across which flow cannot occur, hence, the no-flow designation is thought to be the most valid way to represent natural conditions. The northern edge of this unit is truncated by erosion south of UTR Creek and the free-water surface defines the northern extent to which groundwater can flow.

Aquifer Unit IIB2 - Boundaries to this unit are treated in identical fashion as Aquifer Unit IIB1, no-flow boundaries on three sides and a free-water surface to the north. The groundwater divides in both units are sub-parallel, and hence, the domain extent is representative of these boundaries in both units.

Confining Units IIA-IIB and IIB1-IIB2 - In theory, flow directions in aquitards is nearly vertical, hence, the amount of horizontal flow in the units is negligible. This fact supports the representation of lateral boundaries on the east, south, and west edges of the model domain as no-flow boundaries. At their northern extent each of these units is truncated by erosion south of UTR Creek. In the area north of the "outcrop" position, the vertical hydraulic conductivity for nodes of these layers was increased to the extent where flow is not impeded.

Internal steams - Two tributaries of UTR Creek enter from the south and are dischatge areas of Aquifer Units IIB1 and IIB2 within the model domain. These tributaries are Crouch Branch, located east and north of the EAVDF, and an unnamed branch located west and north of the EAVDF. Measurements of flow rates were taken at multiple locations along each of the steams to delineate rates of gain along different steam segments. Measurements were taken at a relatively dry time period so that measured stream flows would directly reflect groundwater discharge. Model nodes closest to the bed of each of these streams was designated as a "stream node". Initially, constant fluxes were assigned to each of these nodes at a rate equal to the measured stream flow gain. Once calibration was achieved, designations of the stream nodes were changed to constant-heads, set at the elevation of the stream bed.

Hydraulic Characteristics

The five units conceptualized for the groundwater model are assumed to be homogenous and anisotropic. Vertical and horizontal hydraulic conductivity values, K_v and K_h, were assigned uniformly within each layer. In all cases, K_v was assigned at a lower value than K_h, but the ratio was kept constant within each layer. Incorporation of vertical to horizontal

anisotropy is supported by extensive hydrologic and geologic evidence. Values of hydraulic conductivity for the groundwater flow and transport simulations are documented in Table 3.3-6.

Table 3.3-6. Hydraulic conductivities for saturated zone simulations

Hydrologic Unit	Horizontal Hydraulic Conductivity (cm yr^{-1})	Vertical Hydraulic Conductivity (cm yr^{-1})
Aquifer Unit IIB2	4.0×10^4	1.0×10^4
Confining Zone IIB1-IIB2	6.4×10^1	4.3×10^1
Aquifer Unit IIB1	4.1×10^4	3.1×10^4
Confining Unit IIA-IIB	3.0	2.0
Aquifer Unit IIA	4.2×10^5	4.2×10^4

Each of the five units was also assumed to be homogenous with respect to specific storage and porosity. Porosity was set at 0.3 for the aquifer units and at 0.4 for the aquitard units. Specific storage was assumed to be uniform throughout the entire flow field at 0.0001.

Mass Transport

Mass transport in the saturated zone occurs by advective, diffusive, and dispersive processes, but is hindered by sorptive processes. It is assumed that the use of partitioning coefficients, K_d's, which remain constant throughout the simulation is a valid method of representation of the sorption phenomenon for each contaminant species. Although these coefficients are known to vary with changing geochemical conditions, there is no transport code available which can simulate time or spatially-varying K_d's. The K_d's assumed for Aquifer Units IIA, IIB1, and IIB2 are listed in the soil column of Table 3.3-2. For Confining Units IIA-IIB and IIB1-IIB2, the K_d's assumed are listed in the clay column of Table 3.3-2.

Dispersion was simulated by assuming longitudinal and transverse dispersivities of 3 m and 0.3 m, respectively, assigned uniformly in all layers. Diffusion does not significantly contribute to contaminant transport within the saturated zone. Values of the aquifer matrix specific parameters assumed in the mass transport simulations are listed in Table 3.3-7.

Table 3.3-7. Aquifer matrix-specific mass transport parameters

Matrix Property	Property Value Used
Effective diffusion coef.	5×10^{-10} m^2 s^{-1}
Longitudinal dispersivity	3 m
Transverse dispersivity	0.3 m
Matrix dry bulk density	2650 kg m^3
Total porosity	0.40
Effective porosity	0.30

3.3.3 Models for Dose Estimation

As described in Sect. 3.2.3 and 3.2.4, two basic exposure situations are considered in the PA for the EAV. The first is exposure of members of the general public following transport of radionuclides beyond the boundary of the disposal site, and the second is exposure of inadvertent intruders at the disposal site following loss of active institutional control at 100 years after facility closure. In each case, models for calculating radiation dose from estimated concentrations of radionuclides in the environment are required.

3.3.3.1 Models for Estimating Dose to Off-Site Individuals

The different transport pathways for exposure of off-site members of the public following release of radionuclides from the EAV are discussed in Sect. 3.2.2. The two principal pathways of concern are transport in groundwater following mobilization of radionuclides by

infiltrating precipitation and transport in air following releases of volatile radionuclides to the atmosphere. An analysis of the atmospheric pathway is presented in Appendix A.3. This section discusses the analysis for the groundwater pathway beyond the boundary of the 100-m buffer zone around the disposal site.

For transport of radionuclides via the groundwater pathway, an analysis presented in Sect. 3.2.3.3 shows that the only exposure pathway of concern for off-site members of the public is direct consumption of contaminated drinking water obtained from a well located beyond the boundary of the 100-m buffer zone around the disposal site. Either the performance objective for protection of groundwater resources determines allowable releases to groundwater, in which case only the drinking water pathway is of concern, or doses from other pathways involving use of contaminated groundwater are relatively insignificant. Therefore, doses from other exposure pathways involving other use of contaminated groundwater need not be considered in the dose analysis for off-site members of the public.

The model used to estimate dose from the drinking water pathway is presented in Appendix A.4.5.1. The inputs to the model are the maximum concentrations of radionuclides in groundwater at any location beyond the boundary of the 100-m buffer zone at any time after disposal, as obtained from the models for mobilization and transport of radionuclides described in Sect. 3.3.1 and 3.3.2. The model for the drinking water pathway is summarized in Table A.4-6 of Appendix A.4. For each radionuclide, the factor in this table gives the EDE in rem per year from the drinking water pathway for a unit concentration in groundwater of 1 μCi/L. Thus, the annual dose from any radionuclide is simply obtained by multiplying the estimated maximum concentration in groundwater by the factor given in this table.

3.3.3.2 Models for Estimating Dose to Inadvertent Intruders

The different exposure scenarios and exposure pathways for inadvertent intruders assumed for the EAV are discussed in Sect. 3.2.4. The principal exposure scenarios of concern involve direct intrusion into disposal units. Doses to inadvertent intruders resulting from use of contaminated groundwater obtained from a well on the disposal site should be negligible compared with the doses from direct intrusion into solid waste, because the maximum

permissible doses from the groundwater pathway are only a small fraction of the dose limits for inadvertent intruders from all exposure pathways. An analysis in Appendix A.3 discusses doses to inadvertent intruders following release of volatile radionuclides to the atmosphere.

The discussion of possible exposure scenarios for inadvertent intruders in Sect. 3.2.4 shows that only three scenarios need be considered in the analysis for the EAV. All of these scenarios involve chronic exposure and, thus, are subject to a limit on EDE from all exposure pathways of 100 mrem per year. These scenarios include 1) an agriculture scenario involving direct intrusion into disposal units at any time after the concrete vaults and any other engineered barriers above the waste have lost their structural and physical integrity and excavation into the waste becomes credible, 2) a resident scenario involving permanent residence in a home located immediately above an intact concrete roof or other engineered barrier at any time after loss of active institutional control, and 3) a post-drilling scenario involving exhumation of waste from a disposal unit at any time after drilling through a disposal unit becomes credible. The discussion in Sect. 3.2.4 shows that other scenarios involving chronic or acute exposure either are not credible for the EAV, would result in lower doses than the scenarios considered in the analysis, or are subject to a higher dose limit in the case of acute exposure scenarios (i.e., 500 mrem) and, thus, would be less restrictive than the chronic exposure scenarios considered in the analysis.

The models for estimating dose for the three chronic exposure scenarios for inadvertent intruders considered in this analysis are presented in Appendix A.4.5.2. The inputs to the model for each scenario are the maximum concentrations of radionuclides in the disposal facility at any time after the scenario is first assumed to be credible. The concentrations of radionuclides in disposal units over time are estimated using the initial concentrations at disposal corrected for radioactive decay. Depletion of radionuclide inventories in disposal units due to removal by infiltrating water also is considered in some cases, particularly for long-lived isotopes of uranium. In these cases, the ingrowth of radiologically significant decay products at times long after disposal is potentially important in the intruder dose analysis. The models for the agriculture, resident, and post-drilling scenarios are summarized in Tables A.4-14, A.4-15, and A.4-16, respectively, of Appendix A.4. For each radionuclide and exposure scenario, the factor in the appropriate table gives the EDE in rem per year for a unit

concentration in the disposal facility of 1 $\mu Ci/m^3$. Thus, for any scenario, the annual dose from any radionuclide is simply obtained by multiplying the estimated concentration in the disposal facility at the time intrusion is assumed to occur by the factor given in the table for that scenario. The calculation of radionuclide concentrations in disposal facilities on the basis of concentrations in disposed waste is described in Sect. 4.1.5.

3.4 PERFORMANCE ANALYSIS METHODOLOGY

This section describes the computational methods used to implement conceptual models for release and transport of EAV constituents. As discussed previously, the PORFLOW-3D computer code was used for the flow and transport simulations. The simulations were conducted for three time frames: intact (as-built) vault, cracked vault, and failed roof over the vault. Separate analyses were conducted for concrete degradation and resulting structural changes to determine the timing and changes that occur when moving from one time frame to the next.

Analyses of potential pathways of transport of EAV constituents through the environment (Sect. 3.2.2) to receptors (Sect. 3.2.3 and 3.2.4) indicate that soil and groundwater concentrations will dominate the performance of the facility. Thus, the computational analyses focussed on determining concentrations in these media as the vault changes with time, and on doses received as a result of such concentrations.

These analyses were aided by the use of computer codes, which are described in detail in Appendix B. Integration of the results of various computations was accomplished in the manner outlined in Fig. 3.4-1. The manner in which each of the computer codes and analytical techniques were adapted to address the conceptual model is described in detail in the following sections.

3.4.1 Near-Field Model Analysis

Computational software (i.e., WingZ, Mathematica) and sophisticated computer codes (i.e., MINTEQ, PORFLOW) were used in the near-field analysis of the E-Area PA. The software and computer codes were applied to analyze or predict: 1) degradation of the

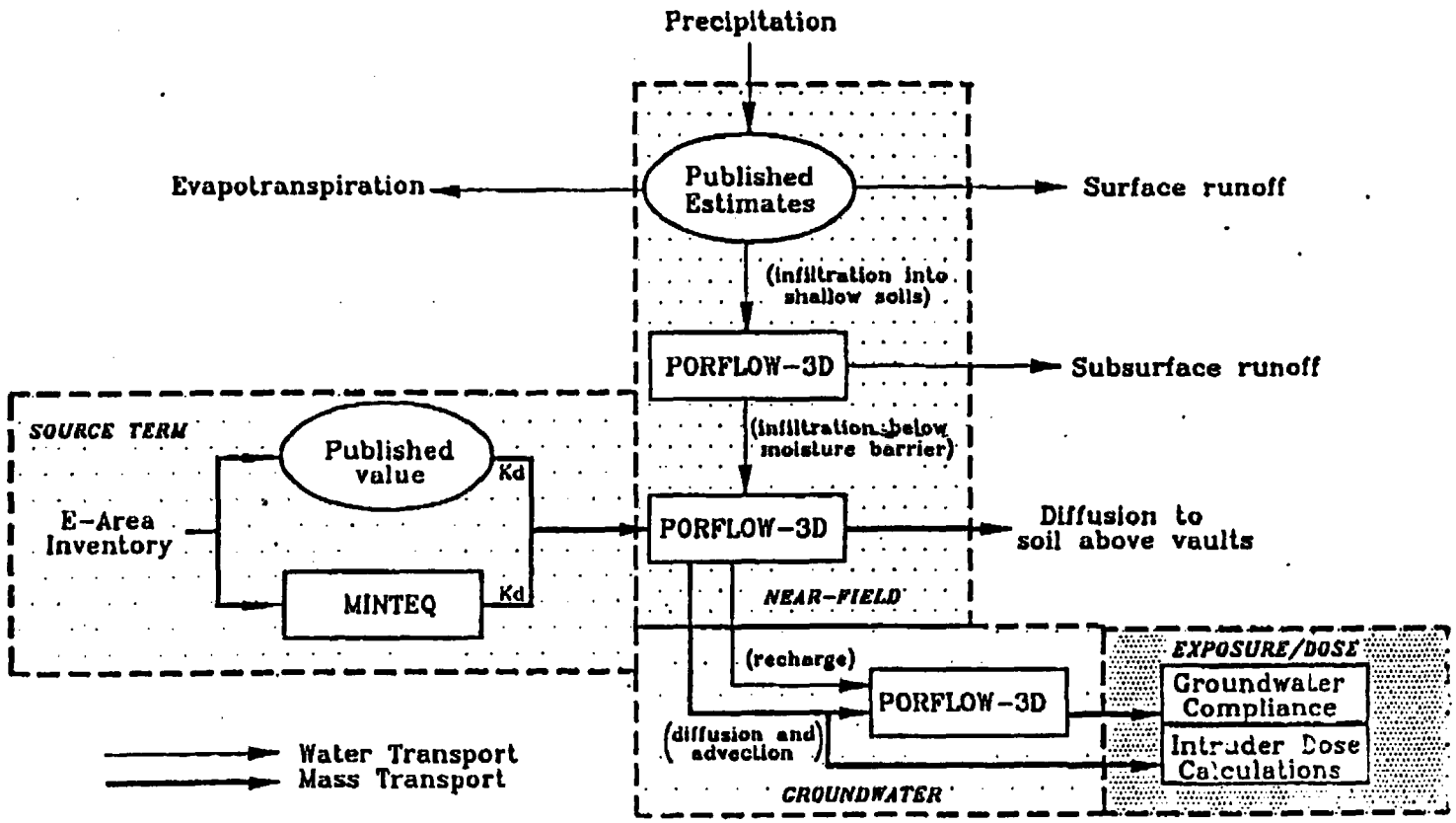

Fig. 3.4-1. Integration of computational methods for the Radiological Performance Assessment of the EAVs.

concrete; 2) screening of insignificant radionuclides; 3) geochemical conditions in the wasteform pore-fluid; 4) water flow patterns and travel-times through the vadose zone; and 5) contaminant migration patterns and fluxes to the aquifer.

A complex sequence of computations and computer simulations were performed to answer the following technical questions:

- Which of the numerous radionuclides in the wasteforms are likely to control the long-term performance of the disposal systems?
- What are the pore-fluid concentrations of the key contaminants in the wasteforms and what geochemical conditions may control the release rates?
- What is the average infiltration rate into the vadose zone?
- What are the likely water flow paths and average travel-times through the cover materials and vaults?
- What rate do the vaults degrade and how does the hydraulic conductivity of the vault change with time?
- As the cover and vaults degrade, what quantities (i.e. concentrations and fluxes) of contaminants will reach the underlying aquifer?

This section describes the computational methods and simulation approaches that were used in the near-field analysis. Methods and approaches have been divided into several sections. Both intact and degraded vault conditions were used in the PA.

Contaminant Inventory Computations

Due to the uncertainty associated with estimating future inventories, an initial activity of one curie within the model domain was used for all radionuclides. This approach was used to establish limits on the quantities of radionuclides that could be placed in the vaults rather than determining if a given inventory was acceptable. In some cases, solubility-limited simulations were made. These cases required an estimate of the initial inventory. The approach for obtaining this inventory is described in Sect. 3.1.

Concrete Degradation Computations

The general methodology of Walton et al. (1990) was used in conjunction with structural calculations to investigate degradation of the structural and hydraulic properties of the vault (Sect. 3.1.3 and Appendix K). The methodology, which consists of empirical relationships and diffusion and structural submodels, provides a basis for predicting the degradation penetration depth. To specialize the methodology for the vaults, mathematical relationships were modified to account for the specific composition of the concrete (e.g., water-to-cement ratio, carbonate content, thickness, etc.) and the pore-water chemistry (pH, carbonate, sulfate and magnesium concentrations, etc.) of the vadose zone.

Infiltration and Fluid Flow Computations

Net moisture flux at the soil surface and through the vadose zone are two primary factors controlling contaminant release and transport rates in the vadose zone. Estimates of the average annual infiltration rate at the site were obtained from previous investigations (Appendix A.1.1). The estimated infiltration rate was then used as a boundary condition for two-dimensional simulations of water flow through the clay and gravel cover and the subsurface region containing the vaults and waste.

Two-dimensional simulations of water flow through the vadose zone were performed using the PORFLOW code. These computations were used, in turn, to:

- estimate the net moisture flux through the cover (i.e., gravel-clay layers),
- define the primary flow paths (i.e., streamlines) from the soil surface, through the cover materials, backfill and vault, to the water table, and
- estimate the water travel-times (i.e., residence times) along the flow paths.

Fluid flow simulations were performed for two distinct subregions of a portion of a single vault. These subregions consisted of: 1) soil, gravel, and clay and 2) backfill, vault, and wasteform. The PORFLOW computer code was used for the flow and transport simulations.

3.4.1.1 Screening Calculations

Screening calculations for the EAVs at the SRS were conducted to limit the scope of future iterations of the PA. For simplicity and efficiency, the approach used for the screening calculations considers site characteristics (in the form of a conservative travel time and distribution coefficients) and excludes the benefits of engineered features of the vault. In this regard, the calculations should be considered conservative. Since E-Area inventories are indeterminate, a set of TVs were calculated using the screening approach. The TVs can be used to identify future waste streams (with larger inventories of given radionuclides) that require more detailed analysis. The TVs are based on extremely conservative calculations, and thus, are not limits for disposal. The simplistic nature of the calculations allowed the use of commercially available spreadsheet software.

3.4.1.2 Flow and Transport Analysis

Implementation of the conceptual near-field model of flow and transport was accomplished in the manner summarized below. Details of the simulation techniques are provided in Appendix A.1.2.

Contaminant Transport Computations

Mass transport simulations were performed to predict the distribution of the key contaminants as a function of such factors as their initial concentrations, solubilities, pore-water velocities and dispersivities. For consistency with the fluid flow computations, the PORFLOW code was used to perform two-dimensional simulations of contaminant transport. These simulations were performed for the two subregions described previously (i.e., engineered barrier and vault) and were carried out until peak concentration was obtained.

Three distinct time periods, corresponding to the stages of vault degradation, were simulated. The three stages correspond to the times when the vault is intact, cracked, and when it completely fails. Hydrologic and transport properties were adjusted at the times when the vault is projected to crack and when it subsequently fails. The timing of the changes in the vault was estimated using the degradation calculations discussed previously. The times used for the base case calculations are best estimates. Appendix K describes the ranges of conditions considered and the resulting ranges of predicted time of failure.

Changes in material properties were estimated using degradation calculations and (or) engineering judgment. The hydraulic conductivity of the cracked concrete is estimated using a semi-analytic solution. The semi-analytic solution assumes a series of equally spaced parallel cracks through the roof and floor of the vault (Sect. 3.3.1.2). Determination of the presence or absence of perched water on a fractured vault is a prerequisite to determining the potential for flow to occur through the cracks. The determination of effective permeability of cracked vaults is necessary to quantify how rapidly the water available above can be conducted through the fractured media. Since the simplified model is steady-state, all fractures are assumed to open at the time of cracking predicted by the structural models. Computational analyses are described in Appendix K.

Pore Fluid Geochemistry Computations

In order to model mass transport in heterogeneous media the concentrations of contaminants in the pore fluid of the wasteforms must be estimated and related to total concentrations in the porous media (contaminant on or in the solid phase plus contaminant in aqueous phase).

The problem of relating total inventory to pore fluid concentrations in wasteforms is complicated by several factors including: 1) precipitation/dissolution reactions involving contaminants; 2) complex formation in solution; and 3) sorption. All of these processes are poorly understood and difficult to quantify.

The chemical complexities of wasteforms were simplified to be consistent with models which consider only reversible linear sorption (i.e., K_d's). Within this context two general approaches are possible:

1) Use theoretical geochemical codes (such as MINTEQ) to estimate K_d's of each contaminant. Assume the contaminants are released from the solid by linear reversible sorption.
2) Obtain K_d's from pertinent literature for each contaminant.

Both of these approaches are used to compute initial pore solutions in the manner described in Sect. A.1.2.2. The results of the first approach are documented in Appendix D. The remainder of the contaminants of interest used only the second approach to address contaminant/cement reactions (see Table 3.3-2 for K_d's obtained).

The primary output of the flow and transport computations were: 1) fluid concentration distributions in the vault for use in intruder calculations, and 2) mass flux histories at the water table. The mass flux histories at the water table were used as input into the mass transport simulations for groundwater (Sect. 3.4.2.). In addition, the transport computations were performed in a manner allowing parametric sensitivity analysis to gain insight regarding:

- impacts of cover effectiveness on performance,
- impact of wasteform distribution coefficients on performance, and
- the impacts of hydrologic parameters on performance.

3.4.2 Groundwater Flow and Mass Transport

The code PORFLOW (Appendix B.4), developed by Analytical and Computational Research, Inc. (ACRI), was used to simulate groundwater flow and contaminant transport in E-Area. In this section, the means by which the conceptual model for groundwater (described in Sect. 3.3.2) was translated into a computer-simulated model are described.

3.4.1.1 Groundwater Flow Simulations

The problem domain consisted of a volume defined by a surface water drainage, a drainage divide, and five hydrostratigraphic units as described in Sect. 3.3.2. The model area was discretized into a three-dimensional model consisting of a 38 by 30 by 28 grid as illustrated in Fig. 3.4-2. The five horizontal zones corresponding to the hydrostratigraphic units of interest, specifically Aquifer Unit IIB2 (water table), Confining Zone IIB1-IIB2 (Tan Clay), Aquifer IIB1 (Barnwell/McBean Aquifer), Confining Unit IIA-IIB (Green Clay), and Aquifer Unit IIA (Congaree Aquifer), were defined in the model input by specifying different hydrologic characteristics for each zone.

The northern model boundary, defined by UTR Creek, was designated as a constant head boundary for all of the hydrostratigraphic units. The tributary streams of Crouch and an unnamed Branch are simulated within the problem domain. The western and eastern boundaries for the problem domain were placed at significant distances to minimize influences and were defined as no-flow boundaries because they coincide approximately with groundwater divides in the upper two aquifers. The southern boundary was located along the watershed divide. For Aquifer Unit IIB2 and IIB1 and Confining Units IIB1-IIB2 and IIA-IIB, the watershed divide was defined as a no-flow boundary consistent with Toth's (1962) approach for defining regional flow. For Aquifer Unit IIA (Congaree Aquifer), the southern boundary was defined as a constant-flux boundary, reflecting the regional flow characteristics of this aquifer. The base of Aquifer Unit IIA was considered as a constant flux boundary reflecting small quantities of recharge from the underlying Ellenton Formation.

Hydraulic parameters used in the model are discussed in Sect. 3.3.2 and A.2. Recharge to the system of 40 cm/year was used based on the analysis in Appendix A.1.1.

Model calibration

Using the saturated flow option of PORFLOW, steady-state groundwater flow conditions were simulated and a potentiometric map for the Aquifer Unit IIB2 (water table aquifer) was generated based on the head values calculated by the model (Fig. 3.4-3). To calibrate the

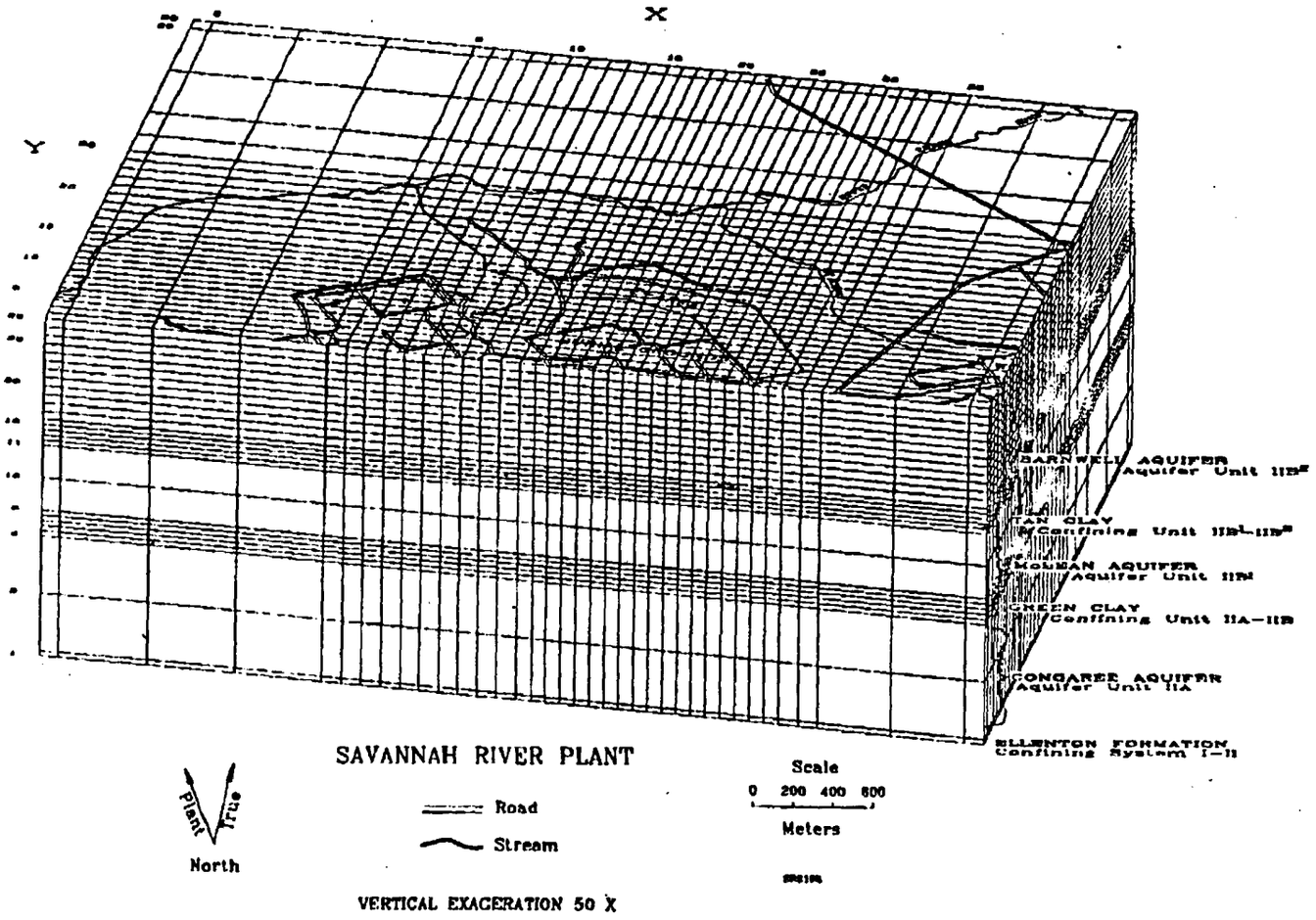

Fig. 3.4-2. Model domain for PORFLOW simulations of groundwater at E-Area.

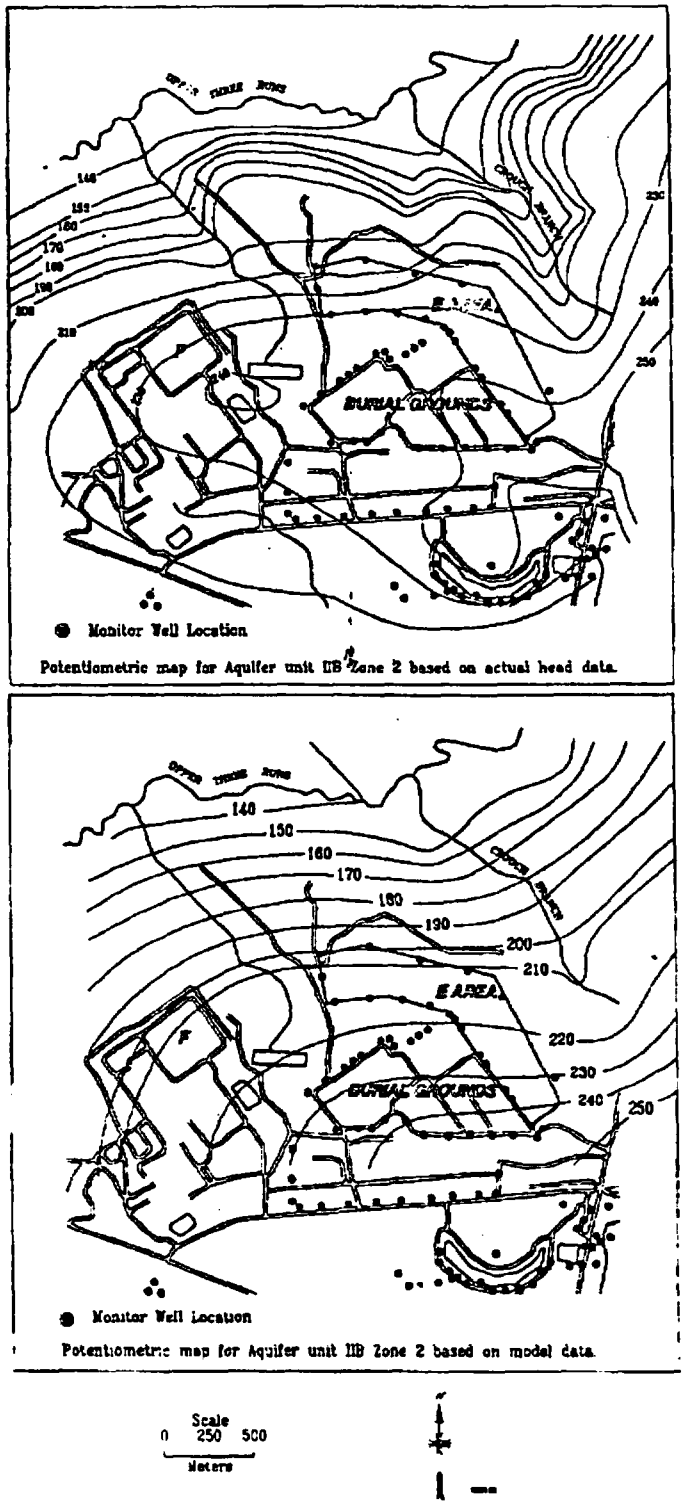

Fig. 3.4-3. Actual potentiometric surface for Aquifer Unit IIB, Zone 2 (water table), and simulated surface for Aquifer Unit IIB, Zone 2.

groundwater flow model, the model-based potentiometric map was compared with potentiometric maps generated from actual water level data from E-Area. Hydraulic parameters were adjusted within the range of observed values to attain the closest comparison between the two types of maps. This calibration process was also completed for Aquifer Unit IIB1 (Barnwell/McBean Aquifer) (Fig. 3.4-4) and for Aquifer Unit IIA (Congaree) (Fig. 3.4-5). The impact of hydraulic parameters in obtaining a calibrated model are discussed in Sect 4.2.2, where a sensitivity analysis of PORFLOW is described.

Model validation

True validation of the calibrated PORFLOW model requires that the model be capable of accurately predicting flow and transport responses when changes in flow conditions occur. Data are not available to carry out such an exercise. However, local stream flow data were obtained at selected locations along the surface creeks (Fig. 3.4-6) using conventional stream gaging techniques and used to evaluate the predictive capability of the groundwater flow model with respect to discharge to the creeks. The data collected are provided in Appendix C.2.

3.4.2.2 Contaminant Transport Simulations

Contaminant transport simulations used to assess the impact of the EAVs on the underlying groundwater system were dependent on the calibrated flow model and the source input values from the overlying unsaturated zone. Data files for contaminant transport simulations relied on the groundwater flow velocity vectors calculated from the steady-state simulations. During actual contaminant transport, the flow simulation portion of the model was disabled and advective movement of the contaminants were calculated from the steady-state velocity values.

Contaminant fluxes at the water table, obtained as described in Sect. 3.4.1, were injected at nodes that corresponded to the water table elevation beneath the vaults. Areas where contamination was injected into the groundwater system are shown in Fig. 3.4-7.

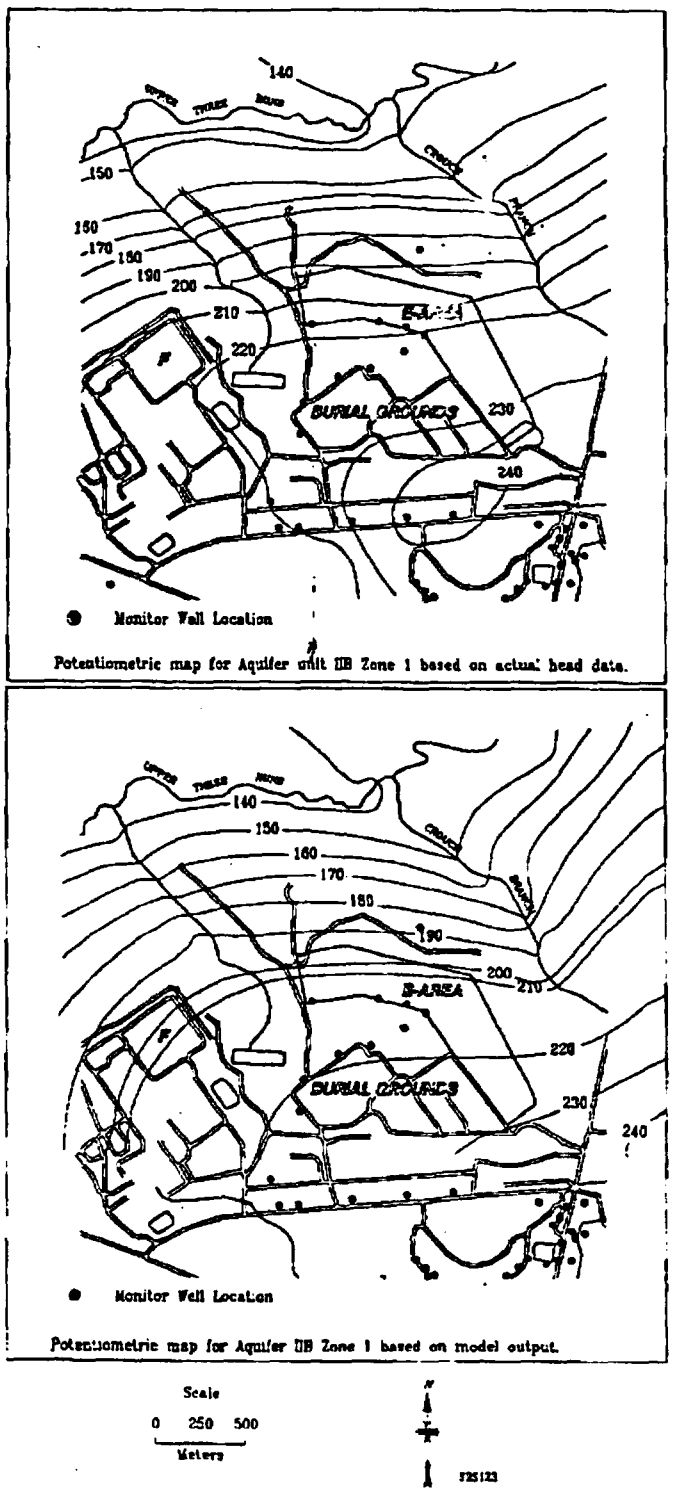

Fig. 3.4-4. Actual potentiometric surface for Aquifer Unit IIB, Zone 1 (Barnwell/McBean), and simulated surface for Aquifer Unit IIB, Zone 1.

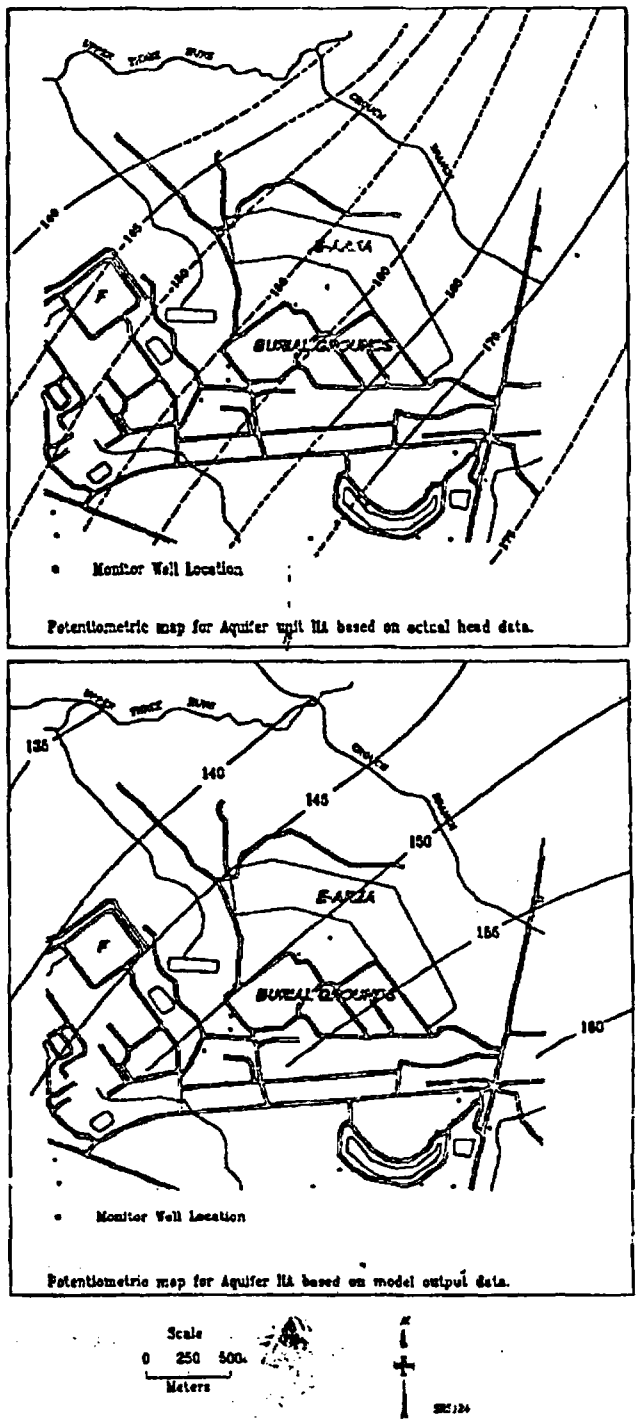

Fig. 3.4-5. Actual potentiometric surface for Aquifer Unit IIA (Congaree) and simulated surface for Aquifer Unit IIA.

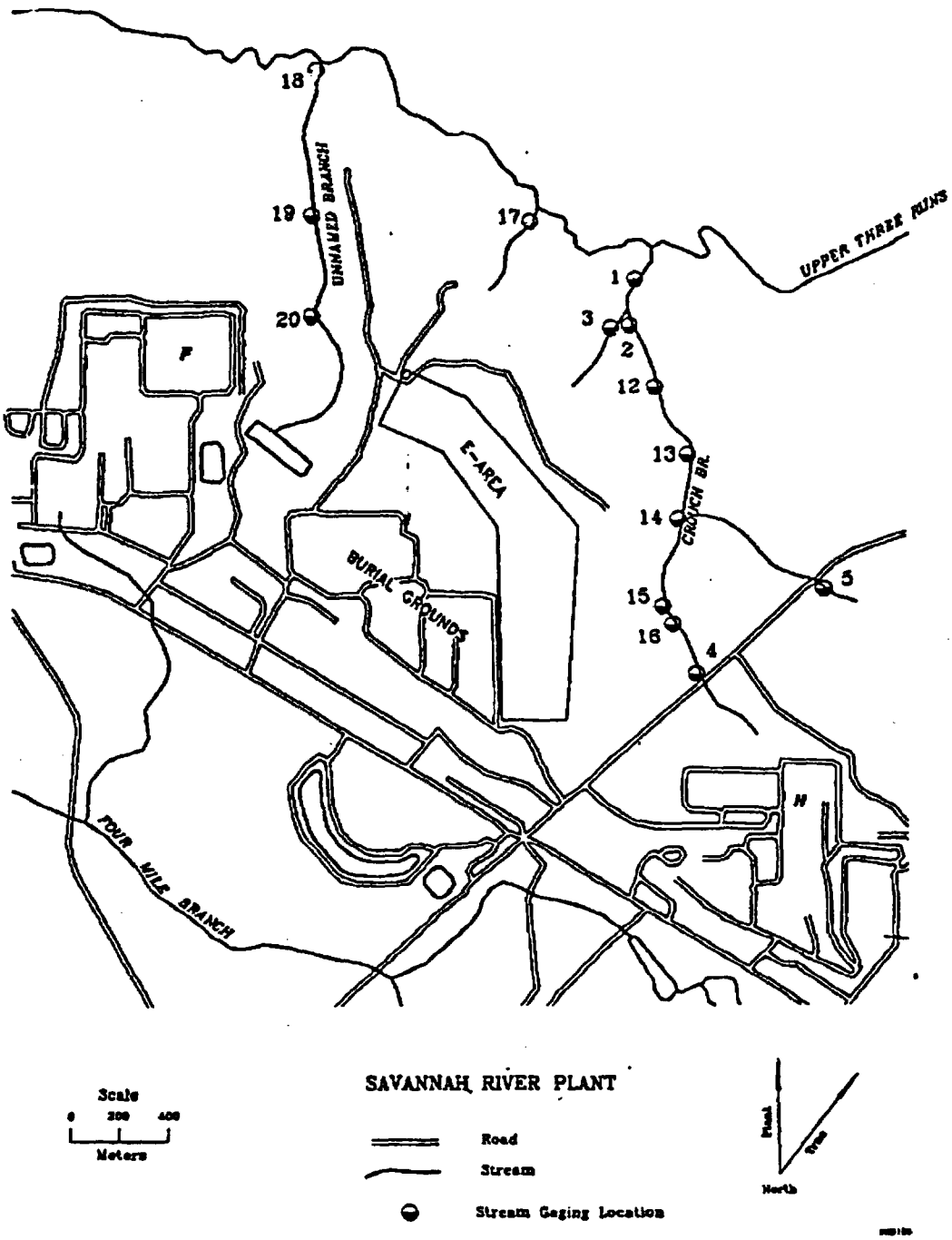

Fig. 3.4-6. Locations of stream-gaging stations in creeks near E-Area.

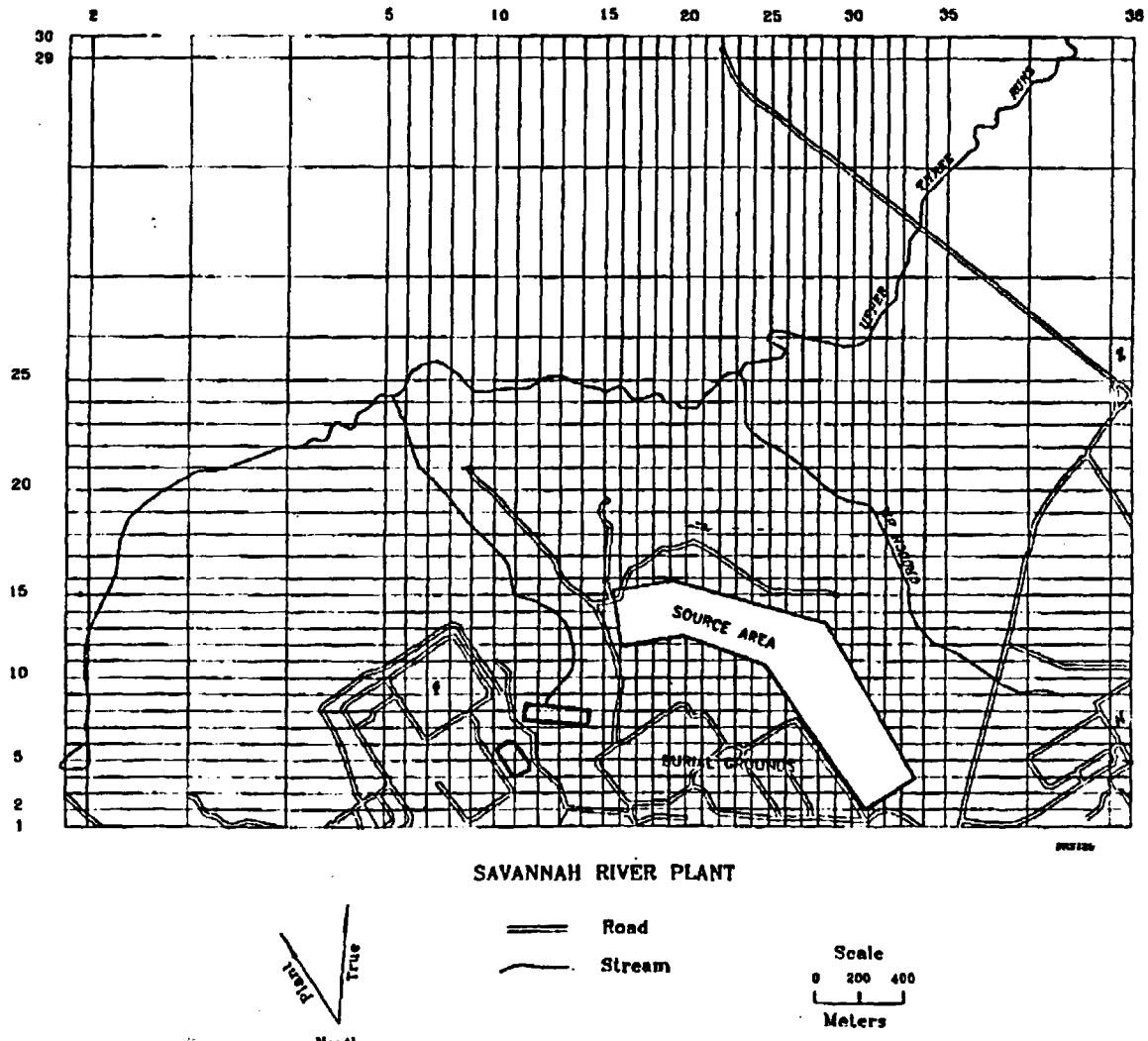

Fig. 3.4-7. Illustration of EAV source area in PORFLOW grid.

3.4.3 Methods for Dose Analysis

3.4.3.1 Protection of Off-Site Individuals and Groundwater

Calculations of the maximum concentrations of radionuclides in groundwater at any location beyond the 100-m buffer zone were obtained from the models to generate source terms and describe transport in the near-field region and groundwater (Sect. 3.4.1 and 3.4.2).

Doses to the off-site members of the public resulting from use of contaminated groundwater beyond the 100-m buffer zone around all disposal units were not directly estimated. Rather, comparisons of maximum perdicted groundwater concentrations with the more restrictive of either MCLs (Table 3.2-1) or allowable concentrations based on the 25-mrem per year performance objective were made. The allowable concentrations were calculated by dividing 25 mrem per year by the EDE per unit concentration in drinking water (Table A.4-6, Sect. A.4). These calculations are simple, were performed by hand, and checked several times for accuracy.

3.4.3.2 Intruder Dose Analysis

Doses to inadvertent intruders into the EAV following loss of active institutional control were estimated. The different exposure scenarios assumed in the analysis are discussed in Sect. 3.2.4 and the models and parameter values are presented in detail in Appendix A.4. Because of the hypothetical and prospective nature of the intruder scenarios and dose estimates, simple multiplicative-chain models which assume that the concentrations of radionuclides are in equilibrium in all parts of the intruder's exposure environment are used in the intruder dose analysis. The use of such models had the advantage that unnecessarily complex computer codes are avoided. The models and data bases presented in Appendix A.4 describe the calculations in their entirety.

In practice, the models are sufficiently simple that all calculations can be performed by hand, and this approach normally was used. The calculations were checked several times for accuracy.

3.5 QUALITY ASSURANCE (QA)

Contributors to this RPA conducted pertinent activities of the project under the guidance of the provisions of the American National Standards Institute (ANSI)/American Society of Mechanical Engineers (ASME) Nuclear Quality Assurance (NQA)-1 Program Requirements for Nuclear Facilities (NRC 1989), as required by the DOE Order 5820.2A (U.S.DOE 1988a). The manner in which the nineteen basic elements of NQA-1 are implemented by Oak Ridge National Laboratory (ORNL), the RPA coordinator, is shown in Table 3.5-1. In this table, the ORNL documented QA procedure which implements the specified element of NQA-1 is listed. Some aspects of all nineteen elements of NQA-1 applied to this RPA. Procedures are documented in the ORNL QA Manual (*Oak Ridge National Laboratory Quality Assurance Manual* current edition), the ORNL Pollutant Assessments Group Procedures Manual (1992), and the Software QA Plan (*Software Quality Assurance Plan for PORFLOW* 1991) produced specifically for the PORFLOW computer code used in this assessment. Table 3.5-2 presents similar information for INEL.

Software QA plans were written by each DOE contractor contributing to this RPA, addressing the provisions of ASME NQA-2a, Part 2.7, *Quality Assurance Requirements of Computer Software for Nuclear Facility Applications*. These QA plans were transmitted to WSRC for review and approval.

Copies of the Software QA Plans submitted are in Appendix F. A surveillance was conducted by WSRC at all contractor sites after the RPA project was underway, for the purpose of evaluating adherence to governing QA procedures described in the submitted QA plans and general project integration. Observations and findings from these surveillances are on file at WSRC. Corrective action was taken in response to these findings, and responses made to observations.

Table 3.3-1. Implementation of NQA-1 by ORNL for the FAVDS RPA

NQA-1 basic element	Implementing ORNL QA procedures[a]	Location of project-specific procedure
1. Organization	QA-L-1-100	a,b,c
2. Quality Assurance Program	QA-L-2-100 QA-L-2-101 QA-L-2-103 QA-L-2-105 QA-L-2-106	a,b,c,d,e
3. Design Control	QA-L-3-100 QA-L-3-101 QA-L-3-102	b,c
4. Procurement Document Control	QA-L-4-100 QA-L-4-101	b,c
5. Instructions, Procedures, and Drawings	QA-L-5-100	b,c
6. Document Control	QA-L-6-100	c
7. Control of Purchased Items and Services	QA-L-7-100 QA-L-7-101 QA-L-7-102	b,c
8. Identification and Control of Items	QA-L-8-100	b,c
9. Control of Processes	QA-L-9-100	b,c
10. Inspection	QA-L-10-100	b,c
11. Test Control	QA-L-11-100	b,c
12. Control of Measuring and Test Equipment	QA-L-12-100	b,c
13. Handling, Storage, and Shipping	QA-L-13-100	b,c
14. Inspection, Test, and Operating Status	QA-L-14-100 QA-L-14-101	b,c

Table 3.5-1. (continued)

NQA-1 basic element	Implementing ORNL QA procedures[a]	Location of project-specific procedure
15. Control of Nonconforming Items	QA-L-15-100	[b,c]
16. Corrective Action	QA-L-16-100 QA-L-16-101 QA-L-16-102 QA-L-16-103	[b,c]
17. Quality Assurance Records	QA-L-17-100	[b,c]
18. Audits and Surveillances	QA-L-18-100 QA-L-18-101 QA-L-18-102	[b,c]
19. Software	QA-L-19-100	[b,c]

[a] *Source: Oak Ridge National Laboratory Quality Assurance Manual* (current edition).

[b] *Source: Software Quality Assurance Plan for PORFLOW-3D* (1991), Appendix F.

[c] *Source: ORNL Pollutant Assessments Group Procedures Manual* (1992).

[d] *Source:* U.S.DOE (1991).

[e] *Source: Quality Assurance Program Requirements for Nuclear Facilities* (1989).

Table 3.5-2. Implementation of NQA-1 by INEL for the EM Work RPA

NQA-1 basic element	Implementing INEL QA procedures*	Location of project-specific procedure
1. Organization	QP-1	*
2. Quality Assurance Program	QP-2 QP-2 QP-2 QP-2 QP-2	*
3. Design Control	QP-3 QP-3 QP-3	*
4. Procurement Document Control	QP-4 QP-4	*
5. Instructions, Procedures, and Drawings	QP-5	*
6. Document Control	QP-6	*
7. Control of Purchased Items and Services	QP-7 QP-7 QP-7	*
8. Identification and Control of Items	QP-8	*
9. Control of Processes	QP-9	*
10. Inspection	QP-10	*
11. Test Control	QP-11	*
12. Control of Measuring and Test Equipment	QP-12	*
13. Handling, Storage, and Shipping	QP-13	*
14. Inspection, Test, and Operating Status	QP-14 QP-14	*

Table 3.5-2. (continued)

NQA-1 basic element	Implementing INEL QA procedures[a]	Location of project-specific procedure
15. Control of Nonconforming Items	QP-15	[a]
16. Corrective Action	QP-16 QP-16 QP-16 QP-16	[a]
17. Quality Assurance Records	QP-17	[a]
18. Audits and Surveillances	QP-18 QP-18 QP-18	[a]
19. Software	EG&G-EELS-106666	[b]

[a] *Source: EG&G Idaho Inc. Quality Manual - Policy and Procedures* (current edition).

[b] *Source: Software Quality Assurance Plan for PORFLOW-3D* (1993), Appendix F.

4. RESULTS OF ANALYSIS

In this chapter, the results of the analysis of performance of the EAV, conducted in accordance with the conceptual models and methodologies described in the previous chapter, are presented. Predicted releases to the environment, resulting concentrations, results of dose analysis, and allowable inventories are presented in Sect. 4.1. The results of the sensitivity and uncertainty analyses that were conducted to gain perspective on the meaning of the results are provided in Sect. 4.2.

4.1 ANALYSIS RESULTS

In this section, results of the computational analyses that estimate the potential radiological impact of the EAV are provided. Maximum concentrations of radionuclides in exposure media and estimated doses based on these maximum values are tabulated. The radionuclide concentrations in groundwater are provided in Sect. 4.1.3.

In Sect. 4.1.1, the results of a screening analysis for the groundwater pathway are presented. Since the specific radionuclides that may be encountered in the waste during disposal operations are not known, a conservative screening method was used to determine the allowable inventories of a large suite of radionuclides, which may be encountered during disposal operations. These limits are called "trigger values" (TVs) and indicate the inventory at which the performance objectives may be exceeded. A detailed, site-specific analysis is recommended for a given radionuclide before additional inventories above the TVs are placed in E-Area for disposal. Radionuclides which have relatively small TVs are included in the detailed site-specific analysis, especially if an inventory above the TV is likely to occur in future waste.

In Sect 4.1.2, the near-field model results are presented. The predicted unsaturated flow field through the facility and estimated fluxes of radionuclide constituents in the waste to the water table are described.

4. RESULTS OF ANALYSIS

In this chapter, the results of the analysis of performance of the EAV, conducted in accordance with the conceptual models and methodologies described in the previous chapter, are presented. Predicted releases to the environment, resulting concentrations, results of dose analysis, and allowable inventories are presented in Sect. 4.1. The results of the sensitivity and uncertainty analyses that were conducted to gain perspective on the meaning of the results are provided in Sect. 4.2.

4.1 ANALYSIS RESULTS

In this section, results of the computational analyses that estimate the potential radiological impact of the EAV are provided. Maximum concentrations of radionuclides in exposure media and estimated doses based on these maximum values are tabulated. The radionuclide concentrations in groundwater are provided in Sect. 4.1.3.

In Sect. 4.1.1, the results of a screening analysis for the groundwater pathway are presented. Since the specific radionuclides that may be encountered in the waste during disposal operations are not known, a conservative screening method was used to determine the allowable inventories of a large suite of radionuclides, which may be encountered during disposal operations. These limits are called "trigger values" (TVs) and indicate the inventory at which the performance objectives may be exceeded. A detailed, site-specific analysis is recommended for a given radionuclide before additional inventories above the TVs are placed in E-Area for disposal. Radionuclides which have relatively small TVs are included in the detailed site-specific analysis, especially if an inventory above the TV is likely to occur in future waste.

In Sect 4.1.2, the near-field model results are presented. The predicted unsaturated flow field through the facility and estimated fluxes of radionuclide constituents in the waste to the water table are described.

Table 4.1-1. Trigger values for radionuclides selected for detailed groundwater analysis.

	Trigger Value (Ci/vault)	
Nuclide	LAWV	ILNT
H-3	2.8×10^{0}	3.4×10^{-1}
C-14	7.0×10^{-1}	8.5×10^{-2}
Ni-59	1.1×10^{3}	1.3×10^{2}
Se-79	4.1×10^{-1}	5.1×10^{-2}
Sr-90	2.5×10^{1}	3.1×10^{0}
Tc-99	2.8×10^{-1}	3.5×10^{-2}
Sn-126	5.2×10^{0}	6.3×10^{-1}
I-129	1.9×10^{-3}	2.3×10^{-4}
Cs-135	9.3×10^{0}	1.1×10^{0}
Th-232	1.6×10^{-1}	1.9×10^{-2}
U-233	1.2×10^{-1}	1.5×10^{-2}
U-234	1.2×10^{-1}	1.5×10^{-2}
U-235	6.3×10^{-2}	7.7×10^{-3}
U-236	1.3×10^{-1}	1.6×10^{-2}
U-238	1.3×10^{-1}	1.6×10^{-2}
Np-237	1.7×10^{-3}	2.1×10^{-4}
Pu-238	3.2×10^{2}	3.9×10^{1}
Pu-239	1.6×10^{-2}	2.0×10^{-3}
Pu-240	2.0×10^{-2}	2.4×10^{-3}
Pu-241	3.1×10^{1}	3.8×10^{0}
Pu-242	1.6×10^{-2}	2.0×10^{-3}
Pu-244	1.7×10^{-2}	2.0×10^{-3}
Am-241	4.4×10^{0}	5.4×10^{-1}
Am-243	2.7×10^{-2}	3.3×10^{-3}
Cm-244	7.3×10^{0}	9.0×10^{-1}
Cm-248	4.2×10^{-3}	5.1×10^{-4}
Cf-252	5.5×10^{2}	6.7×10^{1}

4.1.2.1 Engineered Barrier Simulation

The PORFLOW computer code was used to simulate the engineered barrier's effectiveness in reducing the amount of infiltrating water reaching the vault. The engineered barrier consisted of two soil layers. The upper layer was comprised of highly conductive gravel overlying a layer of low permeability clay; this system was surrounded by native backfill soil. In the design of the barrier these layers are sloped from 2 to 5%. As a measure of conservatism, the slope was taken to be 2%.

The hydraulic characteristics of each of the material types used in the simulation were discussed in Sect. 3.3.1.1. The simulation domain was 1000 cm wide and 600 cm high. Although the barriers will be emplaced over the entire vault system, it was only necessary to simulate the end 500 cm of the barrier in order to determine its performance. The physical domain simulated is shown in Fig. 3.3-2. In this simulation, the orientation of gravity was rotated clockwise in the simulation to account for the 2% slope of the barrier.

The boundary conditions for the simulation consisted of no-flow boundaries for each lateral direction. The left boundary, or boundary away from the barrier, could be considered no-flow since it was far enough away from the barrier so that the flow field was not affected and remained vertical. Admittedly, this is slightly in error due to the orientation of gravity. The placement of the right no-flow boundary is arbitrary; based on the results of the simulation it is adequately placed. Results showed that extending the simulation domain further to the right to include more of the barrier, would not change vertical flow through the barrier. The upper boundary was assigned a prescribed flux of 40 cm/year based on the results of the infiltration study (see Appendix A.1.1). The bottom boundary was also arbitrarily placed far enough away to eliminate any influence on the flow field near the barrier and was assigned a pressure head of zero.

The simulation domain was discretized into a grid of 22 horizontal and 63 vertical nodes. The grid spacing in both the horizontal and vertical directions was variable in order to improve the definition of the flow field near the barrier.

The simulation was carried out in several stages. Initially, the entire domain was treated as if it were all backfill to establish a uniform flow field. Then, the clay layer was included and the simulation was run in a transient mode until equilibrium was achieved. The gravel layer was then added and the simulation was run in a transient mode until the flow field equilibrated. Steady-state saturation is shown in Fig. 4.1-1.

In addition to monitoring the convergence of the flow field to steady state, the total water mass balance for the domain was also monitored. Until the addition of the gravel layer, the mass balance was exactly correct to the third decimal place. Upon placement of the gravel layer, the mass balance gained a slight amount of mass. The water flux in the top was 4.0×10^4 cm/year, which was exactly correct based on the 1000 cm width and the flux of 40 cm/year. The flux out the bottom was 4.014×10^4 cm/year. This corresponds to a mass balance error of 0.35%. We judged this to be adequate for determining the effectiveness of the barrier at diverting water based on these two observations: 1) the numerical techniques of reducing the time step and refining the grid about the barrier were both tried, but neither improved the mass balance; and 2) a close inspection of the numerical solution showed that the slight increase of water in the system occurred within the gravel.

The flux across two planes within the simulation domain was monitored to determine how effective the barrier was at diverting water. One flux plane extended from the left simulation boundary to the edge of the clay layer. The other flux plane went from the edge of the clay layer to the right simulation boundary. The flux through the left and right planes was 3.992×10^4 and 2.218×10^2 cm/year, respectively. The sum of these two fluxes matches the total flux out the bottom of the simulation. So, the barrier diverts approximately 99.4% of the infiltrating water.

To determine the flow rate through the moisture barrier, the gravity corrected vertical fluxes through a plane beneath the clay layer were plotted. The results are shown in Fig. 4.1-2. From this plot, it can be seen that the left boundary was placed far enough away from the edge of the barrier so as not to influence the results, because the flux at the left boundary matches the overall infiltration rate of 40 cm/year. The large amount of water being diverted around the barrier shows up as the large downward dip in the graph. Some

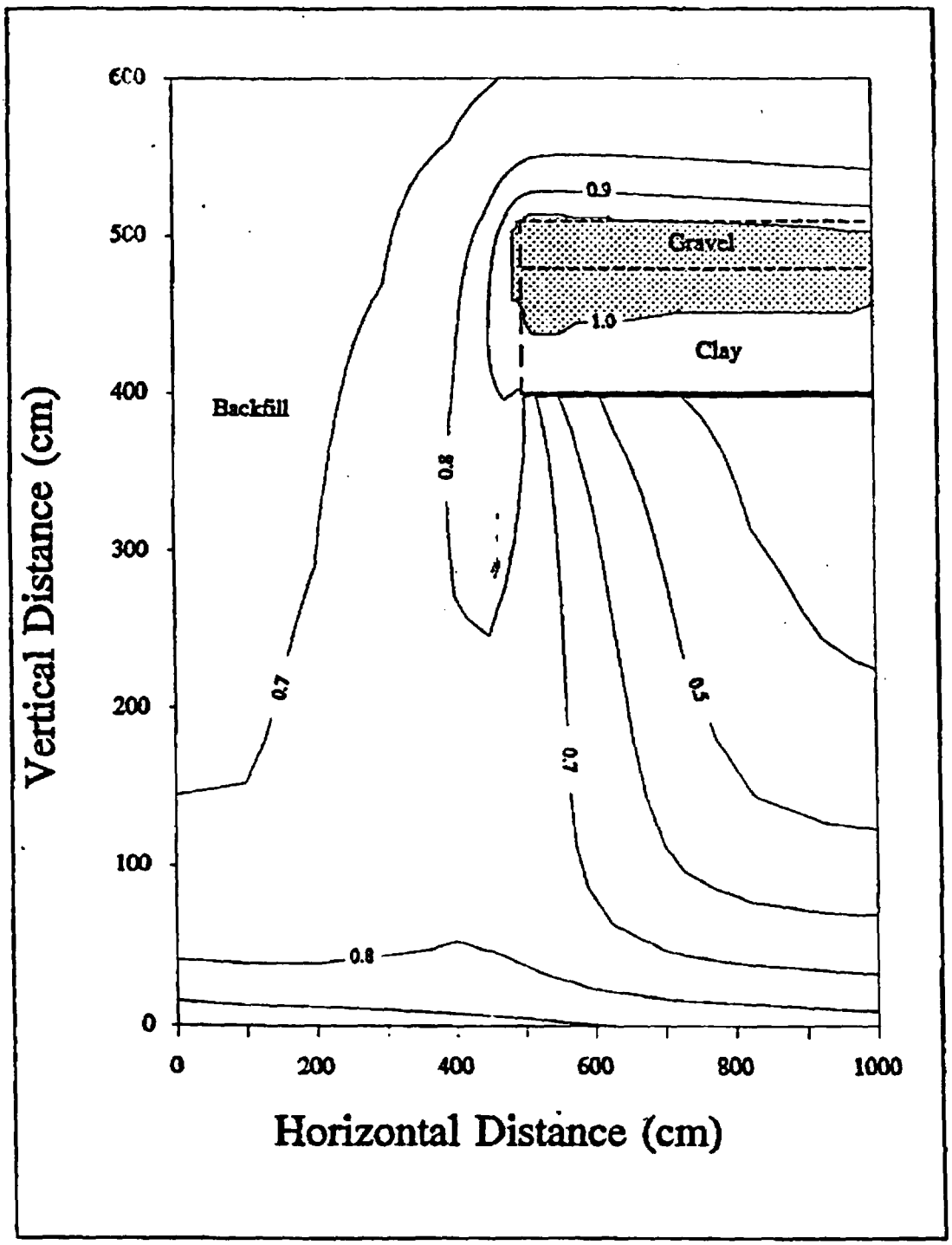

Fig. 4.1-1. Engineered barrier steady-state saturation

Rev. 0

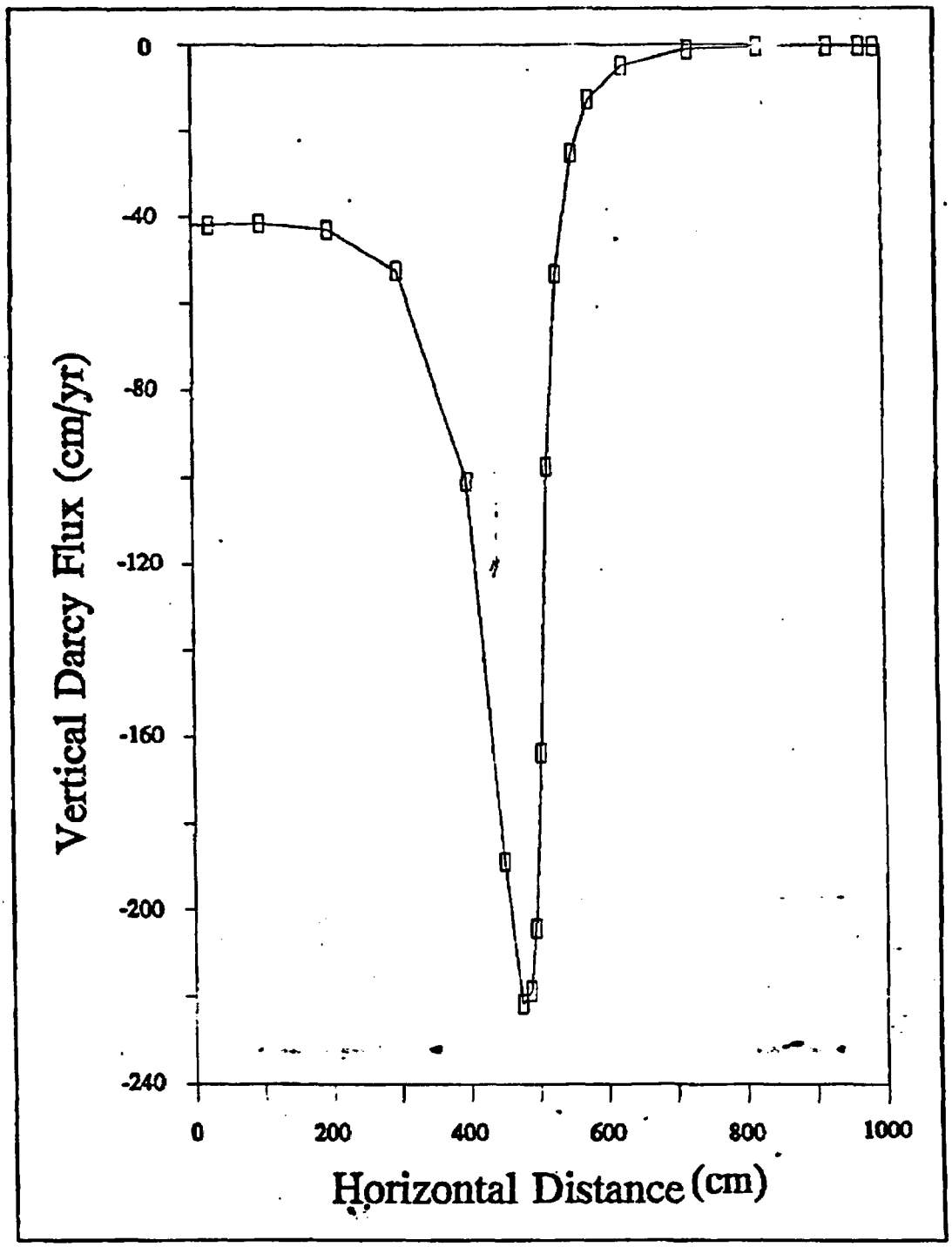

Fig. 4.1-2. Vertical fluxes beneath the engineered barrier.

water infiltrates around the end of the barrier, as can be seen by the elevated infiltration rate, which extends past 500 cm, the beginning of the gravel/clay barrier. And lastly, it appears that 500 cm of the barrier was an adequate length to establish a constant flow rate through the barrier. The vertical flux through the barrier stabilizes about 300 cm in from the end of the barrier at a value of 0.45 cm/year. While it would be appropriate to use this value as the infiltration rate for water reaching the vault, WSRC determined a more conservative value of 4 cm/year should be used as the infiltration rate through the barrier.

4.1.2.2 Vault and Waste Form Simulations

The similarities between the ILNT and ILT allowed the same conceptual design to be used for both types of vaults, whereas, the LAW vault required a different conceptual design (see Sect. 3.3.1.1). Likewise, for the simulations of solute transport the same flow fields were used for the ILNT and ILT vaults and a separate flow field was generated for the LAW vault. The physical domain in the simulation consisted of a vertical half-plane of the vaults and the surrounding backfill soil (see Figs. 3.3-3 and 3.3-4). This domain is rectangular with the vault superimposed on the right side. Since the roof of the vault slopes from the center out to the edge to increase the flow of water around the vault, the gravity vector was shifted to account for the sloped roofs. The domain was discretized into a computational grid of 46 by 72 nodes for the ILNT and ILT vaults. The LAW vault domain was discretized into a computational grid of 71 by 76 nodes. In order to make the transition from one flow field to the next easier, the same computational domain was used for all simulations.

As mentioned previously in Sect. 3.3.1.1, a three-step process was used to simulate the performance of the vaults over time. In the first time period, all engineered systems are assumed to remain intact and function as designed, so the flux into the domain was 4 cm/year. In the second period, some of the engineered barriers are assumed to begin to fail. Specifically, cracks are assumed to penetrate the entire width of the vault walls, floor, and ceiling. This was simulated by increasing the concrete permeability which causes an increase of water flowing through the vault instead of being diverted around the vault. The third and final step of the simulations was a complete failure of the members supporting the vault ceiling, causing

the ceiling to collapse. The failure of the vaults has two significant impacts on the flow of moisture through the domain. The first is the breach in the engineered barrier, causing a higher flux of water (40 cm/year) entering the domain. Second, the loss of integrity of the vault allows more water to flow through the vaults rather than being diverted around by the roof.

The upper boundary for water flow in each simulation is treated as a prescribed flux boundary with the assigned value fixed to 4 cm/year before the collapse of the vaults and increased to 40 cm/year after the failure. Because of symmetry, both lateral boundaries are prescribed as no-flux boundaries. The lateral boundary away from the vault is located halfway between adjacent vaults and the flow field there is strictly vertical. The inner boundary is located at the midpoint of the vault and the flow field is also vertical. The bottom boundary is located at the water table so a prescribed head of 0 cm is appropriate. The boundary conditions for the transport simulations were assigned as follows. Again using symmetry, the lateral boundary conditions are assigned to be no-flux. A conservative approach to the lower boundary condition is to assign a zero concentration, which serves to maximize the diffusive flux out of the domain. The upper boundary condition was also set to zero as it is the most appropriate with the flow boundary condition.

The procedure used for simulating the flow and transport in the vault region consisted of the following:

- First a domain consisting entirely of backfill was simulated with the 4 cm/year upper boundary in order to obtain a uniform initial pressure head and saturation distribution.

- The vault and waste form were then superimposed on the model space, and the upper flow boundary was kept at 4 cm/year. This new system was simulated until it reached steady state. The results of this simulation were used for the first time period in which the vault is assumed to remain intact.

- The next step was to change the hydraulic parameters to those of the cracked vault in the input file and make another flow simulation. The resulting flow field was used for the intermediate time period transport simulations.

- The final flow field was then simulated using hydraulic properties of the collapsed vault. This flow field was used for the final time interval of the transport simulations.

- The flow fields, calculated from the above steps, were used for each step of the transport simulations.

- With the exception of the solubility limited runs, all transport runs simulated a total of 200,000 years. The solubility limited runs continued until all of the mass had dissolved out of the solid phase.

Table 4.1-2 defines the simulation time for each state of the vault. Steady-state saturation fields for each time period are shown in Figs. 4.1-3, 4.1-4, and 4.1-5. The success of the flow simulation was determined by three methods. The first was by monitoring the local convergence of the flow simulation in relation to a specified convergence criterion. The PORFLOW code allows a simulation to proceed even though convergence may not be achieved at a particular time step. This was the case during the initial time steps of the flow simulation. However, as the simulations continued, the results began to converge to the specified convergence criterion. The second method involved monitoring the flow of water through the domain. Monitoring of an internal flux plane around the upper and lower boundaries allows a check to confirm if the correct amount of water was flowing through the domain. Mass balance for each flow field matched exactly (to four significant digits), except for the flow field for the intact LAW vault simulation, where the error was 0.4%, which was judged to be acceptable.

Table 4.1-2. Simulation time for each state of the vault

Vault State	ILNT	LAW
Intact	0 to 575 years	0 to 1400 years
Cracked	575 to 1050 years	1400 to 3100 years
Failed	1050 to end	3100 to end

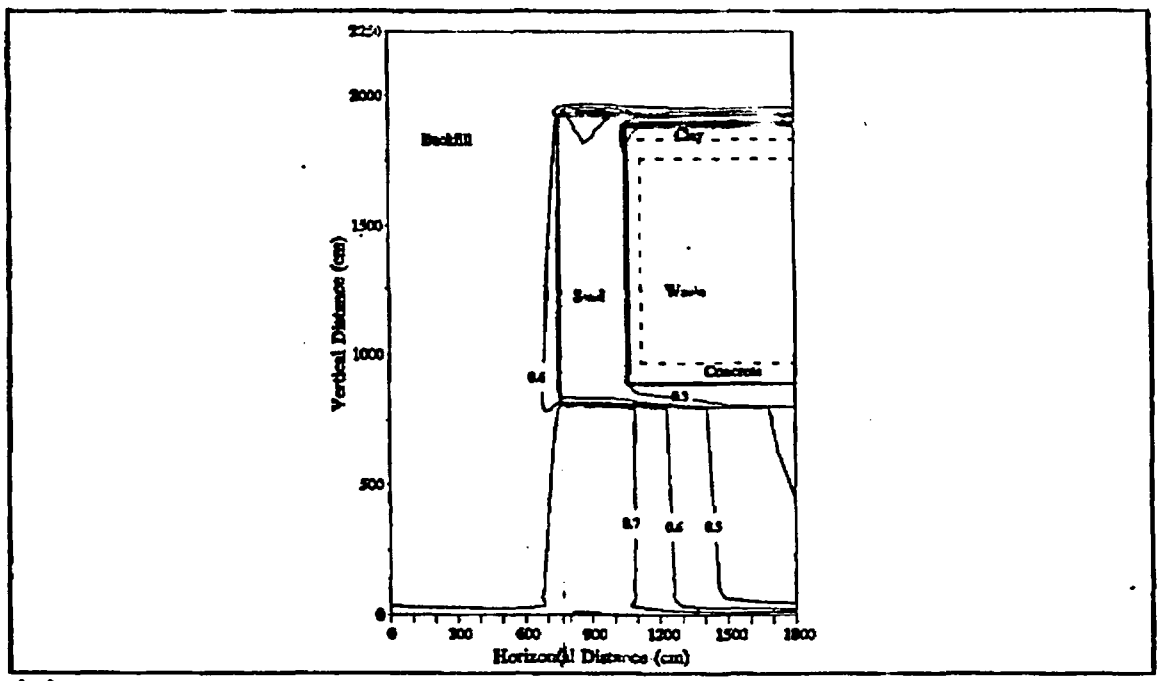

(a)

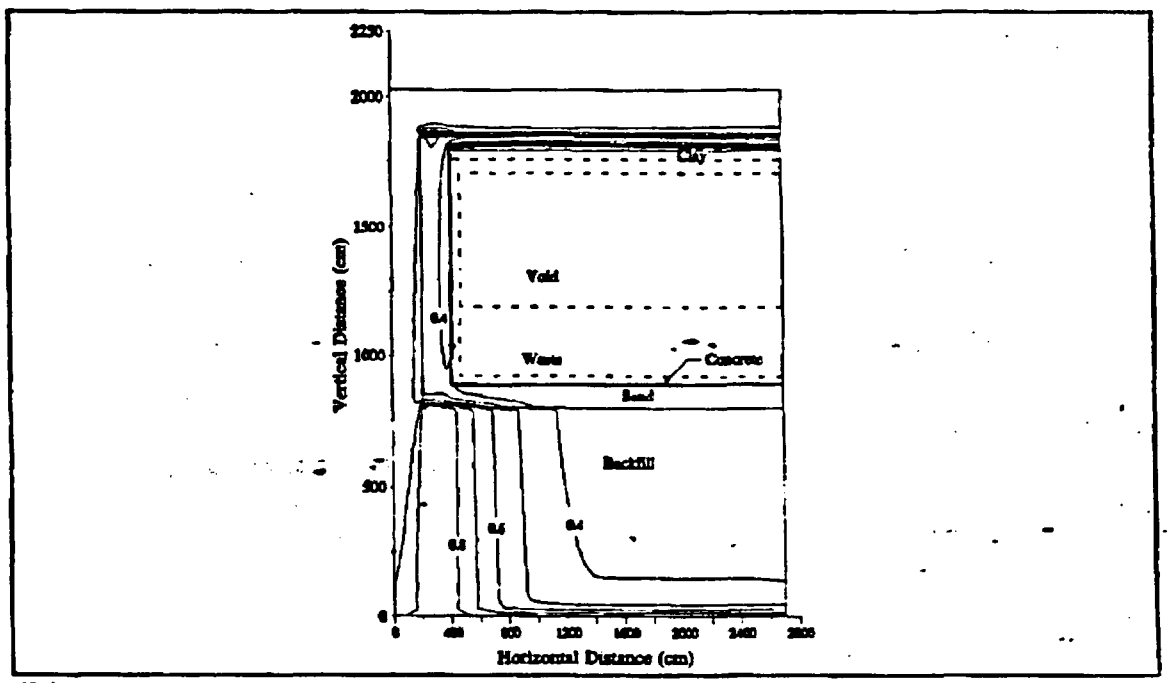

(b)

Fig. 4.1-3. Steady state saturation for the Intact period for the ILNT (a), and LAW (b) vaults.

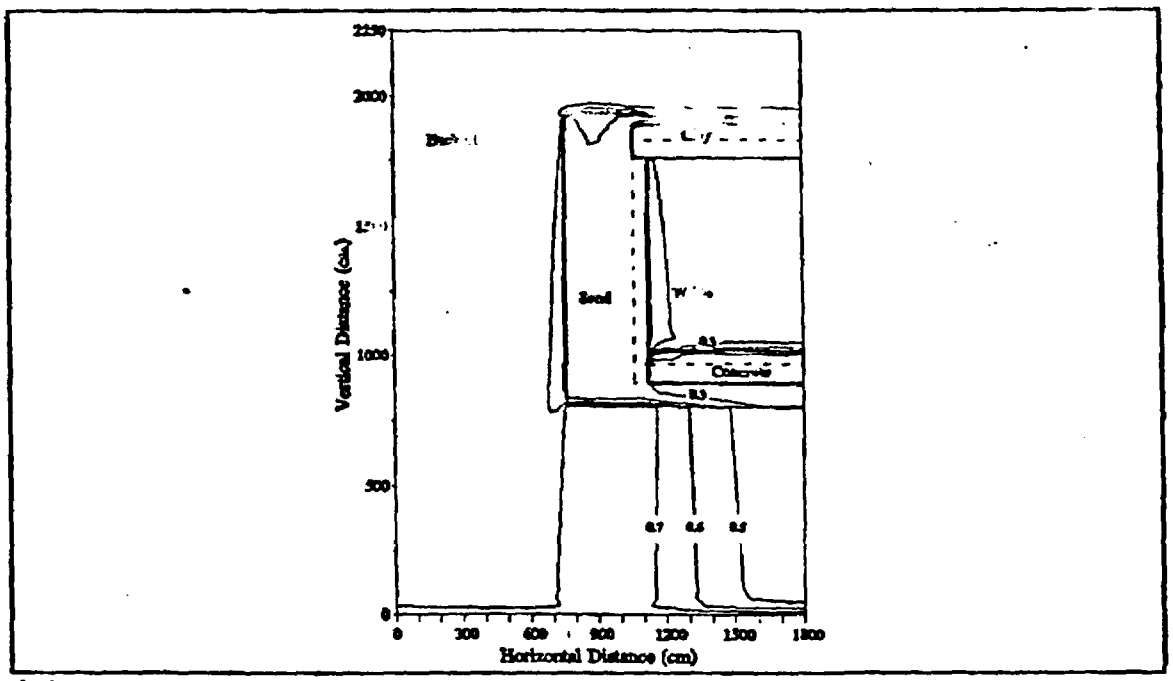

(a)

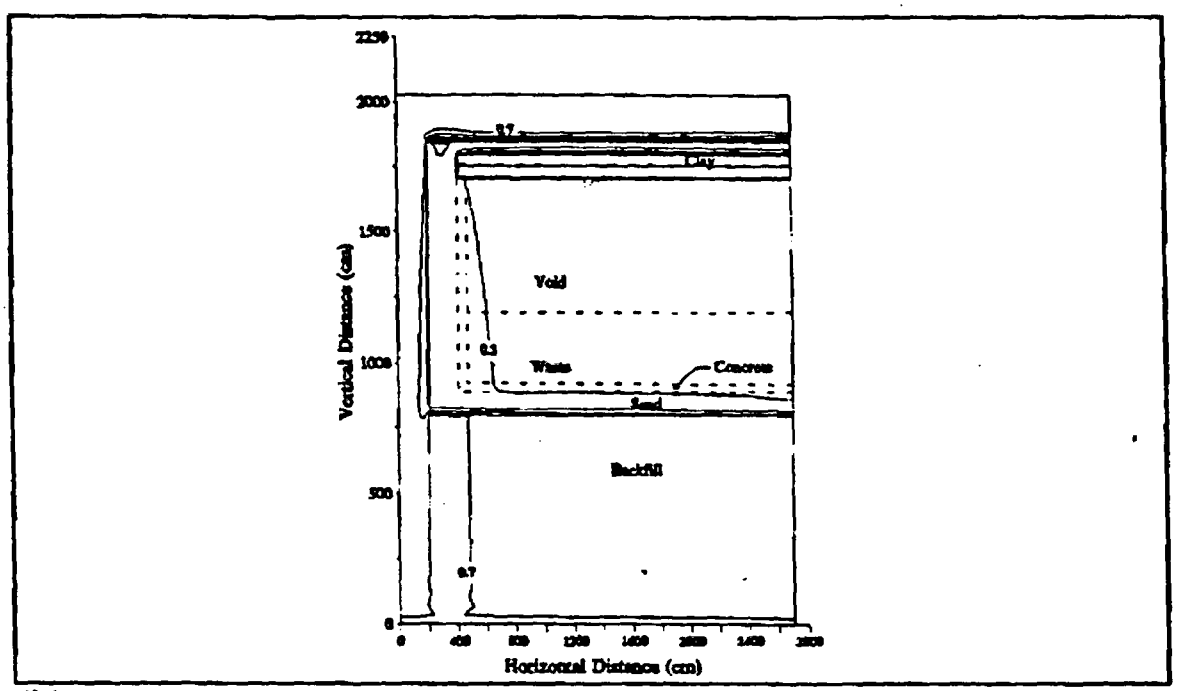

(b)

Fig. 4.1-4. Steady state saturation for the Cracked period for the ILNT (a), and LAW (b) vaults.

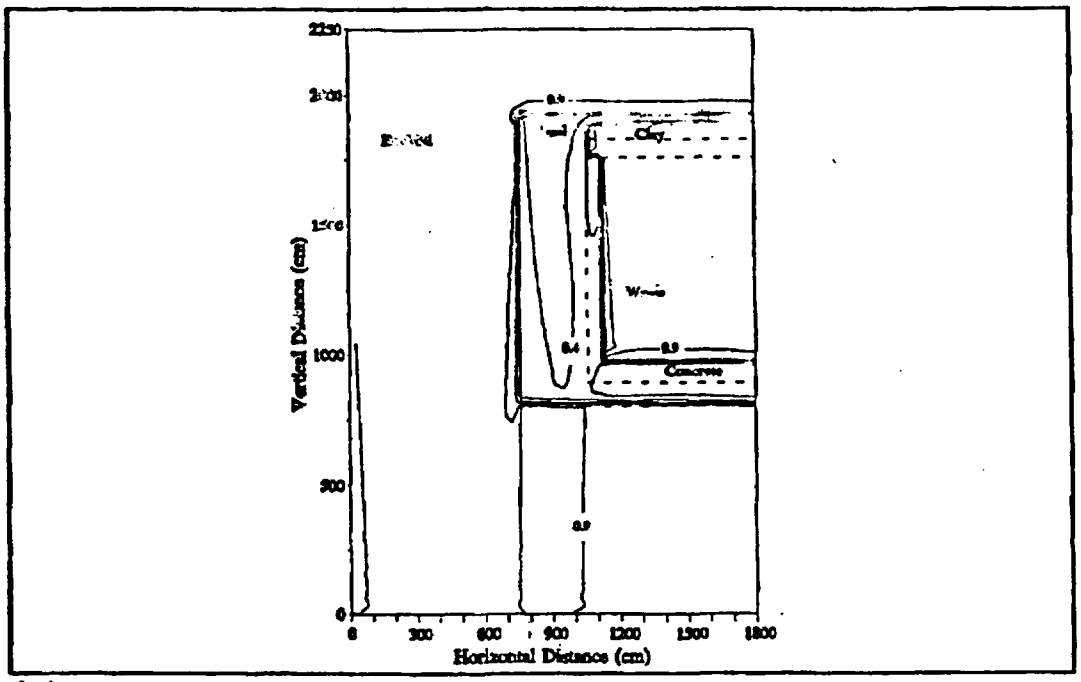

(a)

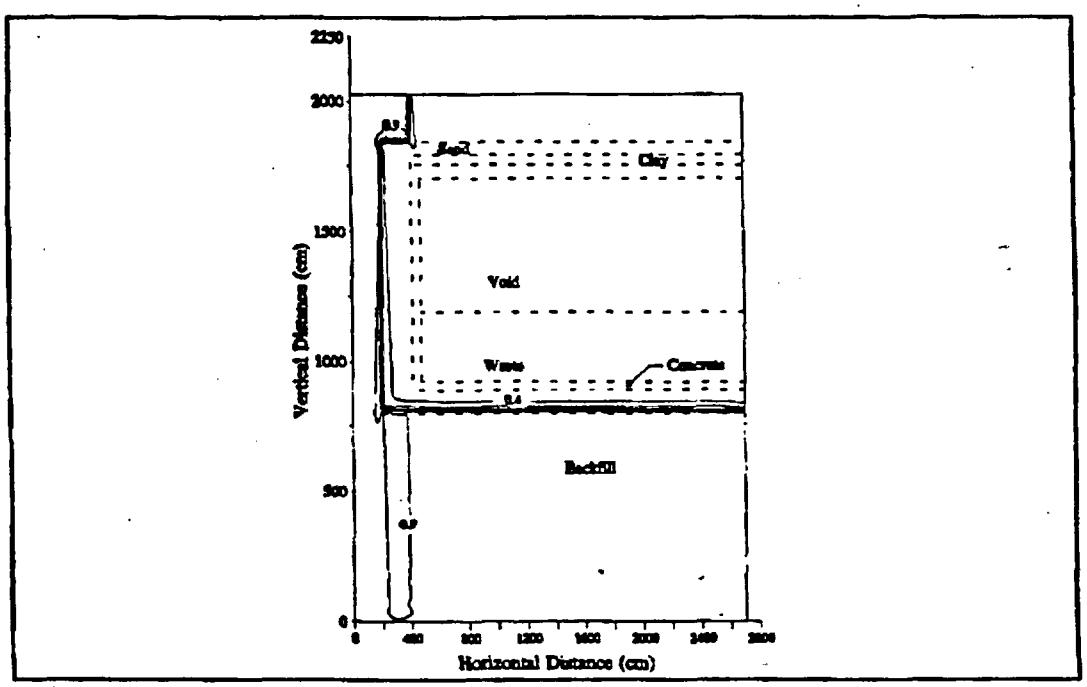

(b)

Fig. 4.1-5. Steady state saturation for the Failed period for the ILNT (a), and LAW (b) vaults.

The third method, in which a flow simulation was judged to be at steady state, was to monitor the maximum and minimum x and y velocities, pressures, and saturations. The simulations were continued until the maximums and minimums remained constant to at least 3 significant digits. The success of the transport simulation was determined through a similar mass balance approach. For each contaminant considered, all the initial mass was contained within the vault. The mass of contaminant leaving the simulation domain, via the top and bottom boundaries, was integrated over the entire simulation. For these two boundaries, the amount that left via the top boundary was always negligible. The sum of the exiting mass and the mass remaining in the domain at the end of the simulation was compared to the initial mass (for those radionuclides with a short enough half life to have an impact decay was factored into the equation). The transport mass balance errors were all less than 1%.

The flux of each radionuclide to the aquifer is needed to predict the groundwater concentration. The peak flux to the water table for each nuclide and its corresponding time are given in Table 4.1-3. Isotopes of U and Pu are not included in this table, as the fluxes of these isotopes were estimated in a different manner described below. Graphical representations of the flux to the aquifer for selected nuclides are given in Appendix A.1.4.1.

Solubility-limited simulations were conducted for isotopes of Pu and U in both vaults. The only modification to the above process for the solubility-limited simulations was to use the estimated solubility limit for each element as described in Appendix D. The initial concentrations for Pu isotopes were based upon an assumed initial inventory of 150 Ci/vault of each nuclide. The initial mass assumed for U isotopes in the transport simulations was 10,000 kg/vault. The assumed initial inventories were chosen to exceed the solubility limit. The solubility limit is the controlling factor in this type of simulation and not the initial mass.

Because the initial mass for each of the nuclides was much greater than the solubility limit, the pore water concentration coming out of the waste form was equal to the solubility-limited concentration for several thousand years. Consequently, the only reduction of the pore water concentration in the waste comes from decay during travel out of the vault and to the water table. Table 4.1-4 lists the solubility limit assumed for each nuclide and the peak flux (Ci/year) entering the aquifer from all of the ILNT and LAW vaults.

Table 4.1-3. Peak fractional mass flux release to the aquifer for EAV radionuclides except isotopes of U and Pu

Nuclide	ILNT Vaults (10)		LAW Vaults (21)	
	Fractional Flux (pCi/year-pCi)	Time (year)	Fractional Flux (pCi/year-pCi)	Time (year)
^{3}H	9.7×10^{-14}	114	5.9×10^{-11}	85
^{14}C	1.7×10^{-06}	12,000	1.4×10^{-04}	4,800
^{59}Ni	5.0×10^{-05}	14,500	2.2×10^{-04}	9,300
^{79}Se	2.9×10^{-04}	2,000	2.3×10^{-03}	3,300
^{90}Sr	1.3×10^{-16}	975	$<1 \times 10^{-20}$	<1,000
^{90}Y	3.2×10^{-19}	975	N/A	N/A
^{99}Tc	7.4×10^{-04}	1,700	1.8×10^{-03}	3,200
^{126}Sn	2.5×10^{-04}	5,600	6.7×10^{-04}	5,100
^{129}I	8.1×10^{-04}	1,100	4.3×10^{-03}	1,700
^{135}Cs	7.7×10^{-04}	2,700	8.6×10^{-04}	4,700
^{232}Th	1.1×10^{-05}	110,000	3.0×10^{-05}	55,800
^{237}Np	2.7×10^{-04}	24,800	2.3×10^{-04}	6,200
^{241}Am	3.0×10^{-11}	7,700	4.0×10^{-11}	7,400
^{243}Am	1.2×10^{-06}	19,700	3.2×10^{-05}	12,400
^{244}Cm	$<1 \times 10^{-20}$	>1,000	$<1 \times 10^{-20}$	<1,000
^{245}Cm	1.0×10^{-06}	24,200	2.8×10^{-05}	14,800
^{246}Cm	2.4×10^{-07}	20,900	1.1×10^{-05}	13,900
^{247}Cm	1.2×10^{-05}	56,500	9.7×10^{-05}	16,000
^{248}Cm	1.0×10^{-05}	48,300	9.4×10^{-05}	16,000
^{249}Bk	N/A	N/A	$<1 \times 10^{-20}$	<1,000
^{249}Cf	4.3×10^{-15}	6,900	2.7×10^{-12}	7,100
^{251}Cf	1.1×10^{-10}	10,600	3.2×10^{-08}	8,900
^{252}Cf	$<1 \times 10^{-20}$	<1,000	$<1 \times 10^{-20}$	<1,000

Table 4.1-4. Solubility limit and peak flux to the aquifer for isotopes of U and Pu*

Nuclide	Solubility Limit, g/cc	ILNT Vaults (10)		[illegible]AW Vaults (21)	
		Flux, Ci/yr	Time, year	Flux, Ci/yr	Time, year
^{233}U	7.2×10^{-11}	1.7×10^{-3}	106,000	4.8×10^{-2}	41,200
^{234}U	7.2×10^{-11}	1.0×10^{-3}	92,900	3.1×10^{-2}	44,200
^{235}U	7.2×10^{-11}	4.0×10^{-7}	83,100	1.3×10^{-6}	44,200
^{236}U	7.2×10^{-11}	1.2×10^{-5}	90,400	3.3×10^{-4}	27,600
^{238}U	7.2×10^{-11}	6.2×10^{-8}	86,600	1.7×10^{-6}	39,200
^{238}Pu	1.0×10^{-13}	6.7×10^{-18}	3,111	6.4×10^{-16}	4,410
^{239}Pu	1.0×10^{-13}	5.3×10^{-6}	64,300	1.8×10^{-5}	21,400
^{240}Pu	1.0×10^{-13}	7.6×10^{-6}	38,800	4.3×10^{-5}	29,100
^{241}Pu	1.0×10^{-13}	$<10^{-50}$	1,050	$<10^{-50}$	522
^{242}Pu	1.0×10^{-13}	5.0×10^{-7}	102,000	1.3×10^{-6}	22,000
^{244}Pu	1.0×10^{-13}	4.7×10^{-9}	99,300	1.3×10^{-7}	18,800

* Based on 150 Ci/vault for Pu and 10,000 kg/vault for U.

4.1.3 Groundwater Concentrations

Groundwater concentrations at the compliance point for groundwater protection were predicted by using the near-field results, which supplied the contaminant flux to the water table as a function of time. Fractional fluxes were specified as the source term to groundwater and the concentrations at the compliance point were specified as pCi/cc-Ci. In other words, the groundwater concentration (pCi/cc) was based upon an initial inventory in each set of vaults of one curie. The results could then be used to determine the allowable inventory limits for the EAVs. For uranium and plutonium isotopes, which are solubility limited, the flux to the water table based on an assumed inventory (Sect. 4.1.2.2) was specified as the source term to the groundwater and the concentrations at the compliance point were specified as pCi/cc. The compliance point is assumed to be the point of maximum concentration in groundwater at least 100 m from the edge of the facility, and was determined by surveying the groundwater simulation results to locate this point. The potential for plume overlap from the ILNT and LAW vaults was evaluated to determine if the overlap of these plumes resulted in a groundwater concentration greater than from ILNT or LAW vaults alone. It was determined that the maximum groundwater concentrations were not located in the area of plume overlap (see Fig. 4.1-6).

Tables 4.1-5 and 4.1-6 provide the maximum predicted contaminant concentrations at the compliance point for groundwater protection, and the time of occurrence. Results for the ILNT and LAW vaults are provided in Tables 4.1-5 and 4.1-6, respectively.

Radioactive daughter contributions to groundwater concentrations were considered in the following ways. For radionuclides that are relatively short-lived (with half-lives less than 1000 years) and that decay to longer-lived radioactive progeny, daughter contributions to groundwater radioactivity per Ci of parent activity originally in all of the vaults were estimated in the following manner. First, it was conservatively assumed that the parent radionuclide decays completely to the daughter in the vaults. This assumption neglects the loss of parent through leaching and the gradual, rather than instantaneous, nature of daughter ingrowth. The initial activity of the daughter per Ci of original inventory of parent was calculated from:

$$A_{D0} = A_{P0} \frac{\lambda_D}{\lambda_P} = \frac{\lambda_D}{\lambda_P}$$

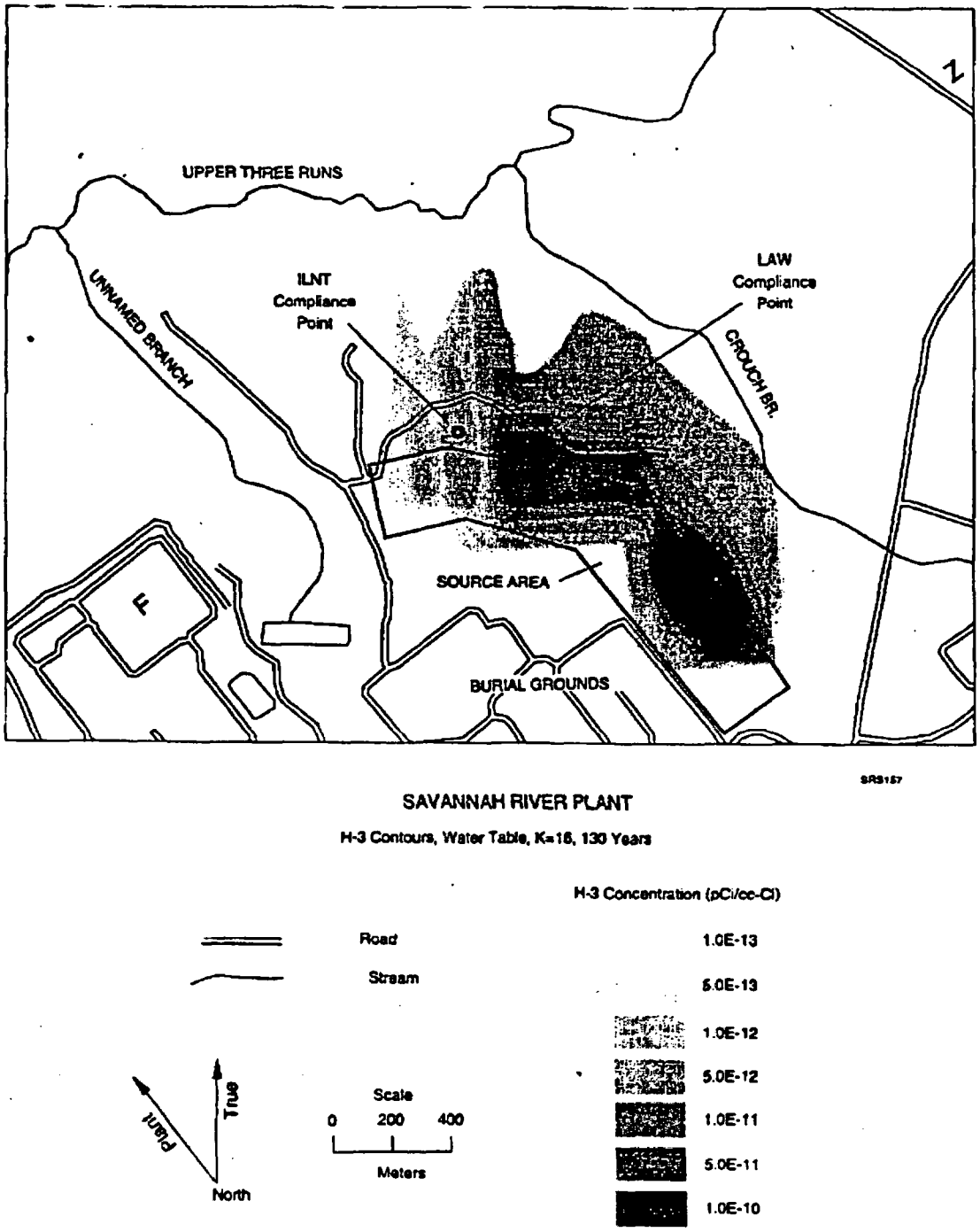

Fig. 4.1-6. Contaminant plume overlap for the LAW and ILNT vaults at E-Area.

Table 4.1-3. Predicted groundwater compliance concentration for the H-Area

Radionuclides	Groundwater Conc. at 10,000 years, (pCi/cc-Ci)[a]	Peak Groundwater Conc., (pCi/cc - Ci)[a]	Time of Peak Groundwater Conc., (years)
Am-241	----[b]	6.4×10^{-12}	9,000
Np-237	8.9×10^{-7} [c]	2.8×10^{-6} [c]	27,000
Am-243	2.3×10^{-7}	1.2×10^{-5}	27,000
Bk-249	----	----	----
Cm-245	3.7×10^{-12} [c]	1.2×10^{-9} [c]	33,000
C-14	6.5×10^{-5}	8.7×10^{-5}	12,300
Cf-249	----[b]	5.9×10^{-16}	7,900
Cm-245	1.5×10^{-9} [c]	5.0×10^{-7} [c]	33,000
Cf-251	4.7×10^{-11}	9.4×10^{-11}	13,000
Cm-247	3.6×10^{-12} [c]	2.1×10^{-8} [c]	76,000
Cf-252	----	----	----
Cm-248	1.0×10^{-12} [c]	2.5×10^{-9} [c]	72,000
Cm-244	----	----	----
Pu-240	7.3×10^{-6} [c,d]	1.2×10^{-4} [c,d]	66,000
Cm-245	3.6×10^{-8}	1.2×10^{-5}	33,000
Cm-246	1.8×10^{-8}	1.9×10^{-6}	27,000
Cm-247	6.2×10^{-8}	3.7×10^{-4}	76,000
Cm-248	1.3×10^{-7}	3.2×10^{-4}	72,000
Cs-135	----[b]	4.2×10^{-3}	6,700
H-3	----[b]	2.7×10^{-12}	130
I-129	----[b]	9.4×10^{-2}	1,400
Ni-59	3.0×10^{-5}	9.4×10^{-4}	32,000
Np-237	4.4×10^{-3}	1.4×10^{-2}	27,000
Se-79	----[b]	7.4×10^{-3}	3,000
Sn-126	2.5×10^{-3}	2.8×10^{-3}	12,000
Sr-90	----[b]	2.7×10^{-17}	1,100
Tc-99	----[b]	4.1×10^{-2}	1,800
Th-232	4.0×10^{-17}	1.5×10^{-4}	300,000

see footnotes at end of table

Table 4.1-5. (continued)

Radionuclides	Groundwater Conc. at 10,000 years, (pCi/cc)	Peak Groundwater Conc., (pCi/cc)	Time of Peak Groundwater Conc. (years)
U-233	3.5×10^{-3}	8.1×10^{-2}	160,000
Th-229	2.3×10^{-11}	—	—
U-234	2.3×10^{-3}	5.5×10^{-2}	150,000
Th-230	4.0×10^{-18}	—	—
Ra-226	3.9×10^{-3}	—	—
U-235	6.9×10^{-6}	1.9×10^{-4}	110,000
Pa-231	3.2×10^{-6} [c]	—	—
U-236	2.4×10^{-5}	5.8×10^{-4}	230,000
Th-232	1.3×10^{-19}	—	—
U-238	1.4×10^{-7}	3.0×10^{-6}	140,000
U-234	$\leq 2.3 \times 10^{-3}$	—	—
Th-230	6.4×10^{-24}	—	—
Ra-226	6.2×10^{-9}	—	—
Pu-238	— [b]	9.7×10^{-20}	3,300
U-234	$\leq 2.3 \times 10^{-3}$	—	—
Th-230	3.5×10^{-24}	—	—
Ra-226	3.4×10^{-9}	—	—
Pu-239	4.7×10^{-6}	1.5×10^{-4}	220,000
U-235	$\leq 6.9 \times 10^{-6}$	—	—
Pa-231	2.1×10^{-11}	—	—
Pu-240	7.3×10^{-6}	1.2×10^{-4}	66,000
Pu-242	2.7×10^{-7}	2.4×10^{-5}	500,000
Pu-244	2.1×10^{-9}	2.5×10^{-7}	400,000

[a] Except for isotopes of plutonium and uranium, for which groundwater concentrations are based on solubility limits, and thus, are expressed in pCi/cc per any inventory in the vaults.

[b] Peak groundwater concentration at the compliance point for groundwater protection occurred before 10,000 years.

[c] Units for radioactive daughters are pCi/cc per Ci of parent activity originally in vaults.

[d] Assumes Pu-240 reaches same concentration based on solubility-limited calculations as a daughter of Cm-244.

[e] Ac-227 daughter accounted for in EDE.

Table 4.1-6. Predicted groundwater compliance concentration for the LAW vaults

Radionuclides	Groundwater Conc. at 10,000 years, (pCi/cc-Ci)[a]	Peak Groundwater Conc., (pCi/cc - Ci)[a]	Time of Peak Groundwater Conc., (years)
Am-241	—[b]	1.1×10^{-12}	8,700
Np-237	3.2×10^{-7} [c]	3.2×10^{-7} [c]	10,000
Am-243	4.2×10^{-6}	3.7×10^{-5}	18,000
Bk-249	—	—	—
Cm-245	1.1×10^{-10} [c]	3.8×10^{-9} [c]	21,000
C-14	—[b]	1.5×10^{-3}	5,400
Cf-249	—[b]	5.0×10^{-14}	8,100
Cm-245	4.5×10^{-8} [c]	1.5×10^{-6} [c]	21,000
Cf-251	3.1×10^{-9}	3.5×10^{-9}	11,000
Cm-247	1.7×10^{-10} [c]	1.3×10^{-8} [c]	23,000
Cf-252	—	—	—
Cm-248	2.3×10^{-11} [c]	1.6×10^{-9} [c]	23,000
Cm-244	—	—	—
Pu-240	1.6×10^{-5} [c,d]	9.5×10^{-5} [c,d]	45,000
Cm-245	1.1×10^{-6}	3.7×10^{-5}	21,000
Cm-246	5.7×10^{-7}	1.0×10^{-5}	19,000
Cm-247	3.0×10^{-6}	2.2×10^{-4}	23,000
Cm-248	3.0×10^{-6}	2.1×10^{-4}	23,000
Cs-135	—[b]	6.7×10^{-4}	8,400
H-3	—[b]	2.1×10^{-10}	97
I-129	—[b]	2.4×10^{-2}	1,800
Ni-59	3.4×10^{-5}	2.1×10^{-4}	21,000
Np-237	1.6×10^{-3}	1.6×10^{-3}	10,000
Se-79	—[b]	5.1×10^{-3}	3,600
Sn-126	4.7×10^{-4}	4.7×10^{-4}	10,000
Sr-90	—[b]	1.5×10^{-22}	520
Tc-99	—[b]	1.9×10^{-2}	3,400
Th-232	1.2×10^{-17}	2.3×10^{-5}	210,000

see footnotes at end of table

Fig. 4.1-6. (continued)

Radionuclide	Groundwater Conc. at 10,000 years, (pCi/cc)	Peak Groundwater Conc., (pCi/cc)	Time of Peak Groundwater Conc., (years)
U-233	1.0×10^{-1}	4.1×10^{-1}	260,000
Th-229	1.4×10^{-11}	—	—
U-234	6.2×10^{-2}	2.9×10^{-1}	200,000
Th-230	1.6×10^{-17}	—	—
Ra-226	2.5×10^{-1}	—	—
U-235	2.0×10^{-5}	1.3×10^{-4}	230,000
Pa-231	2.1×10^{-4} [a]	—	—
U-236	7.0×10^{-4}	3.9×10^{-3}	320,000
Th-232	8.2×10^{-20}	—	—
U-238	3.4×10^{-6}	2.0×10^{-5}	230,000
U-234	$\leq 6.2 \times 10^{-2}$	—	—
Th-230	2.6×10^{-23}	—	—
Ra-226	4.0×10^{-7}	—	—
Pu-238	— [b]	1.2×10^{-18}	4,800
U-234	$\leq 6.2 \times 10^{-2}$	—	—
Th-230	1.3×10^{-23}	—	—
Ra-226	2.1×10^{-7}	—	—
Pu-239	1.0×10^{-5}	6.4×10^{-5}	160,000
U-235	$\leq 2.0 \times 10^{-5}$	—	—
Pa-231	1.3×10^{-9}	—	—
Pu-240	1.6×10^{-5}	9.5×10^{-5}	45,000
Pu-242	7.7×10^{-7}	1.0×10^{-5}	620,000
Pu-244	7.1×10^{-8}	1.5×10^{-6}	660,000

[a] Except for isotopes of plutonium and uranium, for which groundwater concentrations are based on solubility limits, and thus, are expressed in pCi/cc per any inventory in the vaults.

[b] Peak groundwater concentration at the compliance point for groundwater protection occurred before 10,000 years.

[c] Units for radioactive daughters are pCi/cc per Ci of parent activity originally in vaults.

[d] Assumes Pu-240 reaches same concentration based on solubility-limited calculations as a daughter of Cm-244.

[e] Ac-227 daughter accounted for in EDE.

where

A_{D0} = initial activity of the daughter, Ci,

A_{P0} = initial activity of the parent (= 1 Ci),

λ_D = radioactive decay constant ($.693/T_{1/2}$) of the daughter (yr^{-1}), and

λ_P = radioactive decay constant of the parent (yr^{-1}).

The peak concentration of the daughter, per Ci of parent radionuclide, was then calculated by multiplying the initial activity of the daughter per Ci of parent activity (A_{D0}) by the 10,000-year and peak groundwater concentration of the daughter (pCi/cc-Ci). The daughter concentration is expressed in terms of pCi/cc of daughter per Ci of parent activity.

For relatively long-lived radionuclides with short-lived daughters, the EDEs used in this PA (Table A.4-6 of Appendix A.4) consider that short-lived daughters are in secular equilibrium with the parent radionuclide. Therefore, separate accounting of these daughters does not need to be carried out in the groundwater simulations.

Several radionuclides in the inventory lists for both the ILNT and LAW vaults are long-lived parents of potentially radiologically-significant daughters. Radiologically-significant daughters are defined here as radioactive decay products that may reach the groundwater compliance point by 10,000 years in concentrations that are significant with respect to the 10,000-year concentration of the parent. Consideration is given to the fact that the allowable concentration of the daughter may be less than that of the parent, as is the case with some decay products of uranium isotopes. The long-lived parents of decay products that fall into this category include Np-237, Cm-246, Cm-247, Cm-248, isotopes of uranium, and isotopes of plutonium. The following discussion provides the rationale for neglecting or considering decay products of these radionuclides in the groundwater-based dose analysis for off-site individuals.

First, note that for the uranium and plutonium decay products of the long-lived radionuclides listed, solubility limits are applied in the waste. Although uranium and plutonium decay products may also be produced in transit from the waste to the compliance point in groundwater, the production during transport is minimal because transit times are

small compared to half-lives of the parent radionuclides. Therefore, the peak groundwater concentrations calculated for the uranium and plutonium isotopes as parent radionuclides can be assumed to constitute an upper bound on the peak groundwater concentration of these isotopes as decay products.

For Np-237, U-233 is the first daughter of interest, since the short-lived daughter Pa-233 will never exceed the Np-237 concentration in groundwater based on its considerably greater sorption on surfaces (K_d exceeds that of Np by a factor of 100; Sheppard and Thibault 1990). As noted above, uranium is considered to be solubility limited at the source in this assessment, and thus, the compliance-point groundwater concentration of this Np-237 decay product will never exceed the value calculated for U-233 considered as the parent radionuclide. The only decay product of U-233 that is relatively long-lived is Th-229. By 10,000 years, the maximum production of Th-229 is approximately 1% of the original Np-237 activity. Because Th-229 is much more strongly sorbed than Np-237, and can only reach a small fraction of the Np-237 activity in the source, it was not deemed a radiologically-significant radionuclide in the Np-237 decay chain. Therefore, radioactive decay products of Np-237 were not considered further in the analysis.

For Cm-246, the only long-lived decay products are Pu-242 and U-238, which are both considered to be solubility-limited at the source. Thus, radioactive decay products of Cm-246 were not considered further in the groundwater analysis.

For Cm-247, the long-lived decay products are Am-243, Pu-239, and U-235. Am-243 is assumed to sorb similarly to Cm-247 and can be, therefore, assumed to travel at the same rate. At 10,000 years, the activity of Am-243 relative to that of Cm-247 is approximately 60%, and this activity relationship can be assumed to hold at the groundwater compliance point. Therefore, Am-243 should be considered as a potentially radiologically-significant daughter. Aside from solubility-limited uranium and plutonium isotopes in the Cm-247 decay chain, Pa-231 is the only other long-lived radionuclide. However, the ingrowth of Pa-231 in 10,000 years is less than 1×10^{-4}%, because of the very long-lived U-235 intermediary, and thus, is not considered radiologically significant.

For Cm-248, no long-lived radionuclides other than isotopes of uranium and plutonium achieve significant activities relative to that of the parent in this decay chain. Thus, radioactive decay products of Cm-248 were not considered further in the groundwater analysis.

For U-233, which is considered solubility-limited, the long-lived Th-229 decay product is of potential significance. By delaying loss of U-233 from the waste due to solubility limitations, the U-233 source of Th-229 in the waste remains for a long time. By 10,000 years, assuming a negligible amount of U-233 is lost from the waste, the Th-229 activity may reach close to 60% of the U-233 initial activity. Thorium is also slowly leached from the waste due to its high sorption potential (K_d = 3000 mL/g). A conservative estimate of the peak activity of Th-229 in the ILNT vaults in the first 10,000 years after disposal is 5.8×10^5 Ci, based on an initial U-233 content of 10,000 kg in each of 10 vaults. This Th-229 activity is conservatively assumed to be present in the 10 ILNT vaults at the time of disposal. For the LAW vaults, a similar calculation results in an initial activity of the Th-229 daughter in the 21 LAW vaults of 1.2×10^6 Ci of Th-229. Ten thousand-year groundwater concentrations of the Th-229 daughter of U-233 are estimated by multiplying the assumed initial activity of Th-229 by the pCi/cc-Ci concentrations of Th-232 in Tables 4.1-5 and 4.1-6, and are reported with the U-233 parent concentration. Because Th-229 decays more rapidly than Th-232, this adds additional conservatism to the result.

For U-234, potentially radiologically-significant daughters include Th-230, Ra-226, and short-lived decay products. The shorter-lived decay products are included in the EDE for Ra-226. As with U-233, the Th-230 concentration in the waste can be estimated at 10,000 years by assuming negligible loss of U-234 and Th-230 from the waste. However, because Ra-226 is more mobile than Th-230 and solubility-limited U-234, estimating the peak concentration of Ra-226 in the waste up to 10,000 years is more difficult. Therefore, the ingrowth and loss via leaching and decay of these decay products of U-234 were simulated rigorously in the PORFLOW runs for U-234 for the ILNT vaults, and the 10,000-year value is reported as pCi/cc with the U-234 concentration in Table 4.1-5. Observations from the ILNT and LAW vault simulation results allow parallels to be drawn for the Th-230 and Ra-226 contributions to groundwater concentrations for the LAW vaults. For Th-232, the ratio of the 10,000-year peak groundwater concentration for the LAW vaults to the 10,000-year concentration for the ILNT vaults is approximately four. Therefore, assuming this same ratio for the daughter calculations, the groundwater concentration of the Th-230 daughter of U-234 in the LAW vaults was estimated. For Ra-226, no simulations of this isotope were carried out.

However, the overall ratio of 10,000-year groundwater concentrations from LAW to ILNT vaults ranges up to about a factor of 65 (Tables 4.1-5 and 4.1-6). Assuming for Ra-226 that the ratio of 10,000-year groundwater concentrations from LAW to ILNT vaults is 65, the Ra-226 groundwater concentration resulting from decay of U-234 in the LAW vaults was estimated.

For U-235, the only potentially radiologically-significant decay products include Pa-231 and Ac-227. Both of these daughter radionuclides exhibit similar sorption behavior, and thus, can be assumed to travel similarly. Assuming negligible transport of U-235 in 10,000 years, the activity of Pa-231 and Ac-227 can achieve activities approaching 20% of the original U-235 activity. However, the mobility of Pa-231 and Ac-227 will limit the peak activity of the radionuclides in the waste, due to continuous leaching during production by decay. Because the ingrowth and loss via leaching and decay of these decay products are not readily estimated, PORFLOW runs simulating these processes were carried out for the U-235 chain in the ILNT vaults. As with U-234, daughter concentrations arising from U-235 in LAW vaults were estimated from LAW:ILNT vault 10,000-year concentration ratios, assuming an upper-end value of 65 for this ratio.

For U-236, ingrowth of all potentially radiologically-significant decay products is limited by ingrowth of the first member of the decay chain, Th-232, which has a half-life of 1.5×10^{10} years. All other members of the decay chain are short-lived, and can be assumed in equilibrium with Th-232 during transit. Assuming no leaching of the parent, U-236, and no leaching of the daughters, the maximum activity of any daughter is less that 5×10^{-5} % of the initial U-236 activity. Groundwater concentrations of Th-232, as a daughter of U-236, were conservatively estimated by assuming that this 10,000-year activity is present at the time of disposal. Based on the 10,000 kg/vault U-236 initial inventory, this corresponds to an initial activity of 3.3×10^{-3} Ci in the 10 ILNT vaults, and 6.8×10^{-3} Ci of Th-232 in the LAW vaults. Ten thousand-year groundwater concentrations of the Th-232 daughter of U-233 are calculated by multiplying the assumed initial activity of Th-232 by the pCi/cc-Ci concentrations in Tables 4.1-5 and 4.1-6, and are reported with the U-233 parent concentration.

For U-233, the first long-lived radiologically-significant daughter in the decay chain is U-234. The decay products of U-234 are considered for the U-234 parent in the waste. By 10,000 years, assuming no leaching of uranium isotopes, the activity of U-234 will be approximately 3% of that of U-233. Therefore, a conservative estimate of the contribution of the U-234 daughters to the U-238 chain is based on the assumption that the initial activity of the U-234 daughter of U-238 is 1 Ci for the 10 ILNT vaults and 2.1 Ci for the LAW vaults, or 3% of the initial 10,000 kg U-238/vault. Using this method to estimate initial inventory of U-234, the results of the U-234 daughter simulations were scaled to these initial activities to derive groundwater concentrations of Th-230 and Ra-226 arising from U-238.

For Pu-238, the first radiologically-significant decay product is U-234. The peak activity of U-234 in the waste relative to the initial activity of Pu-238 in the waste can be estimated according to the procedures described above for short-lived parents with longer-lived daughters. This method uses the ratio of the half-lives of parent-to-daughter to conservatively estimate ingrowth. Because the ingrowth and loss of decay products of U-234 were simulated with PORFLOW, these results can be used to estimate the groundwater concentrations of the decay products of Pu-238. The initial activity of U-234 in ILNT and LAW vaults arising from decay of Pu-238 was estimated to be 3.6×10^{-4} Ci per Ci of Pu-238 initially present. With 150 Ci of Pu-238 assumed initially in each vault, the total inventory of U-234 arising from Pu-238 is 0.54 Ci for the 10 ILNT vaults, and 1.1 Ci for the LAW vaults. The 10,000-year groundwater concentrations for Th-230 and Ra-226 were calculated by scaling the results of the U-234 daughter calculations to these initial inventories of U-234 in each vault type. The results are presented with the Pu-238 concentrations in Tables 4.1-5 and 4.1-6.

For Pu-239, other than solubility-limited U-235, the potentially radiologically-significant daughters are Pa-231 and Ac-227. Assuming no leaching of Pu-239 or U-235, the activity of U-235 is approximately 9×10^{-5} % of the original activity of Pu-239 at 10,000 years after disposal. This corresponds to U-235 activities of 1.4×10^{-3} Ci for all 10 of the ILNT vaults, and 2.8×10^{-3} Ci for all 21 of the LAW vaults. Conservatively assuming that these activities exist initially, the daughter contributions to groundwater concentrations can be estimated using the results of the U-235 PORFLOW simulations, which consider transport of decay products, described previously.

For Pu-240, Pu-242, and Pu-244, other than solubility-limited uranium isotopes, there are no potentially radiologically-significant decay products. For Pu-240, very long-lived Th-232 limits ingrowth of other decay products to less than 10^{-7}% of the initial activity of Pu-240. For Pu-242, very long-lived U-238 and U-235 limit ingrowth of decay products to less than 10^{-9}% of the initial activity of Pu-242. Finally, for Pu-244, Th-232 again limits ingrowth to less than 10^{-7}% of the initial activity of Pu-244. Therefore, decay products of these radionuclides were not considered further in the groundwater analysis.

4.1.4 Dose Analysis for Off-Site Releases of Radionuclides

As described in Sect. 3.2.3.3, the only exposure pathway of concern for off-site releases of radionuclides via the groundwater pathway is direct consumption of groundwater obtained from a well located beyond the 100-m buffer zone around the disposal units. For beta/gamma-emitting and some alpha-emitting radionuclides, the performance objective for protection of groundwater resources, which requires consideration of the drinking water pathway only, is more restrictive than the performance objective for protection of off-site members of the general public, which requires consideration of all exposure pathways involving use of contaminated groundwater. For some alpha-emitting radionuclides, the performance objective for off-site individuals is more restrictive than the performance objective for groundwater protection, due to the high doses per unit activity intake by ingestion, but in these cases the dose from all exposure pathways involving use of contaminated groundwater is only marginally greater than the dose from the drinking water pathway alone. This conclusion assumes that off-site releases of volatile radionuclides (i.e., H-3 and C-14) also can be neglected in the dose analysis beyond the buffer zone (see Appendix A.3).

In order to determine which performance objective is more restrictive for each radionuclide, the MCLs from Table 3.2-1 were compared to the results of the model for estimating dose from the drinking water pathway for off-site individuals. The annual EDEs, in rem per year, from the drinking water pathway per unit concentration (1 μCi/L) of radionuclides in

groundwater (from Table A.4-6 of Appendix A.4) are summarized in Table 4.1-7. The radionuclides in this table were selected by the screening analysis described in Sect. 4.1.1, and all potentially significant decay products are included.

For comparison to MCLs, the performance objective of 25 mrem per year for off-site individuals is divided by the EDEs in Table 4.1-7 to derive the concentration limit in drinking water for each radionuclide based on this dose limit. The results of this calculation, converted to appropriate units, and the MCLs from Table 3.2-1 are listed in Table 4.1-8 for comparison. These results indicate that the 25 mrem per year performance objective is more restrictive for most of the alpha-emitting radionuclides, with the exception of Ra-226, Th-230, U-235, and U-238.

The dose analysis for the drinking water pathway is based on the predicted maximum concentrations of radionuclides in groundwater at any location beyond the 100-m buffer zone and at any time up to 10,000 years after disposal. These concentrations for the different disposal units in E-Area are presented in Tables 4.1-5 and 4.1-6. The groundwater concentrations in these tables represent activity concentrations per unit activity (Ci) in all (not each) of the 10 ILNT vaults or all (not each) of the 21 LAW vaults, except for the Pu and U isotopes. Maximum groundwater concentrations for Pu and U isotopes are based on solubility limits in the vaults for 150 Ci of each Pu isotope and 10,000 kg of each U isotope initially in each vault of each type.

The allowable inventories derived for the drinking water pathway from off-site releases of radionuclides are given in Table 4.1-9. These inventories (Ci) are calculated for all isotopes except for those of Pu and U in the following manner. First, the most restrictive performance objective based in Table 4.1-8 is selected by choosing the lowest allowable groundwater concentration of the two values given for each radionuclide. Second, the lowest allowable groundwater concentration is divided by the maximum groundwater concentration up to 10,000 years, per Ci of inventory in either the ILNT or LAW vaults. Because U and Pu isotopes are assumed to be solubility limited in the vaults, a linear relationship between groundwater concentration and initial inventory does not exist and the allowable inventory cannot be calculated. However, the calculated groundwater concentrations for Pu and U can

Table 4.1-7. Annual EDEs from drinking water pathway per unit concentration of radionuclides in groundwater[a]

Radionuclide[b]	Annual EDE (rem/y per μCi/L)	Radionuclide[b]	Annual EDE (rem/y per μCi/L)
H-3	4.6×10^{-2}	Pa-231 + d	1.1×10^{1}
C-14	1.5	U-232 + d	1.5×10^{3}
Al-26	9.5	U-233	2.0×10^{2}
Ni-59	1.5×10^{-1}	U-234	1.9×10^{2}
Ni-63	3.9×10^{-1}	U-235	1.8×10^{2}
Se-79	6.1	U-236	1.8×10^{2}
Rb-87	3.5	U-238 + d	1.8×10^{2}
Sr-90 + d	1.0×10^{2}	Np-237	2.8×10^{3}
Zr-93[c]	1.2	Pu-238	2.8×10^{3}
Nb-93m	3.9×10^{-1}	Pu-239	3.1×10^{3}
Tc-99	9.5×10^{-1}	Pu-240	3.1×10^{3}
Pd-107	1.0×10^{-1}	Pu-242	3.0×10^{3}
Cd-113m	1.1×10^{2}	Pu-244	2.9×10^{3}
Sn-121m	9.5×10^{-1}	Am-241	3.3×10^{3}
Sn-126 + d	1.3×10^{1}	Am-242m[e]	3.1×10^{3}
I-129	2.0×10^{2}	Am-243	3.3×10^{3}
Cs-135	5.2	Cm-245	3.3×10^{3}
Sm-151	2.5×10^{-1}	Cm-246	3.3×10^{3}
Pb-210 + d	4.9×10^{3}	Cm-247	3.0×10^{3}
Ra-226 + d[d]	8.0×10^{2}	Cm-248	1.2×10^{4}
Th-229 + d	2.9×10^{3}	Cf-249	7.4×10^{3}
Th-230	3.9×10^{2}	Cf-251	3.4×10^{3}
Th-232 + d	3.5×10^{3}		

[a] Results are obtained from Table A.4-6 of Appendix A.4.

[b] "+ d" denotes short-lived decay products that are assumed to be in secular equilibrium with parent radionuclide; see Table A.4-1 of Appendix A.4 for decay products and branching fractions.

[c] Value does not include possible contributions from Nb-93m decay product.

[d] Value does not include possible contributions from Pb-210 decay product.

[e] Value does not include possible contributions from Pu-238 decay product.

Table 4.1-3 Comparison of MCLs and allowable groundwater concentrations based on the 25 mrem per year performance objective for off-site individuals

Radionuclide	MCL,[a] pCi/L	Allowable Concentration Based on 25 mrem per year, pCi/L
H-3	20,000	540,000
C-14	6,400	16,000
Ni-59	530	160,000
Se-79	660[b]	4,100
Sr-90	8	250
Tc-99	800	26,000
Sn-126	290[b]	1,900
I-129	0.5	120
Cs-135	800	4,800
Ra-226	15	31
Ac-227	5.3	----[c]
Pa-231	2.4	2.3
Th-229	15	8.6
Th-230	15	64
Th-232	15	7.1
U-233	190,000 (20 µg/L)[b]	125
U-234	124,000 (20 µg/L)[b]	132
U-235	428 (20 µg/L)[b]	139
U-236	1,270 (20 µg/L)[b]	139
U-238	6.66 (20 µg/L)[b]	139
Np-237	15	8.9
Pu-238	15	8.9
Pu-239	15	8.1
Pu-240	15	8.1

Table 4.1-8 (continued)

Radionuclide	MCL,[a] pCi/L	Allowable Concentration Based on 25 mrem per year, pCi/L
Pu-242	15	8.3
Pu-244	15	8.6
Am-241	15	7.6
Am-243	15	7.6
Cm-244	15	(based solely on Pu-240) [d]
Cm-245	15	7.6
Cm-246	15	7.6
Cm-247	15	8.3
Cm-248	15	2.1
Bk-249	15	(based solely on Cm-245) [d]
Cf-249	15	3.4
Cf-251	15	7.4
Cf-252	15	(based solely on Cm-248) [d]

[a] Option 1, Table 3.2-1, unless otherwise noted.

[b] Option 3, Table 3.2-1.

[c] EDE of Pa-231 parent considers contribution of Ac-227.

[d] EDE not provided in Table 4.1-7 because groundwater concentration of parent negligible.

Table 4.1-9. Calculated allowable inventories based on the groundwater pathway (for off-site doses up to 10,000 years after disposal)[a]

Radionuclide	ILNT Vaults (10) Inventory, Ci	LAW Vaults (21) Inventory, Ci
H-3	7.4×10^{12}	9.5×10^{10}
C-14	9.9×10^{4}	7.4×10^{4}
Ni-59	1.8×10^{4}	1.6×10^{4}
Se-79	8.9×10^{1}	1.3×10^{2}
Sr-90	3.0×10^{14}	5.3×10^{19}
Tc-99	2.0×10^{1}	4.2×10^{1}
Sn-126	1.2×10^{2}	6.2×10^{2}
I-129	5.3×10^{-3}	2.1×10^{-2}
Cs-135	1.9×10^{2}	1.2×10^{3}
Th-232	1.8×10^{14}	5.9×10^{14}
Np-237	2.0	5.6
Am-241[b]	1.0×10^{4}	2.7×10^{4}
Am-243	3.3×10^{4}	1.8×10^{3}
Cm-244[c]	5.4×10^{4}	5.4×10^{4}
Cm-245	2.1×10^{5}	6.9×10^{3}
Cm-246	4.2×10^{5}	1.3×10^{4}
Cm-247	1.3×10^{5}	2.8×10^{3}
Bk-249[b]	2.1×10^{9}	6.9×10^{7}
Cm-248	1.6×10^{4}	7.0×10^{2}
Cf-249[b]	5.1×10^{6}	1.7×10^{5}
Cf-251[b]	1.6×10^{8}	2.4×10^{6}
Cf-252[b]	2.1×10^{9}	9.1×10^{7}
U-233[b]	Solubility limited[d]	Solubility limited[d]
Th-229[e]	3.6×10^{14} ($>>10^5$ kg)[f]	1.2×10^{15} ($>>2.1 \times 10^5$ kg)[g]
U-234[b]	Solubility limited[d]	Solubility limited[d]
Th-230[e]	1.0×10^{20} ($>>10^5$ kg)[f]	5.2×10^{21} ($>>2.1 \times 10^5$ kg)[g]
Ra-226[e]	8.0×10^{5} ($>10^5$ kg)[f]	2.6×10^{4} ($<2.1 \times 10^5$ kg)[g]
U-235[b]	Solubility limited[d]	Solubility limited[d]
Pa-231[e]	1.6×10^{5} ($>>10^5$ kg)[f]	5.0×10^{3} ($>2.1 \times 10^5$ kg)[g]
U-236[b]	Solubility limited[d]	Solubility limited[d]
Th-232[e]	3.5×10^{20} ($>>10^5$ kg)[f]	1.2×10^{2} ($>>2.1 \times 10^5$ kg)[g]
U-238[b]	Solubility limited[d]	Solubility limited[d]
U-234[e]	Solubility limited[d]	Solubility limited[d]
Th-230[e]	3.4×10^{25} ($>>10^5$ kg)[f]	1.7×10^{25} ($>>2.1 \times 10^5$ kg)[g]
Ra-226[e]	2.7×10^{7} ($>>10^5$ kg)[f]	8.8×10^{5} ($>>2.1 \times 10^5$ kg)[g]
Pu-238[b]	Solubility limited[h]	Solubility limited[h]
U-234[e]	Solubility limited[d]	Solubility limited[d]
Th-230[e]	2.7×10^{25}	1.6×10^{25}
Ra-226[e]	2.2×10^{9}	7.5×10^{7}
Pu-239[b]	Solubility limited[h]	Solubility limited[h]
U-235[e]	Solubility limited[d]	Solubility limited[d]
Pa-231[e]	1.6×10^{11}	5.6×10^{9}
Pu-240	Solubility limited[h]	Solubility limited[h]
Pu-242	Solubility limited[h]	Solubility limited[h]
Pu-244	Solubility limited[h]	Solubility limited[h]

[a] Based on lower of the two allowable concentrations listed in Table 4.1-8.
[b] Includes contributions of potentially radiologically-significant daughter(s).
[c] Based on solubility-limited Pu-240 with a total initial inventory of 150 Ci/vault of Pu-240. Parent inventory based on ratio of half-lives (Sect. 4.1.3).
[d] Assumed initial inventory of 10,000 kg/vault for each uranium isotope.
[e] Inventory limit listed is for U or Pu parent.
[f] Expression in parentheses indicates that the inventory limit, in Ci, always exceeds and usually greatly exceeds, the assumed initial inventory of 10^5 kg U for the 10 ILNT vaults.
[g] Expression in parentheses indicates that the inventory limit, in Ci, always exceeds the assumed initial inventory of 2.1×10^5 kg U for the 21 LAW vaults, with one exception (U-234).
[h] Assumed initial inventory of 150 Ci/vault for each plutonium isotope.

be directly compared to the most restricted allowable groundwater limit from Table 4.1-8 to evaluate whether up to 150 Ci of Pu/vault (for any of the Pu isotopes evaluated) and/or 10,000 kg of U/vault (for any of the U isotopes evaluated) are acceptable for disposal. Inventory limits for U and Pu isotopes based on radiologically significant daughters were calculated by dividing the 10,000-year groundwater concentrations by the assumed initial inventory of the parent (U or Pu isotope), in Ci, and following the procedure described above for the radionuclides other than isotopes of U and Pu.

4.1.5 Dose Analysis for Inadvertent Intruders

As demonstrated in Sect. 3.2.4, the following exposure scenarios are of concern for inadvertent intruders onto the disposal site following loss of active institutional control at 100 years after facility closure:

- an agriculture scenario involving direct excavation into disposal units at times after the engineered barriers above the waste have lost their structural and physical integrity and can be penetrated by normal excavation procedures at the SRS;
- a resident scenario involving permanent residence in a home located either on top of an intact concrete roof or other engineered barrier, which first could occur at any time after loss of active institutional control, or on top of intact but exposed waste at times after all engineered barriers have lost their integrity; and
- a post-drilling scenario involving removal by drilling of waste from a disposal unit at times after drilling through a disposal unit becomes credible. The results of the dose analysis for the different exposure scenarios for inadvertent intruders are presented in the following sections.

The general approach to the dose analysis for any exposure scenario for inadvertent intruders is described below.

Because the isotopic composition of waste intended for disposal in the EAV is not known, the dose analysis for inadvertent intruders is used to estimate limits on inventories of

radionuclides that would be acceptable for disposal. For a known volume of disposal units of the same type, limits on radionuclide inventories are equivalent to limits on average concentrations in disposed waste. The estimated limits on radionuclide inventories are based on the performance objective for protection of inadvertent intruders described in Sect. 1.2, i.e., a limit on EDE of 0.1 rem per year for scenarios involving chronic exposure. The procedure for estimating limits on inventories of radionuclides for the different types of disposal units, based on the dose analysis for each exposure scenario for inadvertent intruders, is described as follows.

For an assumed exposure scenario and particular type of disposal unit, the EDE (rem/year) to an inadvertent intruder from exposure to a given radionuclide can be expressed as

$$H = (I_0/V) \times SDCF \times G \times F, \qquad \text{(Eq. 4.1-1)}$$

where

I_0 = inventory of radionuclide in disposal units at time of disposal (μCi),

V = volume of waste in disposal units (m^3),

SDCF = scenario dose conversion factor for radionuclide (rem/year per μCi/m^3),

G = geometrical correction factor (dimensionless), and

F = fraction of initial inventory of radionuclide remaining in disposal units at time intrusion occurs.

In this equation, scenario dose conversion factor (SDCF) is the annual dose to an inadvertent intruder for the assumed exposure scenario per unit concentration of a radionuclide based on the assumption that intrusion occurs only into the regions of disposal units that are occupied by waste. The SDCFs for the agriculture, resident, and post-drilling scenarios are estimated in Appendix A.4, and the results are summarized in Table 4.1-10, 4.1-11, and 4.1-12, respectively. The correction factors G and F then take into account that the average radionuclide concentration encountered by an inadvertent intruder would be less than the average concentration in disposed waste and that the dose would be correspondingly reduced.

Table A.4-15. S[illegible]s for [illegible]ulture [illegible] for [illegible][a]

Radionuclide[b]	Annual EDE (rem/y per μCi/m^3)	Radionuclide[b]	Annual EDE (rem/y per μCi/m^3)
H-3	3.9×10^{-6}	Pa-231 + d	8.3×10^{1}
C-14	1.5×10^{-5}	U-232 + d[e]	2.3×10^{-3}
Al-26	3.9×10^{-3}	Rn-220	1.0×10^{-2} [f]
Co-60	3.5×10^{-3}	U-233	1.1×10^{-5}
Ni-59	6.8×10^{-8}	U-234	1.1×10^{-5}
Ni-63	1.8×10^{-7}	U-235 + d	1.8×10^{-4}
Se-79	1.2×10^{-6}	U-236	1.0×10^{-5}
Rb-87	1.9×10^{-6}	U-238 + d	3.9×10^{-5}
Sr-90 + d	1.8×10^{-4}	Np-237 + d	5.0×10^{-4}
Zr-93[c]	4.5×10^{-8}	Pu-238	3.4×10^{-5}
Nb-93m	1.9×10^{-8}	Pu-239	4.0×10^{-5}
Tc-99	1.1×10^{-5}	Pu-240	4.0×10^{-5}
Pd-107	3.2×10^{-8}	Pu-241	7.7×10^{-7}
Cd-113m	1.3×10^{-4}	Pu-242	3.8×10^{-5}
Sn-121m	4.7×10^{-7}	Pu-244	3.7×10^{-5}
Sn-126 + d	2.6×10^{-3}	Am-241	5.6×10^{-5}
I-129	8.3×10^{-5}	Am-242m + d	6.0×10^{-5}
Cs-135	1.2×10^{-6}	Am-243 + d	2.5×10^{-4}
Cs-137 + d	7.7×10^{-4}	Cm-243	1.6×10^{-4}
Sm-151	1.4×10^{-8}	Cm-244	2.0×10^{-5}
Eu-154	1.7×10^{-3}	Cm-245	1.1×10^{-4}
Eu-155	4.0×10^{-5}	Cm-246	4.0×10^{-5}
Pb-210 + d	3.0×10^{-4}	Cm-247 + d	4.4×10^{-4}
Ra-226 + d[d,e]	2.7×10^{-3}	Cm-248	1.4×10^{-4}
Rn-222	1.2×10^{-1} [f]	Cf-249	4.6×10^{-4}
Th-229 + d	4.3×10^{-4}	Cf-250	1.7×10^{-5}
Th-230	1.1×10^{-5}	Cf-251	1.6×10^{-4}
Th-232 + d[e]	3.6×10^{-3}		
Rn-220	1.0×10^{-2} [f]		

[a] Results are obtained from Table A.4-14 of Appendix A.4.
[b] "+ d" denotes short-lived decay products that are assumed to be in secular equilibrium with parent radionuclide; see Table A.4-1 for decay products and branching fractions.
[c] Value assumes that Nb-93m is present in secular equilibrium.
[d] Value assumes that Pb-210 is present in secular equilibrium.
[e] Dose from radon decay product is listed separately.
[f] Dose is normalized to unit concentration of parent radionuclide.

Table 4.1-11. SDCFs for resident scenario for inadvertent intruders[a]

Radionuclide[b]	Annual EDE (rem/y per μCi/m^3)		
	No shielding[c]	45-cm shielding[d]	100-cm shielding[e]
Al-26	3.9×10^{-3}	1.1×10^{-4}	2.8×10^{-6}
Co-60	—	8.8×10^{-5}	1.2×10^{-6}
Sn-121m	4.2×10^{-7}	—	—
Sn-126 + d	2.6×10^{-3}	2.2×10^{-5}	8.4×10^{-8}
I-129	2.8×10^{-6}	—	—
Cs-137 + d	7.6×10^{-4}	6.6×10^{-6}	2.2×10^{-8}
Eu-154	—	3.2×10^{-5}	3.5×10^{-7}
Eu-155	—	6.3×10^{-10}	—
Ra-226 + d	2.4×10^{-3}	6.0×10^{-5}	1.3×10^{-6}
Th-229 + d	3.5×10^{-4}	2.6×10^{-6}	3.5×10^{-8}
Th-232 + d	3.5×10^{-3}	1.1×10^{-4}	4.1×10^{-6}
Pa-231 + d	4.2×10^{-4}	1.1×10^{-6}	3.5×10^{-9}
U-232 + d	2.2×10^{-3}	9.2×10^{-5}	3.8×10^{-6}
U-235 + d	1.7×10^{-4}	3.9×10^{-8}	2.3×10^{-12}
U-238 + d	2.9×10^{-5}	3.0×10^{-7}	2.5×10^{-9}
Np-237 + d	2.4×10^{-4}	4.6×10^{-7}	2.8×10^{-10}
Am-241	9.5×10^{-6}	—	—
Am-242m + d	1.5×10^{-5}	6.2×10^{-8}	5.2×10^{-10}
Am-243 + d	2.0×10^{-4}	1.1×10^{-7}	4.2×10^{-11}
Cm-243	1.3×10^{-4}	4.9×10^{-8}	2.0×10^{-11}
Cm-245	7.4×10^{-5}	5.3×10^{-9}	—
Cm-247 + d	4.0×10^{-4}	1.3×10^{-6}	1.3×10^{-9}
Cf-249	4.2×10^{-4}	1.2×10^{-6}	1.1×10^{-9}
Cf-251	1.2×10^{-4}	3.1×10^{-8}	—

[a] Results are obtained from Table A.4-15 of Appendix A.4.
[b] "+ d" denotes short-lived decay products that are assumed to be in secular equilibrium with parent radionuclides; see Table A.4-1 of Appendix A.4 for decay products and branching fractions.
[c] Results apply to ILNT, LAW, and ILT vaults at times long after disposal when all engineered barriers above the waste have lost their integrity.
[d] Results apply to LAW vaults at 100 years after disposal.
[e] Results apply to ILNT and ILT vaults at 100 years after disposal.

Table 4.4-12. SOCFs for post-drilling scenario for [illegible] intruders[a]

Radionuclide[b]	Annual EDE (rem/year per μCi/m^3)	Radionuclide[b]	Annual EDE (rem/year per μCi/m^3)
H-3	3.9×10^{-7}	Pa-231 + d	1.8×10^{-5}
C-14	1.5×10^{-5}	U-232 + d[e]	5.6×10^{-6}
Al-26	1.8×10^{-5}	Rn-220	2.1×10^{-6}[f]
Co-60	1.8×10^{-6}	U-233	7.5×10^{-7}
Ni-59	6.8×10^{-9}	U-234	7.3×10^{-7}
Ni-63	1.8×10^{-8}	U-235 + d	7.9×10^{-7}
Se-79	1.2×10^{-7}	U-236	6.9×10^{-7}
Rb-87	1.9×10^{-7}	U-238 + d	6.6×10^{-7}
Sr-90 + d	1.8×10^{-5}	Np-237	2.4×10^{-5}
Zr-93[c]	3.5×10^{-9}	Pu-238	2.1×10^{-6}
Nb-93m	1.8×10^{-9}	Pu-239	2.5×10^{-6}
Tc-99	1.1×10^{-6}	Pu-240	2.5×10^{-6}
Pd-107	3.2×10^{-9}	Pu-241	4.8×10^{-8}
Cd-113m	1.3×10^{-5}	Pu-242	2.4×10^{-6}
Sn-121m	5.3×10^{-9}	Pu-244	2.3×10^{-6}
Sn-126 + d	1.4×10^{-6}	Am-241	3.1×10^{-6}
I-129	8.1×10^{-6}	Am-242m + d	3.0×10^{-6}
Cs-135	1.2×10^{-7}	Am-243 + d	3.2×10^{-6}
Cs-137 + d	1.2×10^{-6}	Cm-243	1.6×10^{-6}
Sm-151	9.3×10^{-10}	Cm-244	1.3×10^{-6}
Eu-154	8.4×10^{-7}	Cm-245	2.5×10^{-6}
Eu-155	2.6×10^{-8}	Cm-246	2.5×10^{-6}
Pb-210 + d	3.0×10^{-5}	Cm-247 + d	2.5×10^{-6}
Ra-226 + d[d,e]	3.2×10^{-5}	Cm-248	8.9×10^{-6}
Rn-222	1.3×10^{-5}[f]	Cf-249	2.7×10^{-6}
Th-229 + d	2.9×10^{-6}	Cf-250	1.0×10^{-6}
Th-230	3.4×10^{-7}	Cf-251	2.6×10^{-6}
Th-232 + d[e]	5.9×10^{-6}		
Rn-220	2.1×10^{-6}[f]		

[a] Results are obtained from Table A.4-16 of Appendix A.4.
[b] "+ d" denotes short-lived decay products that are assumed to be in secular equilibrium with parent radionuclide; see Table A.4-1 of Appendix A.4 for decay products and branching fractions.
[c] Value assumes that Nb-93m is present in secular equilibrium.
[d] Value assumes that Pb-210 is present in secular equilibrium.
[e] Dose from radon decay product is listed separately.
[f] Dose is normalized to unit concentration of parent radionuclides.

The geometrical correction factor, G, in Eq. 4.1-1 takes into account that a large-scale excavation into disposal units, as assumed in the agriculture and resident scenarios, would involve exposure to uncontaminated material between individual disposal units as well as disposed waste itself. This correction factor assumes, in essence, that excavation into disposal units would occur at random locations. Therefore, the geometrical correction factor is given by the fraction of the land area encompassed by the disposal units of a particular type that contains waste.

The values of the geometrical correction factor for the agriculture and resident scenarios assumed in this analysis for the different disposal types of units are given in Table 4.1-13. These values were estimated for the three vault types and the suspect soil trenches in the following manner. An envelope was drawn around each grouping of each vault type (Fig. 2.5-1) or trench (Fig. 2.6-1), representing the total land area occupied by vaults or trenches and uncontaminated soil between each disposal unit in a grouping. Using known vault and trench dimensions (Figs. 2.5-2, 2.5-3, and 2.6-1) and spacing, the correction factors were estimated by dividing the vault and trench areas in a grouping by the area of the corresponding envelope. The correction factors represent the fraction of land area occupied by the vaults or trenches and soil between these units that actually contains waste. For the post-drilling scenario, the geometrical correction factor is assumed to be unity for all disposal units, because an intruder is assumed to drill only through contaminated regions in each type of disposal unit. Any uncontaminated material above and below the waste that also would be exhumed by drilling is taken into account in estimating the SDCF for the post-drilling scenario in Table 4.1-12.

Table 4.1-13. Geometrical reduction factors (G) used in dose analyses for inadvertent intruders[a]

Disposal Units	Reduction Factor
ILNT vaults	0.4
LAW vaults	0.8
ILT vaults	0.4
Suspect soil trenches	0.6

[a] See Eq. 4.1-1; reduction factors apply to agriculture and resident scenarios but not to post-drilling scenario.

The parameter F in Eq. 4.1-1 takes into account that, between the time of disposal and the time that a scenario for inadvertent intrusion is assumed to occur, the initial inventories of radionuclides in the disposal units would be reduced by radioactive decay and by mobilization and transport in infiltrating water. This correction factor depends on the particular disposal unit as well as the radionuclide.

For any radionuclide in disposed waste, the parameter F is a monotonically decreasing function of time after disposal. Therefore, if a radionuclide does not produce radiologically significant long-lived decay products, the dose to an inadvertent intruder for a given scenario will attain its maximum value at the time after disposal when the scenario first becomes credible. However, if a radionuclide produces radiologically more significant long-lived decay products (e.g., U-238, which produces Ra-226), the maximum dose from the parent radionuclide and its decay products could occur long after the scenario first becomes credible, depending on the rate of buildup of activity of the decay product relative to the rate of removal of the parent radionuclide from the disposal units.

For any radionuclide and type of disposal unit, the value of the parameter F as a function of time after disposal is obtained from calculations performed by the PORFLOW computer code. Again, the fraction of the initial inventory remaining in disposal units at any time after disposal takes into account radioactive decay and removal from the disposal units by infiltrating water. For any radiologically significant long-lived decay products, the simplifying assumption is made that the inventory at any time after disposal is determined by (1) the remaining inventory of the parent radionuclide at that time and (2) the ratio of the activity of the decay product to the initial activity of the parent radionuclide as obtained from the Bateman equations. As described in Sect. 4.1.3, a similar approximation was used in accounting for long-lived decay products in the dose analysis for the groundwater pathway.

Since the objective of the intruder dose analysis is to establish limits on inventories of radionuclides for disposal, Eq. 4.1-1 can be rearranged to give

$$I_0 = (H \times V)/(SDCF \times G \times F).$$

Therefore, for a dose limit for inadvertent intruders of 0.1 rem per year and using a conversion factor for activity of 10^{-6} Ci/μCi, the inventory limit for a radionuclide in a particular type of disposal unit for a given exposure scenario is given by

$$I_0(\text{Ci}) = [10^{-7} \times V(\text{m}^3)]/[\text{SDCF}(\text{rem-m}^3/\mu\text{Ci-y}) \times G \times F]. \qquad \text{(Eq. 4.1-2)}$$

The volume V depends only on the type of disposal unit, the SDCF depends only on the radionuclide and exposure scenario but not on the type of disposal unit, G depends only on the type of disposal unit and exposure scenario, and F depends on the time after disposal at which intrusion is assumed to occur and on the radionuclide and type of disposal unit.

Alternatively, the waste acceptance criteria (WAC) could be expressed in terms of limits on average concentrations of radionuclides in disposed waste. From Eq. 4.1-2, the limit on average concentration of a radionuclide is given by

$$C_0(\mu\text{Ci/m}^3) = 0.1/[\text{SDCF}(\text{rem-m}^3/\mu\text{Ci-y}) \times G \times F]. \qquad \text{(Eq. 4.1-3)}$$

The model in Eqs. 4.1-2 and 4.1-3 for estimating limits on inventories or average concentrations of radionuclides in the different types of disposal units for the different exposure scenarios for inadvertent intruders is implemented in the following sections.

4.1.5.1 Dose Analysis for Agriculture Scenario

The SDCFs obtained from the model for estimating dose to inadvertent intruders for the agriculture scenario are summarized in Table 4.1-10. The remainder of this section discusses application of the results in Table 4.1-10 and the model in Eqs. 4.1-1 through 4.1-3 to the different disposal units in E-Area.

ILNT Vaults

Because of the design of the ILNT vaults, the agriculture scenario involving direct excavation into the waste is not expected to become credible for a considerable period of time

after disposal. Since the waste will be located well below the ground surface, a considerable amount of erosion will need to occur before the waste could be accessed by normal excavation procedures for a home. Then, the concrete roof and layer of uncontaminated grout above the waste are expected to preclude excavation into the waste for as long as they maintain their physical integrity. The assumed performance of the three barriers to excavation into waste is discussed below.

The current closure concept for the disposal units in E-Area calls for an earthen cover above the concrete roof of thickness about 2.9 m. As described in Sect. 2.1.8, the average erosion rate for cropland in the vicinity of the SRS is about 1.4 mm/year. This erosion rate probably is an upper-bound estimate for the earthen cover, because an estimated erosion rate for natural successional forests (see Sect. 2.1.8) is about 0.003 mm/year. Since an excavation for a home normally is assumed to extend no more than about 3 m below the ground surface (NRC 1981; Oztunali and Roles 1986) and since the total thickness of the concrete roof and layer of uncontaminated grout above the waste in the ILNT vaults is expected to be about 1.7 m (see Sect. 2.8), at least 2.7 m of the earthen cover would need to erode before a significant thickness of the waste (about 1 m) would be accessible during excavation and significant exposures according to the agriculture scenario could occur. Using the estimated erosion rates given above, the time required for 2.7 m of cover material to erode is estimated to be nearly 2,000 years and perhaps as long as 900,000 years. The very low erosion rate for natural successional forests is difficult to justify for such a long time period. However, the presence of a gravel layer about 0.9 m below the surface in the current closure concept undoubtedly would inhibit further erosion once the gravel layer is exposed. Therefore, erosion to a depth necessary to permit normal excavation into the waste presumably will not occur for at least several thousand years after disposal.

The models for degradation of the concrete roof are described in Sect. 3.1.3. As indicated in Table 3.3-4, the roof above an ILNT vault is expected to maintain its integrity for about 1,000 years after disposal, and collapse of the roof is expected to occur at about that time. If the roof were in the form of rubble after collapse, which probably represents a worst-case scenario, excavation through the collapsed roof could occur at that time.

After the concrete roof over an ILNT vault fails, the layer of uncontaminated grout above the waste presumably must weather almost entirely to soil-equivalent material before excavation into the waste would become credible. In order to estimate the weathering rate of grout, this material is assumed to resemble carbonate rock (e.g., limestone) in its weathering properties. Available data summarized by Ketelle and Huff (1984) indicate that the weathering rate of carbonate rock in regions near the SRS is in the range 35 to 100 mm per 1,000 years. For purposes of this analysis, a weathering rate for the layer of uncontaminated grout of 100 mm (0.1 m) per 1,000 years is assumed. This value applies to the expected infiltration rate of water in native soil of 40 cm/year (see Appendix A.1.1) and, thus, applies at times after the concrete roof has failed at about 1,000 years after disposal. A weathering rate at the upper end of the range of reported values for carbonate rock is chosen, because grout should have a somewhat higher porosity than average carbonate rock and, thus, should be correspondingly more susceptible to weathering by infiltrating water.

The nominal thickness of the layer of uncontaminated grout above the waste in the ILNT vaults is 3 ft (90 cm). By assuming that essentially all of this grout layer must weather to soil-equivalent material in order for excavation into the waste to become credible, and using the estimated weathering rate given above, the time required for weathering of the grout at the normal infiltration rate of water is estimated to be about 9,000 years. This estimate shows that even in the absence of a concrete roof, the layer of uncontaminated grout above the waste should prevent excavation into the waste for many thousands of years after disposal.

The analysis described above assumes that excavation into the waste could occur as soon as the concrete roof has failed and the layer of uncontaminated grout above the waste has weathered to soil-equivalent material and the waste becomes accessible by excavation. This assumption probably is conservative because the space between waste packages in the ILNT vaults will be backfilled with grout, and the top layer (about 1 m) of this grout presumably must weather to soil-equivalent material before significant excavation into the waste could occur. The weathering rate of this material presumably would be about the same as for the grout layer above the waste described above. Therefore, about 10,000 years presumably would be required for a layer 1 m thick to weather to soil-equivalent material. This time is in addition to the time required for weathering of the grout above the waste.

In summary, an analysis of the expected performance of the earthen cover above the ILNT vaults and the concrete roof and layers of grout in the vaults indicates that excavation into the waste probably is not credible for at least 20,000 years after disposal. The layer of gravel in the earthen cover, which will be placed about 3.5 m above the waste, presumably will be quite erosion resistant, and a typical excavation to a depth of about 3 m below the ground surface would not access waste in the presence of the gravel layer. Even if the gravel layer were subject to the same erosion rate as native soil, the time required for a sufficient thickness of the cover to erode so that about 1 m of waste would be accessible by excavation should be at least several thousand years and could approach one million years if the current erosion rate for natural successional forests at the SRS is maintained.

The concrete roof above the vaults, the layer of uncontaminated grout above the waste, and the grouting of the waste itself also are expected to be effective barriers to excavation into the waste for many thousands of years after disposal. Although the roof is expected to collapse at about 1,000 years after disposal, the presence of large, intact pieces of the roof may preclude excavation for a considerable period of time thereafter. However, even if a collapsed roof were not a deterrent to excavation, the layer of uncontaminated grout above the waste is expected to maintain its integrity for about 10,000 years after disposal (i.e., for about 9,000 years after the roof collapses), and the grouting of the waste itself is expected to preclude excavation into a layer of waste about 1 m thick for about another 10,000 years after disposal.

From the analysis of the earthen cover and engineered barriers for the ILNT vaults presented above, it is clear that only long-lived radionuclides in the waste possibly could be of concern in an analysis of the agriculture scenario for inadvertent intruders. In this analysis, results are presented for three different times after disposal. The first is at 10,000 years after disposal, which is the maximum time of compliance with the performance objective for protection of inadvertent intruders (see Sect. 1.2.1). The analysis at this time is based on the pessimistic assumption that the agriculture scenario reasonably could occur then. Again, however, the scenario may not be credible until long after 10,000 years, based on the expected performance of the earthen cover and engineered barriers. The second time is at

20,000 years after disposal, which is the earliest time that the engineered barriers are expected to have failed sufficiently to permit excavation into a layer of waste about 1 m thick. Again, however, excavation into the waste at this time may be a pessimistic assumption if the gravel layer in the earthen cover prevents erosion to a depth sufficient to permit excavation at the depth of the waste. The third time is far into the future (i.e., at 200,000 to 2,000,000 years) when all barriers to excavation presumably have failed. Results at these far future times are presented only for U-234, U-235, and U-238, and the purpose of the analysis is to capture possible exposures to long-lived decay products which would reach their peak values only at very long times after disposal. A similar analysis was considered for Np-237, but in this case removal of the parent radionuclide from the vaults by mobilization and transport in water is sufficiently rapid to more than compensate for the long-term buildup of U-233 and Th-229 decay products.

The results of the dose analysis for the agriculture scenario at the various times after disposal are given in Table 4.1-14. The results are calculated using Eqs. 4.1-2 and 4.1-3. The SDCFs for the long-lived radionuclides of concern are given in Table 4.1-10, the geometrical reduction factor for the ILNT vaults of 0.4 is obtained from Table 4.1-13, and the fraction of the initial inventory of radionuclides remaining in the vaults at the various times after disposal, which takes into account radioactive decay and mobilization and transport in water, was calculated using the PORFLOW computer code. The results of the analysis are given in two forms, both of which are based on the dose limit for inadvertent intruders of 0.1 rem per year. The first set of results is in the form of limits on average concentrations of radionuclides in the waste. This type of result is useful because the concentrations in individual waste packages cannot exceed the limits for Class-C waste established by the NRC in 10 CFR Part 61 (DOE 1988a). The second set of results is in the form of limits on total activity of radionuclides in each vault.

For Th-232, U-234, and U-238, two sets of concentration and inventory limits are calculated for each time after disposal listed in Table 4.1-13. The first set of results include the contributions to the dose to inadvertent intruders from radon decay products (i.e., Rn-220 for Th-232 and Rn-222 for U-234 and U-238), but the second set of results excludes the contributions from radon. The dose limit for inadvertent intruders in the present performance

Table 4.1-11. Results of dose analysis for intruder agriculture scenario for ILNT vaults[a]

Radionuclide	SDCF[b] (rem/y per μCi/m^3)	Time (y)	F[c]	Concentration Limit[d] (μCi/m^3)	Inventory Limit[e] (Ci)
C-14	1.5×10^{-5}	1×10^4	3.0×10^{-1}	5.6×10^4	3.2×10^2
		2×10^4	8.8×10^{-2}	1.9×10^5	1.1×10^3
Al-26	3.9×10^{-3}	1×10^4	9.9×10^{-1}	6.5×10^1	3.7×10^{-1}
		2×10^4	9.8×10^{-1}	6.5×10^1	3.7×10^{-1}
Ni-59	6.8×10^{-8}	1×10^4	8.3×10^{-1}	4.4×10^6	2.5×10^4
		2×10^4	3.6×10^{-1}	1.0×10^7	5.8×10^4
Se-79	1.2×10^{-6}	1×10^4	3.8×10^{-2}	5.5×10^6	3.1×10^4
		2×10^4	3.4×10^{-2}	6.1×10^6	3.5×10^4
Rb-87	1.9×10^{-6}	1×10^4	1.0	1.3×10^5	7.5×10^2
		2×10^4	1.0	1.3×10^5	7.5×10^2
Zr-93	4.5×10^{-8}	1×10^4	1.0	5.6×10^6	3.2×10^4
		2×10^4	1.0	5.6×10^6	3.2×10^4
Tc-99	1.1×10^{-5}	1×10^4	1.8×10^{-2}	1.3×10^6	7.2×10^3
		2×10^4	1.5×10^{-2}	1.5×10^6	8.6×10^3
Pd-107	3.2×10^{-8}	1×10^4	1.0	7.8×10^6	4.5×10^4
		2×10^4	1.0	7.8×10^6	4.5×10^4
Sn-126	2.6×10^{-3}	1×10^4	5.8×10^{-2}	1.7×10^3	9.5
		2×10^4	4.1×10^{-2}	2.3×10^3	1.3×10^1
I-129	8.3×10^{-5}	1×10^4	2.5×10^{-3}	1.2×10^6 [f]	4.6×10^2
		2×10^4	2.5×10^{-3}	1.2×10^6 [f]	4.6×10^2
Cs-135	1.2×10^{-6}	1×10^4	1.1×10^{-2}	1.9×10^7	1.1×10^5
		2×10^4	1.1×10^{-2}	1.9×10^7	1.1×10^5
Th-232 [g]	1.4×10^{-2}	1×10^4	1.0	1.8×10^1 [g]	1.0×10^{-1} [g]
		2×10^4	1.0	1.8×10^1 [g]	1.0×10^{-1} [g]
Th-232 [h]	3.6×10^{-3}	1×10^4	1.0	6.9×10^1 [h]	4.0×10^{-1} [h]
		2×10^4	1.0	6.9×10^1 [h]	4.0×10^{-1} [h]
U-233	1.1×10^{-5}	1×10^4	9.6×10^{-1}	2.4×10^4	1.3×10^2
		2×10^4	9.2×10^{-1}	2.5×10^4	1.4×10^2
U-234	1.1×10^{-5}	1×10^4	9.7×10^{-1}	3.2×10^1 [g]	1.8×10^{-1} [g]
Th-230	1.1×10^{-5}		8.5×10^{-2}	1.3×10^3 [h]	7.5
Ra-226 [g]	1.2×10^{-1}		6.6×10^{-2}		
Ra-226 [h]	2.7×10^{-3}		6.6×10^{-2}		
U-234	1.1×10^{-5}	2×10^4	9.4×10^{-1}	1.5×10^1 [g]	8.5×10^{-2} [g]
Th-230	1.1×10^{-5}		1.6×10^{-1}	6.4×10^2 [g]	3.7
Ra-226 [g]	1.2×10^{-1}		1.4×10^{-1}		
Ra-226 [h]	2.7×10^{-3}		1.4×10^{-1}		

Table 4.1-14. (continued)

Radionuclide	SDCF[b] (rem/y per μCi/m^3)	Time (y)	F[c]	Concentration Limit[d] (μCi/m^3)	Inventory Limit[e] (Ci)
U-234	1.1×10^{-5}	2×10^{5}	5.7×10^{-1}	3.5 [g]	2.0×10^{-2} [g]
Th-230	1.1×10^{-5}		5.9×10^{-1}	1.6×10^{2} [h]	8.9×10^{-1} [h]
Ra-226 [g]	1.2×10^{-1}		5.9×10^{-1}		
Ra-226 [h]	2.7×10^{-3}		5.9×10^{-1}		
U-235	1.8×10^{-4}	1×10^{4}	1.0	7.4×10^{2}	4.2
Pa-231	8.3×10^{-4}		1.9×10^{-1}		
U-235	1.8×10^{-4}	2×10^{4}	1.0	5.3×10^{2}	3.0
Pa-231	8.3×10^{-4}		3.5×10^{-1}		
U-235	1.8×10^{-4}	1×10^{6}	1.0	2.5×10^{2}	1.4
Pa-231	8.3×10^{-4}		1.0		
U-236	1.0×10^{-5}	1×10^{4}	1.0	2.5×10^{4}	1.4×10^{2}
		2×10^{4}	1.0	2.5×10^{4}	1.4×10^{2}
U-238	3.9×10^{-5}	1×10^{4}	1.0	1.9×10^{3} [g]	1.1×10^{1} [g]
U-234	1.1×10^{-5}		2.8×10^{-2}	6.1×10^{3} [h]	3.4×10^{1} [h]
Th-230	1.1×10^{-5}		1.2×10^{-3}		
Ra-226 [g]	1.2×10^{-1}		7.9×10^{-4}		
Ra-226 [h]	2.7×10^{-3}		7.9×10^{-4}		
U-238	3.9×10^{-5}	2×10^{4}	1.0	5.1×10^{2} [g]	2.9 [g]
U-234	1.1×10^{-5}		5.5×10^{-2}	5.0×10^{3} [h]	2.9×10^{1} [h]
Th-230	1.1×10^{-5}		4.7×10^{-3}		
Ra-226 [g]	1.2×10^{-1}		3.8×10^{-3}		
Ra-226 [h]	2.7×10^{-3}		3.8×10^{-3}		
U-238	3.9×10^{-5}	2×10^{6}	1.0	2.1 [g]	1.2×10^{-2} [g]
U-234	1.1×10^{-5}		1.0	8.9×10^{1} [h]	5.1×10^{-1} [h]
Th-230	1.1×10^{-5}		1.0		
Ra-226 [g]	1.2×10^{-1}		1.0		
Ra-226 [h]	2.7×10^{-3}		1.0		
Np-237	5.0×10^{-4}	1×10^{4}	9.7×10^{-1}	5.1×10^{2}	2.9
U-233	1.1×10^{-5}		4.2×10^{-2}		
Th-229	4.3×10^{-4}		1.5×10^{-2}		
Np-237	5.0×10^{-4}	2×10^{4}	7.4×10^{-1}	6.4×10^{2}	3.7
U-233	1.1×10^{-5}		6.2×10^{-2}		
Th-229	4.3×10^{-4}		3.5×10^{-2}		
Pu-239	4.0×10^{-5}	1×10^{4}	7.5×10^{-1}	8.3×10^{3}	4.8×10^{1}
		2×10^{4}	5.6×10^{-1}	1.1×10^{4}	6.4×10^{1}
Pu-240	4.0×10^{-5}	1×10^{4}	3.4×10^{-1}	1.8×10^{4}	1.0×10^{2}
		2×10^{4}	1.2×10^{-1}	5.2×10^{4}	3.0×10^{2}
Pu-242	3.8×10^{-5}	1×10^{4}	9.8×10^{-1}	6.7×10^{3}	3.8×10^{1}
		2×10^{4}	9.6×10^{-1}	6.9×10^{3}	3.9×10^{1}

Table 4.1-14. (continued)

Radionuclide	SDCF[b] (rem/y per μCi/m^3)	Time (y)	F[c]	Concentration Limit[d] (μCi/m^3)	Inventory Limit[e] (Ci)
Pu-244	3.7×10^{-5}	1×10^4	1.0	6.8×10^3	3.9×10^1
		2×10^4	1.0	6.8×10^3	3.9×10^1
Am-243	2.5×10^{-4}	1×10^4	3.9×10^{-1}	2.6×10^3	1.5×10^1
		2×10^4	1.5×10^{-1}	6.7×10^3	3.8×10^1
Cm-245	1.1×10^{-4}	1×10^4	4.4×10^{-1}	5.2×10^3	2.9×10^1
		2×10^4	2.0×10^{-1}	1.1×10^4	6.5×10^1
Cm-246	4.0×10^{-5}	1×10^4	2.3×10^{-1}	2.7×10^4	1.5×10^2
		2×10^4	5.4×10^{-2}	1.2×10^5	6.6×10^2
Cm-247	4.4×10^{-4}	1×10^4	1.0	5.7×10^2	3.2
		2×10^4	1.0	5.7×10^2	3.2
Cm-248	1.4×10^{-4}	1×10^4	9.8×10^{-1}	1.8×10^3	1.0×10^1
		2×10^4	9.6×10^{-1}	1.9×10^3	1.1×10^1

[a] Concentration and inventory limits are obtained from Eqs. 4.1-2 and 4.1-3.

[b] Values are obtained from Table 4.1-10.

[c] Fraction of initial inventory of radionuclide remaining in disposal units at time scenario is assumed to occur.

[d] Limit on average concentration in disposed waste.

[e] Limit on inventory per vault; volume of each vault is assumed to be 5.7×10^3 m^3.

[f] Value exceeds NRC's Class-C limit in 10 CFR Part 61 of 8×10^4 μCi/m^3, which applies to individual waste packages at DOE disposal sites (U.S.DOE 1988a).

[g] Results include contribution to dose from radon decay product.

[h] Results exclude contribution to dose from radon decay product.

objective in DOE Order 5820.2A (U.S.DOE 1988a) presumably includes contributions from radon. However, as described in Sect. 1.2.3, a revision of the DOE Order is being considered in which the dose limit in the performance objective for inadvertent intruders specifically excludes contributions from radon, and a separate limit on radon flux rate to the atmosphere would be imposed to provide an additional constraint on acceptable disposals of radionuclides that produce radon.

The results in Table 4.1-14 may be interpreted as follows. For all radionuclides except the isotopes of uranium which produce long-lived decay products, the maximum dose would occur at the time after disposal at which the agriculture scenario first becomes credible, and the results at 10,000 or 20,000 years represent lower-bound estimates of limits on average concentrations and inventories of radionuclides in waste. For U-234, U-235, and U-238, the results at times far beyond 10,000 or 20,000 years represent worst-case estimates of concentration and inventory limits at times when the buildup of decay products has reached equilibrium with the parent radionuclide.

LAW Vaults

Because of the presence of an earthen cover and concrete roof above the LAW vaults, the agriculture scenario involving direct excavation into the waste is not expected to become credible for a considerable period of time after disposal. However, these disposal units will not include a layer of uncontaminated grout above the waste, and the waste itself will not be grouted after disposal.

As described previously in the dose analysis for the ILNT vaults, the erosion rate of the earthen cover should be no greater than 1.4 mm/year and could be as low as 0.003 mm/year. For the LAW vaults, the earthen cover also is about 2.9 m thick, and the thickness of the concrete roof is about 50 cm. Thus, for a layer of waste about 1 m thick to be accessible during excavation, about 1.4 m of the cover material would need to be removed by erosion. Based on the erosion rates given above, the time period required for this amount of erosion should be at least 1,000 years and could be as long as 500,000 years. These estimates do not take into account the presence of a gravel layer at about 0.9 m below the surface, which presumably would inhibit erosion once it is exposed.

The models for degradation of the concrete roof indicate that the roof above the LAW vault should maintain its integrity for about 3,000 years after disposal, and collapse of the roof is expected to occur at about that time. If the roof were in the form of rubble after collapse, then excavation through the collapsed roof could occur at that time.

The assumption that excavation through the concrete roof could occur immediately following collapse of the roof would be pessimistic if most of the roof were in large pieces. Excavation through the collapsed roof would become more likely after most of the roof has weathered to soil-equivalent material. As previously described with the ILNT vaults, the weathering rate of concrete is assumed to be about 0.1 m per 1,000 years. Therefore, since a collapsed roof presumably could weather from both top and bottom and the thickness of the roof is about 0.5 m, the time required for essentially all of the concrete to weather to soil is expected to be about 2,000 years. Thus, taking into account that the roof is not expected to collapse for about 3,000 years, the estimated time at which excavation through the roof could occur is about 5,000 years after disposal.

From the analysis of the earthen cover and concrete roof for the LAW vaults presented above, it is again clear that only long-lived radionuclides in the waste possibly could be of concern in an analysis of the agriculture scenario for inadvertent intruders. In this analysis, results are presented for four different times after disposal. The first is at 3,000 years after disposal, and the analysis is based on the pessimistic assumption that the agriculture scenario reasonably could occur at the time that the concrete roof is expected to collapse. This assumption is pessimistic because it assumes that erosion of the cover material below the gravel layer has occurred and that excavation of the collapsed roof would be credible. The second time is at 5,000 years after disposal, when the concrete roof presumably has weathered to soil-equivalent material and excavation into the waste could occur. This assumption is pessimistic again because erosion of the cover material below the gravel layer again is presumed to have occurred. Finally, results are presented for U-234, U-235, and U-238 at 10,000 years after disposal, which is the maximum time of compliance with the performance objective for protection of inadvertent intruders, and at times far into the future (i.e., at 200,000 to 2,000,000 years) when the doses due to buildup of radiologically significant decay products could attain their maximum values. Similar calculations were performed for Np-237

INFORMATION ONLY

and its long-lived decay products, but in this case the maximum dose occurs when the agriculture scenario first becomes credible, due to the rapid depletion of the parent radionuclide in the vaults by mobilization and transport in water compared with the buildup of decay products U-233 and Th-229.

The results of the dose analysis for the agriculture scenario at the various times after disposal are given in Table 4.1-15. These results were obtained as described previously for the ILNT vaults, except the geometrical reduction factor for the LAW vaults is 0.8 (see Table 4.1-13). For Th-232, U-234, and U-238, two sets of results again are given, one including the contributions to dose from radon and the other excluding the contributions from radon. For all radionuclides except U-234, U-235, and U-238, the maximum dose would occur at the time after disposal at which the agriculture scenario first becomes credible, and the results at 3,000 or 5,000 years after disposal represent lower-bound estimates of limits on average concentrations and inventories of radionuclides in waste. For U-234, U-235, and U-238, the results at 10,000 years represent the best estimates of the concentration and inventory limits during the 10,000-year compliance period for protection of inadvertent intruders, and the results at times far beyond 10,000 years represent worst-case estimates of limits at times when the buildup of decay products has reached equilibrium with the parent radionuclide.

ILT Vaults

The ILT vaults will be constructed in the same manner as the ILNT vaults, i.e., with an earthen cover about 2.9 m thick, a concrete roof about 90 cm thick, a layer of uncontaminated grout above the waste about 90 cm thick, and grouting of the waste in the vaults. Therefore, essentially the same assumptions used previously in the analysis of the agriculture scenario for the ILNT vaults apply to the ILT vaults. In particular, the scenario may not be credible until long after 10,000 years due to burial of the waste below the ground surface, the slow erosion rate expected for the earthen cover with a gravel layer, and the slow weathering rate of the layers of grout in the vaults.

Table 4.1-15. Results of [illegible] for intruder agriculture scenario for LAW vault [illegible]

Radionuclide	SDCF[b] (rem/y per μCi/m³)	Time (y)	F[c]	Concentration Limit[d] (μCi/m³)	Inventory Limit[e] (Ci)
C-14	1.5×10^{-5}	3×10^{3}	6.9×10^{-1}	1.2×10^{4}	5.8×10^{2}
		5×10^{3}	4.5×10^{-1}	1.9×10^{4}	8.9×10^{2}
Al-26	3.9×10^{-3}	3×10^{3}	1.0	3.2×10^{1}	1.5
		5×10^{3}	1.0	3.2×10^{1}	1.5
Ni-59	6.8×10^{-8}	3×10^{3}	9.7×10^{-1}	1.9×10^{6}	9.1×10^{4}
		5×10^{3}	9.6×10^{-1}	1.9×10^{6}	9.2×10^{4}
Se-79	1.2×10^{-6}	3×10^{3}	9.3×10^{-1}	1.1×10^{5}	5.4×10^{3}
		5×10^{3}	4.3×10^{-2}	2.4×10^{6}	1.2×10^{5}
Rb-87	1.9×10^{-6}	3×10^{3}	1.0	6.6×10^{4}	3.2×10^{3}
		5×10^{3}	1.0	6.6×10^{4}	3.2×10^{3}
Zr-93	4.5×10^{-8}	3×10^{3}	1.0	2.8×10^{6}	1.3×10^{5}
		5×10^{3}	1.0	2.8×10^{6}	1.3×10^{5}
Tc-99	1.1×10^{-5}	3×10^{3}	8.7×10^{-1}	1.3×10^{4}	6.3×10^{2}
		5×10^{3}	2.2×10^{-2}	5.2×10^{5}	2.5×10^{4}
Pd-107	3.2×10^{-8}	3×10^{3}	1.0	3.9×10^{6}	1.9×10^{5}
		5×10^{3}	1.0	3.9×10^{6}	1.9×10^{5}
Sn-126	2.6×10^{-3}	3×10^{3}	9.8×10^{-1}	4.9×10^{1}	2.4
		5×10^{3}	6.6×10^{-1}	7.3×10^{1}	3.5
I-129	8.3×10^{-5}	3×10^{3}	1.5×10^{-4}	1.0×10^{7} [f]	3.8×10^{3}
		5×10^{3}	1.1×10^{-4}	1.4×10^{7} [f]	3.8×10^{3}
Cs-135	1.2×10^{-6}	3×10^{3}	1.0	1.0×10^{5}	5.0×10^{3}
		5×10^{3}	3.2×10^{-1}	3.3×10^{5}	1.6×10^{4}
Th-232 [g]	1.4×10^{-2}	3×10^{3}	1.0	8.9 [g]	4.3×10^{-1} [g]
		5×10^{3}	1.0	8.9 [g]	4.3×10^{-1} [g]
Th-232 [h]	3.6×10^{-3}	3×10^{3}	1.0	3.5×10^{1} [h]	1.7
		5×10^{3}	1.0	3.5×10^{1} [h]	1.7
U-233	1.1×10^{-5}	3×10^{3}	9.9×10^{-1}	1.1×10^{4}	5.5×10^{2}
		5×10^{3}	9.8×10^{-1}	1.2×10^{4}	5.6×10^{2}
U-234	1.1×10^{-5}	3×10^{3}	9.9×10^{-1}	8.6×10^{1} [g]	4.1 [g]
Th-230	1.1×10^{-5}		2.7×10^{-2}	2.9×10^{3} [h]	1.4×10^{2} [h]
Ra-226 [g]	1.2×10^{-1}		1.2×10^{-2}		
Ra-226 [h]	2.7×10^{-3}		1.2×10^{-2}		
U-234	1.1×10^{-5}	5×10^{3}	9.9×10^{-1}	4.0×10^{1} [g]	1.9 [g]
Th-230	1.1×10^{-5}		4.4×10^{-2}	1.5×10^{3} [h]	7.4×10^{1} [h]
Ra-226 [g]	1.2×10^{-1}		2.6×10^{-2}		
Ra-226 [h]	2.7×10^{-3}		2.6×10^{-2}		
U-234	1.1×10^{-5}	1×10^{4}	9.7×10^{-1}	1.6×10^{1} [g]	7.6×10^{-1} [g]
Th-230	1.1×10^{-5}		8.5×10^{-2}	6.6×10^{2} [h]	3.2×10^{1} [h]
Ra-226 [g]	1.2×10^{-1}		6.6×10^{-2}		
Ra-226 [h]	2.7×10^{-3}		6.6×10^{-2}		

Table 4.1-15. (continued)

Radionuclide	SDCF[b] (rem/y per μCi/m^3)	Time (y)	F[c]	Concentration Limit[d] (μCi/m^3)	Inventory Limit[e] (Ci)
U-234	1.1×10^{-5}	2×10^{5}	5.7×10^{-1}	1.8 [g]	8.5×10^{-2} [g]
Th-230	1.1×10^{-5}		5.9×10^{-1}	7.8×10^{1} [h]	3.8 [h]
Ra-226 [g]	1.2×10^{-1}		5.9×10^{-1}		
Ra-226 [h]	2.7×10^{-3}		5.9×10^{-1}		
U-235	1.8×10^{-4}	3×10^{3}	1.0	5.4×10^{2}	2.6×10^{1}
Pa-231	8.3×10^{-4}		6.2×10^{-2}		
U-235	1.8×10^{-4}	5×10^{3}	1.0	4.8×10^{2}	2.3×10^{1}
Pa-231	8.3×10^{-4}		1.0×10^{-1}		
U-235	1.8×10^{-4}	1×10^{4}	1.0	3.7×10^{2}	1.8×10^{1}
Pa-231	8.3×10^{-4}		1.9×10^{-1}		
U-235	1.8×10^{-4}	1×10^{6}	1.0	1.3×10^{2}	6.0
Pa-231	8.3×10^{-4}		1.0		
U-236	1.0×10^{-5}	3×10^{3}	1.0	1.3×10^{4}	6.0×10^{2}
		5×10^{3}	1.0	1.3×10^{4}	6.0×10^{2}
U-238	3.9×10^{-5}	3×10^{3}	1.0	2.9×10^{3} [g]	1.4×10^{2} [g]
U-234	1.1×10^{-5}		8.5×10^{-3}	3.2×10^{3} [h]	1.5×10^{2} [h]
Th-230	1.1×10^{-5}		1.1×10^{-4}		
Ra-226 [g]	1.2×10^{-1}		3.7×10^{-5}		
Ra-226 [h]	2.7×10^{-3}		3.7×10^{-5}		
U-238	3.9×10^{-5}	5×10^{3}	1.0	2.2×10^{3} [g]	1.1×10^{2} [g]
U-234	1.1×10^{-5}		1.4×10^{-2}	3.1×10^{3} [h]	1.5×10^{2} [h]
Th-230	1.1×10^{-5}		3.1×10^{-4}		
Ra-226 [g]	1.2×10^{-1}		1.4×10^{-4}		
Ra-226 [h]	2.7×10^{-3}		1.4×10^{-4}		
U-238	3.9×10^{-5}	1×10^{4}	1.0	9.3×10^{2} [g]	4.5×10^{1} [g]
U-234	1.1×10^{-5}		2.8×10^{-2}	3.0×10^{3} [h]	1.5×10^{2} [h]
Th-230	1.1×10^{-5}		1.2×10^{-3}		
Ra-226 [g]	1.2×10^{-1}		7.9×10^{-4}		
Ra-226 [h]	2.7×10^{-3}		7.9×10^{-4}		
U-238	3.9×10^{-5}	2×10^{6}	1.0	1.0 [g]	5.0×10^{-2} [g]
U-234	1.1×10^{-5}		1.0	4.5×10^{1} [h]	2.1 [h]
Th-230	1.1×10^{-5}		1.0		
Ra-226 [g]	1.2×10^{-1}		1.0		
Ra-226 [h]	2.7×10^{-3}		1.0		
Np-237	5.0×10^{-4}	3×10^{3}	1.0	2.5×10^{2}	1.2×10^{1}
U-233	1.1×10^{-5}		1.3×10^{-2}		
Th-229	4.3×10^{-4}		1.7×10^{-3}		
Np-237	5.0×10^{-4}	5×10^{3}	8.9×10^{-1}	2.8×10^{2}	1.3×10^{1}
U-233	1.1×10^{-5}		2.0×10^{-2}		
Th-229	4.3×10^{-4}		3.9×10^{-3}		
Pu-239	4.0×10^{-5}	3×10^{3}	9.2×10^{-1}	3.4×10^{3}	1.6×10^{2}
		5×10^{3}	8.7×10^{-1}	3.6×10^{3}	1.7×10^{2}
Pu-240	4.0×10^{-5}	3×10^{3}	7.3×10^{-1}	4.3×10^{3}	2.1×10^{2}
		5×10^{3}	5.9×10^{-1}	5.3×10^{3}	2.5×10^{2}

Table 4.1-15. (continued)

Radionuclide	SDCF[b] (rem/y per μCi/m^3)	Time (y)	F[c]	Concentration Limit[d] (μCi/m^3)	Inventory Limit[e] (Ci)
Pu-242	3.8×10^{-5}	3×10^3	9.9×10^{-1}	3.3×10^3	1.6×10^2
		5×10^3	9.9×10^{-1}	3.3×10^3	1.6×10^2
Pu-244	3.7×10^{-5}	3×10^3	1.0	3.4×10^3	1.6×10^2
		5×10^3	1.0	3.4×10^3	1.6×10^2
Am-241	5.6×10^{-5}	3×10^3	8.1×10^{-3}	2.8×10^5 [i]	—
		5×10^3	3.3×10^{-4}	6.8×10^6 [i]	—
Am-243	2.5×10^{-4}	3×10^3	7.5×10^{-1}	6.7×10^2	3.2×10^1
		5×10^3	6.2×10^{-1}	8.1×10^2	3.9×10^1
Cm-245	1.1×10^{-4}	3×10^3	7.8×10^{-1}	1.5×10^3	7.0×10^1
		5×10^3	6.6×10^{-1}	1.7×10^3	8.3×10^1
Cm-246	4.0×10^{-5}	3×10^3	6.5×10^{-1}	4.8×10^3	2.3×10^2
		5×10^3	4.8×10^{-1}	6.5×10^3	3.1×10^2
Cm-247	4.4×10^{-4}	3×10^3	1.0	2.8×10^2	1.4×10^1
		5×10^3	1.0	2.8×10^2	1.4×10^1
Cm-248	1.4×10^{-4}	3×10^3	9.9×10^{-1}	9.0×10^2	4.3×10^1
		5×10^3	9.9×10^{-1}	9.0×10^2	4.3×10^1
Cf-249	4.6×10^{-4}	3×10^3	2.7×10^{-3}	1.0×10^5 [i]	—
		5×10^3	5.2×10^{-5}	5.2×10^6 [i]	—
Cf-251	1.6×10^{-4}	3×10^3	9.9×10^{-2}	7.9×10^3	3.8×10^2
		5×10^3	2.1×10^{-2}	3.7×10^4	1.8×10^3

[a] Concentration and inventory limits are obtained from Eqs. 4.1-2 and 4.1-3.

[b] Values are obtained from Table 4.1-10.

[c] Fraction of initial inventory of radionuclide remaining in disposal units at time scenario is assumed to occur.

[d] Limit on average concentration in disposed waste.

[e] Limit on inventory per vault; volume of each vault is assumed to be 4.8×10^4 m^3.

[f] Value exceeds NRC's Class-C limit in 10 CFR Part 61 of 8×10^4 μCi/m^3, which applies to individual waste packages at DOE disposal sites (U.S.DOE 1988a).

[g] Results include contributions to dose from radon decay product.

[h] Results exclude contributions to dose from radon decay product.

[i] Limit for individual waste packages at DOE disposal sites is 100 nCi/g (about 2×10^5 μCi/m^3) for all alpha-emitting, transuranic radionuclides with half-lives greater than 5 years (U.S.DOE 1988a).

The results of the dose analysis for the agriculture scenario at various times after disposal are given in Table 4.1-16. The results were obtained as described previously for the ILNT vaults. For Th-232, U-234, and U-238, two sets of results again are given, one including the contributions from radon and the other excluding the contributions from radon. The calculations again were performed at 10,000 and 20,000 years after disposal for all long-lived radionuclides and at 200,000 to 2,000,000 years for U-234, U-235, and U-238, when the dose from buildup of radiologically significant long-lived decay products could attain its maximum value. However, the results at 10,000 years, which is the maximum time of compliance with the performance objective for protection of inadvertent intruders, and at 20,000 years, which is the earliest time that the concrete and grout barriers in the vaults are expected to have failed sufficiently to permit excavation into a significant amount of waste, may be pessimistic based on the expected erosion resistance of the earthen cover, particularly the gravel layer. The only difference between the results for the ILT vaults in Table 4.1-16 and for the ILNT vaults in Table 4.1-14 is the volume of waste per vault, which is used only to convert the limits on average concentrations of radionuclides in disposed waste to limits on inventory per vault.

4.1.5.2 Dose Analysis for Resident Scenario

Two bounding assumptions have been used in the dose analysis for the resident scenario for inadvertent intruders. In the first case, the intruder is assumed to reside in a home located immediately on top of an intact concrete roof or other engineered barrier above a disposal unit, and the scenario is assumed to be credible immediately following loss of active institutional control at 100 years after disposal. In the second case, the home is assumed to be located immediately on top of the waste in a disposal unit, but the scenario is assumed not to occur until the concrete roof and any other engineered barriers above the waste have lost their integrity and can be penetrated during excavation.

In both bounding cases for the resident scenario, the intruder is assumed not to excavate into the waste itself while constructing a home on the disposal site. Thus, the only exposure pathway of concern for this scenario is external exposure to photon-emitting radionuclides in the waste while residing in the home. The only differences between the two bounding cases

Table 4.1-16. Results of dose analysis for intruder agriculture scenario for ILT vaults[a]

Radionuclide	SDCF[b] (rem/y per μCi/m³)	Time (y)	F[c]	Concentration Limit[d] (μCi/m³)	Inventory Limit[e] (Ci)
C-14	1.5×10^{-5}	1×10^{4}	3.0×10^{-1}	5.6×10^{4}	4.4×10^{1}
		2×10^{4}	8.8×10^{-2}	1.9×10^{5}	1.5×10^{2}
Al-26	3.9×10^{-3}	1×10^{4}	9.9×10^{-1}	6.5×10^{1}	5.2×10^{-2}
		2×10^{4}	9.8×10^{-1}	6.5×10^{1}	5.2×10^{-2}
Ni-59	6.8×10^{-8}	1×10^{4}	8.3×10^{-1}	4.4×10^{6}	3.5×10^{3}
		2×10^{4}	3.6×10^{-1}	1.0×10^{7}	8.2×10^{3}
Se-79	1.2×10^{-6}	1×10^{4}	3.8×10^{-2}	5.5×10^{6}	4.4×10^{3}
		2×10^{4}	3.4×10^{-2}	6.1×10^{6}	4.9×10^{3}
Rb-87	1.9×10^{-6}	1×10^{4}	1.0	1.3×10^{5}	1.0×10^{2}
		2×10^{4}	1.0	1.3×10^{5}	1.0×10^{2}
Zr-93	4.5×10^{-8}	1×10^{4}	1.0	5.6×10^{6}	4.4×10^{3}
		2×10^{4}	1.0	5.6×10^{6}	4.4×10^{3}
Tc-99	1.1×10^{-5}	1×10^{4}	1.8×10^{-2}	1.3×10^{6}	1.0×10^{3}
		2×10^{4}	1.5×10^{-2}	1.5×10^{6}	1.2×10^{3}
Pd-107	3.2×10^{-8}	1×10^{4}	1.0	7.8×10^{6}	6.3×10^{3}
		2×10^{4}	1.0	7.8×10^{6}	6.3×10^{3}
Sn-126	2.6×10^{-3}	1×10^{4}	5.8×10^{-2}	1.7×10^{3}	1.3
		2×10^{4}	4.1×10^{-2}	2.3×10^{3}	1.9
I-129	8.3×10^{-5}	1×10^{4}	2.5×10^{-3}	1.2×10^{6} [f]	6.4×10^{1}
		2×10^{4}	2.5×10^{-3}	1.2×10^{6} [f]	6.4×10^{1}
Cs-135	1.2×10^{-6}	1×10^{4}	1.1×10^{-2}	1.9×10^{7}	1.5×10^{4}
		2×10^{4}	1.1×10^{-2}	1.9×10^{7}	1.5×10^{4}
Th-232 [g]	1.4×10^{-2}	1×10^{4}	1.0	1.8×10^{1} [g]	1.4×10^{-2} [g]
		2×10^{4}	1.0	1.8×10^{1} [g]	1.4×10^{-2} [g]
Th-232 [h]	3.6×10^{-3}	1×10^{4}	1.0	6.9×10^{1} [h]	5.5×10^{-2} [h]
		2×10^{4}	1.0	6.9×10^{1} [h]	5.5×10^{-2} [h]
U-233	1.1×10^{-5}	1×10^{4}	9.6×10^{-1}	2.4×10^{4}	1.9×10^{1}
		2×10^{4}	9.2×10^{-1}	2.5×10^{4}	2.0×10^{1}
U-234	1.1×10^{-5}	1×10^{4}	9.7×10^{-1}	3.2×10^{1} [g]	2.5×10^{-2} [g]
Th-230	1.1×10^{-5}		8.5×10^{-2}	1.3×10^{3} [h]	1.0
Ra-226 [g]	1.2×10^{-1}		6.6×10^{-2}		
Ra-226 [h]	2.7×10^{-3}		6.6×10^{-2}		
U-234	1.1×10^{-5}	2×10^{4}	9.4×10^{-1}	1.5×10^{1} [g]	1.2×10^{-2} [g]
Th-230	1.1×10^{-5}		1.6×10^{-1}	6.4×10^{2} [h]	5.1×10^{-1} [h]
Ra-226 [g]	1.2×10^{-1}		1.4×10^{-1}		
Ra-226 [h]	2.7×10^{-3}		1.4×10^{-1}		

Table 4.1-16. (continued)

Radionuclide	SDCF[b] (rem/y per μCi/m^3)	Time (y)	F[c]	Concentration Limit[d] (μCi/m^3)	Inventory Limit[e] (Ci)
U-234	1.1×10^{-5}	2×10^{5}	5.7×10^{-1}	3.5 [g]	2.8×10^{-3} [g]
Th-230	1.1×10^{-5}		5.9×10^{-1}	1.6×10^{2} [h]	1.3×10^{-1} [h]
Ra-226 [g]	1.2×10^{-1}		5.9×10^{-1}		
Ra-226 [h]	2.7×10^{-3}		5.9×10^{-1}		
U-235	1.8×10^{-4}	1×10^{4}	1.0	7.4×10^{2}	5.9×10^{-1}
Pa-231	8.3×10^{-4}		1.9×10^{-1}		
U-235	1.8×10^{-4}	2×10^{4}	1.0	5.3×10^{2}	4.3×10^{-1}
Pa-231	8.3×10^{-4}		3.5×10^{-1}		
U-235	1.8×10^{-4}	1×10^{6}	1.0	2.5×10^{2}	2.0×10^{-1}
Pa-231	8.3×10^{-4}		1.0		
U-236	1.0×10^{-5}	1×10^{4}	1.0	2.5×10^{4}	2.0×10^{1}
		2×10^{4}	1.0	2.5×10^{4}	2.0×10^{1}
U-238	3.9×10^{-5}	1×10^{4}	1.0	1.9×10^{3} [g]	1.5 [g]
U-234	1.1×10^{-5}		2.8×10^{-2}	6.1×10^{3} [h]	4.9 [h]
Th-230	1.1×10^{-5}		1.2×10^{-3}		
Ra-226 [g]	1.2×10^{-1}		7.9×10^{-4}		
Ra-226 [h]	2.7×10^{-3}		7.9×10^{-4}		
U-238	3.9×10^{-5}	2×10^{4}	1.0	5.1×10^{2} [g]	4.0×10^{-1} [g]
U-234	1.1×10^{-5}		5.5×10^{-2}	5.0×10^{3} [h]	4.0 [h]
Th-230	1.1×10^{-5}		4.7×10^{-3}		
Ra-226 [g]	1.2×10^{-1}		3.8×10^{-3}		
Ra-226 [h]	2.7×10^{-3}		3.8×10^{-3}		
U-238	3.9×10^{-5}	2×10^{6}	1.0	2.1 [g]	1.7×10^{-3} [g]
U-234	1.1×10^{-5}		1.0	8.9×10^{1} [h]	7.1×10^{-2} [h]
Th-230	1.1×10^{-5}		1.0		
Ra-226 [g]	1.2×10^{-1}		1.0		
Ra-226 [h]	2.7×10^{-3}		1.0		
Np-237	5.0×10^{-4}	1×10^{4}	9.7×10^{-1}	5.1×10^{2}	4.1×10^{-1}
U-233	1.1×10^{-5}		4.2×10^{-2}		
Th-229	4.3×10^{-4}		1.5×10^{-2}		
Np-237	5.0×10^{-4}	2×10^{4}	7.4×10^{-1}	6.4×10^{2}	5.1×10^{-1}
U-233	1.1×10^{-5}		6.2×10^{-2}		
Th-229	4.3×10^{-4}		3.5×10^{-2}		
Pu-239	4.0×10^{-5}	1×10^{4}	7.5×10^{-1}	8.3×10^{3}	6.7
		2×10^{4}	5.6×10^{-1}	1.1×10^{4}	8.9
Pu-240	4.0×10^{-5}	1×10^{4}	3.4×10^{-1}	1.8×10^{4}	1.5×10^{1}
		2×10^{4}	1.2×10^{-1}	5.2×10^{4}	4.2×10^{1}
Pu-242	3.8×10^{-5}	1×10^{4}	9.8×10^{-1}	6.7×10^{3}	5.4
		2×10^{4}	9.6×10^{-1}	6.9×10^{3}	5.5
Pu-244	3.7×10^{-5}	1×10^{4}	1.0	6.8×10^{3}	5.4
		2×10^{4}	1.0	6.8×10^{3}	5.4

Table 4.1-16. (continued)

Radionuclide	SDCF[b] (rem/y per μCi/m^3)	Time (y)	F[c]	Concentration Limit[d] (μCi/m^3)	Inventory Limit[e] (Ci)
Am-243	2.5×10^{-4}	1×10^4	3.9×10^{-1}	2.6×10^3	2.1
		2×10^4	1.5×10^{-1}	6.7×10^3	5.3
Cm-245	1.1×10^{-4}	1×10^4	4.4×10^{-1}	5.2×10^3	4.1
		2×10^4	2.0×10^{-1}	1.1×10^4	9.1
Cm-246	4.0×10^{-5}	1×10^4	2.3×10^{-1}	2.7×10^4	2.2×10^1
		2×10^4	5.4×10^{-2}	1.2×10^5	9.3×10^1
Cm-247	4.4×10^{-4}	1×10^4	1.0	5.7×10^2	4.5×10^{-1}
		2×10^4	1.0	5.7×10^2	4.5×10^{-1}
Cm-248	1.4×10^{-4}	1×10^4	9.8×10^{-1}	1.8×10^3	1.5
		2×10^4	9.6×10^{-1}	1.9×10^3	1.5

[a] Concentration and inventory limits are obtained from Eqs. 4.1-2 and 4.1-3.

[b] Values are obtained from Table 4.1-10.

[c] Fraction of initial inventory of radionuclide remaining in disposal units at time scenario is assumed to occur.

[d] Limit on average concentration in disposed waste.

[e] Limit on inventory per vault; volume of each vault is assumed to be 8.0×10^2 m^3.

[f] Value exceeds NRC's Class-C limit in 10 CFR Part 61 of 8×10^4 μCi/m^3, which applies to individual waste packages at DOE disposal sites (U.S.DOE 1988a).

[g] Results include contribution to dose from radon decay product.

[h] Results exclude contribution to dose from radon decay product.

are the time at which the scenario is assumed to become credible, as described above, and the amount of shielding between the source region (i.e., the waste) and the receptor location.

The SDCFs obtained from the model for estimating dose to an inadvertent intruder for the resident scenario are summarized in Table 4.1-11. The remainder of this section discusses application of the results in Table 4.1-11 and the model in Eqs. 4.1-1 through 4.1-3 to the different disposal units in E-Area. The resident scenario is potentially relevant for any disposal units constructed with engineered barriers above the waste.

ILNT Vaults

As described previously, the ILNT vaults will be constructed with a concrete roof of average thickness about 90 cm and a layer of uncontaminated grout above the waste of thickness about 90 cm. Thus, the total thickness of the engineered barriers is about 1.8 m, and this thickness of shielding would apply to the resident scenario for the ILNT vaults at 100 years after disposal when all engineered barriers are assumed to be intact and impenetrable by normal excavation procedures.

As described in Appendix A.4.4, the 1.8 m thickness of shielding in the ILNT vaults is sufficient to reduce the external dose to very low levels for any conceivable concentrations of photon-emitting radionuclides in the waste. Therefore, in the dose analysis for the ILNT vaults at 100 years after disposal, the conservative assumption is made that only the layer of uncontaminated grout above the waste is present to provide shielding. For purposes of this analysis, the thickness of the grout layer is assumed to be 100 cm. This value is slightly greater than the planned thickness and is intended to take into account the somewhat greater shielding provided by any metal waste containers and waste forms in the ILNT vaults compared with the shielding provided by soil-equivalent material.

The results of the dose analysis for the resident scenario at 100 years after disposal are given in Table 4.1-17. The results are calculated in the same manner as those for the agriculture scenario using Eqs. 4.1-2 and 4.1-3, and the SDCFs are those for 100 cm of shielding in Table 4.1-11.

Table 4.1-17. Results of worst-case dose analysis for residential scenario for ELNT vaults at 100 years after disposal[a]

Radionuclide	SDCF[b] (rem/y per μCi/m^3)	F[c]	Concentration limit (μCi/m^3)	Inventory limit[e] (Ci)
Al-26	2.8×10^{-6}	1.0	8.9×10^{4}	5.1×10^{2}
Co-60	1.2×10^{-5}	2.0×10^{-5}	1.0×10^{11}	5.9×10^{3}
Sn-126	8.4×10^{-8}	1.0	3.0×10^{6}	1.7×10^{4}
Cs-137	2.2×10^{-8}	1.0×10^{-1}	1.1×10^{8}	6.5×10^{5}
Eu-154	3.5×10^{-7}	3.8×10^{-4}	1.9×10^{9}	1.1×10^{7}
Th-232	4.1×10^{-6}	1.0	6.1×10^{4}	3.5×10^{2}
U-232	3.8×10^{-6}	3.8×10^{-1}	1.7×10^{5}	9.9×10^{2}
U-235	2.3×10^{-12}	1.0	—	—
U-238	2.5×10^{-9}	1.0	—	—
Np-237	2.8×10^{-10}	1.0	[f]	—
Am-242m	5.2×10^{-10}	6.3×10^{-1}	[f]	—
Am-243	4.2×10^{-11}	9.9×10^{-1}	[f]	—
Cm-243	2.0×10^{-11}	8.8×10^{-2}	[f]	—
Cm-247	1.3×10^{-9}	1.0	[f]	—
Cf-249	1.1×10^{-9}	8.2×10^{-1}	[f]	—

[a] Concentration and inventory limits are obtained from Eqs. 4.1-2 and 4.1-3.

[b] Values are obtained from Table 4.1-11 for 100 cm of shielding.

[c] Fraction of initial inventory of radionuclides remaining in disposal units at time scenario is assumed to occur.

[d] Limit on average concentration in disposal waste.

[e] Limit on inventory per vault; volume of each vault is assumed to be 5.7×10^3 m^3.

[f] Limit for individual waste packages at DOE disposal sites is 100 nCi/g (about 2×10^5 μCi/m^3) for all alpha-emitting transuranic radionuclides with half-lives greater than 5 years (U.S.DOE 1988a).

The results in Table 4.1-17 are expected to be quite pessimistic, and thus, the derived concentration and inventory limits are identified as worst-case conditions. As described above, the assumed thickness of shielding of 100 cm for these calculations greatly underestimates the amount of shielding that would be provided by an intact concrete roof and the uncontaminated layer of grout above the waste. For the long-lived isotopes of uranium, the calculated concentration limit is greater than the specific activity, and the calculated limits are not included in the table.

As described previously, the second bounding case for the resident scenario for the ILNT vaults is based on the assumption that the intruder's home is located immediately on top of exposed waste in a disposal unit, but that the excavation for the home does not penetrate into the waste itself, because the grouting at the depth of the top layer of waste is still intact. Therefore, this variation of the resident scenario could not reasonably occur until the concrete roof above the vaults has lost its integrity and the layer of uncontaminated grout above the waste has weathered to soil-equivalent material. An analysis described previously in presenting the results for the agriculture scenario indicates that the second bounding case for the resident scenario first could occur at about 10,000 years after disposal.

The results of the dose analysis for the resident scenario at 10,000 years after disposal are given in Table 4.1-18 and again are obtained using Eqs. 4.1-2 and 4.1-3. The SDCFs in this case are those for no shielding in Table 4.1-11. Only long-lived radionuclides, including long-lived decay products of the isotopes of uranium and neptunium, are of concern at this time.

The assumption that residence on top of exposed waste could occur at 10,000 years after disposal may also be pessimistic for the ILNT vaults. Even if the top layer of the earthen cover would erode to the level of the gravel layer by that time, which would occur only if the erosion rate was comparable to the value presently observed for agriculture lands at the SRS, but was considerably greater than the erosion rate for natural forests at the site, the gravel layer presumably would be quite resistant to further erosion. Since the top of the gravel layer will lie about 3.5 m above the top layer of waste and an excavation for a home is assumed to extend no more than 3 m below the ground surface, an excavation at 10,000 years probably would not extend to the depth of waste, and the additional shielding provided by the remaining layer of uncontaminated material between the bottom of the excavation and the waste has not been taken into account in the dose analysis.

Table 4.1-18. Results of dose analysis for residential scenario for RLWF vaults at 10,000 years after closure[a]

Radionuclide	SDCF[b] (rem/year per μCi/m^3)	F[c]	Concentration limit (μCi/m^3)	Inventory limit[d] (Ci)
Al-26	3.9×10^{-3}	9.9×10^{-1}	6.5×10^{1}	3.7×10^{-1}
Sn-126	2.6×10^{-3}	5.8×10^{-2}	1.7×10^{3}	9.5
I-129	2.8×10^{-6}	2.5×10^{-3}	3.6×10^{7} [f]	4.6×10^{2}
Th-232	3.5×10^{-3}	1.0	7.1×10^{1}	4.1×10^{-1}
U-234 Ra-226	--- 2.4×10^{-3}	9.7×10^{-1} 6.6×10^{-2}	1.6×10^{3}	9.0
U-235 Pa-231	1.7×10^{-4} 4.2×10^{-4}	1.0 1.9×10^{-1}	1.0×10^{3}	5.7
U-238 Ra-226	2.9×10^{-5} 2.4×10^{-3}	1.0 7.9×10^{-4}	8.1×10^{3}	4.6×10^{1}
Np-237 Th-229	2.4×10^{-4} 3.5×10^{-4}	9.7×10^{-1} 1.5×10^{-2}	1.0×10^{3}	5.9
Am-243	2.0×10^{-4}	3.9×10^{-1}	3.2×10^{3}	1.8×10^{1}
Cm-245	7.4×10^{-5}	4.4×10^{-1}	7.7×10^{3}	4.4×10^{1}
Cm-247	4.0×10^{-4}	1.0	6.3×10^{2}	3.6

[a] Concentration and inventory limits are obtained from Eqs. 4.1-2 and 4.1-3.

[b] Values are obtained from Table 4.1-11 for the case of no shielding.

[c] Fraction of initial inventory of radionuclides remaining in disposal units at time scenario is assumed to occur.

[d] Limit on average concentration in disposal waste.

[e] Limit on inventory per vault; volume of each vault is assumed to be 5.7×10^{5} m^3.

[f] Value exceeds NRC's Class-C limit in 10 CFR Part 61 of 8×10^{4} μCi/m^3, which applies to individual waste packages at DOE disposal sites (U.S.DOE 1988a).

In contrast to the dose analysis for the agriculture scenario, there is no need to perform a dose analysis for the resident scenario at times beyond the time at which residence on top of exposed waste first becomes credible. At later times, the top layer of waste presumably would begin to weather to soil-equivalent material and the agriculture scenario, which always results in a higher dose per unit concentration of radionuclides, then becomes the scenario of concern.

LAW Vaults

As described previously, the LAW vaults will be constructed with a concrete roof of average thickness about 50 cm, but without a layer of uncontaminated grout above the waste. This thickness of shielding would apply to the resident scenario for the LAW vaults at 100 years after disposal when the concrete roof is assumed to be intact and impenetrable by normal excavation procedures.

As described in Appendix A.4.4, the nominal thickness of shielding provided by the concrete roof for the LAW vaults is assumed to be 45 cm. This value is slightly less than the planned thickness of the roof and is intended to take into account the somewhat reduced shielding provided by the waste itself due to the presence of void spaces in these disposal units.

The results of the dose analysis for the resident scenario at 100 years after disposal are given in Table 4.1-19. The results are calculated using Eqs. 4.1-2 and 4.1-3, and the SDCFs are those for 45 cm of shielding in Table 4.1-11.

The assumption that the resident scenario could occur at 100 years after disposal probably is reasonable for the LAW vaults, because the thickness of the earthen cover above the vaults is approximately the same as the presumed maximum depth of an excavation in constructing a home. Therefore, significant erosion of the cover material would not be required in order for an excavation to uncover the roof of the vaults.

Table 4.1-19. Results of dose analysis for resident scenario for LAW vaults at 100 years after closure[a]

Radionuclide	SDCF[b] (rem/year per μCi/m^3)	F[c]	Concentration limit (μCi/m^3)	Inventory limit[e] (Ci)
Al-26	1.1×10^{-4}	1.0	1.1×10^{3}	5.5×10^{1}
Co-60	8.8×10^{-5}	2.0×10^{-6}	7.1×10^{3}	3.4×10^{7}
Sn-126	2.2×10^{-5}	1.0	5.7×10^{3}	2.7×10^{2}
Cs-137	6.6×10^{-6}	1.0×10^{-1}	1.9×10^{5}	9.1×10^{3}
Eu-154	3.2×10^{-5}	3.8×10^{-4}	1.0×10^{7}	4.9×10^{5}
Th-232	1.1×10^{-4}	1.0	1.1×10^{3}	5.5×10^{1}
U-232	9.2×10^{-5}	3.8×10^{-1}	3.6×10^{3}	1.7×10^{2}
U-235	3.9×10^{-8}	1.0	----	----
U-238	3.0×10^{-7}	1.0	----	----
Np-237	4.6×10^{-7}	1.0	[f]	----
Am-242m	6.2×10^{-8}	6.3×10^{-1}	[f]	----
Am-243	1.1×10^{-7}	9.9×10^{-1}	[f]	----
Cm-243	4.9×10^{-8}	8.8×10^{-2}	[f]	----
Cm-245	5.3×10^{-9}	9.9×10^{-1}	[f]	----
Cm-247	1.3×10^{-6}	1.0	[f]	----
Cf-249	1.2×10^{-6}	8.2×10^{-1}	[f]	----
Cf-251	3.1×10^{-8}	9.3×10^{-1}	[f]	----

[a] Concentration and inventory limits are obtained from Eqs. 4.1-2 and 4.1-3.

[b] Values are obtained from Table 4.1-11 for 45 cm of shielding.

[c] Fraction of initial inventory of radionuclides remaining in disposal units at time scenario is assumed to occur.

[d] Limit on average concentration in disposal waste.

[e] Limit on inventory per vault; volume of each vault is assumed to be 4.8×10^4 m^3.

[f] Limit for individual waste packages at DOE disposal sites is 100 nCi/g (about 2×10^5 μCi/m^3) for all alpha-emitting transuranic radionuclides with half-lives greater than 5 years (U.S.DOE 1988a).

However, the second bounding case for the resident scenario, based on an assumption that the intruder's home is located immediately on top of exposed but impenetrable waste in a disposal unit, is not relevant for the LAW vaults. This bounding case occurs only at a time when the concrete roof has failed and excavation to the depth of the waste could occur. As described previously, this time at which the concrete roof collapses is expected to be about 3,000 years after disposal for the LAW vaults. By this time, the waste forms and waste packages themselves presumably will have degraded to soil-equivalent material, because the waste in the LAW vaults will not be grouted. Therefore, at times after the concrete roof collapses, the agriculture scenario would become the scenario of concern and the resident scenario would no longer be relevant.

ILT Vaults

As described previously, the ILT vaults will be constructed in the same manner as the ILNT vaults, i.e., with a concrete roof of average thickness about 90 cm, a layer of uncontaminated grout above the waste of thickness about 90 cm, and grouting of the waste vaults. Thus, the dose analysis for the resident scenario for the ILT vaults is essentially the same as the previous analysis for the ILNT vaults. The only difference between the results for these two types of vaults is the assumed volume of waste per vault, which again is used only to convert the limits on average concentrations of radionuclides to limits on inventory per vault.

The results for the two bounding cases for the resident scenario — the first at 100 years after disposal when residence on top of an intact concrete barrier 100 cm thick is assumed to occur, and the second at about 10,000 years when residence on top of unshielded waste is assumed to occur — are given in Tables 4.1-20 and 4.1-21. As in the analysis for the ILNT vaults, the results at 100 years after disposal in Table 4.1-20, are expected to be quite pessimistic, because the assumed thickness of shielding of 100 cm considerably underestimates the thickness of an intact concrete roof and layer of uncontaminated grout above the waste. The analysis for the second bounding case at 10,000 years after disposal also would be pessimistic if the earthen cover above the vaults has eroded only to the level of the gravel layer by that time, because an excavation would not likely extend to the depth of the waste.

Table 4.1-10. Results of worst-case dose analysis for accident scenario for ILT vaults at 100 years after disposal[a]

Radionuclide	SDCF[b] (rem/year per μCi/m^3)[a]	F[c]	Concentration limit (μCi/m^3)	Inventory limit[d] (Ci)
Al-26	2.8×10^{-5}	1.0	8.9×10^{4}	7.1×10^{1}
Co-60	1.2×10^{-6}	2.0×10^{-6}	1.0×10^{11}	8.3×10^{7}
Sn-126	8.4×10^{-8}	1.0	3.0×10^{6}	2.4×10^{3}
Cs-137	2.2×10^{-8}	1.0×10^{-1}	1.1×10^{8}	9.1×10^{4}
Eu-154	3.5×10^{-7}	3.8×10^{-4}	1.9×10^{9}	1.5×10^{6}
Th-232	4.1×10^{-6}	1.0	6.1×10^{4}	4.9×10^{1}
U-232	3.8×10^{-6}	3.8×10^{-1}	1.7×10^{5}	1.4×10^{2}
U-235	2.3×10^{-12}	1.0	—	—
U-238	2.5×10^{-9}	1.0	—	—
Np-237	2.8×10^{-10}	1.0	[f]	—
Am-242m	5.2×10^{-10}	6.3×10^{-1}	[f]	—
Am-243	4.2×10^{-11}	9.9×10^{-1}	[f]	—
Cm-243	2.0×10^{-11}	8.8×10^{-2}	[f]	—
Cm-247	1.3×10^{-9}	1.0	[f]	—
Cf-249	1.1×10^{-9}	8.2×10^{-1}	[f]	—

[a] Concentration and inventory limits are obtained from Eqs. 4.1-2 and 4.1-3.

[b] Values are obtained from Table 4.1-11 for 100 cm of shielding.

[c] Fraction of initial inventory of radionuclides remaining in disposal units at time scenario is assumed to occur.

[d] Limit on average concentration in disposal waste.

[e] Limit on inventory per vault; volume of each vault is assumed to be 8.0×10^{2} m^3.

[f] Limit for individual waste packages at DOE disposal sites is 100 nCi/g (about 2×10^{5} μCi/m^3) for all alpha-emitting transuranic radionuclides with half-lives greater than 5 years (U.S.DOE 1988a).

Table 4.1-21. Results of dose analysis for resident scenario for ILT vaults at 10,000 years after disposal

Radionuclide	SDCF[b] (rem/y per μCi/m^3)	F[c]	Concentration limit (μCi/m^3)	Inventory limit[e] (Ci)
Al-26	3.9×10^{-3}	9.9×10^{-1}	6.5×10^{1}	5.2×10^{-2}
Sn-126	2.6×10^{-3}	5.8×10^{-2}	1.7×10^{3}	1.3
I-129	2.8×10^{-6}	2.5×10^{-3}	3.6×10^{7} [f]	2.9×10^{4}
Th-232	3.5×10^{-3}	1.0	7.1×10^{1}	5.7×10^{-2}
U-234 Ra-226	— 2.4×10^{-3}	9.7×10^{-1} 6.6×10^{-2}	1.6×10^{3}	1.3
U-235 Pa-231	1.7×10^{-4} 4.2×10^{-4}	1.0 1.9×10^{-1}	1.0×10^{3}	8.0×10^{-1}
U-238 Ra-226	2.9×10^{-5} 2.4×10^{-3}	1.0 7.9×10^{-4}	8.1×10^{3}	6.5
Np-237 Th-229	2.4×10^{-4} 3.5×10^{-4}	9.7×10^{-1} 1.5×10^{-2}	1.0×10^{3}	8.3×10^{-1}
Am-243	2.0×10^{-4}	3.9×10^{-1}	3.2×10^{3}	2.6
Cm-245	7.4×10^{-5}	4.4×10^{-1}	7.7×10^{3}	6.1
Cm-247	4.0×10^{-4}	1.0	6.3×10^{2}	5.0×10^{-1}

[a] Concentration and inventory limits are obtained from Eqs. 4.1-2 and 4.1-3.

[b] Values are obtained from Table 4.1-11 for the case of no shielding.

[c] Fraction of initial inventory of radionuclides remaining in disposal units at time scenario is assumed to occur.

[d] Limit on average concentration in disposal waste.

[e] Limit on inventory per vault; volume of each vault is assumed to be 8.0×10^{2} m^3.

[f] Value exceeds NRC's Class-C limit in 10 CFR Part 61 of 8×10^{4} μCi/m^3, which applies to individual waste packages at DOE disposal sites (U.S.DOE 1988a).

4.1.5.3 Dose Analysis for Post-Drilling Scenario

The SDCFs obtained from the model for estimating dose to inadvertent intruders for the post-drilling scenario are summarized in Table 4.1-12. The remainder of this section discusses application of the results in Table 4.1-12 to the different disposal units in E-Area. The model for estimating dose and limits on concentrations and inventories of radionuclides is given by Eqs. 4.1-1 through 4.1-3, except the geometrical correction factor (G) is not relevant for the post-drilling scenario when drilling is assumed to occur through the waste. The post-drilling scenario is potentially relevant for any disposal units constructed with engineered barriers.

ILNT Vaults

The post-drilling scenario assumes that the concrete roof, layer of uncontaminated grout above the waste, and grouting of the waste itself would preclude drilling into the waste for as long as these barriers remain intact. Therefore, since the waste in the ILNT vaults will be grouted, drilling into the waste is not expected to be a credible occurrence until the grout essentially has weathered to soil-equivalent material. Since weathering of the grout also is presumed to be a necessary condition for occurrence of the agriculture scenario involving excavation into the waste, the post-drilling and agriculture scenarios presumably would not occur until approximately the same time after disposal. Therefore, since the agriculture scenario always results in more restrictive disposal limits for radionuclides than the post-drilling scenario when the two scenarios are assumed to occur at the same time, the post-drilling scenario need not be considered further in the ILNT vaults, and limits on concentrations and inventories of radionuclides based on this scenario are not presented.

LAW Vaults

As described in previously, the concrete roof on the LAW vaults is expected to remain intact for about 3,000 years. At the time the roof is expected to collapse, drilling through the disposal units is presumed to be a credible occurrence because, in contrast to the ILNT

vaults, the waste in the LAW vaults will not be grouted and any waste forms and waste packages presumably will be sufficiently degraded that drilling through the waste would not be precluded.

The results of the dose analysis for the post-drilling scenario at 3,000 years after disposal are given in Table 4.1-22. The SDCFs are obtained from Table 4.1-12, and the concentration and inventory limits are calculated from Eqs. 4.1-2 and 4.1-3, except the parameter G is set equal to unity. As in the analysis for the agriculture scenario, results for Th-232, U-234, and U-238 are calculated including and excluding the contribution to the dose from radon decay products. The post-drilling scenario need not be considered at times substantially beyond 3,000 years, because the more restrictive agriculture scenario is presumed to become credible by about 5,000 years. At 3,000 years after disposal, only long-lived radionuclides in the waste are of concern for the post-drilling scenario.

ILT Vaults

The ILT vaults will be constructed in the same manner as the ILNT vaults. Therefore, the applicability of the post-drilling scenario will be the same in the two cases. As described previously in the discussion of the post-drilling scenario for the ILNT vaults, the post-drilling scenario need not be considered in establishing concentration and inventory limits of radionuclides in the ILT vaults, essentially because the more restrictive agriculture scenario could occur at the same time as the first credible occurrence of the post-drilling scenario. Therefore, results for the post-drilling scenario are not presented for the ILT vaults.

4.1.5.4 Summary of Dose Analysis for Inadvertent Intruders

A dose analysis for inadvertent intruders for the EAV has been performed on the basis of three assumed exposure scenarios:

- an agriculture scenario involving direct excavation into disposal units;
- a resident scenario involving residence in a home on top of intact engineered barriers above disposal units or on top of unshielded waste; and
- a post-drilling scenario involving removal of waste from disposal units by drilling.

Table 4.1-24. Results of dose analysis for post-drilling scenario for CAW waste[a]

Radionuclide	SDCF[b] (rem/year per μCi/m^3)	F[c]	Concentration limit[d] (μCi/m^3)	Inventory limit[e] (Ci)
C-14	1.5×10^{-6}	6.9×10^{-1}	9.7×10^{4}	4.6×10^{3}
Al-26	1.8×10^{-6}	1.0	5.5×10^{4}	2.7×10^{3}
Ni-59	6.8×10^{-9}	9.7×10^{-1}	1.5×10^{7}	7.3×10^{5}
Se-79	1.2×10^{-7}	9.3×10^{-1}	9.0×10^{5}	4.3×10^{4}
Zr-93	3.5×10^{-9}	1.0	2.9×10^{7}	1.4×10^{6}
Rb-87	1.9×10^{-7}	1.0	5.3×10^{5}	2.5×10^{4}
Tc-99	1.1×10^{-6}	8.7×10^{-1}	1.0×10^{5}	5.0×10^{3}
Pd-107	3.2×10^{-9}	1.0	3.1×10^{7}	1.5×10^{6}
Sn-126	1.4×10^{-6}	9.8×10^{-1}	7.3×10^{4}	3.5×10^{3}
I-129	8.1×10^{-6}	1.5×10^{-4}	8.2×10^{7} [f]	3.8×10^{3}
Cs-135	1.2×10^{-7}	1.0	8.3×10^{5}	4.0×10^{4}
Th-232 [g]	8.0×10^{-6}	1.0	1.3×10^{4} [g]	6.0×10^{2} [g]
Th-232 [h]	5.9×10^{-6}	1.0	1.7×10^{4} [h]	8.1×10^{2} [h]
U-233	7.5×10^{-7}	9.9×10^{-1}	1.3×10^{5}	6.5×10^{3}
U-234	7.3×10^{-7}	9.9×10^{-1}	7.9×10^{4} [g]	3.8×10^{3} [g]
Th-230	3.4×10^{-7}	2.7×10^{-2}	9.1×10^{4} [h]	4.4×10^{3} [h]
Ra-226 [g]	4.5×10^{-5}	1.2×10^{-2}		
Ra-226 [h]	3.2×10^{-5}	1.2×10^{-2}		
U-235	7.9×10^{-7}	1.0	5.2×10^{4}	2.5×10^{3}
Pa-231	1.8×10^{-5}	6.2×10^{-2}		
U-236	6.9×10^{-7}	1.0	1.4×10^{5}	7.0×10^{3}
U-238	6.6×10^{-7}	1.0	1.5×10^{5} [g]	7.2×10^{3} [g]
U-234	7.3×10^{-7}	8.5×10^{-3}	1.5×10^{5} [h]	7.2×10^{3} [h]
Th-230	3.4×10^{-7}	1.1×10^{-4}		
Ra-226 [g]	4.5×10^{-5}	3.7×10^{-5}		
Ra-226 [h]	3.2×10^{-5}	3.7×10^{-5}		
Np-237	2.4×10^{-5}	1.0	4.2×10^{3}	2.0×10^{2}
U-233	7.5×10^{-7}	1.3×10^{-2}		
Th-229	2.9×10^{-6}	1.7×10^{-3}		
Pu-239	2.5×10^{-6}	9.2×10^{-1}	4.3×10^{4}	2.1×10^{3}

Table 4.1-22. (continued)

Radionuclide	SDCF[b] (rem/year per μCi/m^3)	F[c]	Concentration limit[d] (μCi/m^3)	Inventory limit[e] (Ci)
Pu-240	2.5×10^{-6}	7.3×10^{-1}	5.5×10^{4}	2.6×10^{3}
Pu-242	2.4×10^{-6}	9.9×10^{-1}	4.2×10^{4}	2.0×10^{3}
Pu-244	2.3×10^{-6}	1.0	4.3×10^{4}	2.1×10^{3}
Am-241	3.1×10^{-6}	8.1×10^{-3}	4.0×10^{6} [g]	---
Am-242m	3.0×10^{-6}	1.1×10^{-6}	3.0×10^{10} [i]	—
Am-243	3.2×10^{-6}	7.5×10^{-1}	4.2×10^{4}	2.0×10^{3}
Cm-245	2.5×10^{-6}	7.8×10^{-1}	5.1×10^{4}	2.5×10^{3}
Cm-246	2.5×10^{-6}	6.5×10^{-1}	6.2×10^{4}	3.0×10^{3}
Cm-247	2.5×10^{-6}	1.0	4.0×10^{4}	1.9×10^{3}
Cm-248	8.9×10^{-6}	9.9×10^{-1}	1.1×10^{4}	5.4×10^{2}
Cf-249	2.7×10^{-6}	2.7×10^{-3}	1.4×10^{7} [f]	—
Cf-251	2.6×10^{-6}	9.9×10^{-2}	3.9×10^{5} [i]	—

[a] Concentration and inventory limits are obtained from Eqs. 4.1-2 and 4.1-3 with G set equal to unity. Scenario is assumed to occur at 3,000 years after disposal.

[b] Values are obtained from Table 4.1-12.

[c] Fraction of initial inventory of radionuclides remaining in disposal units at time scenario is assumed to occur.

[d] Limit on average concentration in disposal waste.

[e] Limit on inventory per vault; volume of each vault is assumed to be 4.8×10^4 m^3.

[f] Value exceeds NRC's Class-C limit in 10 CFR Part 61 of 8×10^4 μCi/m^3, which applies to individual waste packages at DOE disposal sites (U.S.DOE 1988a).

[g] Results include contribution to dose from radon decay product.

[h] Results exclude contribution to dose from radon decay product.

[i] Limit for individual waste packages at DOE disposal sites is 100 nCi/g (about 2×10^5 μCi/m^3) for all alpha-emitting transuranic radionuclides with half-lives greater than 5 years (U.S.DOE 1988a).

For each of these scenarios, the performance objective for protection of inadvertent intruders is a limit on EDE of 100 mrem per year. As described in Sect. 1.2.1, this performance objective is assumed to apply for 10,000 years after disposal. However, an intruder dose analysis also has been performed for times beyond 10,000 years if the maximum dose could occur at such times.

Models for estimating dose to inadvertent intruders according to the assumed exposure scenarios were used to derive limits on average concentrations and inventories of radionuclides in the different types of disposal units, based on the performance objective for inadvertent intruders. The results of the analyses for the three exposure scenarios for the different types of disposal units in E-Area are summarized as follows.

ILNT Vaults

For the ILNT vaults, an analysis of the expected performance of the earthen cover above the vaults, the layer of uncontaminated grout above the waste, and the grout surrounding the waste itself has indicated that the agriculture scenario probably is not a credible occurrence until well beyond 10,000 years after disposal. A gravel layer, which should erode at a very slow rate compared with an assumed erosion rate for agriculture land at the SRS, will be located sufficiently far above the top layer of waste that normal excavation into the waste is not expected as long as the gravel layer is in place. Furthermore, the analysis indicates that about 20,000 years will be required for a significant thickness of waste to weather to soil-equivalent material, and thus, be subject to removal by excavation.

In Table 4.1-14, results based on a dose analysis for the agriculture scenario are presented for a sequence of times beginning at 10,000 years after disposal. However, for the purpose of demonstrating compliance with the performance objective for protection of inadvertent intruders, the most reasonable conclusion from the present analysis is that the agriculture scenario would not occur within the 10,000-year compliance period for the performance objective, and thus, would not provide a reasonable basis for establishing limits on concentrations and inventories of radionuclides for disposal.

Since the post-drilling scenario is assumed to be credible only after the concrete roof and grout layers have lost their integrity, this scenario presumably cannot occur for the ILNT vaults until about the same time as the agriculture scenario. Therefore, the post-drilling scenario also would not reasonably occur within the 10,000-year compliance period. Furthermore, the dose per unit concentration of radionuclides for the post-drilling scenario is always less than the value for the agriculture scenario. Therefore, it is reasonable to conclude that the post-drilling scenario also is not relevant for establishing disposal limits for the ILNT vaults.

The resident scenario could occur at 100 years after disposal, when a home could be built on top of an intact concrete roof, or at about 10,000 years after disposal, when an analysis of the performance of the engineered barriers indicates that excavation to the depth of the top of the waste in the vaults could become credible. Thus, of the different exposure scenarios for inadvertent intruders considered in this analysis, only the resident scenario reasonably can be used to establish disposal limits for the ILNT vaults. Results for the two bounding cases for the resident scenario are given in Table 4.1-17 and 4.1-18.

The estimated limits on concentrations and inventories of radionuclides for the ILNT vaults, as obtained from the analysis of the resident scenario at 100 and 10,000 years after disposal, are summarized in Table 4.1-23. The limits for any radionuclide are the more restrictive of the results in Tables 4.1-17 and 4.1-18. With the exception of the relatively short-lived radionuclides Co-60, Cs-137, and U-232, the disposal limits are based on the resident scenario at 10,000 years after disposal, because the shielding between the source and receptor locations is considerably less in the case of residence on unshielded waste compared with residence on an intact concrete barrier above the waste. The disposal limits for Co-60, Cs-137, and U-232 are undoubtedly pessimistic, because the planned thickness of the concrete roof and layer of uncontaminated grout above the waste is about 1.8 m thick but only 1 m of shielding was assumed in the dose analysis. The disposal limits for the other radionuclides also may be pessimistic. Erosion of the earthen cover to a depth below the top of the gravel layer appears unlikely within 10,000 years. If the gravel layer has not eroded away within 10,000 years, then an excavation for a home probably would not extend to the depth of the waste, and the shielding provided by a layer of uncontaminated material between the top of the waste and the bottom of the excavation was not considered in the dose analysis.

Table 4.1-23. Disposal limits of radionuclides for ILNT and ILT vaults based on analyses of exposure scenarios for inadvertent intruders[a]

Radionuclide[b]	Concentration limit[c] (μCi/m^3)	Inventory limit[d] (Ci)
Al-26	6.5×10^{1}	4.2×10^{-1}
Co-60	1.0×10^{11}	6.7×10^{8}
Sn-126	1.7×10^{3}	1.1×10^{1}
I-129	8.0×10^{4} [e]	5.2×10^{2}
Cs-137	1.1×10^{8}	7.4×10^{5}
Eu-154	1.9×10^{9}	1.2×10^{7}
Th-232	7.1×10^{1}	4.7×10^{-1}
U-232	1.7×10^{5}	1.1×10^{3}
U-234	1.6×10^{3}	1.0×10^{1}
U-235	1.0×10^{3}	6.5
U-238	8.1×10^{3}	5.2×10^{1}
Np-237	1.0×10^{3}	6.7
Am-243	3.2×10^{3}	2.1×10^{1}
Cm-245	7.7×10^{3}	5.0×10^{1}
Cm-247	6.3×10^{2}	4.1

[a] Values are more restrictive of limits for resident scenario at 100 and 10,000 years after disposal given in Table 4.1-17, 4.1-18, 4.1-20, and 4.1-21.

[b] For radionuclides not listed, either there are no disposal limits based on scenarios for inadvertent intrusion or concentration limits in individual waste packages are restricted to limits for Class-C wastes specified in NRC's 10 CFR Part 61 (see Table 4.1-24).

[c] Limit on average concentration in disposed waste.

[d] Limit on inventory per vault, sum of ILNT and ILT limits.

[e] Limit for Class-C waste specified in NRC's 10 CFR Part 61; limit applies to individual waste packages.

As indicated in Table 4.1-23, analyses of scenarios for inadvertent intrusion have established disposal limits for only a relatively few of the total number of radionuclides that could occur in the waste. For all other radionuclides of concern with half-lives sufficiently long that they possibly could exist in significant amount at 100 years after disposal when inadvertent intrusion first could occur, either there are no disposal limits based on the intruder dose analysis or the concentrations in individual waste packages are restricted to the limits for Class-C waste specified by the NRC in 10 CFR Part 61. Concentration limits for Class-C waste specified by the NRC are given in Table 4.1-24.

LAW Vaults

For the LAW vaults, all three exposure scenarios for inadvertent intruders are presumed to be credible during the 10,000-year compliance period, primarily because these vaults do not contain a layer of uncontaminated grout above the waste and the waste itself is not grouted. Based on an analysis of the collapse and subsequent degradation of the concrete roof for the LAW vaults, the agriculture scenario is most likely to become credible at about 5,000 years after disposal and the post-drilling scenario could occur at about 3,000 years. The only relevant resident scenario involves residence on an intact concrete roof at 100 years after disposal. Results for the three scenarios are given in Tables 4.1-15, 4.1-19, and 4.1-22.

The estimated limits on concentrations and inventories of radionuclides for the LAW vaults, as obtained from the analyses of the agriculture scenario at 5,000 to 10,000 years after disposal, the resident scenario at 100 years, and the post-drilling scenario at 3,000 years, are summarized in Table 4.1-25. The limits for any radionuclide are the most restrictive of the limits for the relevant scenarios. For most radionuclides, the disposal limits are based on the agriculture scenario at 5,000 to 10,000 years after disposal. However, for Co-60, Cs-137, and U-232, the limits are based on the resident scenario at 100 years after disposal, and the limits for Tc-99 are based on the post-drilling scenario at 3,000 years. Tc-99 represents an unusual case where a large fraction of the initial inventory of waste is predicted to be removed from the vaults by mobilization and transport in water between the times the post-drilling and

Table 4.1-23. Concentration limits of radionuclides for Class-C waste specified in NRC's 10 CFR Part 61[a]

Radionuclide	Concentration limit (μCi/m^3)
C-14 [b]	8.0×10^6
Ni-59 [b]	2.2×10^7
Ni-63 [b]	7.0×10^8
Sr-90	7.0×10^9
Tc-99	3.0×10^6
I-129	8.0×10^4
Cs-137	4.6×10^9
[illegible] [c]	1.0×10^2 [d]
Pu-241	3.5×10^3 [d]
Cm-242	2.0×10^4 [d]

[a] Limits from Table 1 and 2 of 10 CFR Part 61 apply to individual waste packages at DOE disposal sites (U.S.DOE 1988a).

[b] If radionuclide occurs in form of activated metal, concentration limit is increased by factor of 10.

[c] All alpha-emitting transuranic radionuclides with half-lives greater than 5 years.

[d] Units are nCi/g; 1 nCi/g corresponds approximately to 2×10^3 μCi/m^3.

Table 4.1-2i. Disposal limits of radionuclides for LAW vaults based on analyses of exposure scenarios for inadvertent intrusion[a]

Radionuclide[b]	Concentration limit[c] ($\mu Ci/m^3$)	Inventory limit[d] (Ci)
C-14	1.9×10^4	8.9×10^2
Al-26	3.2×10^1	1.5
Co-60	7.1×10^8	3.4×10^7
Ni-59	1.9×10^6	9.2×10^4
Se-79	2.4×10^6	1.2×10^5
Rb-87	6.6×10^4	3.2×10^3
Zr-93	2.8×10^6	1.3×10^5
Tc-99	1.0×10^5	5.0×10^3
Pd-107	3.9×10^6	1.9×10^5
Sn-126	7.3×10^8	3.5
I-129	8.0×10^4 [e]	3.8×10^3
Cs-135	3.3×10^5	1.6×10^4
Cs-137	1.9×10^5	9.1×10^3
Eu-154	1.0×10^7	4.9×10^5
Th-232	8.9 [f] 3.5×10^1 [g]	4.3×10^{-1} [f] 1.7 [g]
U-232	3.6×10^3	1.7×10^2
U-233	1.2×10^4	5.6×10^2
U-234	1.6×10^1 [f] 6.6×10^2 [g]	7.6×10^{-1} [f] 3.2×10^1 [g]
U-235	3.7×10^2	1.8×10^1
U-236	1.3×10^4	6.0×10^2
U-238	9.3×10^2 [f] 3.0×10^3 [g]	4.5×10^1 [f] 1.5×10^2 [g]
Np-237	2.8×10^2	1.3×10^1
Pu-239	3.6×10^3	1.7×10^2
Pu-240	5.3×10^3	2.5×10^2
Pu-242	3.3×10^3	1.6×10^2
Pu-244	3.4×10^3	1.6×10^2

Table 4.1-25. (continued)

Radionuclide[b]	Concentration limit[c] (μCi/m^3)	Inventory limit[d] (Ci)
Am-241	[h]	—
Am-242m	[h]	—
Am-243	8.1×10^2	3.9×10^1
Cm-245	1.7×10^3	8.3×10^2
Cm-246	6.5×10^3	3.1×10^2
Cm-247	2.8×10^2	1.4×10^1
Cm-248	9.0×10^2	4.3×10^1
Cf-249	[h]	—
Cf-251	3.7×10^4	1.8×10^3

[a] Values are most restrictive of limits for agriculture scenario at 5,000 or 10,000 years after disposal given in Table 4.1-14, resident scenario at 100 years after disposal given in Table 4.1-20, or post-drilling scenario at 3,000 years after disposal given in Table 4.1-23.

[b] For radionuclides not listed, either there are no disposal limits based on scenarios for inadvertent intrusion or concentration limits in individual waste packages are restricted to limits for Class-C wastes specified in NRC's 10 CFR Part 61 (see Table 4.1-24).

[c] Limit on average concentration in disposed waste.

[d] Limit on inventory per vault.

[e] Limit for Class-C waste specified in NRC's 10 CFR Part 61; limit applies to individual waste packages.

[f] Results include contributions to dose from radon decay product.

[g] Results exclude contributions to dose from radon decay product.

[h] Limit for individual waste packages is based on requirement that concentration of all alpha-emitting transuranic radionuclides with half-lives greater than 5 years not exceed 100 nCi/g (about 2×10^3 μCi/m^3).

agriculture scenarios are assumed to occur, due to the significant increase in infiltration at times beyond collapse of the vault roof at 3,000 years after disposal. Two sets of concentration and inventory limits are given for Th-232, U-234, and U-238. If exposures to radon decay products are taken into account in estimating doses to inadvertent intruders, which presumably is required by the present performance objective (U.S.DOE 1988a), then the lower of the disposal limits apply for each isotope. However, if the dose limit in the performance objective for protection of inadvertent intruders were to exclude doses from exposure to radon and a separate limit on radon flux rate to the atmosphere were imposed, as is presently being considered in revision of DOE Order 5820.2A, then the higher of the disposal limits apply.

ILT Vaults

The dose analysis for inadvertent intruders is essentially the same for the ILT vaults as for the ILNT vaults, because both types of vaults will be constructed in the same manner. Therefore, as in the case of the ILNT vaults, the only exposure scenario for inadvertent intruders that reasonably could be used to determine disposal limits of radionuclides for the ILT vaults is the resident scenario, evaluated at either 100 or 10,000 years after disposal.

The estimated limits on concentrations and inventories of radionuclides for the ILT vaults, as obtained from the analysis of the resident scenario at 100 and 10,000 years after disposal in Tables 4.1-20 and 4.1-21, are summarized in Table 4.1-26. With the exception of Co-60, Cs-137, and U-232, the disposal limits are based on the resident scenario at 10,000 years after disposal. As described previously for the ILNT vaults, the disposal limits for Co-60, Cs-137, and U-232 are expected to be quite pessimistic, because the amount of shielding between the source and receptor locations has been underestimated by a significant amount, and the disposal limits for the other radionuclides also may be pessimistic, because excavation to the depth of the waste appears unlikely within 10,000 years after disposal.

Table 4.1-26. D[illegible] of radionuclide[illegible] vaults b[illegible] c[illegible] of exposure scenarios for [illegible] intrusion[illegible]

Radionuclide[b]	Concentration limit[c] ($\mu Ci/m^3$)	Inventory limit[d] (Ci)
Al-26	8.9×10^4	7.1×10^1
Co-60	1.0×10^{11}	8.3×10^7
Sn-126	1.7×10^3	1.3
I-129	8.0×10^4 [e]	4.6×10^2
Cs-137	1.1×10^8	9.1×10^4
Eu-154	1.9×10^9	1.5×10^6
Th-232	7.1×10^1	5.7×10^{-2}
U-232	1.7×10^5	1.4×10^2
U-234	1.6×10^3	1.3
U-235	1.0×10^3	8.0×10^{-1}
U-238	8.1×10^3	6.5
Np-237	1.0×10^3	8.6×10^{-1}
Am-243	3.2×10^3	2.6
Cm-245	7.7×10^3	6.1
Cm-247	6.3×10^2	5.0×10^{-1}

[a] Values are more restrictive of limits for resident scenario at 100 and 10,000 years after disposal given in Table 4.1-21 and 4.1-22, respectively.

[b] For radionuclides not listed, either there are no disposal limits based on scenarios for inadvertent intrusion or concentration limits in individual waste packages are restricted to limits for Class-C wastes specified in NRC's 10 CFR Part 61 (see Table 4.1-24).

[c] Limit on average concentration in disposed waste.

[d] Limit on inventory per vault.

[e] Limit for Class-C waste specified in NRC's 10 CFR Part 61; limit applies to individual waste packages.

4.2 SENSITIVITY AND UNCERTAINTY ANALYSES

To interpret the results provided in the previous section (Sect. 4.1), parameters and assumptions to which the results are most sensitive must be identified. The uncertainty associated with these parameters and assumptions must also be considered to determine the degree of confidence in the predicted results. A rigorous quantitative analysis of uncertainty is desirable, but such an analysis is not possible for all aspects of the analyses conducted for this RPA due to: 1) limits of our knowledge with respect to certain physical and functional characteristics or processes; 2) the inability to predict conditions in the future, especially beyond several decades; and 3) the inability to quantify uncertainty associated with the definition of a particular scenario. This last type of uncertainty can dominate the overall uncertainty in some cases.

In this section, sensitivity and uncertainty analyses are discussed separately for the following stages of the overall computational approach: 1) analysis of near-field transport to the water table from the vaults and subsequent groundwater transport; 2) dose analysis for off-site releases; and 3) dose analysis for inadvertent intruders.

4.2.1 Analysis of Near-Field and Groundwater Transport

In this RPA, the fractional fluxes of radionuclides to the water table were simulated in the near-field model with PORFLOW and used as a source to the saturated flow and transport model (also simulated with PORFLOW) to determine groundwater concentrations as a function of time and distance from the EAV. The sensitivity and uncertainty analysis of the near-field groundwater transport model is discussed in this section.

A sensitivity and uncertainty analysis was performed on the near-field and groundwater transport models with respect to selected parameters (Appendix J). The PORFLOW simulations of the ILNT vault system were evaluated in terms of the movement of ^{99}Tc from the vault area through the vadose zone and in groundwater. The study focusses on the sensitivity and uncertainty in model results with respect to the K_ds in the waste form, concrete and soil of the unsaturated zone, and with respect to timing of two different types of vault failure: roof cracking and roof collapse.

Sensitivity of, and uncertainty in, PORFLOW simulations of vault-contained low-level radioactive waste were evaluated in the Z-Area RPA (WSRC 1992b) with respect to variable infiltration rates and hydraulic and diffusive properties of the waste form, vaults, and soil. The results indicated a low sensitivity to infiltration rate, due to the flux-controlling nature of the low-conductivity concrete materials, and a high sensitivity to hydraulic conductivity, especially to that of the material with the lowest conductivity. Ultimately, the amount of water allowed to flow through the waste and reach the water table controls the final groundwater concentration. A large uncertainty in the hydraulic conductivity can translate to a large uncertainty in predicted results. However, the EAVs analysis is expected to be less sensitive to concrete hydraulic conductivities with respect to maximum groundwater concentrations, since most of the radionuclides of concern are long-lived and, thus, are available for transport after vault failure is assumed. Degradation of the low-conductivity concrete is considered to be complete in approximately 1000 years, during which time leaching or radioactive decay for most of the E-Area radionuclides of concern is minimal.

The analysis of the influence of K_d and timing parameters (Appendix J) together resulted in specification of distributions and bounds on values of five factors for the PORFLOW simulations in this analysis. The results of the sensitivity analysis indicated that the peak groundwater concentration was most sensitive to the concrete K_d assumed for ^{99}Tc (accounting for 96% of the response variability). This is likely due to the fact that concrete K_ds specified in this RPA are orders of magnitude larger than the waste or soil K_ds for ^{99}Tc, such that retardation in the concrete is the controlling geochemical factor in the simulations. The time that the peak occurred was also fairly sensitive to the time assumed between vault cracking and roof collapse. The amount of variability, or uncertainty, in the ^{99}Tc results was rather low for the range of parameter values tested. Calculated 95% tolerance limits indicated peak groundwater concentrations to range between 0.008 and 0.192 pCi/cc per Ci of ^{99}Tc in the ILNT vaults, while the time of the peak ranged from 780 to 5500 years with 95% confidence. The peak groundwater concentration of ^{99}Tc from Table 4.1-5 is 0.04 pCi/cc per Ci in the ILNT vaults, occurring at 1800 years, which is approximately the midpoint of these distributions. A cumulative distribution function of the maximum groundwater concentrations calculated in the uncertainty analysis (Fig. 4.2-1) indicated that although 50% of the calculated peak

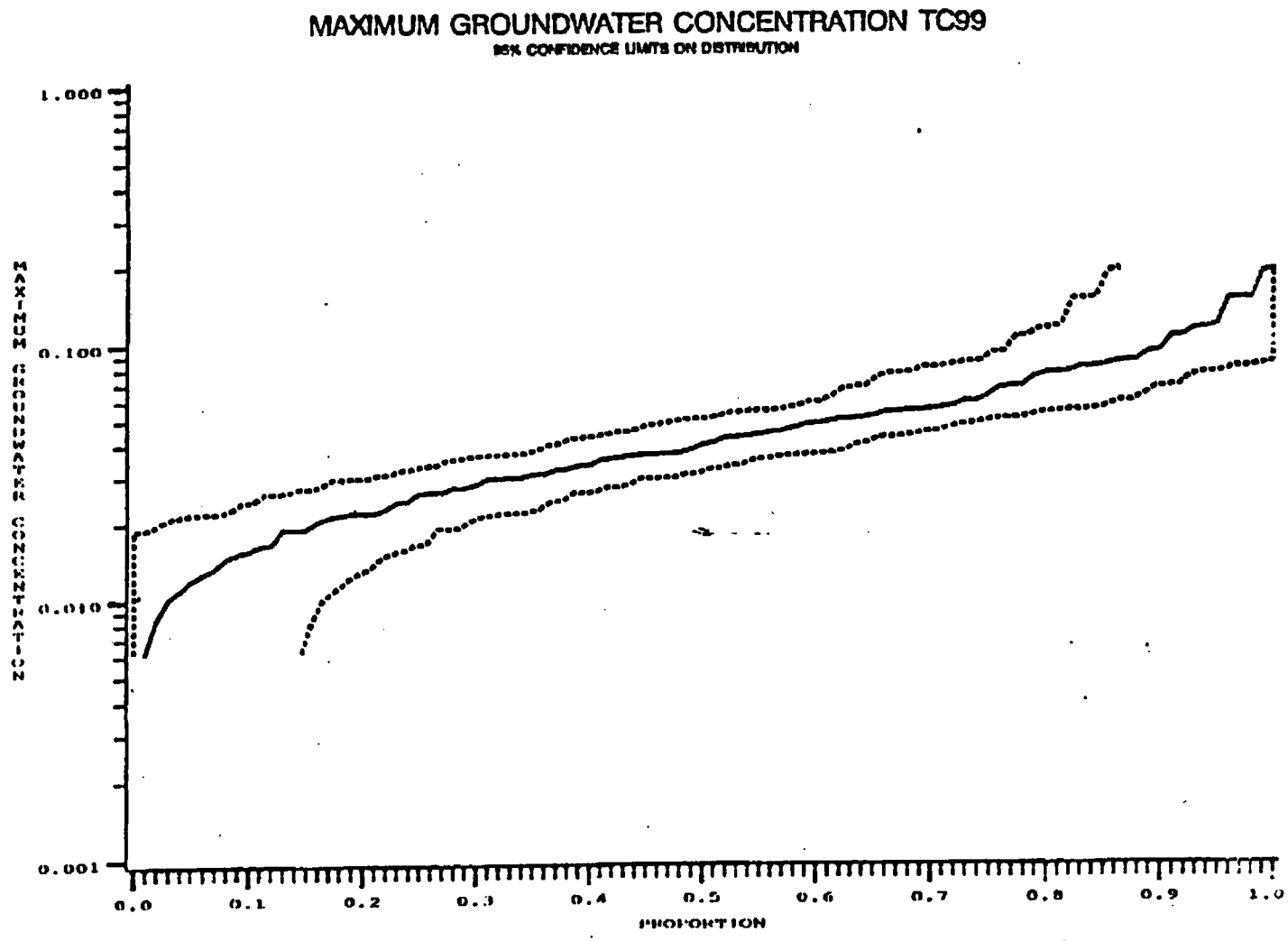

Fig. 4.2-1. Cumulative distribution function for peak groundwater concentration of ^{99}Tc, based on ranges of parameters specified in Appendix J.

groundwater concentrations appear to exceed the 0.24 pCi/cc per Ci inventory, less than 10% exceed 0.1 pCi/cc per Ci. Because the ranges of K_ds and timing of degradation events were specified to be very broad for the uncertainty analysis (Table J.1-1, Appendix J), the results of this analysis lend confidence in the RPA results for near-field transport.

A preliminary sensitivity analysis of the PORFLOW saturated flow and transport model indicates that simulation of flow is sensitive to the amount of recharge assumed and the horizontal and vertical saturated hydraulic conductivities of the five hydrologic units assumed in the model. The simulation of transport by groundwater is directly proportional to the flux of contaminant to the water table, but is insensitive to the diffusion coefficient because the transport in groundwater is advection-dominated. Sensitivity of the model to transverse and longitudinal dispersivities within the reasonable ranges for these parameters is low because the plume originating at the EAV facility is so broad.

Sensitivity to recharge under the facility was tested by varying the recharge rate between 0.2 and 40 cm/year under the area covered by the facility, and assuming 40 cm/year elsewhere in the model domain. Increasing recharge from 0.2 to 2 cm/year under the EAV results in only a slight increase in water levels and hydraulic gradients under the facility, and virtually no change in the contaminant concentration at the compliance point for a given flux of contaminant to the water table. This is likely due to the relative unimportance of either 0.2 or 2 cm/year recharge to the flow system under the facility. When recharge under the EAV is increased to 40 cm/year, the simulated elevation of the groundwater table and hydraulic gradient under the facility are observed to increase more dramatically, but contaminant concentrations at the point of compliance do not decrease as dramatically for a given flux of contaminant to the aquifer.

While the sensitivity and uncertainty analysis with respect to selected parameters for Tc-99 indicates low variability around the reported groundwater concentrations for Tc-99, groundwater concentrations for solubility-limited radionuclides (i.e., isotopes of U and Pu) have an additional type of associated uncertainty - that of the prescribed solubility limits. It is believed that the uncertainty associated with the solubility limits applied is largely governed by the changes in geochemistry that may occur over time, as the vaults degrade. It is very

difficult, if not impossible, to predict these changes and the effect they may have on solubility of U and Pu with a quantifiable degree of certainty because of the multitude of competing geochemical processes involved. Therefore, quantification of uncertainty associated with the groundwater concentrations of U and Pu isotopes was not attempted in this analysis.

4.2.2 Analysis of Dose Model from Off-Site Releases

As described in Sect. 4.1.4 and elsewhere, the drinking water pathway is the primary exposure pathway of concern for releases of radionuclides via the groundwater pathway beyond the 100-m buffer zone around disposal units. In this section, the sensitivity and uncertainty analysis of the model used to estimate dose from the drinking water pathway is discussed.

For a given concentration of a radionuclide in groundwater, the estimated dose from the drinking water pathway is given by Eq. (A.4-1) of Appendix A.4. In this equation, the dose per unit concentration of a radionuclide for the drinking water pathway is directly proportional to two parameters: 1) the consumption rate of drinking water from the affected source and 2) the ingestion DCF for the radionuclide. Both of these parameters are assumed to be fixed values for a reference adult as specified by regulatory authorities or international advisory groups. In this analysis, the assumed consumption rate of water of 2 L/d is the value normally specified by the EPA in demonstrating compliance with DWS for radionuclides; and the ingestion DCFs for radionuclides, which are given in Table A.4-2 of Appendix A.4, are values developed by the International Commission on Radiological Protection. Therefore, for purposes of this analysis, the dose from the drinking water pathway per unit concentration of any radionuclide in groundwater is assumed to be a prescribed value with no uncertainty.

In any population of exposed individuals, the intake rate of water and the ingestion DCFs for radionuclides are variables that could be described by a mean value and standard deviation. However, for the type of dose analysis presented in this report, it is customary to assume, as indicated above, that all exposed members of the general public are reference individuals who experience the same intake rates of water and the same doses per unit activity intakes of radionuclides by ingestion. The assumed intake rate of drinking water of 2 L/day is not likely to be exceeded by most individuals.

Although the dose per unit concentration of a radionuclide in water for a normal population would be subject to some uncertainty, this uncertainty undoubtedly will be much less than the uncertainty associated with estimates of the maximum concentrations of radionuclides in groundwater at any location beyond the 100-m buffer zone. Thus, the assumption of no uncertainty in the model for estimating dose from the drinking water pathway should have no effect on the overall uncertainty in the performance of the disposal facility with regard to meeting the performance objective for protection of groundwater resources.

4.2.3 Analysis of Dose Models for Inadvertent Intruders

The model for estimating dose to an inadvertent intruder, as represented by Eq. 4.1-1, is based on estimates of annual doses per unit concentration of radionuclides in disposed waste, the so-called SDCFs for the agriculture, resident, and post-drilling scenarios summarized in Tables 4.1-10, 4.1-11, and 4.1-12, respectively. This section discusses the sensitivity and uncertainty analysis of the models used to estimate the SDCFs for the different exposure scenarios for inadvertent intruders. The sensitivity and uncertainties in these models do not depend on similar considerations regarding depletion of radionuclide inventories in disposal units due to mobilization and transport in water, which are discussed in Sect. 4.2.1.

For each of the assumed exposure scenarios, the SDCFs for radionuclides are single values based on the models and parameter values presented in Appendix A.4.5. The parameter values adopted for use in the models for the different exposure pathways usually were intended to represent reasonable average conditions that might be experienced, rather than maximum possible conditions that would yield the highest estimates of dose. This approach was used in selecting parameter values related to human activities, such as the annual consumption of foodstuffs, breathing rate, and exposure times, and parameter values describing transport of radionuclides through environmental pathways to man, such as the elemental plant-to-soil concentration ratios and atmospheric mass loading of activity suspended from surface soil.

The exposure pathways considered in the dose analyses for an inadvertent intruder for the different exposure scenarios include consumption of vegetables grown in contaminated garden soil, direct consumption of contaminated garden soil, external exposure while working in the garden or during indoor residence, and inhalation exposure while working in the garden or during indoor residence. In implementing the models for the various exposure pathways, data specific to the SRS generally were not available for such important parameters as the elemental plant-to-soil concentration ratios in vegetables grown in contaminated garden soil and the airborne concentration of suspended radionuclides in particulate form. Therefore, generic parameter values obtained from the literature were used in all exposure pathway models, and the same data can be used to provide crude estimates of uncertainty.

For fission and activation products which do not emit significant intensities of high-energy photons (e.g., Sr-90 and Tc-99), the vegetable pathway is the only significant contributor to the total dose for the agriculture and post-drilling scenarios, and the dose for this pathway is directly proportional to the plant-to-soil concentration ratio. Data available in the literature, which often were obtained under conditions that may not be representative of the SRS, indicate that this parameter could be uncertain by as much as one-to-three orders of magnitude depending upon the radionuclide (Ng et al. 1982; Peterson 1983).

For actinide radioisotopes which do not emit significant intensities of high-energy photons (e.g., Pu-239), the soil ingestion and inhalation pathways are significant contributors to the total dose for the agriculture and post-drilling scenarios. In the model for the soil ingestion pathway, the intake rate of contaminated soil is the only parameter that is subject to variability. There are few data on the distribution of intake rates that could be used to support an uncertainty analysis, but the intake rate presumably is uncertain by at least an order of magnitude. In the model for the inhalation pathway, the dose is proportional to the atmospheric mass loading of suspended activity from surface soil. Generic data indicate that this parameter could be uncertain by two or three orders of magnitude (Anspaugh et al. 1975; Healy 1980).

The dose for the resident scenario is due entirely to external exposure; and, for radionuclides that emit significant intensities of high-energy photons (e.g., Cs-137, Ra-226), this pathway is the only significant contributor to the total dose for the agriculture scenario and is an important contributor to the total dose for the post-drilling scenario. The dose from external exposure depends on the assumed exposure time and the amount of shielding between the source and receptor locations, and it is not particularly meaningful to attempt to quantify uncertainties in these parameters. Particularly in the resident scenario, estimates of external dose could be uncertain by an order of magnitude or more if the assumed thickness of shielding provided by engineered barriers is in error by only a few tens of cm. As described in Appendix A.4.4, the assumed thicknesses of shielding for the types of disposal units constructed with engineered barriers probably result in overestimates of dose. External dose in the resident and agriculture scenarios also depends on the shielding factor for the walls of the home during indoor residence, but this parameter probably is uncertain by no more than a factor of two.

For some important parameters in the exposure pathway models, it is difficult to quantify the uncertainty even on the basis of generic data. An example of a parameter for which the uncertainty appears to be essentially unquantifiable is the assumed dilution factor for mixing of waste exhumed from disposal units with native soil in a vegetable garden. The dose from several exposure pathways in the agriculture scenario and from all exposure pathways in the post-drilling scenario is directly proportional to this dilution factor. An uncertainty analysis for this parameter could be based on estimated uncertainties in the volume of waste exhumed from disposal units, the fraction of exhumed waste that is mixed with soil in a vegetable garden, and the size of the garden. But, except for the assumed size of the garden, there are no data that could be used to support such an uncertainty analysis, essentially because the values are based primarily on assumptions presumed to be reasonable. The uncertainty in this dilution factor is probably an order of magnitude or more. However, it seems likely that the values chosen for use in this analysis tend to overestimate the average concentrations of radionuclides that would be found in contaminated soil in a vegetable garden. The dilution factor of 0.2 assumed in the agriculture scenario probably is conservative because exhumed

waste presumably would not be fertile material and, thus, soil containing a significantly larger fraction of exhumed material would not support plant growth. The dilution factor of 0.02 assumed in the post-drilling scenario is based on reasonable assumptions for the volume of drilling waste and the size of the vegetable garden, and the assumption that all drilling waste is mixed with native soil in the garden clearly is conservative.

The most important source of uncertainty in the estimates of the SDCFs for the different exposure scenarios probably is the definitions of the scenarios themselves, not withstanding any parameter uncertainties that could be quantified and regardless of whether or not the results would reasonably represent the variability in doses that could be experienced at the SRS. The dose analyses for inadvertent intruders are based on assumptions that the exposure scenarios will occur as postulated, but many of the explicit or implicit assumptions used in defining the scenarios are open to question and, furthermore, are likely to be conservative.

In defining exposure scenarios, it seems reasonable to assume that an inadvertent intruder will establish a homestead within the boundary of the disposal facility at some time after loss of active institutional controls. However, several of the assumptions used in developing the particular exposure scenarios used in this analysis are less certain and probably pessimistic. For example, all scenarios assume that individuals will have no knowledge of prior waste disposal activities at the site, but this assumption seems unreasonable for times soon after loss of active institutional controls. Furthermore, even if knowledge of the disposal facility were lost, all exposure scenarios assume that an inadvertent intruder will build a home or drill a well at the location of disposal units, rather than in uncontaminated areas, and that exhumed waste will be mixed with uncontaminated soil in a vegetable garden. Particularly at the SRS, it may also be pessimistic to assume that an intruder would excavate to depths well below the ground surface in constructing a home, because most homes near the site do not have a basement.

By their very definitions, the exposure scenarios for inadvertent intruders assume conditions that probably tend to produce estimates of dose considerably greater than doses that reasonably could be received by most individuals who might come onto the disposal site. Therefore, it is not really the purpose of a dose analysis for inadvertent intruders to provide best estimates of dose that likely would be received and a quantification of uncertainties in

these estimates. Rather, the primary purpose of the analysis is to establish WAC in the form of limits on average concentrations (total inventories) of radionuclides in waste. Furthermore, quantitative estimates of uncertainties in calculated doses (and, thus, in limits on average concentrations or inventories of radionuclides) based on parameter uncertainty analyses may not be meaningful, because the results are conditional on the occurrence of the assumed exposure scenarios. Therefore, the most important factor in determining whether or not the WAC derived from dose analyses for inadvertent intruders are likely to be reasonable is the credibility of the assumed exposure scenarios—i.e., whether the assumed exposure scenarios reasonably could occur at a particular disposal facility—rather than any estimates of uncertainties in the results due to uncertainties in model parameters.

4.3 INTERPRETATION OF RESULTS

The results presented in Sect. 4.1 can be interpreted by comparing the calculated vault inventory limits and an estimated radionuclide inventory for disposal. As stated in Sect. 1, due to the changing nature of operations at SRS, it is impossible to make an accurate estimate at the present time as to the type and quantity of waste that will be disposed of in the EAVDF. However, an estimate based on several years of disposal while SRS was in production has been made (Reed 1992), and that will be used as the basis for the comparison. While this is a good measure of the usefulness of the vault structures as a method of disposal, this alone is not sufficient to address the question of whether there is reasonable assurance that all performance objectives of DOE Order 5820.2A are met. Further interpretation is necessary because limited data exist for performing realistic and definitive uncertainty analyses. Providing reasonable assurance requires consideration of: 1) sensitivities of results to parameters, assumptions and models; 2) uncertainties in models, parameters and scenarios; and 3) conservatisms, or lack thereof, inherent in the calculational approach or scenarios devised. In this section, some of the more significant observations made throughout this report are summarized and results are interpreted in terms of these observations.

Results presented in Sect. 4.1 indicate that the EAVDF will meet the performance objectives of DOE Order 5820.2A. The results are based on a number of assumptions, simplifications, and scenarios that, in most cases, erred on the side of conservatism. Therefore, the results are more likely to underestimate, rather than overestimate, the inventory allowable in each type of disposal.

4.3.1 Off-Site Doses and Groundwater Protection

For off-site releases, groundwater was demonstrated to be the only pathway of concern except for H-3 and C-14, which are limited by atmospheric emission (see Appendix A.3). Nine radionuclides were limited by the groundwater pathway, Ni-59, Se-79, Sr-90, Pd-107, I-129, Cs-135, Np-237, Am-241, and Cf-252 (based on the Cm-248 daughter). Consideration of solubility limitations on U and Pu isotopes prevents them from exceeding their respective MCLs. Although the solubility limits applied are believed to be reasonable for this waste, the long-term geochemistry is impossible to predict. As noted in Sect. 4.2.1, the uncertainty associated with the predicted groundwater concentrations of U and Pu, arising from uncertainty in long-term geochemistry, has not been addressed. Radioactive decay products of U and Pu isotopes that are potentially radiologically significant were not found to limit the inventory of U or Pu below the assumed initial inventory, with the exception of the Ra-226 daughter of U-234 in the LAW vaults. In this one case, it was estimated that U-234 would be limited to 2.6×10^4 Ci for all 21 LAW vaults, or about 200 kg/LAW vault.

As stated in Sect. 1.2, the current MCLs, promulgated under the Safe Drinking Water Act, are used in this RPA to assess compliance with the groundwater protection performance objective of DOE Order 5820.2A. For uranium a compliance limit of 20 µg/L is used (EPA 1991).

Degradation of the vaults and the overlying closure cap were considered in this RPA because the engineered features of the facility are not expected to last indefinitely. An engineering study was commissioned to provide a basis for selecting degradation time for use in the analysis (Appendix K). As stated in Sect. 2.5.2.4, the EAVs were designed to withstand a 0.2 g earthquake after closure. Based on Sect. 2.1.5.2, seismic events are not expected to

produce accelerations at SRS greater than 0.1 g; thus, seismic events were considered less significant than other degradation mechanisms. Although many mechanisms potentially contributing to degradation are identified (Sect. 3.1.3), the impossibility of predicting the timing and magnitude of degradation processes renders the uncertainty associated with the degradation scenario high.

4.3.2 Inadvertent Intruders

Scenarios were developed and dose analyses were completed to estimate exposures to hypothetical inadvertent intruders. Acute exposure scenarios for inadvertent intruders were not included, because they would always be less restrictive in regard to demonstrating compliance with performance objectives than chronic exposure scenarios (Sect. 3.2.4.3). The four chronic exposure scenarios considered were: 1) an agricultural scenario with direct intrusion into the disposal vaults; 2) a resident scenario; 3) a post-drilling scenario; and 4) volatile transport. Some considerations are important for interpretation of the intruder results.

One consideration is the longevity of the engineered structures. If the vaults maintain their integrity for several hundred years then all of the radionuclides with relatively short half-lives decay away before intrusion into the waste is possible. As shown in Appendix K and Sect. 3.1.3.2, even in the conservative analysis presented, the vaults will be effective intruder barriers for at least 1,000 years.

The second consideration is the long-term dose in the agricultural scenario due to the buildup of radium and radon daughters from U-238 and U-234. As shown in Tables 4.1-14 and 4.1.15, doses from these isotopes exceed performance objectives at very long times after disposal. However, as stated in Sect. 1.2, this RPA assumes that only doses calculated out to 10,000 years after disposal are considered for compliance. Also, as stated in Sect. 1.2.3, dose from radon and its decay products will be excluded from inadvertent intruder dose for the purpose of assessing compliance. A separate performance objective for radon (20 pCi/m^2 s) is established. A conservative analysis of the radon exhalation rate from the EAVDF is presented in Appendix A.3.

Yet another consideration is the effect of long-term land use policy at SRS. Draft DOE Order 5820.2B (U.S.DOE 1994) considers the use of inadvertent intruder analyses to determine whether a site should be released for unrestricted use. Also, DOE Headquarters Offices of Environmental Restoration and Waste Management (EM) and Facilities Management (FM) are jointly sponsoring an effort to develop future use plans for each of the DOE sites. The expectation for SRS is that the EAVDF and surrounding land will be zoned for industrial use only and will be controlled in perpetuity. This will eliminate the potential for inadvertent intrusion. Table 4.1-9 presents acceptable inventory limits for the EAVDF derived only from the groundwater protection scenario. Long-term land use plans will be developed and implemented; however, because this effort is only now in the planning stage, this PA will conservatively establish inventory limits based on protection of inadvertent intruders. Future revisions of the PA will take appropriate credit for land use planning.

4.3.3 Disposal Limits for Waste at E-Area

Limiting inventories calculated from the groundwater pathway (Table 4.1-9) and intruder scenarios (Table 4.1-14 and Table 4.1-15) as well as the results of the atmospheric effluent analyses in Appendix A.3, have been combined in Table 4.3-1, which lists for each radionuclide the most restrictive of the three. The limiting inventories in Table 4.3-1 can be compared with an estimated vault inventory which is shown in Table 4.3-2 for the LAW vaults and Table 4.3-3 for the ILNT vaults. The estimated inventory (Reed 1992) is based on the average waste receipts at the SRS burial ground during the three year period 1986 through 1988. The average annual receipts were multiplied by a factor of 2.5 to provide a conservative inventory estimate.

None of the vault limits exceed the estimated inventory. Thus, the limits calculated in this PA are not expected to restrict waste receipts to the EAVDF.

The inventory limits calculated in this analysis are implemented through a set of WAC and managed through the SRS's computerized Waste Information Tracking System (WITS). The operating limits for the EAVs, as documented in the SRS WAC Manual (WSRC 1993), are derived from safety documentation and this PA. The WAC Manual is a compilation of

Table 4.3-1. E-Area Vault Disposal Facility performance-based inventory limits (Ci/vault) and limiting performance objectives

Radionuclide	LAW	ILNT & ILT (ILNT only for ^3H)	ILT
H-3	8.3×10^5 (air)	5.0×10^5 (air)	6.7×10^4 (air) JCW* 4.2×10^7 (air) crucibles
C-14	4.0×10^1 (air)	1.0×10^1 (air)	
Al-26	1.5 (a)	4.2×10^{-1} (r)	
Co-60	3.4×10^7 (r)	6.7×10^2 (r)	
Ni-59	7.6×10^2 (g)	1.8×10^3 (g)	
Se-79	6.2 (g)	8.9 (g)	
Rb-87	3.2×10^3 (a)	No limit #	
Sr-90	2.5×10^{13} (g)	3.0×10^{13} (g)	
Zr-93	1.3×10^5 (a)	No limit #	
Tc-99	2.0 (g)	2.0 (g)	
Pd-107	1.9×10^5 (a)	No limit #	
Sn-126	3.5 (a)	1.1×10^1 (r)	
I-129	1.0×10^{-3} (g)	5.3×10^{-4} (g)	
Cs-135	5.7×10^1 (g)	1.9×10^1 (g)	
Cs-137	9.1×10^3 (r)	7.4×10^5 (r)	
Eu-154	4.9×10^5 (r)	1.2×10^7 (r)	
Th-232	1.7 (a)	4.7×10^{-1} (r)	
U-232	1.7×10^2 (r)	1.1×10^3 (r)	
U-233	5.6×10^2 (a)	3.6×10^{13} (g)	
U-234	3.2×10^1 (a)	1.0×10^1 (r)	
U-235	1.8×10^1 (a)	6.5 (r)	
U-236	6.0×10^2 (a)	3.5×10^{19} (g)	
U-238	1.5×10^2 (a)	5.2×10^1 (r)	
Np-237	2.6×10^{-1} (g)	2.0×10^{-1} (g)	
Pu-239	1.7×10^2 (a)	1.6×10^{10} (g)	
Pu-240	2.5×10^2 (a)	No limit #	
Pu-242	1.6×10^2 (a)	No limit #	
Pu-244	1.6×10^2 (a)	No limit #	
Am-241	2.1×10^3 (g)	1.0×10^3 (g)	
Am-243	3.9×10^1 (a)	2.1×10^1 (r)	
Cm-245	8.3×10^1 (a)	5.0×10^1 (r)	
Cm-246	3.1×10^2 (a)	No limit #	
Cm-247	1.4×10^1 (a)	4.1 (r)	
Cm-248	4.3×10^1 (a)	No limit #	
Cf-249	8.1×10^3 (g)	5.1×10^5 (g)	
Cf-251	1.8×10^3 (a)	1.6×10^7 (g)	
Cf-252	4.3×10^6 (g)	2.1×10^8 (g)	

Note: (air) = atmospheric (Appendix A.3)
(g) = groundwater protection (Table 4.1-9)
(a) = intruder, agricultural scenario (Tables 4.1-14 and 4.1-15)
(r) = intruder, resident scenario (Tables 4.1-17, 4.1-18, and 4.1-19).
(*) = JCW = Job Control Waste
(#) = Intrusion into waste in the Intermediate Level vaults is not credible until after 10,000 years (Sect. 4.1.5.1).

Table 13-2 Comparison of LAW vault calculated disposal limits with estimated inventory

Radionuclide	Disposal Limit Ci/Vault	Estimated Inventory Ci/Vault	Ratio
H-3	8.3×10^{5}	5.0×10^{3}	1.7×10^{2}
C-14	4.0×10^{1}	6.0×10^{-1}	6.7×10^{3}
Al-26	1.5	--------	--------
Co-60	3.4×10^{7}	2.4	1.4×10^{7}
Ni-59	7.6×10^{2}	0	--------
Se-79	6.2	5.5×10^{-5}	1.1×10^{6}
Rb-87	3.2×10^{3}	--------	--------
Sr-90	2.5×10^{12}	7.1×10^{2}	3.5×10^{15}
Zr-93	1.3×10^{5}	2.6×10^{-2}*	5.0×10^{6}
Tc-99	2.0	2.0×10^{-4}	1.0×10^{4}
Pd-107	1.9×10^{5}	2.1×10^{-4}*	9.1×10^{8}
Sn-126	3.5	3.4×10^{-3}	1.0×10^{3}
I-129	1.0×10^{-3}	3.1×10^{-7}	3.2×10^{3}
Cs-135	5.7×10^{1}	1.3×10^{-3}*	4.4×10^{4}
Cs-137	9.1×10^{3}	7.1×10^{2}	1.3×10^{1}
Eu-154	4.9×10^{5}	--------	--------
Th-232	1.7	3.4×10^{-3}	5.0×10^{2}
U-232	1.7×10^{2}	--------	--------
U-233	5.6×10^{2}	1.2×10^{-1}	4.7×10^{3}
U-234	3.2×10^{1}	1.9	1.7×10^{1}
U-235	1.8×10^{1}	1.7×10^{-2}	1.1×10^{3}
U-236	6.0×10^{2}	3.2×10^{-1}	1.9×10^{3}
U-238	1.5×10^{2}	5.5	2.7×10^{1}
Np-237	2.6×10^{-1}	3.2×10^{-7}	8.1×10^{5}
Pu-239	1.7×10^{2}	3.2×10^{1}	5.3
Pu-240	2.5×10^{2}	1.2×10^{-1}	2.1×10^{3}
Pu-242	1.6×10^{2}	2.2×10^{-7}	7.3×10^{8}
Pu-244	1.6×10^{2}	1.2×10^{-1}	1.3×10^{3}
Am-241	2.1×10^{3}	4.0×10^{-4}	3.3×10^{6}
Am-243	3.9×10^{1}	2.1×10^{-7}	1.9×10^{8}
Cm-245	8.3×10^{1}	1.2×10^{-1}	6.9×10^{2}
Cm-246	3.1×10^{2}	1.2×10^{-1}	2.4×10^{3}
Cm-247	1.4×10^{1}	1.2×10^{-1}	1.2×10^{2}
Cm-248	4.3×10^{1}	1.2×10^{-1}	3.6×10^{2}
Cf-249	8.1×10^{3}	1.2×10^{-1}	6.8×10^{4}
Cf-251	1.8×10^{3}	1.2×10^{-1}	1.5×10^{4}
Cf-252	4.3×10^{6}	6.0×10^{-17}	7.2×10^{22}

* Not included in Reed inventory. Calculated by ratio to Cs-137 from Table 2.4 of Cook et al. 1987

Table 4.3-3 Comparison of ILNT and ILT vault calculated disposal limits with estimated inventory

Radionuclide	Disposal Limit Ci/Vault	Estimated Inventory Ci/Vault	Ratio
H-3	5.0×10^{5}	1.0×10^{3}	5.0×10^{2}
C-14	1.0×10^{1}	0	--------
Al-26	4.2×10^{-1}	--------	--------
Co-60	6.7×10^{2}	2.4×10^{4}	2.8×10^{4}
Ni-59	1.8×10^{3}	1.3×10^{1}	1.4×10^{2}
Se-79	8.9	8.0×10^{1}	1.1×10^{4}
Rb-87	--------	--------	--------
Sr-90	3.0×10^{13}	1.3×10^{4}	2.3×10^{9}
Zr-93	--------	--------	--------
Tc-99	2.0	2.6×10^{-2}	7.7×10^{1}
Pd-107	--------	--------	--------
Sn-126	1.1×10^{1}	6.4×10^{-2}	1.7×10^{2}
I-129	5.3×10^{-4}	4.3×10^{-5}	1.2×10^{1}
Cs-135	1.9×10^{1}	2.4×10^{-2}*	7.9×10^{2}
Cs-137	7.4×10^{5}	1.3×10^{4}	5.7×10^{1}
Th-232	4.7×10^{-1}	3.2×10^{-3}	1.5×10^{2}
U-232	1.1×10^{3}	--------	--------
U-233	3.6×10^{13}	2.7	1.3×10^{13}
U-234	1.0×10^{1}	4.4×10^{-2}	2.3×10^{2}
U-235	6.5	8.0×10^{-4}	8.1×10^{3}
U-236	3.5×10^{19}	3.8×10^{-3}	9.2×10^{21}
U-238	5.2×10^{1}	2.2×10^{-3}	2.4×10^{4}
Np-237	2.0×10^{-1}	2.5×10^{-3}	8.0×10^{1}
Pu-239	1.6×10^{10}	4.4×10^{-1}	3.6×10^{10}
Pu-240	--------	--------	--------
Pu-242	--------	--------	--------
Pu-244	--------	--------	--------
Am-241	1.0×10^{3}	5.6×10^{-2}	1.8×10^{4}
Am-243	2.1×10^{1}	2.8×10^{-5}	7.5×10^{5}
Cm-245	5.0×10^{1}	2.8	1.8×10^{1}
Cm-246	--------	--------	--------
Cm-247	4.1	2.8	1.5
Cm-248	--------	--------	--------
Cf-249	5.1×10^{5}	2.8	1.8×10^{5}
Cf-251	1.6×10^{7}	2.8	5.7×10^{6}
Cf-252	2.1×10^{8}	3.7	5.7×10^{7}

* Not included in Reed inventory. Calculated by ratio to Cs-137 from Table 2.4 of Cook et al. 1987

the radionuclide limits from a Safety Analysis Report (SAR), cell criticality limits, 100 nCi/g transuranic concentration limit, NRC Class C limits, and vault performance-based inventory limits. Each of these limits is converted into a hypothetical container limit. For each radionuclide, the most restrictive limit is then implemented as a WAC container limit for the waste generators.

As packages are received for emplacement in the various vaults, their package contents will be entered into WITS. Before emplacement of each package, WITS will compare the package contents with the 100 nCi/g transuranic limits and NRC Class C limits, and calculate the cell inventory (to ensure compliance with the cell criticality limits) and the total vault inventory (to ensure compliance with the PA-based limits). The SAR and PA-based limits are tracked as a sum-of-fractions of the individual radionuclide limits. For the PA-based limits, the total vault inventory for each radionuclide is divided by its corresponding limit. The sum of these fractions will be maintained less than one to ensure compliance with the limits. A similar procedure will be followed to ensure compliance with the SAR limits.

5. PERFORMANCE EVALUATION

The purpose of this site-specific RPA of the EAVDF at the SRS is to fulfill the DOE Order 5820.2A requirement that such an assessment be prepared and maintained for any LLW disposal facility located at a DOE field site. The RPA must provide reasonable assurance that the facility design and method of disposal will comply with the performance objectives of the order, which are concerned with protection of public health and safety, limiting doses to members of the general public and inadvertent intruders, and protecting groundwater resources. In this chapter of the RPA, a summary of how the results of the comprehensive analysis provide reasonable assurance that the performance objectives will be met, followed by consideration of design changes that are based on the results, and recommended data acquisition and research necessary to reduce conservatism in the results are presented.

5.1 COMPARISON TO PERFORMANCE OBJECTIVES

The performance objectives of DOE Order 5820.2A for LLW disposal are listed in Sect. 1.2. In essence, these objectives put forth dose limits for members of the general public and inadvertent intruders that are not to be exceeded at any point in time through consideration of credible pathways. The performance objectives include protection of groundwater resources consistent with Federal, State and local requirements.

For the groundwater protection performance objective, it has been determined that Option 1, as described in Sect. 1.2, is required to be used because of the interpretation of CERCLA regulations by the State of South Carolina. If the proposed drinking water standard is promulgated by the EPA (U.S.EPA 1991), the limits presented in this report must be recalculated.

This PA was prepared using reasonable, but conservative, parameter values to calculate disposal facility inventories that will meet the performance objectives. Implementation of these limits as waste acceptance criteria and a waste certification program will provide reasonable assurance that the performance objectives will be met.

5.2 DESIGN CHANGES REQUIRED TO MEET PERFORMANCE OBJECTIVES

The RPA process assumed the design described for the EAVs in Sect. 2.5 and the closure concept described in Sect. 2.9 of this report. Because the results indicate compliance with performance objectives, no changes to the design of EAVs and suspect soil trenches are recommended. However, the analysis of NR waste presented in Appendix L does not indicate compliance. Rather than indicating the need for design changes, the results presented in Appendix L indicate the need for additional data to reduce conservatism in the analysis (see Sect. 5.3).

However, as noted in Sect. 2.9, a final design for the closure is not now available; a closure concept was analyzed. As the closure design is developed, it's performance for limiting infiltration into the waste will be evaluated versus the performance of the closure concept analyzed in this RPA.

5.3 DATA AND RESEARCH NEEDS

In addition to groundwater monitoring (Sect. 2.9.3 and H.2 - recommendation #6), near-field monitoring will be necessary to validate the predicted performance of the EAVDF. However, technology for accomplishing near-field monitoring, especially in terms of *in-situ* monitoring of non-volatile contaminants, is in a developmental stage. SRS will seek and implement appropriate monitoring technology as it becomes available. Meanwhile, SRS will continue to collect data from the various lysimeter programs at SRS. Such data may be useful for validation.

The analysis of naval reactor waste presented in Appendix L does not indicate compliance with performance objectives. However, as noted in Appendix L, the analysis is very conservative because of a lack of data specific to the NR wasteforms. Obtaining data on the composition and physical configuration of the wasteforms and on the expected lifetime of the welds in the disposal containers should enable the analysis to be revised to indicate compliance. Until the analysis is so revised, NR waste will only be received at E-Area for storage.

Although the RPA has indicated compliance with performance objectives for the EAVs and suspect soil trenches, a number of opportunities have been identified which would decrease the conservatism in the analysis. Because the RPA is to be maintained through time, and thus is a living document, further iterations of the RPA process will benefit greatly if these opportunities are explored. Reducing conservatism in the RPA should enable disposal limits to be increased, thus, enhancing the utility of the EAV. Several opportunities for reducing conservatism are discussed below.

The waste in the vaults could be represented more realistically. Presently, all of the waste containers are assumed to totally degrade immediately and the waste is represented as a single stirred tank. Corrosion rates of waste containers could be developed and incorporated into the RPA to take credit for the waste containers. Also, the waste, after container degradation, could be represented as a series of stirred tanks to more realistically represent the waste volume. Treatment of the waste prior to disposal, such as super-compaction, incineration, vitrification, etc., or addition of additives such as zeolite to waste packages, could be incorporated into the RPA to take credit for improved waste forms.

Because the predicted groundwater concentrations of U and Pu isotopes depend on the applied solubility limits for these elements, further research should be conducted to evaluate the appropriateness of the applied limits over the long-term. Geochemical degradation, although difficult to assess, is potentially an important aspect of PAs. Additional consideration of chemical solubility in the waste form for radionuclides with low disposal limits, such as Np-237, should be done. Geochemical modeling and/or laboratory experimentation will be required to determine solubility values.

Since collapse of the LAW vault roof is a significant contributor to doses from the LAW, any measures to prevent, or reduce the extent of, roof collapse would result in significantly increased vault limits. If for example, the LAW vault design and mode of waste emplacement were altered to enable minimizing voids (or filling voids with an inert material such as sand), the roof collapse scenario would be improved. Also, waste emplacement procedures could be implemented to provide for placement of packages containing higher concentrations of radionuclides of concern in intruder scenarios at the bottom of each vault. Another possibility to be considered is to alter the vault (or other disposal unit) design to provide deeper burial of the waste to deter intrusion. In addition, more realistic representation of the collapsed vault in the intruder scenarios to take credit for the presence of the concrete rubble should be considered. More realistic formulation of intrusion scenarios to take credit for practices in the southeastern USA, such as not generally constructing basements for private homes, should be considered. Credit for longer-term institutional control, such as limiting future land use through the Site Development Plan, should be considered.

Modeling of the degraded vaults could be improved by using a time distribution for the development of cracks and collapse of the roofs. Data would need to be developed to support the distributions.

Doses from I-129 in the RPA have been calculated without regard to the isotopic dilution with stable iodine that will take place. Because assimilated iodine is concentrated in the thyroid, and the thyroid has a limited capacity for iodine, consideration of the expected specific activity of I-129 (curies of I-129 per gram of iodine present in the environment) would lead to a more realistic assessment of the dose from I-129.

More rigorous implementation of the sum-of-fractions rule using the timing of doses to improve waste acceptance criteria from the RPA results should be considered.

Although vault design changes are not needed to meet performance objectives, disposal design could be optimized to ensure cost-effective LLW disposal. Alternative disposal technologies such as trench burial could be employed for certain waste types in addition to suspect soil. Further modeling is necessary to develop the appropriate disposal limits for each disposal technology to ensure that performance objectives will be met.

6. PREPARERS

Below is a list of contributors to this performance assessment effort, and the portions of the assessment for which they are responsible.

COOK, JAMES R., WSRC/SRTC, Geology, Geochemistry

M.S. Geochemistry
B.S. Geology

Experience: Mr. Cook has 15 years of experience at the Savannah Rive Site, 13 of which have been in various aspects of low-level waste research. Research topics have included site selection, site characterization, site closure, and performance assessment. Mr. Cook served on the revision team for Chapter 3 of DOE Order 5820.2A. He is a member of the Performance Assessment Task Team. He serves as the technical lead on the PA advisory team.

Contributions: WSRC Technical Leader of PA team. Screening Calculations.

DICKE, CRAIG A., INEL, Radionuclide Screening, Concrete Degradation, Geochemistry

M.S. Geology
B.S. Geology

Experience: Mr. Dicke has 6 years experience in modeling geochemical processes related to radioactive waste disposal.

Contributions: Analyzed the geochemistry of the vault environments, and provided K_ds for radionuclides in all media.

HIERGESELL, ROBERT A., WSRC/SRTC, Geology, Hydrology

M.S. Hydrology/Hydrogeology
B.S. Geology

Experience: Mr. Hiergesell has 16 years of experience relating to all aspects of groundwater investigations. Specific experience includes data collection and analysis, aquifer testing, and groundwater flow modeling.

Contributions: Participated in development and implementation of the three dimensional saturated zone flow model. Collected field data required to calibrate the saturated flow model.

HORWEDEL, JIM L., ORNL, Computer Analyst, Sensitivity and Uncertainty Analysis

M.A. Math Education

Experience: For the last 9 years, Mr. Horwedel has developed the GRESS software system for automation of sensitivity analysis capability into existing computer codes and has applied GRESS to a wide range of waste management and performance assessment analysis codes. Mr. Horwedel has written several drivers for automating the use of statistical sampling methods, such as Latin Hypercube Sampling, for a variety of computers.

Contributions: Performed all sensitivity and uncertainty analysis runs of PORFLOW for both the saturated and unsaturated models. Developed a driver to carry out these runs based on Latin Hypercube sampling procedures. Developed a post-processor to analyze the output of the multiple PORFLOW runs.

HSU, ROBERT H., WSRC/SRTC, R & D Management

D.E.S. Chemical Engineering
M.S. Chemical Engineering
B.S. Chemical Engineering

Experience: Dr. Hsu has 13 years of industrial experience in chemical processing, R&D, safety analysis and management. In his 10 years at SRS his assignments have included laboratory R&D, NRC-format safety analyses, and management of R&D groups. For the past year, he has managed an R&D group that develops technology for support of environmental restoration (soil and groundwater) and for treating, handling and disposing of low-level radioactive, mixed, hazardous, sanitary, and industrial aqueous wastes. The group has expertise in site closure, environmental transport, groundwater modeling and decontamination.

HUNT, PAUL D.

B.S. Nuclear Engineering

Experience: Mr. Hunt has seven years experience on the Navy's Nuclear Power Program and three years experience at the Savannah River Site. He has served as Manager, Low-Level Waste Cognizant Engineering for two years and is the engineering manager for the E-Area Vaults.

Contribution: Advisor to PA team.

KEARL, PETER M., ORNL/GJ, Groundwater Hydrology

M.S. Hydrology/Hydrogeology
B.S. Geology

Experience: Mr. Kearl has extensive experience (13+ years) with designing and installing groundwater monitoring networks to evaluate contaminant transport and for conducting regional aquifer studies. He has dealt with the hydraulics of fractured media as well as cavernous and porous media, and has conducted vadose zone characterizations. He also has several years experience with numerical modeling of groundwater flow.

Contributions: Evaluated the hydrogeologic environment at E-Area, and developed and implemented a three-dimensional saturated flow and transport model. Collected field data required to calibrate the saturated flow model.

KOCHER, DAVID C., ORNL, Exposure Scenario Development, Dose Calculations

Ph.D. Physics

Experience: Dr. Kocher has over 15 years experience in environmental health physics. He also has served on the Performance Assessment Task Team since its inception, and thus, has considerable insight into performance assessment issues.

Contributions: Developed exposure scenarios for intruders and off-site individuals, computed doses from environmental concentrations, and served in an advisory capacity for several other technical issues.

LANGTON, CHRISTINE A., WSRC/SRTC, Material Science

Ph.D. Material Science
M.S. Geochemistry
B.S. Geology

Experience: Dr. Langton has 10 years experience on developing and testing cement wasteforms and inorganic treatment processes for low-level and mixed wastes.

Contributions: Advisor to PA team.

LEVER, WILLIAM E., ORNL, Task Leader, Sensitivity and Uncertainty Analysis

Ph.D. Statistics

Experience: Dr. Lever has over twenty-five years of experience as a statistical consultant. He has been involved in a large number of physical science problems for both ORNL and the Oak Ridge Y-12 Plant.

Contributions: Determined through the analysis of simulated results from PORFLOW, the K_d and time factors that had the greatest influence on the simulated performance of the vault. The analysis was done through the use of Step-Wise Regression Techniques. The variability of the simulated results was examined through the use of confidence and tolerance intervals.

LORAH, STEVEN A., WSRC/SWME, Chemical Engineering

B.S. Chemical Engineering
B.S. Chemistry
B.S. Applied Mathematics

Experience: Mr. Lorah has 5 years of experience in Solid Waste Management at the Savannah River Site. Responsibilities have included technical support for the closure of F- and H-Area Seepage Basin at the SRS, and for the design and permitting of the Consolidated Incineration Facility (CIF). His most recent assignment has been the engineering support for the startup of E-Area Vaults.

Contributions: Input on the facility descriptions and concrete information in the PA. Advisor to PA team.

LOWE, PAUL E., WSRC/SRTC, Quality Assurance

B.S. Industrial Engineering
Registered Professional Engineer (PE)

Experience: Mr. Lowe has over 20 years of high technology experience in aerospace, commercial nuclear, and DOE facilities. Six of these years have been in Radioactive Waste Program QA. Mr. Lowe has managed major projects and worked for companies such as Hughes Aircraft, Battelle Institute, as well as major nuclear utilities and consulting firms.

Contributions: Interpreted the Quality Assurance requirements of the PA and ensured SRTC and the National Laboratories performed their research in a manner consistent with good QA practice. This was accomplished by reviews and QA surveillances of all the contractors on the project.

MCDOWELL-BOYER, LAURA M., ORNL/GJ, Groundwater Hydrology

Ph.D. Civil/Environmental Engineering
M.S. Radiological Health Physics

Experience: Dr. McDowell-Boyer has eight years experience in radiological exposure assessments, has directed the development of a multi-media environmental transport model, studied mechanisms of subsurface contaminant migration, and modeled groundwater flow and transport.

Contributions: Evaluated the hydrogeologic environment at E-Area, assisted with the development and implementation of a three-dimensional saturated flow and transport model, and coordinated production of the final draft and final report of this PA effort. Co-principal investigator of PA.

MCVAY, CHARLES W., WSRC/SWO, Facility Manager EAV

B.S. Chemistry

Experience: Mr. McVay has 9 years of experience in the nuclear field. Seven years of experience were at the West Valley Demonstration Project in analytical chemistry analysis and laboratory analysis, waste management activities including remediation, and disposal and treatment. The 2 years of experience at Savannah River have been predominantly in startup activities with E-Area Vaults.

Contributions: Reviewed draft PA.

REED, SHAWN R., WSRC/SWME

B.S. Geology
B.S. Mechanical Engineering
M.S. Geophysics

Experience: Mr. Reed has 3½ years of experience in Solid Waste Management at the Savannah River Site. He functioned as the technical support engineer for the E-Area Vaults during the design phase and has been involved with the E-Area Vaults Performance Assessment for 2½ years.

Contributions: Advisor to PA team.

RODDY, NATHANIEL S., WSRC/SRTC, Engineer

B.S. Civil Engineering

Experience: Mr. Roddy has five years of experience at the Savannah River Site in the area of low-level waste programs. Research programs include closure cap evaluation utilizing the HELP computer code. He served as chairperson of the Process Requirements Team for the E-Area Vaults, and was responsible for the preparation of the PR document. Mr Roddy has served as an alternate Operational Readiness Review Board member for the EAV. He co-coordinated the Engineered Low-Level Trench-4 flood recovery. He is a member of the Performance Assessment advisory team.

Contributions: Advisor to PA team.

SEITZ, ROGER R., INEL, Near-Field Degraded Vault Flow and Transport, Radionuclide Screening

B.S. Mathematics
(pursuing M.S. in Chemical Engineering)

Experience: Mr. Seitz has over nine years of experience in conducting performance assessments for high- and low-level waste disposal facilities. His experience is primarily in the area of flow and transport modeling in porous media with some additional experience in radiological dose calculations.

Contributions: Principal investigator for near-field modeling.

SMITH, CARY S., INEL, Unsaturated Zone Conceptual Design and Modeling

B.S. Mathematics

Experience: Mr. Smith's primary area of expertise is applied mathematics and mathematical modeling. Mr. Smith has spent two years working with groundwater flow and contaminant transport modeling. He is doing research on numerical algorithms for fluid flow and transport.

Contributions: Conducted numerical modeling of the fluid flow and contaminant transport for the moisture barrier, concrete vaults, and vadose zone.

SMITH, ROBERT, INEL, Geochemistry

M.S. Geochemistry and Geoscience
Ph.D. Geochemistry and Geoscience

Experience: Dr. Smith specializes in inorganic aqueous geochemistry, with emphasis on the modeling of water-rock system at ambient and elevated temperatures. His work focuses on characterizing chemical processes important in natural systems by the application of thermodynamic principals, kinetic theories and adsorption phenomenon. In addition, Dr. Smith has extensive experience in both domestic and international high-level nuclear waste repository design. He has numerous publications in the areas of geochemistry, mineralogy, and environmental science.

Contributions: Conducted geochemical modeling of the E-Area Vaults.

STEVENS, WILLIAM E., WSRC/SRTC, R & D Management

M.S. Chemical Engineering
B.S. Chemical Engineering

Experience: Mr. Stevens has 17 years of industrial experience in chemical processing, waste management, and environmental restoration. His assignments include process engineering, development engineering, and management of process and project engineering groups, maintenance groups, and R & D groups. For the past four years, he has managed an R & D group that develops technology for support of environmental restoration and minimizing, recycling, treating, handling, and disposing of low-level radioactive, mixed, hazardous, and sanitary waste. The group has expertise in site closure, environmental transport, groundwater modeling, and decontamination. Mr. Stevens is a licensed Professional Engineer.

Contribution: Advisor to PA team.

TAYLOR, GERALD E., WSRC/SWME

B.S. Civil/Structural Engineering

Experience: Mr. Taylor came to the Savannah River Site with 11 years experience at the Tennessee Valley Authority in the Hydraulic Investigations Branch in the Division of Nuclear Engineering. He has functioned as the Disposal Vault Project Engineer for 3 years.

Contribution: Advisor to PA team.

THORNE, DAVID J., ORNL/GJ, Task Group Leader

M.S. Radiological Health Physics
B.S. Geology

Experience: Mr. Thorne has five years experience in radiological transport and dose assessments. His experience includes source term development, contaminant transport modeling, dose and risk assessment, and environmental compliance. He is member of the Performance Assessment Task Team and serves as a research member of the IAEA's research program on Near-Surface Radioactive Waste Disposal Facility Performance Assessments.

Contributions: Integrated results of the various technical tasks and coordinated the production of the initial draft report. Provided technical support to the saturated flow modeling and analysis of volatile emissions release and dose. Co-principal investigator of PA.

WILHITE, ELMER L., WSRC/SRTC, Advisory Scientist

M.S. Inorganic Chemistry
B.S. Chemistry

Experience: Mr. Wilhite has twenty-two years experience at the Savannah River Site. Most of his experience (12 years) has been in low-level waste research. Other experience has included environmental research (3 years), high-level waste research (2 years), and analytical development supervision (3 years). Mr. Wilhite has contributed to the preparation of DOE Order 5820.2A and is currently chairman of the Peer Review Panel.

Contributions: Advisor to PA team.

WORLEY, BRIAN A., ORNL, Task Manager, Sensitivity and Uncertainty Analysis

Ph.D. Nuclear Engineering, Massachusetts Institute of Technology

Experience: Dr. Worley has been involved with reactor physics analysis of advanced reactors since 1977 at ORNL. He has experience in developing methods for sensitivity and uncertainty analysis for reactor systems and waste management systems. He has managed the development of sensitivity and uncertainty analysis work sponsored by ONWI and DOE/LLW since 1985.

Contributions: Provided management and oversight of the sensitivity and uncertainty analysis for the E-Area performance assessment.

YU, ANDREW, WSRC/SRTC, Chemical Engineering

Ph.D. Chemical Engineering

Experience: Dr. Yu has thirteen years experience in modeling enhanced oil recovery processes prior to joining SRS in 1987. At SRS, he and his coworkers have recommended key design features of disposal vaults based on groundwater protection.

Contributions: Advisor to PA team. Participated in various aspects of the vadose zone model development.

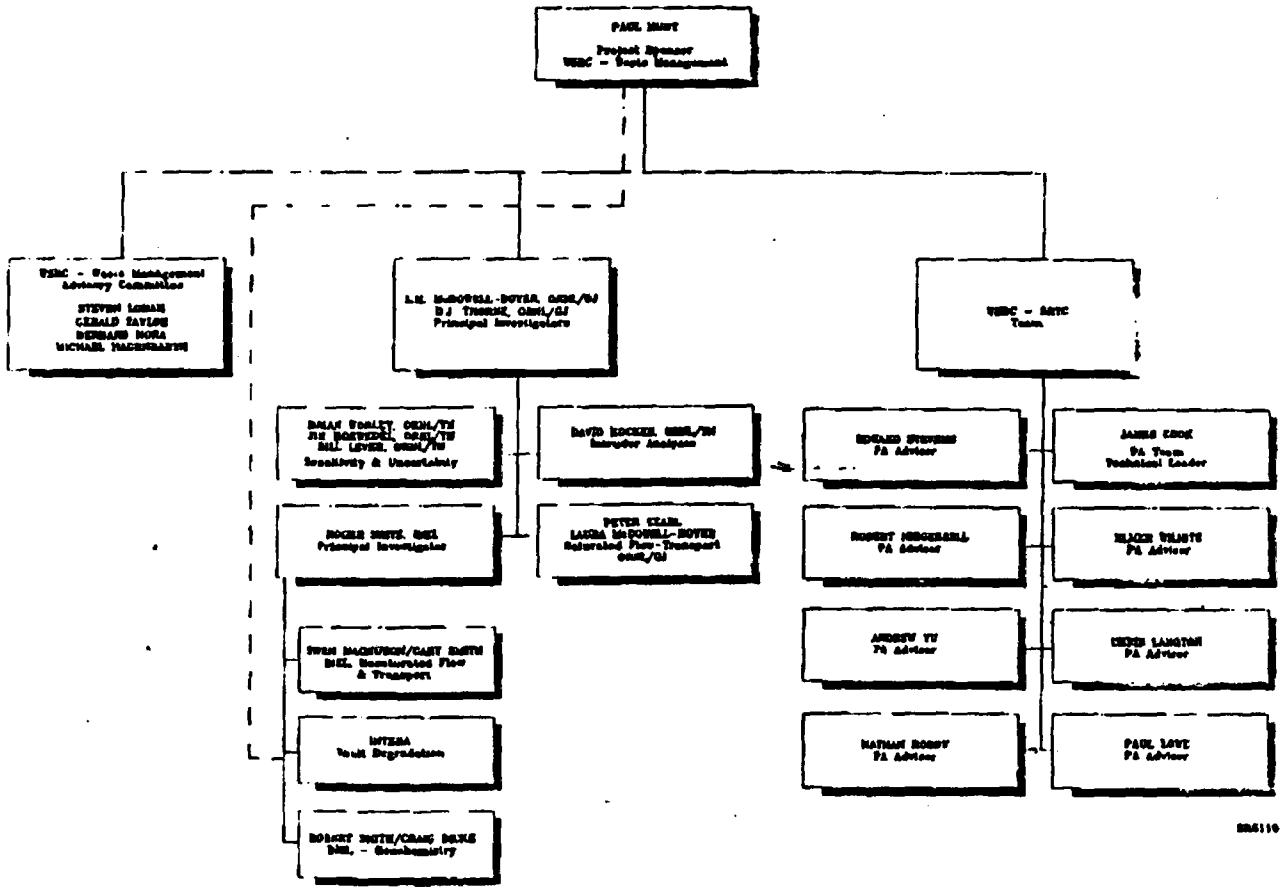

Fig. 6.0-1. E-Area PA organizational chart.

7. REFERENCES

Aadland, R. K. 1990. *Classification of Hydrostratigraphic Units at Savannah River Site, South Carolina.* Savannah River Laboratory, WSRC-RP-90-937. Westinghouse Savannah River Company, Aiken, SC.

ACRI. 1993. *PORFLOW: A Model for Fluid Flow, Heat and Mass Transport in Multifluid, Multiphase Fractured or Porous Media, Version 2.50, Draft User's Manual.* Analytic and Computational Research, Inc., Bel Air, Calif.

Allard, B. 1985. Radionuclide Sorption on Concrete. Nationale Genossenschaft fur die Lagerung Radioaktiver Abfalle report NAGRA-NTB-85-21 (November).

Alter, H. W., and R. A. Oswald. 1988. Nationwide Distribution of Indoor Radon Measurements. *Radiation Protection Practice.* Proceedings of the Seventh International Congress of International Radiation Protection Association, Sydney: Pergamon Press.

Amidon, M. B. 1990. *Re: Historic Water Table High at the Burial Ground Expansion Site (U).* Internal Report. NMP-WMT-900953. Westinghouse Savannah River Company, Savannah River Site, Aiken, SC.

Anspaugh, L. R., J. H. Shinn, P. L. Phelps, and N. C. Kennedy. 1975. Resuspension and Redistribution of Plutonium in Soils. *Health Phys.* 29:571.

Arnett, M. W., L. K. Karapatakis, A. R. Mamatey, and J. L. Todd. 1991. *Savannah River Site Environmental Report for 1991.* WSRC-TR-92-186. Westinghouse Savannah River Company, Savannah River Site, Aiken, S.C.

Atkinson, A., and Hearne. 1984. *An Assessment of the Long-Term Durability of Concrete in Radioactive Waste Repositories.* AERE-R11465. Harwell, U. K.

Baes, C. F. III, and R. D. Sharp. 1983. A Proposal for Estimation of Soil Leaching and Leaching Constants for Use in Assessment Models. *J. Environ. Qual.,* 12:17.

Baes, C. F. III, R. D. Sharp, A. L. Sjoreen, and R. W. Shor. 1984. *A Review and Analysis of Parameters for Assessing Transport of Environmentally Released Radionuclides through Agriculture.* ORNL-5786. Oak Ridge National Laboratory.

Bollinger, G. A., F. C. Davison, Jr., M. S. Sibol, and J. B. Birch. 1989. Magnitude Recurrence Relations for The Southeastern United States and its Subdivisions. *Journal of Geophysical Research*, 94(B3):2857-2873.

Briese, L. A., and M. H. Smith. 1974. Seasonal Abundance and Movement of Nine Species of Small Mammals. *J. Mammal.*, 55:615-629.

Cook, J. R. 1991. *Technical Basis for Non-Vault Disposal of Suspect Soil (U).* WSRC-RP-91-58. Westinghouse Savannah River Company, Savannah River Site, Aiken, S.C.

Cook, J. R., M. W. Grant, and O. A. Towler. 1987. *Environmental Information Document - New Low-Level Radioactive Waste Storage/Disposal Facilities at the Savannah River Plant.* DPST-85-862. Savannah River Laboratory, E. I. du Pont de Nemours & Co., Inc., Aiken, SC.

Cummins, C. L., D. K. Martin, and J. L. Todd. 1990. *Savannah River Site Environmental Report.* WSRC-IM-91-28, Volumes I and II. Westinghouse Savannah River Company, Savannah River Site, Aiken, SC.

Davenport, L. B. 1964. Structure of Two Peromyscus polionotus Populations in Old-Field Ecosystems at the AED Savannah River Plant. *J. Mammal.*, 45:95-113.

Denneby, K. F., D. C. Prowell, and P. B. McMahon. 1989. *Reconnaissance Hydrological Investigation of the Defense Waste Processing Facility and Vicinity.* E. I. du Pont de Nemours and Company Savannah River Laboratory, Aiken, SC.

Dodge, R. L., W. R. Hansen, W. E. Kennedy, Jr., D. W. Layton, D. W. Lee, S. J. Maheras, S. M. Neuder, E. L. Wilhite, R. U. Curl, K. F. Grahn, B. A. Heath, and K. H. Turner. 1991. *Performance Assessment Review Guide for DOE Low-Level Radioactive Waste Disposal Facilities.* Prepared by Dames and Moore for Department of Energy Office of Environmental Restoration and Waste Management (DOE/LLW-93). Radioactive Waste Technical Support Program, Idaho National Engineering Laboratory EG&G Idaho, Inc. Idaho. Idaho.

Eckerman, K. F., A. B. Wohlbarst, and A. C. B. Richardson. 1988. *Limiting Values of Radionuclide Intake and Air Concentration and Dose Conversion Factors for Inhalation, Submersion, and Ingestion.* Federal Guidance Report No. 11. EPA-520/1-88-020. U. S. Environmental Protection Agency, Washington, D.C.

GeoTrans. 1991. *Groundwater Flow Model for the General Separations Area, Savannah River Site.* GeoTrans Project No: 3017-003. GeoTrans Inc., Sterling, Virginia.

Golley, F. B., and J. B. Gentry. 1964. Bioenergetics of the Southern Harvester Ant, Pogonomyrmex badius. *Ecol.*, 45:217-225.

Gruber, P. 1980. *A Hydrologic Study of the Unsaturated Zone Adjacent to a Radioactive-Waste Disposal Site at the Savannah River Plant, Aiken, South Carolina.* M.S. Thesis, University of Georgia, Athens, Georgia.

Hamby, D. M. 1992. Site-Specific Parameter Values for the Nuclear Regulatory Commission's Food Pathway Dose Model. *Health Phys.*, 62:136.

Healy, J. W. 1980. Review of Resuspension Models in *Transuranic Elements in the Environment*, p. 209. DOE/TIC-22800. Ed. by W. C. Hanson. U. S. Department of Energy, Washington, D. C.

Hoeffner, S. L. 1985. *Radionuclide Sorption on Savannah River Plant Burial Ground Soil: A Summary and Interpretation of Laboratory Data.* DP-1702. E. I. du Pont de Nemours and Company, Savannah River Laboratory, Aiken, SC.

Horton, J. H., and E. L. Wilhite. 1978. *Estimated Erosion Rate at the SRP Burial Ground.* DP-1493. E. I. du Pont de Nemours & Co., Inc., Savannah River Laboratory, Aiken, SC.

INTERA. 1989. *Comparison of Unsaturated Flow and Transport Models with Volume and Nitrate Measurements from a Pilot-Scale, In-Situ Lysimeter with Different Geometry Low Level Radioactive Waste Designs.* INTERA Technologies report H01203R014. INTERA Technologies, Inc., Austin, Texas.

ICRP. 1959. *Recommendation of the International Commission on Radiological Protection.* International Commission on Radiological Protection. Publication No. 2. Pergamon Press, New York.

ICRP. 1979. *Limits for Intakes of Radionuclides by Workers.* International Commission on Radiological Protection. Publication 30, Part 1. *Ann. ICRP* 2. No. 3/4. Pergamon Press, Oxford, U.K.

Kennedy, W. E., Jr., and R. A. Peloquin. 1988. *Intruder Scenarios for Site-Specific Low-Level Waste Classification.* DOE/LLW-71T. Idaho Operations Office, U. S. Department of Energy.

Ketelle, R. H, and D. D. Huff. 1984. *Site Characterization of the West Chestnut Ridge Site.* ORNL/TM-9229. Oak Ridge National Laboratory, Oak Ridge, Tenn.

Looney, B. B., Grant, M. W., and King, C. M. 1987. *Estimation of Geochemical Parameters for Assessing Subsurface Transport at the Savannah River Plant. Savannah River Laboratory Environmental Information Document.* DPST-85-904. E. I. du Pont de Nemours and Company, Savannah River Laboratory, Aiken, SC, p. 13.

Marine, I. W. 1976. *Geochemistry of Ground Water at the Savannah River Plant.* DP-1356. E. I. du Pont de Nemours and Co, Savannah River Laboratory, Aiken, SC.

Mualem, Y. 1976. A New Model for Predicting the Hydraulic Conductivity of Unsaturated Porous Media. *Water Resources Research,* 12(3):518-522.

McIntyre, P. F. 1988. *Sorption Properties of Carbon-14 on Savannah River Plant Soil.* DPST-88-900. E. I. du Pont de Nemours and Company, Savannah River Laboratory, Aiken, SC.

McKenzie, D. H., L. L. Cadwell, L. E. Eberhardt, W. E. Kennedy, Jr., R. A. Peloquin, and M. A. Simmons. 1983. *Relevance of Biotic Pathways to the Long-Term Regulation of Nuclear Waste Disposal; Topical Report on Reference Eastern Humid Low-Level Sites.* NUREG/CR-2675, PNL-4241, Vol. 3. Pacific Northwest Laboratory, Richland, Wash.

McKenzie, D. H., L. L. Cadwell, W. E. Kennedy, Jr., L. A. Prohammer, and M. A. Simmons. 1986. *Relevance of Biotic Pathways to the Long-Term Regulation of Nuclear Waste Disposal, Phase II, Final Report.* NUREG/CR-2675, PNL-4241, vol. 6. Pacific Northwest Laboratory, Richland, Wash.

Murphy, C. E., Jr. 1990. *Lysimeter Study of Vegetative Uptake from Saltstone.* WSRC-RP-90-421. Westinghouse Savannah River Company.

NCRP. 1987. *Ionizing Exposure of the Population of the United States.* Washington, D. C., NCRP report No. 93. National Council on Radiation Protection and Measurements.

NCRP. 1989. *Exposure of the U. S. Population from Diagnostic Medical Radiation.* NCRP report No. 100. National Council on Radiation Protection and Measurements, Bethesda, MD.

NRC. 1977. *Regulatory Guide 1.109. Calculation of Annual Doses to Man from Routine Releases of Reactor Effluents for the Purpose of Evaluating Compliance with 10 CFR Part 50, Appendix I.* Nuclear Regulatory Commission.

NRC. 1981. *Draft Environmental Impact Statement on 10 CFR Part 61 "Licensing Requirements for Land Disposal of Radioactive Waste."* NUREG-0782. U. S. Nuclear Regulatory Commission, Washington D. C.

NRC. 1989. *Quality Assurance Program Requirements for Nuclear Facilities.* ASME NQA-1-1989 Edition. The American Society of Mechanical Engineers.

Ng, Y. C., C. S. Colsher, and S. E. Thompson. 1982. *Soil-to-Plant Concentration Factors for Radiological Assessments.* NUREG/CR-4370, UCID-19463. Lawrence Livermore National Laboratory, Livermore, Calif.

Oak Ridge National Laboratory Quality Assurance Manual. Current Edition. Oak Ridge National Laboratory, Oak Ridge, Tenn.

ORNL. 1990. *Performance Assessment for Continuing and Future Operations at SWSA 6.* Internal draft report. Oak Ridge National Laboratory, Oak Ridge, Tenn.

ORNL Pollutant Assessments Group Procedures Manual. 1992. ORNL-6645/V2/R1. Oak Ridge National Laboratory, Oak Ridge, Tenn.

Oakly, D. T. 1972. *Natural Radiation Exposure in the United States.* ORP/SID 72-1. U. S. Environmental Protection Agency, Washington, D. C.

Oblath, S. B. 1985. *Effect of Groundwater on Saltstone Leaching,* Internal Report. DPST-85-504. E. I. du Pont de Nemours and Company, Savannah River Laboratory, Aiken, SC.

Ostundi, O. L., and O. W. Roles. 1986. *Update of Part 61 Impacts Analysis Methodology*. NUREG/CR-4370. U. S. Nuclear Regulatory Commission and Envirosphere Company.

Parizek, R. R., and R. W. Root. 1986. *Development of a Groundwater Velocity Model for the Radioactive Waste Management Facility, Savannah River Plant, South Carolina*. Pennsylvania State University, University Park, Penn.

Peterson, H. T., Jr. 1983. Terrestrial and Aquatic Food Chain Pathways in *Radiological Assessment*. NUREG/CR-3332, ORNL-5968. Ed. by J. E. Till and H. R. Meyer. U. S. Nuclear Regulatory Commission and Oak Ridge National Laboratory, Oak Ridge, Tenn.

Quality Assurance Program Requirements for Nuclear Facilities. 1989. ASME NQA-2a, Part 2.7. The American Society of Mechanical Engineers.

Reed, S. 1992. WER-WMT-929265. Reed-SR-Y5597, Westinghouse Savannah River Company, Aiken, SC.

Rupp, E. M. 1980. Age Dependent Values of Dietary Intake for Assessing Human Exposures to Environmental Pollutants. *Health Phys.*, 39:151.

Salvo, S. K., and Cook, J. R. 1993. Selection and cultivation of final vegetative cover for closed waste sites at the Savannah River Site, S.C. *Waste Management '93 Proceedings*, 2:1635-1637.

Sheppard, M. I. 1985. Radionuclide Partitioning Coefficients in Soils and Plants and Their Correlation. *Health Phys.*, 49:106.

Sheppard, M. I., and D. H. Thibault. 1990. Default Soil Solid/Liquid Partition Coefficients, Kds, for Four Major Soil Types: A Compendium. *Health Physics*, 59:471-482.

Smith, M. H. 1971. Food as a Limiting Factor in the Population Ecology of Peromyscus polionotus (Wagner). *Physiol. Zool.*, 40:31-39.

Stephenson, D. E. 1988. *August 1988 Savannah River Plant Earthquake*. DPST-88-841. E. I. du Pont de Nemours & Company, Inc., Savannah River Laboratory, Aiken, SC.

Stephenson, D. E. 1993. Personal Communication 12/14/93.

Stephenson, D. E., P. Talwani, and J. Rawlins. 1985. *Savannah River Plant Earthquake of June 1985.* DPST-85-583. E. I. du Pont de Nemours & Co., Inc., Savannah River Laboratory, Aiken, SC.

Stone, H. L. 1973. Estimation of Three-Phase Relative Permeability and Residual Oil Data. *Journal of Canadian Petroleum Technology,* October - December.

Thompson, D. G. 1991. *RE: Vault Closure Concept for Saltstone Vaults.* Internal report OPS-DTZ-91-0002. Westinghouse Savannah River Company, Savannah River Site, Aiken, SC.

Ticknor, K. V., and Ruegger, B. 1989. *A Guide to the NEA's Sorption Data Base.* Version 2.0, 19 p.

Toth, J. 1962. A theory of groundwater motion in small drainage basins in central Alberta. *J. Geophys. Res.*, 67:4375-4387.

URS/Blume, J. A. and Associates, Engineers. 1982. *Update of Seismic Criteria for the Savannah River Plant.* 1, Geotechnical, DPE-3699. E.I. du Pont de Nemours and Company, Savannah River Laboratory, Aiken, SC.

U. S. Department of Agriculture. 1985. *Site Specific Cropland Erosion Inventory.* Soil Conservation Service, Columbia, SC.

U. S. Department of Commerce. 1963. *Maximum Permissible Body Burdens and Maximum Permissible Concentrations of Radionuclides in Air and Water for Occupational Exposure.* National Bureau of Standards Handbook 69. NCRP Report No. 22.

U. S. Department of Commerce. 1977. *1974 Census of Agriculture.* Bureau of the Census, Agriculture Division.

U.S.DOE. 1987. Waste Management Activities for Groundwater Protection, Savannah River Plant, Aiken, SC. Final Environmental Impact Statement, DOE/EIS-0120, Vol. 1. U. S. Department of Energy, Savannah River Plant, Aiken, SC.

U.S.DOE. 1988a. *Radioactive Waste Management, Order 5820.2A*, U. S. Department of Energy, Washington, D.C.

U.S.DOE. 1988b. *Internal Dose Conversion Factors for Calculation of Dose to the Public.* DOE/EH-0071. U. S. Department of Energy, Washington, D.C.

U.S.DOE. 1991. *Analysis of the Environmental Impacts Resulting from Modifications in the Defense Waste Processing Facility.* Environmental Division, Savannah River Operations Office, U. S. Department of Energy, Aiken, SC.

U.S.DOE. 1994. *Waste Management* (draft). Order 5820.2B. U. S. Department of Energy, Washington, D.C.

U.S.EPA. 1991. 40 CFR Parts 141 and 142 - National Primary Drinking Water Regulations; Radionuclides; Proposed Rule. *Federal Register,* 56:33050.

van Genuchten, M. Th. 1978. *Calculating the Unsaturated Hydraulic Conductivity with a New Closed-Form Analytic Model.* Report 78-WR-08. Water Resources Program, Department of Civil Engineering, Princeton University, Princeton, NJ.

van Genuchten, M. Th. 1988. *RETC, F77 FORTRAN Code.* June.

Van Pelt, A. F. 1966. Activity and Density of Old-Field Ants of the Savannah River Plant, South Carolina. *J. Elisha Mitchell Sci. Soc.,* 2:343-351.

Walton, J. C., L. E. Plansky, and R. W. Smith. 1990. *Models for Estimation of Service Life of Concrete Barriers in Low-Level Radioactive Waste Disposal.* NUREG/CR-5542, EGG-2597. U.S. Nuclear Regulatory Commission, Washington, D.C.

WSRC. 1991a. *Burial Ground Operation Safety Analysis Report Addendum - E-Area Vaults (U).* DPSTSA-200-10, SUPP-8, Addendum 1. DOE Review Draft. Westinghouse Savannah River Company, Savannah River Site, Aiken, SC.

WSRC. 1991b. *Burial Grounds Expansion (U) - Hydrogeologic Characterization, Savannah River Site.* WSRC-RP-91866. Prepared by Sirrine Environmental, Inc., for Westinghouse Savannah River Company, Aiken, SC.

WSRC. 1992a. *Safety Analysis 200 Area Replacement Tritium Facility.* WSRC-SA-1-1. Savannah River Laboratory, Westinghouse Savannah River Company, Aiken, SC.

WSRC. 1992b. *Radiological Performance Assessment for the Z-Area Saltstone Disposal Facility*. WSRC-RP-92-1360. Savannah River Laboratory, Westinghouse Savannah River Company, Aiken, SC.

WSRC. 1993. *Procedure Manual 1S*. Westinghouse Savannah River Company, Savannah River Site Waste Acceptance Criteria. Chapter 3.10, Rev. 1 Interim.

Yu, A. D., C. A. Langton, and M. G. Serrato. 1993. *Physical Properties Measurements Program*. WSRC-93-894.

487581

[illegible] PERFORMANCE ASSESSMENT FOR THE E-AREA VAULTS DISPOSAL FACILITY (U)

APPENDICES A through M

April 15, 1994

Authenticated
Mary Mullis
5/6/94

Rev. 0

APPENDIX A

DETAILS OF MODELS AND ASSUMPTIONS

A.1 NEAR-FIELD MODELS

Appendix A.1 provides details of models and assumptions that support the information provided in Sect. 3.3 and 3.4 of the main body of the RPA report.

A.1.1 Infiltration

The process of infiltration is defined as the flow of water from the ground surface and into the soil. This is contrasted with the process of evaporation, and transpiration (i.e., evapotranspiration). In order to assess the performance of EAV an estimate of the infiltration rate at SRS is needed.

An idealized cross section of the vadose, or unsaturated soil, zone representing the infiltration area is shown in Fig. A.1-1. Water infiltrates at the surface and either undergoes evapotranspiration back through the surface and out of the domain or it infiltrates down to the underlying aquifer. The upper region in Fig. A.1-1, the dynamic zone, consists of the sediments near the surface where evaporation and transpiration have a dynamic role in reversing the downward movement of water due to gravity. The remaining region consists of the vadose zone. In the vadose zone, soil pores contain gases and water. Water is typically transported downward by gravity and capillarity.

A.1.1.1 Past Infiltration Studies

Past studies of infiltration at or near the SRS offer estimates of average infiltration rates. Hubbard and Englehardt (1987) used the CREAMS computer code to calculate a water balance for the old SRS burial ground (643-G) for the period 1961-1986. The CREAMS code, developed by the U.S. EPA, considers daily rainfall records, site vegetation, climatic characteristics, and soil properties. Daily rainfall records from F Separations Area were used in the simulation. Soils, vegetation, and climatic characteristics of the burial ground site

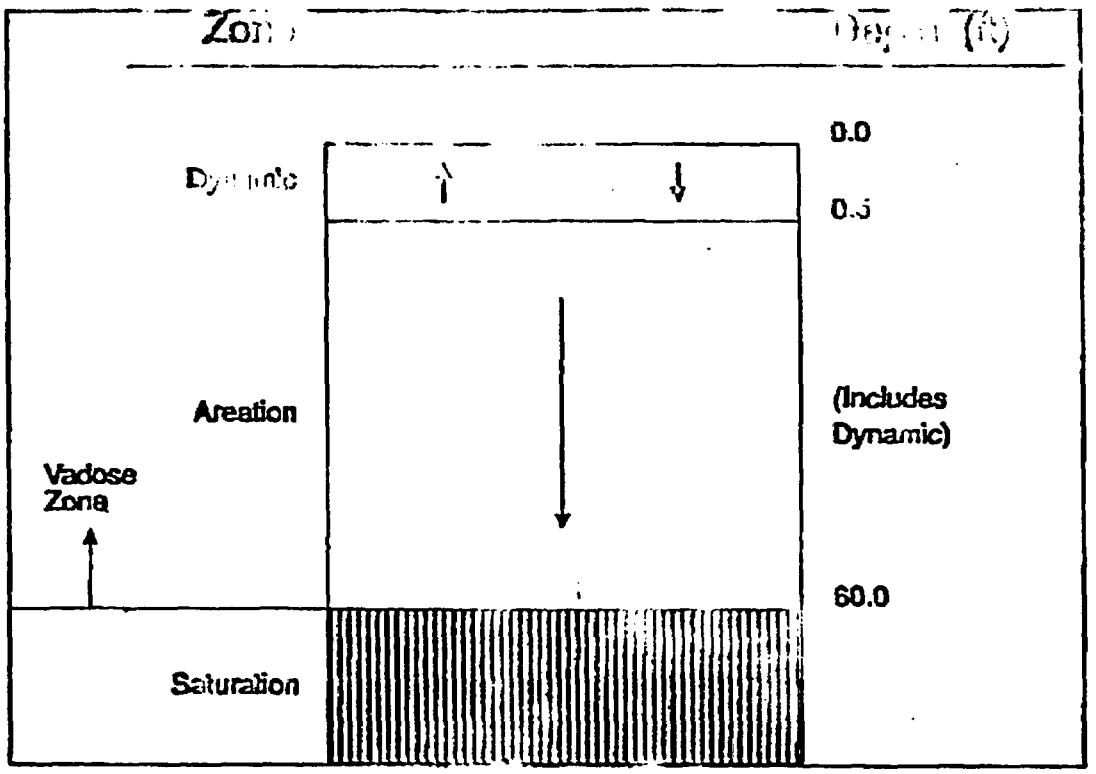

Fig. A.1-1. Idealized cross-section of the SRS vadose zone.

were used for the hydrologic parameters in the model. The average annual infiltration rate was estimated to be 37 cm or about 1/3 of annual average precipitation. Observed extremes for infiltration were 81 cm in 1964 and 10 cm in 1968.

To estimate the net infiltration for time intervals corresponding to pumping of the Tank 24 lysimeter, INTERA Technologies (1986) estimated discrete event evaporation using these bases:

- maximum evaporation is limited to 80% of pan evaporation rates;
- if evaporation exceeds the precipitation by more than 10% of the pan rate, an infiltration deficit can remove water from the soil;
- the maximum infiltration deficit per month is assumed to be 20% of the pan rate; and

- the infiltration deficit accumulates until it is overcome by subsequent precipitation exceeding evaporation.

The algorithm developed from these bases was then used to estimate infiltration rates during discrete periods of precipitation. A yearly infiltration total for the period February 1984 through August 1985 was determined to be approximately 24 cm.

Parizek and Root (1986) used a water balance method, where stream flow measurements were subtracted from annual precipitation to yield an estimated evaporation at 64% of the total annual precipitation. This estimate gives an average annual infiltration value of 45 cm for a grassland and intermittently forested portion of the SRS near the LLW burial site.

Dennehy and McMahon (1987) conducted a field study of water movement in the unsaturated zone at 4 grass-covered test trenches located at the SRP LLW burial site. The study consisted of monitoring actual evapotranspiration, monitoring soil water, and water movement using field techniques and computer simulations. The results of the study relevant to net infiltration were:

- 43 cm of infiltration neglecting runoff occurred between June 1984 and July 1985;
- precipitation on trenches infiltrated the trench cap and moved vertically into the trench backfill; and
- infiltration mainly occurred during the winter and spring.

A.1.1.2 Summary of Infiltration into the Vadose Zone

Past estimates of infiltration at the SRS have ranged from 22 to 45 cm/year. Using the mean of the observed and predicted infiltration studies at the SRS results in an infiltration value of 37 cm/year. This mean infiltration value of 37 cm/year was rounded to one significant figure for the RPA; i.e., 40 cm/year for the infiltration at the EAVs.

A.1.1.3 Infiltration Through the Clay Cap

PORFLOW (ACRI 1993) was used to estimate the average infiltration rate of water through the upper clay cap given the infiltration estimated for the vadose zone in Sect. A.1.1.2. Infiltration rate through the clay cap was determined by simulating a case with a yearly infiltration into the native soil overlying the vault of 40 cm/year. The gravel layer above the vault provides a zone of high conductivity to remove water from above the vaults. Clay underlying the gravel serves as an additional barrier because of its low hydraulic conductivity. The domain of the cover simulation is shown in Fig. A.1-2. The code recorded infiltration over time for several locations under the clay cap. The infiltration rate in the zone below the edge of the cap was used as a conservative estimate of infiltration beneath the cap. Infiltration in the center of the cap may be approximately two orders of magnitude lower than this estimate, based on the hydraulic conductivity of clay.

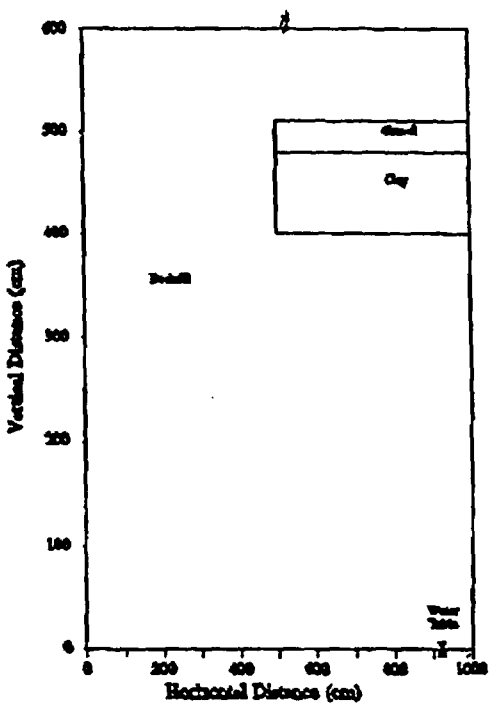

Figure A.1-2. Domain of the cover simulation

A.1.2 Flow and Mass Transport Through Vaults

In this section of Appendix A, details supporting the conceptual near-field model for each state of the vaults, intact, cracked, and failed (briefly described in Sect. 3.3.1.1), and the computational analysis (briefly described in Sect. 3.4.1.1) are provided.

A.1.2.1 Conceptual Model for Near-Field Analysis of the Vaults

As noted in Sect. 3.3.1, the near-field environment is defined as the portion of the subsurface environments extending from the ground surface to the water table. The flow regime in the subsurface was separated into three regions for purposes of analysis. The first region is the sediments near the surface where evaporation and transpiration have a dynamic role in reversing the downward movement of water due to gravity. Below this region, but above the concrete vaults, is the region that includes the engineered moisture barrier, composed of clay and an overlying gravel layer which is expected to divert much of the infiltrating water around the facility. The last region consists of the backfill sediment, soils underlying the EAV, the concrete vault, and the waste form, and extends down to the water table.

Assumptions specific to analysis of flow of water through the first region near the surface are discussed in Appendix A.1.1. The remainder of this section will address assumptions relevant to flow through the moisture barrier and flow and mass transport through the vaults and surrounding soil.

Flow Through the Moisture Barrier

INFORMATION ONLY

Flow through the moisture barrier required assumptions regarding the hydraulic characteristics of the layered clay, gravel, and backfill soil. As noted in Sect. 3.3.1.1, the conceptual model used to provide a framework for the numerical simulation of the near-field movement of water and contaminants from the EAV relies on averaging of spatial properties for these three material types. To the extent possible, characteristics of these materials are site-specific.

Hydraulic properties of each of these porous media can be adequately described by the following hydraulic parameters: saturated hydraulic conductivity, effective porosity, and moisture characteristic curves. Moisture characteristic curves describe the nonlinear relationship between the matrix potential or pressure head, the moisture content, and the hydraulic conductivity. These properties were discussed in Sect. 3.3.1.1.

Flow and Mass Transport Through Waste Form, Vaults, and Surrounding Soil

Like the moisture barrier, flow of water through the concrete vaults and soils surrounding the vaults is a function of the hydraulic properties of the different porous materials present. Hydraulic parameters were defined for these materials in the same manner as for the moisture barrier materials, and the values used are listed in Table 3.3-1. For the backfill sediments and underlying soils, the same parameter definitions used for the backfill portion of the moisture barrier analysis are also used. It is reasonable to expect that all backfill soils will originate from the E-Area vicinity, and will therefore, be similar to native soils underlying the facility. The basis for the hydraulic parameters for all soil types is provided in Sect. 3.3.1. Additionally, a basis for the degradation times and changes in hydraulic conductivity are given in Appendix K.

Mass transport in the near-field model is governed by several processes: diffusion, advection, dispersion, sorption, and radioactive decay. In order to address these processes quantitatively, values for dispersivities, diffusion coefficients, liquid: solid partition coefficients (i.e., K_d's) for the concrete, waste form, clay, sand, and backfill, and half-lives of radioactive decay for all constituents not screened from further consideration in Sect. 3.2.3 and 3.2.4 must be developed.

Longitudinal and transverse dispersion of a contaminant plume will occur, but the degree to which this may occur at E-Area is unknown. Dispersion is largely a function of the heterogeneity of the porous material encountered, which may reduce the concentration in a plume, but may also reduce the travel time of the leading edge of a plume at a downstream location. Although concrete may intuitively seem to be relatively homogeneous, fractures will increase dispersion of a plume passing through this material. The dispersivities assumed for each

material are listed in Table A.1-1. Based on conservation relative to peak plume concentrations, the dispersivities were assigned values as low as possible that still maintained an adequate numerical mass balance.

Table A.1-1. Longitudinal and transverse dispersivities used in the PORFLOW near-field model

Porous Material	Longitudinal Dispersivity (cm)	Transverse Dispersivity (cm)	Eff Diffusion Coefficient (cm^2/year)
Backfill	10	2	110
Concrete	5	1	32

Calculation of the effective diffusive flux of a constituent out of a porous material, requires values of the effective diffusion coefficient (molecular diffusion coefficient corrected for tortuosity of the porous medium). Tortuosity cannot be measured directly, but effective diffusion coefficients can be obtained empirically for conservative (i.e., nonsorbing, non-chemically reactive) compounds. For a given material, it is expected that the effective diffusivities for various radionuclides and non-radioactive compounds would be similar because molecular diffusivities in water do not vary significantly. Table A.1-1 lists the effective diffusion coefficients used for the various materials.

Sorption of radionuclides by the waste form will result in lower initial pore solution concentrations. During mass transport of radionuclides partitioned into the liquid phase, sorption will serve to retard the movement of the contaminants relative to water. Sorption is often characterized by K_ds, which assume linear, reversible, sorption at equilibrium. The K_ds used in this assessment are specific to the material to which they are assigned. K_d values used in this analysis are provided in Sect. 3.3.1.

A.1.2.2 Near-Field Flow and Transport Simulations

As noted in Sect. 3.1.1, computational analysis of the near-field model relied on the PORFLOW (Appendix B.4) computer code to simulate flow and mass transport. This complex code was necessary to address flow through the several adjacent materials in the unsaturated near-field environment, all of which possess different hydraulic properties. Details of the simulations of flow through the moisture barrier and flow and mass transport through the waste forms, vaults, and vadose zone are provided in this section. The PORFLOW code was chosen from a list of three dimensional variably saturated flow codes presently available (Appendix B.4).

Simulation of Flow Through the Moisture Barrier

The simulation of flow through the moisture barrier was performed using the PORFLOW code to determine the effectiveness of the barrier. This engineered barrier consists of a double layer of highly conductive gravel overlying clay. The surrounding material is composed of backfill soil. A 2% slope was used in the simulation as a conservative measure of performance, based on preliminary closure concept information indicating the slope of the clay layer will range between 2 and 5% (Thompson 1991).

The assumed hydraulic characteristics of each of the material types used in the simulations were discussed previously in Sect. 3.3.1.1. The simulation domain was 1000 cm wide and 600 cm high. Although the barriers will be placed over the entire facility, it was only necessary to simulate the end 500 cm of the barrier to determine its performance. This allows consideration of flow around the end of the barrier in addition to flow through the barrier.

The two-dimensional domain developed for the moisture barrier analyses is illustrated in Fig. 4.1-1. This figure also shows simulation results for saturation. It should be noted that the orientation of gravity was rotated clockwise in the simulation to account for the effort of the 2% slope of the barrier on flow rate.

Boundary conditions for this domain are as follows. The upper boundary is a constant flux boundary, representing the average annual infiltration rate into the soil, estimated in Appendix A.1.1 to be 40 cm/year. The lateral boundaries are assumed to be no-flow boundaries. This imposes an assumption that lateral flow in this region can be neglected. This is reasonable, as long as lateral diversion of water by the clay layer simulated occurs far from these boundaries within the domain. The lateral boundary conditions assume only vertical flow parallel to the boundaries, although vertical flow in this case is 2% off from the direction of gravity, due to the orientation of gravity at 2% off the vertical. The placement of the right no-flow boundary at 500 cm from the edge of the moisture barrier was somewhat arbitrary, based on judgement that the edge effect of the barrier would not be significant at this distance. From Fig. 4.1-1, the simulated saturation field supports this judgement, as it appears to be approaching an equilibrium near the right boundary, where saturation contours indicate predominantly vertical flow. The lower boundary was placed far enough away so as not to influence the flow field near the moisture barrier, and was assigned a pressure head of zero, in effect simulating the water table.

The simulation was carried out in several stages. Initially, the entire domain was treated as if it was all backfill, such that a uniform flow field was predicted. Then, the clay layer was included and the simulation was conducted in a transient mode until steady state was achieved. Lastly, the gravel layer was added to the simulation domain, and a simulation was conducted in transient mode until the pressure field (Fig. 4.1-1) maintained constant values.

During the course of these simulations, the predicted pressure field was monitored, as was the total water mass balance for the simulation domain. The maximum water mass balance error observed in these simulations was less than 3%, which was considered adequate for the purpose of determining the effectiveness of the barrier in diverting water. Reasonable efforts to improve the mass balance failed. A close inspection of the numerical solution showed that a slight increase in water in the system originated within the gravel layer, and persisted through the clay.

The flux across two planes (two-dimensional domains assume a unit width in the third dimension, such that a plane is of unit width) within the simulation domain was monitored to determine how effective the barrier was at diverting water. One flux plane extended from the left simulation boundary edge of the clay layer at 500 cm, representing flux through the region not covered by clay, but receiving diverted water from the gravel layer overlying the clay. The other flux plane went from the edge of the clay layer to the right simulation boundary at 1000 cm, representing the region of the domain "protected" by the clay. A comparison of the two fluxes indicated that 99.5% of the total water flux across the upper boundary was being diverted through the plane to the left of the assumed-intact clay layer.

To evaluate the flow rate through the moisture barrier, the vertical fluxes through a plane beneath the clay layer were plotted. The results are shown in Fig. 4.1-2. The results indicated that the left boundary (no-flow condition assumed) was far enough away from the moisture barrier such that the assumption of negligible lateral flow at this boundary from the gravel drainage layer is reasonable. The flux adjacent to this boundary is 40 cm/year in the vertical direction, parallel to the boundary. The large amount of water being diverted around the barrier is represented in Fig. 4.1-2 by the peak flux occurring in approximately the center of the domain. Inspection of Fig. 4.1-2, also indicates that an elevated infiltration rate extends past 500 cm, into the region covered by the clay, representing infiltration around the end of the barrier into the protected region. Finally, it appears that 500 cm of the barrier was an adequate length to establish a constant flow rate through the barrier. The vertical flux through the barrier stabilizes about 300 cm in from the end of the barrier at a value of 0.45 cm/year. While it would be appropriate to use this value as the infiltration rate for water reaching the vault, SRS determined a more conservative value of 4 cm/year should be used as the infiltration rate through the barrier. This is due, in part, to the fact that the hydraulic conductivity of the clay as measured in the laboratory was approximately 1.0×10^{-8} cm/s. It was felt that a more appropriate value for the *in situ* saturated hydraulic conductivity would be 1.0×10^{-7} cm/s, which is consistent with liners in RCRA clay liners. Using this saturated hydraulic conductivity and assuming unit gradient conditions the flux through the cover would be approximately 4 cm/year.

Simulation of Flow and Mass Transport Through the Vadose Zone

The second part of the near-field analysis consisted of simulating water flow and solute transport in the region below the moisture barrier, which includes the vault and waste form. This simulation was performed using the PORFLOW computer code using double precision. The physical domain in the simulation consisted of a vertical half-plane of the vaults and the surrounding backfill soil (Figs. 3.3-3 and 3.3-4). The simulation domain was rectangular with the vault superimposed on the left side. While the actual vaults have sloping roofs to increase the flow of water around the vault, the roof was assumed to be flat in the simulation, for ease of computation. This was conservative because it allowed more water to perch, and thus, penetrate the vault. The process used to simulate the vaults is discussed in Sect. 4.1.2.2.

The ILNT physical domain simulated was 1800 cm wide, 2100 cm high, and LAW vault domain was 2700 cm wide, and 2050 cm high. The computational grids for the ILNT/ILT model was 46 × 72, while the much larger LAW vault was simulated with a grid of 71 × 76 nodes. Spacing of the nodes varied in the domain with a maximum vertical distance in the ILNT/ILT vault of 90 cm in the center of the waste zone, and a maximum of 100 cm in the horizontal direction in the backfill zone at the side of the vault. The minimum node spacing occurred at every soil boundary and was 10 cm for both the vertical and horizontal directions. The maximum node spacing for the LAW vault was 50 cm in both the horizontal and vertical directions, each occurred in the backfill zone. The minimum node spacing in the horizontal direction was 5 cm at the sand-backfill interface, while the minimum node spacing in the vertical direction was 10 cm at each soil interface.

The upper boundary for water flow in each simulation was treated as a prescribed flux boundary with the assigned value dependent on the assumption regarding whether the moisture barrier remained intact. Both lateral boundaries were assumed to be no-flux boundaries. The left lateral boundary, away from the vault, was located halfway between adjacent vaults, where the flow field is essentially vertical. The inner boundary is located at the midpoint of a transverse section of a vault, where the flow field is also essentially vertical. The bottom boundary is located at the water table, such that a prescribed pressure head of zero is appropriate.

The boundary conditions for mass transport (i.e., boundary conditions on concentration, rather than fluid pressure) simulations were assigned as follows. No-flux conditions were assigned at the lateral boundaries, based on assumptions of symmetry between vaults and at the midpoint within the vaults. The lower boundary condition was a prescribed zero concentration, which corresponds to a condition where contaminants are swept away from the water table surface fast enough to render the concentration relatively low. This assumption serves to maximize the simulated diffusive flux through the domain, which is driven by concentration gradients, and thus, is conservative. The upper boundary condition was also specified as a zero concentration boundary, which is reasonable because mass transport is expected to be predominantly downward once contaminants are out of the vaults.

Since the void in the LAW vault is not a porous media, it required special consideration. In order to maintain conservatism, it was necessary to assume the travel time through the void was minimal. However, during the intact time period only a small amount of water is expected to enter the void resulting in small average velocities. Therefore, the saturated hydraulic conductivity in the void was set equal to that of concrete (1.0×10^{-10} cm/s). After cracking, the void's saturated hydraulic conductivity was increased to that of sand (1.0×10^{-3} cm/s). By doing this it was possible to allow the movement of water through the void space to be maximized upon cracking and maintain mass balance during the intact period.

Since the waste containers are expected to corrode and lose their integrity much faster than the vault, it was assumed that upon placement of the waste the boxes were completely corroded and compacted. This required an estimate of the effective height of the waste zone. A brief discussion of the assumptions used to calculate the height of the waste inside the LAW vault is given below.

<u>Assumptions:</u>

A Porosity of 50% is assumed in the waste inside the B-25 boxes.

As the B-25 boxes compact and corrode the volume of pores in the waste decrease by 50%.

LAW vaults are filled to the capacity of 12,000 B-25 boxes.

B-25 boxes are filled to 85% capacity.

Void Inside B-25 Boxes:

Fraction of inside of box that is void = 0.15

Fraction of inside of box that is waste = 0.425

Fraction of inside of box that is pores = 0.425

$$\begin{aligned} Void &= (Initial\ Void) + (Compaction\ Factor)(Initial\ Pore\ Fraction) \\ &= (0.15) + (0.5)(0.425) \\ &= 0.3625 \end{aligned}$$

Void Outside B-25 Boxes:

Volume of B-25 Box: 113 ft^3

Volume of Cell: 159,753 ft^3

$$\begin{aligned} Void &= 1 - \frac{(Volume\ of\ Boxes)}{(Total\ Volume)} \\ &= 1 - \frac{(113\ ft^3/box)(12000\ box/vault)}{(159{,}753\ ft^3/cell)(12\ cell/vault)} \\ &= 0.293 \end{aligned}$$

Total Void:

$$\begin{aligned} Total\ Void &= (Void\ Inside\ Boxes) + (Void\ Outside\ of\ Boxes) \\ &= 0.3625 + 0.293 \\ &= 0.655 \end{aligned}$$

Height of Waste and Void:

Inside height of LAW Vault = 785 cm

$$\begin{aligned} Void\ Depth &= (785\,cm)(0.655) = 514\ cm \\ Waste\ Depth &= (785 - 514)\,cm = 271\ cm \end{aligned}$$

All of the waste was assumed to be uniformly distributed in the bottom 2/1 cm of the LAW vault. The same process was followed for the ILNT/ILT vaults; however, the results indicated that the waste would occupy all but 9% of the total height. Based on this result, it was determined that a void would not be considered for the ILNT/ILT vault system, although collapse of the ILNT/ILT roof was incorporated into the modeling study.

A.2 GROUNDWATER FLOW AND MASS TRANSPORT MODEL AND SIMULATIONS

This section of Appendix A provides details of the conceptual model adopted for simulating flow and mass transport through the saturated hydrologic zones beneath the EAVs (Sect. A.2.1), and details related to simulation of the model using the PORFLOW computer code (Sect. A.2.2).

A.2.1 Conceptual Saturated Flow and Transport Model

Based on the piezometric data at E-Area (Sect. 3.4.2), it is apparent that the groundwater flow field is highly variable within and among the hydrologic units in the vicinity of E-Area. A three-dimensional representation of the groundwater flow system was chosen to allow the divergent lateral flow to be simulated (Fig. A.2-1).

The conceptual model for saturated flow was developed from data obtained in the E-Area wells and available regional data. The E-Area wells shown in Fig. A.2-2, provided site-specific information on the lithology and hydrologic properties of the subsurface units. Lithologic cross-sections (Sect. 2.2.2) developed from site wells were used to identify hydrologic units. Data from single well hydraulic tests and pump tests were used to group units according to similar hydrologic characteristics. Regional hydrogeologic data provided information on potentiometric surfaces, from which hydraulic gradients were estimated. Regional topographic maps were used to estimate pressure heads and gradients in the nearby streams. Local streams were gaged to estimate the quantity of groundwater discharge.

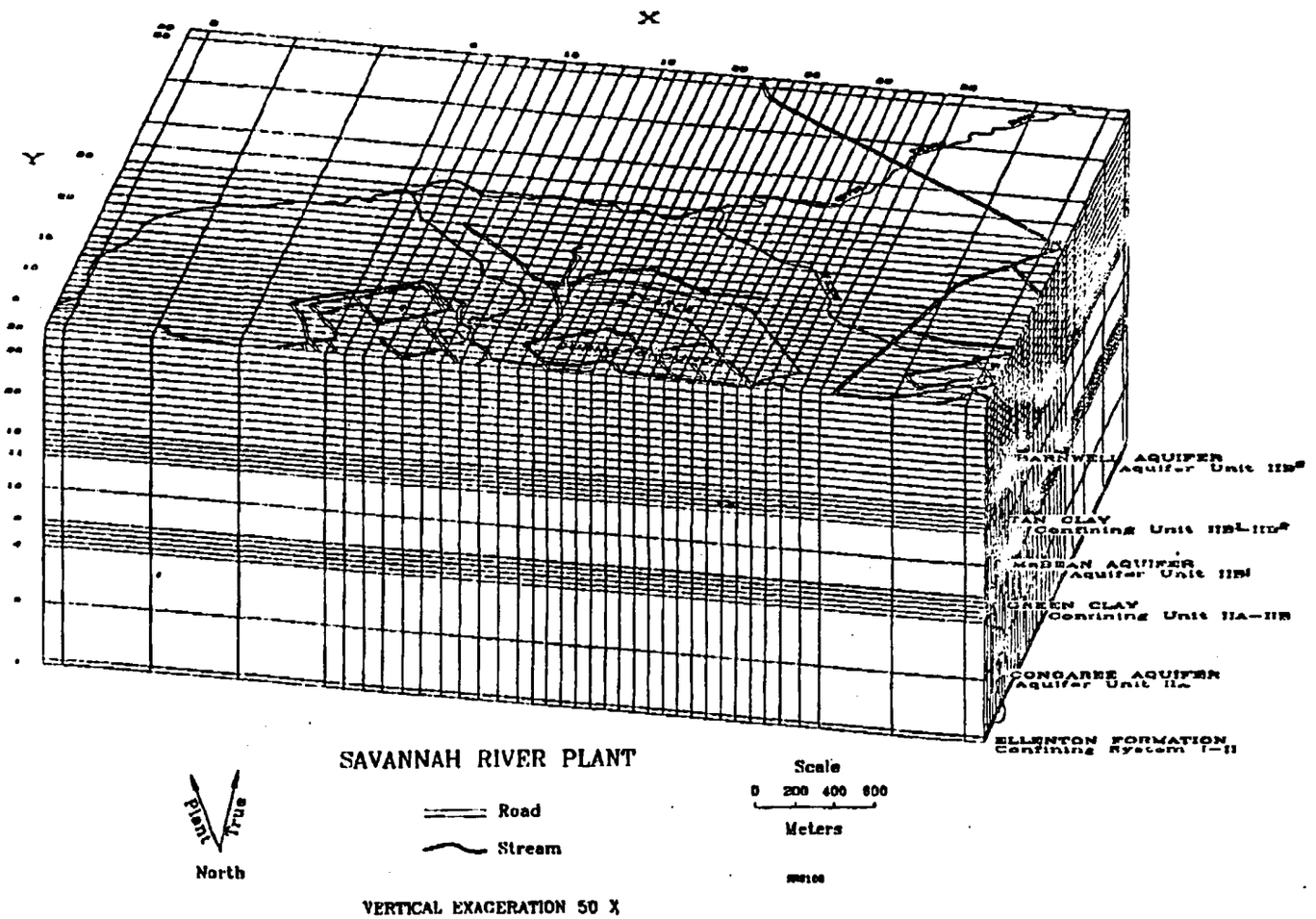

Fig. A.2-1. Model domain for PORFLOW simulation of groundwater in E-Area vicinity.

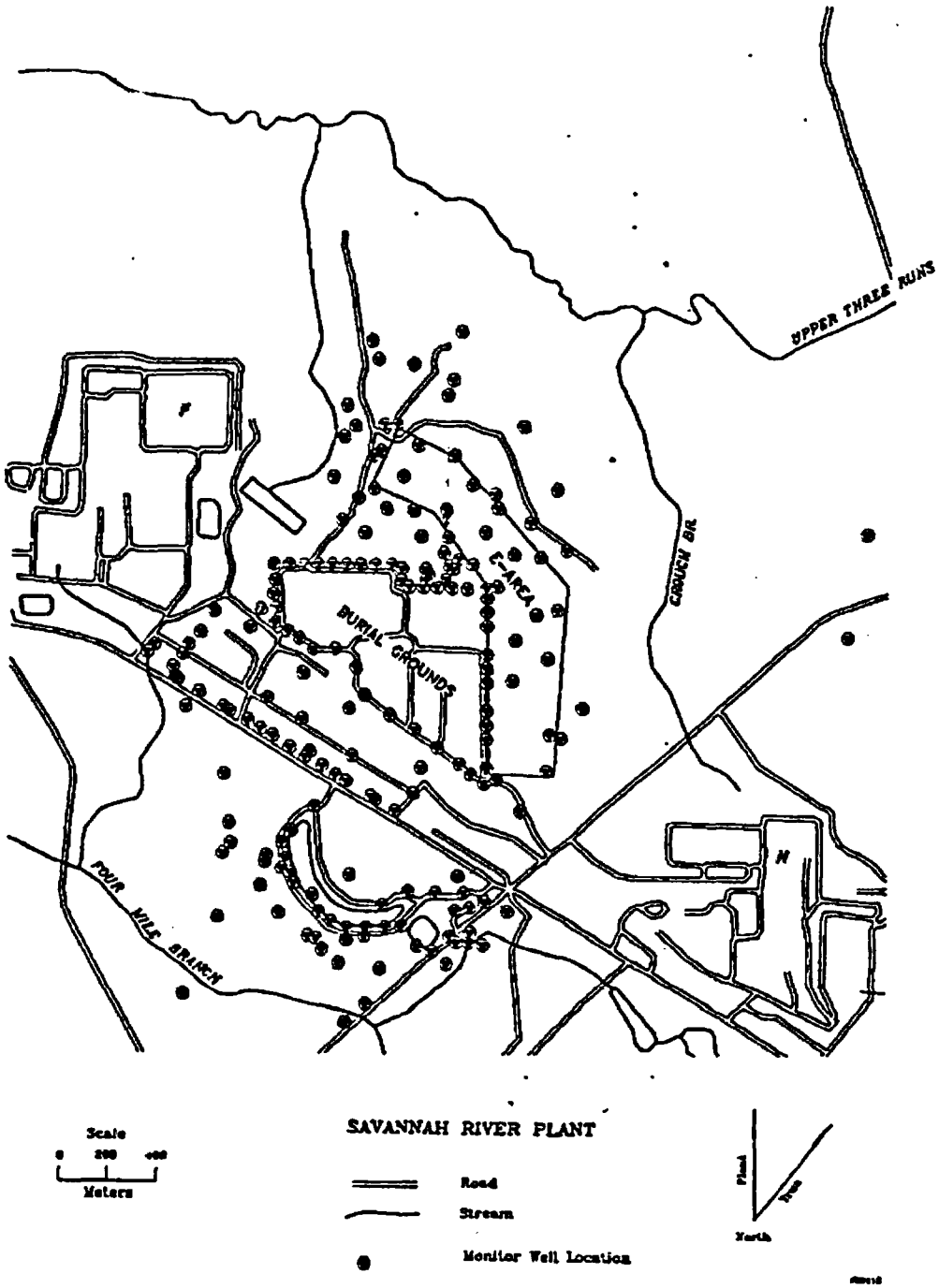

Fig. A.2-2. Location of E-Area groundwater wells.

In Sect. A.2.1.1, the boundaries selected for the model domain are defined and the basis for these boundaries are justified. Section A.2.1.2 identifies the five hydrologic units simulated. Characteristics of these units that affect flow are described in Sect. A.2.1.3. Properties that affect mass transport are described in Sect. A.2.1.4.

A.2.1.1 Model Boundaries

Before a model of the saturated zone beneath the EAVs was conceptualized, the area of potential concern was defined. This was done by: 1) evaluating hydrologic data available for the SRS, particularly for E-Area (Sect. 2.1.5, 2.2.2 and Appendix E), to identify the likely areas of potential contamination and 2) to further limit these boundaries by considering the exposure scenarios of concern, which are outlined in Sect. 3.2.3 and 3.2.4 in this report. The vertical extent of the model is described first according to the lower and upper boundaries of the model domain. The areal extent of the model and its boundaries are then described.

Vertical Extent of Model

The model boundaries for the vertical extent of the E-Area conceptual groundwater model domain are described in terms of the hydrological units underlying E-Area, which were identified in Sect. 2.1.5. According to the regional geological and hydrological data, Aquifer Unit IIA (Congaree Aquifer) is the lowermost hydrostratigraphic unit which could potentially be affected by the planned facility. The lower boundary of the domain (i.e., constant flux boundary) is assumed to be the contact between Aquifer Unit IIA and Confining System I-II (Ellenton Clays) (Fig. 2.1-5). There is a considerable thickness of the low-permeability geologic constituents of Confining System I-II (Sect. 2.1.5) separating the two units. In addition, Christiansen and Gordon (1983) indicated that the lower sand aquifer (Aquifer System I) has a higher piezometric head than the overlying Aquifer Unit IIA, thus forming an effective barrier to downward flow from Aquifer Unit IIA. However, the same quantities of recharge to the Congaree from the underlying formations is expected due to a substantial upward gradient. Consequently, the base of the problem domain is simulated as a constant flux boundary.

The upper boundary limit in the vertical extent of the model domain is defined by the water table, assumed to be a constant flux boundary defined by the average annual recharge. The upper boundary of the vertical domain occurs in Aquifer Unit IIB, Zone 2 (water table).

Lateral extent of the model

The upper hydrologic units included in the model [Aquifer Unit IIB, Zone 2 (water table), and Aquifer Unit IIB, Zone 1 (Barnwell/McBean)] are partially drained by the three creeks surrounding E-Area. Groundwater in these upper units discharges into the creeks around E-Area. Groundwater from Aquifer Unit IIB, Zone 1, discharges through the green clay into the underlying Aquifer Unit IIA (Fig. A.2-1). The lowermost unit, Aquifer Unit IIA, is partially dissected only by UTR Creek.

The eastern and western model boundaries for all hydrologic units are located at a substantial distance from the creek (Fig. A.2-1). As mentioned in Sect. 3.3.2.2, the horizontal extent of the model domain was selected to coincide wherever possible with naturally occurring sub-regional groundwater flow boundaries. Selecting model boundaries so that the streams that are included within the flow field allows simulation of the effect of the creeks on groundwater flow. UTR Creek forms the northern boundary of the problem domain and incises all of these units. Stream gaging surveys indicate significant groundwater discharge from all units to UTR Creek. Flow rates in Crouch and unnamed Branches increase from their upper reaches towards UTR Creek, suggesting significant groundwater discharge from the water-table units which they incise.

The southern boundary is defined by the drainage divide. Measured potentiometric surfaces for Aquifer Units IIB, Zones 1 and 2, in this region (Fig. E.2-2, E.2-4, and E.2-5) indicate that flow is away from this divide and toward the creeks.

The presence of the creeks serve to limit the lateral extent of flow, especially those creeks that completely incise a hydrologic unit. The upper units are completely incised by UTR Creek (Aquifer Units IIB, Zones 1 and 2), (Appendix E) and partially by Crouch and unnamed Branches. Aquifer Unit IIA is partially incised by only UTR Creek. All available hydrogeologic information suggests that the entire contaminant plume will eventually discharge to the surface streams near E-Area.

A.2.1.2 Hydrologic Units

Five simplified hydrologic units (Fig. 2.1-5) are included in the groundwater conceptual model: Aquifer Unit IIB, Zone 2, makes up the upper zone containing the water table aquifer, Confining Unit IIB1-IIB2 (Tan Clay) is a semi-confining unit separating the water table unit and Aquifer Unit IIB, Zone 1 (Barnwell/McBean), Confining Unit IIA-IIB (Green Clay) is a confining zone between Aquifer Unit IIB, Zone 1, and the underlying aquifer, Aquifer Unit IIA (Congaree Aquifer). These five units were identified based on similar lithology and hydrologic characteristics. The five units are characterized by spatially-averaged hydrologic parameters, which are obtained in pump tests. Anisotropy, which is likely to exist as a result of lithologic heterogeneity, is assumed for each unit by assigning vertical hydraulic conductivities that are less than horizontal conductivities. Hydrologic characteristics of the units making up these conceptual units are described in detail in Appendix E.

A.2.1.3 Hydrogeologic Properties

The hydrogeologic properties chosen to represent the five simplified hydrologic units in the groundwater model are based on previous field, laboratory, and modeling studies at SRS.

The existing horizontal hydraulic conductivity data, listed in Table 2.2-1 for all hydrologic units at E-Area, indicate horizontal conductivities ranging over several orders of magnitude for the aquifer units simulated in this RPA. The range, as well as the value used in simulations, are listed in Table A.2-1. Values used in simulations were chosen from the range of measured values, when available, based on the calibration procedure described in Sect. 3.4.2.1.

Table A.2-1. Measured and assumed hydraulic conductivities for saturated hydrologic units

Hydrologic Unit	Horizontal hydraulic conductivity (cm yr^{-1})		Vertical hydraulic conductivity (cm yr^{-1})
	Measured range (Geotrans 1992)	Value used in simulations	Value used in simulations
Aquifer Unit IIB, Zone 2	4.1×10^3 to 1.8×10^4	4.0×10^4	1.0×10^4
Confining Unit IIB1-IIB2	0.19 to 3.8	6.4×10^1	4.3×10^1
Aquifer Unit IIB, Zone 1	2.3×10^3 to 2.3×10^5	4.1×10^4	3.1×10^4
Confining Unit IIA-IIB	0.44 to 5.0	3.0	2.0
Aquifer Unit IIA	2.0×10^4	4.2×10^5	4.2×10^4

A.2.1.4 Properties Affecting Mass Transport

Mass transport in the saturated zone occurs by advective, diffusive, and dispersive processes, but is hindered by sorptive processes. In the saturated zone, advective transport is sufficiently high to render diffusive transport relatively insignificant. Mechanical dispersion,which causes spreading of a contaminant plume, is a property of the aquifer matrix and flow characteristics that have not been measured in aquifers underlying the SRS. Dispersion is not expected to be important for the EAV, however, because the area of the source (i.e., area of the EAV), and thus, the potential area of a contaminant plume originating from the facility, is large. Spreading of the plume from such a large source will not significantly reduce concentrations at a point 100 m from the facility, the compliance point for groundwater protection assumed in this RPA. Thus, reasonable dispersivities for longitudinal and transverse dispersion were selected from a reputable groundwater textbook (Freeze and Cherry 1979). The longitudinal and transverse dispersivities selected are 3 m and 0.3 m respectively.

Other characteristics of the porous media that affect mass transport simulations include density and porosity of the media. Matrix density of the media is a property used by the simulation code PORFLOW to calculate retardation based on sorption coefficients, or K_d's. For the five hydrologic units of interest, a matrix density of 2650 kg/m^3 is used, based on an average value provided by Freeze and Cherry (1979). The total porosity of all units was based on data contained in Table A.2-2. An effective porosity was determined, based on an average value from de Marsily (1986).

Table A.2-2. Total porosities - E-Area

Zone(s)	Total θ (%)
Aquifer Unit IIB, Zone 2	40
Confining Unit IIB1-IIB2	40
Aquifer Unit IIB, Zone 1	40
Confining Unit IIA-IIB	40
Aquifer Unit IIA	40

Characteristics of contaminants that are needed to simulate mass transport are sorption coefficients (Sect. 3.3.1) and half-lives of radioactive decay (Appendix C). Sorption of a continuous source of contaminants on solid surfaces is often viewed as reversible, achieving equilibrium instantaneously, and applies only to immobile surfaces (i.e., sorption on mobile colloids is not considered). This view of sorption is represented by a K_d, and is the view adopted for this RPA. This representation of sorption serves to retard the computed arrival of a plume of contaminants at a given location, rather than lower the ultimate concentration. However, extending the transit time of a contaminant can allow for radioactive decay or microbial degradation processes to reduce the concentration before the plume reaches a critical receptor location. These decay processes will be important for radionuclides with half-lives significantly less than the transit time in groundwater.

The value of K_d varies with the contaminant and the media to a large degree. The values used for the saturated zone are consistent with those used in the near-field model (Table 3.3-2), and were site-specific when possible.

A.2.2 Saturated Flow and Transport Simulations

In this section, the method for simulating the conceptual saturated flow and transport is described in detail. In Sect. A.2.2.1, details of the design of the input file for the PORFLOW computer code simulations are given. In Sect. A.2.2.2, the initial optimization study that was done, to ascertain that code simulations were producing credible results is discussed.

A.2.2.1 Simulation Design

Groundwater flow and mass transport simulations were conducted with PORFLOW based on the conceptual model discussed in Sect. A.2.1. The model was calibrated by comparing hydraulic head values calculated by PORFLOW with actual head values from site monitoring wells. Calibration was based on an average annual recharge of 40 cm. The calibration process is discussed in detail in Sect. 3.4.2.

After completing the groundwater flow simulations, and generating a predicted steady-state flow field, separate input files were developed for transport simulations. These input files consisted of the concentration boundary conditions and transport parameters described in Sect. A.2.1.4 above, and rely on the results of the steady-state flow simulations for the specification of the velocity vectors. The velocity vectors are used in the transport simulations in computing advective and dispersive transport of potential contaminants.

A.3. ANALYSIS OF ATMOSPHERIC EFFLUENT

Volatile emissions, such as HTO (tritiated water vapor), HT, $^{14}CO_2$, and isotopes of radon are expected to occur at LLW disposal facilities in varying quantities that depend on the initial disposal activities of each volatile isotope or radioactive parent, disposal method, and the surrounding physiochemical environment.

The purpose of this section is to estimate an upper bound of the potential impact of ^{3}H and ^{14}C in terms of off-site individual and inadvertent intruder doses associated with the EAVDF. The impacts from the release of radons are described in Sect. A.3.7.

A.3.1 Dose Analysis of Tritium Crucibles in the ILT Vaults

Tritium is produced by irradiation of lithium isotopes by the neutron flux produced in nuclear reactors at the SRS. The ^{3}H is extracted as a gas by vacuum melting irradiated Li-Al alloy targets in stainless steel crucibles such that only a small residual of less than 500 Ci ^{3}H is left in the alloy when the crucibles are discarded. The tritium crucibles are placed into sealed 46-cm-diameter steel pipe overpacks and placed into lined concrete silos in the ILT vaults, with a capacity of 142 crucibles for each vault.

A.3.1.1 Previous Studies

Orebaugh and Wallace (1989) produced a modeling study titled *Quantification of Hazards Associated with the Decay and Storage/Disposal of Tritium Crucibles.* This study evaluated the release of ^{3}H from the crucibles for various scenarios including: Case I, a tritium crucible sealed with moist air inside; Case II, plug shrinkage vents the crucible to moist air; Case III, vented crucibles stored in a sealed concrete vault; and Case IV, Case III with an engineered vent. This study evaluated the impact of the corrosion reaction between Al and H_2O producing H_2 gas. The study provides ^{3}H flux rates from the crucibles, which were used in this RPA to determine the impact to the intruder and off-site individuals from tritiated water vapor released from the EAV ILT vaults.

A.3.1.2 Intruder Dose Analysis

An analysis was performed for the intruder based upon the flux rate determined by Orebaugh and Wallace (1989). Modeling results for Case III of this study were used in which vented crucibles are stored in a sealed concrete vault. This assumes that the vault is not

ventilated, therefore, the source of HTO would be maximized in the vault. The epoxy plugged crucibles are assumed to vent due to shrinkage of the plug. New saturated vault walls were assumed requiring an aqueous diffusion pathway. Wet vault walls were assumed to ensure saturated air at all times in the vault.

The Orebaugh and Wallace (1989) study assumed that: 1) the air in the vault is always water saturated; 2) all 250 plugged crucibles, each containing 500 Ci of ^3H, are releasing hydrogen and tritium to the vault (NOTE: presently only 142 crucibles are planned per vault making this analysis conservative); and 3) hydrogen diffuses out of the vault through an aqueous pathway (i.e., saturated concrete). The hydrogen and tritium diffuse out of the crucibles into the vault, and gradually increase the concentration of both isotopes in the vault atmosphere. The concentration in the soil is assumed to always be zero. The flux through all the vault walls at the time of the maximum tritium concentration in the vault air was less than 1 mCi yr^{-1}.

Assuming that the intruder's house resides directly on top of the vault, the steady-state concentration in the house may be determined simply by:

$$C_{ss} = \frac{\left(\frac{q}{a}\right)}{h} \qquad \text{Eq. A.3.1}$$

where

C_{ss} = steady-state air concentration in house, Ci m^{-3},
q = HTO flux rate into house, Ci m^{-2} yr,
a = air exchange rate in house, 8760 yr^{-1},
h = height of the ceiling in house, 2.4 m.

The inhalation dose to the intruder is calculated as follows:

$$D = C_{ss} * B_I * DCF \qquad \text{Eq. A.3.2}$$

where

D = inhalation dose, mrem yr^{-1},
C_{ss} = steady-state air concentration, Ci m^{-3},
B_r = breathing rate (8000 m^3 yr^{-1}),
DCF = inhalation dose conversion factor (6.3 x 10^4 mrem Ci^{-1}).

Assuming a 1 mCi yr^{-1} flux out of the top of the ILT vault (i.e., 15 m by 7.6 m) enters directly into the house of the intruder, a steady-state concentration was determined to be 4.2 × 10^{-10} Ci m^{-3} using Eq. A.3.1. The inhalation committed EDE to the intruder in the house was determined to be 2.1 × 10^{-1} mrem yr^{-1} using Eq. A.3.2. The dose calculation is for inhalation only; however, it is considered bounding for the all-pathway dose to the intruder since the intruder is assumed to reside in the house all year. Thus, the dose from a more realistic full pathway analysis would result in doses which are equivalent to or less than those determined for the inhalation pathway only.

The tritium inventory limit for the tritium crucibles in the ILT vault is determined from:

$$I = I_0 * \frac{D}{D_0} \qquad \text{Eq. A.3.3}$$

where

I = allowable inventory, Ci $vault^{-1}$,
I_0 = initial inventory used in the calculation, Ci $vault^{-1}$,
D = allowable intruder dose objective, (100 mrem yr^{-1}),
D_0 = dose from the initial inventory, mrem yr^{-1}.

Using Eq. A.3.3, and the assumed initial inventory of 500 Ci per crucible or 1.25 × 10^5 Ci of ^3H, the allowable inventory for tritium crucibles in the ILT vaults was determined to be 6.0 × 10^7 Ci $vault^{-1}$.

The ILT vaults are predicted to crack 575 years post-closure and to fail at 1050 years (Appendix X). These times are sufficiently long to preclude significant individual dose at the time of failure, even for the large allowable inventory calculated below.

A.3.1.3 Off-Site Individual Dose Analysis

The dose to an individual located at the SRS site boundary before the 100 year institutional control period was evaluated using the Orebaugh and Wallace (1989) report for Case IV, which involved a vented engineered vault with barometric pumping. This is the expected scenario for the off-site individual since the vault will be intact during the institutional control period. A vented vault is allowed to breathe, by variations in barometric pressure. The report indicates that daily pressure excursions of 0.01 atm are expected. The resulting concentration of HTO at this pressure was determined to be 5.2×10^{-7} Ci L^{-1} and the release rate through a 1-cm vent pipe of 2.6×10^{1} Ci yr^{-1} from each vault. The release rate is adjusted to account for the ten ILT vaults providing releases of ^{3}H. The nearest off-site individual is assumed to reside continuously at the SRS site boundary located 5 km from E-Area. A maximum EDE dose of 0.06 mrem yr^{-1} was calculated for all pathways by AIRDOS-PC (U.S.EPA 1989) utilizing the August, GA windfile. The AIRDOS-EPA input and output information is provided in Appendix C. The dose results for this analysis indicate that the maximum inventory of ^{3}H crucibles (i.e., 250,000 Ci/vault) in the ILT vaults will not exceed the performance objective of 10 mrem yr^{-1} for an off-site individual from the airborne pathway.

A.3.2 Dose Analysis of ^{3}H in JCW in the ILT Vaults

A.3.2.1 Intruder Dose Analysis

The basis of this analysis is to determine the allowable inventory of ^{3}H in the ILT job control waste vaults. Since ^{3}H in the vapor form is derived from the concentrations in the pore water, the ratio of the concentration in the vapor form to that in the water phase was

determined as follows:

$$H = \frac{C_{vapor}\ (g/m^3\ of\ air)}{C_{water}\ (g/m^3\ of\ water)} \qquad \text{Eq. A.3.4}$$

The concentration of water in air at 10 °C and 100 percent relative humidity can be determined as follows:

$$C\ (g/m^3) = \frac{Avp}{R \times T} \times MW \qquad \text{Eq. A.3.5}$$

where

Avp = actual vapor pressure (0.012 bars),
R = gas constant (8.314×10^{-5} bar m^3 mol^{-1} $^0K^{-1}$),
T = temperature (283 ^0K),
MW = molecular weight (18 g mol^{-1}).

This results in a water concentration in the air of 9.2 g m^{-3}. Assuming that concentration of H-3 in water is equal to the concentration in the vapor:

$$\frac{1\ Ci}{m^3_{(H_2O)}} \times \frac{1\ m^3_{(H_2O)}}{10^6\ g_{(H_2O)}} \times \frac{9.2\ g_{(H_2O)}}{m^3_{(air)}} = \frac{9.2 \times 10^{-6}\ Ci\ H\text{-}3}{m^3_{(air)}}$$

Therefore,

$$H = \frac{9.2 \times 10^{-6}\ Ci/m^3_{(air)}}{1\ Ci/m^3_{(H_2O)}} \qquad \text{Eq. A.3.6}$$

Using this relationship, the ^3H concentration in the vapor phase can be determined from the concentration in the water phase in the vault. It was assumed that the vaults each contained 1.0 Ci $vault^{-1}$ at the time of closure, which results in 3.6×10^{-3} Ci $vault^{-1}$ at the end of institutional control (i.e., 100 years post-closure). The ILT JCW vaults have a volume of

800 m^3 $vault^{-1}$. Assuming that the waste within each ILT vault is saturated and has a porosity of 0.50, the volume of water in each vault would be about 400 m^3 $vault^{-1}$. The corresponding ^3H concentration in the water within the vault is 9.0×10^{-6} Ci m^{-3}. Using the relationship developed in Eq. A.3.6, the ^3H concentration in the vapor phase would be 8.3×10^{-11} Ci m^{-3}. Assuming this vapor concentration is at the top surface of the vault, then the flux at the ground surface is given by Eq. A.3.7:

$$J = D\left(\frac{C_o}{x}\right) \qquad \text{Eq. A.3.7}$$

where

J	=	flux at the soil surface, Ci m^{-2} yr^{-1},
D	=	diffusion coefficient in air, 754 m^2 yr^{-1}, (CRC 1981),
C_o	=	source concentration, Ci m^{-3},
x	=	soil thickness, 1 m.

The allowable ^3H inventory was determined by use of Eq. A.3.2 and A.3.3 to be 6.7×10^4 Ci $vault^{-1}$ based upon an intruder dose of 100 mrem. The dose calculated is for inhalation exposure only; however, it is considered bounding for the all pathway dose to the intruder since the intruder is assumed to reside in the house all year.

A.3.2.2 Off-Site Dose Analysis

The dose to an individual located at the SRS site boundary before the 100 year institutional control period was evaluated in the following manner. Potential exposure is estimated by first calculating the ^3H concentration in pore water per Ci in each vault. Assuming 400 m^3 of pore water per vault, the ^3H concentration in pore water is 2.5×10^{-3} Ci m^{-3}. From Eq. A.3.6, the vapor phase ^3H concentration is 2.3×10^{-8} Ci m^{-3}. The flux at the soil surface was determined using Eq. A.3.7. This results in a flux at the soil surface above the

ILNT vault of 1.7×10^{-5} Ci m^{-2} yr^{-1}. This flux is assumed to occur over all 10 of the ILNT vaults resulting in a release of 1.1×10^{-2} Ci yr^{-1} for an area source of 6.4×10^{2} m^{2}. The off-site atmospheric transport was modeled with the AIRDOS-PC computer code (U.S.EPA 1989) using the Augusta, GA windfile (Appendix C). The nearest off-site individual is assumed to reside continuously at the SRS site boundary located 5 km from E-Area. The maximum EDE from all pathways was determined to be 2.5×10^{-6} mrem yr^{-1}. The AIRDOS-PC input and output file information is provided in Appendix C. The allowable ^{3}H inventory was determined using Eq. A.3.3, and was calculated to be 4.0×10^{6} Ci $vault^{-1}$ based upon the atmospheric performance objective dose of 10 mrem yr^{-1}.

A.3.3 Dose Analysis of ^{3}H in JCW in the ILNT Vaults

A.3.3.1 Intruder Dose Analysis

Using the relationship in Eq. A.3.6, the ^{3}H concentration in the vapor phase can be determined from the concentration in the water phase in the vault. It is assumed that the vaults each contained 1.0 Ci $vault^{-1}$ at the time of closure, which results in 3.6×10^{-3} Ci $vault^{-1}$ at the end of institutional control (i.e., 100 years post-closure). The ILNT vaults have a volume of 5880 m^{3} $vault^{-1}$. Assuming that the waste within each ILNT vault is saturated and has a porosity of 0.50, the volume of water in each vault would be 2940 m^{3} $vault^{-1}$. Therefore, the ^{3}H concentration in the water within the vault is 1.2×10^{-6} Ci m^{-3}. Using the relationship developed in Eq. A.3.6, the ^{3}H concentration in the vapor phase would be 1.1×10^{-11} Ci m^{-3}. Assuming this vapor concentration in Eq. A.3.7 and using Eqs. A.3.1 and A.3.2, the intruder's dose from inhalation would be 2.0×10^{-4} mrem yr^{-1}. The allowable ^{3}H inventory was determined by use of Eq. A.3.3, and was calculated to be 5.0×10^{5} Ci $vault^{-1}$ based upon an intruder dose of 100 mrem. The dose calculated is for inhalation exposure only; however, it is considered bounding for the all pathway dose to the intruder since the intruder is assumed to reside in the house all year.

A.3.3.1 Off-Site Dose Analysis

The dose to an individual located at the SRS site boundary before the 100 year institutional control period was evaluated using the equation for the flux given in Eq. A.3.7. The ^3H concentration in pore water per Ci in each vault is 3.4×10^{-4} Ci m^{-3}, based on 2.94×10^3 m^3 of pore water. From Eq. A.3.6, the vapor phase ^3H concentration is 3.1×10^{-9} Ci m^{-3}. This results in a flux at the soil surface above each ILNT vault of 2.3×10^{-6} Ci m^{-2} yr^{-1}. This flux is assumed to occur over all 10 of the ILNT vaults resulting in a release of 2.0×10^{-2} Ci yr^{-1} for an area source of 8.7×10^3 m^2. The off-site atmospheric transport was modeled with the AIRDOS-PC computer code (U.S.EPA 1989) using the Augusta, GA windfile (Appendix C). The nearest off-site individual is assumed to reside continuously at the SRS site boundary located 5 km from E-Area. The maximum EDE from all pathways was determined to be 4.5×10^{-6} mrem yr^{-1}. The AIRDOS-PC input and output file information is provided in Appendix C. The allowable ^3H inventory was determined using Eq. A.3.3, and was calculated to be 2.2×10^6 Ci vault^{-1} based upon the atmospheric performance objective dose of 10 mrem yr^{-1}.

A.3.4 Dose Analysis of ^{14}C in the ILNT Vaults

The waste form expected to contain ^{14}C in the ILNT vaults is mainly job control waste. C-14 is assumed to be in the form of $^{14}CO_2$ and contained in B-25 boxes.

A.3.4.1 Intruder Dose Analysis

The initial activity of ^{14}C in an ILNT vault containing job control waste is assumed to be 1 Ci. Each ILNT vault has a volume of 5880 m^3. Assuming a porosity within the waste of 0.50, the void volume in each ILNT vault is 2940 m^3. This results in a ^{14}C vault concentration of 3.4×10^{-4} Ci m^{-3} of void space at the end of the institutional control period (i.e., 100

years post-closure). Assuming this is the vapor phase concentration of $^{14}CO_2$, the flux of ^{14}C at the surface of 1 m of overlying soil, determined for the ILNT vault based on Eq. A.3.7 using a diffusion coefficient of 4.4×10^{2} m^2 yr^{-1} (CRC 1981), is 1.5×10^{-1} Ci m^{-2} yr^{-1}.

The projected area of each ILNT vault is 870 m^2. At a flux rate of 1.5×10^{-1} Ci m^{-2} yr^{-1} per Ci of ^{14}C in each ILNT vault, the entire ^{14}C inventory would be released in much less than a year. Therefore, the flux rate was adjusted to reflect total release within the first year. Per Ci of ^{14}C in the ILNT vault, total release in a year gives a flux rate of 1/870 Ci m^{-2} yr^{-1}, or 1.1×10^{-3} Ci m^{-2} yr^{-1}. From Eq. A.3.1, the resulting air concentration in the intruder's house is 5.2×10^{-8} Ci m^{-3}. The dose to the intruder was determined to be 10 mrem yr^{-1}, based upon Eq. A.3.2, using a DCF of 2.4×10^{4} mrem Ci^{-1}. The allowable inventory of ^{14}C in the ILNT vaults was determined to be 10 Ci per vault using Eq. A.3.3 and a performance objective of 100 mrem yr^{-1}. The dose calculated is for inhalation exposure only; however, it is considered bounding for the all-pathway dose to the intruder since the intruder is assumed to reside in the house all year.

A.3.4.2 Off-Site Dose Analysis

The dose to an individual located at the SRS site Boundary before the 100-year institutional control period was evaluated using the ^{14}C flux determined above, i.e., 1.1×10^{-3} Ci m^{-2} yr^{-1}. This flux is assumed to occur over all 10 ILNT vaults resulting in a release of 9.6 Ci yr^{-1} for an area source of 8.7×10^{3} m^2. The off-site atmospheric transport was modeled with the AIRDOS-PC computer code (U.S.EPA 1989) using the Augusta, GA windfile (Appendix C). The nearest off-site individual is assumed to reside continuously at the SRS site boundary located 5 km from E-Area. The maximum EDE from all pathways was determined to be 1.2 $\times 10^{-1}$ mrem yr^{-1}. The AIRDOS-PC input and output file information is provided in Appendix C. The allowable ^{14}C inventory was determined using Eq. A.3.3, and was calculated to be 83 Ci per vault, based upon the atmospheric performance objective dose of 10 mrem yr^{-1}.

A.3.5 Dose Analysis of ^3H in JCW in the LAW Vaults

A.3.5.1 Intruder Dose Analysis

Using the relationship in Eq. A.3.6, the ^3H concentration in the vapor phase can be determined from the concentration in the water phase in the vault. It is assumed that the vaults each contained 1.0 Ci vault^{-1} at the time of closure, which results in 3.6×10^{-3} Ci vault^{-1} at the end of institutional control (i.e., 100 years post-closure). The LAW vaults have a volume of approximately 47,000 m^3 vault^{-1} (for the smaller 2-module vaults). Assuming that the waste in each vault is saturated and has a porosity of 0.50, the volume of water in each vault would be 2.4×10^4 m^3 vault^{-1}. Therefore, the ^3H concentration in the water within each vault is approximately 1.5×10^{-7} Ci m^{-3} (1.0×10^{-7} for the larger vaults). Using the relationship developed in Eq. A.3.6, the ^3H concentration in the vapor phase would be 1.4×10^{-12} Ci m^{-3}. Assuming this vapor concentration in Eq. A.3.7 and using Eqs. A.3.1 and A.3.2, the intruder's dose from inhalation would be 2.5×10^{-5} mrem yr^{-1}. The allowable ^3H inventory was determined by use of Eq. A.3.3, and was calculated to be 4.0×10^6 Ci vault^{-1} based upon an intruder dose of 100 mrem. The dose calculated is for inhalation exposure only; however, it is considered bounding for the all pathway dose to the intruder since the intruder is conservatively assumed to reside in the house all year.

A.3.5.2 Off-Site Dose Analysis

The dose to an individual located at the SRS site boundary before the 100 year institutional control period was evaluated using the equation for the flux given in Eq. A.3.7. The vapor-phase concentration of ^3H is calculated from Eq. A.3.6, assuming an initial pore water ^3H concentration of 4.2×10^{-5} Ci m^{-3} (or 1 Ci divided by 2.4×10^4 m^3 pore water per vault). The ^3H concentration in the vault vapor phase, 3.9×10^{-10} Ci m^{-3}, leads to a ^3H flux at the soil surface above each LAW vault of 2.9×10^{-7} Ci m^{-2} yr^{-1}. This flux was assumed to occur over all 21 of the LAW vaults resulting in a release of 5.2×10^{-2} Ci yr^{-1} for an area source

computer code (U.S.EPA 1989) using the Augusta, GA windfile (Appendix C). The maximum off-site individual is assumed to reside continuously at the SRS site boundary located 5 km from E-Area. The maximum EDE from all pathways was determined to be 1.2 × 10^{-5} mrem yr^{-1}. The AIRDOS-EPA input and output file information is provided in Appendix C. The allowable ^{3}H inventory was determined using Eq. A.3.3, and was calculated to be 8.3 × 10^{5} Ci $vault^{-1}$ based upon the atmospheric performance objective dose of 10 mrem yr^{-1}.

A.3.6 Dose Analysis of ^{14}C in the LAW Vaults

The waste form expected to contain ^{14}C in the LAW vaults is mainly job control waste. C-14 is assumed to be in the form of $^{14}CO_2$ and contained in B-25 boxes.

A.3.6.1 Intruder Dose Analysis

The initial activity of ^{14}C in a LAW vault containing job control waste is assumed to be 1 Ci. Each LAW vault has a volume of approximately 47,000 m^3. Assuming a porosity within the waste of 0.50, the void volume in each LAW vault is 2.4 × 10^4 m^3. This results in a ^{14}C vault concentration of 4.2 × 10^{-5} m^{-3} of void space at the end of the institutional control period (i.e., 100 years post-closure). Assuming this is the vapor phase concentration of $^{14}CO_2$, the flux of ^{14}C at the surface of 1 m of overlying soil, determined for a LAW vault based on Eq. A.3.7 using a diffusion coefficient of 4.4 × 10^2 m^2 yr^{-1} (CRC 1981), is 1.8 × 10^{-2} Ci m^{-2} yr^{-1}.

The projected area of each LAW vault is 8800 m^2. At a flux rate of 1.8 × 10^{-2} Ci m^{-2} yr^{-1} per Ci of ^{14}C in each LAW vault, the entire ^{14}C inventory would be released in less than a year. Therefore, the flux rate was adjusted to reflect total release within the first year. Per Ci of ^{14}C in the LAW vault, total release in a year gives a flux rate of 1/8800 Ci m^{-2} yr^{-1}, or 1.1 × 10^{-4} Ci m^{-2} yr^{-1}. From Eq. A.3.1, the resulting air concentration in the intruder's house is 5.2 × 10^{-9} Ci m^{-3}. The dose to the intruder was determined to be 1 mrem yr^{-1}, based upon Eq. 4.3.2, using a DCF of 2.4 × 10^4 mrem Ci^{-1}. The allowable inventory of ^{14}C in the LAW vaults was determined to be 100 Ci per vault using Eq. A.3.3 and a performance objective of

100 mrem yr^{-1}. The dose calculated is for inhalation exposure only; however, it is considered bounding for the all-pathway dose to the intruder since the intruder is assumed to reside in the house all year.

A.3.6.2 Off Site Dose Analysis

The dose to an individual located at the SRS site Boundary before the 100-year institutional control period was evaluated using the ^{14}C flux determined above, i.e., 1.1×10^{-4} Ci m^{-2} yr^{-1}. This flux is assumed to occur over all 21 LAW vaults resulting in a release of 20 Ci yr^{-1} for an area source of 1.8×10^{5} m^{2}. The off-site atmospheric transport was modeled with the AIRDOS-PC computer code (U.S.EPA 1989) using the Augusta, GA windfile (Appendix C). The nearest off-site individual is assumed to reside continuously at the SRS site boundary located 5 km from E-Area. The maximum EDE from all pathways was determined to be 2.5×10^{-1} mrem yr^{-1}. The AIRDOS-PC input and output file information is provided in Appendix C. The allowable ^{14}C inventory was determined using Eq. A.3.3, and was calculated to be 40 Ci per vault, based upon the atmospheric performance objective dose of 10 mrem yr^{-1}.

A.3.7 Analysis of Radon Flux

The release of radon from the EAVDF was calculated using the PORFLOW code. Besides having the capability to model groundwater flow and transport, the PORFLOW code can also model radioactive decay and diffusion. The case that was modeled was that of the LAW vault at 10,000 years. At this time it is assumed that the vault has failed, and the waste has formed a layer 2.7 m thick with a uniform distribution of waste constituents. A 2-m thick layer of soil was assumed to cover the waste in the failed vault. A unit concentration of U-234 was allowed to decay for 10,000 years through the intermediate daughters, Th-230 and Ra-226, producing Rn-222. The radon was allowed to diffuse upward as it was produced, and the flux of radon emanating from the top of the 2-m soil cover was calculated. The

parameters used in this calculation were:

Rn-222 Half Life:	1.05×10^{-2} year (3.3 days)
Ra-226 Half Life:	1.62×10^{3} year
Th-230 Half Life:	7.70×10^{4} year
U-234 Half Life:	2.45×10^{5} year
Diffusivity of Rn:	2×10^{6} cm^2/year
Density of waste and soil	1.6 g/cm^3
Effective porosity	0.1

The simulation results give a radon flux of 1.0×10^{-6} units per cm^3/year from the soil cover. In order to compare this with a performance objective of 20 pCi/m^2-s, the following unit's conversions had to be made:

If we assume that the initial units were mol/cm^3, converting units gives:

$$1 \text{ mol/cm}^3 = >1.0 \times 10^{-6} \text{ mol/cm}^2\text{-yr} * 222 \text{ g/mol} * 1.5 \times 10^{5} \text{ Ci/g} = 3.3 \times 10^{1} \text{ Ci/cm}^2\text{-yr}$$
$$= >3.3 \times 10^{1} \text{ Ci/cm}^2\text{-yr} * 10^{12} \text{ pCi/Ci} * 10^{4} \text{ cm}^2/\text{m}^2 * 3.2 \times 10^{-8} \text{ yr/s}$$
$$= 1.1 \times 10^{10} \text{ pCi/m}^2\text{-s}$$

Since we now know that 1 mol/cm^3 of U-234 will produce 1.1×10^{10} pCi/m^2-yr as a radon flux, a simple ratio can be used to determine the U-234 concentration, in Ci/m^3, that will produce a Rn-222 flux of 20 pCi/m^2-s.

$$X \text{ mol/cm}^3 / 1 \text{ mol/cm}^3 = 20 \text{ pCi/m}^2\text{-s} / 1.1 \times 10^{10} \text{ pCi/m}^2\text{-s}$$
$$X = 1.8 \times 10^{-9} \text{ mol/cm}^3 * 234 \text{ g/mol} * 6.2 \times 10^{-3} \text{ Ci/g} * 10^{6} \text{ cm}^3/\text{m}^3$$
$$X = 2.6 \times 10^{-3} \text{ Ci/m}^3$$

This is equivalent to 125 Ci per LAW vault with a volume of 4.8×10^{4} m^3, which is about two and a half orders of magnitude greater than the allowable inventory for ^{234}U based on intruder results, which include the dose from Rn-222 (Sect. 4.1.5.2). The conceptual model used here is applicable to failed ILNT vaults as well. The concentration of 2.6×10^{-3} Ci/m^3 would give an inventory limit of 15 Ci per ILNT vault with a volume of 5,880 m^3.

A sensitivity analysis was performed on the effect of the thickness of soil cover over the waste. The results were fluxes of 1.6×10^{-6} and 5.7×10^{-7} for cover thicknesses of 1 m and 3 m, respectively.

The results for 1 m of cover are applicable to trench disposal of suspect soil (Appendix I). If transport of uranium from the trench is conservatively ignored, then using the same analysis as above gives:

$$1\ \text{mol/cm}^3 = >1.6 \times 10^{-6}\ \text{mol/cm}^2\text{-yr} * 222\ \text{g/mol} * 1.5 \times 10^5\ \text{Ci/g} = 5.3 \times 10^1\ \text{Ci/cm}^2\text{-yr}$$
$$= >5.3 \times 10^1\ \text{Ci/cm}^2\text{-yr} * 10^{12}\ \text{pCi/Ci} * 10^4\ \text{cm}^2/\text{m}^2 * 3.2 \times 10^{-8}\ \text{yr/s}$$
$$= 1.7 \times 10^{10}\ \text{pCi/m}^2\text{-s}$$

Since we now know that 1 mol/cm^3 of U-234 will produce 1.7×10^{10} pCi/m^2-yr as a radon flux, a simple ratio can be used to determine the U-234 concentration, in Ci/m^3, that will produce a Rn-222 flux of 20 pCi/m^2-s.

$$X\ \text{mol/cm}^3 / 1\ \text{mol/cm}^3 = 20\ \text{pCi/m}^2\text{-s} / 1.7 \times 10^{10}\ \text{pCi/m}^2\text{-s}$$
$$X = 1.2 \times 10^{-9}\ \text{mol/cm}^3 * 234\ \text{g/mol} * 6.2 \times 10^{-3}\ \text{Ci/g} * 10^6\ \text{cm}^3/\text{m}^3$$
$$X = 1.7 \times 10^{-3}\ \text{Ci/m}^3$$

Since the disposal volume of each trench is 5,200 m^3, the limiting inventory due to radon generation is:

$$1.7 \times 10^{-3}\ \text{Ci/m}^3 * 5{,}200\ \text{m}^3 = 8.8\ \text{Ci per trench}$$

The input file used to produce the 2-m cover case is presented in Fig. A.3-1.

```
/TITLE E-Area Radon Diffusion, 1-D
/ 200 cm of soil on top of 270 cm of waste
/ J. R. Cook, P. S. L[illegible] & A. B. Yu
/ 2/4/94, 2/14/94, 2/22/94
/
/*****************************************************
GRID  3 by  48
SCALE  1.0000
COORDINATE X
     -1.0       0.0       1.0
SCALE  1.0000
COORDINATE Y RANGE 470
/
ZONE 1 is from (  1,   1) to (  3,  48) & soil
/
DATUM = 0. 0.
/
GRAVity components are: 0.0, 0.0
/
DENSity of fluid is constant and equal to 0.01 gm/cc
/
POR  1   Soil
MATerial PROPerties:  rho 1.60 gm/cc, neff = 0.1, ntot = 0.1 , nmif = 0.1
/MULT  VAN   n = 1.70   alpha = 7.5e-2  sr = 0.088
/HYDR  ss = 1.e-3  kx = 315.0  ky = 315.0  kz = 315.0
TRANsport for C  kd =    0.00, D = 0.000, al = 10.0, at = 2.0 & C  is U-234
TRANsport for C2 kd =    0.00, D = 0.000, al = 10.0, at = 2.0 & C  is Th230
TRANsport for C3 kd =    0.00, D = 0.000, al = 10.0, at = 2.0 & C  is Ra226
TRANsport for C4 kd =    0.00, D = 2.e-6, al = 10.0, at = 2.0 & C2 is Rn222
/
LOCAte subregion (  1,   1) to (  3,  48) with ID=SOIL
LOCAte subregion (  1,  21) to (  3,  48) with ID=U234
/
SET C2 to 0.0 in ID=SOIL
SET C3 to 0.0 in ID=SOIL
SET C4 to 0.0 in ID=SOIL
SET C  to 0.0 in ID=SOIL
SET C  to 1.0 in ID=U234
/
DECAy half life for C  is 2.45E+05  transform to Th230 is 1.00
DECAy half life for C2 is 7.70E+04  transform to Ra226 is 1.00
DECAy half life for C3 is 1.62E+03  transform to Rn222 is 1.00
DECAy half life for C4 is 1.04E-02
/
BOUN C  -1   FLUX =   0.
BOUN C  +1   FLUX =   0.
BOUN C  -2   FLUX =   0.
BOUN C  +2   FLUX =   0.
/
BOUN C2 -1   FLUX =   0.
BOUN C2 +1   FLUX =   0.
BOUN C2 -2   FLUX =   0.
BOUN C2 +2   FLUX =   0.
/
BOUN C3 -1   FLUX =   0.
BOUN C3 +1   FLUX =   0.
BOUN C3 -2   FLUX =   0.
BOUN C3 +2   FLUX =   0.
/
BOUN C4 -1   FLUX =   0.
BOUN C4 +1   FLUX =   0.
BOUN C4 -2   VALU =   0.
```

Fig. A.3-1. PORFLOW input file for radon calculations.

```
PROPerty for C C2 C3 C4 is [illegible]
MATRIX in X and Y directions for C and C2 C3 C4 in 3 sweeps usi[illegible]
RELAx P = 0.7
/
DIAGnostic node for C and C4 at ( 2, 20) every  100 steps
OUTPut every 900000 steps
/
/FLUX BALAnce for C  in 'run.flx'  for ID=SOIL  every  50 steps
/FLUX BALAnce for C  in 'run.flx'  for ID=U234  every  50 steps
FLUX BALAnce for C4 in 'run.flx'  for ID=SOIL  every  100 steps
FLUX BALAnce for C4 in 'run.flx'  for ID=U234  every  100 steps
/
TIME=0.
/
CONV for C4 REFE; GLOB mode; value = 1.0e-06, max 5 iter, 2 4
/HISTory for C  (25,  30)  every 20 in 'run.his'
//////////////
DISAble FLOW
//////////////
SOLV  C C2 C3 C4 500000 init 1.e-5 inc 1.005 max 100.0 min 1.e-9 2.0 900000
OUTPut C C2 C3 C4 NOW
/
SAVE  C C4   in 'run.arc'
END
```

Fig. A.3-1. (continued).

A.4 DOSE ANALYSIS FOR OFF-SITE INDIVIDUALS AND INADVERTENT INTRUDERS

A.4.1 Introduction

This appendix presents the models and data bases used to estimate EDEs per unit concentration of radionuclides in particular exposure media following disposal of LLW in the EAV. The dose analysis considers two groups of exposed individuals:

- off-site individuals, i.e., members of the public who reside beyond the boundary of the disposal facility; and
- inadvertent intruders, i.e., individuals who come onto the disposal site following loss of active institutional control.

Off-site individuals may be exposed to radionuclides released from the disposal facility at any time after disposal. During the period of active institutional control over the disposal site, which is assumed to last for 100 years after facility closure (U.S.DOE 1988a), off-site individuals are assumed to be restricted to locations beyond the present boundary of the SRS. However, after the period of active institutional control, off-site individuals could be located anywhere beyond the boundary of the buffer zone around the disposal facility, which is assumed to be no more than 100 m from the disposal units. Inadvertent intrusion onto the disposal site is assumed to be precluded by active institutional control until 100 years after facility closure. No credit is taken in this analysis for any passive institutional controls (e.g., marker systems at the disposal site, public records of land use) that could prevent inadvertent intrusion for some time after the period of active institutional control.

The PA for the EAV assumes that releases of radionuclides to groundwater due to infiltration of precipitation through disposal units is the principal mechanism for transport of radionuclides to off-site locations. However, potential doses to off-site individuals resulting from airborne releases of radionuclides also were considered (see Appendix A.3). Potential doses to inadvertent intruders are estimated by assuming that certain scenarios for direct intrusion into disposal units occur.

The following sections discuss the exposure scenarios and exposure pathways assumed for off-site individuals or inadvertent intruders and the models and parameter values used in calculating annual EDEs to these groups of individuals for each exposure pathway. For exposures to contaminated groundwater, the results of the dose analysis are summarized in the form of annual EDEs per unit concentration of radionuclides in water. For exposures resulting from direct intrusion into disposal units, the results are summarized in the form of annual EDEs per unit concentration of radionuclides in solid waste at the time intrusion is assumed to occur.

A.4.2. Radionuclides of Importance for Dose Analyses

As indicated in Appendix C, waste in the EAV potentially contains a large number of radionuclides. However, only a relatively few radionuclides are potentially important in the dose analyses for off-site individuals or inadvertent intruders. Most of the radionuclides either could occur only in very low concentrations or are sufficiently short-lived that they would decay to innocuous levels before off-site transport via the groundwater pathway or inadvertent intrusion onto the disposal site could occur.

The radionuclides which have been considered in the dose analyses for the EAV, either for off-site individuals or for inadvertent intruders, are listed in Table A.4-1. These radionuclides were selected on the basis of conservative screening analyses for exposures of off-site individuals via the groundwater pathway and exposures of inadvertent intruders, as described in Sects. 3.2.3.4 and 3.2.4.4, respectively. The exposure scenarios which have been considered for each radionuclide are indicated in the table and are described in Sect. A.4.3. All other radionuclides listed in Appendix C can be neglected in the dose analyses for off-site individuals and inadvertent intruders, because their concentrations would be sufficiently low that they could not result in doses that exceed a very small fraction of the applicable limits for either group of individuals.

Table A.11. Radionuclides selected in dose analyses for off-site individuals and for intruders

Radionuclide[a]	Half-life[b]		Applicable scenarios[c]
H-3	12.28	y	1,2,4
C-14	5730	y	1,2,4
Al-26	7.2×10^5	y	1,2,3,4
Co-60	5.271	y	2,3,4
Ni-59	7.5×10^4	y	1,2,4
Ni-63	100.1	y	1,2,4
Se-79	6.5×10^4	y	1,2,4
Rb-87	4.73×10^{10}	y	1,2,4
Sr-90	28.6	y	1,2,4
Y-90 (1.0)	64.1	h	
Zr-93	1.53×10^6	y	1,2,4
Nb-93m	14.6	y	1,2,4
Tc-99	2.13×10^5	y	1,2,4
Pd-107	6.5×10^6	y	1,2,4
Cd-113m	13.7	y	1,2,4
Sn-121m	55	y	1,2,4
Sn-126	1.0×10^5	y	1,2,3,4
Sb-126m (1.0)	19.0	m	
Sb-126 (0.14)	12.4	d	
I-129	1.57×10^7	y	1,2,4
Cs-135	2.3×10^6	y	1,2,4
Cs-137	30.17	y	1,2,3,4
Ba-137m (0.946)	2.552	m	
Sm-151	90	y	1,2,4
Eu-154	8.8	y	2,3,4
Eu-155	4.96	y	2,3,4
Pb-210	22.26	y	1,2,4
Po-210 (1.0)	138.378	d	

See end of table for footnotes.

Table A.4-1. (continued)

Radionuclide[a]	Half-life[b]		Applicable scenarios[c]
Ra-226	1600	y	1,2,3,4
Rn-222 (1.0)	3.8235	d	
Pb-214 (1.0)	26.8	m	
Bi-214 (1.0)	19.9	m	
Th-229	7.34×10^3	y	1,2,3,4
Ra-225 (1.0)	14.8	d	
Ac-225 (1.0)	10.0	d	
Fr-221 (1.0)	4.8	m	
Bi-213 (1.0)	45.65	m	
Tl-209 (0.0216)	2.20	m	
Th-230	7.7×10^4	y	1,2,4
Th-232	1.405×10^{10}	y	1,2,3,4
Ra-228 (1.0)	5.75	y	
Ac-228 (1.0)	6.13	h	
Th-228 (1.0)	1.9132	y	
Ra-224 (1.0)	3.62	d	
Rn-220 (1.0)	55.61	s	
Pb-212 (1.0)	10.643	h	
Bi-212 (1.0)	60.55	m	
Tl-208 (0.3593)	3.053	m	
Pa-231	3.276×10^4	y	1,2,3,4
Ac-227 (1.0)	21.773	y	
Th-227 (0.9862)	18.718	d	
Ra-223 (1.0)	11.434	d	
Pb-211 (1.0)	36.1	m	
Bi-211 (1.0)	2.13	m	
Tl-207 (0.99727)	4.77	m	
U-232[d]	72	y	1,2,3,4
U-233	1.5952×10^5	y	1,2,4

See end of table for footnotes.

Table A.4-1. (continued)

Radionuclide[a]	Half-life[b]		Applicable scenarios[c]
U-234	2.445×10^5	y	1,2,4
U-235	7.038×10^8	y	1,2,3,4
Th-231 (1.0)	25.52	h	
U-236	2.3415×10^7	y	1,2,4
U-238	4.468×10^9	y	1,2,3,4
Th-234 (1.0)	24.10	d	
Pa-234m (1.0)	1.17	m	
Pa-234 (0.0016)	6.70	h	
Np-237	2.14×10^6	y	1,2,3,4
Pa-233 (1.0)	27.0	d	
Pu-238	87.75	y	1,2,4
Pu-239	24,131	y	1,2,4
Pu-240	6569	y	1,2,4
Pu-241	14.4	y	1,2,4
Pu-242	3.758×10^5	y	1,2,4
Pu-244	8.26×10^7	y	1,2,4
Am-241	432.2	y	1,2,3,4
Am242m	152	y	1,2,3,4
Am-242 (0.99524)	16.02	h	
Cm-242 (0.823)	163.2	d	
Np-238 (0.00476)	2.117	d	
Am-243	7.38×10^3	y	1,2,3,4
Np-239 (1.0)	2.355	d	
Cm-243	28.5	y	2,3,4
Cm-244	18.11	y	2,4
Cm-245	8.5×10^3	y	1,2,3,4
Cm-246	4.75×10^3	y	1,2,4
Cm-247	1.56×10^7	y	1,2,3,4
Pu-243 (1.0)	4.956	h	

See end of table for footnotes.

Table A.1-1. (continued)

Radionuclide[a]	Half-life[b]	Applicable scenarios[c]
Cm-248	3.39×10^5 y	1,2,4
Cf-249	350.6 y	1,2,3,4
Cf-250	13.08 y	2,4
Cf-251	900 y	1,2,3,4

[a] Indented entries are radiologically significant short-lived decay products of parent radionuclide listed. With each decay product, branching fraction in decay of parent radionuclide is given in parentheses.

[b] Values from Kocher (1981).

[c] 1 = groundwater transport pathway, off-site individuals;
2 = agriculture scenario, inadvertent intruders;
3 = resident scenario, inadvertent intruders;
4 = post-drilling scenario, inadvertent intruders.

[d] Short-lived decay products Th-228, Ra-224, Rn-220, Pb-212, Bi-212, and Tl-208 are listed under Th-232.

As indicated in Table A.4-1, some radionuclides included in the dose analyses decay to short-lived radionuclides that are potentially important for at least one exposure pathway. In all such cases, the doses from a parent radionuclide and its short-lived decay products are combined by assuming that the decay products are in secular equilibrium with the parent, and the activity concentrations of the decay products take into account the decay branching fractions given in Table A.4-1. Long-lived decay products of uranium and Np-237 that could be significant in the dose analyses (i.e., Ra-226, Th-229, Th-230, Pa-231, and U-233) also are included in the table. However, these radionuclides are not assumed to be in secular equilibrium with their respective parent radionuclides, because buildup of the activity of decay products occurs over a very long time. Thus, in these cases, the activity of the long-lived decay products over time should be considered explicitly in the dose analyses, as is also the case when a radionuclide produces a longer-lived decay product.

A.4.3 Assumed Exposure Scenarios and Exposure Pathways

This section briefly describes the exposure scenarios and exposure pathways assumed in the dose analyses for off-site individuals and inadvertent intruders. A more detailed description of the assumed exposure scenarios, including the justification for neglecting other scenarios in the dose analyses, is given in Sects. 3.2.3 and 3.2.4. The model equations and parameter values for each exposure pathway then are presented in Sect. A.4.5.

A.4.3.1 Exposure Scenarios and Pathways for Off-Site Individuals

The PA for the EAV assumes that radionuclides are transported to off-site locations principally via the groundwater pathway. Off-site transport via atmospheric releases also was considered (see Appendix A.3).

As described in Sect. 3.2.3, off-site individuals are assumed to use contaminated groundwater for domestic purposes, and the following exposure pathways involving use of contaminated water are assumed to occur: 1) direct ingestion of the contaminated drinking

water; 2) ingestion of milk and meat from dairy and beef cattle that drink contaminated water; 3) ingestion of vegetables grown in garden soil irrigated with contaminated water; 4) direct ingestion of contaminated soil in conjunction with intakes of vegetables from the garden; 5) external exposure to contaminated soil while working in the garden; and 6) inhalation of radionuclides suspended into air from contaminated soil while working in the garden. Irrigation of pasture grass consumed by dairy and beef cattle is assumed to be unimportant, because irrigation of pasture is not widely practiced near the SRS. The relative importance of the different exposure pathways for off-site individuals is summarized below.

As described in Sect. 3.2.3.1 and 3.2.3.2, off-site releases of radionuclides via the groundwater pathway are assumed to be subject to two dose limits that are consistent with the performance objectives for LLW disposal (U.S.DOE 1988a): 1) a limit on EDE of 25 mrem per year from all exposure pathways and 2) a limit on EDE of 4 mrem per year from consumption of 2 L/day of drinking water from a contaminated source. The latter performance objective is used to limit concentrations of radionuclides in groundwater at locations beyond the 100-m buffer zone around the disposal units.

In Sect. 3.2.3.3, an analysis was performed to compare the importance of the two performance objectives for off-site releases of radionuclides listed above. The analysis showed that, at the SRS, the performance objective for protection of groundwater is expected to be more restrictive for any radionuclide than the performance objective for protection of off-site individuals from all exposure pathways. That is, if the lower dose limit for direct consumption of contaminated groundwater is met, then the higher dose limit for all exposure pathways also will be met without the need for further analysis of the pathways involving use of contaminated groundwater other than direct consumption of drinking water.

Therefore, in the dose analysis for off-site individuals, only the following exposure pathway needs to be considered:

- direct ingestion of contaminated drinking water from a source of groundwater beyond the 100-m buffer zone around disposal units.

The exposure pathway must be considered at any time after disposal. Therefore, for example, in the analysis of groundwater transport for U-234/U-238 and Np-237 in disposed waste, buildup of the long-lived decay products Th-230/Ra-226 and U-233/Th-229, respectively, must be taken into account in the analysis for the groundwater pathway.

A.4.3.2 Exposure Scenarios and Pathways for Inadvertent Intruders

In estimating doses to inadvertent intruders after the period of active institutional control (i.e., at any time beyond 100 years after closure of the disposal facility), it is assumed that such individuals could establish a permanent homestead on the site. Furthermore, it is assumed that an intruder has no *a priori* knowledge of waste disposal activities at the site. Inadvertent intruders are assumed to receive radiation exposures from use of contaminated groundwater obtained from a well on the disposal site and from direct intrusion into waste disposal units. Exposures of inadvertent intruders to volatile releases of H-3 and C-14 are considered separately in Appendix A.3. However, exposures to radon and its short-lived decay products are considered in this appendix.

Exposures of inadvertent intruders to radionuclides in contaminated groundwater are assumed to occur in conjunction with any of the scenarios involving direct intrusion into waste disposal units described below, and the exposure pathways involving use of contaminated groundwater are assumed to be the same as those listed in Sect. A.4.3.1 for off-site individuals. However, because the requirement for protection of groundwater beyond the 100-m buffer zone (i.e., the limit on EDE of 4 mrem per year from direct consumption of groundwater) is much more stringent than the dose limits for protection of inadvertent intruders taking into account all exposure pathways (i.e., limits on EDE of 100 mrem per year for chronic exposures and 500 mrem for a single acute exposure), exposures to contaminated groundwater can be neglected in the dose analysis for inadvertent intruders (see Sect. 3.2.4.1).

For direct intrusion into disposal units after loss of active institutional control, exposures are assumed to occur according to one of three scenarios, which are called the agriculture, resident, and post-drilling scenarios. Other scenarios which were considered but shown to be less important are discussed in Sect. 3.2.4. The three scenarios considered in this analysis and their associated exposure pathways are described as follows.

In the agriculture scenario, an intruder is assumed to build a home directly on top of disposal units, and the foundation is assumed to extend into the units themselves. Radioactive wastes exhumed during excavation for the foundation are assumed to be indistinguishable from native soil, and some of the exhumed waste is assumed to be mixed with native soil in the intruder's vegetable garden. The following pathways involving exposure to radionuclides in solid waste then are assumed to occur:

- ingestion of vegetables grown in contaminated garden soil;
- direct ingestion of contaminated soil, primarily in conjunction with intakes of vegetables from the garden;
- external exposure to contaminated soil while working in the garden or residing in the home on top of the disposal units;
- inhalation of radionuclides attached to soil particles that are suspended into air from contaminated soil while working in the garden or residing in the home; and
- inhalation of volatile radionuclides released into air from contaminated soil while working in the garden or residing in the home.

Inhalation of the volatile radionuclides H-3 and C-14 while working in the garden or residing in the home is considered separately in Appendix A.3. Inhalation of radon and its short-lived decay products is considered in this appendix.

In the resident scenario, an intruder also is assumed to excavate at the location of disposal units, but is assumed to encounter an intact engineered barrier (e.g., a reinforced concrete roof) used in constructing the disposal units which cannot readily be penetrated by the types of excavation equipment normally used near the SRS. Therefore, instead of excavating into the waste, the intruder is assumed to build a home immediately on top of the intact engineered barrier. Since waste in the disposal facility is not directly accessed during excavation, due to the assumed impenetrability of the engineered barriers, the only exposure pathway of concern for this scenario is external exposure to photon-emitting radionuclides in the waste while residing in the home. While exposure to radon could occur during residence

on top of intact engineered barriers, such exposures presumably would be much less than those occurring in the agriculture scenario when residence on top of unshielded waste is assumed to be credible. Therefore, potential exposures to radon are ignored in the resident scenario but are captured in the agriculture scenario.

In the post-drilling scenario, an intruder is assumed to access solid waste by drilling through a disposal unit, e.g., for the purpose of constructing a well for the intruder's domestic water supply. During drilling, a small volume of waste is brought to the surface, and all of the drilling waste is assumed to be mixed with native soil in the intruder's vegetable garden. The following pathways involving exposure to radionuclides in the solid waste then are assumed to occur:

- ingestion of vegetables grown in contaminated soil;
- direct ingestion of contaminated soil, primarily in conjunction with intakes of vegetables from the garden;
- external exposure to contaminated soil while working in the garden;
- inhalation of radionuclides attached to soil particles that are suspended into air from contaminated soil while working in the garden; and
- inhalation of volatile radionuclides released into air from contaminated soil while working in the garden.

As in the agriculture scenario, inhalation of the volatile radionuclides H-3 and C-14 while working in the garden is considered in Appendix A.3, and inhalation of radon and its short-lived decay products is considered in this appendix.

The pathways listed above for the post-drilling scenario correspond to some of the pathways for the agriculture scenario. However, in the post-drilling scenario, external and inhalation exposures while residing in the home are not relevant, because all drilling waste is assumed to be mixed with soil in the intruder's vegetable garden and the intruder's home is not located on top of disposal units.

A.4.4 Dose Conversion Factors for Internal and External Exposure

From the descriptions of the assumed exposure scenarios and pathways given in Sect. A.4.3, doses to off-site individuals and inadvertent intruders are assumed to result from ingestion, inhalation, and external exposure. This section presents the factors used in the dose analyses to convert intakes of radionuclides via ingestion and inhalation to internal doses and to convert concentrations of radionuclides in the environment to external dose rates.

The internal DCFs for ingestion and inhalation of radionuclides are given in Tables A.4-2 and A.4-3, respectively. These factors give 50-year committed EDEs per unit activity intake. The entries for any short-lived decay products of a longer-lived radionuclide do not take into account the branching fraction in the decay of the parent radionuclide; i.e., the values for each decay product assume the same unit intake of activity (1 μCi). Dose conversion factors are listed for a short-lived decay product only if ingestion or inhalation of the decay product would contribute significantly to the dose from intakes of the parent radionuclide and the decay product in secular equilibrium. Dose conversion factors for inhalation of isotopes of radon and their short-lived decay products are not listed in Table A.4-3. Rather, as described with the agriculture scenario in Sect. A.4.5.2, a natural analog model based on the known doses from exposure to radon per unit concentration of Ra-226 or Th-232 in soil is used to estimate inhalation doses from radon in waste. The internal DCFs in Table A.4-3 are those currently recommended for use by the U.S.DOE (1988b) in assessing radiation doses to the public.

For some radionuclides, more than one DCF for ingestion or inhalation has been tabulated by the U.S.DOE (1988b). Whenever ingestion DCFs are given for two GI-tract absorption fractions, the value corresponding to the higher absorption fraction is adopted in Table A.4-2, because radionuclides that are transported in water or through terrestrial food-chains should be in relatively soluble form and more easily absorbed in the GI tract. This choice does not always give the higher ingestion DCF, but the value corresponding to the lower GI-tract absorption fraction differs from the adopted value in such cases by less than 10%. If inhalation DCFs are given for more than one lung clearance class, the clearance class

Table A.1-2. Internal dose conversion factors for ingestion of radionuclides[a]

Radionuclide[b]	f_1[c]	Rem/μCi ingested	Radionuclide[b]	f_1[c]	Rem/μCi ingested
H-3	1.0	6.3×10^{-5}	Th-229	0.0002	3.5
C-14	---	2.1×10^{-3}	Ra-225	0.2	3.1×10^{-1}
Al-26	0.01	1.3×10^{-2}	Ac-225	0.001	9.5×10^{-2}
Co-60	0.3	2.6×10^{-2}	Th-230	0.0002	5.3×10^{-1}
Ni-59	0.05	2.0×10^{-4}	Th-232	0.0002	2.8
Ni-63	0.05	5.4×10^{-4}	Ra-228	0.2	1.2
Se-79	0.8	8.3×10^{-3}	Th-228	0.0002	3.8×10^{-1}
Rb-87	1.0	4.8×10^{-3}	Ra-224	0.2	3.3×10^{-1}
Sr-90	0.3	1.3×10^{-1}	Pb-212	0.2	4.1×10^{-2}
Y-90	0.0001	1.0×10^{-2}	Pa-231	0.001	1.1×10^{-1}
Zr-93	0.002	1.6×10^{-3}	Ac-227	0.001	1.4×10^{1}
Nb-93m	0.01	5.3×10^{-4}	Ra-223	0.2	5.5×10^{-1}
Tc-99	0.8	1.3×10^{-3}	U-232[d]	0.05	1.3
Pd-107	0.005	1.4×10^{-4}	U-233	0.05	2.7×10^{-1}
Cd-113m	0.05	1.5×10^{-1}	U-234	0.05	2.6×10^{-1}
Sn-121m	0.02	1.3×10^{-3}	U-235	0.05	2.5×10^{-1}
Sn-126	0.02	1.7×10^{-2}	U-236	0.05	2.5×10^{-1}
Sb-126	0.1	9.0×10^{-3}	U-238	0.05	2.3×10^{-1}
I-129	1.0	2.8×10^{-1}	Th-234	0.0002	1.3×10^{-2}
Cs-135	1.0	7.1×10^{-3}	Np-237	0.001	3.9
Cs-137	1.0	5.0×10^{-2}	Pu-238	0.001	3.8
Sm-151	0.0003	3.4×10^{-4}	Pu-239	0.001	4.3
Eu-154	0.001	9.1×10^{-3}	Pu-240	0.001	4.3
Eu-155	0.001	1.3×10^{-3}	Pu-241	0.001	8.6×10^{-2}
Pb-210	0.2	5.1	Pu-242	0.001	4.1
Po-210	0.1	1.6	Pu-244	0.001	4.0
Ra-226	0.2	1.1	Am-241	0.001	4.5

See end of table for footnotes.

Table A.1-2 (continued)

Radionuclide[b]	f_1[c]	Rem/μCi ingested	Radionuclide[b]	f_1[c]	Rem/μCi ingested
Am-242m	0.001	4.2	Cm-246	0.001	4.5
Cm-242	0.001	1.1×10^{-1}	Cm-247	0.001	4.1
Am-243	0.001	4.5	Cm-248	0.001	1.6×10^{1}
Cm-243	0.001	2.9	Cm-249	0.001	4.6
Cm-244	0.001	2.3	Cm-250	0.001	1.9
Cm-245	0.001	4.5	Cm-251	0.001	4.6

[a] Values adopted by U.S.DOE (1988b) give 50-year committed EDEs per unit activity ingested.
[b] Indented entries are radiologically significant short-lived decay products of parent radionuclide listed. Dose-rate conversion factors for decay products do not take into account branching fraction in decay of parent.
[c] Fraction of ingested radionuclide absorbed into blood from GI tract.
[d] Entries for short-lived decay products Th-228, Ra-224, and Pb-212 are listed under Th-232.

Table A.13. Internal dose conversion factors for inhalation of radionuclides[a]

Radionuclide[b]	Clearance Class[c]	Rem/μCi inhaled	Radionuclide[b]	Clearance Class[c]	Rem/μCi inhaled
H-3		6.3×10^{-5}	Ra-226	W	7.9
C-14[d]		2.1×10^{-3}	Rn-222[f]		
Al-26	D	7.9×10^{-2}	Th-229	Y	1.7×10^{3}
Co-60	Y	1.5×10^{-1}	Th-230	Y	2.6×10^{2}
Ni-59[e]	D	1.3×10^{-3}	Th-232	Y	1.1×10^{3}
Ni-63[e]	D	3.0×10^{-3}	Th-228	Y	3.1×10^{2}
Se-79	W	8.9×10^{-3}	Rn-220[f]		
Rb-87	D	3.3×10^{-3}	Pa-231	W	1.3×10^{3}
Sr-90	D	2.3×10^{-1}	Ac-227	D	6.7×10^{3}
Y-90	Y	8.2×10^{-3}	U-232[d]	Y	6.7×10^{2}
Zr-93	D	3.2×10^{-1}	U-233	Y	1.3×10^{2}
Nb-93m	Y	2.8×10^{-2}	U-234	Y	1.3×10^{2}
Tc-99	D	8.4×10^{-4}	U-235	Y	1.2×10^{2}
Pd-107	Y	1.3×10^{-2}	U-236	Y	1.2×10^{2}
Cd-113m	D	1.6	U-238	Y	1.2×10^{2}
Sn-121m	D	5.8×10^{-3}	Np-237	W	4.9×10^{2}
Sn-126	D	8.6×10^{-2}	Pu-238	W	4.6×10^{2}
Sb-126	D	4.6×10^{-3}	Pu-239	W	5.1×10^{2}
I-129	D	1.8×10^{-1}	Pu-240	W	5.1×10^{2}
Cs-135	D	4.5×10^{-3}	Pu-241	W	1.0×10^{1}
Cs-137	D	3.2×10^{-2}	Pu-242	W	4.8×10^{2}
Sm-151	W	2.9×10^{-2}	Pu-244	W	4.8×10^{2}
Eu-154	W	2.6×10^{-1}	Am-241	W	5.2×10^{2}
Eu-155	W	3.9×10^{-2}	Am-242m	W	5.1×10^{2}
Pb-210	D	1.3×10^{1}	Cm-242	W	1.7×10^{2}
Po-210	W	8.1	Am-243	W	5.2×10^{2}

See end of table for footnotes.

Table A.4-1. (continued)

Radionuclide[b]	Clearance Class[c]	Rem/μCi inhaled	Radionuclide[b]	Clearance Class[c]	Rem/μCi inhaled
Cm-243	W	3.5×10^2	Cm-246	W	5.4×10^2
Cm-244	W	2.7×10^2	Cm-247	W	4.9×10^2
Cm-245	W	5.4×10^2			

[a] Values adopted by U.S.DOE (1988) give 50-year committed EDEs per unit activity inhaled.
[b] Indented entries are radiologically significant short-lived decay products of parent radionuclide listed. Dose-rate conversion factors for decay products do not take into account branching fraction in decay of parent.
[c] Clearance from respiratory passages for radionuclides in particulate form in a matter of days (D), weeks (W), or years (Y).
[d] Radionuclide is assumed to be in organic form.
[e] Radionuclide is assumed to be in inorganic form.
[f] Inhalation doses from radon and its short-lived decay products are estimated using model described with agriculture scenario in Sect. A.4.5.2.
[g] Entries for short-lived decay products Th-228 and Rn-220 are listed under Th-232.

giving the highest value usually is adopted in Table A.1-3, because there is little information for most elements on the expected chemical forms and their solubilities in waste or soil and the choice of the highest inhalation DCF may result in conservative overestimates of inhalation dose. However, Sr-90 and Tc-99 are assumed to be Class D because their solubility in the environment is expected to be relatively high, and all isotopes of Th are assumed to be Class Y because Th in the environment is expected to be highly insoluble.

Dose conversion factors for external exposure give dose-equivalent rates per unit concentration of radionuclides in the environment. These factors depend on the distribution of radionuclides in the source region, the amount of self-shielding provided by material in the source region, and the shielding provided by any uncontaminated material between the source region and the location of an exposed individual. Therefore, separate sets of DCFs are required for the assumed pathways involving external exposure to 1) activity in contaminated soil while working in the vegetable garden in the agriculture and post-drilling scenarios, 2) activity in exposed waste while residing in the home at the disposal site in the agriculture and resident scenarios, and 3) activity in waste shielded by intact engineered barriers while residing in the home at the disposal site in the resident scenario.

For external exposure to radionuclides in disposal units or in soil in the vegetable garden, the source region is assumed to be a uniformly contaminated slab of infinite lateral extent. Depending upon the particular exposure scenario and pathway, the slab is assumed to have either finite or infinite thickness, and the shielding provided by any uncontaminated material between the source and receptor locations is taken into account. The idealized distributions of radionuclides in the source region assumed in the dose analysis are reasonable, because radionuclides should be dispersed throughout the source regions and only about 1 m of soil-equivalent material between the source and receptor locations provides essentially complete shielding (Kocher and Sjoreen 1985).

In all calculations of external dose, an exposed individual is assumed to be located at a distance of 1 m above ground. In all cases, the shielding provided by 1 m of air is negligible compared with the shielding provided by the material in the source region itself or by the thickness of any uncontaminated material (e.g., an intact concrete roof) between the source and receptor locations.

For external exposure while working in the vegetable garden, the source region is assumed to be a uniformly contaminated slab of soil with a thickness of 15 cm, which is a typical depth of a plowed layer in a garden. The external dose-rate conversion factors for this case are given in Table A.4-4.

For external exposure while residing in the home in the agriculture scenario, the source region is assumed to be a slab of soil-equivalent material of essentially infinite thickness. This is a good approximation because sources more than 1 m below the surface would not contribute significantly to the dose (Kocher and Sjoreen 1985). No shielding is assumed between the source region and the receptor location other than that provided by the material in the source region itself. Shielding provided by the walls of the home during indoor residence is taken into account in the dose analysis itself (see Eq. A.4-8). The external dose-rate conversion factors for this case are given in the column in Table A.4-5 labeled "No shielding".

For external exposure while residing in the home in the resident scenario, the source region also is assumed to be a slab of soil-equivalent material of infinite thickness. As described in Sect. 3.2.4.2, the maximum external dose in the resident scenario can be bounded by considering two limiting cases. The first involves exposure to both shorter- and longer-lived photon-emitting radionuclides and photon-emitting daughters at the time active institutional control ceases at 100 years after facility closure when an intact concrete roof and any other engineered barriers on top of the waste provide a considerable amount of shielding. The second case involves exposure only to longer-lived photon-emitting radionuclides and photon-emitting daughters at a time long after disposal when the concrete roof and any other engineered barriers above the waste have lost their physical integrity and exposure to waste with no external shielding could occur.

As described in Sect. 2.9, the closure concept for the ILNT and ILT vaults includes a layer of uncontaminated grout about 3 ft (90 cm) thick on top of the waste and a concrete roof of variable thickness, the average thickness being about 3 ft (90 cm). The closure concept for the LAW vaults does not include a layer of uncontaminated grout on top of the waste, and the concrete roof is about 50 cm thick.

Table A.4-4. Effective dose-rate conversion factors for radionuclides uniformly distributed in 15 cm of surface soil[a]

Radionuclide[b]	Dose-rate factor (rem/y per μCi/m³)	Radionuclide[b]	Dose-rate factor (rem/y per μCi/m³)
Al-26	9.0×10^{-3}	Pa-231	1.1×10^{-4}
Co-60	8.5×10^{-3}	Th-227	3.1×10^{-4}
Sn-121m	1.2×10^{-6}	Ra-223	3.6×10^{-4}
Sn-126	9.2×10^{-5}	Pb-211	1.7×10^{-4}
Sb-126m	5.2×10^{-3}	Bi-211	1.5×10^{-4}
Sb-126	9.5×10^{-3}	Tl-207	1.1×10^{-5}
I-129	8.1×10^{-6}	U-232[c]	---
Cs-137	---	U-235	4.4×10^{-4}
Ba-137m	2.0×10^{-3}	Th-231	2.3×10^{-5}
Eu-154	4.1×10^{-3}	U-238	---
Eu-155	1.1×10^{-4}	Th-234	1.5×10^{-5}
Ra-226	---	Pa-234m	4.9×10^{-5}
Pb-214	7.8×10^{-4}	Pa-234	6.3×10^{-3}
Bi-214	5.1×10^{-3}	Np-237	4.9×10^{-5}
Th-229	2.0×10^{-4}	Pa-233	6.0×10^{-4}
Ra-225	6.9×10^{-6}	Am-241	2.7×10^{-5}
Ac-225	3.9×10^{-5}	Am-242m	1.1×10^{-6}
Fr-221	9.2×10^{-5}	Am-242	3.1×10^{-5}
Bi-213	4.4×10^{-4}	Np-238	1.8×10^{-3}
Tl-209	6.8×10^{-3}	Am-243	8.9×10^{-5}
Th-232	---	Np-239	4.6×10^{-4}
Ac-228	3.2×10^{-3}	Cm-243	3.5×10^{-4}
Pb-212	4.2×10^{-4}	Cm-245	2.1×10^{-4}
Bi-212	6.3×10^{-4}	Cm-247	1.0×10^{-3}
Tl-208	1.1×10^{-2}	Pu-243	4.9×10^{-5}
		Cf-249	1.1×10^{-3}
		Cf-251	3.2×10^{-4}

[a] Values from Eckerman and Ryman (1993) give EDE rates from external exposure per unit activity concentration in soil at distance of 1 m from source region.

[b] Indented entries are radiologically significant short-lived decay products of parent radionuclide listed. Dose-rate conversion factors for decay products do not take into account branching fraction in decay of parent.

[c] Entries for short-lived decay products Pb-212, Bi-212, and Tl-208 are listed under Th-232.

Table A-4-5. External dose-rate conversion factors for radionuclides uniformly distributed in infinite thickness of soil-equivalent material

Radionuclide[a]	Dose-rate factor (rem/y per μCi/m^3)		
	No shielding[b]	45-cm shielding[c]	100-cm shielding[c]
Al-26	1.1×10^{-2}	3.2×10^{-4}	7.9×10^{-6}
Co-60	1.0×10^{-2}	2.5×10^{-4}	3.3×10^{-6}
Sn-121m	1.2×10^{-6}	—	—
Sn-126	9.2×10^{-5}	—	—
Sb-126m	5.8×10^{-3}	4.9×10^{-5}	1.8×10^{-7}
Sb-126	1.1×10^{-2}	9.7×10^{-5}	4.3×10^{-7}
I-129	8.1×10^{-6}	—	—
Cs-137	—	—	—
Ba-137m	2.3×10^{-3}	2.0×10^{-5}	6.6×10^{-8}
Eu-154	4.8×10^{-3}	9.0×10^{-5}	1.0×10^{-6}
Eu-155	1.1×10^{-4}	1.8×10^{-9}	—
Ra-226	—	—	—
Pb-214	8.4×10^{-4}	—	—
Bi-214	6.1×10^{-3}	1.7×10^{-4}	3.8×10^{-6}
Th-229	2.0×10^{-4}	2.4×10^{-8}	—
Ra-225	6.9×10^{-6}	—	—
Ac-225	4.0×10^{-5}	1.2×10^{-8}	—
Fr-221	9.6×10^{-5}	4.1×10^{-8}	—
Bi-213	4.8×10^{-4}	2.5×10^{-6}	7.5×10^{-9}
Tl-209	8.1×10^{-3}	2.2×10^{-4}	4.3×10^{-6}

See end of table for footnotes.

Table A.4-5. (continued)

Radionuclide[a]	Dose-rate factor (rem/y per pCi/m³)		
	No shielding[b]	45 cm shielding[c]	100-cm shielding[c]
Th-232	—	—	—
Ac-228	3.7×10^{-3}	6.1×10^{-5}	7.2×10^{-7}
Pb-212	4.4×10^{-4}	—	—
Bi-212	7.3×10^{-1}	1.4×10^{-5}	2.1×10^{-7}
Tl-208	1.4×10^{-2}	6.9×10^{-4}	3.0×10^{-5}
Pa-231	1.2×10^{-4}	1.6×10^{-7}	8.0×10^{-11}
Th-227	3.3×10^{-4}	3.6×10^{-7}	1.6×10^{-10}
Ra-223	3.8×10^{-4}	4.6×10^{-7}	2.9×10^{-10}
Pb-211	1.9×10^{-4}	1.7×10^{-6}	8.3×10^{-9}
Bi-211	1.6×10^{-4}	4.4×10^{-7}	3.4×10^{-10}
Tl-207	1.2×10^{-5}	1.2×10^{-7}	8.2×10^{-10}
U-232[d]	—	—	—
U-235	4.5×10^{-4}	1.1×10^{-7}	6.5×10^{-12}
Th-231	2.3×10^{-5}	—	—
U-238	—	—	—
Th-234	1.5×10^{-5}	—	—
Pa-234m	5.6×10^{-5}	6.8×10^{-7}	5.2×10^{-9}
Pa-234	7.2×10^{-3}	1.1×10^{-4}	1.2×10^{-6}
Np-237	4.9×10^{-5}	—	—
Pa-233	6.4×10^{-4}	1.3×10^{-6}	7.9×10^{-10}
Am-241	2.7×10^{-5}	2.9×10^{-13}	—
Am-242m	1.1×10^{-6}	—	—
Am-242	3.1×10^{-5}	—	—
Np-238	2.1×10^{-3}	3.7×10^{-5}	3.1×10^{-7}

See end of table for footnotes.

Table A4-5. (continued)

Radionuclide[a]	Dose-rate factor (rem/y per μCi/m^3)		
	No shielding[b]	45-cm shielding[c]	100-cm shielding[c]
Am-243	8.9×10^{-5}	2.5×10^{-10}	—
Np-239	4.7×10^{-5}	3.2×10^{-7}	1.2×10^{-10}
Cm-243	3.6×10^{-4}	1.4×10^{-7}	5.8×10^{-11}
Cm-245	2.1×10^{-4}	1.5×10^{-8}	—
Cm-247	1.1×10^{-3}	3.6×10^{-6}	3.6×10^{-9}
Pu-243	5.0×10^{-5}	2.8×10^{-8}	—
Cf-249	1.2×10^{-3}	3.4×10^{-6}	3.0×10^{-9}
Cf-251	3.3×10^{-4}	8.8×10^{-9}	—

[a] Indented entries are radiologically significant short-lived decay products of parent radionuclide listed. Dose-rate conversion factors for decay products do not take into account branching fraction in decay of parent.

[b] Values from Eckerman and Ryman (1993) give EDE rates from external exposure per unit activity concentration in soil at distance of 1 m from source region.

[c] Values give EDE rates from external exposure per unit activity concentration in soil at distance of 1 m from source region and are based on calculations for monoenergetic photon sources (Kocher and Sjoreen 1985) and energies and intensities of photons emitted in decay of radionuclides (Kocher 1981).

[d] Entries for short-lived decay products Pb-212, Bi-212, and Tl-208 are listed under Th-232.

For the case of external exposure to waste shielded by engineered barriers at 100 years after disposal in the resident scenario, the total thickness of the concrete roof and layer of uncontaminated grout for the ILNT and ILT vaults thus is about 1.3 m. The thickness of shielding for these vaults is sufficient to reduce the external dose from the waste to minimal levels for any possible concentrations of photon-emitting radionuclides (Kocher and Sjoreen 1985). Therefore, in order to evaluate the need for the concrete roof in limiting external dose at 100 years after disposal for the resident scenario, the dose analysis for the ILNT and ILT vaults at this time is based on the assumption that only the layer of uncontaminated grout is present to provide shielding. The nominal thickness of the grout is assumed to be 100 cm. This value is slightly higher than the planned thickness of the grout layer and is intended to take into account the somewhat greater shielding provided by the metal waste containers and waste forms in the ILNT and ILT vaults compared with the shielding provided by soil-equivalent material.

For the LAW vaults, the nominal thickness of the concrete roof at 100 years after disposal is assumed to be 45 cm. This value is slightly less than the planned thickness of the concrete roof and is intended to take into account the somewhat reduced shielding provided by the waste itself, compared with soil-equivalent material, due to the presence of void spaces in the vaults.

Thus, in Table A.4-5, the external dose-rate conversion factors for the resident scenario at 100 years after disposal are given in the column labeled "45-cm shielding" for the LAW vaults and the column labeled "100-cm shielding" for the ILNT and ILT vaults. Again, the assumed thickness of shielding for the ILNT and ILT vaults should provide considerable over-estimates of external dose, because the planned thickness of the concrete roof on top of the vaults is ignored.

For the case of external exposure to unshielded waste in the resident scenario, the external dose-rate conversion factors are given in the column in Table A.4-5 labeled "No shielding". These data apply to all disposal units. Although exposure to unshielded waste is expected to become credible only at times long after disposal, due to the expected lifetime of the engineered barriers above the waste, dose-rate factors for the case of no shielding are

provided for the shorter-lived radionuclides as well. Inclusion of these radionuclides permits an evaluation of the time period over which the engineered barriers must maintain their integrity and prevent access to unshielded waste in the agriculture and resident scenarios. Again, at any time after disposal, shielding provided by the walls of the home during indoor residence is taken into account in the dose analysis itself.

The external dose-rate conversion factors in Table A.4-4 and in the column labeled "No shielding" in Table A.4-5 were obtained from calculations of Eckerman and Ryman (1993). The external dose-rate conversion factors for the two thicknesses of shielding in Table A.4-5 were obtained from calculations of absorbed dose rates in air from monoenergetic photon sources in soil (Kocher and Sjoreen 1985), the spectrum of photons emitted in the decay of each radionuclide (Kocher 1981), and the assumption that absorbed doses in air can be converted to EDEs by multiplying by a factor of 0.8. The entries for any short-lived decay products of a longer-lived radionuclide do not take into account the branching fraction in the decay of the parent radionuclide; i.e., the values for each decay product assume exposure to the same unit activity concentration (1 μCi/m^3).

On the basis of a direct comparison of results from Eckerman and Ryman (1993) and Kocher and Sjoreen (1985) for the case in Table A.4-5 of an infinitely thick source region with no shielding, the results from Kocher and Sjoreen for the two thicknesses of shielding in Table A.4-5 could be in error by as much as 25 to 30% in some cases. However, since the results from Kocher and Sjoreen appear to provide conservative overestimates of dose in almost all cases and the magnitude of the possible error is not large, these results reasonably can be used in this analysis. The calculations needed in this analysis for the different thicknesses of shielding between the source region and receptor location were not performed by Eckerman and Ryman.

A.4.5 Models and Parameter Values for Exposure Pathways

This section presents the models used to calculate doses to off-site individuals and inadvertent intruders for the various exposure pathways considered in this analysis involving use of contaminated groundwater or direct intrusion into disposal units. In each case, the

parameter values assumed in implementing the models also are presented. For each exposure pathway, the model results are presented in summary tables which give annual EDEs per unit concentration of radionuclides in water or in disposal units. For scenarios for direct intrusion into disposal units, the unit concentrations to which the dose estimates are normalized are the concentrations at the time exposures are assumed to occur, rather than the concentrations at the time of disposal.

A.4.5.1 Exposure Pathways for Off-Site Individuals

As discussed in Sect. 3.2.3.3 and A.4.3.1, direct consumption of drinking water from a source of contaminated groundwater is the only exposure pathway that needs to be considered in the dose analysis for off-site individuals, because the assumed limit on EDE of 4 mrem per year from the drinking water pathway only is expected to be more restrictive for any radionuclide than the limit on EDE of 25 mrem per year from all exposure pathways.

The annual EDE (rem/year) from direct ingestion of radionuclide i in drinking water (w) is given by

$$H_{iw} = C_{iw} U_w D_i, \tag{A.4-1}$$

where

C_{iw} = concentration of radionuclide i in drinking water (μCi/L),
U_w = annual consumption of drinking water (L/year), and
D_i = DCF for ingestion of radionuclide i (rem/μCi).

In implementing the model, a daily consumption of contaminated drinking water of 2 L, i.e., an annual consumption of 730 L, is assumed.

The model for estimating dose from the drinking water pathway is summarized in Table A.4-6. The radionuclides listed in this table include those selected on the basis of a screening analysis for the groundwater pathway described in Sect. 4.1.1 and the long-lived decay products of U-234/U-238, Np-237, Pu-239, and Pu-241 that could occur in significant concentrations in groundwater at various times in the future. The annual dose per unit concentration of a radionuclide in water is obtained by multiplying the assumed annual consumption of drinking water by the ingestion DCF given in Table A.4-2.

A.4.5.2 Exposure Pathways for Inadvertent Intruders

As described in Sects. 3.2.4 and A.4.3.2, exposures of inadvertent intruders resulting from direct intrusion into disposal units are assumed to occur according to the agriculture, resident, or post-drilling scenarios. This section presents the models and parameter values used to estimate doses to inadvertent intruders for each of these scenarios.

Agriculture Scenario

In the agriculture scenario, exposures of inadvertent intruders are assumed to occur after an intruder exhumes waste from disposal units while excavating to build a foundation for a home on top of the disposal facility and some of the exhumed waste is mixed with native soil in a vegetable garden. The exposure pathways assumed for this scenario then include: 1) ingestion of vegetables grown in contaminated garden soil; 2) direct ingestion of contaminated soil in conjunction with vegetable intakes; 3) external exposure to contaminated soil while working in the garden and residing in the home on top of the disposal units; and 4) inhalation of suspended activity in particulate form and inhalation of isotopes of radon and their short-lived decay products while working in the garden and residing in the home. The model for each exposure pathway is described below. The radionuclides included in the dose analysis for the agriculture scenario were selected on the basis of a screening analysis described in Sect. 3.2.4.4. Long-lived decay products of U-234/U-238, U-235, and Np-237 that could occur in significant concentrations in disposal units at times far in the future also are included in the dose analysis.

Table A.4-6. Annual EDEs from drinking water pathway per unit concentration of radionuclides in water

Radionuclide[a]	Annual EDEs (rem/y per μCi/L)
H-3	4.6×10^{-3}
C-14	1.5
Al-26	9.5
Co-60	1.9×10^{1}
Ni-59	1.5×10^{-1}
Ni-63	3.9×10^{-1}
Se-79	6.1
Rb-87	3.5
Sr-90 + d	1.0×10^{2}
Zr-93[b]	1.2
Nb-93m	3.9×10^{-1}
Tc-99	9.5×10^{-1}
Pd-107	1.0×10^{-1}
Cd-113m	1.1×10^{2}
Sn-121m	9.5×10^{-1}
Sn-126 + d	1.3×10^{1}
I-129	2.0×10^{2}
Cs-135	5.2
Cs-137	3.7×10^{1}
Sm-151	2.5×10^{-1}
Pb-210 + d	4.9×10^{3}
Ra-226 + d[c]	8.0×10^{2}
Th-229 + d	2.9×10^{3}
Th-230	3.9×10^{2}
Th-232 + d	3.5×10^{3}
Pa-231 + d	1.1×10^{4}

See end of table for footnotes.

Table A4-6. (continued)

Radionuclide[a]	Annual ADRs (rem/y per μCi/L)
U-232 + d	1.5×10^3
U-233	2.0×10^2
U-234	1.9×10^2
U-235	1.8×10^2
U-236	1.8×10^2
U-238 + d	1.8×10^2
Np-237	2.8×10^3
Pu-238	2.8×10^3
Pu-239	3.1×10^3
Pu-240	3.1×10^3
Pu-242	3.0×10^3
Pu-244	2.9×10^3
Am-241	3.3×10^3
Am-242m + d	3.1×10^3
Am-243	3.3×10^3
Cm-245	3.3×10^3
Cm-246	3.3×10^3
Cm-247	3.0×10^3
Cm-248	1.2×10^4
Cf-249	3.4×10^3
Cf-251	3.4×10^3

[a] " + d" denotes short-lived decay products that are assumed to be in secular equilibrium with parent radionuclide; see Table A4-1 for decay products and branching fractions.

[b] Entry does not include possible contribution from Nb-93m decay product.

[c] Entry does not include possible contribution from Pb-210 decay product.

Vegetable Pathway. The annual EDE (rem/year) from ingestion of radionuclide i in vegetables (v) is given by

$$H_{iv} = C_{iv} U_v D_i, \tag{A.4-2}$$

where

C_{iv} = concentration of radionuclide i in vegetables (μCi/kg),
U_v = annual consumption of vegetables (kg fresh weight per year), and
D_i = DCF for ingestion of radionuclide i (rem/μCi).

Radionuclides are assumed to be transferred to vegetables via root uptake from the contaminated garden soil, and the radionuclide concentrations in vegetables are given by

$$\begin{aligned} C_{iv} &= B_{iv} C_{is} / \rho_s \\ &= B_{iv} f_s C_{ii} / \rho_s, \end{aligned} \tag{A.4-3}$$

where

B_{iv} = plant-to-soil concentration ratio for radionuclide i (μCi/kg fresh weight in vegetation per μCi/kg dry weight in soil),
C_{is} = concentration of radionuclide i in soil in vegetable garden (μCi/m^3),
ρ_s = bulk density of soil (kg/m^3),
C_{ii} = concentration of radionuclide i in exhumed waste (μCi/m^3), and
f_s = dilution factor for mixing of radionuclides in exhumed waste into soil in vegetable garden.

In implementing the model, the assumed plant-to-soil concentration ratios in vegetables are given in Table A.4-7. Since site-specific data generally are lacking, the adopted values for all elements are based entirely on published evaluations and compilations which are generic in nature. The adopted values for almost all elements were obtained from the evaluation of published data by Baes et al. (1984). Although selection of these concentration ratios for use at the SRS clearly is judgmental, the use of data from a single source at least ensures some degree of consistency among the adopted values for the different elements.

Baes et al. (1984) give concentration ratios for vegetative portions of food crops, which would apply to leafy vegetables, and for nonvegetative (reproductive) portions, which would apply to nonleafy vegetables. The values for nonvegetative portions of food crops were adopted for use in this analysis, because consumption of nonleafy vegetables is expected to be considerably greater than consumption of leafy vegetables (Baes et al. 1984; Hamby 1992). The reported concentration ratios on a dry-weight basis for nonleafy vegetation were converted to a fresh-weight basis by multiplying by a factor of 0.43, which represents the average conversion factor for all types of nonleafy vegetables (Baes et al. 1984).

The other parameter values assumed in the model for the vegetable pathway are as follows: a dilution factor for mixing of radionuclides in exhumed waste into native soil in the vegetable garden of 0.2 (Napier et al. 1984), a bulk density of soil of 1,400 kg/m^3 (Baes and Sharp 1983), and an annual fresh-weight consumption of contaminated vegetables of 90 kg. The assumed dilution factor for mixing of exhumed waste with native soil in a vegetable garden of 0.2 is based on a typical depth and area of an excavation for a home and the reasonable assumption that only a relatively small fraction of the soil in the vegetable garden could contain exhumed waste in order for the garden to be productive; this dilution factor is consistent with previous assumptions for the agriculture scenario (NRC 1981; Oztunali and Roles 1986). The assumed yearly consumption of vegetables of 90 kg is based on data obtained near the SRS (Hamby 1992), which indicate a total yearly consumption of all vegetables by an average adult of 180 kg, and the assumption that half of an intruder's total intake of vegetables is obtained from the home garden. An assumption that an intruder's entire intake of all vegetables would be obtained from the home garden is regarded as unreasonably conservative.

Table A.4-7. Elemental plant-to-soil concentration ratios[a] vegetables[a]

Element	B_v[b]	Element	B_v[b]
H	4.8[c]	Cs	1.3×10^{-2}
C	5.6×10^{-1} [d]	Sm	1.7×10^{-3}
Al	2.8×10^{-1}	Eu	1.7×10^{-3}
Co	3.0×10^{-3}	Pb	3.9×10^{-3}
Ni	2.6×10^{-2}	Po	1.7×10^{-4}
Se	1.1×10^{-2}	Ra	6.5×10^{-4}
Rb	3.0×10^{-2}	Ac	1.5×10^{-4}
Sr	1.1×10^{-1}	Th	3.7×10^{-5}
Zr	2.2×10^{-4}	Pa	1.1×10^{-4}
Nb	2.2×10^{-3}	U	1.7×10^{-3}
Tc	6.5×10^{-1}	Np	4.3×10^{-3}
Pd	1.7×10^{-2}	Pu	1.9×10^{-5}
Cd	6.5×10^{-2}	Am	1.1×10^{-4}
Sn	2.6×10^{-3}	Cm	6.6×10^{-6}
Sb	1.3×10^{-2}	Cf[e]	6.6×10^{-6}
I	2.2×10^{-2}		

[a] μCi/kg fresh weight in vegetation per μCi/kg dry weight in soil.

[b] Except as noted, values are based on concentration ratios reported on basis of dry weight of vegetation given in Fig. 2.2 of Baes et al. (1984) multiplied by a factor of 0.43 to convert to fresh weight of vegetation (Baes et al. 1984).

[c] Value obtained from Table E-1 of NRC (1977).

[d] Value based on measurement of Sheppard et al. (1991) for carbonate form in acidic soil with low organic matter content. Reported value for dry weight of vegetation is converted to fresh weight by multiplying by factor of 0.43 (Baes et al. 1984).

[e] Value is assumed to be the same as value for Cm.

The model for estimating dose from the vegetable pathway is summarized in Table A.4-8. The annual dose per unit concentration of a radionuclide in exhumed waste from a disposal unit at the time intrusion occurs is based on the model and parameter values described above and the ingestion DCFs given in Table A.4-2.

Soil Ingestion Pathway. The annual EDE (rem/year) from direct ingestion of radionuclide i in contaminated soil (s) is given by

$$H_{is} = C_{is} U_s D_i \qquad \text{(A.4-4)}$$

where

C_{is} = concentration of radionuclide i in soil in vegetable garden (μCi/kg),
U_s = annual consumption of contaminated soil (kg/year), and
D_i = DCF for ingestion of radionuclide i (rem/μCi).

Ingestion of contaminated soil is assumed to occur primarily as a result of incomplete washing of vegetables from the garden before consumption. Since the SRS is a humid site with extensive vegetation, ingestion of contaminated soil from sources other than the garden should be relatively unimportant for an average adult. Radionuclide concentrations in soil in the vegetable garden are given by

$$C_{is} = f_s C_{iv} / \rho_s \qquad \text{(A.4-5)}$$

where

C_{iv} = concentration of radionuclide i in exhumed waste (μCi/m^3),
f_s = dilution factor for mixing of radionuclides in exhumed waste into soil in vegetable garden, and
ρ_s = bulk density of soil (kg/m^3).

Table A4-8. Annual EDEs from vegetable pathway per unit concentration of radionuclides in [illegible] wastes for agriculture [illegible]

Radionuclide[a]	Annual EDE (rem/y per μCi/m^3)
H-3	3.9×10^{-6}
C-14	1.5×10^{-5}
Al-26	4.7×10^{-8}
Co-60	1.0×10^{-6}
Ni-59	6.7×10^{-8}
Ni-63	1.8×10^{-7}
Se-79	1.2×10^{-6}
Rb-87	1.9×10^{-6}
Sr-90	1.8×10^{-4}
Zr-93[b]	2.4×10^{-8}
Nb-93m	1.5×10^{-8}
Tc-99	1.1×10^{-5}
Pd-107	3.1×10^{-8}
Cd-113m	1.3×10^{-4}
Sn-121m	4.4×10^{-8}
Sn-126 + d	7.8×10^{-7}
I-129	7.9×10^{-5}
Cs-135	1.2×10^{-6}
Cs-137	8.4×10^{-6}
Sm-151	7.5×10^{-9}
Eu-154	2.0×10^{-7}
Eu-155	2.9×10^{-8}
Pb-210 + d	2.6×10^{-4}
Ra-226 + d[c]	2.7×10^{-4}
Th-229 + d	4.5×10^{-6}
Th-230	2.5×10^{-7}
Th-232 + d	1.6×10^{-5}
Pa-231 + d	3.2×10^{-5}
U-232 + d	3.4×10^{-5}

See end of table for footnotes.

Table A.4-8. (continued)

Radionuclide[a]	Annual EDE (rem/y per µCi/m³)
U-233	5.9×10^{-6}
U-234	5.7×10^{-6}
U-235	5.5×10^{-6}
U-236	5.5×10^{-6}
U-238	5.0×10^{-6}
Np-237	2.2×10^{-4}
Pu-238	9.3×10^{-7}
Pu-239	1.1×10^{-6}
Pu-240	1.1×10^{-6}
Pu-241	2.1×10^{-8}
Pu-242	1.0×10^{-6}
Pu-244	9.8×10^{-7}
Am-241	6.4×10^{-6}
Am-242m	6.0×10^{-6}
Am-243	6.4×10^{-6}
Cm-243	2.5×10^{-7}
Cm-244	2.0×10^{-7}
Cm-245	3.8×10^{-7}
Cm-246	3.8×10^{-7}
Cm-247	3.5×10^{-7}
Cm-248	1.4×10^{-6}
Cf-249	3.9×10^{-7}
Cf-250	1.6×10^{-7}
Cf-251	3.9×10^{-7}

[a] " + d" denotes short-lived decay products that are assumed to be in secular equilibrium with parent radionuclide; see Table A.4-1 for decay products and branching fractions.

[b] Value assumes that Nb-93m is present in secular equilibrium.

[c] Value assumes that Pb-210 is present in secular equilibrium.

In implementing the model, a dilution factor for mixing of radionuclides in exhumed waste into native soil in the vegetable garden of 0.2 and a soil bulk density of 1,400 kg/m^3 are assumed, as in the model for the vegetable pathway. A daily consumption of contaminated soil from the vegetable garden of 0.1 g, i.e., an annual consumption of 0.037 kg, also is assumed (U.S.EPA 1989b).

The model for estimating dose from the soil ingestion pathway is summarized in Table A.4-9. The annual dose per unit concentration of a radionuclide in exhumed waste from a disposal unit at the time intrusion occurs is based on the model and parameter values described above and the ingestion DCFs given in Table A.4-2.

External Exposure Pathways. For external exposure (e) to contaminated soil while working in the vegetable garden, the annual EDE (rem/year) from radionuclide i is given by

$$H_{ie} = C_{ie} U_e D_{ie}, \qquad \text{(A.4-6)}$$

where

C_{ie} = concentration of radionuclide i in soil in vegetable garden (μCi/m^3),

U_e = fraction of the year during which external exposure to contaminated soil in vegetable garden occurs, and

D_{ie} = dose-rate conversion factor for external exposure to radionuclide i in garden soil (rem/y per μCi/m^3).

As in the models for the vegetable and soil ingestion pathways, the radionuclide concentrations in soil in the vegetable garden are given by

$$C_{ie} = f_s C_{iv}, \qquad \text{(A.4-7)}$$

Table A.4-9. Annual EDEs from soil ingestion pathway per unit concentration of all radionuclides in disposed waste for agricultural scenario

Radionuclide[a]	Annual EDE (rem/y per μCi/m^3)
H-3	3.3×10^{-10}
C-14	1.1×10^{-9}
Al-26	6.9×10^{-8}
Co-60	1.4×10^{-7}
Ni-59	1.1×10^{-9}
Ni-63	2.9×10^{-9}
Se-79	4.4×10^{-8}
Rb-87	2.5×10^{-8}
Sr-90 + d	7.4×10^{-7}
Zr-93[b]	1.1×10^{-8}
Nb-93m	2.8×10^{-9}
Tc-99	6.9×10^{-9}
Pd-107	7.4×10^{-10}
Cd-113m	7.9×10^{-7}
Sn-121m	6.9×10^{-9}
Sn-126 + d	9.7×10^{-8}
I-129	1.5×10^{-6}
Cs-135	3.8×10^{-8}
Cs-137	2.6×10^{-7}
Sm-151	1.8×10^{-9}
Eu-154	4.8×10^{-8}
Eu-155	6.9×10^{-9}
Pb-210 + d	3.5×10^{-5}
Ra-226 + d[c]	4.1×10^{-5}
Th-229 + d	2.1×10^{-5}
Th-230	2.8×10^{-6}
Th-232 + d	2.5×10^{-5}
Pa-231 + d	1.4×10^{-4}
U-232 + d	1.1×10^{-5}

See end of table for footnote.

Table A.4-9. (continued)

Radionuclide[a]	Annual EDE (rem/year per $\mu Ci/m^3$)
U-233	1.4×10^{-5}
U-234	1.4×10^{-6}
U-235	1.3×10^{-6}
U-236	1.3×10^{-6}
U-238 + d	1.3×10^{-6}
Np-237	2.1×10^{-5}
Pu-238	2.0×10^{-5}
Pu-239	2.3×10^{-5}
Pu-240	2.3×10^{-5}
Pu-241	4.5×10^{-7}
Pu-242	2.2×10^{-5}
Pu-244	2.1×10^{-5}
Am-241	2.4×10^{-5}
Am-242m + d	2.3×10^{-5}
Am-243	2.4×10^{-5}
Cm-243	1.5×10^{-5}
Cm-244	1.2×10^{-5}
Cm-245	2.4×10^{-5}
Cm-246	2.4×10^{-5}
Cm-247	2.2×10^{-5}
Cm-248	8.5×10^{-5}
Cf-249	2.4×10^{-5}
Cf-250	1.0×10^{-5}
Cf-251	2.4×10^{-5}

[a] " + d" denotes short-lived decay products that are assumed to be in secular equilibrium with parent radionuclide; see Table A.4-1 for decay products and branching fractions.

[b] Value assumes that Nb-93m is present in secular equilibrium.

[c] Value assumes that Pb-210 is present in secular equilibrium.

where

C_{it} = concentration of radionuclide i in exhumed waste ($\mu Ci/m^3$), and

f_s = dilution factor for mixing of radionuclides in exhumed waste into soil in vegetable garden.

In implementing the model, a dilution factor for mixing of radionuclides in exhumed waste into native soil in the vegetable garden of 0.2 is assumed, as in the models for the vegetable and soil ingestion pathways. The fraction of the year during which exposure while working in the garden occurs is assumed to be 0.01 (Oztunali et al. 1981); i.e., the assumed exposure time is about 100 h/year.

The model for estimating external dose while working in the garden is summarized in Table A.4-10. The annual dose per unit concentration of a radionuclide in exhumed waste from a disposal unit at the time intrusion occurs is based on the model and parameter values described above and the external dose-rate conversion factors given in Table A.4-4.

For external exposure during residence in a home on top of exposed disposal units, the annual EDE (rem/year) from radionuclide i is given by

$$H_{ie} = C_{it} U_h D_{it} S, \qquad \text{(A.4-8)}$$

where

C_{it} = concentration of radionuclide i in disposal unit ($\mu Ci/m^3$),

U_h = fraction of the year during which external exposure while residing in the home occurs,

D_{it} = dose-rate conversion factor for external exposure to radionuclide i in disposal unit (rem/y per $\mu Ci/m^3$), and

S = shielding factor for radionuclides during indoor residence.

Table A.4-10. Annual EDE from ingestion of [illegible] per unit concentration of radionuclides in channel water for agriculture [illegible]

Radionuclide[a]	Annual EDE (rem/y per pCi/m³)
Al-26	1.8×10^{-5}
Co-60	1.7×10^{-5}
Sn-121m	2.4×10^{-9}
Sn-126 + d	1.3×10^{-5}
I-129	1.6×10^{-8}
Cs-137 + d	3.8×10^{-6}
Eu-154	8.2×10^{-6}
Eu-155	2.2×10^{-7}
Ra-226 + d	1.2×10^{-5}
Th-229 + d	1.8×10^{-6}
Th-232 + d	1.6×10^{-5}
Pa-231 + d	2.2×10^{-6}
U-232 + d	1.0×10^{-5}
U-235 + d	9.3×10^{-7}
U-238 + d	1.5×10^{-7}
Np-237 + d	1.3×10^{-6}
Am-241	5.4×10^{-8}
Am-242m + d	8.2×10^{-8}
Am-243 + d	1.1×10^{-6}
Cm-243	7.0×10^{-7}
Cm-245	4.2×10^{-7}
Cm-247 + d	2.1×10^{-6}
Cf-249	2.2×10^{-6}
Cf-251	6.4×10^{-7}

[a] "+ d" denotes short-lived decay products that are assumed to be in secular equilibrium with parent radionuclide; see Table A.4-1 for decay products and branching fractions.

The shielding factor takes into account the reduction in external dose provided by the walls and floor of the home.

In implementing the model, the fraction of the year during which exposure in the home is assumed to occur is 0.5 (Oztunali et al. 1981); i.e., the assumed exposure time is about 4,000 h/year. A shielding factor during indoor residence of 0.7 is assumed for all radionuclides (NRC 1977).

The model for estimating external dose during indoor residence is summarized in Table A.4-11. The annual dose per unit concentration of a radionuclide in a disposal unit at the time intrusion occurs is based on the model and parameter values described above and the external dose-rate conversion factors for sources uniformly distributed in an infinite thickness of soil-equivalent material given in the column in Table A.4-5 labeled "No shielding".

Inhalation Pathways. While working in the vegetable garden or residing in the home, the annual EDE (rem/year) from inhalation of radionuclide i suspended into air (a) in particulate form is given by

$$H_{ia} = C_{ia} f_a U_a D_i, \qquad \text{(A.4-9)}$$

where

C_{ia} = concentration of radionuclide i in air (μCi/m^3),
f_a = fraction of the year during which inhalation exposure occurs,
U_a = annual air intake (m^3/year), and
D_i = DCF for inhalation of radionuclide i (rem/μCi).

Airborne concentrations of suspended radionuclides in particulate form are estimated using a mass-loading model (Anspaugh et al. 1975), which is based on observations of airborne concentrations of naturally occurring materials, such as uranium and thorium, relative to their

Table A.1-11. Annual EDEs from external exposure per unit concentration of radionuclides in dispersal units for agricultural scenario

Radionuclide[a]	Annual EDE (rem/y per $\mu Ci/m^3$)
Al-26	3.9×10^{-3}
Co-60	3.5×10^{-3}
Sn-121m	4.2×10^{-7}
Sn-126 + d	2.6×10^{-3}
I-129	2.8×10^{-6}
Cs-137 + d	7.6×10^{-4}
Eu-154	1.7×10^{-3}
Eu-155	3.9×10^{-5}
Ra-226 + d	2.4×10^{-3}
Th-229 + d	3.5×10^{-4}
Th-232 + d	3.5×10^{-3}
Pa-231 + d	4.2×10^{-4}
U-232 + d	2.2×10^{-3}
U-235 + d	1.7×10^{-4}
U-238 + d	2.9×10^{-5}
Np-237 + d	2.4×10^{-4}
Am-241	9.5×10^{-6}
Am-242m + d	1.5×10^{-5}
Am-243 + d	2.0×10^{-4}
Cm-243	1.3×10^{-4}
Cm-245	7.4×10^{-5}
Cm-247 + d	4.0×10^{-4}
Cf-249	4.2×10^{-4}
Cf-251	1.2×10^{-4}

[a] "+ d" denotes short-lived decay products that are assumed to be in secular equilibrium with parent radionuclide; see Table A.4-1 for decay products and branching fractions.

concentrations in surface soils. In this model, airborne concentrations of [illegible] radionuclides in particulate form are given by

$$C_{is} = C_i L_s / \rho_s \qquad \text{(A.4-10)}$$

where

C_{is} = concentration of radionuclide i in surface soil (μCi/m^3),
L_s = atmospheric mass loading of surface soil (kg/m^3), and
ρ_s = bulk density of soil (kg/m^3).

The model described above is applied to all radionuclides except Rn-222, Rn-220, and their short-lived decay products. The model for estimating inhalation doses from exposure to radon is described later in this section.

For inhalation exposure while working in the vegetable garden, the concentration of radionuclide i in soil again is given by

$$C_{is} = f_s C_{it} \qquad \text{(A.4-11)}$$

where

C_{it} = concentration of radionuclide i in exhumed waste (μCi/m^3), and
f_s = dilution factor for mixing of radionuclides in exhumed waste into soil in vegetable garden.

In implementing the model, a dilution factor for mixing of radionuclides in exhumed waste into native soil in the garden of 0.2, a soil bulk density of 1,400 kg/m^3, and a fraction of the year during which exposure while working in the garden occurs of 0.01 (about 100 h/year) again are assumed, and the annual air intake is assumed to be 8,000 m^3 (NRC 1977). Finally, the atmospheric mass loading of contaminated soil while working in the garden is assumed to be 10^{-7} kg/m^3.

The assumed atmospheric mass loading of contaminated soil while working in the vegetable garden of 10^{-7} kg/m^3 is a somewhat conservative approximation of the average background dust loading for nonurban locations in the U.S. of about 4×10^{-7} kg/m^3 (Anspaugh et al. 1975) and, furthermore, is in good agreement with an average dust loading of 6×10^{-8} kg/m^3 measured above two agricultural fields at the SRS (Shinn et al. 1982). The choice of an atmospheric mass loading for this exposure pathway is based on these data and the following considerations. Although some gardening activities (e.g., tilling and hoeing) presumably would increase atmospheric concentrations of suspended soil above background levels, it probably is unreasonable to assume that the average concentration during all gardening activities would be substantially above the average background level in the U.S. First, the average background level of suspended soil originating from the SRS should be substantially lower than the average level in the U.S. because of the high annual precipitation, extensive vegetation, and low average wind speed at the site. Second, at any location, airborne concentrations of suspended surface soil consist of material originating from a wide area, not just from the particular location where exposures occur. Finally, the model assumes that all suspended soil particles are respirable; but, particularly during more vigorous gardening activities that could result in above-average atmospheric mass loadings, some particles are likely to be too large to be respirable. Taking into account all of these factors, the choice of 10^{-7} kg/m^3 to represent the average mass loading during gardening activities at the SRS seems reasonable.

The model for estimating inhalation dose while working in the vegetable garden is summarized in Table A.4-12. The annual dose per unit concentration of a radionuclide in exhumed waste from a disposal unit at the time intrusion occurs is based on the model and parameter values described above and the inhalation DCFs given in Table A.4-3. Again, the results for Rn-222 and Rn-220 are estimated using a different model described later in this section.

For inhalation exposure while residing in the home, the airborne concentration of radionuclide i is given by

$$C_{ia} = C_{ir} L_a / \rho_{ar} \qquad \text{(A.4-12)}$$

Table A.1-12. Annual EDEs from inhalation exposure in vegetable gardens [illegible] concentration of radionuclides in exhumed waste for agricultural [illegible]

Radionuclide[a]	Annual EDE (rem/y per μCi/m^3)	Radionuclide[a]	Annual EDE (rem/y per μCi/m^3)
H-3	7.2×10^{-11}	Pa-231 + d	9.1×10^{-5}
C-14	2.7×10^{-12}	U-232 + d[d]	7.6×10^{-7}
Al-26	9.0×10^{-11}	Ra-220	2.1×10^{-5} [e]
Co-60	1.7×10^{-10}	U-233	1.5×10^{-7}
Ni-59	1.5×10^{-12}	U-234	1.5×10^{-7}
Ni-63	3.4×10^{-12}	U-235	1.4×10^{-7}
Se-79	1.0×10^{-11}	U-236	1.4×10^{-7}
Rb-87	3.8×10^{-12}	U-238	1.4×10^{-7}
Sr-90 + d	2.7×10^{-10}	Np-237	5.6×10^{-7}
Zr-93[b]	4.0×10^{-10}	Pu-238	5.2×10^{-7}
Nb-93m	3.2×10^{-11}	Pu-239	5.8×10^{-7}
Tc-99	9.6×10^{-13}	Pu-240	5.8×10^{-7}
Pd-107	1.5×10^{-11}	Pu-241	1.1×10^{-8}
Cd-113m	1.8×10^{-9}	Pu-242	5.5×10^{-7}
Sn-121m	6.6×10^{-12}	Pu-244	5.5×10^{-7}
Sn-126 + d	9.9×10^{-11}	Am-241	5.9×10^{-7}
I-129	2.1×10^{-10}	Am-242m + d	5.9×10^{-7}
Cs-135	5.1×10^{-12}	Am-243	5.9×10^{-7}
Cs-137	3.6×10^{-11}	Cm-243	4.0×10^{-7}
Sm-151	3.3×10^{-11}	Cm-244	3.1×10^{-7}
Eu-154	3.0×10^{-10}	Cm-245	6.2×10^{-7}
Eu-155	4.5×10^{-11}	Cm-246	6.2×10^{-7}
Pb-210 + d	2.4×10^{-8}	Cm-247	5.6×10^{-7}
Ra-226 + d[c,d]	3.3×10^{-8}	Cm-248	2.2×10^{-6}
Rn-222	1.3×10^{-4} [e]	Cf-249	6.3×10^{-7}
Th-229	1.9×10^{-6}	Cf-250	2.5×10^{-7}
Th-230	3.0×10^{-7}	Cf-251	6.4×10^{-7}
Th-232 + d[d]	1.6×10^{-6}		
Rn-220	2.1×10^{-5} [e]		

[a] "+ d" denotes short-lived decay products that are assumed to be in secular equilibrium with parent radionuclide; see Table A.4-1 for decay products and branching fractions.
[b] Value assumes that Nb-93m is present in secular equilibrium.
[c] Value assumes that Pb-210 is present in secular equilibrium.
[d] Dose from radon decay product is listed separately.
[e] Dose is normalized to unit concentration of parent radionuclide.

where

C_{ti} = concentration of radionuclide i in disposal unit ($\mu Ci/m^3$),
L_s = atmospheric mass loading of surface soil (kg/m^3), and
ρ_s = bulk density of soil (kg/m^3).

In implementing the model, a fraction of the year during which exposure in the home occurs of 0.5 (i.e., about 4,000 h/year), a soil bulk density of 1,400 kg/m^3, and an annual air intake of 8,000 m^3 again are assumed. The atmospheric mass loading of contaminated soil at the location of the home on top of the disposal facility is assumed to be 10^{-8} kg/m^3, which is approximately one-fourth of the average background dust loading in the U.S. (Anspaugh et al. 1975). On the basis of the previous discussion of the atmospheric mass loading while working in the vegetable garden, it seems unreasonable to assume that the atmospheric mass loading of largely undisturbed surface soil at the SRS would be as high as the average dust loading in the U.S. The assumption that the atmospheric mass loading of contaminated soil at the disposal site is about one-fourth of the average background level in the U.S. is intended to take into account the abundant precipitation, extensive vegetation, and low average wind speed at the site, compared with average conditions in the U.S., as well as the presence of uncontaminated soil suspended from other locations and the possibility that some suspended soil particles may not be respirable. In addition, the model for inhalation exposure indoors does not take into account the possibility that indoor concentrations of suspended soil particles may be somewhat less than the concentrations outdoors, due to such factors as filtering of air entering the home through windows and doorways and enhanced deposition on indoor surfaces.

The model for estimating inhalation dose during indoor residence is summarized in Table A.4-13. The annual dose per unit concentration of a radionuclide in a disposal unit at the time intrusion occurs is based on the model and parameter values described above and the inhalation DCFs given in Table A.4-3. The results for Rn-222 and Rn-220 are estimated using the model described below.

Table A.4-11. Annual EDEs from inhalation exposure in [illegible] per unit concentration of radionuclide in the [illegible] units for [illegible] scenario

Radionuclide[a]	Annual EDE (rem/y per μCi/m³)	Radionuclide[a]	Annual EDE (rem/y per μCi/m³)
H-3	1.8×10^{-12}	Pa-231 + d	2.3×10^{-1}
C-14	6.0×10^{-11}	U-232 + d [d]	1.9×10^{-5}
Al-26	2.3×10^{-9}	Rn-220	1.0×10^{-2} [e]
Co-60	4.3×10^{-9}	U-233	3.7×10^{-6}
Ni-59	3.7×10^{-11}	U-234	3.7×10^{-6}
Ni-63	8.6×10^{-11}	U-235	3.4×10^{-6}
Se-79	2.5×10^{-10}	U-236	3.4×10^{-6}
Rb-87	9.4×10^{-11}	U-238	3.4×10^{-6}
Sr-90 + d	6.8×10^{-9}	Np-237	1.4×10^{-5}
Zr-93 [b]	1.0×10^{-8}	Pu-238	1.3×10^{-5}
Nb-93m	8.0×10^{-10}	Pu-239	1.5×10^{-5}
Tc-99	2.4×10^{-11}	Pu-240	1.5×10^{-5}
Pd-107	3.7×10^{-10}	Pu-241	2.9×10^{-7}
Cd-113m	4.6×10^{-8}	Pu-242	1.4×10^{-5}
Sn-121m	1.7×10^{-10}	Pu-244	1.4×10^{-5}
Sn-126 + d	2.5×10^{-9}	Am-241	1.5×10^{-5}
I-129	5.1×10^{-9}	Am-242m + d	1.5×10^{-5}
Cs-135	1.3×10^{-10}	Am-243	1.5×10^{-5}
Cs-137	9.2×10^{-10}	Cm-243	1.0×10^{-5}
Sm-151	8.3×10^{-10}	Cm-244	7.7×10^{-6}
Eu-154	7.4×10^{-9}	Cm-245	1.5×10^{-5}
Eu-155	1.1×10^{-9}	Cm-246	1.5×10^{-5}
Pb-210 + d	6.0×10^{-7}	Cm-247	1.4×10^{-5}
Ra-226 + d [c,d]	8.3×10^{-7}	Cm-248	5.4×10^{-5}
Rn-222	1.2×10^{-1} [e]	Cf-249	1.6×10^{-5}
Th-229	4.9×10^{-5}	Cf-250	6.3×10^{-6}
Th-230	7.4×10^{-6}	Cf-251	1.6×10^{-5}
Th-232 + d [d]	4.0×10^{-5}		
Rn-220	1.0×10^{-2} [e]		

[a] "+ d" denotes short-lived decay products that are assumed to be in secular equilibrium with parent radionuclide; see Table A.4-1 for decay products and branching fractions.
[b] Value assumes that Nb-93m is present in secular equilibrium.
[c] Value assumes that Pb-210 is present in secular equilibrium.
[d] Dose from radon decay product is listed separately.
[e] Dose is normalized to unit concentration of parent radionuclide.

In this analysis, inhalation doses from Rn-222, Rn-220, and their short-lived decay products while working in the vegetable garden containing contaminated soil or while residing in the home on top of a disposal unit are estimated using a natural analog model. Specifically, estimated average doses to the general population from exposure to Rn-222 and Rn-220, both indoors and outdoors, which result from known average concentrations of their parent radionuclides Ra-226 and Th-232, respectively, in surface soil, are used to estimate doses from radon per unit concentration of its parent radionuclide in waste for the inhalation pathways of concern for the agriculture scenario. This approach has the advantage compared, for example, with using a mechanistic diffusion model to predict radon emanation rates to the atmosphere that the natural analog model is based on environmental measurements and it implicitly takes into account all factors that relate concentrations of radium or thorium in soil to average exposures to indoor radon (e.g., average residence time in basements and other living areas). The analysis based on the natural analog model proceeds as follows.

The NCRP (1987) has estimated that the average EDE from exposure to radon in the U.S. is about 0.2 rem per year. This dose estimate applies only to Rn-222 and its short-lived decay products in homes and, furthermore, assumes continuous residence indoors. The estimated dose from Rn-222 indoors results from an average concentration of the parent radionuclide Ra-226 in surface soil of 0.6 pCi/g (NCRP 1984) which, for an assumed bulk density of soil of 1.4 g/cm^3 (Baes and Sharp 1983), corresponds to a concentration of 0.84 μCi/m^3. Therefore, for continuous residence indoors, the EDE from exposure to Rn-222 and its short-lived decay products per unit concentration of Ra-226 in surface soil is estimated as:

Rn-222, continuous residence indoors -

$$(0.2 \text{ rem/y}) / (0.84\ \mu\text{Ci/m}^3) = 0.24 \text{ rem/y per } \mu\text{Ci/m}^3.$$

The dose per unit concentration from Rn-222 during indoor residence derived above can be applied directly to the inhalation pathway during indoor residence in a home located on top of a disposal unit containing Ra-226. The only correction needed is to take into account the assumption for this pathway in the agriculture scenario that the fraction of the year during

which residence in the home at the disposal site occurs is 0.5. Thus, for inhalation exposure while residing in the home on a disposal unit in the agriculture scenario, the EDE from Rn-222 and its short-lived decay products per unit concentration of Ra-226 in the disposal unit is estimated as:

Rn-222, indoor residence in agriculture scenario -

$$(0.24 \text{ rem/y per } \mu\text{Ci/m}^3)(0.5) = 0.12 \text{ rem/y per } \mu\text{Ci/m}^3.$$

This dose estimate for Rn-222 is given in Table A.4-13.

The dose from Rn-222 per unit concentration of Ra-226 in soil while working in the vegetable garden is obtained as follows. The United Nations Scientific Committee on the Effects of Atomic Radiation (UNSCEAR 1988) has estimated that, for continuous exposure, the average EDE from exposure to Rn-222 outdoors would be 28% of the average dose from exposure to Rn-222 indoors. Therefore, for continuous residence outdoors, the EDE from exposure to Rn-222 and its short-lived decay products per unit concentration of Ra-226 in surface soil can be estimated from the previous result for continuous residence indoors as:

Rn-222, continuous residence outdoors -

$$(0.24 \text{ rem/y per } \mu\text{Ci/m}^3)(0.28) = 0.067 \text{ rem/y per } \mu\text{Ci/m}^3.$$

The dose per unit concentration from Rn-222 during outdoor residence derived above can be applied directly to the inhalation pathway while working in the vegetable garden containing Ra-226. Two corrections are needed in applying this result to the agriculture scenario. The first is the fraction of the year that an intruder spends working in the vegetable garden, which is assumed to be 0.01. The second is the dilution factor for mixing of radionuclides in exhumed waste from a disposal unit into soil in the garden, which is assumed to be 0.2. Thus, for inhalation exposure while working in the garden in the agriculture scenario, the EDE from Rn-222 and its short-lived decay products per unit concentration of Ra-226 in

e[illegible]ed waste is estimated as:

Rn-222, residence in vegetable garden in agriculture scenario -

(0.067 rem/y per μCi/m^3)(0.01)(0.2) = 1.3 × 10^{-4} rem/y per μCi/m^3.

This dose estimate for Rn-222 is given in Table A.4-12. This estimate may be somewhat conservative because the natural analog model is based on a distribution of radium to depths well below the ground surface, whereas the radium in garden soil in the agriculture scenario is assumed to be confined to a layer of surface soil 15 cm thick.

The dose analysis for inhalation exposure to Rn-220 and its short-lived decay products during outdoor residence and while working in the garden is based on the data on average doses from Rn-222 both indoors and outdoors presented previously and the following information. First, for continuous residence, the average dose from indoor Rn-220 would be 14% of the average dose from indoor Rn-222, and the average dose from outdoor Rn-220 would be about 26% of the average dose from outdoor Rn-222 (UNSCEAR 1988). Second, the doses from Rn-220 result from an average concentration of Th-232 in surface soil of 1 pCi/g (NCRP 1984), which corresponds to a concentration of 1.4 μCi/m^3. Th-232 can be regarded as the parent radionuclide for Rn-220 because the intermediate decay products Ra-228, Ac-228, Th-228, and Ra-224 all are sufficiently short-lived (see Table A.4-1) that they should be in secular equilibrium with Th-232 at any time following loss of active institutional control at 100 years after disposal.

Using the data on doses indoors and outdoors from Rn-222 presented previously, the information on Rn-220 and Th-232 given above, and the assumptions for the indoor and outdoor residence times and dilution factor for mixing of waste in the vegetable garden for the agriculture scenario, the following dose estimates for Rn-220 are obtained. For inhalation during indoor residence, the EDE from exposure to Rn-220 and its short-lived decay products per unit concentration of Th-232 in a disposal unit is estimated as:

Rn-220, indoor residence in agriculture scenario -

(0.2 rem/y)(0.14)(0.5) / (1.4 μCi/m^3) = 0.010 rem/y per μCi/m^3.

This dose estimate is given in Table A.4-13. For inhalation while working in the vegetable garden, the dose from exposure to Rn-220 per unit concentration of Th-232 in exhumed waste is estimated as:

- Rn-220, residence in vegetable garden in agriculture scenario -

  $(0.2\ \text{rem/y})(0.28)(0.26)(0.01)(0.2) / (1.4\ \mu\text{Ci/m}^3) =$

  2.1×10^{-5} rem/y per μCi/m^3.

This dose estimate is given in Table A.4-12. As described previously for Rn-222, this estimate may be somewhat conservative.

Decay of the long-lived isotopes U-235 and Pa-231 considered in the intruder dose analysis produces Rn-219. However, the 3.96-s half-life of this isotope (Kocher 1981) is too short for its production in surface soil to result in a significant inhalation exposure. Therefore, inhalation doses from Rn-219 and its short-lived decay products can be ignored in the dose analysis for the agriculture scenario.

All Pathways. For the agriculture scenario, the annual EDEs from all exposure pathways per unit concentration of radionuclides in disposal units at the time intrusion is assumed to occur are summarized in Table A.4-14. For each radionuclide the total dose is the sum of the doses from the vegetable, soil ingestion, external exposure, and inhalation pathways given in Tables A.4-8 through A.4-13.

Given the models and parameter values assumed in the dose analysis for the agriculture scenario, the most important exposure pathways depend on the particular radionuclide. For many of the fission and activation products, the vegetable pathway is by far the most important. However, for the photon-emitting radionuclides Co-60, Sn-126, and Cs-137, external exposure while residing in the home is the only important pathway. For Sm-151, the soil ingestion pathway is a minor contributor to the total dose. Finally, the inhalation pathways are never important for any fission and activation products. For Ra-226 and the actinide radionuclides, the vegetable and soil ingestion pathways and inhalation exposure while residing in the home usually are important contributors to the total dose, except the soil ingestion and

Table A4-11. Annual EDEs per unit concentration for radionuclides in [illegible] all exposure pathways for agricultural scenario[a]

Radionuclide[a]	Annual EDE (rem/y per μCi/m³)	Radionuclide[a]	Annual EDE (rem/y per μCi/m³)
H-3	3.9×10^{-6}	Th-232 + d [d]	3.5×10^{-3}
C-14	1.5×10^{-5}	Rn-220	1.0×10^{-2} [e]
Al-26	3.9×10^{-3}	Pa-231 + d	8.3×10^{-4}
Co-60	3.5×10^{-3}	U-232 + d [d]	2.3×10^{-3}
Ni-59	6.8×10^{-8}	Rn-220	1.0×10^{-2} [e]
Ni-63	1.8×10^{-7}	U-233	1.1×10^{-5}
Se-79	1.2×10^{-6}	U-234	1.1×10^{-5}
Rb-87	1.9×10^{-6}	U-235 + d	1.8×10^{-4}
Sr-90 + d	1.8×10^{-4}	U-236	1.0×10^{-5}
Zr-93 [b]	4.5×10^{-8}	U-238 + d	3.9×10^{-5}
Nb-93m	1.9×10^{-8}	Np-237 + d	5.0×10^{-4}
Tc-99	1.1×10^{-5}	Pu-238	3.4×10^{-5}
Pd-107	3.2×10^{-8}	Pu-239	4.0×10^{-5}
Cd-113m	1.3×10^{-4}	Pu-240	4.0×10^{-5}
Sn-121m	4.7×10^{-7}	Pu-241	7.7×10^{-7}
Sn-126 + d	2.6×10^{-3}	Pu-242	3.8×10^{-5}
I-129	8.3×10^{-5}	Pu-244	3.7×10^{-5}
Cs-135	1.2×10^{-6}	Am-241	5.6×10^{-5}
Cs-137 + d	7.7×10^{-4}	Am-242 + d	6.0×10^{-5}
Sm-151	1.0×10^{-8}	Cm-243	1.6×10^{-4}
Eu-154	1.7×10^{-3}	Cm-244	2.0×10^{-5}
Eu-155	4.0×10^{-5}	Cm-245	1.1×10^{-4}
Pb-210 + d	3.0×10^{-4}	Cm-246	4.0×10^{-5}
Ra-226 + d [c,d]	2.7×10^{-3}	Cm-247 + d	4.4×10^{-4}
Rn-222	1.2×10^{-1} [e]	Cm-248	1.4×10^{-4}
Th-229 + d	4.3×10^{-4}	Cf-249	4.6×10^{-4}
Th-230	1.1×10^{-5}	Cf-250	1.7×10^{-5}
		Cf-251	1.6×10^{-4}

[a] "+ d" denotes short-lived decay products that are assumed to be in secular equilibrium with parent radionuclide; see Table A.4-1 for decay products and branching fractions.

[b] Value assumes that Nb-93m is present in secular equilibrium.

[c] Value assumes that Pb-210 is present in secular equilibrium.

[d] Dose from radon decay product is listed separately.

[e] Dose is normalized to unit concentration of parent radionuclide.

inhalation pathways are of lesser importance when external exposure while residing in the home is a significant contributor to the total dose. For isotopes of Th and Pu, which are assumed to have a low plant-to-soil concentration ratio, the soil ingestion pathway is more important than the vegetable pathway.

The models for the exposure pathways involving mixing of exhumed waste with native soil in a vegetable garden may be somewhat conservative for radionuclides that are highly mobile in surface soil, because the models assume that the concentration in soil during the first year after mixing is not reduced as a result of leaching and transport to deeper soil layers by infiltrating precipitation. Thus, for mobile radionuclides, the average concentration in surface soil during the first year after mixing, which is the appropriate concentration for calculating the maximum annual dose to an intruder, could be substantially less than the initial concentration after mixing, and the annual dose per unit concentration in exhumed waste could be correspondingly overestimated.

The radionuclides in Table A.4-14 for which leaching and transport from surface soil in a vegetable garden by infiltrating precipitation could reduce the annual dose per unit concentration in exhumed waste include H-3 and Tc-99. In each case, a leaching model described in Sect. 3.2.3.3 (Baes and Sharp 1983) could be used to estimate the average concentration in surface soil during the first year after mixing of exhumed waste with native soil in the garden.

For H-3, which is expected to be removed from the soil root zone (i.e., the first 30 cm of surface soil) at the same rate as infiltrating water, the leaching correction described above would reduce the annual dose per unit concentration in exhumed waste by about a factor of five. This correction is not applied to the dose estimate for H-3 in Table A.4-14, but it could be taken into account in the dose analysis if estimated doses from H-3 are a significant fraction of the performance objective for protection of inadvertent intruders.

For Tc-99, the assumption of a small but non-zero distribution coefficient (K_d) in surface soil, such as given in Sect. 3.2.3.3, would reduce the annual dose per unit concentration in exhumed waste by less than a factor of two. Thus, the leaching correction undoubtedly is considerably less than the uncertainty in the plant-to-soil concentration ratio (B_v), which is the most important parameter in determining the dose from Tc-99 in the agriculture scenario.

Furthermore, there is evidence that the usual assumption of a low distribution coefficient for Tc-99 may overestimate considerably the removal rate from the soil root zone for a substantial fraction of the activity initially mixed into surface soil (Vandecasteele et al. 1989). Therefore, application of a leaching correction may not be valid in this case.

Resident scenario

In the resident scenario, exposures of inadvertent intruders are assumed to occur after an intruder encounters an intact and impenetrable engineered barrier (e.g., a concrete roof) while excavating to build a foundation for a home at the disposal site. An intruder then is assumed to build a home immediately on top of the intact engineered barrier and receives an external exposure while residing in the home. Ingestion and inhalation exposures are precluded when the waste is assumed to be inaccessible during excavation. The radionuclides included in the dose analysis for the resident scenario were selected on the basis of a screening analysis described in Sect. 3.2.4.4.

External dose during indoor residence for the resident scenario is estimated using the model given in Eq. (A.4-8). In implementing the model, the fraction of the year for indoor residence is assumed to be 0.5 and the shielding factor during indoor residence is assumed to be 0.7, as in the agriculture scenario. The dose-rate conversion factor for each radionuclide is the external dose rate per unit concentration in disposal units taking into account the shielding provided by the material in the source region (i.e., the waste itself) and by an intact concrete roof and/or layer of uncontaminated grout above the waste.

As described in Sect. 3.2.4.1 and A.4.4, only two bounding cases need to be considered in evaluating potential doses for the resident scenario. The first is exposure to both shorter-lived and long-lived photon-emitting radionuclides at 100 years after disposal when all engineered barriers in disposal units are assumed to be intact. The second case is exposure only to long-lived photon-emitting radionuclides in unshielded waste at a time long after disposal when all engineered barriers have lost their physical integrity and weathered to soil-equivalent material. However, as described in Sect. A.4.4, shorter-lived radionuclides also are included in the dose analysis for exposure to unshielded waste in order to evaluate the time period over which the engineered barriers must maintain their integrity and prevent access to the waste.

The model for calculating external dose in the resident scenario is summarized in Table A.4-15, which gives the annual EDE per unit concentration of radionuclides in the disposal units at the time intrusion occurs for different assumed thicknesses of shielding above the waste (see Sect. A.4.1). The results are obtained from the assumed exposure time and shielding factor during indoor residence and the external dose-rate conversion factors for the radionuclides of concern given in Table A.4-5. The results for 45-cm and 100-cm shielding apply to the bounding case of intact engineered barriers described above. The results for no shielding apply to the bounding case of no engineered barriers above the waste and are the same as the dose estimates during indoor residence for the agriculture scenario given in Table A.4-11.

In Table A.4-15, the calculations for no shielding apply to all disposal units, the calculations for 45-cm shielding apply to the LAW vaults, and the calculations for 100-cm shielding apply to the ILNT and ILT vaults. For the case of 45-cm shielding, results are presented only for those radionuclides selected by the screening analysis for the LAW vaults (see Sect. 3.2.4.4). For 100-cm shielding, no entry is given for Am-241 because the dose per unit concentration is too low to be of concern for any possible concentrations of this radionuclide in waste.

Post-drilling scenario

In the post-drilling scenario, exposures of inadvertent intruders are assumed to occur after an intruder drills through a disposal unit, e.g., for the purpose of constructing a well for a domestic water supply. The entire amount of drilling waste is assumed to be mixed with native soil in a vegetable garden, and the exposure pathways assumed for this scenario then include: 1) ingestion of vegetables grown in contaminated garden soil; 2) direct ingestion of contaminated soil in conjunction with vegetable intakes; 3) external exposure to contaminated soil while working in the garden; and 4) inhalation of suspended activity in particulate form and inhalation of isotopes of radon and their short-lived decay products while working in the garden. The radionuclides included in the dose analysis for the post-drilling scenario were selected on the basis of a screening analysis described in Sect. 3.2.4.4.

Table A.4-15. Annual EDEs per unit [illegible] radionuclides [illegible]

Radionuclide[a]	Annual EDE (rem/y per nCi/m³)		
	No shielding[b]	45 cm shielding[c]	100-cm shielding[d]
Al-26	3.9×10^{-3}	1.1×10^{-4}	2.3×10^{-6}
Co-60	—	8.8×10^{-5}	1.2×10^{-6}
Sn-121m	4.2×10^{-7}	—	—
Sn-126 + d	2.6×10^{-3}	2.2×10^{-5}	8.4×10^{-8}
I-129	2.8×10^{-6}	—	—
Cs-137 + d	7.6×10^{-4}	6.6×10^{-6}	2.2×10^{-8}
Eu-154	—	3.2×10^{-5}	3.5×10^{-7}
Eu-155	—	6.3×10^{-10}	—
Ra-226 + d	2.4×10^{-3}	6.0×10^{-5}	1.3×10^{-6}
Th-229 + d	3.5×10^{-4}	2.6×10^{-6}	3.5×10^{-8}
Th-232 + d	3.5×10^{-3}	1.1×10^{-4}	4.1×10^{-6}
Pa-231 + d	4.2×10^{-4}	1.1×10^{-6}	3.5×10^{-9}
U-232 + d	2.2×10^{-3}	9.2×10^{-5}	3.8×10^{-6}
U-235 + d	1.7×10^{-4}	3.9×10^{-8}	2.3×10^{-12}
U-238 + d	2.9×10^{-5}	3.0×10^{-7}	2.5×10^{-9}
Np-237 + d	2.4×10^{-4}	4.6×10^{-7}	2.8×10^{-10}
Am-241	9.5×10^{-6}	—	—
Am-242m + d	1.5×10^{-5}	6.2×10^{-8}	5.2×10^{-10}
Am-243 + d	2.0×10^{-4}	1.1×10^{-7}	4.2×10^{-11}
Cm-243	1.3×10^{-4}	4.9×10^{-8}	2.0×10^{-11}
Cm-245	7.4×10^{-5}	5.3×10^{-9}	—
Cm-247 + d	4.0×10^{-4}	1.3×10^{-6}	1.3×10^{-9}
Cf-249	4.2×10^{-4}	1.2×10^{-6}	1.1×10^{-9}
Cf-251	1.2×10^{-4}	3.1×10^{-8}	—

[a] "+ d" denotes short-lived decay products that are assumed to be in secular equilibrium with parent radionuclide; see Table A.4-1 for decay products and branching fractions.

[b] Results apply to all disposal units and at times long after disposal when engineered barriers above the waste are assumed to have lost their physical integrity and residence on unshielded waste becomes credible.

[c] Results apply to LAW vaults at 100 years after facility closure when engineered barriers are assumed to be intact and residence on unshielded waste is precluded.

[d] Results apply to ILNT and ILT vaults at 100 years after facility closure when engineered barriers are assumed to be intact and residence on unshielded waste is precluded.

The exposure pathways for the post drilling scenario are the same as the corresponding pathways for the agriculture scenario described previously, but external and inhalation exposures during indoor residence do not occur in the post drilling scenario since all of the exhumed waste is assumed to be mixed with native soil in the vegetable garden and the intruder's home is not located on top of exposed disposal units. Therefore, the models given by Eqs. (A.4-2) and (A.4-3) for the vegetable pathway, Eqs. (A.4-4) and (A.4-5) for the soil ingestion pathway, Eqs. (A.4-6) and (A.4-7) for external exposure while working in the garden, and Eqs. (A.4-9) through (A.4-11) for inhalation exposure to radionuclides in particulate form while working in the garden, as well as the natural analog model for estimating dose from exposure to radon while working in the garden, also apply to the post-drilling scenario.

In implementing the models for the different exposure pathways, most of the parameter values for the post-drilling scenario would be the same as the values assumed for the agriculture scenario. The one important exception is the dilution factor for mixing of radionuclides in exhumed waste with native soil in the vegetable garden, which is denoted by f_v. For all exposure pathways in the post-drilling scenario, the dose per unit concentration of a radionuclide in exhumed waste is directly proportional to this dilution factor.

In the post-drilling scenario, the volume of contaminated drilling waste is assumed to be 0.5 m^3 (Kennedy et al. 1983), and this material is assumed to be mixed to a depth of 15 cm in a vegetable garden of area about 200 m^2. The assumed area of the garden reasonably could provide half of the entire yearly intake of all vegetables by an intruder, which is the value assumed in this analysis. Therefore, the volume of soil in the garden into which the drilling waste is mixed is about 30 m^3, and the resulting dilution factor is about 0.02. The assumed dilution factor for the post-drilling scenario thus is a factor of ten less than the value 0.2 assumed for the agriculture scenario. Therefore, for any exposure pathway in the post-drilling scenario, the dose per unit concentration of a radionuclide in exhumed waste is a factor of ten less than the corresponding value for the same pathway in the agriculture scenario.

For the post-drilling scenario, the annual EDE from all exposure pathways per unit concentration of radionuclides in exhumed waste at the time intrusion occurs, as obtained from the models and parameter values described above, is summarized in Table A.4-16. The

Table A-4-16. Annual EDE per unit concentration of radionuclides in contaminated soil for post-drilling scenario[a]

Radionuclide[b]	Annual EDE (rem/yr per µCi/m³)
H-3	3.9×10^{-7}
C-14	1.5×10^{-6}
Al-26	1.8×10^{-5}
Co-60	1.8×10^{-6}
Ni-59	6.8×10^{-9}
Ni-63	1.8×10^{-8}
Se-79	1.2×10^{-7}
Rb-87	1.9×10^{-7}
Sr-90 + d	1.8×10^{-5}
Zr-93 [c]	3.5×10^{-9}
Nb-93m	1.8×10^{-9}
Tc-99	1.1×10^{-6}
Pd-107	3.2×10^{-9}
Cd-113m	1.3×10^{-5}
Sn-121m	5.3×10^{-9}
Sn-126 + d	1.4×10^{-6}
I-129	8.1×10^{-6}
Cs-135	1.2×10^{-7}
Cs-137 + d	1.2×10^{-6}
Sm-151	9.3×10^{-10}
Eu-154	8.4×10^{-7}
Eu-155	2.6×10^{-8}
Pb-210 + d	3.0×10^{-5}
Ra-226 + d [d,e]	3.2×10^{-5}
Rn-222	1.3×10^{-5} [f]
Th-229 + d	2.9×10^{-6}
Th-230	3.4×10^{-7}
Th-232 + d [e]	5.9×10^{-6}
Rn-220	2.1×10^{-6}
Pa-231 + d	1.8×10^{-5}
U-232 + d [e]	5.6×10^{-6}
Rn-220	2.1×10^{-6}

See end of table for footnotes.

Table A.4-16. (continued)

Radionuclide[b]	Annual EDE (rem/y per μCi/m³)
U-233	7.5×10^{-7}
U-234	7.3×10^{-7}
U-235 + d	7.9×10^{-7}
U-236	6.9×10^{-7}
U-238 + d	6.6×10^{-7}
Np-237	2.4×10^{-5}
Pu-238	2.1×10^{-6}
Pu-239	2.5×10^{-6}
Pu-240	2.5×10^{-6}
Pu-241	4.8×10^{-8}
Pu-242	2.4×10^{-6}
Pu-244	2.3×10^{-6}
Am-241	3.1×10^{-6}
Am-242m + d	3.0×10^{-6}
Am-243 + d	3.2×10^{-6}
Cm-243	1.6×10^{-6}
Cm-244	1.3×10^{-6}
Cm-245	2.5×10^{-6}
Cm-246	2.5×10^{-6}
Cm-247 + d	2.5×10^{-6}
Cm-248	8.9×10^{-6}
Cf-249	2.7×10^{-6}
Cf-250	1.0×10^{-6}
Cf-251	2.6×10^{-6}

[a] Values are one-tenth the sum of doses for agriculture scenario in Tables A.4-8 through A.4-10 and A.4-12.

[b] "+ d" denotes short-lived decay products that are assumed to be in secular equilibrium with parent radionuclide; see Table A.4-1 for decay products and branching fractions.

[c] Value assumes that Nb-93m is present in secular equilibrium.

[d] Value assumes that Pb-210 is present in secular equilibrium.

[e] Dose from radon decay product is listed separately.

[f] Dose is normalized to unit concentration of parent radionuclide.

dose per unit concentration from the vegetable, soil ingestion, external exposure, and inhalation pathways again is one-tenth of the corresponding values for the agriculture scenario in Tables A.4-8 through A.4-10 and A.4-12, respectively.

Since all of the exposure pathways for the post-drilling scenario involve mixing of exhumed waste into surface soil in a vegetable garden, the leaching correction for H-3 discussed previously with the agriculture scenario also could be applied in this case. However, for the reasons previously discussed, a leaching correction will be applied in the dose analysis for the post-drilling scenario only if the dose from H-3 is expected to be significant.

A.4.6 Summary

This appendix has presented the models and data bases used in estimating annual EDEs to 1) off-site individuals resulting from exposure to radionuclides in contaminated groundwater and 2) inadvertent intruders resulting from direct intrusion into the EAV. In each case, particular exposure scenarios and associated exposure pathways have been assumed. The scenarios and pathways chosen for analysis and the radionuclides selected for the dose analysis for each scenario were based on considerations discussed in Sect. 3.2.3 and 3.2.4. For each exposure pathway, simple models for estimating dose have been developed, and annual doses per unit concentration of radionuclides in groundwater or in disposal units have been estimated on the basis of assumed parameter values for the particular pathway models.

For each exposure scenario, the annual doses per unit concentration of a radionuclide for each exposure pathway have been combined to obtain the total dose per unit concentration from all pathways. The following tables give the total dose per unit concentration at the time intrusion occurs for the different exposure scenarios:

- Table A.4-6, exposure of off-site individuals to radionuclides in contaminated groundwater via the drinking water pathway;
- Table A.4-14, agriculture scenario for exposure of inadvertent intruders to radionuclides in disposal units;
- Table A.4-15, resident scenario for exposure of inadvertent intruders to photon-emitting radionuclides in disposal units; and

- Table A.4-16, post drilling scenario for exposure of inadvertent intruders to radionuclides in disposal units.

The dose analyses for each exposure scenario and exposure pathway were based on certain model parameters, some of which are radionuclide- or element-specific and others of which are independent of radionuclide. The radionuclide- or element-specific parameter values are given in Tables A.4-2 through A.4-5 and A.4-7. The parameter values that are independent of radionuclide are summarized in Table A.4-17.

For the three scenarios involving direct intrusion into the EAV, the radionuclide concentrations in the disposal units to which the annual doses obtained in this analysis are normalized are the concentrations at the time intrusion is assumed to occur, rather that the concentrations at the time of disposal. That is, the dose analysis for these scenarios presented in this appendix does not include any assumptions about the time after disposal at which intrusion occurs, except in the case of the resident scenario where bounding calculations based on intrusion at 100 years after disposal or at times long after disposal were performed. In most cases, assumptions about the time intrusion occurs are applied when the results of the intruder dose analyses in this appendix are combined with the results of the PAs for the disposal facility, which yield predictions of the concentrations of radionuclides remaining in the disposal units as a function of time after disposal.

Table A.1-17. Summary of radionuclide-independent parameter values used in dose analyses for off-site individuals and inadvertent intruders

Parameter description	Symbol	Parameter value
Consumption of contaminated drinking water[a]	U_w	730 L/year
Consumption of contaminated vegetables[b]	U_v	90 kg (fresh weight) per year
Density of soil[b]	ρ_s	1,400 kg/m^3
Dilution factor for mixing of exhumed waste with native soil in vegetable garden	f_s	0.2[c] 0.02[d]
Consumption of contaminated soil[b]	U_s	0.037 kg/year
Exposure times -		
working in garden[b]	U_g	1% per year
residing in home[e]	U_h	50% per year
Shielding factor for external exposure during indoor residence[e]	S	0.7
Air intake (breathing rate)[b]	U_a	8,000 m^3/year
Atmospheric mass loading of contaminated surface soil -	L_a	
working in garden[b]		10^{-7} kg/m^3
residing in home[e]		10^{-8} kg/m^3

[a] Parameter applies to exposure of off-site individuals.

[b] Parameter applies to agriculture and post-drilling scenarios for inadvertent intruders.

[c] Parameter applies to agriculture scenario for inadvertent intruders.

[d] Parameter applies to post-drilling scenario for inadvertent intruders.

[e] Parameter applies to agriculture and resident scenarios for inadvertent intruders.

APPENDIX A REFERENCES

ACRI. 1993. *POLYFLOW: A Model for Fluid Flow, Heat and Mass Transport in Multifluid, Multiphase Fractured or Porous Media, Users Manual, Version 2.5.* Draft. Analytic and Computational Research, Inc., Los Angeles, Calif.

Anspaugh, L. R., J. H. Shinn, P. L. Phelps, and N. C. Kennedy. 1975. Resuspension and Redistribution of Plutonium in Soils. *Health Physics.*, 29:571.

Baes, C. F. III, and R. D. Sharp. 1983. A Proposal for Estimation of Soil Leaching Constants for Use in Assessment Models. *Journal of Environmental Quality,* 12:17.

Baes, C. F. III, R. D. Sharp, A. L. Sjoreen, and R. W. Shor. 1984. *A Review and Analysis of Parameters for Assessing Transport of Environmentally Released Radionuclides Through Agriculture.* ORNL-5786. Oak Ridge National Laboratory.

Christiansen, E. J., and D. E. Gordon. 1983. *Technical Summary of Groundwater Quality Protection Program at Savannah River Plant.* DPST-83-829, Vol. 1. E. I. Du Pont de Nemours & Co., Inc., Savannah River Laboratory, Aiken, S.C.

CRC Press, Inc. 1981. *CRC Handbook of Chemistry and Physics.* Robert C. Weast and Melvin J. Astle, eds. Baca Raton, FL.

de Marsily, G. 1986. *Quantitative Hydrogeology.* Academic Press, Inc., New York, NY.

Dennehy, K. F., and P. B. McMahon. 1987. *Water Movement in the Unsaturated Zone at a Low-Level Radioactive-Waste Burial Site Near Barnwell, South Carolina.* U. S. Geological Survey Open-File Report 87-46, p.66.

Eckerman, K. F., and J. C. Ryman. 1993. *External Exposure to Radionuclides in Air, Water, and Soil.* Federal Guidance Report No. 12. EPA 402-R-93-081. Oak Ridge National Laboratory and U. S. Environmental Protection Agency.

Freeze, R. A., and J. A. Cherry. 1979. *Groundwater,* Prentice-Hall, Inc., N.J.

Geotrans. 1992. *Groundwater Flow Model for the General Separations Area, Savannah River Plant.* Draft Report. Geotrans, Inc., Sterling, Va.

Hamby, D. M. 1992. Site-Specific Parameter Values for the Nuclear Regulatory Commission's Food Pathway Dose Model. *Health Physics,* 62:136.

Hubbard, J. E., and M. Engelhardt. 1987. *Calculation of Groundwater Recharge at the Old SRP Burial Ground Using the CREAMS Model (1961-1986).* July 31, 1987, Memorandum from J. E. Hubbard and M. Engelhardt, Department of Earth Sciences, State University of New York, College at Brockport, N.Y.

INTERA. 1986. *Validation of Unsaturated Flow Models Using Tank 24 Lysimeter Data.* INTERA Technologies report H01203R005, INTERA Technologies, Inc., Austin, Texas.

Kennedy, W. E. Jr., B. A. Napier, and J. K. Soldat. 1983. Advanced Disposal Systems for Transuranic Waste: Preliminary Disposal Criteria for Plutonium-239 at Hanford. *Nuclear Chemical Waste Management,* 4:103.

Kocher, D. C. 1981. *Radioactive Decay Data Tables.* DOE/TIC-11026. U. S. Department of Energy.

Kocher, D. C., and A. L. Sjoreen. 1985. Dose-Rate Conversion Factors for External Exposure to Photon Emitters in Soil. *Health Physics,* 48:193.

Napier, B. A., R. A. Peloquin, W. E. Kennedy, Jr., and S. M. Neuder. 1984. *Intruder Dose Pathway Analysis for the Onsite Disposal of Radioactive Waste: The ONSITE/MAXII Computer Program.* NUREG/CR-3620, PNL-4054. Pacific Northwest Laboratory.

NCRP. 1984. *Exposures from the Uranium Series with Emphasis on Radon and Its Daughters.* NCRP Report No. 77. National Council on Radiation Protection and Measurements, Bethesda, MD.

NCRP. 1987. *Exposure of the Population in the United States and Canada from Natural Background Radiation.* NCRP Report No. 94. National Council on Radiation Protection and Measurements, Bethesda, MD.

NRC. 1977. *Regulatory Guide 1.109. Calculation of Annual Doses to Man from Routine Releases of Reactor Effluents for the Purpose of Evaluating Compliance with 10 CFR Part 50, Appendix I.* U. S. Nuclear Regulatory Commission, Washington, D.C.

NRC. 1981. *Draft Environmental Impact Statement on 10 CFR Part 61 "Licensing Requirements for Land Disposal of Radioactive Waste".* NUREG-0945, Vol. 1. U. S. Nuclear Regulatory Commission, Washington, D.C.

Orebaugh, E. G., and R. M. Wallace. 1989. *Quantification of Hazards Associated with the Decay Storage/Disposal of Tritium Crucibles (U)*. WSRC-RP-89-1226.

Oztunali, O. I., G. C. Re, P. M. Moskowitz, E. D. Picano, and C. J. Pitt. 1981. *Data Base for Radioactive Waste Management*. NUREG/CR-1759, Vol. 3. Dames and Moore, Inc.

Oztunali, O. I., and G. W. Roles. 1986. *Update of Part 61 Impacts Analysis Methodology*. NUREG/CR-4370. U. S. Nuclear Regulatory Commission and Envirosphere Company.

Parizek, R. R., and R. W. Root. 1986. *Development of a Ground-Water Velocity Model for the Radioactive Waste Management Facility, Savannah River Plant, South Carolina*. College of Earth and Mineral Sciences, Pennsylvania State University, University Park, Penn.

Sheppard, M. I., S. C. Sheppard, and B. D. Amiro. 1991. Mobility and Plant Uptake of Inorganic ^{14}C and ^{14}C-Labelled PCB in Soils of High and Low Retention. *Health Physics*, 61:481.

Shinn, J. H., D. N. Homan, and D. D. Gay. 1982. Plutonium Aerosol Fluxes and Pulmonary Exposure Rates During Resuspension from Bare Soils Near a Chemical Separation Facility, p. 1131 in *Precipitation Scavenging, Dry Deposition, and Resuspension*. Vol. 2. Ed. by H. R. Pruppacher, R. G. Semonin, and W. G. N. Slinn, Elsevier Science Publishing Co., New York, N.Y.

Thompson, D. G. 1991. *RE: Vault Closure Concept for Saltstone Vaults*. Internal Report OPS-DTZ-91-0002. Westinghouse Savannah River Co., Savannah River Site, Aiken, S.C.

UNSCEAR. 1988. *Sources, Effects and Risks of Ionizing Radiation*. United Nations Scientific Committee on the Effects of Atomic Radiation, New York, N.Y.

U.S.DOE. 1988a. Management of Low-Level Waste, Chapter III in *Radioactive Waste Management*. Order 5820.2A, U. S. Department of Energy.

U.S.DOE. 1988b. *Internal Dose Conversion Factors for Calculation of Dose to the Public*. DOE/EH-0071. U. S. Department of Energy.

U.S EPA. 1989a. *User's Guide for AIRDOS-PC*. EPA/520/6-89-035. U. S. Environmental Protection Agency, Office of Radiation Programs, Las Vegas Facility, Las Vegas, Nev.

U.S. EPA. 1989b. *Risk Assessment Guidance for Superfund. Volume I. Human Health Evaluation Manual (Part A).* EPA/540/1-89/002. U. S. Environmental Protection Agency, Washington, D. C.

Vandecasteele, C. M., J. P. Dehut, S. Van Laer, D. Deprins, and C. Myttenaere. 1989. Long-Term Availability of Tc Deposited on Soil after Accidental Releases. *Health Physics*, 57:247.

APPENDIX B

COMPUTER CODES

B.1. CODE SELECTION CRITERIA AND CONSIDERATIONS

Listed below are criteria that were considered in selecting computer codes for use in the RPA of the MAV at the Savannah River Plant. The first list, which follows directly, consists of absolute requirements for any code (1R = #1, Required); any code not meeting any one of these requirements was rejected.

1R. The theoretical framework of the selected computer code(s) should be based on appropriate fundamental principles of chemistry and physics (e.g., conservation of mass, momentum, and energy) and well established constitutive equations (e.g., Darcy's law, Fick's law, etc.).

2R. The selected code(s) should be verified (i.e., simulation results compared against known analytical solutions of the underlying equations) to demonstrate correctness of the source code. Such verification should be fully documented in a technical report made available, at a minimum, to SRS and the Peer Review Panel.

3R. The selected code should be documented in a technical report and contain descriptions of: 1) model theory, governing equations and assumptions, 2) computational techniques and algorithms, and 3) example applications.

4R. All simulation codes(s) selected for use in the PAs must be maintained under a software QA and management program that assures that modifications and updates are traceable, auditable and documented, and that all production versions have been verified and validated.

This second list contains criteria describing attributes of computer codes that, though desirable, may not be presently attainable (1S = #1, Suggested). Consideration was given to these criteria, and justification for using a code not meeting them is given in this appendix.

1S. The code(s) should allow site- and facility-specific applications; i.e., be capable of simulating the hydrologic, geologic and/or geochemical setting of the site, as well as specific design features of the facility over time.

2S. A contaminant transport code should be capable of: 1) tracking waste inventory over time, including radioactive daughter products, and 2) computing the contaminant fluxes at designated locations as a function of driving hydrologic processes and mass transport phenomena.

3S. The code(s) should be validated (e.g., simulation results compared with field data) for a system similar to that being modeled whenever possible. Benchmarking (i.e., code-to-code comparisons) is also useful in demonstrating code capabilities.

4S. The degree of complexity of the computer code(s) should be consistent with the quantity and quality of data, and the objectives of the computation. Screening calculations and sensitivity analyses should be used to simplify conceptual models, and ultimately direct code selection.

5S. Hardware requirements for the selected code should not be exotic (i.e., codes should run on readily accessible mainframe, mini, or personal computers (PC); convertibility is highly desirable).

6S. Proprietary codes should be used only if they provide a distinct advantage over public domain codes and only if the author(s)/custodian(s) allow inspection and verification of the source code. If a proprietary code is used, it must be made available by lease or purchase to WSRC-IWT.

7S. Consideration must be given to the ease of interfacing code output with other codes. For example, it is often desirable to use a groundwater code that simulates unsaturated and saturated flow, as well as mass transport, as coupling of output from each simulation type has already been accomplished.

8). Familiarity with the code(s) should also be a consideration in selection, in light of time constraints that may be imposed for completion of a given Performance Assessment, and the need to revise the code if problems arise.

B.2 GEOCHEMICAL COMPUTER CODE

The composition of EAV pore fluids was estimated using the MINTEQ geochemical code.

I. Code Description - MINTEQ

Purpose and Scope: MINTEQ is a geochemical computer code used to predict and evaluate the equilibrium behavior of inorganic pollutants in a variety of geochemical environments. The code can model complex equilibrium relationships that exist among soluble species, insoluble solids, gases, and adsorbed species. The code can also be used to calculate the consequences of equilibrium mass transfer between aqueous and solid phases. However, the code does not have the capability to calculate reaction path models nor can it calculate reaction kinetics. MINTEQ is useful for calculating the source term concentrations and speciation of inorganic contaminants. In addition, MINTEQ contains algorithms that predict the sorption of contaminants on soils and sediments. The sorption algorithms include: activity K_d, Langmuir isotherm, Freundlich isotherm, ion exchange, and surface complexation models. The code incorporates a Newton-Raphson iteration scheme to solve the set of mass-action and mass-balance expressions.

Development History: The MINTEQ code was originally developed at Pacific Northwest Laboratory (Felmy et al. 1984a) by combining the mathematical structure of the MINEQL and the geochemical attributes of the WATEQ geochemical codes. MINTEQ was developed to solve geochemical equilibria problems by applying fundamental principles of

thermodynamics. Changes to the code since its creation have been confined to improving ease of input and the flexibility of the output. Additional thermodynamic data has also been added to the database.

Code Attributes: The code is written in FORTRAN 77 programming language and includes several input data files containing data necessary for the operation of the code, such as: thermodynamic data, component identification numbers, ion charge and size, and formula weights.

Computer Requirements: Many applications of MINTEQ can be performed effectively and efficiently on a PC with a 286 central processor unit (cpu). More complex calculations will be more efficiently processed on a PC with a 386 cpu or on a work station. MINTEQ can also be run on mainframe computer systems.

Restrictions: The MINTEQ code was developed by Pacific Northwest Laboratory for the U.S. NRC and the EPA; the code is public domain software. The code is documented in Felmy et al. (1984a), Brown and Allison (1987), and Peterson et al. (1987).

II. Code Selection Basis

General Critique: MINTEQ is one of several computer codes that has been developed to calculate equilibrium aqueous speciation and mineral mass transfer. Mechanistic adsorption models are included in the MINTEQ code, a major advantage over other geochemical codes such as EQ3/EQ6. The fundamental limitation of MINTEQ and other equilibrium based geochemical codes is that equilibrium conditions are often not obtained in low temperature systems. Furthermore, metastable conditions may persist for long periods of times in experimental systems, and experimentally observed concentrations may differ from those predicted by the code.

Code Verification: MINTEQ calculates the equilibrium speciation for an aqueous composition. Verification can be performed by using the MINTEQ output and hand calculations to evaluate equilibrium. In addition, the MINTEQ code was verified during its development by comparison calculations against WATEQ4 (Felmy et al. 1984a, b)

Code Benchmarking: The code has been benchmarked using the river water test case of Nordstrom et. al. (1979; see Peterson et al. 1987). In addition, the code was benchmarked against WATEQ4 during development (Krupka and Morrey 1985).

Code Validation: The MINTEQ code has been partially validated for aqueous systems containing Cu(II), Pu, and U (Krupka and Morrey 1985).

III. Theoretical Framework

Governing Equation and Assumptions: The MINTEQ code calculates equilibrium speciation of aqueous phases. Speciation is defined as the chemical form of an element in an aqueous solution. The code solves mass balance expressions for each component ion (e.g., Ca^{2+}, HCO_3^-, Na^+, etc.) using mass action relationships and equilibrium constants relating each species (such as CO_3^{2-}, a species of the HCO_3^- component) to MINTEQ components. Equilibrium constants for species are provided in the THERMO.DAT data base for calculations at a reference temperature of 25°C and infinite dilution. For temperatures that differ from 25°C, equilibrium constants are calculated either by using the Van't Hoff equation and enthalpies of reaction included in the data base or from analytical expressions relating equilibrium constants to temperature (Smith 1988). The concentration dependence of equilibrium constants is derived from individual ion activity coefficients calculated from the modified Debye-Huckel equation (Trusdell and Jones 1974), the Davies equation (Trusdell and Jones 1974), or the B-dot equation (Smith 1988).

Initial Conditions: The algorithm used in MINTEQ requires estimated starting values for the activities of component species. If these activity estimates are too far from the true values, the algorithm may fail to converge.

Numerical Techniques: MINTEQ uses a Newton-Raphson iteration method to simultaneously solve the non-linear mass balance equations.

IV. Code Inputs and Outputs

Input Data Structure: To execute the MINTEQ computer code, an input data file is prepared for each problem. The data file consists of

- title or run identifier,
- analytical units and temperature,
- run-specific user options,
- component identification and concentrations, and
- component modifications (e.g., concentration of H^+ fixed by pH).

Output Options: The MINTEQ code outputs the following:

- Echo of the data file input
- progress of the Newton-Raphson iterations
- full speciation of the input water composition
- charge balance and ionic strength for the aqueous composition
- saturation state of the water with respect to minerals in the data base

The user can also specify that the thermodynamic data base be printed. Debugging printing options are supported.

B.3 VAULT DEGRADATION COMPUTER CODE

I. Code Description - Concrete Degradation and Steel Reinforcement Corrosion

Purpose and Scope: The code used to estimate concrete degradation and rebar corrosion is designed to model the important degradation processes that can affect the long-term performance of concrete barriers. The processes modeled include: 1) concrete attack by sulfate and magnesium, 2) concrete leaching (both concrete and geologically controlled), 3) carbonation, and 4) rebar corrosion.

Development History: The current model consists of analytical solutions for concrete degradation processes. These solutions were selected as the best available means of predicting long-term concrete barrier performance.

Code Attributes: The code is written in Mathematica programming language (Wolfram 1988) and consists of four separate modules. Three of the modules are used to estimate concrete degradation and one is used to predict corrosion of steel reinforcement.

Sulfate and magnesium attack on concrete is described by an empirical relationship determined by Atkinson and Hearne (1984). Leaching of concrete components is described by a shrinking core model, in the case of concrete-controlled leaching, and by diffusional mass transport for geologic-controlled leaching (Atkinson and Hearne 1984). Walton et al. (1990) derived a shrinking core model to describe concrete carbonation. Rebar corrosion is described by an empirical correlation to determine time to onset of corrosion from chloride attack (Clear 1976) and a one dimensional diffusion calculation for actual corrosion (Walton et al. 1990).

Computer Requirements: The code was developed on an Apple Macintosh™ IIcx and has also been run using a NEXT workstation. The code will run on any workstation, mainframe or PC that runs Mathematica. The degradation code will run on any system running the Mathematica software package. The Macintosh, Version 1.2.2, recommends a minimum of 4 megabytes of RAM.

Restrictions: The code has been developed in the Mathematica software package and is therefore restricted by the purchase of the software.

II. Code Selection Basis

General Critique: The code is a compilation of analytical solutions for important concrete degradation processes (Clear 1976; Atkinson and Hearne 1984; Walton et al. 1990) selected based on the work of Walton et al. (1990). These analytical solutions are considered to be the best available means of predicting concrete degradation. The equations that are used to represent the degradation processes are based on observed conditions (i.e., sulfate, magnesium, chloride and dissolved oxygen concentrations in groundwater, etc.). However, in some cases the conditions encountered in a PA are very different from the conditions on which the empirical relationships are based. Also, the observations that form the basis of the equation are for much shorter periods of time (tens of years) than is needed for PAs (thousands of years).

Code Verification: The Mathematica's version of the code has been verified against the results of Walton et al. 1990.

Code Benchmarking: The code is made up of analytical solutions, therefore the benchmarking process does not apply.

Code Validation: The code is made up of analytical solutions, therefore the validation process does not apply.

III. Theoretical Formulation

Governing Equation and Assumptions:

Sulfate and Magnesium Attack. The equations that form the basis for the calculations are based on chemical reactions between concrete and rebar with chemical constituents from the waste and/or the geologic media surrounding the vault. Sulfate attack on concrete is the result of reactions of sulfate with hydrated tricalcium aluminate (C_3A) and portlandite [$Ca(OH)_2$] to form compounds of larger volume leading to expansion and disruption of the concrete. The reactions between sulfate and cement compounds can be written as

Gypsum:

$$Ca(OH)_2 + SO_4^{2-} + 2H_2O \Longrightarrow CaSO_4 \cdot 2H_2O + 2OH^-$$

Monosulphoaluminate:

$$3CaO \cdot Al_2O_3 \cdot 6H_2O + CaSO_4 + 6H_2O \Longrightarrow 3CaO \cdot Al_2O_3(CaSO_4) \cdot 12H_2O$$

Ettringite:

$$3CaO \cdot Al_2O_3(CaSO_4) \cdot 12H_2O + 2CaSO_4 + 20H_2O \Longrightarrow 3CaO \cdot Al_2O_3 \cdot 3(CaSO_4) \cdot 32H_2O$$

An example of a reaction between cement paste and magnesium sulfate is

Brucite:

$$3CaO \cdot 2SiO_2 + 3MgSO_4 \cdot 7H_2O \Longrightarrow 3CaSO_4 \cdot 2H_2O + 3Mg(OH)_2 + 2SiO_2 + 2H_2O$$

The low solubility of $Mg(OH)_2$ causes the reaction to proceed to completion, making the attack more severe.

The depth of sulfate and magnesium attack is described by the equation

$$x = 0.55\ C_a\ (Mg^{2+} + SO_4^{2-})t$$

where

x = depth of deterioration (cm),
C_a = weight percent of C_3A in non-hydrated cement,
Mg^{2+} = concentration of magnesium in the bulk solution (mol/L),
SO_4^{2-} = concentration of sulfate in the bulk solution (mol/L), and
t = time (years).

Assumptions: The rate of attack is proportional to sulfate and magnesium concentration in the solution and C_3A content of the cement.

Limitations: Correlations are only valid over the time/system parameters tested. Application outside this range is highly questionable.

The empirical correlation does not include the impacts of advective transport and/or the known importance of water to cement ratio (WCR) on durability. Application of the model is not clearly conservative.

Concrete-Controlled Leaching of Calcium Hydroxide. Cement components will be leached from concrete in environments in contact with water and have significant percolation rates. The alkalis are the first components to be leached followed by calcium hydroxide. The leaching of calcium hydroxide from the cement is described by

$$Ca(OH)_2 \Longrightarrow Ca^{2+} + 2OH^-$$

The equation that describes concrete controlled leaching is

$$x = [2D_i \{(C_i - C_{gw})/C_s\}t]^{1/2}$$

where

- x = depth of leaching (cm),
- D_i = intrinsic diffusion coefficient of Ca^{2+} in concrete solid (cm^2/s),
- C_i = concentration of Ca^{2+} in concrete pore water (mol/cm^3),
- C_{gw} = concentration of Ca^{2+} in the groundwater or soil moisture (mol/cm^3),
- C_s = bulk concentration of Ca^{2+} in the concrete solid (mol/cm^3), and
- t = time (s).

Assumptions: The rate of calcium removal from the exterior of the concrete is assumed to be rapid relative to the movement of calcium ions through the concrete. Therefore, diffusion controls the transport rate of the calcium.

Limitations: Diffusional mass transport is considered, but advection through and around the concrete is not considered.

D_i for the leached portion of the concrete will be substantially higher than D_i for intact concrete. Permeability of the concrete will increase as leaching proceeds leading to greater flow rates through the leached area. Diffusional control may no longer be valid under these conditions.

Geology-Controlled Leaching of Calcium Hydroxide. Geology-controlled leaching occurs as a result of the diffusion being controlled by the geologic material surrounding the concrete. The resulting equation is

$$x = 2 \text{ phi } [(C_i - C_{gw} / C_b] [(R_d D_E t) / \pi]^{1/2}$$

where

x	= depth of leaching (cm),
phi	= porosity of the geologic material (cm^3 voids/cm^3 total),
C_1	= concentration of Ca^{2+} in concrete pore water (mol/cm^3),
C_{gw}	= concentration of Ca^{2+} in the groundwater or soil moisture (mol/cm^3),
C_b	= concentration of Ca^{2+} in the bulk concrete (solid+pore) (mol/cm^3),
R_d	= retardation factor for Ca^{2+} in the geologic material,
D_E	= effective dispersivity/diffusivity of Ca^{2+} in geologic material (cm^2/s), and
t	= time (s).

Assumptions: Diffusion into the surrounding geologic material controls leaching. Leaching is highest in low calcium concentration environments.

Limitations: Parameters for geologic material are needed (R_d, D_E, phi).

Concrete Carbonation. Carbonation is typically thought of as the reaction between calcium hydroxide and carbon dioxide as represented by

$$Ca(OH)_2 + CO_2 ==> CaCO_3 + H_2O$$

Carbonation can occur only as rapidly as dissolved carbonate can diffuse through the concrete. Carbonation rate is dependent on the moisture content of the concrete and the relative humidity of the ambient medium and the concentration of CO_2 in the ambient medium. If diffusion in the concrete is too slow, an equilibrium is reached where the diffusion of CO_2 and carbonation are stopped or severely reduced.

Carbonation rate is dependent on the moisture content of the concrete. As relative humidity changes from 0 to 100%, the rate of carbonation passes through a maximum.

Because the pH in concrete is high (>12), the carbonation reaction actually occurs as

$$Ca(OH)_2 + CO_3^{2-} ==> CaCO_3 + 2OH^-$$

The relationship between carbonation depth and groundwater concentration, portlandite in the concrete, and intrinsic diffusion coefficient of calcium is:

$$x = [2D_i (C_{gw}/C_s) t]^{1/2}$$

where

- x = depth of carbonation (cm),
- D_i = intrinsic diffusion coefficient of Ca^{2+} in concrete (cm^2/s),
- C_{gw} = concentration of total inorganic carbon in the groundwater (mol/cm^3),
- C_s = bulk concentration of $Ca(OH)_2$ in the concrete solid (mol/cm^3), and
- t = time (s).

Assumptions: Concrete is saturated with water.

Limitations: The type of cement ultimately affects the depth of carbonation. This relationship becomes increasingly invalid as the relative humidity of the concrete decreases from 100% to 50%; below this level, the reaction rates decline rapidly resulting in a reduction in carbonation rate.

Reinforcement Corrosion/Chloride Attack. The alkaline environment of the concrete and the isolation it provides from external corrosive agents protects the steel reinforcement from corrosion by forming a protective oxide layer on the metal surface. The passive oxide layer may undergo attack by corrosive agents as the concrete deteriorates. Historically, aqueous chloride is the corrosive agent associated with the break up of the passive layer.

Reinforcement corrosion may also be associated with reduction of concrete alkalinity in the absence of elevated chloride levels. Carbonation and leaching can cause a decrease in the concrete pH with eventual loss of passivity.

Chloride attack is modeled in two stages (a) time to breakup of the passive layer and initiation of corrosion and (b) corrosion rate subsequent to breakup of the passive layer. An

empirical correlation for the time to passive layer breakup is

$$t_c = (129\ x_c^{1.22})/(WCR\ Cl^{0.42})$$

where

t_c = time to onset of corrosion (years),
x_c = thickness of concrete over the rebar (in.),
WCR = water to cement ratio (by mass), and
Cl = chloride ion concentration in groundwater (ppm).

Assumptions: The time to onset of corrosion is related to the water to cement ratio, depth of cement cover, and chloride concentration in groundwater.

Limitations: Applicability to conditions outside the observed chloride concentrations on which the equation is based is questionable.

The simplest method of estimating the corrosion rate subsequent to initiation of corrosion is a one dimensional diffusion calculation assuming limitation of the corrosion rate by oxygen diffusion. The percent of reinforcement remaining at any time is given by

$$\%\ \text{remaining} = 100[(4*9.4\ sD_iC_{gw}t)/(\text{pi}\ d^2\ \text{delta}\ x)]$$

where

s = spacing between reinforcement bars (cm),
D_i = intrinsic diffusion coefficient of O_2 in concrete (cm^2/s),
C_{gw} = concentration of oxygen in the groundwater (mol/cm^3),
delta x = depth of reinforcement below surface (cm), and
t = time (s).

Assumptions: The corrosion rate is limited by oxygen diffusion.

Limitations: Applicable only if oxygen diffusion controls corrosion.

Initial Conditions: Not applicable.

Numerical Techniques: Not applicable.

IV. Code Inputs and Outputs

Input Data Structure: Input for the calculations is contained in the Mathematica file for degradation calculations. The values may be changed from within Mathematica and the file is evaluated as needed.

Output Options: Output can be in the form of numeric values, tables, two- or three-dimensional plots, and contour plots. Mathematica allows many forms of output to be displayed within the package and exported for use in other graphics packages.

B.4 SATURATED/UNSATURATED FLOW AND TRANSPORT CODE

I. General Code Description

Purpose and Scope. The PORFLOW computer code was selected and applied to predict the isolation performance of the EAVs in the vadose zone, to predict transport of radionuclides released to the underlying aquifer, and to predict contaminant transport in the aquifer. Specifically, the computer code was used to model water flow through the backfill, gravel-clay barrier, vault structure, and EAV waste forms. The code was then used to model the release of contaminants from the waste form, migration through the vault structure, surrounding soils and underlying formations. The simulation results generated by the

PORFLOW code were then post-processed to obtain predictions of

- water pathlines and travel times to the aquifer,
- contaminant plume distributions in the vadose zone,
- contaminant fluxes to the aquifer, and
- contaminant plume distributions in the aquifer's saturated zone.

These results are then used to characterize the isolation performance of the EAV.

Development History. The original version of the PORFLOW code (Runchal et al. 1985) was developed to analyze the isolation performance of deep geologic repositories. This early version was limited to saturated conditions and two-dimensional porous domains, and was extensively verified and benchmarked by Eyler and Budden (1984). The code was later extended to model variably saturated flow in three-dimensions and was therefore renamed PORFLO-3, Version 1.0 (Sagar and Runchal 1990). Version 1.0 of the three-dimensional computer code was independently verified and benchmarked by Magnuson et al. (1990) against FEMWATER, FLASH, TRACR3D, and MAGNUM-2D for some applications. The code has been used in practical applications at the Hanford Site to model various waste disposal problems (Smoot and Sagar 1990), at an experimental waste trench site in Las Cruces, NM to evaluate the solute transport simulation capabilities (Rockhold and Wurstner 1991), and at the INEL to model a large organic vapor plume (Baca et al. 1988).

A newer version of PORFLO-3 (Version 2.3) was recently developed which has a number of enhancements and new options. For example, one of the new features of Version 2.3 is the capability to model multiphase flow. The commercial version of PORFLO-3 which was used to model the EAVs, suspect soil and NR waste performance in the vadose and saturated zones is PORFLOW, Version 2.5 (ACRI 1993). This later version has been verified and benchmarked to a greater degree than the previous one (ACRI 1994).

Code Attributes. The PORFLOW, Version 2.5, computer code is written in Fortran 77 programming language. Some of the unique attributes of this version are

- capability to model either single or multiphase flow,
- applicable to one-, two-, or three-dimensional geometries in Cartesian or cylindrical coordinate systems,
- alternate solver techniques (such as point successive over relaxation, Cholesky decomposition, Gauss elimination, and reduced system conjugate gradient) can be selected,
- multiple porosity representations can be used, and
- discrete features (such as fractures) can be represented by line or plate elements.

The computer program is relatively portable and can be run on PCs, workstations and mainframe computers.

Computer Requirements. Practical applications of the PORFLOW code to realistic multidimensional flow and transport problems require the availability of a high performance workstation or mainframe computer. The vault and vadose zone simulations presented in this report were performed on an IBM workstation. Complex simulation problems such as those performed for the EAVs often require double precision, and are cumbersome for PCs. For saturated flow, a PC with a 486 processor was sufficient to simulate the flow and mass transport regime.

Restrictions. Version 2.3 of PORFLO-3 was originally developed for the U.S. DOE and is therefore in the public domain. All versions of the PORFLO-3 code are copyright protected. Commercial versions of the code, PORFLOW, which include updates of the Version 2.3, are available from Analytic and Computational Research, Inc. (ACRI), Los Angeles, California.

II. Code Selection Basis

The code selection criteria put forth in Sect. B.1 of this appendix were used to select PORFLOW for use in the EAV RPA. The procedure followed was to identify several codes meeting requirements 1R - 4R, and subsequently evaluate those codes in terms of the remaining eight desirable criteria (1S - 8S). Table B.4.1 summarizes the results of this procedure. A more detailed explanation is given below.

General Critique. At present, there are relatively few general computer codes that have the capability to adequately simulate variably-saturated flow and transport in a multidimensional system. Such codes are scarce because the governing equations for flow in the unsaturated zone are highly nonlinear, and very difficult to solve. In addition to nonlinearity, this numerical difficulty is caused by such factors as:

- large contrasts in soil-hydraulic properties,
- high recharge rates and broad range of saturation conditions,
- contrasting thicknesses of soil strata, and
- advection dominated mass transport.

Advanced computational techniques (Celia et al. 1990 and Fletcher 1988) can overcome some of these difficulties; however, obtaining stable and accurate numerical solutions on a routine basis is still a modeling goal.

A number of computer codes with a demonstrated capability to model flow and transport were considered for application to the EAV study. The principal codes considered were: 1) PORFLOW (ACRI 1993); 2) FEMWATER/FEMWASTE (Yeh and Ward 1979; Yeh and Ward 1981; Yeh 1987); 3) FLASH (Baca and Magnuson 1992); 4) SUTRA (Voss 1984); 5) TRACR3D (Travis 1985); and 6) VAM3D-CG (Huyakorn and Panday 1990). All of these codes, with the possible exception of FEMWATER/FEMWASTE meet the first four requirements (1R-4R, see Table B4.1). The availability of documentation of the most recent version of FEMWATER was in question, as was support by the primary developer of the code. Thus, this code was not considered further.

The remaining codes were evaluated with respect to their probability of satisfying the eight suggested criteria (1S - 8S, Sect. B-1). Reviews of available computer codes useful to PAs (Kozak et al. 1989, Case et al. 1989) were consulted to assess this probability. The results are summarized in Table B.4.1. From this table, the lack of familiarity with SUTRA, TRACR3D, and VAM3D-CG is the only distinguishing characteristic between these codes and FLASH and PORFLOW. Because of time constraints, this latter criteria was deemed important to code selection.

The PORFLOW computer code was ultimately selected over FLASH for these reasons:

- previous successful applications to modeling waste sites (Smoot and Sagar 1990);
- quality and completeness of code documentation (ACRI 1993; Sagar and Runchal 1990);
- favorable results of independent verification and benchmark testing of an earlier version (Magnuson et al. 1990);
- flexibility of the code, computational efficiency and ease of use;
- rigorous testing the source code has undergone using Fortran analyzers.

Applicability to EAVs. The hydrogeologic setting at the SRS is uniquely characterized by relatively high recharge rates, drainable soils, and a shallow vadose, or unsaturated, zone. In contrast, the vault and barrier components are typically low permeability. The PORFLOW computer code allows for consideration of heterogeneity and anisotropy, and employs various numerical techniques to enhance stability under the diverse conditions encountered. PORFLOW also has options for considering planar geologic features such as fractures, which is important to evaluating the possibility of vault failure during the time for which performance is being assessed.

Table B.1.1. Evaluation of identified alternative subsurface flow and transport codes

Selection Criteria (by number)[a]	Code Meets Criterion?					
	POLLOW[b]	FEMWATER FEMWASTE[c]	FLASH[d]	SUTRA[e]	TRACRJD[f]	VAM3D-CG[g]
1R	yes	yes	yes	yes	yes	yes
2R	yes	yes	yes	yes	yes	yes
3R	yes	no	yes	yes	yes	yes
4R[h]	yes	yes	yes	yes	yes	yes
1S	yes	yes	yes	yes	yes	yes
2S	yes	no	yes	yes	yes	not known
3S	yes	not known	yes	not known	yes	not known
4S	yes	yes	yes	yes	yes	yes
5S	yes	yes	yes	yes	yes	yes
6S	yes	yes	yes	not known	yes	not known
7S	yes	yes	yes	yes	yes	yes
8S	yes	no	yes	no	no	no

[a] Described in Appendix B-1.
[b] ACRI 1993.
[c] Yeh, G. T. 1987; Yeh, G. T. and D. S. Ward 1981.
[d] Baca, R. G. and S. O. Magnuson 1992.
[e] Voss, C. I. 1984
[f] Travis, B. J. 1985.
[g] Huyakorn, P. S. and S. Panday 1990.
[h] Satisfying this criteria ensured by user.

Code Verification. Version 1.0 of the PORFLOW computer code has been verified by comparing the numerical solutions against known analytical solutions. In particular, the unsaturated flow component of the code has been verified against the Philip's (1957) analytical solutions for unsaturated flow in vertical and horizontal soil columns. In a like manner, the mass transport component has been verified against a number of analytical solutions for contaminant movement in steady-state flow fields. Results of the code verification are documented in Magnuson et al. (1990).

Version 2.5 of PORFLOW has been verified by ACRI (1994) using the same files compiled by Magnuson (1990).

Code Benchmarking. Version 1.0 of the PORFLOW code has been benchmarked by making code-to-code comparison for various flow and transport simulations. A number of hypothetical flow and transport situations were postulated and were simulated with PORFLOW and other independent computer codes. The hypothetical test problems were formulated to be representative of typical waste sites with realistic hydrogeologic settings. The PORFLOW code has been benchmark tested against such codes as TRACR3D (Travis 1985), FEMWATER (Yeh and Ward 1979), SUTRA (Voss 1984), and FLASH (Baca and Magnuson 1992). Results of the benchmark testing is documented in Magnuson et al. (1990).

Benchmarking of Version 2.5 was recently completed by ACRI (1994) and is in draft form at this writing.

Code Validation. At the present time, the PORFLOW code has not been validated by comparison to laboratory or field data. There is a definite need to perform such comparisons against experimental data collected at the SRS.

III. Theoretical Framework

Governing Equations and Assumptions. The governing equations solved in the PORFLOW code are based on the conservation principles of continuum mechanics. These equations describe fluid flow and mass transport processes in a heterogeneous and anisotropic

porous medium. The equations are well accepted mathematical representations and are found in such texts as Bear and Bachmat (1990), Freeze and Cherry (1979), and Huyakorn and Pinder (1983). The specific partial differential equation solved in PORFLOW for isothermal fluid flow around and through the EAVs is

$$S_s \frac{\partial H}{\partial t} = \frac{\partial}{\partial x_i}\left[K_{ij}\left(\frac{\partial H}{\partial x_j} - \delta_{i3}\right)\right] + m_v \tag{B4.1}$$

where

S_s is the fluid storage term (i.e., specific storage or moisture capacity term),
H is the total or hydraulic head,
K_{ij} is the hydraulic conductivity tensor,
δ_{i3} is the buoyancy vector, and
m_v is the fluid source or sink term,
t is time, and
x_i is distance in the ith direction.

The quantity H is defined by:

$$H = h + z - z^* \tag{B4.2}$$

where

h = pressure head,
z = elevation head, and
z^* = reference datum.

and the quantity S_e is defined by

$$S_e = S(\alpha_s + \theta_E \alpha_f) + \theta_E \frac{\partial S}{\partial H} \tag{B4.3}$$

where

S = the saturation level,

α_s and α_f = the solid and fluid compressibilities normalized by the specific weight of the fluid, and

θ_E = the effective porosity.

Some of the basic assumptions made in the above mathematical formulations are:

- fluid flow is laminar, slightly compressible, and single phase;
- fluid flow obeys Darcy's law for porous flow, where specific discharge is proportional to the hydraulic gradient;
- fluid viscosity is a function of temperature only;
- hydraulic properties of the porous continuum are volume averages; and
- osmotic effects are negligible.

In general, these assumptions are satisfied in the hydrogeologic environment of EAVs.

The specific partial differential equation solved in PORFLOW for contaminant transport from EAVs is

$$R_D \phi_D \frac{\partial C}{\partial t} + \frac{\partial}{\partial x_i}(V_i C) = \frac{\partial}{\partial x_i}\left[\Gamma^C_{ij} \frac{\partial C}{\partial x_j}\right] - \phi_D R_D \lambda C + S_C + \sum_D \phi_D R^P_D \sigma^P \lambda^{mp} C \tag{B4.4}$$

where

C = contaminant concentration,

V_i = fluid pore velocities,

R_D = retardation factor,

Γ^C_{ij} = hydrodynamic dispersivity tensor,

λ = decay rate,

S_c = mass source term,

σ^p = fraction of decay of the parent mass species which generates the current species, and the superscript p refers to the parent mass species.

The last term in equation B4.4 represents ingrowth of mass species. The quantity R_D is defined by:

$$R_D = \left[1 + \frac{(1-\theta_T)\,\rho_s k_d}{\phi_D}\right], \tag{B4.5}$$

where

ρ_s is bulk density,

θ_T is total porosity,

ϕ_D is water filled diffusive porosity, and

k_d is sorption coefficient,

and Γ^C_{ij} is defined by,

$$\Gamma^C_{ij} = \phi_D \tau_{ij} D_M + \phi_E D_{ij}, \tag{B4.6}$$

where

ϕ_e is the effective pore space saturated with water,

τ_{ij} is the tortuosity tensor,

D_M is the molecular diffusion coefficient, and

D_{ij} is the mechanical dispersion tensor.

All other coefficients are as previously defined.

Some of the key assumptions that limit the applicability of the above formulation are as follows:

- contaminant concentrations are low enough that the fluid flow is independent of mass transport, i.e., concentrations do not affect the density or viscosity of the fluid;
- diffusion of the contaminants through the fluid obeys Fick's first law, where mass flux is proportional to the concentration gradient with the constant of proportionality being the diffusion coefficient;
- mechanical dispersion is described by Scheidegger's equation, (Scheidegger 1961);
- adsorption (and desorption) of contaminants onto the porous medium is an equilibrium process described by a linear isotherm.

The model formulation is applicable to both unsaturated and saturated flow conditions.

Initial and Boundary Conditions. The PORFLOW code accommodates the specification of standard mathematical boundary conditions. These include: 1) Dirichlet, i.e., fixed head or concentration), 2) Neumann, i.e., specified flux, and 3) Robin, i.e., mixed, boundary conditions. Detailed information on boundary condition options is given in ACRI (1993).

Numerical Techniques. In the PORFLOW code, the governing equations for flow and transport are solved using a method referred to as the Nodal Point Integration, a variation of the finite volume or integrated finite difference technique (Runchal and Sagar 1992). In

this method, the difference approximations to the governing equations are derived on a staggered grid system. The state variables are computed at the grid nodes whereas the fluid velocities and fluxes are computed at the cell faces (located midway between adjacent grid nodes). Three discretization schemes, or basis functions to be integrated, are provided. The user may select which of the three schemes is to be used to maximize accuracy and stability.

The system of algebraic equations produced by the finite volume method are solved in the PORFLOW code using any one of five techniques

- Point successive over relaxation (Bear and Verruijt 1987),
- Alternating direction implicit (Peaceman and Rachford 1955),
- Cholesky decomposition (de Marsily 1986),
- Gauss elimination (Remson et al. 1971), or
- Reduced system conjugate gradient method (Hestenes and Stiefel 1952).

The nonlinearity of the governing equation for variably saturated flow is solved using a Picard iteration method.

IV. Code Inputs and Outputs

Input Data Structure. Input data files for the PORFLOW code are relatively easy to prepare and check. The code uses a free-form input which allows the user to document the input data deck. The input file uses a keyword approach to define primary input data groups. For typical flow and transport simulations, the data groups consist of

- Title card and comments,
- Finite difference grid specification, i.e., number of grid nodes in each direction,
- Lists of grid node coordinates,
- Zone definitions that specify the grid locations of distinct strata,
- Rock and hydraulic property specifications,
- Convergence and iteration parameters,

- Initial pressures and concentrations,
- Boundary values and/or fluxes,
- Mass properties including effective diffusion coefficients and K_ds,
- Source specifications, and
- Time step and output specifications.

Simulations of multidimensional flow and transport can be performed in either steady-state or time-dependent mode.

Output Options. Results from the PORFLOW simulation consist of total head, saturation, contaminant concentration, and Darcy velocities for each grid block in the computational grid. The user can select to print out any or all of the output variables. Each of these variables can be post-processed to produce graphical output.

Post-Processor Programs. A number of post-processor programs have been written by EG&G Idaho, Inc. which may be used to graph the simulation results. These post-processor programs are DISSPLA based routines that plot profiles, contours, streamlines and travel times, and time histories. These programs have been used extensively by EG&G Idaho on various projects. However, no formal documentation currently exists. Analytic and Computational Research, Inc. also distributes a PLOT88-based post-processor for use with the 486 PC versions of PORFLOW, documented by Runchal (1991).

Documentation of Users Instructions. The PORFLOW, Version 2.5, is documented in ACRI (1993). This report describes the mathematical theory and numerical techniques of this version, serves as a user's manual, and provides detailed information on the code organization, selection of computational grids and time steps, input structure and key-word definitions.

APPENDIX C REFERENCES

ACRI. 1993. *PORFLOW: A Model for Fluid Flow, Heat and Mass Transport in Multifluid, Multiphase Fractured or Porous Media, Users Manual, Version 2.5.* Draft. Analytic and Computational Research, Inc., Los Angeles, Calif.

ACRI. 1994. *Verification and Benchmarking of PORFLOW.* Analytic and Computational Research, Inc., draft (in review).

Atkinson, A., and J.A. Hearne. 1984. *An Assessment of the Long-Term Durability of Concrete in Radioactive Waste Repositories.* AERE-R11465, Harwell, U.K.

Baca, R. G., J. C. Walton, and A. S. Rood. 1988. Organic Contaminant Release from a Mixed Waste Disposal Site: Analysis of Vapor Transport through the Vadose Zone and Site Remediation. *Proceedings of Tenth Annual DOE Low-Level Waste Management Conference.* Denver, Colo.

Baca, R. G. and S. O. Magnuson. 1992. *FLASH - Finite Element Computer Code for Variably Saturated Flow.* EGG-GEO-10274. EG&G Idaho, Inc., Idaho Falls, ID.

Bear, J., and A. Verruijt. 1987. *Modeling Groundwater Flow and Pollution.* D. Reidel Publishing Co., Boston, Mass.

Bear, J., and Y. Bachmat. 1990. *Introduction to Modeling of Transport Phenomena in Porous Media.* Kluwer Academic Publishers, Boston, Mass.

Brown, D. S., and J. D. Allison. 1987. *MINTEQA1.* An Equilibrium Metal Speciation Model: User's Manual. EPA-600/3-87/012. U. S. Environmental Protection Agency, Athens, GA.

Case, M. J., S. J. Maheras, M. D. Otis, and R. G. Baca. 1989. *A Review and Selection of Computer Codes for Establishing of the Performance Assessment Center.* DOE/LLW-83. EG&G Idaho, Inc.

Celia, M. A., E. T. Bouloutas, and R. L. Zarba. 1990. A General Mass-Conservative Numerical Solution for the Unsaturated Flow Equation. *Water Resources Research,* 26(7):1483-1496.

Clear, K.C. 1976. Time to Corrosion of Reinforcing Steel in Concrete Slabs, Vol. 3. Performance After 830 Daily Salt Applications. Federal Highway Administration Report No. FHWA-RD-76-70, NTIS PB-258 446.

de Marsily, G. 1986. *Quantitative Hydrogeology.* Academic Press, Inc., New York, NY.

Eyler, L. L., and M. J. Budden. 1984. *Verification and Benchmarking PORFLO: An Equivalent Porous Continuum Code for Repository Scale Analysis.* PNL-5044. Pacific Northwest Laboratory, Richland, Wash.

Felmy, A. R., D. C. Girvin, and E. A. Jenne. 1984a. *MINTEQ*: A Computer Program for Calculating Aqueous Geochemical Equilibria. (NTIS PB84-157148) EPA-600/3-84-032. National Technical Information Service, Springfield, VA.

Felmy A. R., S. M. Brown, Y. Onishi, S. B. Yabusaki, and R. S. Argo. 1984b. *MEXAMS--The Metals Exposure Analysis Modeling System.* EPA-600/3-84-031 (NTIS PB84-157155). U. S. Environmental Protection Agency, Athens, GA.

Fletcher, C. A. J. 1988. *Computational Techniques for Fluid Dynamics.* Vols I & II, Springer-Verlag, New York, NY.

Freeze, R. A. and J. A. Cherry. 1979. *Groundwater.* Prentice-Hall, Inc. Englewood Cliffs, NJ.

Hestenes, M. R., and E. Stiefel. 1952. Methods of conjugate gradients for solving linear systems. *NBS J. Res.*, 49:409-436.

Huyakorn, P. S., and G. F. Pinder. 1983. *Computational Methods in Subsurface Flow.* Academic Press, Inc., New York, NY.

Huyakorn, P. S., and S. Panday. 1990. *VAM3D-CG - Variably Saturated Analysis Model in Three-dimensions with Preconditioned Conjugate Gradient Matrix Solvers, Documentation and User's Guide, Version 2.1.* HGL/89-02, Hydrogeologic, Inc., Herndon, VA.

Kozak, M. W., M. S. Y. Chu, C. P. Harlan, and P. A. Mattingly. 1989. *Identification and Recommendation of Computer Codes for Low-Level Waste Performance Assessment.* Subtasks 3.0 and 4.1 of the Final Letter Report to the USNRC (August).

Krupka, K. M., and J. R. Morrey. 1985. MINTEQ Geochemical Reaction Code: Status and Applications. *Proceedings of a Conference on the Application of Geochemical models to High-Level Nuclear Waste Repository Assessment.* G.K. Jacobs, and S. K. Whatley, Eds. NUREG/CP-0062. U.S. Nuclear Regulatory Commission, Washington, D.C.

Magnuson, S. O., R. G. Baca, and A. J. Sondrup. 1990. *Independent Verification and Benchmark Testing of the PORFLO-3 Computer Code, Version 1.0.* EGG-BG-9175. EG&G Idaho, Inc., ID.

Nordstrom, D. K., L. N. Plummer, T. M. L. Wigley, T. J. Wolery, J. W. Ball, E. A. Jenne, R. L. Basset, D. A. Crerarm, T. M. Florence, B. Fritz, M. Morel, M. M. Reddy, G. Sposito, and J. Thrailkill. 1979. A Comparison of Computerized Chemical Models foe Equilibrium Calculations in Aqueous Systems. *Chemical Modeling in Aqueous Systems.* E. A. Jenne, Ed. (ACS Symp. Series 93, American Chemical Society, Washington D.C.), pp. 857-892.

Peaceman, D. W., and H. H. Rachford, Jr. 1955. The numerical solution of parabolic and elliptic differential equations. *J. Soc. of Industrial and Applied Mathematics.* 3:28-41.

Peterson, S. R., C. J. Hostetler, W. J. Deutsch, and C. E. Cowan. 1987. MINTEQ User's Manual. (NUREG/CR-4808) PNL-6106. U.S. Nuclear Regulatory Commission, Washington, D.C.

Philip, J. R. 1957. Numerical Solution of Equations of the Diffusion Type with Diffusivity Concentration-Dependent II. *Australian Journal of Physics*, 10(2):29-42.

Remson, I., G. M. Hornberger, and R. F. Molz. 1971. *Numerical Methods in Subsurface Hydrology.* Wiley-Interscience, New York, NY.

Rockhold, M. L, and S. K. Wurstner. 1991. *Simulation of Unsaturated Flow and Solute Transport at the Las Cruces Trench Site Using the PORFLO-3 Computer Code.* PNL-7562. Pacific Northwest Laboratory, Richland, Wash.

Runchal, A. K., B. Sagar, R. G. Baca, and N. W. Kline. 1985. *PORFLO - A Continuum Model for Fluid Flow, Heat Transfer, Mass Transport in Porous Media.* RHO-BW-CR-150P. Rockwell Hanford Operations, Richland, Wash.

Runchal, A. K. 1991. *acaPLOT - A General Purpose Plotting Package, User's Manual - Version 3.00.* ACRi/014/Rev. A. Analytic and computational Research, Inc., Los Angeles, Calif.

Sagar, B., and A. K. Runchal. 1990. *PORFLO-3: A Mathematical Model for Fluid Flow, Heat and Mass Transport in Variably Saturated Geologic Media, Theory and Numerical Methods, Version 1.0.* WHC-EP-0042. Westinghouse Hanford Operations, Richland, Wash.

Scheidegger, A. E. 1961. General Theory of Dispersion in Porous Media. *J. Geophys. Res.* 66(10):3273-3278.

Smith, R. W. 1988. Calculation of Equilibria at Elevated Temperatures Using the MINTEQ Geochemical Code. PNL-6700. Pacific Northwest Laboratory, Richland, Wash.

Smoot, J. L., and B. Sagar. 1990. *Three-dimensional Contaminant Plume Dynamics in the Vadose Zone: Simulation of the 241-T-106 Single-Shell Tank Leak at Hanford.* PNL-7221. Pacific Northwest Laboratories, Richland, Wash.

Travis, B. 1985. *TRACR3D: A Model of Flow and Transport in Porous Media.* LA-9667-MS. Los Alamos National Laboratory, Los Alamos, NM.

Trusdell, A. H., and B. F. Jones. 1974. WATEQ, a Computer Program for Calculating Chemical Equilibria of Natural Waters." *J. Research U.S. Geol. Survey*, 2:233-348.

Voss, C. I. 1984. *A Finite-Element Simulation Model for Saturated-Unsaturated, Fluid-Density-Dependent Ground-Water Flow and Energy Transport or Chemically-Reactive Single-Species Solute Transport.* U. S. Geological Survey, Reston, VA.

Walton, J. C., L. E. Plansky, and R. W. Smith. 1990. *Models for Estimation of Service Life of Concrete Barriers in Low-Level Radioactive Waste Disposal.* Prepared for Division of Engineering Office of Nuclear Regulatory Research, U.S. Nuclear Regulatory Commission, Washington, DC 20555, NRC FIN A6858, NUREG/CR-5542, EGG-2597, RW,CC, 38 p.

Wolfram, S. 1988. *Mathematica: A System for Doing Mathematics by Computer.* Addison-Wesley Publishing Company, Inc., USA, 749 p.

Yeh, G. T., and D. S. Ward. 1979. *FEMWATER: A Finite-Element Model of Water Flow Through Saturated-Unsaturated Porous Media.* ORNL-5567. Oak Ridge National Laboratory, Oak Ridge, Tenn.

Yeh, G. T., and D. S. Ward. 1981. *FEMWASTE: A Finite-Element Model of WASTE Transport Through Saturated-Unsaturated Porous Media.* ORNL-5601. Oak Ridge National Laboratory, Oak Ridge, Tenn.

Yeh, G. T. 1987. *FEMWATER: a Finite-Element Model of WATER Flow Through Saturated-Unsaturated Porous Media - First Revision".* ORNL-5567/R1. Oak Ridge National Laboratory, Oak Ridge, Tenn.

APPENDIX C

DATA TABULATION

C.1 RADIONUCLIDE SCREENING AND TRIGGER LEVEL RESULTS

The screening calculations and trigger levels determined for each vault type at the EAV disposal facility are provided in Tables C.1-1 through C.1-4.

Table C.1-1. Screening calculations and trigger levels for the ILT vaults

Nuclide	T1/2 (years)	DCF (mrem/pCi)	Lambda (1/year)	Kd (cm**3/gm)	Rf	ILT GW Trigger (Ci/vault)	ILT Int Trigger (Ci/vault)
H-3	1.23e+01	6.3e-08	5.62e-02	0	1	1.3e+01	2.7e 01
Be-7	1.47e-01	1.1e-07	4.72e+00	0	1	>1E20	>1E20
Be-10	1.60e+06	4.2e-06	4.33e-07	0	1	5.2e-04	8.0e-04
C-11	3.86e-05	1.2e-08	1.80e+04	2	11	>1E20	>1E20
C-14	5.73e+03	2.1e-06	1.21e-04	2	11	1.2e-02	8.1e-04
F-18	2.14e-04	1.0e-04	3.25e+03	0	1	>1E20	>1E20
Na-22	2.58e+00	1.2e-05	2.69e-01	0	1	3.3e+08	3.7e+08
Na-24	1.71e-03	1.4e-06	4.05e+02	0	1	>1E20	>1E20
Mg-28	2.40e-03	7.5e-06	2.89e+02	0	1	>1E20	>1E20
Al-26	7.40e+05	1.3e-05	9.37e-07	0	1	1.7e-04	8.0e-04
Si-31	2.99e-04	5.4e-07	2.32e+03	0	1	>1E20	>1E20
Si-32	6.50e+02	1.7e-06	1.07e-03	0	1	1.4e-03	8.9e-04
P-32	3.89e-02	7.7e-06	1.78e+01	0	1	>1E20	>1E20
P-33	6.84e-02	8.8e-07	1.01e+01	0	1	>1E20	>1E20
S-35	2.39e-01	4.3e-07	2.90e+00	0	1	>1E20	>1E20
Cl-36	3.01e+05	3.0e-06	2.30e-06	0	1	7.3e-04	8.0e-04
Cl-38	7.07e-05	2.0e-07	9.80e+03	0	1	>1E20	>1E20
Cl-39	1.06e-04	1.4e-07	6.57e+03	0	1	>1E20	>1E20
K-40	1.28e+09	1.9e-05	5.42e-10	0	1	1.2e-04	8.0e-04
K-42	1.41e-03	1.1e-06	4.92e+02	0	1	>1E20	>1E20
K-43	2.56e-03	7.8e-07	2.71e+02	0	1	>1E20	>1E20
K-44	4.18e-05	1.5e-07	1.66e+04	0	1	>1E20	>1E20
K-45	3.04e-05	9.3e-08	2.28e+04	0	1	>1E20	>1E20
Ca-41	1.30e+05	1.2e-06	5.33e-06	0	1	1.8e-03	8.0e-04
Ca-45	4.46e-01	3.0e-06	1.55e+00	0	1	>1E20	>1E20
Ca-47	1.24e-02	6.2e-06	5.58e+01	0	1	>1E20	>1E20
Sc-43	4.47e-04	7.3e-07	1.55e+03	0	1	>1E20	>1E20
Sc-44m	6.68e-03	9.9e-06	1.04e+02	0	1	>1E20	>1E20
Sc-44	4.47e-04	1.4e-06	1.55e+03	0	1	>1E20	>1E20
Sc-46	2.29e-01	5.6e-06	3.02e+00	0	1	>1E20	>1E20
Sc-47	9.39e-03	1.9e-06	7.38e+01	0	1	>1E20	>1E20
Sc-48	5.03e-03	6.4e-06	1.38e+02	0	1	>1E20	>1E20
Sc-49	1.09e-04	2.4e-07	6.34e+03	0	1	>1E20	>1E20

Table C.1-1. (continued)

Nuclide	T1/2 (year)	[illegible] (uCi/g-Ci)	Lambda (1/year)	Kd (cm^3/gm)	Rf	HTC GW Trigger (Ci/y unit)	HTC Gas Trigger (Ci/vault)
Ti-44	4.80e+01	1.9e-05	1.44e-02	0	1	5.2e-04	3.4e-03
Ti-45	3.52e-04	5.7e-07	1.97e+03	0	1	>1E20	>1E20
V-47	6.27e-05	1.6e-07	1.10e+04	0	1	>1E20	>1E20
V-48	4.41e-02	7.5e-06	1.57e+01	0	1	>1E20	>1E20
V-49	9.03e-01	5.4e-08	7.67e-01	0	1	>1E20	>1E20
Cr-48	2.62e-03	8.2e-07	2.64e+02	40	201	>1E20	>1E20
Cr-49	7.97e-05	1.7e-07	8.70e+03	40	201	>1E20	>1E20
Cr-51	7.58e-02	1.3e-07	9.14e+00	40	201	>1E20	>1E20
Mn-51	8.56e-05	2.5e-07	8.10e+03	50	251	>1E20	>1E20
Mn-52m	3.99e-05	1.5e-07	1.74e+04	50	251	>1E20	>1E20
Mn-52	1.52e-02	6.9e-06	4.56e+01	50	251	>1E20	>1E20
Mn-53	2.00e+06	9.9e-08	3.47e-07	50	251	5.6e+00	8.0e-04
Mn-54	7.97e-01	2.7e-06	8.70e-01	50	251	>1E20	>1E20
Mn-56	2.94e-04	9.5e-07	2.36e+03	50	251	>1E20	>1E20
Fe-52	9.35e-04	5.4e-06	7.41e+02	0	1	>1E20	>1E20
Fe-55	2.70e+00	5.8e-07	2.57e-01	0	1	1.9e+09	1.1e+08
Fe-59	1.22e-01	6.6e-06	5.68e+00	0	1	>1E20	>1E20
Fe-60	3.00e+05	1.5e-04	2.31e-06	0	1	1.5e-05	8.0e-04
Co-55	2.08e-03	4.1e-06	3.34e+02	10	51	>1E20	>1E20
Co-56	2.11e-01	1.2e-05	3.29e+00	10	51	>1E20	>1E20
Co-57	7.39e-01	1.1e-05	9.38e-01	10	51	>1E20	>1E20
Co-58m	1.03e-03	8.8e-08	6.75e+02	10	51	>1E20	>1E20
Co-58	1.95e-01	3.5e-06	3.55e+00	10	51	>1E20	>1E20
Co-60m	2.00e-05	3.6e-09	3.47e+04	10	51	>1E20	>1E20
Co-60	5.27e+00	2.6e-05	1.32e-01	10	51	8.1e+17	4.1e+02
Co-61	1.88e-04	2.6e-07	3.68e+03	10	51	>1E20	>1E20
Co-62m	3.04e-06	9.6e-08	2.28e+05	10	51	>1E20	>1E20
Ni-56	1.67e-02	3.5e-06	4.15e+01	300	1501	>1E20	>1E20
Ni-57	4.11e-03	3.3e-06	1.69e+02	300	1501	>1E20	>1E20
Ni-59	8.00e+04	2.0e-07	8.66e-06	300	1501	1.8e+01	8.0e-04
Ni-63	1.00e+02	5.4e-07	6.93e-03	300	1501	>1E20	1.6e-03
Ni-65	2.87e-04	6.1e-07	2.41e+03	300	1501	>1E20	>1E20
Ni-66	6.23e-03	1.1e-05	1.11e+02	300	1501	>1E20	>1E20
Cu-60	4.37e-05	1.7e-07	1.59e+04	25	126	>1E20	>1E20

Table C.1-1. (continued)

Nuclide	T1/2 (sec)	DCF (mrem/pCi)	Lambda (1/sec)	Kd (cm³/g)	Rf	ILT GW Trigger (Ci/vault)	ILT Int Trigger (Ci/vault)
Cu-51	3.[illegible]e-04	4.1e-07	1.[illegible]e+03	25	126	>1E20	>1E20
Cu-64	1.15e-03	4.3e-07	4.78e+02	25	126	>1E20	>1E20
Cu-67	7.06e-03	1.1e-06	9.82e+01	25	126	>1E20	>1E20
Zn-62	1.04e-03	3.4e-06	6.64e+02	16	81	>1E20	>1E20
Zn-63	7.30e-05	2.0e-07	9.49e+03	16	81	>1E20	>1E20
Zn-65	6.67e-01	1.4e-05	1.04e+00	16	81	>1E20	>1E20
Zn-69m	1.57e-03	1.2e-05	4.40e+02	16	81	>1E20	>1E20
Zn-69	1.08e-04	8.5e-08	6.40e+03	16	81	>1E20	>1E20
Zn-71m	4.56e-04	8.3e-07	1.52e+03	16	81	>1E20	>1E20
Zn-72	1.27e-01	4.9e-06	5.44e+00	16	81	>1E20	>1E20
Ga-65	2.89e-05	7.8e-08	2.40e+04	0	1	>1E20	>1E20
Ga-66	1.07e-03	4.7e-06	6.46e+02	0	1	>1E20	>1E20
Ga-67	8.91e-03	7.2e-07	7.78e+01	0	1	>1E20	>1E20
Ga-68	1.30e-04	3.3e-07	5.34e+03	0	1	>1E20	>1E20
Ga-70	4.01e-05	7.1e-08	1.73e+04	0	1	>1E20	>1E20
Ga-72	1.61e-03	4.4e-06	4.31e+02	0	1	>1E20	>1E20
Ga-73	1.34e-02	1.0e-06	5.19e+01	0	1	>1E20	>1E20
Ge-66	1.07e-03	2.1e-07	6.46e+02	0	1	>1E20	>1E20
Ge-67	3.61e-05	1.1e-07	1.92e+04	0	1	>1E20	>1E20
Ge-68	7.86e-01	1.1e-06	8.82e-01	0	1	>1E20	>1E20
Ge-69	4.45e-03	3.6e-07	1.56e+02	0	1	>1E20	>1E20
Ge-71	3.12e-02	9.6e-09	2.22e+01	0	1	>1E20	>1E20
Ge-75	1.57e-04	7.3e-08	4.40e+03	0	1	>1E20	>1E20
Ge-77	1.29e-03	5.6e-07	5.38e+02	0	1	>1E20	>1E20
Ge-78	1.65e-04	2.1e-07	4.19e+03	0	1	>1E20	>1E20
As-69	2.85e-05	1.1e-07	2.43e+04	3	16	>1E20	>1E20
As-70	1.01e-04	3.4e-07	6.88e+03	3	16	>1E20	>1E20
As-71	7.07e-03	1.3e-06	9.80e+01	3	16	>1E20	>1E20
As-72	2.97e-03	5.6e-06	2.34e+02	3	16	>1E20	>1E20
As-73	2.20e-01	6.1e-07	3.15e+00	3	16	>1E20	>1E20
As-74	3.29e-02	3.3e-06	2.11e+01	3	16	>1E20	>1E20
As-76	3.00e-03	4.8e-06	2.31e+02	3	16	>1E20	>1E20
As-77	1.06e-01	1.1e-06	6.53e+00	3	16	>1E20	>1E20
As-78	1.73e-04	6.5e-07	4.01e+03	3	16	>1E20	>1E20

Table C.1-1. (continued)

Nuclide	T1/2 (year)	DCF (mrem/pCi)	Lambda (1/year)	Kd (cm^3/gm)	Rf	ILT Gas Trigger (Ci/vault)	ILT Liq Trigger (Ci/vault)
Se-70	8.37e-05	4.9e-07	8.29e+03	5	26	>1E20	>1E20
Se-73m	7.99e-05	1.5e-07	8.68e+03	5	26	>1E20	>1E20
Se-73	8.10e-01	1.5e-06	8.56e+02	5	26	>1E20	>1E20
Se-75	3.30e-01	8.8e-06	2.10e+00	5	26	>1E20	>1E20
Se-79	6.50e+04	8.3e-06	1.07e-05	5	26	6.9e-03	8.0e-04
Se-81m	1.09e-04	2.1e-07	6.36e+03	5	26	>1E20	>1E20
Se-81	4.30e-05	6.1e-08	1.61e+04	5	26	>1E20	>1E20
Se-83	4.28e-05	1.5e-07	1.62e+04	5	26	>1E20	>1E20
Br-74m	7.89e-05	2.2e-07	8.78e+03	0	1	>1E20	>1E20
Br-74	6.84e-05	1.4e-07	1.01e+04	0	1	>1E20	>1E20
Br-75	1.94e-04	1.3e-07	3.57e+03	0	1	>1E20	>1E20
Br-76	1.84e-03	1.4e-06	3.77e+02	0	1	>1E20	>1E20
Br-77	6.50e-03	3.1e-07	1.07e+02	0	1	>1E20	>1E20
Br-80m	5.04e-04	2.3e-07	1.37e+03	0	1	>1E20	>1E20
Br-80	3.37e-05	5.5e-08	2.06e+04	0	1	>1E20	>1E20
Br-82	4.03e-03	1.7e-06	1.72e+02	0	1	>1E20	>1E20
Br-83	2.74e-04	7.3e-08	2.53e+03	0	1	>1E20	>1E20
Br-84	6.05e-05	1.5e-07	1.15e+04	0	1	>1E20	>1E20
Rb-79	3.99e-05	8.7e-08	1.74e+04	0	1	>1E20	>1E20
Rb-81m	6.08e-05	1.8e-08	1.14e+04	0	1	>1E20	>1E20
Rb-81	5.36e-04	1.3e-07	1.29e+03	0	1	>1E20	>1E20
Rb-82m	7.30e-04	4.2e-07	9.49e+02	0	1	>1E20	>1E20
Rb-83	2.27e-01	7.7e-06	3.05e+00	0	1	>1E20	>1E20
Rb-84	9.31e-02	1.0e-05	7.45e+00	0	1	>1E20	>1E20
Rb-86	5.09e-02	9.4e-06	1.36e+01	0	1	>1E20	>1E20
Rb-87	4.80e+10	4.8e-06	1.44e-11	0	1	4.6e-04	8.0e-04
Rb-88	3.37e-05	1.6e-07	2.06e+04	0	1	>1E20	>1E20
Rb-89	2.89e-05	8.0e-08	2.40e+04	0	1	>1E20	>1E20
Sr-80	1.94e-04	5.2e-09	3.57e+03	10	51	>1E20	>1E20
Sr-81	5.51e-05	2.2e-07	1.26e+04	10	51	>1E20	>1E20
Sr-83	3.76e-03	2.3e-06	1.84e+02	10	51	>1E20	>1E20
Sr-85m	1.29e-04	2.4e-08	5.39e+03	10	51	>1E20	>1E20
Sr-85	1.79e-01	1.9e-06	3.88e+00	10	51	>1E20	>1E20
Sr-87m	3.21e-04	1.2e-07	2.16e+03	10	51	>1E20	>1E20

Table C.1-1. (continued)

Nuclide	T1/2 (years)	DCF (mrem/pCi)	Lambda (1/year)	Kd (cm**3/gm)	Rf	ILT GW Trigger (Ci/vault)	ILT Int Trigger (Ci/vault)
Sr-89	1.23e-01	8.7e-06	5.01e+00	10	51	>1E20	>1E20
Sr-90	2.86e+01	1.3e-04	2.42e-02	10	51	4.7e+00	9.1e-03
Sr-91	1.08e-03	3.0e-06	6.41e+02	10	51	>1E20	>1E20
Sr-92	3.09e-04	1.9e-06	2.24e+03	10	51	>1E20	>1E20
Y-86m	9.13e-05	2.4e-07	7.60e+03	10	51	>1E20	>1E20
Y-86	1.67e-03	4.1e-06	4.16e+02	10	51	>1E20	>1E20
Y-87	9.13e-03	2.2e-06	7.60e+01	10	51	>1E20	>1E20
Y-88	2.88e-01	5.2e-06	2.41e+00	10	51	>1E20	>1E20
Y-90m	3.64e-04	6.6e-07	1.90e+03	10	51	>1E20	>1E20
Y-90	2.86e+01	1.0e-05	2.42e-02	10	51	6.1e+01	9.1e-03
Y-91m	9.51e-05	3.9e-08	7.29e+03	10	51	>1E20	>1E20
Y-91	1.67e-01	8.9e-06	4.15e+00	10	51	>1E20	>1E20
Y-92	4.03e-04	1.9e-06	1.72e+03	10	51	>1E20	>1E20
Y-93	1.16e-03	4.5e-06	5.96e+02	10	51	>1E20	>1E20
Y-94	3.61e-05	1.8e-07	1.92e+04	10	51	>1E20	>1E20
Y-95	2.00e-05	9.7e-08	3.47e+04	10	51	>1E20	>1E20
Zr-86	1.88e-03	3.5e-06	3.68e+02	0	1	>1E20	>1E20
Zr-88	2.33e-01	1.3e-06	2.98e+00	0	1	>1E20	>1E20
Zr-89	8.94e-03	3.1e-06	7.75e+01	0	1	>1E20	>1E20
Zr-93	1.50e+06	1.6e-06	4.62e-07	0	1	1.4e-03	8.0e-04
Zr-95	1.75e-01	3.4e-06	3.96e+00	0	1	>1E20	>1E20
Zr-97	1.92e-03	8.0e-06	3.62e+02	0	1	>1E20	>1E20
Nb-88	2.66e-05	7.2e-08	2.60e+04	0	1	>1E20	>1E20
Nb-89(66m)	1.25e-04	4.6e-07	5.52e+03	0	1	>1E20	>1E20
Nb-89(122m)	2.32e-04	1.0e-06	2.99e+03	0	1	>1E20	>1E20
Nb-90	1.67e-03	4.9e-06	4.16e+02	0	1	>1E20	>1E20
Nb-93m	1.01e+01	5.3e-07	6.84e-02	0	1	5.5e+00	7.5e-01
Nb-94	2.00e+04	5.1e-06	3.47e-05	0	1	4.3e-04	8.1e-04
Nb-95m	9.88e-03	2.0e-06	7.02e+01	0	1	>1E20	>1E20
Nb-95	9.58e-02	2.2e-06	7.23e+00	0	1	>1E20	>1E20
Nb-96	2.67e-03	4.4e-06	2.60e+02	0	1	>1E20	>1E20
Nb-97	1.40e-04	2.3e-07	4.95e+03	0	1	>1E20	>1E20
Nb-98	8.87e-08	3.4e-07	7.81e+06	0	1	>1E20	>1E20
Mo-90	6.50e-04	2.5e-06	1.07e+03	0	1	>1E20	>1E20

Table C.1-1. (continued)

Nuclide	T1/2 (years)	DCF (mrem/pCi)	Lambda (1/year)	Kd (cm³/g)	Rf	ILT GW Trigger (Ci/vault)	ILT Int Trigger (Ci/vault)
Mo-93m	7.37e-01	1.1e-06	8.81e+02	0	1	>1E20	>1E20
Mo-93	3.50e+03	1.3e-05	1.94e-04	0	1	1.7e-03	8.2e-04
Mo-99	7.53e-03	4.4e-06	9.20e+01	0	1	>1E20	>1E20
Mo-101	2.78e-05	9.2e-08	2.50e+04	0	1	>1E20	>1E20
Tc-93m	8.18e-05	7.1e-08	8.48e+03	0.36	2.8	>1E20	>1E20
Tc-93	3.08e-04	1.6e-07	2.25e+03	0.36	2.8	>1E20	>1E20
Tc-94m	1.01e-04	2.5e-07	6.88e+03	0.36	2.8	>1E20	>1E20
Tc-94	5.57e-04	5.8e-07	1.24e+03	0.36	2.8	>1E20	>1E20
Tc-96m	9.89e-05	3.1e-08	7.01e+03	0.36	2.8	>1E20	>1E20
Tc-96	1.18e-02	2.7e-06	5.89e+01	0.36	2.8	>1E20	>1E20
Tc-97m	2.46e-01	1.1e-06	2.81e+00	0.36	2.8	>1E20	>1E20
Tc-97	2.60e+06	1.5e-07	2.67e-07	0.36	2.8	4.1e-02	8.0e-04
Tc-98	1.50e+06	4.8e-06	4.62e-07	0.36	2.8	1.3e-03	8.0e-04
Tc-99m	6.87e-04	6.0e-08	1.01e+03	0.36	2.8	>1E20	>1E20
Tc-99	2.11e+05	1.3e-06	3.29e-06	0.36	2.8	4.7e-03	8.0e-04
Tc-101	2.70e-05	3.8e-08	2.57e+04	0.36	2.8	>1E20	>1E20
Tc-104	3.42e-05	1.6e-07	2.03e+04	0.36	2.8	>1E20	>1E20
Ru-94	1.08e-04	3.3e-07	6.40e+03	100	501	>1E20	>1E20
Ru-97	7.91e-03	6.4e-07	8.76e+01	100	501	>1E20	>1E20
Ru-103	1.08e-01	2.7e-06	6.43e+00	100	501	>1E20	>1E20
Ru-105	5.07e-04	1.0e-06	1.37e+03	100	501	>1E20	>1E20
Ru-106	9.99e-01	2.1e-05	6.94e-01	100	501	>1E20	>1E20
Rh-99m	5.36e-04	2.8e-07	1.29e+03	0	1	>1E20	>1E20
Rh-99	4.38e-02	2.0e-06	1.58e+01	0	1	>1E20	>1E20
Rh-100	2.28e-03	3.1e-06	3.04e+02	0	1	>1E20	>1E20
Rh-101m	1.23e-02	8.8e-07	5.63e+01	0	1	>1E20	>1E20
Rh-101	3.10e+00	2.3e-06	2.24e-01	0	1	1.5e+07	4.1e+06
Rh-102m	2.90e+00	3.5e-06	2.39e-01	0	1	5.0e+07	1.9e+07
Rh-102	5.75e-01	5.5e-06	1.21e+00	0	1	>1E20	>1E20
Rh-103m	1.06e-04	0.00000001	6.51e+03	0	1	>1E20	>1E20
Rh-105	4.05e-03	1.4e-06	1.71e+02	0	1	>1E20	>1E20
Rh-106m	2.49e-04	6.1e-07	2.79e+03	0	1	>1E20	>1E20
Rh-107	4.13e-05	5.4e-08	1.68e+04	0	1	>1E20	>1E20

C-8 W3

[illegible]	1.1[illegible]	[illegible]	5[illegible]	0	1	>	
[illegible]	9.5[illegible]	[illegible]	7[illegible]	0	1	>	
[illegible]	4.5[illegible]	4[illegible]	1.[illegible]	0	1	>[illegible]	
[illegible]	6.[illegible]e-05	1.[illegible]	1.0[illegible]	0	1	1.[illegible]	
10[illegible]	1.53e-03	2.1e-05	1.53e[illegible]	0	1	>1[illegible]	>
-102[illegible]	2.85e-03	7.9e-[illegible]	2.[illegible]	10	51	>1E20	>[illegible]
-103	1.25e-04	1.4e-07	5.52e+03	10	51	>1E20	>1[illegible]
g-104m	5.70e-05	1.5e-07	1.22e+04	10	51	>1E20	>1[illegible]
g-104	1.27e-04	2.3e-07	5.44e+03	10	51	>1E20	>1E[illegible]
g-105	1.10e-01	1.9e-06	6.33e+00	10	51	>1E20	>[illegible]
Ag-106m	2.27e-02	6.1e-06	3.05e+01	10	51	>1E20	>1[illegible]
Ag-106	4.56e-05	7.6e-08	1.52e+04	10	51	>1E20	>[illegible]
Ag-108m	1.30e+02	7.5e-06	5.33e-03	10	51	9.9e-02	
Ag-110m	6.90e-01	1.1e-05	1.00e+00	10	51	>1E20	>1[illegible]
Ag-111	2.05e-02	4.5e-06	3.39e+01	10	51	>1E20	>1[illegible]
Ag-112	3.57e-04	1.6e-06	1.94e+03	10	51	>1E20	>1[illegible]
Ag-115	3.99e-05	1.5e-07	1.74e+04	10	51	>1E20	>1[illegible]
Cd-104	1.08e-04	2.3e-07	6.40e+03	8	41	>1E20	>1[illegible]
Cd-107	7.42e-04	2.4e-07	9.35e+02	8	41	>1E20	>1[illegible]
Cd-109	1.24e+00	1.2e-05	5.59e-01	8	41	>1E20	>1[illegible]
Cd-113m	1.46e+01	1.5e-04	4.75e-02	8	41	1.2e+03	[illegible]
Cd-113	9.30e+15	1.6e-04	7.45e-17	8	41	5.6e-04	[illegible]
Cd-115m	1.36e-01	1.5e-05	5.11e+00	8	41	>1E20	>[illegible]
Cd-115	6.10e-03	4.7e-06	1.14e+02	8	41	>1E20	>[illegible]
Cd-117m	3.88e-04	1.1e-06	1.79e+03	8	41	>1E20	>1E[illegible]
Cd-117	2.97e-04	1.1e-06	2.34e+03	8	41	>1E20	>1[illegible]
In-109	4.91e-04	2.7e-07	1.41e+03	0	1	>1E20	>1E[illegible]
In-110(69m)	1.27e-04	3.3e-07	5.44e+03	0	1	>1E20	>1[illegible]
In-111	7.69e-03	1.2e-06	9.01e+01	0	1	>1E20	>1[illegible]
In-112	2.66e-05	0.00000002	2.60e+04	0	1	>1E20	>1[illegible]
In-113m	1.89e-04	1.0e-07	3.66e+03	0	1	>1E20	>1[illegible]
In-114m	1.36e-01	0.000015	5.11e+00	0	1	>1E20	>1E[illegible]
In-115m	5.13e-04	3.4e-07	1.35e+03	0	1	>1E20	>1E[illegible]
In-115	4.60e+15	1.4e-04	1.51e-16	0	1	1.6e-05	[illegible]

********** PRINTER ERROR RECOVERY **********

COMPLEX PAGE TOO BIG TO STORE FOR AUTOMATIC RECOVERY REPRINT

THIS PAGE WAS SUBSTITUTED SO THAT PRINTING COULD CONTINUE.

PLEASE RESUBMIT PAGE FOR PRINT.

********** PRINTER ERROR RECOVERY **********

COMPLEX PAGE TOO BIG TO STORE FOR AUTOMATIC RECOVERY REPRINT

THIS PAGE WAS SUBSTITUTED SO THAT PRINTING COULD CONTINUE.

PLEASE RESUBMIT PAGE FOR PRINT.

Table C.1-1. (continued)

Nuclide	T1/2 (year)	DCF (mrem/pCi)	Lambda (1/year)	Kd (cm**3/gm)	Rf	ILT GW Trigger (Ci/vault)	ILT Int Trigger (Ci/vault)
Sb-129	4.76e-03	1.7e-05	1.40e+03	10	51	>1E20	>1E20
Sb-130	1.25e-05	2.6e-07	5.52e+04	10	51	>1E20	>1E20
Sb-131	4.37e-05	2.9e-07	1.59e+04	10	51	>1E20	>1E20
Te-118	1.64e-02	6.7e-07	4.22e-01	0	1	>1E20	>1E20
Te-121m	4.11e-01	6.7e-06	1.69e+00	0	1	>1E20	>1E20
Te-121	4.65e-02	1.5e-06	1.49e+01	0	1	>1E20	>1E20
Te-123m	3.28e-01	5.1e-06	2.12e+00	0	1	>1E20	>1E20
Te-123	1.20e+13	4.1e-06	5.78e-14	0	1	5.4e-04	8.0e-04
Te-125m	1.59e-01	3.4e-06	4.37e+00	0	1	>1E20	>1E20
Te-127m	2.98e-01	7.9e-06	2.32e+00	0	1	>1E20	>1E20
Te-127	1.07e-03	6.9e-07	6.46e+02	0	1	>1E20	>1E20
Te-129m	9.14e-02	9.9e-06	7.58e+00	0	1	>1E20	>1E20
Te-129	1.33e-04	1.9e-07	5.21e+03	0	1	>1E20	>1E20
Te-131m	3.42e-03	1.5e-05	2.03e+02	0	1	>1E20	>1E20
Te-131	4.75e-05	2.0e-07	1.46e+04	0	1	>1E20	>1E20
Te-132	8.76e-03	7.4e-06	7.91e+01	0	1	>1E20	>1E20
Te-133m	1.05e-04	7.6e-07	6.58e+03	0	1	>1E20	>1E20
Te-133	2.38e-05	1.6e-07	2.92e+04	0	1	>1E20	>1E20
Te-134	7.99e-05	2.1e-07	8.68e+03	0	1	>1E20	>1E20
I-120m	1.01e-04	3.9e-07	6.88e+03	0.6	4	>1E20	>1E20
I-120	1.48e-04	6.7e-07	4.67e+03	0.6	4	>1E20	>1E20
I-121	2.40e-04	1.8e-07	2.89e+03	0.6	4	>1E20	>1E20
I-123	1.52e-03	4.9e-07	4.57e+02	0.6	4	>1E20	>1E20
I-124	1.15e-02	3.1e-05	6.03e+01	0.6	4	>1E20	>1E20
I-125	1.64e-01	3.8e-05	4.22e+00	0.6	4	>1E20	>1E20
I-126	3.64e-02	7.1e-05	1.90e+01	0.6	4	>1E20	>1E20
I-128	4.75e-05	8.5e-08	1.46e+04	0.6	4	>1E20	>1E20
I-129	1.72e+07	2.8e-04	4.02e-08	0.6	4	3.1e-05	8.0e-04
I-130	1.41e-03	4.3e-06	4.90e+02	0.6	4	>1E20	>1E20
I-131	2.22e-02	5.3e-05	3.13e+01	0.6	4	>1E20	>1E20
I-132m	1.58e-04	4.7e-07	4.39e+03	0.6	4	>1E20	>1E20
I-132	2.60e-04	3.3e-07	2.66e+03	0.6	4	>1E20	>1E20
I-133	2.37e-03	5.4e-06	2.92e+02	0.6	4	>1E20	>1E20
I-134	1.00e-04	1.9e-07	6.93e+03	0.6	4	>1E20	>1E20

Table C.1-1. (continued)

Nuclide	T1/2 (years)	DCF (mrem/pCi)	Lambda (1/year)	Kd (cm**3/gm)	Rf	ILT GW Trigger (Ci/vault)	ILT [illegible] Trigger (Ci/vault)
I-135	7.51e-03	2.0e-05	9.23e+02	0.6	4	>1E20	>1E20
Cs-125	8.56e-05	5.5e-08	8.10e+03	100	501	>1E20	>1E20
Cs-127	7.07e-04	8.0e-08	9.80e+02	100	501	>1E20	>1E20
Cs-129	3.65e-03	2.7e-07	1.90e+02	100	501	>1E20	>1E20
Cs-130	5.70e-05	4.9e-08	1.22e+01	100	501	>1E20	>1E20
Cs-131	2.66e-02	2.4e-07	2.61e+01	100	501	>1E20	>1E20
Cs-132	1.80e-02	1.9e-06	3.85e+01	100	501	>1E20	>1E20
Cs-134m	3.31e-04	4.2e-08	2.10e+03	100	501	>1E20	>1E20
Cs-134	2.06e+00	7.4e-05	3.36e-01	100	501	>1E20	3.3e+11
Cs-135m	1.01e-04	4.9e-08	6.88e+03	100	501	>1E20	>1E20
Cs-135	2.30e+06	7.1e-06	3.01e-07	100	501	1.6e-01	8.0e-04
Cs-136	3.53e-02	1.1e-05	1.96e+01	100	501	>1E20	>1E20
Cs-137	3.01e+01	5.0e-05	2.30e-02	100	501	>1E20	8.0e-03
Cs-138	6.12e-05	1.6e-07	1.13e+04	100	501	>1E20	>1E20
Ba-126	1.84e-04	9.0e-07	3.76e+03	5	26	>1E20	>1E20
Ba-128	6.57e-03	1.0e-05	1.05e+02	5	26	>1E20	>1E20
Ba-131m	2.78e-05	9.7e-07	2.50e+04	5	26	>1E20	>1E20
Ba-131	3.20e-02	1.6e-06	2.16e+01	5	26	>1E20	>1E20
Ba-133m	4.44e-03	2.0e-06	1.56e+02	5	26	>1E20	>1E20
Ba-133	1.07e+01	3.2e-06	6.48e-02	5	26	5.3e+04	5.2e-01
Ba-135m	3.27e-03	1.6e-06	2.12e+02	5	26	>1E20	>1E20
Ba-137m	4.85e-06	0.0	1.43e+05	5	26	>1E20	>1E20
Ba-139	1.58e-04	3.9e-07	4.38e+03	5	26	>1E20	>1E20
Ba-140	3.50e-02	8.4e-06	1.98e+01	5	26	>1E20	>1E20
Ba-141	3.48e-05	2.0e-07	1.99e+04	5	26	>1E20	>1E20
Ba-142	2.03e-05	1.0e-07	3.41e+04	5	26	>1E20	>1E20
La-131	1.12e-04	1.1e-07	6.18e+03	100	501	>1E20	>1E20
La-132	5.13e-04	1.5e-06	1.35e+03	100	501	>1E20	>1E20
La-135	2.22e-03	1.3e-07	3.12e+02	100	501	>1E20	>1E20
La-137	6.00e+04	4.3e-07	1.16e-05	100	501	2.6e+00	8.0e-04
La-138	1.06e+11	5.9e-06	6.54e-12	100	501	1.9e-01	8.0e-04
La-140	4.59e-03	7.7e-06	1.51e+02	100	501	>1E20	>1E20
La-141	4.41e-04	1.4e-06	1.57e+03	100	501	>1E20	>1E20
La-142	1.76e-04	8.3e-07	3.95e+03	100	501	>1E20	>1E20

Table C.1-1. (continued)

Nuclide	T1/2 (years)	DCF (rem/pCi)	Lambda (1/year)	Kd (cm**3/gm)	Rf	ILT GW Trigger (Ci/vault)	ILT Int Trigger (Ci/vault)
Ce-133	2.[illegible]e-05	1.[illegible]e-07	2.60e+04	100	501	>1E20	>1E20
Ce-134	8.21e-03	8.[illegible]e-06	8.44e+01	10	51	>1E20	>1E20
Ce-135	1.96e-03	3.2e-06	3.53e+02	10	51	>1E20	>1E20
Ce-137m	3.92e-03	2.0e-06	1.77e+02	10	51	>1E20	>1E20
Ce-137	1.03e-03	9.8e-03	6.75e+02	10	51	>1E20	>1E20
Ce-139	3.77e-01	1.1e-06	1.84e+00	10	51	>1E20	>1E20
Ce-141	8.90e-02	2.6e-06	7.79e+00	10	51	>1E20	>1E20
Ce-143	3.76e-03	4.2e-06	1.84e+02	10	51	>1E20	>1E20
Ce-144	7.94e-01	2.0e-05	8.73e-01	10	51	>1E20	>1E20
Pr-136	1.25e-04	6.8e-08	5.52e+03	10	51	>1E20	>1E20
Pr-137	1.71e-04	1.3e-07	4.05e+03	100	501	>1E20	>1E20
Pr-138m	2.40e-04	4.9e-07	2.89e+03	100	501	>1E20	>1E20
Pr-139	5.13e-04	1.2e-07	1.35e+03	100	501	>1E20	>1E20
Pr-142m	2.72e-05	6.3e-08	2.55e+04	100	501	>1E20	>1E20
Pr-142	2.18e-03	5.1e-06	3.18e+02	100	501	>1E20	>1E20
Pr-143	3.75e-02	4.5e-06	1.85e+01	100	501	>1E20	>1E20
Pr-144	3.29e-05	1.1e-07	2.11e+04	100	501	>1E20	>1E20
Pr-145	6.82e-04	1.5e-06	1.02e+03	100	501	>1E20	>1E20
Pr-147	2.28e-05	5.7e-08	3.04e+04	100	501	>1E20	>1E20
Nd-136	9.64e-05	3.3e-07	7.19e+03	100	501	>1E20	>1E20
Nd-138	4.18e-05	2.5e-06	1.66e+04	100	501	>1E20	>1E20
Nd-139m	6.27e-04	1.0e-06	1.10e+03	100	501	>1E20	>1E20
Nd-139	5.93e-04	5.7e-08	1.17e+03	100	501	>1E20	>1E20
Nd-141	2.85e-04	3.2e-08	2.43e+03	100	501	>1E20	>1E20
Nd-147	3.01e-02	3.9e-06	2.30e+01	100	501	>1E20	>1E20
Nd-149	1.97e-03	4.6e-07	3.51e+02	100	501	>1E20	>1E20
Nd-151	2.36e-05	7.4e-08	2.94e+04	100	501	>1E20	>1E20
Pm-141	4.18e-05	8.4e-08	1.66e+04	100	501	>1E20	>1E20
Pm-143	7.26e-01	9.5e-07	9.55e-01	100	501	>1E20	>1E20
Pm-144	8.22e-01	3.9e-06	8.43e-01	100	501	>1E20	>1E20
Pm-145	1.77e+01	4.6e-07	3.92e-02	100	501	>1E20	4.0e-02
Pm-146	1.94e+00	3.2e-06	3.57e-01	100	501	>1E20	2.5e+12
Pm-147	2.52e+00	9.5e-07	2.75e-01	100	501	>1E20	7.2e+08
Pm-148m	1.14e-01	7.0e-06	6.06e+00	100	501	>1E20	>1E20

Table C.1-1. (continued)

Nuclide	T1/2 (years)	DCF (mrem/pCi)	Lamda (1/year)	Kd (cm**3/gm)	Rf	ILT GW Trigger (Ci/vault)	ILT Int Trigger (Ci/vault)
Pm-148	1.37e-02	9.5e-06	4.71e+01	100	501	>1E20	>1E20
Pm-149	6.06e-03	3.6e-06	1.14e+02	100	501	>1E20	>1E20
Pm-150	3.06e-04	9.8e-07	2.27e+03	100	501	>1E20	>1E20
Pm-151	3.24e-03	2.8e-06	2.14e+02	100	501	>1E20	>1E20
Sm-141m	4.30e-05	1.8e-07	1.61e+04	100	501	>1E20	>1E20
Sm-141	1.94e-05	8.4e-08	3.57e+04	100	501	>1E20	>1E20
Sm-142	1.37e-04	6.0e-07	5.06e+03	100	501	>1E20	>1E20
Sm-145	9.31e-01	8.5e-07	7.45e-01	100	501	>1E20	>1E20
Sm-146	7.00e+07	2.0e-04	9.90e-09	100	501	5.5e-03	8.0e-04
Sm-147	1.06e+11	1.8e-04	6.54e-12	100	501	6.1e-03	8.0e-04
Sm-151	9.00e+01	3.4e-07	7.70e-03	100	501	1.7e+09	1.7e-03
Sm-153	5.33e-03	2.6e-06	1.30e+02	100	501	>1E20	>1E20
Sm-155	4.22e-05	6.6e-08	1.64e+04	100	501	>1E20	>1E20
Sm-158	8.37e-05	1.0e-06	8.29e+03	100	501	>1E20	>1E20
Eu-145	1.62e-02	3.2e-05	4.29e+01	100	501	>1E20	>1E20
Eu-146	1.26e-02	5.1e-06	5.50e+01	100	501	>1E20	>1E20
Eu-147	6.02e-02	1.8e-06	1.15e+01	100	501	>1E20	>1E20
Eu-148	1.48e-01	5.2e-06	4.69e+00	100	501	>1E20	>1E20
Eu-149	2.90e-01	4.2e-07	2.39e+00	100	501	>1E20	>1E20
Eu-150(12h)	1.37e-03	1.5e-06	5.06e+02	100	501	>1E20	>1E20
Eu-150(34y)	3.40e+01	6.2e-06	2.04e-02	100	501	>1E20	6.2e-03
Eu-152m	1.07e-03	1.9e-06	6.51e+02	100	501	>1E20	>1E20
Eu-152	1.34e+01	6.0e-06	5.17e-02	100	501	>1E20	1.4e-01
Eu-154	8.20e+00	9.1e-06	8.45e-02	100	501	>1E20	3.8e+00
Eu-155	1.70e+00	1.3e-06	4.08e-01	100	501	>1E20	4.1e+14
Eu-156	4.22e-02	8.7e-06	1.64e+01	100	501	>1E20	>1E20
Eu-157	1.73e-03	2.3e-06	4.00e+02	100	501	>1E20	>1E20
Eu-158	8.73e-05	2.6e-07	7.94e+03	100	501	>1E20	>1E20
Gd-145	4.75e-05	1.1e-07	1.46e+04	100	501	>1E20	>1E20
Gd-146	1.26e-02	3.8e-06	5.50e+01	100	501	>1E20	>1E20
Gd-147	3.99e-03	2.6e-06	1.74e+02	100	501	>1E20	>1E20
Gd-148	1.30e+02	2.1e-04	5.33e-03	100	501	5.7e+03	1.4e-03
Gd-149	2.46e-02	1.8e-06	2.81e+01	100	501	>1E20	>1E20
Gd-151	3.29e-01	7.7e-07	2.11e+00	100	501	>1E20	>1E20

Table C.1-1. (continued)

Nuclide	T1/2 (sec)	DCF (mrem/pCi)	Lambda (1/year)	K1 (cm*3/s)	Rf	ILT GW Trigger (Ci/vault)	ILT Int Trigger (Ci/vault)
Gd-152	1.10e+14	1.5e-04	6.30e-15	100	501	7.[illegible]e-03	8.0e-04
Gd-153	6.61e 01	1.1e-06	1.05e+00	100	501	>1E20	>1E20
Gd-159	2.12e-03	1.9e-06	3.27e+02	100	501	>1E20	>1E20
Tb-147	4.56e-05	5.6e-07	1.52e+04	100	501	>1E20	>1E20
Tb-149	4.68e-04	9.5e-07	1.48e+03	100	501	>1E20	>1E20
Tb-150	3.54e-04	9.7e-07	1.96e+03	100	501	>1E20	>1E20
Tb-151	2.05e-03	1.4e-06	3.38e+02	100	501	>1E20	>1E20
Tb-153	6.27e-03	9.9e-07	1.10e+02	100	501	>1E20	>1E20
Tb-154	9.70e-04	2.8e-06	7.15e+02	100	501	>1E20	>1E20
Tb-155	1.53e-02	8.2e-07	4.52e+01	100	501	>1E20	>1E20
Tb-156m(24h)	2.74e-03	7.0e-07	2.53e+02	100	501	>1E20	>1E20
Tb-156m(5h)	6.27e-04	3.2e-07	1.10e+03	100	501	>1E20	>1E20
Tb-156	1.48e-02	4.6e-06	4.69e+01	100	501	>1E20	>1E20
Tb-157	1.50e+02	1.0e-07	4.62e-03	100	501	1.9e+06	1.3e-03
Tb-158	1.20e+03	4.0e-06	5.78e-04	100	501	1.2e+00	8.5e-04
Tb-160	1.98e-01	6.4e-06	3.50e+00	100	501	>1E20	>1E20
Tb-161	1.88e-02	2.6e-06	3.68e+01	100	501	>1E20	>1E20
Dy-155	1.20e-03	5.6e-07	5.79e+02	100	501	>1E20	>1E20
Dy-157	9.24e-04	2.7e-07	7.50e+02	100	501	>1E20	>1E20
Dy-159	3.94e-01	4.0e-07	1.76e+00	100	501	>1E20	>1E20
Dy-165	2.66e-04	3.6e-07	2.61e+03	100	501	>1E20	>1E20
Dy-166	9.31e-03	6.2e-06	7.45e+01	100	501	>1E20	>1E20
Ho-155	9.51e-05	1.2e-07	7.29e+03	100	501	>1E20	>1E20
Ho-157	2.66e-05	1.9e-08	2.60e+04	100	501	>1E20	>1E20
Ho-159	6.27e-05	2.3e-08	1.10e+04	100	501	>1E20	>1E20
Ho-161	2.85e-04	4.7e-08	2.43e+03	100	501	>1E20	>1E20
Ho-162m	1.29e-04	9.0e-08	5.36e+03	100	501	>1E20	>1E20
Ho-162	2.85e-05	6.7e-09	2.43e+04	100	501	>1E20	>1E20
Ho-164m	7.13e-05	4.9e-08	9.72e+03	100	501	>1E20	>1E20
Ho-164	7.03e-05	2.4e-08	9.85e+03	100	501	>1E20	>1E20
Ho-166m	1.20e+03	7.8e-06	5.78e-04	100	501	6.4e-01	8.5e-04
Ho-166	3.06e-03	5.5e-06	2.27e+02	100	501	>1E20	>1E20
Ho-167	3.54e-04	3.2e-07	1.96e+03	100	501	>1E20	>1E20
Er-161	3.54e-04	3.3e-07	1.96e+03	100	501	>1E20	>1E20

Table C.1-1. (continued)

Nuclide	T1/2 (years)	D[illegible] (mm/year)	Lambda (1/year)	Kd (cm^3/gm)	Rf	ILT GW Trigger (Ci/vault)	ILT Int Trigger (Ci/vault)
Er-165	1.1[illegible]e+03	7.9e-08	5.86e+02	100	501	>1E20	>1E20
Er-169	2.57e-02	1.4e-06	2.69e+01	100	501	>1E20	>1E20
Er-171	8.58e-04	1.4e-06	8.08e+02	100	501	>1E20	>1E20
Er-172	5.59e-03	3.7e-06	1.24e+02	100	501	>1E20	>1E20
Tm-162	1.46e-04	7.0e-08	4.73e+03	100	501	>1E20	>1E20
Tm-166	8.78e-04	1.2e-06	7.89e+02	100	501	>1E20	>1E20
Tm-167	2.63e-02	2.1e-06	2.64e+01	100	501	>1E20	>1E20
Tm-170	3.53e-01	5.0e-06	1.96e+00	100	501	>1E20	>1E20
Tm-171	1.92e+00	3.9e-07	3.61e-01	100	501	>1E20	3.8e+12
Tm-172	7.26e-03	6.0e-06	9.55e+01	100	501	>1E20	>1E20
Tm-173	9.35e-04	1.2e-06	7.41e+02	100	501	>1E20	>1E20
Tm-175	3.80e-05	5.4e-08	1.82e+04	100	501	>1E20	>1E20
Yb-162	3.59e-05	7.0e-08	1.93e+04	100	501	>1E20	>1E20
Yb-165	1.90e-05	3.8e-06	3.65e+04	100	501	>1E20	>1E20
Yb-167	3.42e-05	1.7e-08	2.03e+04	100	501	>1E20	>1E20
Yb-169	8.76e-02	2.8e-06	7.91e+00	100	501	>1E20	>1E20
Yb-175	1.15e-02	1.6e-06	6.04e+01	100	501	>1E20	>1E20
Yb-177	2.17e-04	3.1e-07	3.20e+03	100	501	>1E20	>1E20
Yb-178	1.40e-04	3.9e-07	4.94e+03	100	501	>1E20	>1E20
Lu-169	3.88e-03	2.0e-06	1.79e+02	100	501	>1E20	>1E20
Lu-170	5.48e-03	4.3e-06	1.27e+02	100	501	>1E20	>1E20
Lu-171	2.27e-02	2.6e-06	3.05e+01	100	501	>1E20	>1E20
Lu-172	1.83e-02	5.0e-06	3.78e+01	100	501	>1E20	>1E20
Lu-173	1.37e+00	9.7e-07	5.06e-01	100	501	>1E20	>1E20
Lu-174m	3.83e-01	1.8e-06	1.81e+00	100	501	>1E20	>1E20
Lu-174	3.60e+00	9.9e-07	1.93e-01	100	501	>1E20	1.8e+05
Lu-176m	4.21e-04	6.3e-07	1.65e+03	100	501	>1E20	>1E20
Lu-176	3.00e+10	6.6e-06	2.31e-11	100	501	1.7e-01	8.0e-04
Lu-177m	4.41e-02	6.8e-06	1.57e+01	100	501	>1E20	>1E20
Lu-177	1.84e-02	2.0e-06	3.77e+01	100	501	>1E20	>1E20
Lu-178m	3.80e-05	8.8e-08	1.82e+04	100	501	>1E20	>1E20
Lu-178	5.70e-05	1.2e-07	1.22e+04	100	501	>1E20	>1E20
Lu-179	5.25e-04	8.1e-07	1.32e+03	100	501	>1E20	>1E20
Hf-170	1.39e-03	1.2e-05	4.98e+02	100	501	>1E20	>1E20

Table C.1-1. (continued)

Nuclide	T1/2 (years)	DCF (mrem/pCi)	Lambda (1/year)	Kd (cm³/g)	Rf	ILT GW Trigger (Ci/vault)	ILT Int Trigger (Ci/vault)
Hf-172	5.[illegible]+00	4.1e-06	1.39e-01	100	501	>1E[illegible]	8.[illegible]-02
Hf-173	2.60e-03	9.6e-07	2.57e+02	100	501	>1E20	>1E20
Hf-175	1.92e-01	1.6e-06	3.62e+00	100	501	>1E20	>1E20
Hf-177m	9.77e-05	2.5e-07	7.09e+03	100	501	>1E20	>1E20
Hf-178m	3.10e+01	2.0e-05	2.24e-02	100	501	>1E20	7.5e-03
Hf-179m	6.87e-02	4.8e-06	1.01e+01	100	501	>1E20	>1E20
Hf-180m	6.27e-04	8.9e-07	1.10e+03	100	501	>1E20	>1E20
Hf-181	1.16e-01	4.3e-06	5.97e+00	100	501	>1E20	>1E20
Hf-182m	1.18e-04	1.4e-07	5.88e+03	100	501	>1E20	>1E20
Hf-182	9.00e+06	1.4e-05	7.70e-08	100	501	7.9e-02	8.0e-04
Hf-183	1.25e-04	2.5e-07	5.52e+03	100	501	>1E20	>1E20
Hf-184	4.68e-04	2.1e-06	1.48e+03	100	501	>1E20	>1E20
Ta-172	8.37e-05	1.4e-07	8.29e+03	0	1	>1E20	>1E20
Ta-173	4.22e-04	7.4e-07	1.64e+03	0	1	>1E20	>1E20
Ta-174	1.48e-04	1.9e-07	4.67e+03	0	1	>1E20	>1E20
Ta-175	1.20e-03	8.8e-07	5.79e+02	0	1	>1E20	>1E20
Ta-176	9.13e-04	1.3e-06	7.60e+02	0	1	>1E20	>1E20
Ta-177	6.46e-03	4.1e-07	1.07e+02	0	1	>1E20	>1E20
Ta-178	1.79e-05	2.9e-07	3.88e+04	0	1	>1E20	>1E20
Ta-179	2.40e-04	2.5e-07	2.89e+03	0	1	>1E20	>1E20
Ta-180m	9.24e-04	2.1e-07	7.50e+02	0	1	>1E20	>1E20
Ta-180	1.00e+13	3.3e-06	6.93e-14	0	1	6.7e-04	8.0e-04
Ta-182m	3.02e-05	2.4e-08	2.29e+04	0	1	>1E20	>1E20
Ta-182	3.15e-01	6.0e-06	2.20e+00	0	1	>1E20	>1E20
Ta-183	1.40e-02	4.6e-06	4.96e+01	0	1	>1E20	>1E20
Ta-184	9.92e-04	2.7e-06	6.98e+02	0	1	>1E20	>1E20
Ta-185	9.51e-05	2.0e-07	7.29e+03	0	1	>1E20	>1E20
Ta-186	2.00e-05	6.7e-08	3.47e+04	0	1	>1E20	>1E20
W-176	2.85e-04	4.8e-07	2.43e+03	0	1	>1E20	>1E20
W-177	2.57e-04	2.4e-07	2.70e+03	0	1	>1E20	>1E20
W-178	5.89e-02	9.3e-07	1.18e+01	0	1	>1E20	>1E20
W-179	7.22e-05	9.0e-09	9.59e+03	0	1	>1E20	>1E20
W-181	3.31e-01	3.1e-07	2.09e+00	0	1	>1E20	>1E20
W-185	2.06e-01	1.9e-06	3.37e+00	0	1	>1E20	>1E20

Table C.1-1. (continued)

Nuclide	T1/2 (year)	DCF (mrem/µCi)	Lambda (1/year)	Kd (cm**3/gm)	Rf	ILT GW Trigger (Ci/mult)	ILT Lu Trigger (Ci/mult)
W-137	2.73e-03	2.6e-06	2.54e+02	0	1	>1E20	>1E20
W-138	1.89e-01	9.0e-06	3.67e+00	0	1	>1E20	>1E20
Re-177	3.23e-05	4.4e-08	2.14e+04	0	1	>1E20	>1E20
Re-178	2.85e-05	4.8e-08	2.43e+04	0	1	>1E20	>1E20
Re-181	2.05e-03	1.0e-06	3.38e+02	0	1	>1E20	>1E20
Re-182(64h)	7.30e-03	3.4e-06	9.49e+01	0	1	>1E20	>1E20
Re-182(12h)	1.45e-03	7.4e-07	4.78e+02	0	1	>1E20	>1E20
Re-184m	4.63e-01	2.4e-06	1.50e+00	0	1	>1E20	>1E20
Rm-184	1.04e-02	2.2e-06	6.66e+01	0	1	>1E20	>1E20
Re-186m	2.00e+05	3.3e-06	3.47e-06	0	1	6.7e-04	8.0e-04
Re-186	1.03e-02	2.6e-06	6.71e+01	0	1	>1E20	>1E20
Re-187	7.00e+10	8.3e-09	9.90e-12	0	1	2.7e-01	8.0e-04
Re-188m	3.54e-05	6.2e-08	1.96e+04	0	1	>1E20	>1E20
Re-188	1.91e-03	2.8e-06	3.64e+02	0	1	>1E20	>1E20
Re-189	2.74e-03	1.5e-06	2.53e+02	0	1	>1E20	>1E20
Os-180	4.13e-05	4.7e-08	1.68e+04	0	1	>1E20	>1E20
Os-181	4.37e-05	3.5e-07	1.59e+04	0	1	>1E20	>1E20
Os-182	2.51e-03	2.2e-06	2.76e+02	0	1	>1E20	>1E20
Os-185	2.57e-01	2.1e-06	2.69e+00	0	1	>1E20	>1E20
Os-189m	6.84e-04	6.6e-08	1.01e+03	0	1	>1E20	>1E20
Os-191m	1.48e-03	3.6e-07	4.67e+02	0	1	>1E20	>1E20
Os-191	4.19e-02	2.0e-06	1.65e+01	0	1	>1E20	>1E20
Os-193	3.48e-03	3.1e-06	1.99e+02	0	1	>1E20	>1E20
Os-194	6.00e+00	9.1e-06	1.16e-01	0	1	4.5e+01	8.4e+01
Ir-182	2.85e-05	1.2e-07	2.43e+04	0	1	>1E20	>1E20
Ir-184	3.65e-04	6.4e-07	1.90e+03	0	1	>1E20	>1E20
Ir-185	1.60e-03	1.1e-06	4.34e+02	0	1	>1E20	>1E20
Ir-186	1.83e-03	2.1e-06	3.80e+02	0	1	>1E20	>1E20
Ir-187	1.20e-03	4.8e-07	5.79e+02	0	1	>1E20	>1E20
Ir-188	4.68e-03	2.7e-06	1.48e+02	0	1	>1E20	>1E20
Ir-189	3.64e-02	9.3e-07	1.90e+01	0	1	>1E20	>1E20
Ir-190m	3.65e-04	3.0e-08	1.90e+03	0	1	>1E20	>1E20
Ir-190	3.01e-02	4.9e-06	2.30e+01	0	1	>1E20	>1E20
Ir-192m	2.74e-06	1.5e-06	2.53e+05	0	1	>1E20	>1E20

Table C.1-1. (continued)

Nuclide	T1/2 (year)	DCF (mrem/pCi)	Lambda (1/year)	Kd (cm**3/gm)	Rf	ILT GW Trigger (Ci/vault)	ILT Int Trigger (Ci/vault)
Ir-192	2.03e-01	5.3e-06	3.41e+00	0	1	>1E20	>1E20
Ir-194m	4.63e-01	8.1e-06	1.48e+00	0	1	>1E20	>1E20
Ir-194	2.22e-01	5.1e-06	3.12e+02	0	1	>1E20	>1E20
Ir-195m	4.45e-04	6.4e-07	1.56e+03	0	1	>1E20	>1E20
Ir-195	4.79e-04	3.4e-07	1.45e+03	0	1	>1E20	>1E20
Pt-186	3.42e-04	3.7e-07	2.03e+03	0	1	>1E20	>1E20
Pt-188	2.79e-02	3.0e-06	2.48e+01	0	1	>1E20	>1E20
Pt-189	1.24e-03	4.9e-07	5.57e+02	0	1	>1E20	>1E20
Pt-191	1.24e-03	1.3e-06	5.57e+02	0	1	>1E20	>1E20
Pt-193m	1.18e-02	1.7e-06	5.89e+01	0	1	>1E20	>1E20
Pt-193	5.00e+01	1.1e-07	1.39e-02	0	1	8.6e-02	3.2e-03
Pt-195m	1.10e-02	2.2e-06	6.30e+01	0	1	>1E20	>1E20
Pt-197m	1.79e-04	3.1e-07	3.88e+03	0	1	>1E20	>1E20
Pt-197	2.09e-03	1.5e-06	3.32e+02	0	1	>1E20	>1E20
Pt-199	5.86e-05	1.0e-07	1.18e+04	0	1	>1E20	>1E20
Pt-200	1.31e-03	4.5e-06	5.28e+02	0	1	>1E20	>1E20
Au-193	1.83e-03	6.0e-07	3.80e+02	0	1	>1E20	>1E20
Au-194	4.51e-03	2.0e-06	1.54e+02	0	1	>1E20	>1E20
Au-195	5.01e-01	1.1e-06	1.38e+00	0	1	>1E20	>1E20
Au-198m	6.30e-03	5.7e-06	1.10e+02	0	1	>1E20	>1E20
Au-198	7.38e-03	2.3e-06	9.39e+01	0	1	>1E20	>1E20
Au-199	8.60e-03	1.8e-06	8.06e+01	0	1	>1E20	>1E20
Au-200m	2.13e-03	4.6e-06	3.25e+02	0	1	>1E20	>1E20
Au-200	9.20e-05	1.9e-07	7.53e+03	0	1	>1E20	>1E20
Au-201	4.94e-05	5.7e-08	1.40e+04	0	1	>1E20	>1E20
Hg-193m	1.14e-03	1.6e-06	6.08e+02	1000	5001	>1E20	>1E20
Hg-193	6.84e-04	3.3e-07	1.01e+03	1000	5001	>1E20	>1E20
Hg-194	1.90e+00	6.0e-06	3.65e-01	1000	5001	>1E20	5.6e+12
Hg-195m	4.56e-03	2.2e-06	1.52e+02	1000	5001	>1E20	>1E20
Hg-195	1.08e-03	3.8e-07	6.40e+02	1000	5001	>1E20	>1E20
Hg-197m	2.72e-03	1.7e-06	2.55e+02	1000	5001	>1E20	>1E20
Hg-197	7.31e-03	9.1e-07	9.48e+01	1000	5001	>1E20	>1E20
Hg-199m	8.10e-05	8.5e-08	8.56e+03	1000	5001	>1E20	>1E20
Hg-203	1.28e-01	2.1e-06	5.43e+00	1000	5001	>1E20	>1E20

Table C.1-1. (continued)

Nuclide	T1/2 (years)	DCF (mrem/pCi)	Lambda (1/year)	Kd (cm^3/gm)	Rf	ILT OW Trigger (Ci/vault)	ILT Int Trigger (Ci/vault)
Tl-194m	6.21e-05	7.1e-08	1.11e+04	0	1	>1E20	>1E20
Tl-194	6.27e-05	1.9e-08	1.10e+04	0	1	>1E20	>1E20
Tl-195	1.37e-04	7.7e-08	5.06e+03	0	1	>1E20	>1E20
Tl-197	3.19e-04	6.9e-08	2.17e+03	0	1	>1E20	>1E20
Tl-198m	2.13e-04	1.6e-07	3.25e+03	0	1	>1E20	>1E20
Tl-198	6.05e-04	2.6e-07	1.15e+03	0	1	>1E20	>1E20
Tl-199	8.44e-04	8.2e-08	8.21e+02	0	1	>1E20	>1E20
Tl-200	2.98e-03	6.7e-07	2.33e+02	0	1	>1E20	>1E20
Tl-201	8.33e-03	2.9e-07	8.32e+01	0	1	>1E20	>1E20
Tl-202	3.29e-02	1.5e-06	2.11e+01	0	1	>1E20	>1E20
Tl-204	3.77e+00	3.2e-06	1.84e-01	0	1	1.7e+05	7.8e+04
Pb-195m	2.85e-05	8.5e-08	2.43e+04	100	501	>1E20	>1E20
Pb-198	2.74e-04	1.6e-07	2.53e+03	100	501	>1E20	>1E20
Pb-199	1.71e-04	2.2e-07	4.05e+03	100	501	>1E20	>1E20
Pb-200	2.45e-03	1.5e-06	2.83e+02	100	501	>1E20	>1E20
Pb-201	1.07e-03	6.7e-07	6.46e+02	100	501	>1E20	>1E20
Pb-202m	4.13e-04	5.5e-07	1.68e+03	100	501	>1E20	>1E20
Pb-202	3.00e+05	3.9e-05	2.31e-06	100	501	2.8e-02	8.0e-04
Pb-203	5.94e-03	9.6e-07	1.17e+02	100	501	>1E20	>1E20
Pb-205	1.40e+07	1.5e-06	4.95e-08	100	501	7.4e-01	8.0e-04
Pb-209	6.24e-06	9.0e-08	1.11e+05	100	501	>1E20	>1E20
Pb-210	2.23e+01	5.1e-03	3.11e-02	100	501	>1E20	1.8e-02
Pb-211	6.86e-05	4.4e-07	1.01e+04	100	501	>1E20	>1E20
Pb-212	1.21e-03	4.1e-05	5.71e+02	100	501	>1E20	>1E20
Pb-214	5.10e-05	5.8e-07	1.36e+04	100	501	>1E20	>1E20
Bi-200	6.65e-05	1.7e-07	1.04e+04	0	1	>1E20	>1E20
Bi-201	2.05e-04	4.5e-07	3.38e+03	0	1	>1E20	>1E20
Bi-202	1.81e-04	3.6e-07	3.84e+03	0	1	>1E20	>1E20
Bi-203	1.35e-03	2.1e-06	5.15e+02	0	1	>1E20	>1E20
Bi-205	4.19e-02	3.7e-06	1.65e+01	0	1	>1E20	>1E20
Bi-206	1.71e-02	8.0e-06	4.06e+01	0	1	>1E20	>1E20
Bi-207	7.94e+00	4.9e-06	8.73e-02	0	1	4.3e+00	5.0e+00
Bi-210m	3.50e+06	8.6e-05	1.98e-07	0	1	2.6e-05	8.0e-04
Bi-210	1.37e-02	5.9e-06	5.06e+01	0	1	>1E20	>1E20

Table C.1-1. (continued)

Nuclide	T1/2 (years)	DCF (rem/pCi)	Lambda (1/year)	Kd (cm³/g)	Rf	ILT GW Trigger (Ci/vault)	ILT Int Trigger (Ci/vault)
Bi-211	1.15e-04	9.[illegible]e-07	6.02e+0[illegible]	0	1	>1E20	>1E20
Bi-213	8.68e-05	6.0e-07	7.99e+0[illegible]	0	1	>1E20	>1E20
Bi-214	3.76e-05	2.4e-07	1.84e+04	0	1	>1E20	>1E20
Po-203	7.99e-05	2.0e-07	8.68e+03	0	1	>1E20	>1E20
Po-205	2.05e-04	2.4e-07	3.38e+03	0	1	>1E20	>1E20
Po-207	6.50e-04	6.1e-07	1.07e+03	0	1	>1E20	>1E20
Po-210	3.79e-01	1.6e-03	1.83e+00	0	1	>1E20	>1E20
At-207	2.05e-04	8.9e-07	3.38e+03	0	1	>1E20	>1E20
At-211	8.22e-04	4.1e-05	8.43e+02	0	1	>1E20	>1E20
Fr-222	2.81e-05	2.5e-06	2.46e+04	0	1	>1E20	>1E20
Fr-223	4.18e-05	8.6e-06	1.66e+04	0	1	>1E20	>1E20
Ra-223	3.13e-02	5.5e-04	2.21e+01	500	2501	>1E20	>1E20
Ra-224	9.91e-03	3.3e-04	6.99e+01	500	2501	>1E20	>1E20
Ra-225	4.05e-02	3.1e-04	1.71e+01	500	2501	>1E20	>1E20
Ra-226	1.62e+03	1.1e-03	4.27e-04	500	2501	1.1e+00	8.4e-04
Ra-227	7.83e-05	2.2e-07	8.85e+03	500	2501	>1E20	>1E20
Ra-228	5.75e+00	1.2e-03	1.21e-01	500	2501	>1E20	1.4e+02
Ac-224	3.31e-04	2.6e-06	2.10e+03	150	751	>1E20	>1E20
Ac-225	2.74e-02	9.5e-05	2.53e+01	150	751	>1E20	>1E20
Ac-226	3.31e-03	4.0e-05	2.10e+02	150	751	>1E20	>1E20
Ac-227	2.18e+01	1.4e-02	3.18e-02	150	751	>1E20	1.9e-02
Ac-228	6.99e-04	2.1e-06	9.91e+02	150	751	>1E20	>1E20
Th-226	5.87e-05	9.2e-07	1.18e+04	3000	15001	>1E20	>1E20
Th-227	5.13e-02	3.6e-05	1.35e+01	3000	15001	>1E20	>1E20
Th-228	1.91e+00	3.8e-04	3.62e-01	3000	15001	>1E20	4.4e+12
Th-229	7.43e+03	3.5e-03	9.33e-05	3000	15001	1.0e+01	8.1e-04
Th-230	7.70e+04	5.3e-04	9.00e-06	3000	15001	1.2e-01	8.0e-04
Th-231	2.91e-03	1.3e-06	2.38e+02	3000	15001	>1E20	>1E20
Th-232	1.41e+10	2.8e-03	4.93e-11	3000	15001	1.2e-02	8.0e-04
Th-234	6.60e-02	1.3e-05	1.05e+01	3000	15001	>1E20	>1E20
Pa-227	7.28e-05	1.3e-06	9.52e+03	10	51	>1E20	>1E20
Pa-228	2.97e-03	4.0e-06	2.34e+02	10	51	>1E20	>1E20
Pa-230	4.85e-02	5.6e-06	1.43e+01	10	51	>1E20	>1E20
Pa-231	3.28e+04	1.1e-02	2.12e-05	10	51	1.0e-05	8.1e-04

Table C.1-1. (continued)

Nuclide	T1/2 (year)	DCF (mrem/pCi)	Lambda (1/year)	Kd (cm**3/gm)	Rf	ILT (Ci/yr) Tris... (Ci/vault)	ILT (Ci/yr) Tri... (Ci/vault)
Pa-232	3.5[illegible]e-03	3.4e-06	1.9[illegible]e+02	10	51	>1E20	>1E20
Pa-233	7.39e-02	3.3e-06	9.38e+00	10	51	>1E20	>1E20
Pa-234	7.[illegible]e-04	2.1e-06	9.07e+02	10	51	>1E20	>1E20
U-230	5.69e-02	8.4e-04	1.22e+01	50	251	>1E20	>1E20
U-231	4.30e+00	1.1e-06	1.61e-01	50	251	>1E20	8.0e+03
U-232	7.20e+01	1.3e-03	9.63e-03	50	251	2.0e+02	2.1e-03
U-233	1.60e+05	2.7e-04	4.35e-06	50	251	2.1e-03	8.0e-04
U-234	2.45e+05	2.6e-04	2.83e-06	50	251	2.1e-03	8.0e-04
U-235	7.04e+08	2.5e-04	9.85e-10	50	251	2.2e-03	8.0e-04
U-236	2.34e+07	2.5e-04	2.96e-08	50	251	2.2e-03	8.0e-04
U-237	1.85e-02	2.7e-06	3.75e+01	50	251	>1E20	>1E20
U-238	4.47e+09	2.3e-04	1.55e-10	50	251	2.4e-03	8.0e-04
U-239	4.47e-05	7.6e-08	1.55e+04	50	251	>1E20	>1E20
U-240	1.61e-03	4.1e-06	4.31e+02	50	251	>1E20	>1E20
Np-232	2.47e-05	2.4e-08	2.80e+04	10	51	>1E20	>1E20
Np-233	6.65e-05	5.6e-09	1.04e+04	10	51	>1E20	>1E20
Np-234	1.20e-02	1.7e-06	5.75e+01	10	51	>1E20	>1E20
Np-235	1.12e+00	2.1e-07	6.17e-01	10	51	>1E20	>1E20
Np-236(1E5y)	1.10e+05	7.9e-04	6.30e-06	10	51	1.4e-04	8.0e-04
Np-236(22h)	2.51e-03	9.5e-07	2.76e+02	10	51	>1E20	>1E20
Np-237	2.14e+06	3.9e-03	3.24e-07	10	51	2.9e-05	8.0e-04
Np-238	5.80e-03	3.4e-06	1.20e+02	10	51	>1E20	>1E20
Np-239	6.38e-03	2.9e-06	1.09e+02	10	51	>1E20	>1E20
Np-240	1.20e-04	2.0e-07	5.79e+03	10	51	>1E20	>1E20
Pu-234	1.03e-03	1.2e-06	6.75e+02	100	501	>1E20	>1E20
Pu-235	4.94e-05	1.4e-08	1.40e+04	100	501	>1E20	>1E20
Pu-236	2.85e+00	1.3e-03	2.43e-01	100	501	>1E20	2.9e+07
Pu-237	1.24e-01	1.0e-06	5.58e+00	100	501	>1E20	>1E20
Pu-238	8.78e+01	3.8e-03	7.90e-03	100	501	2.5e+05	1.8e-03
Pu-239	2.41e+04	4.3e-03	2.87e-05	100	501	2.8e-04	8.1e-04
Pu-240	6.57e+03	4.3e-03	1.06e-04	100	501	3.4e-04	8.1e-04
Pu-241	1.44e+01	8.6e-05	4.81e-02	100	501	>1E20	9.9e-02
Pu-242	3.76e+05	4.1e-03	1.84e-06	100	501	2.7e-04	8.0e-04
Pu-243	5.65e-04	3.3e-07	1.23e+03	100	501	>1E20	>1E20

Table C.1-1. (continued)

Nuclide	T1/2 (years)	DCF (mrem/pCi)	Lambda (1/year)	Kd (cm^3/gm)	Rf	ILT GW Trigger (Ci/vault)	ILT Int Trigger (Ci/vault)
Pu-244	8.10e+07	4.0e-03	8.56e-09	100	501	2.8e-04	8.0e-04
Pu-245	1.14e-04	2.4e-06	6.08e+02	100	501	>1E20	>1E20
Am-237	1.48e-04	7.4e-08	4.67e+03	150	751	>1E20	>1E20
Am-238	2.17e-04	1.7e-07	3.20e+03	150	751	>1E20	>1E20
Am-239	1.38e-03	1.0e-06	5.02e+02	150	751	>1E20	>1E20
Am-240	5.82e-03	2.9e-06	1.19e+02	150	751	>1E20	>1E20
Am-241	4.32e+02	4.5e-03	1.60e-03	150	751	1.8e-01	9.4e-04
Am-242m	1.52e+02	4.2e-03	4.56e-03	150	751	1.7e+04	1.3e-03
Am-242	1.83e-03	1.2e-06	3.80e+02	150	751	>1E20	>1E20
Am-243	7.37e+03	4.5e-03	9.40e-05	150	751	5.3e-04	8.1e-04
Am-244m	4.94e-05	6.8e-08	1.40e+04	150	751	>1E20	>1E20
Am-244	1.15e-03	2.0e-06	6.02e+02	150	751	>1E20	>1E20
Am-245	2.40e-04	1.8e-07	2.89e+03	150	751	>1E20	>1E20
Am-246m	4.75e-05	8.4e-08	1.46e+04	150	751	>1E20	>1E20
Am-246	4.75e-05	1.5e-07	1.46e+04	150	751	>1E20	>1E20
Cm-238	2.85e-04	3.6e-07	2.43e+03	100	501	>1E20	>1E20
Cm-240	7.34e-02	6.3e-05	9.45e+00	100	501	>1E20	>1E20
Cm-241	9.58e-02	4.6e-06	7.23e+00	100	501	>1E20	>1E20
Cm-242	4.46e-01	1.1e-04	1.56e+00	100	501	>1E20	>1E20
Cm-243	2.85e+01	2.9e-03	2.43e-02	100	501	>1E20	9.1e-03
Cm-244	1.81e+01	2.3e-03	3.83e-02	100	501	>1E20	3.7e-02
Cm-245	8.50e+03	4.5e-03	8.15e-05	100	501	3.0e-04	8.1e-04
Cm-246	4.70e+03	4.5e-03	1.47e-04	100	501	3.6e-04	8.2e-04
Cm-247	1.60e+07	4.1e-03	4.33e-08	100	501	2.7e-04	8.0e-04
Cm-248	3.50e+05	1.6e-02	1.98e-06	100	501	6.9e-05	8.0e-04
Cm-249	1.24e-04	9.5e-08	5.61e+03	100	501	>1E20	>1E20
Bk-245	1.36e-02	2.3e-06	5.08e+01	100	501	>1E20	>1E20
Bk-246	4.93e-03	1.9e-06	1.41e+02	100	501	>1E20	>1E20
Bk-247	1.40e+03	2.3e-03	4.95e-04	100	501	1.7e-03	8.4e-04
Bk-249	8.80e-01	6.0e-06	7.88e-01	100	501	>1E20	>1E20
Bk-250	3.67e-04	5.0e-07	1.89e+03	100	501	>1E20	>1E20
Cf-244	4.75e-05	1.5e-07	1.46e+04	100	501	>1E20	>1E20
Cf-246	4.11e-03	1.2e-05	1.69e+02	100	501	>1E20	>1E20
Cf-248	9.86e-01	2.8e-04	7.03e-01	100	501	>1E20	>1E20

Table C.1-1. (continued)

Nuclide	T1/2 (year)	DCF (mrem/μCi)	Lambda (1/year)	Xd (cm³/g)	RC	ILT GW Trigger (Ci/vault)	ILT [illegible] Trigger (Ci/vault)
Cf-249	3.51e+02	4.6e-03	1.97e-03	100	501	4.1e-02	9.8e-04
Cf-250	1.31e+01	1.9e-03	5.29e-02	100	501	>1E20	1.6e-01
Cf-251	9.00e+02	4.6e-03	7.70e-04	100	501	1.8e-03	8.7e-04
Cf-252	2.62e+00	9.4e-01	2.65e-01	100	501	>1E20	2.5e+03
Cf-253	4.87e-02	9.2e-06	1.42e+01	100	501	>1E20	>1E20
Cf-254	1.66e-01	2.5e-03	4.18e+00	100	501	>1E20	>1E20
Es-250	9.13e-04	9.5e-08	7.60e+02	100	501	>1E20	>1E20
Es-251	4.11e-03	6.7e-07	1.69e+02	100	501	>1E20	>1E20
Es-253	5.60e-02	2.4e-05	1.24e+01	100	501	>1E20	>1E20
Es-254m	4.48e-03	1.5e-05	1.55e+02	100	501	>1E20	>1E20
Es-254	7.56e-01	1.5e-04	9.17e-01	100	501	>1E20	>1E20
Fm-252	2.62e-03	9.9e-06	2.64e+02	100	501	>1E20	>1E20
Fm-253	8.21e-03	3.5e-06	8.44e+01	100	501	>1E20	>1E20
Fm-254	3.70e-04	1.6e-06	1.88e+03	100	501	>1E20	>1E20
Fm-255	2.29e-03	9.7e-06	3.02e+02	100	501	>1E20	>1E20
Fm-257	2.19e-01	7.3e-05	3.16e+00	100	501	>1E20	>1E20
Md-257	3.42e-04	5.4e-07	2.03e+03	100	501	>1E20	>1E20
Md-258	1.53e-01	6.1e-05	4.52e+00	100	501	>1E20	>1E20

Table C.1 [illegible]. Screening calculations and trigger levels for the ILNT [illegible]

Nuclide	T1/2 (year)	DCF (mrem/pCi)	Lambda (1/year)	Kd (cm**3/gm)	Rf	ILNT GW Trigger (Ci/cult)	ILNT Int Trigger (Ci/cult)
H-3	1.23e+01	6.3e-08	5.62e-02	0	1	3.4e-01	1.6e+00
Be-7	1.47e-01	1.1e-07	4.72e+00	0	1	2.6e+00	>1E20
Be-10	1.60e+06	4.2e-06	4.33e-07	0	1	3.8e-03	5.9e-03
C-11	3.86e-05	1.2e-08	1.80e+04	2	11	>1E20	>1E20
C-14	5.73e+03	2.1e-06	1.21e-04	2	11	8.5e-02	6.0e-03
F-18	2.14e-04	1.0e-04	3.25e+03	0	1	>1E20	>1E20
Na-22	2.58e+00	1.2e-05	2.69e-01	0	1	5.1e-03	2.7e+09
Na-24	1.71e-03	1.4e-06	4.05e+02	0	1	>1E20	>1E20
Mg-28	2.40e-03	7.5e-06	2.89e+02	0	1	>1E20	>1E20
Al-26	7.40e+05	1.3e-05	9.37e-07	0	1	1.2e-03	5.9e-03
Si-31	2.99e-04	5.4e-07	2.32e+03	0	1	>1E20	>1E20
Si-32	6.50e+02	1.7e-06	1.07e-03	0	1	9.5e-03	6.5e-03
P-32	3.89e-02	7.7e-06	1.78e+01	0	1	>1E20	>1E20
P-33	6.84e-02	8.8e-07	1.01e+01	0	1	>1E20	>1E20
S-35	2.39e-01	4.3e-07	2.90e+00	0	1	7.6e+04	>1E20
Cl-36	3.01e+05	3.0e-06	2.30e-06	0	1	5.4e-03	5.9e-03
Cl-38	7.07e-05	2.0e-07	9.80e+03	0	1	>1E20	>1E20
Cl-39	1.06e-04	1.4e-07	6.57e+03	0	1	>1E20	>1E20
K-40	1.28e+09	1.9e-05	5.42e-10	0	1	8.5e-04	5.9e-03
K-42	1.41e-03	1.1e-06	4.92e+02	0	1	>1E20	>1E20
K-43	2.56e-03	7.8e-07	2.71e+02	0	1	>1E20	>1E20
K-44	4.18e-05	1.5e-07	1.66e+04	0	1	>1E20	>1E20
K-45	3.04e-05	9.3e-08	2.28e+04	0	1	>1E20	>1E20
Ca-41	1.30e+05	1.2e-06	5.33e-06	0	1	1.3e-02	5.9e-03
Ca-45	4.46e-01	3.0e-06	1.55e+00	0	1	1.3e+01	>1E20
Ca-47	1.24e-02	6.2e-06	5.58e+01	0	1	>1E20	>1E20
Sc-43	4.47e-04	7.3e-07	1.55e+03	0	1	>1E20	>1E20
Sc-44m	6.68e-03	9.9e-06	1.04e+02	0	1	>1E20	>1E20
Sc-44	4.47e-04	1.4e-06	1.55e+03	0	1	>1E20	>1E20
Sc-46	2.29e-01	5.6e-06	3.02e+00	0	1	1.0e+04	>1E20
Sc-47	9.39e-03	1.9e-06	7.38e+01	0	1	>1E20	>1E20
Sc-48	5.03e-03	6.4e-06	1.38e+02	0	1	>1E20	>1E20
Sc-49	1.09e-04	2.4e-07	6.34e+03	0	1	>1E20	>1E20

Table C.1-2. (continued)

Nuclide	T1/2 (years)	DCF (mrem/pCi)	Lambda (1/year)	Kd (cm^3/gm)	RF	ILNT GW Trigger (Ci/month)	ILNT Inv Trigger (Ci/month)
Ti-44	4.2[illegible]e+01	1.9e-05	1.44e-02	0	1	9.1e-04	2.5e-02
Ti-45	3.5[illegible]e-04	5.7e-07	1.97e+03	0	1	>1E20	>1E20
V-47	6.27e-05	1.6e-07	1.1[illegible]e+04	0	1	>1E20	>1E20
V-48	4.41e-02	7.5e-06	1.57e+01	0	1	>1E20	>1E20
V-49	9.03e-01	5.4e-08	7.67e-01	0	1	1.4e+01	>1E20
Cr-48	2.62e-03	8.2e-07	2.64e+02	40	201	>1E20	>1E20
Cr-49	7.97e-05	1.7e-07	8.70e+03	40	201	>1E20	>1E20
Cr-51	7.58e-02	1.3e-07	9.14e+00	40	201	>1E20	>1E20
Mn-51	8.56e-05	2.5e-07	8.10e+03	50	251	>1E20	>1E20
Mn-52m	3.99e-05	1.5e-07	1.74e+04	50	251	>1E20	>1E20
Mn-52	1.52e-02	6.9e-06	4.56e+01	50	251	>1E20	>1E20
Mn-53	2.00e+06	9.9e-08	3.47e-07	50	251	4.1e+01	5.9e-03
Mn-54	7.97e-01	2.7e-06	8.70e-01	50	251	>1E20	>1E20
Mn-56	2.94e-04	9.5e-07	2.36e+03	50	251	>1E20	>1E20
Fe-52	9.35e-04	5.4e-06	7.41e+02	0	1	>1E20	>1E20
Fe-55	2.70e+00	5.8e-07	2.57e-01	0	1	1.0e-01	8.3e+08
Fe-59	1.22e-01	6.6e-06	5.68e+00	0	1	5.2e+09	>1E20
Fe-60	3.00e+05	1.5e-04	2.31e-06	0	1	1.1e-04	5.9e-03
Co-55	2.08e-03	4.1e-06	3.34e+02	10	51	>1E20	>1E20
Co-56	2.11e-01	1.2e-05	3.29e+00	10	51	>1E20	>1E20
Co-57	7.39e-01	1.1e-05	9.38e-01	10	51	>1E20	>1E20
Co-58m	1.03e-03	8.8e-08	6.75e+02	10	51	>1E20	>1E20
Co-58	1.95e-01	3.5e-06	3.55e+00	10	51	>1E20	>1E20
Co-60m	2.00e-05	3.6e-09	3.47e+04	10	51	>1E20	>1E20
Co-60	5.27e+00	2.6e-05	1.32e-01	10	51	1.2e+13	3.0e+03
Co-61	1.88e-04	2.6e-07	3.68e+03	10	51	>1E20	>1E20
Co-62m	3.04e-06	9.6e-08	2.28e+05	10	51	>1E20	>1E20
Ni-56	1.67e-02	3.5e-06	4.15e+01	300	1501	>1E20	>1E20
Ni-57	4.11e-03	3.3e-06	1.69e+02	300	1501	>1E20	>1E20
Ni-59	8.00e+04	2.0e-07	8.66e-06	300	1501	1.3e+02	5.9e-03
Ni-63	1.00e+02	5.4e-07	6.93e-03	300	1501	>1E20	1.2e-02
Ni-65	2.87e-04	6.1e-07	2.41e+03	300	1501	>1E20	>1E20
Ni-66	6.23e-03	1.1e-05	1.11e+02	300	1501	>1E20	>1E20
Cu-60	4.37e-05	1.7e-07	1.59e+04	25	126	>1E20	>1E20

Table C.1-2 (continued)

Nuclide	T1/2 (year)	DCF (mrem/pCi)	Lambda (1/year)	Kd (cm^3/gm)	Rf	ILNT GW Trigger (Ci/vault)	ILNT Int Trigger (Ci/vault)
Cu-61	3.69e-04	4.1e-07	1.77e+03	25	126	>1E20	>1E20
Cu-64	1.45e-03	4.2e-07	4.78e+02	25	126	>1E20	>1E20
Cu-67	7.06e-03	1.1e-06	9.82e+01	25	126	>1E20	>1E20
Zn-62	1.04e-03	3.4e-06	6.64e+02	16	81	>1E20	>1E20
Zn-63	7.30e-05	2.0e-07	9.49e+03	16	81	>1E20	>1E20
Zn-65	6.67e-01	1.4e-05	1.04e+00	16	81	>1E20	>1E20
Zn-69m	1.57e-03	1.2e-05	4.40e+02	16	81	>1E20	>1E20
Zn-69	1.08e-04	8.5e-08	6.40e+03	16	81	>1E20	>1E20
Zn-71m	4.56e-04	8.3e-07	1.52e+03	16	81	>1E20	>1E20
Zn-72	1.27e-01	4.9e-06	5.44e+00	16	81	>1E20	>1E20
Ga-65	2.89e-05	7.8e-08	2.40e+04	0	1	>1E20	>1E20
Ga-66	1.07e-03	4.7e-06	6.46e+02	0	1	>1E20	>1E20
Ga-67	8.91e-03	7.2e-07	7.78e+01	0	1	>1E20	>1E20
Ga-68	1.30e-04	3.3e-07	5.34e+03	0	1	>1E20	>1E20
Ga-70	4.01e-05	7.1e-08	1.73e+04	0	1	>1E20	>1E20
Ga-72	1.61e-03	4.4e-06	4.31e+02	0	1	>1E20	>1E20
Ga-73	1.34e-02	1.0e-06	5.19e+01	0	1	>1E20	>1E20
Ge-66	1.07e-03	2.1e-07	6.46e+02	0	1	>1E20	>1E20
Ge-67	3.61e-05	1.1e-07	1.92e+04	0	1	>1E20	>1E20
Ge-68	7.86e-01	1.1e-06	8.82e-01	0	1	1.2e+00	>1E20
Ge-69	4.45e-03	3.6e-07	1.56e+02	0	1	>1E20	>1E20
Ge-71	3.12e-02	9.6e-09	2.22e+01	0	1	>1E20	>1E20
Ge-75	1.57e-04	7.3e-08	4.40e+03	0	1	>1E20	>1E20
Ge-77	1.29e-03	5.6e-07	5.38e+02	0	1	>1E20	>1E20
Ge-78	1.65e-04	2.1e-07	4.19e+03	0	1	>1E20	>1E20
As-69	2.85e-05	1.1e-07	2.43e+04	3	16	>1E20	>1E20
As-70	1.01e-04	3.4e-07	6.88e+03	3	16	>1E20	>1E20
As-71	7.07e-03	1.3e-06	9.80e+01	3	16	>1E20	>1E20
As-72	2.97e-03	5.6e-06	2.34e+02	3	16	>1E20	>1E20
As-73	2.20e-01	6.1e-07	3.15e+00	3	16	>1E20	>1E20
As-74	3.29e-02	3.3e-06	2.11e+01	3	16	>1E20	>1E20
As-76	3.00e-03	4.8e-06	2.31e+02	3	16	>1E20	>1E20
As-77	1.06e-01	1.1e-06	6.53e+00	3	16	>1E20	>1E20
As-78	1.73e-04	6.5e-07	4.01e+03	3	16	>1E20	>1E20

Table C.1-2. (continued)

Nuclide	T1/2 (years)	DCF (mrem/pCi)	Lambda (1/year)	Kd (cm^3/gm)	Rf	ILCF Trigger (Ci/vault)	ILCF Trigger (Ci/vault)
Se-70	8.37e-05	4.2e-07	8.29e+03	5	26	>1E20	>1E20
Se-73m	7.59e-05	1.5e-07	8.68e+03	5	26	>1E20	>1E20
Se-73	8.10e-04	1.5e-06	8.56e+02	5	26	>1E20	>1E20
Se-75	3.30e-01	8.8e-06	2.10e+00	5	26	>1E20	>1E20
Se-79	6.50e+04	8.2e-06	1.07e-05	5	26	5.1e-02	5.9e-03
Se-81m	1.09e-04	2.1e-07	6.36e+03	5	26	>1E20	>1E20
Se-81	4.30e-05	6.1e-08	1.61e+04	5	26	>1E20	>1E20
Se-83	4.28e-05	1.5e-07	1.62e+04	5	26	>1E20	>1E20
Br-74m	7.89e-05	2.2e-07	8.78e+03	0	1	>1E20	>1E20
Br-74	6.84e-05	1.4e-07	1.01e+04	0	1	>1E20	>1E20
Br-75	1.94e-04	1.3e-07	3.57e+03	0	1	>1E20	>1E20
Br-76	1.84e-03	1.4e-06	3.77e+02	0	1	>1E20	>1E20
Br-77	6.50e-03	3.1e-07	1.07e+02	0	1	>1E20	>1E20
Br-80m	5.04e-04	2.3e-07	1.37e+03	0	1	>1E20	>1E20
Br-80	3.37e-05	5.5e-08	2.06e+04	0	1	>1E20	>1E20
Br-82	4.03e-03	1.7e-06	1.72e+02	0	1	>1E20	>1E20
Br-83	2.74e-04	7.3e-08	2.53e+03	0	1	>1E20	>1E20
Br-84	6.05e-05	1.5e-07	1.15e+04	0	1	>1E20	>1E20
Rb-79	3.99e-05	8.7e-08	1.74e+04	0	1	>1E20	>1E20
Rb-81m	6.08e-05	1.8e-08	1.14e+04	0	1	>1E20	>1E20
Rb-81	5.36e-04	1.3e-07	1.29e+03	0	1	>1E20	>1E20
Rb-82m	7.30e-04	4.2e-07	9.49e+02	0	1	>1E20	>1E20
Rb-83	2.27e-01	7.7e-06	3.05e+00	0	1	8.8e+03	>1E20
Rb-84	9.31e-02	1.0e-05	7.45e+00	0	1	2.4e+13	>1E20
Rb-86	5.09e-02	9.4e-06	1.36e+01	0	1	>1E20	>1E20
Rb-87	4.80e+10	4.8e-06	1.44e-11	0	1	3.4e-03	5.9e-03
Rb-88	3.37e-05	1.6e-07	2.06e+04	0	1	>1E20	>1E20
Rb-89	2.89e-05	8.0e-08	2.40e+04	0	1	>1E20	>1E20
Sr-80	1.94e-04	5.2e-09	3.57e+03	10	51	>1E20	>1E20
Sr-81	5.51e-05	2.2e-07	1.26e+04	10	51	>1E20	>1E20
Sr-83	3.76e-03	2.3e-06	1.84e+02	10	51	>1E20	>1E20
Sr-85m	1.29e-04	2.4e-08	5.39e+03	10	51	>1E20	>1E20
Sr-85	1.79e-01	1.9e-06	3.88e+00	10	51	>1E20	>1E20
Sr-87m	3.21e-04	1.2e-07	2.16e+03	10	51	>1E20	>1E20

Table C.1-2 (continued)

Nuclide	T1/2 (years)	DCF (mrem/pCi)	Lambda (1/year)	Kd (cm^3/gm)	Rf	[illegible] Trigger (Ci/vault)	[illegible] Trigger (Ci/vault)
Sr-89	1.32e-01	8.7e-06	5.05e+00	10	51	>1E20	>1E20
Sr-90	2.86e+01	1.3e-04	2.42e-02	10	51	3.1e+00	6.6e-02
Sr-91	1.03e-03	3.0e-06	6.41e+02	10	51	>1E20	>1E20
Sr-92	3.09e-04	1.9e-06	2.24e+03	10	51	>1E20	>1E20
Y-86m	9.13e-05	2.4e-07	7.60e+03	10	51	>1E20	>1E20
Y-86	1.67e-03	4.1e-06	4.16e+02	10	51	>1E20	>1E20
Y-87	9.13e-03	2.2e-06	7.60e+01	10	51	>1E20	>1E20
Y-88	2.88e-01	5.2e-06	2.41e+00	10	51	>1E20	>1E20
Y-90m	3.64e-04	6.6e-07	1.90e+03	10	51	>1E20	>1E20
Y-90	2.86e+01	1.0e-05	2.42e-02	10	51	4.0e+01	6.6e-02
Y-91m	9.51e-05	3.9e-08	7.29e+03	10	51	>1E20	>1E20
Y-91	1.67e-01	8.9e-06	4.15e+00	10	51	>1E20	>1E20
Y-92	4.03e-04	1.9e-06	1.72e+03	10	51	>1E20	>1E20
Y-93	1.16e-03	4.5e-06	5.96e+02	10	51	>1E20	>1E20
Y-94	3.61e-05	1.8e-07	1.92e+04	10	51	>1E20	>1E20
Y-95	2.00e-05	9.7e-08	3.47e+04	10	51	>1E20	>1E20
Zr-86	1.88e-03	3.5e-06	3.68e+02	0	1	>1E20	>1E20
Zr-88	2.33e-01	1.3e-06	2.98e+00	0	1	3.6e+04	>1E20
Zr-89	8.94e-03	3.1e-06	7.75e+01	0	1	>1E20	>1E20
Zr-93	1.50e+06	1.6e-06	4.62e-07	0	1	1.0e-02	5.9e-03
Zr-95	1.75e-01	3.4e-06	3.96e+00	0	1	1.8e+06	>1E20
Zr-97	1.92e-03	8.0e-06	3.62e+02	0	1	>1E20	>1E20
Nb-88	2.66e-05	7.2e-08	2.60e+04	0	1	>1E20	>1E20
Nb-89(66m)	1.25e-04	4.6e-07	5.52e+03	0	1	>1E20	>1E20
Nb-89(122m)	2.32e-04	1.0e-06	2.99e+03	0	1	>1E20	>1E20
Nb-90	1.67e-03	4.9e-06	4.16e+02	0	1	>1E20	>1E20
Nb-93m	1.01e+01	5.3e-07	6.84e-02	0	1	4.3e-02	5.5e+00
Nb-94	2.00e+04	5.1e-06	3.47e-05	0	1	3.2e-03	5.9e-03
Nb-95m	9.88e-03	2.0e-06	7.02e+01	0	1	>1E20	>1E20
Nb-95	9.58e-02	2.2e-06	7.23e+00	0	1	3.7e+13	>1E20
Nb-96	2.67e-03	4.4e-06	2.60e+02	0	1	>1E20	>1E20
Nb-97	1.40e-04	2.3e-07	4.95e+03	0	1	>1E20	>1E20
Nb-98	8.87e-08	3.4e-07	7.81e+06	0	1	>1E20	>1E20
Mo-90	6.50e-04	2.5e-06	1.07e+03	0	1	>1E20	>1E20

Table C.1-2 (continued)

Nuclide	T1/2 (year)	DCF (rem/yr/Ci)	Leach (1/year)	K (cm³/g)	Rf	ILNT GW Trigger (Ci/vault)	ILNT Int Trigger (Ci/vault)
Mo-93m	7.87e-04	1.1e-06	8.81e+02	0	1	>1E20	>1E20
Mo-93	3.50e+03	1.2e-06	1.98e-04	0	1	1.2e-02	6.0e-03
Mo-99	7.53e-03	4.4e-06	9.20e+01	0	1	>1E20	>1E20
Mo-101	2.78e-05	9.2e-08	2.50e+04	0	1	>1E20	>1E20
Tc-93m	8.18e-05	7.1e-08	8.48e+03	0.36	2.8	>1E20	>1E20
Tc-93	3.08e-04	1.6e-07	2.25e+03	0.36	2.8	>1E20	>1E20
Tc-94m	1.01e-04	2.5e-07	6.88e+03	0.36	2.8	>1E20	>1E20
Tc-94	5.57e-04	5.8e-07	1.24e+03	0.36	2.8	>1E20	>1E20
Tc-96m	9.89e-05	3.1e-08	7.01e+03	0.36	2.8	>1E20	>1E20
Tc-96	1.18e-02	2.7e-06	5.89e+01	0.36	2.8	>1E20	>1E20
Tc-97m	2.46e-01	1.1e-06	2.81e+00	0.36	2.8	5.2e+15	>1E20
Tc-97	2.60e+06	1.5e-07	2.67e-07	0.36	2.8	3.0e-01	5.9e-03
Tc-98	1.50e+06	4.8e-06	4.62e-07	0.36	2.8	9.4e-03	5.9e-03
Tc-99m	6.87e-04	6.0e-08	1.01e+03	0.36	2.8	>1E20	>1E20
Tc-99	2.11e+05	1.3e-06	3.29e-06	0.36	2.8	3.5e-02	5.9e-03
Tc-101	2.70e-05	3.8e-08	2.57e+04	0.36	2.8	>1E20	>1E20
Tc-104	3.42e-05	1.6e-07	2.03e+04	0.36	2.8	>1E20	>1E20
Ru-94	1.08e-04	3.3e-07	6.40e+03	100	501	>1E20	>1E20
Ru-97	7.91e-03	6.4e-07	8.76e+01	100	501	>1E20	>1E20
Ru-103	1.08e-01	2.7e-06	6.43e+00	100	501	>1E20	>1E20
Ru-105	5.07e-04	1.0e-06	1.37e+03	100	501	>1E20	>1E20
Ru-106	9.99e-01	2.1e-05	6.94e-01	100	501	>1E20	>1E20
Rh-99m	5.36e-04	2.8e-07	1.29e+03	0	1	>1E20	>1E20
Rh-99	4.38e-02	2.0e-06	1.58e+01	0	1	>1E20	>1E20
Rh-100	2.28e-03	3.1e-06	3.04e+02	0	1	>1E20	>1E20
Rh-101m	1.23e-02	8.8e-07	5.63e+01	0	1	>1E20	>1E20
Rh-101	3.10e+00	2.3e-06	2.24e-01	0	1	2.1e-02	3.0e+07
Rh-102m	2.90e+00	3.5e-06	2.39e-01	0	1	1.5e-02	1.4e+08
Rh-102	5.75e-01	5.5e-06	1.21e+00	0	1	1.2e+00	>1E20
Rh-103m	1.06e-04	0.00000001	6.51e+03	0	-1	>1E20	>1E20
Rh-105	4.05e-03	1.4e-06	1.71e+02	0	1	>1E20	>1E20
Rh-106m	2.49e-04	6.1e-07	2.79e+03	0	1	>1E20	>1E20
Rh-107	4.13e-05	5.4e-08	1.68e+04	0	1	>1E20	>1E20
Pd-100	1.10e-02	3.8e-06	6.33e+01	0	1	>1E20	>1E20

Table C.1-2 (continued)

Nuclide	T1/2 (years)	DCF (mrem/pCi)	Emanation (1/year)	Xd (cm**3/gm)	Rf	ILNT GW Trigger (Ci/vault)	ILNT Int Trigger (Ci/vault)
Pd-101	9.58e-04	3.[illegible]e-07	7.23e+02	0	1	>1E20	>1E20
Pd-103	4.65e-02	6.9e-07	1.49e+01	0	1	>1E20	>1E20
Pd-107	6.50e+06	1.4e-07	1.07e-07	0	1	1.2e-01	5.9e-03
Pd-109	1.53e-03	2.1e-06	4.53e+02	0	1	>1E20	>1E20
Ag-102	2.85e-05	7.5e-08	2.43e+04	10	51	>1E20	>1E20
Ag-103	1.25e-04	1.4e-07	5.52e+03	10	51	>1E20	>1E20
Ag-104m	5.70e-05	1.5e-07	1.22e+04	10	51	>1E20	>1E20
Ag-104	1.27e-04	2.3e-07	5.44e+03	10	51	>1E20	>1E20
Ag-105	1.10e-01	1.9e-06	6.33e+00	10	51	>1E20	>1E20
Ag-106m	2.27e-02	6.1e-06	3.05e+01	10	51	>1E20	>1E20
Ag-106	4.56e-05	7.6e-08	1.52e+04	10	51	>1E20	>1E20
Ag-108m	1.30e+02	7.5e-06	5.33e-03	10	51	4.3e-01	1.0e-02
Ag-110m	6.98e-01	1.1e-05	1.00e+00	10	51	>1E20	>1E20
Ag-111	2.05e-02	4.5e-06	3.39e+01	10	51	>1E20	>1E20
Ag-112	3.57e-04	1.6e-06	1.94e+03	10	51	>1E20	>1E20
Ag-115	3.99e-05	1.5e-07	1.74e+04	10	51	>1E20	>1E20
Cd-104	1.08e-04	2.3e-07	6.40e+03	8	41	>1E20	>1E20
Cd-107	7.42e-04	2.4e-07	9.35e+02	8	41	>1E20	>1E20
Cd-109	1.24e+00	1.2e-05	5.59e-01	8	41	>1E20	>1E20
Cd-113m	1.46e+01	1.5e-04	4.75e-02	8	41	7.4e+01	6.8e-01
Cd-113	9.30e+15	1.6e-04	7.45e-17	8	41	4.1e-03	5.9e-03
Cd-115m	1.36e-01	1.5e-05	5.11e+00	8	41	>1E20	>1E20
Cd-115	6.10e-03	4.7e-06	1.14e+02	8	41	>1E20	>1E20
Cd-117m	3.88e-04	1.1e-06	1.79e+03	8	41	>1E20	>1E20
Cd-117	2.97e-04	1.1e-06	2.34e+03	8	41	>1E20	>1E20
In-109	4.91e-04	2.7e-07	1.41e+03	0	1	>1E20	>1E20
In-110(69m)	1.27e-04	3.3e-07	5.44e+03	0	1	>1E20	>1E20
In-111	7.69e-03	1.2e-06	9.01e+01	0	1	>1E20	>1E20
In-112	2.66e-05	0.00000002	2.60e+04	0	1	>1E20	>1E20
In-113m	1.89e-04	1.0e-07	3.66e+03	0	1	>1E20	>1E20
In-114m	1.36e-01	0.000015	5.11e+00	0	1	1.4e+08	>1E20
In-115m	5.13e-04	3.4e-07	1.35e+03	0	1	>1E20	>1E20
In-115	4.60e+15	1.4e-04	1.51e-16	0	1	1.2e-04	5.9e-03
In-116m	1.03e-04	2.1e-07	6.73e+03	0	1	>1E20	>1E20

Table C.1-2 (continued)

Nuclide	T1/2 (years)	DCF (mrem/pCi)	Inhalation (1/year)	χ/Q (cm^3/μm)	RF	ILNT GW Trigger (Ci/vault)	ILNT Int Trigger (Ci/vault)
In-117m	2.24e-04	4.2e-07	3.12e+03	0	1	>1E20	>1E20
In-117	8.37e-05	8.7e-08	8.29e+03	0	1	>1E20	>1E20
In-119m	3.44e-05	1.0e-07	2.03e+04	0	1	>1E20	>1E20
Sn-110	4.55e-04	1.5e-06	1.52e+03	130	651	>1E20	>1E20
Sn-111	6.65e-05	6.7e-08	1.04e+04	130	651	>1E20	>1E20
Sn-113	3.15e-01	2.7e-06	2.20e+00	130	651	>1E20	>1E20
Sn-117m	3.83e-02	2.6e-06	1.81e+01	130	651	>1E20	>1E20
Sn-119m	8.02e-01	1.2e-05	8.64e-01	130	651	>1E20	>1E20
Sn-121m	7.60e+01	1.3e-06	9.12e-03	130	651	6.3e+13	1.5e-02
Sn-121	3.08e-03	8.9e-07	2.25e+02	130	651	>1E20	>1E20
Sn-123m	7.61e-05	1.0e-07	9.11e+03	130	651	>1E20	>1E20
Sn-123	3.53e-01	7.7e-06	1.96e+00	130	651	>1E20	>1E20
Sn-125	2.64e-02	1.1e-05	2.62e+01	130	651	>1E20	>1E20
Sn-126	1.00e+05	1.7e-05	6.93e-06	130	651	6.3e-01	5.9e-03
Sn-127	2.42e-04	7.4e-07	2.87e+03	130	651	>1E20	>1E20
Sn-128	1.12e-04	5.2e-07	6.18e+03	130	651	>1E20	>1E20
Sb-115	5.89e-05	6.3e-08	1.18e+04	10	51	>1E20	>1E20
Sb-116m	1.14e-04	2.4e-07	6.08e+03	10	51	>1E20	>1E20
Sb-116	2.85e-05	5.6e-08	2.43e+04	10	51	>1E20	>1E20
Sb-117	3.19e-04	7.4e-08	2.17e+03	10	51	>1E20	>1E20
Sb-118m	5.82e-04	9.3e-07	1.19e+03	10	51	>1E20	>1E20
Sb-119	4.33e-03	3.4e-07	1.60e+02	10	51	>1E20	>1E20
Sb-120(16m)	3.04e-05	3.0e-08	2.28e+04	10	51	>1E20	>1E20
Sb-120(6d)	1.59e-02	5.4e-06	4.37e+01	10	51	>1E20	>1E20
Sb-122	7.45e-03	6.3e-06	9.31e+01	10	51	>1E20	>1E20
Sb-124m	1.77e-04	2.0e-08	3.92e+03	10	51	>1E20	>1E20
Sb-124	1.65e-01	9.3e-06	4.20e+00	10	51	>1E20	>1E20
Sb-125	2.40e+00	2.6e-06	2.89e-01	10	51	>1E20	2.0e+10
Sb-126m	3.61e-05	7.3e-08	1.92e+04	10	51	>1E20	>1E20
Sb-126	3.39e-02	9.6e-06	2.04e+01	10	51	>1E20	>1E20
Sb-127	1.04e-02	6.6e-06	6.66e+01	10	51	>1E20	>1E20
Sb-128(9h)	1.03e-03	4.3e-06	6.75e+02	10	51	>1E20	>1E20
Sb-128(10m)	1.90e-05	5.0e-08	3.65e+04	10	51	>1E20	>1E20
Sb-129	4.95e-04	1.7e-06	1.40e+03	10	51	>1E20	>1E20

Table C.1-2 (continued)

Nuclide	T1/2 (year)	DCF (mrem/pCi)	Lambda (1/year)	Kd (cm**3/gm)	Rf	Hazard GW Trigger (Ci/vault)	Hazard Int Trigger (Ci/vault)
Sb-130	1.25e-05	2.[illegible]e-07	5.52e+[illegible]	10	51	>1E20	>1E20
Sb-131	4.37e-05	2.9e-07	1.59e+04	10	51	>1E20	>1E20
Te-116	1.64e-02	6.7e-07	4.22e+01	0	1	>1E20	>1E20
Te-121m	4.11e-01	6.7e-06	1.68e+00	0	1	1.1e+01	>1E20
Te-121	4.65e-02	1.5e-06	1.49e+01	0	1	>1E20	>1E20
Te-123m	3.28e-01	5.1e-06	2.12e+00	0	1	1.2e+02	>1E20
Te-123	1.20e+13	4.1e-06	5.78e-14	0	1	3.9e-03	5.9e-03
Te-125m	1.59e-01	3.4e-06	4.37e+00	0	1	1.4e+07	>1E20
Te-127m	2.98e-01	7.9e-06	2.32e+00	0	1	2.3e+02	>1E20
Te-127	1.07e-03	6.9e-07	6.46e+02	0	1	>1E20	>1E20
Te-129m	9.14e-02	9.9e-06	7.58e+00	0	1	4.7e+13	>1E20
Te-129	1.33e-04	1.9e-07	5.21e+03	0	1	>1E20	>1E20
Te-131m	3.42e-03	1.5e-05	2.03e+02	0	1	>1E20	>1E20
Te-131	4.75e-05	2.0e-07	1.46e+04	0	1	>1E20	>1E20
Te-132	8.76e-03	7.4e-06	7.91e+01	0	1	>1E20	>1E20
Te-133m	1.05e-04	7.6e-07	6.58e+03	0	1	>1E20	>1E20
Te-133	2.38e-05	1.6e-07	2.92e+04	0	1	>1E20	>1E20
Te-134	7.99e-05	2.1e-07	8.68e+03	0	1	>1E20	>1E20
I-120m	1.01e-04	3.9e-07	6.88e+03	0.6	4	>1E20	>1E20
I-120	1.48e-04	6.7e-07	4.67e+03	0.6	4	>1E20	>1E20
I-121	2.40e-04	1.8e-07	2.89e+03	0.6	4	>1E20	>1E20
I-123	1.52e-03	4.9e-07	4.57e+02	0.6	4	>1E20	>1E20
I-124	1.15e-02	3.1e-05	6.03e+01	0.6	4	>1E20	>1E20
I-125	1.64e-01	3.8e-05	4.22e+00	0.6	4	>1E20	>1E20
I-126	3.64e-02	7.1e-05	1.90e+01	0.6	4	>1E20	>1E20
I-128	4.75e-05	8.5e-08	1.46e+04	0.6	4	>1E20	>1E20
I-129	1.72e+07	2.8e-04	4.02e-08	0.6	4	2.3e-04	5.9e-03
I-130	1.41e-03	4.3e-06	4.90e+02	0.6	4	>1E20	>1E20
I-131	2.22e-02	5.3e-05	3.13e+01	0.6	4	>1E20	>1E20
I-132m	1.58e-04	4.7e-07	4.39e+03	0.6	4	>1E20	>1E20
I-132	2.60e-04	3.3e-07	2.66e+03	0.6	4	>1E20	>1E20
I-133	2.37e-03	5.4e-06	2.92e+02	0.6	4	>1E20	>1E20
I-134	1.00e-04	1.9e-07	6.93e+03	0.6	4	>1E20	>1E20
I-135	7.51e-04	2.0e-05	9.23e+02	0.6	4	>1E20	>1E20

Table C.1-2. (continued)

Nuclide	T1/2 (year)	DCF (mrem/pCi)	Lambda (1/year)	Kd (cm**3/gm)	RF	ILNT GW Trigger (Ci/vault)	ILNT Cat Trigger (Ci/vault)
Cs-125	8.56e-05	5.5e-03	8.10e+03	100	501	>1E20	>1E20
Cs-127	7.07e-04	8.0e-08	9.80e+02	100	501	>1E20	>1E20
Cs-129	3.65e-03	2.2e-07	1.90e+02	100	501	>1E20	>1E20
Cs-130	5.70e-05	4.9e-08	1.22e+04	100	501	>1E20	>1E20
Cs-131	2.66e-02	2.4e-07	2.61e+01	100	501	>1E20	>1E20
Cs-132	1.80e-02	1.9e-06	3.85e+01	100	501	>1E20	>1E20
Cs-134m	3.31e-04	4.2e-08	2.10e+03	100	501	>1E20	>1E20
Cs-134	2.06e+00	7.4e-05	3.36e-01	100	501	>1E20	2.4e+12
Cs-135m	1.01e-04	4.9e-08	6.88e+03	100	501	>1E20	>1E20
Cs-135	2.30e+06	7.1e-06	3.01e-07	100	501	1.1e+00	5.9e-03
Cs-136	3.53e-02	1.1e-05	1.96e+01	100	501	>1E20	>1E20
Cs-137	3.01e+01	5.0e-05	2.30e-02	100	501	>1E20	5.9e-02
Cs-138	6.12e-05	1.6e-07	1.13e+04	100	501	>1E20	>1E20
Ba-126	1.84e-04	9.0e-07	3.76e+03	5	26	>1E20	>1E20
Ba-128	6.57e-03	1.0e-05	1.05e+02	5	26	>1E20	>1E20
Ba-131m	2.78e-05	9.7e-07	2.50e+04	5	26	>1E20	>1E20
Ba-131	3.20e-02	1.6e-06	2.16e+01	5	26	>1E20	>1E20
Ba-133m	4.44e-03	2.0e-06	1.56e+02	5	26	>1E20	>1E20
Ba-133	1.07e+01	3.2e-06	6.48e-02	5	26	5.9e+02	3.8e+00
Ba-135m	3.27e-03	1.6e-06	2.12e+02	5	26	>1E20	>1E20
Ba-137m	0.000005		1.43e+05	5	26	>1E20	>1E20
Ba-139	1.58e-04	3.9e-07	4.38e+03	5	26	>1E20	>1E20
Ba-140	3.50e-02	8.4e-06	1.98e+01	5	26	>1E20	>1E20
Ba-141	3.48e-05	2.0e-07	1.99e+04	5	26	>1E20	>1E20
Ba-142	2.03e-05	1.0e-07	3.41e+04	5	26	>1E20	>1E20
La-131	1.12e-04	1.1e-07	6.18e+03	100	501	>1E20	>1E20
La-132	5.13e-04	1.5e-06	1.35e+03	100	501	>1E20	>1E20
La-135	2.22e-03	1.3e-07	3.12e+02	100	501	>1E20	>1E20
La-137	6.00e+04	4.3e-07	1.16e-05	100	501	1.9e+01	5.9e-03
La-138	1.06e+11	5.9e-06	6.54e-12	100	501	1.4e+00	5.9e-03
La-140	4.59e-03	7.7e-06	1.51e+02	100	501	>1E20	>1E20
La-141	4.41e-04	1.4e-06	1.57e+03	100	501	>1E20	>1E20
La-142	1.76e-04	8.3e-07	3.95e+03	100	501	>1E20	>1E20
La-143	2.66e-05	1.4e-07	2.60e+04	100	501	>1E20	>1E20

Table C.1-2 (continued)

Nuclide	T1/2 (year)	DCF (mrem/pCi)	Lambda (1/day)	Kd (cm**3/gm)	Rf	ILNT GW Trigger (Ci/vol)	ILNT Int Trigger (Ci/vol)
Ce-134	8.21e-03	8.9e-06	8.11e+01	10	51	>1E20	>1E20
Ce-135	1.94e-03	3.2e-06	3.53e+02	10	51	>1E20	>1E20
Ce-137m	3.92e-03	2.0e-06	1.77e+02	10	51	>1E20	>1E20
Ce-137	1.03e-03	9.8e-08	6.75e+02	10	51	>1E20	>1E20
Ce-139	3.77e-01	1.1e-06	1.84e+00	10	51	>1E20	>1E20
Ce-141	8.90e-02	2.6e-06	7.79e+00	10	51	>1E20	>1E20
Ce-143	3.76e-03	4.2e-06	1.84e+02	10	51	>1E20	>1E20
Ce-144	7.94e-01	2.0e-05	8.73e-01	10	51	>1E20	>1E20
Pr-136	1.25e-04	6.8e-08	5.52e+03	10	51	>1E20	>1E20
Pr-137	1.71e-04	1.3e-07	4.05e+03	100	501	>1E20	>1E20
Pr-138m	2.40e-04	4.9e-07	2.89e+03	100	501	>1E20	>1E20
Pr-139	5.13e-04	1.2e-07	1.35e+03	100	501	>1E20	>1E20
Pr-142m	2.72e-05	6.3e-08	2.55e+04	100	501	>1E20	>1E20
Pr-142	2.18e-03	5.1e-06	3.18e+02	100	501	>1E20	>1E20
Pr-143	3.75e-02	4.5e-06	1.85e+01	100	501	>1E20	>1E20
Pr-144	3.29e-05	1.1e-07	2.11e+04	100	501	>1E20	>1E20
Pr-145	6.82e-04	1.5e-06	1.02e+03	100	501	>1E20	>1E20
Pr-147	2.28e-05	5.7e-08	3.04e+04	100	501	>1E20	>1E20
Nd-136	9.64e-05	3.3e-07	7.19e+03	100	501	>1E20	>1E20
Nd-138	4.18e-05	2.5e-06	1.66e+04	100	501	>1E20	>1E20
Nd-139m	6.27e-04	1.0e-06	1.10e+03	100	501	>1E20	>1E20
Nd-139	5.93e-04	5.7e-08	1.17e+03	100	501	>1E20	>1E20
Nd-141	2.85e-04	3.2e-08	2.43e+03	100	501	>1E20	>1E20
Nd-147	3.01e-02	3.9e-06	2.30e+01	100	501	>1E20	>1E20
Nd-149	1.97e-03	4.6e-07	3.51e+02	100	501	>1E20	>1E20
Nd-151	2.36e-05	7.4e-08	2.94e+04	100	501	>1E20	>1E20
Pm-141	4.18e-05	8.4e-08	1.66e+04	100	501	>1E20	>1E20
Pm-143	7.26e-01	9.5e-07	9.55e-01	100	501	>1E20	>1E20
Pm-144	8.22e-01	3.9e-06	8.43e-01	100	501	>1E20	>1E20
Pm-145	1.77e+01	4.6e-07	3.92e-02	100	501	>1E20	3.0e-01
Pm-146	1.94e+00	3.2e-06	3.57e-01	100	501	>1E20	1.8e+13
Pm-147	2.52e+00	9.5e-07	2.75e-01	100	501	>1E20	5.3e+09
Pm-148m	1.14e-01	7.0e-06	6.06e+00	100	501	>1E20	>1E20
Pm-148	1.47e-02	9.5e-06	4.71e+01	100	501	>1E20	>1E20

Table C.1-2 (continued)

Nuclide	T1/2 (year)	DCF (mrem/pCi)	Lambda (1/year)	Kd (cm**3/gm)	PF	ILCR GW Target (Ci/vault)	ILCR Air Target (Ci/vault)
Pm-149	6.06e-03	3.6e-06	1.14e+02	100	501	>1E20	>1E20
Pm-150	3.06e-04	9.3e-07	2.27e+03	100	501	>1E20	>1E20
Pm-151	3.24e-03	2.8e-06	2.14e+02	100	501	>1E20	>1E20
Sm-141m	4.30e-05	1.8e-07	1.61e+04	100	501	>1E20	>1E20
Sm-141	1.94e-05	8.4e-08	3.57e+04	100	501	>1E20	>1E20
Sm-142	1.37e-04	6.0e-07	5.06e+03	100	501	>1E20	>1E20
Sm-145	9.31e-01	8.5e-07	7.45e-01	100	501	>1E20	>1E20
Sm-146	7.00e+07	2.0e-04	9.90e-09	100	501	4.0e-02	5.9e-03
Sm-147	1.06e+11	1.8e-04	6.54e-12	100	501	4.5e-02	5.9e-03
Sm-151	9.00e+01	3.4e-07	7.70e-03	100	501	5.7e+09	1.3e-02
Sm-153	5.33e-03	2.6e-06	1.30e+02	100	501	>1E20	>1E20
Sm-155	4.22e-05	6.6e-08	1.64e+04	100	501	>1E20	>1E20
Sm-158	8.37e-05	1.0e-06	8.29e+03	100	501	>1E20	>1E20
Eu-145	1.62e-02	3.2e-05	4.29e+01	100	501	>1E20	>1E20
Eu-146	1.26e-02	5.1e-06	5.50e+01	100	501	>1E20	>1E20
Eu-147	6.02e-02	1.8e-06	1.15e+01	100	501	>1E20	>1E20
Eu-148	1.48e-01	5.2e-06	4.69e+00	100	501	>1E20	>1E20
Eu-149	2.90e-01	4.2e-07	2.39e+00	100	501	>1E20	>1E20
Eu-150(12h)	1.37e-03	1.5e-06	5.06e+02	100	501	>1E20	>1E20
Eu-150(34y)	3.40e+01	6.2e-06	2.04e-02	100	501	>1E20	4.5e-02
Eu-152m	1.07e-03	1.9e-06	6.51e+02	100	501	>1E20	>1E20
Eu-152	1.34e+01	6.0e-06	5.17e-02	100	501	>1E20	1.0e+00
Eu-154	8.20e+00	9.1e-06	8.45e-02	100	501	>1E20	2.8e+01
Eu-155	1.70e+00	1.3e-06	4.08e-01	100	501	>1E20	>1E20
Eu-156	4.22e-02	8.7e-06	1.64e+01	100	501	>1E20	>1E20
Eu-157	1.73e-03	2.3e-06	4.00e+02	100	501	>1E20	>1E20
Eu-158	8.73e-05	2.6e-07	7.94e+03	100	501	>1E20	>1E20
Gd-145	4.75e-05	1.1e-07	1.46e+04	100	501	>1E20	>1E20
Gd-146	1.26e-02	3.8e-06	5.50e+01	100	501	>1E20	>1E20
Gd-147	3.99e-03	2.6e-06	1.74e+02	100	501	>1E20	>1E20
Gd-148	1.30e+02	2.1e-04	5.33e-03	100	501	2.4e+04	1.0e-02
Gd-149	2.46e-02	1.8e-06	2.81e+01	100	501	>1E20	>1E20
Gd-151	3.29e-01	7.7e-07	2.11e+00	100	501	>1E20	>1E20
Gd-152	1.10e+14	1.5e-04	6.30e-15	100	501	5.4e-02	5.9e-03

Table C.1-2. (continued)

Nuclide	T1/2 (sec)	DCF (mrem/pCi)	Lambda (1/sec)	X1 (cm^3/g/µm)	RF	ILNT Gov Trigger (Ci/yrd)	Hot Spot Trigger (Ci/yrd)
Gd-153	6.61e-01	1.1e-06	1.05e+00	100	501	>1E20	>1E20
Gd-159	2.12e-03	1.9e-06	3.27e+02	100	501	>1E20	>1E20
Tb-147	4.56e-05	5.6e-07	1.52e+04	100	501	>1E20	>1E20
Tb-149	4.68e-04	9.5e-07	1.48e+03	100	501	>1E20	>1E20
Tb-150	3.54e-04	9.7e-07	1.96e+03	100	501	>1E20	>1E20
Tb-151	2.05e-03	1.4e-06	3.38e+02	100	501	>1E20	>1E20
Tb-153	6.27e-03	9.9e-07	1.10e+02	100	501	>1E20	>1E20
Tb-154	9.70e-04	2.8e-06	7.15e+02	100	501	>1E20	>1E20
Tb-155	1.53e-02	8.2e-07	4.52e+01	100	501	>1E20	>1E20
Tb-156m(24h)	2.74e-03	7.0e-07	2.53e+02	100	501	>1E20	>1E20
Tb-156m(5h)	6.27e-04	3.2e-07	1.10e+03	100	501	>1E20	>1E20
Tb-156	1.48e-02	4.6e-06	4.69e+01	100	501	>1E20	>1E20
Tb-157	1.50e+02	1.0e-07	4.62e-03	100	501	8.6e+06	9.3e-03
Tb-158	1.20e+03	4.0e-06	5.78e-04	100	501	8.6e+00	6.2e-03
Tb-160	1.98e-01	6.4e-06	3.50e+00	100	501	>1E20	>1E20
Tb-161	1.88e-02	2.6e-06	3.68e+01	100	501	>1E20	>1E20
Dy-155	1.20e-03	5.6e-07	5.79e+02	100	501	>1E20	>1E20
Dy-157	9.24e-04	2.7e-07	7.50e+02	100	501	>1E20	>1E20
Dy-159	3.94e-01	4.0e-07	1.76e+00	100	501	>1E20	>1E20
Dy-165	2.66e-04	3.6e-07	2.61e+03	100	501	>1E20	>1E20
Dy-166	9.31e-03	6.2e-06	7.45e+01	100	501	>1E20	>1E20
Ho-155	9.51e-05	1.2e-07	7.29e+03	100	501	>1E20	>1E20
Ho-157	2.66e-05	1.9e-08	2.60e+04	100	501	>1E20	>1E20
Ho-159	6.27e-05	2.3e-08	1.10e+04	100	501	>1E20	>1E20
Ho-161	2.85e-04	4.7e-08	2.43e+03	100	501	>1E20	>1E20
Ho-162m	1.29e-04	9.0e-08	5.36e+03	100	501	>1E20	>1E20
Ho-162	2.85e-05	6.7e-09	2.43e+04	100	501	>1E20	>1E20
Ho-164m	7.13e-05	4.9e-08	9.72e+03	100	501	>1E20	>1E20
Ho-164	7.03e-05	2.4e-08	9.85e+03	100	501	>1E20	>1E20
Ho-166m	1.20e+03	7.8e-06	5.78e-04	100	501	4.4e+00	6.2e-03
Ho-166	3.06e-03	5.5e-06	2.27e+02	100	501	>1E20	>1E20
Ho-167	3.54e-04	3.2e-07	1.96e+03	100	501	>1E20	>1E20
Er-161	3.54e-04	3.3e-07	1.96e+03	100	501	>1E20	>1E20
Er-165	1.18e-03	7.9e-08	5.86e+02	100	501	>1E20	>1E20

Table C.1-2 (continued)

Nuclide	T1/2 (yrs)	DCF (rem/pCi)	Lambda (1/yr)	Xd (cm**3/gm)	Rf	ILNT GW Trigger (Ci/vault)	ILNT Int Trigger (Ci/vault)
Er-169	2.57e-02	1.4e-06	2.69e+01	100	501	>1E20	>1E20
Er-171	8.58e-04	1.4e-06	8.08e+02	100	501	>1E20	>1E20
Er-172	5.59e-03	3.7e-06	1.24e+02	100	501	>1E20	>1E20
Tm-162	1.46e-04	7.0e-08	4.73e+03	100	501	>1E20	>1E20
Tm-166	8.78e-04	1.2e-06	7.89e+02	100	501	>1E20	>1E20
Tm-167	2.63e-02	2.1e-06	2.64e+01	100	501	>1E20	>1E20
Tm-170	3.53e-01	5.0e-06	1.96e+00	100	501	>1E20	>1E20
Tm-171	1.92e+00	3.9e-07	3.61e-01	100	501	>1E20	2.8e+13
Tm-172	7.26e-03	6.0e-06	9.55e+01	100	501	>1E20	>1E20
Tm-173	9.35e-04	1.2e-06	7.41e+02	100	501	>1E20	>1E20
Tm-175	3.80e-05	5.4e-08	1.82e+04	100	501	>1E20	>1E20
Yb-162	3.59e-05	7.0e-08	1.93e+04	100	501	>1E20	>1E20
Yb-165	1.90e-05	3.8e-06	3.65e+04	100	501	>1E20	>1E20
Yb-167	3.42e-05	1.7e-08	2.03e+04	100	501	>1E20	>1E20
Yb-169	8.76e-02	2.8e-06	7.91e+00	100	501	>1E20	>1E20
Yb-175	1.15e-02	1.6e-06	6.04e+01	100	501	>1E20	>1E20
Yb-177	2.17e-04	3.1e-07	3.20e+03	100	501	>1E20	>1E20
Yb-178	1.40e-04	3.9e-07	4.94e+03	100	501	>1E20	>1E20
Lu-169	3.88e-03	2.0e-06	1.79e+02	100	501	>1E20	>1E20
Lu-170	5.48e-03	4.3e-06	1.27e+02	100	501	>1E20	>1E20
Lu-171	2.27e-02	2.6e-06	3.05e+01	100	501	>1E20	>1E20
Lu-172	1.83e-02	5.0e-06	3.78e+01	100	501	>1E20	>1E20
Lu-173	1.37e+00	9.7e-07	5.06e-01	100	501	>1E20	>1E20
Lu-174m	3.83e-01	1.8e-06	1.81e+00	100	501	>1E20	>1E20
Lu-174	3.60e+00	9.9e-07	1.93e-01	100	501	>1E20	1.4e+06
Lu-176m	4.21e-04	6.3e-07	1.65e+03	100	501	>1E20	>1E20
Lu-176	3.00e+10	6.6e-06	2.31e-11	100	501	1.2e+00	5.9e-03
Lu-177m	4.41e-02	6.8e-06	1.57e+01	100	501	>1E20	>1E20
Lu-177	1.84e-02	2.0e-06	3.77e+01	100	501	>1E20	>1E20
Lu-178m	3.80e-05	8.8e-08	1.82e+04	100	501	>1E20	>1E20
Lu-178	5.70e-05	1.2e-07	1.22e+04	100	501	>1E20	>1E20
Lu-179	5.25e-04	8.1e-07	1.32e+03	100	501	>1E20	>1E20
Hf-170	1.39e-03	1.2e-05	4.98e+02	100	501	>1E20	>1E20
Hf-172	5.00e+00	4.1e-06	1.39e-01	100	501	>1E20	6.2e+03

Table C.1-2 (continued)

Nuclide	T1/2 (sec)	DCF (mrem/pCi)	Lambda (1/sec)	Kd (cm^3/gm)	Rf	ILNT GW Trigger (Ci/vault)	ILNT [illegible] Trigger (Ci/vault)
Hf-173	2.6[illegible]e+03	9.[illegible]e-07	2.57e-02	100	501	>1E20	>1E20
Hf-175	1.9[illegible]e+01	1.6e-[illegible]	3.6[illegible]e+00	100	501	>1E20	>1E20
Hf-177m	9.77e-05	2.5e-07	7.0[illegible]e+03	100	501	>1E20	>1E20
Hf-178m	3.10e+01	2.0e-05	2.2[illegible]e-02	100	501	>1E20	5.5e-02
Hf-179m	6.87e-02	4.8e-06	1.01e+01	100	501	>1E20	>1E20
Hf-180m	6.27e-04	8.9e-07	1.10e+03	100	501	>1E20	>1E20
Hf-181	1.16e-01	4.3e-06	5.97e+00	100	501	>1E20	>1E20
Hf-182m	1.18e-04	1.4e-07	5.88e+03	100	501	>1E20	>1E20
Hf-182	9.00e+06	1.4e-05	7.70e-08	100	501	5.8e-01	5.9e-03
Hf-183	1.25e-04	2.5e-07	5.52e+03	100	501	>1E20	>1E20
Hf-184	4.68e-04	2.1e-06	1.48e+03	100	501	>1E20	>1E20
Ta-172	8.37e-05	1.4e-07	8.29e+03	0	1	>1E20	>1E20
Ta-173	4.22e-04	7.4e-07	1.64e+03	0	1	>1E20	>1E20
Ta-174	1.48e-04	1.9e-07	4.67e+03	0	1	>1E20	>1E20
Ta-175	1.20e-03	8.8e-07	5.79e+02	0	1	>1E20	>1E20
Ta-176	9.13e-04	1.3e-06	7.60e+02	0	1	>1E20	>1E20
Ta-177	6.46e-03	4.1e-07	1.07e+02	0	1	>1E20	>1E20
Ta-178	1.79e-05	2.9e-07	3.88e+04	0	1	>1E20	>1E20
Ta-179	2.40e-04	2.5e-07	2.89e+03	0	1	>1E20	>1E20
Ta-180m	9.24e-04	2.1e-07	7.50e+02	0	1	>1E20	>1E20
Ta-180	1.00e+13	3.3e-06	6.93e-14	0	1	4.9e-03	5.9e-03
Ta-182m	3.02e-05	2.4e-08	2.29e+04	0	1	>1E20	>1E20
Ta-182	3.15e-01	6.0e-06	2.20e+00	0	1	1.6e+02	>1E20
Ta-183	1.40e-02	4.6e-06	4.96e+01	0	1	>1E20	>1E20
Ta-184	9.92e-04	2.7e-06	6.98e+02	0	1	>1E20	>1E20
Ta-185	9.51e-05	2.0e-07	7.29e+03	0	1	>1E20	>1E20
Ta-186	2.00e-05	6.7e-08	3.47e+04	0	1	>1E20	>1E20
W-176	2.85e-04	4.8e-07	2.43e+03	0	1	>1E20	>1E20
W-177	2.57e-04	2.4e-07	2.70e+03	0	1	>1E20	>1E20
W-178	5.89e-02	9.3e-07	1.18e+01	0	1	>1E20	>1E20
W-179	7.22e-05	9.0e-09	9.59e+03	0	1	>1E20	>1E20
W-181	3.31e-01	3.1e-07	2.09e+00	0	1	1.8e+03	>1E20
W-185	2.06e-01	1.9e-06	3.37e+00	0	1	1.8e+05	>1E20
W-187	2.73e-03	2.6e-06	2.54e+02	0	1	>1E20	>1E20

Table C.1-2. (continued)

Nuclide	T1/2 (year)	DCF (mrem/pCi)	Lambda (1/year)	Fd (cm^3/g)	Rf	ILNT Gw Table (Ci/mg/l)	ILNT Int Table (Ci/mg/l)
W-178	1.8[illegible]e-01	9.0e-06	3.67e+00	0	1	1.7e+05	>1E20
Re-177	3.2[illegible]e-05	4.4e-08	2.14e+04	0	1	>1E20	>1E20
Re-178	2.85e-05	4.8e-[illegible]	2.43e+04	0	1	>1E20	>1E20
Re-181	2.05e-03	1.0e-06	3.38e+02	0	1	>1E20	>1E20
Re-184(64h)	7.30e-03	3.4e-06	9.49e+01	0	1	>1E20	>1E20
Re-182(12h)	1.45e-03	7.4e-07	4.78e+02	0	1	>1E20	>1E20
Re-184m	4.63e-01	2.4e-06	1.50e+00	0	1	1.2e+01	>1E20
Rm-184	1.04e-02	2.2e-06	6.66e+01	0	1	>1E20	>1E20
Re-186m	2.00e+05	3.3e-06	3.47e-06	0	1	4.9e-03	5.9e-03
Re-186	1.03e-02	2.6e-06	6.71e+01	0	1	>1E20	>1E20
Re-187	7.00e+10	8.3e-09	9.90e-12	0	1	1.9e+00	5.9e-03
Re-188m	3.54e-05	6.2e-08	1.96e+04	0	1	>1E20	>1E20
Re-188	1.91e-03	2.8e-06	3.64e+02	0	1	>1E20	>1E20
Re-189	2.74e-03	1.5e-06	2.53e+02	0	1	>1E20	>1E20
Os-180	4.13e-05	4.7e-08	1.68e+04	0	1	>1E20	>1E20
Os-181	4.37e-05	3.5e-07	1.59e+04	0	1	>1E20	>1E20
Os-182	2.51e-03	2.2e-06	2.76e+02	0	1	>1E20	>1E20
Os-185	2.57e-01	2.1e-06	2.69e+00	0	1	5.4e+03	>1E20
Os-189m	6.84e-04	6.6e-08	1.01e+03	0	1	>1E20	>1E20
Os-191m	1.48e-03	3.6e-07	4.67e+02	0	1	>1E20	>1E20
Os-191	4.19e-02	2.0e-06	1.65e+01	0	1	>1E20	>1E20
Os-193	3.48e-03	3.1e-06	1.99e+02	0	1	>1E20	>1E20
Os-194	6.00e+00	9.1e-06	1.16e-01	0	1	3.2e-03	6.1e+02
Ir-182	2.85e-05	1.2e-07	2.43e+04	0	1	>1E20	>1E20
Ir-184	3.65e-04	6.4e-07	1.90e+03	0	1	>1E20	>1E20
Ir-185	1.60e-03	1.1e-06	4.34e+02	0	1	>1E20	>1E20
Ir-186	1.83e-03	2.1e-06	3.80e+02	0	1	>1E20	>1E20
Ir-187	1.20e-03	4.8e-07	5.79e+02	0	1	>1E20	>1E20
Ir-188	4.68e-03	2.7e-06	1.48e+02	0	1	>1E20	>1E20
Ir-189	3.64e-02	9.3e-07	1.90e+01	0	1	>1E20	>1E20
Ir-190m	3.65e-04	3.0e-08	1.90e+03	0	1	>1E20	>1E20
Ir-190	3.01e-02	4.9e-06	2.30e+01	0	1	>1E20	>1E20
Ir-192m	2.74e-06	1.5e-06	2.53e+05	0	1	>1E20	>1E20
Ir-192	2.03e-01	5.3e-06	3.41e+00	0	1	7.8e+04	>1E20

Table C.1-2 (continued)

Nuclide	T1/2 (Ci/g)	DCF (mrem/hr/Ci)	Lambda (1/yr)	Kd (cm**3/gm)	RF	ILNT GW Trigger (Ci/vault)	ILNT Inv Trigger (Ci/vault)
Ir-192m	4.6[illegible]e-01	8.1e-06	1.[illegible]e+00	0	1	3.[illegible]e+00	>1E20
Ir-194	2.22e-03	5.1e-06	3.12e+02	0	1	>1E20	>1E20
Ir-195m	4.45e-04	6.4e-07	1.5[illegible]e+03	0	1	>1E20	>1E20
Ir-195	4.7[illegible]e-03	3.4e-07	1.45e+03	0	1	>1E20	>1E20
Pt-186	3.42e-04	3.7e-07	2.03e+03	0	1	>1E20	>1E20
Pt-188	2.79e-02	3.0e-06	2.48e+01	0	1	>1E20	>1E20
Pt-189	1.24e-03	4.9e-07	5.57e+02	0	1	>1E20	>1E20
Pt-191	1.24e-03	1.3e-06	5.57e+02	0	1	>1E20	>1E20
Pt-193m	1.18e-02	1.7e-06	5.89e+01	0	1	>1E20	>1E20
Pt-193	5.00e+01	1.1e-07	1.39e-02	0	1	1.6e-01	2.4e-02
Pt-195m	1.10e-02	2.2e-06	6.30e+01	0	1	>1E20	>1E20
Pt-197m	1.79e-04	3.1e-07	3.88e+03	0	1	>1E20	>1E20
Pt-197	2.09e-03	1.5e-06	3.32e+02	0	1	>1E20	>1E20
Pt-199	5.86e-05	1.0e-07	1.18e+04	0	1	>1E20	>1E20
Pt-200	1.31e-03	4.5e-06	5.28e+02	0	1	>1E20	>1E20
Au-193	1.83e-03	6.0e-07	3.80e+02	0	1	>1E20	>1E20
Au-194	4.51e-03	2.0e-06	1.54e+02	0	1	>1E20	>1E20
Au-195	5.01e-01	1.1e-06	1.38e+00	0	1	1.5e+01	>1E20
Au-198m	6.30e-03	5.7e-06	1.10e+02	0	1	>1E20	>1E20
Au-198	7.38e-03	2.3e-06	9.39e+01	0	1	>1E20	>1E20
Au-199	8.60e-03	1.8e-06	8.06e+01	0	1	>1E20	>1E20
Au-200m	2.13e-03	4.6e-06	3.25e+02	0	1	>1E20	>1E20
Au-200	9.20e-05	1.9e-07	7.53e+03	0	1	>1E20	>1E20
Au-201	4.94e-05	5.7e-08	1.40e+04	0	1	>1E20	>1E20
Hg-193m	1.14e-03	1.6e-06	6.08e+02	1000	5001	>1E20	>1E20
Hg-193	6.84e-04	3.3e-07	1.01e+03	1000	5001	>1E20	>1E20
Hg-194	1.90e+00	6.0e-06	3.65e-01	1000	5001	>1E20	4.1e+13
Hg-195m	4.56e-03	2.2e-06	1.52e+02	1000	5001	>1E20	>1E20
Hg-195	1.08e-03	3.8e-07	6.40e+02	1000	5001	>1E20	>1E20
Hg-197m	2.72e-03	1.7e-06	2.55e+02	1000	5001	>1E20	>1E20
Hg-197	7.31e-03	9.1e-07	9.48e+01	1000	5001	>1E20	>1E20
Hg-199m	8.10e-05	8.5e-08	8.56e+03	1000	5001	>1E20	>1E20
Hg-203	1.28e-01	2.1e-06	5.43e+00	1000	5001	>1E20	>1E20
Tl-194m	6.24e-05	7.1e-08	1.11e+04	0	1	>1E20	>1E20

Table C.1-2 (continued)

Nuclide	T1/2 (year)	DCF (mrem/pCi)	Inventory (Ci/year)	Kd (cm^3/gm)	Rf	ILNT GW Trigger (Ci/vault)	ILNT Int Trigger (Ci/vault)
Tl-194	6.27e-05	1.[illegible]	1.10e+04	0	1	>1E20	>1E20
Tl-195	1.37e-04	7.7e-08	5.06e+03	0	1	>1E20	>1E20
Tl-197	3.19e-04	6.9e-08	2.17e+03	0	1	>1E20	>1E20
Tl-198m	2.12e-04	1.6e-07	3.25e+03	0	1	>1E20	>1E20
Tl-198	6.05e-04	2.6e-07	1.15e+03	0	1	>1E20	>1E20
Tl-199	8.44e-04	8.2e-08	8.21e+02	0	1	>1E20	>1E20
Tl-200	2.98e-03	6.7e-07	2.33e+02	0	1	>1E20	>1E20
Tl-201	8.33e-03	2.9e-07	8.32e+01	0	1	>1E20	>1E20
Tl-202	3.29e-02	1.5e-06	2.11e+01	0	1	>1E20	>1E20
Tl-204	3.77e+00	3.2e-06	1.84e-01	0	1	1.3e-02	5.7e+05
Pb-195m	2.85e-05	8.5e-08	2.43e+04	100	501	>1E20	>1E20
Pb-198	2.74e-04	1.6e-07	2.53e+03	100	501	>1E20	>1E20
Pb-199	1.71e-04	2.2e-07	4.05e+03	100	501	>1E20	>1E20
Pb-200	2.45e-03	1.5e-06	2.83e+02	100	501	>1E20	>1E20
Pb-201	1.07e-03	6.7e-07	6.46e+02	100	501	>1E20	>1E20
Pb-202m	4.13e-04	5.5e-07	1.68e+03	100	501	>1E20	>1E20
Pb-202	3.00e+05	3.9e-05	2.31e-06	100	501	2.1e-01	5.9e-03
Pb-203	5.94e-03	9.6e-07	1.17e+02	100	501	>1E20	>1E20
Pb-205	1.40e+07	1.5e-06	4.95e-08	100	501	5.4e+00	5.9e-03
Pb-209	6.24e-06	9.0e-08	1.11e+05	100	501	>1E20	>1E20
Pb-210	2.23e+01	5.1e-03	3.11e-02	100	501	>1E20	1.3e-01
Pb-211	6.86e-05	4.4e-07	1.01e+04	100	501	>1E20	>1E20
Pb-212	1.21e-03	4.1e-05	5.71e+02	100	501	>1E20	>1E20
Pb-214	5.10e-05	5.8e-07	1.36e+04	100	501	>1E20	>1E20
Bi-200	6.65e-05	1.7e-07	1.04e+04	0	1	>1E20	>1E20
Bi-201	2.05e-04	4.5e-07	3.38e+03	0	1	>1E20	>1E20
Bi-202	1.81e-04	3.6e-07	3.84e+03	0	1	>1E20	>1E20
Bi-203	1.35e-03	2.1e-06	5.15e+02	0	1	>1E20	>1E20
Bi-205	4.19e-02	3.7e-06	1.65e+01	0	1	>1E20	>1E20
Bi-206	1.71e-02	8.0e-06	4.06e+01	0	1	>1E20	>1E20
Bi-207	7.94e+00	4.9e-06	8.73e-02	0	1	5.1e-03	3.6e+01
Bi-210m	3.50e+06	8.6e-05	1.98e-07	0	1	1.9e-04	5.9e-03
Bi-210	1.37e-02	5.9e-06	5.06e+01	0	1	>1E20	>1E20
Bi-212	1.15e-04	9.9e-07	6.02e+03	0	1	>1E20	>1E20

Table C.1-2 (continued)

Nuclide	T1/2 (year)	DCF (mrem/pCi)	Lambda (1/year)	Kd (cm^3/g)	Rf	ILNT GW Trigger (Ci/cm^3)	ILNT Int Trigger (Ci/cm^3)
Bi-213	8.58e-05	6.7e-07	7.99e+03	0	1	>1E20	>1E20
Bi-214	3.70e-05	2.1e-07	1.84e+04	0	1	>1E20	>1E20
Po-203	7.99e-05	2.0e-07	8.68e+03	0	1	>1E20	>1E20
Po-205	2.05e-04	2.4e-07	3.38e+03	0	1	>1E20	>1E20
Po-207	6.50e-04	6.1e-07	1.07e+03	0	1	>1E20	>1E20
Po-210	3.79e-01	1.6e-03	1.83e+00	0	1	9.5e-02	>1E20
At-207	2.05e-04	8.9e-07	3.38e+03	0	1	>1E20	>1E20
At-211	8.22e-04	4.1e-05	8.43e+02	0	1	>1E20	>1E20
Fr-222	2.81e-05	2.5e-06	2.46e+04	0	1	>1E20	>1E20
Fr-223	4.18e-05	8.6e-06	1.66e+04	0	1	>1E20	>1E20
Ra-223	3.13e-02	5.5e-04	2.21e+01	500	2501	>1E20	>1E20
Ra-224	9.91e-03	3.3e-04	6.99e+01	500	2501	>1E20	>1E20
Ra-225	4.05e-02	3.1e-04	1.71e+01	500	2501	>1E20	>1E20
Ra-226	1.62e+03	1.1e-03	4.27e-04	500	2501	7.7e+00	6.1e-03
Ra-227	7.83e-05	2.2e-07	8.85e+03	500	2501	>1E20	>1E20
Ra-228	5.75e+00	1.2e-03	1.21e-01	500	2501	>1E20	1.0e+03
Ac-224	3.31e-04	2.6e-06	2.10e+03	150	751	>1E20	>1E20
Ac-225	2.74e-02	9.5e-05	2.53e+01	150	751	>1E20	>1E20
Ac-226	3.31e-03	4.0e-05	2.10e+02	150	751	>1E20	>1E20
Ac-227	2.18e+01	1.4e-02	3.18e-02	150	751	>1E20	1.4e-01
Ac-228	6.99e-04	2.1e-06	9.91e+02	150	751	>1E20	>1E20
Th-226	5.87e-05	9.2e-07	1.18e+04	3000	15001	>1E20	>1E20
Th-227	5.13e-02	3.6e-05	1.35e+01	3000	15001	>1E20	>1E20
Th-228	1.91e+00	3.8e-04	3.62e-01	3000	15001	>1E20	3.2e+13
Th-229	7.43e+03	3.5e-03	9.33e-05	3000	15001	7.6e+01	5.9e-03
Th-230	7.70e+04	5.3e-04	9.00e-06	3000	15001	9.0e-01	5.9e-03
Th-231	2.91e-03	1.3e-06	2.38e+02	3000	15001	>1E20	>1E20
Th-232	1.41e+10	2.8e-03	4.93e-11	3000	15001	1.9e-02	5.9e-03
Th-234	6.60e-02	1.3e-05	1.05e+01	3000	15001	>1E20	>1E20
Pa-227	7.28e-05	1.3e-06	9.52e+03	10	51	>1E20	>1E20
Pa-228	2.97e-03	4.0e-06	2.34e+02	10	51	>1E20	>1E20
Pa-230	4.85e-02	5.6e-06	1.43e+01	10	51	>1E20	>1E20
Pa-231	3.28e+04	1.1e-02	2.12e-05	10	51	7.5e-05	5.9e-03
Pa-232	3.59e-03	3.4e-06	1.93e+02	10	51	>1E20	>1E20

Table C.1-2 (continued)

Nuclide	T1/2 (C[illegible])	DCF (mrem/pCi)	L[illegible] (1/[illegible])	K1 (cm[illegible]/pCi)	RF	ILNT GW Trigger (Ci/vault)	ILNT Air Trigger (Ci/vault)
Pa-233	7.3[illegible]e+02	3.2e-06	9.2[illegible]e+00	10	51	>1[illegible]20	>1E20
Pa-234	7.6[illegible]e+04	2.1e-06	9.07e+02	10	51	>1E20	>1E20
U-230	5.6[illegible]e+02	8.4e-04	1.22e+01	50	251	>1E20	>1E20
U-231	4.30e+00	1.1e-06	1.61e+01	50	251	>1E20	5.9e+04
U-232	7.20e+01	1.3e-03	9.63e-03	50	251	5.5e+02	1.5e-02
U-233	1.60e+05	2.7e-04	4.35e-06	50	251	1.5e-02	5.9e-03
U-234	2.45e+05	2.6e-04	2.83e-06	50	251	1.5e-02	5.9e-03
U-235	7.04e+08	2.5e-04	9.85e-10	50	251	7.7e-03	5.9e-03
U-236	2.34e+07	2.5e-04	2.96e-08	50	251	1.6e-02	5.9e-03
U-237	1.85e-02	2.7e-06	3.75e+01	50	251	>1E20	>1E20
U-238	4.47e+09	2.3e-04	1.55e-10	50	251	1.6e-02	5.9e-03
U-239	4.47e-05	7.6e-08	1.55e+04	50	251	>1E20	>1E20
U-240	1.61e-03	4.1e-06	4.31e+02	50	251	>1E20	>1E20
Np-232	2.47e-05	2.4e-08	2.80e+04	10	51	>1E20	>1E20
Np-233	6.65e-05	5.6e-09	1.04e+04	10	51	>1E20	>1E20
Np-234	1.20e-02	1.7e-06	5.75e+01	10	51	>1E20	>1E20
Np-235	1.12e+00	2.1e-07	6.17e-01	10	51	>1E20	>1E20
Np-236(1E5y)	1.10e+05	7.9e-04	6.30e-06	10	51	1.0e-03	5.9e-03
Np-236(22h)	2.51e-03	9.5e-07	2.76e+02	10	51	>1E20	>1E20
Np-237	2.14e+06	3.9e-03	3.24e-07	10	51	2.1e-04	5.9e-03
Np-238	5.80e-03	3.4e-06	1.20e+02	10	51	>1E20	>1E20
Np-239	6.38e-03	2.9e-06	1.09e+02	10	51	>1E20	>1E20
Np-240	1.20e-04	2.0e-07	5.79e+03	10	51	>1E20	>1E20
Pu-234	1.03e-03	1.2e-06	6.75e+02	100	501	>1E20	>1E20
Pu-235	4.94e-05	1.4e-08	1.40e+04	100	501	>1E20	>1E20
Pu-236	2.85e+00	1.3e-03	2.43e-01	100	501	>1E20	2.1e+08
Pu-237	1.24e-01	1.0e-06	5.58e+00	100	501	>1E20	>1E20
Pu-238	8.78e+01	3.8e-03	7.90e-03	100	501	3.9e+01	1.3e-02
Pu-239	2.41e+04	4.3e-03	2.87e-05	100	501	2.0e-03	5.9e-03
Pu-240	6.57e+03	4.3e-03	1.06e-04	100	501	2.4e-03	5.9e-03
Pu-241	1.44e+01	8.6e-05	4.81e-02	100	501	3.8e+00	7.2e-01
Pu-242	3.76e+05	4.1e-03	1.84e-06	100	501	2.0e-03	5.9e-03
Pu-243	5.65e-04	3.3e-07	1.23e+03	100	501	>1E20	>1E20
Pu-244	8.10e+07	4.0e-03	8.56e-09	100	501	2.0e-03	5.9e-03

Table C.1-2 (continued)

Nuclide	T1/2 (years)	DCF (mrem/Ci)	Inventory (Ci/mg)	Kd (cm**3/g)	Kf	ILCOW Trigger (Ci/mult)	ILNT Trigger (Ci/mult)
Pu-[illegible]	1.14e-01	2.[illegible]	6.[illegible]e+02	100	501	>1E20	>1E20
Am-237	1.48e-04	7.4e-03	4.67e+03	150	751	>1E20	>1E20
Am-238	2.17e-04	1.7e-07	3.20e+03	150	751	>1E20	>1E20
Am-239	1.38e-03	1.0e-[illegible]	5.02e+02	150	751	>1E20	>1E20
Am-240	5.82e-03	2.9e-06	1.19e+02	150	751	>1E20	>1E20
Am-241	4.32e+02	4.5e-03	1.60e-03	150	751	5.4e-01	6.9e-03
Am-242m	1.52e+02	4.2e-03	4.56e-03	150	751	7.9e+04	9.3e-03
Am-242	1.83e-03	1.2e-06	3.80e+02	150	751	>1E20	>1E20
Am-243	7.37e+03	4.5e-03	9.40e-05	150	751	3.3e-03	5.9e-03
Am-244m	4.94e-05	6.8e-08	1.40e+04	150	751	>1E20	>1E20
Am-244	1.15e-03	2.0e-06	6.02e+02	150	751	>1E20	>1E20
Am-245	2.40e-04	1.8e-07	2.89e+03	150	751	>1E20	>1E20
Am-246m	4.75e-05	8.4e-08	1.46e+04	150	751	>1E20	>1E20
Am-246	4.75e-05	1.5e-07	1.46e+04	150	751	>1E20	>1E20
Cm-238	2.85e-04	3.6e-07	2.43e+03	100	501	>1E20	>1E20
Cm-240	7.34e-02	6.3e-05	9.45e+00	100	501	>1E20	>1E20
Cm-241	9.58e-02	4.6e-06	7.23e+00	100	501	>1E20	>1E20
Cm-242	4.46e-01	1.1e-04	1.56e+00	100	501	>1E20	>1E20
Cm-243	2.85e+01	2.9e-03	2.43e-02	100	501	>1E20	6.7e-02
Cm-244	1.81e+01	2.3e-03	3.83e-02	100	501	9.0e-01	2.7e-01
Cm-245	8.50e+03	4.5e-03	8.15e-05	100	501	2.2e-03	5.9e-03
Cm-246	4.70e+03	4.5e-03	1.47e-04	100	501	2.6e-03	6.0e-03
Cm-247	1.60e+07	4.1e-03	4.33e-08	100	501	2.0e-03	5.9e-03
Cm-248	3.50e+05	1.6e-02	1.98e-06	100	501	5.1e-04	5.9e-03
Cm-249	1.24e-04	9.5e-08	5.61e+03	100	501	>1E20	>1E20
Bk-245	1.36e-02	2.3e-06	5.08e+01	100	501	>1E20	>1E20
Bk-246	4.93e-03	1.9e-06	1.41e+02	100	501	>1E20	>1E20
Bk-247	1.40e+03	2.3e-03	4.95e-04	100	501	1.2e-02	6.2e-03
Bk-249	8.80e-01	6.0e-06	7.88e-01	100	501	>1E20	>1E20
Bk-250	3.67e-04	5.0e-07	1.89e+03	100	501	>1E20	>1E20
Cf-244	4.75e-05	1.5e-07	1.46e+04	100	501	>1E20	>1E20
Cf-246	4.11e-03	1.2e-05	1.69e+02	100	501	>1E20	>1E20
Cf-248	9.86e-01	2.8e-04	7.03e-01	100	501	>1E20	>1E20
Cf-249	3.51e+02	4.6e-03	1.97e-03	100	501	2.5e-01	7.2e-03

Table C.1-2 (continued)

Nuclide	T1/2 (year)	DCF (mrem/pCi)	Lambda (1/year)	Kd (cm^3/gm)	Rf	ILNT GW Trigger (Ci/vault)	ILNT Int Trigger (Ci/vault)
Cf-250	1.30e+01	1.9e-03	5.29e-02	100	501	>1E20	1.2e+00
Cf-251	9.00e+02	4.6e-03	7.70e-04	100	501	1.2e-02	6.4e-03
Cf-252	2.62e+00	9.4e-04	2.65e-01	100	501	6.7e+01	1.8e+09
Cf-253	4.87e-02	9.2e-06	1.42e+01	100	501	>1E20	>1E20
Cf-254	1.65e-01	2.5e-03	4.18e+00	100	501	>1E20	>1E20
Es-250	9.13e-04	9.5e-08	7.60e+02	100	501	>1E20	>1E20
Es-251	4.11e-03	6.7e-07	1.69e+02	100	501	>1E20	>1E20
Es-253	5.60e-02	2.4e-05	1.24e+01	100	501	>1E20	>1E20
Es-254m	4.48e-03	1.5e-05	1.55e+02	100	501	>1E20	>1E20
Es-254	7.56e-01	1.5e-04	9.17e-01	100	501	>1E20	>1E20
Fm-252	2.62e-03	9.9e-06	2.64e+02	100	501	>1E20	>1E20
Fm-253	8.21e-03	3.5e-06	8.44e+01	100	501	>1E20	>1E20
Fm-254	3.70e-04	1.6e-06	1.88e+03	100	501	>1E20	>1E20
Fm-255	2.29e-03	9.7e-06	3.02e+02	100	501	>1E20	>1E20
Fm-257	2.19e-01	7.3e-05	3.16e+00	100	501	>1E20	>1E20
Md-257	3.42e-04	5.4e-07	2.03e+03	100	501	>1E20	>1E20
Md-258	1.53e-01	6.1e-05	4.52e+00	100	501	>1E20	>1E20

Table C.1-3. Screening calculations and trigger levels for the LAW vaults

Nuclide	T1/2 (years)	DCF (mrem/pCi)	Lambda (1/year)	Kd (cm^3/g)	Rf	LAW Vault Trigger (Ci/vault)	LAW Tot Trigger (Ci/vault)
H-3	1.23e+01	6.3e-08	5.62e-02	0	1	2.8e+00	1.3e+01
Be-7	1.47e-01	1.1e-07	4.72e+00	0	1	2.2e+10	>1E
Be-10	1.60e+06	4.2e-06	4.33e-07	0	1	3.1e 02	4.8e 02
C-11	3.86e-05	1.2e-08	1.80e+04	2	11	>1E20	>1E20
C-14	5.73e+03	2.1e-06	1.21e-04	2	11	7.0e-01	4.9e-02
F-18	2.14e-04	1.0e-04	3.25e+03	0	1	>1E20	>1E20
Na-22	2.58e+00	1.2e-05	2.69e-01	0	1	4.2e-02	2.2e+10
Na-24	1.71e-03	1.4e-06	4.05e+02	0	1	>1E20	>1E20
Mg-28	2.40e-03	7.5e-06	2.89e+02	0	1	>1E20	>1E20
Al-26	7.40e+05	1.3e-05	9.37e-07	0	1	1.0e-02	4.8e-02
Si-31	2.99e-04	5.4e-07	2.32e+03	0	1	>1E20	>1E20
Si-32	6.50e+02	1.7e-06	1.07e-03	0	1	7.8e-02	5.4e-02
P-32	3.89e-02	7.7e-06	1.78e+01	0	1	>1E20	>1E20
P-33	6.84e-02	8.8e-07	1.01e+01	0	1	>1E20	>1E20
S-35	2.39e-01	4.3e-07	2.90e+00	0	1	6.2e+05	>1E20
Cl-36	3.01e+05	3.0e-06	2.30e-06	0	1	4.4e-02	4.8e-02
Cl-38	7.07e-05	2.0e-07	9.80e+03	0	1	>1E20	>1E20
Cl-39	1.06e-04	1.4e-07	6.57e+03	0	1	>1E20	>1E20
K-40	1.28e+09	1.9e-05	5.42e-10	0	1	6.9e-03	4.8e-02
K-42	1.41e-03	1.1e-06	4.92e+02	0	1	>1E20	>1E20
K-43	2.56e-03	7.8e-07	2.71e+02	0	1	>1E20	>1E20
K-44	4.18e-05	1.5e-07	1.66e+04	0	1	>1E20	>1E20
K-45	3.04e-05	9.3e-08	2.28e+04	0	1	>1E20	>1E20
Ca-41	1.30e+05	1.2e-06	5.33e-06	0	1	1.1e-01	4.8e-02
Ca-45	4.46e-01	3.0e-06	1.55e+00	0	1	1.0e+02	>1E20
Ca-47	1.24e-02	6.2e-06	5.58e+01	0	1	>1E20	>1E20
Sc-43	4.47e-04	7.3e-07	1.55e+03	0	1	>1E20	>1E20
Sc-44m	6.68e-03	9.9e-06	1.04e+02	0	1	>1E20	>1E20
Sc-44	4.47e-04	1.4e-06	1.55e+03	0	1	>1E20	>1E20
Sc-46	2.29e-01	5.6e-06	3.02e+00	0	1	8.6e+04	>1E20
Sc-47	9.39e-03	1.9e-06	7.38e+01	0	1	>1E20	>1E20
Sc-48	5.03e-03	6.4e-06	1.38e+02	0	1	>1E20	>1E20
Sc-49	1.09e-04	2.4e-07	6.34e+03	0	1	>1E20	>1E20

Table C.1-3. (continued)

Nuclide	T1/2 (years)	DCF (mrem/pCi)	Lambda (1/year)	Kd (cm**3/gm)	Rf	LAW GW Trigger (Ci/vault)	LAW GW Trigger (Ci/vault)
Ti-44	4.80e+01	1.9e-05	1.44e-02	0	1	7.5e-03	2.0e-01
Ti-45	3.52e-04	5.7e-07	1.97e+03	0	1	>1E20	>1E20
V-47	6.27e-05	1.6e-07	1.10e+04	0	1	>1E20	>1E20
V-48	4.41e-02	7.5e-06	1.57e+01	0	1	>1E20	>1E20
V-49	9.03e-01	5.4e-08	7.67e-01	0	1	1.1e+02	>1E20
Cr-48	2.62e-03	8.2e-07	2.64e+02	40	201	>1E20	>1E20
Cr-49	7.97e-05	1.7e-07	8.70e+03	40	201	>1E20	>1E20
Cr-51	7.58e-02	1.3e-07	9.14e+00	40	201	>1E20	>1E20
Mn-51	8.56e-05	2.5e-07	8.10e+03	50	251	>1E20	>1E20
Mn-52m	3.99e-05	1.5e-07	1.74e+04	50	251	>1E20	>1E20
Mn-52	1.52e-02	6.9e-06	4.56e+01	50	251	>1E20	>1E20
Mn-53	2.00e+06	9.9e-08	3.47e-07	50	251	3.3e+02	4.8e-02
Mn-54	7.97e-01	2.7e-06	8.70e-01	50	251	>1E20	>1E20
Mn-56	2.94e-04	9.5e-07	2.36e+03	50	251	>1E20	>1E20
Fe-52	9.35e-04	5.4e-06	7.41e+02	0	1	>1E20	>1E20
Fe-55	2.70e+00	5.8e-07	2.57e-01	0	1	8.2e-01	6.8e+09
Fe-59	1.22e-01	6.6e-06	5.68e+00	0	1	4.2e+10	>1E20
Fe-60	3.00e+05	1.5e-04	2.31e-06	0	1	8.8e-04	4.8e-02
Co-55	2.08e-03	4.1e-06	3.34e+02	10	51	>1E20	>1E20
Co-56	2.11e-01	1.2e-05	3.29e+00	10	51	>1E20	>1E20
Co-57	7.39e-01	1.1e-05	9.38e-01	10	51	>1E20	>1E20
Co-58m	1.03e-03	8.8e-08	6.75e+02	10	51	>1E20	>1E20
Co-58	1.95e-01	3.5e-06	3.55e+00	10	51	>1E20	>1E20
Co-60m	2.00e-05	3.6e-09	3.47e+04	10	51	>1E20	>1E20
Co-60	5.27e+00	2.6e-05	1.32e-01	10	51	9.5e+13	2.5e+04
Co-61	1.88e-04	2.6e-07	3.68e+03	10	51	>1E20	>1E20
Co-62m	3.04e-06	9.6e-08	2.28e+05	10	51	>1E20	>1E20
Ni-56	1.67e-02	3.5e-06	4.15e+01	300	1501	>1E20	>1E20
Ni-57	4.11e-03	3.3e-06	1.69e+02	300	1501	>1E20	>1E20
Ni-59	8.00e+04	2.0e-07	8.66e-06	300	1501	1.1e+03	4.8e-02
Ni-63	1.00e+02	5.4e-07	6.93e-03	300	1501	>1E20	9.6e-02
Ni-65	2.87e-04	6.1e-07	2.41e+03	300	1501	>1E20	>1E20
Ni-66	6.23e-03	1.1e-05	1.11e+02	300	1501	>1E20	>1E20
Cu-60	4.37e-05	1.7e-07	1.59e+04	25	126	>1E20	>1E20

Table C.1-3. (continued)

Nuclide	T1/2 (year)	DCF (mrem/pCi)	Lambda (1/year)	Kd (cm^3/gm)	Rf	LAW Trigger (Ci/vault)	LAW Trigger (Ci/vault)
Cu-61	3.38e-04	4.1e-07	1.78e+03	25	126	>1E20	>1E20
Cu-64	1.45e-03	4.3e-07	4.78e+02	25	126	>1E20	>1E20
Cu-67	7.06e-03	1.1e-06	9.82e+01	25	126	>1E20	>1E20
Zn-62	1.04e-03	3.4e-06	6.64e+02	16	81	>1E20	>1E20
Zn-63	7.30e-05	2.0e-07	9.49e+03	16	81	>1E20	>1E20
Zn-65	6.67e-01	1.4e-05	1.04e+00	16	81	>1E20	>1E20
Zn-69m	1.57e-03	1.2e-05	4.40e+02	16	81	>1E20	>1E20
Zn-69	1.08e-04	8.5e-08	6.40e+03	16	81	>1E20	>1E20
Zn-71m	4.56e-04	8.3e-07	1.52e+03	16	81	>1E20	>1E20
Zn-72	1.27e-01	4.9e-06	5.44e+00	16	81	>1E20	>1E20
Ga-65	2.89e-05	7.8e-08	2.40e+04	0	1	>1E20	>1E20
Ga-66	1.07e-03	4.7e-06	6.46e+02	0	1	>1E20	>1E20
Ga-67	8.91e-03	7.2e-07	7.78e+01	0	1	>1E20	>1E20
Ga-68	1.30e-04	3.3e-07	5.34e+03	0	1	>1E20	>1E20
Ga-70	4.01e-05	7.1e-08	1.73e+04	0	1	>1E20	>1E20
Ga-72	1.61e-03	4.4e-06	4.31e+02	0	1	>1E20	>1E20
Ga-73	1.34e-02	1.0e-06	5.19e+01	0	1	>1E20	>1E20
Ge-66	1.07e-03	2.1e-07	6.46e+02	0	1	>1E20	>1E20
Ge-67	3.61e-05	1.1e-07	1.92e+04	0	1	>1E20	>1E20
Ge-68	7.86e-01	1.1e-06	8.82e-01	0	1	9.9e+00	>1E20
Ge-69	4.45e-03	3.6e-07	1.56e+02	0	1	>1E20	>1E20
Ge-71	3.12e-02	9.6e-09	2.22e+01	0	1	>1E20	>1E20
Ge-75	1.57e-04	7.3e-08	4.40e+03	0	1	>1E20	>1E20
Ge-77	1.29e-03	5.6e-07	5.38e+02	0	1	>1E20	>1E20
Ge-78	1.65e-04	2.1e-07	4.19e+03	0	1	>1E20	>1E20
As-69	2.85e-05	1.1e-07	2.43e+04	3	16	>1E20	>1E20
As-70	1.01e-04	3.4e-07	6.88e+03	3	16	>1E20	>1E20
As-71	7.07e-03	1.3e-06	9.80e+01	3	16	>1E20	>1E20
As-72	2.97e-03	5.6e-06	2.34e+02	3	16	>1E20	>1E20
As-73	2.20e-01	6.1e-07	3.15e+00	3	16	>1E20	>1E20
As-74	3.29e-02	3.3e-06	2.11e+01	3	16	>1E20	>1E20
As-76	3.00e-03	4.8e-06	2.31e+02	3	16	>1E20	>1E20
As-77	1.06e-01	1.1e-06	6.53e+00	3	16	>1E20	>1E20
As-78	1.73e-04	6.5e-07	4.01e+03	3	16	>1E20	>1E20

Table C.1-3. (continued)

Nuclide	T1/2 (years)	DCF (mrem/pCi)	Inventory (Ci/year)	Kd (cm**3/gm)	Rf	LAW GW Trigger (Ci/vault)	LAW Int Trigger (Ci/vault)
Se-70	8.31e-05	4.8e-07	8.[illegible]e+03	5	26	>1E20	>1E20
Se-73m	7.9[illegible]e-05	1.5e-07	8.[illegible]e+03	5	26	>1E20	>1E20
Se-73	8.10e-04	1.5e-06	8.56e+02	5	26	>1E20	>1E20
Se-75	3.30e-01	8.8e-06	2.10e+00	5	26	>1E20	>1E20
Se-79	6.50e+04	8.3e-06	1.07e-05	5	26	4.1e-01	4.8e-02
Se-81m	1.09e-04	2.1e-07	6.36e+03	5	26	>1E20	>1E20
Se-81	4.30e-05	6.1e-08	1.61e+04	5	26	>1E20	>1E20
Se-83	4.28e-05	1.5e-07	1.62e+04	5	26	>1E20	>1E20
Br-74m	7.89e-05	2.2e-07	8.78e+03	0	1	>1E20	>1E20
Br-74	6.84e-05	1.4e-07	1.01e+04	0	1	>1E20	>1E20
Br-75	1.94e-04	1.3e-07	3.57e+03	0	1	>1E20	>1E20
Br-76	1.84e-03	1.4e-06	3.77e+02	0	1	>1E20	>1E20
Br-77	6.50e-03	3.1e-07	1.07e+02	0	1	>1E20	>1E20
Br-80m	5.04e-04	2.3e-07	1.37e+03	0	1	>1E20	>1E20
Br-80	3.37e-05	5.5e-08	2.06e+04	0	1	>1E20	>1E20
Br-82	4.03e-03	1.7e-06	1.72e+02	0	1	>1E20	>1E20
Br-83	2.74e-04	7.3e-08	2.53e+03	0	1	>1E20	>1E20
Br-84	6.05e-05	1.5e-07	1.15e+04	0	1	>1E20	>1E20
Rb-79	3.99e-05	8.7e-08	1.74e+04	0	1	>1E20	>1E20
Rb-81m	6.08e-05	1.8e-08	1.14e+04	0	1	>1E20	>1E20
Rb-81	5.36e-04	1.3e-07	1.29e+03	0	1	>1E20	>1E20
Rb-82m	7.30e-04	4.2e-07	9.49e+02	0	1	>1E20	>1E20
Rb-83	2.27e-01	7.7e-06	3.05e+00	0	1	7.2e+04	>1E20
Rb-84	9.31e-02	1.0e-05	7.45e+00	0	1	1.9e+14	>1E20
Rb-86	5.09e-02	9.4e-06	1.36e+01	0	1	>1E20	>1E20
Rb-87	4.80e+10	4.8e-06	1.44e-11	0	1	2.7e-02	4.8e-02
Rb-88	3.37e-05	1.6e-07	2.06e+04	0	1	>1E20	>1E20
Rb-89	2.89e-05	8.0e-08	2.40e+04	0	1	>1E20	>1E20
Sr-80	1.94e-04	5.2e-09	3.57e+03	10	51	>1E20	>1E20
Sr-81	5.51e-05	2.2e-07	1.26e+04	10	51	>1E20	>1E20
Sr-83	3.76e-03	2.3e-06	1.84e+02	10	51	>1E20	>1E20
Sr-85m	1.29e-04	2.4e-08	5.39e+03	10	51	>1E20	>1E20
Sr-85	1.79e-01	1.9e-06	3.88e+00	10	51	>1E20	>1E20
Sr-87m	3.21e-04	1.2e-07	2.16e+03	10	51	>1E20	>1E20

Table C.1-3. (continued)

Nuclide	T1/2 (year)	DCF (mrem/μCi)	Lambda (1/year)	Kd (cm**3/gm)	BF	LAW Grout Trigger (Ci/vault)	LAW Int Trigger (Ci/vault)
Sr-89	1.38e-01	8.7e-06	5.01e+00	10	51	>1E20	>1E20
Sr-90	2.86e+01	1.3e-04	2.42e-02	10	51	2.5e+01	5.4e-01
Sr-91	1.08e-03	3.0e-06	6.41e+02	10	51	>1E20	>1E20
Sr-92	3.09e-04	1.9e-06	2.24e+03	10	51	>1E20	>1E20
Y-86m	9.13e-05	2.4e-07	7.60e+03	10	51	>1E20	>1E20
Y-86	1.67e-03	4.1e-06	4.16e+02	10	51	>1E20	>1E20
Y-87	9.13e-03	2.2e-06	7.60e+01	10	51	>1E20	>1E20
Y-88	2.88e-01	5.2e-06	2.41e+00	10	51	>1E20	>1E20
Y-90m	3.64e-04	6.6e-07	1.90e+03	10	51	>1E20	>1E20
Y-90	2.86e+01	1.0e-05	2.42e-02	10	51	3.2e+02	5.4e-01
Y-91m	9.51e-05	3.9e-08	7.29e+03	10	51	>1E20	>1E20
Y-91	1.67e-01	8.9e-06	4.15e+00	10	51	>1E20	>1E20
Y-92	4.03e-04	1.9e-06	1.72e+03	10	51	>1E20	>1E20
Y-93	1.16e-03	4.5e-06	5.96e+02	10	51	>1E20	>1E20
Y-94	3.61e-05	1.8e-07	1.92e+04	10	51	>1E20	>1E20
Y-95	2.00e-05	9.7e-08	3.47e+04	10	51	>1E20	>1E20
Zr-86	1.88e-03	3.5e-06	3.68e+02	0	1	>1E20	>1E20
Zr-88	2.33e-01	1.3e-06	2.98e+00	0	1	3.0e+05	>1E20
Zr-89	8.94e-03	3.1e-06	7.75e+01	0	1	>1E20	>1E20
Zr-93	1.50e+06	1.6e-06	4.62e-07	0	1	8.2e-02	4.8e-02
Zr-95	1.75e-01	3.4e-06	3.96e+00	0	1	1.5e+07	>1E20
Zr-97	1.92e-03	8.0e-06	3.62e+02	0	1	>1E20	>1E20
Nb-88	2.66e-05	7.2e-08	2.60e+04	0	1	>1E20	>1E20
Nb-89(66m)	1.25e-04	4.6e-07	5.52e+03	0	1	>1E20	>1E20
Nb-89(122m)	2.32e-04	1.0e-06	2.99e+03	0	1	>1E20	>1E20
Nb-90	1.67e-03	4.9e-06	4.16e+02	0	1	>1E20	>1E20
Nb-93m	1.01e+01	5.3e-07	6.84e-02	0	1	3.5e-01	4.5e+01
Nb-94	2.00e+04	5.1e-06	3.47e-05	0	1	2.6e-02	4.8e-02
Nb-95m	9.88e-03	2.0e-06	7.02e+01	0	1	>1E20	>1E20
Nb-95	9.58e-02	2.2e-06	7.23e+00	0	1	3.1e+14	>1E20
Nb-96	2.67e-03	4.4e-06	2.60e+02	0	1	>1E20	>1E20
Nb-97	1.40e-04	2.3e-07	4.95e+03	0	1	>1E20	>1E20
Nb-98	8.87e-08	3.4e-07	7.81e+06	0	1	>1E20	>1E20
Mo-90	6.50e-04	2.5e-06	1.07e+03	0	1	>1E20	>1E20

Table C.1-3. (continued)

Nuclide	T1/2 (years)	DCF (mrem/pCi)	Lambda (1/year)	Kd (cm³/gm)	Rf	LAW GW Trigger (Ci/vault)	LAW Int Trigger (Ci/vault)
Mo-93m	7.37e-04	1.1e-06	8.81e+02	0	1	>1E20	>1E20
Mo-93	3.50e+03	1.3e-06	1.98e-04	0	1	1.0e-01	4.9e-02
Mo-99	7.53e-03	4.4e-06	9.20e+01	0	1	>1E20	>1E20
Mo-101	2.78e-05	9.2e-08	2.50e+04	0	1	>1E20	>1E20
Tc-93m	8.18e-05	7.1e-08	8.48e+03	0.36	2.8	>1E20	>1E20
Tc-93	3.08e-04	1.6e-07	2.25e+03	0.36	2.8	>1E20	>1E20
Tc-94m	1.01e-04	2.5e-07	6.88e+03	0.36	2.8	>1E20	>1E20
Tc-94	5.57e-04	5.8e-07	1.24e+03	0.36	2.8	>1E20	>1E20
Tc-96m	9.89e-05	3.1e-08	7.01e+03	0.36	2.8	>1E20	>1E20
Tc-96	1.18e-02	2.7e-06	5.89e+01	0.36	2.8	>1E20	>1E20
Tc-97m	2.46e-01	1.1e-06	2.81e+00	0.36	2.8	4.3e+16	>1E20
Tc-97	2.60e+06	1.5e-07	2.67e-07	0.36	2.8	2.5e+00	4.8e-02
Tc-98	1.50e+06	4.8e-06	4.62e-07	0.36	2.8	7.7e-02	4.8e-02
Tc-99m	6.87e-04	6.0e-08	1.01e+03	0.36	2.8	>1E20	>1E20
Tc-99	2.11e+05	1.3e-06	3.29e-06	0.36	2.8	2.8e-01	4.8e-02
Tc-101	2.70e-05	3.8e-08	2.57e+04	0.36	2.8	>1E20	>1E20
Tc-104	3.42e-05	1.6e-07	2.03e+04	0.36	2.8	>1E20	>1E20
Ru-94	1.08e-04	3.3e-07	6.40e+03	100	501	>1E20	>1E20
Ru-97	7.91e-03	6.4e-07	8.76e+01	100	501	>1E20	>1E20
Ru-103	1.08e-01	2.7e-06	6.43e+00	100	501	>1E20	>1E20
Ru-105	5.07e-04	1.0e-06	1.37e+03	100	501	>1E20	>1E20
Ru-106	9.99e-01	2.1e-05	6.94e-01	100	501	>1E20	>1E20
Rh-99m	5.36e-04	2.8e-07	1.29e+03	0	1	>1E20	>1E20
Rh-99	4.38e-02	2.0e-06	1.58e+01	0	1	>1E20	>1E20
Rh-100	2.28e-03	3.1e-06	3.04e+02	0	1	>1E20	>1E20
Rh-101m	1.23e-02	8.8e-07	5.63e+01	0	1	>1E20	>1E20
Rh-101	3.10e+00	2.3e-06	2.24e-01	0	1	1.8e-01	2.5e+08
Rh-102m	2.90e+00	3.5e-06	2.39e-01	0	1	1.2e-01	1.2e+09
Rh-102	5.75e-01	5.5e-06	1.21e+00	0	1	9.9e+00	>1E20
Rh-103m	1.06e-04	0.00000001	6.51e+03	0	1	>1E20	>1E20
Rh-105	4.05e-03	1.4e-06	1.71e+02	0	1	>1E20	>1E20
Rh-106m	2.49e-04	6.1e-07	2.79e+03	0	1	>1E20	>1E20
Rh-107	4.13e-05	5.4e-08	1.68e+04	0	1	>1E20	>1E20
Pd-100	1.10e-02	3.8e-06	6.33e+01	0	1	>1E20	>1E20

Table C.1-3. (continued)

Nuclide	T1/2 (years)	DCF (mrem/pCi)	Lambda (1/year)	Kd (cm^3/gm)	Rf	LAW GW Trigger (Ci/vault)	LAW Int Trigger (Ci/vault)
Pd-101	9.5[illegible]e-04	3.2e-07	7.2[illegible]e+02	0	1	>1E[illegible]	>1E20
Pd-103	4.6[illegible]e-02	6.9e-07	1.4[illegible]e+01	0	1	>1E20	>1E20
Pd-107	6.50e+06	1.4e-07	1.07e-07	0	1	9.4e-01	4.8e-02
Pd-109	1.53e-03	2.1e-06	4.53e+02	0	1	>1E20	>1E20
Ag-102	2.85e-05	7.9e-08	2.43e+04	10	51	>1E20	>1E20
Ag-103	1.25e-04	1.4e-07	5.52e+03	10	51	>1E20	>1E20
Ag-104m	5.70e-05	1.5e-07	1.22e+04	10	51	>1E20	>1E20
Ag-104	1.27e-04	2.3e-07	5.44e+03	10	51	>1E20	>1E20
Ag-105	1.10e-01	1.9e-06	6.33e+00	10	51	>1E20	>1E20
Ag-106m	2.27e-02	6.1e-06	3.05e+01	10	51	>1E20	>1E20
Ag-106	4.56e-05	7.6e-08	1.52e+04	10	51	>1E20	>1E20
Ag-108m	1.30e+02	7.5e-06	5.33e-03	10	51	3.5e+00	8.2e-02
Ag-110m	6.90e-01	1.1e-05	1.00e+00	10	51	>1E20	>1E20
Ag-111	2.05e-02	4.5e-06	3.39e+01	10	51	>1E20	>1E20
Ag-112	3.57e-04	1.6e-06	1.94e+03	10	51	>1E20	>1E20
Ag-115	3.99e-05	1.5e-07	1.74e+04	10	51	>1E20	>1E20
Cd-104	1.08e-04	2.3e-07	6.40e+03	8	41	>1E20	>1E20
Cd-107	7.42e-04	2.4e-07	9.35e+02	8	41	>1E20	>1E20
Cd-109	1.24e+00	1.2e-05	5.59e-01	8	41	>1E20	>1E20
Cd-113m	1.46e+01	1.5e-04	4.75e-02	8	41	6.1e+02	5.6e+00
Cd-113	9.30e+15	1.6e-04	7.45e-17	8	41	3.4e-02	4.8e-02
Cd-115m	1.36e-01	1.5e-05	5.11e+00	8	41	>1E20	>1E20
Cd-115	6.10e-03	4.7e-06	1.14e+02	8	41	>1E20	>1E20
Cd-117m	3.88e-04	1.1e-06	1.79e+03	8	41	>1E20	>1E20
Cd-117	2.97e-04	1.1e-06	2.34e+03	8	41	>1E20	>1E20
In-109	4.91e-04	2.7e-07	1.41e+03	0	1	>1E20	>1E20
In-110(69m)	1.27e-04	3.3e-07	5.44e+03	0	1	>1E20	>1E20
In-111	7.69e-03	1.2e-06	9.01e+01	0	1	>1E20	>1E20
In-112	2.66e-05	0.00000002	2.60e+04	0	1	>1E20	>1E20
In-113m	1.89e-04	1.0e-07	3.66e+03	0	1	>1E20	>1E20
In-114m	1.36e-01	0.000015	5.11e+00	0	1	1.1e+09	>1E20
In-115m	5.13e-04	3.4e-07	1.35e+03	0	1	>1E20	>1E20
In-115	4.60e+15	1.4e-04	1.51e-16	0	1	9.4e-04	4.8e-02
In-116m	1.03e-04	2.1e-07	6.73e+03	0	1	>1E20	>1E20

Table C.1-3. (continued)

Nuclide	T1/2 (year)	DCF (mrem/pCi)	Lambda (1/year)	Kd (cm³/g)	Rf	LAW GW Trigger (Ci/vault)	LAW Int Trigger (Ci/vault)
In-114m	2.21e-01	4.2e-07	3.13e+03	0	1	>1E20	>1E20
In-117	8.37e-05	8.7e-08	8.29e+03	0	1	>1E20	>1E20
In-119m	3.42e-05	1.0e-07	2.03e+04	0	1	>1E20	>1E20
Sn-110	4.56e-04	1.5e-06	1.52e+03	130	651	>1E20	>1E20
Sn-111	6.65e-05	6.7e-08	1.04e+04	130	651	>1E20	>1E20
Sn-113	3.15e-01	2.7e-06	2.20e+00	130	651	>1E20	>1E20
Sn-117m	3.83e-02	2.6e-06	1.81e+01	130	651	>1E20	>1E20
Sn-119m	8.02e-01	1.2e-05	8.64e-01	130	651	>1E20	>1E20
Sn-121m	7.60e+01	1.3e-06	9.12e-03	130	651	5.2e+14	1.2e-01
Sn-121	3.08e-03	8.9e-07	2.25e+02	130	651	>1E20	>1E20
Sn-123m	7.61e-05	1.0e-07	9.11e+03	130	651	>1E20	>1E20
Sn-123	3.53e-01	7.7e-06	1.96e+00	130	651	>1E20	>1E20
Sn-125	2.64e-02	1.1e-05	2.62e+01	130	651	>1E20	>1E20
Sn-126	1.00e+05	1.7e-05	6.93e-06	130	651	5.2e+00	4.8e-02
Sn-127	2.42e-04	7.4e-07	2.87e+03	130	651	>1E20	>1E20
Sn-128	1.12e-04	5.2e-07	6.18e+03	130	651	>1E20	>1E20
Sb-115	5.89e-05	6.3e-08	1.18e+04	10	51	>1E20	>1E20
Sb-116m	1.14e-04	2.4e-07	6.08e+03	10	51	>1E20	>1E20
Sb-116	2.85e-05	5.6e-08	2.43e+04	10	51	>1E20	>1E20
Sb-117	3.19e-04	7.4e-08	2.17e+03	10	51	>1E20	>1E20
Sb-118m	5.82e-04	9.3e-07	1.19e+03	10	51	>1E20	>1E20
Sb-119	4.33e-03	3.4e-07	1.60e+02	10	51	>1E20	>1E20
Sb-120(16m)	3.04e-05	3.0e-08	2.28e+04	10	51	>1E20	>1E20
Sb-120(6d)	1.59e-02	5.4e-06	4.37e+01	10	51	>1E20	>1E20
Sb-122	7.45e-03	6.3e-06	9.31e+01	10	51	>1E20	>1E20
Sb-124m	1.77e-04	2.0e-08	3.92e+03	10	51	>1E20	>1E20
Sb-124	1.65e-01	9.3e-06	4.20e+00	10	51	>1E20	>1E20
Sb-125	2.40e+00	2.6e-06	2.89e-01	10	51	>1E20	1.7e+11
Sb-126m	3.61e-05	7.3e-08	1.92e+04	10	51	>1E20	>1E20
Sb-126	3.39e-02	9.6e-06	2.04e+01	10	51	>1E20	>1E20
Sb-127	1.04e-02	6.6e-06	6.66e+01	10	51	>1E20	>1E20
Sb-128(9h)	1.03e-03	4.3e-06	6.75e+02	10	51	>1E20	>1E20
Sb-128(10m)	1.90e-05	5.0e-08	3.65e+04	10	51	>1E20	>1E20
Sb-129	4.95e-04	1.7e-06	1.40e+03	10	51	>1E20	>1E20

Table C.1-3. (continued)

Nuclide	T1/2 (years)	DCF (mrem/pCi)	Lambda (1/year)	Kd (cm**3/gm)	Rf	LAW Trench (Curies)	LAW Tumulus (Curies)
Sb-130	1.25e-05	2.[illegible]e-07	5.5[illegible]e+04	10	51	>1E20	>1E20
Sb-131	4.37e-05	2.9e-07	1.59e+04	10	51	>1E20	>1E20
Te-118	1.61e-02	6.7e-07	4.2[illegible]e+01	0	1	>1E20	>1E20
Te-121m	4.11e-01	6.7e-06	1.69e+00	0	1	9.1e+01	>1E20
Te-121	4.65e-02	1.5e-06	1.49e+01	0	1	>1E20	>1E20
Te-123m	3.28e-01	5.1e-06	2.12e+00	0	1	1.0e+03	>1E20
Te-123	1.20e+13	4.1e-06	5.78e-14	0	1	3.2e-02	4.8e-02
Te-125m	1.59e-01	3.4e-06	4.37e+00	0	1	1.2e+08	>1E20
Te-127m	2.98e-01	7.9e-06	2.32e+00	0	1	1.8e+03	>1E20
Te-127	1.07e-03	6.9e-07	6.46e+02	0	1	>1E20	>1E20
Te-129m	9.14e-02	9.9e-06	7.58e+00	0	1	3.8e+14	>1E20
Te-129	1.33e-04	1.9e-07	5.21e+03	0	1	>1E20	>1E20
Te-131m	3.42e-03	1.5e-05	2.03e+02	0	1	>1E20	>1E20
Te-131	4.75e-05	2.0e-07	1.46e+04	0	1	>1E20	>1E20
Te-132	8.76e-03	7.4e-06	7.91e+01	0	1	>1E20	>1E20
Te-133m	1.05e-04	7.6e-07	6.58e+03	0	1	>1E20	>1E20
Te-133	2.38e-05	1.6e-07	2.92e+04	0	1	>1E20	>1E20
Te-134	7.99e-05	2.1e-07	8.68e+03	0	1	>1E20	>1E20
I-120m	1.01e-04	3.9e-07	6.88e+03	0.6	4	>1E20	>1E20
I-120	1.48e-04	6.7e-07	4.67e+03	0.6	4	>1E20	>1E20
I-121	2.40e-04	1.8e-07	2.89e+03	0.6	4	>1E20	>1E20
I-123	1.52e-03	4.9e-07	4.57e+02	0.6	4	>1E20	>1E20
I-124	1.15e-02	3.1e-05	6.03e+01	0.6	4	>1E20	>1E20
I-125	1.64e-01	3.8e-05	4.22e+00	0.6	4	>1E20	>1E20
I-126	3.64e-02	7.1e-05	1.90e+01	0.6	4	>1E20	>1E20
I-128	4.75e-05	8.5e-08	1.46e+04	0.6	4	>1E20	>1E20
I-129	1.72e+07	2.8e-04	4.02e-08	0.6	4	1.9e-03	4.8e-02
I-130	1.41e-03	4.3e-06	4.90e+02	0.6	4	>1E20	>1E20
I-131	2.22e-02	5.3e-05	3.13e+01	0.6	4	>1E20	>1E20
I-132m	1.58e-04	4.7e-07	4.39e+03	0.6	4	>1E20	>1E20
I-132	2.60e-04	3.3e-07	2.66e+03	0.6	4	>1E20	>1E20
I-133	2.37e-03	5.4e-06	2.92e+02	0.6	4	>1E20	>1E20
I-134	1.00e-04	1.9e-07	6.93e+03	0.6	4	>1E20	>1E20
I-135	7.51e-04	2.0e-05	9.23e+02	0.6	4	>1E20	>1E20

Table C.1-3. (continued)

Nuclide	T1/2 (year)	DCF (mrem/pCi)	Leach (1/year)	Kd (cm**3/gm)	Rf	LAW GW Trigger (Ci/vault)	LAW Int Trigger (Ci/vault)
Cs-125	8.50e-05	5.5e-03	8.10e+03	100	501	>1E20	>1E20
Cs-127	7.07e-04	8.0e-03	9.80e+02	100	501	>1E20	>1E20
Cs-129	3.65e-03	2.2e-07	1.90e+02	100	501	>1E20	>1E20
Cs-130	5.70e-05	4.9e-03	1.22e+04	100	501	>1E20	>1E20
Cs-131	2.66e-02	2.4e-07	2.61e+01	100	501	>1E20	>1E20
Cs-132	1.80e-02	1.9e-06	3.85e+01	100	501	>1E20	>1E20
Cs-134m	3.31e-04	4.2e-08	2.10e+03	100	501	>1E20	>1E20
Cs-134	2.06e+00	7.4e-05	3.36e-01	100	501	>1E20	2.0e+13
Cs-135m	1.01e-04	4.9e-08	6.88e+03	100	501	>1E20	>1E20
Cs-135	2.30e+06	7.1e-06	3.01e-07	100	501	9.3e+00	4.8e-02
Cs-136	3.53e-02	1.1e-05	1.96e+01	100	501	>1E20	>1E20
Cs-137	3.01e+01	5.0e-05	2.30e-02	100	501	>1E20	4.8e-01
Cs-138	6.12e-05	1.6e-07	1.13e+04	100	501	>1E20	>1E20
Ba-126	1.84e-04	9.0e-07	3.76e+03	5	26	>1E20	>1E20
Ba-128	6.57e-03	1.0e-05	1.05e+02	5	26	>1E20	>1E20
Ba-131m	2.78e-05	9.7e-07	2.50e+04	5	26	>1E20	>1E20
Ba-131	3.20e-02	1.6e-06	2.16e+01	5	26	>1E20	>1E20
Ba-133m	4.44e-03	2.0e-06	1.56e+02	5	26	>1E20	>1E20
Ba-133	1.07e+01	3.2e-06	6.48e-02	5	26	4.9e+03	3.1e+01
Ba-135m	3.27e-03	1.6e-06	2.12e+02	5	26	>1E20	>1E20
Ba-137m	0.000005		1.43e+05	5	26	>1E20	>1E20
Ba-139	1.58e-04	3.9e-07	4.38e+03	5	26	>1E20	>1E20
Ba-140	3.50e-02	8.4e-06	1.98e+01	5	26	>1E20	>1E20
Ba-141	3.48e-05	2.0e-07	1.99e+04	5	26	>1E20	>1E20
Ba-142	2.03e-05	1.0e-07	3.41e+04	5	26	>1E20	>1E20
La-131	1.12e-04	1.1e-07	6.18e+03	100	501	>1E20	>1E20
La-132	5.13e-04	1.5e-06	1.35e+03	100	501	>1E20	>1E20
La-135	2.22e-03	1.3e-07	3.12e+02	100	501	>1E20	>1E20
La-137	6.00e+04	4.3e-07	1.16e-05	100	501	1.6e+02	4.8e-02
La-138	1.06e+11	5.9e-06	6.54e-12	100	501	1.1e+01	4.8e-02
La-140	4.59e-03	7.7e-06	1.51e+02	100	501	>1E20	>1E20
La-141	4.41e-04	1.4e-06	1.57e+03	100	501	>1E20	>1E20
La-142	1.76e-04	8.3e-07	3.95e+03	100	501	>1E20	>1E20
La-143	2.66e-05	1.4e-07	2.60e+04	100	501	>1E20	>1E20

INFORMATION ONLY

Table C.1-3. (continued)

Nuclide	T1/2 (years)	DCF (mrem/pCi)	Limit (pCi/mL)	Kd (cm^3/g)	Rf	LAW GTV Trigger (Ci/vault)	LAW Int Trigger (Ci/vault)
Ce-134	8.21e-03	8.2e-06	8.[illegible]e-01	10	51	>1E20	>1E20
Ce-135	1.90e-03	3.2e-06	3.53e+02	10	51	>1E20	>1E20
Ce-137m	3.92e-03	2.0e-06	1.77e+02	10	51	>1E20	>1E20
Ce-137	1.03e-03	9.8e-08	6.75e+02	10	51	>1E20	>1E20
Ce-139	3.77e-01	1.1e-06	1.84e+00	10	51	>1E20	>1E20
Ce-141	8.90e-02	2.6e-06	7.79e+00	10	51	>1E20	>1E20
Ce-143	3.76e-03	4.2e-06	1.84e+02	10	51	>1E20	>1E20
Ce-144	7.94e-01	2.0e-05	8.73e-01	10	51	>1E20	>1E20
Pr-136	1.25e-04	6.8e-08	5.52e+03	10	51	>1E20	>1E20
Pr-137	1.71e-04	1.3e-07	4.05e+03	100	501	>1E20	>1E20
Pr-138m	2.40e-04	4.9e-07	2.89e+03	100	501	>1E20	>1E20
Pr-139	5.13e-04	1.2e-07	1.35e+03	100	501	>1E20	>1E20
Pr-142m	2.72e-05	6.3e-08	2.55e+04	100	501	>1E20	>1E20
Pr-142	2.18e-03	5.1e-06	3.18e+02	100	501	>1E20	>1E20
Pr-143	3.75e-02	4.5e-06	1.85e+01	100	501	>1E20	>1E20
Pr-144	3.29e-05	1.1e-07	2.11e+04	100	501	>1E20	>1E20
Pr-145	6.82e-04	1.5e-06	1.02e+03	100	501	>1E20	>1E20
Pr-147	2.28e-05	5.7e-08	3.04e+04	100	501	>1E20	>1E20
Nd-136	9.64e-05	3.3e-07	7.19e+03	100	501	>1E20	>1E20
Nd-138	4.18e-05	2.5e-06	1.66e+04	100	501	>1E20	>1E20
Nd-139m	6.27e-04	1.0e-06	1.10e+03	100	501	>1E20	>1E20
Nd-139	5.93e-04	5.7e-08	1.17e+03	100	501	>1E20	>1E20
Nd-141	2.85e-04	3.2e-08	2.43e+03	100	501	>1E20	>1E20
Nd-147	3.01e-02	3.9e-06	2.30e+01	100	501	>1E20	>1E20
Nd-149	1.97e-03	4.6e-07	3.51e+02	100	501	>1E20	>1E20
Nd-151	2.36e-05	7.4e-08	2.94e+04	100	501	>1E20	>1E20
Pm-141	4.18e-05	8.4e-08	1.66e+04	100	501	>1E20	>1E20
Pm-143	7.26e-01	9.5e-07	9.55e-01	100	501	>1E20	>1E20
Pm-144	8.22e-01	3.9e-06	8.43e-01	100	501	>1E20	>1E20
Pm-145	1.77e+01	4.6e-07	3.92e-02	100	501	>1E20	2.4e+00
Pm-146	1.94e+00	3.2e-06	3.57e-01	100	501	>1E20	1.5e+14
Pm-147	2.52e+00	9.5e-07	2.75e-01	100	501	>1E20	4.3e+10
Pm-148m	1.14e-01	7.0e-06	6.06e+00	100	501	>1E20	>1E20
Pm-148	1.47e-02	9.5e-06	4.71e+01	100	501	>1E20	>1E20

Table C.1-3. (continued)

Nuclide	T1/2 (year)	DCF (mrem/pCi)	Lambda (1/year)	Kd (cm**3/gm)	Rf	LAW GW Trigger (Ci/vault)	LAW Int Trigger (Ci/vault)
Pm-149	6.06e-03	3.6e-06	1.14e+02	100	501	>1E20	>1E20
Pm-150	3.06e-04	9.8e-07	2.27e+03	100	501	>1E20	>1E20
Pm-151	3.24e-03	2.8e-06	2.14e+02	100	501	>1E20	>1E20
Sm-141m	4.30e-05	1.8e-07	1.61e+04	100	501	>1E20	>1E20
Sm-141	1.94e-05	8.4e-08	3.57e+04	100	501	>1E20	>1E20
Sm-142	1.37e-04	6.0e-07	5.06e+03	100	501	>1E20	>1E20
Sm-145	9.31e-01	8.5e-07	7.45e-01	100	501	>1E20	>1E20
Sm-146	7.00e+07	2.0e-04	9.90e-09	100	501	3.3e-01	4.8e-02
Sm-147	1.06e+11	1.8e-04	6.54e-12	100	501	3.7e-01	4.8e-02
Sm-151	9.00e+01	3.4e-07	7.70e-03	100	501	4.6e+10	1.0e-01
Sm-153	5.33e-03	2.6e-06	1.30e+02	100	501	>1E20	>1E20
Sm-155	4.22e-05	6.6e-08	1.64e+04	100	501	>1E20	>1E20
Sm-158	8.37e-05	1.0e-06	8.29e+03	100	501	>1E20	>1E20
Eu-145	1.62e-02	3.2e-05	4.29e+01	100	501	>1E20	>1E20
Eu-146	1.26e-02	5.1e-06	5.50e+01	100	501	>1E20	>1E20
Eu-147	6.02e-02	1.8e-06	1.15e+01	100	501	>1E20	>1E20
Eu-148	1.48e-01	5.2e-06	4.69e+00	100	501	>1E20	>1E20
Eu-149	2.90e-01	4.2e-07	2.39e+00	100	501	>1E20	>1E20
Eu-150(12h)	1.37e-03	1.5e-06	5.06e+02	100	501	>1E20	>1E20
Eu-150(34y)	3.40e+01	6.2e-06	2.04e-02	100	501	>1E20	3.7e-01
Eu-152m	1.07e-03	1.9e-06	6.51e+02	100	501	>1E20	>1E20
Eu-152	1.34e+01	6.0e-06	5.17e-02	100	501	>1E20	8.5e+00
Eu-154	8.20e+00	9.1e-06	8.45e-02	100	501	>1E20	2.3e+02
Eu-155	1.70e+00	1.3e-06	4.08e-01	100	501	>1E20	>1E20
Eu-156	4.22e-02	8.7e-06	1.64e+01	100	501	>1E20	>1E20
Eu-157	1.73e-03	2.3e-06	4.00e+02	100	501	>1E20	>1E20
Eu-158	8.73e-05	2.6e-07	7.94e+03	100	501	>1E20	>1E20
Gd-145	4.75e-05	1.1e-07	1.46e+04	100	501	>1E20	>1E20
Gd-146	1.26e-02	3.8e-06	5.50e+01	100	501	>1E20	>1E20
Gd-147	3.99e-03	2.6e-06	1.74e+02	100	501	>1E20	>1E20
Gd-148	1.30e+02	2.1e-04	5.33e-03	100	501	2.0e+05	8.2e-02
Gd-149	2.46e-02	1.8e-06	2.81e+01	100	501	>1E20	>1E20
Gd-151	3.29e-01	7.7e-07	2.11e+00	100	501	>1E20	>1E20
Gd-152	1.10e+14	1.5e-04	6.30e-15	100	501	4.4e-01	4.8e-02

Table C.1-3. (continued)

Nuclide	T1/2 (years)	DCF (mrem/pCi)	Lambda (1/year)	Kd (cm^3/gm)	Rf	LAW GW Tr (Ci/year)	LAW Gr Trigger (Ci/year)
Cd-113	6.61e-01	1.1e-06	1.05e+00	100	501	>1E20	>1E20
Cd-139	2.12e-03	1.9e-06	3.27e+02	100	501	>1E20	>1E20
Tb-147	4.56e-05	5.6e-07	1.52e+04	100	501	>1E20	>1E20
Tb-149	4.68e-04	9.5e-07	1.48e+03	100	501	>1E20	>1E20
Tb-150	3.54e-04	9.7e-07	1.96e+03	100	501	>1E20	>1E20
Tb-151	2.05e-03	1.4e-06	3.38e+02	100	501	>1E20	>1E20
Tb-153	6.27e-03	9.9e-07	1.10e+02	100	501	>1E20	>1E20
Tb-154	9.70e-04	2.8e-06	7.15e+02	100	501	>1E20	>1E20
Tb-155	1.53e-02	8.2e-07	4.52e+01	100	501	>1E20	>1E20
Tb-156m(24h)	2.74e-03	7.0e-07	2.53e+02	100	501	>1E20	>1E20
Tb-156m(5h)	6.27e-04	3.2e-07	1.10e+03	100	501	>1E20	>1E20
Tb-156	1.48e-02	4.6e-06	4.69e+01	100	501	>1E20	>1E20
Tb-157	1.50e+02	1.0e-07	4.62e-03	100	501	7.0e+07	7.6e-02
Tb-158	1.20e+03	4.0e-06	5.78e-04	100	501	7.0e+01	5.1e-02
Tb-160	1.98e-01	6.4e-06	3.50e+00	100	501	>1E20	>1E20
Tb-161	1.88e-02	2.6e-06	3.68e+01	100	501	>1E20	>1E20
Dy-155	1.20e-03	5.6e-07	5.79e+02	100	501	>1E20	>1E20
Dy-157	9.24e-04	2.7e-07	7.50e+02	100	501	>1E20	>1E20
Dy-159	3.94e-01	4.0e-07	1.76e+00	100	501	>1E20	>1E20
Dy-165	2.66e-04	3.6e-07	2.61e+03	100	501	>1E20	>1E20
Dy-166	9.31e-03	6.2e-06	7.45e+01	100	501	>1E20	>1E20
Ho-155	9.51e-05	1.2e-07	7.29e+03	100	501	>1E20	>1E20
Ho-157	2.66e-05	1.9e-08	2.60e+04	100	501	>1E20	>1E20
Ho-159	6.27e-05	2.3e-08	1.10e+04	100	501	>1E20	>1E20
Ho-161	2.85e-04	4.7e-08	2.43e+03	100	501	>1E20	>1E20
Ho-162m	1.29e-04	9.0e-08	5.36e+03	100	501	>1E20	>1E20
Ho-162	2.85e-05	6.7e-09	2.43e+04	100	501	>1E20	>1E20
Ho-164m	7.13e-05	4.9e-08	9.72e+03	100	501	>1E20	>1E20
Ho-164	7.03e-05	2.4e-08	9.85e+03	100	501	>1E20	>1E20
Ho-166m	1.20e+03	7.8e-06	5.78e-04	100	501	3.6e+01	5.1e-02
Ho-166	3.06e-03	5.5e-06	2.27e+02	100	501	>1E20	>1E20
Ho-167	3.54e-04	3.2e-07	1.96e+03	100	501	>1E20	>1E20
Er-161	3.54e-04	3.3e-07	1.96e+03	100	501	>1E20	>1E20
Er-165	1.18e-03	7.9e-08	5.86e+02	100	501	>1E20	>1E20

Table C.1-3. (continued)

Nuclide	T1/2 (year)	DCF (mr/yr/Ci)	Lambda (1/year)	Kd (cm^3/gm)	Rf	LAW GW Trigger (Ci/vault)	LAW Int Trigger (Ci/vault)
Er-169	2.57e-02	1.1e-06	2.69e+01	100	501	>1E20	>1E20
Er-171	8.58e-04	1.4e-06	8.09e+02	100	501	>1E20	>1E20
Er-172	5.59e-03	3.7e-06	1.24e+02	100	501	>1E20	>1E20
Tm-162	1.46e-04	7.0e-08	4.73e+03	100	501	>1E20	>1E20
Tm-166	8.78e-04	1.2e-06	7.89e+02	100	501	>1E20	>1E20
Tm-167	2.63e-02	2.1e-06	2.64e+01	100	501	>1E20	>1E20
Tm-170	3.53e-01	5.0e-06	1.96e+00	100	501	>1E20	>1E20
Tm-171	1.92e+00	3.9e-07	3.61e-01	100	501	>1E20	2.3e+14
Tm-172	7.26e-03	6.0e-06	9.55e+01	100	501	>1E20	>1E20
Tm-173	9.35e-04	1.2e-06	7.41e+02	100	501	>1E20	>1E20
Tm-175	3.80e-05	5.4e-08	1.82e+04	100	501	>1E20	>1E20
Yb-162	3.59e-05	7.0e-08	1.93e+04	100	501	>1E20	>1E20
Yb-165	1.90e-05	3.8e-06	3.65e+04	100	501	>1E20	>1E20
Yb-167	3.42e-05	1.7e-08	2.03e+04	100	501	>1E20	>1E20
Yb-169	8.76e-02	2.8e-06	7.91e+00	100	501	>1E20	>1E20
Yb-175	1.15e-02	1.6e-06	6.04e+01	100	501	>1E20	>1E20
Yb-177	2.17e-04	3.1e-07	3.20e+03	100	501	>1E20	>1E20
Yb-178	1.40e-04	3.9e-07	4.94e+03	100	501	>1E20	>1E20
Lu-169	3.88e-03	2.0e-06	1.79e+02	100	501	>1E20	>1E20
Lu-170	5.48e-03	4.3e-06	1.27e+02	100	501	>1E20	>1E20
Lu-171	2.27e-02	2.6e-06	3.05e+01	100	501	>1E20	>1E20
Lu-172	1.83e-02	5.0e-06	3.78e+01	100	501	>1E20	>1E20
Lu-173	1.37e+00	9.7e-07	5.06e-01	100	501	>1E20	>1E20
Lu-174m	3.83e-01	1.8e-06	1.81e+00	100	501	>1E20	>1E20
Lu-174	3.60e+00	9.9e-07	1.93e-01	100	501	>1E20	1.1e+07
Lu-176m	4.21e-04	6.3e-07	1.65e+03	100	501	>1E20	>1E20
Lu-176	3.00e+10	6.6e-06	2.31e-11	100	501	1.0e+01	4.8e-02
Lu-177m	4.41e-02	6.8e-06	1.57e+01	100	501	>1E20	>1E20
Lu-177	1.84e-02	2.0e-06	3.77e+01	100	501	>1E20	>1E20
Lu-178m	3.80e-05	8.8e-08	1.82e+04	100	501	>1E20	>1E20
Lu-178	5.70e-05	1.2e-07	1.22e+04	100	501	>1E20	>1E20
Lu-179	5.25e-04	8.1e-07	1.32e+03	100	501	>1E20	>1E20
Hf-170	1.39e-03	1.2e-05	4.98e+02	100	501	>1E20	>1E20
Hf-172	5.00e+00	4.1e-06	1.39e-01	100	501	>1E20	5.0e+04

Table C.1-3. (continued)

Nuclide	T1/2 (year)	DCF (mrem/pCi)	Lambda (1/year)	Xd (cm**3/gm)	Rf	LAW Off Trigger (Ci/vault)	LAW Int Trigger (Ci/vault)
Hf-173	2.6[illegible]-03	9.[illegible]e-07	2.57e+02	100	501	>1E20	>1E20
Hf-175	1.92e-01	1.6e-06	3.62e+00	100	501	>1E[illegible]	>1E20
Hf-177m	9.77e-05	2.5e-07	7.09e+03	100	501	>1E20	>1E20
Hf-178m	3.10e+01	2.0e-05	2.24e-02	100	501	>1E20	4.5e-01
Hf-179m	6.37e-02	4.8e-06	1.01e+01	100	501	>1E20	>1E20
Hf-180m	6.27e-04	8.9e-07	1.10e+03	100	501	>1E20	>1E20
Hf-181	1.16e-01	4.3e-06	5.97e+00	100	501	>1E20	>1E20
Hf-182m	1.18e-04	1.4e-07	5.88e+03	100	501	>1E20	>1E20
Hf-182	9.00e+06	1.4e-05	7.70e-08	100	501	4.7e+00	4.8e-02
Hf-183	1.25e-04	2.5e-07	5.52e+03	100	501	>1E20	>1E20
Hf-184	4.68e-04	2.1e-06	1.48e+03	100	501	>1E20	>1E20
Ta-172	8.37e-05	1.4e-07	8.29e+03	0	1	>1E20	>1E20
Ta-173	4.22e-04	7.4e-07	1.64e+03	0	1	>1E20	>1E20
Ta-174	1.48e-04	1.9e-07	4.67e+03	0	1	>1E20	>1E20
Ta-175	1.20e-03	8.8e-07	5.79e+02	0	1	>1E20	>1E20
Ta-176	9.13e-04	1.3e-06	7.60e+02	0	1	>1E20	>1E20
Ta-177	6.46e-03	4.1e-07	1.07e+02	0	1	>1E20	>1E20
Ta-178	1.79e-05	2.9e-07	3.88e+04	0	1	>1E20	>1E20
Ta-179	2.40e-04	2.5e-07	2.89e+03	0	1	>1E20	>1E20
Ta-180m	9.24e-04	2.1e-07	7.50e+02	0	1	>1E20	>1E20
Ta-180	1.00e+13	3.3e-06	6.93e-14	0	1	4.0e-02	4.8e-02
Ta-182m	3.02e-05	2.4e-08	2.29e+04	0	1	>1E20	>1E20
Ta-182	3.15e-01	6.0e-06	2.20e+00	0	1	1.3e+03	>1E20
Ta-183	1.40e-02	4.6e-06	4.96e+01	0	1	>1E20	>1E20
Ta-184	9.92e-04	2.7e-06	6.98e+02	0	1	>1E20	>1E20
Ta-185	9.51e-05	2.0e-07	7.29e+03	0	1	>1E20	>1E20
Ta-186	2.00e-05	6.7e-08	3.47e+04	0	1	>1E20	>1E20
W-176	2.85e-04	4.8e-07	2.43e+03	0	1	>1E20	>1E20
W-177	2.57e-04	2.4e-07	2.70e+03	0	1	>1E20	>1E20
W-178	5.89e-02	9.3e-07	1.18e+01	0	1	>1E20	>1E20
W-179	7.22e-05	9.0e-09	9.59e+03	0	1	>1E20	>1E20
W-181	3.31e-01	3.1e-07	2.09e+00	0	1	1.5e+04	>1E20
W-185	2.06e-01	1.9e-06	3.37e+00	0	1	1.5e+06	>1E20
W-187	2.73e-03	2.6e-06	2.54e+02	0	1	>1E20	>1E20

Table C.1-3. (continued)

Nuclide	T1/2 (year)	DCF (mrem/pCi)	Lambda (1/year)	Kd (cm^3/gm)	Rf	LAW Grout Trigger (Ci/vault)	LAW Int Trigger (Ci/vault)
W-188	1.[illegible]e+01	9.0e-06	3.67e+00	0	1	1.[illegible]e+06	>1E20
Re-177	3.[illegible]	4.4e-08	2.1[illegible]e+04	0	1	>1E20	>1E20
Re-178	2.85e-05	4.8e-08	2.43e+04	0	1	>1E20	>1E20
Re-181	2.05e-03	1.0e-06	3.38e+02	0	1	>1E20	>1E20
Re-182(64h)	7.30e-03	3.4e-06	9.49e+01	0	1	>1E20	>1E20
Re-182(12h)	1.45e-03	7.4e-07	4.78e+02	0	1	>1E20	>1E20
Re-184m	4.63e-01	2.4e-06	1.50e+00	0	1	9.8e+01	>1E20
Rm-184	1.04e-02	2.2e-06	6.66e+01	0	1	>1E20	>1E20
Re-186m	2.00e+05	3.3e-06	3.47e-06	0	1	4.0e-02	4.8e-02
Re-186	1.03e-02	2.6e-06	6.71e+01	0	1	>1E20	>1E20
Re-187	7.00e+10	8.3e-09	9.90e-12	0	1	1.6e+01	4.8e-02
Re-188m	3.54e-05	6.2e-08	1.96e+04	0	1	>1E20	>1E20
Re-188	1.91e-03	2.8e-06	3.64e+02	0	1	>1E20	>1E20
Re-189	2.74e-03	1.5e-06	2.53e+02	0	1	>1E20	>1E20
Os-180	4.13e-05	4.7e-08	1.68e+04	0	1	>1E20	>1E20
Os-181	4.37e-05	3.5e-07	1.59e+04	0	1	>1E20	>1E20
Os-182	2.51e-03	2.2e-06	2.76e+02	0	1	>1E20	>1E20
Os-185	2.57e-01	2.1e-06	2.69e+00	0	1	4.4e+04	>1E20
Os-189m	6.84e-04	6.6e-08	1.01e+03	0	1	>1E20	>1E20
Os-191m	1.48e-03	3.6e-07	4.67e+02	0	1	>1E20	>1E20
Os-191	4.19e-02	2.0e-06	1.65e+01	0	1	>1E20	>1E20
Os-193	3.48e-03	3.1e-06	1.99e+02	0	1	>1E20	>1E20
Os-194	6.00e+00	9.1e-06	1.16e-01	0	1	2.6e-02	5.0e+03
Ir-182	2.85e-05	1.2e-07	2.43e+04	0	1	>1E20	>1E20
Ir-184	3.65e-04	6.4e-07	1.90e+03	0	1	>1E20	>1E20
Ir-185	1.60e-03	1.1e-06	4.34e+02	0	1	>1E20	>1E20
Ir-186	1.83e-03	2.1e-06	3.80e+02	0	1	>1E20	>1E20
Ir-187	1.20e-03	4.8e-07	5.79e+02	0	1	>1E20	>1E20
Ir-188	4.68e-03	2.7e-06	1.48e+02	0	1	>1E20	>1E20
Ir-189	3.64e-02	9.3e-07	1.90e+01	0	1	>1E20	>1E20
Ir-190m	3.65e-04	3.0e-08	1.90e+03	0	1	>1E20	>1E20
Ir-190	3.01e-02	4.9e-06	2.30e+01	0	1	>1E20	>1E20
Ir-192m	2.74e-06	1.5e-06	2.53e+05	0	1	>1E20	>1E20
Ir-192	2.03e-01	5.3e-06	3.41e+00	0	1	6.4e+05	>1E20

Table C.1-3. (continued)

Nuclide	T1/2 (years)	DCF (mrem/pCi)	Lambda (1/year)	Kd (cm^3/g)	Rf	LAW GW Trigger (Ci/vault)	LAW Int Trigger (Ci/vault)
Ir-194m	4.58e-01	8.1e-06	1.[illegible]+00	0	1	2.7e+01	>1[illegible]
Ir-194	2.22e-03	5.1e-06	3.12e+02	0	1	>1E20	>1E20
Ir-195m	4.45e-04	6.4e-07	1.56e+03	0	1	>1E20	>1E20
Ir-195	4.79e-04	3.4e-07	1.45e+03	0	1	>1E20	>1E20
Pt-186	3.42e-04	3.7e-07	2.03e+03	0	1	>1E20	>1E20
Pt-188	2.79e-02	3.0e-06	2.48e+01	0	1	>1E20	>1E20
Pt-189	1.24e-03	4.9e-07	5.57e+02	0	1	>1E20	>1E20
Pt-191	1.24e-03	1.3e-06	5.57e+02	0	1	>1E20	>1E20
Pt-193m	1.18e-02	1.7e-06	5.89e+01	0	1	>1E20	>1E20
Pt-193	5.00e+01	1.1e-07	1.39e-02	0	1	1.3e+00	1.9e-01
Pt-195m	1.10e-02	2.2e-06	6.30e+01	0	1	>1E20	>1E20
Pt-197m	1.79e-04	3.1e-07	3.88e+03	0	1	>1E20	>1E20
Pt-197	2.09e-03	1.5e-06	3.32e+02	0	1	>1E20	>1E20
Pt-199	5.86e-05	1.0e-07	1.18e+04	0	1	>1E20	>1E20
Pt-200	1.31e-03	4.5e-06	5.28e+02	0	1	>1E20	>1E20
Au-193	1.83e-03	6.0e-07	3.80e+02	0	1	>1E20	>1E20
Au-194	4.51e-03	2.0e-06	1.54e+02	0	1	>1E20	>1E20
Au-195	5.01e-01	1.1e-06	1.38e+00	0	1	1.2e+02	>1E20
Au-198m	6.30e-03	5.7e-06	1.10e+02	0	1	>1E20	>1E20
Au-198	7.38e-03	2.3e-06	9.39e+01	0	1	>1E20	>1E20
Au-199	8.60e-03	1.8e-06	8.06e+01	0	1	>1E20	>1E20
Au-200m	2.13e-03	4.6e-06	3.25e+02	0	1	>1E20	>1E20
Au-200	9.20e-05	1.9e-07	7.53e+03	0	1	>1E20	>1E20
Au-201	4.94e-05	5.7e-08	1.40e+04	0	1	>1E20	>1E20
Hg-193m	1.14e-03	1.6e-06	6.08e+02	1000	5001	>1E20	>1E20
Hg-193	6.84e-04	3.3e-07	1.01e+03	1000	5001	>1E20	>1E20
Hg-194	1.90e+00	6.0e-06	3.65e-01	1000	5001	>1E20	3.4e+14
Hg-195m	4.56e-03	2.2e-06	1.52e+02	1000	5001	>1E20	>1E20
Hg-195	1.08e-03	3.8e-07	6.40e+02	1000	5001	>1E20	>1E20
Hg-197m	2.72e-03	1.7e-06	2.55e+02	1000	5001	>1E20	>1E20
Hg-197	7.31e-03	9.1e-07	9.48e+01	1000	5001	>1E20	>1E20
Hg-199m	8.10e-05	8.5e-08	8.56e+03	1000	5001	>1E20	>1E20
Hg-203	1.28e-01	2.1e-06	5.43e+00	1000	5001	>1E20	>1E20
Tl-194m	6.24e-05	7.1e-08	1.11e+04	0	1	>1E20	>1E20

Table C.1-3. (continued)

Nuclide	T1/2 (year)	DCF (mrem/pCi)	Lambda (1/year)	Kd (cm^3/g)	Rf	LAW GW Trigger (Ci/vault)	LAW fat Trigger (Ci/vault)
Tl-194	6.27e-05	1.9e-08	1.10e+04	0	1	>1E20	>1E20
Tl-195	1.37e-04	7.7e-08	5.06e+03	0	1	>1E20	>1E20
Tl-197	3.12e-04	6.9e-08	2.17e+03	0	1	>1E20	>1E20
Tl-198m	2.12e-04	1.6e-07	3.25e+03	0	1	>1E20	>1E20
Tl-198	6.05e-04	2.6e-07	1.15e+03	0	1	>1E20	>1E20
Tl-199	8.44e-04	8.2e-08	8.21e+02	0	1	>1E20	>1E20
Tl-200	2.98e-03	6.7e-07	2.33e+02	0	1	>1E20	>1E20
Tl-201	8.33e-03	2.9e-07	8.32e+01	0	1	>1E20	>1E20
Tl-202	3.29e-02	1.5e-06	2.11e+01	0	1	>1E20	>1E20
Tl-204	3.77e+00	3.2e-06	1.84e-01	0	1	1.0e-01	4.6e+06
Pb-195m	2.85e-05	8.5e-08	2.43e+04	100	501	>1E20	>1E20
Pb-198	2.74e-04	1.6e-07	2.53e+03	100	501	>1E20	>1E20
Pb-199	1.71e-04	2.2e-07	4.05e+03	100	501	>1E20	>1E20
Pb-200	2.45e-03	1.5e-06	2.83e+02	100	501	>1E20	>1E20
Pb-201	1.07e-03	6.7e-07	6.46e+02	100	501	>1E20	>1E20
Pb-202m	4.13e-04	5.5e-07	1.68e+03	100	501	>1E20	>1E20
Pb-202	3.00e+05	3.9e-05	2.31e-06	100	501	1.7e+00	4.8e-02
Pb-203	5.94e-03	9.6e-07	1.17e+02	100	501	>1E20	>1E20
Pb-205	1.40e+07	1.5e-06	4.95e-08	100	501	4.4e+01	4.8e-02
Pb-209	6.24e-06	9.0e-08	1.11e+05	100	501	>1E20	>1E20
Pb-210	2.23e+01	5.1e-03	3.11e-02	100	501	>1E20	1.1e+00
Pb-211	6.86e-05	4.4e-07	1.01e+04	100	501	>1E20	>1E20
Pb-212	1.21e-03	4.1e-05	5.71e+02	100	501	>1E20	>1E20
Pb-214	5.10e-05	5.8e-07	1.36e+04	100	501	>1E20	>1E20
Bi-200	6.65e-05	1.7e-07	1.04e+04	0	1	>1E20	>1E20
Bi-201	2.05e-04	4.5e-07	3.38e+03	0	1	>1E20	>1E20
Bi-202	1.81e-04	3.6e-07	3.84e+03	0	1	>1E20	>1E20
Bi-203	1.35e-03	2.1e-06	5.15e+02	0	1	>1E20	>1E20
Bi-205	4.19e-02	3.7e-06	1.65e+01	0	1	>1E20	>1E20
Bi-206	1.71e-02	8.0e-06	4.06e+01	0	1	>1E20	>1E20
Bi-207	7.94e+00	4.9e-06	8.73e-02	0	1	4.2e-02	3.0e+02
Bi-210m	3.50e+06	8.6e-05	1.98e-07	0	1	1.5e-03	4.8e-02
Bi-210	1.37e-02	5.9e-06	5.06e+01	0	1	>1E20	>1E20
Bi-212	1.15e-04	9.9e-07	6.02e+03	0	1	>1E20	>1E20

Table C.1-3. (continued)

Nuclide	T1/2 (year)	DCF (mrem/pCi)	Lambda (1/year)	Kd (cm^3/g)	Rf	LAW GW Trigger (Ci/vault)	LAW Int Trigger (Ci/vault)
Bi-213	8.68e-05	6.8e-07	7.99e+03	0	1	>1E20	>1E20
Bi-214	3.76e-05	2.4e-07	1.84e+04	0	1	>1E20	>1E20
Po-203	7.99e-05	2.0e-07	8.68e+03	0	1	>1E20	>1E20
Po-205	2.05e-04	2.4e-07	3.38e+03	0	1	>1E20	>1E20
Po-207	6.50e-04	6.1e-07	1.07e+03	0	1	>1E20	>1E20
Po-210	3.79e-01	1.6e-03	1.83e+00	0	1	7.7e-01	>1E20
At-207	2.05e-04	8.9e-07	3.38e+03	0	1	>1E20	>1E20
At-211	8.22e-04	4.1e-05	8.43e+02	0	1	>1E20	>1E20
Fr-222	2.81e-05	2.5e-06	2.46e+04	0	1	>1E20	>1E20
Fr-223	4.18e-05	8.6e-06	1.66e+04	0	1	>1E20	>1E20
Ra-223	3.13e-02	5.5e-04	2.21e+01	500	2501	>1E20	>1E20
Ra-224	9.91e-03	3.3e-04	6.99e+01	500	2501	>1E20	>1E20
Ra-225	4.05e-02	3.1e-04	1.71e+01	500	2501	>1E20	>1E20
Ra-226	1.62e+03	1.1e-03	4.27e-04	500	2501	6.3e+01	5.0e-02
Ra-227	7.83e-05	2.2e-07	8.85e+03	500	2501	>1E20	>1E20
Ra-228	5.75e+00	1.2e-03	1.21e-01	500	2501	>1E20	8.3e+03
Ac-224	3.31e-04	2.6e-06	2.10e+03	150	751	>1E20	>1E20
Ac-225	2.74e-02	9.5e-05	2.53e+01	150	751	>1E20	>1E20
Ac-226	3.31e-03	4.0e-05	2.10e+02	150	751	>1E20	>1E20
Ac-227	2.18e+01	1.4e-02	3.18e-02	150	751	>1E20	1.2e+00
Ac-228	6.99e-04	2.1e-06	9.91e+02	150	751	>1E20	>1E20
Th-226	5.87e-05	9.2e-07	1.18e+04	3000	15001	>1E20	>1E20
Th-227	5.13e-02	3.6e-05	1.35e+01	3000	15001	>1E20	>1E20
Th-228	1.91e+00	3.8e-04	3.62e-01	3000	15001	>1E20	2.6e+14
Th-229	7.43e+03	3.5e-03	9.33e-05	3000	15001	6.2e+02	4.9e-02
Th-230	7.70e+04	5.3e-04	9.00e-06	3000	15001	7.3e+00	4.8e-02
Th-231	2.91e-03	1.3e-06	2.38e+02	3000	15001	>1E20	>1E20
Th-232	1.41e+10	2.8e-03	4.93e-11	3000	15001	1.6e-01	4.8e-02
Th-234	6.60e-02	1.3e-05	1.05e+01	3000	15001	>1E20	>1E20
Pa-227	7.28e-05	1.3e-06	9.52e+03	10	51	>1E20	>1E20
Pa-228	2.97e-03	4.0e-06	2.34e+02	10	51	>1E20	>1E20
Pa-230	4.85e-02	5.6e-06	1.43e+01	10	51	>1E20	>1E20
Pa-231	3.28e+04	1.1e-02	2.12e-05	10	51	6.1e-04	4.8e-02
Pa-232	3.59e-03	3.4e-06	1.93e+02	10	51	>1E20	>1E20

Table C.1-3. (continued)

Nuclide	T1/2 (year)	DCF (mrem/pCi)	Lambda (1/year)	Kd (cm**3/gm)	Rf	LAW GW Trigger (Ci/vault)	LAW Int Trigger (Ci/vault)
Pa-233	7.30e-02	3.1e-06	9.23e+00	10	51	>1E20	>1E20
Pa-234	7.64e-04	2.1e-06	9.07e+02	10	51	>1E20	>1E20
U-230	5.69e-02	8.4e-04	1.22e+01	50	251	>1E20	>1E20
U-231	4.30e+00	1.1e-06	1.61e-01	50	251	>1E20	4.8e+05
U-232	7.20e+01	1.3e-03	9.63e-03	50	251	4.5e+03	1.3e-01
U-233	1.60e+05	2.7e-04	4.35e-06	50	251	1.2e-01	4.8e-02
U-234	2.45e+05	2.6e-04	2.83e-06	50	251	1.2e-01	4.8e-02
U-235	7.04e+08	2.5e-04	9.85e-10	50	251	6.3e-02	4.8e-02
U-236	2.34e+07	2.5e-04	2.96e-08	50	251	1.3e-01	4.8e-02
U-237	1.85e-02	2.7e-06	3.75e+01	50	251	>1E20	>1E20
U-238	4.47e+09	2.3e-04	1.55e-10	50	251	1.3e-01	4.8e-02
U-239	4.47e-05	7.6e-08	1.55e+04	50	251	>1E20	>1E20
U-240	1.61e-03	4.1e-06	4.31e+02	50	251	>1E20	>1E20
Np-232	2.47e-05	2.4e-08	2.80e+04	10	51	>1E20	>1E20
Np-233	6.65e-05	5.6e-09	1.04e+04	10	51	>1E20	>1E20
Np-234	1.20e-02	1.7e-06	5.75e+01	10	51	>1E20	>1E20
Np-235	1.12e+00	2.1e-07	6.17e-01	10	51	>1E20	>1E20
Np-236(1E5y)	1.10e+05	7.9e-04	6.30e-06	10	51	8.5e-03	4.8e-02
Np-236(22h)	2.51e-03	9.5e-07	2.76e+02	10	51	>1E20	>1E20
Np-237	2.14e+06	3.9e-03	3.24e-07	10	51	1.7e-03	4.8e-02
Np-238	5.80e-03	3.4e-06	1.20e+02	10	51	>1E20	>1E20
Np-239	6.38e-03	2.9e-06	1.09e+02	10	51	>1E20	>1E20
Np-240	1.20e-04	2.0e-07	5.79e+03	10	51	>1E20	>1E20
Pu-234	1.03e-03	1.2e-06	6.75e+02	100	501	>1E20	>1E20
Pu-235	4.94e-05	1.4e-08	1.40e+04	100	501	>1E20	>1E20
Pu-236	2.85e+00	1.3e-03	2.43e-01	100	501	>1E20	1.8e+09
Pu-237	1.24e-01	1.0e-06	5.58e+00	100	501	>1E20	>1E20
Pu-238	8.78e+01	3.8e-03	7.90e-03	100	501	3.2e+02	1.1e-01
Pu-239	2.41e+04	4.3e-03	2.87e-05	100	501	1.6e-02	4.8e-02
Pu-240	6.57e+03	4.3e-03	1.06e-04	100	501	2.0e-02	4.9e-02
Pu-241	1.44e+01	8.6e-05	4.81e-02	100	501	3.1e+01	5.9e+00
Pu-242	3.76e+05	4.1e-03	1.84e-06	100	501	1.6e-02	4.8e-02
Pu-243	5.65e-04	3.3e-07	1.23e+03	100	501	>1E20	>1E20
Pu-244	8.10e+07	4.0e-03	8.56e-09	100	501	1.7e-02	4.8e-02

Table C.1-3. (continued)

Nuclide	T1/2 (years)	D[illegible] (mrem/pCi)	Lambda (1/year)	Kd (cm^3/gm)	RF	LAW Trigger (Ci/vault)	LAW Trigger (Ci/vault)
Pu-245	1.1[illegible]e-01	2.4e-06	6.08e+02	100	501	>1E20	>1E20
Am-237	1.48e-01	7.4e-08	4.67e+03	150	751	>1E20	>1E20
Am-238	2.17e-01	1.7e-07	3.20e+03	150	751	>1E20	>1E20
Am-239	1.38e-03	1.0e-06	5.02e+02	150	751	>1E20	>1E20
Am-240	5.82e-03	2.9e-06	1.19e+02	150	751	>1E20	>1E20
Am-241	4.32e+02	4.5e-03	1.60e-03	150	751	4.4e+00	5.7e-02
Am-242m	1.52e+02	4.2e-03	4.56e-03	150	751	6.4e+05	7.6e-02
Am-242	1.83e-03	1.2e-06	3.80e+02	150	751	>1E20	>1E20
Am-243	7.37e+03	4.5e-03	9.40e-05	150	751	2.7e-02	4.9e-02
Am-244m	4.94e-05	6.8e-08	1.40e+04	150	751	>1E20	>1E20
Am-244	1.15e-03	2.0e-06	6.02e+02	150	751	>1E20	>1E20
Am-245	2.40e-04	1.8e-07	2.89e+03	150	751	>1E20	>1E20
Am-246m	4.75e-05	8.4e-08	1.46e+04	150	751	>1E20	>1E20
Am-246	4.75e-05	1.5e-07	1.46e+04	150	751	>1E20	>1E20
Cm-238	2.85e-04	3.6e-07	2.43e+03	100	501	>1E20	>1E20
Cm-240	7.34e-02	6.3e-05	9.45e+00	100	501	>1E20	>1E20
Cm-241	9.58e-02	4.6e-06	7.23e+00	100	501	>1E20	>1E20
Cm-242	4.46e-01	1.1e-04	1.56e+00	100	501	>1E20	>1E20
Cm-243	2.85e+01	2.9e-03	2.43e-02	100	501	>1E20	5.5e-01
Cm-244	1.81e+01	2.3e-03	3.83e-02	100	501	7.3e+00	2.2e+00
Cm-245	8.50e+03	4.5e-03	8.15e-05	100	501	1.8e-02	4.9e-02
Cm-246	4.70e+03	4.5e-03	1.47e-04	100	501	2.1e-02	4.9e-02
Cm-247	1.60e+07	4.1e-03	4.33e-08	100	501	1.6e-02	4.8e-02
Cm-248	3.50e+05	1.6e-02	1.98e-06	100	501	4.2e-03	4.8e-02
Cm-249	1.24e-04	9.5e-08	5.61e+03	100	501	>1E20	>1E20
Bk-245	1.36e-02	2.3e-06	5.08e+01	100	501	>1E20	>1E20
Bk-246	4.93e-03	1.9e-06	1.41e+02	100	501	>1E20	>1E20
Bk-247	1.40e+03	2.3e-03	4.95e-04	100	501	9.9e-02	5.1e-02
Bk-249	8.80e-01	6.0e-06	7.88e-01	100	501	>1E20	>1E20
Bk-250	3.67e-04	5.0e-07	1.89e+03	100	501	>1E20	>1E20
Cf-244	4.75e-05	1.5e-07	1.46e+04	100	501	>1E20	>1E20
Cf-246	4.11e-03	1.2e-05	1.69e+02	100	501	>1E20	>1E20
Cf-248	9.86e-01	2.8e-04	7.03e-01	100	501	>1E20	>1E20
Cf-249	3.51e+02	4.6e-03	1.97e-03	100	501	2.0e+00	5.9e-02

Table C.1-3. (continued)

Nuclide	T1/2 (years)	DCF (mrem/pCi)	Limit (l/year)	Kd (cm^3/gm)	Rf	LAW GW Tier (Ci/unit)	LAW Inv Tier (Ci/unit)
Cf-250	1.31e+01	1.9e-03	5.80e-02	100	501	>1E20	9.5e+00
Cf-251	9.00e+02	4.6e-03	7.70e-04	100	501	9.9e-02	5.2e-02
Cf-252	2.62e+00	9.4e-04	2.65e-01	100	501	5.5e+02	1.5e+10
Cf-253	4.87e-02	9.2e-06	1.42e+01	100	501	>1E20	>1E20
Cf-254	1.66e-01	2.5e-03	4.18e+00	100	501	>1E20	>1E20
Es-250	9.13e-04	9.5e-08	7.60e+02	100	501	>1E20	>1E20
Es-251	4.11e-03	6.7e-07	1.69e+02	100	501	>1E20	>1E20
Es-253	5.60e-02	2.4e-05	1.24e+01	100	501	>1E20	>1E20
Es-254m	4.48e-03	1.5e-05	1.55e+02	100	501	>1E20	>1E20
Es-254	7.56e-01	1.5e-04	9.17e-01	100	501	>1E20	>1E20
Fm-252	2.62e-03	9.9e-06	2.64e+02	100	501	>1E20	>1E20
Fm-253	8.21e-03	3.5e-06	8.44e+01	100	501	>1E20	>1E20
Fm-254	3.70e-04	1.6e-06	1.88e+03	100	501	>1E20	>1E20
Fm-255	2.29e-03	9.7e-06	3.02e+02	100	501	>1E20	>1E20
Fm-257	2.19e-01	7.3e-05	3.16e+00	100	501	>1E20	>1E20
Md-257	3.42e-04	5.4e-07	2.03e+03	100	501	>1E20	>1E20
Md-258	1.53e-01	6.1e-05	4.52e+00	100	501	>1E20	>1E20

Table C.1.1. Weighted dose conversion factors for radionuclides with multiple daughters

Parent	Progeny	DCF rem/uCi	Rf	Time (year)	Activity Fraction @ Ar. Time	Weighted DCF
Th-232		2.8E+00	15001	75005	1.0E+00	1.9E-04
	Ra-228	1.5E+00	2501		1.0E+00	6.0E-04
	Th-228	7.2E-01	15001	1.0E+00	4.8E-05	
Th-232 Ingrowth Factor (rem/uCi) = >						8.3E-04
U-234		2.6E-01	251	1255	1.0E+00	1.0E-03
	Th-230	5.3E-01	15001	1.1E-01	3.9E-06	
	Ra-226	1.1E+00	2501		2.6E-03	1.1E-06
	Pb-210	6.7E+00	501		2.5E-03	3.3E-05
U-234 Ingrowth Factor (rem/uCi) =>						1.1E-03
U-235		2.6E-01	251	1255	1.0E+00	1.0E-03
	Pa-231	1.1E+00	51		2.6E-02	5.7E-04
	Ac-227	1.5E+01	751		2.6E-02	5.0E-04
U-235 Ingrowth Factor (rem/uCi) =>						2.1E-03
U-236		2.5E-01	251	1255	1.0E+00	1.0E-03
	Th-232	2.8E+00	15001	6.2E-08	1.2E-11	
	Ra-228	1.2E+00	2501		6.2E-08	3.0E-11
	Th-228	7.5E-01	15001	6.1E-08	3.1E-12	
U-236 Ingrowth Factor (rem/uCi) =>						1.0E-03
U-238		2.5E-01	251	1255	1.0E+00	9.8E-04
	U-234	2.6E-01	251		3.6E-03	3.7E-06
	Th-230	5.3E-01	15001	2.0E-05	7.1E-10	
	Ra-226	1.1E+00	2501		3.2E-06	1.4E-09
	Pb-210	6.7E+00	501		3.0E-06	4.0E-08
U-238 Ingrowth Factor (rem/uCi) =>						9.8E-04
Np-237		3.9E+00	51	255	1.0E+00	7.6E-02
	U-233	2.7E-01	251		1.1E-03	1.2E-06
	Th-229	3.9E+00	15001	1.3E-05	3.4E-09	
Np-237 Ingrowth Factor (rem/uCi) =>						7.6E-02
Pu-238		3.8E+00	501	2505	2.6E-09	1.9E-11
	U-234	2.6E-01	251		3.6E-04	3.7E-07
	Th-230	5.3E-01	15001	7.6E-06	2.7E-10	
	Ra-226	1.1E+00	2501		2.9E-06	1.3E-09
	Pb-210	6.7E+00	501		2.8E-06	3.8E-08
Pu-238 Ingrowth Factor (rem/uCi) =>						4.1E-07

Table C.1.4. (continued)

Parent	Progeny	DCF rem/uCi	Rf	Time (year)	Arrival Fraction @ Ar. Time	Weighted DCF
Pu-239		4.3E+00	501	2505	9.3E-01	8.0E-03
	U-235	2.6E-01	251		2.4E-06	2.4E-09
	Pa-231	1.1E+00	51		6.3E-08	1.4E-08
	Ac-227	1.5E+01	751		6.1E-08	1.2E-09
Pu-239 Ingrowth Factor (rem/uCi) =>						8.0E-03
Pu-241		8.6E-02	501	2505	4.3E-53	7.4E-57
	Am-241	4.5E+00	751		6.2E-04	3.7E-06
	Np-237	3.9E+00	51		6.2E-04	3.7E-06
	U-233	2.7E-01	251		5.5E-08	5.9E-11
	Th-229	3.9E+00	15001	5.0E-09	1.3E-12	
Pu-241 Ingrowth Factor (rem/uCi) =>						4.2E-06
Pu-242		4.1E+00	501	2505	1.0E+00	8.1E-03
	U-238	2.5E-01	251		3.9E-07	3.8E-10
	U-234	2.6E-01	251		1.4E-09	1.4E-12
	Th-230	5.3E-01	15001	1.0E-11	3.6E-16	
	Ra-226	1.1E+00	2501		2.3E-12	1.0E-15
	Pb-210	6.7E+00	501		2.2E-12	2.9E-14
Pu-242 Ingrowth Factor (rem/uCi) =>						8.1E-03
Am-241		4.5E+00	751	3755	2.4E-03	1.5E-05
	Np-237	3.9E+00	51		2.0E-04	1.5E-05
	U-233	2.7E-01	251		2.7E-06	2.9E-09
	Th-229	3.9E+00	15001	3.8E-07	9.9E-11	
Am-241 Ingrowth Factor (rem/uCi) =>						3.0E-05
Am-243		4.5E+00	751	3755	7.0E-01	4.2E-03
	Pu-239	4.3E+00	501		8.6E-02	7.4E-04
	U-235	2.6E-01	251		1.7E-07	1.7E-10
	Pa-231	1.1E+00	51		4.6E-09	1.0E-09
	Ac-227	1.5E+01	751		4.5E-09	8.8E-11
Am-243 Ingrowth Factor (rem/uCi) =>						4.9E-03
Cm-244		2.3E+00	501	2505	2.3E-42	1.1E-44
	Pu-240	2.1E-03	501		2.1E-03	1.8E-05
	U-236	2.5E-01	251		1.8E-07	1.8E-10
	Th-232	2.8E+00	15001	1.1E-14	2.1E-18	
	Ra-228	1.2E+00	2501		1.1E-14	5.4E-18
	Th-228	7.5E-01	15001	1.1E-14	5.7E-19	
Cm-244 Ingrowth Factor (rem/uCi) =>						1.8E-05

Table C.1-1. (continued)

Parent	Progeny	DCF rem/uCi	RF	Time (year)	Arrival Fraction @ Ar. Time	Weighted DCF
Cf-252		9.4E-01	501	2505	0.0E+00	0.0E+00
	Cm-248	1.6E+01	501		7.5E-06	2.4E-07
	Pu-244	4.0E+00	501		1.5E-10	1.2E-12
	Pu-240	2.1E-03	501		1.8E-11	1.5E-13
	U-236	2.5E-01	251		4.4E-16	4.4E-19
	Th-232	2.8E+00	15001	1.4E-23	6.5E-27	
	Ra-228	1.2E+00	2501		1.4E-23	6.5E-27
	Th-228	7.5E-01	15001	1.4E-23	6.8E-28	
Cf-252 Ingrowth Factor (rem/uCi) =>						2.4E-07

C.2 E-AREA STREAM FLOW DATA

The gauging results for SRS creeks in the vicinity of E-Area are presented in Table C.2-1. In Fig. C.2-1, the location of stream flow measurements supporting these results is shown.

Table C.2-1. Stream gaging results for SRS creeks in the vicinity of [illegible]
(field measurements taken on January 27, [illegible] by Peter Xeud)

Location Number	Location Description (refer to Fig. C.2-1)	Flow, cfs
1	Crouch, near Upper Three Runs	1.78
2	Tributary to Crouch, near Upper Three Runs	1.42
3	Crouch, just above confluence with tributary	0.15
12	Crouch, 50 ft from stream stage measurement station	1.21
13	Crouch, upstream from station 12	0.78
14	Crouch, upstream from station 13	0.44
15	Crouch, upstream from station 14	0.014
16	Crouch, upstream from station 15	0.48
4	Crouch, just below road and NPDES sample site	0.137
17	Lower end of tributary to Upper Three Runs	0.33
18	Unnamed branch, just upstream from railroad crossing near Upper Three Runs	0.68
19	Unnamed branch, upstream from station 18	0.44
20	Unnamed branch, upstream from station 19	0.10

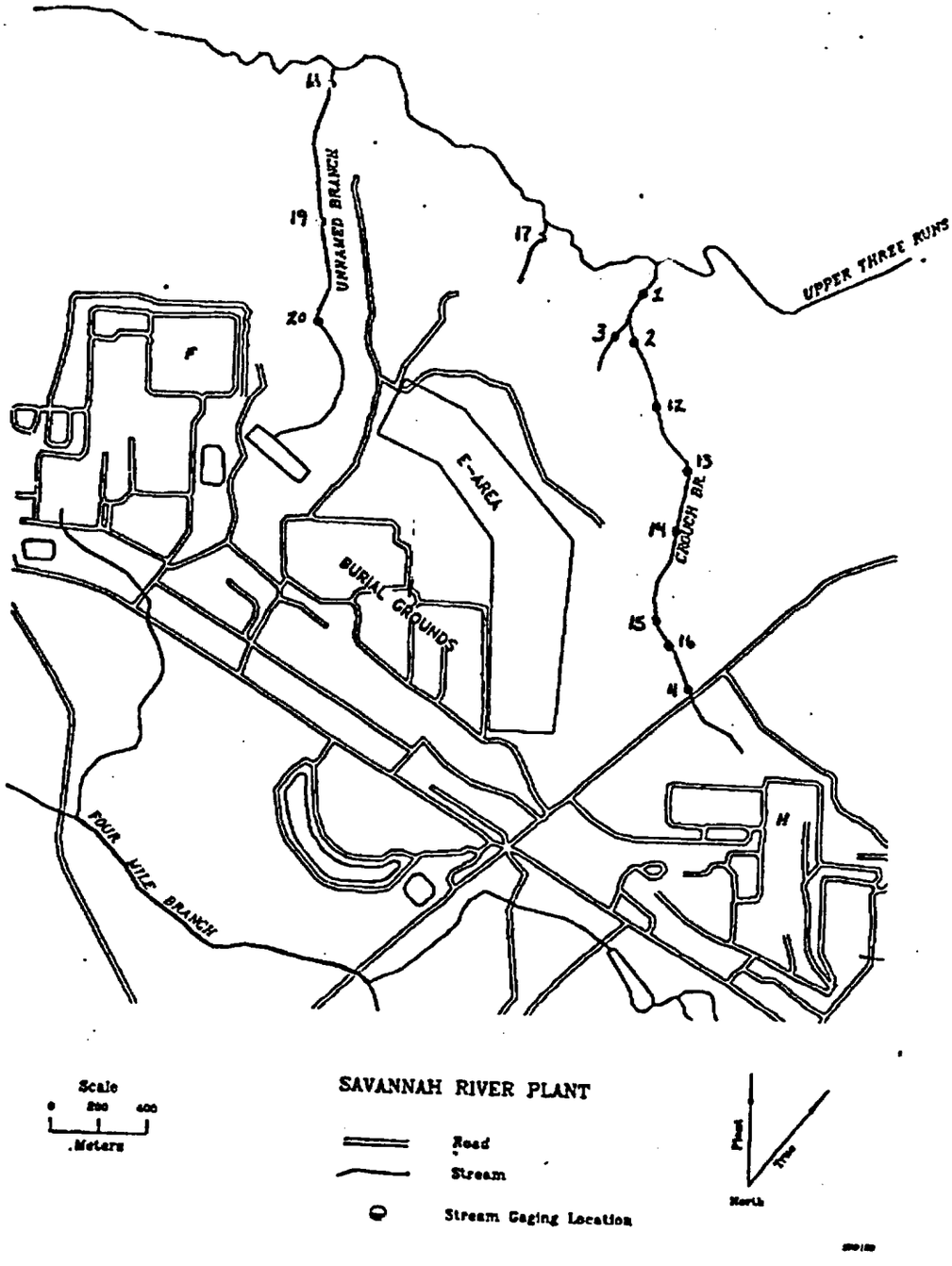

Fig. C.2-1. Locations of stream-gaging stations in creeks near E-Area.

C.3 RADIONUCLIDE SCREENING RESULTS FOR SUSPECT SOIL

The screening results for radionuclides potentially present suspect soil are given in Table C.3-1.

Table C3-1. Screening calculations and trigger values for the suspect soil trenches

Nuclide	T1/2 (year)	DCF (mrem/pCi)	Lambda (1/year)	Kd (cm^3/gm)	Rf	SUSP GW Trigger (Ci/trench)	SUSP Int Trigger (Ci/trench)
H-3	1.23e+01	6.3e-08	5.62e-02	0	1	3.3e-01	2.4e-03
Be-7	1.47e-01	1.1e-07	4.72e+00	0	1	2.6e+09	>1E20
Be-10	1.60e+06	4.2e-06	4.33e-07	0	1	3.8e-03	8.6e-06
C-11	3.86e-05	1.2e-08	1.80e+04	2	11	>1E20	>1E20
C-14	5.73e+03	2.1e-06	1.21e-04	2	11	8.3e-02	8.7e-06
F-18	2.14e-04	1.0e-04	3.25e+03	0	1	>1E20	>1E20
Na-22	2.58e+00	1.2e-05	2.69e-01	0	1	5.0e-03	4.0e+06
Na-24	1.71e-03	1.4e-06	4.05e+02	0	1	>1E20	>1E20
Mg-28	2.40e-03	7.5e-06	2.89e+02	0	1	>1E20	>1E20
Al-26	7.40e+05	1.3e-05	9.37e-07	0	1	1.2e-03	8.6e-06
Si-31	2.99e-04	5.4e-07	2.32e+03	0	1	>1E20	>1E20
Si-32	6.50e+02	1.7e-06	1.07e-03	0	1	9.3e-03	9.6e-06
P-32	3.89e-02	7.7e-06	1.78e+01	0	1	>1E20	>1E20
P-33	6.84e-02	8.8e-07	1.01e+01	0	1	>1E20	>1E20
S-35	2.39e-01	4.3e-07	2.90e+00	0	1	7.4e+04	>1E20
Cl-36	3.01e+05	3.0e-06	2.30e-06	0	1	5.3e-03	8.6e-06
Cl-38	7.07e-05	2.0e-07	9.80e+03	0	1	>1E20	>1E20
Cl-39	1.06e-04	1.4e-07	6.57e+03	0	1	>1E20	>1E20
K-40	1.28e+09	1.9e-05	5.42e-10	0	1	8.3e-04	8.6e-06
K-42	1.41e-03	1.1e-06	4.92e+02	0	1	>1E20	>1E20
K-43	2.56e-03	7.8e-07	2.71e+02	0	1	>1E20	>1E20
K-44	4.18e-05	1.5e-07	1.66e+04	0	1	>1E20	>1E20
K-45	3.04e-05	9.3e-08	2.28e+04	0	1	>1E20	>1E20
Ca-41	1.30e+05	1.2e-06	5.33e-06	0	1	1.3e-02	8.6e-06
Ca-45	4.46e-01	3.0e-06	1.55e+00	0	1	1.2e+01	>1E20
Ca-47	1.24e-02	6.2e-06	5.58e+01	0	1	>1E20	>1E20
Sc-43	4.47e-04	7.3e-07	1.55e+03	0	1	>1E20	>1E20
Sc-44m	6.68e-03	9.9e-06	1.04e+02	0	1	>1E20	>1E20
Sc-44	4.47e-04	1.4e-06	1.55e+03	0	1	>1E20	>1E20
Sc-46	2.29e-01	5.6e-06	3.02e+00	0	1	1.0e+04	>1E20
Sc-47	9.39e-03	1.9e-06	7.38e+01	0	1	>1E20	>1E20
Sc-48	5.03e-03	6.4e-06	1.38e+02	0	1	>1E20	>1E20
Sc-49	1.09e-04	2.4e-07	6.34e+03	0	1	>1E20	>1E20

Table C3-1. (continued)

Nuclide	T1/2 (years)	DCF (mrem/pCi)	Lambda (1/year)	Kd (cm**3/gm)	Rf	SUSP Int Trigger (Ci/trench)	SUSP Int Trigger (Ci/trench)
Ti-44	4.[illegible]e+01	1.9e-05	1.44e-02	0	1	3.[illegible]e+01	3.7e-05
Ti-45	3.5[illegible]e-04	5.7e-07	1.97e+03	0	1	>1E20	>1E20
V-47	6.27e-05	1.6e-07	1.10e+04	0	1	>1E20	>1E20
V-48	4.41e-02	7.5e-06	1.57e+01	0	1	>1E20	>1E20
V-49	9.03e-01	5.4e-08	7.67e-01	0	1	1.4e+01	>1E20
Cr-48	2.62e-03	8.2e-07	2.64e+02	40	201	>1E20	>1E20
Cr-49	7.97e-05	1.7e-07	8.70e+03	40	201	>1E20	>1E20
Cr-51	7.58e-02	1.3e-07	9.14e+00	40	201	>1E20	>1E20
Mn-51	8.56e-05	2.5e-07	8.10e+03	50	251	>1E20	>1E20
Mn-52m	3.99e-05	1.5e-07	1.74e+04	50	251	>1E20	>1E20
Mn-52	1.52e-02	6.9e-06	4.56e+01	50	251	>1E20	>1E20
Mn-53	2.00e+06	9.9e-08	3.47e-07	50	251	4.0e+01	8.6e-06
Mn-54	7.97e-01	2.7e-06	8.70e-01	50	251	>1E20	>1E20
Mn-56	2.94e-04	9.5e-07	2.36e+03	50	251	>1E20	>1E20
Fe-52	9.35e-04	5.4e-06	7.41e+02	0	1	>1E20	>1E20
Fe-55	2.70e+00	5.8e-07	2.57e-01	0	1	9.8e-02	1.2e+06
Fe-59	1.22e-01	6.6e-06	5.68e+00	0	1	5.1e+09	>1E20
Fe-60	3.00e+05	1.5e-04	2.31e-06	0	1	1.1e-04	8.6e-06
Co-55	2.08e-03	4.1e-06	3.34e+02	10	51	>1E20	>1E20
Co-56	2.11e-01	1.2e-05	3.29e+00	10	51	>1E20	>1E20
Co-57	7.39e-01	1.1e-05	9.38e-01	10	51	>1E20	>1E20
Co-58m	1.03e-03	8.8e-08	6.75e+02	10	51	>1E20	>1E20
Co-58	1.95e-01	3.5e-06	3.55e+00	10	51	>1E20	>1E20
Co-60m	2.00e-05	3.6e-09	3.47e+04	10	51	>1E20	>1E20
Co-60	5.27e+00	2.6e-05	1.32e-01	10	51	1.1e+13	4.4e+00
Co-61	1.88e-04	2.6e-07	3.68e+03	10	51	>1E20	>1E20
Co-62m	3.04e-06	9.6e-08	2.28e+05	10	51	>1E20	>1E20
Ni-56	1.67e-02	3.5e-06	4.15e+01	300	1501	>1E20	>1E20
Ni-57	4.11e-03	3.3e-06	1.69e+02	300	1501	>1E20	>1E20
Ni-59	8.00e+04	2.0e-07	8.66e-06	300	1501	1.3e+02	8.6e-06
Ni-63	1.00e+02	5.4e-07	6.93e-03	300	1501	>1E20	1.7e-05
Ni-65	2.87e-04	6.1e-07	2.41e+03	300	1501	>1E20	>1E20
Ni-66	6.23e-03	1.1e-05	1.11e+02	300	1501	>1E20	>1E20
Cu-60	4.37e-05	1.7e-07	1.59e+04	25	126	>1E20	>1E20

Table C.3-1. (continued)

Nuclide	T1/2 (years)	DCF (mrem/pCi)	Inhalation (1/year)	Kd (cm**3/gm)	IF	SUSP (HW Trigger (Ci/trench)	SUSP Int Trigger (Ci/trench)
Cu-61	3.39e-04	4.1e-07	1.78e+03	25	126	>1E20	>1E20
Cu-64	1.35e-03	4.2e-07	4.78e+02	25	126	>1E20	>1E20
Cu-67	7.06e-03	1.1e-06	9.82e+01	25	126	>1E20	>1E20
Zn-62	1.04e-03	3.4e-06	6.64e+02	16	81	>1E20	>1E20
Zn-63	7.30e-05	2.0e-07	9.49e+03	16	81	>1E20	>1E20
Zn-65	6.67e-01	1.4e-05	1.04e+00	16	81	>1E20	>1E20
Zn-69m	1.57e-03	1.2e-05	4.40e+02	16	81	>1E20	>1E20
Zn-69	1.08e-04	8.5e-08	6.40e+03	16	81	>1E20	>1E20
Zn-71m	4.56e-04	8.3e-07	1.52e+03	16	81	>1E20	>1E20
Zn-72	1.27e-01	4.9e-06	5.44e+00	16	81	>1E20	>1E20
Ga-65	2.89e-05	7.8e-08	2.40e+04	0	1	>1E20	>1E20
Ga-66	1.07e-03	4.7e-06	6.46e+02	0	1	>1E20	>1E20
Ga-67	8.91e-03	7.2e-07	7.78e+01	0	1	>1E20	>1E20
Ga-68	1.30e-04	3.3e-07	5.34e+03	0	1	>1E20	>1E20
Ga-70	4.01e-05	7.1e-08	1.73e+04	0	1	>1E20	>1E20
Ga-72	1.61e-03	4.4e-06	4.31e+02	0	1	>1E20	>1E20
Ga-73	1.34e-02	1.0e-06	5.19e+01	0	1	>1E20	>1E20
Ge-66	1.07e-03	2.1e-07	6.46e+02	0	1	>1E20	>1E20
Ge-67	3.61e-05	1.1e-07	1.92e+04	0	1	>1E20	>1E20
Ge-68	7.86e-01	1.1e-06	8.82e-01	0	1	1.2e+00	>1E20
Ge-69	4.45e-03	3.6e-07	1.56e+02	0	1	>1E20	>1E20
Ge-71	3.12e-02	9.6e-09	2.22e+01	0	1	>1E20	>1E20
Ge-75	1.57e-04	7.3e-08	4.40e+03	0	1	>1E20	>1E20
Ge-77	1.29e-03	5.6e-07	5.38e+02	0	1	>1E20	>1E20
Ge-78	1.65e-04	2.1e-07	4.19e+03	0	1	>1E20	>1E20
As-69	2.85e-05	1.1e-07	2.43e+04	3	16	>1E20	>1E20
As-70	1.01e-04	3.4e-07	6.88e+03	3	16	>1E20	>1E20
As-71	7.07e-03	1.3e-06	9.80e+01	3	16	>1E20	>1E20
As-72	2.97e-03	5.6e-06	2.34e+02	3	16	>1E20	>1E20
As-73	2.20e-01	6.1e-07	3.15e+00	3	16	>1E20	>1E20
As-74	3.29e-02	3.3e-06	2.11e+01	3	16	>1E20	>1E20
As-76	3.00e-03	4.8e-06	2.31e+02	3	16	>1E20	>1E20
As-77	1.06e-01	1.1e-06	6.53e+00	3	16	>1E20	>1E20
As-78	1.73e-04	6.5e-07	4.01e+03	3	16	>1E20	>1E20

Table C3-1. (continued)

Nuclide	T1/2 (year)	DCF (mrem/pCi)	Lambda (1/year)	Kd (cm**3/gm)	Rf	SUSP GW Trigger (Ci/trench)	SUSP Int Trigger (Ci/trench)
Se-70	8.37e-05	4.2e-07	8.29e+03	5	26	>1E20	>1E20
Se-73m	7.99e-05	1.5e-07	8.68e+03	5	26	>1E20	>1E20
Se-73	8.10e-01	1.5e-06	8.56e+02	5	26	>1E20	>1E20
Se-75	3.30e-01	8.8e-06	2.10e+00	5	26	>1E20	>1E20
Se-79	6.50e+04	8.3e-06	1.07e-05	5	26	5.0e-02	8.6e-06
Se-81m	1.09e-04	2.1e-07	6.36e+03	5	26	>1E20	>1E20
Se-81	4.30e-05	6.1e-08	1.61e+04	5	26	>1E20	>1E20
Se-83	4.28e-05	1.5e-07	1.62e+04	5	26	>1E20	>1E20
Br-74m	7.89e-05	2.2e-07	8.78e+03	0	1	>1E20	>1E20
Br-74	6.84e-05	1.4e-07	1.01e+04	0	1	>1E20	>1E20
Br-75	1.94e-04	1.3e-07	3.57e+03	0	1	>1E20	>1E20
Br-76	1.84e-03	1.4e-06	3.77e+02	0	1	>1E20	>1E20
Br-77	6.50e-03	3.1e-07	1.07e+02	0	1	>1E20	>1E20
Br-80m	5.04e-04	2.3e-07	1.37e+03	0	1	>1E20	>1E20
Br-80	3.37e-05	5.5e-08	2.06e+04	0	1	>1E20	>1E20
Br-82	4.03e-03	1.7e-06	1.72e+02	0	1	>1E20	>1E20
Br-83	2.74e-04	7.3e-08	2.53e+03	0	1	>1E20	>1E20
Br-84	6.05e-05	1.5e-07	1.15e+04	0	1	>1E20	>1E20
Rb-79	3.99e-05	8.7e-08	1.74e+04	0	1	>1E20	>1E20
Rb-81m	6.08e-05	1.8e-08	1.14e+04	0	1	>1E20	>1E20
Rb-81	5.36e-04	1.3e-07	1.29e+03	0	1	>1E20	>1E20
Rb-82m	7.30e-04	4.2e-07	9.49e+02	0	1	>1E20	>1E20
Rb-83	2.27e-01	7.7e-06	3.05e+00	0	1	8.6e+03	>1E20
Rb-84	9.31e-02	1.0e-05	7.45e+00	0	1	2.3e+13	>1E20
Rb-86	5.09e-02	9.4e-06	1.36e+01	0	1	>1E20	>1E20
Rb-87	4.80e+10	4.8e-06	1.44e-11	0	1	3.3e-03	8.6e-06
Rb-88	3.37e-05	1.6e-07	2.06e+04	0	1	>1E20	>1E20
Rb-89	2.89e-05	8.0e-08	2.40e+04	0	1	>1E20	>1E20
Sr-80	1.94e-04	5.2e-09	3.57e+03	10	51	>1E20	>1E20
Sr-81	5.51e-05	2.2e-07	1.26e+04	10	51	>1E20	>1E20
Sr-83	3.76e-03	2.3e-06	1.84e+02	10	51	>1E20	>1E20
Sr-85m	1.29e-04	2.4e-08	5.39e+03	10	51	>1E20	>1E20
Sr-85	1.79e-01	1.9e-06	3.88e+00	10	51	>1E20	>1E20
Sr-87m	3.21e-04	1.2e-07	2.16e+03	10	51	>1E20	>1E20

Table C.3-1. (continued)

Nuclide	T1/2 (yrs)	DCF (mrem/pCi)	Lambda (1/yrs)	Kd (cm^3/gm)	Rf	SUSP GW Trigger (Ci/treach)	SUSP Int Trigger (Ci/treach)
Sr-89	1.[illegible]e-01	8.7e-06	5.01e+00	10	51	>1E20	>1E20
Sr-90	2.[illegible]e-01	1.3e-04	2.42e-02	10	51	3.0e+00	9.8e-05
Sr-91	1.0[illegible]e-03	3.0e-06	6.41e+02	10	51	>1E20	>1E20
Sr-92	3.0[illegible]e-04	1.9e-06	2.24e+03	10	51	>1E20	>1E20
Y-86m	9.13e-05	2.4e-07	7.60e+03	10	51	>1E20	>1E20
Y-86	1.67e-03	4.1e-06	4.16e+02	10	51	>1E20	>1E20
Y-87	9.13e-03	2.2e-06	7.60e+01	10	51	>1E20	>1E20
Y-88	2.88e-01	5.2e-06	2.41e+00	10	51	>1E20	>1E20
Y-90m	3.64e-04	6.6e-07	1.90e+03	10	51	>1E20	>1E20
Y-90	2.86e+01	1.0e-05	2.42e-02	10	51	3.9e+01	9.8e-05
Y-91m	9.51e-05	3.9e-08	7.29e+03	10	51	>1E20	>1E20
Y-91	1.67e-01	8.9e-06	4.15e+00	10	51	>1E20	>1E20
Y-92	4.03e-04	1.9e-06	1.72e+03	10	51	>1E20	>1E20
Y-93	1.16e-03	4.5e-06	5.96e+02	10	51	>1E20	>1E20
Y-94	3.61e-05	1.8e-07	1.92e+04	10	51	>1E20	>1E20
Y-95	2.00e-05	9.7e-08	3.47e+04	10	51	>1E20	>1E20
Zr-86	1.88e-03	3.5e-06	3.68e+02	0	1	>1E20	>1E20
Zr-88	2.33e-01	1.3e-06	2.98e+00	0	1	3.6e+04	>1E20
Zr-89	8.94e-03	3.1e-06	7.75e+01	0	1	>1E20	>1E20
Zr-93	1.50e+06	1.6e-06	4.62e-07	0	1	9.9e-03	8.6e-06
Zr-95	1.75e-01	3.4e-06	3.96e+00	0	1	1.8e+06	>1E20
Zr-97	1.92e-03	8.0e-06	3.62e+02	0	1	>1E20	>1E20
Nb-88	2.66e-05	7.2e-08	2.60e+04	0	1	>1E20	>1E20
Nb-89(66m)	1.25e-04	4.6e-07	5.52e+03	0	1	>1E20	>1E20
Nb-89(122m)	2.32e-04	1.0e-06	2.99e+03	0	1	>1E20	>1E20
Nb-90	1.67e-03	4.9e-06	4.16e+02	0	1	>1E20	>1E20
Nb-93m	1.01e+01	5.3e-07	6.84e-02	0	1	4.2e-02	8.1e-03
Nb-94	2.00e+04	5.1e-06	3.47e-05	0	1	3.1e-03	8.7e-06
Nb-95m	9.88e-03	2.0e-06	7.02e+01	0	1	>1E20	>1E20
Nb-95	9.58e-02	2.2e-06	7.23e+00	0	1	3.7e+13	>1E20
Nb-96	2.67e-03	4.4e-06	2.60e+02	0	1	>1E20	>1E20
Nb-97	1.40e-04	2.3e-07	4.95e+03	0	1	>1E20	>1E20
Nb-98	8.87e-08	3.4e-07	7.81e+06	0	1	>1E20	>1E20
Mo-90	6.50e-04	2.5e-06	1.07e+03	0	1	>1E20	>1E20

Table C.3-1. (continued)

Nuclide	T1/2 (years)	DCF (mrem/pCi)	Lambda (1/year)	Kd (cm^3/g)	Rf	SUSP GW Trigger (Curies/cm)	SUSP for Trigger (Curies/cm)
Mo-91m	7.87e-04	1.1e-06	8.81e+02	0	1	>1E20	>1E20
Mo-93	3.50e+01	1.3e-06	1.98e-04	0	1	1.2e-02	8.6e-06
Mo-99	7.52e-03	4.1e-06	9.20e+01	0	1	>1E20	>1E20
Mo-101	2.73e-05	9.2e-03	2.50e+04	0	1	>1E20	>1E20
Tc-93m	8.18e-05	7.1e-03	8.48e+03	0.36	2.8	>1E20	>1E20
Tc-93	3.08e-04	1.6e-07	2.25e+03	0.36	2.8	>1E20	>1E20
Tc-94m	1.01e-04	2.5e-07	6.88e+03	0.36	2.8	>1E20	>1E20
Tc-94	5.57e-04	5.8e-07	1.24e+03	0.36	2.8	>1E20	>1E20
Tc-96m	9.89e-05	3.1e-08	7.01e+03	0.36	2.8	>1E20	>1E20
Tc-96	1.18e-02	2.7e-06	5.89e+01	0.36	2.8	>1E20	>1E20
Tc-97m	2.46e-01	1.1e-06	2.81e+00	0.36	2.8	5.1e+15	>1E20
Tc-97	2.60e+06	1.5e-07	2.67e-07	0.36	2.8	2.9e-01	8.6e-06
Tc-98	1.50e+06	4.8e-06	4.62e-07	0.36	2.8	9.2e-03	8.6e-06
Tc-99m	6.87e-04	6.0e-08	1.01e+03	0.36	2.8	>1E20	>1E20
Tc-99	2.11e+05	1.3e-06	3.29e-06	0.36	2.8	3.4e-02	8.6e-06
Tc-101	2.70e-05	3.8e-08	2.57e+04	0.36	2.8	>1E20	>1E20
Tc-104	3.42e-05	1.6e-07	2.03e+04	0.36	2.8	>1E20	>1E20
Ru-94	1.08e-04	3.3e-07	6.40e+03	100	501	>1E20	>1E20
Ru-97	7.91e-03	6.4e-07	8.76e+01	100	501	>1E20	>1E20
Ru-103	1.08e-01	2.7e-06	6.43e+00	100	501	>1E20	>1E20
Ru-105	5.07e-04	1.0e-06	1.37e+03	100	501	>1E20	>1E20
Ru-106	9.99e-01	2.1e-05	6.94e-01	100	501	>1E20	>1E20
Rh-99m	5.36e-04	2.8e-07	1.29e+03	0	1	>1E20	>1E20
Rh-99	4.38e-02	2.0e-06	1.58e+01	0	1	>1E20	>1E20
Rh-100	2.28e-03	3.1e-06	3.04e+02	0	1	>1E20	>1E20
Rh-101m	1.23e-02	8.8e-07	5.63e+01	0	1	>1E20	>1E20
Rh-101	3.10e+00	2.3e-06	2.24e-01	0	1	2.1e-02	4.4e+04
Rh-102m	2.90e+00	3.5e-06	2.39e-01	0	1	1.5e-02	2.1e+05
Rh-102	5.75e-01	5.5e-06	1.21e+00	0	1	1.2e+00	>1E20
Rh-103m	1.06e-04	0.00000001	6.51e+03	0	1	>1E20	>1E20
Rh-105	4.05e-03	1.4e-06	1.71e+02	0	1	>1E20	>1E20
Rh-106m	2.49e-04	6.1e-07	2.79e+03	0	1	>1E20	>1E20
Rh-107	4.13e-05	5.4e-08	1.68e+04	0	1	>1E20	>1E20
Pd-100	1.10e-02	3.8e-06	6.33e+01	0	1	>1E20	>1E20

Table C3-1. (continued)

Nuclide	T1/2 (years)	DCF (mrem/pCi)	Lambda (1/year)	Xd (cm**3/gm)	Rf	SUSP GW Tolerance (Ci/cubic m)	SUSP Int Tolerance (Ci/cubic m)
Pd-101	9.52e-04	3.3e-07	7.23e+02	0	1	>1E20	>1E20
Pd-103	4.65e-02	6.9e-07	1.49e+01	0	1	>1E20	>1E20
Pd-107	6.50e+06	1.4e-07	1.07e-07	0	1	1.1e-01	8.6e-06
Pd-109	1.53e-03	2.1e-06	4.53e+02	0	1	>1E20	>1E20
Ag-102	2.85e-05	7.9e-08	2.43e+04	10	51	>1E20	>1E20
Ag-103	1.25e-04	1.4e-07	5.52e+03	10	51	>1E20	>1E20
Ag-104m	5.70e-05	1.5e-07	1.22e+04	10	51	>1E20	>1E20
Ag-104	1.27e-04	2.3e-07	5.44e+03	10	51	>1E20	>1E20
Ag-105	1.10e-01	1.9e-06	6.33e+00	10	51	>1E20	>1E20
Ag-106m	2.27e-02	6.1e-06	3.05e+01	10	51	>1E20	>1E20
Ag-106	4.56e-05	7.6e-08	1.52e+04	10	51	>1E20	>1E20
Ag-108m	1.30e+02	7.5e-06	5.33e-03	10	51	4.2e-01	1.5e-05
Ag-110m	6.90e-01	1.1e-05	1.00e+00	10	51	>1E20	>1E20
Ag-111	2.05e-02	4.5e-06	3.39e+01	10	51	>1E20	>1E20
Ag-112	3.57e-04	1.6e-06	1.94e+03	10	51	>1E20	>1E20
Ag-115	3.99e-05	1.5e-07	1.74e+04	10	51	>1E20	>1E20
Cd-104	1.08e-04	2.3e-07	6.40e+03	8	41	>1E20	>1E20
Cd-107	7.42e-04	2.4e-07	9.35e+02	8	41	>1E20	>1E20
Cd-109	1.24e+00	1.2e-05	5.59e-01	8	41	>1E20	>1E20
Cd-113m	1.46e+01	1.5e-04	4.75e-02	8	41	7.3e+01	1.0e-03
Cd-113	9.30e+15	1.6e-04	7.45e-17	8	41	4.0e-03	8.6e-06
Cd-115m	1.36e-01	1.5e-05	5.11e+00	8	41	>1E20	>1E20
Cd-115	6.10e-03	4.7e-06	1.14e+02	8	41	>1E20	>1E20
Cd-117m	3.88e-04	1.1e-06	1.79e+03	8	41	>1E20	>1E20
Cd-117	2.97e-04	1.1e-06	2.34e+03	8	41	>1E20	>1E20
In-109	4.91e-04	2.7e-07	1.41e+03	0	1	>1E20	>1E20
In-110(69m)	1.27e-04	3.3e-07	5.44e+03	0	1	>1E20	>1E20
In-111	7.69e-03	1.2e-06	9.01e+01	0	1	>1E20	>1E20
In-112	2.66e-05	0.00000002	2.60e+04	0	1	>1E20	>1E20
In-113m	1.89e-04	1.0e-07	3.66e+03	0	1	>1E20	>1E20
In-114m	1.36e-01	0.000015	5.11e+00	0	1	1.3e+08	>1E20
In-115m	5.13e-04	3.4e-07	1.35e+03	0	1	>1E20	>1E20
In-115	4.60e+15	1.4e-04	1.51e-16	0	1	1.1e-04	8.6e-06
In-116m	1.03e-04	2.1e-07	6.73e+03	0	1	>1E20	>1E20

Table C.3-1. (continued)

Nuclide	T1/2 (yrs)	DCF (mrem/pCi)	Lambda (1/year)	Kd (cm^3/gm)	Rf	SUSP C/W Trigger (Ci/trench)	SUSP Int Trigger (Ci/trench)
In-117m	2.21e-03	4.2e-07	3.13e+03	0	1	>1E20	>1E20
In-117	8.37e-05	8.7e-08	8.29e+03	0	1	>1E20	>1E20
In-119m	3.42e-05	1.0e-07	2.02e+04	0	1	>1E20	>1E20
Sn-110	4.56e-04	1.5e-06	1.52e+03	130	651	>1E20	>1E20
Sn-111	6.65e-05	6.7e-08	1.04e+04	130	651	>1E20	>1E20
Sn-113	3.15e-01	2.7e-06	2.20e+00	130	651	>1E20	>1E20
Sn-117m	3.83e-02	2.6e-06	1.81e+01	130	651	>1E20	>1E20
Sn-119m	8.02e-01	1.2e-05	8.64e-01	130	651	>1E20	>1E20
Sn-121m	7.60e+01	1.3e-06	9.12e-03	130	651	6.2e+13	2.2e-05
Sn-121	3.08e-03	8.9e-07	2.25e+02	130	651	>1E20	>1E20
Sn-123m	7.61e-05	1.0e-07	9.11e+03	130	651	>1E20	>1E20
Sn-123	3.53e-01	7.7e-06	1.96e+00	130	651	>1E20	>1E20
Sn-125	2.64e-02	1.1e-05	2.62e+01	130	651	>1E20	>1E20
Sn-126	1.00e+05	1.7e-05	6.93e-06	130	651	6.2e-01	8.6e-06
Sn-127	2.42e-04	7.4e-07	2.87e+03	130	651	>1E20	>1E20
Sn-128	1.12e-04	5.2e-07	6.18e+03	130	651	>1E20	>1E20
Sb-115	5.89e-05	6.3e-08	1.18e+04	10	51	>1E20	>1E20
Sb-116m	1.14e-04	2.4e-07	6.08e+03	10	51	>1E20	>1E20
Sb-116	2.85e-05	5.6e-08	2.43e+04	10	51	>1E20	>1E20
Sb-117	3.19e-04	7.4e-08	2.17e+03	10	51	>1E20	>1E20
Sb-118m	5.82e-04	9.3e-07	1.19e+03	10	51	>1E20	>1E20
Sb-119	4.33e-03	3.4e-07	1.60e+02	10	51	>1E20	>1E20
Sb-120(16m)	3.04e-05	3.0e-08	2.28e+04	10	51	>1E20	>1E20
Sb-120(6d)	1.59e-02	5.4e-06	4.37e+01	10	51	>1E20	>1E20
Sb-122	7.45e-03	6.3e-06	9.31e+01	10	51	>1E20	>1E20
Sb-124m	1.77e-04	2.0e-08	3.92e+03	10	51	>1E20	>1E20
Sb-124	1.65e-01	9.3e-06	4.20e+00	10	51	>1E20	>1E20
Sb-125	2.40e+00	2.6e-06	2.89e-01	10	51	>1E20	3.0e+07
Sb-126m	3.61e-05	7.3e-08	1.92e+04	10	51	>1E20	>1E20
Sb-126	3.39e-02	9.6e-06	2.04e+01	10	51	>1E20	>1E20
Sb-127	1.04e-02	6.6e-06	6.66e+01	10	51	>1E20	>1E20
Sb-128(9h)	1.03e-03	4.3e-06	6.75e+02	10	51	>1E20	>1E20
Sb-128(10m)	1.90e-05	5.0e-08	3.65e+04	10	51	>1E20	>1E20
Sb-129	4.95e-04	1.7e-06	1.40e+03	10	51	>1E20	>1E20

Table C3-1. (continued)

Nuclide	T1/2 (years)	DCF (mrem/pCi)	Lambda (1/year)	Kd (cm³/g)	Rf	SUSP OW Trigger (Ci/trench)	SUSP Int Trigger (Ci/trench)
Sb-130	1.25e-03	2.6e-07	5.5[illegible]e+04	10	51	>1E20	>1E20
Sb-131	4.37e-05	2.9e-07	1.59e+04	10	51	>1E20	>1E20
Te-113	1.64e-02	6.7e-07	4.22e+01	0	1	>1E20	>1E20
Te-121m	4.11e-01	6.7e-06	1.69e+00	0	1	1.1e+01	>1E20
Te-121	4.65e-02	1.5e-06	1.49e+01	0	1	>1E20	>1E20
Te-123m	3.28e-01	5.1e-06	2.12e+00	0	1	1.2e+02	>1E20
Te-123	1.20e+13	4.1e-06	5.78e-14	0	1	3.8e-03	8.6e-06
Te-125m	1.59e-01	3.4e-06	4.37e+00	0	1	1.4e+07	>1E20
Te-127m	2.98e-01	7.9e-06	2.32e+00	0	1	2.2e+02	>1E20
Te-127	1.07e-03	6.9e-07	6.46e+02	0	1	>1E20	>1E20
Te-129m	9.14e-02	9.9e-06	7.58e+00	0	1	4.6e+13	>1E20
Te-129	1.33e-04	1.9e-07	5.21e+03	0	1	>1E20	>1E20
Te-131m	3.42e-03	1.5e-05	2.03e+02	0	1	>1E20	>1E20
Te-131	4.75e-05	2.0e-07	1.46e+04	0	1	>1E20	>1E20
Te-132	8.76e-03	7.4e-06	7.91e+01	0	1	>1E20	>1E20
Te-133m	1.05e-04	7.6e-07	6.58e+03	0	1	>1E20	>1E20
Te-133	2.38e-05	1.6e-07	2.92e+04	0	1	>1E20	>1E20
Te-134	7.99e-05	2.1e-07	8.68e+03	0	1	>1E20	>1E20
I-120m	1.01e-04	3.9e-07	6.88e+03	0.6	4	>1E20	>1E20
I-120	1.48e-04	6.7e-07	4.67e+03	0.6	4	>1E20	>1E20
I-121	2.40e-04	1.8e-07	2.89e+03	0.6	4	>1E20	>1E20
I-123	1.52e-03	4.9e-07	4.57e+02	0.6	4	>1E20	>1E20
I-124	1.15e-02	3.1e-05	6.03e+01	0.6	4	>1E20	>1E20
I-125	1.64e-01	3.8e-05	4.22e+00	0.6	4	>1E20	>1E20
I-126	3.64e-02	7.1e-05	1.90e+01	0.6	4	>1E20	>1E20
I-128	4.75e-05	8.5e-08	1.46e+04	0.6	4	>1E20	>1E20
I-129	1.72e+07	2.8e-04	4.02e-08	0.6	4	2.3e-04	8.6e-06
I-130	1.41e-03	4.3e-06	4.90e+02	0.6	4	>1E20	>1E20
I-131	2.22e-02	5.3e-05	3.13e+01	0.6	4	>1E20	>1E20
I-132m	1.58e-04	4.7e-07	4.39e+03	0.6	4	>1E20	>1E20
I-132	2.60e-04	3.3e-07	2.66e+03	0.6	4	>1E20	>1E20
I-133	2.37e-03	5.4e-06	2.92e+02	0.6	4	>1E20	>1E20
I-134	1.00e-04	1.9e-07	6.93e+03	0.6	4	>1E20	>1E20
I-135	7.51e-04	2.0e-05	9.23e+02	0.6	4	>1E20	>1E20

Table C.3-1. (continued)

Nuclide	T1/2 (years)	DCF (mrem/pCi)	Landfill (L/year)	Kd (cm^3/gm)	Rf	SUSP GW Trigger (Ci/trench)	SUSP Int Trigger (Ci/trench)
Cs-125	8.56e-05	5.5e-08	8.10e+03	100	501	>1E20	>1E20
Cs-127	7.07e-04	8.0e-08	9.80e+02	100	501	>1E20	>1E20
Cs-129	3.65e-03	2.2e-07	1.90e+02	100	501	>1E20	>1E20
Cs-130	5.70e-05	4.9e-08	1.22e+04	100	501	>1E20	>1E20
Cs-131	2.66e-02	2.4e-07	2.61e+01	100	501	>1E20	>1E20
Cs-132	1.80e-02	1.9e-06	3.85e+01	100	501	>1E20	>1E20
Cs-134m	3.31e-04	4.2e-08	2.10e+03	100	501	>1E20	>1E20
Cs-134	2.06e+00	7.4e-05	3.36e-01	100	501	>1E20	3.5e+09
Cs-135m	1.01e-04	4.9e-08	6.88e+03	100	501	>1E20	>1E20
Cs-135	2.30e+06	7.1e-06	3.01e-07	100	501	1.1e+00	8.6e-06
Cs-136	3.53e-02	1.1e-05	1.96e+01	100	501	>1E20	>1E20
Cs-137	3.01e+01	5.0e-05	2.30e-02	100	501	>1E20	8.6e-05
Cs-138	6.12e-05	1.6e-07	1.13e+04	100	501	>1E20	>1E20
Ba-126	1.84e-04	9.0e-07	3.76e+03	5	26	>1E20	>1E20
Ba-128	6.57e-03	1.0e-05	1.05e+02	5	26	>1E20	>1E20
Ba-131m	2.78e-05	9.7e-07	2.50e+04	5	26	>1E20	>1E20
Ba-131	3.20e-02	1.6e-06	2.16e+01	5	26	>1E20	>1E20
Ba-133m	4.44e-03	2.0e-06	1.56e+02	5	26	>1E20	>1E20
Ba-133	1.07e+01	3.2e-06	6.48e-02	5	26	5.8e+02	5.6e-03
Ba-135m	3.27e-03	1.6e-06	2.12e+02	5	26	>1E20	>1E20
Ba-137m	0.000005		1.43e+05	5	26	>1E20	>1E20
Ba-139	1.58e-04	3.9e-07	4.38e+03	5	26	>1E20	>1E20
Ba-140	3.50e-02	8.4e-06	1.98e+01	5	26	>1E20	>1E20
Ba-141	3.48e-05	2.0e-07	1.99e+04	5	26	>1E20	>1E20
Ba-142	2.03e-05	1.0e-07	3.41e+04	5	26	>1E20	>1E20
La-131	1.12e-04	1.1e-07	6.18e+03	100	501	>1E20	>1E20
La-132	5.13e-04	1.5e-06	1.35e+03	100	501	>1E20	>1E20
La-135	2.22e-03	1.3e-07	3.12e+02	100	501	>1E20	>1E20
La-137	6.00e+04	4.3e-07	1.16e-05	100	501	1.9e+01	8.6e-06
La-138	1.06e+11	5.9e-06	6.54e-12	100	501	1.3e+00	8.6e-06
La-140	4.59e-03	7.7e-06	1.51e+02	100	501	>1E20	>1E20
La-141	4.41e-04	1.4e-06	1.57e+03	100	501	>1E20	>1E20
La-142	1.76e-04	8.3e-07	3.95e+03	100	501	>1E20	>1E20
La-143	2.66e-05	1.4e-07	2.60e+04	100	501	>1E20	>1E20

Table C3-1. (continued)

Nuclide	T1/2 (years)	DCF (mrem/pCi)	Lambda (1/year)	Kd (cm**3/gm)	Rf	SUSP GW Trigger (Ci/trench)	SUSP Int Trigger (Ci/trench)
Ce-134	8.21e-05	8.5e-06	8.44e+01	10	51	>1E20	>1E20
Ce-135	1.96e-03	3.2e-06	3.53e+02	10	51	>1E20	>1E20
Ce-137m	3.92e-03	2.0e-06	1.77e+02	10	51	>1E20	>1E20
Ce-137	1.03e-03	9.8e-08	6.75e+02	10	51	>1E20	>1E20
Ce-139	3.77e-01	1.1e-06	1.84e+00	10	51	>1E20	>1E20
Ce-141	8.90e-02	2.6e-06	7.79e+00	10	51	>1E20	>1E20
Ce-143	3.76e-03	4.2e-06	1.84e+02	10	51	>1E20	>1E20
Ce-144	7.94e-01	2.0e-05	8.73e-01	10	51	>1E20	>1E20
Pr-136	1.25e-04	6.8e-08	5.52e+03	10	51	>1E20	>1E20
Pr-137	1.71e-04	1.3e-07	4.05e+03	100	501	>1E20	>1E20
Pr-138m	2.40e-04	4.9e-07	2.89e+03	100	501	>1E20	>1E20
Pr-139	5.13e-04	1.2e-07	1.35e+03	100	501	>1E20	>1E20
Pr-142m	2.72e-05	6.3e-08	2.55e+04	100	501	>1E20	>1E20
Pr-142	2.18e-03	5.1e-06	3.18e+02	100	501	>1E20	>1E20
Pr-143	3.75e-02	4.5e-06	1.85e+01	100	501	>1E20	>1E20
Pr-144	3.29e-05	1.1e-07	2.11e+04	100	501	>1E20	>1E20
Pr-145	6.82e-04	1.5e-06	1.02e+03	100	501	>1E20	>1E20
Pr-147	2.28e-05	5.7e-08	3.04e+04	100	501	>1E20	>1E20
Nd-136	9.64e-05	3.3e-07	7.19e+03	100	501	>1E20	>1E20
Nd-138	4.18e-05	2.5e-06	1.66e+04	100	501	>1E20	>1E20
Nd-139m	6.27e-04	1.0e-06	1.10e+03	100	501	>1E20	>1E20
Nd-139	5.93e-04	5.7e-08	1.17e+03	100	501	>1E20	>1E20
Nd-141	2.85e-04	3.2e-08	2.43e+03	100	501	>1E20	>1E20
Nd-147	3.01e-02	3.9e-06	2.30e+01	100	501	>1E20	>1E20
Nd-149	1.97e-03	4.6e-07	3.51e+02	100	501	>1E20	>1E20
Nd-151	2.36e-05	7.4e-08	2.94e+04	100	501	>1E20	>1E20
Pm-141	4.18e-05	8.4e-08	1.66e+04	100	501	>1E20	>1E20
Pm-143	7.26e-01	9.5e-07	9.55e-01	100	501	>1E20	>1E20
Pm-144	8.22e-01	3.9e-06	8.43e-01	100	501	>1E20	>1E20
Pm-145	1.77e+01	4.6e-07	3.92e-02	100	501	>1E20	4.3e-04
Pm-146	1.94e+00	3.2e-06	3.57e-01	100	501	>1E20	2.6e+10
Pm-147	2.52e+00	9.5e-07	2.75e-01	100	501	>1E20	7.7e+06
Pm-148m	1.14e-01	7.0e-06	6.06e+00	100	501	>1E20	>1E20
Pm-148	1.47e-02	9.5e-06	4.71e+01	100	501	>1E20	>1E20

Table C3-1. (continued)

Nuclide	T1/2 (years)	DCF (mrem/pCi)	Lambda (1/year)	Xd (mrem/J/gm)	Rf	SUSP GW Trigger (Ci/mrem/h)	SUSP Air Trigger (Ci/mrem/h)
Pm-149	6.06e-02	3.6e-05	1.14e+02	100	501	>1E20	>1E20
Pm-150	3.06e-04	9.2e-07	2.27e+03	100	501	>1E20	>1E20
Pm-151	3.24e-03	2.8e-06	2.14e+02	100	501	>1E20	>1E20
Sm-141m	4.30e-05	1.8e-07	1.61e+04	100	501	>1E20	>1E20
Sm-141	1.94e-05	8.4e-08	3.57e+04	100	501	>1E20	>1E20
Sm-142	1.37e-04	6.0e-07	5.06e+03	100	501	>1E20	>1E20
Sm-145	9.31e-01	8.5e-07	7.45e-01	100	501	>1E20	>1E20
Sm-146	7.00e+07	2.0e-04	9.90e-09	100	501	4.0e-02	8.6e-06
Sm-147	1.06e+11	1.8e-04	6.54e-12	100	501	4.4e-02	8.6e-06
Sm-151	9.00e+01	3.4e-07	7.70e-03	100	501	5.6e+09	1.9e-05
Sm-153	5.33e-03	2.6e-06	1.30e+02	100	501	>1E20	>1E20
Sm-155	4.22e-05	6.6e-08	1.64e+04	100	501	>1E20	>1E20
Sm-158	8.37e-05	1.0e-06	8.29e+03	100	501	>1E20	>1E20
Eu-145	1.62e-02	3.2e-05	4.29e+01	100	501	>1E20	>1E20
Eu-146	1.26e-02	5.1e-06	5.50e+01	100	501	>1E20	>1E20
Eu-147	6.02e-02	1.8e-06	1.15e+01	100	501	>1E20	>1E20
Eu-148	1.48e-01	5.2e-06	4.69e+00	100	501	>1E20	>1E20
Eu-149	2.90e-01	4.2e-07	2.39e+00	100	501	>1E20	>1E20
Eu-150(12h)	1.37e-03	1.5e-06	5.06e+02	100	501	>1E20	>1E20
Eu-150(34y)	3.40e+01	6.2e-06	2.04e-02	100	501	>1E20	6.6e-05
Eu-152m	1.07e-03	1.9e-06	6.51e+02	100	501	>1E20	>1E20
Eu-152	1.34e+01	6.0e-06	5.17e-02	100	501	>1E20	1.5e-03
Eu-154	8.20e+00	9.1e-06	8.45e-02	100	501	>1E20	4.1e-02
Eu-155	1.70e+00	1.3e-06	4.08e-01	100	501	>1E20	>1E20
Eu-156	4.22e-02	8.7e-06	1.64e+01	100	501	>1E20	>1E20
Eu-157	1.73e-03	2.3e-06	4.00e+02	100	501	>1E20	>1E20
Eu-158	8.73e-05	2.6e-07	7.94e+03	100	501	>1E20	>1E20
Gd-145	4.75e-05	1.1e-07	1.46e+04	100	501	>1E20	>1E20
Gd-146	1.26e-02	3.8e-06	5.50e+01	100	501	>1E20	>1E20
Gd-147	3.99e-03	2.6e-06	1.74e+02	100	501	>1E20	>1E20
Gd-148	1.30e+02	2.1e-04	5.33e-03	100	501	2.4e+04	1.5e-05
Gd-149	2.46e-02	1.8e-06	2.81e+01	100	501	>1E20	>1E20
Gd-151	3.29e-01	7.7e-07	2.11e+00	100	501	>1E20	>1E20
Gd-152	1.10e+14	1.5e-04	6.30e-15	100	501	5.3e-02	8.6e-06

Table C.3-1. (continued)

Nuclide	T1/2 (year)	DCF (mrem/µCi)	Lambda (1/year)	Kd (cm**3/gm)	Rf	SUSP GW Trigger (Cy/month)	SUSP Int Trigger (Cy/month)
Gd-[illegible]	6.6[illegible]-01	1.1[illegible]-06	1.05e+00	100	501	>1E20	>1E20
Gd-159	2.12e-03	1.9[illegible]-06	3.27e+02	100	501	>1E20	>1E20
Tb-147	4.56e-05	5.6e-07	1.52e+04	100	501	>1E20	>1E20
Tb-149	4.68e-04	9.5e-07	1.48e+03	100	501	>1E20	>1E20
Tb-150	3.54e-04	9.7e-07	1.96e+03	100	501	>1E20	>1E20
Tb-151	2.05e-03	1.4e-06	3.38e+02	100	501	>1E20	>1E20
Tb-153	6.27e-03	9.9e-07	1.10e+02	100	501	>1E20	>1E20
Tb-154	9.70e-04	2.8e-06	7.15e+02	100	501	>1E20	>1E20
Tb-155	1.53e-02	8.2e-07	4.52e+01	100	501	>1E20	>1E20
Tb-156m(24h)	2.74e-03	7.0e-07	2.53e+02	100	501	>1E20	>1E20
Tb-156m(5h)	6.27e-04	3.2e-07	1.10e+03	100	501	>1E20	>1E20
Tb-156	1.48e-02	4.6e-06	4.69e+01	100	501	>1E20	>1E20
Tb-157	1.50e+02	1.0e-07	4.62e-03	100	501	8.4e+06	1.4e-05
Tb-158	1.20e+03	4.0e-06	5.78e-04	100	501	8.4e+00	9.2e-06
Tb-160	1.98e-01	6.4e-06	3.50e+00	100	501	>1E20	>1E20
Tb-161	1.88e-02	2.6e-06	3.68e+01	100	501	>1E20	>1E20
Dy-155	1.20e-03	5.6e-07	5.79e+02	100	501	>1E20	>1E20
Dy-157	9.24e-04	2.7e-07	7.50e+02	100	501	>1E20	>1E20
Dy-159	3.94e-01	4.0e-07	1.76e+00	100	501	>1E20	>1E20
Dy-165	2.66e-04	3.6e-07	2.61e+03	100	501	>1E20	>1E20
Dy-166	9.31e-03	6.2e-06	7.45e+01	100	501	>1E20	>1E20
Ho-155	9.51e-05	1.2e-07	7.29e+03	100	501	>1E20	>1E20
Ho-157	2.66e-05	1.9e-08	2.60e+04	100	501	>1E20	>1E20
Ho-159	6.27e-05	2.3e-08	1.10e+04	100	501	>1E20	>1E20
Ho-161	2.85e-04	4.7e-08	2.43e+03	100	501	>1E20	>1E20
Ho-162m	1.29e-04	9.0e-08	5.36e+03	100	501	>1E20	>1E20
Ho-162	2.85e-05	6.7e-09	2.43e+04	100	501	>1E20	>1E20
Ho-164m	7.13e-05	4.9e-08	9.72e+03	100	501	>1E20	>1E20
Ho-164	7.03e-05	2.4e-08	9.85e+03	100	501	>1E20	>1E20
Ho-166m	1.20e+03	7.8e-06	5.78e-04	100	501	4.3e+00	9.2e-06
Ho-166	3.06e-03	5.5e-06	2.27e+02	100	501	>1E20	>1E20
Ho-167	3.54e-04	3.2e-07	1.96e+03	100	501	>1E20	>1E20
Er-161	3.54e-04	3.3e-07	1.96e+03	100	501	>1E20	>1E20
Er-165	1.18e-03	7.9e-08	5.86e+02	100	501	>1E20	>1E20

Table C3-1. (continued)

Nuclide	T1/2 (years)	DCF (mrem/pCi)	Lambda (1/year)	Kd (cm^3/gm)	Rf	SUSP GW Trigger (Ci/trench)	SUSP Int Trigger (Ci/trench)
Er-169	2.57e-02	1.4e-06	2.[illegible]e+01	100	501	>1E20	>1E20
Er-171	8.58e-01	1.4e-06	8.03e+02	100	501	>1E20	>1E20
Er-172	5.59e-03	3.7e-06	1.21e+02	100	501	>1E20	>1E20
Tm-162	1.46e-04	7.0e-08	4.73e+03	100	501	>1E20	>1E20
Tm-166	8.78e-04	1.2e-06	7.89e+02	100	501	>1E20	>1E20
Tm-167	2.63e-02	2.1e-06	2.64e+01	100	501	>1E20	>1E20
Tm-170	3.53e-01	5.0e-06	1.96e+00	100	501	>1E20	>1E20
Tm-171	1.92e+00	3.9e-07	3.61e-01	100	501	>1E20	4.1e+10
Tm-172	7.26e-03	6.0e-06	9.55e+01	100	501	>1E20	>1E20
Tm-173	9.35e-04	1.2e-06	7.41e+02	100	501	>1E20	>1E20
Tm-175	3.80e-05	5.4e-08	1.82e+04	100	501	>1E20	>1E20
Yb-162	3.59e-05	7.0e-08	1.93e+04	100	501	>1E20	>1E20
Yb-165	1.90e-05	3.8e-06	3.65e+04	100	501	>1E20	>1E20
Yb-167	3.42e-05	1.7e-08	2.03e+04	100	501	>1E20	>1E20
Yb-169	8.76e-02	2.8e-06	7.91e+00	100	501	>1E20	>1E20
Yb-175	1.15e-02	1.6e-06	6.04e+01	100	501	>1E20	>1E20
Yb-177	2.17e-04	3.1e-07	3.20e+03	100	501	>1E20	>1E20
Yb-178	1.40e-04	3.9e-07	4.94e+03	100	501	>1E20	>1E20
Lu-169	3.88e-03	2.0e-06	1.79e+02	100	501	>1E20	>1E20
Lu-170	5.48e-03	4.3e-06	1.27e+02	100	501	>1E20	>1E20
Lu-171	2.27e-02	2.6e-06	3.05e+01	100	501	>1E20	>1E20
Lu-172	1.83e-02	5.0e-06	3.78e+01	100	501	>1E20	>1E20
Lu-173	1.37e+00	9.7e-07	5.06e-01	100	501	>1E20	>1E20
Lu-174m	3.83e-01	1.8e-06	1.81e+00	100	501	>1E20	>1E20
Lu-174	3.60e+00	9.9e-07	1.93e-01	100	501	>1E20	2.0e+03
Lu-176m	4.21e-04	6.3e-07	1.65e+03	100	501	>1E20	>1E20
Lu-176	3.00e+10	6.6e-06	2.31e-11	100	501	1.2e+00	8.6e-06
Lu-177m	4.41e-02	6.8e-06	1.57e+01	100	501	>1E20	>1E20
Lu-177	1.84e-02	2.0e-06	3.77e+01	100	501	>1E20	>1E20
Lu-178m	3.80e-05	8.8e-08	1.82e+04	100	501	>1E20	>1E20
Lu-178	5.70e-05	1.2e-07	1.22e+04	100	501	>1E20	>1E20
Lu-179	5.25e-04	8.1e-07	1.32e+03	100	501	>1E20	>1E20
Hf-170	1.39e-03	1.2e-05	4.98e+02	100	501	>1E20	>1E20
Hf-172	5.00e+00	4.1e-06	1.39e-01	100	501	>1E20	9.1e+00

Table C3-1. (continued)

Nuclide	T1/2 (years)	DCF (mrem/pCi)	Lambda (1/year)	Kd (cm^3/gm)	Rf	SUSP GW Trigger (Ci/trench)	SUSP Int Trigger (Ci/trench)
Hf-175	2.69e-03	9.5e-07	2.57e+02	100	501	>1E20	>1E20
Hf-175	1.92e-01	1.6e-06	3.62e+00	100	501	>1E20	>1E20
Hf-177m	9.77e-05	2.5e-07	7.09e+03	100	501	>1E20	>1E20
Hf-178m	3.10e+01	2.0e-05	2.24e-02	100	501	>1E20	8.1e-05
Hf-179m	6.87e-02	4.8e-06	1.01e+01	100	501	>1E20	>1E20
Hf-180m	6.27e-04	8.9e-07	1.10e+03	100	501	>1E20	>1E20
Hf-181	1.16e-01	4.3e-06	5.97e+00	100	501	>1E20	>1E20
Hf-182m	1.18e-04	1.4e-07	5.88e+03	100	501	>1E20	>1E20
Hf-182	9.00e+06	1.4e-05	7.70e-08	100	501	5.6e-01	8.6e-06
Hf-183	1.25e-04	2.5e-07	5.52e+03	100	501	>1E20	>1E20
Hf-184	4.68e-04	2.1e-06	1.48e+03	100	501	>1E20	>1E20
Ta-172	8.37e-05	1.4e-07	8.29e+03	0	1	>1E20	>1E20
Ta-173	4.22e-04	7.4e-07	1.64e+03	0	1	>1E20	>1E20
Ta-174	1.48e-04	1.9e-07	4.67e+03	0	1	>1E20	>1E20
Ta-175	1.20e-03	8.8e-07	5.79e+02	0	1	>1E20	>1E20
Ta-176	9.13e-04	1.3e-06	7.60e+02	0	1	>1E20	>1E20
Ta-177	6.46e-03	4.1e-07	1.07e+02	0	1	>1E20	>1E20
Ta-178	1.79e-05	2.9e-07	3.88e+04	0	1	>1E20	>1E20
Ta-179	2.40e-04	2.5e-07	2.89e+03	0	1	>1E20	>1E20
Ta-180m	9.24e-04	2.1e-07	7.50e+02	0	1	>1E20	>1E20
Ta-180	1.00e+13	3.3e-06	6.93e-14	0	1	4.8e-03	8.6e-06
Ta-182m	3.02e-05	2.4e-08	2.29e+04	0	1	>1E20	>1E20
Ta-182	3.15e-01	6.0e-06	2.20e+00	0	1	1.6e+02	>1E20
Ta-183	1.40e-02	4.6e-06	4.96e+01	0	1	>1E20	>1E20
Ta-184	9.92e-04	2.7e-06	6.98e+02	0	1	>1E20	>1E20
Ta-185	9.51e-05	2.0e-07	7.29e+03	0	1	>1E20	>1E20
Ta-186	2.00e-05	6.7e-08	3.47e+04	0	1	>1E20	>1E20
W-176	2.85e-04	4.8e-07	2.43e+03	0	1	>1E20	>1E20
W-177	2.57e-04	2.4e-07	2.70e+03	0	1	>1E20	>1E20
W-178	5.89e-02	9.3e-07	1.18e+01	0	1	>1E20	>1E20
W-179	7.22e-05	9.0e-09	9.59e+03	0	1	>1E20	>1E20
W-181	3.31e-01	3.1e-07	2.09e+00	0	1	1.8e+03	>1E20
W-185	2.06e-01	1.9e-06	3.37e+00	0	1	1.7e+05	>1E20
W-187	2.73e-03	2.6e-06	2.54e+02	0	1	>1E20	>1E20

Table C.3-1. (continued)

Nuclide	T1/2 (years)	DCF (mrem/pCi)	Lambda (1/year)	Kd (cm**3/gm)	Pf	SUSP Tap (C/m-sch)	SUSP Tap (C/m-sch)
W-188	1.89e-01	9.0e-06	3.67e+00	0	1	1.0e-05	>1E20
Re-177	3.23e-05	4.4e-08	2.14e+04	0	1	>1E20	>1E20
Re-178	2.85e-05	4.8e-08	2.43e+04	0	1	>1E20	>1E20
Re-181	2.05e-03	1.0e-06	3.38e+02	0	1	>1E20	>1E20
Re-182(64h)	7.30e-03	3.4e-06	9.49e+01	0	1	>1E20	>1E20
Re-182(12h)	1.45e-03	7.4e-07	4.78e+02	0	1	>1E20	>1E20
Re-184m	4.63e-01	2.4e-06	1.50e+00	0	1	1.2e+01	>1E20
Rm-184	1.04e-02	2.2e-06	6.66e+01	0	1	>1E20	>1E20
Re-186m	2.00e+05	3.3e-06	3.47e-06	0	1	4.8e-03	8.6e-06
Re-186	1.03e-02	2.6e-06	6.71e+01	0	1	>1E20	>1E20
Re-187	7.00e+10	8.3e-09	9.90e-12	0	1	1.9e+00	8.6e-06
Re-188m	3.54e-05	6.2e-08	1.96e+04	0	1	>1E20	>1E20
Re-188	1.91e-03	2.8e-06	3.64e+02	0	1	>1E20	>1E20
Re-189	2.74e-03	1.5e-06	2.53e+02	0	1	>1E20	>1E20
Os-180	4.13e-05	4.7e-08	1.68e+04	0	1	>1E20	>1E20
Os-181	4.37e-05	3.5e-07	1.59e+04	0	1	>1E20	>1E20
Os-182	2.51e-03	2.2e-06	2.76e+02	0	1	>1E20	>1E20
Os-185	2.57e-01	2.1e-06	2.69e+00	0	1	5.3e+03	>1E20
Os-189m	6.84e-04	6.6e-08	1.01e+03	0	1	>1E20	>1E20
Os-191m	1.48e-03	3.6e-07	4.67e+02	0	1	>1E20	>1E20
Os-191	4.19e-02	2.0e-06	1.65e+01	0	1	>1E20	>1E20
Os-193	3.48e-03	3.1e-06	1.99e+02	0	1	>1E20	>1E20
Os-194	6.00e+00	9.1e-06	1.16e-01	0	1	3.1e-03	9.0e-01
Ir-182	2.85e-05	1.2e-07	2.43e+04	0	1	>1E20	>1E20
Ir-[illegible]	3.65e-04	6.4e-07	1.90e+03	0	1	>1E20	>1E20
Ir-[illegible]	1.60e-03	1.1e-06	4.34e+02	0	1	>1E20	>1E20
Ir-186	1.83e-03	2.1e-06	3.80e+02	0	1	>1E20	>1E20
Ir-187	1.20e-03	4.8e-07	5.79e+02	0	1	>1E20	>1E20
Ir-188	4.68e-03	2.7e-06	1.48e+02	0	1	>1E20	>1E20
Ir-189	3.64e-02	9.3e-07	1.90e+01	0	1	>1E20	>1E20
Ir-190m	3.65e-04	3.0e-08	1.90e+03	0	1	>1E20	>1E20
Ir-190	3.01e-02	4.9e-06	2.30e+01	0	1	>1E20	>1E20
Ir-192m	2.74e-06	1.5e-06	2.53e+05	0	1	>1E20	>1E20
Ir-192	2.03e-01	5.3e-06	3.41e+00	0	1	7.6e+04	>1E20

Table C.4-1. (continued)

Nuclide	T1/2 (years)	DCF (mrem/pCi)	Lambda (1/year)	Kd (cm³/g)	Rf	SUSP GW Trigger (Ci/mrem)	SUSP Int Trigger (Ci/mrem)
Ir-194m	4.8[illegible]-01	8.1e-06	1.42e+00	0	1	3.2e+00	>1E20
Ir-194	2.2[illegible]-03	5.1e-06	3.12e+02	0	1	>1E20	>1E20
Ir-195m	4.45e-04	6.4e-07	1.56e+03	0	1	>1E20	>1E20
Ir-195	4.79e-04	3.4e-07	1.45e+03	0	1	>1E20	>1E20
Pt-186	3.42e-04	3.7e-07	2.03e+03	0	1	>1E20	>1E20
Pt-188	2.79e-02	3.0e-06	2.48e+01	0	1	>1E20	>1E20
Pt-189	1.24e-03	4.9e-07	5.57e+02	0	1	>1E20	>1E20
Pt-191	1.24e-03	1.3e-06	5.57e+02	0	1	>1E20	>1E20
Pt-193m	1.18e-02	1.7e-06	5.89e+01	0	1	>1E20	>1E20
Pt-193	5.00e+01	1.1e-07	1.39e-02	0	1	1.5e-01	3.5e-05
Pt-195m	1.10e-02	2.2e-06	6.30e+01	0	1	>1E20	>1E20
Pt-197m	1.79e-04	3.1e-07	3.88e+03	0	1	>1E20	>1E20
Pt-197	2.09e-03	1.5e-06	3.32e+02	0	1	>1E20	>1E20
Pt-199	5.86e-05	1.0e-07	1.18e+04	0	1	>1E20	>1E20
Pt-200	1.31e-03	4.5e-06	5.28e+02	0	1	>1E20	>1E20
Au-193	1.83e-03	6.0e-07	3.80e+02	0	1	>1E20	>1E20
Au-194	4.51e-03	2.0e-06	1.54e+02	0	1	>1E20	>1E20
Au-195	5.01e-01	1.1e-06	1.38e+00	0	1	1.4e+01	>1E20
Au-198m	6.30e-03	5.7e-06	1.10e+02	0	1	>1E20	>1E20
Au-198	7.38e-03	2.3e-06	9.39e+01	0	1	>1E20	>1E20
Au-199	8.60e-03	1.8e-06	8.06e+01	0	1	>1E20	>1E20
Au-200m	2.13e-03	4.6e-06	3.25e+02	0	1	>1E20	>1E20
Au-200	9.20e-05	1.9e-07	7.53e+03	0	1	>1E20	>1E20
Au-201	4.94e-05	5.7e-08	1.40e+04	0	1	>1E20	>1E20
Hg-193m	1.14e-03	1.6e-06	6.08e+02	1000	5001	>1E20	>1E20
Hg-193	6.84e-04	3.3e-07	1.01e+03	1000	5001	>1E20	>1E20
Hg-194	1.90e+00	6.0e-06	3.65e-01	1000	5001	>1E20	6.0e+10
Hg-195m	4.56e-03	2.2e-06	1.52e+02	1000	5001	>1E20	>1E20
Hg-195	1.08e-03	3.8e-07	6.40e+02	1000	5001	>1E20	>1E20
Hg-197m	2.72e-03	1.7e-06	2.55e+02	1000	5001	>1E20	>1E20
Hg-197	7.31e-03	9.1e-07	9.48e+01	1000	5001	>1E20	>1E20
Hg-199m	8.10e-05	8.5e-08	8.56e+03	1000	5001	>1E20	>1E20
Hg-203	1.28e-01	2.1e-06	5.43e+00	1000	5001	>1E20	>1E20
Tl-194m	6.24e-05	7.1e-08	1.11e+04	0	1	>1E20	>1E20

Table C.3-1. (continued)

Nuclide	T1/2 (year)	DCF (mrem/pCi)	Lambda (1/year)	Kd (cm^3/gm)	Rf	SUSP GW Tri[illegible] (Ci/cubic m)	SU[illegible] int Tr[illegible] (Ci/cubic m)
Tl-194	6.27e-05	1.9e-08	1.10e+04	0	1	>1E20	>1E20
Tl-195	1.37e-04	7.7e-08	5.06e+03	0	1	>1E20	>1E20
Tl-197	3.19e-04	6.9e-08	2.17e+03	0	1	>1E20	>1E20
Tl-198m	2.13e-04	1.6e-07	3.25e+03	0	1	>1E20	>1E20
Tl-198	6.05e-04	2.6e-07	1.15e+03	0	1	>1E20	>1E20
Tl-199	8.44e-04	8.2e-08	8.21e+02	0	1	>1E20	>1E20
Tl-200	2.98e-03	6.7e-07	2.33e+02	0	1	>1E20	>1E20
Tl-201	8.33e-03	2.9e-07	8.32e+01	0	1	>1E20	>1E20
Tl-202	3.29e-02	1.5e-06	2.11e+01	0	1	>1E20	>1E20
Tl-204	3.77e+00	3.2e-06	1.84e-01	0	1	1.2e-02	8.3e+02
Pb-195m	2.85e-05	8.5e-08	2.43e+04	100	501	>1E20	>1E20
Pb-198	2.74e-04	1.6e-07	2.53e+03	100	501	>1E20	>1E20
Pb-199	1.71e-04	2.2e-07	4.05e+03	100	501	>1E20	>1E20
Pb-200	2.45e-03	1.5e-06	2.83e+02	100	501	>1E20	>1E20
Pb-201	1.07e-03	6.7e-07	6.46e+02	100	501	>1E20	>1E20
Pb-202m	4.13e-04	5.5e-07	1.68e+03	100	501	>1E20	>1E20
Pb-202	3.00e+05	3.9e-05	2.31e-06	100	501	2.0e-01	8.6e-06
Pb-203	5.94e-03	9.6e-07	1.17e+02	100	501	>1E20	>1E20
Pb-205	1.40e+07	1.5e-06	4.95e-08	100	501	5.3e+00	8.6e-06
Pb-209	6.24e-06	9.0e-08	1.11e+05	100	501	>1E20	>1E20
Pb-210	2.23e+01	5.1e-03	3.11e-02	100	501	>1E20	1.9e-04
Pb-211	6.86e-05	4.4e-07	1.01e+04	100	501	>1E20	>1E20
Pb-212	1.21e-03	4.1e-05	5.71e+02	100	501	>1E20	>1E20
Pb-214	5.10e-05	5.8e-07	1.36e+04	100	501	>1E20	>1E20
Bi-200	6.65e-05	1.7e-07	1.04e+04	0	1	>1E20	>1E20
Bi-201	2.05e-04	4.5e-07	3.38e+03	0	1	>1E20	>1E20
Bi-202	1.81e-04	3.6e-07	3.84e+03	0	1	>1E20	>1E20
Bi-203	1.35e-03	2.1e-06	5.15e+02	0	1	>1E20	>1E20
Bi-205	4.19e-02	3.7e-06	1.65e+01	0	1	>1E20	>1E20
Bi-206	1.71e-02	8.0e-06	4.06e+01	0	1	>1E20	>1E20
Bi-207	7.94e+00	4.9e-06	8.73e-02	0	1	5.0e-03	5.3e-02
Bi-210m	3.50e+06	8.6e-05	1.98e-07	0	1	1.8e-04	8.6e-06
Bi-210	1.37e-02	5.9e-06	5.06e+01	0	1	>1E20	>1E20
Bi-212	1.15e-04	9.9e-07	6.02e+03	0	1	>1E20	>1E20

Table C3-1. (continued)

Nuclide	T1/2 (years)	DCF (mrem/pCi)	Lambda (1/year)	Kd (cm^3/gm)	Rf	SUSP GW Trigger (Ci/trench)	SUSP Int Trigger (Ci/trench)
Bi-213	8.68e-[illegible]	6.[illegible]e-07	7.99e+03	0	1	>1E20	>1E20
Bi-214	3.76e-05	2.4e-07	1.84e+04	0	1	>1E20	>1E20
Po-203	7.99e-05	2.0e-07	8.68e+03	0	1	>1E20	>1E20
Po-205	2.05e-04	2.4e-07	3.38e+03	0	1	>1E20	>1E20
Po-207	6.50e-04	6.1e-07	1.07e+03	0	1	>1E20	>1E20
Po-210	3.79e-01	1.6e-03	1.83e+00	0	1	9.3e-02	>1E20
At-207	2.05e-04	8.9e-07	3.38e+03	0	1	>1E20	>1E20
At-211	8.22e-04	4.1e-05	8.43e+02	0	1	>1E20	>1E20
Fr-222	2.81e-05	2.5e-06	2.46e+04	0	1	>1E20	>1E20
Fr-223	4.18e-05	8.6e-06	1.66e+04	0	1	>1E20	>1E20
Ra-223	3.13e-02	5.5e-04	2.21e+01	500	2501	>1E20	>1E20
Ra-224	9.91e-03	3.3e-04	6.99e+01	500	2501	>1E20	>1E20
Ra-225	4.05e-02	3.1e-04	1.71e+01	500	2501	>1E20	>1E20
Ra-226	1.62e+03	1.1e-03	4.27e-04	500	2501	7.5e+00	9.0e-06
Ra-227	7.83e-05	2.2e-07	8.85e+03	500	2501	>1E20	>1E20
Ra-228	5.75e+00	1.2e-03	1.21e-01	500	2501	>1E20	1.5e+00
Ac-224	3.31e-04	2.6e-06	2.10e+03	150	751	>1E20	>1E20
Ac-225	2.74e-02	9.5e-05	2.53e+01	150	751	>1E20	>1E20
Ac-226	3.31e-03	4.0e-05	2.10e+02	150	751	>1E20	>1E20
Ac-227	2.18e+01	1.4e-02	3.18e-02	150	751	>1E20	2.1e-04
Ac-228	6.99e-04	2.1e-06	9.91e+02	150	751	>1E20	>1E20
Th-226	5.87e-05	9.2e-07	1.18e+04	3000	15001	>1E20	>1E20
Th-227	5.13e-02	3.6e-05	1.35e+01	3000	15001	>1E20	>1E20
Th-228	1.91e+00	3.8e-04	3.62e-01	3000	15001	>1E20	4.7e+10
Th-229	7.43e+03	3.5e-03	9.33e-05	3000	15001	7.4e+01	8.7e-06
Th-230	7.70e+04	5.3e-04	9.00e-06	3000	15001	8.8e-01	8.6e-06
Th-231	2.91e-03	1.3e-06	2.38e+02	3000	15001	>1E20	>1E20
Th-232	1.41e+10	2.8e-03	4.93e-11	3000	15001	8.5e-02	8.6e-06
Th-234	6.60e-02	1.3e-05	1.05e+01	3000	15001	>1E20	>1E20
Pa-227	7.28e-05	1.3e-06	9.52e+03	10	51	>1E20	>1E20
Pa-228	2.97e-03	4.0e-06	2.34e+02	10	51	>1E20	>1E20
Pa-230	4.85e-02	5.6e-06	1.43e+01	10	51	>1E20	>1E20
Pa-231	3.28e+04	1.1e-02	2.12e-05	10	51	7.4e-05	8.7e-06
Pa-232	3.59e-03	3.4e-06	1.93e+02	10	51	>1E20	>1E20

Table C.3-1. (continued)

Nuclide	T1/2 (years)	DCF (mrem/pCi)	Lambda (1/year)	Xd (cm^3/J/gm)	Rf	SUSP GW Trigger (Ci/trench)	SUSP Int Trigger (Ci/trench)
Pa-233	7.39e-02	3.3e-06	9.2[illegible]e+00	10	51	>1E20	>1E20
Pa-234	7.64e-01	2.1e-06	9.07e+01	10	51	>1E20	>1E20
U-230	5.69e-02	8.4e-04	1.22e+01	50	251	>1E20	>1E20
U-231	4.30e+00	1.1e-06	1.61e-01	50	251	>1E20	8.7e+01
U-232	7.20e+01	1.3e-03	9.62e-03	50	251	5.4e+02	2.3e-05
U-233	1.60e+05	2.7e-04	4.35e-06	50	251	1.5e-02	8.6e-06
U-234	2.45e+05	2.6e-04	2.83e-06	50	251	1.5e-02	8.6e-06
U-235	7.04e+08	2.5e-04	9.85e-10	50	251	1.6e-02	8.6e-06
U-236	2.34e+07	2.5e-04	2.96e-08	50	251	1.6e-02	8.6e-06
U-237	1.85e-02	2.7e-06	3.75e+01	50	251	>1E20	>1E20
U-238	4.47e+09	2.3e-04	1.55e-10	50	251	1.7e-02	8.6e-06
U-239	4.47e-05	7.6e-08	1.55e+04	50	251	>1E20	>1E20
U-240	1.61e-03	4.1e-06	4.31e+02	50	251	>1E20	>1E20
Np-232	2.47e-05	2.4e-08	2.80e+04	10	51	>1E20	>1E20
Np-233	6.65e-05	5.6e-09	1.04e+04	10	51	>1E20	>1E20
Np-234	1.20e-02	1.7e-06	5.75e+01	10	51	>1E20	>1E20
Np-235	1.12e+00	2.1e-07	6.17e-01	10	51	>1E20	>1E20
Np-236(1E5y)	1.10e+05	7.9e-04	6.30e-06	10	51	1.0e-03	8.6e-06
Np-236(22h)	2.51e-03	9.5e-07	2.76e+02	10	51	>1E20	>1E20
Np-237	2.14e+06	3.9e-03	3.24e-07	10	51	2.1e-04	8.6e-06
Np-238	5.80e-03	3.4e-06	1.20e+02	10	51	>1E20	>1E20
Np-239	6.38e-03	2.9e-06	1.09e+02	10	51	>1E20	>1E20
Np-240	1.20e-04	2.0e-07	5.79e+03	10	51	>1E20	>1E20
Pu-234	1.03e-03	1.2e-06	6.75e+02	100	501	>1E20	>1E20
Pu-235	4.94e-05	1.4e-08	1.40e+04	100	501	>1E20	>1E20
Pu-236	2.85e+00	1.3e-03	2.43e-01	100	501	>1E20	3.2e+05
Pu-237	1.24e-01	1.0e-06	5.58e+00	100	501	>1E20	>1E20
Pu-238	8.78e+01	3.8e-03	7.90e-03	100	501	8.2e+05	1.9e-05
Pu-239	2.41e+04	4.3e-03	2.87e-05	100	501	2.0e-03	8.7e-06
Pu-240	6.57e+03	4.3e-03	1.06e-04	100	501	2.4e-03	8.7e-06
Pu-241	1.44e+01	8.6e-05	4.81e-02	100	501	>1E20	1.1e-03
Pu-242	3.76e+05	4.1e-03	1.84e-06	100	501	1.9e-03	8.6e-06
Pu-243	5.65e-04	3.3e-07	1.23e+03	100	501	>1E20	>1E20
Pu-244	8.10e+07	4.0e-03	8.56e-09	100	501	2.0e-03	8.6e-06

Table C.3-1. (continued)

Nuclide	T1/2 (years)	DCF (mrem/pCi)	Limit's (1/year)	Kd (cm**3/gm)	Rf	SUSP GW Trigger (Ci/trench)	SOIL Int Trigger (Ci/trench)
Pu-235	1.1[illegible]e-03	2.[illegible]e-06	6.0[illegible]e+02	100	501	>1E20	>1E20
Am-237	1.42e-04	7.[illegible]e-08	4.67e+03	150	751	>1E20	>1E20
Am-238	2.17e-04	1.7e-07	3.20e+03	150	751	>1E20	>1E20
Am-239	1.38e-03	1.0e-06	5.02e+02	150	751	>1E20	>1E20
Am-240	5.82e-03	2.9e-06	1.19e+02	150	751	>1E20	>1E20
Am-241	4.32e+02	4.5e-03	1.60e-03	150	751	1.1e+00	1.0e-05
Am-242m	1.52e+02	4.2e-03	4.56e-03	150	751	7.7e+04	1.4e-05
Am-242	1.83e-03	1.2e-06	3.80e+02	150	751	>1E20	>1E20
Am-243	7.37e+03	4.5e-03	9.40e-05	150	751	3.7e-03	8.7e-06
Am-244m	4.94e-05	6.8e-08	1.40e+04	150	751	>1E20	>1E20
Am-244	1.15e-03	2.0e-06	6.02e+02	150	751	>1E20	>1E20
Am-245	2.40e-04	1.8e-07	2.89e+03	150	751	>1E20	>1E20
Am-246m	4.75e-05	8.4e-08	1.46e+04	150	751	>1E20	>1E20
Am-246	4.75e-05	1.5e-07	1.46e+04	150	751	>1E20	>1E20
Cm-238	2.85e-04	3.6e-07	2.43e+03	100	501	>1E20	>1E20
Cm-240	7.34e-02	6.3e-05	9.45e+00	100	501	>1E20	>1E20
Cm-241	9.58e-02	4.6e-06	7.23e+00	100	501	>1E20	>1E20
Cm-242	4.46e-01	1.1e-04	1.56e+00	100	501	>1E20	>1E20
Cm-243	2.85e+01	2.9e-03	2.43e-02	100	501	>1E20	9.8e-05
Cm-244	1.81e+01	2.3e-03	3.83e-02	100	501	>1E20	4.0e-04
Cm-245	8.50e+03	4.5e-03	8.15e-05	100	501	2.2e-03	8.7e-06
Cm-246	4.70e+03	4.5e-03	1.47e-04	100	501	2.5e-03	8.8e-06
Cm-247	1.60e+07	4.1e-03	4.33e-08	100	501	1.9e-03	8.6e-06
Cm-248	3.50e+05	1.6e-02	1.98e-06	100	501	5.0e-04	8.6e-06
Cm-249	1.24e-04	9.5e-08	5.61e+03	100	501	>1E20	>1E20
Bk-245	1.36e-02	2.3e-06	5.08e+01	100	501	>1E20	>1E20
Bk-246	4.93e-03	1.9e-06	1.41e+02	100	501	>1E20	>1E20
Bk-247	1.40e+03	2.3e-03	4.95e-04	100	501	1.2e-02	9.1e-06
Bk-249	8.80e-01	6.0e-06	7.88e-01	100	501	>1E20	>1E20
Bk-250	3.67e-04	5.0e-07	1.89e+03	100	501	>1E20	>1E20
Cf-244	4.75e-05	1.5e-07	1.46e+04	100	501	>1E20	>1E20
Cf-246	4.11e-03	1.2e-05	1.69e+02	100	501	>1E20	>1E20
Cf-248	9.86e-01	2.8e-04	7.03e-01	100	501	>1E20	>1E20
Cf-249	3.51e+02	4.6e-03	1.97e-03	100	501	2.4e-01	1.1e-05

Table C.3-1. (continued)

Nuclide	T1/2 (year)	DCF (mrem/pCi)	Lambda (1/year)	Kd (cm**3/gm)	Rf	SUSP Crit Trigger (Cutrench)	SUSP Int Trigger (Cutrench)
Cf-250	1.31e+01	1.5e-03	5.2[illegible]e-02	100	501	>1E20	1.7e-03
Cf-251	9.00e+02	4.6e-03	7.70e-04	100	501	1.2e-02	9.[illegible]e-06
Cf-252	2.62e+00	9.4e-04	2.65e-01	100	501	>1E20	2.7e-06
Cf-253	4.87e-02	9.2e-06	1.42e+01	100	501	>1E20	>1E20
Cf-254	1.66e-01	2.5e-03	4.18e+00	100	501	>1E20	>1E20
Es-250	9.13e-04	9.5e-08	7.60e+02	100	501	>1E20	>1E20
Es-251	4.11e-03	6.7e-07	1.69e+02	100	501	>1E20	>1E20
Es-253	5.60e-02	2.4e-05	1.24e+01	100	501	>1E20	>1E20
Es-254m	4.48e-03	1.5e-05	1.55e+02	100	501	>1E20	>1E20
Es-254	7.56e-01	1.5e-04	9.17e-01	100	501	>1E20	>1E20
Fm-252	2.62e-03	9.9e-06	2.64e+02	100	501	>1E20	>1E20
Fm-253	8.21e-03	3.5e-06	8.44e+01	100	501	>1E20	>1E20
Fm-254	3.70e-04	1.6e-06	1.88e+03	100	501	>1E20	>1E20
Fm-255	2.29e-03	9.7e-06	3.02e+02	100	501	>1E20	>1E20
Fm-257	2.19e-01	7.3e-05	3.16e+00	100	501	>1E20	>1E20
Md-257	3.42e-04	5.4e-07	2.03e+03	100	501	>1E20	>1E20
Md-258	1.53e-01	6.1e-05	4.52e+00	100	501	>1E20	>1E20

C.4 NEAR-FIELD RESULTS

Figures C.4-1 through C.4-12 show the time histories of fluxes to the water table. The fluxes are given in the yearly fraction of a unit inventory in each vault released to the water table.

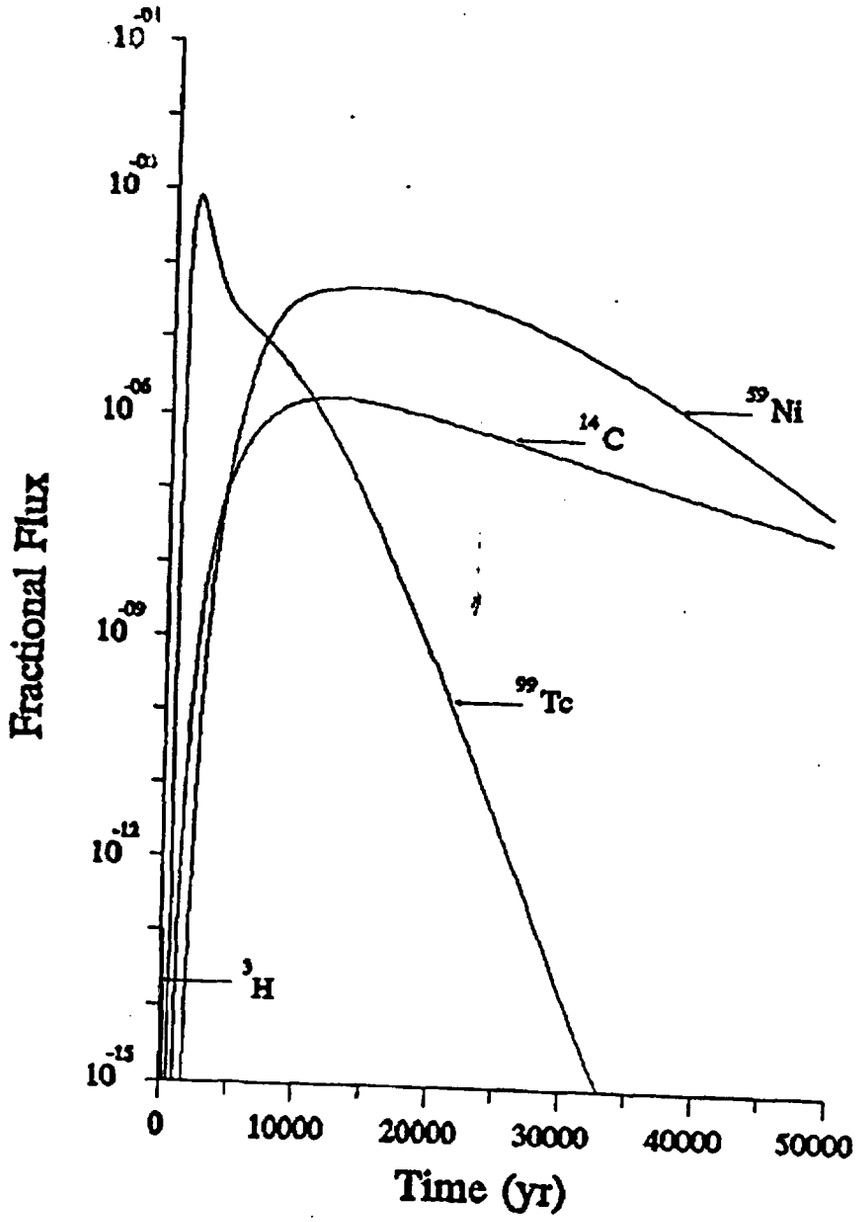

Fig. C.4-1. Fractional flux to the water table from the ILNT vaults.

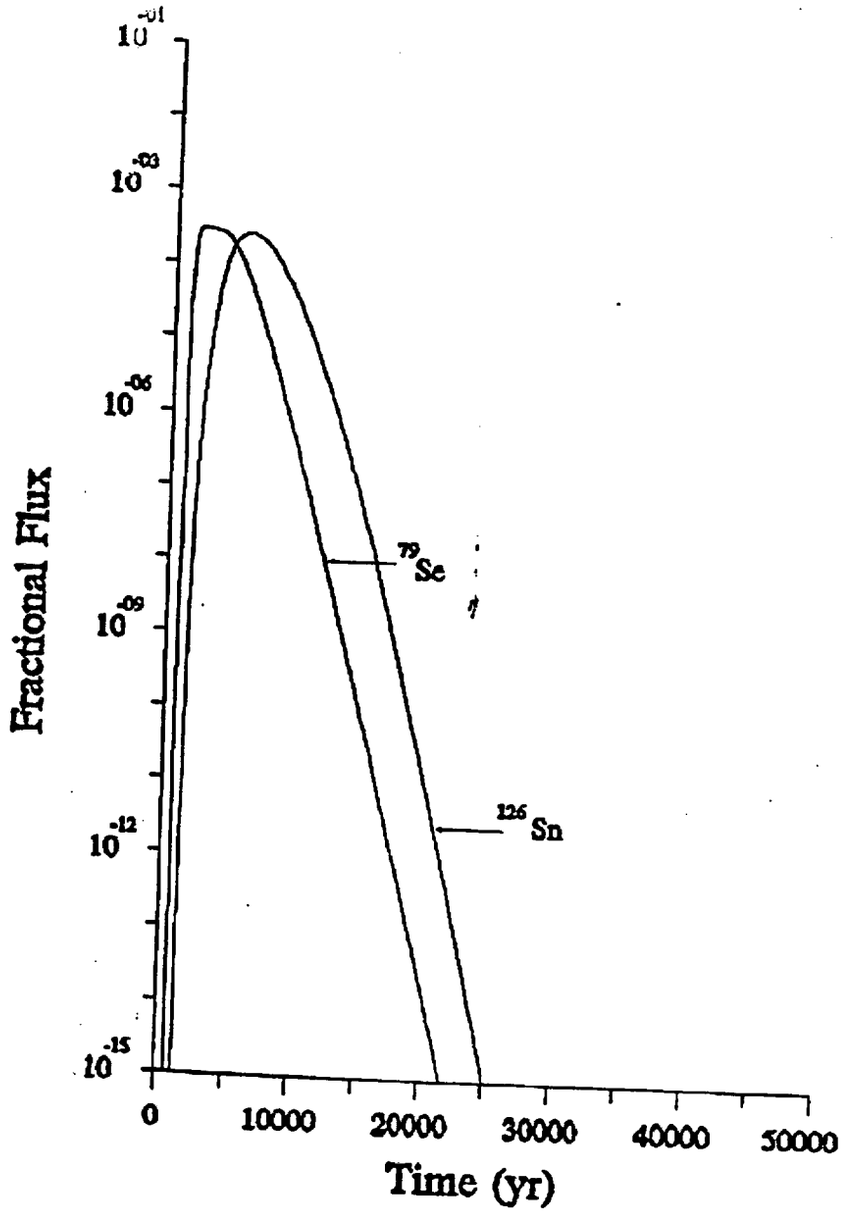

Fig. C.4-2. Fractional flux to the water table from the ILNT vaults.

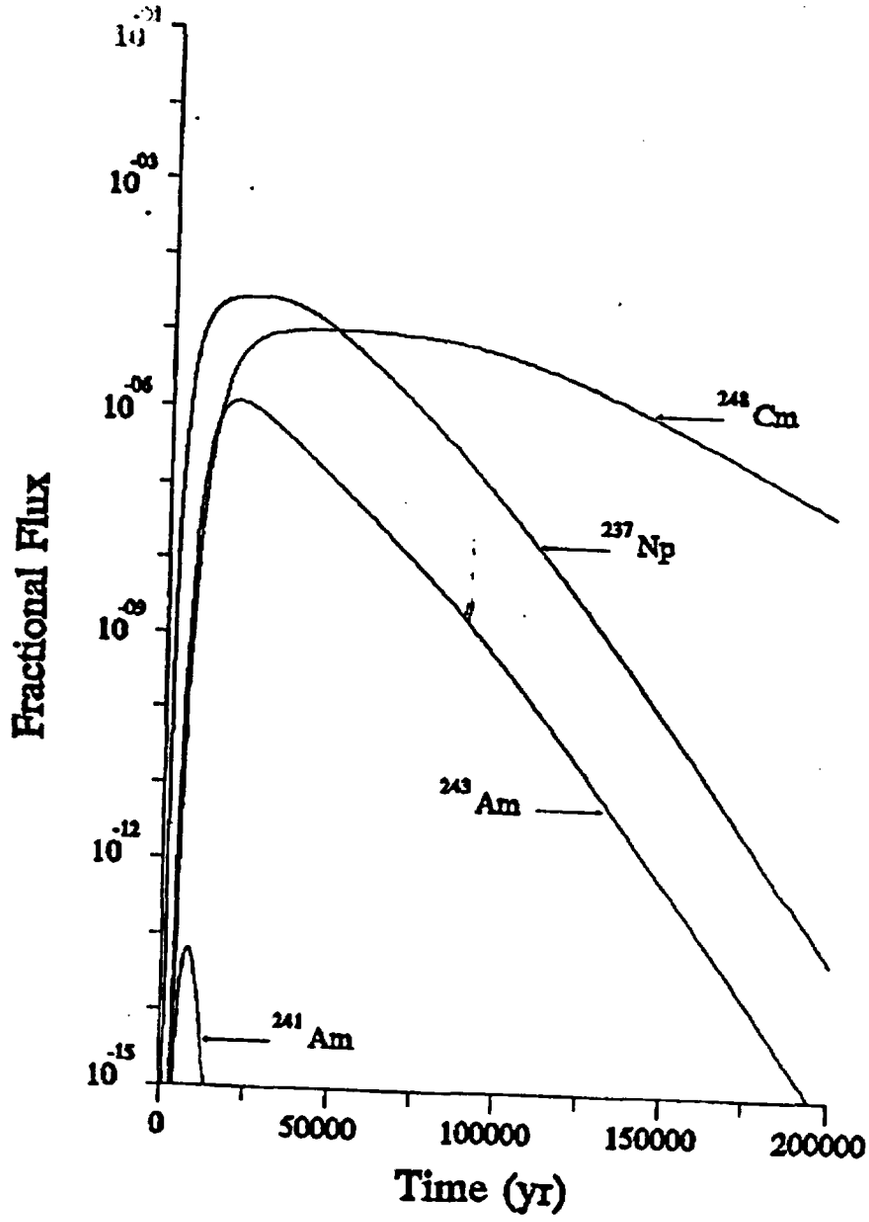

Fig. C.4-3. Fractional flux to the water table from the ILNT vaults.

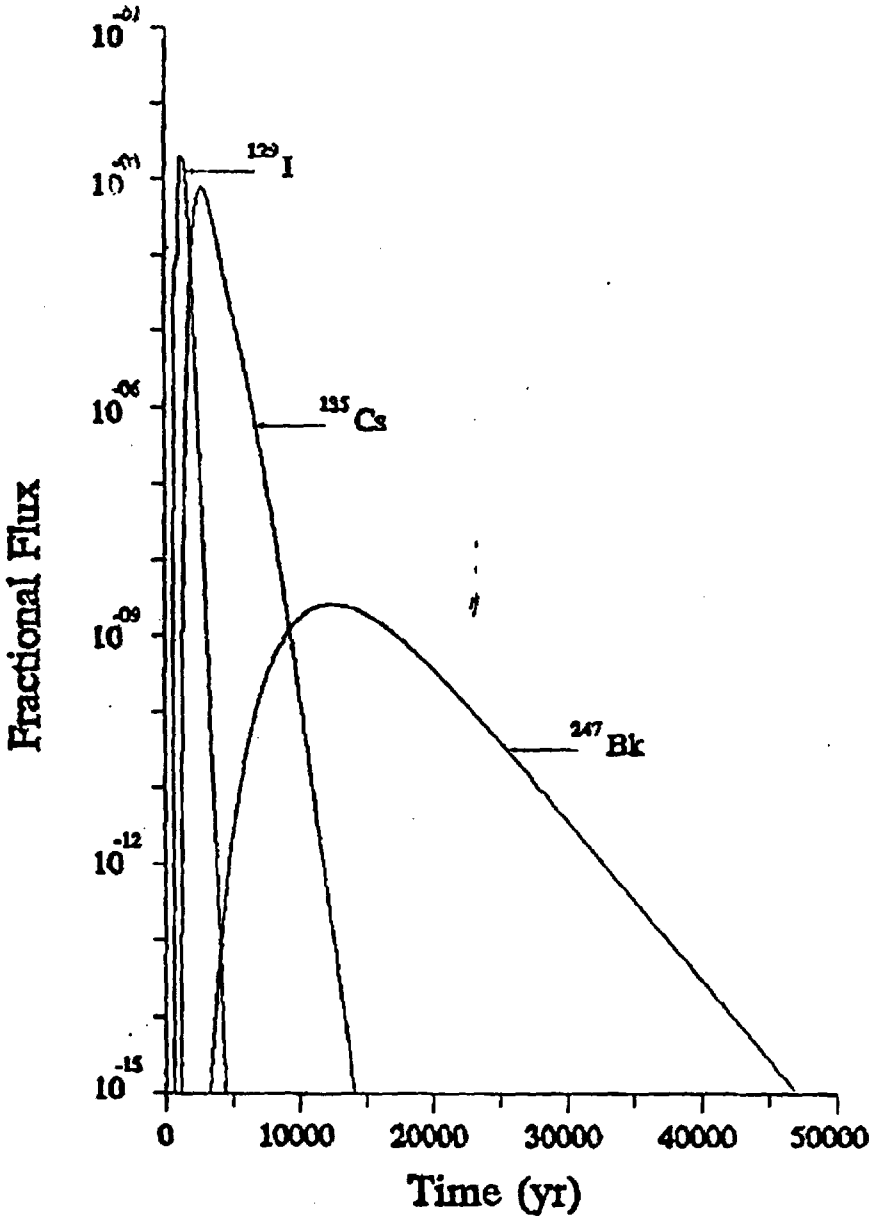

Fig. C.4-4. Fractional flux to the water table from the ILNT vaults.

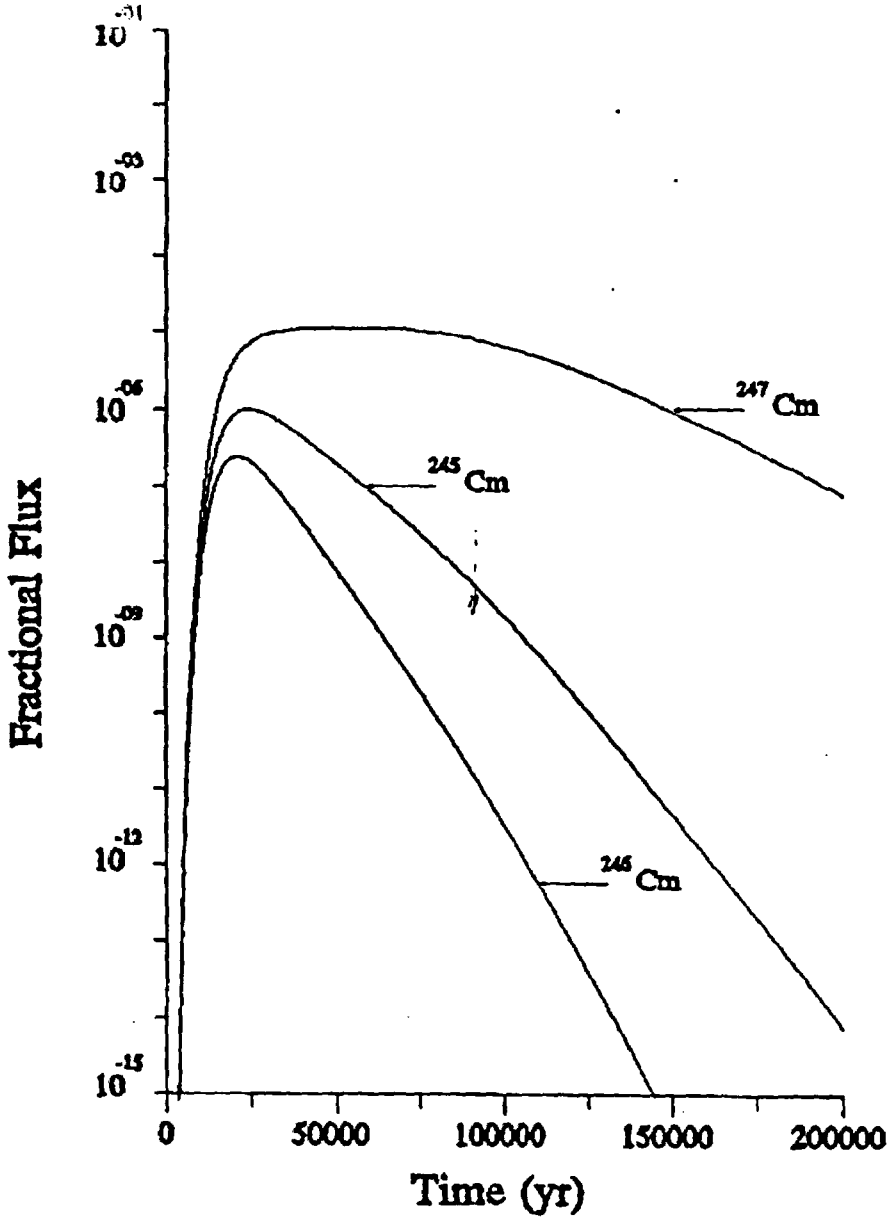

Fig. C.4-5. Fractional flux to the water table from the ILNT vaults.

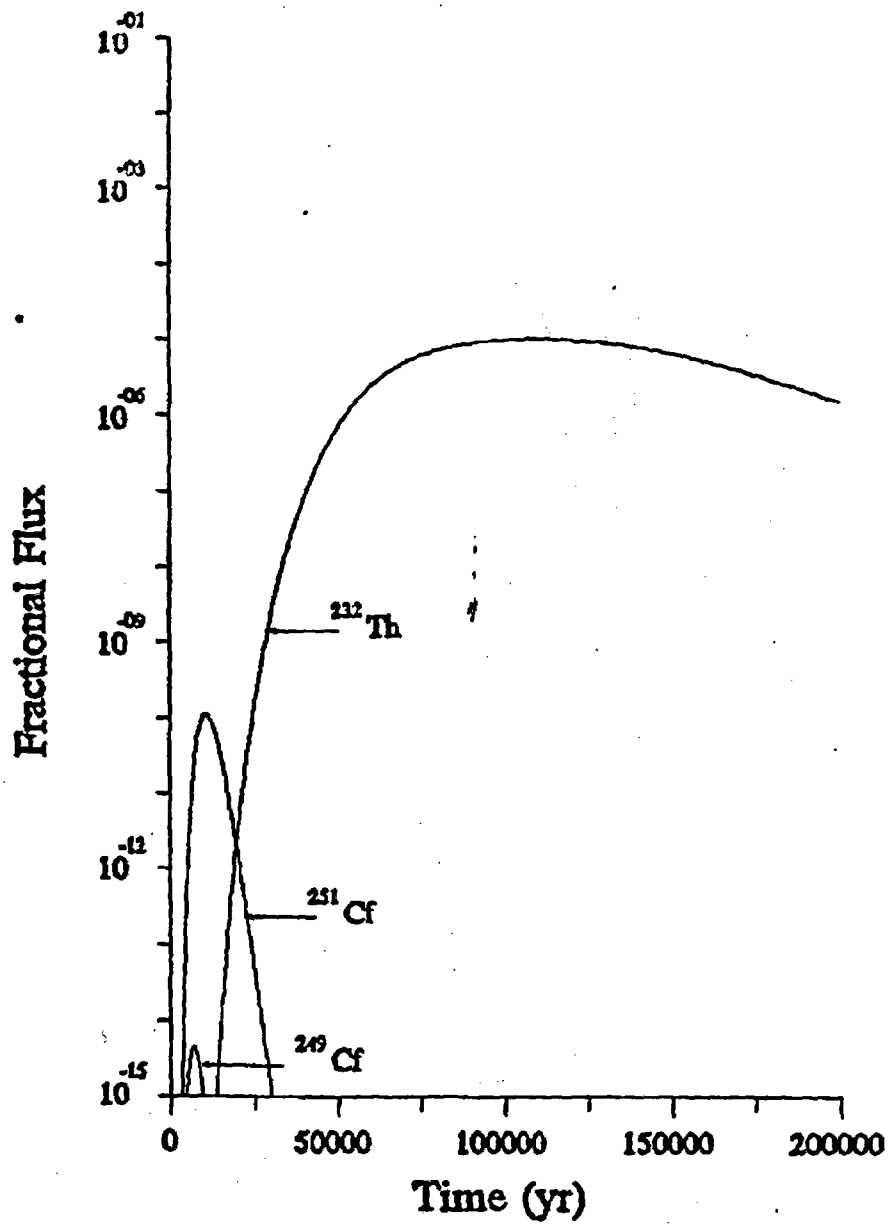

Fig. C.4-6. Fractional flux to the water table from the ILNT vaults.

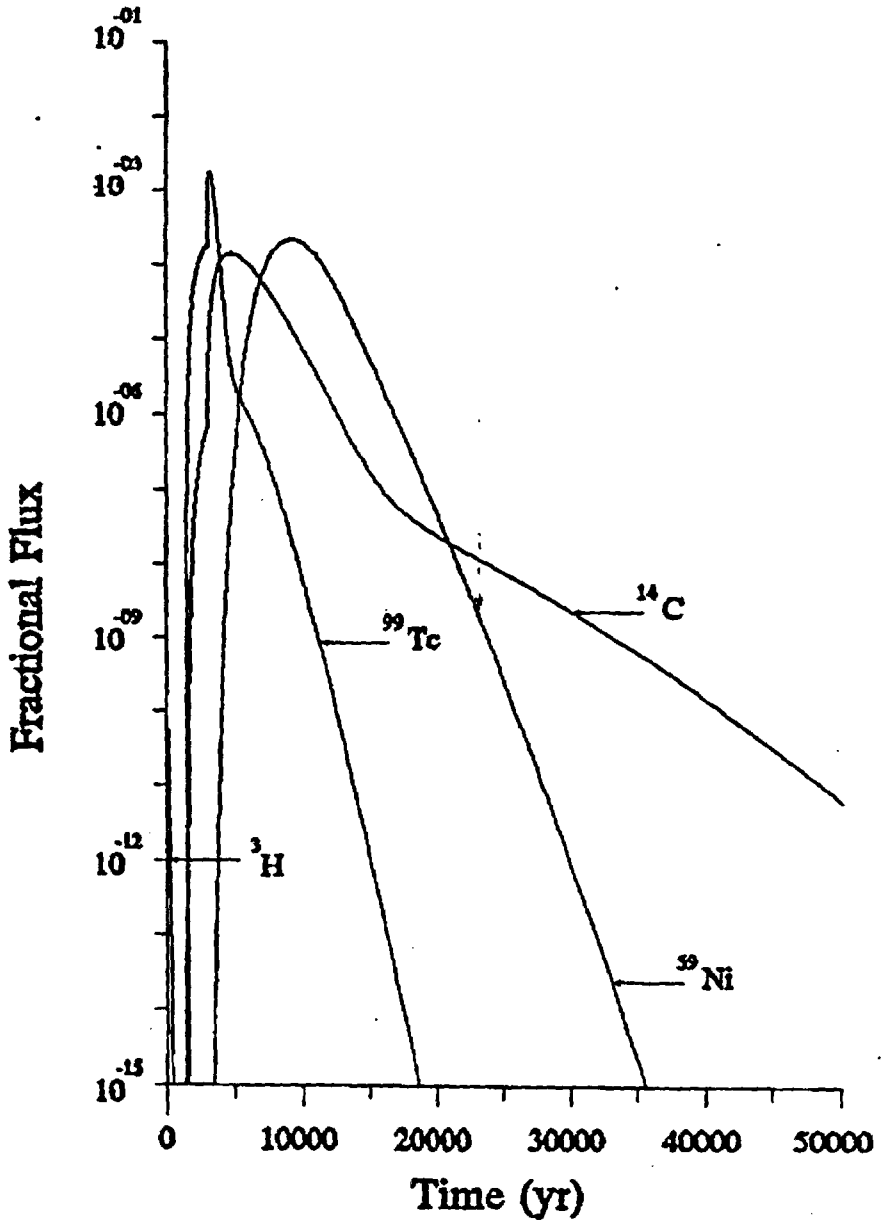

Fig. C.4-7. Fractional flux to the water table from the LAW vaults.

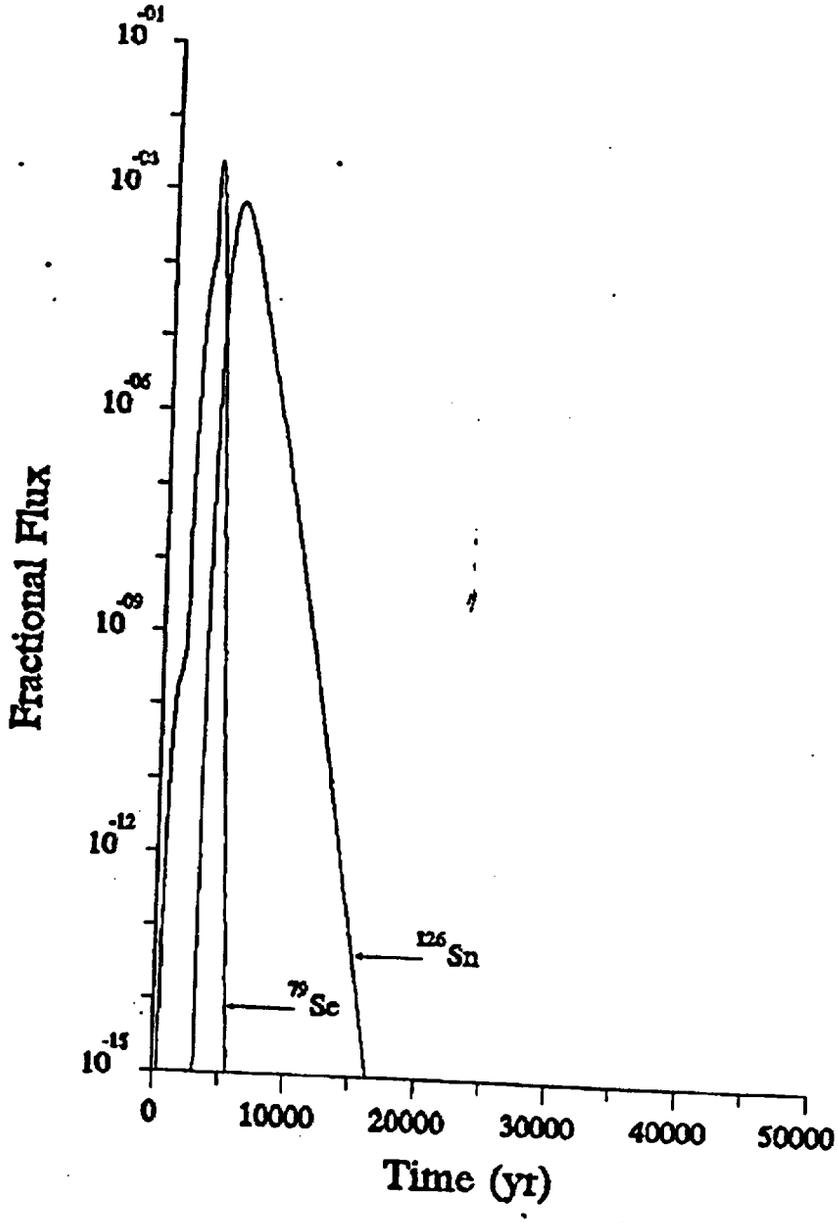

Fig. C.4-8. Fractional flux to the water table from the LAW vaults.

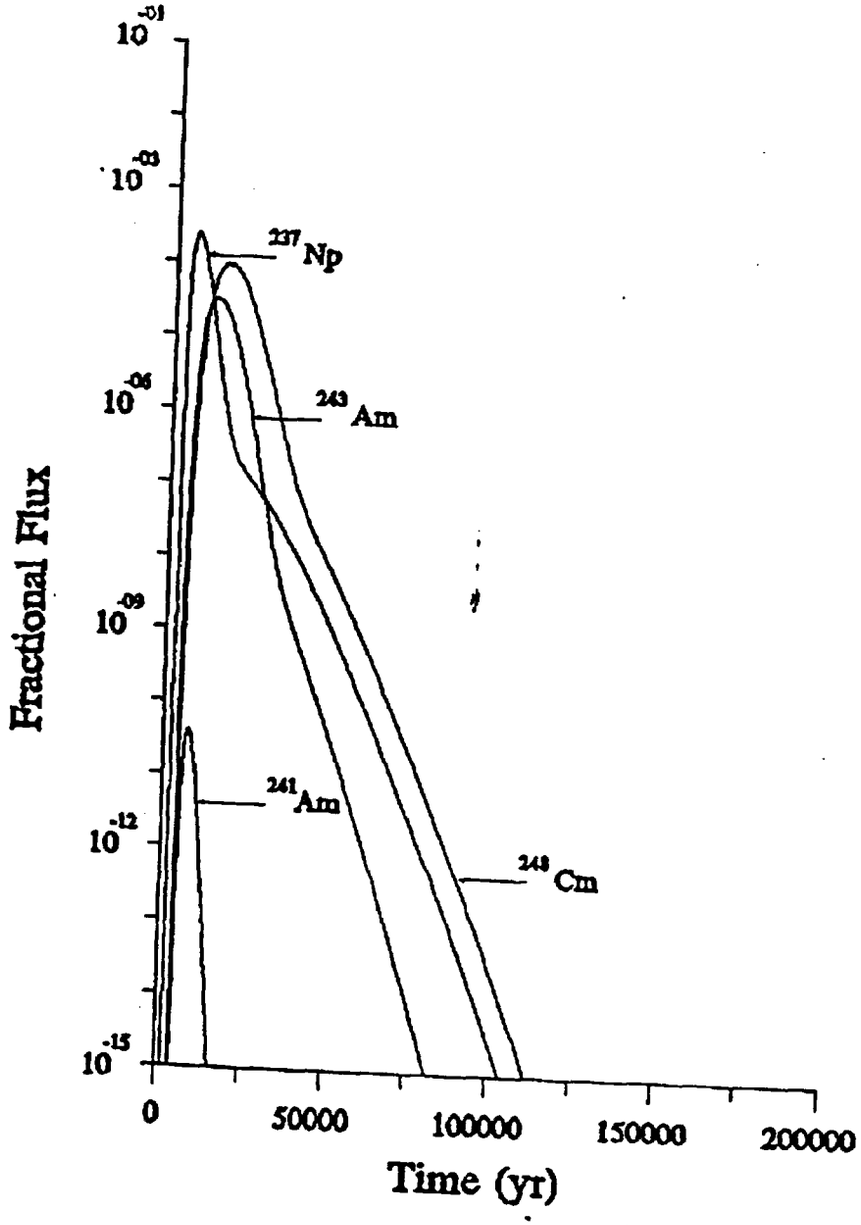

Fig. C.4-9. Fractional flux to the water table from the LAW vaults.

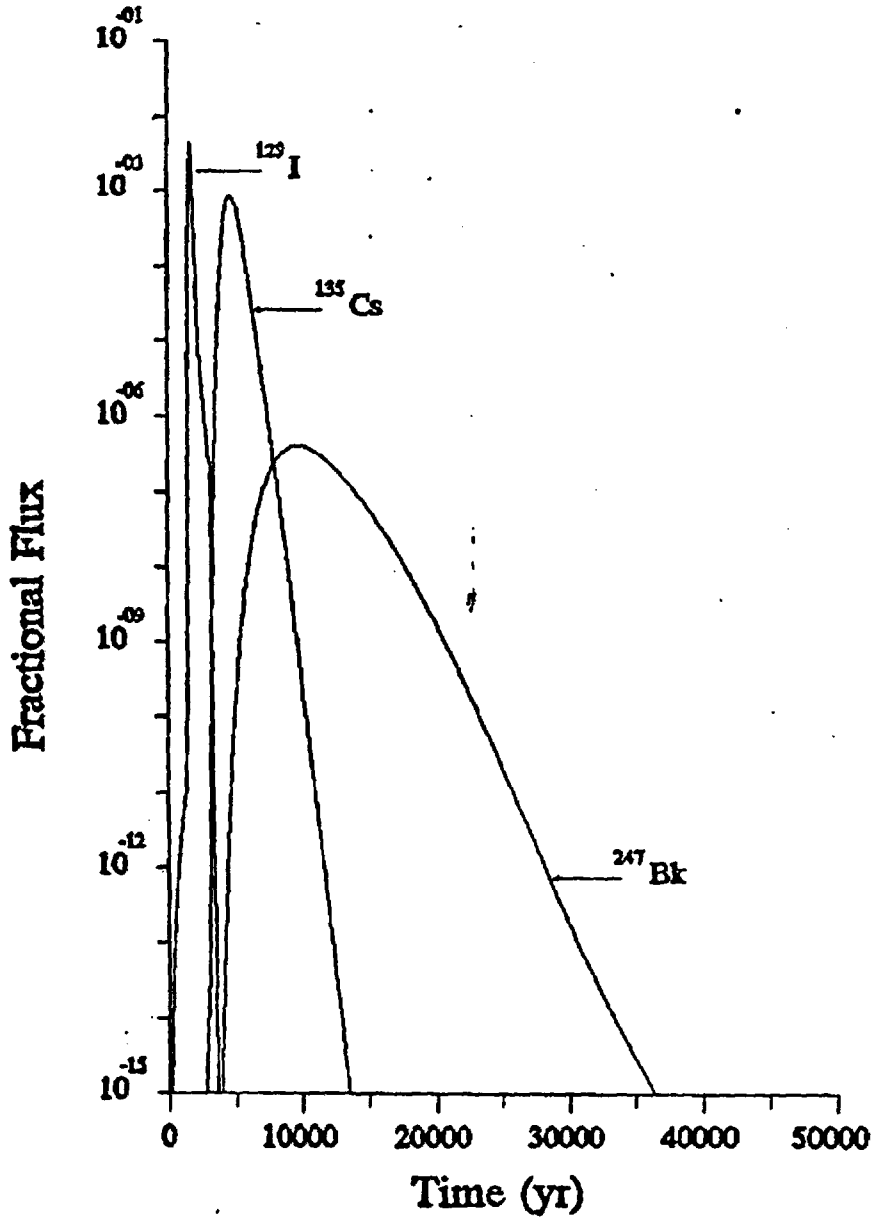

Fig. C.4-10. Fractional flux to the water table from the LAW vaults.

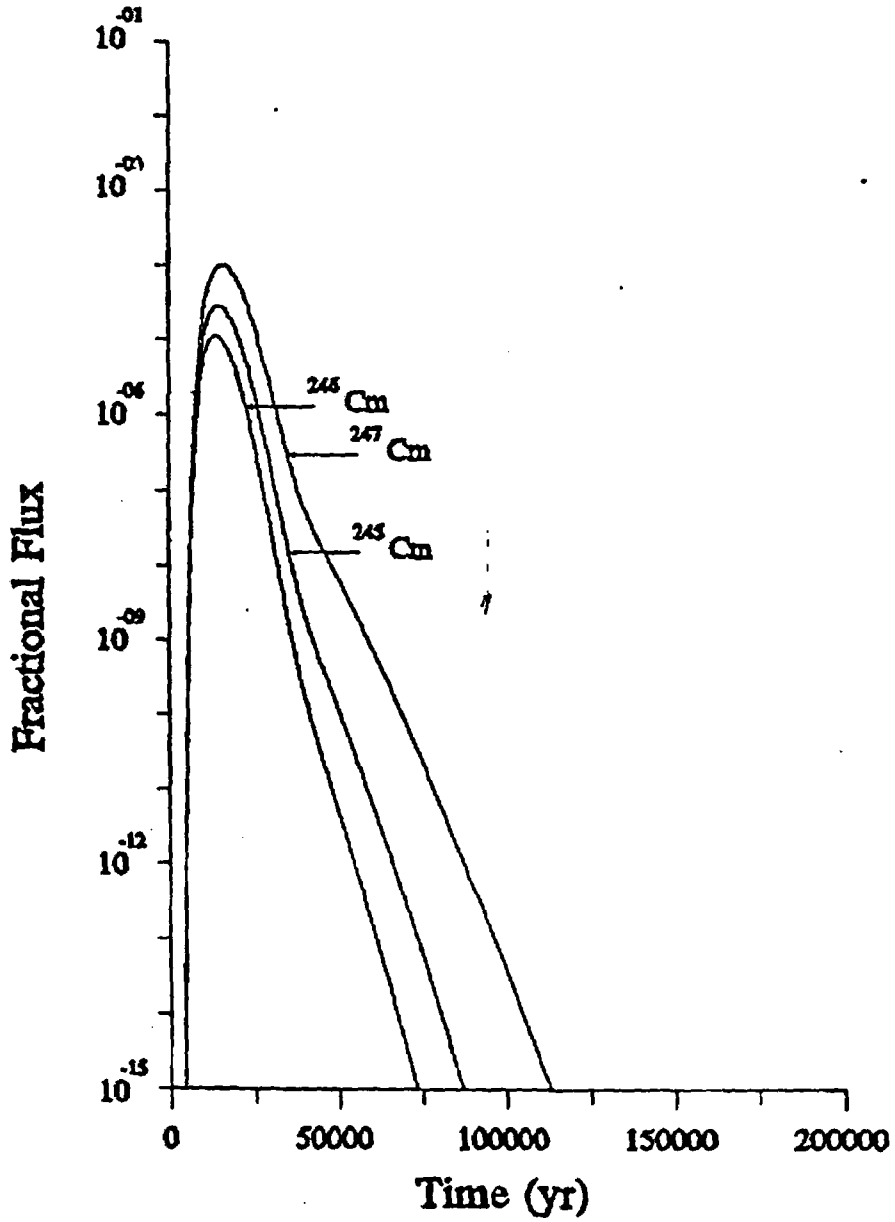

Fig. C.4-11. Fractional flux to the water table from the LAW vaults.

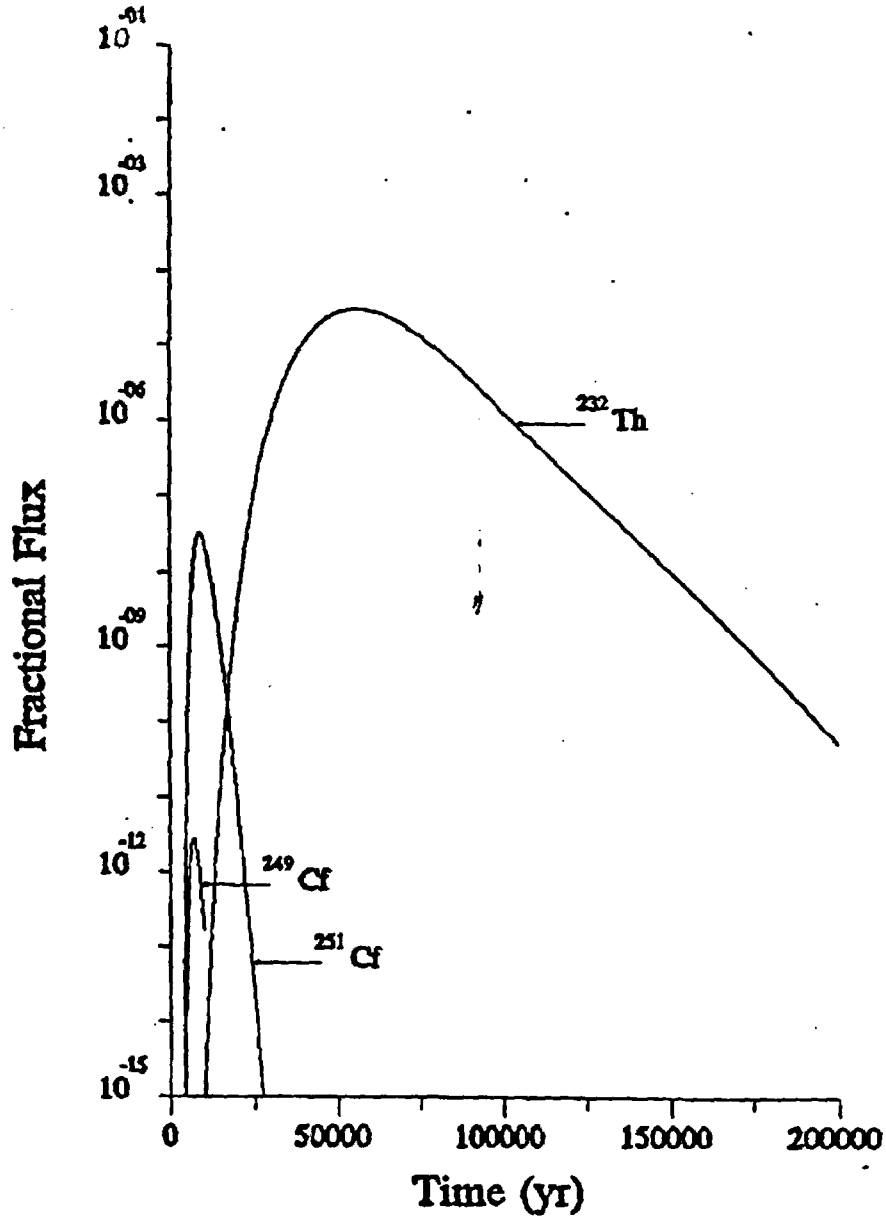

Fig. C.4-12. Fractional flux to the water table from the LAW vaults.

C.5 GROUNDWATER RESULTS

The fluxes given in Sect. C.4 were used in the groundwater transport simulations to estimate groundwater concentrations at the compliance point for groundwater protection. The groundwater concentrations are given in Figs. C.5-1 through C.5-31. The groundwater concentrations are given in units of concentration (pCi/cc) per Ci in each vault except for uranium and plutonium isotopes, which are solubility limited; for these isotopes, concentrations are given in units of pCi/cc.

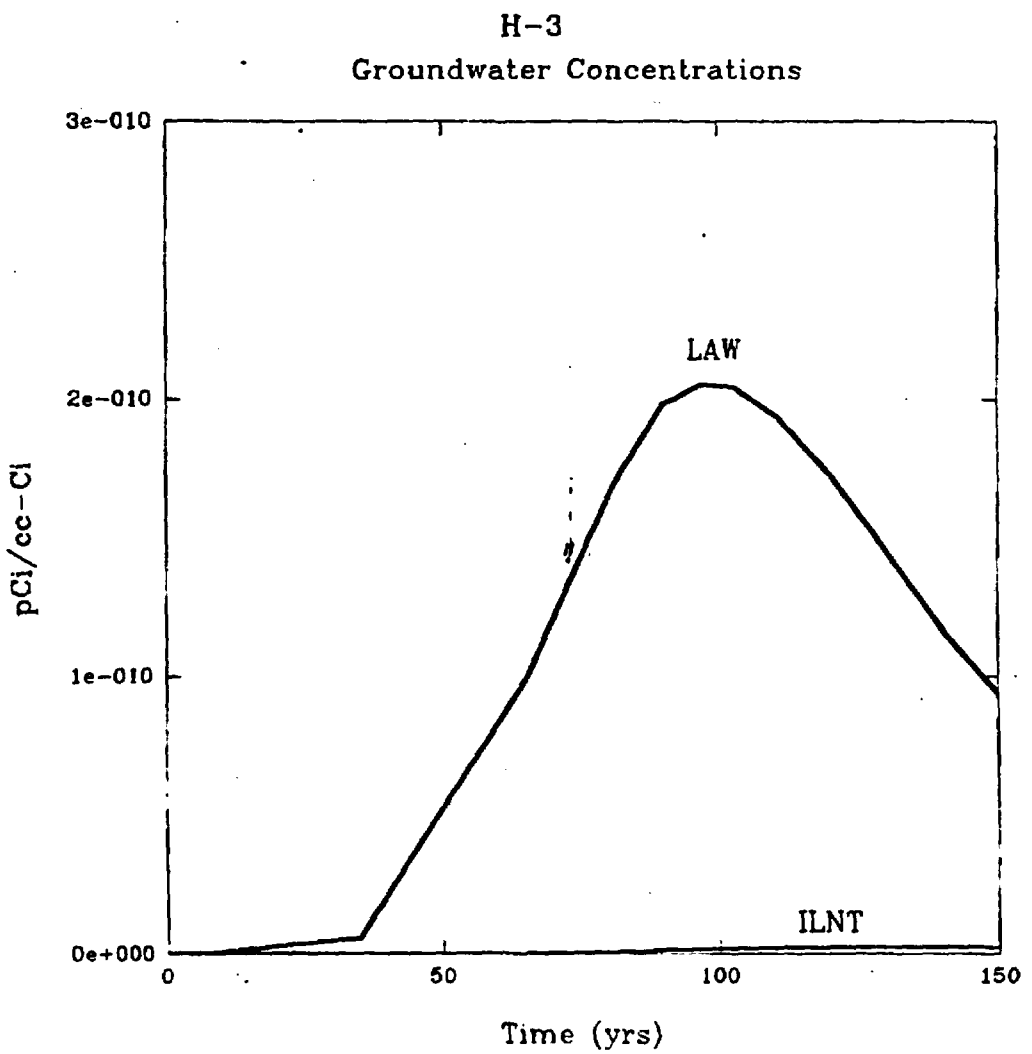

	Peak Concentration	Time (yrs)
LAW	2 10 e-010	9 7 e+001
ILNT	2.70 e-012	1 30 e+002

h3 spg

Fig. C.5-1. Predicted groundwater concentration of H-3 as a function of time.

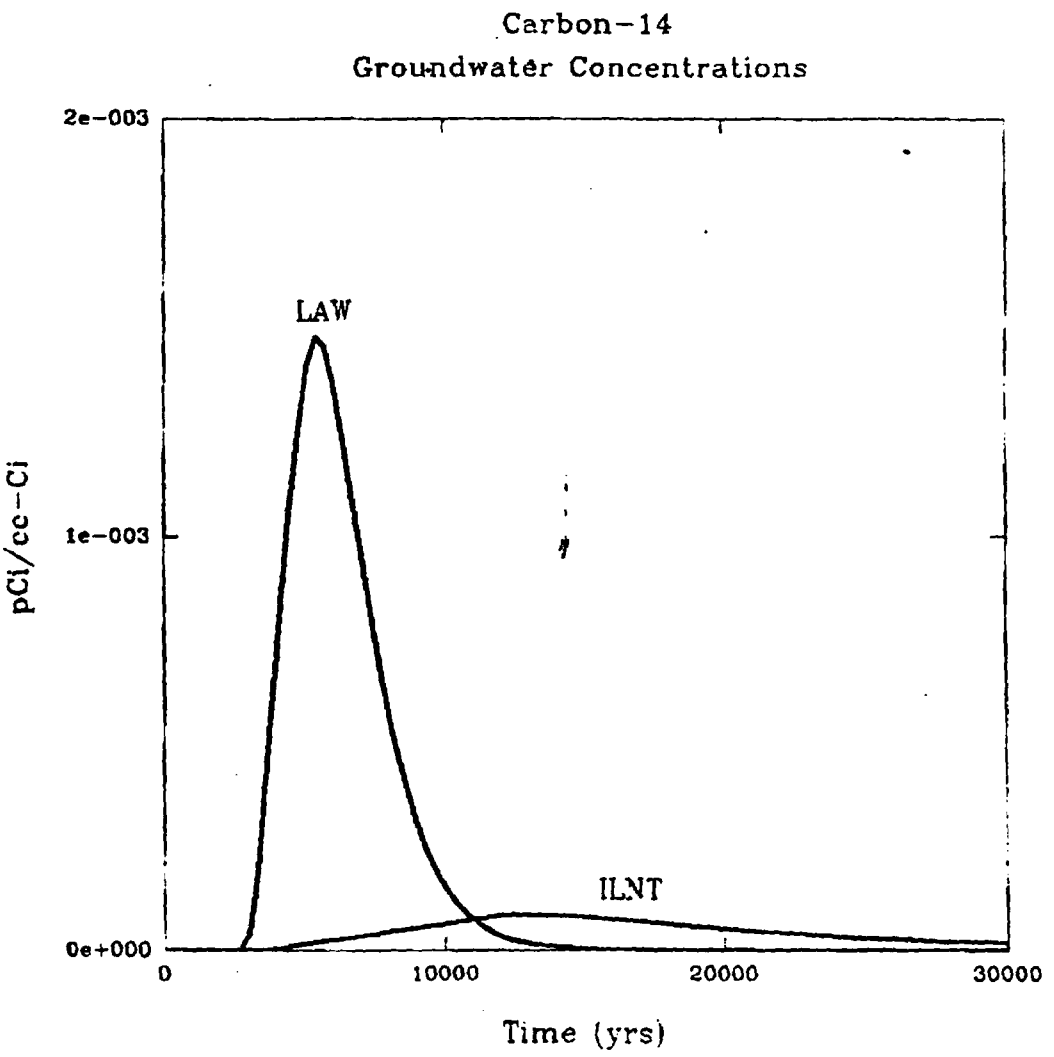

	Peak Concentration	Time (yrs)
LAW	1.50 e-003	5.40 e+003
ILNT	8.70 e-005	1.20 e+004

c14.spg

Fig. C.5-2. Predicted groundwater concentration of C-14 as a function of time.

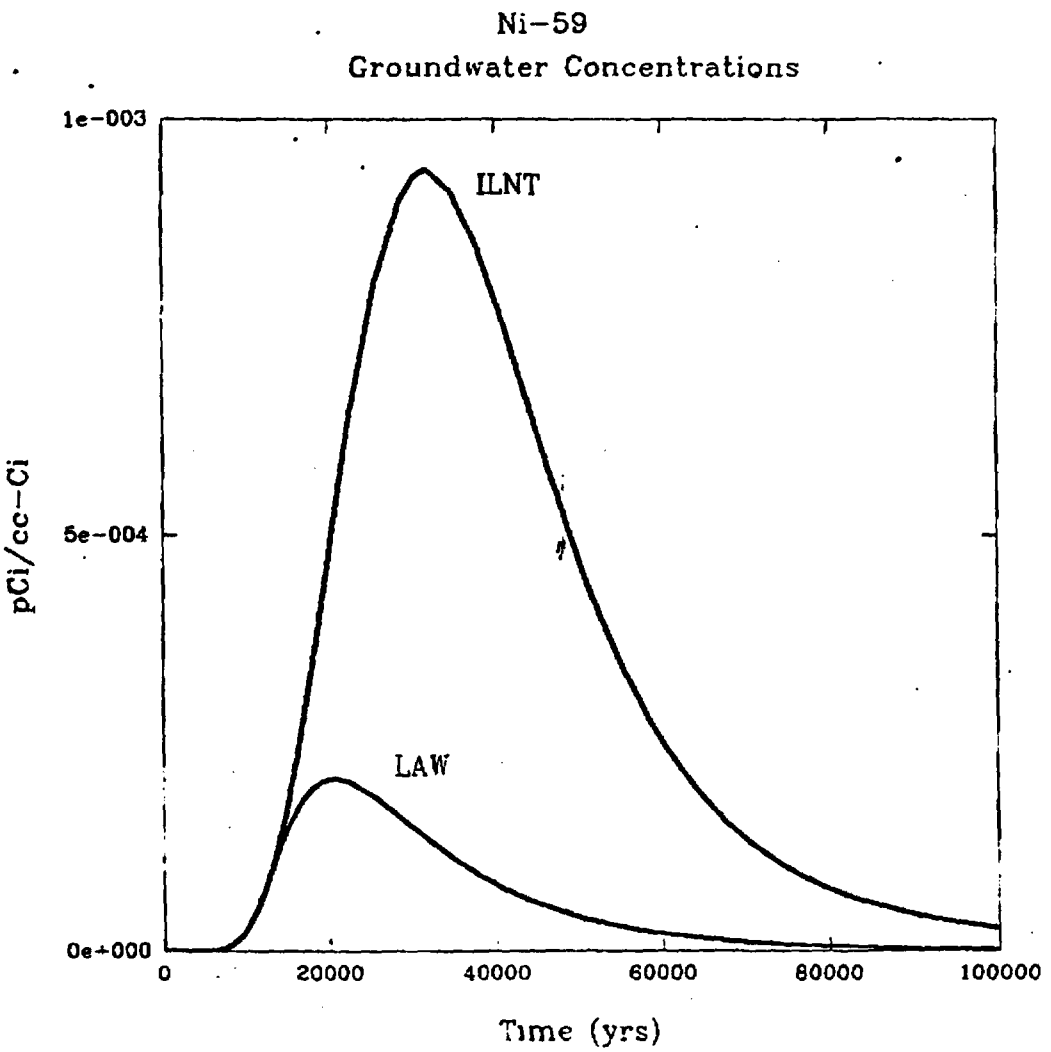

	Peak Concentration	Time (yrs)
LAW	2.10 e-004	2 10 e+004
ILNT	9.4 e-004	3.20 e+004

ni59.spg

Fig. C.5-3. Predicted groundwater concentration of Ni-59 as a function of time.

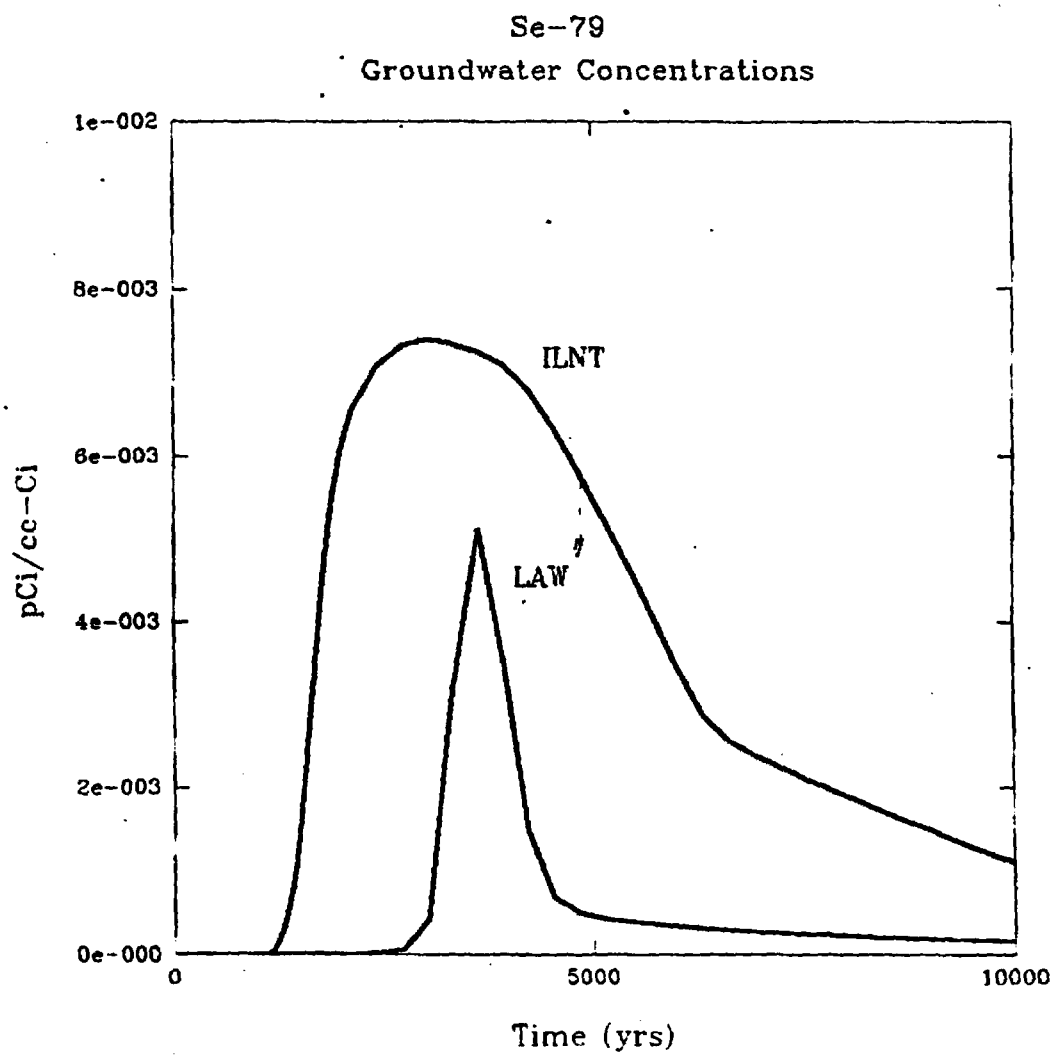

	Peak Concentration	Time (yrs)
LAW	5.10 e-003	3.60 e+003
ILNT	7.40 e-003	3.00 e+003

se79.spg

Fig. C.5-4. Predicted groundwater concentration of Se-79 as a function of time.

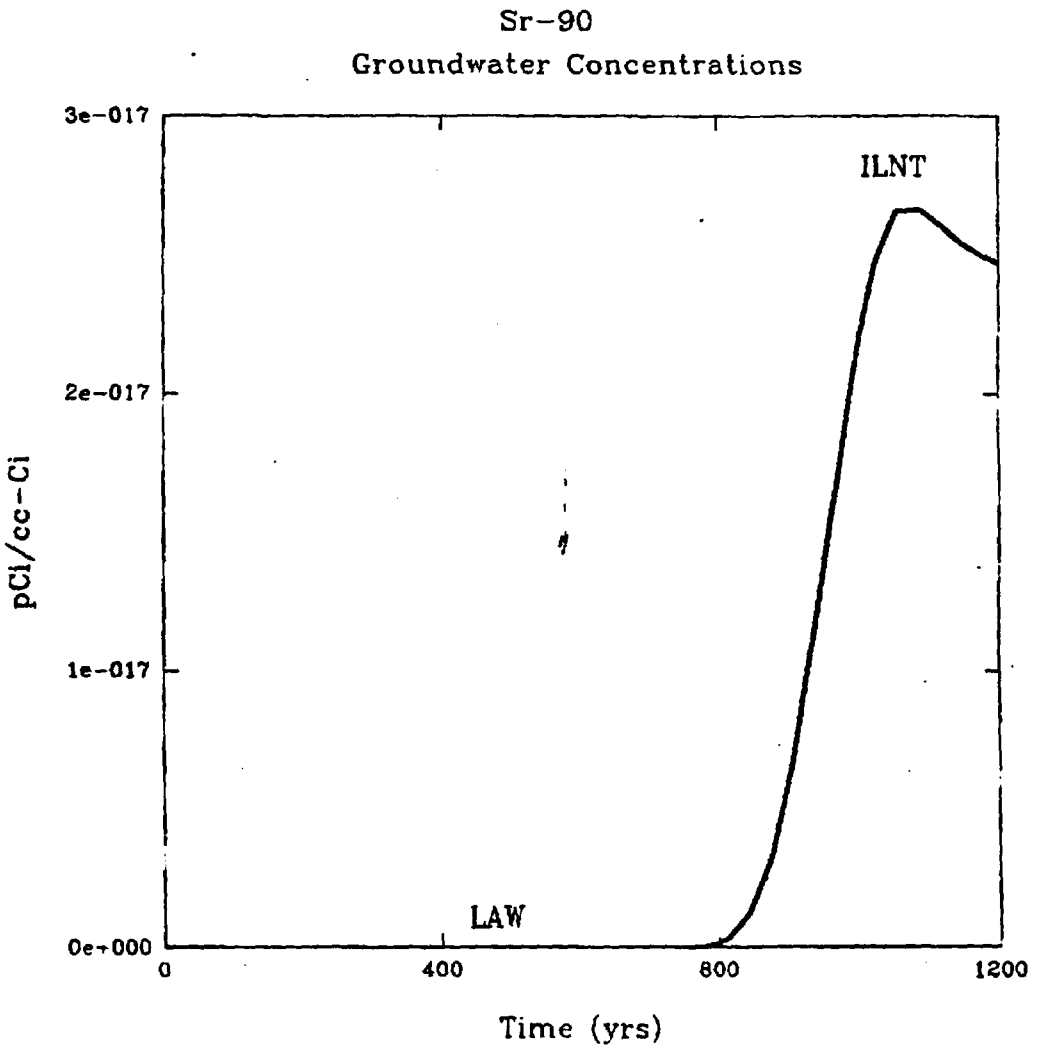

	Peak Concentration	Time (yrs)
LAW	1.50 e-022	5.20 e+002
ILNT	2.70 e-017	1.10 e+003

sr90.spg

Fig. C.5-5. Predicted groundwater concentration of Sr-90 as a function of time.

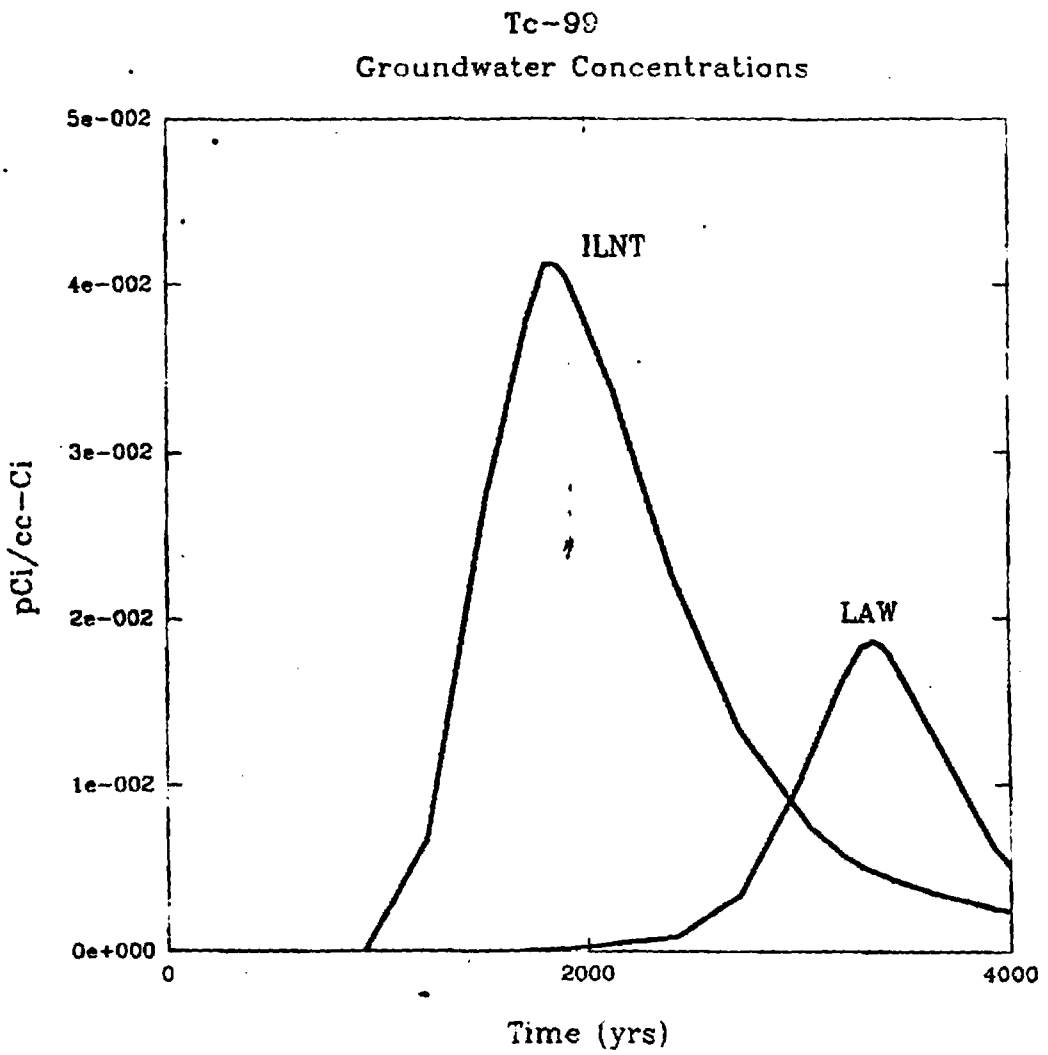

	Peak Concentration	Time (yrs)
LAW	1.90 e-002	3.30 e+003
ILNT	4.10 e-002	1.80 e+003

tc99.spg

Fig. C.5-6. Predicted groundwater concentration of Tc-99 as a function of time.

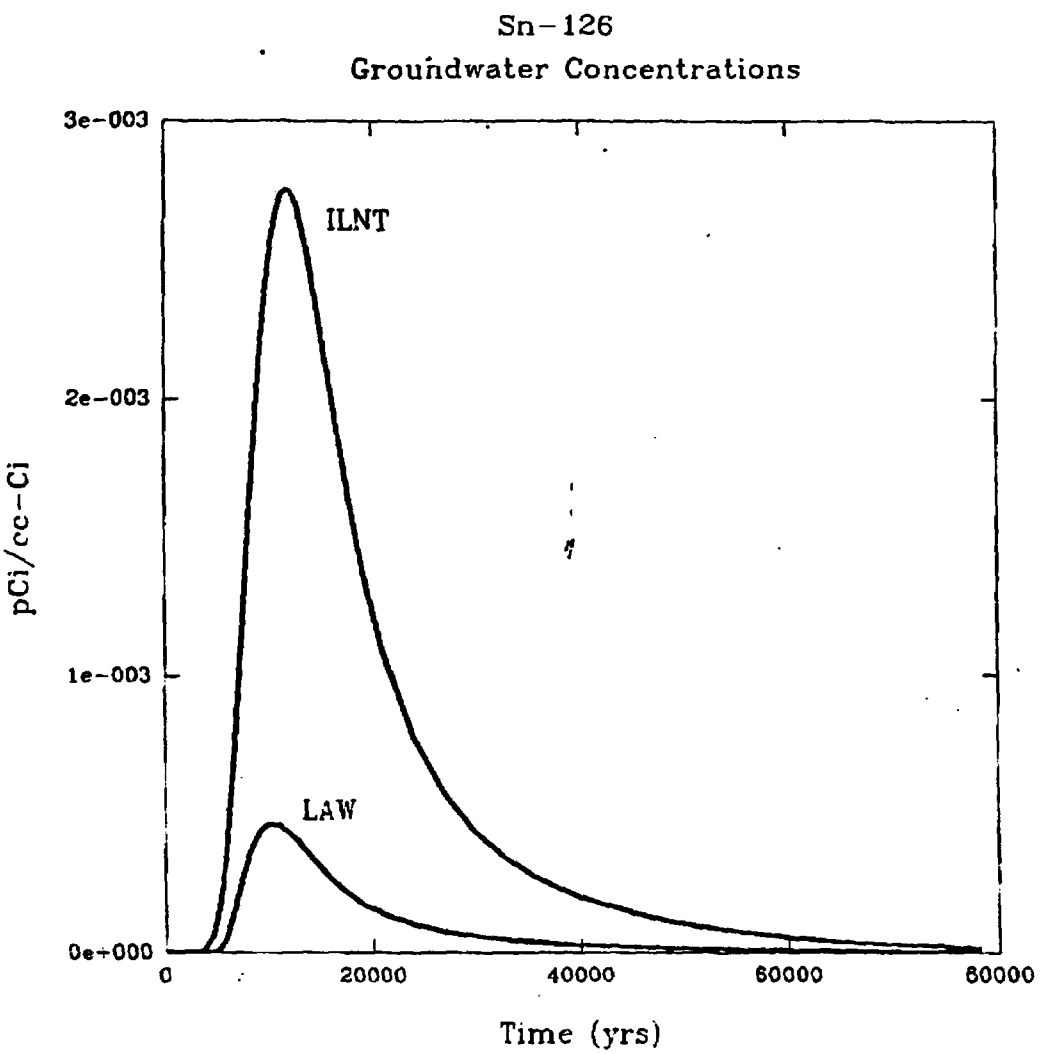

	Peak Concentration	Time (yrs)
LAW	4 70 e-004	1 00 e+004
ILNT	2 80 e-003	1 20 e+004

sn126 spg

Fig. C.5-7. Predicted groundwater concentration of Sn-126 as a function of time.

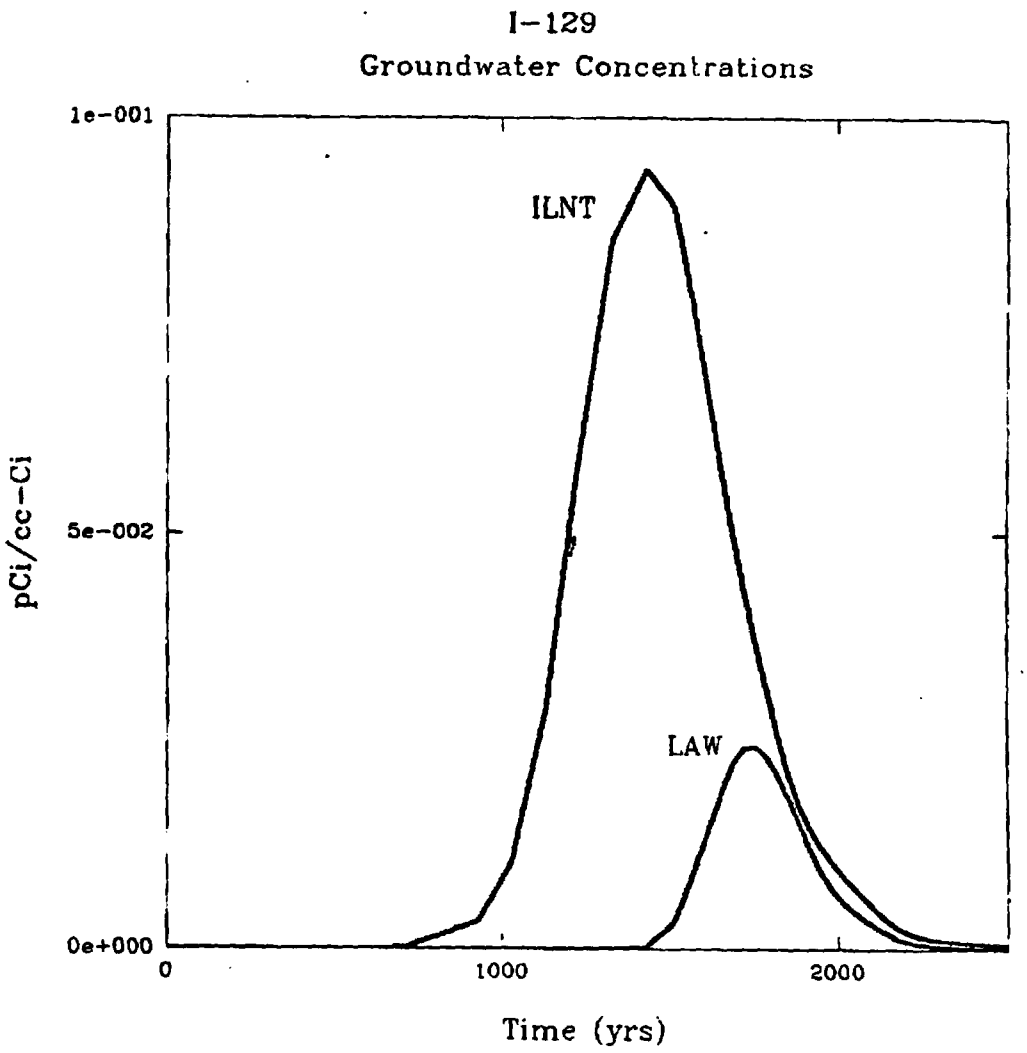

	Peak Concentration	Time (yrs)
LAW	2.40 e-002	1.70 e+003
ILNT	9.40 e-002	1.40 e-003

i129.spg

Fig. C.5-8. Predicted groundwater concentration of I-129 as a function of time.

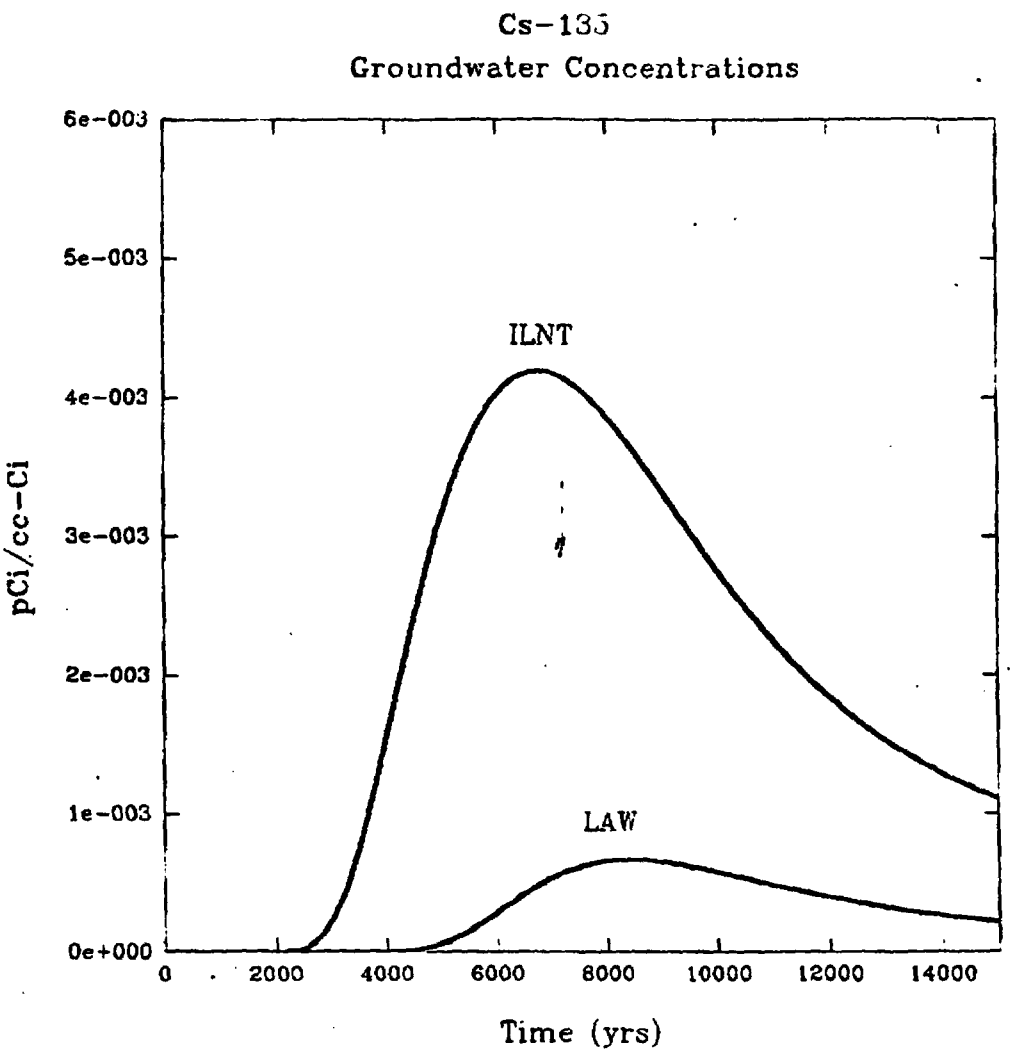

	Peak Concentration	Time (yrs)
LAW	6.70 e-004	8.40 e+003
ILNT	4.20 e-003	6.70 e+003

cs135.spg

Fig. C.5-9. Predicted groundwater concentration of Cs-135 as a function of time.

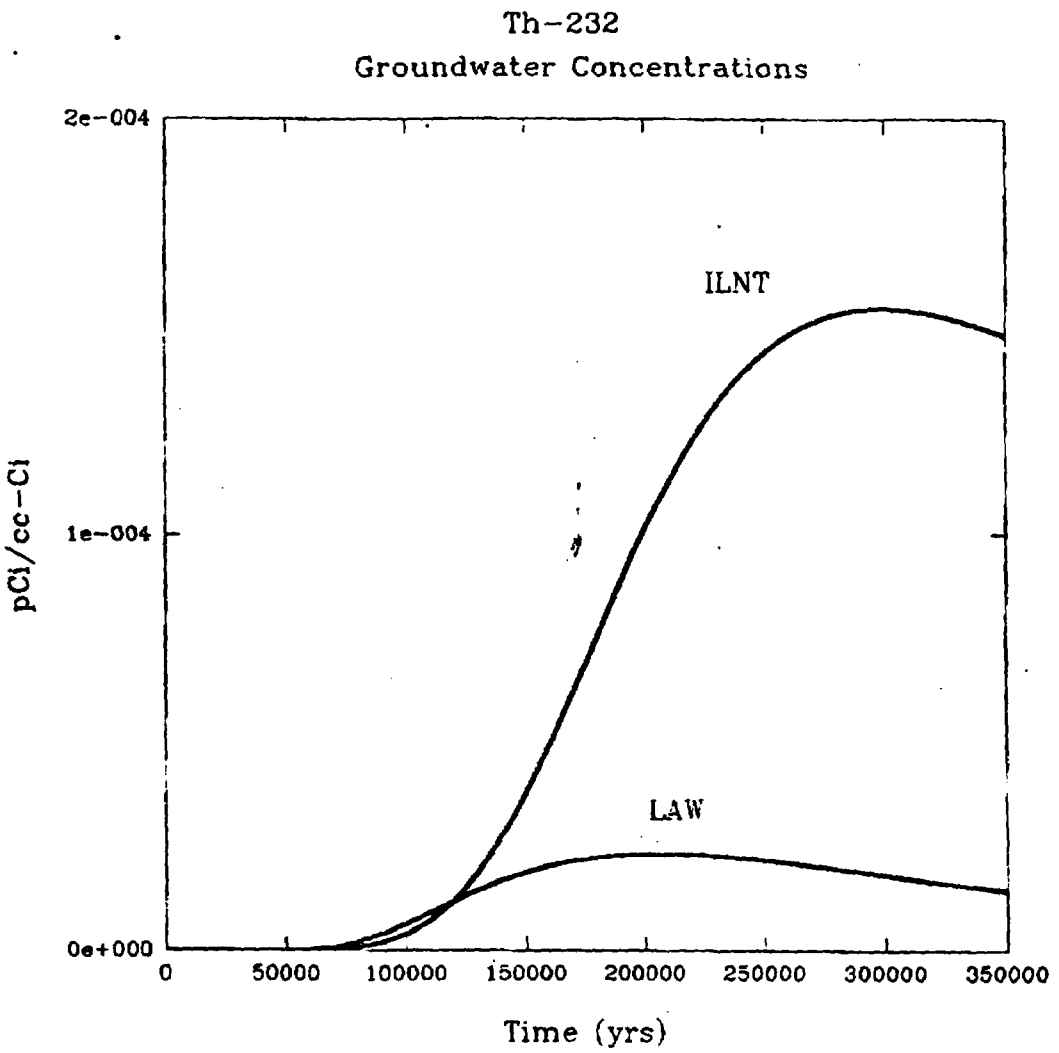

	Peak Concentration	Time (yrs)
LAW	2.30 e-005	2.10 e+005
ILNT	1.50 e-004	3.00 e+005

th232.spg

Fig. C.5-10. Predicted groundwater concentration of Th-232 as a function of time.

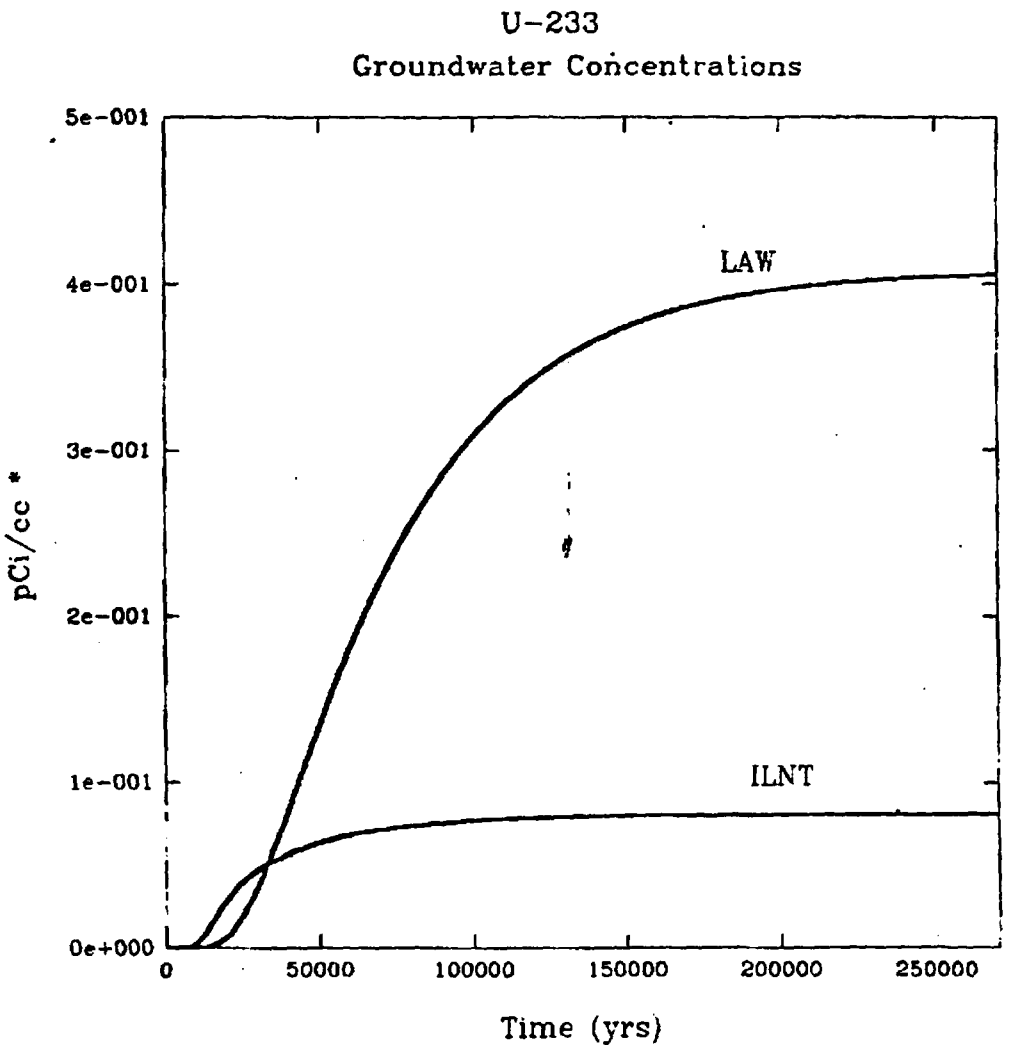

	Peak Concentration	Time (yrs)
LAW	4.10 e-001	2.61 e+005
ILNT	8.10 e-002	1.62 e+005

* Based on 10,000 kg U-233 per vault

u233.spg

Fig. C.5-11. Predicted groundwater concentration of U-233 as a function of time.

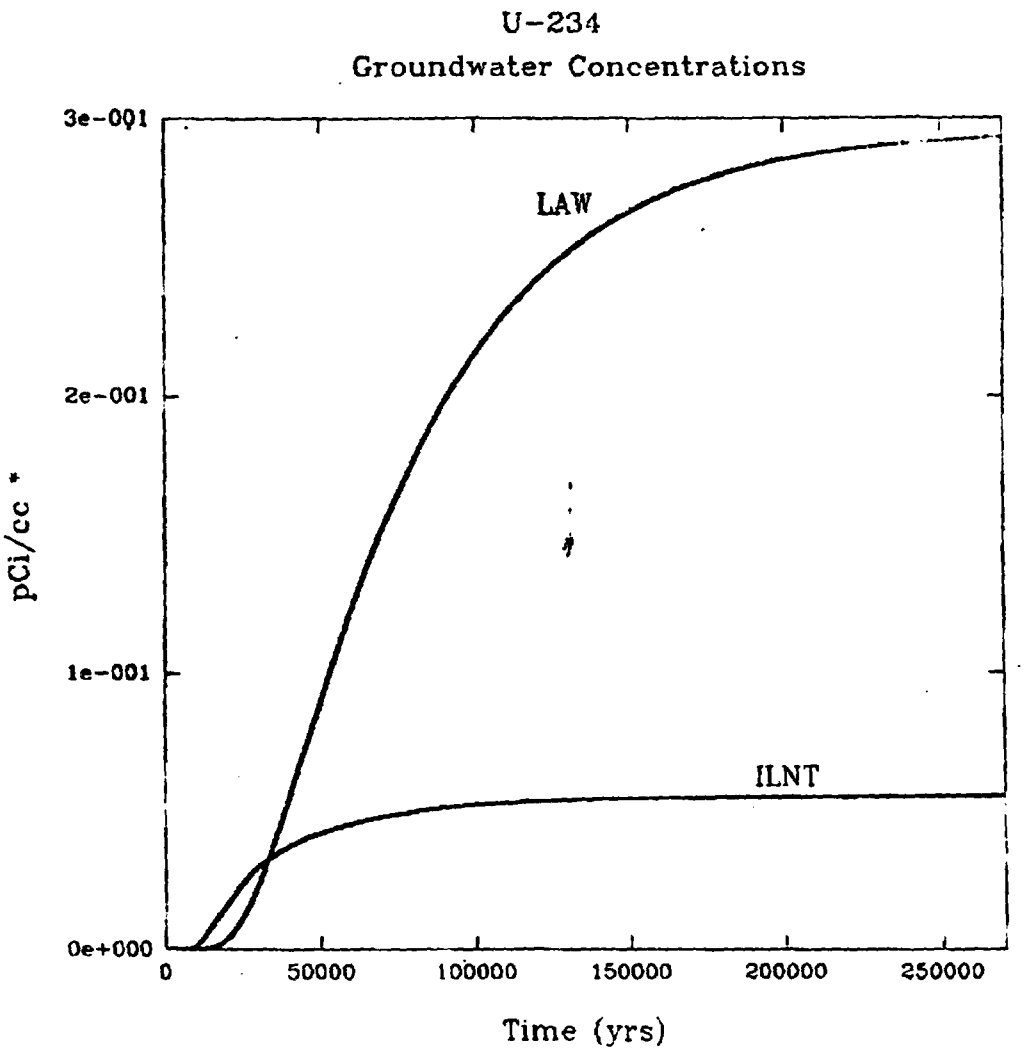

	Peak Concentration	Time (yrs)
LAW	2.90 e-001	2.01 e+005
ILNT	5.50 e-002	1.53 e+005

* Based on 10,000 kg U-234 per vault

u234.spg

Fig. C.5-12. Predicted groundwater concentration of U-234 as a function of time.

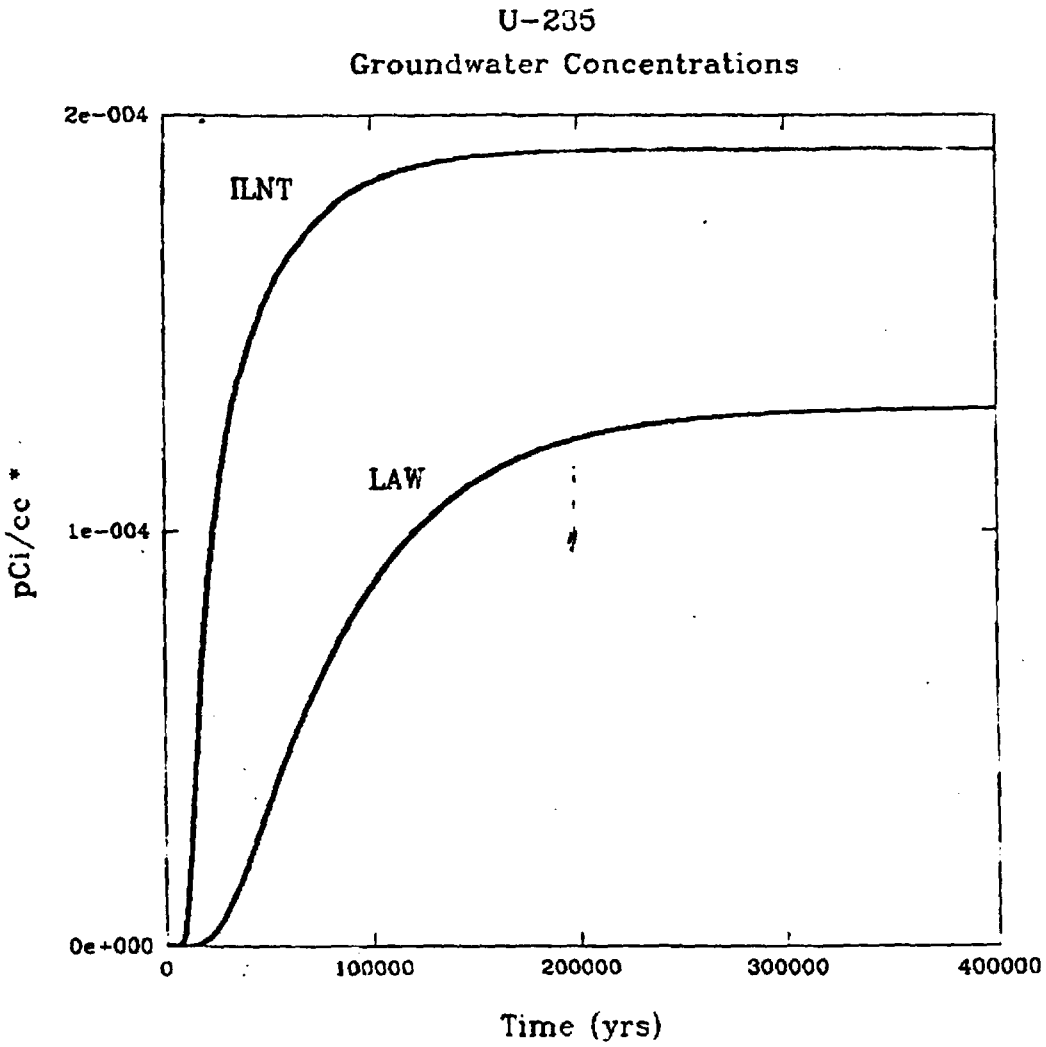

	Peak Concentration	Time (yrs)
LAW	1.30 e-004	2.30 e+005
ILNT	1.90 e-004	1.10 e+005

* Based on 10,000 kg U-235 per vault

U235.SPG

Fig. C.5-13. Predicted groundwater concentration of U-235 as a function of time.

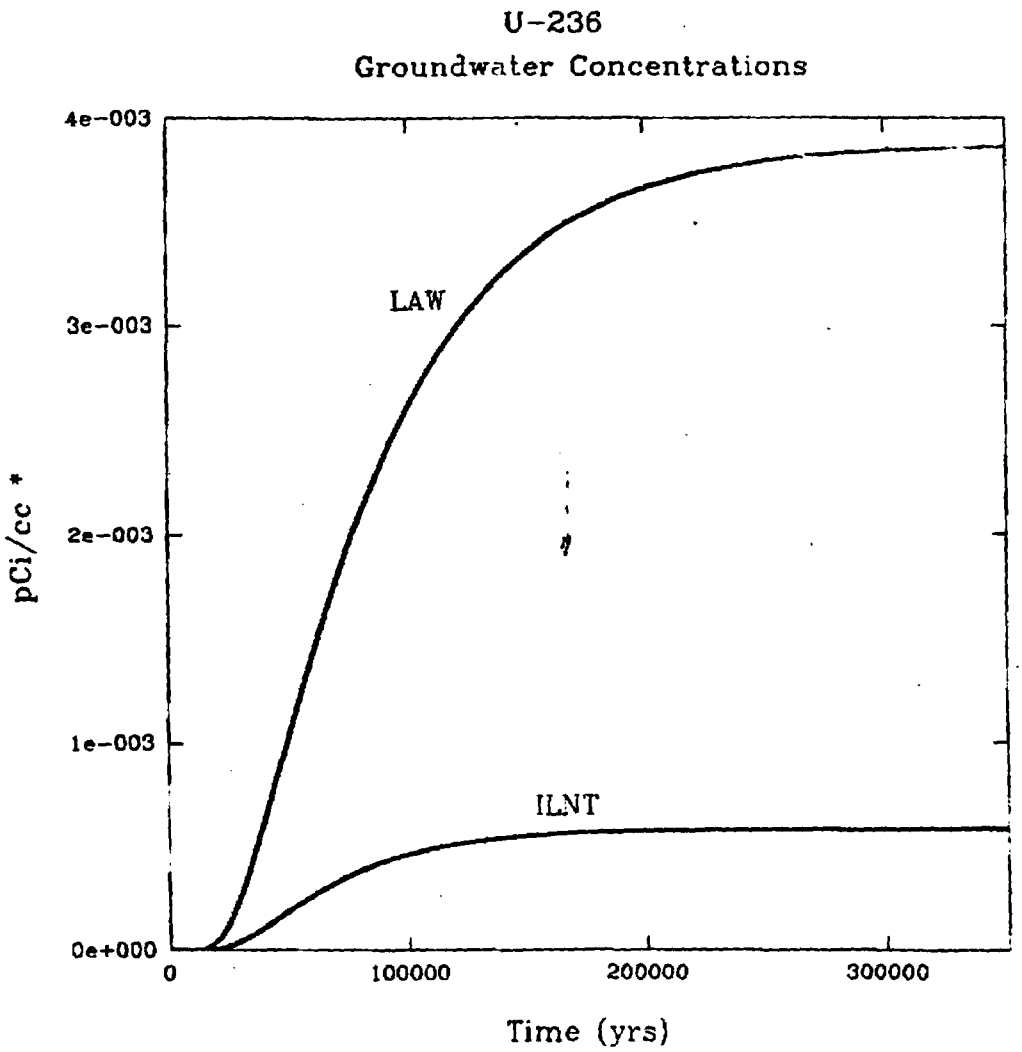

	Peak Concentration	Time (yrs)
LAW	3.90 e-003	3.24 e+005
ILNT	5.80 e-004	2.28 e+005

* Based on 10,000 kg U-236 per vault

u236.spg

Fig. C.5-14. Predicted groundwater concentration of U-236 as a function of time.

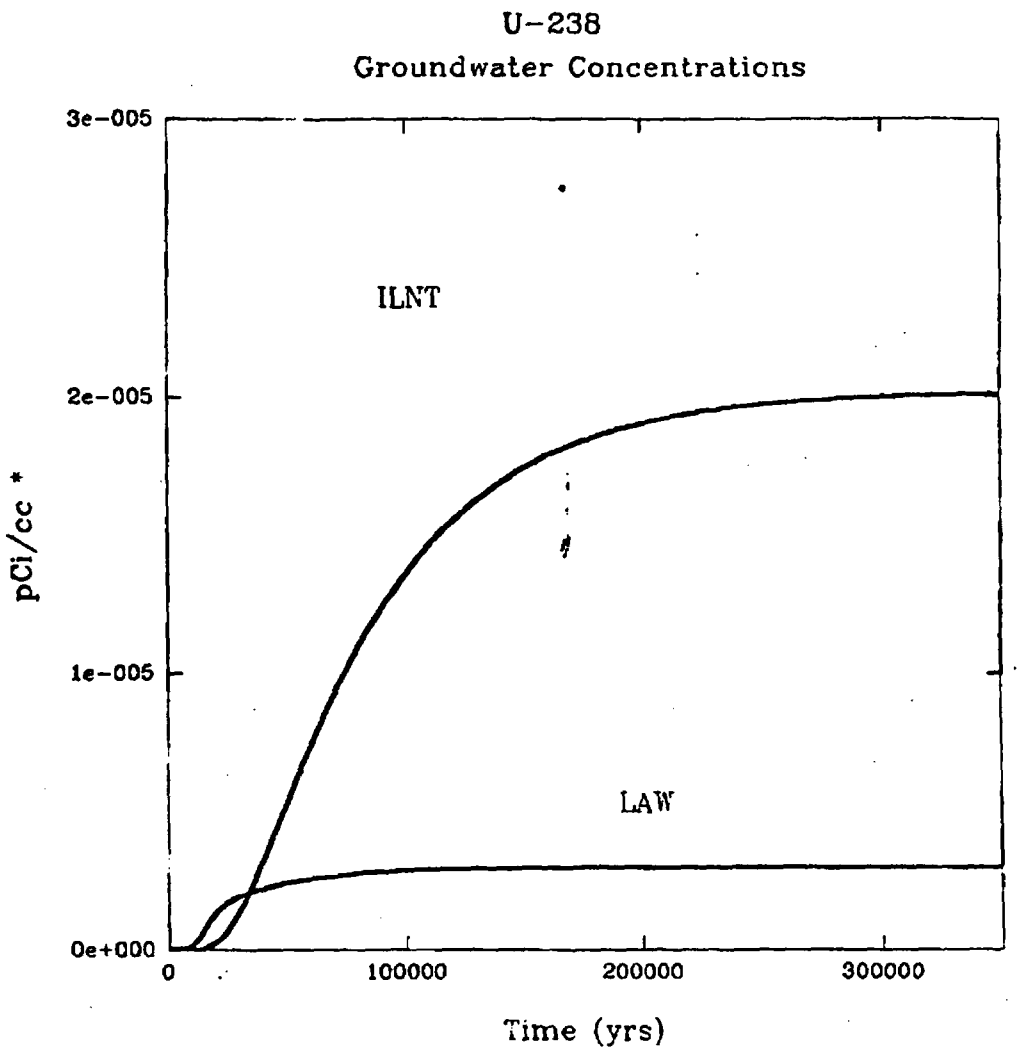

	Peak Concentration	Time (yrs)
LAW	2.00 e-005	2.31 e+005
ILNT	3.00 e-006	1.44 e+005

* Based on 10,000 kg U-238 per vault

u238.spg

Fig. C.5-15. Predicted groundwater concentration of U-238 as a function of time.

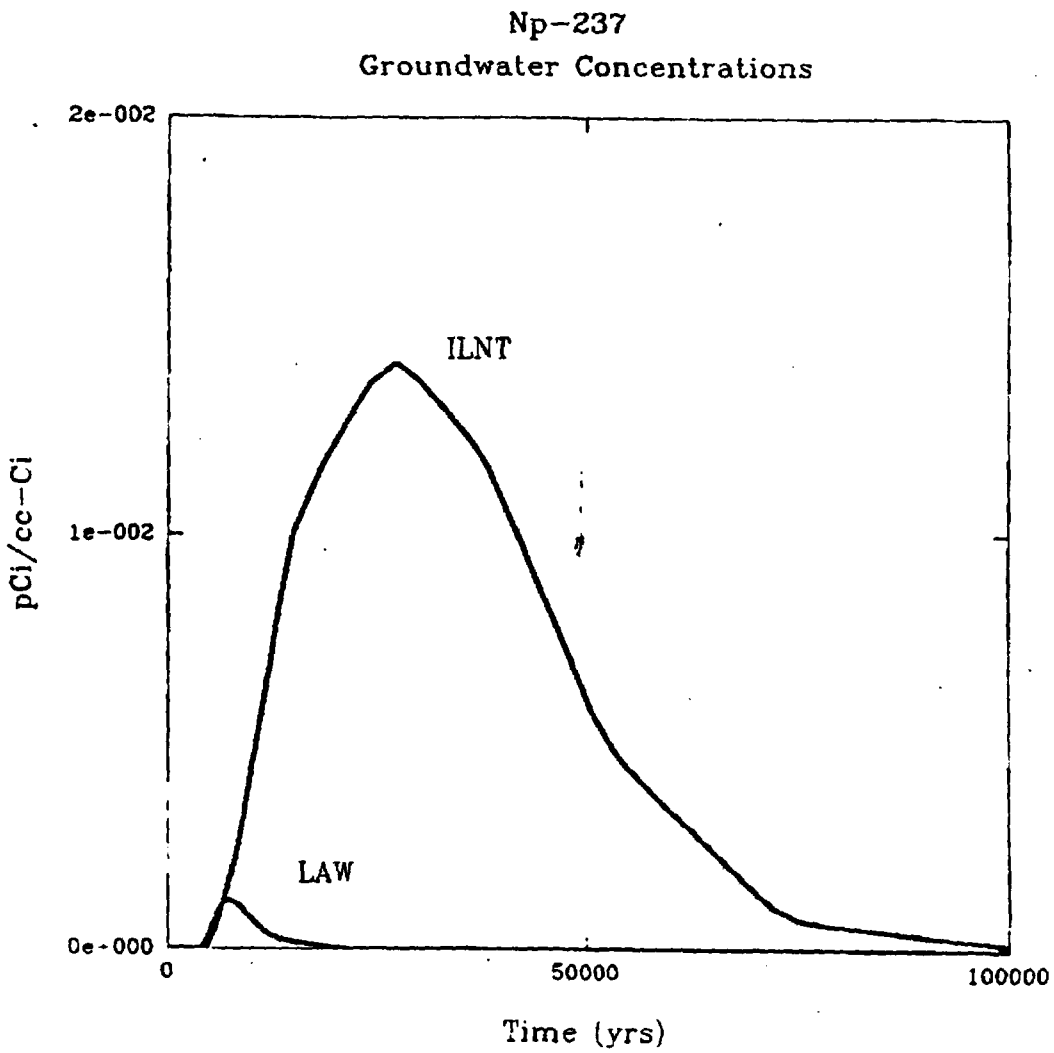

	Peak Concentration	Time (yrs)
LAW	1.60 e-003	1.00 e+004
ILNT	1.40 e-002	2.70 e+004

np237.spg

Fig. C.5-16. Predicted groundwater concentration of Np-237 as a function of time.

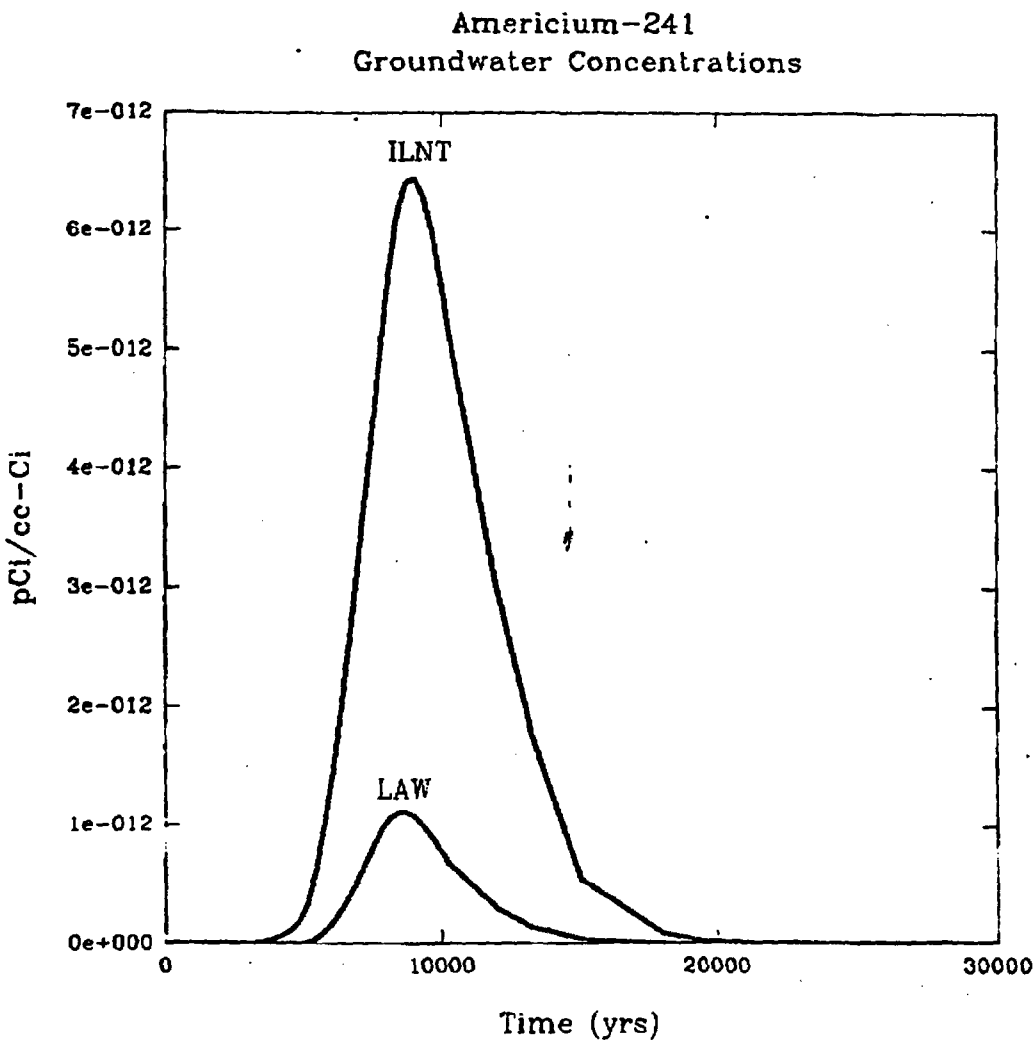

	Peak Concentration	Time (yrs)
LAW	1.10 e-012	8.70 e+003
ILNT	6.40 e-012	9.00 e+003

* Without radioactive daughter contributions.

am241.spg

Fig. C.5-17. Predicted groundwater concentration of Am-241 as a function of time.

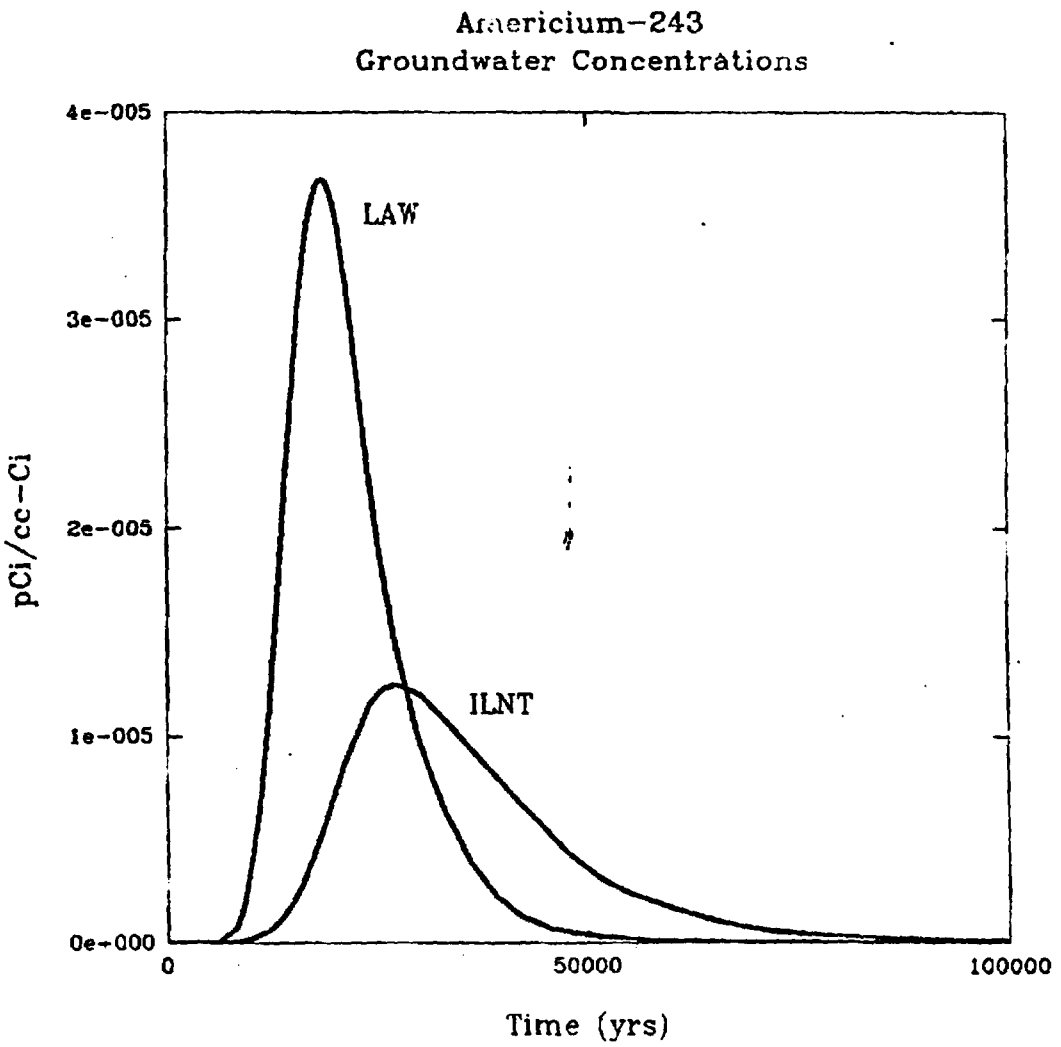

	Peak Concentration	Time (yrs)
LAW	3.70 e-005	1.80 e+004
ILNT	1.20 e-005	2.70 e+004

am243.spg

Fig. C.5-18. Predicted groundwater concentration of Am-243 as a function of time.

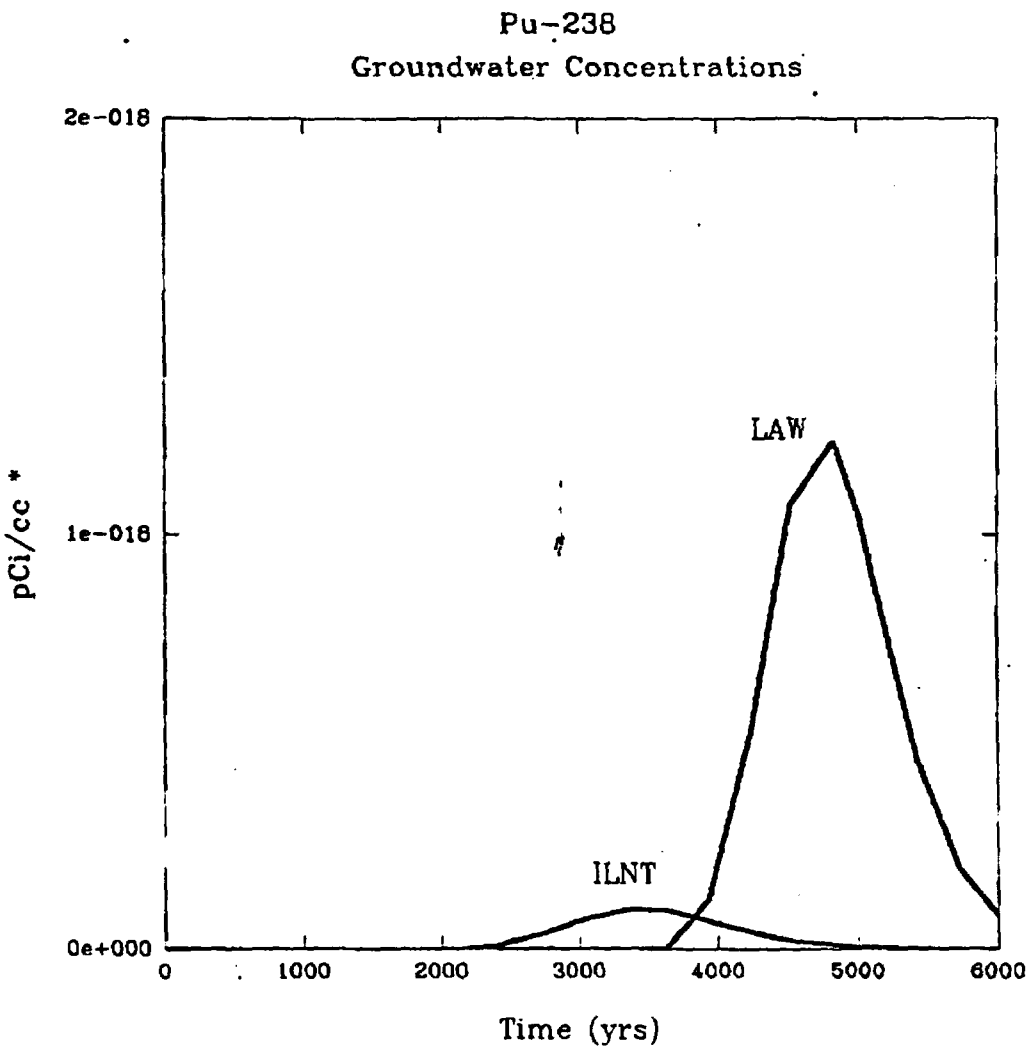

	Peak Concentration	Time (yrs)
LAW	1.20 e-018	4.83 e+003
ILNT	9.70 e-020	3.33 e+003

* Based on 150 Ci Pu-238 per vault

pu238.spg

Fig. C.5-19. Predicted groundwater concentration of Pu-238 as a function of time.

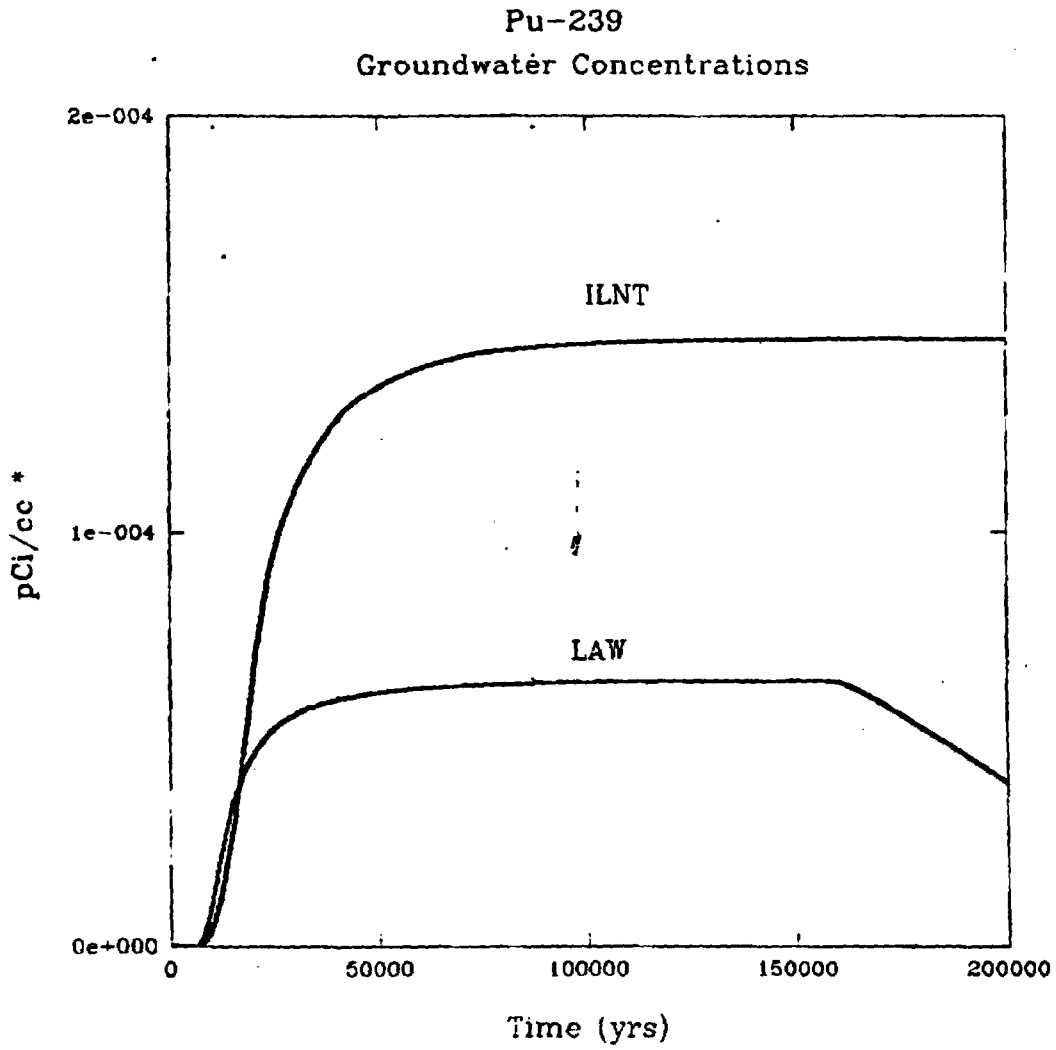

	Peak Concentration	Time (yrs)
LAW	6.40 e-005	1.60 e+005
ILNT	1.50 e-004	2.20 e+005

* Based on 150 Ci Pu-239 per vault

Fig. C.5-20. Predicted groundwater concentration of Pu-239 as a function of time.

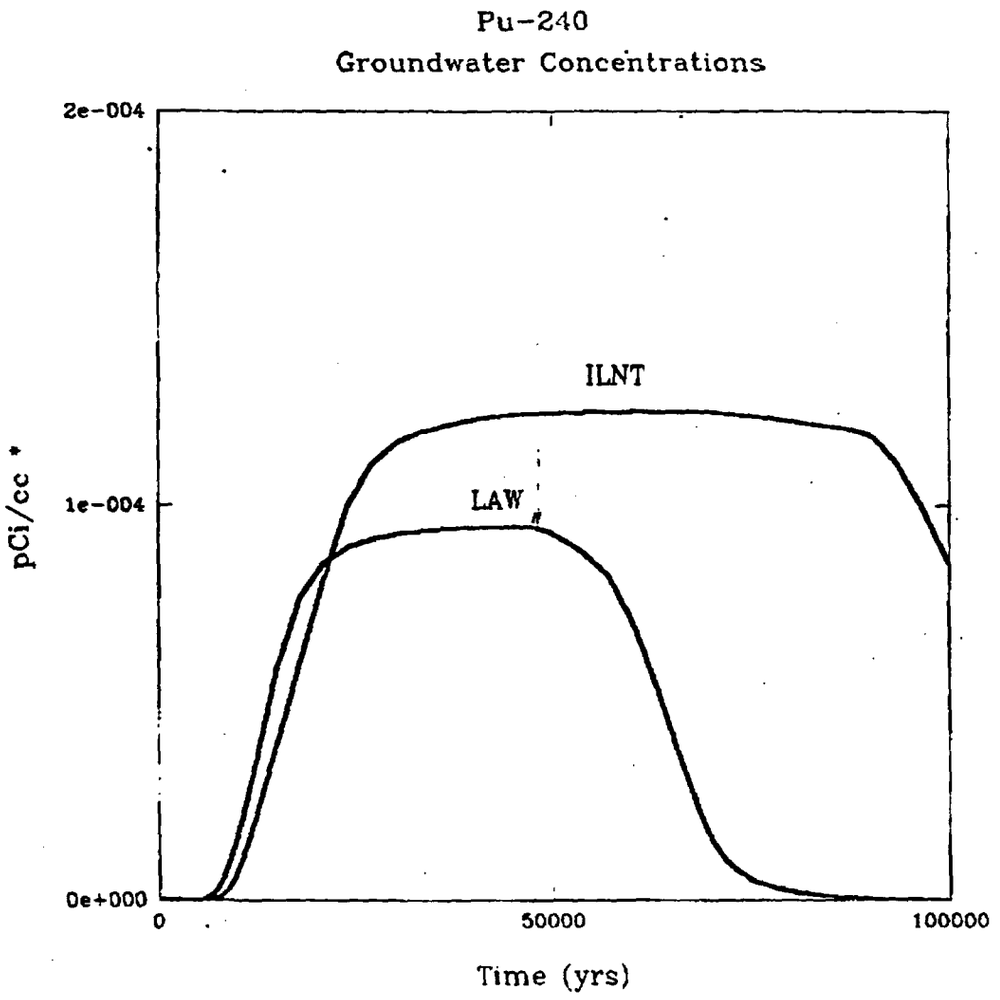

	Peak Concentration	Time (yrs)
LAW	9.50 e-005	4.50 e+004
ILNT	1.20 e-004	6.60 e+004

* Based on 150 Ci Pu-240 per vault

Fig. C.5-21. Predicted groundwater concentration of Pu-240 as a function of time.

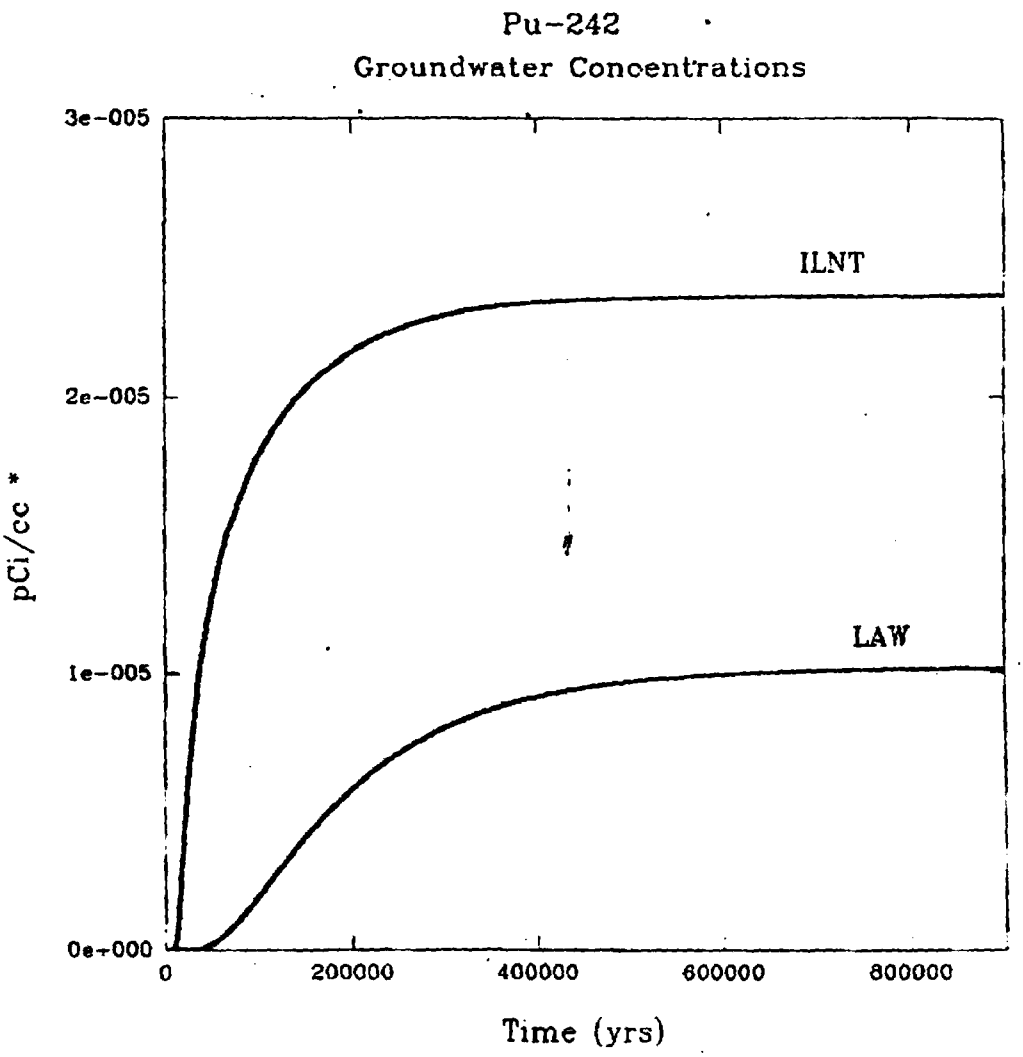

	Peak Concentration	Time (yrs)
LAW	1.00 e-005	6.15 e+005
ILNT	2.40 e-005	4.98 e+005

* Based on 150 Ci Pu-242 per vault

Fig. C.5-22. Predicted groundwater concentration of Pu-242 as a function of time.

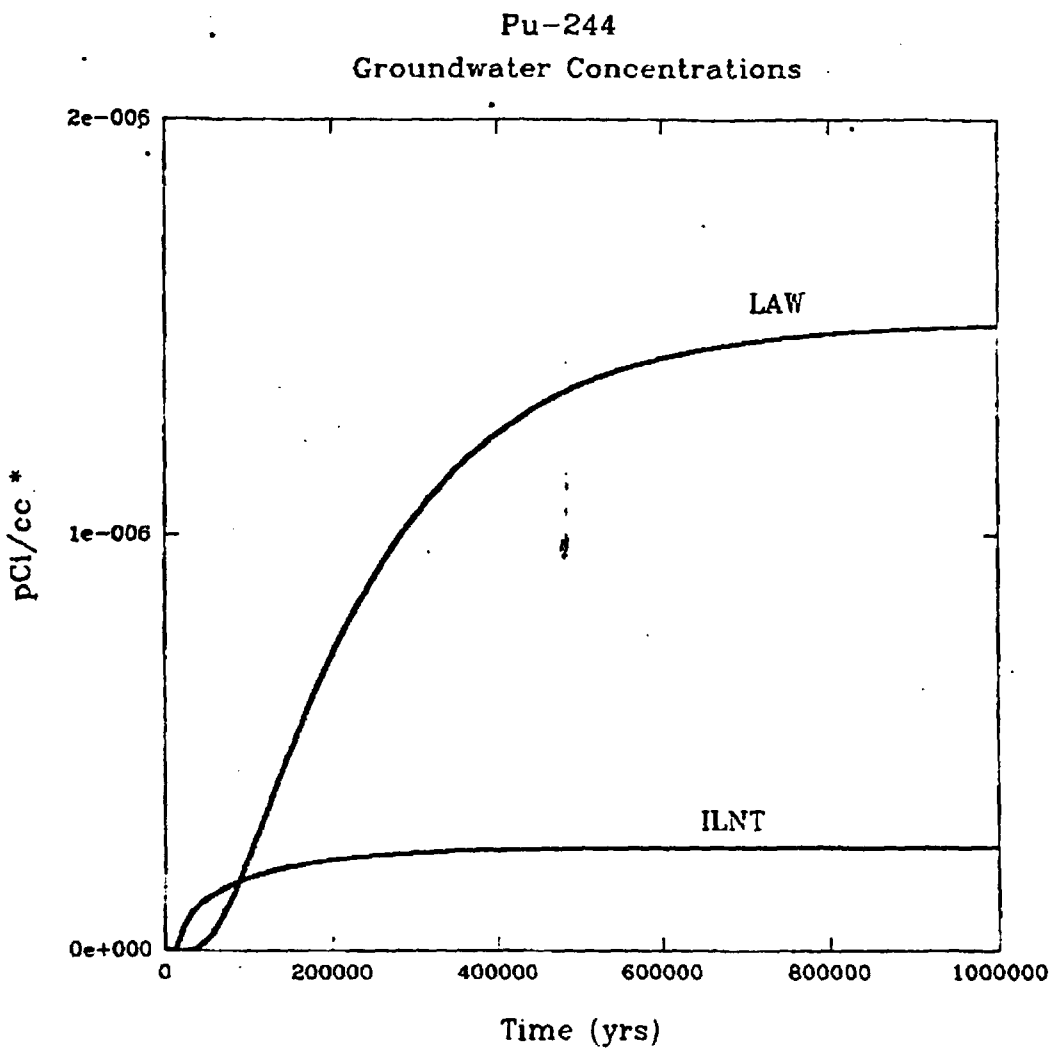

	Peak Concentration	Time (yrs)
LAW	1.50 e-006	6.60 e+005
ILNT	2.50 e-007	4.08 e+005

* Based on 150 Ci Pu-244 per vault

Fig. C.5-23. Predicted groundwater concentration of Pu-244 as a function of time.

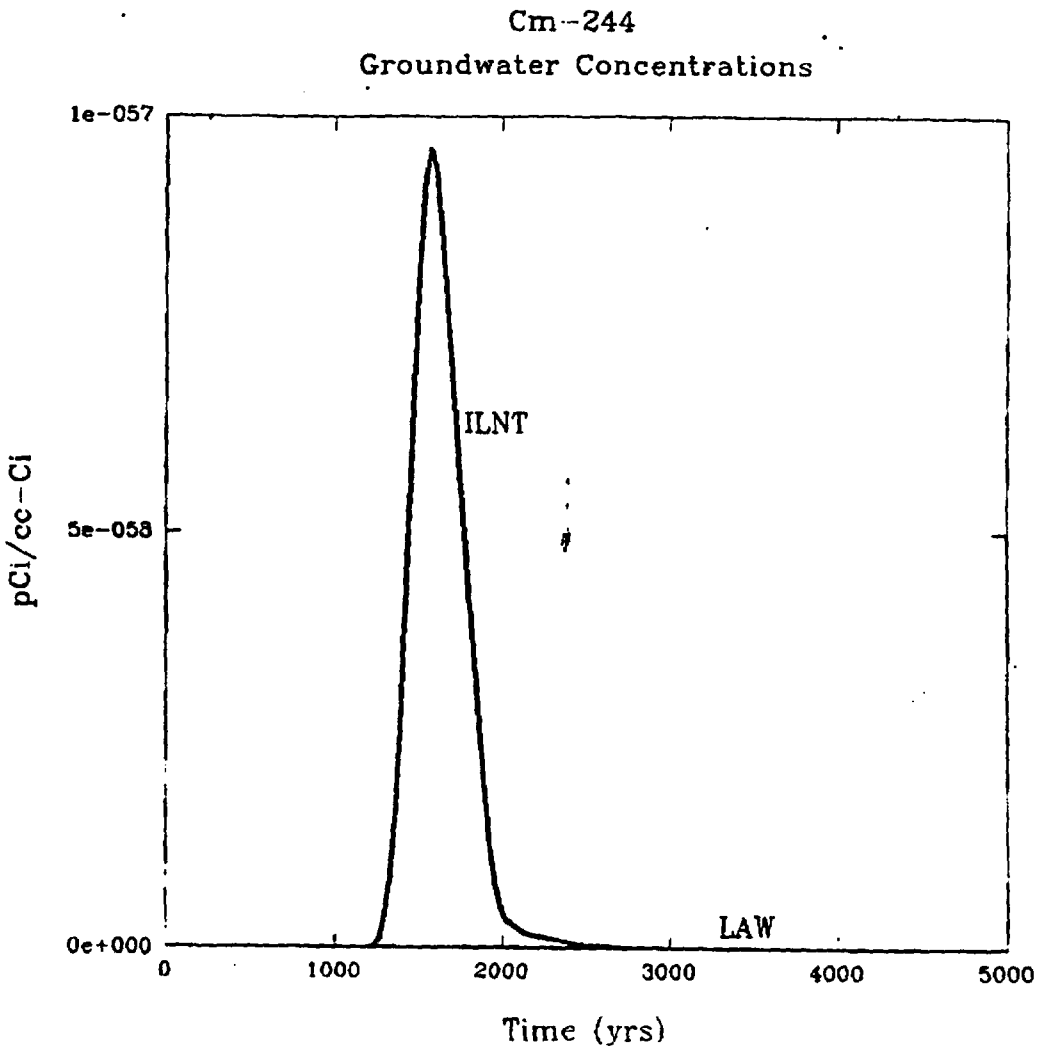

	Peak Concentration	Time (yrs)
LAW	1.10 e-066	7.30 e+002
ILNT	9.60 e-058	1.60 e+003

cm244.spg

Fig. C.5-24. Predicted groundwater concentration of Cm-244 as a function of time.

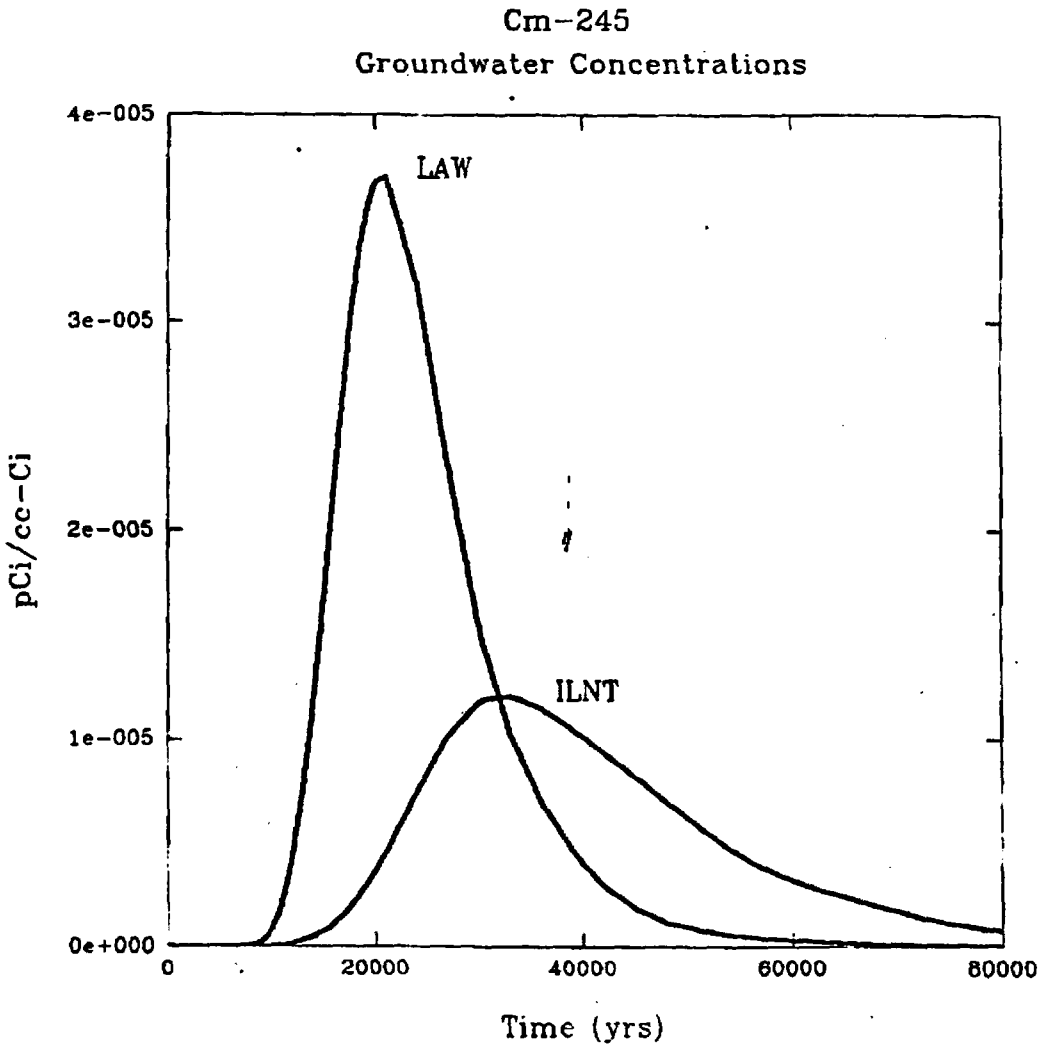

	Peak Concentration	Time (yrs)
LAW	3.70 e-005	2.10 e+004
ILNT	1.20 e-005	3.30 e+004

cm245.spg

Fig. C.5-25. Predicted groundwater concentration of Cm-245 as a function of time.

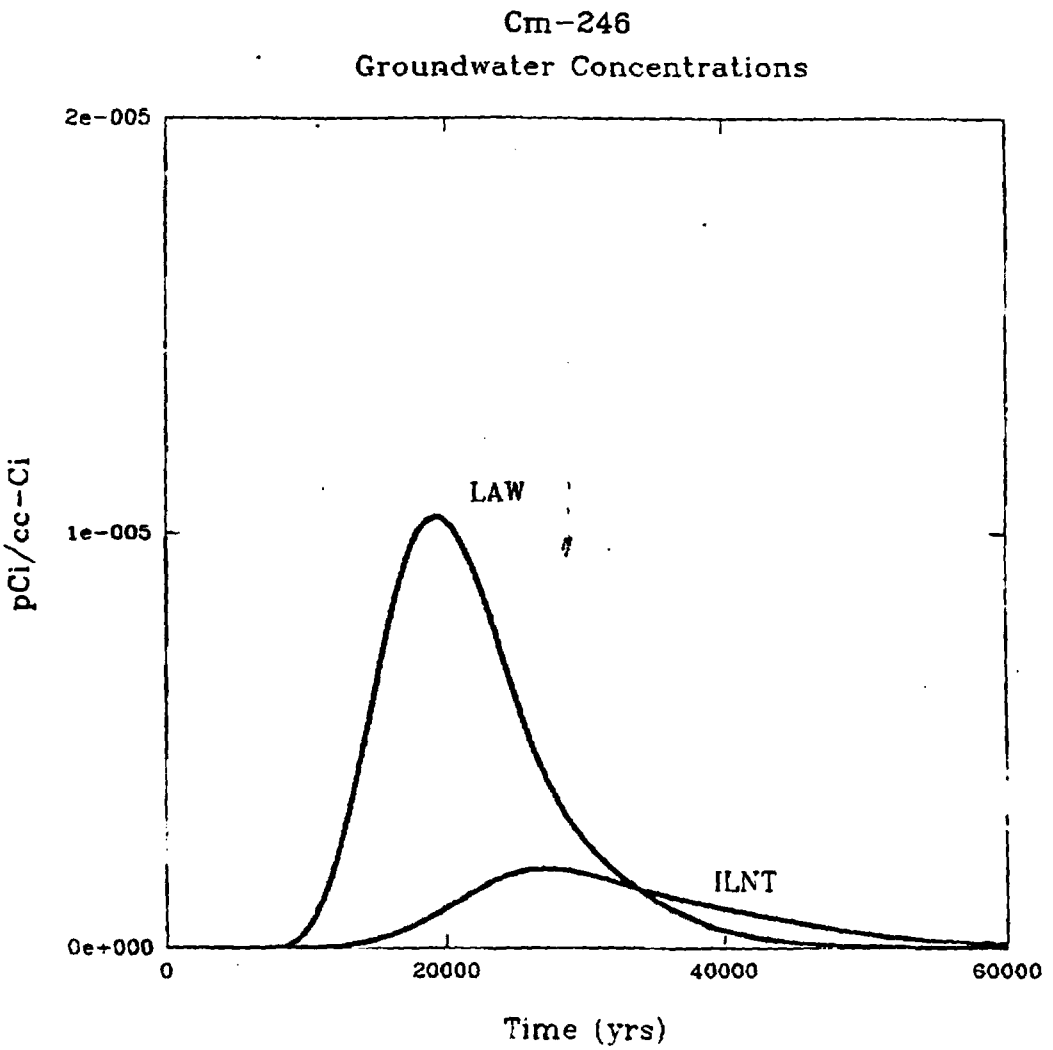

	Peak Concentration	Time (yrs)
LAW	1.00 e-005	2.00 e+004
ILNT	1.90 e-006	2.70 e+004

cm246.spg

Fig. C.5-26. Predicted groundwater concentration of Cm-246 as a function of time.

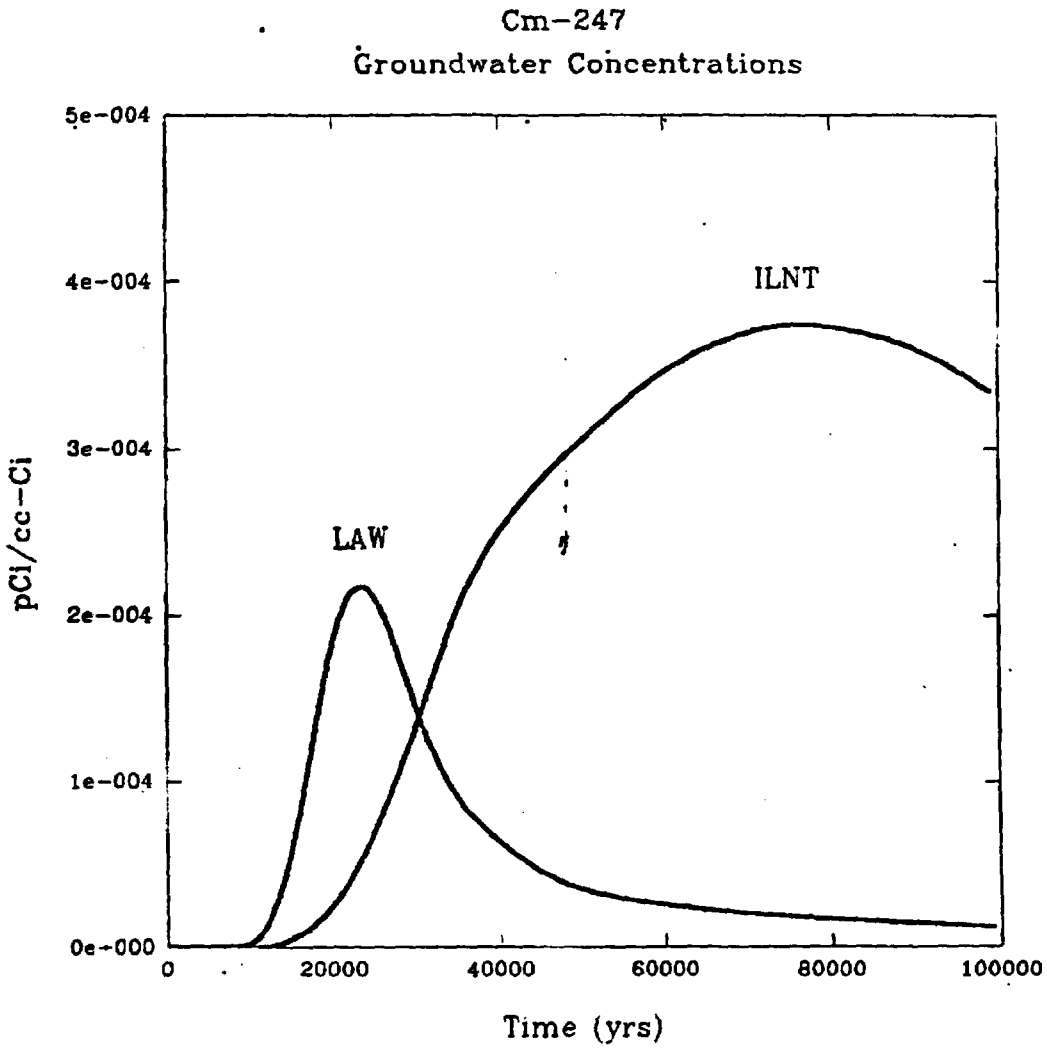

	Peak Concentration	Time (yrs)
LAW	2.20 e-004	2.30 e+004
ILNT	3.70 e-004	7.60 e+004

cm247.spg

Fig. C.5-27. Predicted groundwater concentration of Cm-247 as a function of time.

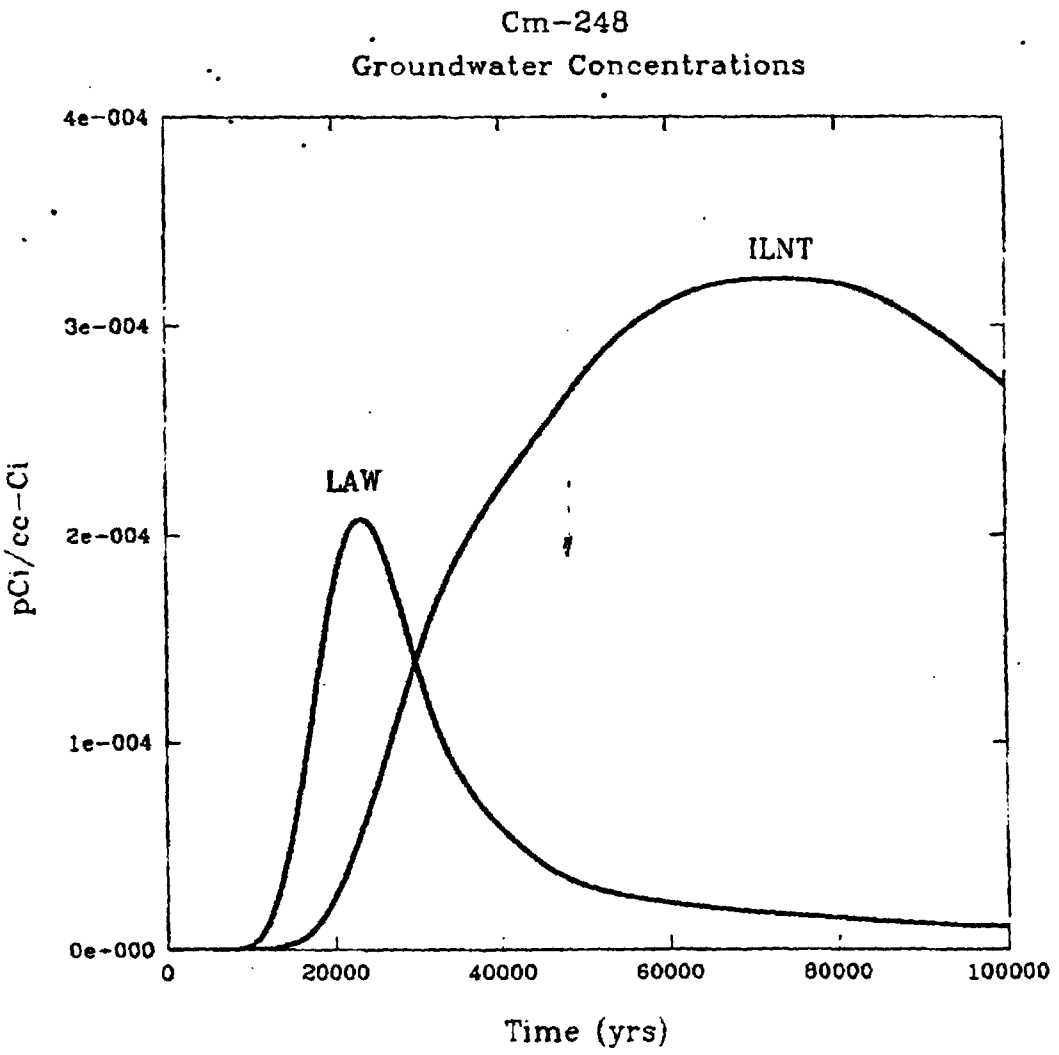

	Peak Concentration	Time (yrs)
LAW	2.10 e-004	2.30 e+004
ILNT	3.20 e-004	7.20 e+004

* Without radioactive daughter contributions.

cm248.spg

Fig. C.5-28. Predicted groundwater concentration of Cm-248 as a function of time.

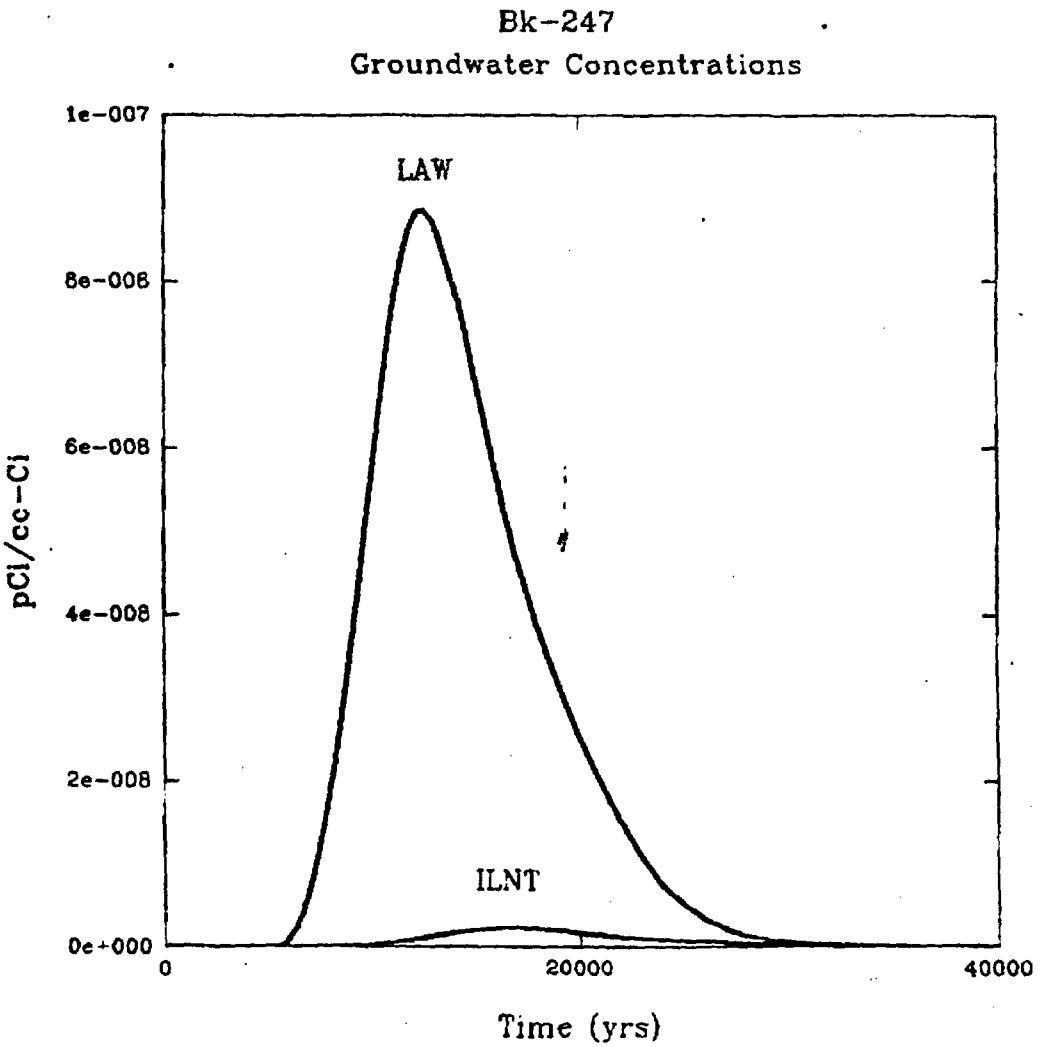

	Peak Concentration	Time (yrs)
LAW	8.90 e-008	1.30 e+004
ILNT	4.40 e-009	1.60 e+004

bk247.spg

Fig. C.5-29. Predicted groundwater concentration of Bk-247 as a function of time.

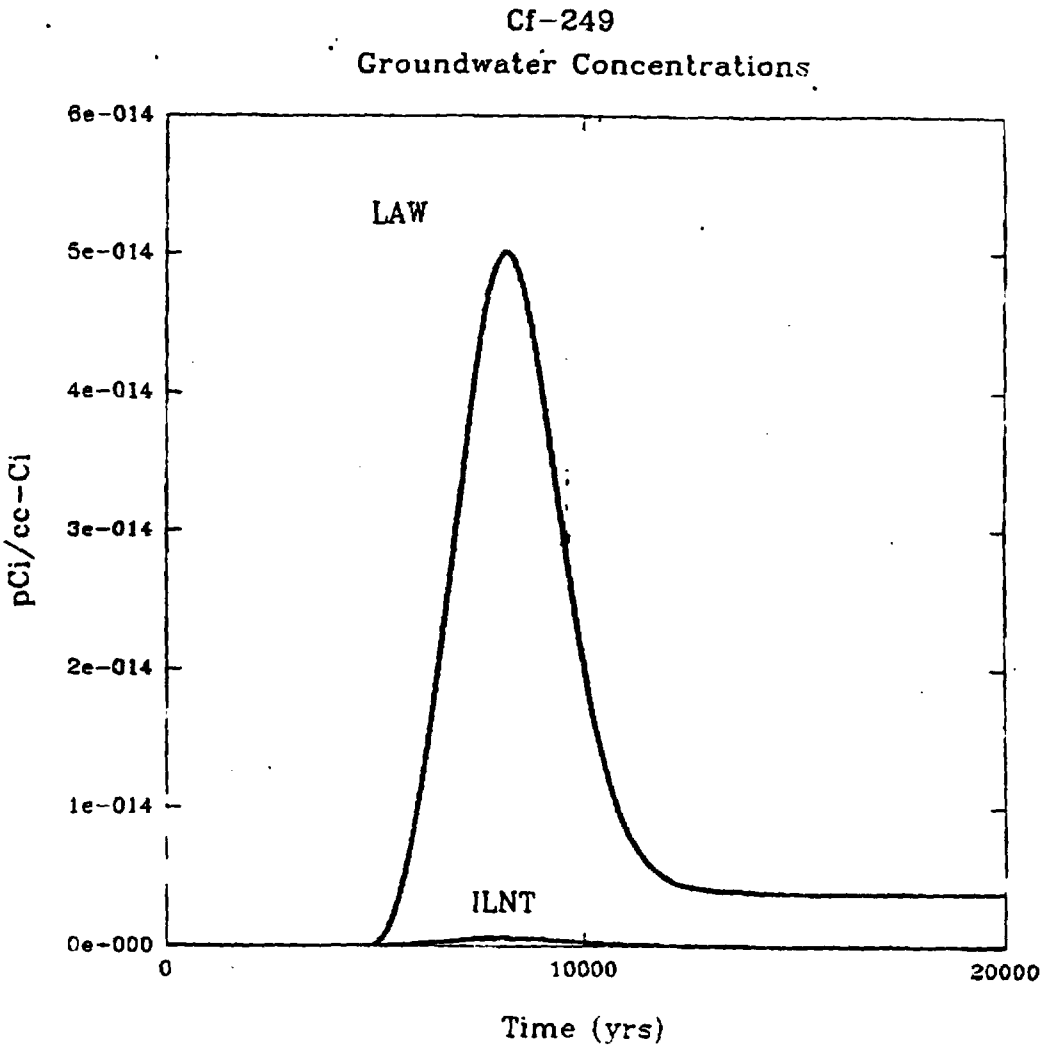

	Peak Concentration	Time (yrs)
LAW	5.00 e-014	8.10 e+003
ILNT	5.90 e-016	7.90 e+003

cf249.spg

Fig. C.5-30. Predicted groundwater concentration of Cf-249 as a function of time.

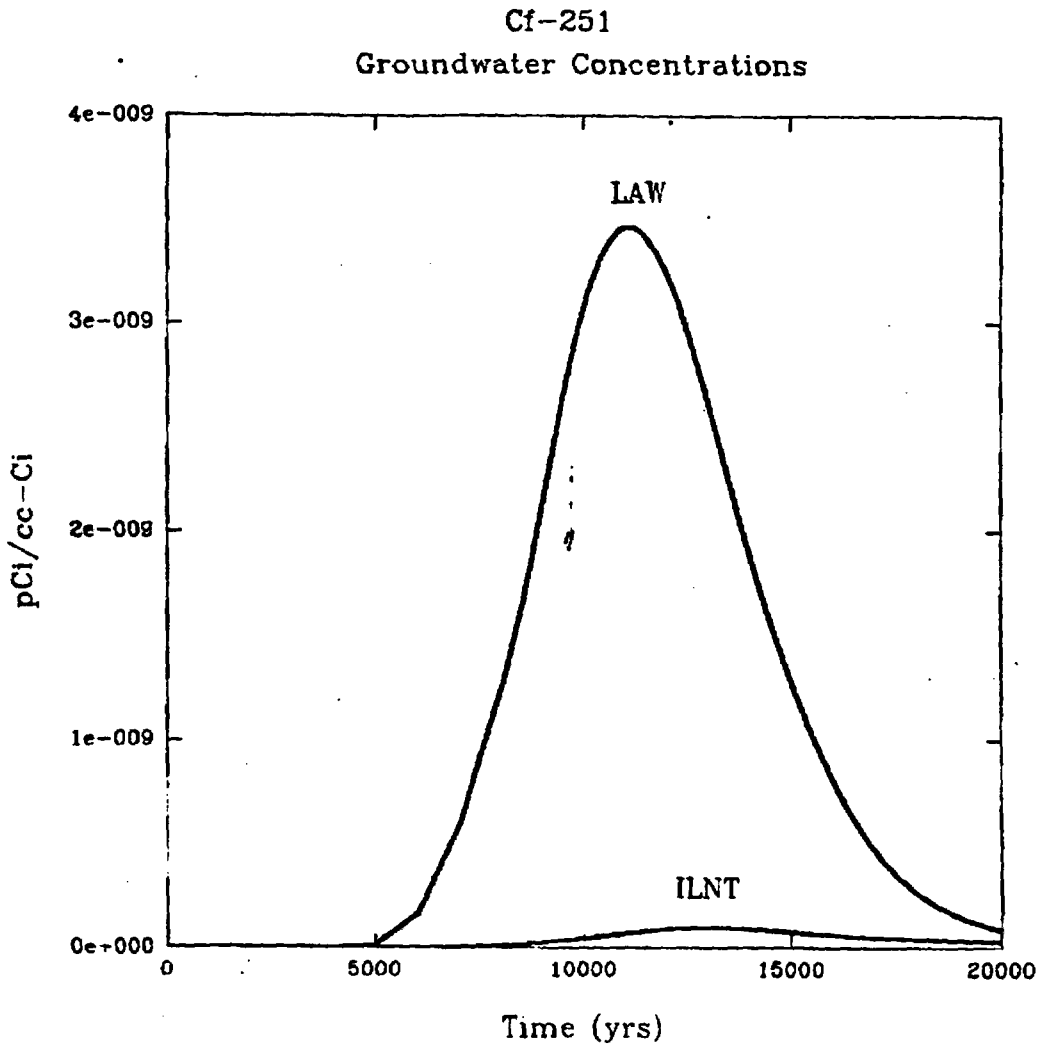

	Peak Concentration	Time (yrs)
LAW	3.50 e-009	1.10 e+004
ILNT	9.40 e-011	1.30 e+004

cf251.spg

Fig. C.5-31. Predicted groundwater concentration of Cf-251 as a function of time.

C.6 ATMOSPHERIC TRANSPORT

The atmospheric transport and dose results are given in Table C.6-1.

Table C.6-1. AIRDOS-PC data for the volatile radionuclide pathway

FREQUENCIES OF WIND DIRECTIONS AND TRUE-AVERAGE WIND SPEEDS

WIND TOWARD	FREQUENCY	WIND SPEEDS FOR EACH STABILITY CLASS (METERS/SEC)						
		A	B	C	D	E	F	G
N	0.089	1.77	2.21	3.56	4.14	3.08	1.71	0.77
NNW	0.048	1.93	2.08	3.04	3.76	2.87	1.65	0.77
NW	0.084	1.95	2.34	3.24	3.69	3.03	1.72	0.77
WNW	0.043	1.85	2.35	3.25	3.64	2.71	1.59	0.77
W	0.052	2.00	2.40	3.55	3.60	2.74	1.69	0.77
WSW	0.041	2.09	2.21	3.12	3.21	2.87	1.73	0.77
SW	0.056	2.39	2.46	3.57	3.79	3.23	1.80	0.77
SSW	0.052	1.49	2.23	3.48	3.88	3.31	1.47	0.77
S	0.068	2.08	2.28	3.36	3.41	3.05	1.68	0.77
SSE	0.049	1.65	2.36	3.54	3.34	3.06	2.02	0.77
SE	0.058	1.87	2.21	3.56	4.39	3.44	1.94	0.77
ESE	0.060	2.42	2.85	3.86	5.71	4.02	1.96	0.77
E	0.101	1.93	2.54	4.15	5.82	3.95	1.88	0.77
ENE	0.080	2.39	2.35	3.98	4.97	3.57	1.91	0.77
NE	0.072	2.09	2.65	4.00	4.65	3.25	1.63	0.77
NNE	0.049	2.35	2.67	3.52	4.42	3.28	1.68	0.77

FREQUENCY OF ATMOSPHERIC STABILITY CLASSES FOR EACH DIRECTION

SECTOR	FRACTION OF TIME IN EACH STABILITY CLASS						
	A	B	C	D	E	F	G
N	0.0043	0.0560	0.0920	0.3666	0.1142	0.1839	0.1831
NNW	0.0110	0.0664	0.0922	0.3408	0.1281	0.1663	0.1953
NW	0.0162	0.1169	0.0898	0.3789	0.1055	0.1513	0.1415
WNW	0.0105	0.1247	0.1462	0.4085	0.1026	0.1092	0.0982
W	0.0176	0.1525	0.1478	0.3968	0.0690	0.1192	0.0971
WSW	0.0090	0.1421	0.1606	0.4678	0.0719	0.0814	0.0673
SW	0.0109	0.1324	0.1330	0.4765	0.0975	0.0915	0.0582
SSW	0.0103	0.1296	0.1377	0.5041	0.0745	0.0725	0.0714
S	0.0113	0.1266	0.1486	0.4282	0.0762	0.1303	0.0789
SSE	0.0201	0.1049	0.1135	0.2989	0.1086	0.2111	0.1429
SE	0.0040	0.0892	0.1217	0.3122	0.1215	0.2218	0.1297
ESE	0.0038	0.0666	0.1185	0.4218	0.1329	0.1122	0.1440
E	0.0053	0.0545	0.1103	0.4107	0.1405	0.1257	0.1530
ENE	0.0037	0.0797	0.1222	0.3300	0.1316	0.1669	0.1658
NE	0.0052	0.0761	0.1172	0.3445	0.0918	0.1541	0.2112
NNE	0.0016	0.0644	0.0822	0.3732	0.1302	0.1622	0.1863

Table C.6-1. (continued)

CLEAN AIR ACT COMPLIANCE REPORT 12/28/93 10:57 AM

Facility: ILT H-3 crucibles
Address: City: State:
Comments: H-3 releases to the off-site individual for ILT crucible vaults.
Year:

	Dose Equivalent Rates to Nearby Individuals (mrem/year)
Effective Dose Equivalent	0.0580
Highest Organ Dose is to REMAINDER	0.0680

EMISSION INFORMATION

Radio-nuclide	Class	Amad	Stack #1 (Ci/y)
H-3	*	0.0	2.6E+02
Stack Height (m)			1.00
Stack Diameter (m)			0.03
Buoyant (cal/s)			0.0E-01

SITE INFORMATION

Wind Data	AGS1018.WND	Temperature (C)	20
Food Source	LOCAL	Rainfall (cm/y)	100
Distance to Individuals (m)	5000	Lid Height (m)	1000

*NOTE: The results of this computer model are dose estimates. They are only to be used for the purpose of determining compliance and reporting per 40 CFR 61.93 and 40 CFR 61.94.

Table C.6-1. (continued)

CLEAN AIR ACT COMPLIANCE REPORT 2/ 9/94 10:40 AM

Facility: ILT Vaults JCW
Address: City: State:
Comments: H-3 releases to the off-site individual for the ILT vaults.
Year:

	Dose Equivalent Rates to Nearby Individuals (mrem/year)
Effective Dose Equivalent	2.46E-06
Highest Organ Dose is to REMAINDER	2.90E-06

EMISSION INFORMATION

Radio-nuclide	Class	Amad	Area #1 (Ci/y)
H-3	*	0.0	1.1E-02
Total Area (m**2)			6.4E+02

SITE INFORMATION

Wind Data	AGS1016.WND	Temperature (C)	20
Food Source	LOCAL	Rainfall (cm/y)	100
Distance to Individuals (m)	5000	Lid Height (m)	1000

*NOTE: The results of this computer model are dose estimates. They are only to be used for the purpose of determining compliance and reporting per 40 CFR 61.93 and 40 CFR 61.94.

Table C.6-1. (continued)

CLEAN AIR ACT COMPLIANCE REPORT 2/ 9/94 10:43 AM

Facility: ILNT Vaults JCV
Address: City: State:
Comments: H-3 releases to the off-site individual for the ILNT vaults.
Year:

	Dose Equivalent Rates to Nearby Individuals (mrem/year)
Effective Dose Equivalent	4.47E-06
Highest Organ Dose is to REMAINDER	5.27E-06

EMISSION INFORMATION

Radio-nuclide	Class	Amad	Area #1 (Ci/y)
H-3	*	0.0	2.0E-02
Total Area (m**2)			8.7E+03

SITE INFORMATION

Wind Data	AGS1018.WND	Temperature (C)	20
Food Source	LOCAL	Rainfall (cm/y)	100
Distance to Individuals (m)	5000	Lid Height (m)	1000

*NOTE: The results of this computer model are dose estimates. They are only to be used for the purpose of determining compliance and reporting per 40 CFR 61.93 and 40 CFR 61.94.

Table C.6-1. (continued)

CLEAN AIR ACT COMPLIANCE REPORT 2/ 9/94 2:30 PM

Facility: ILNT Vaults JCW
Address: City: State:
Comments: C-14 releases to the off-site individual for the ILNT vaults.
Year:

	Dose Equivalent Rates to Nearby Individuals (mrem/year)
Effective Dose Equivalent	0.1200
Highest Organ Dose is to ENDOSTEUM	0.5100

----------EMISSION INFORMATION----------

Radio-nuclide	Class	Amad	Area #1 (Ci/y)
C-14	*	0.0	1.0E+01
Total Area (m**2)			8.7E+03

----------SITE INFORMATION----------

Wind Data	AGS1018.WND	Temperature (C)	20
Food Source	LOCAL	Rainfall (cm/y)	100
Distance to Individuals (m)	5000	Lid Height (m)	1000

*NOTE: The results of this computer model are dose estimates. They are only to be used for the purpose of determining compliance and reporting per 40 CFR 61.93 and 40 CFR 61.94.

Table C.6-1. (continued)

CLEAN AIR ACT COMPLIANCE REPORT 2/ 9/94 2:32 PM

Facility: LAW Vaults JCW
Address: City: State:
Comments: H-3 releases to the off-site individual for the LAW vaults.
Year:

	Dose Equivalent Rates to Nearby Individuals (mrem/year)
Effective Dose Equivalent	1.17E-05
Highest Organ Dose is to REMAINDER	1.37E-05

----------EMISSION INFORMATION----------

Radio-nuclide	Class	Amad	Area #1 (Ci/y)
H-3	*	0.0	5.2E-02
Total Area (m**2)			1.8E+05

----------SITE INFORMATION----------

Wind Data	AGS1018.WND	Temperature (C)	20
Food Source	LOCAL	Rainfall (cm/y)	100
Distance to Individuals (m)	5000	Lid Height (m)	1000

*NOTE: The results of this computer model are dose estimates. They are only to be used for the purpose of determining compliance and reporting per 40 CFR 61.93 and 40 CFR 61.94.

Table C.6-1. (continued)

CLEAN AIR ACT COMPLIANCE REPORT 2/ 9/94 2:34 PM

Facility: LAW Vaults C-14
Address: City: State:
Comments: C-14 releases to the off-site individual for the LAW vaults.
Year:

	Dose Equivalent Rates to Nearby Individuals (mrem/year)
Effective Dose Equivalent	0.2600
Highest Organ Dose is to ENDOSTEUM	1.1

----------EMISSION INFORMATION----------

Radio-nuclide	Class	Amad	Area #1 (Ci/y)
C-14	*	0.0	2.1E+01
Total Area (m**2)			1.6E+05

----------SITE INFORMATION----------

Wind Data	AGS1018.WND	Temperature (C)	20
Food Source	LOCAL	Rainfall (cm/y)	100
Distance to Individuals (m)	5000	Lid Height (m)	1000

*NOTE: The results of this computer model are dose estimates. They are only to be used for the purpose of determining compliance and reporting per 40 CFR 61.93 and 40 CFR 61.94.

Table C.6-1. (continued)

CLEAN AIR ACT COMPLIANCE REPORT 2/ 9/94 2:37 PM

Facility: Suspect Soil Trenches
Address: City: State:
Comments: H-3 releases for the suspect soil trenches (off-site individual)
Year:

	Dose Equivalent Rates to Nearby Individuals (mrem/year)
Effective Dose Equivalent	6.48E-06
Highest Organ Dose is to REMAINDER	7.64E-06

EMISSION INFORMATION

Radio-nuclide	Class	Amad	Area #1 (Ci/y)
H-3	*	0.0	2.9E-02
Total Area (m**2)			6.0E+03

SITE INFORMATION

Wind Data	AGS1018.WND	Temperature (C)	20
Food Source	LOCAL	Rainfall (cm/y)	100
Distance to Individuals (m)	5000	Lid Height (m)	1000

*NOTE: The results of this computer model are dose estimates. They are only to be used for the purpose of determining compliance and reporting per 40 CFR 61.93 and 40 CFR 61.94.

Table C.6-1. (continued)

CLEAN AIR ACT COMPLIANCE REPORT 2/ 9/94 2:39 PM

Facility: Suspect Soil Trenches
Address: City: State:
Comments: C-14 releases for the suspect soil trenches (off-site individual)
Year:

	Dose Equivalent Rates to Nearby Individuals (mrem/year)
Effective Dose Equivalent	0.0120
Highest Organ Dose is to ENDOSTEUM	0.0510

EMISSION INFORMATION

Radio-nuclide	Class	Amad	Area #1 (Ci/y)
C-14	*	0.0	1.0E+00
Total Area (m**2)			6.0E+03

SITE INFORMATION

Wind Data	AGS1018.WND	Temperature (C)	20
Food Source	LOCAL	Rainfall (cm/y)	100
Distance to Individuals (m)	5000	Lid Height (m)	1000

*NOTE: The results of this computer model are dose estimates. They are only to be used for the purpose of determining compliance and reporting per 40 CFR 61.93 and 40 CFR 61.94.

Table C.6-1. (continued)

CLEAN AIR ACT COMPLIANCE REPORT 2/ 9/94 2:41 PM

Facility: Naval Reactor Waste
Address: City: State:
Comments: H-3 releases for the Naval Reactor Waste (off-site individual)
Year:

	Dose Equivalent Rates to Nearby Individuals (mrem/year)
Effective Dose Equivalent	0.0002
Highest Organ Dose is to REMAINDER	0.0002

----------EMISSION INFORMATION----------

Radio-nuclide	Class	Amad	Area #1 (Ci/y)
H-3	*	0.0	7.2E-01
Total Area (m**2)			8.0E+02

----------SITE INFORMATION----------

Wind Data	AGS1018.WND	Temperature (C)	20
Food Source	LOCAL	Rainfall (m/y)	100
Distance to Individuals (m)	5000	Lid Height (m)	1000

*NOTE: The results of this computer model are dose estimates. They are only to be used for the purpose of determining compliance and reporting per 40 CFR 61.93 and 40 CFR 61.94.

Table C.6-1. (continued)

CLEAN AIR ACT COMPLIANCE REPORT 2/ 9/94 2:[illegible] PM

Facility: Naval Reactor Waste
Address: City: State:
Comments: C-14 releases for the Naval Reactor Waste (off-site individual)
Year:

	Dose Equivalent Rates to Nearby Individuals (mrem/year)
Effective Dose Equivalent	1.2
Highest Organ Dose is to ENDOSTEUM	5.1

EMISSION INFORMATION

Radio-nuclide	Class	Amad	Area #1 (Ci/y)
C-14	*	0.0	1.0E+02
Total Area (m**2)			8.0E+02

SITE INFORMATION

Wind Data	AGS1018.WND	Temperature (C)	20
Food Source	LOCAL	Rainfall (cm/y)	100
Distance to Individuals (m)	5000	Lid Height (m)	1000

*NOTE: The results of this computer model are dose estimates. They are only to be used for the purpose of determining compliance and reporting per 40 CFR 61.93 and 40 CFR 61.94.

APPENDIX D

GEOCHEMICAL INTERACTIONS

D.1 INTRODUCTION

Predicting the release of radionuclides from the E-Area disposal facility is difficult because of the large variety of contaminated material that will be disposed of in the vaults. Conceptually, waste within steel boxes (B-12 and B-25) or activated metals disposed in the vaults will remain immobile until contacted by water that has leaked into the vaults. Defensible prediction of water and contaminant movement in the vaults and the effectiveness of boxes and activated metals in retarding waste release is not possible without development of a conservative simplified conceptual model. The key features of the conceptual model are summarized below.

Waste is immobile until contacted by water.

1) Water entering the vault will have a composition that can be represented as a mixture of concrete pore fluid and local groundwater equilibrated with soil levels of carbon dioxide gas.
2) Steel and activated metals present in the vaults will result in the formation of corrosion products (i.e., hydrous Fe[III] oxides) and lead to reducing conditions inside the vaults.
3) Entire vault inventory is available to react with the reducing water inside the vault.
4) Aqueous radionuclide concentrations are controlled by sorption (represent with a K_d or isotherm) onto corrosion products (LAW vault) or grout (ILT and ILNT vaults) with a solubility limited (oxide and hydroxide phases) upper concentration limit.
5) Contaminated water exiting the vault will interact with the concrete vault and radionuclides will be chemically retarded by the vault wall.

D.2 RADIONUCLIDES CONSIDERED

The radionuclides considered in detail for the LAW vaults are H-3, C-14, Ni-59, Se-79, Ra-226, Th-232, Sn-126, Tc-99, I-129, Cs-135, Sr-90, Y-90, Am-241, 243, Cm-244, 245, 246, 247, 248, Bk-247, 249, Cf-249, 251, 252, Np-237, Pu-238, 239, 240, 241, 242, 244, and U-234, 235, 236, 238. These radionuclides were selected for detailed numerical transport simulations based on the screening calculations discussed in Sect. 4.1.1. The anionic radionuclides C, Tc, and I, as well as tritium are weakly sorbed to corrosion products. If conditions in the vault are reducing enough, the anion Tc(VII) may be reduced to insoluble Tc(IV). Tritium release from tritium crucibles in the ILT vaults was found to be limited by transport through the vault sufficiently that no leach rate calculations were required to reach adequate performance. Distribution coefficients for the remaining radionuclides were developed based on hydrous ferric oxide (HFO) adsorption.

D.3 VAULT WATER COMPOSITION

Water compositions inside the vaults will reflect the interaction of concrete pore water and vadose water. The composition of the vault water will be dominated by concrete interactions even under conditions of fracture flow through the vault shell. The presence of CO_2 gas in the soil and calcite present as a weathering product in the cement will buffer the pH of the vault water to between 7 and 8.

D.4 RADIONUCLIDE SORPTION BEHAVIOR

Wastes disposed of in the LAW vaults will be contained in steel boxes (B-12 and B-25). The basic assumption of the method used to derive distribution coefficients for the LAW vault waste form is that the corrosion of the boxes will result in the formation of HFO, (e.g., goethite) and that any water contaminated with radionuclides must pass over the corroded area of the box.

Distribution coefficients (K_d) based on surface area of the adsorbent for the selected radionuclides were estimated by assuming that adsorption occurs exclusively on the corrosion products (HFO) of these boxes. The total potential concentration of HFO in the vault is 0.07 g/cm^3 [based on 9730 B-25 at 350 lbs and 4330 B-12 boxes at 300 lbs in a 1,700,000 ft^3 vault (Harley 1990a,b)]. The surface area of goethite in the vault is predicted to be 32,000 cm^2/cm^3 based on a specific surface area of goethite of 450,000 cm^2/g (Hsi and Langmuir 1985).

Numerous adsorption studies of metal and radionuclides onto hydrous metal oxides are reported in the literature (see Dzombak and Morel 1990). Specific studies for key radionuclides (summarized below) were used to estimate K_d values at pH 8 for the waste assuming HFO is the only reactive phase. Distribution coefficients for radionuclides that lack adsorption experiments were estimated using elemental analogs. The K_d is calculated by relating the experimental data (i.e. fraction adsorbed and suspension concentration) to the waste in the vaults (i.e surface area and bulk density of waste). This is accomplished by using the following equation.

$$K_d = SA\ X / r\ SA_{exp}\ (1-X) \qquad \text{(Eq. 1)}$$

where

SA is the specific surface area of the waste (32,000 cm^2/cm^3)
X is the fraction adsorbed
r is the bulk density of the waste (1.6 g/cm^3)
SA_{exp} is the concentration of solid in the adsorption experiment (cm^2/mL)

Estimated K_d values for the LAW vaults are summarized below (Table D.4-1).

Table D.1-1. Summary of distribution coefficients for selected radionuclides on goethite (pH =3.0).

Radionuclide	Chemical Form	Distribution Coefficient (mL/g)
H-3	HTO	0
C-14	CO_3^{2-}	0
Tc-99	TcO_4^-	0
I-129	I^-	0
Cs-135	Cs^+	0
Sr-90	Sr^{2+}	3
Y-90	Y^{3+}	3
Sn-126	Sn^{2+}	55
Ra-226	Ra^{2+}	60
Se-79	SeO_3^{2-}	170
Ni-59	Ni^{2+}	1200
Th-232	Th^{4+}	2200
U-234, 235, 236, 238	UO_2^{2+}	6000
Np-237	NpO_2^+	750
Pu-238, 239, 240, 241, 242, 244	Pu^{4+}	2000
Am-241, 243	Am^{3+}	3700
Cm-244, 245, 246, 247, 248	Cm^{3+}	3700
Bk-247, 249	Bk^{3+}	3700
Cf-249, 251, 252	Cf^{3+}	3700

Plutonium

Aqueous plutonium speciation is a very complex because it may be simultaneously present in four oxidation states (III, IV, V, VI). The dominant oxidation states of plutonium in oxygenated waters are Pu(V) and Pu(VI) based on calculations and analyses (Nelson and Lovett 1978 and 1981; Nelson and Orlandini 1979; Bondietti and Trabalka 1980). Because of the large amount of reducing material, conditions inside the E-Area vaults will not be oxidizing enough to support Pu(VI) species. The predominant oxidation states expected are Pu(V) and Pu(IV).

Plutonium adsorption on synthetic goethite as functions of pH, ionic strength, carbonate alkalinity, and dissolved organic carbon was measured by Sanchez et al. (1985). The experiments consisted of a synthetic goethite suspension with a surface area of 285 cm^2/mL in a borosilicate glass reaction vessel. Hydrogen activity was controlled using HCl or NaOH. Adsorption of Pu(IV) is much stronger than Pu(V) on goethite because it is more strongly hydrolyzed. The adsorption edge for Pu(IV) occurs from pH 3 to 5 (Fig. D.4-1a) with relatively rapid kinetics (equilibrium reached in 1 h). Pu(V) adsorption is much slower and equilibrium was not achieved after 20 days (Fig. D.4-1b). The Pu(V) adsorption edge changes with time from pH 7 to pH 5 over the 20 day period. Although Pu(V) is predicted to be stable based on thermodynamic calculations the slow shift of the adsorption edge toward that of Pu(IV) suggests that Pu(V) may be reduced to Pu(IV). The reduction may take place on the goethite surface after adsorption of the Pu(V) or Pu(V) may be reduced as it nears the goethite surface and the Pu(IV) state is adsorbed (Sanchez et al. 1985).

Adsorption of Pu(IV) or Pu(V) was not significantly affected by ionic strength in the range of 0.1 to 3 M $NaNO_3$ or NaCl (see Table D.4-2). A decrease in Pu adsorption on goethite occurs with increased carbonate alkalinity. However, this occurs at much higher alkalinity levels than will be found in the E-Area vaults (Fig. D.4-2).

The data used to estimate Pu adsorption for the LAW vault waste is for a pH of 7 (negligible change from pH 7 to 8) and a total Pu concentration of 10^{-11} M. At these conditions 97.1% of the Pu is on the solid (Table D.4-2). This sorption fraction is consistent with a K_d of 2,000 mL/g for expected bulk density and HFO content in the vaults using Eq. 1.

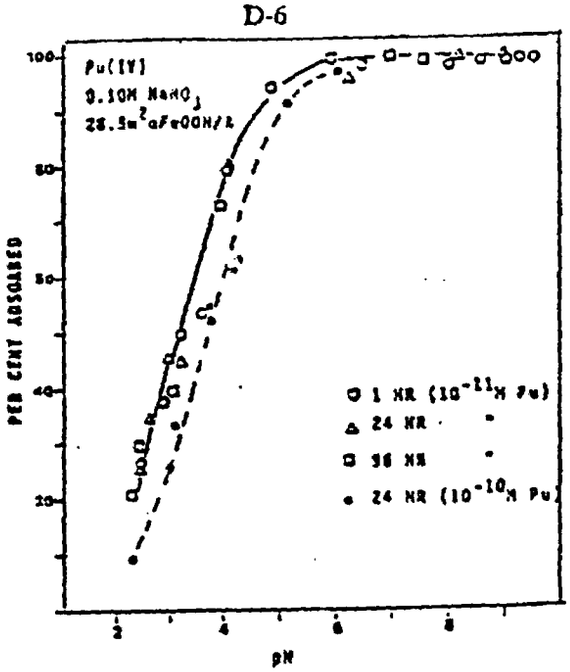

a)

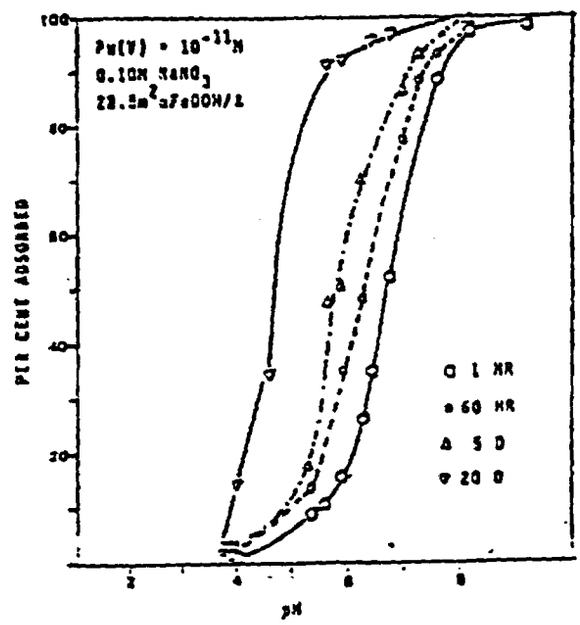

b)

Fig. D.4-1. Adsorption of Pu on goethite as a function of pH at two plutonium concentrations (from Sanchez et al. 1985). a) Pu(IV), b) Pu(V).

Table D.4-2. Adsorption of Pu(IV) on goethite as a function of ionic strength (pH =7.0, Total Pu = 10^{-11} M) from Sanchez et al. 1983

Electrolyte Solution	Percent Adsorbed at Equilibrium
0.1 M $NaNO_3$	97
0.5 M $NaNO_3$	97
1.0 M $NaNO_3$	98
3.0 M $NaNO_3$	98
0.5 M $NaNO_3$	98
3.0 M $NaNO_3$	97
0.03 M $NaNO_3$	97
0.15 M $NaNO_3$	97
0.30 M $NaNO_3$	95
Mean	97.1

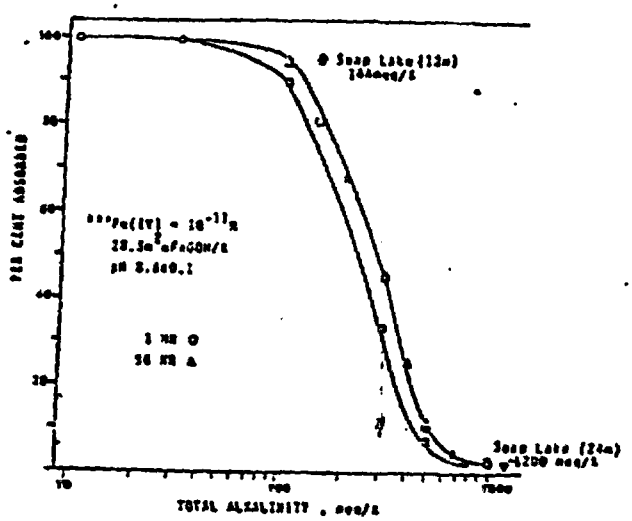

Fig. D.4-2. The effect of carbonate alkalinity on the adsorption of Pu(IV) on goethite (from Sanchez et al. 1985). Alkalinity in the vault will be approximately 60 meq/L.

Uranium

Uranium partitioning onto HFO under varying pH, ionic strength, competing cation and complexing anions is described by Hsi and Langmuir (1985). The HFO used by Hsi and Langmuir were amorphous ferric oxyhydroxide, goethite, and hematite. Uranyl species were strongly adsorbed to all three of the iron oxides considered at pHs above 5 to 6. The most adsorptive oxide considered was the amorphous ferric oxyhydroxide with natural hematite providing the least amount of adsorption. These differences in adsorption result from the difference in specific surface area of the polymorphs. We have calculated the adsorption of uranium in the waste based on goethite representing the steel corrosion product.

The surface area of the goethite suspension was 450 cm^2/mL. HNO_3 and NaOH were used to maintain pH with a total uranyl concentration of 10^{-5} m. Goethite removes over 99% of the U from solution above pH 6 (Fig. D.4-3a). Uranyl adsorption was not affected by the presence of calcium and magnesium at total solution concentrations of 10^{-3} M. The vault pore fluid concentrations of Ca^{2+} and Mg^{2+} are anticipated to be lower than this and therefore should not result in reduced uranyl adsorption.

Total carbonate concentration influences the adsorption of uranium (VII) on goethite. Higher CO_3^{2-} content in solution results in increased uranyl carbonate complexation, predominantly $UO_2(CO_3)_2^{2-}$ and $UO_2(CO_3)_3^{4-}$, and decreases adsorption of UO_2^{2+} above pH 6 (Fig. D.4-3b). The affect of total carbonate on the adsorption of UO_2^{2+} is very evident in plots of soluble uranium versus pH with varying carbonate concentrations (Fig. D.4-3c). The dissolved uranium concentration at pH 7 for a carbonate concentration of 10^{-3} M was selected for use in the K_d estimation because this carbonate concentration and pH match the expected vault pore fluid conditions. A K_d for the LAW vault waste of 6000 mL/g was calculated using Eq. 1.

Strontium

Adsorption of strontium onto hydrous ferric oxides has been studied by Kolarik (1961), Kinniburgh et al. (1975), and Kinniburgh et al. (1976). These experiments indicate that strontium ion adsorbs rapidly and is not significantly impacted by variations in the Na^+

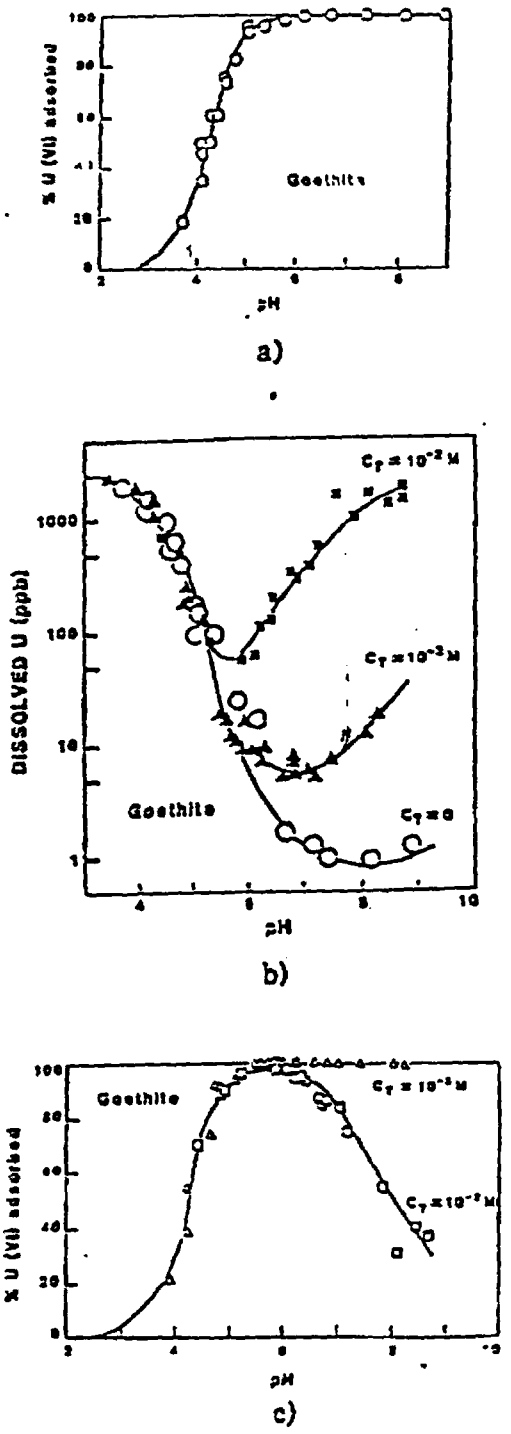

Fig. D.4-3. Adsorption of uranyl on a 1 g/L goethite suspension as a function of pH in a 0.1 M $NaNO_3$ solution (from Hsi and Langmuir 1985). a) uranyl at 10^{-5} M, b) dissolved uranium at 10^{-5} M and varying total carbonate, c) effect of changes in total carbonate on the adsorption of uranyl.

concentration in the solution. These experiments also show that there is no selectivity for Ca^{2+} over Sr^{2+} (Kinniburgh et al. 1975). The adsorption edge for Sr^{2+} on the iron oxide (Kinniburgh et al. 1975) was between pH 6 and 7.5.

Dzombak and Morel (1990) provide a summary of adsorption data for Sr^{2+} on HFO. The experiments used to determine the adsorption of strontium on HFO are from Kinniburgh et al. (1975) and Kolarik (1961). The HFO was prepared by the addition of NaOH to $Fe(NO_3)_3$ solution and the ionic strength of the solution was held at 1.0 m $NaNO_3$. The adsorption curves used to estimate strontium adsorption at pH 8 are shown in Fig. D.4-4a to k and the data are summarized in Table D.4-3. The total strontium in the experiments ranged from 10^{-2} to 10^{-7} M and HFO surface area ranged from 10700 to 106620 cm^2/mL. An average Sr^{2+} K_d for LAW vault waste of 3 mL/g was calculated from Eq. 1.

Nickel

Dzombak and Morel (1990) provide a summary of adsorption data for Ni^{2+} on HFO. The experiment used to determine the adsorption curve for nickel on HFO is from Leckie et al. (1984). The HFO was prepared by the addition of NaOH to $Fe(NO_3)_3$ solution and the ionic strength of the solution was held at 0.1 M $NaNO_3$. The adsorption edge is located between pH 6.5 and 7.5 (Fig. D.4-5) for the experiment used to estimate nickel adsorption. The total nickel in the system is 10^{-7} M and HFO surface area is 533 cm^2/mL. Approximately 97% of the nickel is adsorbed to the goethite surface at pH 8. A Ni^{2+} K_d for LAW vault waste of 1200 mL/g was calculated from Eq. 1.

Selenite

Selenium geochemistry is strongly controlled by the geochemistry of iron (Howard 1977). In the pH range from 2 to 8 selenite (SeO_3^{2-}) is strongly adsorbed and decreases from pH 8 to 11. Dzombak and Morel (1990) provide a summary of adsorption data for SeO_3^{2-} on HFO. The experiment used to determine the adsorption curve for selenite on HFO is from Plotnikov (1958). The HFO was prepared by the addition of NH_4OH to $Fe(NO_3)_3$ solution

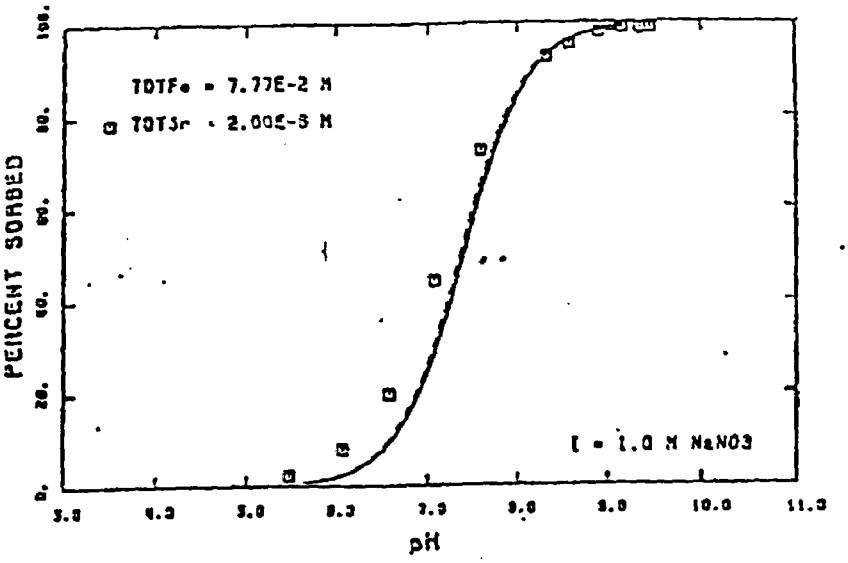

a)

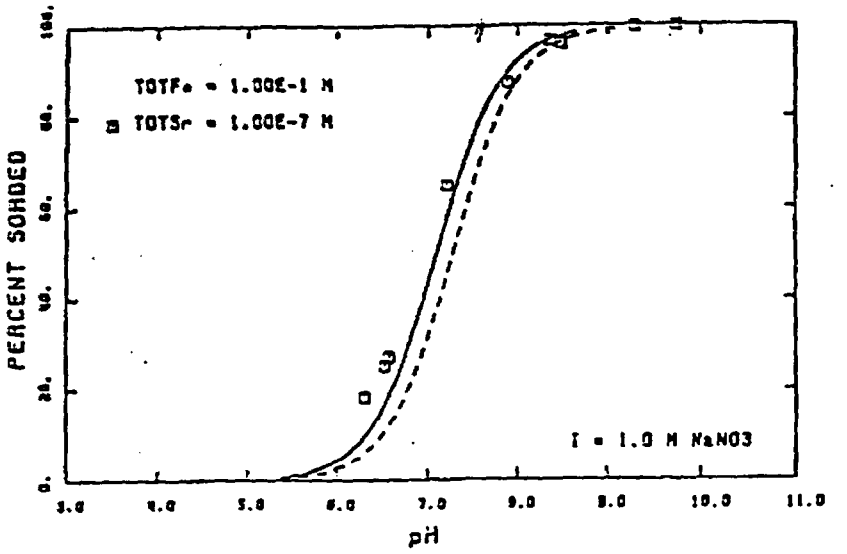

b)

Fig. D.4-4. Adsorption of Sr^{2+} on goethite as a function of pH in a 1.0 M $NaNO_3$ solution (from Dzombak and Morel 1990). a) 6.9 g goethite/L, b) 8.9 g goethite/L, c) 8.9 g goethite/L, d) 8.9 g goethite/L, e) 8.9 g goethite/L, f) 8.9 g goethite/L, g) 8.9 g goethite/L, h) 1.8 g goethite/L, i) 4.4 g goethite/L, j) 8.9 g goethite/L, k) 17.8 g goethite/L.

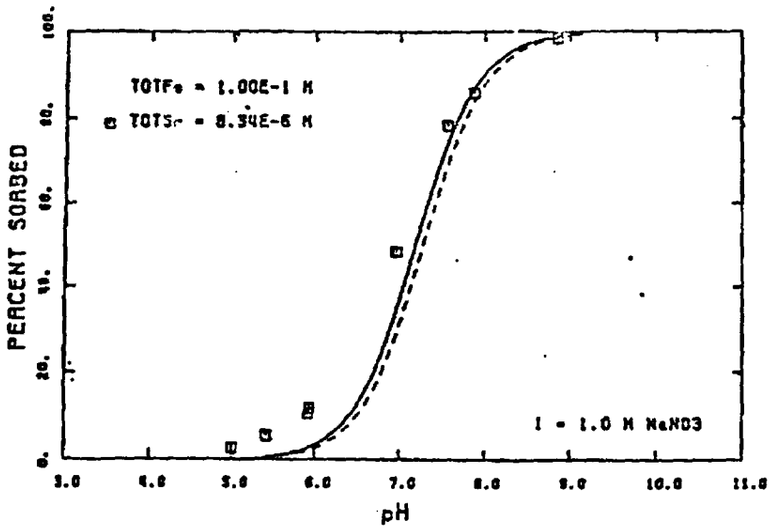

c)

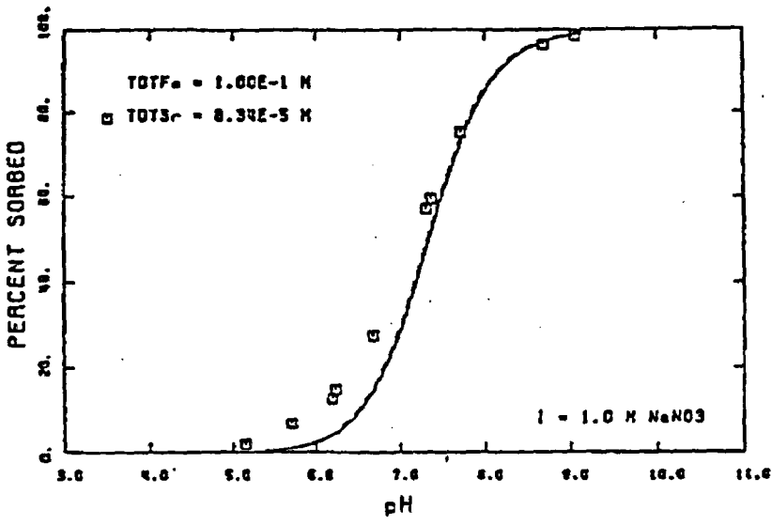

d)

Fig. D.4-4. (continued).

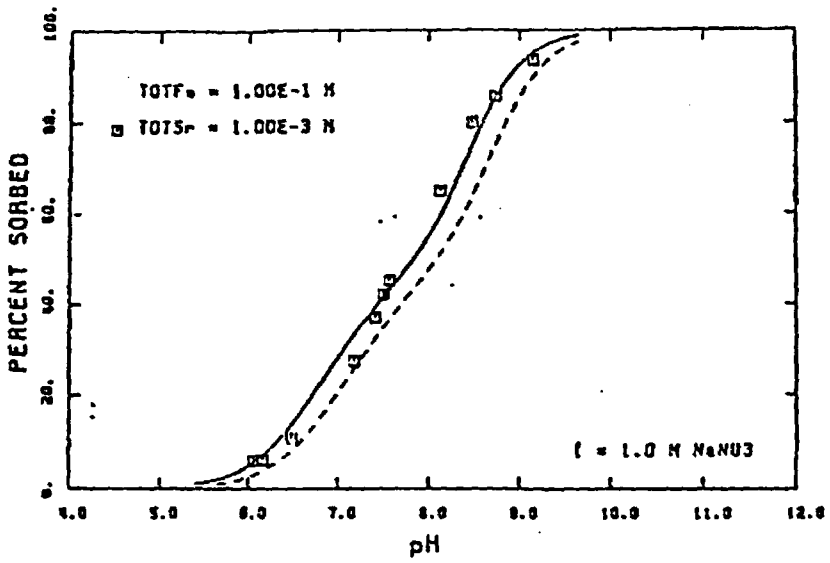

e)

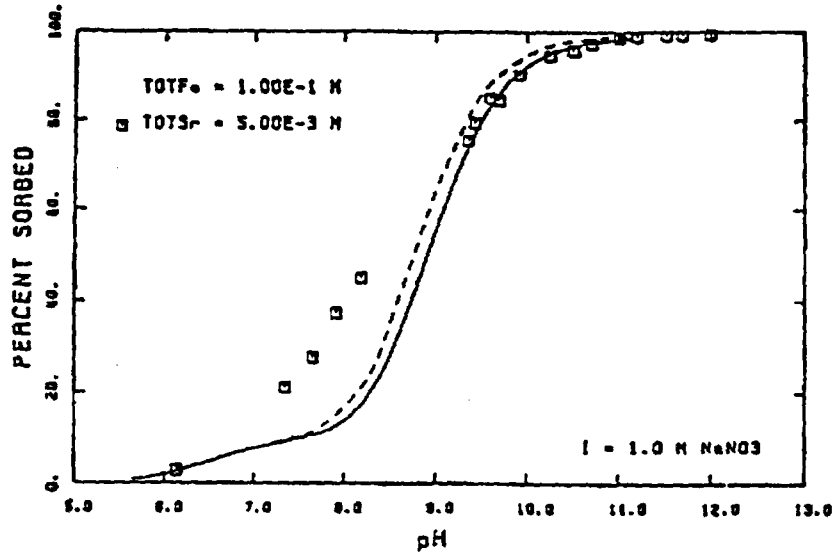

f)

Fig. D.4-4. (continued).

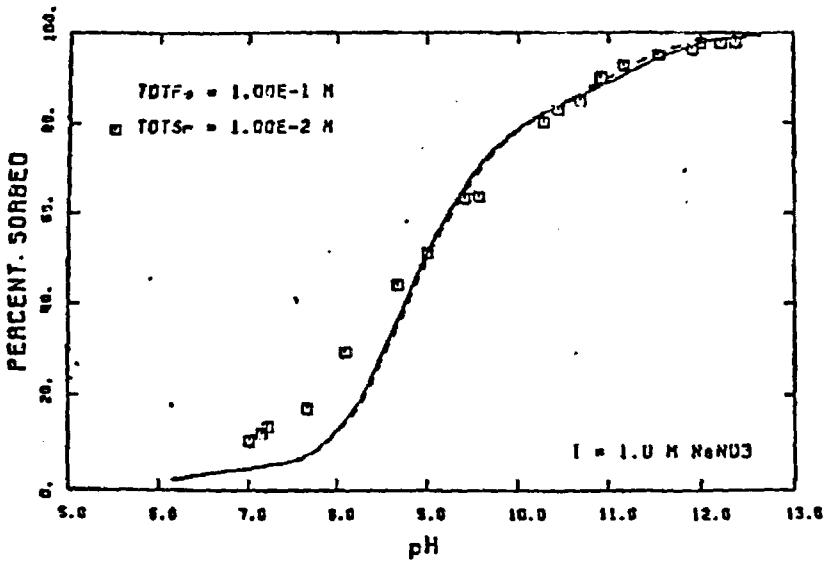

g)

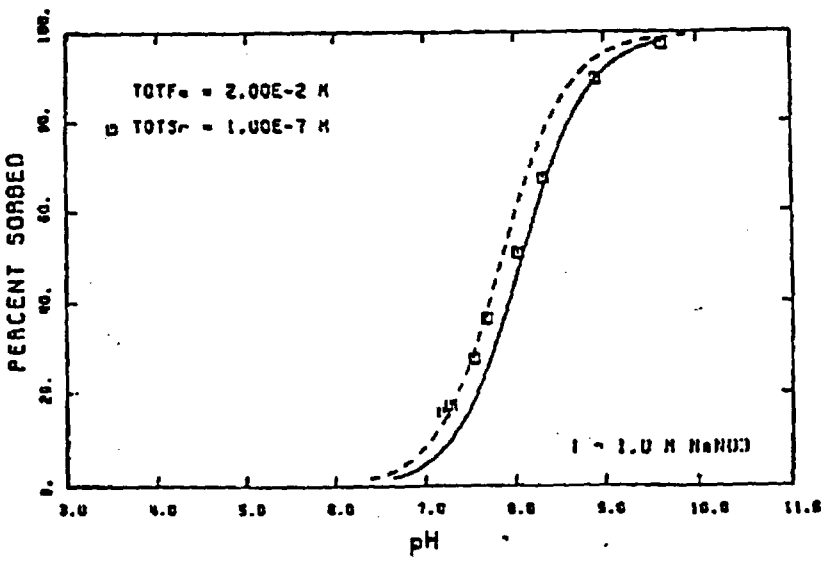

h)

Fig. D.4-4. (continued).

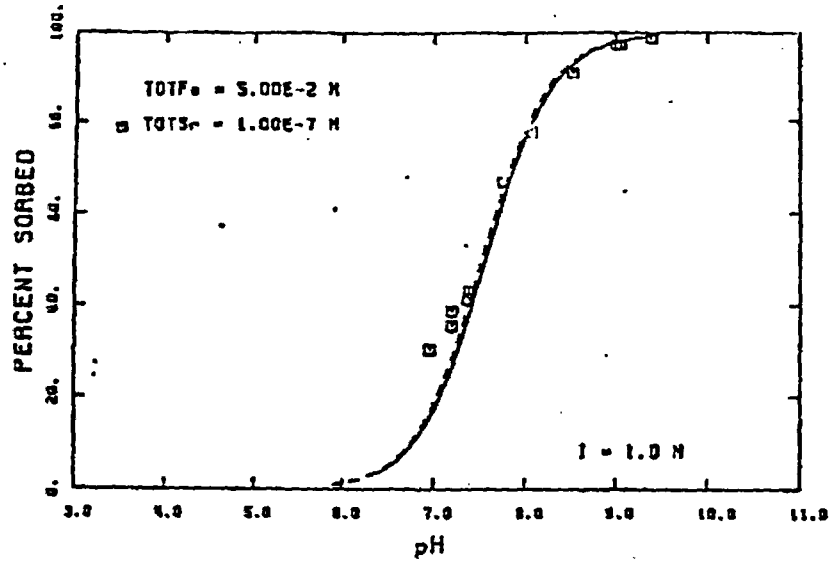

i)

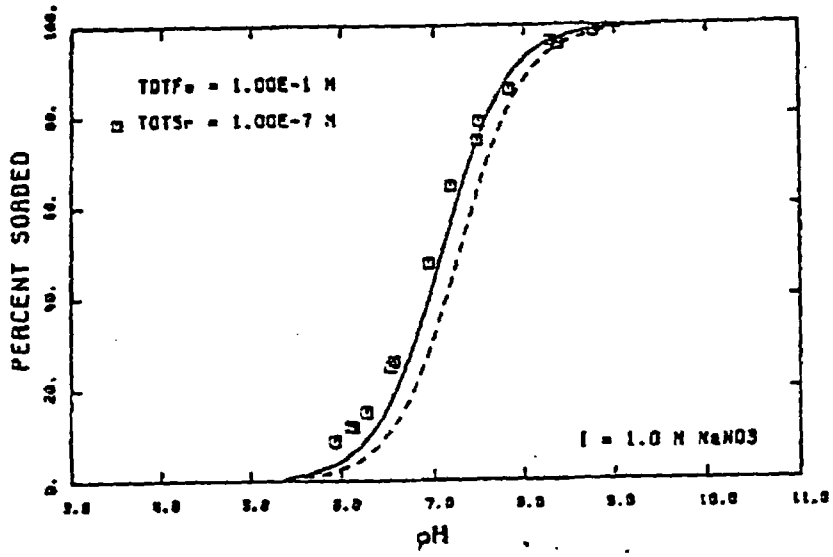

j)

Fig. D.4-4. (continued).

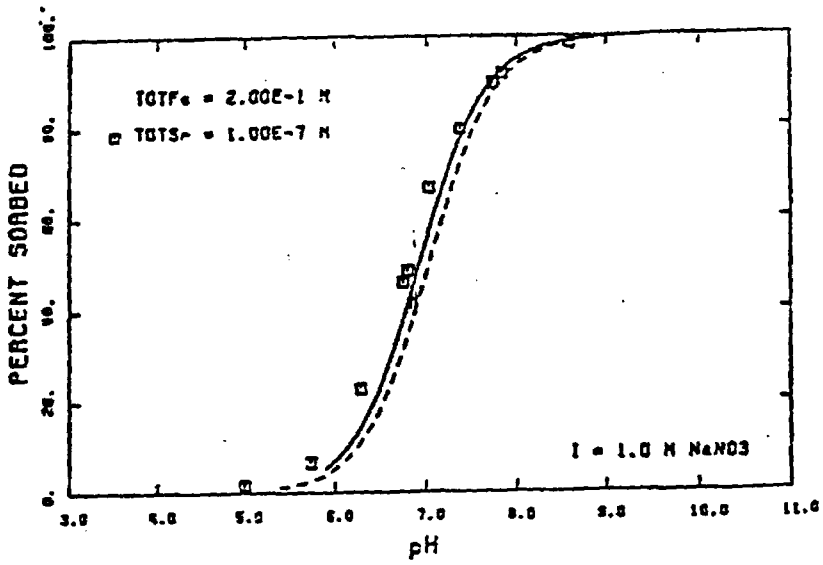

k)

Fig. D.4-4. (continued).

Table D.4-3. Adsorption data for strontium used to estimate K_d

Total Sr (M)	Surface Area (cm^2/mL)	Percent Adsorbed	K_d (mL/g)
$2.00\ 10^{-5}$	41,420	87	3.2
$1.00\ 10^{-7}$	53,000	90	3.4
$8.34\ 10^{-6}$	53,000	90	3.4
$8.34\ 10^{-5}$	53,000	88	2.8
$1.00\ 10^{-3}$	53,000	58	0.5
$5.00\ 10^{-3}$	53,000	40	0.3
$1.00\ 10^{-2}$	53,000	30	0.2
$1.00\ 10^{-7}$	10,700	51	1.9
$1.00\ 10^{-7}$	26,700	80	3.0
$1.00\ 10^{-7}$	53,300	93	5.0
$1.00\ 10^{-7}$	106,620	95	3.6

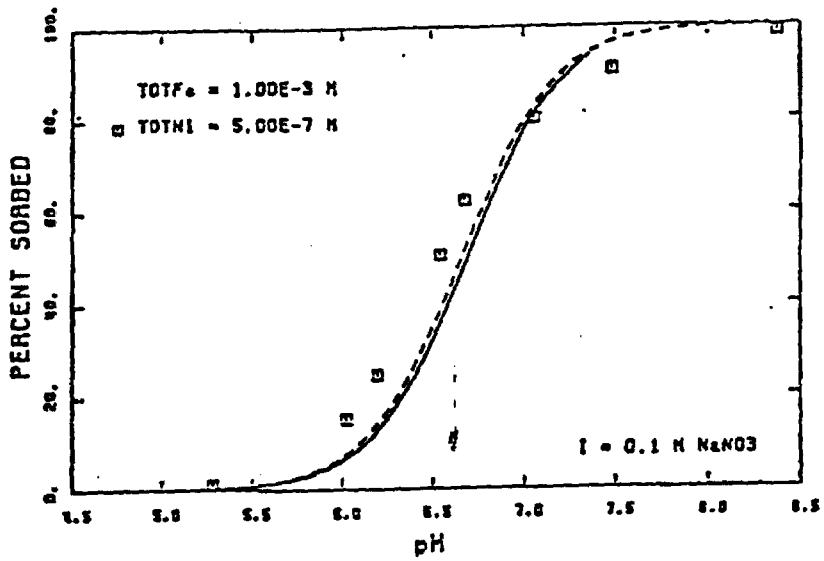

Fig. D.4-5. Adsorption of nickel on goethite as a function of pH in a 0.1 M $NaNO_3$ solution (from Dzombak and Morel 1990).

and the ionic strength of the solution was held at 0.5 M NH_4NO_3. The adsorption curve (Fig. D.4-6) was used to estimate selenite adsorption at pH 8. The total selenite in the system is 1.27 10^{-5} M and HFO surface area is 3806 cm^2/mL. At this pH, 97% of the selenite is adsorbed to the goethite surface. A Se^{4+} K_d for LAW vault waste of 170 mL/g was calculated from Eq. 1.

Radium

No information is available for radium adsorption on HFO. However, Dzombak and Morel (1990) provide a summary of adsorption data for barium ion on HFO. This barium data will be used as an analog for radium. The experiments used to determine the adsorption curves for barium on HFO are from Kurbatov (1949) and Duval and Kurbatov (1952). Kurbatov (1949) prepared HFO by the addition of NH_4OH to $FeCl_3$ solution at ionic strengths of 0.0038, 0.033, and 0.3 M NH_4Cl. Duval and Kurbatov (1952) prepared HFO by the addition of NH_4OH to $FeCl_3$ solution at an ionic strength of 0.0.0087 N NH_4Cl. The adsorption curves (Fig. D.4-7a,b,c,d,e) were used to estimate barium adsorption at pH 8. The total barium, HFO surface areas, and percentage Ba^{2+} adsorbed at pH 8 are shown in Table D.4-4. An average Ba^{2+} K_d for LAW vault waste of 60 mL/g was calculated for radium from Eq. 1.

Thorium

Hunter et al. (1988) conducted Th adsorption studies on goethite that show the characteristic adsorption edge of hydrolyzable metal ions on oxides. Adsorption was found to involve $Th(OH)_2(^{2+})$, $Th(OH)_3(^{+})$, and $Th(OH)_4$. Experiments were focused on determining the effects of the major ions Mg^{2+}, Ca^{2+}, and SO_4^{2-} on the adsorption of Th on goethite as compared to adsorption in a NaCl electrolyte. Adsorbent and adsorbate concentrations were also varied to determine if these concentrations effect Th adsorption.

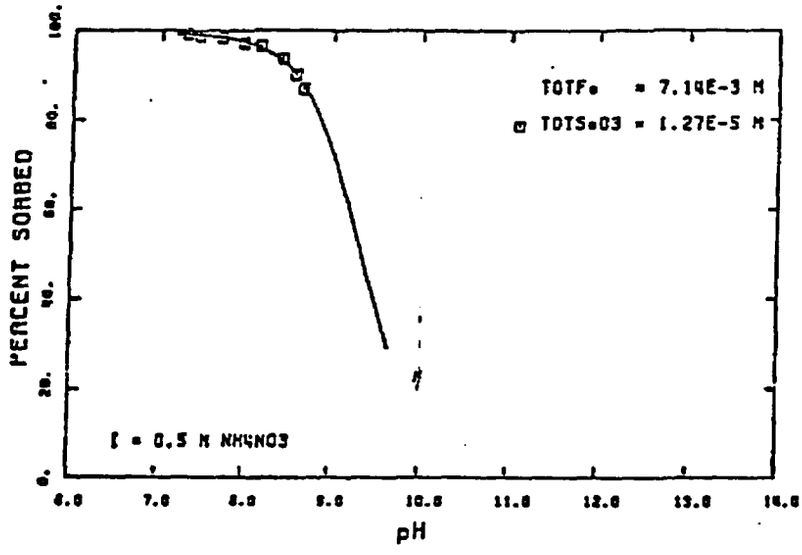

Fig. D.4-6. Adsorption of selenite on goethite as a function of pH in a 0.5 M NH_4NO_3 solution (from Dzombak and Morel 1990).

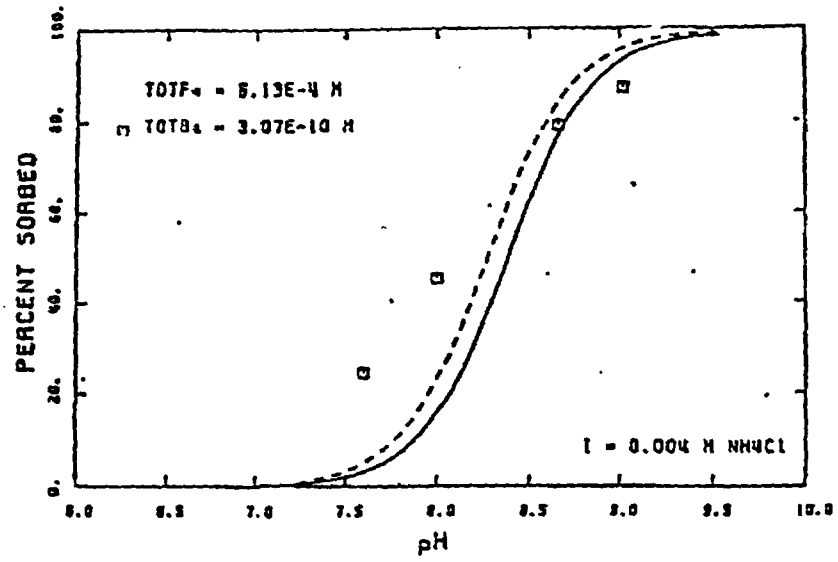

a)

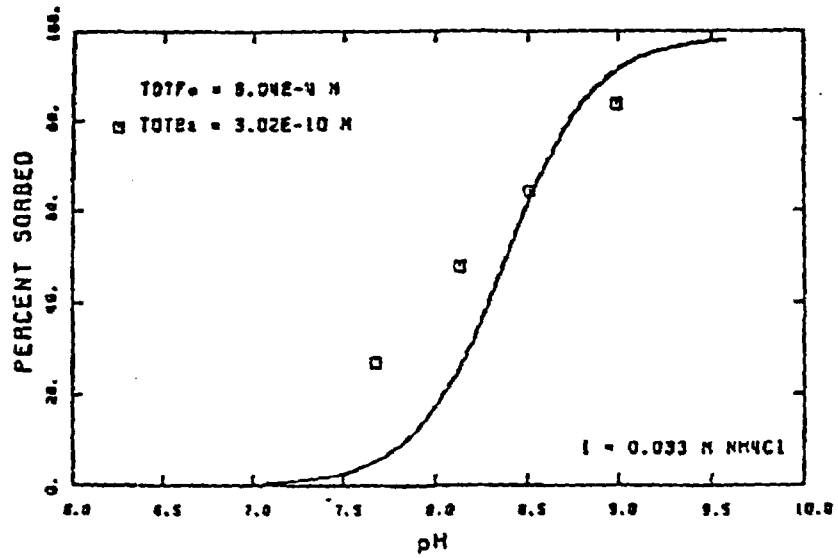

b)

Fig. D.4-7. Adsorption of barium on goethite as a function of pH as an analog for radium (from Dzombak and Morel 1990). a) 0.05 g goethite/L, b) 0.05 g goethite/L, c) 0.01 g goethite/L, d) 0.06 g goethite/L, e) 0.2 g goethite/L.

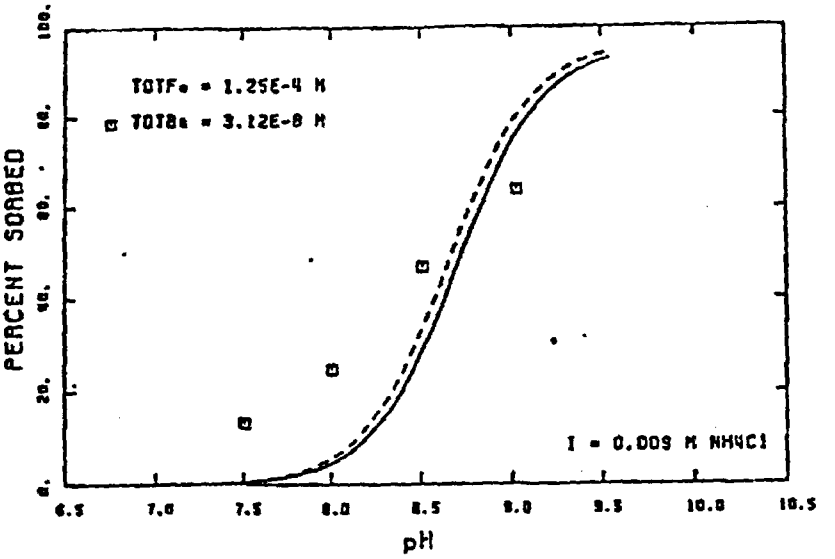

c)

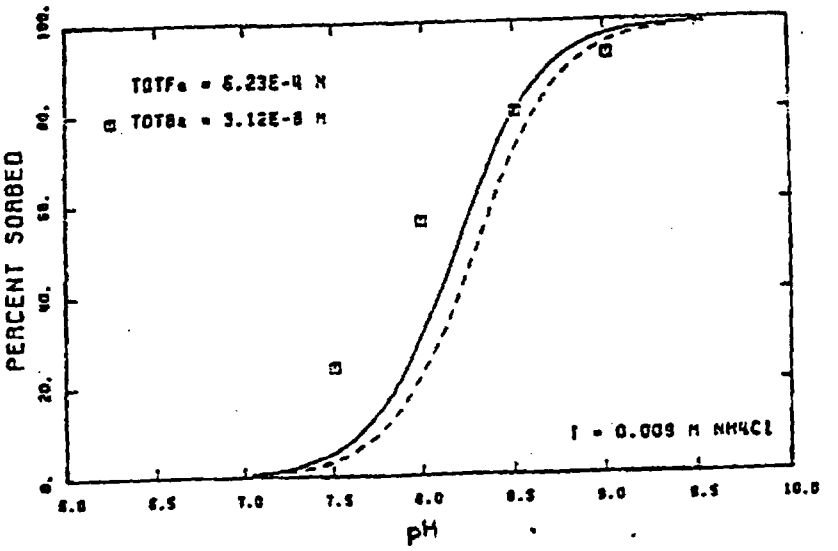

d)

Fig. D.4-7. (continued).

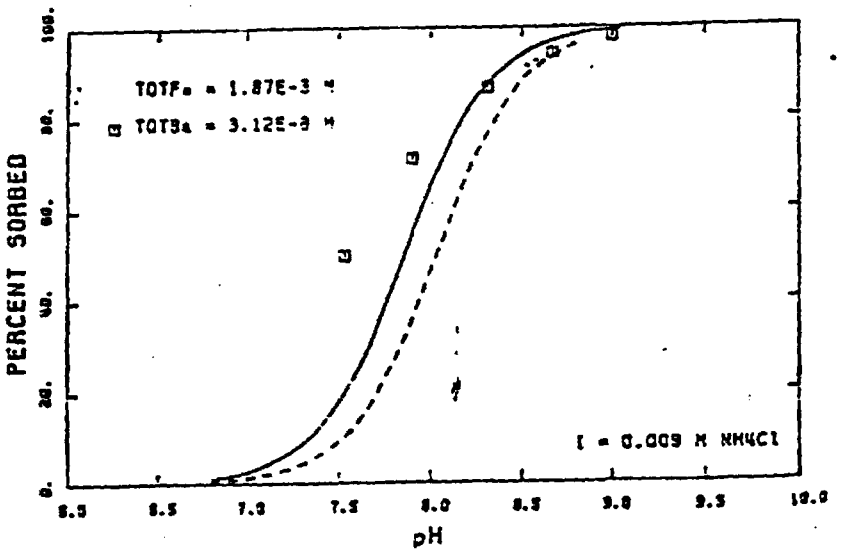

e)

Fig. D.4-7. (continued).

Table D.4-4. Adsorption data for barium used to estimate radium K_d

Total Ba (M)	Surface Area (cm^2/mL)	Percent Adsorbed	K_d (mL/g)
$3.07\ 10^{-10}$	330	46	52
$3.02\ 10^{-10}$	320	39	40
$3.12\ 10^{-8}$	70	23	85
$3.12\ 10^{-8}$	330	53	68
$3.12\ 10^{-8}$	1000	74	57

The HFO was prepared by the addition of KOH to $Fe(NO_3)_3$ solution and the ionic strength of the solution was held at 0.1 M $NaNO_3$. The adsorption curve (Fig. D.4-8) was used to estimate thorium adsorption at pH 8. The total thorium in the system is 6.6 10^{-5} M and HFO surface area is 80 cm^2/mL. At this pH, 90% of the thorium is adsorbed to the goethite surface. A Th K_d for LAW vault waste of 2200 mL/g was calculated from Eq. 1.

Neptunium

Neptunium has been identified in the aqueous phase in the IV, V, and VI oxidations states with Np(V) being most common for waters in contact with atmospheric oxygen between pH 5 and 11. Girvin et al. (1991) conducted Np(V) adsorption studies on synthetic iron oxyhydroxide. The HFO was prepared by the addition of NaOH to $Fe(NO_3)_3$ solution and the ionic strength of the solution was held at 0.1 M $NaNO_3$. The adsorption curve (Fig. D.4-9) was used to estimate neptunium adsorption at pH 8. The total neptunium in the system is 4.7 10^{-12} M and HFO surface area is 5330 cm^2/mL. At this pH, 99.5% of the Np is adsorbed to the goethite surface. A Np K_d for LAW vault waste of 750 mL/g was calculated from Eq. 1.

Tin

No tin adsorption data is available for iron oxides. However, Dzombak and Morel (1990) provide a summary of adsorption data for Hg on HFO. The Hg experimental data of Avotins (1975) was used to determine the analog adsorption curve for tin on HFO. The HFO was prepared by the addition of NaOH to $Fe(ClO_4)_3$ solution and the ionic strength of the solution was held at 0.1 M $NaClO_4$. The adsorption curves (Fig. D.4-10a,b) for mercury were used to estimate tin adsorption at pH 8. The total Hg in the system is 3.41 10^{-5} M and HFO sur-face area is 300 cm^2/mL. At this pH, 97% of the mercury is adsorbed to the goethite surface.

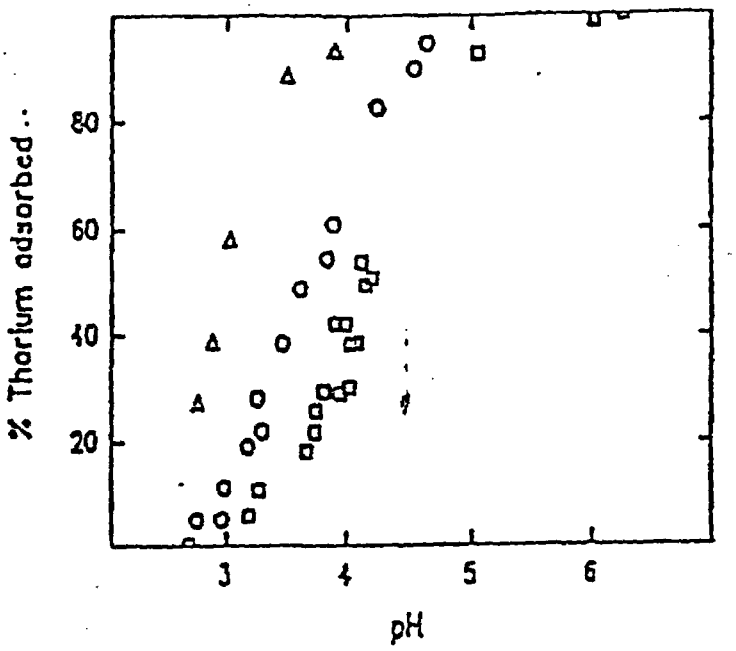

Fig. D.4-8. Adsorption of thorium on goethite as function of pH in 0.422 mol/Kg NaCl electrolyte at different thorium/oxide ratios (Hunter et al. 1988). Triangles: 9 micromol/L Th, 8.6 g/L goethite; Circles: 9 micromol/L Th, 0.54 g/L goethite; Squares: 45 micromol/L Th, 0.54 g/L goethite.

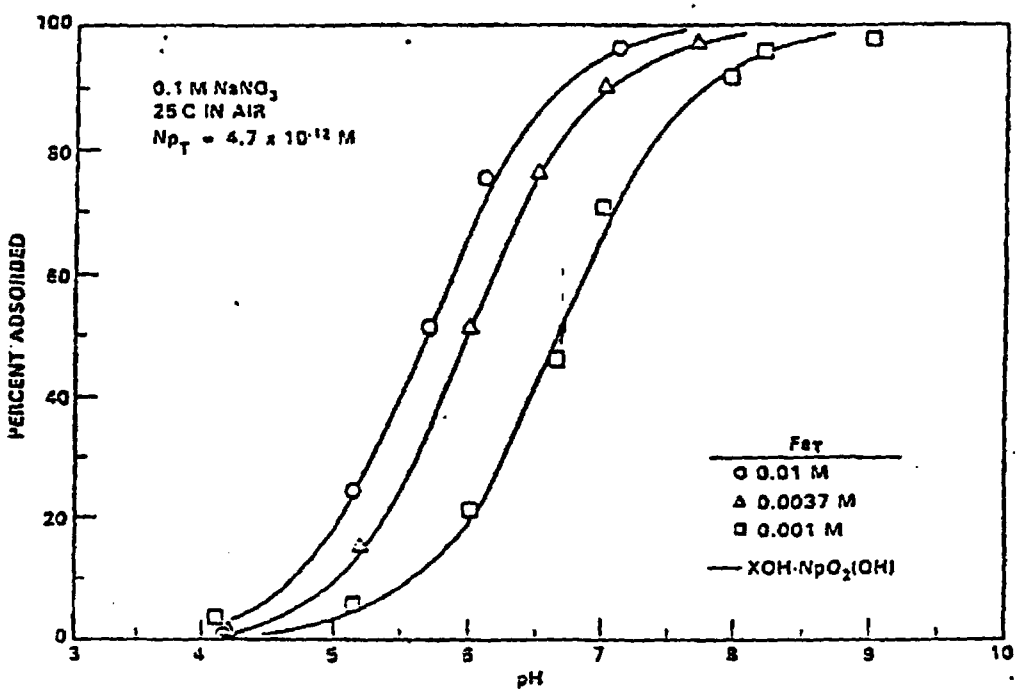

Fig. D.4-9. Adsorption of neptunium on goethite as function of pH (Girvin et al. 1991). Triangles: 0.3 g/L goethite; Circles: 0.9 g/L goethite; Squares: 0.09 g/L goethite.

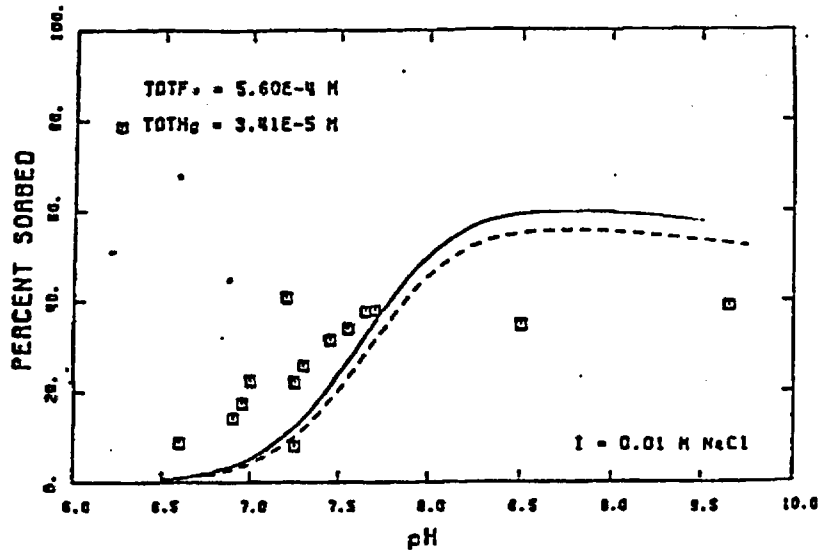

a)

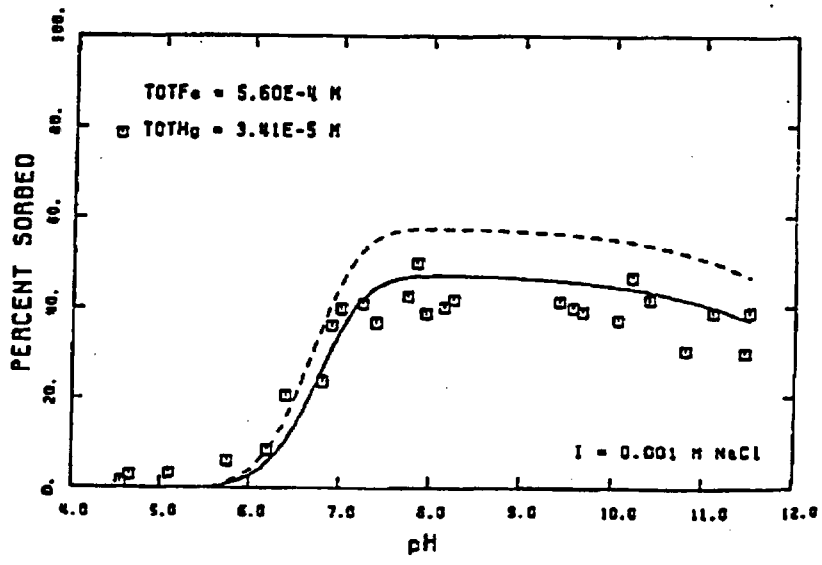

b)

Fig. D.4-10. Adsorption of mercury on goethite as function of pH as an analog for tin (from Dzombak and Morel 1990). a) 0.05 g/L goethite, b) 0.05 g/L goethite.

An average tin K_d for LAW vault waste of 55 mL/g was calculated from Eq. 1.

Americium and Other Transplutonic Elements

Americium in aqueous environments can be found in the III, IV, V, and VI oxidation states. Am (III) is the most predominant oxidation state. No americium adsorption data was available for HFO so Cr(III) adsorption data summarized by Dzombak and Morel (1990) was used as an analog for americium. The HFO was used by prepared by the addition of NaOH to $Fe(NO_4)_3$ solution and the ionic strength of the solution was held at 0.1 M $NaNO_3$ (Leckie et al. 1980). The adsorption curve (Fig. D.4-11) was used to estimate Am adsorption at pH 8. The total Cr in the system is 5.0 10^{-6} M and HFO surface area is 530 cm^2/mL. At this pH, 99% of the chromium is adsorbed to the goethite surface. An americium K_d for LAW vault waste of 3700 mL/g was calculated from Eq. 1. Due to chemical similarities of the transplutonic elements, this K_d was also used for Cm(III), Bk(III), and Cf(III).

D.5 RADIONUCLIDE SOLUBILITY LIMITS

The release of radionuclides from the ILNT and ILT vaults will depend on the vault aqueous chemistry, solubility, and sorption behavior of the relevant radionuclides. The chemical conditions in the vaults will be controlled by the dissolution of the soluble constituents of the cement and by the corrosion of the iron waste containers and activated metals (Ewart et al. 1992). Corrosion of the waste containers and infiltration of water through the vaults will cause slow changes in the vault chemical conditions. Work conducted by Ewart et al. (1992) has shown that the pH of concrete repositories will remain above 10.5 for extended periods of time and Sharland et al. (1986) have shown that the oxidation potential throughout the near field will become reducing approximately 100 years after saturation. Ewart et al. (1992) have shown that the carbonate concentration in the near-field groundwater remain at a constant level of about 10^{-4} M to 10^{-5} M by the relatively high calcium concentration. These conditions provide low solubilities for actinides and provide

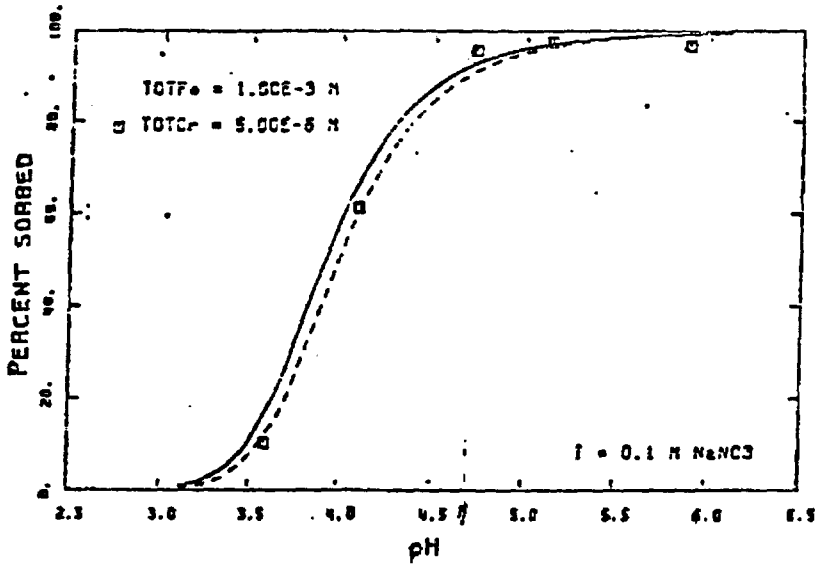

Fig. D.4-11. Adsorption of chromium III on goethite as function of pH as an analog for americium (from Dzombak and Morel 1990).

a valuable chemical component of the multi-barrier containment of the waste. This section discusses the solubility limits for plutonium and uranium in the ILNT and ILT vault environments. Adsorption has been discussed in previous sections.

Plutonium

The tetravalent state of plutonium will predominate under the chemical conditions in the vaults. Solubility of plutonium was estimated assuming the controlling solid phase is amorphous $Pu(OH)_4$ with the plutonium hydroxides (i.e. $Pu(OH)^{3+}$, $Pu(OH)_2^{2+}$, $Pu(OH)_3^+$, and $Pu(OH)_4^*$) comprising the soluble species.

A large variance, up to 16 orders of magnitude, in the solubility product values has been shown in experimental or theoretical techniques. Kim and Kanellakopulos (1989) have redone the experiments in order to provide a more substantiated solubility product value. A solubility product of $\log K_{sp} = -57.85 \pm 0.05$ for amorphous $Pu(OH)_4$ was determined in a 1 M $HClO_4$ solution (Kim and Kanellakopulos 1989). This is the lowest value ever measured for amorphous $Pu(OH)_4$ because the experiment includes the spectroscopic speciation to measure only the Pu^{4+} concentration (Kim and Kanellakopulos 1989). The formation constants for $Pu(OH)^{3+}$, $Pu(OH)_2^{2+}$, $Pu(OH)_3^+$, and $Pu(OH)_4^*$ were taken from Ewart et al. (1992). The reactions and constants used in the model are listed below in Table D.5-1.

Solubility calculations based on these thermodynamic data show a solubility limit of approximately 4.4×10^{-13} M for Pu(IV) at pH greater than 7. This value was used in the PORFLOW transport simulations. The solubility limit value does not change significantly above pH 7 (Fig. D.5-1). The solubility limit calculated here is lower than the average value reported by Ewart et al. (1992) of 7×10^{-11} M at high pH because a lower solubility product was used. The $Pu(OH)_5^-$ species was not considered in the solubility calculations. Experimental observations by Ewart et al. (1992) indicate that this should not impact the calculations because $Pu(OH)_5^-$ does not form to a significant extent.

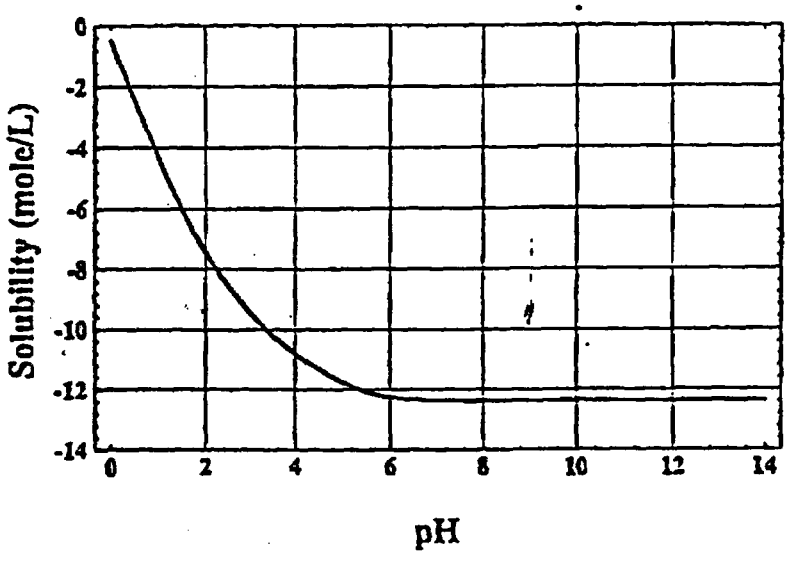

Fig. D.5-1. Estimated Pu(IV) solubility under E-Area conditions.

Table D.5-1. Plutonium reactions considered

Reactions						log K	References
$Pu(OH)_4$	+ $4H^+$	==	Pu^{4+}	+ $4H_2O$		-1.86	Kim and Kanellakopulos 1989
Pu^{4+}	+ H_2O	==	$PuOH^{3+}$	+ H^+		-0.9	Ewart et al. 1992
Pu^{4+}	+ $2H_2O$	==	$Pu(OH)_2^{2+}$	+ $2H^+$		-2.2	Ewart et al. 1992
Pu^{4+}	+ $3H_2O$	==	$Pu(OH)_3^+$	+ $3H^+$		-5.1	Ewart et al. 1992
Pu^{4+}	+ $4H_2O$	==	$Pu(OH)_4^\circ$	+ $4H^+$		-10.54	Ewart et al. 1992

Uranium

Uranium may be present in more than one oxidation state under the conditions found in the vaults. The solubility of uranium for both tetravalent and hexavalent states has been studied. The dominant oxidation state in the high pH and reducing conditions in the vault will be U(IV). The controlling solid selected for the calculations is uraninite, crystalline UO_2, which is stable under the vault conditions (Brookins 1988) and is also present in nature. The value used for solubility limited transport calculations were generated by Orebaugh (1993) and confirmed for higher pH.

Orebaugh modeled uranium solubility using version 3.0 of ESP software from OLI Systems (OLI 1993). The calculations were based on the thermodynamic data provided with the software (based on Phillips et al., 1988). The oxidation state of the uranium was assumed to be reducing based on the presence of large amounts of iron in the vaults. The calculations were made for the major species U(IV) and U(VI) at concentrations of 10^{-6} M for each oxidation state at pH's between 4 and 8. Iron was present in equal amounts of 10^{-4} M for Fe(II) and Fe(III) and the redox couple is described by the equation:

$$UO_2^{2+} + 2Fe^{2+} + 4H^+ \;\; <=====> \;\; U^{4+} + 2Fe^{3+} + 2H_2O$$

Above pH 7 the solubility is controlled primarily by $U(OH)_4$ in equilibrium with crystalline UO_2. A total solubility for uranium of 3×10^{-10} M at pH 7 was used to model the release of uranium from the vaults in PORFLOW (Fig. D.5-2).

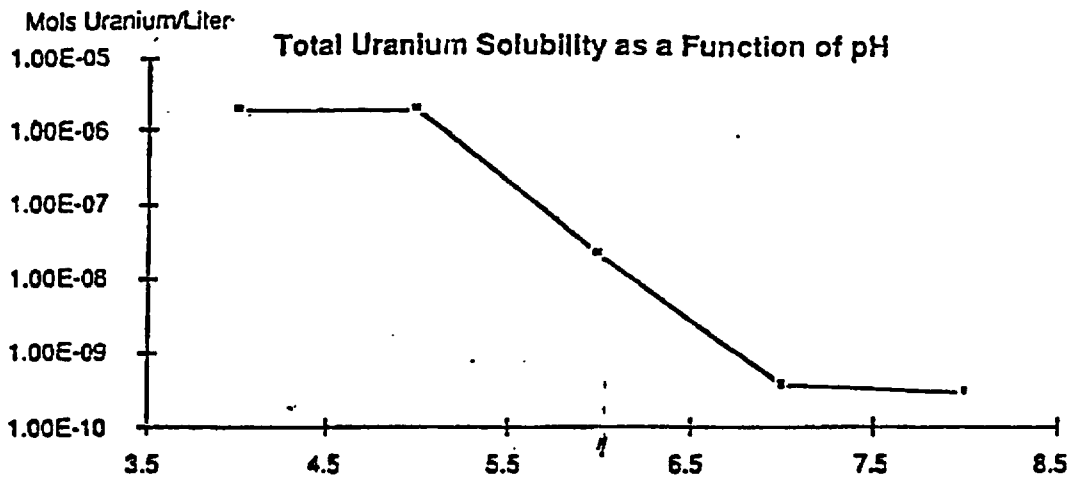

Fig. D.5-2. Estimated total uranium solubility under E-Area conditions (*Source:* Orebaugh 1993).

Solubility calculations conducted for U(IV) using Mathematica with uraninite as the controlling solid phase gave a similar solubility to that calculated by Orebaugh (1993) for the pH range of 7 to 12. Using the formation constants of Rai et al. (1990) and solubility product from Parks and Pohl (1988) a solubility of 3×10^{-10} M was calculated (Table D.5-2).

Table D.5-2. Uranium reactions considered

Reactions	log K	Reference
$UO_2 + 4H^+ == U^{4+} + 2(H_2O)$	2.5	Parks and Pohl 1988
$U^{4+} + H_2O == UOH^{3+} + H^+$	-0.5	Rai et al. 1990
$U^{4+} + 2H_2O == U(OH)_2^{2+} + 2H^+$	-4.0	Rai et al. 1990
$U^{4+} + 3H_2O == U(OH)_3^{+} + 3H^+$	-8.0	Rai et al. 1990
$U^{4+} + 4H_2O == U(OH)_4^{\circ} + 4H^+$	-12.0	Rai et al. 1990
$U^{4+} + 5H_2O == U(OH)_4^{-} + 5H^+$	-26.0	Rai et al. 1990

The Orebaugh (1993) solubility calculations and Mathematica solubility calculations based on the thermodynamic data for U(IV) from Rai et al. (1990) and Parks and Pohl (1988) are in good agreement (Fig. D.5-3) above pH 7. Variation in the results below pH 7 is due to disregarding U(VI) in the Mathematica solubility calculation. This is not significant because the pH in the vaults should remain above pH 7 due to the high alkalinity of the concrete.

D.6 SORPTION IN SOILS

There has not been a need to generate K_d's using iron oxide content of the soils. The K_d's used in the PA are documented in tables within the text. Additional material may be added as required during the course of the PA.

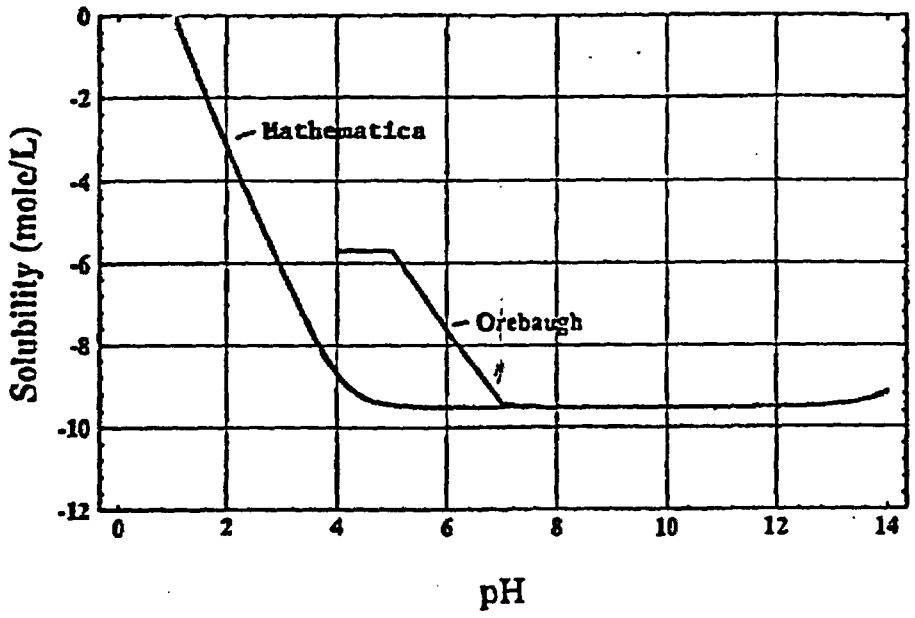

Fig. D.5-3. Comparison of uranium solubilities under E-Area conditions.

APPENDIX D
REFERENCES

Avotins, P. V. 1975. *Adsorption and Coprecipitation Studies of Mercury on Hydrous Iron Oxide.* Ph.D. thesis. Stanford University, Stanford, Calif.

Bondietti, E. A., and J. R. Trabalka. 1980. Evidence for Plutonium(V) in an Alkaline, Freshwater Pond. *Radiochem. Radioanal. Letters*, 42:169-176.

Brookins, D. G. 1988. *Eh-pH Diagrams for Geochemistry.* Springer-Verlag, New York. p. 176.

Duval, J. E., and M. H. Kurbatov. 1952. The Adsorption of Cobalt and Barium Ions by Hydrous Ferric Oxide at Equilibrium. *J. Phys. Chem*, 56(982-984).

Dzombak, D. A., and F. M. M. Morel. 1990. *Surface Complexation Modeling: Hydrous Ferric Oxide.* Wiley-Interscience Publication, John Wiley & Sons, Inc.

Ewart, F. T., J. L. Smith-Briggs, H. P. Thomason, and S. J. Williams. 1992. The Solubility of Actinides in a Cementitious Near-Field Environment. *Waste Management*, 12:241-252.

Girvin, D. C., L. L. Ames, A. P. Schwab, and J. E. McGarrah. 1991. Neptunium Adsorption on Synthetic Amorphous Iron Oxyhydroxide. *Journal of Colloid and Interface Science*, 141:67-78.

Harley, J. P., Jr. 1990a. *Specifications for Procurement of Low-Level Waste Burial Box.* Procurement Specification No. S4-G-183.

Harley, J. P., Jr. 1990b. *Specifications for Procurement of 45 ft3 Disposal/Storage Box.* Procurement Specification No. S4-G-858.

Hingston, F. J., A. M. Posner, and J. P. Quirk. 1968. *Adsorption of Selenite by Goethite.* In Adsorption from Aqueous Solution, Advances in Chemistry Series, American Chemical Society, pp. 82-90.

Howard, J. H., III. 1977. Geochemistry of Selenium: Formation of Ferroselite and Selenium Behavior in the Vicinity of Oxidizing Sulfide and Uranium Deposits. *Geochimica et Cosmochimica Acta*, 41(1665-1678).

Hsi, C. K. D., and D. Langmuir. 1985. Adsorption of Uranyl onto Ferric Oxyhydroxides: Application of the Surface Complexation Site-Binding Model. *Geochemica et Cosmochimica Acta*, 49(1931-1941).

Hunter, K. A., D. J. Hawke, and L. K. Choo. 1988. Equilibrium Adsorption of Thorium by Metal Oxides in Marine Electrolytes. *Geochimica et Cosmochimica Acta*, 52(627-636).

Kim, J. I., and B. Kanellakopulos. 1989. Solubility Products of Plutonium(IV) Oxide and Hydroxide. *Radiochimica Acta*, 48:145-150.

Kinniburgh, D. G., J. K. Syers, and M. L. Jackson. 1975. Specific Adsorption of Trace Amounts of Calcium and Strontium by Hydrous Oxides of Iron and Aluminum. *Soil Science Society of America Proceedings*, 39(464-470).

Kinniburgh, D. G., M. L. Jackson, and J. K. Syers. 1976. Adsorption of Alkaline Earth, Transition, and Heavy Metal Cations by Hydrous Oxide Gels of Iron and Aluminum. *Soil Science Society of America Proceedings*, 40(796-799).

Kolarik, Z. 1961. Sorption Radioaktiver Isotopen an Niederschlagen. VI. System Eisen(II)-Hydroxyd-Strontiumnitratlosung und die allgemeinen gesetzmassigkeiten der Sorption am Eisen(III)-Hydroxyd. *Collection Czech. Chem. Commun.*, 27(938-949).

Kurbatov, M. H. 1949. Rate of Adsorption of Barium Ions in Extreme Dilution by Hydrous Ferric Oxide. *Journal of American Chemical Society*, 71(858-863).

Leckie, J. O., M. M. Benjamin, K. F. Hayes, G. Kaufman, and S. Altamann. 1980. *Adsorption/Coprecipitation of Trace Elements from Water with Iron Oxyhydroxide*. EPRI RP-910-1. Electric Power Research Institute, Palo Alto, CA.

Leckie, J. O., A. R. Appleton, N. B. Ball, K. F. Hayes, and B. D. Honeyman. 1984. *Adsorptive Removal of Trace Elements from Fly-Ash Pond Effluents onto Iron Oxyhydroxide*. EPRI RP-910-1. Electric Power Research Institute, Palo Alto, CA.

Nelson, D. M., and M. B. Lovett. 1978. Oxidation State of Plutonium in the Irish Sea. *Nature*, 236(599-601).

Nelson, D. M., and M. B. Lovett. 1981. Measurements of the Oxidation State and Concentration of Plutonium in Interstitial Waters of the Irish Sea. In *Impacts of Radionuclide Releases into the Marine Environment*, Proc., Symp., Otaniemi, June 30-July 4, 1975. IAEA, Vienna.

Nelson, D. M., and K. A. Orlandini. 1979. Identification of Pu(V) in Natural Waters. In *Radiological and Environmental Research Division Annual Report*, ANL-79-65, Part III, pp. 57-59.

OLI. 1993. *ESP Version 3 Manual.* OLI Systems, Inc., Morris Plains, NJ.

Orebaugh, E. G. 1993. *Modeling Uranium Solubility in Aged Vault Disposal.* WSRC-RP-93-1318. E. I. du Pont de Nemours and Company, Savannah River Laboratory, Aiken, SC.

Parks, G. A., and Pohl, D. C. 1988. Hydrothermal solubility of uraninite. *Geochimica et Cosmochimica Acta*, 52:863-875.

Phillips, S. L., Hale, F. V., Silvester, L. F., and Siegel, M. D. 1988. *Thermodynamic Tables for Nuclear Waste Isolation.* Aqueous Solution Database, NUREG/CR-4864, p. 138.

Plotnikov, V. I. 1958. *Coprecipitation of Small Quantities of Selenium with Ferric Hydroxide.* Russian Journal of Inorganic Chemicals, 3(8):1761-1766.

Rai, D., Felmy, A. R., and Ryan, J. L. 1990. Uranium(IV) Hydrolysis Constants and Solubility Product of UO2 xH2O(am). *Inorganic Chemistry*, 29:260-264.

Sanchez, A. L., J. W. Murray, and T. H. Sibley. 1985. The Adsorption of Plutonium IV and V on Goethite. *Geochemica et Cosmochimica Acta*, 49(2297-2307).

Sharland, S. M., P. W. Tasker, and C. J. Tweed. 1986. *The Evolution of Eh in the Pore Water of a Model Nuclear Waste Repository.* UKAEA Report AERE-R12442. Harwell Laboratory, UK.

APPENDIX E

HYDROGEOLOGY OF THE SRS

E.1 GEOLOGY

The surface of the Upper Atlantic Coastal Plain on which SRS is located slopes gently seaward. The province is underlain by a seaward dipping wedge of unconsolidated and semi-consolidated sediments that extends from the Fall Line to the seaward edge of the continental shelf. Sediment thickness increases from zero at the Fall Line, where the crystalline Piedmont province gives way to the Coastal Plain, to more than 1.2 km near the coast of South Carolina. The SRS is underlain by about 180 to 370 m of Coastal Plain sediments. The Coastal Plain sediments vary in age from Late Cretaceous to Recent. The Coastal Plain sediments are divided into several groups based principally on age and lithology. These groups are described briefly below. An in-depth treatment of the stratigraphy of the SRS is given in the Replacement Tritium Facility Draft Safety Analysis Report (WSRC 1992).

E.1.1 Late Cretaceous Lumbee Group

The Late Cretaceous sediments constitute the Lumbee Group, which includes, from oldest to youngest, the Cape Fear, Middendorf, Black Creek, and Peedee Formations (Fig. E.1-1). This group has also been referred to as the Tuscaloosa Formation (INTERA 1986). The thickness of the Lumbee Group varies across SRS from 120 m in the northwest to more than 230 m near the southeastern boundary.

The Cape Fear Formation is composed of poorly sorted silty-to-clayey quartz sands and interbedded clays. Bedding thicknesses range from 1.5 to 6 m, with sand beds being thicker than clay beds. The formation is about 9 m thick at the northwestern boundary of SRS, and it increases to more than 55 m near the southeastern boundary. This formation has not been observed to outcrop in the vicinity of the SRS.

The Middendorf Formation, which overlies the Cape Fear Formation, is composed mostly of medium and coarse quartz sand that is cleaner and less indurated than the underlying sediments. Clay casts and pebbly zones occur in several places in the

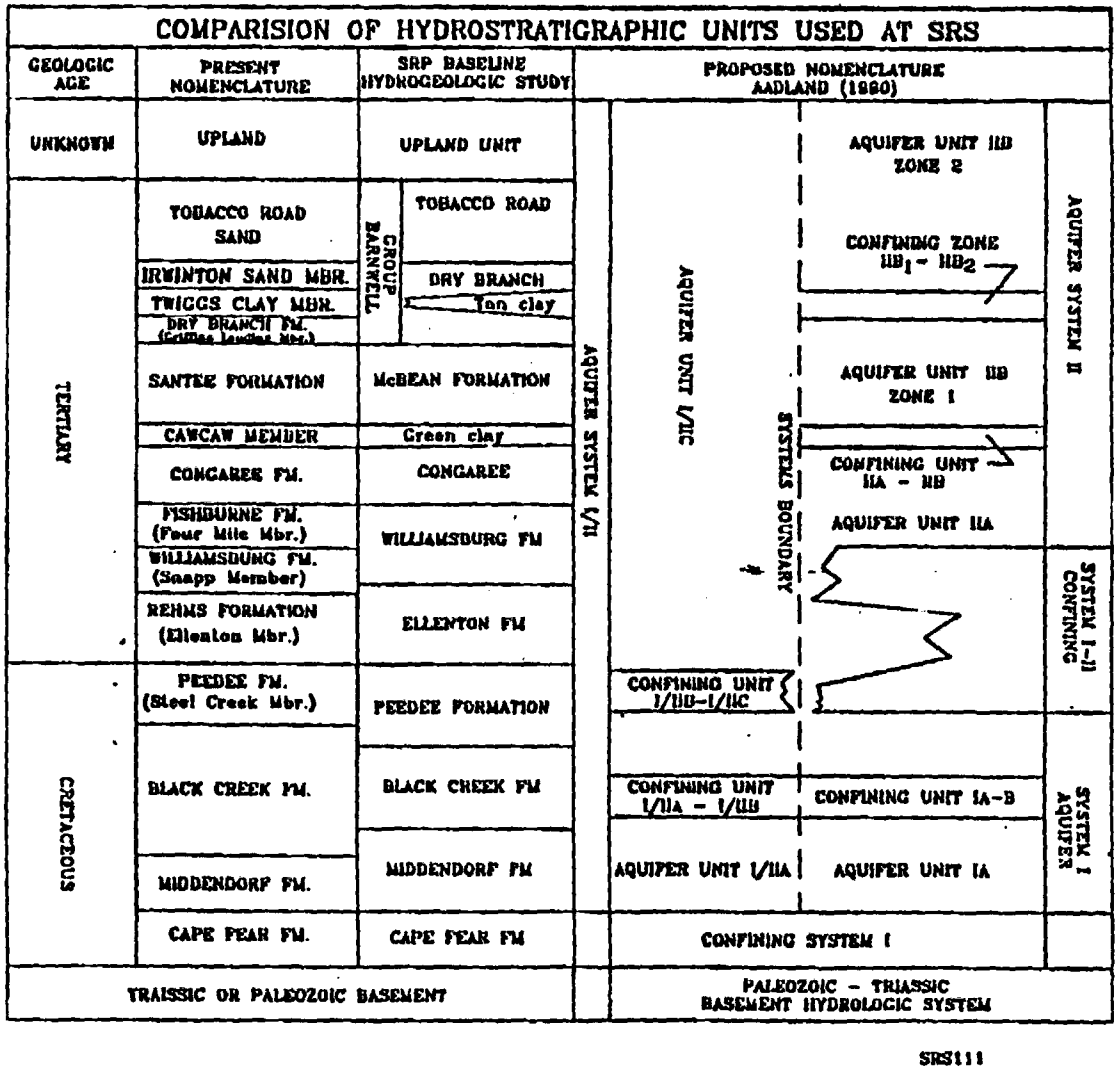

Fig. E.1-1. Hydrologic and stratigraphic units underlying the SRS.

Middendorf Formation. A clay zone up to 24 m thick forms the top of this formation over much of the SRS. In total, the Middendorf Formation ranges from approximately 40 to 55 m thick from the northwestern to southeastern boundary of the SRS. Outcrops of this formation have been identified northwest of the SRS.

The Black Creek Formation consists of quartz sands, silts and clays. The lower section consists of fine- to coarse-grained sands, with layers of pebbles and clay casts. The upper section changes in composition as it crosses the SRS from northwest to southeast; from massive clay to silty sand with interbeds of clay. Thickness of the Black Creek Formation under the SRS ranges from 34 m in the northwest to 76 m in the southeast. Outcropping in the vicinity of the SRS has not been confirmed.

The uppermost formation in the Lumbee Group is the Peedee Formation, which consists of fine-grained sandstone and siltstone with marine fossils. This formation is subtitled as the Steel Creek Member in Fig. E.1-1 to distinguish this formation from the Peedee Formation in southwestern South Carolina that is comparable in age, but lithologically distinct. The lower portion of this formation consists of fine- to coarse-grained quartz sand and silty sand, with a pebble-rich zone at its base. Pebbly zones and clay casts are common throughout the lower portion of the Peedee Formation. The upper portion of this formation is a clay that varies from more than 15 m to less than 1 m in thickness at the SRS. The Peedee Formation is about 34 m thick at the northwestern SRS boundary, and about 40 m thick at the southeastern boundary. No nearby outcropping has been identified.

E.1.2 Paleocene-Eocene Black Mingo Group

The Paleocene-Early Eocene sediments make up the Black Mingo Group. This group consists of the Early Paleocene Rhems Formation, the Late Paleocene Williamsburg Formation, and the Early Eocene Fishburne Formation (Fig. E.1-1). This group is about 21 m thick at the northwestern SRS boundary, thickens to about 46 m near the southeastern boundary, and is about 210 m thick at the coast.

The Rhems Formation has also been called the Ellenton Formation (INCERA 1986), but is now believed to be the time-equivalent to the Rhems Formation with some lithological differences in the vicinity of SRS. Thus, it is now designated as the Ellenton Member of the Rhems Formation (Fig. E.1-1). The Ellenton Member consists mostly of gray, poorly sorted, micaceous, lignitic, silty and clayey quartz sand interbedded with gray clays. It is approximately 12 m thick at the northwestern boundary of the SRS and thickens to about 30 m near the southeastern boundary. This formation outcrops about four miles northwest of the SRS.

The deposits near the SRS that are time equivalent to the Williamsburg Formation differ from the type Williamsburg and are designated as the Snapp Member of the Williamsburg Formation. The sediments are typically silty, medium- to coarse-grained quartz sand interbedded with clay. The Snapp Member is about 9 m thick at the northwestern SRS boundary and thickens to about 15 m near the southeastern boundary. Sediments of this formation have not been identified to outcrop northwest of the SRS. Although the Fishburne Formation exists in southwestern South Carolina, only one Early Eocene fossil assemblage has been found at the SRS. The distribution of any Fishburne equivalent at the SRS is not known at this time.

E.1.3 Middle Eocene Orangeburg Group

The Middle Eocene sediments make up the Orangeburg Group, which consists of the lower Middle Eocene Congaree Formation and the upper Middle Eocene Santee Limestone Formation. The sediments thicken from about 30 m at the northwestern SRS boundary to about 49 m near the southeastern boundary. The dip of the upper surface of this formation is about .002 m/m to the southeast across the site. The Orangeburg Group is about 100 m thick at the coast. The group outcrops at lower elevations in many places near and on the SRS.

The Congaree Formation consists of fine to coarse quartz sands. Thin clay laminae occur throughout with pebbly layers, clay casts, and glauconite present in places. A glauconitic clay encountered in some wells on the SRS may be at or near the base of this formation. In many places at the SRS, the upper part of the Congaree Formation is

cemented with silica, while in other places it is slightly calcareous. The well-sorted sands, glauconite, and a few fossils indicate that the Congaree is a shallow marine deposit. The formation is about 18 m thick at the northwestern boundary of the SRS and about 26 m thick near the southeastern boundary.

The Santee Limestone Formation consists of carbonates, calcareous quartz sands, quartz sands, glauconitic sands, and clays. The sediments comprising this formation have been referred to in the past as the McBean and Lisbon Formations. However, more recently (WSRC 1992), these sediments are considered to be one of three members of the Santee Limestone Formation. A fine-grained sandstone occurs at the base of the Santee Limestone Formation at several locations across the SRS. This sandstone is referred to as the Warley Hill Member. Green clay, which also occurs near the base of this formation, is referred to as the Caw Caw Member of the Santee Limestone. The remainder of the Santee Limestone Formation is assigned to the McBean Member, which dominates the formation and is made up of micritic, calcarenitic, and shelly limestone, calcareous quartz sand, and noncalcareous, generally fine-grained quartz sand. Previous investigations in the nearby vicinity (Z-Area) indicate that the green clay is not a discrete clay bed, but rather a series of thin clays interlayered with sandy clays (Dennehy et al. 1989). Therefore, the green clay tends to thicken and thin, and grade laterally into the sands of the overlying McBean Member (Dennehy et al. 1989).

Above the green clay, the McBean Member is comprised of 13 m of poorly sorted multi-colored clayey sand with clay lenses. Calcareous components of the McBean Member are rare in the northwestern part of the SRS, more abundant in central portions, and increase to the southeast across the SRS where they are widespread and thick. Siple (1967) noted that voids and loosely compacted sediments were encountered during well drilling and mentioned that large amounts of cement grout were used to stabilize the subsurface before construction of heavy structures, suggesting that dissolution of calcareous material in the Santee Limestone has occurred at the SRS. The Formation is about 12 m thick at the northwestern boundary and thickens to more than 24 m near the southeastern boundary. All three members of the Santee Limestone Formation outcrop within the SRS boundary.

E.1.1 Late Eocene Barnwell Group

The Late Eocene sediments make up the Barnwell Group, which consists of the Clinchfield, Dry Branch, and Tobacco Road Sand Formations (Fig. E.1-1). The Clinchfield Formation, the oldest of the three, is made up of quartz sand and has been identified only when the contrasting carbonates of the Dry Branch and Santee Limestone Formations are present, with the sand of the Clinchfield Formation sandwiched between them. It has been identified at several areas within the SRS, where it is up to 8 m thick, but it cannot be mapped with available data.

The Dry Branch Formation consists of three distinguishable members: the Griffins Landing Member, the Irwinton Sand Member and the Twiggs Clay Member. The latter member does not appear to be mappable within the SRS, but lithologically similar clay is present at various levels within this formation. The composition of the tan clay, varies from a dark brown to tan clayey sand to a red to dark brown sandy clay. There is no geologic evidence suggesting a discrete clay layer for the Twiggs Clay Member. Rather, this member is apparently a series of intercalated clay and sand layers.

The carbonate of the Griffins Landing Member is up to 14 m thick in the southeastern part of the SRS. This member consists mostly of calcilutite and calcarenite, calcareous quartz sand, and slightly calcareous clay. It occurs sporadically at the SRS and is not known to be present northwest of Tinker Creek and UTR Creek within the SRS boundaries. The Griffins Landing Member has previously been considered to be part of the "McBean Formation" (Siple 1967; INTERA 1986). The remainder of the Dry Branch Formation within the SRS is made up of the Irwinton Sand Member, which is composed of moderately sorted quartz sand, with interlaminated clays abundant in places. The Dry Branch formation is about 15 m thick at the northwestern SRS boundary, and thickens to 24 m near the southeastern boundary. It outcrops in many places around and within the SRS.

The Tobacco Road Sand overlies the Dry Branch Formation. The base of this unit is marked by a coarse layer that can contain flat quartz pebbles. The rest of the formation is made up of moderately to poorly sorted quartz sands. The sediments have the characteristics of a shallow marine deposit. The upper surface of this formation is irregular due to an incision that accompanied deposition of the overlying "Upland" unit and later erosion. The

thickness is variable as a result of erosive processes, but is at least 15 m in places. The Tobacco Road Sand of Barnwell Group (INTERA 1986), is widely exposed at the SRS. The combined thickness of the Dry Branch and Tobacco Road formations at the coast is almost 120 m.

E.1.5 "Upland Unit"

The "Upland Unit" is an informal stratigraphic term applied to terrestrial deposits that occur at higher elevations in some places in the southwestern South Carolina Coastal Plain. This unit occurs at the surface at higher elevations in many places around and within the SRS, but it is not present at all higher elevations. The sediments are poorly sorted, clayey-to-silty sands, with lenses and layers of conglomerates, pebbly sands, and clays. Clay casts are abundant. The "Upland" unit is up to 21 m thick in parts of the SRS. Much of this unit corresponds to the Hawthorne Formation and the Tertiary alluvial gravels identified in previous documents (INTERA 1986).

E.1.6 Quaternary Deposits

Cooke (1936) identified seven marine terraces in the region near the SRS, although the highest three are extensively eroded and are not easily recognized. The terrace deposits are a few tens of feet thick. The origin of these deposits is not definitive. Recent alluvium occurs in the main and tributary channels of the Savannah River and other streams in the vicinity of the SRS.

E.2 GROUNDWATER HYDROLOGY

An alpha-numeric system of hydrostratigraphic nomenclature was developed by Aadland (1990) for SRS. Figure E.1-1 illustrates the alphanumeric system and compares it to other systems developed in previous studies.

E.2.1 Aquifer System I

The lowermost aquifer system, referred to as Aquifer System I, is regional in nature and includes the Middendorf Formation, the Black Creek Formation, and the Peedee Formation (Fig. E.1.1). These formations are of Cretaceous age and consists of beds of sands, silts, and clays. Aquifer System I is further divided into aquifer zones and confining zones depending upon hydraulic properties. This system serves as a major source of water for SRS and the region.

E.2.2 Confining System I-II

Confining System I-II separates Aquifer System I from Aquifer System II (Fig. E.1.1). Greater than 30 m thick, it is comprised of the Ellenton Clays. Hydraulically, it restricts flow between Aquifer System I and Aquifer System II.

E.2.3 Aquifer System II

Because of relative hydrologic isolation due to Confining System I, only the uppermost system of the two major aquifer systems is of interest for contamination studies at E-Area. This aquifer system, referred to as Aquifer System II, is divided into individual units and further subdivided into zones. These units and zones primarily relate to hydrogeological characteristics. The units and zones which comprise the aquifer system are as follows:

Nomenclature of Aadland (1990)	Common Nomenclature
Aquifer System II	
Aquifer Unit IIB, Zone 2	Water Table Aquifer
Confining Unit IIB1-IIB2	Tan Clay
Aquifer Unit IIB, Zone 1	Barnwell/McBean Aquifer
Confining Unit IIA-IIB	Green Clay
Aquifer Unit IIA	Congaree Aquifer
Confining System I-II	Ellenton Clays

E-Area is located within the GSA of the SRS. The GSA includes the present buried grounds and S-Area.

E.2.3.1 Confining System I-II

Confining System I-II (Ellenton Clays) is a silty to sandy lignitic, micaceous clay interbedded with fine to coarse quartz sand. Individual layers of clays, silts, and sandy clays range in thickness from 0.6 to 6.7 m. Individual layers of clayey sands range in thickness from 0.3 to 4.6 m. Clay and silt lenses of Confining System I-II consist of buff and light gray to black clay and sandy clay. The interbeds of clayey sands and sands are generally fine to coarse grained and range from moderate to very poorly sorted. Grains are subangular to angular (GeoTrans 1992).

Confining System I-II attains a thickness of over 30 m in the GSA. The unit appears to occur no further northwest than the northwest boundary of SRS where it is about 12 m in thickness. Regionally, the unit thickens to the southeast.

E.2.3.2 Aquifer Unit IIA

Aquifer Unit IIA (Congaree Aquifer) unconformably overlies Confining System I-II (Ellenton Clays) and ranges from 15.8 to 32.6 m thick within the GSA. The unit dips at 1.5 to 1.7 m per km to the south and southeast. Additionally, the unit thickens in the western portion of the GSA and to a minor extent, thickens to the southeast.

Clayey layers are encountered to some degree at all depths throughout the formation. However, by far the majority of such layers occur below an elevation of 24 m MSL which corresponds to the lower and middle portions of the formation. The unit consists predominantly of sands and clayey sands with small interbeds of sandy clays, clays, and calcareous sands. The sands and clayey sands range in thickness from 0.6 to 25.6 m while the sandy clays and clays range in thickness from 0.3 to 2.7 m. Calcareous sands range in thickness from 0.6 to 0.9 m. Sands and clayey sands of Aquifer Unit IIA are largely yellow to orange in color and consists of fine to coarse grained, subangular to subrounded quartz. The sands vary from well to poorly sorted.

Groundwater flow in the aquifer at E-Area is to the west toward UTR Creek (Fig. E.2-1). A local potentiometric map of Aquifer Unit IIA was developed based upon water level data from E-Area wells (Fig. E.2-2) which indicates the flow direction. A regional potentiometric map of Aquifer Unit IIA is provided in Fig. E.2-3 for comparison purposes. The horizontal gradient of the aquifer is estimated to be 0.006 in the GSA area. Based on a slug test (WSRC 1991) the hydraulic conductivity of the aquifer was estimated to be 6.46×10^{-4} cm/s in the GSA area.

E.2.3.3 Confining Unit IIA-IIB

Confining Unit IIA-IIB (Green Clay) separates Aquifer Unit IIA and Aquifer Unit IIB. This confining unit is locally known as the Green Clay. Recent investigations have indicated that this unit is comprised of several lenses of green clay that thicken, thin, and pinch out abruptly. Thickness can be variable, from 0.6 to 9 m. Although Confining Unit IIA-IIB does not always appear during drilling to be a significant geologic feature, wells screened above and below the layer routinely have very different heads. Thus, Confining Unit IIA-IIB retards downward vertical leakage from Aquifer Unit IIB, Zone 1 (Barnwell/McBean Aquifer), into Aquifer Unit IIA (Congaree Aquifer). The unit is thin to the west and southeast, becoming thicker to the north. Structural lows in the unit tend to correspond to areas of carbonate accumulation in the overlying sediments. In addition, the clays of the unit thin or truncate in these areas.

Confining Unit IIA-IIB consists predominantly of clays, sandy clays, and clayey sands. Locally, beds of calcareous mud contribute significant thickness to the unit. Minor interbeds of sands are also present. The clay and sandy clay lenses in the unit range in thickness from 0.6 to 3.6 m. The clayey sand beds range in thickness from 0.3 to 4.2 m. Calcareous muds range in thickness from 0.9 to 3.3 m and the sand beds range in thickness from 0.3 to 1.8 m (GeoTrans 1992).

The clayey sands are generally moderately to poorly sorted with grain sizes ranging from medium to very coarse. They are described as light tan to orange in color, fine to very fine grained, well sorted and occasionally indurated. Grains are usually subangular and in some layers cemented with silica.

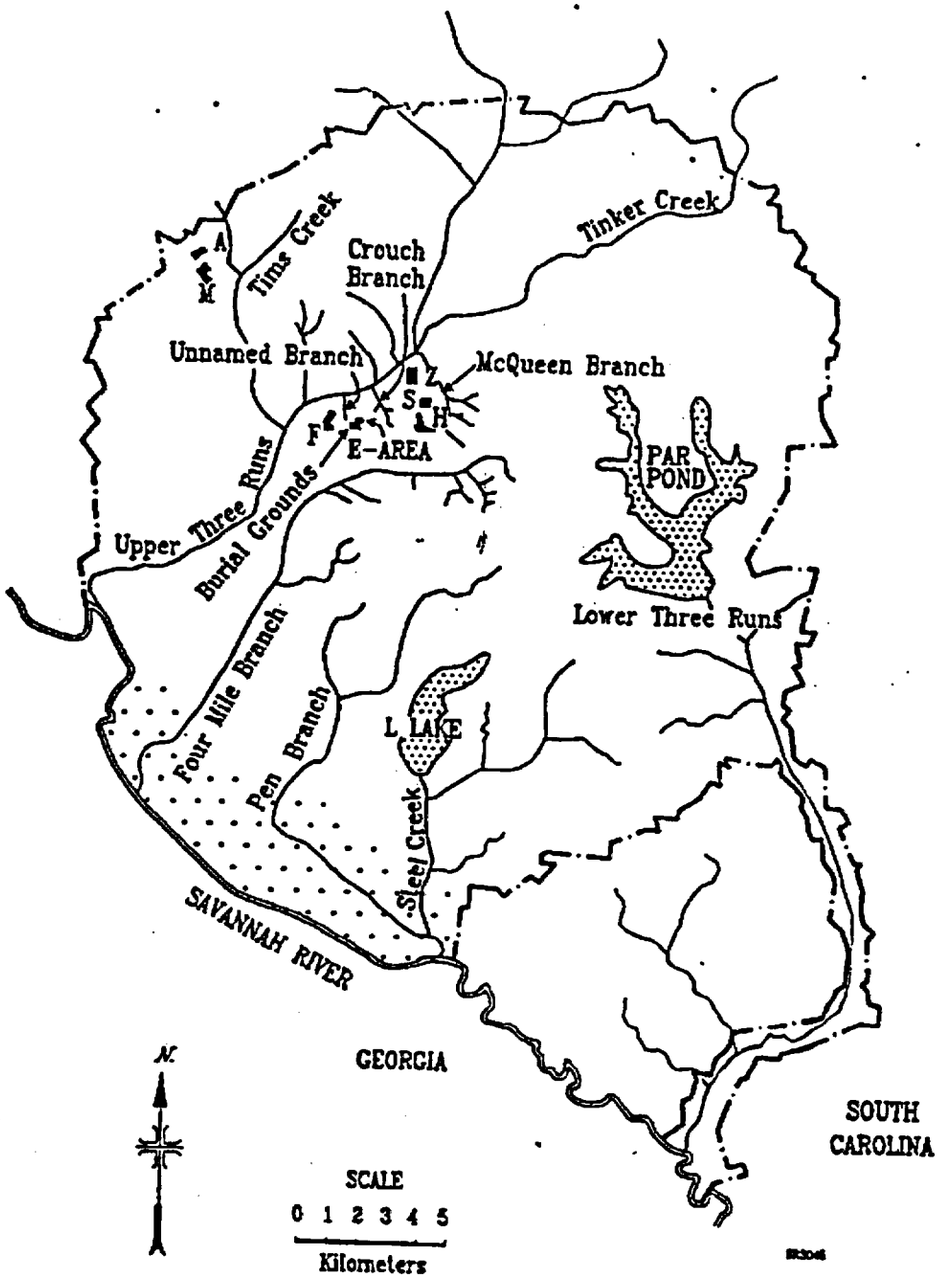

Fig. E.2-1. Surface drainage map of the SRS.

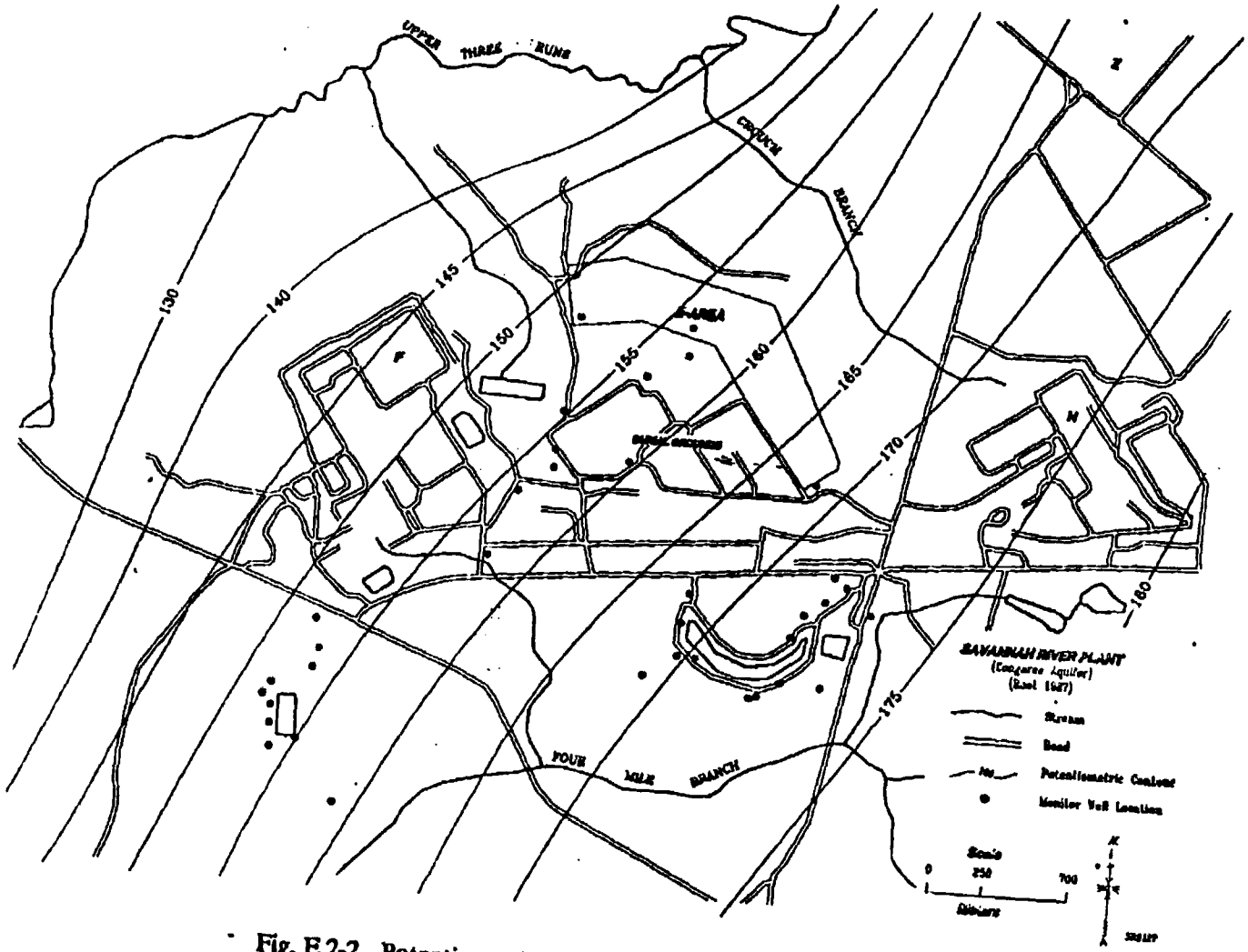

Fig. E.2-2. Potentiometric surface of Aquifer Unit IIA at E-Area.

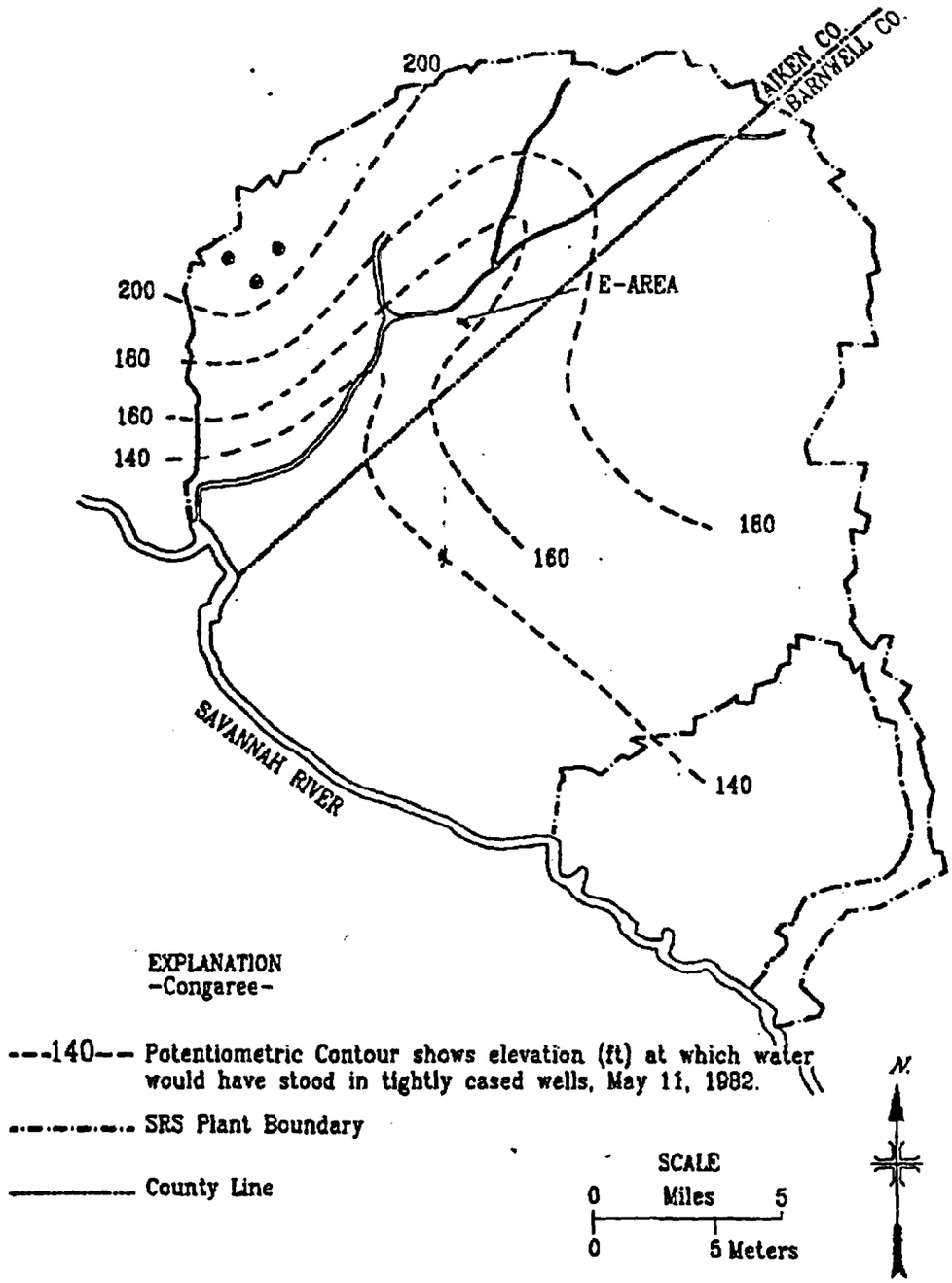

Fig. E.2-3. Regional potentiometric surface of Aquifer Unit IIA (Christensen and Gordon 1983).

SRS077

From laboratory tests of undisturbed samples, the hydraulic conductivity of Confining Unit IIA-IIB has been determined to range from 1.4×10^{-8} to 1.6×10^{-7} cm/s (horizontal) and 6.5×10^{-9} to 7.4×10^{-8} cm/s (vertical). The vertical gradient has been estimated to be 5.5 m/m (WSRC 1991).

E.2.3.4 Aquifer Unit IIB1

Aquifer Unit IIB, Zone 1 (Barnwell/McBean Aquifer), overlies Confining Unit IIA-IIB (Green Clay) and underlies Confining Unit IIB1-IIB2 (Tan Clay). This zone ranges in thickness from 11.9 to 27.7 m. It thins toward the western portion of the GSA, in the vicinity of the F-Area Seepage Basins. Thickening of the zone occurs to the southeast, in the vicinity of the H-Area Seepage Basins. Aquifer Unit IIB, Zone 1, dips approximately 1.5 to 1.7 m/km to the southeast (GeoTrans 1992).

This aquifer zone consists predominantly of sand and clayey sand sequences with localized zones of abundant calcareous sands, sandy and muddy limestones, and limestones. Minor interbeds of clay and sandy clay are also present. Sands and clayey sands within the zone range in thickness from 0.6 to 18 m. Calcareous sands range in thickness from 0.6 to 10 m. Sandy and muddy limestones, and limestones range in thickness from 0.9 to 9 m.

The sand and clayey sand beds are generally yellow to tan, occasionally greenish brown to light brown. The sand is fine to coarse grained, moderately to well sorted, and generally subangular. The calcareous sands are white to buff in color and contain up to 50% calcareous materials. The sandy and muddy limestones and limestones are white to buff in color and contain greater than 80 percent calcareous material. The interbeds of the clays and sandy clays in this unit are light tan to orange in color. Sand is quartz, fine to medium grained, subangular, and well to moderately sorted.

The hydraulic conductivity of the zone ranges from 7.39×10^{-5} to 7.2×10^{-3} cm/s. The horizontal hydraulic gradient within the zone is estimated to be 0.01 m/m. The vertical gradient in Aquifer Unit IIB1 is estimated to be 0.058 m/m (WSRC 1991). A potentiometric surface for Aquifer Unit IIB, Zone 1, was developed based upon water level data taken from E-Area wells and is provided in Fig. E.2-4.

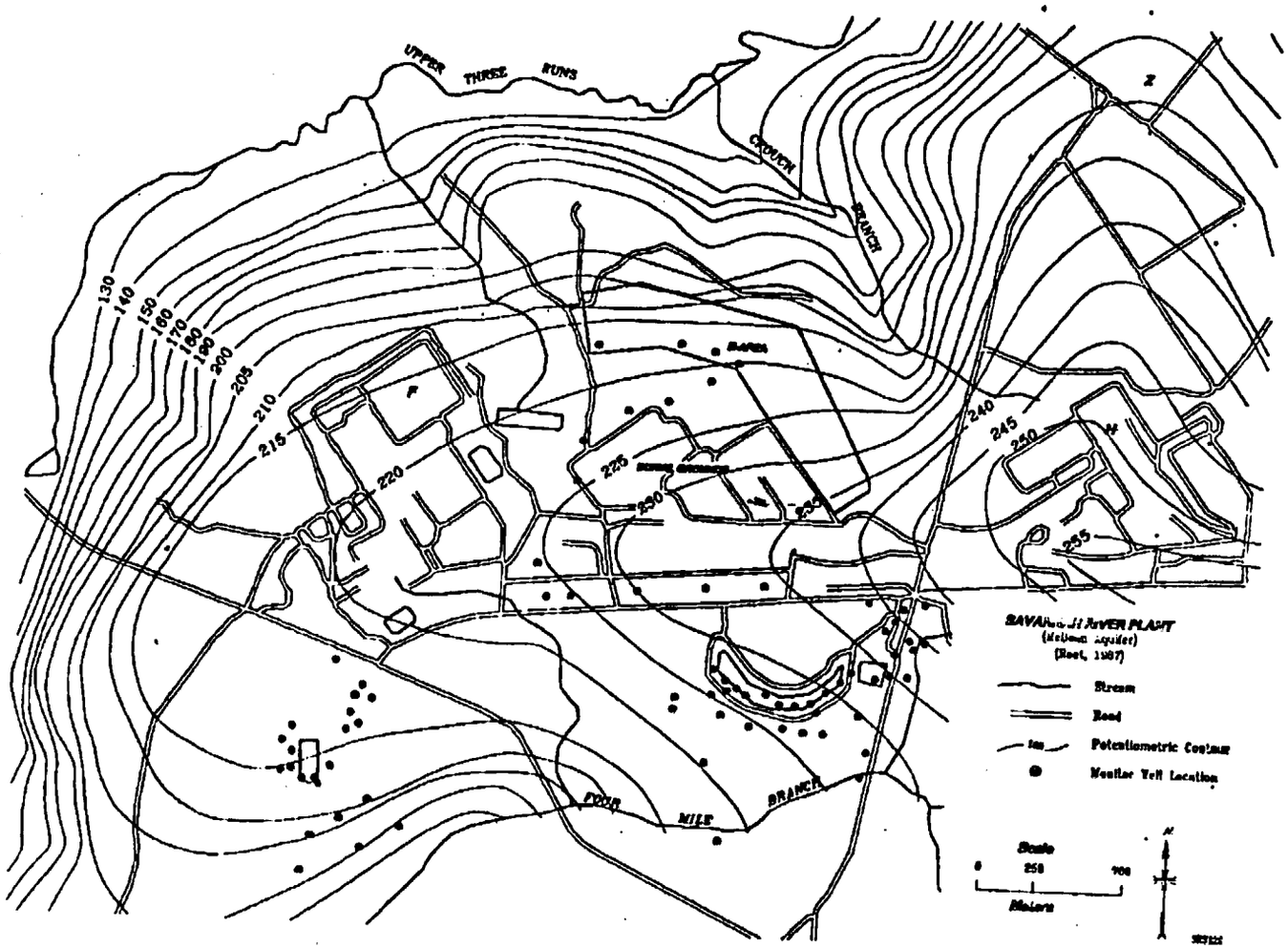

Fig. E.2-4. Potentiometric surface of Aquifer Unit IIB, Zone 1, at E-Area.

E.2.3.5 Confining Zone IIB1-IIB2

Confining Zone IIB1-IIB2 (Tan Clay) consists of multiple, discontinuous clay layers, which separates underlying Aquifer Unit IIB, Zone 1 (Barnwell/McBean), from overlying Aquifer Unit IIB, Zone 2 (water table). The two aquifer zones are in direct contact where this confining zone is absent. Thickness varies from 0 to 10 m. Confining Zone IIB1-IIB2 is not always clearly observed during drilling. Where the zone is present in the GSA, however, head differences between wells screened above and below the zone range from 0.9 to 1.5 m (GeoTrans 1992).

Confining Zone IIB1-IIB2 consists predominantly of clays and sandy clay with minor to equal interbeds of clayey sands and sands. Clays and sandy clays range in thickness from 0.3 to 3.3 m. Clayey sands and sands range in thickness from 0.3 to 2.4 m.

The clays, clayey sands, and sands within Confining Zone IIB1-IIB2 are light tan to light orange in color. The sands are predominantly medium to coarse grained with a moderate degree of sorting. Grain size tends to coarsen upward.

Laboratory analyses of undisturbed samples of Confining Zone IIB1-IIB2 yielded a range of hydraulic conductivities from 6.0×10^{-9} to 1.2×10^{-7} cm/s in the horizontal direction and 1.2×10^{-9} to 4.0×10^{-7} cm/s in the vertical direction (WSRC 1991).

E.2.3.6 Aquifer Unit IIB, Zone 2

Aquifer Unit IIB, Zone 2 (water table), is the uppermost aquifer. Although sometimes referred to as "water table", it is defined stratigraphically, not by the degree of saturation. In portions of the GSA this aquifer is completely desaturated. It overlies Confining Zone IIB1-IIB2 (Tan Clay) where the confining zone is present and Aquifer Unit IIB, Zone 1 (Barnwell/McBean), where the confining zone is absent. This aquifer zone attains a maximum thickness of 33.5 m within the GSA. The aquifer zone ranges from 0 to 20 m in thickness along Four Mile Branch which partially incises it within the GSA. Additionally, the aquifer zone dips at a rate of 1.5 to 1.7 m/km to the southeast (GeoTrans 1992).

Aquifer Unit IIB, Zone 2, consists predominantly of sands and clayey sands with lesser or equal amount of clay and sandy clay. Gravel and pebble layers occur locally. The sands and clayey sands within the zone range in thickness from 6.1 to 32.6 m while the clays and

sandy clays range in thickness from 0.3 to 5.4 m. Gravel and pebble layers range in thickness from 0.3 to 1.5 m.

Sands and clayey sands are tan to red to purple and are often highly variegated in color. Sands are fine to very coarse, subangular to angular and moderately to poorly sorted.

Hydraulic conductivities for Aquifer Unit IIB, Zone 2, range from 1.3×10^{-4} to 5.8×10^{-4} cm/s. The horizontal gradient ranges from 0.0035 to 0.018 m/m with the flow direction to the north and northwest toward UTR Creek (WSRC 1991). A potentiometric surface based upon water level data from wells located at E-Area is provided in Fig. E.2-5 for Aquifer Unit IIB, Zone 2.

E.2.4 Hydrologic Characteristics of the Unsaturated Zone

Hydraulic characteristics of unsaturated soil in E-Area were investigated by Gruber (1980) and in nearby Z-Area, by Quisenberry (1985). Soil water content - soil water pressure relationships for soil in both areas were developed, as were relationships between hydraulic conductivity and water content. Characteristic curves illustrating the relationship between moisture content and soil pressure head (m), and between moisture content and hydraulic conductivity (m s^{-1}), for soils in E-Area are presented in Fig. E.2-6 and E.2-7. The plotted data were obtained by Gruber for undisturbed soil cores. Saturated hydraulic conductivity of these soils was estimated by Gruber to be on the order of 1×10^{-6} m s^{-1}, with porosity on the order of 0.47 to 0.52, and bulk density on the order of 1.6 g cm^{-3}.

Results for the undisturbed soil in Z-Area are presented in Figs. E.2-8 and E.2-9. A relationship similar to that depicted in Fig. E.2-8 for undisturbed soil cores was found for disturbed soil, with a somewhat steeper gradient as soil water pressure approached zero. For the undisturbed soil cores, at pressures less than -1 m, little additional decrease in soilwater content was measured as pressures were decreased to -5 m. Saturated hydraulic conductivity of the Z-Area soils tested was estimated by Quisenberry to be 2×10^{-7} m s^{-1}, with a porosity of 0.37 and corresponding bulk density of 1.7 g cm^{-3}. It is noted by Quisenberry that the field measurements were made in three well-drained areas. The difference between both investigator's curves illustrate the heterogeneous nature of soils in the vicinity of E-Area.

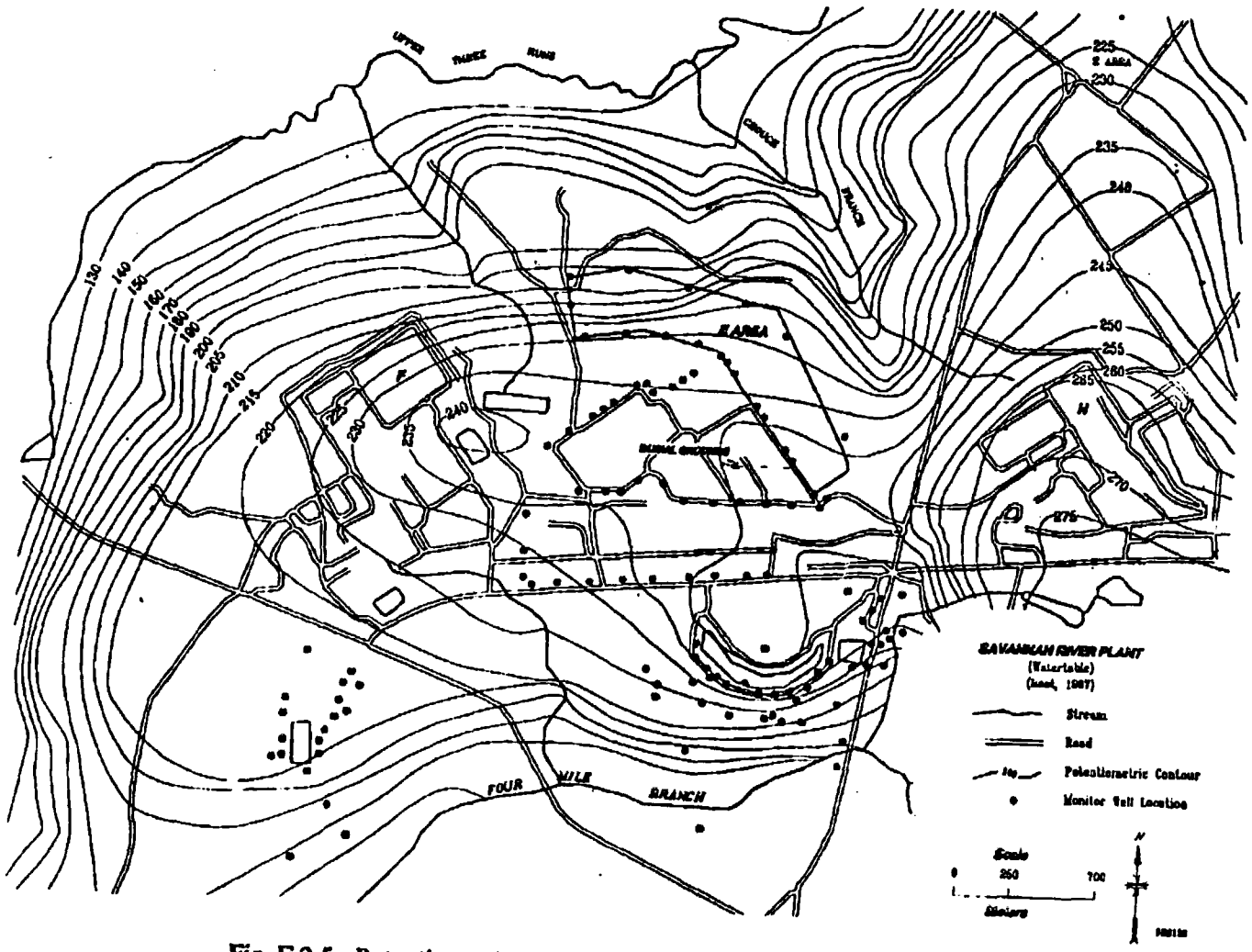

Fig. E.2-5. Potentiometric surface for Aquifer Unit IIB, Zone 2, at E-Area.

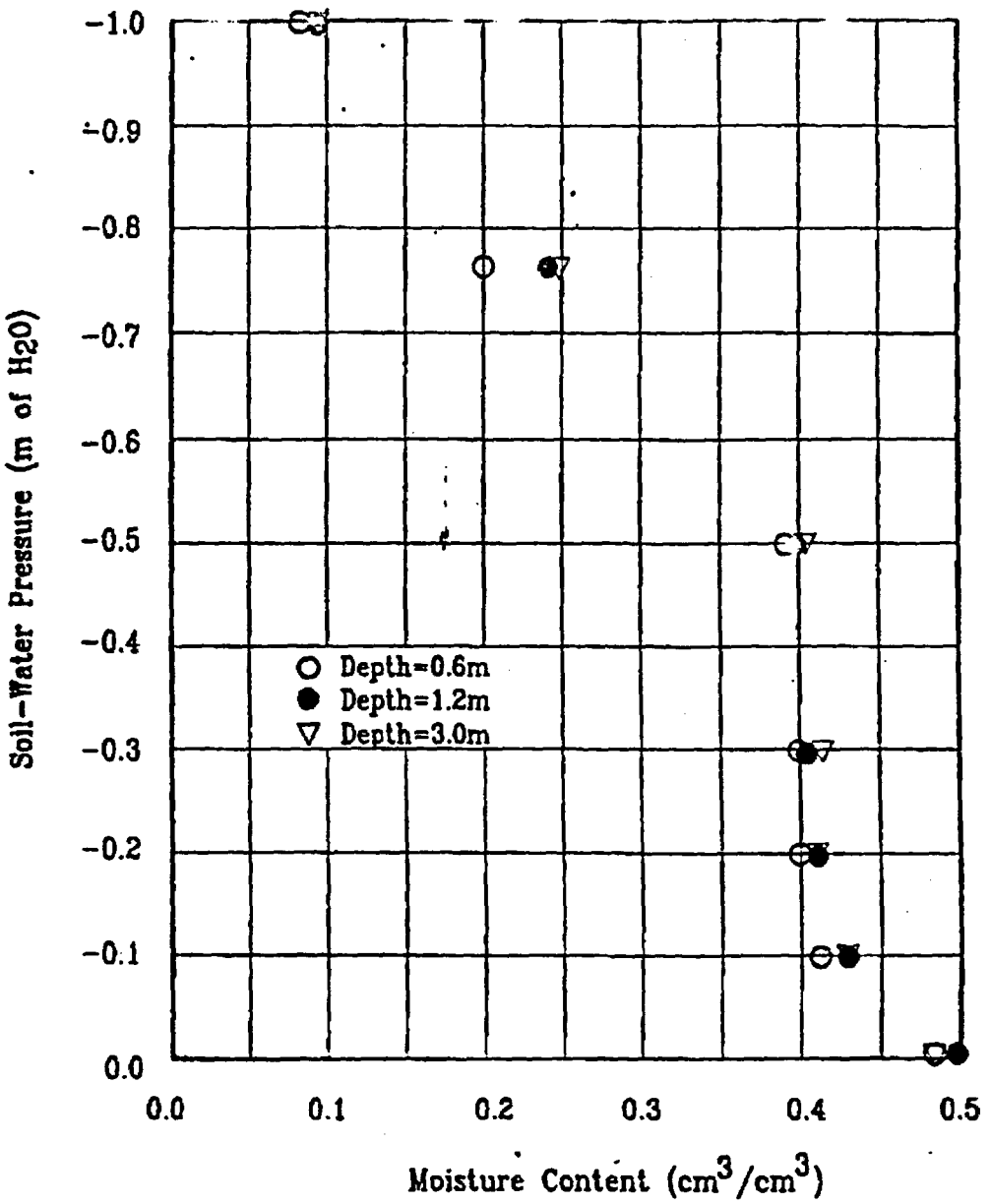

Fig. E.2-6. Soil water content - pressure relationships for undisturbed soils at SRS burial grounds (Gruber 1980). SRS075

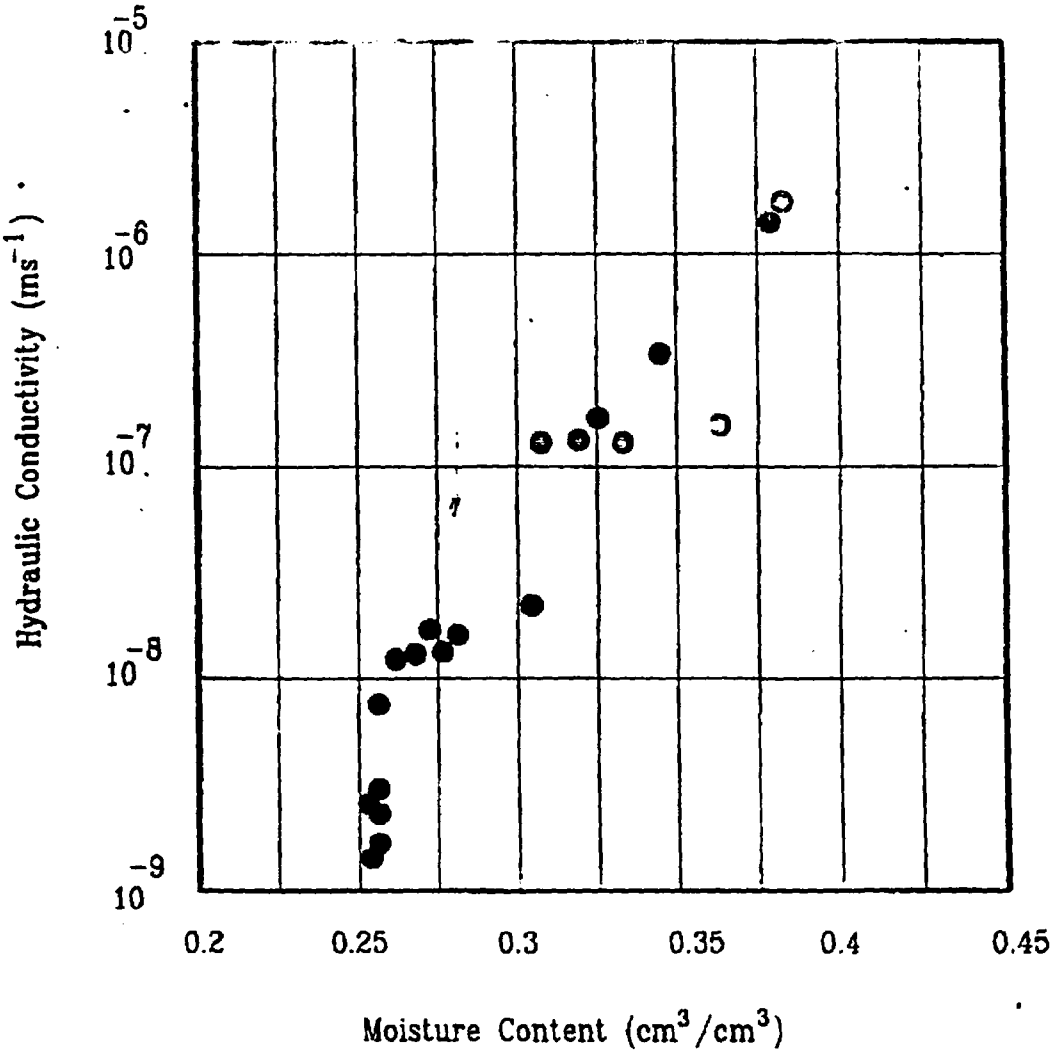

Fig. E.2-7. Unsaturated hydraulic conductivity as a function of moisture content at SRS burial grounds (Gruber 1980).

SRS076

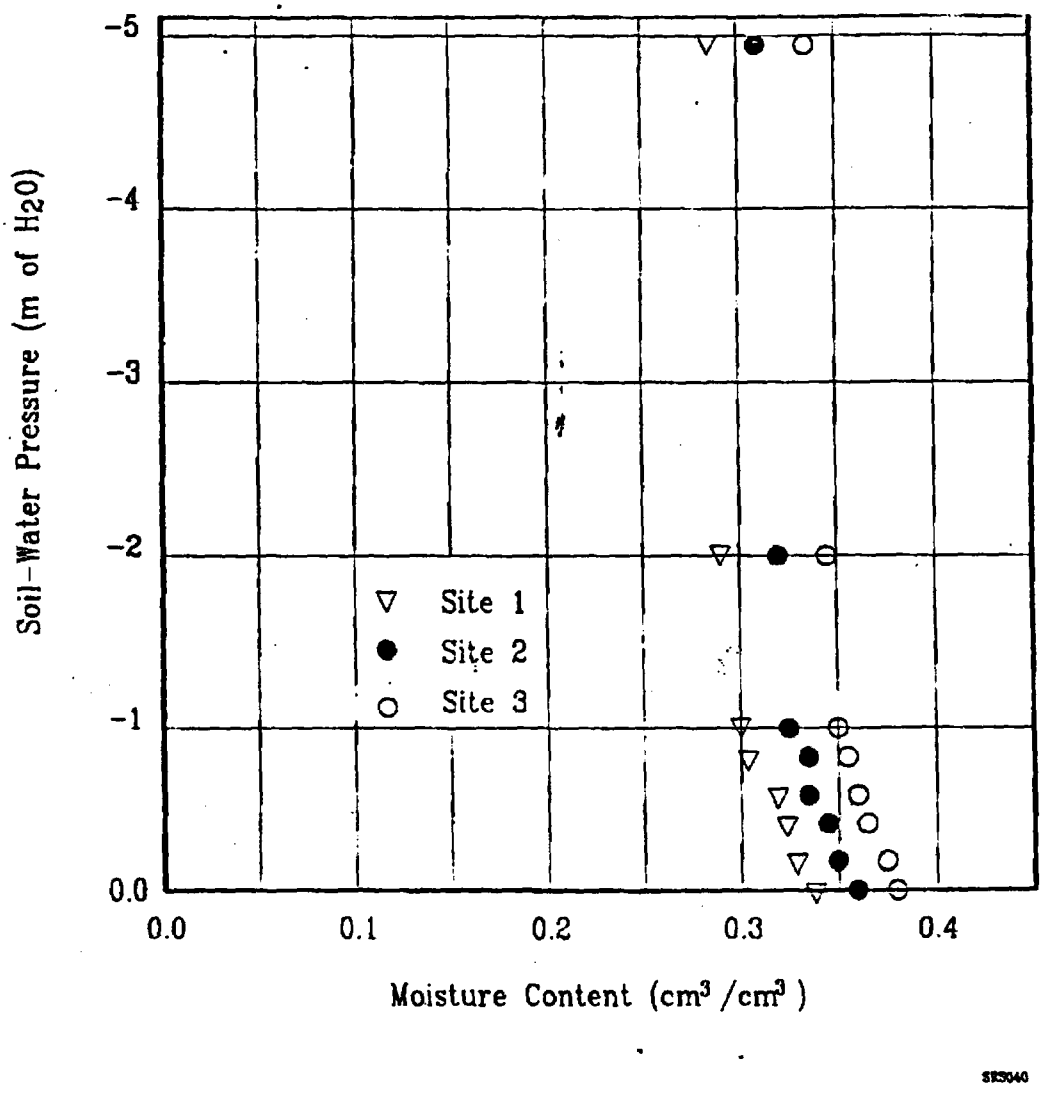

Fig. E.2-8. Soil water content-pressure relationships for undisturbed soils in Z-Area (Quisenberry 1985).

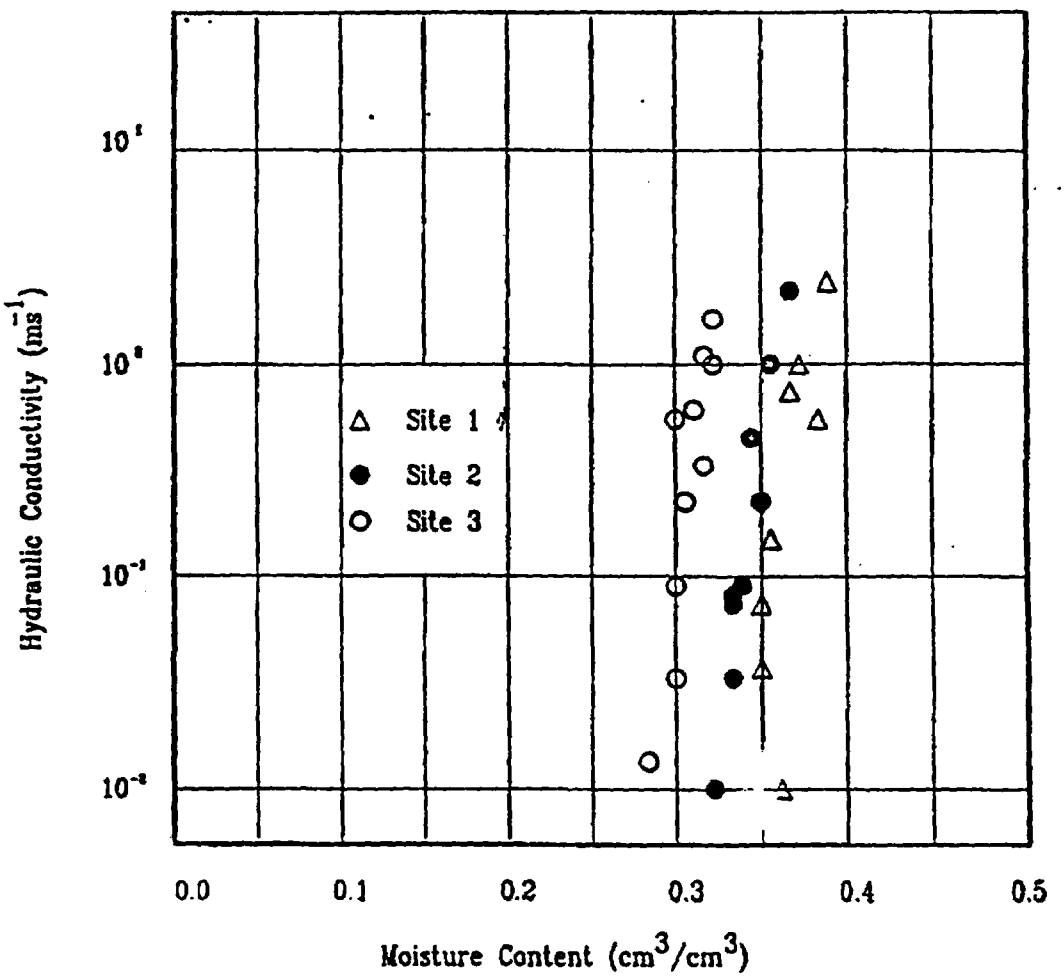

Fig. E.2-9. Unsaturated hydraulic conductivity as a function of moisture content at Z-Area (Quisenberry 1985).

APPENDIX E REFERENCES

Aadland, R. K. 1990. *Classification of Hydrostratigraphic Units at Savannah River Site, South Carolina.* Savannah River Laboratory, WSRC-RP-90-981, Westinghouse Savannah River Company, Aiken, SC.

Christensen, E. J., and D. E. Gordon. 1983. *Technical Summary of Groundwater Quality Protection Program at Savannah River Plant, Volume I.* DPST-83-829. Savannah River Laboratory, E. I. du Pont de Nemours & Co., Inc., Aiken, South Carolina.

Cooke, C. W. 1936. Geology of the Coastal Plain of South Carolina. *U. S. Geological Survey Bull. 867,* U. S. Geological Survey.

Dennehy, K. F., D. C. Prowell, and P. B. McMahon. 1989. *Reconnaissance Hydrological Investigation of the Defense Waste Processing Facility and Vicinity.* E. I. du Pont de Nemours & Co., Inc., Savannah River Laboratory, Aiken, SC.

GeoTrans. 1992. *Groundwater Flow Model for the General Separations Area, Savannah River Site.* GeoTrans Project No. 3017-003, GeoTrans Inc., Sterling, Va.

Gruber, P. 1980. *A Hydrologic Study of the Unsaturated Zone Adjacent to a Radioactive-Waste Disposal Site at the Savannah River Plant, Aiken, South Carolina.* M. S. Thesis, University of Georgia, Athens, Ga.

INTERA. 1986. *Z-Area Site Assessment.* INTERA Technologies, Inc., for E. I. du Pont de Nemours & Co., Inc., Savannah Research Laboratory, Aiken, SC.

Quisenberry, V. 1985. *Hydraulic Properties of Saltstone and Z-Area Soil.* DPST 85-263. Savannah River Laboratory, E. I. du Pont de Nemours & Co., Inc., Aiken, SC.

Siple, G. E. 1967. *Geology and Ground Water of the Savannah River Plant and Vicinity, South Carolina.* Geological Survey Water-Supply Paper 1984, U. S. Atomic Energy Commission.

WSRC. 1991. *Burial Grounds Expansion (U) - Hydrogeologic Characterization, Savannah River Site.* WSCR-RP-91-866. Prepared by Sirrine Environmental, Inc. for Westinghouse Savannah River Company, Aiken, SC.

WSRC. 1992. *Safety Analysis 200 Area Replacement Tritium Facility.* WSRC-SA-1-1. Savannah River Laboratory, Aiken, SC.

INFORMATION ONLY

APPENDIX F

SOFTWARE QA PLANS

OAK RIDGE NATIONAL LABORATORY/GRAND JUNCTION OFFICE

SOFTWARE QUALITY ASSURANCE PLAN FOR PORFLOW 3D

1.0 PURPOSE

This plan describes the steps taken by Oak Ridge National Laboratory's (ORNL) Pollutants Assessment Group (PAG) to implement software quality assurance (SQA) procedures, developed with consideration of the ORNL Quality Assurance Manual (ref. 10.1), the Martin Marietta Automated Data Processing Systems Development Methodology (ref. 10.2), and ASME NQA-2a (ref. 10.3) for the acquired computer code PORFLOW-3D (ref. 10.4).

2.0 SCOPE

The SQA plan applies to life-cycle phases of PORFLOW-3D as it is used in conducting radiological performance assessments at the Savannah River Site (SRS), including identification and acquisition, installation, testing, operation and maintenance, and retirement of this pre-existing custom software. Configuration control and quality control procedures are also included in the plan.

3.0 TERMS/DEFINITIONS

COMPUTER PROGRAMMING ASSISTANT
The Computer Programming Assistant assists the Computer Services Manager in assignment and management of software.

COMPUTER SECURITY OFFICER (CSO)
The Computer Security Officer is the person who ensures computer and software security, and passwords.

COMPUTER SERVICES MANAGER (CSM)
The Computer Services Manager is the person who oversees procurement and assignment of computer hardware and software, who works to ensure compatibility of existing and newly acquired products, and who ensures systems have adequate backup.

CONFIGURATION CONTROL
Configuration control is the process of identifying and defining the configuration items in the PORFLOW-3D software system, controlling the release and change of these items throughout the system life cycle, and recording and reporting the status of configuration items and change requests.

PERFORMANCE ASSESSMENT PRINCIPAL INVESTIGATOR (PI)
The Principal Investigator is the person having overall technical responsibility for the radiological performance assessment (PA) project.

PORFLOW-3D
PORFLOW-3D is a commercially-available computer code acquired by ORNL for use in simulating unsaturated and saturated flow of mass transport in the subsurface. Simulation results will provide concentrations of radionuclides originating in low-level waste (LLW) facilities in groundwater. By sponsor (Westinghouse Savannah River Company) directive, it is subject to NQA-2a, and thus is considered a Category 4 software, from QA Procedure No. QA-L-19-100 entitled "Software Quality Assurance" in the ORNL QA Program.

SOFTWARE
Computer programs, procedures, associated procedure manuals, computer source codes and program disks.

CUSTOM SOFTWARE
Software developed to address a specific technical problem, as opposed to commercially-available wide-usage software such as a word processor or database manager.

SOFTWARE VALIDATION
Validation of software refers to the testing of the software with respect to the accuracy of decisions or assumptions incorporated into the software.

SOFTWARE VERIFICATION
Verification of software refers to the testing of the software with respect to accuracy of numerical algorithms.

4.0 RESPONSIBILITIES FOR SQA

PERFORMANCE ASSESSMENT PRINCIPAL INVESTIGATOR
The principal investigator (PI) for the radiological performance assessments for which PORFLOW-3D was acquired is responsible for defining software needs. Upon acquisition, the PI is responsible for overseeing that the software life cycle procedures are correctly implemented and for overseeing configuration control and quality control procedures. The PI is also responsible for maintaining documentation of SQA procedures.

COMPUTER SERVICES MANAGER
The Computer Services Manager (CSM) is responsible for assisting the PI, when requested, with identifying software needs, as well as determining software compatibility with existing or acquired hardware, the operating system, network system and other software that it may have to interface with.

COMPUTER SECURITY OFFICER
Software protection measures are defined by and overseen by the Computer Security Officer (CSO).

5.0 SOFTWARE LIFE CYCLE

5.1 Identification of Software Requirements

The PI shall examine, in detail, the performance assessment problem(s) that necessitate software acquisition, and define the purpose, objectives, scope and constraints of the software need. A feasibility study shall be done to identify alternative pre-existing custom software solutions.

When a code, such as PORFLOW-3D, is identified as a solution, the PI must define all significant requirements of PORFLOW-3D pertinent to its:

1) Function - verifiable simulations to be accomplished,
2) Performance - time efficiency,
3) External Interfaces - interactions with hardware, other software, and available trained operators,
4) Attributes - adequacy of documentation, security, particular attributes specified by sponsor.

Documentation of identified requirements of PORFLOW-3D will be provided in the Procedural Logbook, and in an appendix of the performance assessment report.

5.2 Software Installation

Because PORFLOW-3D is pre-existing software, installation must be preceded by tests to assure the software is complete and free of viruses that may infect the computer system on which it is installed. Backup copies of the original software shall be made, and used for installation. Installation will take place in accordance with the installation instructions provided by the provider of PORFLOW-3D.

Once installed, the original software and the backup copy is stored and protected from theft, loss and environmental damage. The Configuration Control Logbook shall be initiated, in which date of installation, version installed, and installation notes are recorded. This Logbook shall contain the name and telephone number of the PI responsible for PORFLOW-3D and the name of the performance assessment project for which it was acquired. Source code listing, software documentation and user's manuals will be stored in a location accessible to designated users of the software, and shall not be removed without permission of the PI.

5.3 Software Testing

Testing is required to confirm that PORFLOW-3D satisfies the objectives and requirements defined in Section 5.1, Identification of Software Requirements. Verification testing, described in Section 5.3.1, below, is a demonstration of whether PORFLOW-3D meets the requirements specified regarding function, performance, external interfaces and attributes.

5.3.1 Verification

The capabilities of PORFLOW-3D must be verified by comparing analytical solutions of the desired simulation equations for a defined problem to PORFLOW-3D output to evaluate the accuracy of numerical algorithms. Comparison of software simulation results with results from previously verified versions or codes (termed benchmarking) is acceptable.

5.3.2 Validation or Benchmarking

Validation of PORFLOW-3D requires data from SRS that are not available in sufficient quantity or quality to provide meaningful results. Benchmarking of PORFLOW-3D will therefore be carried out by comparing the results to software that has gained high acceptability by acknowledged experts.

5.3.3 Documentation of Testing

Results of verification and benchmarking of PORFLOW-3D shall be recorded in the Procedural Logbook which is initiated when requirements are identified (Sect. 5.1), and in an appendix of the performance assessment report.

5.4 Software Operation and Maintenance

5.4.1 Operation

Operation of PORFLOW-3D will be conducted by personnel approved by the PI, who in the PI's judgement, are appropriately trained. These individuals will have access to the user's manual of the code, the Procedural Logbook, and the Configuration Control Logbook.

Operational tests will be performed whenever PORFLOW-3D is installed on a different computer, or when configurational changes are made to the software or hardware system. The results of these tests will be documented in the Configuration Control Logbook.

5.4.2 Maintenance

Maintenance to correct software errors or adapt to changes in requirements or the operating environments will be made only with the PI's approval, documented in the Procedural Logbook. Written requests for maintenance actions will be kept in a specified location by the PI.

5.5 Software Retirement

Once the life cycle of PORFLOW-3D is over, it will be retired according to the developer's requirements, in order to assure future use is in accord with applicable licensing agreements. All documents pertaining to the life cycle of PORFLOW-3D will be archived, and a caretaker will be designated by the PI to ensure that the retired software is not made available for unrestricted use. Documentation of retirement procedures followed will be made in the Procedural Logbook.

6.0 CONFIGURATION CONTROL

6.1 Configuration Identification

A configuration baseline shall be defined for PORFLOW-3D, in input data sets including test cases, simulation results, and hardware as the tested and approved configuration. A labeling system will be implemented for each of these components of the system, such that each item is uniquely identified and that configurations resulting from revisions of each item are uniquely identified.

6.2 Configuration Change Control

Changes to configuration items, including the PORFLOW-3D code, input data sets, simulation results and hardware shall be formally documented under the following guidelines.

6.2.1 Changes to PORFLOW-3D

Changes to the baseline version of PORFLOW-3D must be approved by the PI. Verification shall be performed to ensure that changes are properly reflected in documentation of the code, and that the changed document is properly archived.

6.2.2 Changes to /Creation of Data Sets and Simulation Results

Changes to, or creation of new, data sets must be documented in a manner that uniquely identifies each set and corresponding simulation results set.

6.2.3 Changes in Hardware Configuration

Changes to hardware may affect the operation of PORFLOW-3D. Therefore, such changes shall be reflected in the archiving, or tracking procedure, and in the documentation.

6.3 Configuration Control Documentation

Configuration control documentation shall contain the information needed to manage the PORFLOW-3D configuration and accompanying data sets, simulation results and hardware requirements. This information shall identify the approved configuration (via a well documented naming conventions for software, data sets, and simulation results) and will be kept in the Configuration Control Logbook. This Logbook shall be easily decipherable with respect to reflecting modifications made to the various configurations.

7.0 QUALITY CONTROL

7.1 Technical Review of Software

The PI shall periodically review the approach and key assumptions, and evaluate input data sets to assure that QA procedures have been applied and that proper documentation is being generated throughout the life cycle of PORFLOW-3D. When necessary, the PI will call on others to review assumptions and input data to verify their appropriateness and accuracy.

7.2 Sign-off and Approvals

The sign-off and formal approvals on key assumptions and input data will be accomplished with cover letters transmitting the information being approved. Individuals whose approval is sought will be identified by the PI, and will include QA personnel from ORNL and from SRS, as well as those with particular knowledge of the specific information from both organizations, and appropriate managers.

7.3 Quality Control Documentation

Documentation of Quality Control procedures will be kept in the form of the sign-off and approval cover letters that transmit information that has submitted to these procedures. These signature forms and attached information will be kept in a separate notebook, entitled Quality Control Notebook.

8.0 PROBLEM REPORTING AND CORRECTIVE ACTION

A formal procedure of software problems and corrective action reporting shall be established by the PI for PORFLOW-3D errors and failures. The reporting system shall assure that problems and corrective actions taken are promptly reported to affected organizations, such as Idaho National Engineering Laboratory and SRS. Problems and corrective actions shall be reported in the form of letters to affected individuals and organizations, and will be described in the Procedural Logbook.

9.0 RECORDS

The following documents will be retained as records:

1) SQA Plan;

2) Procedural Logbook containing information on software requirements, code testing results, maintenance actions, and retirement procedures followed;

3) Configuration Control Logbook containing installation information, results of testing when configurational changes are made, and identification of approved or defined configuration items, including the PORFLOW-3D version, input data sets, simulation results and hardware;

4) Documentation of PORFLOW-3D, including user's manual; and

5) Quality Control Notebook including documentation of approvals on input data and major assumptions made.

10.0 REFERENCES

Oak Ridge National Laboratory. *Quality Assurance Manual.* Current Edition. Oak Ridge National Laboratory, Oak Ridge, Tenn.

Martin Marietta for Department of Energy. 1987. *Automated Data Processing Systems Development Methodology Volume I.* K/CSD/INF/86-3, Vol. 1 & 2, R3, (ADP SDM), August.

ASME NQA-2a. Part 2.6, *Quality Assurance Requirements of Computer Software for Nuclear Facility Applications.*

Runchal, A. K., and B. Saggar. 1991. *PORFLOW: A Model For Fluid Flow, Heat and Mass Transport in Mustifluid, Multiphase Fractured or Porous Media; User's Manual - Version 2.34.* Analytic and Computational Research, Inc., West Los Angeles, Calif.

EGG-EELS-10606

EG&G Idaho, Inc.

SOFTWARE QUALITY ASSURANCE PLAN FOR PORFLOW-3D

Steven J. Maheras

March 1993

Rev. 0

SOFTWARE QUALITY ASSURANCE PLAN FOR PORFLOW-3D

1. PURPOSE

This plan describes the steps taken by the Idaho National Engineering Laboratory (INEL) Subsurface and Environmental Modeling (SEM) Unit personnel to implement software quality assurance procedures consistent with the EG&G Idaho Quality Manual Section QP-21 "Computer Software Configuration Management," and ASME NQA-2a-1990 Part 2.7 "Quality Assurance Requirements of Computer Software for Nuclear Facility Applications," for the computer code PORFLOW-3D (Runchal and Saggar 1991).

2. SCOPE

The software quality assurance plan applies to life-cycle phases of PORFLOW-3D as it is used in conducting radiological performance assessments at the Savannah River Site (SRS) including acquisition, installation, testing, operation, maintenance, and retirement. Configuration control and quality assurance procedures are also included or referenced in this plan.

3. TERMS/DEFINITIONS

COMPUTER CODE CUSTODIAN - The designated individual with responsibility for coordinating the control of computer codes and related documentation.

CONFIGURATION CONTROL - Configuration control is the process of identifying and defining the configuration items in the PORFLOW-3D software system, controlling the release and change of these items throughout the system life cycle, and recording and reporting the status of configuration items and change requests.

PERFORMANCE ASSESSMENT PRINCIPAL INVESTIGATOR - The Principal Investigator (PI) is the person having overall technical responsibility for the radiological performance assessment project.

PORFLOW-3D - PORFLOW-3D is a commercially-available computer code acquired by the INEL for use in simulating unsaturated and saturated flow and mass transport in the subsurface. Simulation results will provide concentrations of radionuclides originating the low-level waste facilities in ground water. By sponsor [Westinghouse Savannah River Company (WSRC)] directive, it is considered "High Impact" software (QAP-20-1, Rev 1., 10/01/90). This is equivalent to EG&G Idaho Quality Level B software".

SOFTWARE - Computer programs, procedures, associated procedure manuals, computer source code, and program disks.

SOFTWARE VALIDATION - Software validation refers to the testing of the accuracy of decisions or assumptions incorporated into the software.

SOFTWARE VERIFICATION - Software verification refers to testing the accuracy of numerical algorithms contained in the software.

4. RESPONSIBILITIES FOR SQA

PERFORMANCE ASSESSMENT PRINCIPAL INVESTIGATOR - The PI for the radiological performance assessment for which PORFLOW-3D was acquired is responsible for software quality assurance. Upon acquisition, the PI is responsible for overseeing that the software life-cycle procedures are correctly implemented and for overseeing configuration control and quality control procedures. The PI is also responsible for maintaining documentation of software quality assurance procedures. The PI may delegate the configuration control responsibility to the computer code custodian.

---

a. Quality Level B software failure would degrade the performance or reliability of operations, data acquisition, or deliverables.

5. SOFTWARE LIFE CYCLE

5.1 Software Installation

Because PORFLOW-3D is pre-existing, commercially available software, life cycle steps associated with the development of the software are the responsibility of the computer code vendor. Installation will take place in accordance with the instructions provided by the PORFLOW-3D vendor. A backup copy of the original software shall be made and stored under version control. Because PORFLOW-3D is stored under version control on the INEL CRAY, it is protected against theft, loss, and environmental damage.

After installation, PORFLOW-3D will be installed in the INEL Version Control System (Miller et al. 1991). The INEL Version Control System provides for automated change control and logging, therefore, a separate configuration control logbook is not required.

5.2 Software Testing

Testing is required to confirm that PORFLOW-3D functions as the code vendors assert. Once installed, a FORTRAN analyzer is typically run on the code to look for potential programming errors. Marshall and Marwil (1991) contains a description of a typical FORTRAN analyzer. No programming errors were identified in PORFLOW-3D.

5.2.1 Verification

The capabilities of PORFLOW-3D must be verified by comparing analytical solutions of the desired simulation equations for a defined problem to PORFLOW-3D output to evaluate the accuracy of numerical algorithms. Comparison of software simulation results with results from previously verified versions or codes (termed benchmarking) is acceptable. An independent verification of an earlier version of PORFLOW has been performed (Magnuson et al. 1990).

5.2.2 Validation or Benchmarking

Validation of PORFLOW-3D requires data from SRS that are not available in sufficient quantity or quality to provide meaningful results. Therefore, PORFLOW-3D will be benchmarked by comparing PORFLOW-3D results to results obtained using other software that has gained high acceptability from acknowledged experts. An independent benchmarking of an earlier version of PORFLOW has been performed (Magnuson et al. 1990).

5.2.3 Documentation of Testing

The results of the verification and benchmarking of PORFLOW-3D are documented in Magnuson et al. (1990). The verification and benchmark testing of PORFLOW was conducted using Version 1. However, the version of PORFLOW used on this project was PORFLOW-3D. The test problems used to verify and benchmark Version 1 have been run using PORFLOW-3D and equivalent results were obtained.

5.3 Software Operation and Maintenance

5.3.1 Operation

Operation of PORFLOW-3D will be conducted by personnel approved by the PI, who in the PI's judgement, are appropriately trained. These individuals will have access to the user's manual of the code.

Operational tests will be performed whenever PORFLOW-3D is installed on a computer with a different operating system, or when configuration changes are made to the software or hardware system.

5.3.2 Maintenance

Maintenance to correct software errors or adapt to changes in requirements or the operating environments will be made only with the PI's approval. However, the PI may delegate this authority to the code custodian.

The changes will be logged in the Version Control System. Because the Version Control System provides an automated log of changes to the source code, no separate maintenance log will be required.

5.4 Software Retirement

Once the life cycle of PORFLOW-3D is over, it will be retired according to the code developer's requirements in order to assure future use is in accordance with applicable licensing agreements. All documents pertaining to the life cycle of PORFLOW-3D at the INEL will be archived. During the retirement phase of the software life cycle, the routine use of PORFLOW-3D will be prevented. The retirement procedures followed will be documented.

6. CONFIGURATION CONTROL

PORFLOW-3D is maintained under configuration control using the INEL Version Control System. The Configuration Management Plan for PORFLOW-3D is part of a larger Configuration Management Plan documented in Matthews (1992), that meets the requirements of the EG&G Idaho Quality Manual, QP-21, "Computer Software Configuration Management".

7. QUALITY ASSURANCE

The PI shall periodically review the approach and assumptions and evaluate input data sets to ensure that quality assurance procedures have been applied and that proper documentation is being generated throughout the life cycle of PORFLOW-3D. When necessary, the PI will call on others to review assumptions and input data to verify their appropriateness and accuracy.

Key assumptions (those critical to the project) will be evaluated by WSRC, Oak Ridge National Laboratory - Grand Junction (ORNL-GJ), and INEL; a consensus on each key assumption will be reached.

Project notebooks will be used to document day-to-day project activities. Formal documentation of analyses conducted using PORFLOW-3D will

be accomplished using the EG&G Idaho Engineering Design File (EDF) format. The EDF format provides for formal approval of input data, assumptions, and output by the author, reviewer (technical), and approver (managerial) of the calculations. The EG&G Idaho Quality Manual, "Design Control," QP-3, Section 4.2.15, describes the elements required in the documentation of a design analysis. The EDF's generated during this project will be transmitted to SRS as part of the project documentation.

8. ERROR REPORTING AND CORRECTIVE ACTION

Any errors found in the code will be reported to the code author and other affected organizations such as SRS and ORNL-GJ. The error and its corrective action will be documented in the project logbook maintained by the analyst.

9. RECORDS

The following documents will be retained as records that will be turned over to WSRC:

1. Software Quality Assurance
2. Version Control System change log for PORFLOW-3D.
3. Documentation of PORFLOW-3D, including user's manual.
4. EDFs containing results generated using PORFLOW-3D.
5. Project notebooks.

10. REFERENCES

ASME NQA-2a-1990, Part 2.7, Quality Assurance Requirements of Computer Software for Nuclear Facility Applications.

EG&G Idaho, Inc., 1992, Quality Manual, Sections QP-3, "Design Control," and QP-21, "Computer Software Configuration Management".

Magnuson, S. O., R. G. Baca, A. J. Sondrup, 1990, Independent Verification and Benchmark Testing of the PORFLO-3 Computer Code, Version 1.0, EGG-BG-9175.

Marshall, N. H. and E. S. Marwil, 1991, Cross Reference Analysis of FORTRAN (CRAFT), EGG-CATT-9198.

Matthews, S. D., 1992, Software Configuration Management Plan for Controlled Code Support System, EGG-CATT-10196.

Miller, G. V., D. G. Barber, E. S. Marwil, 1991, Software Quality Assurance Plan for the Version Control System, Release 2, EGG-CATT-9821.

Runchal, A. K. and B. Saggar, 1991, PORFLOW: A Model for Fluid Flow, Heat and Mass Transport in Multifluid, Multiphase Fractured or Porous Media: User's Manual - Version 2.34, Analytic and Computational Research, Inc., West Los Angeles, CA.

APPENDIX G

COMPLETENESS REVIEW GUIDE

APPENDIX G

COMPLETENESS REVIEW GUIDE

An attempt was made to address all items identified in DOE/LLW-93 Performance Assessment Review Guide for DOE Low-Level Radioactive Waste Disposal Facilities and to specifically address these items in the E-Area Disposal Facility Performance Assessment. A table has been prepared which summarizes all items identified within the guidance document and connects each item with the appropriate section(s) of the Performance Assessment. In some cases the required items are addressed in two or more sections of the report. Additional details are sometimes presented in an Appendix. This table is provided as an aid to the reviewers in their completeness review of the E-Area Performance Assessment.

DOE/LLW-93 REVIEW GUIDE SECTIONS	E-AREA PERFORMANCE ASSESSMENT SECTIONS
DISPOSAL FACILITY DESCRIPTION	Sect. 2
Site Characteristics	Sect. 2.1 and Sect 2.2
Hydrogeology (Regional/Site Specific)	Sect. 2.1.4, Sect. 2.2.2, and Appendix E.2
Ecology and Biotic Conditions	Sect. 2.1.9
Natural Resources, Land and Water Use	Sect. 2.1.6 and Sect. 2.2.1
Geography and Demography	Sect. 2.1.1 and Sect. 2.1.2
Climate and Meteorology	Sect. 2.1.3
Geology (Regional/Site Specific)	Sect. 2.1.4, Sect. 2.2.2, and Appendix E.1
Seismology	Sect. 2.1.5
Natural Radiation Background	Sect. 2.1.10 and Sect. 2.2.5
Waste Generation Process	Sect. 2.3 and Sect. 2.4
Waste Characteristics	Sect. 2.4
Volumes	Sect. 2.4
Radionuclide Concentration and Inventory	Sect. 2.4.3 and Sect. 2.6
Chemical and Physical Form	Sect. 2.4
Packaging	Sect. 2.4.2
ANALYSIS OF PERFORMANCE	Sect. 3
Background	
Source Term	Sect. 3.1
Transport/Pathways/Scenarios	Sect. 3.2
Assumptions/Methodologies	Sect. 3.3 and Sect. 3.4
Dose Conversion Factors	Sect. 3.4.3
Computer Modeling Codes	Sect. 3.4.1, Sect. 3.4.2, Appendix A and B
RESULTS OF ANALYSIS	Sect. 4
Dose to Public and Intruder	Sect. 4.1.4 and Sect. 4.1.5
Sensitivity and Uncertainty Analysis	Sect. 4.2
QUALITY ASSURANCE/QUALITY CONTROL	Appendix F

APPENDIX H

PERFORMANCE ASSESSMENT PEER REVIEW PANEL RECOMMENDATIONS

H.1 INTRODUCTION

The Performance Assessment Peer Review Panel met on May 26-27, 1993 at the Savannah River Site to conduct a preliminary review of the radiological performance assessment (RPA) for the Savannah River Site E-Area Vaults Disposal Facility. Recommendations for improving this assessment were made by the Panel based on a review of an earlier version of the draft of this report and on presentations that were made to the Panel during the review. The Panel reached consensus on 19 recommendations which were presented to SRS, and are listed verbatim in Sect. H.2. How those recommendations which suggested action were adopted for improving this report are discussed immediately below each recommendation.

H.2 RECOMMENDATIONS OF THE PERFORMANCE ASSESSMENT PEER REVIEW PANEL

Recommendation #1

"The Peer Review Panel (PRP) is once again very appreciative of the courteous reception, generous hospitality, and openness of discussion provided by DOE's Savannah River Field Office, the Westinghouse Savannah River Company, and all review contributors."

Response:

No action requested.

Recommendation #2

"The PRP would like to commend the fine efforts of Westinghouse Savannah River Company for producing a high quality preliminary draft report, of comparable high quality to the Saltstone preliminary draft report. The basic elements of establishing a conceptual model, the early application of screening methods to establish the significant radionuclides, pathways, and scenarios, and the effort to establish waste acceptance criteria consistent with the PA methods and data are noteworthy."

Response:

No action requested.

Recommendation #3

"Again, the multidisciplinary 'team work' approach has been applied and is credited with the production of this high quality draft. The PRP feels that this preliminary review successfully met its expectations and objectives and hopes that our comments will be useful to the development of the final PA."

Response:

No action requested.

Recommendation #4

"The PRP notes that our final review of the Saltstone PA suffered because of the decision by the preparers to defer a final editorial review until after distribution to the PRP. The resulting errata pages and additional analyses that must be considered during the final review are somewhat awkward to handle. The PRP recommends that the time be spent on the E-Area PA to conduct a final internal editorial and technical review prior to release to the Panel."

Response:

The schedule of issuance of the final E-Area PA was adjusted to provide time to conduct a final internal editorial and technical review. The review included two separate reviews by WSRC and the PA Team and a review by DOE-SR and their subcontractor. Results of these reviews have been incorporated in this final PA.

Recommendation #5

"The PRP is concerned that no mention has been made in this PA of the disposal of post 1988 waste in the existing burial ground."

Response:

In the Implementation Plan for DOE Order 5820.2A, DOE-SR indicated that, for continuity of SRS operations, shallow land burial of low-level waste would continue until the E-Area vault disposal facility was available. The Implementation Plan also indicated that a radiological performance assessment would be conducted only for the E-Area vault facility. Consistent with this decision, no mention of post-1988 waste disposal in the existing burial ground is in the E-Area Vaults Performance Assessment.

Recommendation #5

"How are existing plumes and future E-Area plumes covered by this PA going to be differentiated by the near-term monitoring program?"

Response:

Differentiating future EAV Facility (EAVF) contaminant plumes from previously existing plumes will be based upon deviation from groundwater quality trends that will previously have been established.

Numerous groundwater monitoring wells have been installed in the vicinity of the EAVF to permit monitoring of contaminant plumes emanating from existing facilities. These wells are currently being sampled on a routine basis to define the current extent of contaminant plumes and to establish groundwater quality trends.

Several of these wells are situated close to the EAVF, both in the upgradient and downgradient directions. These wells are capable of detecting the presence of contaminants in the groundwater which might originate upgradient of the EAVF and flow beneath it. Data obtained from these wells indicates that contaminants originating at other facilities has already migrated beneath the EAVF (see Sect. 2.2.5).

Continued monitoring of these wells will allow establishment of future trends such that deviations due to EAVF operation will be apparent. Statistical analysis methodology will form the basis for making such a determination. An adequate methodology has not yet been developed, but is expected to be developed for analysis of groundwater at the Z-Area. The methodology will be described in a "Statistical Analysis Plan" which is required to obtain an Industrial Waste Permit from SCDHEC for operation of the Saltstone Facility. When the methodology is developed it will serve as a precedent that can be utilized at the EAVF.

Recommendation #7

"The PRP is concerned that the cumulative effects of the future hazardous waste/mixed waste disposal facility must be integrated with those in the E-Area PA."

Response:

The cumulative effects of the planned Hazardous Waste/Mixed Waste Disposal Facility and the E-Area Vaults will be addressed in the Performance Assessment for the HWMW facility. The HWMW PA is currently in the planning stage, but the actual project to design and construct the facility has not received funding. Integration of the HWMW and EAV PA results will be an important part of the analysis.

Recommendation #8

"The screening analysis used to determine significant radionuclides seems to focus on near term effects important during operations and the first few hundred years. By contrast, radionuclides important to low-level waste PAs are often long-lived mobile radionuclides that may be present in trace quantities (i.e., less than 1% of the total inventory) at the time of disposal. Efforts should be made to confirm, document, and justify the results of the inventory screening analysis. This is especially important in light of the changing mission with future inclusion of decommissioning wastes containing long-lived activation products."

Response:

The screening analysis, for both groundwater and intruder scenarios, was revised to include all 730 radionuclides assigned dose conversion factors in the DOE Compendium of dose conversion factors (DOE/EH-0071, "Internal Dose Conversion Factors for Calculation of Dose to the Public", July, 1988). This approach assures that any radionuclide with the potential to have an impact, either long-term or short-term, would be identified. The screening analyses are discussed in Sects. 3.2.3.4 and 3.2.4.4.

Recommendation #9

"Provide a discussion and justification of the methodology and criteria used to select the radionuclides considered in the initial inventory. For example, why were Fe-59, Fe-55, and Eu-152 not included?"

Response:

See the response to comment #8, above.

Recommendation #10

"The PRP is concerned about the allocation of activity in the inventory for the 'other' alpha and beta-gamma categories of Pu-239 and Sr-90/Cs-137. A review of the groundwater screening results presented indicates that Np-237 and Sn-126 should not be excluded."

Response:

The "Other Alpha" and "Other Beta-Gamma" categories have been removed from the Performance Assessment. The comprehensive screening analysis eliminated the need for these categories.

Recommendation #11

"The presentation material implied that the ILNT and LAW waste could contain less than 10 Ci of H-3 per package. However, table 2.4-1 shows relatively low H-3 activity levels for the ILNT and LAW vault categories (i.e., 1,000 and 5,000 Ci, respectively). It is not clear if H-3 is being assigned a value of zero for a portion of these inventories."

Response:

The present analysis no longer relies on estimated initial radionuclide inventories, which were presented in Table 2.4-1 in the original draft report. The methodology in the present RPA uses unit activity inventories or concentrations of radionuclides to determine the allowable inventory in a given vault type based upon the performance objectives for dose. Details of this methodology are provided in Sect. 3.1.1., 3.3, 3.4, and 4.1.

The reference inventories for the non-tritium vaults (ILNT and LAW) were increased based on 10 curies per B-25 container, 12,000 Ci for LAW vaults and 10,000 Ci for ILNT vaults.

Recommendation #12

"Although the PRP applauds the early application of screening methods to make decisions regarding design features and the choice of data and analysis methods for conducting the PA, we caution that efforts must be made to replace the screening methods with a justified site-specific approach. The current analysis may be overly conservative and is likely to be of little use beyond making initial decisions. For example, the high groundwater concentrations are apparently a result of conservative assumptions regarding degraded performance and attempts to simplify a complicated transport analysis. For the final PA, a more site-specific approach must be developed, justified and applied."

Response:

The preparers agree that a site-specific approach must be developed, justified, and applied. This has been done. A more rigorous analysis of vault degradation has been performed (Appendix K) and incorporated into the near-field conceptual model (Sect. 3.3.1, 3.4.1, and 4.1.2). A detailed site-specific three dimensional groundwater flow and transport model to determine the groundwater contaminant concentrations at the compliance point. Details of this model are presented in Sect. 3.3.2, 3.4.2, and 4.1.3.

Recommendation #13

"Provide a description of the conceptual model of how the vaults degrade and the environment evolves to provide an envelope of degraded conditions. The application of the conceptual model to the numerical methods must be described."

Response:

A special modeling study was conducted on the degradation of the concrete vaults in E-Area and the study is provided in Appendix X. The incorporation of this detailed site-specific degradation study into the near-field conceptual model is described in Sect. 3.3.1, 3.4.1, and 4.1.2.

Recommendation #14

"Consider the effects of increased infiltration beyond 40 cm/yr in the degraded scenario for the LAW vault facility after the subsidence event (roof collapse) has occurred."

Response:

An additional run of the unsaturated zone model of the LAW vault was made with the infiltration rate set at 120 cm/year, the total average annual precipitation at SRS, at the time of vault failure. Cs-135 and Th-232 were selected for this analysis. The calculated flux to the water table increased by a factor of about 3, the amount of increase in the infiltration. The results, in fractional flux to the water table, were:

	40 cm/year	120 cm/year
Cs-135	8.6E-04	2.6E-03
Th-232	3.0E-05	9.5E-05

Recommendation #15

"The treatment of the waste in the LAW vaults needs to be better described (i.e., the lifetime of the waste boxes, the void spaces, and the assignment of soil properties to the degraded waste forms)."

Response:

Additional detail has been added to the report to address treatment of the void (see Sect. 3.3.1.1 and Appendix A.1.2.2). Essentially, the boxes are assumed to collapse to a height assuming that the voids in the waste are no longer present, thus increasing the void above the

waste. The void above the boxes is assumed to behave as a high permeability porous media. No effective life is assumed for the waste boxes as it is assumed that the boxes will fail before the vault significantly increases in permeability and the boxes provide no structural support. The degraded boxes are also assumed to be a source of iron oxides (rust) that are used to determine K_ds for selected radionuclides.

A sensitivity analysis was conducted for the hydraulic conductivity of the waste and grout in the ILNT vault. Increases in hydraulic conductivity of the waste form of 4 orders of magnitude initially and a 2 order of magnitude increase for the degraded conditions were considered based on the reference waste form values for the different time periods specified by Andy Yu. These changes yielded an increase of roughly 3 orders of magnitude in the peak release rate for H-3. The impact was minimal on releases of C-14, Tc-99, and Ni-59. The results for the ILNT vault described above suggest that the properties of the waste form can have a significant impact on the release rate of H-3. Additional sensitivity cases for the LAW vault are being conducted, but are proving to be difficult to run. Work is continuing on the additional cases as time permits.

Recommendation #16

"The intruder scenario assumptions need to be further discussed. In particular, there needs to be clear descriptions and justifications of the construction of the house foundation or basement with respect to the waste material, the potential dilution factors applied, and the geometry selected for external dose calculations."

Response:

The assumptions for the intruder scenarios are described qualitatively in Sect. 3.2.4. and in more detail, including a description of the parameter values, in Appendix A.4. As described in the appendix, the assumptions regarding construction of a house foundation or basement that extends into the waste itself and the dilution factor for mixing of exhumed waste into native soil in an intruder's vegetable garden, essentially are the same as those used by the NRC in developing its regulations for low-level waste disposal in 10 CFR Part 61. The geometry selected for the external dose calculations also was used by the NRC. The assumption in estimating external dose of a uniform distribution of activity over the source region is reasonable for the kinds of disposal units in E-Area, particularly when one considers that intrusion onto the site will occur at random locations. It should also be borne in mind that while the assumptions for an intruder dose analysis should be reasonable for the conditions of the site and disposal facility, the primary purpose of the analysis is to establish waste acceptance criteria in the form of limits on concentrations, rather than to provide realistic estimates of dose that might be experienced by future inadvertent intruders. Therefore, it is entirely appropriate to develop simplifying assumptions for idealized exposure situations for inadvertent intruders as long as the assumptions are reasonably credible. This is particularly the case when one realizes that most assumptions will tend to result in estimates of dose that would exceed those that likely would be experienced by most individuals who might intrude onto the disposal site.

Recommendation #17

"The intruder scenarios should be evaluated using an inventory corrected for radioactive decay and leaching. This correction may reduce the importance of radon in the long-term dose assessment."

Response:

The preparers agree that a leaching correction should be applied to reduce the concentrations of radionuclides to which an inadvertent intruder would be exposed at times long after disposal. The dose analysis in Sect. 4.1.5 has been recast to display this correction explicitly (see page 4-30). However, because the engineered barriers to be used in the disposal units are expected to maintain their integrity and preclude direct intrusion into the waste for long time periods after disposal (e.g., for perhaps thousands of years or more), uranium is probably the only radionuclide for which consideration of leaching would be important in increasing significantly the concentration limit for acceptable disposals. As noted by the Peer Review Panel, consideration of leaching for uranium is potentially important in reducing the dose estimates from radon at times long after disposal. However, a solubility limit for uranium has also been implemented (see Sect. 4.1.2.2 and Appendix D). This results in minimal leaching of uranium over the 10,000-year compliance period.

Recommendation #18

"The methods used to estimate doses from radon should be evaluated and justified. For example, the computed ratio of household radon concentration to the radium concentration is highly variable (not a fixed value). In addition, the concentration in basements is generally higher than in upper floors. Finally, a comparison of household radon to the concentrations derived using the ratio to radium in soil should be compared to concentrations estimated using diffusion models."

Response:

The fundamental difficulty with performance assessment for low-level waste disposal is the paucity of data that can be used to validate or justify the assumptions for the various aspects of system behavior. Therefore, when there are opportunities to use real environmental data in a dose analysis, these opportunities clearly should be embraced. Data on exposures of the public to radon due to radium in soil represent such an opportunity. As noted by the Peer Review Panel, the ratio of indoor radon exposure to radium concentration in soil is a variable quantity, depending on many factors, and the concentration of indoor radon varies with location within a house. However, the assumptions used in the dose analysis for the E-Area vaults take this variability into account; i.e., the assumptions represent average conditions taking into account a large body of data. Since it is not the purpose of a dose analysis for low-level waste disposal to estimate the real dose that might result from

a dose analysis for low-level waste disposal to estimate the real dose that might result from placing a real house on top of waste at the Savannah River Site, the use of average assumptions clearly is reasonable. It would be desirable to base the analysis for radon on average levels of indoor radon and average levels of radium in surface soil in the vicinity of the Savannah River Site, but the existence of such a data base is not known to the preparers. Regarding the request by the Peer Review Panel to use a diffusion model to estimate indoor radon levels, it is difficult for the preparers to see how this approach could produce a useful result for the purposes of this analysis. A diffusion model would involve many highly uncertain assumptions that could only be validated by direct comparison with the type of natural analog model used in this analysis. If a diffusion model could be justified only by comparison with existing environmental data, then there is no reason not to use the environment data as the model as in the present analysis.

It should also be noted (see Sect. 1.2 and Appendix A.3) that, although doses from radon and its decay products are presented in the results of intruder analyses, they are no longer considered in assessing compliance to the intruder performance objective. Rather, a radon exhalation rate is estimated and compared with the performance objective of 20 pCi/m^{2}s.

Recommendation #19

"The likelihood of the long-term intruder scenario will be influenced by the depression in the ground surface resulting from subsidence of the LAW vault roof structure. This should be considered and discussed in the final analysis."

Response:

The development of a significant depression in the ground surface due to collapse of the LAW vault roof could affect the likelihood that an inadvertent intruder would excavate at the site. However, even after the roof collapses, the concrete presumably would be in the form of large, relatively intact pieces, in which case excavation into the waste would be precluded until most of the concrete has degraded to soil-like material. This process presumably would require at least a few hundred years, by which time the ground surface could assume a more normal contour due to normal weathering at the site. Therefore, the preparers believe it is reasonable to assume that collapse of the LAW vault roof should not effect the assumptions used in the intruder dose analysis, especially since exposure to longer-lived radionuclides at times long after disposal is the primary concern. Again, it must be borne in the mind that the primary purpose of the intruder dose analysis is to establish waste acceptance criteria, and the assumptions used in this process need not replicate actual exposure situations that might occur. Of course, collapse of the vault roof is potentially quite important in estimating releases from the vaults, and this factor is taken into account in the analysis.

APPENDIX I

SUSPECT SOIL PERFORMANCE ANALYSIS

APPENDIX I
SUSPECT SOIL PERFORMANCE ANALYSIS

I.1 DESCRIPTION OF SUSPECT SOIL TRENCHES

Between 2800 and 5600 m^3 of soil from regulated areas at the SRS is designated annually as potentially contaminated soil (henceforth referred to in this appendix as "suspect soil", Cook 1991). Disposal of a portion of this soil in unlined trenches is being considered for the EAV facility. The performance of these proposed suspect soil trenches is analyzed in this appendix.

I.1.1 Physical Characteristics of Suspect Soil

The suspect soil at the SRS has not specifically been characterized, but can be assumed to have general characteristics similar to the soil horizons across the site. The SRS soils were described in Sect. 2.1.8. In general, the SRS soils are sandy, and underlain by a loamy or clayey subsoil. Excavation activities may result in mixing of the sandy soils with the subsoil. Therefore, it is likely that the suspect soil characteristics are representative of a mixture of the soil horizons present at the SRS.

I.1.2 Layout and Capacity of the Trenches

For this performance analysis, it is assumed that five below-grade trenches exist within the EAV facility. The conceptual configuration and dimensions of the trenches are shown in Fig. I.1-1. The width of the top of each trench is 6 m, and the bottom is 4.8 m wide. Each trench is 200 m long and 6 m deep, but the top 1.2 m of soil in each trench will be clean soil. The disposal capacity of each of the five trenches is approximately 5200 m^3 of suspect soil. The base of the trenches is assumed to lie approximately 9 m above the water table at an elevation similar to that of the base of the LAW vaults.

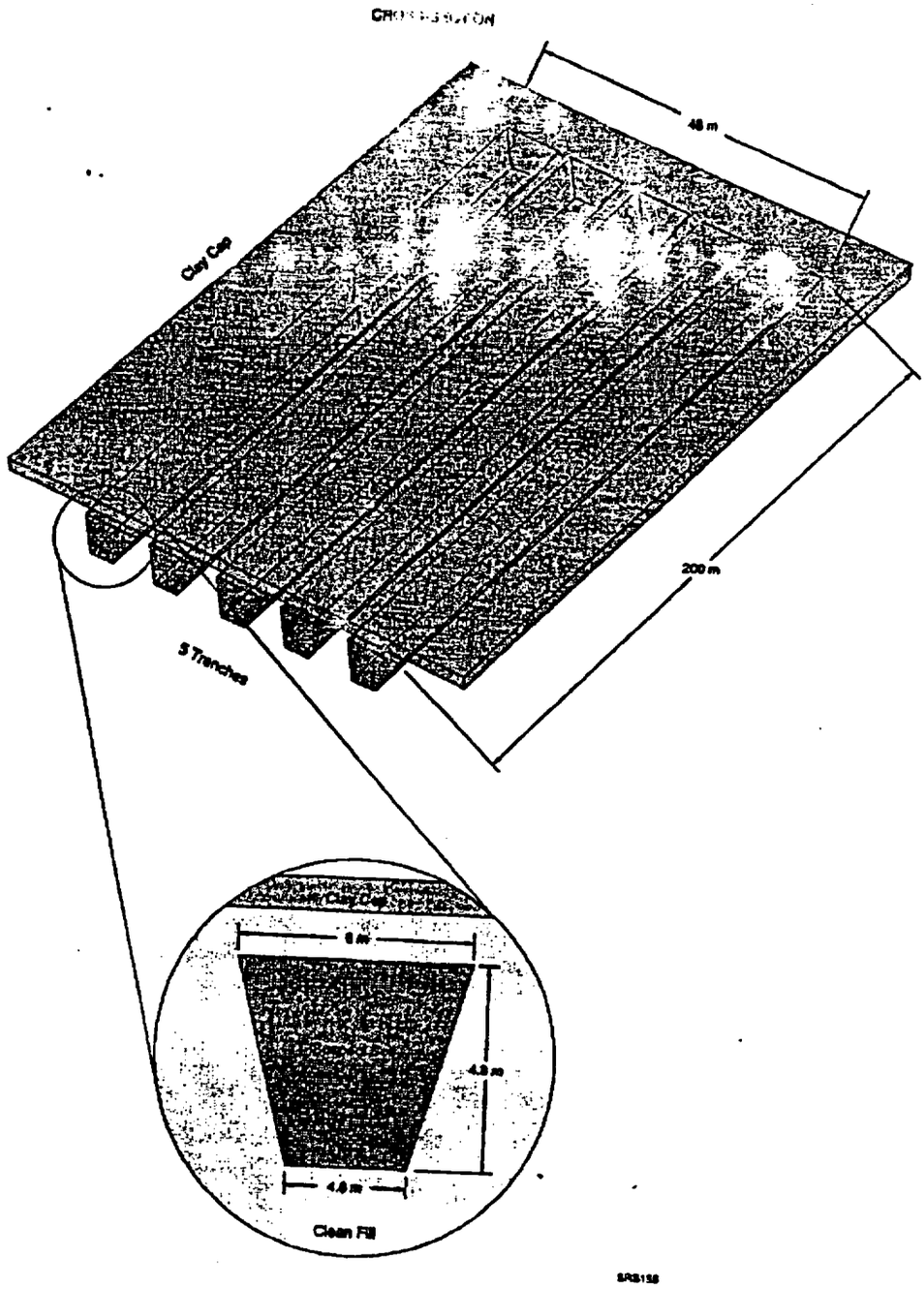

Fig. L1-1. Conceptual drawing of proposed suspect soil trenches.

I.1.3 Radioactive Inventory of Suspect Soil

The inventory of radionuclides in suspect soil is not known. Therefore, a list of radionuclides that are possibly present was generated. These 730 radionuclides are listed in Table C.3-1. The level of contamination of suspect soil is unknown; therefore, the performance assessment of the suspect soil trenches will address allowable inventories that will meet performance objectives described in Sect. 1.2.

I.1.4 Closure Concept

Because the suspect soil trenches will be placed within the EAV facility, final closure will be the same as that for the entire facility. For the purposes of this assessment, the same closure concept as for the EAVs (Sect. 2.9) is assumed. Briefly, backfill of Burma Road sand is assumed to be placed over the filled trenches, above which a laterally extensive moisture barrier is assumed to be placed. The moisture barrier consists of 0.76 m of clay overlain by 0.3 m of gravel and a geotextile fabric. Over this moisture barrier, 0.76 m of backfill is assumed, followed by 0.15 m of topsoil. As a result, a minimum of 2.9 m of cover material is assumed to overlie the suspect soil trenches at closure. Revegetation and drainage ditches are assumed to constitute final closure, for the purposes of stabilizing soil, preventing pine tree growth, and diverting excess water from the gravel layer.

I.2 ANALYSIS OF PERFORMANCE OF SUSPECT SOIL

The methods used to analyze the long-term performance of the suspect soil trenches within the EAV facility are described in this section. A description of the radionuclide source term posed by the trenches is provided in Sect. I.2.1. Pathways to exposure of human receptors are considered in Sect. I.2.2. The conceptual models developed and computational approach used to assess the performance of the suspect soil trenches are described in Sect. I.2.3.

I.2.1 Source Term

The suspect soil trenches provide a source of radionuclides to the geosphere. To characterize this source, it is necessary to evaluate the mechanisms of release. Release of radionuclides from the soil matrix may result from desorption from soil particles, dissolution of precipitated material within the soil matrix, or volatilization into soil gas. Subsequent release to the geosphere occurs as a result of advective and diffusive processes. Advective processes arise as a consequence of the infiltration of water through the trenches. Diffusive processes are driven by the concentration gradient that exists between pore fluids of the trenches and pores of the surrounding uncontaminated soil.

Degradation of the engineered cover will affect release to the geosphere through the effect on infiltration of water into the trenches. As was described in Sect. 3.1.3.1, a reasonable scenario for degradation of the cover is that the cover may be degraded to the gravel layer approximately 900 years after closure of the E-Area facility. Before that time, it is possible that infiltration may increase through the clay layer as a result of head buildup in the gravel layer, if for example the drains fail to divert sufficient water, or disturbance of the clay layer by roots or burrowing animals.

I.2.2 Pathways and Scenarios

In this section, the pathways to human exposure to potential suspect soil constituents are addressed. The time periods of concern for human exposure are identical to those described in Sect. 3.2.1.

I.2.2.1 Transport Pathways

Radionuclides released from the suspect soil trenches to the geosphere have the potential of reaching humans through numerous pathways. Most conceivable pathways for a buried LLW source such as the suspect soil trenches are described in Sect. 3.2.2.1. The same rationale as was applied in pathway screening for the EAVs applies to the suspect soil

trenches, with the result that only pathways related to contaminated air and groundwater are considered to be of potential consequence. These pathways include volatilization of H-3, C-14, and Rn-222, leaching of suspect soil, resulting in contamination of groundwater local to E-Area, and contamination of agricultural crops and animals as a result of irrigation with contaminated groundwater.

I.2.2.2 Exposures of Off-Site Members of the Public and Protection of Groundwater

According to the discussion in Sect. 3.2.3.3, the drinking water pathway is the only pathway that needs to be considered for off-site releases of radionuclides in groundwater. In cases where the MCL in groundwater corresponds to a dose equivalent less than the performance objective for off-site individuals of 25 mrem per year from all exposure pathways, compliance with the MCL would ensure that the dose to off-site individuals would be substantially less than the performance objective. In cases where the MCL in groundwater corresponds to a dose equivalent greater than the performance objective for off-site individuals, the dose from all exposure pathways other than drinking water would be insignificant compared with the dose from the drinking water pathway, particularly when the uncertainties in estimating maximum concentrations of radionuclides in groundwater at locations more than 100 m from any disposal units are taken into account.

In order to reduce the number of radionuclides for which a detailed analysis of potential groundwater concentrations is necessary, a screening analysis was carried out with respect to groundwater protection requirements. This analysis is essentially the same analysis that was applied to the list of radionuclides that was screened for the EAVs. The screening analysis is described in Sect. 3.2.3.4. Of the 730 radionuclides originally listed in Table C.3-1 of that report, 50 radionuclides were identified for which a more detailed analysis was needed. Radioactive daughters were considered in the screening analysis. These radionuclides are listed in Table I.2-1.

Radionuclides for which radioactive progeny were considered in the detailed groundwater analysis were selected based on the potential for significant ingrowth and mobilization of the progeny. For example, radioactive daughters of Pu-239 were not considered significant for several reasons, including: 1) decay of the parent is slow enough to limit the daughter activities available for transport to less than 0.001% of the initial Pu-239 activity during the first

Table I.2-1. Radionuclides considered in the detailed groundwater analysis for suspect soil [illegible]

H-3	U-235 (Pa-231)[a]
C-14	U-236
Al-26	U-233
Ni-59	Np-237
Ni-63	Pu-238 (U-234)[b]
Se-79	Pu-239
Rb-87	Pu-240
Sr-90	Pu-241 (Am-241, Np-237)[b]
Zr-93	Pu-242
Tc-99	Pu-244
Pd-107	Am-241 (Np-237)[b]
Cd-113m	Am-242m (U-234)[b]
Sn-121m	Am-243 (Pu-239)[a]
Sn-126	Cm-242 (Pu-238)[a]
I-129	Cm-243 (Pu-239)[a]
Cs-135	Cm-244 (Pu-240)[a]
Sm-151	Cm-245
Ra-226	Cm-246 (Pu-242)[a]
Th-229	Cm-247 (Am-243, Pu-239)[a]
Th-230 (Ra-226)[a]	Cm-248
Th-232	Bk-249 (Cf-249)[b]
Pa-231	Cf-249 (Cm-245)[b]
U-232	Cf-250 (Cm-246)[b]
U-233 (Th-229)[a]	Cf-251 (Cm-247, Am-243, Pu-239)[a]
U-234 (Th-230, Ra-226)[a]	Cf-252 (Cm-248)[b]

[a] Radioactive daughter(s), in parentheses, are potentially significant and are considered, along with their differential transport, in the groundwater analysis.

[b] Radioactive daughter(s), in parentheses, are longer-lived than the relatively short-lived parent, and the groundwater analysis considers the daughter concentrations.

10,000 years, even when leaching of Pu-239 is neglected; 2) progeny of Pu-239 are generally less mobile than Pu-239, with the exception of U-238; and 3) although U-238 is more mobile (i.e., has a lower K_d), U-238 has a very low specific activity relative to that of Pu-239 and, thus, is not radiologically significant in this decay chain. For Np-237, the activity of the U-233 daughter fairly quickly approaches that of Np-237 if leaching of Np-237 from the suspect soil trenches is neglected. However, Np-237 is fairly mobile (K_d = 5 mL/g), and is leached from the trenches before significant ingrowth can occur, based on groundwater transport simulations for the Np-237 parent.

The radionuclides for which ingrowth of daughters is believed to be insignificant, either up to 10,000 years or before the parent radionuclide has been leached from the trenches, are Np-237, Pu-239, Pu-240, Pu-242, Pu-244, U-236, U-238, Cm-245, and Cm-248. Radioactive progeny of other radionuclides listed in Table I.2.1 are included in the effective dose equivalents for the parent radionuclides, from which allowable concentrations in groundwater are calculated.

I.2.2.3 Exposure Scenarios for Inadvertent Intruders

Chronic and acute exposure scenarios were developed in Sect. 3.2.4 for inadvertent intruders. The scenarios developed were based on low-level radioactive waste disposal in vaults. The conclusions of Sect. 3.2.4 were that chronic exposure scenarios will always be more restrictive than acute scenarios in terms of compliance with performance objectives for protection of intruders, and that an agriculture scenario, a resident scenario and a post-drilling scenario should be considered. The same arguments apply for the suspect soil trenches, but only the agriculture scenario needs to be considered here according to the following reasoning.

The suspect soil trenches will be constructed without engineered barriers that could preclude excavation or drilling into the waste. Therefore, only the agriculture and post-drilling scenarios for inadvertent intruders are relevant. However, since both scenarios could occur beginning at 100 years after disposal, when active institutional control over the disposal site is assumed to be lost, and since the dose per unit concentration of radionuclides always

is greater for the agriculture scenario than for the post-drilling scenario, only the agriculture scenario needs to be considered in estimating dose to an inadvertent intruder and limits on concentrations and inventories of radionuclides that would be acceptable for disposal.

The agriculture scenario is described in detail in Sect. 3.2.4.1. This scenario assumes that an intruder comes onto the site after active institutional control ceases and establishes a permanent homestead, including on-site sources of water and foodstuffs. Suspect soil is assumed to be accessed when an intruder constructs a home directly on top of a disposal trench, with the foundation of the home extending into the trench itself, and some waste is assumed to be mixed with native soil in the intruder's vegetable garden. Ingestion, inhalation, and external exposure pathways are evaluated.

Screening of the list of 730 radionuclides listed in Table C.3-1 with respect to intruder doses was conducted in the manner described in Sect. 3.2.4.4. In addition to the radionuclides listed in Table I.2-1, Co-60, Nb-93m, Cs-137, Eu-154, Eu-155, Pb-210, Ra-228, and Ac-227 were considered in the intruder analysis. Radionuclides not on the list could not pose a significant dose with respect to any performance objectives, due to their short half-lives and/or other factors affecting intruder exposures.

I.2.3 Models and Assumptions

In Sect. I.2.1 and I.2.2, the potential mechanisms of release of radionuclides from the suspect soil trenches were defined, the radionuclides believed to be most significant to this RPA identified, and the relevant human exposure scenarios were described. In this section, the models adopted, and assumptions made, to carry out the computations necessary to estimate doses are described.

I.2.3.1 Near-Field Model

The near-field model for the suspect soil trenches addresses release of radionuclides from the trenches to the surrounding unsaturated soils of the vadose zone, and subsequent transport to the water table. The conceptual models implemented to describe flow and transport are described below.

Flow of water through the trenches is limited by the amount of infiltration through the overlying cover and the characteristics of the suspect soil and surrounding soil. Using the trench design described in Sect. I.1.2, a two-dimensional computational grid was designed to represent the trenches and surrounding soil for simulations carried out with PORFLOW, Version 2.5 (ACRI 1993). The model domain is shown in Fig. I.2-1, and represents a vertical, longitudinal slice through the trenches and surrounding soil. The domain extends vertically from the water table to the ground surface. The trenches are represented within this domain by a zone which is 200 m long and 4.8 m high. In two dimensions, the thickness of the slice is assumed to be of unit thickness, or 1 cm in this case.

The amount of infiltration entering the top of the domain shown in Fig. I.2-1 was assumed to be 40 cm per year, which represents the average infiltration without an engineered cover over the trenches. Although the cover will likely limit infiltration for hundreds of years if undisturbed, there is considerable uncertainty in the timing and extent of degradation. Therefore, for this analysis, no credit was taken for reductions in infiltration brought about by the cover. This is a conservative approach, because flux of radionuclides to the water table is directly proportional to the amount of water available to flow through the system. Therefore, with an intact cover, and the resulting 4 cm per year infiltration (Sect. 4.1.2.1), the flux to the water table is expected to be an order of magnitude lower than the fluxes estimated with a fully degraded cover. Test simulations were carried out at the lower infiltration rate, and confirmation of this proportional reduction in the flux rate was achieved.

Simulation of the path of water through the domain necessitated assumptions of moisture profiles in the suspect soil and surrounding soil. For this analysis, it was assumed that the suspect soil and surrounding soil were essentially the same hydraulically, and that the hydraulic properties described in Sect. 3.3.1.1 for native soil at the SRS are appropriate for these soils. The moisture characteristic data tabulated by Gruber (1980) were used to define the unsaturated hydraulic conductivity and matrix potential as a function of moisture content (Fig. E.2-6, Appendix E). Because the trench soil and surrounding backfill and native soil were assumed to have identical hydraulic properties, water is assumed to be neither diverted

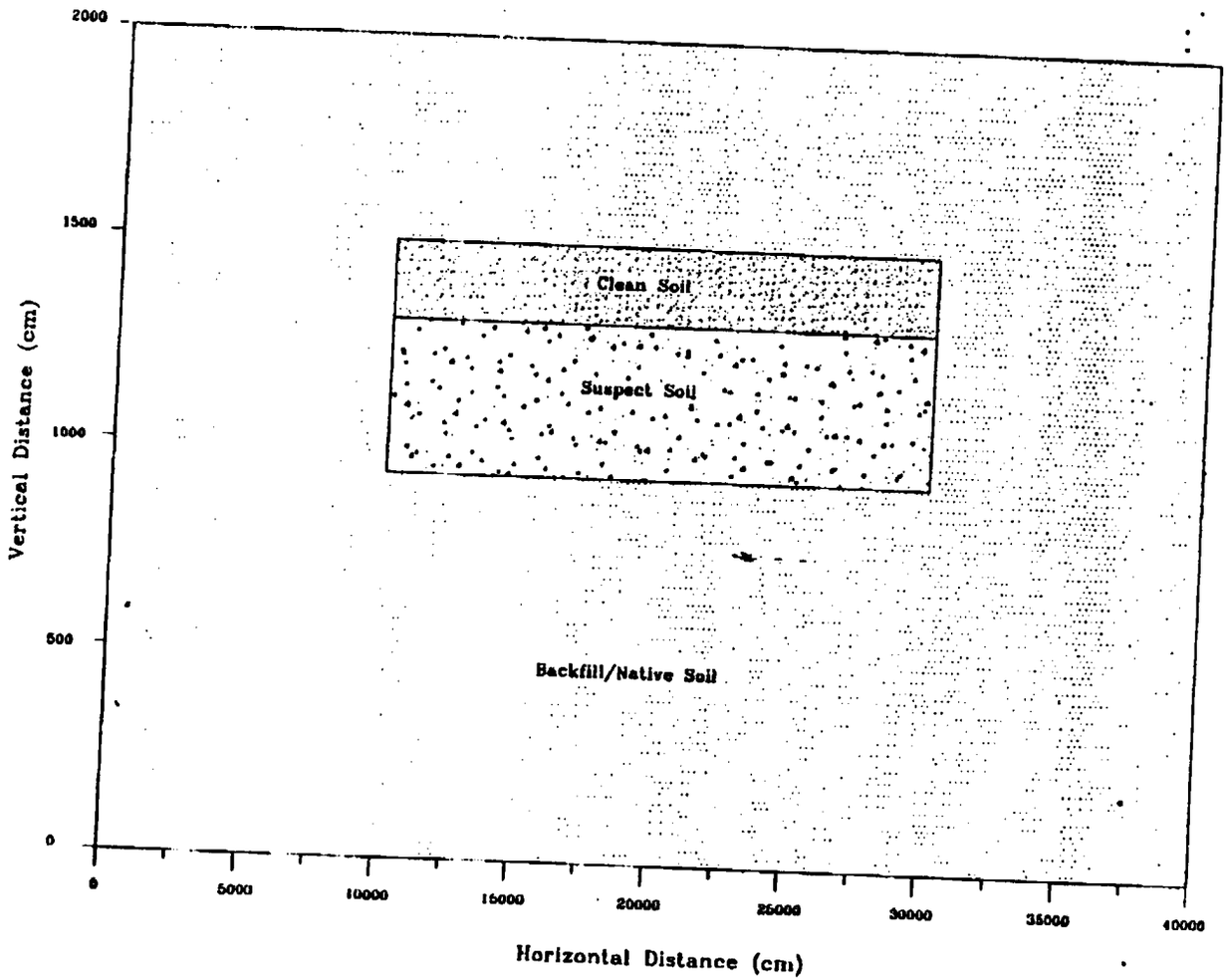

Fig. I.2-1. Simulation domain for the suspect soil trenches in the vadose zone.

into or out of the trenches, but to flow vertically through. Under steady-state hydrologic conditions, the amount of water flowing out of the domain at the water table is equal to the amount of water entering via infiltration; thus, the steady-state flux of water through the suspect soil trenches and surrounding soil was 40 cm/year. Flow simulations were carried out with the computer code PORFLOW, for the two-dimensional domain described above. The PORFLOW input file for these simulations is provided in Fig. I.5-1. The steady-state flow field was subsequently used in mass transport simulations to analyze the advective flux from the trenches.

Release of radionuclides to the geosphere may result from desorption or dissolution processes, as noted in Sect. I.2.1. Advective and diffusive processes act to mobilize the radionuclides in the pore waters of the trenches. For the suspect soil analysis, radionuclides were assumed to be completely soluble, and sorption was considered to be a fully-reversible linear process at equilibrium. Equilibrium partitioning between solid (sorbed) and liquid phases was characterized by the elemental distribution coefficients (K_d's) listed in Table I.2-2. The K_d values in this table are average values taken from site-specific literature, when available, and from a review article by Sheppard and Thibault (1990).

The computer code, PORFLOW, was used to simulate advection and diffusion from the trenches. The steady-state flow field provided flow rates through the trenches and to the water table (at the bottom of the domain, Fig. I.2-1), and K_d's, effective diffusion and dispersion coefficients, and radioactive decay constants provided the necessary information for simulating advective-diffusive transport. An example input file is shown in Fig. I.5-2. Effective diffusion (i.e., molecular diffusion corrected for tortuosity of a porous medium) and dispersion coefficients are not radionuclide-specific, and the values used for these parameters in the PORFLOW simulations were: 1) longitudinal dispersivity = 3 m; 2) transverse dispersivity = 0.3 cm; and 3) effective diffusion coefficient = 158 $cm^2 \cdot yr^{-1}$. No data are available for dispersivities in the unconsolidated sediments of the SRS. In the unsaturated zone, where flow velocities are very low, dispersion, which is directly proportional to flow velocity, is likely to be fairly insignificant with respect to plume movement. The values chosen for these simulations are believed to be reasonable based on a discussion of field-scale dispersivity in a reputable groundwater textbook (Freeze and Cherry 1979). Small values of dispersivity are

Table I.2-2. Distribution coefficients assumed for elements in aquifer soil [illegible]

Radionuclide	K_d Value Assumed (ml/g)		Literature Source	
	Soil	Clay	Soil	Clay
Al	1500	1500	Bates and Sharp 1983	assumed same as soil
Am	1900	8400	Hoeffner 1985	Sheppard and Thibault 1990
Bk	1900	8400	same as Americium	same as Americium
C	2	1	McIntyre 1988	Sheppard and Thibault 1990
Cd	80	560	Sheppard and Thibault 1990	Sheppard and Thibault 1990
Cf	1900	8400	same as Americium	same as Americium
Cm	1900	6000	same as Americium	Sheppard and Thibault 1990
Co	10	550	Hoeffner 1985	Sheppard and Thibault 1990
Cs	330	1900	Hoeffner 1985	Sheppard and Thibault 1990
Eu	245	—	assumed the same as Sm	—
H	0	0	Sheppard and Thibault 1990	Sheppard and Thibault 1990
I	0.6	1	Hoeffner 1984	Sheppard and Thibault 1990
Nb	160	900	Sheppard and Thibault 1990	Sheppard and Thibault 1990
Ni	400	650	Sheppard and Thibault 1990	Sheppard and Thibault 1990
Np	5	55	Sheppard and Thibault 1990	Sheppard and Thibault 1990
Pa	550	2700	Sheppard and Thibault 1990	Sheppard and Thibault 1990
Pb	270	550	Sheppard and Thibault 1990	Sheppard and Thibault 1990
Pd	55	270	Sheppard and Thibault 1990	Sheppard and Thibault 1990
Pu	100	5100	Hoeffner 1985	Sheppard and Thibault 1990
Ra	500	9100	Sheppard and Thibault 1990	Sheppard and Thibault 1990
Rb	55	270	Sheppard and Thibault 1990	Sheppard and Thibault 1990
Se	5	740	Ticknor and Ruegger 1989	Sheppard and Thibault 1990
Sm	245	1300	Sheppard and Thibault 1990	Sheppard and Thibault 1990
Sn	130	670	Sheppard and Thibault 1990	Sheppard and Thibault 1990
Sr	10	110	Hoeffner 1985	Sheppard and Thibault 1990
Tc	0.36	1	Oblath 1982	Sheppard and Thibault 1990
Th	3000	5800	Sheppard and Thibault 1990	Sheppard and Thibault 1990
U	35	1600	Sheppard and Thibault 1990	Sheppard and Thibault 1990
Zr	600	3300	Sheppard and Thibault 1990	Sheppard and Thibault 1990

conservative for radionuclides which do not decay significantly before reaching the water table, as is the case with the great majority of radionuclides in the suspect soil analysis, because less spreading of the plume occurs with small values and the intruder exposures are maximized with the smaller loss from the trenches. Large values of dispersivity are conservative for radionuclides that decay significantly during transport to the water table, as the arrival time at the water table will be earlier and thus less radioactive decay can occur.

I.2.3.2 Groundwater Transport Model

To simulate transport of radionuclides that are released from the suspect soil trenches to the water table, the conceptual saturated zone transport model described in Sect. 3.3.2 was adopted. The flow field established by PORFLOW simulations, which implemented this conceptual model, was used in the suspect soil analysis. Therefore, the groundwater transport model was identical to that described in Sect. 3.3.2 with the exception that the source zone was smaller (2 suspect soil source nodes versus 4 nodes for the ILNT vaults and 35 nodes for the LAW vaults). The smaller source zone represents the relatively smaller source area presented by the suspect soil trenches. An example PORFLOW input file for four radionuclides is shown in Fig. I.5-3.

I.2.3.3 Atmospheric Release Model for Volatile Components

Potential atmospheric release of volatile forms of H-3 and C-14 must be considered in order to consider all potentially significant pathways of exposure to radionuclides from the suspect soil trenches. Inadvertent intruders may be exposed to air within residences built on top of the soil above the trenches, and off-site individuals may be exposed to concentrations transported to or beyond the SRS boundary. The model described below was used to screen this pathway, with the purpose of determining whether a more detailed analysis of the potential significance of this pathway with respect to the 100 mrem per year performance objective for inadvertent intruders and the 10 mrem per year performance objective for off-site individuals (Sect. 1.2) was necessary.

To estimate fluxes of potentially volatile radionuclides, H-3 and C-14, from the suspect soil trenches, the model developed to conservatively estimate fluxes of these radionuclides arising from the LAW vaults (Sect. A.3.5 and A.3.6) was used. For H-3, the vapor phase concentration in the trenches is first calculated by assuming that the concentration of H-3 in water vapor in the trenches is the same as the H-3 concentration in the pore water of the suspect soil. The ideal gas law is used to estimate the ambient concentration of water vapor in air in the trenches, the result being 9.2 g m^{-3} at 10°C and 100% relative humidity. Converting to activity concentration units, the H-3 concentration in air in the trenches, in Ci m^{-3}, is 9.2×10^{-6} times the H-3 concentration in pore water. For C-14, all of this radionuclide was conservatively assumed to exist as $^{14}CO_2$ in the air in the trenches.

For off-site individuals, diffusion of H-3, C-14, and Rn-222 through soil overlying the suspect soil trenches, and subsequent transport to the site boundary were considered. One meter of soil was assumed to cover the suspect soil, although initially approximately 4 m of soil will overly the trenches with the engineered cover in place. Per Ci of H-3 initially in the trenches, the concentration in the air-filled voids of the trenches is calculated from:

$$C_{T,H\text{-}3} = \frac{1\ Ci}{1460\ m^3} \times \frac{9.2\times10^{-6}\ Ci/m^3{}_{(air)}}{1\ Ci/m^3{}_{(H_2O)}}$$

where 1460 m^3 represents the amount of pore fluid in the trenches. This pore fluid content is based on the 5200 m^3 disposal capacity of the trenches (Sect. I.1.2), a total assumed porosity of 0.40, and a saturation of approximately 0.7 in the trenches, based on flow simulations with PORFLOW. The resulting trench air concentration is 6.3×10^{-9} Ci m^{-3}. The flux of H-3 at the soil surface ($J_{H\text{-}3}$ in Ci m^{-2} yr^{-1}) is calculated from:

$$J_{H\text{-}3} = D_a \left(\frac{C_{T,H\text{-}3}}{x} \right)$$

where D_a is the molecular diffusion coefficient in air (754 m^2 yr^{-1} for water vapor, CRC 1981) and x is the soil thickness, assumed to be one meter. The initial flux of H-3 (i.e., at closure) from the soil is conservatively estimated to be 4.8×10^{-6} Ci m^{-2} yr^{-1} over an area of 6000 m^2, per Ci of H-3 disposed of in the suspect soil trenches.

For inadvertent intruders, a similar calculation of H-3 flux from soil above the trenches can be made, but 100-year radioactive decay is first considered because institutional control is assumed to preclude intrusion before 100 years. Per Ci of H-3 in the trenches, no more than 3.5×10^{-3} Ci would remain at 100 years after closure based on consideration of radioactive decay alone. Leaching is neglected. At 100 years, the concentration of H-3 in the trench air is calculated to be 2.3×10^{-11} Ci m^{-3}. The flux of H-3 at the soil surface ($J_{H\text{-}3}$ in Ci m^{-2} yr^{-1}) at 100 years is estimated to be 1.7×10^{-8} Ci m^{-2} yr^{-1} over an area of 6000 m^2.

Similarly, for C-14, the concentration in the trench air ($C_{T,C\text{-}14}$), in Ci m^{-3} per Ci C-14 in the suspect soil trenches, is calculated based on a 100-year Ci content of the trenches of one; that is, decay has been insignificant and leaching is neglected. The trench air concentration of 1.6×10^{-3} Ci m^{-3} was derived from the assumption of an unwetted void space of 624 m^3 in the trenches. The flux at the surface, $J_{C\text{-}14}$, is calculated in the same manner as was done for H-3, using a diffusion coefficient in air of 440 m^2 yr^{-1} (CRC 1981). The flux of C-14 from the soil overlying the suspect soil trenches is conservatively estimated to be 7.0×10^{-1} Ci m^{-2} yr^{-1} over an area of 6000 m^2. A C-14 flux of 7.0×10^{-1} Ci m^{-2} yr^{-1} over an area of 6000 m^2 corresponds to loss of the initial 1 Ci inventory in much less than one year. Therefore, the annual flux of C-14 was assumed to be 1 Ci per 6000 m^2, or 1.6×10^{-4} Ci m^{-2} yr^{-1} for every Ci of C-14 initially in the suspect soil trenches. This flux represents both the initial flux for determining off-site exposures and the 100-year flux, for estimating intruder exposures.

The flux of Rn-222 through one meter of overlying soil was considered in Sect. A.3.7. The estimated Rn-222 flux, per Ci of U-234 in the trenches, is 2.3 pCi m^{-2} s^{-1}.

I.2.3.4 Models for Dose Estimation

Doses to off-site members of the public resulting from use of contaminated groundwater beyond the 100-m buffer zone around the suspect soil trenches were not directly estimated. Rather, comparisons of maximum predicted groundwater concentrations with the more restrictive of either MCLs or allowable concentrations based on 25-mrem per year performance objective were made. The allowable concentrations were calculated by dividing 25 mrem per year by the EDE per unit concentration in drinking water (Table A.4-6, Sect. A.4). These calculations are simple, were performed by hand, and checked several times for accuracy.

Other than the contaminated groundwater, the air pathway is the only potentially significant means of exposure that is considered for off-site individuals in E-Area suspect soil analysis (Sect. I.2.2.2). Doses to off-site individuals were calculated in the manner described in Sect. A.3.1.3. This methodology utilizes the source term described in Sect. I.2.3.3 above, in Ci yr^{-1} of H-3 or C-14, and the AIRDOS-PC atmospheric dispersion model to estimate the all-pathway dose to an individual residing continuously at the SRS site boundary located 5 km from E-Area. The AIRDOS-PC input and output file information is provided in Appendix C.

To estimate dose to the intruder from potentially volatile H-3 and C-14 compounds released from the suspect soil trenches, the same procedure described in Sect. A.3.1.2 was used. Assuming that the intruder's house resides directly on top of soil, 1 m in thickness, overlying the suspect soil trenches, the steady-state air concentration (C_{air}), in Ci m^{-3}, of H-3 or C-14 to which the intruder is exposed is estimated from:

$$C_{air} = \frac{Ja}{h}$$

where

J = flux rate of volatile H-3 or C-14 from soil and into house, Ci m^{-2} yr^{-1},

a = air exchange rate in house, assumed to be 8760 yr^{-1}, and

h = height of the ceiling in house, 2.4 m.

Conservative estimates of the flux rates were provided in Sect. I.2.3.3 above. The inhalation dose to the intruder (D_{ii}) was calculated from:

$$D_{ii} = C_{air} \times B_r \times DCF_i$$

where

B_r = breathing rate (8000 m^3 yr^{-1}), and

DCF_i = inhalation dose conversion factor for H-3 or C-14, (mrem Ci^{-1}).

Doses to inadvertent intruders from the agriculture scenario were estimated according to the procedures described in Sect. A.4.5.2.

I.2.4 Performance Analysis Methodology

The models and assumptions described in Sect. I.2.3 were applied to analyze the performance of the suspect soil trenches. Doses to off-site individuals and inadvertent intruders and groundwater concentrations at the compliance point for groundwater resource protection per Ci of each radionuclide listed in Table I.2-1 were estimated. Because inventories of radionuclides are not known for the suspect soil trenches, the computational results are used to calculate inventory limits for each radionuclide based on performance objectives of the RPA.

Specifically, the near-field model was implemented, using the PORFLOW computer code, to estimate fluxes of radionuclides to the water table over time and to track the inventory in the trenches as a function of time. The results of the two-dimensional PORFLOW simulations were obtained in terms of fraction of the initial inventory in the simulation domain that leaves the bottom boundary of the domain over time, the bottom boundary representing the water table. Because the simulation domain represents a "slice" through the trenches and surrounding soil, a correction was made to the results to account for losses of radionuclides through the faces at the sides of the trenches. This correction assumes that the radionuclide loss from the trenches through these faces is geometrically related to the loss through the ends of the trenches. The losses through the ends are accounted for in the PORFLOW simulations. By calculating the ratio of the side planes (or faces) to the area of the end planes of the trenches, and multiplying this ratio by the PORFLOW-simulated losses through the end planes, the results are corrected by adding this additional amount to the flux at the bottom of the domain. This correction, although necessary, did not significantly alter the flux results for the near-field model because the overwhelmingly significant losses from the trenches are from the base.

Following estimation of flux to the water table for the trenches, the groundwater model was implemented, again using PORFLOW, to estimate the time dependent groundwater concentrations of each radionuclide at the compliance point for groundwater resource protection. The compliance point was selected from the groundwater simulation results as the node with the highest concentration which is at least 100 m from the edge of the suspect soil trenches. For radionuclides that are relatively short-lived (with half-lives less than 1000 years) and that decay to longer-lived radioactive progeny, daughter contributions to groundwater radioactivity per Ci of parent activity originally in the suspect soil trenches were estimated in the manner described in Sect. 4.1.3. The parent radionuclide is assumed to decay completely to the daughter in the trenches. Loss of the parent through leaching during the decay process is neglected. The initial activity of the daughter per Ci of original inventory of parent

is calculated from:

$$A_{D0} = A_{P0} \frac{\lambda_D}{\lambda_P} = \frac{\lambda_D}{\lambda_P}$$

where

A_{D0} = initial activity of the daughter, Ci,

A_{P0} = initial activity of the parent (= 1 Ci),

λ_D = radioactive decay constant ($0.693/T_{1/2}$) of the daughter (yr^{-1}), and

λ_P = radioactive decay constant of the parent (yr^{-1}).

The peak concentration of the daughter, per Ci of parent radionuclide, is calculated by multiplying the initial activity of the daughter per Ci of parent activity (A_{D0}) by the 10,000-year and peak groundwater concentration of the daughter (pCi/cc-Ci), which is determined with PORFLOW simulations. Inventory limits based on groundwater protection requirements and on the 25 mrem per year performance objective for off-site individuals were calculated for the most restrictive requirement. For other radionuclides for which daughters were considered (Table I.2-1), daughter ingrowth and transport were considered explicitly in the vadose zone and groundwater simulations. Again, the results are expressed as pCi/cc of daughter radionuclide per Ci of parent originally in the trenches.

The air pathway was considered by carrying out the calculations described in Sect. I.2.3.3 to calculate fluxes of H-3, C-14, and Rn-222 from the top of the trenches, assuming the approximately 3-m engineered moisture barrier had been removed or eroded away. For H-3 and C-14, these fluxes were then used to conservatively estimate doses to intruders residing over the trenches, or doses to off-site individuals per unit activity in the trenches. Inventory limits were calculated for the air pathway for H-3 and C-14 based on the performance objectives of 10 mrem per year for off-site individuals, and 100 mrem per year for inadvertent intruders. For U-234, inventory limits are based on the performance objective of 20 pCi/m^2-s of Rn-222 in addition to consideration of groundwater concentrations of U-234, Th-230, and Ra-226.

Intruder doses from the agriculture scenario were calculated using the models referenced in Sect. I.2.3.4 above, for a unit inventory of each radionuclide. Inventory limits were calculated for intruders based on the performance objective of 100 mrem per year chronic exposure.

I.2.5 Quality Assurance

As described in Sect. 3.5, this analysis was conducted under the guidance of the provision of the ANSI/ASME NQA-1 Program Requirements for Nuclear Facilities (NRC 1989), as required by DOE Order 5820.2A (U.S.DOE 1988a). Pertinent elements of NQA-1 and relevant documentation are cited in that section of the RPA, and apply directly to the suspect soil analysis.

I.3 RESULTS OF SUSPECT SOIL ANALYSIS

In this section, the results of the analysis of performance of the suspect soil trenches are presented. Predicted releases to the environment (atmospheric releases and releases to the water table), resulting concentrations, results of dose analyses, and allowable inventories in the suspect soil trenches are presented in Sect. I.3.1. The results are interpreted in Sect. I.3.2.

I.3.1 Analysis Results

I.3.1.1 Near-Field Model Results

Table I.3-1 lists the PORFLOW simulation results for the near-field model. The fluxes provided represent the peak flux to the water table per pCi inventory of radionuclide in the suspect soil trenches (i.e., peak fractional flux). These fluxes are based on a 40 cm per year infiltration rate through the trenches, as was noted in Sect. I.2.3.1.

I.3.1.2 Groundwater Concentrations

The results of the groundwater transport simulations are listed in Table I.3-2. The values listed in this table represent peak groundwater concentration per Ci of radionuclide in the suspect soil trenches, at the compliance point for groundwater protection. If the peak occurs at a time greater than 10,000 years after closure, the 10,000 year compliance point concentration is also provided. The compliance point is considered to be the point of maximum groundwater concentration at least 100 m from the edge of the suspect soil trenches.

I.3.1.3 Dose Analysis for Off-Site Releases of Radionuclides

As described in Sect. 3.2.3.3, the only performance objective of concern for off-site release of radionuclides are those pertinent to consumption of groundwater, provided doses from airborne release of radionuclides are insignificant.

The groundwater concentrations per Ci inventory in the trenches are compared to allowable groundwater concentrations to derive inventory limits based on consideration of groundwater resource protection and the 25 mrem-per-year performance objective for off-site individuals. Inventory limits are based on the more restrictive of the two requirements. In order to determine which performance objective is more restrictive for each radionuclide, the MCLs from Table 3.2-1 were compared to the results of the model for estimating dose from the drinking water pathway for off-site individuals. The annual EDEs, in rem per year, from the drinking water pathway per unit concentration (1 μCi/L) of radionuclide in groundwater are summarized in Table 4.1-7.

Table I.3-1. Peak flux to the water table from [illegible] soil trench

Radionuclide	Predicted Peak Fractional Flux (pCi/year-pCi)	Time of Peak Flux (year)
H-3	1.0×10^{-1}	3.4
C-14	8.3×10^{-3}	65
Al-26	1.3×10^{-5}	34,000
Ni-59	4.7×10^{-5}	8,900
Ni-63	1.7×10^{-10}	840
Se-79	3.7×10^{-3}	140
Rb-87	3.7×10^{-4}	1,300
Sr-90	6.7×10^{-5}	100
Zr-93	3.3×10^{-5}	14,000
Tc-99	3.4×10^{-2}	15
Pd-107	3.7×10^{-4}	1,300
Cd-113m	7.4×10^{-11}	130
Sn-121m	8.4×10^{-9}	400
Sn-126	1.5×10^{-4}	3,000
I-129	2.3×10^{-2}	23
Cs-135	6.2×10^{-5}	7,700
Sm-151	2.3×10^{-9}	680
Ra-226	2.2×10^{-6}	4,600
Th-229	2.0×10^{-7}	25,000
Th-230 Ra-226[a]	3.8×10^{-6} 5.3×10^{-7}	56,000 45,000
Th-232	6.7×10^{-6}	71,000
Pa-231	2.9×10^{-5}	11,000
U-232	1.0×10^{-5}	280
U-233 Th-229[a]	5.7×10^{-4} 4.1×10^{-8}	840 3,200
U-234 Th-230[a] Ra-226[a]	5.7×10^{-4} 3.1×10^{-8} 3.9×10^{-9}	840 5,000 9,700

Table I3-1. (continued)

Radionuclide	Predicted Peak Fractional Flux (pCi/year-pCi)	Time of Peak Flux (year)
U-235 Pa-231[a]	5.7×10^{-4} 6.3×10^{-11}	840 3,900
U-236	5.7×10^{-4}	840
U-238	5.7×10^{-4}	840
Np-237	3.7×10^{-3}	140
Pu-238 U-234[a]	2.6×10^{-7} 2.0×10^{-7}	480 840
Pu-239	1.9×10^{-3}	2,300
Pu-240	1.6×10^{-4}	2,100
Pu-241 Am-241[a] Np-237[a]	1.7×10^{-11} 7.0×10^{-13} 2.5×10^{-8}	140 3,700 140
Pu-242	2.0×10^{-4}	2,300
Pu-244	2.0×10^{-4}	2,300
Am-241 Np-237[a]	2.1×10^{-11} 7.5×10^{-7}	3,700 140
Am-242m U-234[a]	1.7×10^{-14} 3.5×10^{-7}	1,700 840
Am-243 Pu-239[a]	8.5×10^{-7} 5.5×10^{-5}	19,000 6,600
Cm-242 Pu-238[a]	4.2×10^{-40} 1.3×10^{-9}	7.6 480
Cm-243 Pu-239[a]	9.0×10^{-21} 2.2×10^{-6}	400 2,300
Cm-244 Pu-240[a]	1.4×10^{-22} 4.4×10^{-7}	250 2,100
Cm-245	1.1×10^{-6}	21,000
Cm-246 Pu-242[a]	3.4×10^{-7} 8.1×10^{-5}	16,000 6,000
Cm-247 Am-243[a] Pu-239[a]	1.1×10^{-5} 5.0×10^{-9} 3.6×10^{-8}	44,000 45,000 29,000
Cm-248	9.8×10^{-6}	42,000
Bk-249 Cf-249[a]	5.4×10^{-37} 1.5×10^{-14}	18 3,200

Table I.3-1. (continued)

Radionuclide	Predicted Peak Fractional Flux (pCi/year-pCi)	Time of Peak Flux (year)
Cf-249	5.8×10^{-12}	3,200
Cf-250	5.8×10^{-24}	190
Cm-246[a]	9.4×10^{-10}	16,000
Cf-251	1.1×10^{-9}	6,100
Cm-247[a]	1.1×10^{-5}	44,000
Am-243[a]	5.0×10^{-9}	46,000
Pu-239[a]	3.5×10^{-8}	30,000
Cf-252	2.7×10^{-31}	42
Cm-248[a]	7.6×10^{-11}	42,000

[a] Fractional Flux and Time of Peak Flux given for radioactive daughter is per pCi of parent radionuclide.

Table I.3-2. Predicted groundwater compliance concentration for the suspect soil trench

Radionuclide	Groundwater Concentration at 10,000 years (pCi/cc-Ci)	Peak Groundwater Concentration	
		pCi/cc-Ci	Time of peak (year)
H-3	---- [a]	1.8	13
C-14	---- [a]	3.2×10^{-1}	185
Al-26	9.6×10^{-8}	3.4×10^{-4}	130,000
Ni-59	1.9×10^{-4}	1.3×10^{-3}	30,000
Ni-63	---- [a]	1.8×10^{-16}	1,800
Se-79	---- [a]	9.2×10^{-2}	370
Rb-87	---- [a]	9.2×10^{-3}	4,400
Sr-90	---- [a]	2.6×10^{-5}	190
Zr-93	3.3×10^{-5}	9.4×10^{-4}	45,000
Tc-99	---- [a]	8.8×10^{-1}	35
Pd-107	---- [a]	9.8×10^{-3}	3,900
Cd-113m	---- [a]	1.0×10^{-10}	2,400
Sn-121m	---- [a]	3.4×10^{-11}	610
Sn-126	---- [a]	4.3×10^{-3}	9,600
I-129	---- [a]	7.6×10^{-1}	65
Cs-135	4.4×10^{-4}	1.7×10^{-3}	24,000
Sm-151	---- [a]	7.7×10^{-12}	1,000
Ra-226	---- [a]	4.1×10^{-5}	2,700
Th-229	1.4×10^{-10}	5.7×10^{-8}	45,000
Th-230 Ra-226[b]	3.4×10^{-10} 2.0×10^{-6}	3.3×10^{-5} 2.3×10^{-4}	180,000 160,000
Th-232	3.6×10^{-10}	2.2×10^{-4}	240,000
Pa-231	4.1×10^{-5}	4.8×10^{-4}	33,000
U-232	---- [a]	2.1×10^{-6}	500

Table I.3-2. (continued)

Radionuclide	Groundwater Concentration at 10,000 years (pCi/cc-Ci)	Peak Groundwater Concentration	
		pCi/cc-Ci	Time of peak (year)
U-233	—[a]	1.2×10^{-2}	2,400
Th-229[b]	8.8×10^{-5}	1.1×10^{-4}	16,000
U-234	—[a]	1.2×10^{-2}	2,400
Th-230[b]	1.2×10^{-5}	2.9×10^{-5}	43,000
Ra-226[b]	3.8×10^{-5}	9.7×10^{-5}	49,000
U-235	—[a]	1.2×10^{-2}	2,400
Pa-231[b]	1.3×10^{-4}	1.7×10^{-4}	25,000
U-236	—[a]	1.2×10^{-2}	2,400
U-238	—[a]	1.2×10^{-2}	2,400
Np-237	—[a]	8.1×10^{-2}	330
Pu-238	—[a]	8.1×10^{-9}	790
U-234[b]	—[a]	5.0×10^{-6}	2,400
Pu-239	—[a]	4.2×10^{-3}	6,600
Pu-240	—[a]	2.6×10^{-3}	6,000
Pu-241	—[a]	4.8×10^{-15}	220
Am-241[b]	—[a]	6.7×10^{-16}	5,400
Np-237[b]	—[a]	5.5×10^{-7}	330
Pu-242	—[a]	5.0×10^{-3}	6,900
Pu-244	—[a]	5.1×10^{-3}	6,900
Am-241	—[a]	2.0×10^{-14}	5,400
Np-237[b]	—[a]	1.6×10^{-5}	330
Am-242m	—[a]	8.3×10^{-19}	2,400
U-234[b]	—[a]	8.7×10^{-6}	2,400
Am-243	5.0×10^{-9}	4.0×10^{-7}	40,000
Pu-239[b]	4.6×10^{-4}	5.1×10^{-4}	13,000
Cm-242	—[a]	—[c]	—
Pu-238[b]	—[a]	4.1×10^{-11}	790
Cm-243	—[a]	3.6×10^{-27}	520
Pu-239[b]	—[a]	5.0×10^{-6}	6,600
Cm-244	—[a]	1.4×10^{-28}	340
Pu240[b]	—[a]	7.2×10^{-6}	6,000
Cm-245	7.6×10^{-9}	7.4×10^{-7}	48,000

Table I3-2. (continued)

Radionuclide	Groundwater Concentration at 10,000 years (pCi/cc-Ci)	Peak Groundwater Concentration	
		pCi/cc-Ci	Time of peak (year)
Cm-246	2.9×10^{-9}	6.4×10^{-8}	31,000
Pu-242[b]	3.0×10^{-5}	3.3×10^{-5}	13,000
Cm-247	1.3×10^{-8}	2.8×10^{-4}	150,000
Am-243[b]	7.8×10^{-9}	2.8×10^{-4}	160,000
Pu-239[b]	1.6×10^{-4}	8.7×10^{-4}	40,000
Cm-248	1.9×10^{-8}	2.6×10^{-4}	170,000
Bk-249	—[a]	—[c]	—
Cf-249[b]	—[a]	7.8×10^{-18}	4,500
Cm-245[b]	7.8×10^{-13}	7.6×10^{-11}	48,000
Cf-249	—[a]	3.1×10^{-15}	4,500
Cm-245[b]	3.1×10^{-10}	3.1×10^{-8}	48,000
Cf-250	—[a]	2.2×10^{-31}	280
Cm-246[b]	1.1×10^{-11}	2.7×10^{-10}	30,000
Cf-251	—[a]	5.7×10^{-12}	9,300
Cm-247[b]	7.6×10^{-13}	1.6×10^{-8}	160,000
Am-243[b]	4.1×10^{-13}	1.5×10^{-8}	160,000
Pu-239[b]	6.3×10^{-9}	4.7×10^{-8}	40,000
Cf-252	—[a]	—[c]	—
Cm-248[b]	1.5×10^{-13}	2.0×10^{-9}	170,000

[a] Peak occurs before 10,000 years.
[b] Concentration given is pCi/cc of the daughter per Ci of the parent. Time of peak applies to that of the daughter.
[c] Fractional flux less than 10^{-30} per year; groundwater concentration not calculated.

For comparison to MCLs, the performance objective of 25 mrem per year for off-site individuals is divided by the EDCs in Table 4.1-7 to derive the concentration limit in drinking water of each radionuclide based on this dose limit. The results of this calculation, converted to appropriate units, and the appropriate MCLs from Table 3.2-1 are listed in Table I.3-3 for comparison. These results indicate that the 25 mrem per year performance objective is more restrictive for most of the alpha-emitting radionuclides, with the exception of Ra-226, Th-230, Am-242m, U-235, and U-238.

The allowable inventories derived for the drinking water pathway from off-site releases of radionuclides are given in Table I.3-4. These inventories (Ci) are calculated in the following manner. First, the most restrictive performance objective from Table I.3-3 is selected by choosing the lowest allowable groundwater concentration of the two values given for each radionuclide. Second, the lowest allowable groundwater concentration is divided by the maximum groundwater concentration up to 10,000 years, per Ci of inventory in the suspect soil trenches.

In order to evaluate the significance of the air pathway for the potentially volatile H-3 and C-14 radionuclides, doses were estimated using the fluxes derived in Sect. I.2.3.3 and the inhalation exposure model described in Sect. I.2.3.4. For Rn-222, the flux derived in Sect. A.3.7 was compared to the performance objective of 20 pCi m^{-2} s^{-1} for Rn-222 to calculate a disposal limit for U-234. The disposal limit of 8.8 Ci per trench (Sect. A.3.7) translates to a total of 44 Ci in all five trenches. The estimated fluxes from the soil per Ci of H-3, C-14, and U-234 present in the trenches, the corresponding inhalation doses per unit activity (mrem/Ci), the appropriate performance objectives (mrem/year) and the inventory limits (Ci) based on the air pathway are given in Table I.3-5. The doses for H-3 and C-14 are based on 50-year committed dose equivalent factors for inhalation of 6.3×10^4 mrem per Ci for ^3H_2O and 2.4×10^4 mrem per Ci for $^{14}CO_2$ (U.S.DOE 1988b).

I.3.1.4 Dose Analysis for Inadvertent Intruders

The results of the dose analysis for the agriculture scenario for the suspect soil trenches are given in Table I.3-6. The limits on concentrations and inventories of radionuclides are

Table I.3-3. Comparison of MCLs and allowable groundwater concentrations based on the 25 mrem per year performance objective for offsite individuals

Radionuclide	MCL[a] pCi/L	Allowable Concentration Based on 25 mrem per year,[b] pCi/L
H-3	20,000	540,000
C-14	6,400	16,000
Al-26	420 [c]	2,600
Ni-59	530	160,000
Ni-63	80	64,000
Se-79	660 [c]	4,100
Rb-87	270	7,100
Sr-90	8	250
Zr-93	2,100	21,000
Tc-99	800	26,000
Pd-107	36,600	250,000
Cd-113m	40	230
Sn-121m	2,260 [c]	26,000
Sn-126	290 [c]	1,900
I-129	0.5	120
Cs-135	800	4,800
Sm-151	1,100	100,000
Ra-226	5	31
Th-229	15	8.6
Th-230	15	64
Th-232	15	7.1
Pa-231	2.4	2.3
U-232	4.3×10^{20} (20 µg/L) [c]	17
U-233	190,000 (20 µg/L) [c]	125
U-234	124,000 (20 µg/L) [c]	132
U-235	42.8 (20 µg/L) [c]	139

Table I.3-3. (continued)

Radionuclide	MCL[a] pCi/L	Allowable Concentration Based on 25 mrem per year,[b] pCi/L
U-236	1,270 (20 µg/L)[c]	139
U-238	6.66 (20 µg/L)[c]	139
Np-237	15	8.9
Pu-238	15	8.9
Pu-239	15	8.1
Pu-240	15	8.1
Pu-241	(based solely on Np-237)[d]	(based solely on Np-237)[d]
Pu-242	15	8.3
Pu-244	15	8.6
Am-241	15	7.6
Am-242m	1.27[e]	8.1
Am-243	15	7.6
Cm-242	(based solely on Pu-238)[e]	(based solely on Pu-238)[e]
Cm-243	(based solely on Pu-239)[e]	(based solely on Pu-239)[e]
Cm-244	(based solely on Pu-240)[e]	(based solely on Pu-240)[e]
Cm-245	15	7.6
Cm-246	15	7.6
Cm-247	15	8.3
Cm-248	15	2.1
Bk-249	(based solely on Cm-245)[e]	(based solely on Cm-245)[e]
Cf-249	15	3.4
Cf-250	(based solely on Cm-246)[e]	(based solely on Cm-246)[e]
Cf-251	15	7.4
Cf-252	(based solely on Cm-248)[e]	(based solely on Cm-248)[e]

[a] Option 1, Table 3.2-1, unless otherwise noted.
[b] Calculated by dividing 25 mrem per year performance objective by EDE in Table 4.1-7.
[c] Option 3, Table 3.2-1.
[d] Np-237 daughter has significantly higher calculated groundwater concentration than Am-241 or Pu-241, due to greater mobility, long half-life, and conservative method of accounting for daughters. Therefore, MCL and allowable concentrations based solely on this daughter.
[e] EDE not provided in Table 4.1-7 because groundwater concentration of parent is negligible.

Table I3-1. Groundwater-based disposal limits for the suspect soil trenches[a]

Radionuclide	Compliance Point Groundwater Concentration (pCi/cc-Ci)	Allowable Groundwater Concentration[a]	Suspect Soil Trench Inventory Limit (Ci)
H-3	1.8	20,000 pCi/L	1.1×10^{1}
C-14	3.2×10^{-1}	6,400 pCi/L	2.0×10^{1}
Al-26	9.6×10^{-8} [b]	420 pCi/L [c]	4.4×10^{6}
Ni-59	1.9×10^{-4} [b]	530 pCi/L	2.8×10^{3}
Ni-63	1.8×10^{-16}	80 pCi/L	4.4×10^{14}
Se-79	9.2×10^{-2}	660 pCi/L [d]	7.2
Rb-87	9.2×10^{-3}	270 pCi/L	2.9×10^{1}
Sr-90	2.6×10^{-5}	8 pCi/L	3.1×10^{2}
Zr-93	3.3×10^{-5} [b]	2,100 pCi/L	6.4×10^{4}
Tc-99	8.8×10^{-1}	800 pCi/L	9.1×10^{-1}
Pd-107	9.8×10^{-3}	36,600 pCi/L	3.7×10^{3}
Cd-113m	1.0×10^{-10}	40 pCi/L [e]	4.0×10^{8}
Sn-121m	3.4×10^{-11}	2,260 pCi/L [e]	6.6×10^{10}
Sn-126	4.3×10^{-3}	290 pCi/L [e]	7.4×10^{1}
I-129	7.6×10^{-1}	0.5 pCi/L	6.6×10^{-4}
Cs-135	4.4×10^{-4} [e]	800 pCi/L	1.8×10^{3}
Sm-151	7.7×10^{-12}	1,100 pCi/L	1.4×10^{11}
Ra-226	4.1×10^{-5}	5 pCi/L [f]	1.2×10^{2}
Th-229	1.4×10^{-10} [b]	8.6 pCi/L	6.1×10^{7}
Th-230 [g] Ra-226	3.4×10^{-10} [b] 2.0×10^{-6} [b]	15 pCi/L 5 pCi/L [f]	2.5×10^{3}
Th-232	3.6×10^{-10} [b]	7.1 pCi/L	2.0×10^{7}
Pa-231	4.1×10^{-5} [b]	2.3 pCi/L	5.6×10^{1}
U-232	2.1×10^{-6}	17 pCi/L	8.1×10^{3}
U-233 [g] Th-229	1.2×10^{-2} 8.8×10^{-5} [b]	125 pCi/L 8.6 pCi/L	8.9

Table I3-4. (continued)

Radionuclide	Compliance Point Groundwater Concentration (pCi/cc-Ci)	Allowable Groundwater Concentration [a]	Suspect Soil Trench Inventory Limit (Ci)
U-234 [c] Th-230 Ra-226	1.4×10^{-2} 1.2×10^{-5} [b] 3.8×10^{-5} [b]	132 pCi/L 15 PCi/L 5 pCi/L [f]	9.4
U-235 [g] Pa-231	1.4×10^{-2} 1.3×10^{-4} [b]	20 µg/L [e,h] 2.3 pCi/L	3.1
U-236	1.4×10^{-2}	139 pCi/L	9.9
U-238	1.4×10^{-2}	20 µg/L [e,h]	4.8×10^{-1}
Np-237	8.1×10^{-2}	8.9 pCi/L	1.1×10^{-1}
Pu-238 [g] U-234	8.1×10^{-9} 5.0×10^{-6}	8.9 pCi/L 132 pCi/L	2.6×10^{4}
Pu-239	4.2×10^{-3}	8.1 pCi/L	1.9
Pu-240	2.6×10^{-3}	8.1 pCi/L	3.1
Pu-241 [g] Am-241 Np-237	4.8×10^{-15} 6.7×10^{-16} 5.5×10^{-7}	---- ---- 8.9 pCi/L	1.6×10^{4}
Pu-242	5.0×10^{-3}	8.3 pCi/L	1.7
Pu-244	5.1×10^{-3}	8.6 pCi/L	1.7
Am-241 [g] Np-237	2.0×10^{-14} 1.6×10^{-5}	7.6 pCi/L 8.9 pCi/L	5.6×10^{2}
Am-242m [g] U-234	8.3×10^{-19} 8.7×10^{-6}	1.27 pCi/L [e] 132 pCi/L	1.5×10^{4}
Am-243 [g] Pu-239	6.7×10^{-9} [b] 4.6×10^{-4} [b]	7.6 pCi/L 8.1 pCi/L	1.8×10^{1}
Cm-242 [g] Pu-238	---- [i] 4.1×10^{-11}	---- 8.9 pCi/L	2.2×10^{2}
Cm-243 [g] Pu-239	---- [i] 5.0×10^{-6}	---- 8.1 pCi/L	1.6×10^{3}
Cm-244 [g] Pu-240	---- [i] 7.2×10^{-6}	---- 8.1 pCi/L	1.1×10^{3}
Cm-245	7.6×10^{-9} [b]	7.6 pCi/L	1.0×10^{6}

Table I.3-4. (continued)

Radionuclide	Compliance Point Groundwater Concentration (pCi/cc-Ci)	Allowable Groundwater Concentration [a]	Suspect Soil Trench Inventory Limit (Ci)
Cm-246 [g] Pu-242	3.9×10^{-9} [b] 3.0×10^{-5} [b]	7.6 pCi/L 8.3 pCi/L	2.8×10^{2}
Cm-247 [c] Am-243 Pu-239	1.9×10^{-8} [b] 7.8×10^{-9} [b] 1.6×10^{-4} [b]	8.3 pCi/L 7.6 pCi/L 8.1 pCi/L	5.1×10^{1}
Cm-248	1.9×10^{-8} [b]	2.1 pCi/L	1.1×10^{5}
Bk-249 [g] Cf-249 Cm-245	---- [i] 7.8×10^{-18} 7.8×10^{-13}	--- 3.4 pCi/L 7.6 pCi/L	1.0×10^{10}
Cf-249 Cm-245	3.1×10^{-15} 3.1×10^{-10}	3.4 pCi/L 7.6 pCi/L	2.5×10^{7}
Cf-250 [g] Cm-246	---- [i] 1.1×10^{-11} [b]	--- 7.6 pCi/L	6.9×10^{3}
Cf-251 Cm-247 Am-243 Pu-239	7.2×10^{-12} 7.6×10^{-13} [b] 4.1×10^{-13} [b] 6.3×10^{-9} [b]	7.4 pCi/L 8.3 pCi/L 7.6 pCi/L 8.1 pCi/L	1.3×10^{6}
Cf-252 [g] Cm-248	---- [i] 1.5×10^{-13} [b]	--- 2.1 pCi/L	1.4×10^{11}

[a] Limit on inventory in all five trenches; total volume of trenches is assumed to be 2.6×10^{6} m^3.
[b] Selected from Table I.3-3 as the lower of either the MCL or 25 mrem-per-year based allowable concentration.
[c] Peak occurred after 10,000 year. Value given is the 10,000-year concentration.
[d] Option 3, Table 3.2-1.
[e] Not available in reference for Option 3. Calculated from CEDE in U.S.DOE 1988b to be 660 pCi/L.
[f] Not available in reference for Option 3. Calculated from CEDE in U.S.DOE 1988b to be 40 pCi/L.
[g] MCL is 5 pCi/L for Ra-226 *plus* Ra-228, but the inventory limit is calculated separately here.
[h] Inventory limit reflects contribution of daughters listed.
[i] Limit applies to total uranium.
[j] Insignificant (less than 10^{-26} pCi/cc-Ci).

Table I3-5. Suspect soil disposal limits based on the air pathway*

Radionuclide	Flux from Soil ($Ci\ m^{-2}\ yr^{-1}$) per Ci in trenches	Dose per unit radioactivity (mrem/year·Ci inventory)	Performance Objective (mrem/yr)	Inventory Limit (Ci)
H-3				
Off-site	4.8×10^{-6}	6.5×10^{-6}	10	1.5×10^{6}
Intruder	1.7×10^{-8}	4.1×10^{-4}	100	2.4×10^{5}
C-14				
Off-site	1.7×10^{-4}	1.2×10^{-2}	10	8.3×10^{2}
Intruder	1.7×10^{-4}	1.6	100	6.3×10^{1}
Rn-222				
Flux limit	2.3 $pCi\ m^{-2}\ s^{-1}$	—	20 $pCi\ m^{-2}\ s^{-1}$	44 (of U-234)

* Limit on inventory in all five trenches; total volume of trenches is assumed to be $2.6 \times 10^{4}\ m^{3}$.

Table I3-6. Results of dose analysis for intruder agriculture scenario for [illegible] trenches

Radionuclide	SDCF[b] (rem/year per µCi/m³)	F[c]	Concentration Limit[a,d] (µCi/m³)	Inventory Limit[a,e] (Ci)
H-3	3.9×10^{-6}	1.5×10^{-12}	--	--
C-14	1.5×10^{-5}	6.9×10^{-2}	1.6×10^{5}	4.2×10^{3}
Al-26	3.9×10^{-3}	9.4×10^{-1}	4.5×10^{1}	1.2
Co-60	3.5×10^{-3}	2.0×10^{-6}	2.4×10^{7}	6.2×10^{5}
Ni-59	6.8×10^{-8}	8.8×10^{-1}	2.8×10^{6}	7.2×10^{4}
Ni-63	1.8×10^{-7}	4.5×10^{-1}	2.1×10^{6}	5.3×10^{4}
Se-79	1.2×10^{-6}	2.1×10^{-1}	6.6×10^{5}	1.7×10^{4}
Rb-87	1.9×10^{-6}	6.8×10^{-1}	1.3×10^{5}	3.4×10^{3}
Sr-90	1.8×10^{-4}	4.4×10^{-2}	2.1×10^{4}	5.5×10^{2}
Zr-93	4.5×10^{-8}	9.1×10^{-1}	4.1×10^{6}	1.1×10^{5}
Nb-93m	1.9×10^{-8}	8.7×10^{-3}	1.0×10^{9}	2.6×10^{7}
Tc-99	1.1×10^{-5}	2.8×10^{-4}	5.4×10^{7}[f]	--
Pd-107	3.2×10^{-8}	6.7×10^{-1}	7.8×10^{6}	2.0×10^{5}
Cd-113m	1.3×10^{-4}	6.3×10^{-3}	2.0×10^{5}	5.3×10^{3}
Sn-121m	4.7×10^{-7}	2.8×10^{-1}	1.3×10^{6}	3.3×10^{4}
Sn-126	2.6×10^{-3}	7.9×10^{-1}	8.1×10^{1}	2.1
I-129	8.3×10^{-5}	3.3×10^{-3}	6.1×10^{5}[g]	--
Cs-135	1.2×10^{-6}	8.7×10^{-1}	1.6×10^{5}	4.2×10^{3}
Cs-137	7.7×10^{-4}	1.0×10^{-1}	2.2×10^{3}	5.6×10^{1}
Sm-151	1.0×10^{-8}	4.6×10^{-1}	3.6×10^{7}	9.4×10^{5}
Eu-154	1.7×10^{-3}	3.8×10^{-4}	2.6×10^{5}	6.7×10^{3}
Eu-155	4.0×10^{-5}	8.5×10^{-7}	4.9×10^{9}	1.3×10^{8}
Pb-210	3.0×10^{-4}	4.4×10^{-2}	1.3×10^{4}	3.3×10^{2}

Table I.3-6. (continued)

Radionuclide	SDCF [b] (rem/year per µCi/m³)	F [c]	Concentration Limit [a,d] (µCi/m³)	Inventory Limit [a,e] (Ci)
Ra-226 [h]	1.2×10^{-1}	8.6×10^{-1}	1.6 [h]	4.2×10^{-2} [h]
Ra-226 [i]	2.7×10^{-3}	8.6×10^{-1}	7.2×10^{1} [i]	1.9 [i]
Th-229	4.3×10^{-4}	9.5×10^{-1}	4.1×10^{2}	1.1×10^{1}
Th-230	1.1×10^{-5}	9.6×10^{-1}	1.6×10^{4}	4.1×10^{2}
Th-232 [h]	1.4×10^{-2}	9.6×10^{-1}	1.2×10^{1} [h]	3.2×10^{-1} [h]
Th-232 [i]	3.6×10^{-3}	9.6×10^{-1}	4.8×10^{1}	1.3 [i]
Pa-231	8.3×10^{-4}	9.0×10^{-1}	2.2×10^{2}	5.8
U-232 [h]	1.2×10^{-2}	2.5×10^{-1}	5.6×10^{1} [h]	1.4 [h]
U-232 [i]	2.3×10^{-3}	2.5×10^{-1}	2.9×10^{2}	7.5 [i]
U-233	1.1×10^{-5}	6.0×10^{-1}	2.5×10^{4}	6.6×10^{2}
U-234 [j]	1.1×10^{-5}	6.6×10^{-2}	5.1×10^{3} [h]	1.3×10^{2} [h]
Th-230	1.1×10^{-5}	9.4×10^{-4}	—	—
Ra-226 [h]	1.2×10^{-1}	2.6×10^{-4}	—	—
U-234 [i]	1.1×10^{-5}	6.0×10^{-1}	2.5×10^{4} [i]	6.6×10^{2} [i]
U-235	1.8×10^{-4}	6.0×10^{-1}	1.5×10^{3}	4.0×10^{1}
U-236	1.0×10^{-5}	6.0×10^{-1}	2.8×10^{4}	7.2×10^{2}
U-238	3.9×10^{-5}	6.0×10^{-1}	7.1×10^{3}	1.9×10^{2}
Np-237	5.0×10^{-4}	2.1×10^{-1}	1.6×10^{2}	4.1×10^{1}
Pu-238	3.4×10^{-5}	3.6×10^{-1}	1.4×10^{4}	3.5×10^{2}
Pu-239	4.0×10^{-5}	7.6×10^{-1}	5.5×10^{3}	1.4×10^{2}
Pu-240	4.0×10^{-5}	7.6×10^{-1}	5.5×10^{3}	1.4×10^{2}
Pu-241	7.7×10^{-7}	6.2×10^{-3}	1.1×10^{5} [h]	2.9×10^{3} [h]
Pu-242	3.8×10^{-5}	7.6×10^{-1}	5.8×10^{3}	1.5×10^{2}
Pu-244	3.7×10^{-5}	7.6×10^{-1}	5.9×10^{3}	1.5×10^{2}
Am-241	5.6×10^{-5}	8.1×10^{-1}	3.7×10^{3}	9.6×10^{1}

Table I3-6. (continued)

Radionuclide	SDCF [b] (rem/year per μCi/m³)	F [c]	Concentration Limit [a,d] (μCi/m³)	Inventory Limit [a,e] (Ci)
Am-242m	6.0×10^{-5}	6.2×10^{-1}	3.4×10^{3} [m]	8.8×10^{1} [m]
Am-243	2.5×10^{-4}	9.4×10^{-1}	7.1×10^{2}	1.8×10^{1}
Cm-243	1.6×10^{-4}	8.3×10^{-2}	1.3×10^{4}	3.3×10^{2}
Cm-244	2.0×10^{-5}	2.1×10^{-2}	4.0×10^{5} [n]	--
Cm-245	1.1×10^{-4}	9.4×10^{-1}	1.6×10^{3}	4.2×10^{1}
Cm-246	4.0×10^{-5}	9.3×10^{-1}	4.5×10^{3}	1.2×10^{2}
Cm-247	4.4×10^{-4}	9.5×10^{-1}	4.0×10^{2}	1.0×10^{1}
Cm-248	1.4×10^{-4}	9.5×10^{-1}	1.3×10^{3}	3.3×10^{1}
Cf-249	4.6×10^{-4}	8.2×10^{-1}	4.4×10^{2}	1.1×10^{1}
Cf-250	1.7×10^{-5}	5.0×10^{-3}	8.2×10^{6} [n]	--
Cf-251	1.6×10^{-4}	9.3×10^{-1}	1.1×10^{3}	2.9×10^{1}

[a] Concentration and inventory limits are obtained from Eqs. (4.1-2) and (4.1-3). Limits are calculated for intrusion at 100 years after disposal, except as noted.
[b] Values are obtained from Table 4.1-10.
[c] Fraction of initial inventory of radionuclide remaining in disposal units at time scenario is assumed to occur.
[d] Limit on average concentration in disposed waste.
[e] Limit on inventory in all trenches; total volume of trenches is assumed to be 2.6×10^{4} m³.
[f] Value exceeds NRC's Class-C limit in 10 CFR Part 61 of 3×10^{6} μCi/m³, which applies to individual waste packages at DOE sites (U.S.DOE 1988a).
[g] Value exceeds NRC's Class-C limit in 10 CFR Part 61 of 8×10^{4} μCi/m³, which applies to individual waste packages at DOE disposal sites (U.S.DOE 1988a).
[h] Results include contribution to dose from radon decay product.
[i] Results exclude contribution to dose from radon decay product.
[j] Disposal limits are based on calculations at 1,600 years after disposal, taking into account buildup of long-lived decay products.
[k] Disposal limits are based on buildup of Am-241 decay product.
[m] Limit takes into account contribution to dose from ingrowth of Pu-238 decay product.
[n] Limit for individual waste packages at DOE disposal sites is 100 nCi/g (about 2×10^{5} μCi/m³) for all alpha-emitting transuranic radionuclides with half-lives greater than 5 years (U.S.DOE 1988a).

calculated using Eqs. I.1-2 and I.1-3. The SDCF for each radionuclide is obtained from Table 4.1-10, the geometrical reduction factor (G) for the subject soil trenches of 0.6 is obtained from Table 4.1-13, and the fraction of the initial inventory of radionuclides remaining in the trenches at the time the agriculture scenario is assumed to occur, taking into account radioactive decay and mobilization and transport in water, was calculated using the PORFLOW computer code. For relatively mobile radionuclides (e.g., H-3 and Tc-99), the calculations indicate that the disposal limits are increased substantially when mobilization and transport in water is taken into account. Since the calculated concentration limit for H-3 exceeds the specific activity of this isotope, there are no limits for disposal based on a dose analysis for inadvertent intruders.

For Ra-226, Th-232, U-232, and U-234, two sets of concentration and inventory limits are calculated and listed in Table I.3-6. The first set of results includes the contributions from radon decay products (i.e., Rn-222 for Ra-226 and U-234 and Rn-220 for Th-232 and U-232), but the second set of calculations excludes the contributions from radon. As described in Sects. 1.2.3 and 4.1.5.1, the two options for accounting for radon decay products are consistent with the present performance objective for protection of inadvertent intruders at DOE LLW disposal sites and a revision of the performance objective that is being considered at the present time.

For most radionuclides, the results in Table I.3-6 are based on the SDCF for the radionuclide in disposed waste and depletion of the initial inventory of the radionuclide over 100 years due to radioactive decay and mobilization and transport in water, because the radionuclide concentrations, and thus the dose for the agriculture scenario, decrease monotonically with time after 100 years. However, there are a few exceptions to this case, which are described below.

For U-234, the calculations indicate that the maximum dose would occur at about 1,600 years after disposal, taking into account buildup of radiologically significant long-lived decay products, principally Ra-226 and its decay product Rn-222, as well as depletion of the initial inventory of the parent radionuclide due to mobilization and transport in water. However, for U-235, U-238, and Np-237, which also decay to radiologically significant long-lived decay

products, the maximum dose nonetheless is predicted to occur at 100 years after disposal and is due primarily to the parent radionuclide only, because depletion of the parent radionuclide due to mobilization and transport in water beyond 100 years more than compensates for any increase in dose due to buildup of the decay products. If the dose from Rn-222 is not included, the maximum dose for U-234 also occurs at 100 years.

The concentration and inventory limits for Am-242m take into account buildup of the Pu-238 decay product. Given the half-lives of 152 years for Am-242m, 87.75 years for Pu-238, and the assumed rate of depletion of Am-242m due to mobilization of water, the maximum dose in this case is predicted to occur at 100 years after disposal because the decrease in the inventory of Am-242m after 100 years more than compensates for the buildup of Pu-238. At this time, about 75% of the estimated dose is due to Am-242m with the remaining 25% due to Pu-238.

For Pu-241, Am-241, Cm-243, Cm-244, and Cf-250, the disposal limits are estimated taking into account buildup of the longer-lived decay products Am-241, Np-237, Pu-239, Pu-240, and Cm-246, respectively. For each of these radionuclides, the disposal limits are the more restrictive of the results obtained from two calculations. The first is a calculation for the parent radionuclide only at 100 years after disposal, taking into account radioactive decay and mobilization and transport in water. In the second calculation, the Bateman equations are used to estimate the maximum inventory of the decay product that would be produced in the decay of the parent radionuclide. This inventory is approximately equal to the initial unit inventory of the parent radionuclide times the ratio of the half-lives of the parent and decay product. This inventory of the decay product then is conservatively assumed to be produced at time $t = 0$, and the disposal limits for the decay product only are calculated for 100 years after disposal. This procedure is the same as that used by the NRC in calculating the concentration limits for Pu-241 and Cm-242 in 10 CFR Part 61.

If the procedure described above is applied to the radionuclides that produce longer-lived radiologically significant isotopes, only for Pu-241 are the disposal limits based on buildup of the decay product. In this case, the maximum inventory of the decay product Am-241 is about 30 times less than the initial inventory of the parent, but the dose per unit concentration of the decay product is nearly two orders of magnitude greater than the value for the

parent. For the other isotopes of concern, the parent radionuclide rather than the decay product determines the disposal limits for the parent radionuclide, because the maximum inventory of the decay product is at least two orders of magnitude less than the initial inventory of the parent but the dose per unit concentration of the decay product is within an order of magnitude of the value for the parent.

I.3.2 Interpretation of Results

The results presented in Sect. I.3.1 are summarized in Table I.3-7. The most restrictive pathway is identified, along with the corresponding inventory limit for each radionuclide. Actinium-227 and Ra-228 were removed from further consideration for intruders because the dose is accounted for in the analysis for the parent radionuclides Pa-231 and Th-232, respectively. Of the 56 radionuclides listed, none are potentially limited by the air pathway, 30 are limited by considerations of inadvertent intruders, and 26 are limited by the groundwater pathway.

These derived inventory limits are generally believed to be low-end estimates of the allowable inventory in the suspect soil trenches, as uncertainties encountered in data or models were generally addressed by choosing a conservative assumption. For example, for the groundwater pathway, no credit was taken for reduced infiltration by the engineered cover due to uncertainties in the long-term performance of this cover.

I.4 PERFORMANCE EVALUATION

I.4.1 Comparison to Performance Objectives

The results of the suspect soil analysis are presented in terms of disposal limits, in lieu of reliable estimates of the expected inventory in the trenches. Therefore, if the disposal limits listed in Table I.3-7 are not exceeded, and if the cumulative dose from all radionuclides is considered, this PA provides reasonable assurance that performance objectives will be met.

Table I3-7. Summary of disposal limits for the suspect soil trenches.[a]

Radionuclide	Limiting Pathway	Suspect Soil Trench Inventory Limit (Ci)
H-3	Groundwater	1.1×10^{1}
C-14	Groundwater	2.0×10^{1}
Al-26	Intruder	1.2
Co-60	Intruder	6.2×10^{5}
Ni-59	Groundwater	2.8×10^{3}
Ni-63	Intruder	5.3×10^{4}
Se-79	Groundwater	7.2
Rb-87	Groundwater	2.9×10^{1}
Sr-90	Groundwater	3.1×10^{2}
Zr-93	Groundwater	6.4×10^{4}
Nb-93m	Intruder	2.6×10^{7}
Tc-99	Groundwater	9.1×10^{-1}
Pd-107	Groundwater	3.7×10^{3}
Cd-113m	Intruder	5.3×10^{3}
Sn-121m	Intruder	3.3×10^{4}
Sn-126	Intruder	2.1
I-129	Groundwater	6.6×10^{-4}
Cs-135	Groundwater	1.8×10^{5}
Cs-137	Intruder	5.6×10^{1}
Sm-151	Intruder	9.4×10^{5}
Eu-154	Intruder	6.7×10^{3}
Eu-155	Intruder	1.3×10^{8}
Pb-210	Intruder	3.3×10^{2}
Ra-226	Intruder	4.2×10^{-2} [b] 1.9 [c]
Th-229	Intruder	1.1×10^{1}
Th-230	Intruder	4.1×10^{2}
Th-232	Intruder	3.2×10^{-1} [b] 1.3 [c]
Pa-231	Intruder	5.8
U-232	Intruder	1.4 [b] 7.5 [c]

Table L3-7. (continued)

Radionuclide	Limiting Pathway	Suspect Soil Trench Inventory Limit (Ci)
U-233	Groundwater	8.9
U-234	Groundwater	9.1
U-235	Groundwater	3.1
U-236	Groundwater	9.9
U-238	Groundwater	4.8×10^{-1}
Np-237	Groundwater	1.1×10^{-1}
Pu-238	Intruder	3.5×10^{2}
Pu-239	Groundwater	1.9
Pu-240	Groundwater	3.1
Pu-241	Intruder	2.9×10^{3}
Pu-242	Groundwater	1.7
Pu-244	Groundwater	1.7
Am-241	Intruder	9.6×10^{1}
Am-242m	Intruder	8.8×10^{1}
Am-243	Intruder/Groundwater	1.8×10^{1}
Cm-242	Groundwater	2.2×10^{5}
Cm-243	Intruder	3.3×10^{2}
Cm-244	Groundwater	1.1×10^{3}
Cm-245	Intruder	5.1×10^{1}
Cm-246	Intruder	1.4×10^{2}
Cm-247	Intruder	1.2×10^{1}
Cm-248	Intruder	3.9×10^{1}
Bk-249	Groundwater	1.0×10^{10}
Cf-249	Intruder	1.1×10^{1}
Cf-250	Groundwater	6.9×10^{5}
Cf-251	Intruder	2.9×10^{1}
Cf-252	Groundwater	1.4×10^{11}

[a] Limit on inventory in all five trenches; total volume of trenches is assumed to be 2.6×10^{4} m^3.
[b] Considers contribution to dose from radon decay product.
[c] Neglects contribution to dose from radon decay product.

I.12 Design Changes Required to Meet Performance Objectives

Because a reliable estimate of the expected inventory of the suspect soil trenches does not presently exist, design changes for the suspect soil trenches are not indicated. In general, the inventory limits for these trenches are estimated to be one to two orders of magnitude lower than for vault-disposed waste.

I.13 Data and Research Needs

The most important information that would improve the assessment of performance of the suspect soil trenches is an estimate of the expected inventory. Because there are no engineered barriers designed for the suspect soil trenches, and credit was not taken for the engineered cover, analysis of performance of these trenches is a fairly straight-forward procedure involving fewer uncertain parameters than for vault disposal. One critical assumption is, however, that water flow through the trenches is similar to that in the surrounding soil. During and after emplacement of soil in trenches, care must be taken to test the validity of that assumption. If the trenches are more hydraulically conductive than surrounding geologic materials, an increased flux of water and radionuclides over that predicted in this analysis may result.

I.5 PORFLOW Input File

```
TITLE SUSPECT SOIL; 40 cm/yr infiltration
/ PORFLOW-3D, Version 2.50
/ File to establish flow field in vadose zone for suspect soil trenches
/
/L. M. McDowell-Boyer, last revised January 20, 1994
/
GRID 38 x 39
/
COORdinate X:
 -500.  500.  1500.  3000.  4500.  6000.  7500.  9000.
 9500.  9750.  10000.  10250.  10500.  11000.  12500.  14000.
15500. 17000.  18500.  20000.  21500.  23000.  24500.  26000.
27500. 29000.  29500.  29750.  30000.  30250.  30500.  31000.
32500. 34000.  35500.  38500.  39500.  40500.
/
COORdinate Y:
 -100.  100.   200.   300.   400.   500.   600.   700.
  800.  850.   875.   885.   895.   900.   905.   915.
  925.  950.   1000.  1100.  1200.  1300.  1350.  1375.
 1380. 1385.   1400.  1450.  1500.  1550.  1650.  1700.
 1750. 1800.   1850.  1900.  1950.  1995.  2005.
/
MATErial type 1 is from (1,34) to (38,39)  &Top Permeable layer
MATErial type 2 is from (1,1) to (38,33)   $Backfill
MATErial type 3 is from (11,14) to (29,29)  $Suspect Soil Trench
/
DATUm = 0. 0.
/
FOR 1:  $ Top permeable layer to allow infiltration into domain
ROCK bulk density 2.65 gm/cc, neff=0.38, ntot=0.38, ndif=0.38
HYDRaulic prop. ss=1.e-3, Kx=1.6e7, Ky=1.6e7 cm per yr
MULTiphase flow: VAN Genuchten: n=3.70, alpha = 0.0819, Sr = 0.01
/
FOR 2:  $Backfill
ROCK bulk density 1.60 gm/cc, neff=0.439, ntot=0.439, ndif=0.439
HYDRaulic prop. ss=1.e-3, Kx=333., Ky=333. cm per yr
/ Moisture characteristic curves entered in table format
MULTiphase flow: TABLe option, 79 sets
/  saturation potential in cm
      0.22    378.3312
      0.23    366.3198
      0.24    354.5856
      0.25    343.125
      0.26    331.9344
```

Fig. I.5-1. PORFLOW input file - flow in the vadose zone.

0.27	321.0102
0.28	310.3433
0.29	299.9466
0.3	289.8
0.31	279.9054
0.32	270.2592
0.33	260.8573
0.34	251.6976
0.35	242.775
0.36	234.0864
0.37	225.6282
0.38	219.3968
0.39	209.3886
0.4	201.6
0.41	194.0274
0.42	186.6672
0.43	179.5158
0.44	172.5696
0.45	165.825
0.46	159.2784
0.47	152.9262
0.48	146.7648
0.49	140.7906
0.5	135.
0.51	129.3894
0.52	123.9552
0.53	118.6938
0.54	113.6016
0.55	108.675
0.56	103.9104
0.57	99.3042
0.58	94.8528
0.59	90.5526
0.6	86.4
0.61	82.3914
0.62	78.5232
0.63	74.7918
0.64	71.1936
0.65	67.725
0.66	63.3824
0.67	61.1622
0.68	58.0608
0.69	55.0746
0.7	52.2
0.71	49.4334
0.72	46.7712

Fig. I.5-1. (cont.).

```
    0.73   44.2098
    0.74   41.7456
    0.75   39.575
    0.76   37.0944
    0.77   34.9002
    0.78   32.7438
    0.79   30.7566
    0.8    28.8
    0.81   26.9154
    0.82   25.0992
    0.83   23.3478
    0.84   21.6576
    0.85   20.025
    0.86   18.4464
    0.87   16.9182
    0.88   15.4368
    0.89   13.9986
    0.9    12.6
    0.91   11.2374
    0.92   9.9072
    0.93   8.6058
    0.94   7.3296
    0.95   6.075
    0.96   4.8384
    0.97   3.6162
    0.98   2.4048
    0.99   1.2006
    1.0    0.0000
MULTiphase flow: COND TABLe option, 79 sets
/  saturation relative conductivity
    0.22   0.0000e+00
    0.23   2.7016e-08
    0.24   4.3226e-07
    0.25   2.1883e-06
    0.26   6.9161e-06
    0.27   1.6885e-05
    0.28   3.5013e-05
    0.29   6.4864e-05
    0.3    1.1066e-04
    0.31   1.7725e-04
    0.32   2.7016e-04
    0.33   3.9552e-04
    0.34   5.6020e-04
    0.35   7.7160e-04
    0.36   1.0378e-03
    0.37   1.3677e-03
```

Fig. I.5-1. (cont.).

0.38	1.7705e-03
0.39	2.2564e-03
0.4	2.8360e-03
0.41	3.5208e-03
0.42	4.3226e-03
0.43	5.2541e-03
0.44	6.3287e-03
0.45	7.5602e-03
0.46	8.9633e-03
0.47	1.0553e-02
0.48	1.2346e-02
0.49	1.4357e-02
0.5	1.6606e-02
0.51	1.9108e-02
0.52	2.1883e-02
0.53	2.4950e-02
0.54	2.8328e-02
0.55	3.2039e-02
0.56	3.6102e-02
0.57	4.0541e-02
0.58	4.5377e-02
0.59	5.0632e-02
0.6	5.6322e-02
0.61	6.2500e-02
0.62	6.9161e-02
0.63	7.6341e-02
0.64	8.4066e-02
0.65	9.2362e-02
0.66	1.0126e-01
0.67	1.1078e-01
0.68	1.2096e-01
0.69	1.3183e-01
0.7	1.4341e-01
0.71	1.5574e-01
0.72	1.6885e-01
0.73	1.8277e-01
0.74	1.9753e-01
0.75	2.1317e-01
0.76	2.2972e-01
0.77	2.4721e-01
0.78	2.6569e-01
0.79	2.8518e-01
0.8	3.0573e-01
0.81	3.2736e-01
0.82	3.5013e-01
0.83	3.7406e-01

Fig. I.5-1. (cont.).

```
      0.84   3.9920e-01
      0.85   4.2558e-01
      0.86   4.5335e-01
      0.87   4.8225e-01
      0.88   5.1262e-01
      0.89   5.4440e-01
      0.9    5.7764e-01
      0.91   6.1234e-01
      0.92   6.4865e-01
      0.93   6.8652e-01
      0.94   7.2602e-01
      0.95   7.6721e-01
      0.96   8.1012e-01
      0.97   8.5480e-01
      0.98   9.0131e-01
      0.99   9.4970e-01
      1.0    1.0000e+00
/
FOR 3:  $Suspect Soil
ROCK bulk density 1.60 cm/cc, neff=0.439, ntot=0.439, ndif=0.439
HYDRaulic prop. ss=1.e-3, Kx=333., Ky=333.  zone 2
/ Moisture characteristic curves entered in table format
MULTiphase flow: TABLe option, 79 sets
/  saturation potential in cm
      0.22   378.3312
      0.23   366.3198
      0.24   354.5856
      0.25   343.125
      0.26   331.9344
      0.27   321.0102
      0.28   310.3488
      0.29   299.9466
      0.3    289.8
      0.31   279.9054
      0.32   270.2592
      0.33   260.8578
      0.34   251.6976
      0.35   242.775
      0.36   234.0864
      0.37   225.6282
      0.38   219.3968
      0.39   209.3886
      0.4    201.6
      0.41   194.0274
      0.42   186.6672
      0.43   179.5158
```

Fig. I.5-1. (cont.).

0.44	172.[illegible]96
0.45	165.[illegible]25
0.46	159.2784
0.47	152.9262
0.48	146.7648
0.49	140.7906
0.5	135.
0.51	129.3894
0.52	123.9552
0.53	118.6938
0.54	113.6016
0.55	108.675
0.56	103.9104
0.57	99.3042
0.58	94.8528
0.59	90.5526
0.6	86.4
0.61	82.3914
0.62	78.5232
0.63	74.7918
0.64	71.1936
0.65	67.725
0.66	63.3824
0.67	61.1622
0.68	58.0608
0.69	55.0746
0.7	52.2
0.71	49.4334
0.72	46.7712
0.73	44.2098
0.74	41.7456
0.75	39.375
0.76	37.0944
0.77	34.9002
0.78	32.7888
0.79	30.7566
0.8	28.8
0.81	26.9154
0.82	25.0992
0.83	23.3478
0.84	21.6576
0.85	20.025
0.86	18.4464
0.87	16.9182
0.88	15.4368
0.89	13.9986

Fig. I.5-1. (cont.).

```
    0.9     12.6
    0.91    11.2374
    0.92    9.5072
    0.93    8.5053
    0.94    7.3256
    0.95    6.075
    0.96    4.8384
    0.97    3.6162
    0.98    2.4048
    0.99    1.2006
    1.0     0.0000
MULTiphase flow: COND TABLe option, 79 sets
/  saturation relative conductivity
    0.22    0.0000e+00
    0.23    2.7016e-08
    0.24    4.3226e-07
    0.25    2.1883e-06
    0.26    6.9161e-06
    0.27    1.6885e-05
    0.28    3.5013e-05
    0.29    6.4864e-05
    0.3     1.1066e-04
    0.31    1.7725e-04
    0.32    2.7016e-04
    0.33    3.9552e-04
    0.34    5.6020e-04
    0.35    7.7160e-04
    0.36    1.0378e-03
    0.37    1.3677e-03
    0.38    1.7705e-03
    0.39    2.2564e-03
    0.4     2.8360e-03
    0.41    3.5208e-03
    0.42    4.3226e-03
    0.43    5.2541e-03
    0.44    6.3287e-03
    0.45    7.5602e-03
    0.46    8.9633e-03
    0.47    1.0553e-02
    0.48    1.2346e-02
    0.49    1.4357e-02
    0.5     1.6606e-02
    0.51    1.9108e-02
    0.52    2.1883e-02
    0.53    2.4950e-02
    0.54    2.8328e-02
```

Fig. I.5-1. (cont.).

0.55	3.2030e-02
0.56	3.6102e-02
0.57	4.0541e-02
0.58	4.5377e-02
0.59	5.0632e-02
0.6	5.6322e-02
0.61	6.2500e-02
0.62	6.9161e-02
0.63	7.6341e-02
0.64	8.4066e-02
0.65	9.2362e-02
0.66	1.0126e-01
0.67	1.1078e-01
0.68	1.2096e-01
0.69	1.3183e-01
0.7	1.4341e-01
0.71	1.5574e-01
0.72	1.6885e-01
0.73	1.8277e-01
0.74	1.9753e-01
0.75	2.1317e-01
0.76	2.2972e-01
0.77	2.4721e-01
0.78	2.6569e-01
0.79	2.8518e-01
0.8	3.0573e-01
0.81	3.2736e-01
0.82	3.5013e-01
0.83	3.7406e-01
0.84	3.9920e-01
0.85	4.2558e-01
0.86	4.5325e-01
0.87	4.8225e-01
0.88	5.1262e-01
0.89	5.4440e-01
0.9	5.7764e-01
0.91	6.1238e-01
0.92	6.4865e-01
0.93	6.8652e-01
0.94	7.2602e-01
0.95	7.6721e-01
0.96	8.1012e-01
0.97	8.5480e-01
0.98	9.0131e-01
0.99	9.4970e-01
1.0	1.0000e+00

Fig. I.5-1. (cont.).

```
/
/ Boundary Conditions for flow simulations
/
SET S = 0.7
BOUN P -1  FLUX=  0.0
BOUN P +1  FLUX=  0.0
BOUN P -2  NODE=  0.0
BOUN P +2  FLUX= -40.0
/
PROPerty for P is HARM mean
MATRIX  for P in 3 sweeps using ADI
CONVergence for P; GLOBal 1.0e-2 max 1 iterations
CONVergence for FLOW REFE GLOB 1.0e-2 max 3 interations
/
DIAGnostic node for P and V at (21,28) every 20 steps
OUTPut every 10000 steps
/
FLUX BALAnce for P in 'fluxp2.out' every 200 steps
/
/ Simulate steady state flow field
/
SOLVe P AUTO 50 1. 1.1 max 1 min 1.e-10 2.0 100000
SAVE U, V, P, S NOW in 'flow40.bkg'
/
END
```

Fig. I.5-1. (cont.).

```
TITLE SUSPECT SOIL; 40 cm/yr infiltration
/ PORFLOW-3D, Version 2.40  File 'u234d40.dat'
/ File to simulate mass transport out of suspect soil trenches
/ U-234 plus daughters
/
/L. M. McDowell-Boyer, March 8, 1994
/
GRID 38 x 39.
/
COORdinate X:
 -500.   500.   1500.   3000.   4500.   6000.   7500.   9000.
 9500.  9750.  10000.  10250.  10500.  11000.  12500.  14000.
15500. 17000.  18500.  20000.  21500.  23000.  24500.  26000.
27500. 29000.  29500.  29750.  30000.  30250.  30500.  31000.
32500. 34000.  35500.  38500.  39500.  40500.
/
COORdinate Y:
 -100.   100.   200.   300.   400.   500.   600.   700.
  800.   850.   875.   885.   895.   900.   905.   915.
  925.   950.  1000.  1100.  1200.  1300.  1350.  1375.
 1380.  1385.  1400.  1450.  1500.  1550.  1650.  1700.
 1750.  1800.  1850.  1900.  1950.  1995.  2005.
/
/ read in flow field for 40 cm/yr infiltration
/
READ 'flow40.bkg'
/
MATErial type 1 is from (1,34) to (38,39)  &Top Permeable layer
MATErial type 2 is from (1,1) to (38,33)   $Backfill
MATErial type 3 is from (11,14) to (29,29)  $Suspect Soil Trench
MATErial type 10 from (1,38) to (38,39)  $No diffusion out top of domain
/
DATUm = 0. 0.
/
LOCAte MATErial type 1 in subregion ID=BKFL
LOCAte MATErial type 2 in subregion ID=BKFL
LOCAte subregion (11,14) to (29,25) with ID=SUSPect soil
LOCAte subregion (1,1) to (38,39) with ID=DOMAin
/
/Specification for mass species C; U-234
/
FOR 1:
TRANsport properties for C Kd = 35., md = 158., Ld = 300., Td= 30.
ROCK density = 2.65; porosity = .30, .40, .30   $entire domain
FOR 2:
TRANsport properties for C Kd = 35., md = 158., Ld = 300., Td= 30.
ROCK density = 2.65; porosity = .30, .40, .30   $entire domain
```

Fig. L5-2. Example PORFLOW input file - mass transport in vadose zone.

```
FOR 3:
TRANsport properties for C Kd = 35., md = 158., Ld = 300., Td = 30.
ROCK density = 2.65; porosity = .30, .40, .30   $entire domain
FOR 10:
TRANsport properties for C Kd = 35., md = 0., Ld = 0., Td = 0.
ROCK density = 2.65; porosity = .30, .40, .30   $entire domain
/
DECAy half life of C is 2.45e5 years, branching ratio is 1.0
/
/Specification for mass species C2; Th-230
/
FOR 1:
TRANsport properties for C2 Kd = 3200., md = 158., Ld = 300., Td= 30.
ROCK density = 2.65; porosity = .30, .40, .30   $entire domain
FOR 2:
TRANsport properties for C2 Kd = 3200., md = 158., Ld = 300., Td= 30.
ROCK density = 2.65; porosity = .30, .40, .30   $entire domain
FOR 3:
TRANsport properties for C2 Kd = 3200., md = 158., Ld = 300., Td= 30.
ROCK density = 2.65; porosity = .30, .40, .30   $entire domain
FOR 10:
TRANsport properties for C2 Kd = 3200., md = 0., Ld = 0., Td= 0.
ROCK density = 2.65; porosity = .30, .40, .30   $entire domain
/
DECAy half life of C2 is 7.7e4 years, branching ratio is 1.0
/
/Specification for mass species C3; Ra-226
/
FOR 1:
TRANsport properties for C3 Kd = 500., md = 158., Ld = 300., Td= 30.
ROCK density = 2.65; porosity = .30, .40, .30   $entire domain
FOR 2:
TRANsport properties for C3 Kd = 500., md = 158., Ld = 300., Td= 30.
ROCK density = 2.65; porosity = .30, .40, .30   $entire domain
FOR 3:
TRANsport properties for C3 Kd = 500., md = 158., Ld = 300., Td= 30.
ROCK density = 2.65; porosity = .30, .40, .30   $entire domain
FOR 10:
TRANsport properties for C3 Kd = 500., md = 0., Ld = 0., Td= 0.
ROCK density = 2.65; porosity = .30, .40, .30   $entire domain
/
DECAy half life of C3 is 1.6e3 years
/
/ Initial and boundary conditions
/
SET C = 0.0 for ID=BKFL
SET C = 1.0 for ID=SUSP
BOUNdary C at -1 FLUX =0.0
BOUNdary C at +1 FLUX =0.0
BOUNdary C at -2 GRAD =0.0
BOUNdary C at +2 FLUX =0.0
```

Fig. I.5-2. (cont.).

```
/
SET C2 = 0.0 for ID=BKFL
SET C2 = 0.0 for ID=SUSP
BOUNdary C2 at -1 FLUX =0.0
BOUNdary C2 at +1 FLUX =0.0
BOUNdary C2 at -2 GRAD =0.0
BOUNdary C2 at +2 FLUX =0.0
/
SET C3 = 0.0 for ID=BKFL
SET C3 = 0.0 for ID=SUSP
BOUNdary C3 at -1 FLUX =0.0
BOUNdary C3 at +1 FLUX =0.0
BOUNdary C3 at -2 GRAD =0.0
BOUNdary C3 at +2 FLUX =0.0
/
/   Specify flux output
/
FLUX for C ID=DOMA in 'flux.out' every 2 step
FLUX for C ID=SUSP in 'flux.out' every 2 step
FLUX for C2 ID=DOMA in every 2 step
FLUX for C2 ID=SUSP in every 2 step
FLUX for C3 ID=DOMA in every 2 step
FLUX for C3 ID=SUSP in every 2 step
/
/   Specify solution criteria
/
MATRIX in X and Y directions for C, C2, and C3 in 1 sweep using ADI
CONVergence for C REFE LOCAl 1.e-2, max iterations = 3
PROPerty for C, C2, C3 is HARM mean
/
/   Specify output
/
DIAGnostic U, C at (20,20) every 20 steps   $center of suspect soil
HISTory for C, C2, C3 TABLE at (20,20) (20,2) (20,30) frequency=5
OUTPUT C, C2, C3 every 1000 steps
TIME = 0.0
/
/ Simulate mass transport with 40 cm/yr infiltration
/
DISAble FLOW
SOLVe C, C2, C3 AUTO 10000 10. 1.01 max 10. min 1.e-10 2.0 100000
SAVE C, C2, C3 NOW in 'eu234d40.arc' $10000 years
/
END
```

Fig. I.5-2. (cont.).

```
TITLe CONTAMINANT TRANSPORT FOR E-AREA
/File u234.inp  March 17, 1994
/ PORFLOW version 2.50
/
/Contaminant transport modeling for Suspect Soil - saturated zone
/U-234 plus Th-230 and Ra-226 daughters
/
GRID 38 by 30 by 28
/units are in cm's
COORdinate X   -10000,     0,  45000,  90000, 135000, 145000, 155000,
          165000, 175000, 185000, 195000, 205000, 215000, 225000,
          235000, 245000, 250000, 257500, 265000, 272500, 280000,
          287500, 295000, 302500, 310000, 317500, 325000, 332500,
          340000, 347500, 355000, 362500, 370000, 380000, 390000,
          427500, 465000, 475000,
/
COORdinate Y   -7500,     0,   7500,  15000,  22500,  30000,  37500,
          45000,  52500,  60000,  67500,  75000,  82500,  90000,
          97500, 105000, 115000, 125000, 135000, 145000, 155000,
          165000, 175000, 185000, 195000, 215000, 242500, 292500,
          342500, 352500,
/
COORdinate Z     610,   732,  2073,  3414,  3536,  3658,  3780,
          3901,  4023,  4785,  5547,  5669,  5791,  5913,
          6035,  6157,  6370,  6553,  6751,  6949,  7148,
          7346,  7544,  7742,  7940,  8138,  8336,  8534,
/
/
READ 'eflow40.arc' $40 cm/yr through vault regions
/
/identify a no-diffusion zone at top of domain to allow mass conservation
MATErial type 10 from (1,1,21) to (38,30,28)
/
FOR 1:
ROCK density = 2.65; porosity = .30, .40, .30
TRANsport properties for C Kd = 35., md = 158., Ld = 300., Td= 30.
TRANsport properties for C2 Kd = 3000., md = 158., Ld = 300., Td= 30.
TRANsport properties for C3 Kd = 500., md = 158., Ld = 300., Td= 30.
FOR 2:
ROCK density = 2.65; porosity = .30, .40, .30
TRANsport properties for C Kd = 1600., md = 158., Ld = 300., Td= 30.
TRANsport properties for C2 Kd = 5800., md = 158., Ld = 300., Td= 30.
TRANsport properties for C3 Kd = 9100., md = 158., Ld = 300., Td= 30.
FOR 3:
ROCK density = 2.65; porosity = .30, .40, .30
TRANsport properties for C Kd = 35., md = 158., Ld = 300., Td= 30.
TRANsport properties for C2 Kd = 3000., md = 158., Ld = 300., Td= 30.
TRANsport properties for C3 Kd = 500., md = 158., Ld = 300., Td= 30.
```

Fig. I.5-3. Example PORFLOW input file - mass transport in groundwater.

```
FOR 4:
ROCK density = 2.65; porosity = .20, .40, .20
TRANsport properties for C Kd = 1500., md = 158., Ld = 300., Td= 20.
TRANsport properties for C2 Kd = 5900., md = 158., Ld = 300., Td= 20.
TRANsport properties for C3 Kd = 9100., md = 158., Ld = 300., Td= 20.
FOR 5:
ROCK density = 2.65; porosity = .30, .40, .30
TRANsport properties for C Kd = 35., md = 158., Ld = 300., Td= 30.
TRANsport properties for C2 Kd = 3000., md = 158., Ld = 300., Td= 30.
TRANsport properties for C3 Kd = 500., md = 158., Ld = 300., Td= 30.
FOR 8:
ROCK density = 2.65; porosity = .30, .40, .30
TRANsport properties for C Kd = 35., md = 158., Ld = 300., Td= 30.
TRANsport properties for C2 Kd = 3000., md = 158., Ld = 300., Td= 30.
TRANsport properties for C3 Kd = 500., md = 158., Ld = 300., Td= 30.
FOR 10:
ROCK density = 2.65; porosity = .30, .40, .30
TRANsport properties for C Kd = 35., md = 158., Ld = 300., Td= 30.
TRANsport properties for C2 Kd = 3000., md = 158., Ld = 300., Td= 30.
TRANsport properties for C3 Kd = 500., md = 158., Ld = 300., Td= 30.
/
/Specification for mass species C; U-234
/
DECAy half life of C is 2.45e5 years, branching ratio is 1.0
INITial C = 0.0 everywhere
BOUNdary C at -1 FLUX =0.0
BOUNdary C at +1 FLUX =0.0
BOUNdary C at -2 FLUX =0.0
BOUNdary C at +2 FLUX =0.0
BOUNdary C at -3 FLUX =0.0
BOUNdary C at +3 FLUX =0.0
/
/Specifications for mass species C2; Th-230
/
DECAy half-life of C2 is 7.7e4 years, branching ratio is 1.0
INITial C2 = 0.0 everywhere
BOUNdary C2 at -1 FLUX =0.0
BOUNdary C2 at +1 FLUX =0.0
BOUNdary C2 at -2 FLUX =0.0
BOUNdary C2 at +2 FLUX =0.0
BOUNdary C2 at -3 FLUX =0.0
BOUNdary C2 at +3 FLUX =0.0
/
/Specifications for mass species C3; Ra-226
/
DECAy half-life of C3 is 1.6e3 years
INITial C3 = 0.0 everywhere
```

Fig. I.5-3. (cont.).

```
BOUNdary C3 at -1 FLUX =0.0
BOUNdary C3 at +1 FLUX =0.0
BOUNdary C3 at -2 FLUX =0.0
BOUNdary C3 at +2 FLUX =0.0
BOUNdary C3 at -3 FLUX =0.0
BOUNdary C3 at +3 FLUX =0.0
/
DISAble FLOW
DIAGnostic U, C at (28,12,20)   $under Suspect soil trenches
/Material type 6 from (17,14,20) to (17,14,20)
/Material type 6 from (19,13,20) to (19,15,20)
/LOCAte material type 6 as ID=ILNT
/Material type 7 is LAW vaults
/MATErial type 7 from (21,14,20) to (23,14,20)
/MATErial type 7 from (21,12,20) to (27,13,20)
/MATErial type 7 from (27,9,20) to (27,9,20)
/MATErial type 7 from (28,7,20) to (28,10,20)
/MATErial type 7 from (29,6,20) to (29,9,20)
/MATErial type 7 from (30,4,20) to (30,8,20)
/MATErial type 7 from (31,3,20) to (31,6,20)
/LOCAte material type 7 as subregion ID=LAWV
/
/MATErial type 8 is Suspect Soil Trenches
/MATErial type 9 is Naval Reactor Components
MATErial type 8 from (28,12,20) to (28,13,20)
LOCAte material type 8 as subregion ID=SUS
/
***  U-234 parent ***
SOURce C  for ID=SUS per VOLUme TABLe 31 sets      $mole per yr per mole U-234
    1.8750E+01    3.5650E-19
    5.3750E+01    1.0155E-17
    9.0000E+01    1.1504E-16
    1.2625E+02    5.2530E-16
    1.6250E+02    1.4269E-15
    1.9875E+02    2.8602E-15
    2.3500E+02    4.7421E-15
    2.7125E+02    6.9266E-15
    3.0625E+02    9.1811E-15
    3.4564E+02    1.1739E-14
    3.9312E+02    1.4679E-14
    4.5151E+02    1.7891E-14
    5.2491E+02    2.1118E-14
    6.1410E+02    2.3827E-14
    7.0743E+02    2.5406E-14
    8.1689E+02    2.6016E-14
    1.0143E+03    2.4939E-14
    1.3069E+03    2.1094E-14
    1.7991E+03    1.4069E-14
    2.4277E+03    7.6597E-15
    3.0749E+03    3.9274E-15
```

Fig. I.5-3. (cont.).

3.7[illegible]E+03	1.[illegible]E-15
4.4177E+03	9.[illegible]E-16
5.1193E+03	4.4[illegible]E-16
5.2069E+03	2.1051[illegible]E-16
6.1973E+03	9.9937E-17
7.1878E+03	4.7[illegible]E-17
7.8964E+03	2.2080E-17
8.5869E+03	1.0484E-17
9.2842E+03	4.9396E-18
9.9999E+03	2.2818E-18

*** Th-230 daughter ***

SOURce C2 for ID=SUS per VOLUme TABLe 31 sets $mole per yr per mole U-234

1.8750E+01	1.1206E-25
6.1250E+01	6.9486E-24
1.0500E+02	1.3894E-22
1.4875E+02	9.2337E-22
1.9250E+02	3.3150E-21
2.3625E+02	8.3331E-21
2.8000E+02	1.6747E-20
3.2438E+02	2.9161E-20
3.7737E+02	4.9208E-20
4.4485E+02	8.2429E-20
5.3359E+02	1.3702E-19
6.4220E+02	2.1557E-19
7.6302E+02	3.1129E-19
9.2271E+02	4.4097E-19
1.1444E+03	6.1212E-19
1.4811E+03	8.3246E-19
2.0031E+03	1.0729E-18
2.5786E+03	1.2283E-18
3.1790E+03	1.3138E-18
3.7938E+03	1.3571E-18
4.4177E+03	1.3751E-18
5.0293E+03	1.3815E-18
5.5706E+03	1.3804E-18
6.1157E+03	1.3773E-18
6.6790E+03	1.3720E-18
7.2241E+03	1.3667E-18
7.7692E+03	1.3604E-18
8.3325E+03	1.3540E-18
8.8805E+03	1.3477E-18
9.4310E+03	1.3403E-18
9.9999E+03	1.3340E-18

*** Ra-226 daughter ***

SOURce C3 for ID=SUS per VOLUme TABLe 31 sets $mole per year per mole U-234

1.8750E+01	6.9302E-29
7.0000E+01	1.0438E-26
1.2125E+02	3.5701E-25
1.7250E+02	3.3822E-24
2.2375E+02	1.5822E-23
2.7500E+02	4.9185E-23

Fig. I.5-3. (cont.).

```
   3.2848E+02   1.2225E-22
   3.9318E+02   2.8737E-22
   4.7976E+02   6.9109E-22
   5.5844E+02   1.6720E-21
   7.3253E+02   3.4647E-21
   9.1221E+02   7.0469E-21
   1.1335E+03   1.4775E-20
   1.6314E+03   3.1796E-20
   2.2786E+03   6.0067E-20
   2.9712E+03   8.8795E-20
   3.6880E+03   1.1357E-19
   4.4177E+03   1.3291E-19
   5.1732E+03   1.4760E-19
   5.9159E+03   1.5763E-19
   6.6608E+03   1.6448E-19
   7.4058E+03   1.6891E-19
   8.1508E+03   1.7165E-19
   8.8988E+03   1.7311E-19
   9.6512E+03   1.7374E-19
   9.7063E+03   1.7373E-19
   9.7614E+03   1.7373E-19
   9.8164E+03   1.7373E-19
   9.8715E+03   1.7373E-19
   9.9265E+03   1.7373E-19
   9.9999E+03   1.7373E-19
HISTory for C, C2, C3 TABLE at (28,12,20)(28,15,20)(28,15,18)
  (28,15,17)(28,15,16)(28,15,10)(26,13,16)
  (30,13,18)(30,13,16)(30,13,10) frequency=3 on 'utr.hst'
OUTPUT C, C2, C3
CONVergence for C REFE 1.e-3, max iterations = 3
DIAGnostic U, C at (28,12,20)   Sunder Suspect soil trenches
SOLVE C, C2, C3 AUTO 1.e3,DT=1.,fac=2.,mx=10,mn=1.e-8,df=2,nx=100000
SAVE C, C2, C3 NOW in 'utr.arc' $1000 yr
SOLVE C, C2, C3 AUTO 1.e3,DT=10.,fac=2.,mx=100,mn=1.e-8,df=2,nx=100000
SAVE C, C2, C3 NOW in 'utr.arc' $2000 yr
SOLVE C, C2, C3 AUTO 2.e3,DT=50.,fac=2.,mx=100,mn=1.e-8,df=2,nx=100000
SAVE C, C2, C3 NOW in 'utr.arc' $4000 yr
SOLVE C, C2, C3 AUTO 2.e3,DT=50.,fac=2.,mx=100,mn=1.e-8,df=2,nx=100000
SAVE C, C2, C3 NOW in 'utr.arc' $6000 yr
SOLVE C, C2, C3 AUTO 2.e3,DT=50.,fac=2.,mx=100,mn=1.e-8,df=2,nx=100000
SAVE C, C2, C3 NOW in 'utr.arc' $8000 yr
SOLVE C, C2, C3 AUTO 2.e3,DT=100.,fac=2.,mx=100,mn=1.e-8,df=2,nx=100000
SAVE C, C2, C3 NOW in 'utr.arc' $10000 yr
SOLVE C, C2, C3 AUTO 4.e4,DT=100.,fac=2.,mx=1000,mn=1.e-8,df=2,nx=100000
SAVE C, C2, C3 NOW in 'utr.arc' $50000 yr
END
```

Fig. I.5-3. (cont.).

APPENDIX I
REFERENCES

ACRI. 1993. *PORFLOW, A Model for Fluid Flow, Heat and Mass Transport in Multifluid, Multiphase Fractures or Porous Media, Version 2.50.* Draft User's Manual. Analytic & Computational Research, Inc., Bel Air, California.

Baes, C. F., III, and R. D. Sharp. 1983. A proposal for estimation of soil leaching and leaching constants for use in assessment models. *Journal of Environmental Qual.*, 12:17.

Cook, J. R. 1991. *Technical Basis for Non-Vault Disposal of Suspect Soil (U).* WSRC-RP-91-58. Westinghouse Savannah River Company, Savannah River Site, Aiken, S.C.

CRC Press, Inc. 1981. *CRC Handbook of Chemistry and Physics.* Robert C. Weast and Melvin J. Astle, eds. Baca Raton, FL.

Freeze, R. A., and J. A. Cherry. 1979. *Groundwater.* Prentice-Hall, Inc., New Jersey.

Gruber, P. 1980. *A Hydrologic Study of the Unsaturated Zone Adjacent to a Radioactive-Waste Disposal Site at the Savannah River Plant, Aiken, South Carolina.* M. S. Thesis, University of Georgia, Athens, Georgia.

Hoeffner, S. L. 1985. *Radionuclide Sorption on Savannah River Plant Burial Ground Soil: A Summary and Interpretation of Laboratory Data.* DP-1702. E. I. du Pont de Nemours and Company, Savannah River Laboratory, Aiken, SC.

McIntyre, P. F. 1988. *Sorption Properties of Carbon-14 on Savannah River Plant Soil.* DPST-88-900, E. I. du Pont de Nemours and Company, Savannah River Laboratory, Aiken, SC.

NRC. 1989. *Quality Assurance Program Requirements for Nuclear Facilities.* ASME NQA-1-1989 edition. The American Society of Mechanical Engineers.

Oblath, S. R. 1982. *Migration of TcO_4^- in SRP Soil.* DPST-82-815. E. I. duPont de Nemours and Company, Savannah River Laboratory, Aiken, SC.

Sheppard, M. I., and Thibault, D. H. 1990. Default Soil Solid/Liquid Partition Coefficients, K_ds, for Four Major Soil Types: A Compendium. *Health Physics*, 59:471-482.

Tickner, K. V., and Ruegger, B. 1989. *A Guide to the NEA's Sorption Data Base.* Version 2.0. Nuclear Energy Agency, Paris, France.

U.S.DOE. 1988a. *Radioactive Waste Management, Order 5820.2A.* U. S. Department of Energy, Washington, D.C.

U.S.DOE. 1988b. *Internal Dose Conversion Factors for Calculation of Dose to the Public.* DOE/EH-0071. U. S. Department of Energy, Washington, D.C.

APPENDIX J

SENSITIVITY/UNCERTAINTY ANALYSIS

J.1 INTRODUCTION

The sensitivity and uncertainty of the PORFLOW simulations of the ILNT vault system were evaluated in terms of the movement of ^{99}Tc from the vault area through the vadose zone and in groundwater. The movement of contaminated water through the system is principally governed by: 1) infiltration; 2) hydraulic properties of the waste form, vaults, and soil; 3) depth to the water table; and 4) retention of contaminants by various materials in the waste, vaults and soil. Sensitivity and uncertainty of PORFLOW simulations of vault-contained low-level radioactive waste were evaluated in the Z-Area Radiological Performance Assessment (WSRC 1992) with respect to variable infiltration rates and hydraulic and diffusive properties of the waste form, vaults, and soil. The results indicated a low sensitivity to infiltration rate, due to the flux-controlling nature of the low-conductivity concrete materials, and a high sensitivity to hydraulic conductivity. This study focusses on the sensitivity and uncertainty in model results with respect to the parameter representing retention of contaminants in the waste form, concrete, and soil, which is the solid/liquid partition coefficient, or K_d.

Since a radionuclide will move through each of the three media (i.e., waste form, concrete vault, and soil) differently according to its K_d in each material, three K_ds, and appropriate probability distributions, were specified for ^{99}Tc. In addition to the K_ds, the time to cracking and time to collapse of the vaults roof were specified. The time-to-roof collapse was the sum of the time-to-roof cracking and the time between roof cracking and roof collapse, both of which were varied.

The K_d and time parameters together resulted in five factors being specified for the PORFLOW simulations in this analysis. Since there is considerable uncertainty associated with these five factors, they are considered to be random variables and distributions were specified for each factor. Based on the available literature, the K_ds are assumed to be observations from log-normal distributions. The bounds of the K_d distributions were estimated from available literature. The times associated with roof cracking and time between cracking and roof collapse are assumed to be distributed uniformly. The bounds of the time-

to-failure distributions were estimated by assuming the baseline values in Appendix K are approximately the midpoint of the ranges, and by considering the sensitivity data provided in Table 10 of that appendix.

The distributions and their limits for the five factors were entered into a Latin Hypercube Sample (LHS) generation program (Iman and Shortencarier 1984), which creates a sample based on the principles of LHS Theory. Table J.1-1 provides the factor information needed for the sample generation routine.

Table J.1-1. Factor specification for Latin Hypercube Sample generation

Factor	Distribution	Lower Limit	Upper Limit
K_d ^{99}Tc waste form	log normal	1.0	6.2
K_d ^{99}Tc concrete	log normal	70	7000
K_d ^{99}Tc soil	log normal	0.01	0.4
Time to roof cracking	uniform	150 years	950 years
Time between roof cracking and collapse	uniform	175 years	775 years

J.2 PRELIMINARY SAMPLE

Initially a data file containing the necessary information for a pre-sample of ten LHS runs was set up and electronically transferred to the PORFLOW program. These runs were given in terms of five parameters, three K_ds and the two vault failure times. The general purpose of these initial ten runs was the identification of sampling and analysis problems.

These results were analyzed using linear regression analysis. An examination of the data indicated the possibility of several linear trends in terms of log responses versus the logs of the K_d or the log response versus the time factors. So the data analysis was directed towards the log-transform of the response data.

The data vector consisted of three responses; the maximum groundwater concentration of ^{99}Tc observed, the number of years after vault disposal that the maximum occurred, and the location of the sampling point where the maximum was observed.

Since the analysis of the initial ten runs did not raise the possibility of any real data problems, the study proceeded with the 100 runs.

J.3 SENSITIVITY ANALYSIS

The analysis of the full 100 runs involved the consideration of a full five factor multiple regression model with all interaction terms and quadratic effects. The form of this multiple regression model was the following:

Multiple Regression Model

Log(Response) = A0 + A1*X1 + A2*X2 +A3*X3 + A4*X4 + A5*X5 + A12*X1*X2 + A13*X1*X3 + A14*X1*X4 + A15*X1*X5 + A23*X2*X3 + A24*X2*X4 + A25*X2*X5 + A34*X3*X4 + A35*X3*X5 + A45*X4*X5 + A11*X1*X1 + A22*X2*X2 + A33*X3*X3 + A44*X4*X4 + A55*X5*X5 + error.

The definitions of these factors are given in Table J.3-1. An inspection of the data showed that 85 of the 100 ^{99}Tc results occurred at the same node within the simulation domain. Thus, the location of the response was not included as a variable in the analysis.

Table J.3-1. Variable definitions for multiple regression model

Variable	Definition
X1	Log(K_d Waste Form)
X2	Log(K_d Concrete)
X3	Log(K_d Soil)
X4	Time to Roof Cracking
X5	Time Between Roof Cracking and Roof Collapse

The selection of the important factors combinations was done in terms of the amount of variation that a group of factors would explain. These groups of factor combinations were selected by the use of a statistical procedure called step-wise regression. This procedure selects factor combinations in groups of one, two, three, etc., that explain the largest portion of the existing variation in the data. The intent was to obtain the smallest set of factor combinations that would explain the most variation. The set of factors combinations was allowed to increase only if the additional factor combination showed a real increase in the amount of variation explained by the linear model.

For example, for the log(max GW ^{99}Tc) response, the linear model involving only the term X2*X2 explains about 96% of the total variation in the data; the addition of any other factor combinations did not make any real increase in the amount of variation explained by the model. Thus one can say that the peak groundwater concentration of ^{99}Tc is most sensitive to X2, or the K_d in concrete, of the parameters considered.

The factors combinations that have the most influence on the log responses are given in Table J.3-2.

Table J.3-2. Important variable combinations

Response	Important Variable Combinations	Percent of Variation Explained by Important Variables
Max GW ^{99}Tc	X2*X2	96%
Years to Max GW ^{99}Tc	X4 X2*X2	96%

J.4 UNCERTAINTY ANALYSIS

The amount of variability present in the simulated response data has been illustrated in two ways. The widths of the 95% confidence intervals for the means of the response distributions, Table J.4-1, and the width of the tolerance intervals for the response distributions. The tolerance intervals were computed in terms of 95% coverage of the response distributions, with 95% confidence, as shown in Table J.4-2. In both cases the intervals were based on the entire sample of 100 simulations. While the limits for the means are relatively tight, the limits for distributions are rather broad.

Table J.4-1. Confidence intervals for mean

Response	95% Confidence Limits	
	Lower	Upper
Max GW ^{99}Tc	0.035	0.046
Years to Max GW ^{99}Tc	1897	2254

Table J.4-2. Tolerance limits on response distribution

Response	95% Confidence that 95% of Distribution Covered by Interval	
	Lower Limit	Upper Limit
Max GW ^{99}Tc	0.008	0.192
Years to Max GW ^{99}Tc	783	5460

The plots of the response against the simulation variables, which are given in Sect. J.7, indicate that the variation in the ^{99}Tc groundwater results was dominated by the magnitude of the concrete K_d (X2) values. The dominance for the maximum groundwater concentration is total, while the time to occurrence of the maximum is also influenced by a small positive trend associated with the time to cracking of the roof (X4). The variation present in the ^{99}Tc concentrations are also illustrated by the estimated cumulative distribution functions (plus 95% confidence limits) of the concentrations (Sect. J.6).

J.5 SUMMARY

In general one can say that the ^{99}Tc responses are dominated by the concrete K_d, with some additional influence of the time-to-roof cracking. The K_ds for waste form and soil, along with the time between roof cracking and collapse do not seem to have any real effect on these responses.

J.6 RESPONSE PLOTS AND CUMULATIVE PROBABILITY DISTRIBUTION

MAXIMUM GROUNDWATER CONCENTRATION TC99

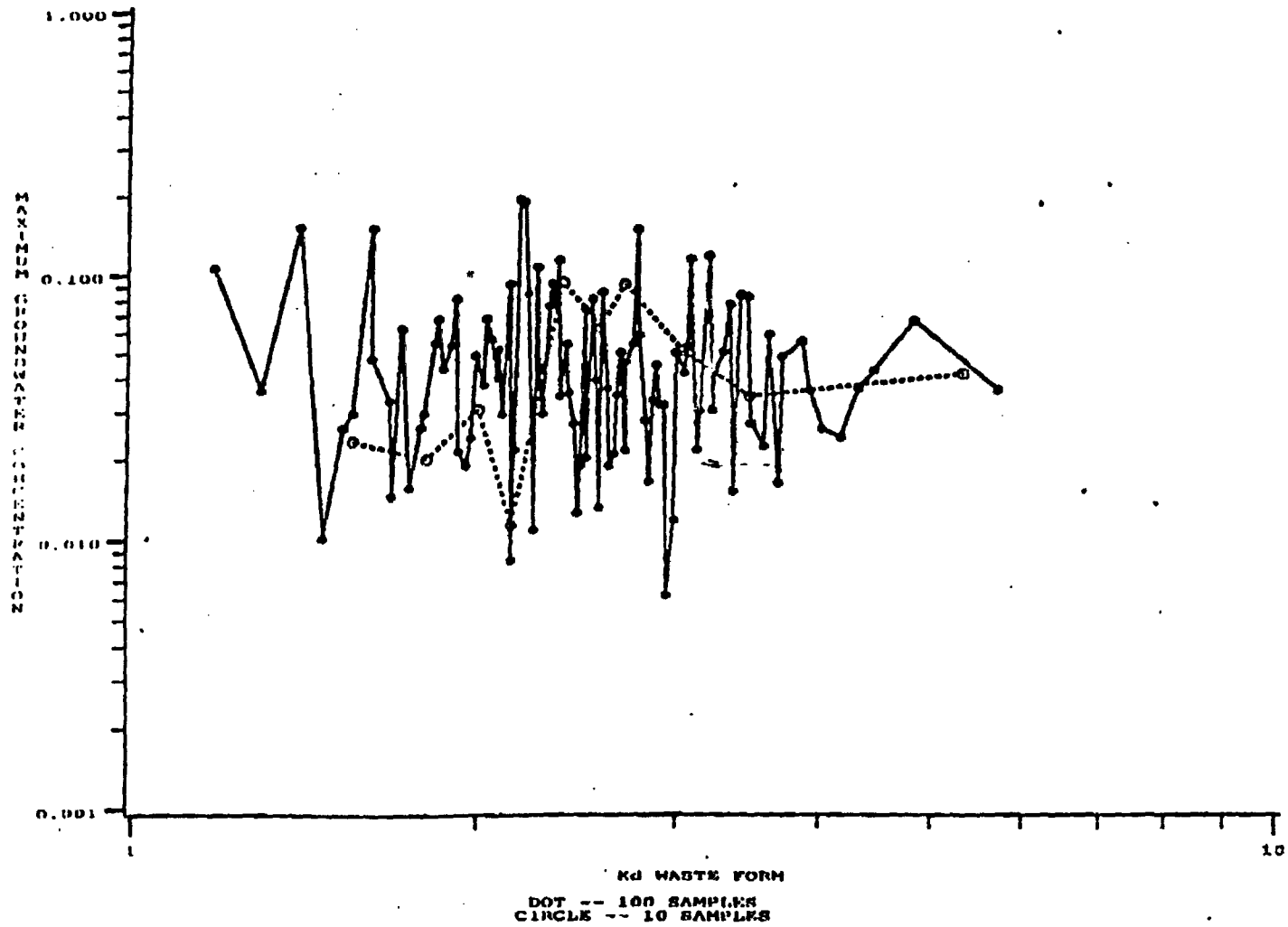

MAXIMUM GROUNDWATER CONCENTRATION TC99

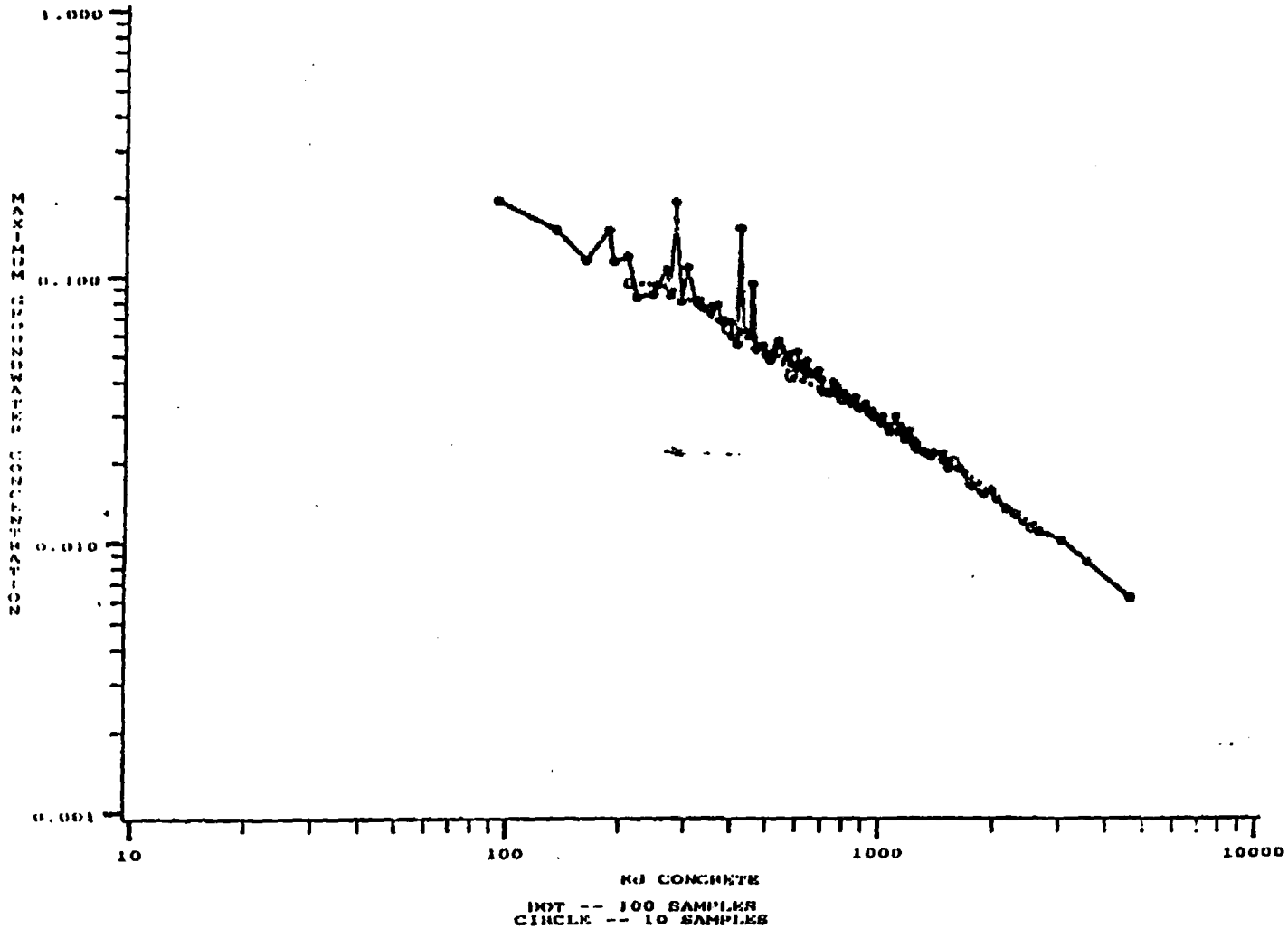

MAXIMUM GROUNDWATER CONCENTRATION TC99

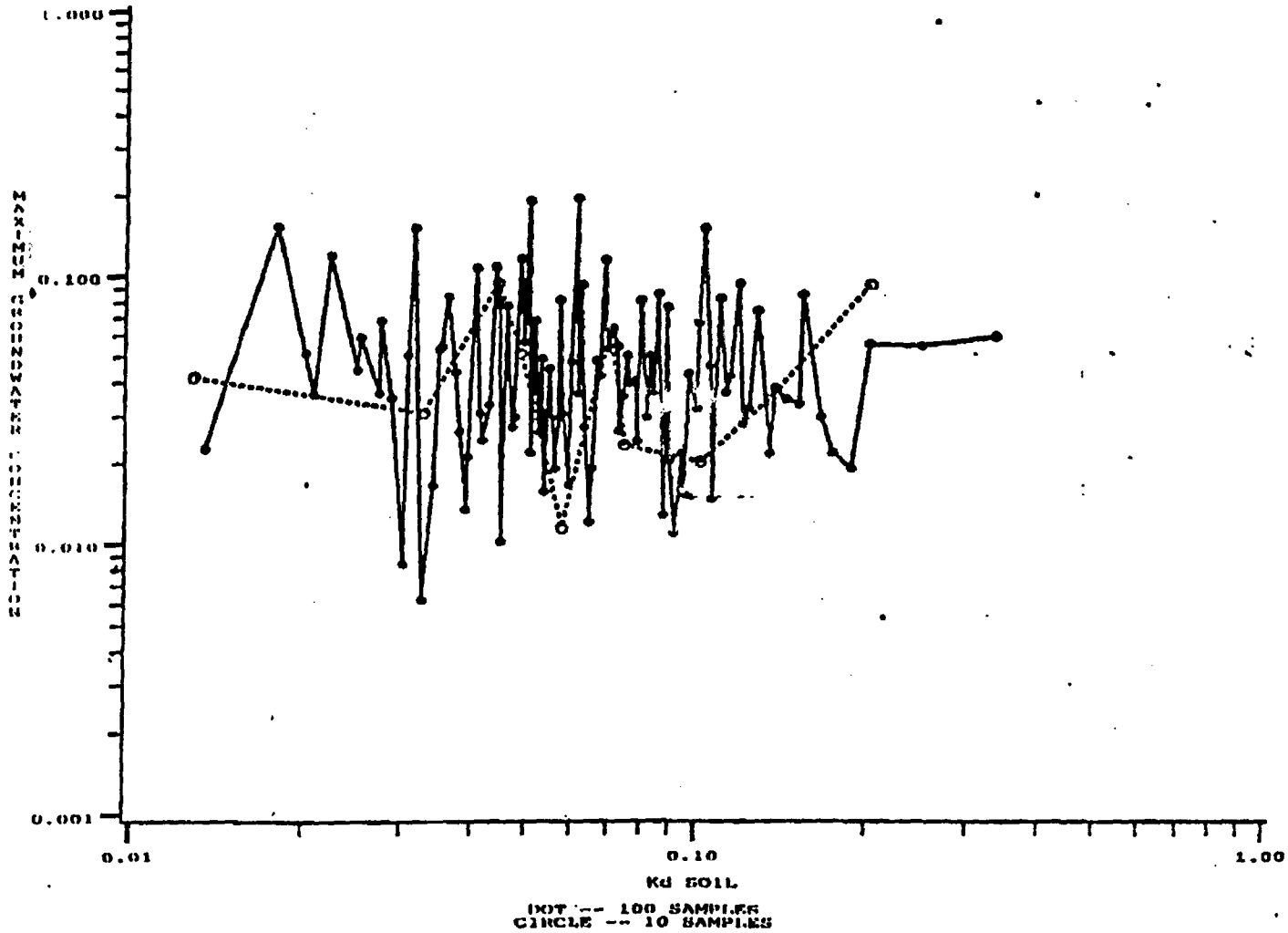

MAXIMUM GROUNDWATER CONCENTRATION TC99

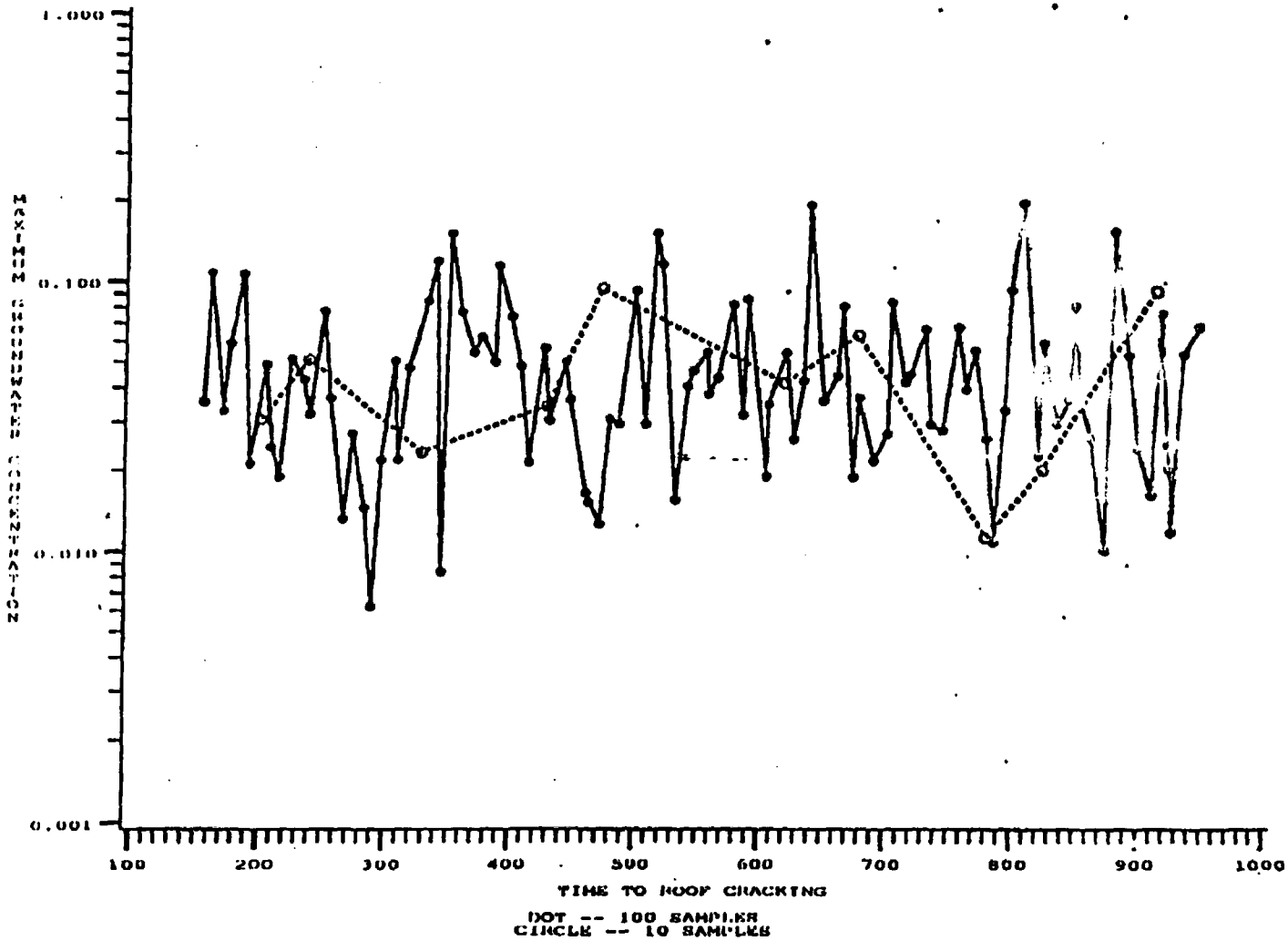

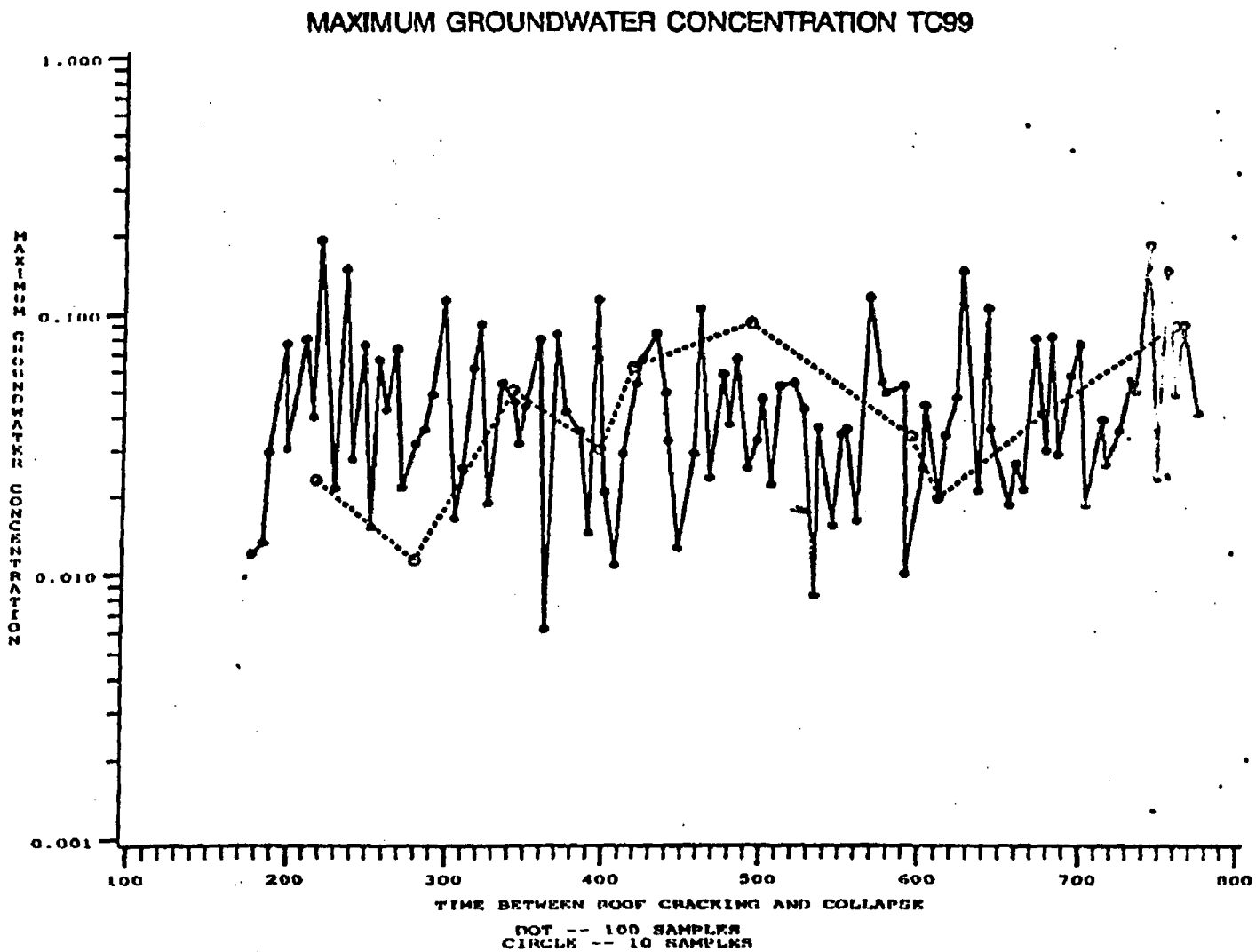
MAXIMUM GROUNDWATER CONCENTRATION TC99
MAXIMUM CONCENTRATION
1.000
0.100
0.010
0.001
100
200
300
400
500
600
700
800
TIME BETWEEN ROOF CRACKING AND COLLAPSE
DOT -- 100 SAMPLES
CIRCLE -- 10 SAMPLES

YEARS TO OCCURRENCE OF MAXIMUM TC99

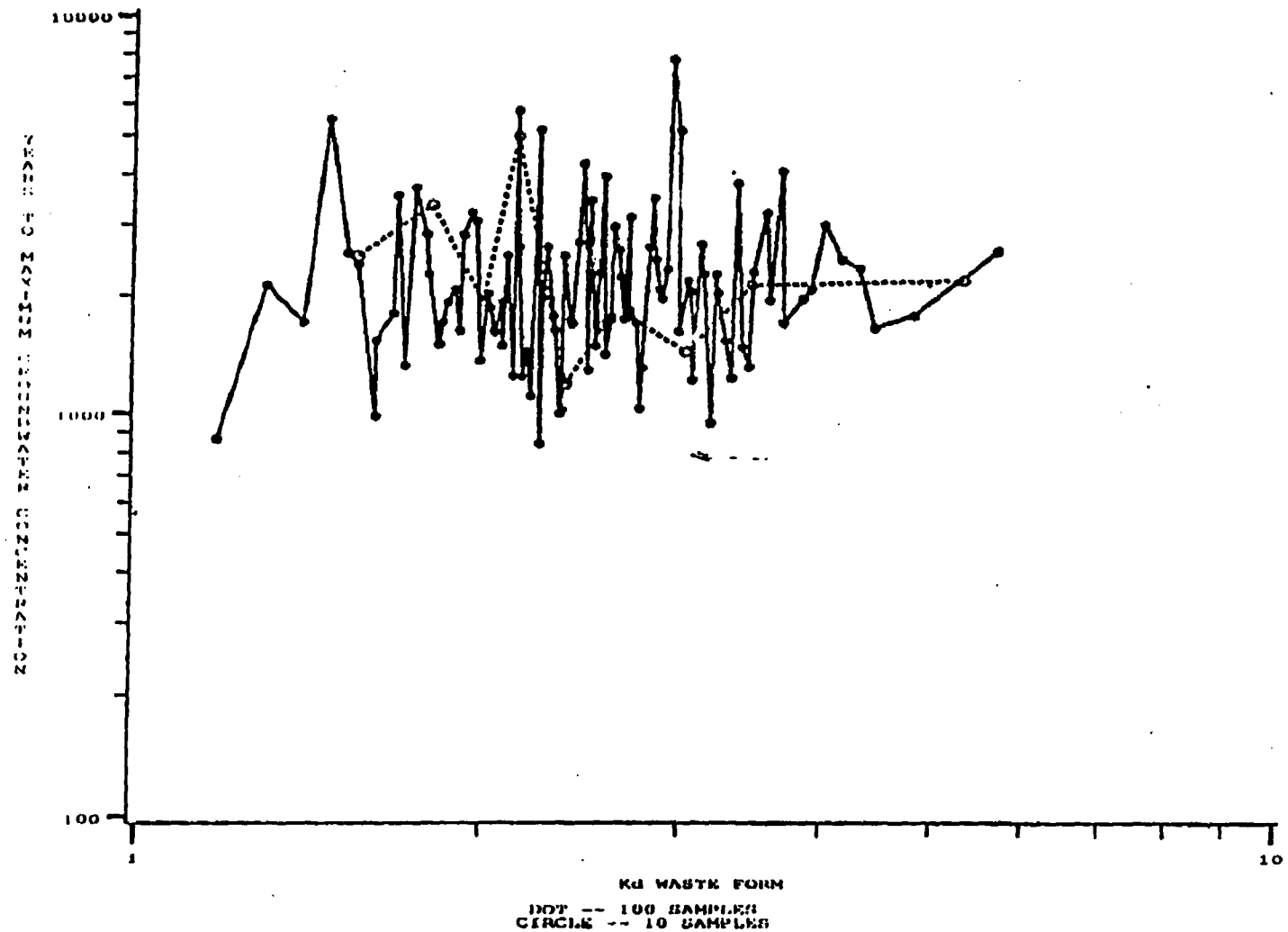

YEARS TO OCCURRENCE OF MAXIMUM TC99

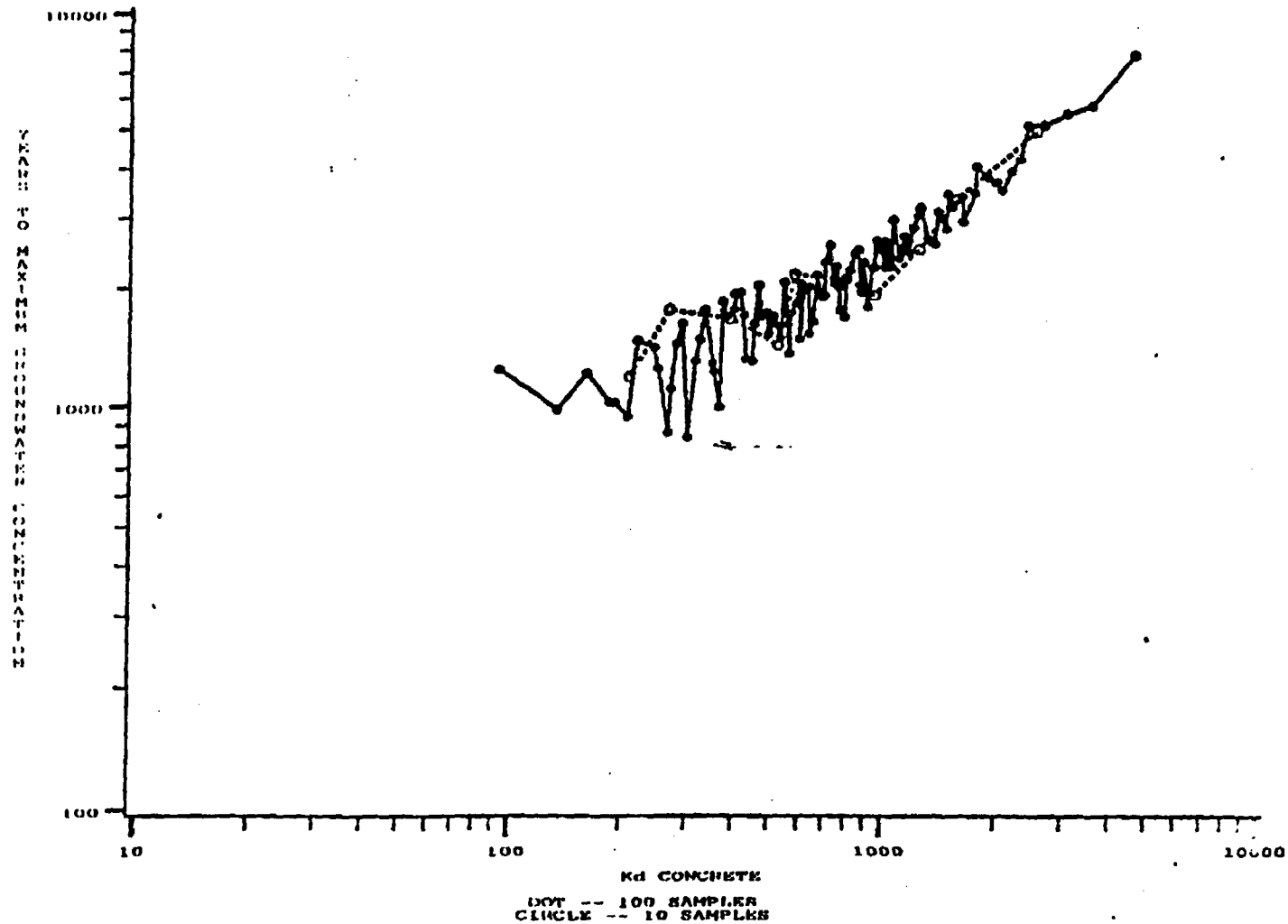

YEARS TO OCCURRENCE OF MAXIMUM TC99

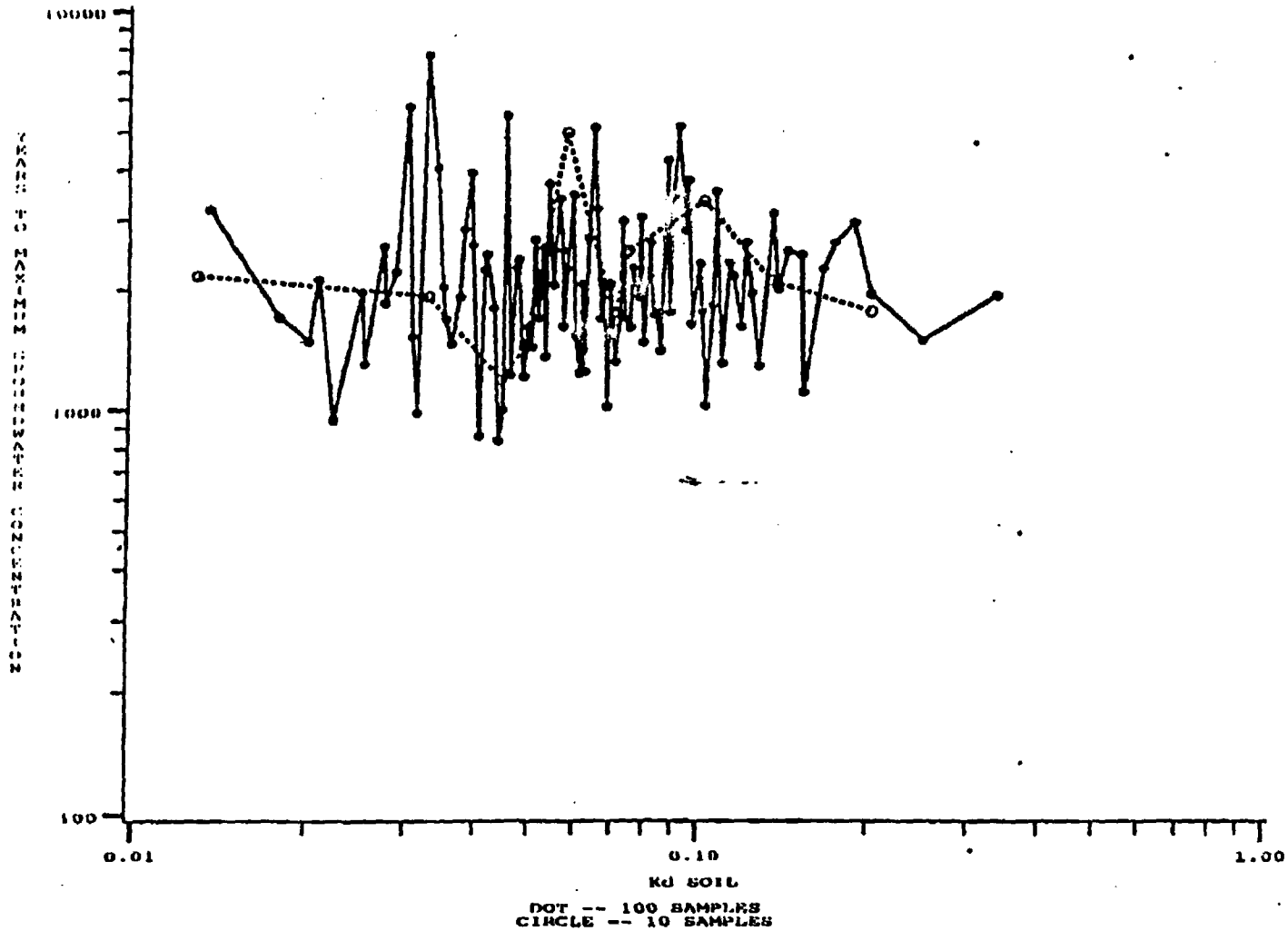

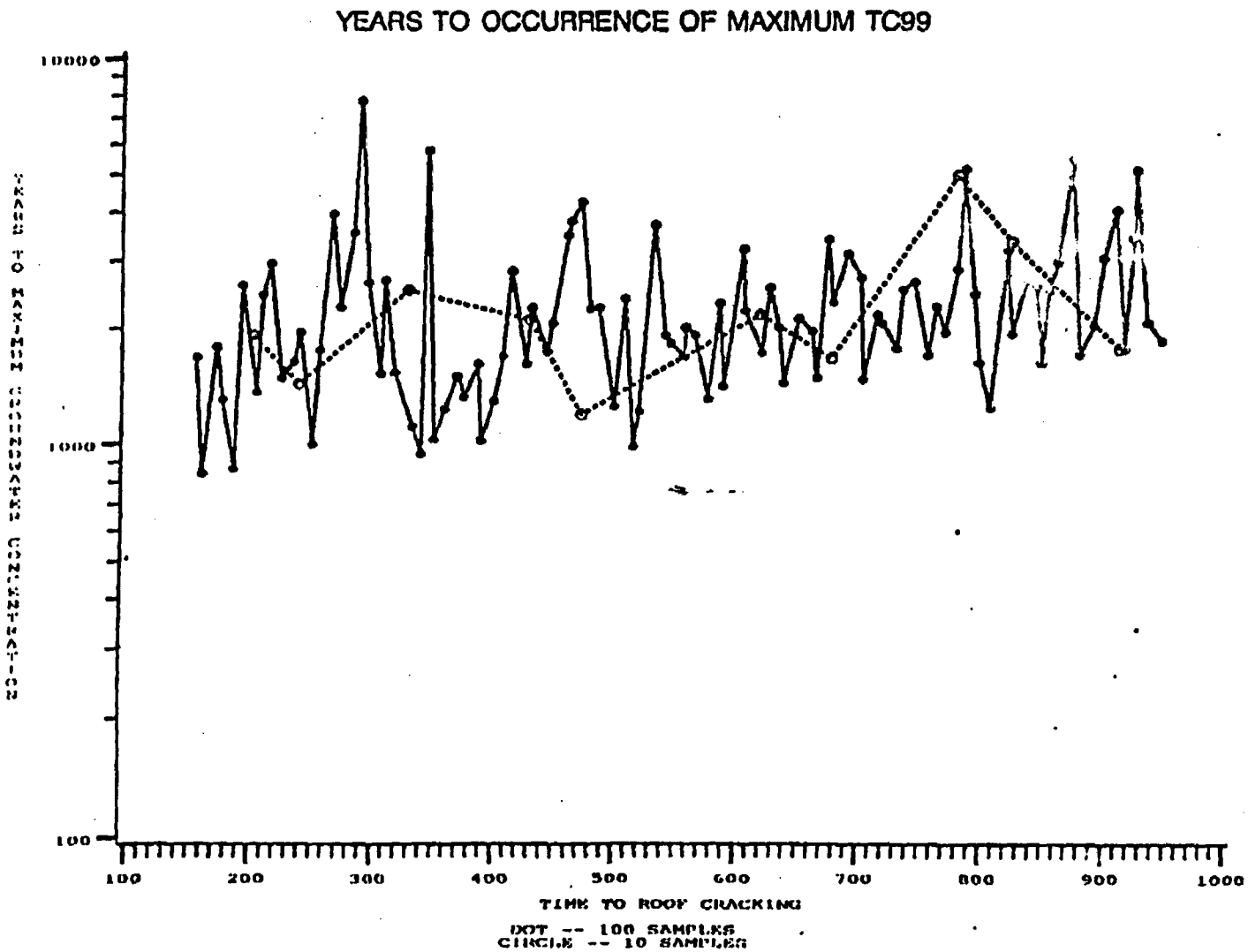
YEARS TO OCCURRENCE OF MAXIMUM TC99
10000
1000
100
YEARS TO MAXIMUM CONCENTRATION
100
200
300
400
500
600
700
800
900
1000
TIME TO ROOF CRACKING
DOT -- 100 SAMPLES
CIRCLE -- 10 SAMPLES

YEARS TO OCCURRENCE OF MAXIMUM TC99

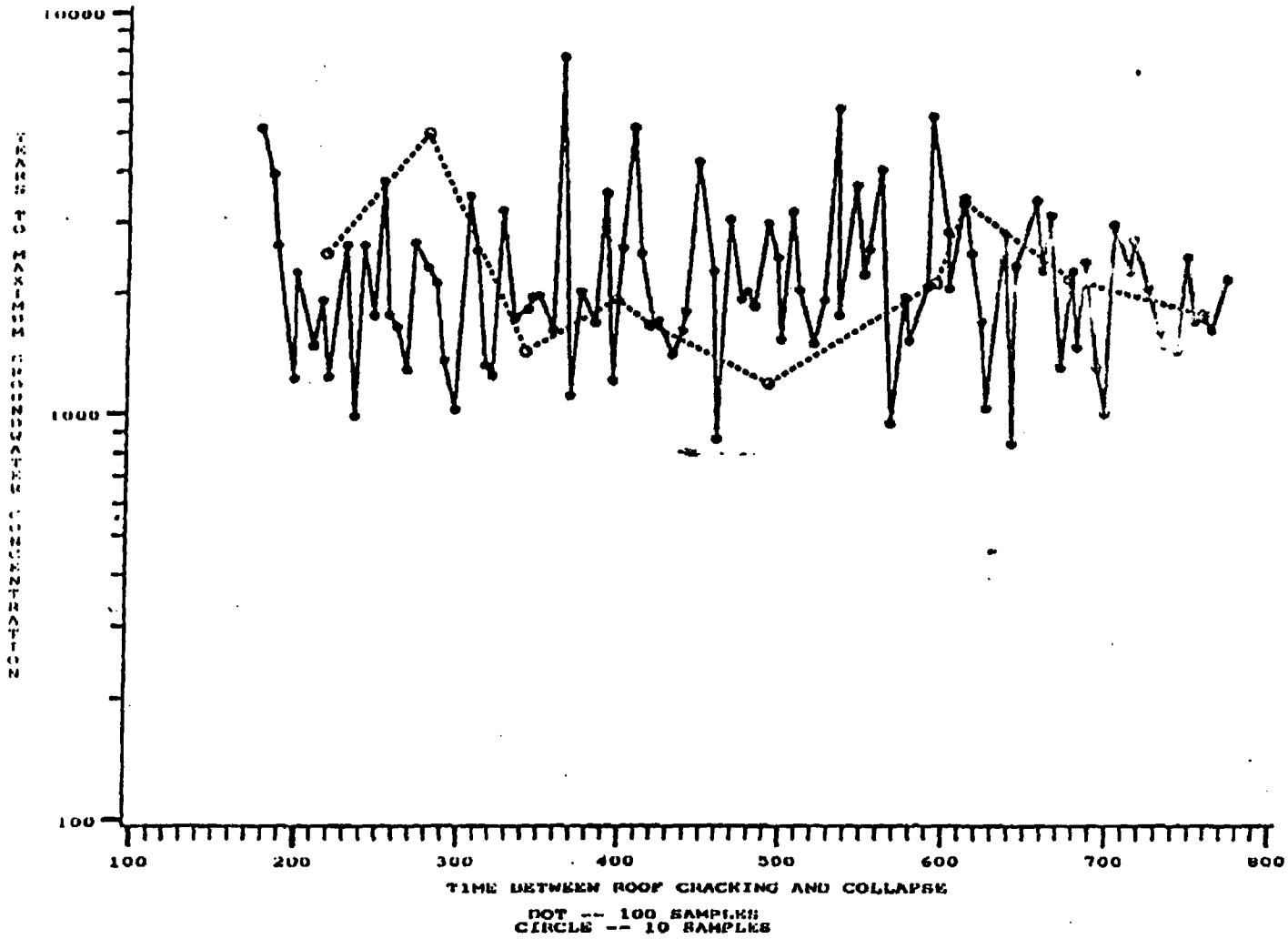

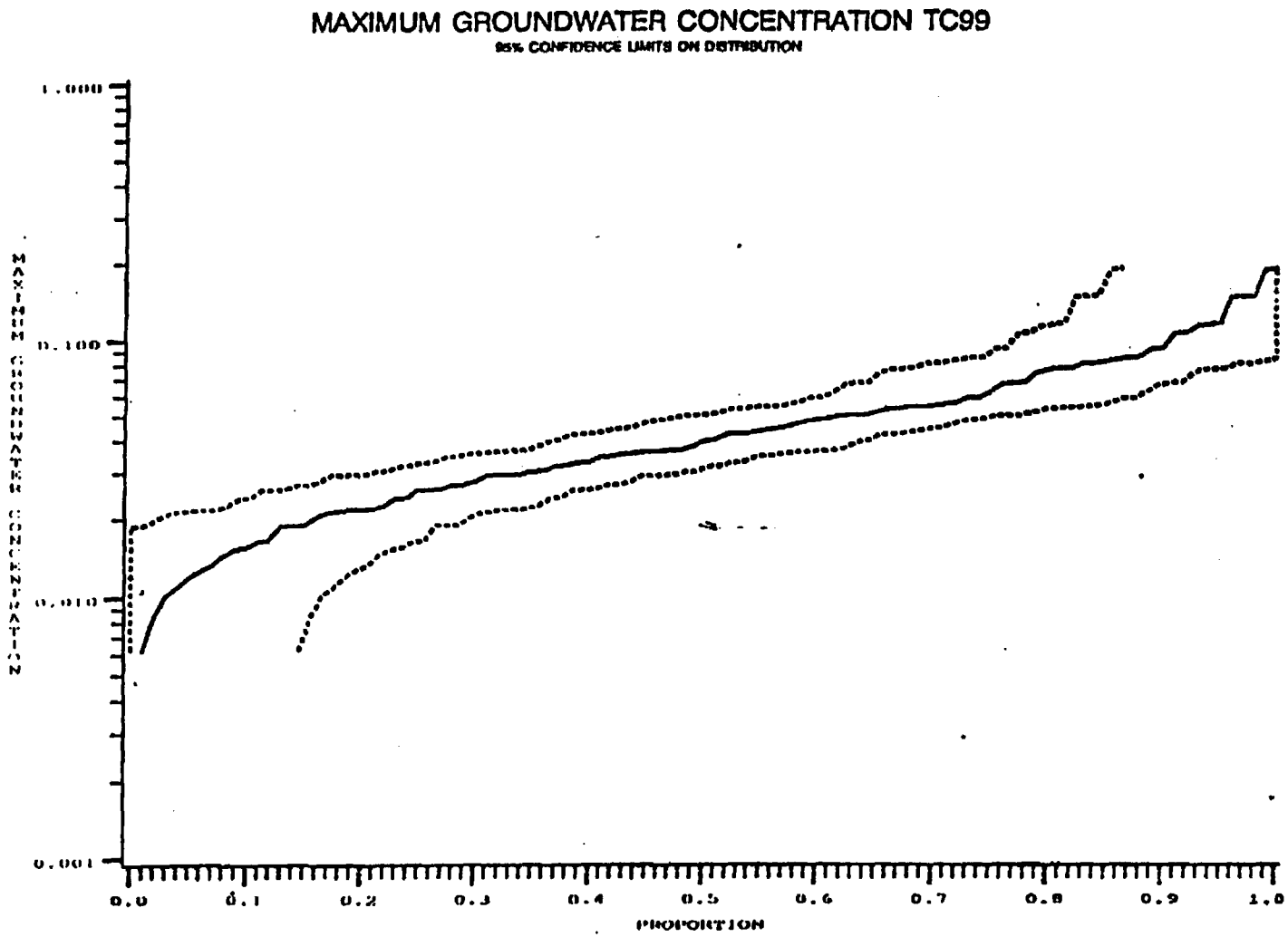
MAXIMUM GROUNDWATER CONCENTRATION TC99
95% CONFIDENCE LIMITS ON DISTRIBUTION
MAXIMUM GROUNDWATER CONCENTRATION
1.000
0.100
0.010
0.001
0.0
0.1
0.2
0.3
0.4
0.5
0.6
0.7
0.8
0.9
1.0
PROPORTION

APPENDIX J
REFERENCES

Iman, R. L., and M. J. Shortencarier. 1984. *A Fortran 77 Program and User's Guide for the Generation of Latin Hypercube and Random Samples for Use with Computer Models.* NUREG/CR-3624, SAND83-2365. Sandia National Laboratory.

WSRC. 1992. *Radiological Performance Assessment for the Z-Area Saltstone Disposal Facility.* WSRC-RP-92-1360. Savannah River Site, Westinghouse Savannah River Company, Aiken, SC.

APPENDIX K

E-AREA VAULTS
VAULT DEGRADATION STUDY

E-AREA VAULTS VAULT DEGRADATION STUDY

FINAL REPORT

INTERA

September 30, 1993

Prepared for Westinghouse Savannah River Company, Aiken, SC 29802

E-AREA VAULTS
VAULT DEGRADATION STUDY

FINAL REPORT

Prepared For:

Westinghouse Savannah River Company
Aiken, SC 29803

Prepared By
Erich R. Brandstetter
Jim L. Lolcama

INTERA Inc.
501 Greene Street, Suite 200-D
Augusta, GA 30901
Tel.: (706)722-2356
Fax: (706)724-2583

September 30, 1993

EXECUTIVE SUMMARY

The primary focus of this study was to determine the possible rates of roof and wall failure and the times to structural collapse of the roof and walls of three vault designs: the Intermediate Level Non-Tritium (ILNT), Intermediate Level Tritium (ILT) and Low Activity Waste (LAW) Vaults at the Department of Energy's Savannah River Site near Aiken, South Carolina. Failure was defined as a loss of ability to divert soil water around the vault. Collapse was defined as the total loss of structural integrity of the vault. Failure and eventual collapse of the three vault types results from concrete deterioration under stress, in the presence of corrosive soil water. Degradation rates for reinforced concrete were utilized, and the resultant changes in properties (such as strength, thickness, cracking and hydraulic conductivity) were evaluated. Baseline times to failure and collapse of the walls and roof components were modeled, and sensitivity analyses were conducted to provide boundaries on these estimated times. Thus, the goal of the project was to provide a bounding analysis of the time to roof and wall failure and potential collapse, rather than an actual prediction of the time to failure and collapse. The overall approach was to develop an executive model which linked various pre-existing models of degradation of reinforced concrete and to integrate that model with structural engineering models which estimate stress in the structure, for the bounding analysis of failure and collapse.

Degradation processes considered were magnesium and sulfate attack, calcium leaching, carbonation, and rebar corrosion due to both oxygen diffusion to the rebar (including breakdown of the passivating layer that initially prevents corrosion of rebar) and due to the "hydrogen evolution" reaction. Existing empirical models for the individual degradation processes were combined into a single model to create an overall model of the degradation of reinforced concrete. The state of stress in the concrete and rebar was calculated and the roof components and walls fractured in order to eliminate excessive stress which cannot be borne by the degraded structure. Crack aperture and spacing were computed and used to estimate hydraulic conductivity.

For each type of vault, a sensitivity analysis was performed to bound the predictions. After an initial rough sensitivity analysis on a large number of factors, six factors were selected for detailed sensitivity analysis: rate of rebar corrosion due to the "hydrogen evolution" reaction, rebar diameter, depth of concrete cover over the rebar, size of AASHTO "bridge" beams used to support the vault roof in the LAW vault design, and depth of soil cover over the vaults, and concrete strength.

The ILNT Vault design consists of 7 rectangular cells, each approximately 48.5' long by 27' wide by 29.75' high. The ILT is a similar design, the main differences being that it consists of only 2 cells and utilizes a slightly thicker roof. The LAW vault consists of 4 cells, each approximately 145' x 53' x 26'. It utilizes a significantly different design in that AASHTO "bridge" beams are used to support the roof span. Baseline times to failure and collapse for the ILNT vault were 570 and 1,045 years, respectively. The thicker roof and two-cell design of the ILT vault result in longer times to failure and collapse for the ILT vault; 790

and 1,300 years respectively. For the LAW vault, failure and collapse are predicted to occur in 1,420 and 3,100 years. The following table summarizes the baseline results for each vault type:

Summary of Baseline Results

Vault	Cracks Penetrate Roof/Failure (years)	Cracks Penetrate Walls (Mid-Height) (years)	Roof Collapse (years)
ILNT	570	800	1,045
ILT	790	1,080	1,300
LAW	1,420	2,235	3,100

Sensitivity analysis indicated that the rate of rebar corrosion due to the hydrogen evolution reaction is the most critical and uncertain model parameter. Variation within the bounds of acceptable values reported in the literature can result in the times to failure and collapse varying hundreds to thousands of years. For example, for the ILNT vault, the time to failure varied from 285 years to 2,775 years, based on variation in the hydrogen evolution corrosion rate. Similarly, the time to collapse varied from 525 years to beyond the 3,000-year duration of the simulation for the ILNT vault.

Variation in depth of concrete cover over rebar and in concrete strength within design constraints resulted in variation in times to failure and collapse of less than 100 years. Variation in depth of soil cover within design constraints resulted in variation in times to failure and collapse on the order of 100 to 400 years. Changing the rebar diameter has the potential to significantly impact the longevity of the vaults. For example, changing the bar designation by 1 (for example, from #8 to #7 or to #9) changes the time to failure and collapse on the order of 300 to 400 years. Changing the size of AASHTO beams has a similar impact on the time to collapse of the LAW vault. Utilizing a smaller beam, however, would result in cracks penetrating the vault (i.e., failure) immediately upon soil loading.

This study has combined pre-existing models for the degradation of reinforced concrete with proven structural engineering models to create a performance assessment code capable of predicting the time to failure (loss of ability to divert water) and collapse (loss of structural integrity) of buried concrete vaults. This code can also be used to estimate the impact of changes in design parameters on the longevity of reinforced concrete structures, and therefore has potential for application as a design aid tool for below-ground concrete storage facilities. The current mandate at DOE facilities to move in the direction of below-ground disposal in concrete-engineered structures makes this code a potentially important performance assessment tool.

TABLE OF CONTENTS

EXECUTIVE SUMMARY ii

LIST OF TABLES vi

LIST OF FIGURES vii

1. INTRODUCTION 1

2. DESCRIPTION OF THE CLOSED ILT, ILNT AND LAW VAULTS 3
   2.1 INTERMEDIATE-LEVEL VAULTS 3
      2.1.1 ILNT Vaults 3
      2.1.2 ILT Vaults 3
   2.2 LAW VAULT 4
   2.3 VAULT CLOSURE 4

3. MODELS OF CHEMICAL DEGRADATION AND STRUCTURAL ANALYSIS 5
   3.1 CHEMICAL ATTACK 5
      3.1.1 Sulfate and Magnesium Attack 5
      3.1.2 Alkali and Calcium Hydroxide Leaching 6
      3.1.3 Carbonation 7
      3.1.4 Rebar corrosion 8
      3.1.5 Vault Interiors 10
   3.2 STRUCTURAL/ENGINEERING ANALYSIS 11
      3.2.1 Application to the ILNT/ILT Vaults 12
      3.2.2 Application to the LAW Vault 13

4. MODELING APPROACH 16
   4.1 COMPUTER CODES 16
   4.2 LINKING BETWEEN DEGRADATION AND STRUCTURAL MODELS 16
   4.3 HYDRAULIC CONDUCTIVITY 16
      4.3.1 Vault Roofs 16
      4.3.2 Vault Walls 18
   4.4 MODEL OUTPUT 18
   4.5 DEFINITION OF FAILURE 18
   4.6 SUMMARY OF CONSERVATIVISM 19

5. INPUT SUMMARY 21

6. MODEL RESULTS 22

7. SENSITIVITY ANALYSIS 24
7.1 SELECTION OF PARAMETERS AND VALUES 24
7.2 OUTPUT SUMMARY 25
7.2.1 HLNT Vault Sensitivity Analysis 26
7.2.2 HLC Vault Sensitivity Analysis 27
7.2.3 LAW Vault Sensitivity Analysis 27
7.3 SUMMARY OF THE IMPACT OF DESIGN CHANGES 29

8. FUTURE RESEARCH AREAS 32

9. SUMMARY AND CONCLUSIONS 34

REFERENCES 56

ACRONYMS AND ABBREVIATIONS 58

APPENDIX: QUALITY ASSURANCE 59
A.1 IMPLEMENTATION OF THE PROJECT QUALITY ASSURANCE PLAN 59
A.2 PROJECT QUALITY ASSURANCE PLAN 62

LIST OF TABLES

Page

Table 1. Summary of Output Parameters 36
Table 2. Structural Input for the ILNT Vault 37
Table 3. Structural Input for the ILT Vault 38
Table 4. Structural Input for the LAW Vault 39
Table 5. Design Drawings Used 40
Table 6. Summary of Degradation Model Variables and Values 44
Table 7. Summary of Rebar Stress (ksi) in ILT Baseline Scenario 49
Table 8. Summary of Rebar Stress (ksi) in ILNT Baseline Scenario 50
Table 9. Summary of Baseline Results 51
Table 10. Summary of ILNT Vault Sensitivity Analyses 52
Table 11. Summary of ILT Vault Sensitivity Analyses 53
Table 12. Summary of LAW Vault Sensitivity Analyses 54
Table 13. Summary of Baseline Results Assuming High-pH Concrete 55

LIST OF FIGURES

Figure 1	Schematic of ILNT Vault
Figure 2	Schematic of ILT Vault
Figure 3	Schematic of LAW Vault
Figure 4	Portion of Vault Cross Section; Cracks Indicate Critical Stress Regions
Figure 5	LAW Vault Roof, Showing Cracking Due to Curvature Over Wall
Figure 6	Cross-Section of ILNT Vault Roof Showing Degradation at 400 Years
Figure 7	Effective Hydraulic Conductivity of Vault Roof; ILNT Vault Design
Figure 8	Effective Hydraulic Conductivity of Vault Roof; ILT Vault Design
Figure 9	Effective Hydraulic Conductivity of Vault Roof; LAW Design
Figure 10	ILNT Vault Time to Crack Penetration of Roof; Sensitivity to Hydrogen Evolution Corrosion Rate (cm/yr)
Figure 11	ILNT Vault Time to Crack Penetration of Walls; Sensitivity to Hydrogen Evolution Corrosion Rate (cm/yr)
Figure 12	ILNT Vault Time to Roof Collapse; Sensitivity to Hydrogen Evolution Corrosion Rate (cm/yr)
Figure 13	ILNT Vault Time to Crack Penetration of Roof; Sensitivity to Depth of Soil Cover
Figure 14	ILNT Vault Time to Crack Penetration of Walls; Sensitivity to Depth of Soil Cover
Figure 15	ILNT Vault Time to Roof Collapse; Sensitivity to Depth of Soil Cover
Figure 16	ILNT Vault Time to Crack Penetration of Roof; Sensitivity to Rebar Size
Figure 17	ILNT Vault Time to Crack Penetration of Walls; Sensitivity to Rebar Size
Figure 18	ILNT Vault to Roof Collapse; Sensitivity to Rebar Size

LIST OF FIGURES (Continued)

Figure 19 ILNT Vault Time to Crack Penetration of Roof; Sensitivity to Depth of Concrete Cover Over Rebar

Figure 20 ILNT Vault Time to Crack Penetration of Walls; Sensitivity to Depth of Concrete Cover Over Rebar

Figure 21 ILNT Vault Time to Roof Collapse; Sensitivity to Depth of Concrete Cover Over Rebar

Figure 22 ILNT Vault Time to Crack Penetration of Roof; Sensitivity to Concrete Strength

Figure 23 ILNT Vault Time to Crack Penetration of Roof; Sensitivity to Concrete Strength

Figure 24 ILNT Vault Time to Roof Collapse; Sensitivity to Concrete Strength

Figure 25 ILT Vault Time to Crack Penetration of Roof; Sensitivity to Hydrogen Evolution Corrosion Rate (cm/yr)

Figure 26 ILT Vault Time to Crack Penetration of Walls; Sensitivity to Hydrogen Evolution Corrosion Rate (cm/yr)

Figure 27 ILT Vault Time to Roof Collapse; Sensitivity to Hydrogen Evolution Corrosion Rate (cm/yr)

Figure 28 ILT Vault Time to Crack Penetration of Roof; Sensitivity to Depth of Soil Cover

Figure 29 ILT Vault Time to Crack Penetration of Walls; Sensitivity to Depth of Soil Cover

Figure 30 ILT Vault Time to Roof Collapse; Sensitivity to Depth of Soil Cover

Figure 31 ILT Vault Time to Crack Penetration of Roof; Sensitivity to Rebar Size

Figure 32 ILT Vault Time to Crack Penetration of Walls; Sensitivity to Rebar Size

Figure 33 ILT Vault Time to Roof Collapse; Sensitivity to Rebar Size

Figure 34 ILT Vault Time to Crack Penetration of Roof; Sensitivity to Depth of Concrete Cover Over Rebar

LIST OF FIGURES (continued)

Figure 35 ILT Vault Time to Crack Penetration of Walls; Sensitivity to Depth of Concrete Cover Over Rebar

Figure 36 ILT Vault Time to Roof Collapse; Sensitivity to Depth of Concrete Cover Over Rebar

Figure 37 ILT Vault Time to Crack Penetration of Roof; Sensitivity to Concrete Strength

Figure 38 ILT Vault Time to Crack Penetration of Walls; Sensitivity to Concrete Strength

Figure 39 ILT Vault Time to Roof Collapse; Sensitivity to Concrete Strength

Figure 40 LAW Vault Time to Crack Penetration of Roof; Sensitivity to Hydrogen Evolution Corrosion Rate (cm/yr)

Figure 41 LAW Vault Time to Crack Penetration of Walls; Sensitivity to Hydrogen Evolution Corrosion Rate (cm/yr)

Figure 42 LAW Vault Time to Roof Collapse; Sensitivity to Hydrogen Evolution Corrosion Rate (H2rate; cm/yr) and Depth of Soil Cover

Figure 43 LAW Vault Time to Crack Penetration of Walls; Sensitivity to Depth of Soil Cover

Figure 44 LAW Vault Time to Crack Penetration of Roof; Sensitivity to Rebar Size

Figure 45 LAW Vault Time to Crack Penetration of Walls; Sensitivity to Rebar Size

Figure 46 LAW Vault Time to Roof Collapse; Sensitivity to Hydrogen Evolution Corrosion Rate (H2rate; cm/yr) and Beam Type

Figure 47 Cross-Section of Vault Roof Assuming Use of High-pH Concrete; Degradation at 50 Years

Figure 48 Cross-Section of Vault Roof Assuming Use of High-pH Concrete; Degradation at 400 Years

1. INTRODUCTION

The E-Area Vaults (EAV), which are the focus of this study, are located at the Savannah River Site (SRS) in South Carolina. The EAV designs which will be discussed in this report are the Intermediate Level Non-Tritium (ILNT), Intermediate Level Tritium (ILT) and Low Activity Waste (LAW) Vaults. Westinghouse Savannah River Company (WSRC) operates this site and is currently developing a Radiological Performance Assessment (RPA) for the EAV. The vault degradation study is a supporting study for this RPA.

The EAV site is located on a 200-acre site immediately north of Building 643-7E at the SRS. The original SRS Solid Waste Disposal Facility (SWDF) and the added EAV site are centrally located between the two chemical separations areas near the center of the SRS, between Upper Three Runs Creek on the north and Four Mile Creek on the south. Of this 200 acre tract, only 100 acres have been developed at this time. The nearest site boundary to the SWDF is about seven miles to the west. The SWDF is in a relatively level highland region of the SRS at about 300 ft above sea level.

The E-Area Vaults are reinforced concrete structures intended for below ground storage of low-activity and intermediate-level wastes. Each of the EAV designs are intended to house designated waste types. The LAW vaults, which are located at a separate facility from the ILT and ILNT vaults, are designed to receive and store low-activity waste radiating less than 200 mR/hr at 5 cm from an unshielded container and containing only incidental quantities of tritium. One section of the Intermediate Level facility is designated as the ILNT vault and receives waste radiating greater than 200 mR/hr at 5 cm in engineered metal containers. The remaining section is designated as the ILT vault and receives tritium-bearing waste contained in engineered metal containers or as overpacked tritium crucibles with most of the tritium removed. These two vault sections are adjacently located, share waste package handling equipment and are to be closed as one facility. The LAW vault facility will be closed separately. A third facility, also a part of the EAV Project, designated as the Long-Lived Waste Storage Building (LLWSB) has not been considered as part of this degradation study.

Closure of the vaults will be via below ground burial under about 8 feet of soil cover. The placement of the soil cover and soil backfill around the vaults will result in loading of the roof and walls of each unit. Chemical attack on the buried reinforced concrete will weaken the concrete, and the roof and walls of each vault type could be expected to fail and collapse over time. Failure is defined as a loss of ability to divert water around the vault. Degradation of concrete by sulfate attack can cause thinning, calcium hydroxide leaching results in weakening of the concrete, carbonation lowers the pH of the matrix-bound water, and oxic ("oxygen") and anoxic ("hydrogen evolution") rebar corrosion weakens the reinforced concrete mass. Failure of the vault would result in infiltrating ground water entering the interior of the vault rather than being diverted around its exterior.

INTERA's approach to this performance assessment problem for the E-Area Vaults has been to construct a mathematical model which integrates structural loading calculations with chemical degradation calculations. This model runs on a PC-platform and utilizes, as subroutines, pre-existing empirical models for the chemical degradation calculations, and an American Concrete Institute code for the design of reinforced concrete structures to calculate the [illegible] of stress within the structure. Adopting this modeling approach facilitates sensitivity analyses on different design components of the vaults.

This report presents the chemical degradation mechanisms which have been modeled for degradation of the concrete of each of the vault designs, describes the structural design model and the approach for integrating these models into one code, and finally, presents the results of the performance assessment calculations on the three vaults types for baseline (base case) and variant configurations of several of the design components. Further work which will likely be accomplished under a separate task will include evaluating the performance of the vault floors for the three vault designs, and extending the sensitivity analyses beyond six parameters.

2. DESCRIPTION OF THE CLOSED ILT, ILNT AND LAW VAULTS

The FAV Project consists of three types of facilities to house four designated waste types and the necessary roadways to allow waste container delivery. This section describes in brief the three vault types.

2.1 INTERMEDIATE-LEVEL VAULTS

The intermediate-level vaults consist of two separate, subsurface reinforced concrete vault structures. The individual vaults are adjacently located, share a similar design, and are closed as a single unit. The vaults are identified as the Intermediate Level Tritium (ILT) Vault, and the Intermediate Level Non-tritium (ILNT) Vault.

2.1.1 ILNT Vaults

Each ILNT Vault consists of seven cells or subdivided sections within the vault structure (Figure 1) and provides a total of approximately 200,000 ft^3 of waste storage capacity. The vaults are subsurface concrete structures approximately 189 ft long, 48.5 ft wide, and 29.75 ft deep. Exterior end walls are 2½ ft thick, side walls are 2 ft thick, and interior walls (between the cells) are 1½ ft thick. All walls are structurally mated to a base slab which is approximately 2½ ft thick and extends past the outside of the exterior walls approximately 2 ft. The base slab rests on two layers of crushed stone placed on the compacted subsurface. The crushed stone drains to a collection sump to prevent a positive water head against the vault exterior.

Concrete is reinforced with deformed steel bars. All concrete construction joints are located at defined control joints with no horizontal joints in any vertical wall. All concrete joints include a waterstop seal which is continuous around all corners and intersections. All exterior concrete surfaces exposed to soil are coated with a coal tar-based waterproofing.

2.1.2 ILT Vaults

Each ILT Vault consists of two cells or subdivided sections within the vault structure (Figure 2) and provides approximately 57,000 ft^3 of waste storage capacity. One cell will in most cases be fitted with a silo system to permit the disposal of tritium crucibles. The ILT Vaults are structurally very similar to the ILNT, with slight differences such as wall height and thickness of the (proposed) roof slab. The ILT Vaults are approximately 57 feet long, 48.5 ft wide, and 28.5 feet deep. Wall arrangement, slab and slab base, and concrete are all identical for the two-cell configuration ILT vault and the seven-cell configuration ILNT vault.

2.2 LAW VAULT

Each LAW Vault consists of either two or three major subdivisions, or modules. Each module provides approximately 566,500 ft^3 storage capacity and will accommodate more than 4,000 B-25 boxes. Figure 3 illustrates one module of a LAW Vault. Each module is approximately 214.5 ft long and 115 ft wide. Height of the vaults varies from approximately 26 to 27 feet. End, side, and interior walls of each module are all 2 ft thick. All walls are structurally mated to a 30-inch footer that is continuous under all cells in each module.

A reinforced concrete roof is supported by prestressed, concrete beams. The beams run between each wall the length of the vault. The end walls of each module have recessed beam seats to support a beam end, and the interior walls are equipped with bearing pads allowing beam ends to rest on the wall. The beams rest on elastomeric bearings which allow the bases of the beams to move towards each other as soil load and progressive deterioration of the structure causes the roof system to bend.

The slightly peaked roof is composed of 3½-inch thick, prestressed, concrete deck panels installed directly on the roof beams providing a base for a 16-inch, cast-in-place roof slab. The roof slab has 2-in. wide expansion joints between module walls. Each expansion joint has flashing installed to provide waterproofing. The roof slab is covered with a bonded-in-place layer of fiberboard insulation and a layer of waterproof membrane roofing.

2.3 VAULT CLOSURE

Final closure of the vaults consists of placing an earthen cover with an engineered clay cap over the entire 21-vault area. The final closure cap will consist of a 2-foot thick compacted clay layer, on top of which will be a clay geomembrane or clay/geotextile composite. This will be overlain with a 1-foot thick granular drainage layer. Above the drainage layer will be a geotextile filter fabric. The uppermost layer of the closure cap will be a 2-foot thick topsoil cover. The slope of each of these layers will be 3% over the ILNT and ILT Vaults, and 3% or 4.3% (depending on location) over the LAW Vaults. The total thickness of the soil layer will be between 8.5 and 9 ft. The "final closure cap" thus accounts for 5 ft of this thickness. The remaining volume will utilize compacted fill material. In addition, in order to reduce the hydraulic conductivity of the layered soil/vault system, a clay layer will be placed immediately adjacent to the vault roofs.

3. MODELS OF CHEMICAL DEGRADATION AND STRUCTURAL ANALYSIS

The selection of chemical degradation mechanisms for concrete was based on a process of eliminating mechanisms which demonstrated little or no effect under chemical conditions of the soil or concrete mix. The chemical degradation models which were included in the assessment were: SO_4 and Mg attack, $Ca(OH)_2$ leaching, carbonation, and rebar corrosion in oxic and anoxic conditions. Below we have presented the models for chemical degradation processes, some empirical and some analytic, and have provided a description of the attack mechanisms for which the models were derived. These mechanisms have been modeled independently. For example, thinning of the concrete surface will not result in an increased rate of reinforcing steel corrosion due to faster diffusion of oxygen through the decreased cover. In addition, the structural analysis modeling is described.

3.1 CHEMICAL ATTACK

3.1.1 Sulfate and Magnesium Attack

Sulfate and magnesium are naturally occurring elements at the Savannah River Site, input to the soil water from rainfall and weathering of rock minerals. Sulfate reacts with tri-calcium aluminate (C_3A) to form calcium aluminum sulfates leading to expansion and cracking of the surface of the concrete (Walton et al., 1990). A related problem is the reaction of magnesium with the cement to form Brucite [$Mg(OH)_2$]. As the concrete cracks, its hydraulic conductivity increases, and water penetrates more easily into the interior, accelerating the deterioration of the concrete. Sulfate attack also results in a progressive loss of strength and mass due to deterioration in the cohesiveness of the cement hydration products. The reaction products have considerably greater volume than the reactants. This causes the expansion of the concrete which, in turn, results in cracking, spalling, and loss of strength. In addition, formation of gypsum causes a deterioration of the cement paste which results in a reduction in stiffness and strength, followed by more expansion, cracking, and loss of cohesiveness. Empirical studies indicate that the rate of attack by magnesium sulfate is twice that of sodium sulfate, and that the rate of attack is reduced by low water to cement ratio and by low C_3A content. The rate of surface loss due to sulfate attack was calculated according to:

$$X = 0.55\, C_s (C_{Mg} + C_{SO_4})\, t \quad ,$$

where:

X =	distance of corrosion into concrete (cm),
C_s =	C_3A concentration in solid (mole/cm^3), and
C_{Mg} =	Mg concentration in solution (mole/cm^3),
C_{SO_4} =	SO_4 concentration in solution (mole/cm^3), and
t =	time (s).

3.1.2 Alkali and Calcium Hydroxide Leaching

When concrete is exposed to water, constituents in the concrete are leached. Alkalis are leached first, followed by calcium hydroxide. This process can be described in four stages:

1. Initially, the pH of standard concrete is approximately 13 due to the presence of alkali metal oxides and hydroxides. These alkali metals leach first.

2. After the alkali metals are leached, the pH is controlled at 12.5 by solid calcium hydroxide. Free (not bound by C-S-H gel) calcium hydroxide is leached first.

3. Following loss of free calcium hydroxide, calcium hydroxide is leached at a slower rate from the C-S-H gel. The C-S-H gel dissolves incongruously, while the pH drops to 10.5 and the calcium to silicon ratio drops to 0.85.

4. The pH is held to 10.5 by congruent dissolution of the C-S-H gel.

The loss of calcium results in a decrease in strength of approximately 1.5% for every 1% loss of total calcium content. The rate of calcium hydroxide leaching depends primarily on the flow of water through the concrete, but also on diffusion into the surrounding geology, and diffusion across a reaction zone in the concrete. Advective transport of leached calcium hydroxide from the concrete structure will dominate only under high rates of groundwater flow, and preferential flow of groundwater through the structure.

Atkinson and Hearne (1984) applied a shrinking core model to calcium hydroxide leaching. This model assumes that removal of calcium from the exterior of the concrete is rapid relative to movement of calcium through the concrete. Thus, leaching is controlled by conditions in the concrete and properties of the concrete, and so this process is referred to as "concrete-controlled leaching". As an alternative approach, Atkinson and Hearne also developed a leach model controlled by the surrounding geology ("geology-controlled leaching"). This model uses an equation for diffusion from a fixed concentration into a semi-infinite domain, with concentrations described by an error function (as in Crank, 1975), and allows for an analytic solution of the amount of calcium lost in a given amount of time. Both models predict that it will take over 1,000 years before calcium hydroxide leaching penetrates the upper 0.05 cm of the concrete. Both analytic models have been added to the degradation model. The equations used to approximate concrete-controlled and geology-controlled leaching, respectively, are:

$$X_C = \left(2 D_l \frac{C_l - C_{fw}}{C_s} t\right)^{1/2}$$

and

$$X_G = 2\phi \frac{C_i - C_{gw}}{C_s} \left(\frac{R_d D_E t}{\pi} \right)^{1/2} ,$$

where,

X_C =	depth of leach penetration due to concrete-controlled leaching (cm),
X_G =	depth of leach penetration due to geology-controlled leaching (cm),
D_i =	intrinsic diffusion coefficient of Ca^{++} in concrete (cm^2/s),
C_i =	Ca^{++} concentration in concrete pore water ($mole/cm^3$),
C_{gw} =	Ca^{++} concentration in ground/soil water ($mole/cm^3$),
C_s =	bulk Ca^{++} concentration in concrete solid ($mole/cm^3$),
ϕ =	porosity of soil (unitless),
R_d =	retardation coefficient (unitless), and
D_E =	effective dispersivity/diffusivity of Ca^{++} in the surrounding geologic material (cm^2/s).

A conservative estimate of the depth of leach penetration was obtained by summing X_C and X_G.

3.1.3 Carbonation

Carbonation is the reaction of carbon dioxide with cement to form calcium carbonate according to the reaction,

$$Ca(OH)_2 + H_2O + CO_2 \Rightarrow CaCO_3 + 2H_2O .$$

Sources of carbon dioxide are atmospheric gases and soil gases. Carbonation occurs most aggressively when the concrete is less than fully saturated with water, allowing CO_2 to diffuse through the air space in the concrete up to the reaction front within the concrete. At the reaction front, CO_2 dissolves in pore water and combines with calcium to precipitate calcium carbonate. From Walton et al. (1990), the depth of carbonation is proportional to the square root of time as shown in the equation below. The rate of carbonation depends on the moisture content of the concrete and its relative humidity, and ultimately on the type of cement used in the concrete mix.

Carbonation does not render the concrete less durable. Some fully-carbonated Roman concretes has survived to modern times. Shrinkage of the concrete may occur with carbonation as will a drop in the pH of the pore water. Carbonation of hydrated Portland-cement pastes also results in reduced hydraulic conductivity and increased hardness

(Verbeck, 1958). The pH shift can be from over 12 to about 8. At this lower pH, enhanced corrosion of steel reinforcing in the concrete may occur.

The rate of carbonation is dependent upon water saturation or relative humidity of the concrete. As relative humidity increases from 0 to 100%, the rate of carbonation passes through a maximum. Since water is required in the carbonation reaction, partially saturated conditions promote the reaction of CO_2 and $Ca(OH)_2$ to form $CaCO_3$, however increasing the water content above that required for this reaction to proceed will slow the diffusion rate of CO_2 through the concrete and limit the carbonation reaction. Typical subsurface environments approach 100% relative humidity, resulting in a water saturated concrete matrix. Therefore slow rates of carbonation are commonly found. The following analytic expression was employed for estimating carbonation rate in the degradation model:

$$X = \left(2D_i \frac{C_{iw}}{C_s} t\right)^{1/2},$$

where,

X = depth of penetration of carbonation (cm)
D_i = intrinsic diffusion coefficient of Ca^{++} in concrete (cm^2/s)
C_{iw} = total inorganic carbon in ground water or soil moisture ($mole/cm^3$)
C_s = $Ca(OH)_2$ bulk concentration in concrete solid ($mole/cm^3$) and
t = time (s)

Inherent in the use of this expression is the assumption that the concrete is water-saturated, and that the concrete is in direct contact with moisture containing a constant concentration of dissolved inorganic carbon.

3.1.4 Rebar corrosion

Corrosion of steel reinforcement results in a loss of strength due to loss of cross-sectional area of the rebar. In addition, a reinforced-concrete structure may suffer structural damage due to the loss of the bond between steel and concrete. Corrosion of the rebar produces a reaction product of greater volume than the rebar. Since the concrete surrounding the reinforcement prevents free expansion, this expansion exerts pressure on the concrete, and thus causes cracking and potentially spalling of the concrete structure, with consequent loss of strength. In the alkaline environment of standard concrete (low alkaline specialty concrete is used for the EAV construction), the rebar is protected from corrosion by the formation of a passivating layer around the rebar. This passivating layer, however, may be destroyed by the diffusion of chloride ions to the embedded steel (i.e., depassivation). Water to cement ratio and depth of concrete cover over the rebar are the most important factors in concrete construction that effect the time to depassivation. In the corrosion reaction, oxygen is electrochemically reduced and iron electrochemically oxidized, followed by conversion of the iron to iron oxides. The reaction rate is generally limited by diffusion of oxygen through

the concrete to the rebar, with oxygen diffusion increasing over time as processes, such as calcium hydroxide leaching and sulfate attack, decrease the diffusion limiting concrete cover over the rebar.

Thus, the corrosion of reinforcing steel due to oxygen diffusion occurs in two steps. First, the passivating layer must be broken down before the onset of corrosion. The time to onset of corrosion was approximated by:

$$t_c = \frac{129\, X_c^{1.22}}{WCR + Cl^{0.12}} \ ,$$

where,

t_c =	time to onset of corrosion (yr),
X_c =	thickness of concrete over rebar (inches),
WCR =	water-cement ratio in concrete (kg/kg), and
Cl =	chloride ion concentration in groundwater (ppm).

The reaction then proceeds, with a loss of reinforcing steel volume approximated by:

$$\%\ \text{Rebar Remaining} = 100\left(1 - \frac{4 * 9.4\left(\frac{cm^3}{mole}\right) s\, D_i\, C_w\, (t - t_c)}{\pi\, d^2\, \Delta X}\right) ,$$

where,

s =	spacing between reinforcement bars (cm),
D_i =	oxygen diffusion coefficient in concrete (cm^2/s),
C_w =	oxygen concentration in groundwater ($mole/cm^3$),
t =	time (s),
d =	diameter of rebar (cm), and
ΔX =	depth of rebar below surface (in).

Another mechanism of reinforcing steel corrosion is via the hydrogen evolution reaction. In this mechanism, H^+ ion from the water molecule is used as the source of oxidant for corrosion. H_2 is a by-product of this reaction. If we assume a low, constant rate of hydrogen evolution corrosion (i.e., a number from the low end of the literature range is adopted), then the relative volume of steel remaining is:
where,

$$\frac{V_{H_2}}{V_{Fe}} = \frac{2at - d^2}{d^2}$$

a = corrosion rate from hydrogen evolution reaction (cm/yr),
t = time (yr), and
d = diameter of rebar (cm).
V_{H2} = volume of steel after H_2 corrosion
V_{Fe} = initial volume of steel

Literature review of hydrogen evolution corrosion rates indicated a pH-dependance in the reaction rate. In the high pH range of typical concrete, the reaction rate is on the order of 1.5E-4 to 1E-5 cm/yr. If the pH drops below approximately 9, the reaction rate increases to values on the order of 1E-3 to 1E-4 cm/yr.

A bounding analysis for corrosion will be utilized by combining the rates due to oxygen-based corrosion and hydrogen evolution corrosion.

3.1.5 Vault Interiors

The degradation mechanisms that were considered for the walls and roof in contact with site soil are: Mg + SO_4 attack, $Ca(OH)_2$ leaching, concrete carbonation, and oxic and anoxic corrosion of the re-bar. Several of these mechanisms will not operate under the conditions anticipated inside the vaults or will occur so slowly that their net effect over the life of the vaults will be insignificant. Only anoxic ("hydrogen evolution") corrosion is anticipated as significant degradation process originating inside the vault, as discussed below.

Magnesium and sulfate attack requires a source of dissolved Mg and SO_4 in contact with the concrete such as would be provided by a moist soil. There is no continuous source of Mg and SO_4 in contact with the concrete in the vault interior, and therefore this mechanism is not anticipated to operate.

Two forms of calcium hydroxide leaching were considered: concrete controlled and geology controlled leaching. The concrete controlled leaching mechanism assumed a zero-concentration boundary condition at the surface of the concrete, a condition which would require ground water to flow over the concrete surface and "sweep" the calcium away from the surface as it diffuses out of the concrete. Inside the vaults, during the period of performance prior to collapse, there is no recognizable mechanism to create this zero-concentration boundary. As a result, a chemical diffusion gradient from the interior of the concrete towards the concrete surface will not be established and diffusion will not occur.

Geology controlled leaching assumes that a concentration gradient can be established into the (soil) material adjacent to the concrete. This is physically impossible in the LAW vault because of the lack of in-filling material and in the case of the ILW and ILNW vaults, where cement grout will contact the walls, the calcium concentration in the grout porewater will be identical to that in the concrete at all times. These conditions prevent a concentration gradient from forming outwards away from the concrete.

Concrete carbonation occurs in the presence of dissolved carbonate and calcium in the porewater of the concrete. Leaching of calcium hydroxide provides a source of calcium and diffusion of carbonate ion from soil water in contact with the concrete provides a source of carbonate. The carbonate in the soil water is replenished from dissolution of CO_2 gas from the soil air. Inside the LAW vault, the air space will contain CO_2, although most likely at concentrations much less than in a biologically-active soil; differences of one to two orders of magnitude would be a reasonable estimate. Carbonation would most likely occur, however with only atmospheric levels of CO_2 driving the reaction, the carbonation front would advance at a much slower rate than for the outer surfaces of the vaults. From the empirical relationship that INTERA has been using to describe carbonation, a slowing of the movement of the carbonation front by an order of magnitude would be possible.

Corrosion of the reinforcing bar in concrete under oxygenated conditions requires an initial depassivation of the steel surface. The mechanism that has been invoked in our modeling relies on diffusion of chloride to the passivating layer. Depassivation is followed by oxidation of the exposed steel. The interior of the vaults does not provide a source of chloride for the depassivation mechanism. Degradation modeling of the interior of the vaults should therefore not include oxic corrosion of rebar, unless the concrete mix is such that the pH of the concrete is below 9.

Anoxic corrosion of rebar will occur in the presence of moisture in the concrete. Since water- saturated concrete has been assumed for the modeling of degradation, this mechanism would proceed at a rate approximately the same as for the exterior surfaces of the vault. Adjustments to the rate caused by a decrease in pH at the corroding surface following carbonation of the local concrete will not be required.

In summary, the dominant degradation mechanism for the interior surfaces of the vaults will likely be anoxic corrosion of re-bar. Carbonation is also likely to occur, however, the rate of advance of the carbonation front will be significantly less than for exterior surfaces. The effect of carbonation on anoxic corrosion will likely not be an important consideration.

3.2 STRUCTURAL/ENGINEERING ANALYSIS

The RCPC.DHelper models (Furlong, 1991) used as the basis for the structural analysis portion of this study are available commercially through the American Concrete Institute

Software Sales Department. The programs have been in use for the past 4 years by approximately 300 engineering offices. The programs are intended to serve as a design aid in accordance with governing design documents, the principal one of which is the Building Code of the American Concrete Institute ACI 318-[illegible]. The Building Code is a strength design document with considerations for serviceability, but the [illegible] for design is the limit strength of reinforced concrete members. Consequently, the computer design aids focus on decisions related to strength design instead of service load performance.

Strength design employs results from elastic analyses of frame response to the many different types and configurations of load that concrete structures support. An analytic routine known as the Portland Cement Association Two-Cycle Method is used for the interpretation of worst effects from pattern loading on beams. The analytic tools in RCPC.DHelper are just as appropriate for serviceability analyses as for strength design. The RCPC.DHelper programs apply required load factors and incorporate appropriate reliability factors in the logic required for design. These programs were modified to bypass load factors and reliability factors in order simply to use response to service load forces (load and reliability factors = 1) for estimates of service load stress in steel reinforcement and shear stress in concrete slabs. Steel stress was computed assuming that the concrete had cracked.

The program most appropriate for Vault Study is the Continuous Beam program in RCPC.DHelper. That program was prepared for design of floor beams in two-dimensional rigid frames. The Vault study involved two structures that consisted of roof slabs cast as rigid and monolithic with supporting walls. The structure represented by a unit width of wall and roof slab is a two-dimensional rigid frame. Distances between supports were adjusted such that the actual clear distances between faces of framing elements remained the same as those in the finished structure.

3.2.1 Application to the ILNT/ILT Vaults

Because the ILNT and ILT vaults are virtually identical in their design, the same approach was used to analyze the two structures. The only changes required were changes in input parameters such as height of the structure and roof thickness. The structures were represented by a 1-ft wide span of walls and roof in the direction of maximum stress. The direction of maximum stress in the short direction of each cell, or, for example, along the 189-ft length of the ILNT vault. Hand calculations indicated that this approach is accurate to within approximately 3% of the full 2-way slab analysis (Furlong, 1993). Parameter values were selected to correspond to the respective height, thickness, amount of rebar, etc. in the walls and roof of each vault.

Stress in concrete and rebar was computed at the locations which experience the maximum stress. Maximum stress occurs over the walls, in the exterior face rebar, and at midspan, in the interior face rebar (Figure 4). After the stress in the rebar was calculated, the roof components and walls may fracture in order to eliminate excessive stress which cannot be borne by the degraded structure. When the stress in the rebar at a particular location

exceeds 40 ksi, cracks are assumed to penetrate the concrete. The approach to the calculation of stress in rebar assumes that the concrete has cracked. Crack width and spacing were computed as functions of the distance between the neutral axis[1] and the lower face of the concrete, the distance between the neutral axis and the center of the reinforcing steel, the diameter of the reinforcing steel, the concrete cover over the reinforcing steel, and the strain on the reinforcing steel.

When the stress in the rebar at a particular location reaches the yield strength of the rebar (60 ksi), the rebar will yield. In most cells, yield strength is reached first at the midspan region. Excess moment is then transferred to other regions in the cell. In the case of the midspan region reaching yield strength first, excess moment is transferred to the regions over the walls. This, in turn, increases the stress levels in the rebar over the walls. When the rebar reaches its yield strength at all three locations, a "hinge" is created. This will allow the roof to sag, and it is presumed that structural integrity will be lost at this point. Therefore, the point in time at which this occurs has been defined as the time of collapse. This process can be summarized as follows:

1. Rebar at center of span reaches yield strength.
2. Excess moment (and corresponding stress) transferred to region over walls.
3. Rebar over walls reaches yield strength, resulting in severe cracking and collapse.

For cells 3, 4, and 5 of the ILNT vault, the rebar reaches yield strength in the regions over the walls before reaching yield strength at midspan. In this case, the order is reversed:

1. Rebar over walls reaches yield strength.
2. Excess moment (and corresponding stress) transferred to midspan.
3. Rebar at midspan reaches yield strength, resulting in severe cracking and collapse.

3.2.2 Application to the LAW Vault

The 3" thick prestressed slabs in the LAW Vault roof design serve to hold the cast-in-place slab, and are therefore ignored in subsequent calculations. The soil and self weight (of the slab and the AASHTO beams) will cause the beams to move on the elastomeric bearings. As the beams move, the upper ends of the precast girders remain separated by a fixed distance at the slab atop the girders (Figure 5). Only the bases of the beams move toward each other, leaving at the end of each beam an angle of rotation each side of the supporting

[1]When a slab deforms under loading, part of the slab will be in compression and part of the slab will be in tension (e.g., at mid-span, the upper portion of the slab is in compression, and the lower portion in tension). The neutral axis is the location in the slab where compression changes to tension; it is therefore an axis of zero strain.

wall. The angle of rotation remains essentially constant as long as the flexural stiffness of the girders remains constant under soil loading. Based upon the soil load and self load of the slab and beams, a curvature (in the roof, over the wall) of 0.35 rad/inch was calculated. This will result in a stress of 2.8 ksi in the concrete, sufficient to crack the concrete. This curvature was then used to calculate the moment in the slab, and stresses in the cracked concrete and rebar. In the LAW Vault design, the stress level in the rebar increases relatively slowly as the structure degrades, and generally does not reach the 40-ksi limit. Therefore, the depth of the neutral axis was calculated in order to approximate the depth of crack penetration. As the structure degrades, the neutral axis, and therefore the cracks, penetrate further into the concrete. When the depth of the neutral axis moves to within 1 inch of the interior surface of the roof, cracks are assumed to penetrate the roof slab.

Due to the difference in roof design, the LAW Vault roof could not be analyzed in the same manner as the intermediate level vaults. The roof slab has only 5 ft of unsupported span between the AASHTO beams. Preliminary calculations indicated that the 16-inch concrete slab can support soil loads across the slab even after significant degradation of the steel. Therefore, collapse of the vault will be determined by the ability of the AASHTO beams to support the structure. A moment arm calculation was used to calculate the moment at mid-span of the beams after soil loading. This was then compared to the ultimate moment[2] of the beams. Because the moment is approximately proportional to the steel area, the ratio of actual moment to ultimate moment is approximately equal to the amount of steel area that can be lost before collapse:

$$A_{crit} = A_{init} * \frac{M_{pred}}{M_u} ,$$

where:

A_{crit} =	critical steel area (the minimum area of steel in the AASHTO beams which is capable of supporting the soil load),
A_{init} =	initial steel area in the AASHTO beams (7.01 inch^2),
M_{pred} =	predicted moment in beam after soil loading, and
M_u =	ultimate moment in beam.

In the model, then, collapse occurs when the steel area in the beams is reduced to A_{crit}.

The NAWY models (Nawy, 1989) were used to calculate loss in prestress in the beams due to elasticity loss, creep, shrinkage and relaxation. The model predicted that 90% of the prestress loss occurs in the first 10 years after release, and was in agreement with the prestress loss calculations by Tindall Concrete Georgia, Inc. (hereafter referred to as

[2]The ultimate moment is the maximum moment that the system can support before collapse.

"Tindall Concrete"). A value of 22% prestress loss was used as a conservative upper bound in the above calculations.

The LAW Vault walls were analyzed using the same RCPC-based code that was used for the intermediate level vaults. To do so, an equivalent roof slab was formulated for input into the code. After the roof slab of the LAW vault is cast, the system gains redundancy as a continuous, composite beam. The earth load was analyzed with the RCPC model using end span and wall models similar to that used for the intermediate level vaults. An equivalent roof slab width was computed to use a rectangular beam of 70-inch depth (the depth of the composite roof slab/AASHTO beam system) and produce the same moment as the composite slab and beam:

$$b = \frac{886200 * 12}{70^3} = 31 \text{ in},$$

where:

b = equivalent slab width;
886200 = I value of composite slab and beam system (from Tindall, 1993).

In this manner the RCPC-based code can be used to analyze stresses in the LAW vault walls.

4. MODELING APPROACH

4.1 COMPUTER CODES

The RCPC code (Furlong, 1991), as it is commercially available, is an interactive program; all input is typed in as the program runs, and output can be directed to the screen and/or a printer. In order to facilitate multiple model runs during the sensitivity analysis, and to maintain adequate Quality Assurance, the model was first modified to a file-based input/output system. In addition, minor modifications were added to compute stresses in rebar.

The NAWY models (Nawy, 1989) were used to evaluate prestress loss in the AASHTO beams and to confirm various calculations performed by Tindall Concrete. In addition to calculating time-dependent prestress loss, the NAWY models capabilities include service load analysis, strength analysis and design in flexure, shear reinforcement selection, and time dependent deflection of prestressed concrete beams.

4.2 LINKING BETWEEN DEGRADATION AND STRUCTURAL MODELS

The degradation model and structural model (modified RCPC) were combined, and a time loop was added so that the state of the structure through time could be modeled. The time loop was implemented as follows: First, the structural model is run at time zero on the (undegraded) structure. Next, the degradation model is run to determine the impact of degradation mechanisms on the physical state (thickness of concrete, diameter of reinforcing rebar, etc.) of the structure using a user-specified time step. After the degradation model is run, a temporary file is created that contains the modified concrete and reinforcing steel specifications. This file is then used as input for the next run of the structural model. Following the structural model run, the degradation model is run again, and the temporarily file is updated. This process of alternating between the structural and degradation models continues until the user-specified end of the simulation (e.g., 1,000 years). The state of the structure is printed at a user-specified time interval (e.g., 50 years).

4.3 HYDRAULIC CONDUCTIVITY

4.3.1 Vault Roofs

Walton (1993), presents a calculational method for Effective Hydraulic Conductivity (K_{eff}) of the vault roof. This method considers the adjacent porous media overlying the concrete roof. We have applied Walton's method in our K_{eff} determination. The closure design for each of the three vault designs considered in this report places a clay barrier over the roof to divert infiltration away from the roof. The infiltration flows laterally away from the vault through a granular drain layer which directly overlies the clay barrier. Only a very small amount of the infiltration will penetrate the intact clay barrier. During the period of

performance in which the concrete contains no cracks or during which the cracks do not fully penetrate the roof, the infiltration which penetrates the clay barrier will drain off of the sloped roof. The limiting barrier to flow will be the reinforced concrete. With cracking of the roof under applied stresses, the clay barrier will limit the infiltration to the roof, and any infiltration passing through the clay will likely enter the vault through penetrating cracks. The clay barrier is assumed to stay intact until collapse of the vault structure.

K_{eff} of the clay barrier and the concrete roof of the vault were derived using separate equations. The calculation of K_{eff} assumes steady, saturated flow through a set of equally spaced, parallel fractures in the concrete. The following equations after Walton (1993) derive the K_{eff} of the clay layer in the presence of fully penetrating cracks in the concrete.

$$K_{eff} = \zeta K_{clay} \text{ , and}$$

$$\zeta = \left\{ \frac{1}{2} + \frac{\tanh\left[a + b\ln\left(\frac{1}{x}\right) + c\ln(z)\right]}{2} \right\}^{d} ,$$

where

K_{clay}	= hydraulic conductivity of the clay layer (m/s),
ψ	= 1/2 of crack width (m),
x	= X/ψ = dimensionless crack spacing,
z	= Z/ψ = dimensionless thickness of the clay layer,
H	= depth of perched water on top of the vault (m),
X	= 1/2 of the crack spacing (m),
Z	= thickness of the clay layer (m),
a	= 0.0477, b = 0.606, c = 0.479, and d = 0.845.

The assumption of steady saturated flow through the clay layer can be demonstrated by calculating the depth of perched water above the clay layer in the granular drain. The analytic solutions for these equations are provided by McEnroe (1993). For the EAV geometry and hydraulic conductivity of the clay and granular drainage layer, a perched water table equal to the thickness of the granular drain was calculated, thereby verifying our assumptions.

The calculations of K_{eff} assume that the cracks are not infilled with porous material. Infilling of the cracks would result in much lower hydraulic conductivity of the clay/concrete layered system when the cracks have fully penetrated the concrete.

4.3.2 Vault Walls

The model for the hydraulic conductivity of the vault roofs assumes that the soil adjacent to the roof will be saturated. This will generally not be the case for the vault walls. Similar models to estimate the hydraulic conductivity of a cracked wall/unsaturated soil system are not available at this time. Nevertheless, the hydraulic conductivity of the walls will be limited by the conductivity of the adjacent material. Therefore, the unsaturated hydraulic conductivity of the adjacent backfill material can be used as an upper bound for the hydraulic conductivity of the cracked wall/soil system (just as the saturated hydraulic conductivity of the adjacent clay was the limiting value for the hydraulic conductivity of the cracked roof/soil system). The unsaturated hydraulic conductivity of the backfill material (or any soil) is a function of its moisture content. The Idaho National Engineering Laboratory is in the process of conducting flow and transport modeling for the vaults. They utilized a VanGenuchten approach to generate a moisture characteristic curve for the backfill material. This curve provides the relationship between moisture content and hydraulic conductivity. Model results indicate that the backfill will have a greater moisture content near the top of the vault, and therefore it will have a correspondingly greater hydraulic conductivity. For the intermediate level vaults, the unsaturated hydraulic conductivity of the backfill material adjacent to the walls was estimated as 7.5E-4 cm/s near the top of the walls, 6.7E-4 cm/s at mid-height of the walls, and 6.9E-4 cm/s near the bottom of the walls. For the LAW Vault, the unsaturated hydraulic conductivity was estimated as 7E-4 cm/s near the top of the walls, and 6.3E-4 cm/s at mid-height and at the bottom of the walls. Thus, a value of 7.5E-4 cm/s can be taken as a worst-case assumption for the hydraulic conductivity of the vault walls.

4.4 MODEL OUTPUT

Model output can be divided into two broad classes; degradation output and structural output. Structural output for the LAW vault includes additional parameters specific to the calculation of stress and cracking in the roof slab due to curvature over the walls. Output parameters are summarized in Table 1. Output is directed to two files. One file contains a summary of all structural parameters at each print interval. In order to facilitate plotting and interpretation, the second file contains one line per print interval. Rebar stress in the first 4 spans (for example, the first wall and the first three cell roof spans) and all degradation parameters are sent to this file.

4.5 DEFINITION OF FAILURE

Failure of a vault can be defined in three ways:

- Loss of ability to resist penetration from drilling.
- Loss of ability to divert water around the vault.

- Structural failure (collapse) of the vault.

Resistance to drill penetration is necessary to avoid accidental intrusion after the period of institutional control, for example, from a future resident attempting to put in a drilling [illegible] well. The geology in the vicinity of the vaults, to depths of approximately [illegible] ft, is made up of soft sediments only. Therefore, drill equipment is not outfitted for hard rock penetration. In the event that an attempt was made to drill over the vaults, the supervising geologist would almost certainly pull up and move over until a normal amount of resistance was encountered. Even in the event that the vault was highly degraded (for example, without rebar and with the consistency of limestone), the supervising geologist would again probably decide to pull up and move. This information on drilling equipment and procedures was obtained through a phone conversation with an experienced geologist in drilling oversight at the Savannah River Site (Asquith, 1993). Thus, drill penetration of the vaults is not expected to be of concern.

Intact concrete generally has a very low hydraulic conductivity; the E-Area Vaults concrete has a hydraulic conductivity of at most 10^{-12} m/s. Therefore, virtually all of the conductivity of the degraded structure will be through fractures. Calculations by INTERA indicate that, once fractures have penetrated the roof slab, the hydraulic conductivity will be very close to that of the clay overlying the vaults, or 10^{-9} m/s. Thus, loss of ability to divert water coincides with crack penetration of the roof.

The modeling approach to collapse of the vaults has been described previously. When a vault roof collapses, the engineered soil cap will also be compromised due to subsidence of the vault roof. This, in turn, will result in a very dramatic increase in hydraulic conductivity of the vault/soil cap system.

4.6 SUMMARY OF CONSERVATIVISM

This section summarizes the conservative assumptions made and approaches taken during the development and application of the performance assessment model. One of the assumptions having the greatest impact on model results was that the concrete was at a relatively low pH (at most 9.5). This results in more rapid degradation of the structure (basically due to more rapid rebar corrosion rates), and causes the estimated service life (i.e., time to crack penetration and collapse) to be several hundred years less than that of high-pH concrete. The sulfate attack rate is based upon empirical experiments using blocks of concrete. The equation was based on the observed attack rate at the location of greatest corrosion (at the corners of the blocks). Rebar corrosion will generally proceed via either anoxic or oxic corrosion. However, because it is not known at this time which mechanism will dominate at any given time, the rates were summed to estimate the rebar corrosion rate. This is clearly conservative because the sum will be greater than either rate individually. The soil cover was assumed to be of constant depth throughout the simulation. In reality, some erosion will take place in the 1,000 to 3,000-year period simulated, resulting in less load on the vaults and therefore lower stress levels and longer service life. In the structural model,

a 1-way analysis was used. This examines the stress in a beam supported at each end (Figure 4). Because the roof is supported by four walls, a cross-section receives some support from adjacent walls as well as the walls at each end. Thus, estimated stress levels will be slightly (approximately 3%) higher than those estimated by a 2-way analysis. The structural analysis also assumed that there would be no interior support provided by the contents. Clearly, if the contents provided some support, there would be less deflection and therefore less stress in the concrete members. In determining the prestressed bridge beams in the LAW vault, a 22% loss in prestressing was assumed. This was considered to be a maximum loss of prestress. Actual losses can be expected to be less, particularly in the first 5-10 years after release. Cracks were assumed to penetrate the UNH and UHT vault roofs and walls, and the LAW walls, when stress in rebar reached 40 ksi. This was estimated to be a conservative estimation of when crack depth would be sufficient to penetration the concrete members. For the LAW vault roof, crack depth was based upon a calculation of the depth of the neutral axis. To add conservatism to the estimation, cracks were assumed to penetrate when the depth of the neutral axis reached within 1 inch of the bottom of the roof slab. The approach for estimating the hydraulic conductivity of the cracked concrete assumed that cracks were evenly spaced across the entire surface of the concrete. In reality, the concrete can be expected to crack in fairly localized regions. This is particularly evident in the LAW vault roof, which is expected to crack only within a less than 2-foot wide region over the walls. This assumption is not expected to have a large impact on the calculated hydraulic conductivity, however, because a few cracks are sufficient to cause large changes in hydraulic conductivity. In contrast to the model assumptions, most of the input parameters for the baseline case utilized on average or typical values. For example, all chemical concentrations in groundwater were based on average values, reaction rates were based on the midpoint of the range of values found in the literature, and roof thickness and wall height used were the average (where variation existed).

5. INPUT SUMMARY

Model input for the structural analyses are listed in Table 2 - Table 4 for the three vault types. Structural input essentially consisted of the dimensions of the vaults (wall height and thickness, roof span and thickness), the size and spacing of the rebar, the depth of cover over the rebar, the compressive strength of the concrete, and the yield strength of the rebar. The required information was obtained from the design drawings for the E-Area Vaults. A list of the drawings used is provided in Table 5.

Input required by the degradation portion of the model is listed in Table 6. Where available and applicable, ranges of values for the input parameters are presented. Input requirements include concentrations of corrosive components of the adjacent groundwater, concentrations of components in the concrete, and reaction rates.

A baseline run was defined to determine a best estimate of the times to crack penetration and failure of the three vault designs. In the baseline case, average values of environmental parameters were used (for example, sulfate concentration of the groundwater). Actual or proposed design parameters (such as rebar size or depth of soil cover) were used. Where design parameters were variable (such as roof thickness in the intermediate level vaults), average values were used.

Soil loading in the baseline case assumed a 9-foot depth of soil cover. A value of 1.7 g/cm^3 (106 lb/ft^3) was used for the density of soil. In order to calculate the self-weight of the vault roofs, a concrete density of 2.34 g/cm^3 (146 lb/ft^3) was used. Lateral soil pressure on the walls was computed using a modified Rankine approach (Das, 1985).

6. MODEL RESULTS

Figure 5 is a cross-section of the ILNT Vault after [illegible] years of [illegible]. The [illegible] mechanism has removed an average of 0.19 [illegible] from the [illegible] of the concrete, and the rebar radius has been reduced from 1.25 cm to 1.05 cm, [illegible] to a radius somewhat less than that of a #7 bar. Figures 7 through 9 present the effective hydraulic conductivity of the three vault designs. Prior to crack penetration, the hydraulic conductivity remains that of intact concrete, 10^{-11} m/s. When cracks penetrate the roof of the vault, the hydraulic conductivity of the (cracked) concrete increases to a conductivity near that of the surrounding clay, 10^{-9} m/s, followed by a gradual increase in hydraulic conductivity as crack apertures and the number of cracks increase, up to a theoretical maximum of 10^{-9} m/s.

Table 7 and Table 8 present summaries of the rebar stress for the baseline cases of the ILT and ILNT vaults, respectively. Each column in the tables represents a particular location in the vault. In this summary presentation, rebar stresses are tabulated at each time step for which an "event" occurs, with an event defined as crack penetration at some location in the vault, or collapse of a cell. Shading in the tables indicates that cracks have penetrated at that location. A box created with thick table lines indicates the time of roof collapse for each cell.

The ILT scenario is fairly straight-forward. Maximum rebar stress occurs at mid-span in the roof, due to the fact that there is twice as much rebar in the region over the walls as there is at mid-span. Rebar stress is slightly less over the interior wall than at midspan. Thus, crack penetration occurs first at mid-span in the roof (year 790) , and soon thereafter over the interior wall (year 850). Rebar stress in the walls is much less than that in the roof, primarily because the lateral soil pressure on the walls is much less than the vertical soil pressure on the roof (lateral pressure is approximately one-third that of vertical). Thus, cracks do not penetrate the center region of the wall, or mid-height of the wall, until year 1,080. The rebar stress level in the roof rebar at mid-span and over the interior wall reaches its yield strength in years 1,125 and 1,150, respectively (not shown). As moment is transferred to the remaining rebar stress point at the exterior wall, this causes a rapid increase in rebar stress levels at this point, and cracks penetrate the roof over the exterior wall at year 1,225. The rapid increase in roof rebar stress over the exterior wall continues, and collapse of the roof occurs in year 1,300. With the loss of support from the roof, it is reasonable to assume that, although rebar stress in the walls near the roof and floor have not reached the levels indicative of crack penetration, the walls at this point will also fail and collapse.

Stress patterns in the ILNT Vault are similar to those in the ILT Vault, in that the rebar stress in the roof span of the exterior cells (cells 1 and 7 of Figure 1) over the exterior wall is much less than that over the interior wall of the same cell. In the first interior cell (cells 2 and 6), this effect is mediated somewhat, and in the remaining cells the rebar stress levels

are equal over each wall for a given cell. The lower stress level over the exterior wall results in higher rebar stress levels at mid-span of the exterior cell. Thus, crack penetration occurs first at mid-span of the exterior cell (year 570), followed by the first interior wall (year 675). Next cracks penetrate over the remaining walls (year 750), followed soon thereafter by crack penetration at mid-span of the remaining cells (year 775). Cracks do not penetrate the roof over the exterior walls until year 1,000. The first cells to collapse are the first interior cells (cells 2 and 6), in year 1,045, followed soon by the remaining interior cells in year 1,075. The exterior cells collapse in year 1,125. In the ILNT vault, the walls are slightly higher than the ILT vault, so the stress levels are correspondingly greater, with the result that cracks penetrate at mid-height in year 800, and near the top of the vault in year 1,050. Stress levels at the bottom of the walls have not reached the levels indicative of crack penetration at the point at which the roof has collapsed in all cells (year 1,125).

Due to the different design and consequent different approach to the analysis, the same type of table cannot be generated to summarize the LAW vault progression through failure and collapse. While crack penetration in the walls is indicated in the same manner (i.e., rebar stress above 40 ksi) as in the intermediate level vaults, crack penetration in the roof is indicated by depth of the neutral axis. Collapse is indicated by the area of prestressed steel in the AASHTO beams dropping below a critical level. The scenario can be described as follows: Cracks penetrate the roof due to curvature over the walls in year 1,420. Next, cracks penetrate at the top, mid-height, and bottom of the walls in years 2,015, 2,235 and 2,300, respectively. Finally, prestress steel loss is sufficient to cause collapse of the roof in year 3,110.

7. SENSITIVITY ANALYSIS

There are three classes of model input that could be considered in the sensitivity analysis. First, sensitivity analysis could be conducted for physical parameters, such as water chemistry or infiltration rates, which are represented by mean values, and are used in the models for the degradation of concrete. Second, sensitivity analysis could be performed for concrete degradation model parameters, such as reaction rates for any of the various degradation reactions. Finally, sensitivity analysis could be conducted on design parameters, such as depth of soil cover, thickness of roof slab, or diameter of rebar. All sensitivity analyses were conducted by varying a single parameter from the baseline case and leaving all other parameters unchanged. This section presents the rationale behind the selection of parameters to be included in the sensitivity analysis, and the results of the analysis.

7.1 SELECTION OF PARAMETERS AND VALUES

Calcium hydroxide is one of the primary buffers that contribute to the high pH of concrete. Based on an X-ray diffraction analysis of a sample of the E-Area Vault concrete, the concrete used for the E-Area Vaults contains no calcium hydroxide. This can be explained by a combination of two factors. First, the cement used in the concrete has a very low calcium hydroxide content. Second, the concrete is designed so that the calcium hydroxide will be removed via a reaction with slag in the concrete. Calculations by Chris Langton of the Savannah River Technology Center determined that the pH of the E-Area Vault concrete is approximately 8, that it is at most around 9 to 9.5, and that it may be as low as 7. Because the E-Area Vault concrete has essentially no calcium hydroxide content and a relatively low pH, the only degradation mechanisms that apply to the concrete are oxic and anoxic ("hydrogen evolution") corrosion of rebar, and sulfate attack. While varying the parameters relevant to the sulfate attack mechanism caused noticeable changes in the amount of surface loss due to sulfate attack, the impact on steel stress was minimal. The oxic corrosion rate has a slightly greater impact on steel stress, but the anoxic corrosion rate by far dominates the rebar corrosion. Thus, for low-pH concrete in the Savannah River Site environment, the only degradation process of interest in terms of the sensitivity analysis is hydrogen evolution corrosion of rebar. This process is modeled using only one parameter, the hydrogen evolution corrosion rate. Therefore, this parameter was selected for inclusion in the uncertainty analysis. Based on a literature review, the low-pH hydrogen evolution corrosion rate was varied between 1E-3 and 1E-4 cm/yr, and the high-pH of hydrogen evolution corrosion between 1.5E-4 and 1E-5 cm/yr. It is important to note that the low-pH assumption is generally conservative, in that most degradation mechanisms proceed at higher rates in the low-pH environment. The only exception is that, with calcium hydroxide leaching, there can be some decrease in concrete strength. Since the E-Area Vault concrete has no calcium hydroxide available for leaching, the concrete strength is assumed to remain constant throughout the simulation.

A preliminary sensitivity analysis was performed to help determine parameters for which to conduct a detailed sensitivity analysis. Of the parameters included in the initial sensitivity analysis, hydrogen evolution corrosion rate (discussed above) and depth of concrete cover over rebar was selected for detailed analysis. Design constraints limited the range of allowable cover to between 1½ and 3 inch. In addition, thickness of vault roofs and numerous parameters related to degradation mechanisms were considered in the initial sensitivity analysis, but not selected for detailed analysis.

- New parameters selected for detailed analysis were rebar diameter, size of AASHTO beams (LAW Vault only), concrete strength, and depth of soil cover over the vaults. Rebar diameter was varied approximately to the minimum and maximum allowable according to ACI 318. The limits varied between vaults and between walls and roofs depending on the values of the relevant design parameters. Standard AASHTO beam sizes were used in the sensitivity analysis. Because changing the size by only one increment is very significant both in cost and in strength of beam, only types III, IV, and V beams were analyzed for the sensitivity analysis. Finally, a minimum soil cover of 8 ft is required to meet performance requirements. This was varied up to a maximum of 16 ft. For all parameters, intermediate values (i.e., between the extremes and the baseline) were selected as appropriate.

7.2 OUTPUT SUMMARY

In the sensitivity analysis, the first time of crack penetration of the roof and wall of the intermediate level vaults are reported, and, for the ILNT vault, the first cell to collapse. The first crack penetration occurs at mid-span of the exterior cell (for the ILT vault, the two cells are equivalent). The first cells to collapse in the ILNT vault are the first interior cells towards each end (cells 2 and 6). Collapse in a cell is indicated when the rebar reaches yield strength at mid-span and over the adjacent walls of that cell. In cells 2 and 6, the first location at which the rebar reaches yield is at mid-span, followed by the wall towards the exterior end of the vault. Collapse, then, occurs when the rebar in the roof reaches yield strength at the remaining location, over the wall towards the interior of the vault. Thus, for the sensitivity analysis of the ILNT Vault, this is the location of interest. By observing the stress in the roof rebar at this location, the time to collapse can be determined. Similarly, for the ILT vault, the last location in the cells to reach yield strength in the rebar is over the exterior wall. Finally, crack penetration of the walls at mid-height was used to indicate crack penetration of walls.

For the LAW Vault, collapse is indicated by prestress steel in the AASHTO beams reaching a critical level. Therefore, observing changes in the area of prestress steel will provide the determination of time to collapse. Crack penetration of the roof is indicated by the neutral axis approaching to within 1 inch of the bottom of the roof slab. As in the case of the intermediate-level vaults, crack penetration at mid-height of the walls was selected to indicate crack penetration of the walls.

Thus, for each vault, three critical output parameters have been selected on which to base the sensitivity analysis of the six input parameters. The output parameters can be used to determine the time to crack penetration of the roof, time to crack penetration of the walls, and collapse of the vaults. These pivotal times are summarized for the baseline case in Table 9.

Table 10 through Table 12 summarize the same pivotal times for each sensitivity run. For the LAW Vault, differences existed in some of the parameters between the different vault components, and these differences are indicated in the left-hand column of Table 12. For example, the AASHTO beams are made of a high-pH concrete. Therefore, they will be subject to the slower, high-pH rate of hydrogen evolution rebar corrosion. Furthermore, since they are on the interior of the vault, there are no corrosive processes available to lower the pH of the beam concrete and thereby increase the reaction rate. In addition, the rebar used in the roof and walls are different. In order to understand the dynamics of the vaults in greater detail, plots of steel stress vs. time are also presented for most of the sensitivity runs.

7.2.1 ILNT Vault Sensitivity Analysis

Pivotal times (time to crack penetration of the roof, time to crack penetration of the walls, and time to collapse) for the ILNT vault are summarized in Table 10.

All pivotal times are sensitive to hydrogen evolution corrosion rate (Figures 10, 11 and 12). Varying the corrosion rate over a range of one order of magnitude changed the pivotal times by an order of magnitude as well. The change in pivotal times is very close to proportional to the ratio of the baseline corrosion rate divided by the new corrosion rate. Increasing the corrosion rate from 5E-4 to 1E-3 changed the time to crack penetration (of the roof) from 570 years to 285 years, a decrease of 285 years, and decreasing the corrosion rate to 1E-4 increased the time to crack penetration to 2,775 years, an increase of over 280%. Decreasing the corrosion rate to only 2.5E-4 almost doubled the time to crack penetration of the roof.

Altering the depth of the soil has less impact on the pivotal times (Figures 13, 14 and 15). Decreasing the soil cover from 9 ft to 8 ft increases the pivotal times by approximately 50 to 100 years. Increasing the soil cover to 12 ft decreases the pivotal times by approximately 200 years, and increasing to 16 ft decreases the pivotal times by 300 to 400 years from the baseline values.

Changing the rebar size has the potential to create large changes in the pivotal times. Reducing the bar size to #6 would result in cracks penetrating the roof immediately upon soil loading (Figure 16), and the wall after 175 years (Figure 17); collapse would occur in 425 years (Figure 18). Using a #7 instead of the present #8 would result in crack penetration of the roof after 250 years, and collapse after 735 years. Increasing the rebar size has

similarly dramatic effects. Using #9 rebar would increase the pivotal times to on the order of 1,000 years, and #11 to on the order of 2,000 years.

Depth of concrete cover over the rebar has little impact on the longevity of low-pH vaults (Figures 19, 20 and 21). Note that this statement applies to the range of 1½ to 3½ inch depth of concrete cover. Further decreasing the depth of cover further could have significant effects. Also, concrete cover over rebar can have very significant impacts if high-pH concrete is used; with increased cover reducing corrosion and thus extending the service life of the vault. Stress is slightly higher with greater depth of cover, and remains so throughout the simulation. Analysis of high-pH concrete (not shown) by INTERA demonstrated that depth of concrete cover over rebar can be very important. In high-pH concrete, several diffusion-limited processes become important. The result is that rebar with greater depth of cover degrades at significantly slower rates, and therefore, in the long term, experiences lower stress levels.

Concrete strength also has little impact on the longevity of the vault (Figures 22, 23, and 24). The reason for this is that concrete has very low tensile strength, and the rebar therefore provides the majority of the tensile strength in reinforced concrete. Thus, increasing the concrete strength decreases the stress levels in the rebar only slightly. High-strength concrete provides other advantages, however, such as resistance to shear stress and reduced hydraulic conductivity.

7.2.2 ILT Vault Sensitivity Analysis

Pivotal times for the ILT Vault are summarized in Table 11. The results are qualitatively very similar to those of the ILNT vault, with quantitative differences caused by the slight differences in some of the design parameters. Again, changes in pivotal times are roughly proportional to changes in hydrogen evolution corrosion rates. At the lowest rate, cracks did not penetrate the ILT Vault prior to the end of the 3,000-year simulation (Figures 25, 26 and 27). At the minimum depth of soil cover, pivotal times decreased by approximately 50 years, and at the maximum, decreased by 300 to 400 years (Figures 28, 29 and 30). Due to the thicker roof in the ILT Vault, #6 rebar did not result in crack penetration of the roof until year 155 (Figure 31). Otherwise (Figures 32 and 33), changing rebar size had similarly dramatic effects on the ILT Vault as was the case with the ILNT vault. Due to the overall more conservative design of the ILT Vault, depth of concrete cover over rebar (Figures 34, 35 and 36) and concrete strength (Figures 37, 38 and 39) had even less impact on the ILT vault than on the ILNT vault.

7.2.3 LAW Vault Sensitivity Analysis

Pivotal times for the LAW Vault sensitivity analysis are summarized in Table 12. Figure 40 shows the location of the neutral axis as a function of time for various rates of hydrogen evolution rebar corrosion. The depth is given in terms of the distance from the interior surface of the slab. This is done for two reasons. First, at the same time that the neutral

axis is moving to lower positions in the slab, sulfate attack is removing surface material from the top of the slab. Therefore, indicating the depth of the neutral axis as a distance from the exterior would be misleading, and, at best, confusing. Second, cracks are assumed to penetrate the roof slab when the depth of the neutral axis exceeds 1 inch. Thus, displaying the depth of the neutral axis in this manner provides a graphical interpretation of the State to crack penetration. In spite of the differences in design between the LAW and the intermediate level vaults, and the resultant differences in the structural calculations, the changes in the time to crack penetration of the roof remain roughly proportional to the changes in the corrosion rate. Crack penetration of the LAW walls also maintains this proportionality (Figure 41).

Figure 42 shows the results of the sensitivity of time to roof collapse of the LAW vault for both hydrogen evolution corrosion rate and depth of soil. The curves represent the area of prestressed steel remaining for different hydrogen evolution corrosion rates, as a function of time. The horizontal lines indicate the area of prestressed steel required to support different depths of soil. The intersection of a curve with a line, then indicates the point in time at which collapse will occur for a given combination of corrosion rate and soil depth. To interpret the impact of hydrogen evolution corrosion rate, consider the horizontal line corresponding to the baseline soil depth (9 ft), and disregard the other horizontal lines. This line indicates the rebar area necessary to support the weight of the vault and 9 ft of soil. When a particular curve crosses that line, that point in time is the time of collapse for that hydrogen evolution rate and the baseline (9 ft) depth of soil. These are the times that are presented under "Hydrogen Evolution Corrosion Rate" in Table 12. The proportionalities is maintained here as well, but not quite as close as in the other cases. At the highest corrosion rate, collapse is predicted at 1,600 years, and, at the lowest rate, the vault did not collapse prior to the end of the 10,000-year simulation.

Because crack penetration of the roof is based upon a neutral axis calculation, and the depth of the neutral axis is not calculated as a function of loading, soil loading does not change the time to crack penetration of the roof. In reality, because increased soil loads will increase the stress level in the rebar, changing soil depth would be expected to have a small impact on the depth of cracks, and therefore on the time to crack penetration. It may appear from the graph of wall stress for different soil depths (Figure 43) that soil load has less impact on LAW walls than on the walls of the intermediate-level vaults. The absolute change, however, remains close to that of the intermediate level vaults: pivotal times are approximately 100 years greater than baseline times for the minimum depth of soil, and 200 to 300 years less for the maximum depth of soil. To examine the impact of soil depth on collapse of the vault, return to Figure 42. This time, consider the baseline hydrogen evolution rate (8E-5) curve only, and neglect the other curves. When the baseline curve crosses the horizontal line for a particular soil depth, that indicates the time to collapse for that depth of soil. These are the values tabulated in Table 12 under "Depth of Soil Cover" (of course, other corrosion rate/soil depth combinations can also be interpreted from this graph). Depth of soil has a much more dramatic impact on time to LAW Vault collapse than on any other pivotal time (for the LAW Vault and the intermediate level vaults). At the

minimum depth of soil, roof collapse increases by almost 200 years, and at the maximum, decreases by over 1,000 years.

Figure 44 shows the impact of changing rebar size on the time to crack penetration of the roof, using the same format as Figure 40. Because the rebar in the roof slab is close to the ACI minimum, only one increment smaller (from #6 to #5) was used in the sensitivity analysis. Again, the effects are significant, decreasing the time to crack penetration by approximately 900 years. Nevertheless, this is still several hundred years greater than the time to crack penetration of the roof in the intermediate level vaults. Increasing the rebar size also has a significant impact on the time to crack penetration of the roof. Increasing to a #8 bar increases the time to crack penetration by 600 years, and, to #14, by approximately 2,400 years. Note that, in this case, the roof will collapse due to structural failure of the AASHTO beams before cracks penetrate the roof. Changes in crack penetration of the walls (Figure 45) are similarly dramatic, with a change of approximately 300 years for every unit increment in bar size. Because roof collapse is determined by the AASHTO beams, changing the bar size in the roof slab has no impact on time to collapse.

Increasing the size of the AASHTO beams from the current Type IV to Type V will have a relatively slight impact on the depth of cracks and therefore on the time to crack penetration. This is due to the neutral axis' lack of dependance on load factors and on the moment in the AASHTO beams. Due to the decreased stress levels in the roof slab rebar (not shown), some decrease in the time to crack penetration would be expected. Decreasing to Type III beams will result in increased stress levels in the roof slab rebar, caused by increased curvature over the walls. Stress levels will be sufficient to cause cracks to penetrate the roof slab (that is, greater than 40 ksi) immediately upon soil loading. Therefore, use of smaller beams is not recommended unless spacing between beams is decreased to compensate. Figure 46 illustrates the impact of using different sized AASHTO beams on the time to collapse, using the same format as Figure 42. The curves for various hydrogen evolution corrosion rates have been retained in order to maximize the amount of information available in the graph. In Figure 46, however, the horizontal lines represent the area of prestress steel required to maintain the structure for the different sizes of AASHTO beams. Using a larger beam results in a smaller requirement in terms of the area of prestress steel required. Using the baseline hydrogen evolution corrosion rate, changing the beam size changes the time to collapse by approximately 300 to 400 years.

7.3 SUMMARY OF THE IMPACT OF DESIGN CHANGES

Within the range of values selected (3,000 to 6,000 psi), concrete strength has little impact on the service life of the vaults, due to the fact that it is predominately the rebar that resists tensile stresses. It is important to note that concrete strength has other important contributions to the vaults, such as reducing permeability and resisting shear stress. Depth of concrete cover over rebar also had little impact on the service life of the vaults. There are two significant caveats to this statement, however. First, this statement applies to the range of 1½- to 3-inch depth of concrete cover. Further decreasing the depth of cover

further could have significant effects. Second, concrete cover over rebar can have very significant impacts if high-pH concrete is used, with increased cover [illegible] ing corrosion and thus extending the service life of the vault.

Rebar size has notable impacts on the service life of the vaults. Increasing or decreasing the rebar by one increment (for example, from #8 to #9 or #7) will increase or decrease, respectively, the service life of the vaults by from 200 to 300 years. Further increments in rebar size have similar effects. This is due to the increased cross-section [illegible] of the rebar. Thus, increasing or decreasing the rebar spacing would be expected to have impacts of the same type and magnitude.

The size of the AASHTO bridge beams that are used for the roof system in the LAW vaults has a significant influence on serviceability. In addition to the Type IV beams now used, smaller Type III and larger Type V beams were considered for this study. It was assumed that the spacing, amount of prestress steel, and amount of prestress applied were the same for each beam type. The nominal stiffness of beams is reflected by the I value. The ratio between Type III and Type IV beams is 125,390/260,741 = 0.48. After the 16-inch slab is cast for composite action with the girders, the relative stiffness ratios will be higher, perhaps 0.6 to 0.7. The curvature of the slab over supports will be 30 to 40% larger as the smaller girders rotate at supports more than the Type IV girders when soil is placed over the hardened slabs. Consequent cracking will result in larger and deeper cracks over supports, and probable crack penetration upon soil loading. The limit strength at midspan will be proportional to the overall depth from the top surface of the slab to the centroid of prestressed strands at midspan. As a consequence, roof collapse is predicted to occur approximately 400 years earlier if the smaller beams are used. The ratio between the nominal stiffness of Type V and Type IV beams is 521,100/260,741 = 2.0. After the 16-inch roof slab is added, the stiffness ratio will become 1.6 to 1.8. With greater stiffness, the deeper girders will rotate at supports through smaller angles than will Type IV beams, and the curvature in the slabs will be smaller for slabs supported on deeper girders. Cracking from such smaller curvatures will be smaller and less deep than those for the slabs supported on Type IV beams, although the neutral axis calculation indicates the same depth of cracking. The time to collapse is extended by slightly over 300 years using the larger girders. In summary, the use of the smaller Type III beams is not recommended. Although some of the increased curvature could be compensated for by closer spacing of the beams, it is not likely that this will be practical, as the beam spacing is already relatively small. On the other hand, increasing the beam size will likely have only a slight impact on the time to crack penetration, and a relatively small impact on the time to collapse (increased from 3,110 years to 3,430 years, or by about 10%). Thus, the present beam size seems to be appropriate. It may be possible to alter the beam spacing, however, and retain adequate service life. Larger beam spacing would result in greater curvature and thus decrease the time to crack penetration; and, of course, decrease the time to collapse. In addition, consideration would need to be given to whether the 16-inch roof span could support the larger distance between girders, particularly as the structure degrades. Nevertheless, it

seems likely that beam spacing could be altered and the vaults still satisfy the performance criteria.

Finally, depth of soil cover has significant impacts on the service life of the vaults. Decreasing the soil cover from the assumed 9 ft to the minimum of 3 ft increased the service life of the vaults by 50 to 100 years. Increasing the soil cover to the maximum considered, 16 ft, decreased the service life by approximately 200 to 400 years. The notable exception to this is the time to collapse of the LAW Vault, which decreased by over 1,000 years when the soil cover was increased.

8. FUTURE RESEARCH AREAS

This study was limited to the roof and walls of the ILT, ILNT and LAW vault types. If cracks penetrate the roof or walls of a vault before cracks penetrate the floor, there is the potential for infiltration water to [illegible] in the vault, resulting in leaching of the vault contents. When the floor does crack, toxic substances could then be released. Clearly, in order to accurately assess flow out of the vaults, it is necessary to estimate the time to crack penetration of the vault floors. This should be the first priority for additional work in this area.

This project has demonstrated the ability of the model to evaluate the impact of changes in design parameters on the longevity of reinforced concrete structures. A number of other design parameters were not considered in this study due to time and budget limitations. Additional sensitivity analyses could be conducted for structural parameters such as roof thickness, rebar spacing, AASHTO beam spacing, length, width and height of the vaults, and wall thickness, as well as degradation model inputs such as oxygen diffusion rate in the concrete, leach rate, carbonation rate, or time to depassivation of the rebar.

One issue that has not been addressed in this project is the potential for loss of bonding between the concrete and rebar as the rebar degrades. Corrosion products have greater volume than the rebar, and this can result in cracking or spalling of the concrete, or other mechanisms may result in loss of bonding.

If high-pH concrete is to be considered, sensitivity analysis should be conducted for other corrosion processes as well. Figures 47 and 48 demonstrate the importance of other processes in the corrosion of high-pH concrete. Figure 47 shows a worst-case degradation scenario at 50 years after burial. Sulfate attack has caused some surface loss. Oxic corrosion has caused the exterior face rebar to corrode at a slightly greater rate than the interior face rebar, which will remain passivated (and thus not subject to oxic corrosion) throughout the simulation. Leaching has resulted in a low-pH zone to a depth of 5.9 cm into the concrete. At 400 years (Figure 48), the low-pH zone has encompassed the exterior face rebar. This causes the hydrogen evolution corrosion reaction to proceed at an accelerated rate, resulting in significant corrosion of the exterior face rebar. The interior face rebar, still protected from oxic corrosion, corrodes much more slowly, at the high-pH rate of hydrogen evolution corrosion. In a low-pH concrete, both exterior and interior rebar corrode at the higher hydrogen evolution corrosion rate. Thus, the high-pH concrete has two basic differences in terms of its corrosion rates: First, there is a delay, both before the onset of oxic corrosion (minor impact) and before the high rate of hydrogen evolution corrosion (major impact). Second, the interior rebar corrodes only at the lower rate of hydrogen evolution corrosion throughout the simulation (major impact). Because of this, carbonation (which, in some scenarios, may be the mechanism for lowering pH), leach penetration, and time to depassivation of the rebar all become important. Table 13 presents the results of a baseline analysis of baseline results for the different vault types, under the assumption that

high-pH concrete is used. This can be compared to Table 9. LAW Vault results for high-pH concrete are not presented because changes were made to the LAW approach such that the initial high-pH results are not directly comparable with the final low-pH results. With high-pH concrete, the time to crack penetration of the roof increases by approximately [illegible] years for both intermediate level vaults, and the time to collapse increases by approximately 800 years.

An issue that was beyond the scope of this project was the performance of the clay layer overlying the vault. It may be worthwhile to investigate whether cracks in the concrete can result in cracks in the clay. This would increase the hydraulic conductuctivity of the clay layer and therefore of the clay/roof system. Furthermore, the clay layer is assumed to maintain the same thickness and size over the long time frames of the simulation. The accuracy of this should be investigated, as well as the impact of changes in the clay layer on the performance of the vaults.

Other issues not addressed in this project include the long-term performance of waterstops and control joints, of waterproof coatings placed on the exterior of the vaults, and the longevity of the sealed shrinkage cracks.

Finally, the hydrogen evolution corrosion rate is a significant source of uncertainty in the model. Any work that could determine this rate with greater accuracy would decrease the uncertainty in the model predictions.

9. SUMMARY AND CONCLUSIONS

This study has demonstrated a capability to estimate the degradation of the Tuffera Vault structures and to utilize information on the degraded vaults to predict the times to failure (loss of ability to divert water) and collapse of the structures. The primary source of uncertainty in the model is the rate of rebar corrosion due to the anodic hydrogen evolution reaction, which results in uncertainty of approximately one order of magnitude.

- Degradation processes considered were magnesium and sulfate attack, calcium leaching, carbonation, and rebar corrosion due to both oxygen diffusion to the rebar (including breakdown of the passivating layer that initially prevents corrosion of rebar) and due to the "hydrogen evolution" reaction. Existing empirical models for the individual degradation processes were combined into a single model to create an overall model of the degradation of reinforced concrete. The degradation processes were used to predict the condition of the concrete, including its strength, thickness and hydraulic conductivity. The evaluation of structural response to loads and other influences (e.g., slow and steady degradation of reinforced concrete) is made on the basis of the equilibrium of forces and compatibility of deformation within the structure and in the surrounding media using the RCPC computer code as a foundation. In addition, the NAWY models were used to calculate loss in prestress in the beams due to elasticity loss, creep, shrinkage and relaxation. The state of stress in the concrete was calculated and the roof components and walls fractured in order to eliminate excessive stress which cannot be borne by the degraded structure. Crack width and spacing were also computed. By combining the degradation and structural models into a single performance assessment tool, sensitivity analysis can be conducted to determine the impact both of variation in important degradation processes and of changes in design parameters on the service life of the vaults.

Structural data for each vault type was based on a review of design drawings provided to INTERA by WSRC. Relevant environmental data (such as sulfate concentration in groundwater) were obtained through the Idaho National Engineering Laboratory (INEL). Corrosion rates were based upon an extensive literature review. All structural and degradation parameters were reviewed by WSRC and INEL. Structural analysis and calculations were reviewed by an expert structural engineer who specializes in the field of design of reinforced concrete structures.

For each type of vault, sensitivity analysis was performed to bound the predictions. After an initial rough sensitivity analysis on a large number of factors, six factors were selected for detailed sensitivity analysis: rate of rebar corrosion due to the "hydrogen evolution" reaction, rebar diameter, depth of concrete cover over the rebar, size of AASHTO "bridge" beams used to support the vault roof in the LAW vault design, and depth of soil cover over the vaults, and concrete strength. Output parameters for the sensitivity analysis were the time to first crack penetration of the vault roof, time to first crack penetration of the vault walls, and time to structural failure (collapse) of the vault roof. Times to crack penetration

are important because the hydraulic conductivity increases by approximately 3 orders of magnitude (over that of intact concrete) upon crack penetration.

From the calculations in this study, we have concluded:

That concrete strength, and, for the low-pH concrete being used in the E-Area vaults, depth of concrete cover over the rebar, have little impact on the vault performance. Depth of soil cover can alter the service life of the vaults on the order of hundreds of years, and rebar size can alter the service life of the vaults on the order of hundreds to thousands of years. Changing the size of the AASHTO beams in the LAW Vaults will change the time to collapse of the vaults on the order of several hundred years. Using a smaller beam, however, is not recommended (unless beam spacing is decreased appropriately), as stress levels in the roof-slab-rebar over the walls will result in crack penetration of the roof upon soil loading.

Future work should include a similar analysis of cracking of the vault floors; in order to accurately assess flow out of the vaults, it is necessary to estimate the time to crack penetration of the vault floors. Sensitivity analyses beyond those conducted for this study could be conducted for structural parameters such as roof thickness, rebar spacing, AASHTO beam spacing, length, width and height of the vaults, and wall thickness, as well as degradation model inputs such as oxygen diffusion rate in the concrete, leach rate, carbonation rate, or time to depassivation of the rebar. In addition, if high-pH concrete is used, additional sensitivity analysis should be conducted on degradation mechanisms important in high-pH concrete. Mechanisms that may result in loss of bonding between rebar and concrete should be investigated and quantified. In addition, performance of the clay layer overlying the vault, of waterstops and control joints, of waterproof coatings placed on the exterior of the vaults, and the longevity of the sealed shrinkage cracks all could warrant further study. Finally, any work that could determine the anoxic (hydrogen evolution) corrosion rate in rebar with greater accuracy would decrease the uncertainty in the model predictions.

This project has demonstrated the ability of the code to estimate the impact of changes in design parameters on the longevity of reinforced concrete structures. The code therefore has potential for application as a design aid tool for below-ground concrete storage facilities. The current mandate at DOE facilities to move in the direction of below-ground disposal in concrete-engineered structures makes this code a potentially important performance assessment tool.

Table 1. Summary of Output Parameters

Parameter Description	Units
Degradation Parameters	
% of rebar volume lost due to the oxygen-diffusion limited reaction	%
% of rebar volume lost due to the hydrogen evolution reaction	%
total loss of rebar at the exterior and interior face of the slab	% volume loss remaining diameter (cm)
depth of SO_4 penetration	cm
$Ca(OH)_2$ leach penetration via the concrete-controlled assumption	cm
$Ca(OH)_2$ leach penetration via the geology-controlled assumption	cm
total leach $Ca(OH)_2$ penetration	cm
depth of carbonation penetration	cm
fracture aperture	mm
fracture spacing	m
effective hydraulic conductivity	m/s
Structural Parameters	
moments at critical stress regions	ft-kip
shear at critical stress regions	kip
concrete stresses at critical stress regions	psi
rebar stress at critical stress regions	ksi
concrete cracking stress	psi
concrete shear limit stress	psi
LAW Vault Curvature Parameters	
curvature over walls	radians/in
depth of neutral axis	inch and cm
stress in rebar due to curvature	ksi

Table 2. Structural Input for the ILNT Vault

variable	"mean"	range	justification
[illegible]			
[illegible]	[illegible]	[illegible]	[illegible]
roof center to first wall center	27 ft		
inner wall center to center	26.5 ft		
roof thickness .	33 inches	27 - 39 inches	
columns			
outer wall thickness	30 inches		
inner wall thickness	18 inches		
misc			
concrete cover over rebar	2.375 inches	1.5 - 3 inches	2.375 actual on blueprint, 2-3 accepted range; may want to go to 4
exterior face bar area	1.58 in^2		
interior face bar area	.79 in^2		
concrete compressive strength	4750 psi		midpoint of minimum spec (4,000) and minimum test (5,500)
rebar yield strength	60 ksi		
degradation			
maximum spacing (outside, at stress points)	12 inches		
rebar diameter	1 inches = 2.5cm		

(1) based on 29'8" wall and 2'3" to 3'3" roof thickness

Table 3. Structural Input for the ILT Vault

Variable	baseline	range	justification
Spans			
wall center to wall center	30.5 - 32 ft	30.25 - 32.75 ft	[illegible]
roof center to first wall center	27 ft		
inner wall center to center	N.A.		
roof thickness	48 inches	42 - 54 inches	
columns			
outer wall thickness	30 inches		
inner wall thickness	18 inches		
misc			
concrete cover over rebar	2.375 inches	1.5 - 3 inches	allowable range
exterior face rebar area	1.58 in^2		
interior face rebar area	.79 in^2		
concrete compressive strength	4750 psi		midpoint of minimum spec (4,000) and minimum test (5,500)
rebar yield strength	60 ksi		
degradation			
maximum spacing (outside, at stress points)	12 inches		
rebar diameter	1 inches = 2.5cm		

(1) based on 28'6" wall and 3'6" to 4'6" roof thickness

Table 4. Structural Input for the LAW Vault

Variable	Value	Source
AASHTO I-Beams		
Length of I-beam	52'	Tindall
Top flange width	20"	Tindall
Top flange depth	11"	Tindall
Bottom flange width	26"	Tindall
Bottom flange depth	8"	Tindall
Total depth	54"	Tindall
Web width	8"	Tindall
Concrete compressive strength at 28 days	6,000 psi	Tindall
Concrete compressive strength at prestress	5,000 psi	Tindall
Eccentricity at midspan	17.13	Tindall
Eccentricity at support	12	Tindall
Ultimate strength of prestress steel	250,000 psi	Tindall
Initial prestress	202,500 psi	Tindall
Yield strength of prestress steel	240,000 psi	Tindall
Young's modulus of prestress steel	28,700,000	Tindall
Area of prestress steel	7.01 $inch^2$	Tindall
Number of tendons	42	Tindall
Thickness of roof panels	3"	Design drawings
Thickness of roof slab	16"	Design drawings
rebar area in roof slab	0.88 in^2/foot	Design drawings
prestress loss	22%	Tindall, confirmed by NAWY10

Table 5. Design Drawings Used

Drawing Number	Revision Number	Title
AA981BC-11-A-TCJ		AASHTO BEAMS AND ROOF PANELS (BY TINDALL CONCRETE, INC.)
SE5-6-2003303	2	BURIAL GROUND EXPANSION ILT VAULT JOINTS LOCATIONS & DETAILS (U) CONCRETE
SE5-6-2003304	1	BURIAL GROUND EXPANSION ILT VAULT BASE SLAB PLANS (U) CONCRETE
SE5-6-2003305	0	BURIAL GROUND EXPANSION ILT VAULT WALLS REINFORCING ELEVATIONS CONCRETE
SE5-6-2003306	0	BURIAL GROUND EXPANSION ILT VAULT WALLS SECTIONS & DETAILS CONCRETE
SE5-6-2003307	0	BURIAL GROUND EXPANSION ILT VAULT WALLS & CRANE RUNWAY PLAN AND SECTIONS CONCRETE
SE5-6-2003308	2	BURIAL GROUND EXPANSION ILNT VAULT JOINTS LOCATIONS & DETAILS (U) CONCRETE
SE5-6-2003309	0	BURIAL GROUND EXPANSION ILNT VAULT BASE SLAB PLANS CONCRETE
SE5-6-2003310	1	BURIAL GROUND EXPANSION ILNT VAULT WALLS REINF'G ELEVATIONS (U) CONCRETE
SE5-6-2003311	1	BURIAL GROUND EXPANSION ILNT VAULT WALLS SECTIONS & DETAILS (U) CONCRETE
SE5-6-2003315	0	BURIAL GROUND EXPANSION ILT VAULT PERMANENT ROOF SLAB PLAN & SECTIONS (FUTURE) CONCRETE

Drawing Number	Revision Number	Title
SE5-6-2008317	0	BURIAL GROUND EXPANSION LAW VAULT PERMANENT ROOF SLAB PLAN & SECTIONS (FUTURE) CONCRETE
SE5-6-2008313	2	BURIAL GROUND EXPANSION LAW VAULTS GENERAL NOTES AND LEGEND (U) CONCRETE
SE5-6-2008800	1	BURIAL GROUND EXPANSION LAW VAULT JOINTS LOCATIONS & DETAILS CONCRETE
SE5-6-2008801	1	BURIAL GROUND EXPANSION LAW VAULT GENERAL NOTES AND LEGEND CONCRETE
SE5-6-2008802	0	BURIAL GROUND EXPANSION LAW VAULT FOUNDATION, SLAB & ROOF FRAMING KEY PLANS CONCRETE
SE5-6-2008803	1	BURIAL GROUND EXPANSION LAW VAULT FOUNDATION & FLOOR SLAB PLAN - MODULE 1 CONCRETE
SE5-6-2008806	0	BURIAL GROUND EXPANSION LAW VAULT ROOF FRAMING & SLAB PLAN - MODULE 1 CONCRETE
SE5-6-2008809	0	BURIAL GROUND EXPANSION LAW VAULT WALLS ELEVATIONS SHEET 1 CONCRETE
SE5-6-2008810	1	BURIAL GROUND EXTENSION LAW VAULT WALLS ELEVATIONS SHEET 2 CONCRETE
SE5-6-2008811	0	BURIAL GROUND EXPANSION LAW VAULT WALLS ELEVATIONS SHEET 3 CONCRETE
SE5-6-2008812	1	BURIAL GROUND EXPANSION LAW VAULT WALLS SECTIONS & DETAILS SHEET 1 CONCRETE

Drawing Number	Revision Number	Title
SE5-6-2008813	1	BURIAL GROUND EXPANSION LAW VAULT WALLS SECTIONS & DETAILS SHEET 2 CONCRETE
SE5-6-2008814	1	BURIAL GROUND EXPANSION LAW VAULT WALLS SECTIONS & DETAILS SHEET 3 (FUTURE) CONCRETE
SE5-6-2008815	1	BURIAL GROUND EXPANSION LAW VAULT WALLS SECTIONS & DETAILS SHEET 4 CONCRETE
SE5-6-2008816	0	BURIAL GROUND EXPANSION LAW VAULT ROOF FRAMING & SLAB SECTIONS & DETAILS CONCRETE
SE5-6-2008817	0	BURIAL GROUND EXPANSION LAW VAULT PRESTRESSED ROOF BEAMS SECTIONS & DETAILS CONCRETE
W2017824	C	BURIAL GROUND EXPANSION ILT, ILNT & LAW VAULTS CLOSURE CONCEPT SITE PLAN CIVIL
W2017825		BURIAL GROUND EXPANSION ILT & ILNT VAULTS CLOSURE CONCEPT SITE CROSS SECTIONS CIVIL
W2017826	B	BURIAL GROUND EXPANSION LAW VAULTS CLOSURE CONCEPT SITE CROSS SECTIONS CIVIL
W2017827		BURIAL GROUND EXPANSION ILT & ILNT VAULTS CLOSURE CONCEPT PLAN AND SECTIONS CIVIL
W2017828	B	BURIAL GROUND EXPANSION LAW VAULTS CLOSURE CONCEPT PLAN & SELECTIONS CIVIL
W2020320	1	BURIAL GROUND EXPANSION ILT VAULT CRUCIBLE SILOS PLAN AND SECTIONS CONCRETE

Drawing Number	Revision Number	Title
W2020372	B	BURIAL GROUND EXPANSION LAW VAULTS CONSTRUCTION STRATEGY SITE CROSS SECTIONS CIVIL
W2020422	1	BURIAL GROUND EXPANSION ILT VAULT CRUCIBLE SILOS DETAILS CONCRETE

Table 6. Summary of Degradation Model Variables and Values

Variable	Definition	Scenario	Min/ Mean/ Median/ Maximum	Reference
Hydrogen Evolution Rebar Corrosion				
H2RATE1	Rate of rebar corrosion due to hydrogen evolution (cm/yr) at high pH (before calcium leaching or carbonation penetrate to rebar).	Minimum	1E-5	(6)
		Baseline	8E-5	(6)
		Maximum	1.5E-4	(6)
H2RATE2	Rate of rebar corrosion due to hydrogen evolution (cm/yr) at low pH (after calcium leaching or carbonation penetrate to rebar).	Minimum	1E-4	(6)
		Baseline	5E-4	(6)
		Maximum	1E-3	(6)
Chloride Initiation of Oxygen-based Rebar Corrosion				
COV	Required clear cover over bars (cm).	Minimum	7.62	design drawings
		Baseline	6.03	design drawings
		Maximum	5.08	design drawings
CLSOIL	Chloride ion concentration in groundwater (ppm).	Minimum	0.44	(1), p.2
		Baseline	1.3	(1), p.2
		Maximum	5.3	(1), p.2

WCR	Water to cement ratio (kg/kg).	Minimum	0.40	Assumed
		Baseline	0.44	(2), p.4
		Maximum	0.48	Assumed
Oxygen Corrosion of Rebar				
COV	Required clear cover over bars (cm).	Minimum	7.62	Design drawings
		Baseline	6.03	Design drawings
		Maximum	5.08	Design drawings
O2DICONC	Oxygen diffusion coefficient in concrete (cm^2/s).	Minimum	2E-8	(1), p.4; from (2)
		Baseline	1E-7	(2), p.4
		Maximum	2E-6	(2), p.4
O2SOIL	Oxygen concentration in groundwater ($mole/cm^3$).	Minimum	1.25E-7	(2), p.4
		Baseline	2.47E-7	(2), p.4
		Maximum	3.125E-7	(2), p.4
Concrete Controlled Leaching				
CADICONC	Intrinsic diffusion coefficient of Ca++ in concrete (cm^2/s).	All	1E-7	(2), p.4

CASOIL	Ca++ concentration in ground-soil water (mole/cm³).	Minimum	4.82E-7	(1), p.7
		Baseline	2.35E-8	(1), p.7
		Maximum	2.5E-9	(1), p.7
CASOLID	Bulk Ca++ concentration in concrete solid (mole/cm³).	Minimum*	0.0035	(2), p.4
		Baseline*	0.003	(2), p.4
		Maximum*	0.0025	(2), p.4
	Geology-Controlled Leaching			
CADICONC	Intrinsic diffusion coefficient of Ca++ in concrete (cm²/s).	All	1E-7	(2), p.4
CAPORE	Ca++ concentration in concrete pore liquid (mole/cm³).	All	2.7E-6	(2), p.4
CASOIL	Ca++ concentration in ground-soil water (mole/cm³).	Minimum	4.82E-7	(1), p.7
		Baseline	2.35E-8	(1), p.7
		Maximum	2.5E-5	(1), p.7
CASOLID	Bulk Ca++ concentration in concrete solid (mole/cm³).	Minimum*	0.0025	(2), p.4
		Baseline*	0.003	(2), p.4
		Maximum*	0.0035	(2), p.4
DE	Effective dispersivity/diffusivity of Ca in geologic material (cm²/s).	Minimum	1E-6	(2), p.5
		Baseline	2E-6	(2), p.5
		Maximum	3E-6	(2), p.5

RD	Retardation factor of Ca in geologic material (ml/cm³).	Minimum	2	(2), p.4
		Baseline	3	(2), p.4
		Maximum	5	(2), p.4
Carbonation				
CODICONC	Diffusion coefficient of CO_2 in concrete (cm²/s)	all	1E-7	(2)
CSOIL	Inorganic carbon content in the soil (mole/cm³)	minimum	1.83E-7	(2)
		baseline	4.33E-7	(2)
		maximum	6.78E-7	(2)
CAOHCONC	$Ca(OH)_2$ concentration in concrete (mole/cm³)	minimum	0.0072	(2)
		baseline	.001485	average
		maximum	0.03225	(2)
Sulfate Attack				
C3A	C3A content in concrete (weight %; e.g. 8 for 8%).	minimum	7	assumed
		baseline	8	(1), p.6; (2), p.4
		maximum	9	assumed
SO4MGSOL	Sum of SO4 and Mg concentrations in soil solution (mole/l).	minimum	1.51E-5	(1), p.6
		baseline	1.08E-4	(1), p.6
		maximum	3.77E-4	(1), p.6

(1) Dicke, 1993.
(2) Walton and Dicke, 1993.
(3) Walton, Plansky, and Smith, 1990.
(4) Walton, J.C. 1993. Unpublished.
(5) Langton, Chris. 1993. Personal communication.
(6) Summarized from Grauer, *et al.*, 1991, Hansson, 1985, Marsh and Taylor, 1988, and Morley, 1986.
(7) Seitz, 1993.
* CASOLID acts in opposite directions for geology-controlled and concrete-controlled leaching; therefore it is not possible to maximize or minimize <u>both</u> leach rates in the <u>same</u> simulation run.

Table 7. Summary of Rebar Stress (ksi) in ILT Baseline Scenario

Time (years)	Walls			Roof Spans		
	Bottom	Mid-Height	Top	Over Exterior Wall	Mid-Span	Over Interior Wall
800	14.2	27.9	16.9	16.9	40.8	38.1
850	15.1	29.6	18.0	18.0	43.3	[illegible]
1,100	20.9	41.0	24.9	24.9	59.8	[illegible]
1,225	25.3	49.3	30.0	44.0	60.0	[illegible]
1,300	28.5	55.6	33.9	61.4	60.0	[illegible]

Table 8. Summary of Rebar Stress (ksi) in ILNT Baseline Scenario

Time (years)	Walls			Exterior Cell			First Interior Cell			Central Cells		
	Bottom	Mid-Height	Top	Over Exterior Wall	Mid-Span	Over Interior Wall	Over Wall Towards Exterior	Mid-Span	Over Wall Towards Interior	Over Wall	Mid-Span	Over Wall
575	16.0	31.3	23.4	23.4	40.3	36.7	36.2	33.1	33.9	33.9	33.1	33.9
675	17.8	34.8	25.9	25.9	44.7	40.7	40.1	36.8	37.6	37.6	35.[illegible]	37.6
750	19.3	37.8	28.1	28.1	48.6	[illegible]	43.6	39.9	40.8	40.8	35.5	[illegible]
775	19.8	38.9	28.9	28.9	50.1	45.9	[illegible]	41.1	42.0	42.0	[illegible]	[illegible]
800	20.4	40.0	29.8	29.8	51.4	46.7	46.1	42.3	43.2	43.2	[illegible]	[illegible]
1,000	26.1	51.2	38.1	41.0	60.0	60.0	58.9	54.1	55.2	55.2	[illegible]	55.2
1,050	27.9	54.7	40.7	49.4	60.0	60.0	62.0	60.0	61.0	59.0	[illegible]	[illegible]
1,075	28.8	56.6	42.1	54.9	60.0	60.0				61.8	[illegible]	[illegible]
1,125	31.4	60.0	45.6	65.1	60.0	79.[illegible]						

(1) "Central Cells" refers to cells 3, 4, and 5 in Figure 1.

Table 9. Summary of Baseline Results

Vault	Cracks Penetrate the Roof (years)	Cracks Penetrate Walls (Mid-Height) (years)	Roof Collapse (years)
IGNT	570	800	1,045
ILT	790	1,080	1,300
LAW	1,420	2,235	3,100

Table 10. Summary of ILNL Vault Sensitivity Analyses

Scenario	Cracks Penetrate Roof	Cracks Penetrate Walls (Mid-Height)	Roof Collapse
Baseline	570	800	1,045
Hydrogen Evolution Corrosion Rate (Baseline = 5E-4 cm/yr)			
1E-3	285	400	525
7.5E-4	380	535	700
2.5E-4	1,130	1,590	2,075
1E-4	2,775	3,000+	3,000+
Depth of Soil Cover (Baseline = 9 feet)			
8 feet	680	850	1,130
12 feet	400	590	925
16 feet	130	360	725
Rebar Size (Baseline = #8)			
#6	0	175	425
#7	250	485	735
#9	875	1,105	1,350
#11	1,785	1,965	2,150
#18	3,000+	3,000+	3,000+
Depth of Concrete Cover Over Rebar (Baseline = 2⅜")			
1½"	600	825	1,060
3"	550	780	1,030
Concrete Strength (Baseline = 4,750 psi)			
3,000 psi	570	800	1,040
6,000 psi	570	800	1,045

A "+" indicates that the event did not occur prior to the end of the simulation.

Table 11. Summary of ILT Vault Sensitivity Analyses

Scenario	Cracks Penetrate Roof	Cracks Penetrate Walls (Mid-Height)	Roof Collapse
Baseline	790	1,080	1,300
Hydrogen Evolution Corrosion Rate (Baseline = 5E-4 cm/yr)			
1E-3	395	535	655
7.5E-4	525	725	865
2.5E-4	1,560	2,155	2,565
1E-4	3,000+	3,000+	3,000+
Depth of Soil Cover (Baseline = 9 feet)			
8 feet	850	1,140	1,340
12 feet	625	940	1,180
16 feet	415	735	1,035
Rebar Size (Baseline = #8)			
#6	155	460	680
#7	470	770	985
#9	1,190	1,380	1,600
#11	1,950	2,185	2,340
#18	3,000+	3,000+	3,000+
Depth of Concrete Cover Over Rebar (Baseline = 2⅜")			
1½"	800	1,100	1,300
3"	775	1,075	1,290
Concrete Strength (Baseline = 4,750 psi)			
3,000 psi	790	1,080	1,300
6,000 psi	790	1,080	1,300

A "+" indicates that the event did not occur prior to the end of the simulation.

Table 12. Summary of LAW Vault Sensitivity Analyses

Scenario	Cracks Penetrate Roof	Cracks Penetrate Walls			Roof Collapse
		Top	Mid-Height	Bottom	
Baseline	1,420	2,015	2,235	2,300	3,110
Roof/Roof & Walls	Hydrogen Evolution Corrosion Rate (Baseline = 8E-5/5.0E-4 cm/yr)				
1.5E-4/1E-3	710	1,010	1,150	1,150	1,600
1.15E-4/7.5E-4	950	1,350	1,550	1,550	2,100
4.5E-5/2.5E-4	2,820	4,000	4,480	4,550	5,400
1E-5/1E-4	6,900	9,750	10,000+	10,000+	10,000+
Depth of Soil Cover (Baseline = 9 feet)					
8 feet	1,420	2,100	2,360	2,410	3,290
12 feet	1,420	1,900	2,185	2,235	2,610
16 feet	1,420	1,730	2,050	2,115	2,060
Walls/Roof Slab	Rebar Size (Baseline = #10/#6)				
#7/#5	1,120	1,100	1,325	1,400	3,110
#9/-	-	1,700	1,940	2,000	3,110
#14/#8	2,020	(3,150)	(3,410)	(3,450)	3,110
#18/#14	(3,800)	(4,440)	(4,710)	(4,750)	3,110
AASHTO Beam Size (Baseline = Type IV)					
Type III	0	2,015	2,235	2,300	2,700
Type V	1,420	2,015	2,235	2,300	3,430
Depth of Concrete Cover Over Rebar (Baseline = 2⅜")					
1½"	1,420	2,015	2,250	2,300	3,110
3"	1,415	2,015	2,250	2,300	3,110
Concrete Strength (Baseline = 4,750 psi)					
3,000 psi	1,420	2,015	2,235	2,300	3,110
6,000 psi	1,420	2,015	2,235	2,300	3,110

A "+" indicates that the event did not occur prior to the end of the simulation.
Values in parentheses () indicate that roof collapse will occur prior to the indicated crack penetration.

Table 13. Summary of Baseline Results Assuming High-pH Concrete

Vault	Cracks Penetrate Roof (years)	Roof collapse (years)
ILLW	1,200	1,840
ILT	1,375	2,225
LAW	Not Available	

REFERENCES

Asquith, S. 1993. Personal Communication. Conversation June 29, 1993 between Jim L. Lolcama of INTERA, Inc. and Shawn Asquith of Rust E and I.

Atkinson, A. and Hearne, J.A. 1984. "An Assessment of the Long Term Durability of Concrete in Radioactive Waste Repositories". AERE-R11465, Harwell, UK.

Crank, J. 1975. *The Mathematics of Diffusion.* Oxford University Press, Oxford.

Das, B.M. 1985. *Principles of Geotechnical Engineering.* PWS Puvliahwea, Boston, MA. 571p.

Dicke, C. 1993. FAX of 3/29/93.

Furlong, R.W. 1991. *Reinforced Concrete Personal Computer Design Handbook.* Prince, Davidson, & Wilson. Austin, TX. 77 pages.

Furlong, R.W. 1993. "Uniform Loading of Rectangular Flat Plates." Unpublished correspondence, June 3, 1993.

Grauer, P., Knecht, B., Kreiss, P. and Simpson, J.P. 1991. "Hydrogen Evolution from Corrosion of Iron and Steel in Intermediate Level Waste Repositories." *Material Research Society Symposium Proceedings* 212:295-302.

Hansson, C.M. 1985. "The Corrosion of Steel and Zirconium in Anaerobic Concrete." *Material Research Society Symposium Proceedings* 50:475-482.

Harrison, W.H. and Teychenne, D.C. 1981. *Sulphate Resistance of Buried Concrete: Second Interim Report on Long Term Investigation at Northwick Park.* Building Research Establishment, Her Majesty's Stationery Office, London.

Marine, I.W. 1976. *Geochemistry of Groundwater at the Savannah River Plant.* DP-1356. September, 1976. E. I. du Pont de Nemours and Company, Savannah River Laboratory, Aiken, SC.

Marsh, G.P. and Taylor, K.J. 1988. "An Assessment of Carbon Steel Containers for Radioactive Waste Disposal." *Corrosion Science* 28.3:289-320.

McEnroe, B.M. 1993. "Maximum Saturated Depth Over Landfill Liner." Journal of Environmental Engineering 119.2.

Morley, J. 1986. "Corrosion of Steel Foundation Caissons from the Old Redheugh Bridge in Newcastle upon Tyne." *British Corrosion Journal* 21.3:177-183.

Nawy, E.G. 1989. *Prestressed Concrete Computer Programs in BASIC*. Prentice Hall. New Jersey.

Seitz, R.R. 1993. FAX of March 22, 1993.

Tindall Concrete. 1993. "Design Calculations for LAW Vault Expansion Modules Two and Three. Prepared for the United States Department of Energy, Savannah River Site. February 12, 1993, P.O. AA98143C, Project S-2[illegible]/4466, Job No. 52-106.

Walton, J.C. 1993. "E-Area Vault Effective Permeability and Reinforcement Corrosion". Unpublished correspondence, July 6, 1993.

Walton, J.C. 1993. "Degradation of Reinforced Concrete." Unpublished.

Walton, J.C. and Dicke, C. 1993. "E-Area Notebook for ILNT/ILT Vaults: Degradation Calculations, (4-13-93) latest mix design data."

Walton, J.C., Plansky, L.E. and Smith, R.W. 1990. *Models for Estimation of Service Life of Concrete Barriers in Low-Level Radioactive Waste Disposal*. Idaho National Engineering Laboratory. NUREG/CR-5542, EGG-2597.

ACRONYMS AND ABBREVIATIONS

ACI	American Concrete Institute
cm	centimeter
C_3A	tri-calcium aluminate
EAV	Ex-Area Vaults
ft	feet
in	inch
ILNT	intermediate-level non-tritium
ILT	intermediate-level tritium
INEL	Idaho National Engineering Laboratory
kip	1,000 pounds
ksi	1,000 pounds per square inch
LAW	low-activity waste
LLWSB	Long-Lived Waste Storage Building
m	meter
mm	millimeter
ppm	parts per million
psi	pounds per square inch
s	second
SRS	Savannah River Site
WSRC	Westinghouse Savannah River Company
yr	year

APPENDIX: QUALITY ASSURANCE

This Appendix is divided into three parts. First, the implementation of the Project Quality Assurance Plan is discussed. Next, the letter report describing INTERA's plan and procedures for software and technical reporting quality assurance for the E-Area Vaults Degradation Study is provided. Finally, forms used in maintaining Quality Assurance Control during the project are provided.

A.1 IMPLEMENTATION OF THE PROJECT QUALITY ASSURANCE PLAN

The RCPC.DHelper models (Furlong, 1991) used as the basis for the structural analysis portion of this study are available commercially through the American Concrete Institute Software Sales Department. The programs have been in use for the past 4 years by approximately 300 engineering offices.

The RCPC computer software for the analysis of reinforced concrete structures has formed the basis for this project. This software has been validated by the author. The software is divided into five main subroutines which do not interact, with each subroutine appropriate for a particular application. For the E-Area Vaults, the "Continuous Beams" program was utilized. This program was tested by using a sample data set available in the manual (Furlong, 1991), and comparing the computed results with results printed in the manual. All results were identical. Another program, NAWY10, was used to analyze the time-dependant loss of prestress in the AASHTO beams. In the same way, a sample data set available in the manual (Nawy, 1989) was used for testing the program. Computed results matched results printed in the manual.

There were four main revisions to the RCPC code:

1. Original program was designed for screen-based input and output. In order to facilitate the multiple runs necessary for the sensitivity analysis and calculation of stress levels through time, the program was modified to utilize file-based input and output.

2. Degradation subroutine was added.

3. A time loop was added to recursively calculate the vault condition through time.

4. For the LAW vault case, a section was added to compute the stress due to curvature and the depth of the neutral axis in the roof slab.

After the code was modified to utilize file-based input and output, an additional test was performed using the manual-supplied input and output. In addition, a data set was created appropriate for the E-Area Vaults. This data set was run in both the original model and in the modified model. Again, all results were identical.

Next the degradation subroutine and time loop were added. Degradation model components included:

- Time to depassivation of rebar.
- Oxic corrosion of rebar.
- Anoxic ("hydrogen-evolution") corrosion of rebar.
- Sulfate attack.
- Calcium hydroxide leaching.
- Carbonation.
- Calculation of fracture aperture and spacing.

Testing of this modification consisted of two phases. First, results of the degradation model were compared to results obtained by modeling performed at INEL. There were extremely slight differences between INEL model results and INTERA results, easily attributed to rounding error. Next, testing was performed on the structural component of the code. The time zero results for the code were compared to the results obtained from the unmodified RCPC code. Because no degradation has taken place at time zero, these results should be, and were, the same. For the LAW vault modifications to calculate stress due to curvature in the roof, testing was performed by comparing model results to spreadsheet calculations.

All changes are documented in detail within the modified code, both at the point of modification and, in chronological order, at the top of the code.

Performance and Design Specifications were generated for the modifications to the RCPC.DHelper code, in order to incorporate concrete degradation, and were established as controlled documents (i.e., they were approved by the program manager and quality assurance manager and had a control date assigned). Performance and Design Specifications for RCPC.DHelper and NAWY10 were taken from the documentation for these codes and established as controlled documents. Performance Specifications for both acquired codes and modifications included the following components:

- a general description of RCPC.DHelper, NAWY10, and modifications to the RCPC.DHelper code, and the intended use of information expected from the codes, including relevant contract specifications.
- a description of physical and chemical phenomena accounted for and any important phenomena neglected.
- statement of relevant mathematical equations and derivations.

- statement and rationalization of applicable assumptions, limitations and simplifications.

- a general description of the type of output information.

- a general description of the type of input information.

- references.

Design Specifications for both acquired codes and modifications included the following components:

- Description of numerical techniques used to solve governing equations.

- Statement of relevant discretized (or otherwise transformed for numerical solution) equations and derivations.

- Statement and rationalization of applicable assumptions and limitations.

- Description of the structure and organization of the computer programs, including logic flow.

- Description of program input and output.

- Description of code/system interfaces.

- Glossary of model variables.

RCPC.DHelper and NAWY10 software was baselined (i.e., entered into the Control File Index at our Austin, TX headquarters). Modifications to software were identified, documented, and tracked through the Control File Index. All data and results which were used in formal code testing and applications were baselined. The project report was baselined and subjected to internal (i.e., within INTERA) review before being submitted to WSRC. The review was documented in the form of required changes, recommended changes and other observations, in writing on a copy of the draft document. After changes were made in response to the internal review, the report was again baselined and submitted to WSRC with the subtitle "Draft Report." All comments in response to WSRC review were received verbally only. Therefore, INTERA prepared a memo summarizing the review comments and distributed copies to WSRC and to the Control File Index at INTERA headquarters. After response to WSRC comments was completed, the report was again baselined and submitted to WSRC as the final report for this Task #7.

INFORMATION ONLY

A.2 PROJECT QUALITY ASSURANCE PLAN

Mr. Shawn Reed
WSRC
Savannah River Technology Center
Solid Waste Engineering
#742-7G
Aiken, SC 29802

May 20, 1993

Re: Quality Assurance Procedures for Software and Technical Reports Under Contract #AA20130P-Task Order 7

Dear Mr. Reed:

The following letter report describes INTERA's plan and procedures for software and technical reporting quality assurance for the E-Area Vaults Degradation Study. This letter report is intended to satisfy Paul Lowe's request at the May 10 status meeting for a summary QA plan for the structural analysis software currently being used on this project and report deliverables. Software for this project has been developed primarily outside of INTERA. The software is two structural analysis codes for concrete structures obtained from the University of Texas at Austin and Rutgers University. Through a co-operative effort between the code authors and INTERA-AUGUSTA the codes are currently being modified to allow, (1) input of concrete thickness and re-bar spacing, (2) the use of file handling for input and output rather than the interactive default mode, and (3) chemical degradation of the reinforced concrete.

The QA plan and procedures for computer software and report deliverables have been taken from INTERA's Project Quality Assurance Manual prepared for the Westinghouse Savannah River Company (Draft; December 20, 1990). This NQA-1 manual has been submitted for approval with WSRC, however this approval is pending. We anticipate a review of the manual prior to the end of the current fiscal year.

PART A PROJECT QUALITY ASSURANCE PLAN

Quality assurance calls for baselining software and supporting documentation through the assignment of Control Identification Numbers (CIN's) and entry into the project Control File Index (CFI). The QA plan requires, for codes developed outside of INTERA, review, verification, validation (when possible) and documentation of software modification activities. Changes to baselined software shall also be identified and tracked through the CFI and shall be subject to review, approval, verification and validation as appropriate. Changes to baselined software shall require documentation and this documentation shall be entered into the CFI. In addition, procedures for the revision of baselined software shall require

identification of any baselines which might require changes as a result of the revision, and that users of affected software be notified of any revisions.

INTERA shall verify the suitability of previously developed computer codes by:

1. Reviewing previous applications of the code(s);

2. Performing a validation of the code(s) for the contract application by inputing data representative of the application;

3. Exercising the code(s) under expected use conditions; and

4. Evaluating the limitations of the code(s).

Results of the validation process shall be documented and entered into the project CFI. A summary report of the results shall be provided to the client.

The structural analysis code(s) adapted for this project are considered proprietary to the author, Dr. Richard Furlong, University of Texas at Austin and Dr. Edward Nawy, Rutgers University. The source code and documentation have been provided to INTERA for adaptation and use on this project without cost to WSRC.

PART B PROJECT QUALITY ASSURANCE PROCEDURES

TITLE: QA Control File and Index

The INTERA - AUGUSTA staff will be responsible for preparing and documenting records that will enter the QA Control File at our Corporate Headquarters in Austin. We will also be responsible for filing QA documents and documentation of client communications with the QA Administrator in Austin.

The INTERA - AUSTIN QA Administrator will be responsible for reviewing control documents, maintaining proper records storage, and maintaining the Control File Index.

TITLE: Baselining and Revising Baselined Specifications

Performance, Design, and Test Specifications shall be baselined for the major codes acquired and applied on this project.

When revising a code, Performance, Design, and Test Specifications shall be developed, baselined, and established as controlled documents (i.e., be approved by the program manager and quality assurance manager and have a control date and [illegible]).

An example of a QA Control Document which shall be completed for Specifications has been included as an attachment.

TITLE: Baselining and Revising Baselined Codes

All structural analysis codes shall be documented following acquisition for the project and during modification and testing. The documentation of the unmodified code(s) shall include: Test Data, Test Results, Validation History (if any), Code Abstract and Users Manual. Modifications which are completed by INTERA-AUGUSTA to the codes to allow, (1) the use of file handling for input and output rather than the interactive default mode, and (2) chemical degradation of the reinforced concrete will be documented with brief performance specifications, design specifications, and a comparison of the code output with empirical results from INEL.

In addition, each code should be accompanied by the following documentation, as appropriate: Code Name and Version Number, Brief Description of Code, Original Source Code and Original Author(s), Brief History of Major Modifications, Proprietary Details, Disclaimer, Language and Level, Machine Where Operative, and References.

An example of a QA Control Document which shall be completed for Computer Codes has been included as an attachment.

TITLE: Baselining and Revising Baselined Test, Application and Other Data

All data which are to be used in formal (i.e., documented) code testing or in code applications shall be baselined. Data should be characterized in detail. The documentation should include, at a minimum, the following: source and method of acquisition, appropriateness for the intended model application, and derivation of input data (processed data) from raw data.

All test and application data baselines shall be written to diskette with copies furnished to the QA Administrator.

Baseline data shall be revised as necessary to correct problems or to improve/ensure quality. Revised baselines shall include justification for the revision.

An example of a QA Control Document which shall be completed for Test/Application/Other Data has been included as an attachment.

TITLE: Baselining and Revising Baselined Test Results

All output data from the code testing phase shall be baselined. Testing of the unmodified structural analysis codes shall be limited to execution of the test problem provided with the code on the PC with which the structural analysis is to be completed. A formal review by the project engineer of the Test Results shall be completed to ensure the accuracy of the installed code.

Testing of the code modifications concerning deterioration of the reinforced concrete shall be limited to accurate reproduction of empirical data provided by INEL. Formal testing shall be reviewed by person(s) not involved in the modification of the code(s). Test Results shall be analyzed for satisfaction of Test Specifications.

The Test Results, and the analyses thereof, must be documented and baselined. A print-out of the Test Results and the Test Data shall be filed with the QA Administrator when Results are baselined.

An example of a QA Control Document which shall be completed for Test/Application Results has been included as an attachment.

TITLE: Baselining Application Results

The results of all code applications to be transmitted outside of, or relied upon by, INTERA or which yield significant information about the code's capabilities or limitations, or about measured data, or about the system or process being modeled shall be baselined.

Where possible input data should be printed in conjunction with the corresponding Application Results output. A copy of the Application Results and Application Data shall be filed with the QA Administrator when results are baselined.

TITLE: Baselining and Revising Baselined Technical Reports and Code Documentation

All Reports which are considered deliverables shall be baselined before transmission outside of INTERA. Code Documentation shall be baselined for internal control. For proprietary reasons, these Baselines will not be allowed outside of INTERA.

Topical Reports and Letter Reports which are specified as contract deliverables shall undergo formal technical review. Baselined reports shall be revised as necessary to correct problems, improve quality, or expand scope.

An example of a QA Control Document which shall be completed for Report/Code Documentation has been included as an attachment.

TTS 3: Technical Reviews.

Each Technical Report, Model Documentation Report, Letter Report, or other document containing technical information that is a project deliverable prepared to satisfy contract requirements shall be the subject of one of more technical reviews before being transmitted outside INTERA.

Documents and data shall be baselined before being submitted for technical review.

Reviews of reports and other documents should consider, as a minimum, the following items:

- Organization, clarity, and conciseness of the material presented;
- Correctness of any assumptions that are made;
- Adequacy of the discussion of variables;
- Validity of the conclusions and recommendations;
- Adequacy of illustrations, graphs, tabular data, etc.; and
- Appropriate acknowledgement of contributions and referenced material.

Reviews shall be documented with written comments in the form of required changes, recommended changes, and other observations. The review shall also document the material being reviewed (title or description), the author of the material, date of the review, and persons performing the review.

Review comments must be stated in terms which will clearly convey the meaning of the comment to others knowledgeable on the subject.

Review comments may be in the form of annotations on the document being reviewed if the comment can be adequately recorded in this manner. When such annotation is inadequate or inappropriate, the comment(s) shall be recorded on separate sheets.

Each review comment shall be responded to and resolved and the response/resolution shall be documented. When review comments are recorded on the document being reviewed, responses may also be recorded on the document.

All review comments recorded on separate sheets shall be responded to either on the review sheets or on separate sheets.

Editorial recommendations may be acknowledged in summary fashion, e.g., "implemented where possible".

When the technical reviewer is unable to accept the task manager's response to one or more required changes, the program manager shall be called upon to resolve the issue unless the program manager is involved in the disagreement, in which case one of the program manager's peers shall resolve the issue.

An example of a QA Control Document which shall be completed for Technical Reviews has been included as an attachment.

cc: Paul Lowe
Jim Cook
Keith Dykes

00/00/00

QA CIN: | --- | - | -- | - | --- | - |

YY MM DD

Control Date (OAAA Only): | -- | -- | -- |

SPECIFICATION BASELINE

☐ Original Baseline (Complete Section 1 only)

☐ Revision to Previous Baseline (Complete Sections 1 and 2)

Project Title: Project Number:

Contract No.:

CFI Description: _____

Section 1 - Baseline

1. Code Name: _____ Code CIN: _____

2. Source (Check one and complete):

This ☐ baseline ☐ revision was developed by: _____

Signature/Printed Name

This ☐ baseline ☐ revision was acquired from: _____

Printed Name/Organization

3. Specification Type (check one only):

☐ A. Peformance Specs.

☐ B. Design Specs.

☐ D. Test Specs.

4. Reference and Location of Specification (if not attached): _____

_____

5. Cross-Reference to other Specifications for this code: (where possible):

QA CIN _____ Control Date: _____

QA CIN _____ Control Date: _____

QA Control Document

00/00/00

QA CIN: ---- - -- - ---- -

YY MM DD

Control Date (QAAA Only): -- -- --

Section 2 - Baseline Revision

1. Reason for Revision:

a. ☐ Response to Review QA CIN: _____ Control Date: _____

b. ☐ Problem Report/ Corrective Action QA CIN: _____ Control Date: _____

c. ☐ Code Enhancement

d. ☐ Other: _____

2. Description of Revision:

3. Baselines which may require revision as a result of this revision:

Recommended by: _____ PM Date: YY MM DD -- -- --

Approved by: _____ QAM Date: YY MM DD -- -- --

QA Control Document

08/15/90

QA CIN: | _ _ _ | _ | _ _ | C | _ _ _ | _ |

YY MM DD

Control Date (QAAA Only): | _ _ | _ _ | _ _ |

CODE (C)

☐ Original Baseline (Complete Section 1 only)

☐ Revision to Baseline (Complete Sections 1 and 2)

Project Name: Project Number:
Contract No.:

CFI Description: _____

Section 1: Code Baseline

1. Code Name: _____

   ☐ Major Code ☐ Minor Code ☐ Commercial Utility Code

2. Source (check one and complete):

   a. This ☐ baseline ☐ revision was developed by: _____
   Signature(s)/Printed Name

   b. This ☐ baseline ☐ revision was acquired from: _____
   Printed Name

3. References:

   a. ☐ Performance Specs. QA CIN: _____ Control Date: _____

   b. ☐ Design Specs. QA CIN: _____ Control Date: _____

   c. ☐ Test Specs. QA CIN: _____ Control Date: _____

   d. ☐ Test Data QA CIN: _____ Control Date: _____

   e. ☐ Test Results QA CIN: _____ Control Date: _____

5. Hardware:

   a. ☐ PC b. ☐ Other (Specify): _____

   c. Special Requirements: _____

6. Compiler/Linker Options:

   a. ☐ FORTRAN a. ☐ PASCAL c. ☐ Other (Specify): _____

   d. Compiler & Options: _____ e. Linker & Options: _____

QA CIN: | --- | - | -- | C - | --- | -

7. Code Storage:

a. ☐ Tape Tape No: _____ Source File Title: _____
Executable File Title: _____ Format: _____

b. ☐ Disk Disk No: _____ Source File Title: _____
Executable File Title: _____ Format: _____

c. ☐ Other (give details): _____

Section 2: Code Revision

1. Reason for Revision:

a. ☐ Response to Review QA CIN: _____ Control Date: _____

b. ☐ Problem Report/ Corrective Action QA CIN: _____ Control Date: _____

c. ☐ Code Enhancement/Evolution

d. ☐ Other: _____

2. Description of Revision:

3. Baselines which may require changes as a result of this revision:

4. Revision approved by Code Custodian: _____ Date: _____
Signature

Recommended by: _____ PM Date: YY MM DD | -- | -- | --

Approved by: _____ QAM Date: YY MM DD | -- | -- | --

QA Control Document
08/15/90

QA CIN: | --- | - | -- | E - | --- | - |
YY MM DD

Control Date (OAAA Only): | -- | -- | -- |

TEST/APPLICATION/OTHER DATA (-)

☐ Original Baseline (Complete Section 1 only)

☐ Revision to Previous Baseline (Complete Sections 1 and 2)

Project Title: Project Number:
Contract No.:
CFI Description: _____

Section 1 - Data Baseline

1. Data Type (check one):

a. ☐ Test Data
Code Name: _____

b. ☐ Application Data
QA CIN: _____ Control Date: _____

c. ☐ Library Data

d. ☐ Generic Data (describe): _____

2. Source of Data:

a. ☐ Documented internally by: _____
Signature/Printed Name

_____
Signature/Printed Name

References made to: ☐ Laboratory ☐ Field ☐ Model ☐ Literature ☐ Judgement

Reference(s) to source(s) (if not attached): _____

_____

b. ☐ Acquired From: _____
Printed Name

3. Data Storage

a. ☐ Tape/Disk
i. Tape/Disk Number: _____
ii. File Names: _____
iii. Format: _____

b. ☐ Other: _____

QA Control Document
08/15/90

QA CIN: | - - - | - | - - | E - | - - - | - |

4. Data Documentation Description (if not attached):

Section 2: Data Revision

1. Reason for Revision

a. ☐ Response to Review QA CIN: _____ Control Date: _____

b. ☐ Problem Report/ Corrective Action QA CIN: _____ Control Date: _____

c. ☐ Other:

2. Description of Revision:

3. Baselines which may require changes as a result of this revision:

Recommended by: _____ PM Date: YY MM DD | - - | - - | - - |

Approved by: _____ QAM Date: YY MM DD | - - | - - | - - |

QA Control Document
08/15/90

QA CIN: | --- | - | -- | F - | --- | - |
YY MM DD

Control Date (QAAA Only): | -- | -- | -- |

TEST/APPLICATION RESULTS (F)

☐ Test Results (Complete Section 1 only)
☐ Application Results (Complete Section 2)

Project Name: Project Number:

Contract No.:

CFI Description: _____

Section 1: Test Results

1. Code Name: _____
2. Code QA CIN: _____ Control Date: _____
3. Test Data QA CIN: _____ Control Date: _____
4. Library Data QA CIN: _____ Control Date: _____
   (if applicable)
5. Description of Test(s) (if not attached):
6. Analysis and Interpretation of Results (if not attached):
7. Storage of Results:
   a. ☐ Tape/Disk
      i. Tape/Disk Number: _____
      ii. File Names: _____
      iii. Format: _____
   b. ☐ Other: _____

QA Control Document
08/15/90

QA CIN: | --- | - | -- | F - | --- | -

8. Test Performed by: _____ Date: _____
Signature/Printed Name

9. Results and Analysis Verified by: _____ Date: _____
Signature/Printed Name

Section 2: Application Results

1. Code Name: _____

2. Code QA CIN: _____ Control Date: _____

3. Test Data QA CIN: _____ Control Date: _____

4. Test Results QA CIN: _____ Control Date: _____

5. Application Data QA CIN: _____ Control Date: _____

6. Description of Application (if not attached):

7. Analysis and Interpretation of results (if not attached):

8. Storage of Results:

a. ☐ Tape/Disk i. Tape/Disk Number: _____
ii. File Names: _____
iii. Format: _____

b. ☐ Other: _____

9. Application Performed by: _____ Date: _____
Signature/Printed Name

10. If known, give references to documents where results will be presented:

	Description	QA CIN (if known)
a.	_____	_____
b.	_____	_____
c.	_____	_____

Recommended by: _____ PM Date: YY MM DD | -- | -- | --

Approved by: _____ QAM Date: YY MM DD | -- | -- | --

QA Control Document
08/15/90

QA CIN: | --- | - | -- | G | --- | - |

YY MM DD

Control Date (QAAA Only): | -- | -- | -- |

REPORT/CODE DOCUMENTATION (G)

☐ Original Baseline (Complete Section 1 only)

☐ Revision to Baseline (Complete Sections 1 and 2)

Project Name: Project Number:
Contract No.:

CFI Description: _____

Section 1: Baseline

1. Report Type:

   a. ☐ Topical Report

   b. ☐ Letter Report

   c. ☐ Model Documentation: Code QA CIN: _____ Control Date: _____

2. Title (or Subject): _____

3. This ☐ baseline ☐ revision was developed by: _____
   Signature/Printed Name

   _____
   Signature/Printed Name

   _____
   Signature/Printed Name

4. This ☐ baseline ☐ revision was acquired from: _____
   Printed Name

5. References:

   a. ☐ No reference to baselined data or results

   b. ☐ Reference is made to data/results with the following baseline QA CIN's:

QA Control Document
08/15/90

QA CIN: | - - - | - | - - | G - | - - - | - |

Section 2: Baseline Revision

1. Reason for Revision:

   a. ☐ Response to Review QA CIN: _____ Control Date: _____

   b. ☐ Corrective Action QA CIN: _____ Control Date: _____

   c. ☐ Other:

2. Description of Revision:

3. Baselines which may require changes as a result of this revision:

Recommended by: _____ PM Date: YY MM DD | - - | - - | - - |

Approved by: _____ QAM Date: YY MM DD | - - | - - | - - |

QA Control Document
08/15/90

QA CIN: | --- | - | -- | I - | --- | -
YY MM DD

Control Date (QAAA Only): | -- | -- | --

REVIEW (I)

Project Name: Project Number:

Contract No.:

CFI Description: _____

1. Title or Description of Baseline Reviewed: _____

2. Author/Originator: _____

3. QA CIN of Baseline Reviewed: _____ Control Date: _____

4. Location of Review Comments: ☐ On Document ☐ Review Form

Reviewed by: _____
Printed Name/Signature

Date: _____

5. Brief Review Comments:

Recommended by: _____ PM Date: YY MM DD | -- | -- | --

Approved by: _____ QAM Date: YY MM DD | -- | -- | --

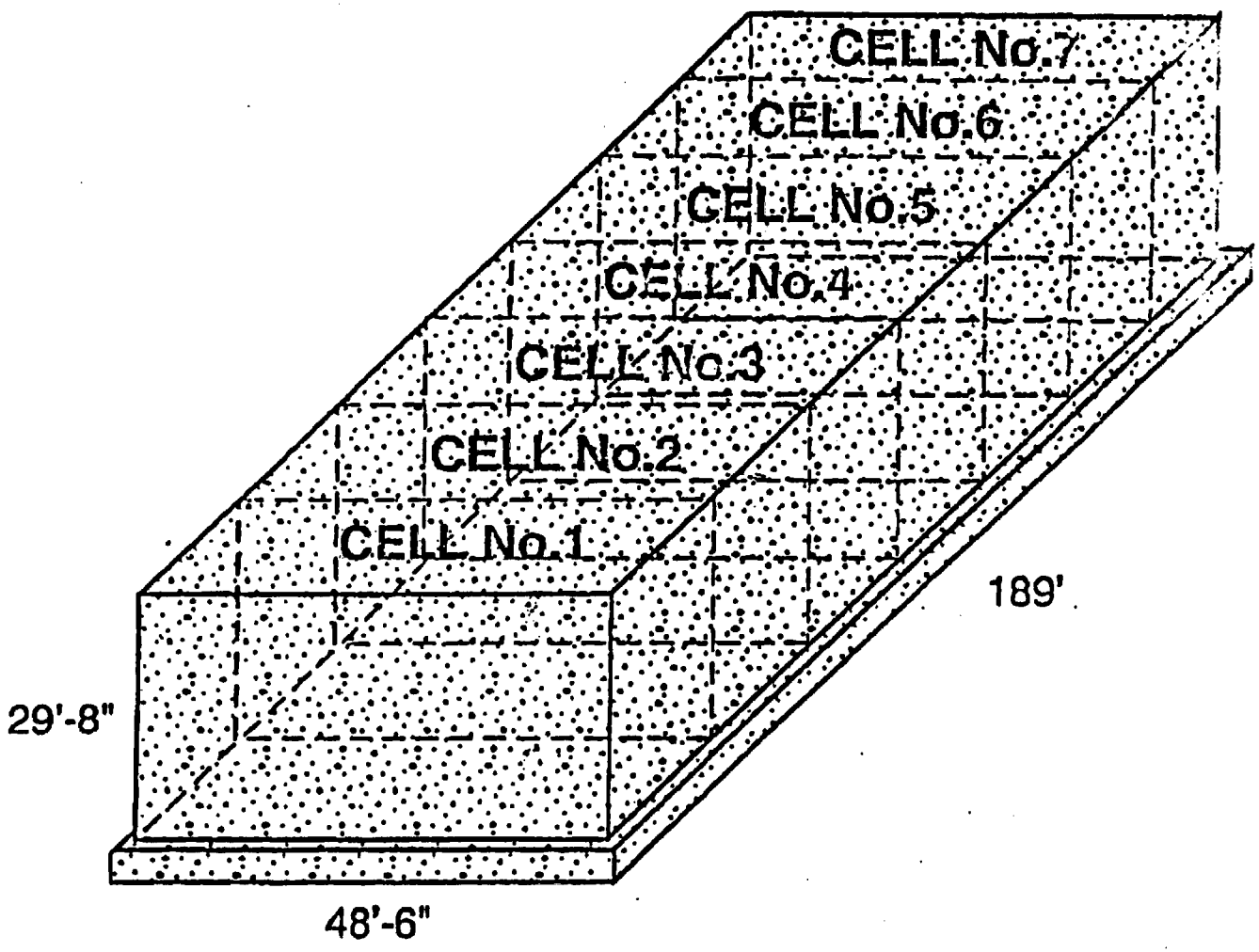

INTERA	Schematic of ILNT Vault	Figure 1

1025-007 9/1/93

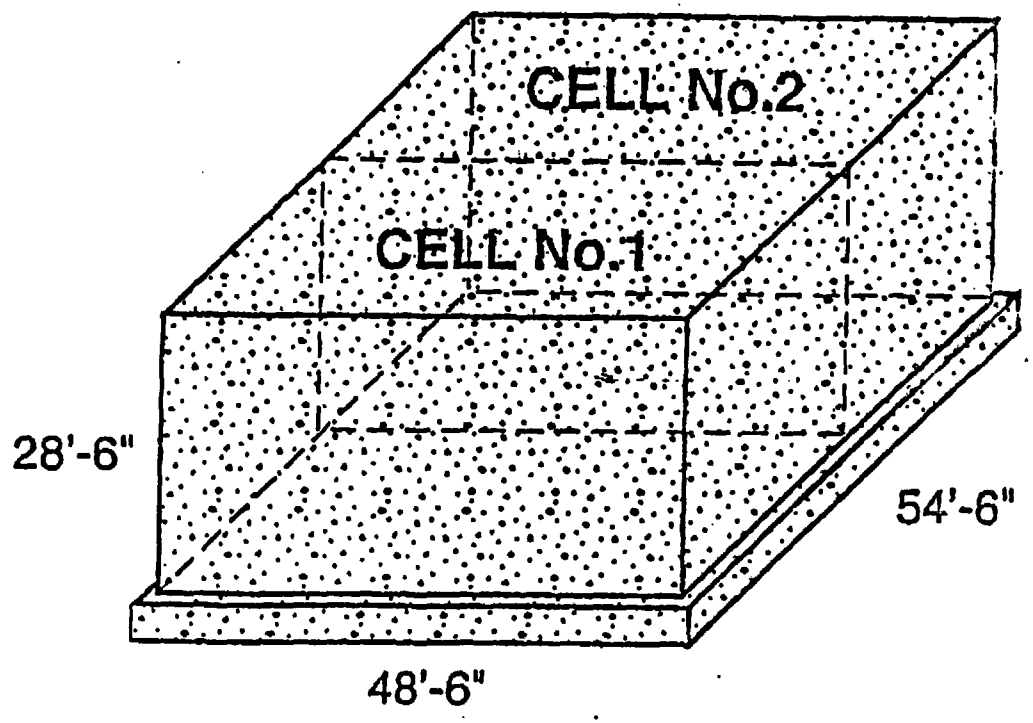

INTERA	Schematic of ILT Vault	Figure 2

1025-007 9/1/93

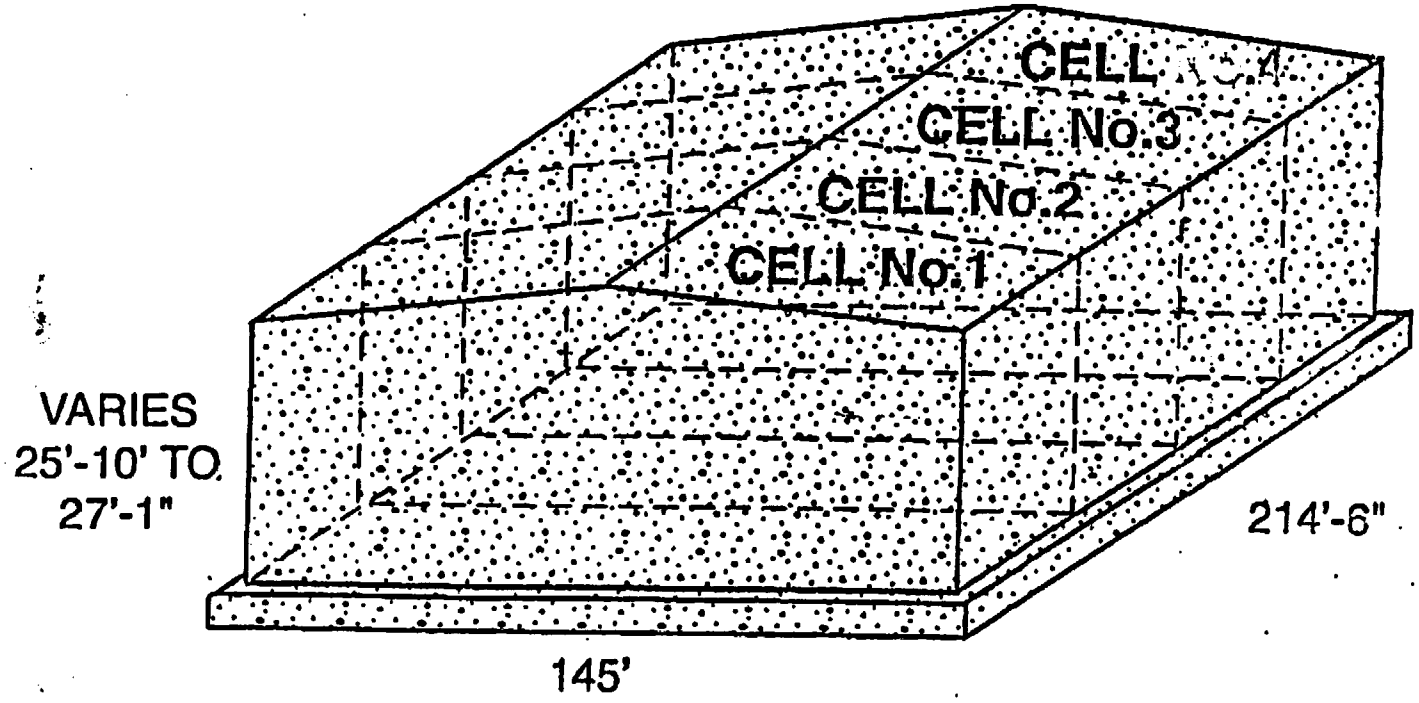

INTERA	Schematic of LAW Vault	Figure 3

1025-007 9/1/93

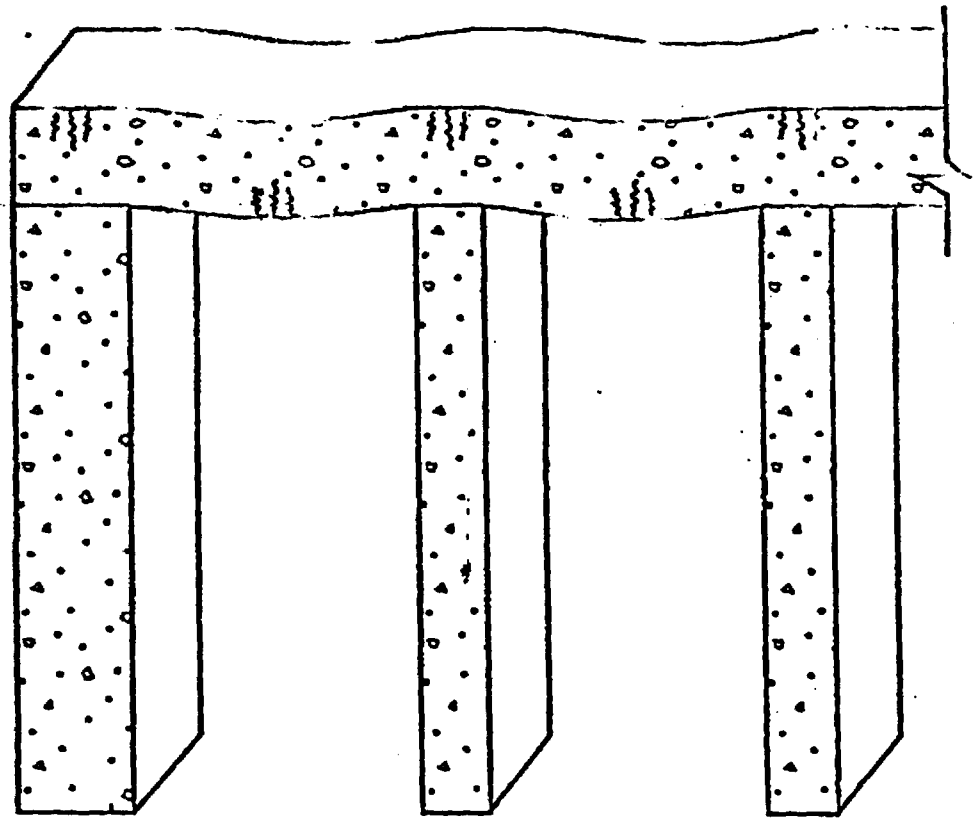

NOT TO SCALE
DEFLECTION HAS BEEN EXAGGERATED FOR EMPHASIS

DATE: 9/7/93 REF: #1025-007	Portion of Vault Cross Section; Cracks Indicate Critical Stress Regions	
INTERA		Figure 4

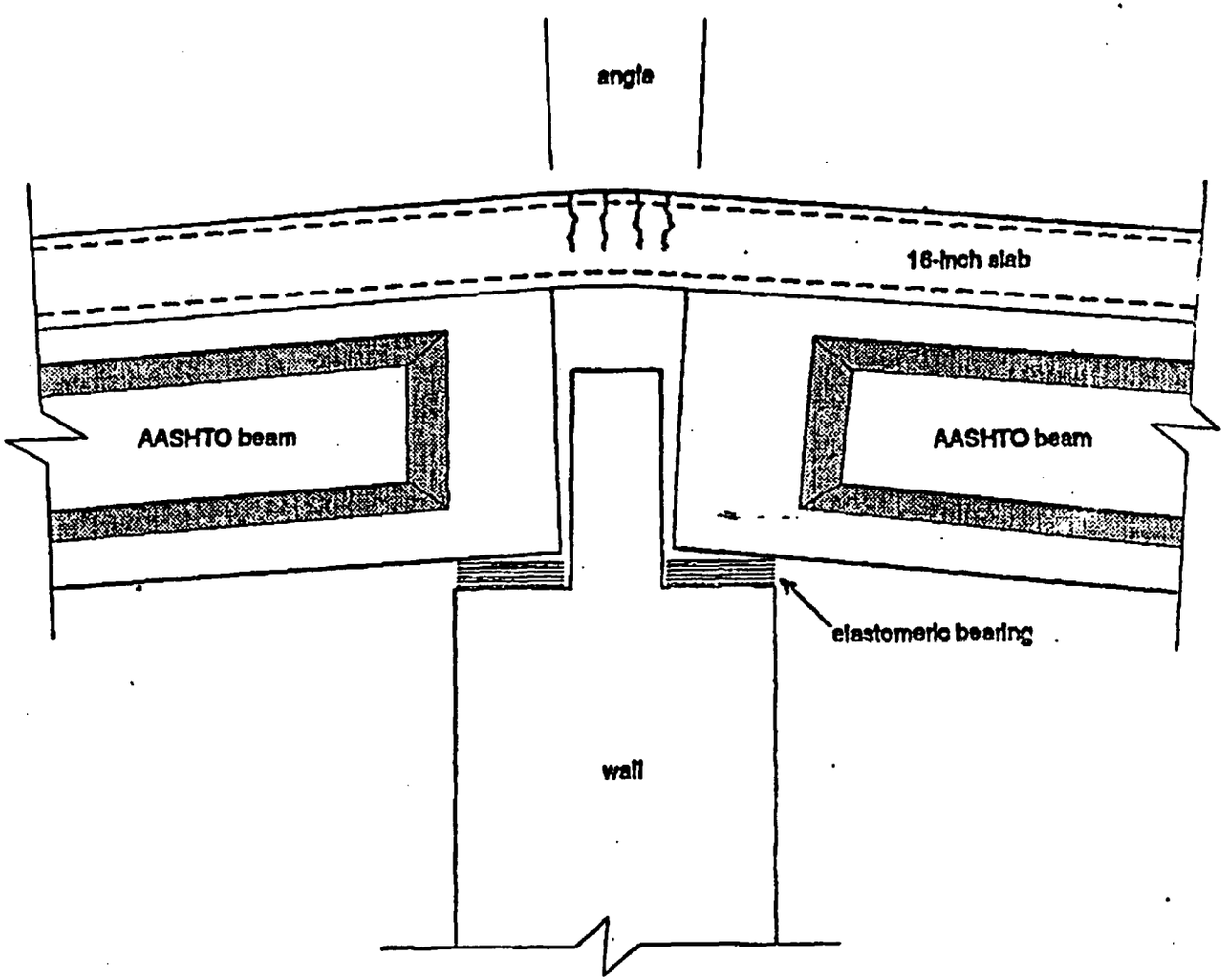

INTERA

LAW Vault Roof, Showing Cracking Due to Curvature Over Wall

Figure 5

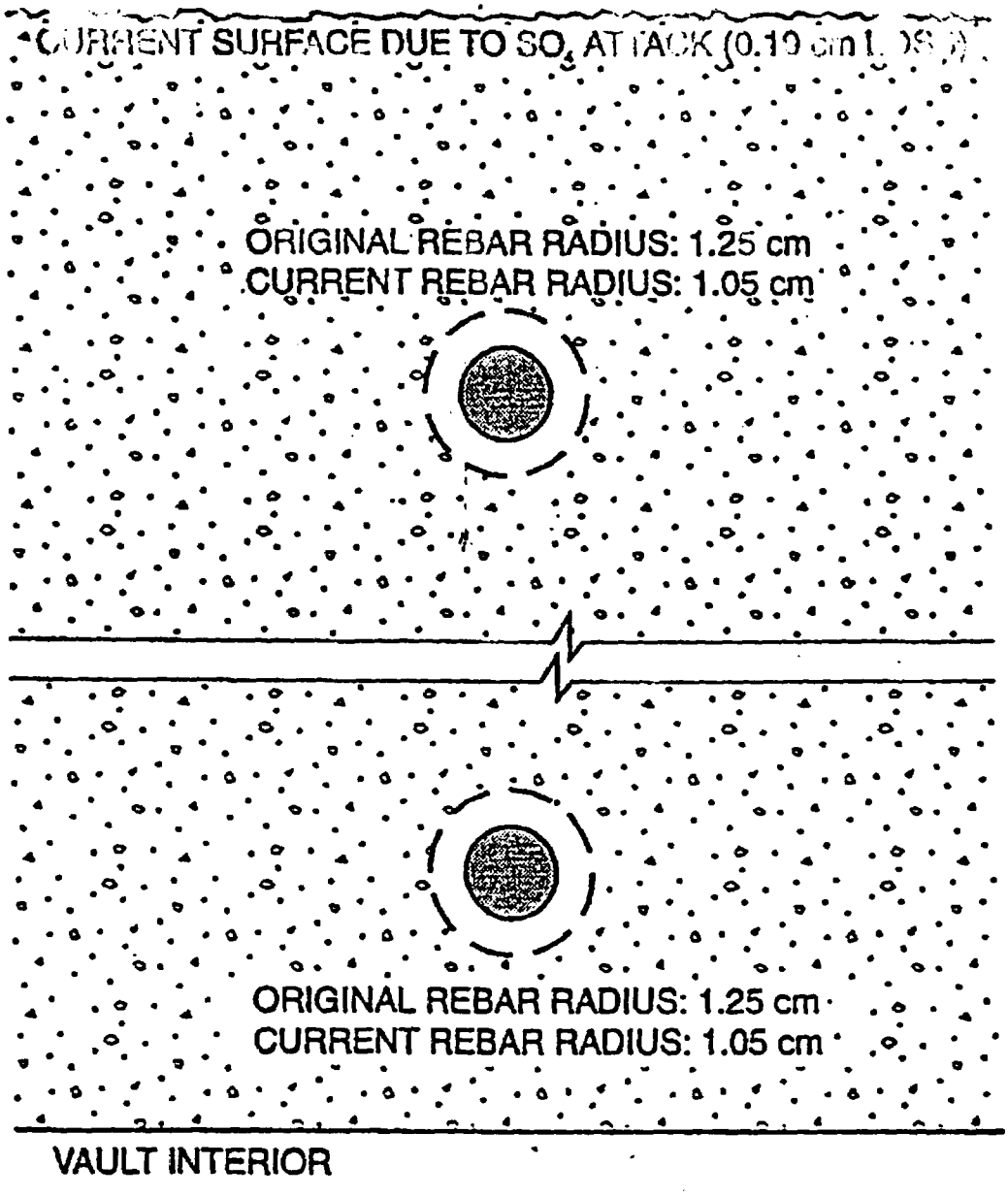

DATE: 9/7/93	Cross-Section of ILNT Vault Roof Showing Degradation at 400 Years
REF: #1025-007	
INTERA	Figure 6

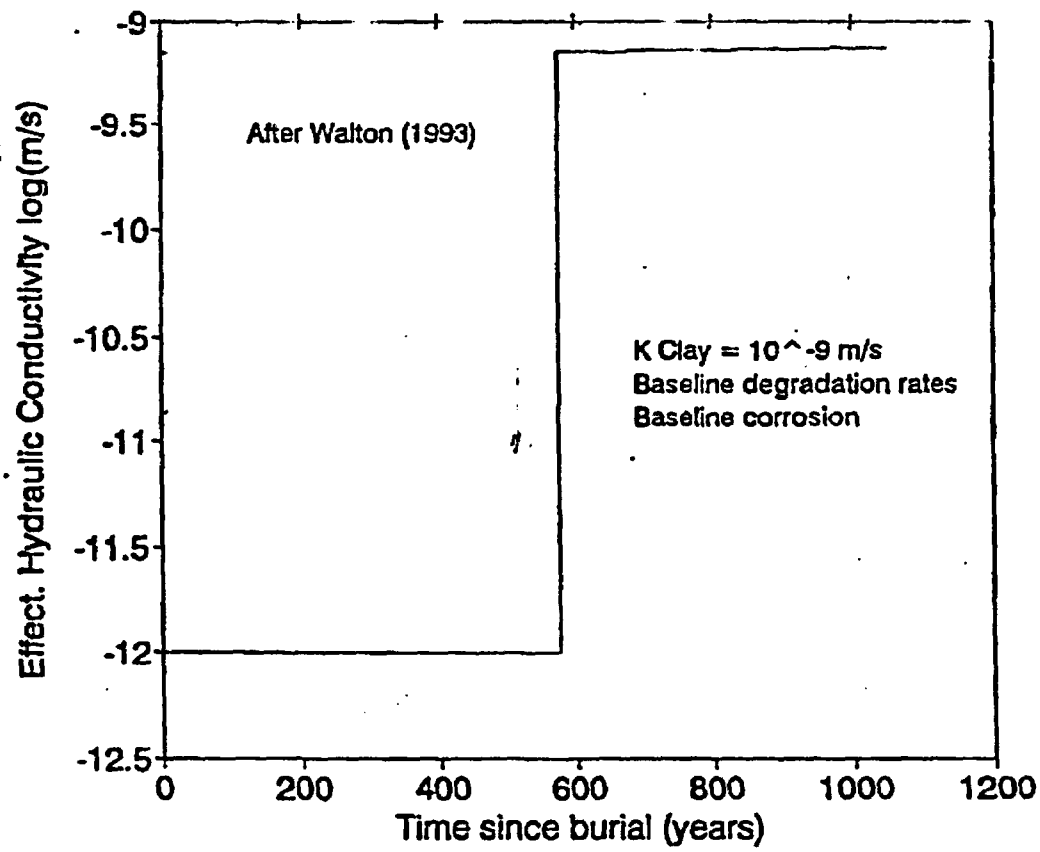

DATE: 9/7/93	Effective Hydraulic Conductivity of Vault Roof; ILNT Vault Design	
REF: #1025-007		
INTERA		Figure 7

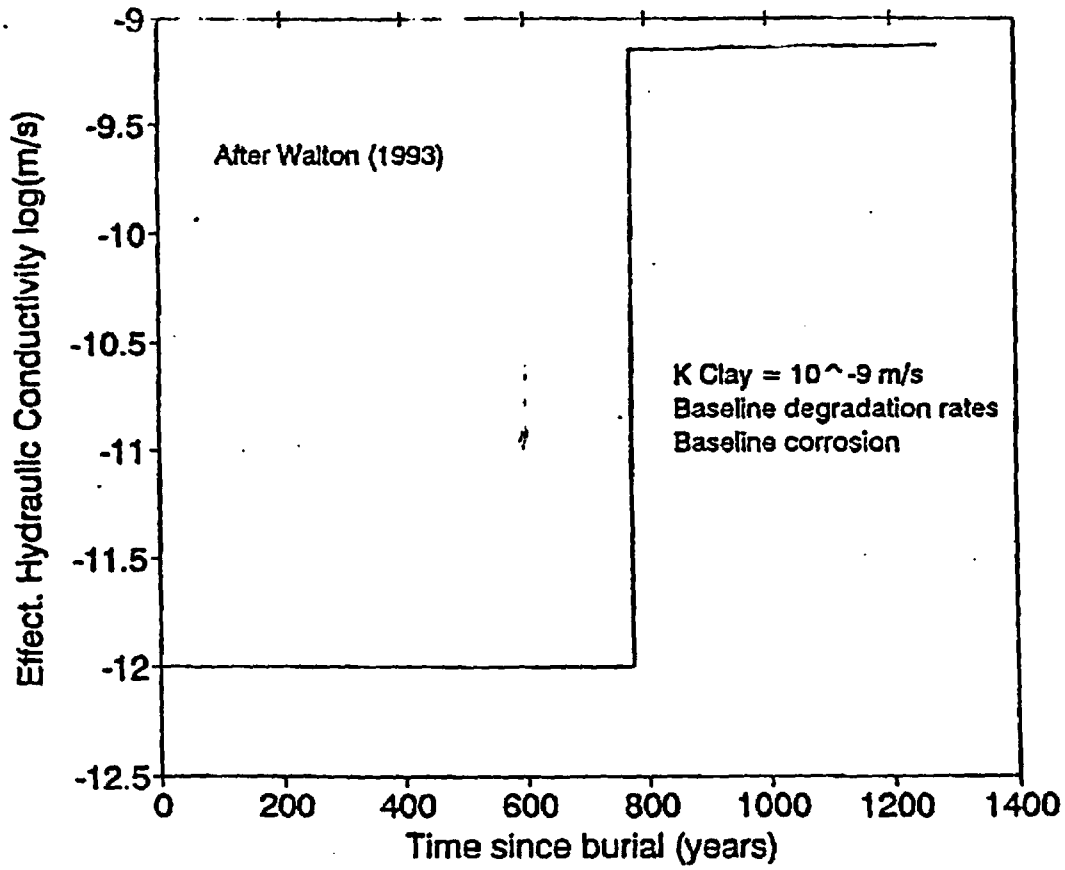

DATE: 9/7/93	Effective Hydraulic Conductivity of Vault Roof; ILT Vault Design	
REF: #1025-007		
INTERA		Figure 8

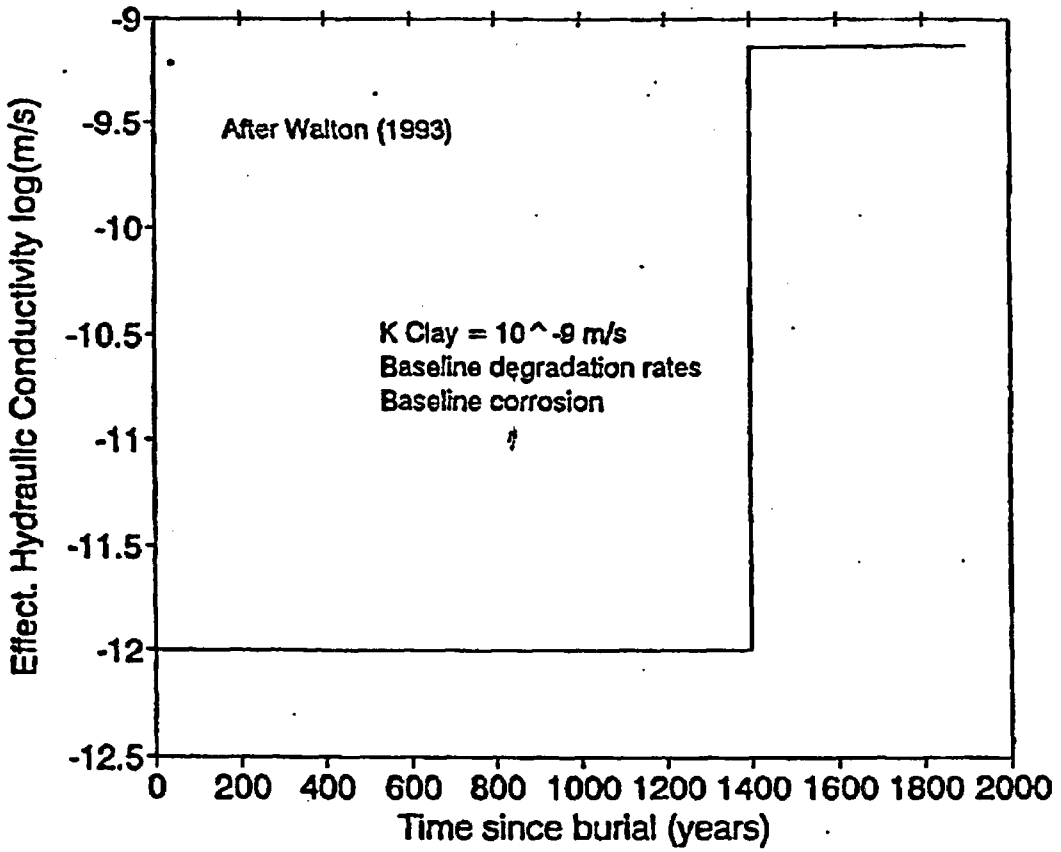

DATE: 9/7/93	Effective Hydraulic Conductivity of Vault Roof; LAW Vault Design
REF: #1025-007	
INTERA	Figure 9

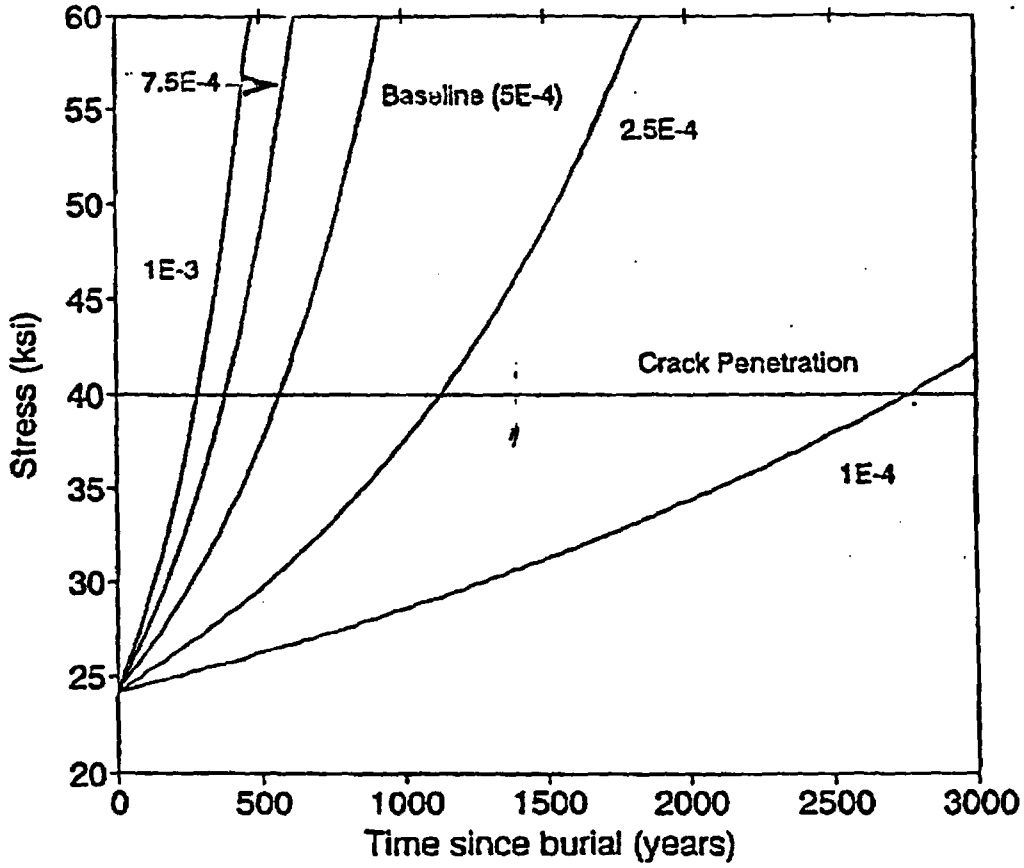

DATE: 9/7/93	ILNT Vault Time to Crack Penetration of Roof; Sensitivity to Hydrogen Evolution Corrosion Rate (cm/yr)
REF: #1025-007	
INTERA	Figure 10

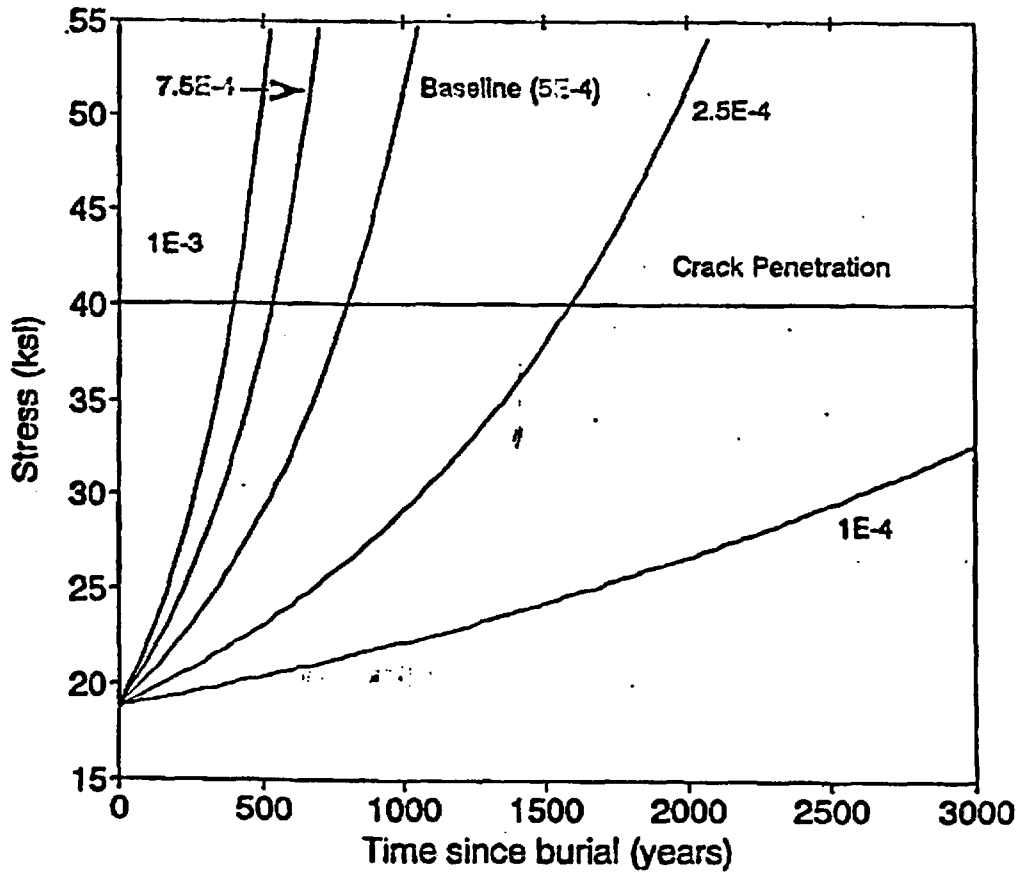

DATE: 9/7/93	ILNT Vault Time to Crack Penetration of Walls; Sensitivity to Hydrogen Evolution Corrosion Rate (cm/yr)
REF: #1025-007	
LITERA	Figure 11

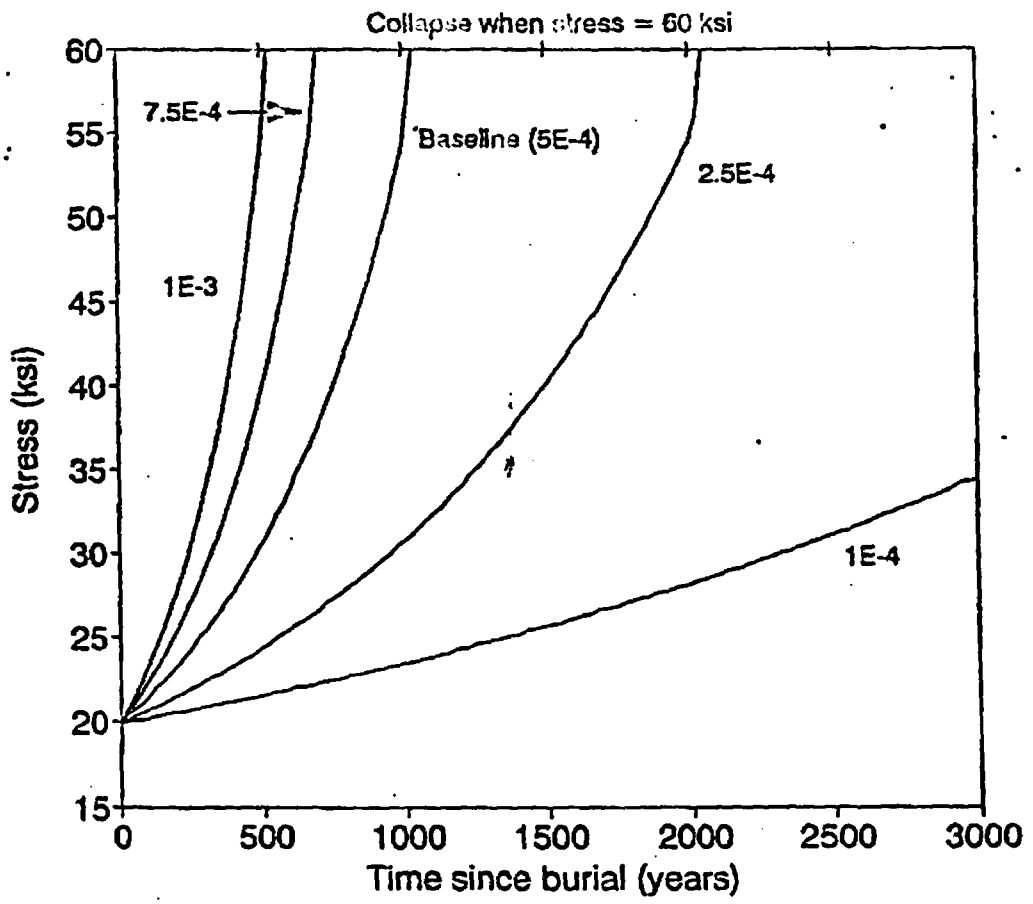

DATE: 9/7/93	ILNT Vault Time to Roof Collapse; Sensitivity to Hydrogen Evolution Corrosion Rate (cm/yr)
REF: #1025-007	
INTERA	Figure 12

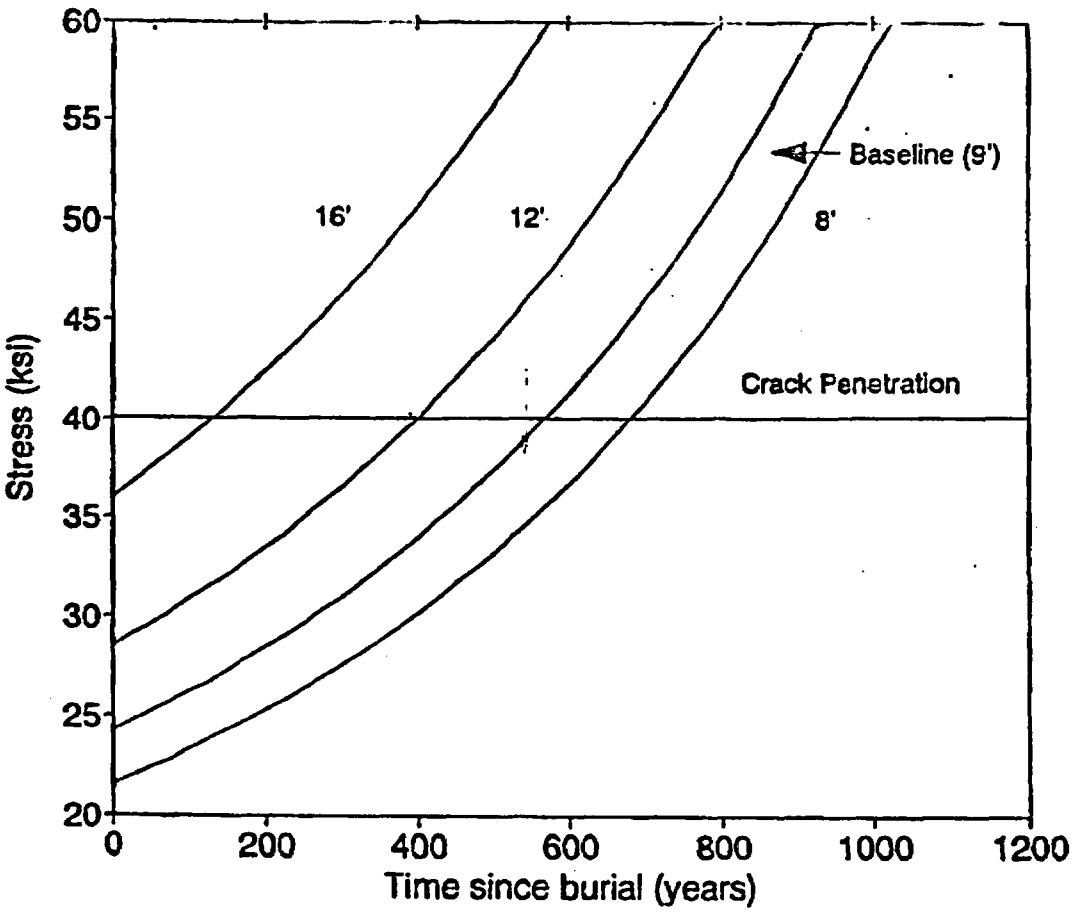

DATE: 9/7/93	ILNT Vault Time to Crack Penetration of Roof; Sensitivity to Depth of Soil Cover
REF: #1025-007	
INTERA	Figure 13

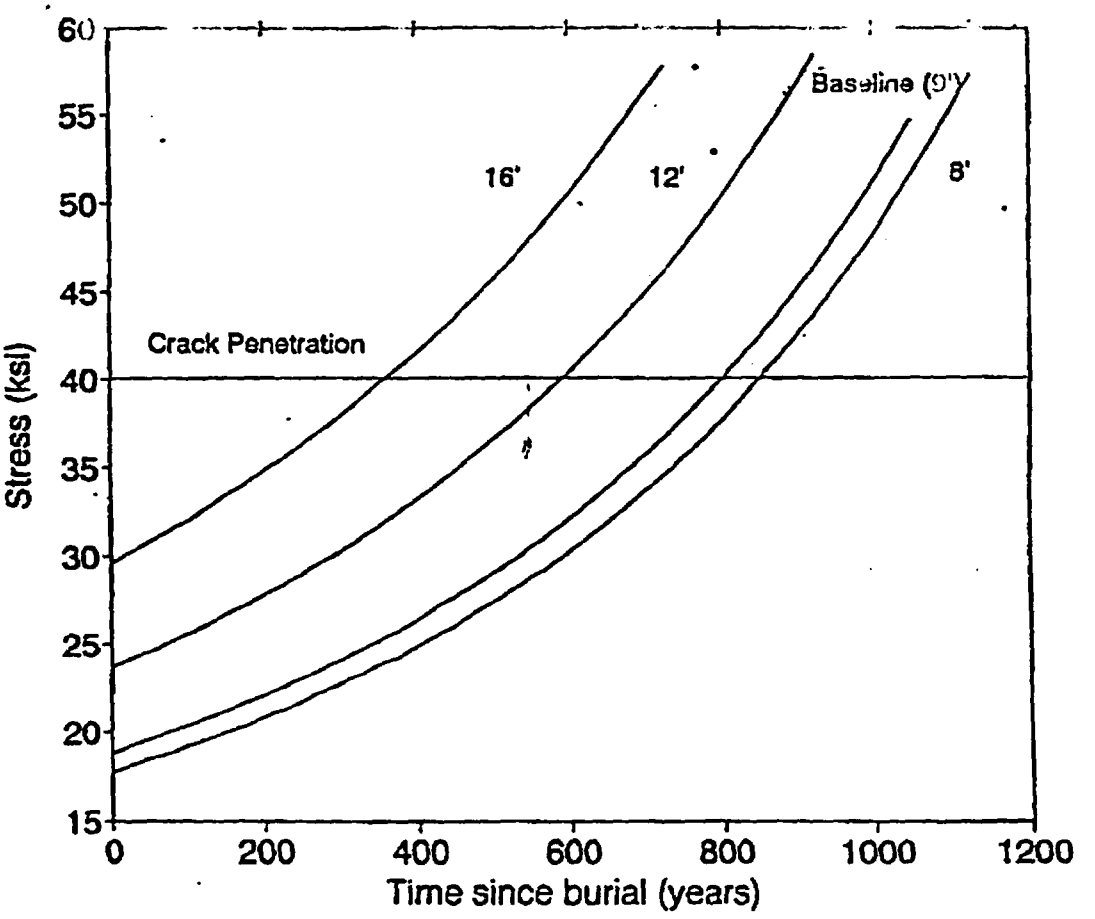

DATE: 9/7/93	ILNT Vault Time to Crack Penetration of Walls; Sensitivity to Depth of Soil Cover	
REF: #1025-007		
INTERA		Figure 14

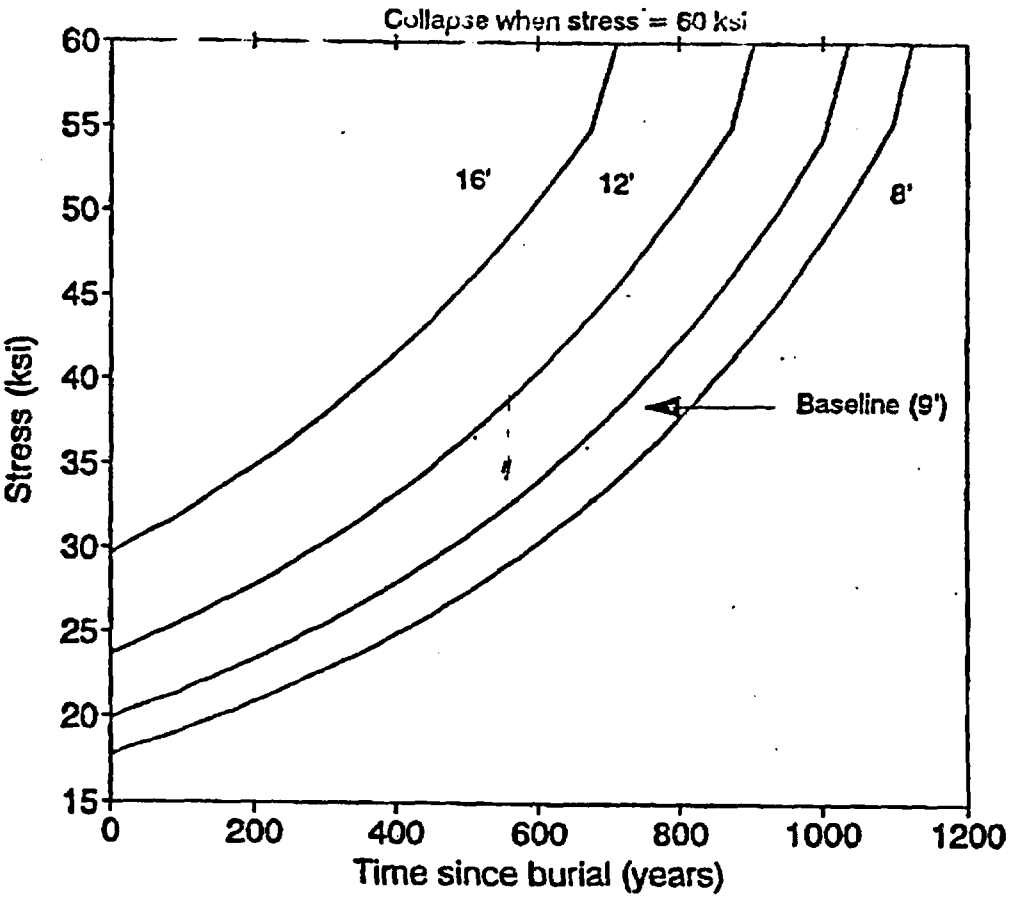

DATE: 9/7/93 REF: #1025-007	ILNT Vault Time to Roof Collapse; Sensitivity to Depth of Soil Cover	
INTERA		Figure 15

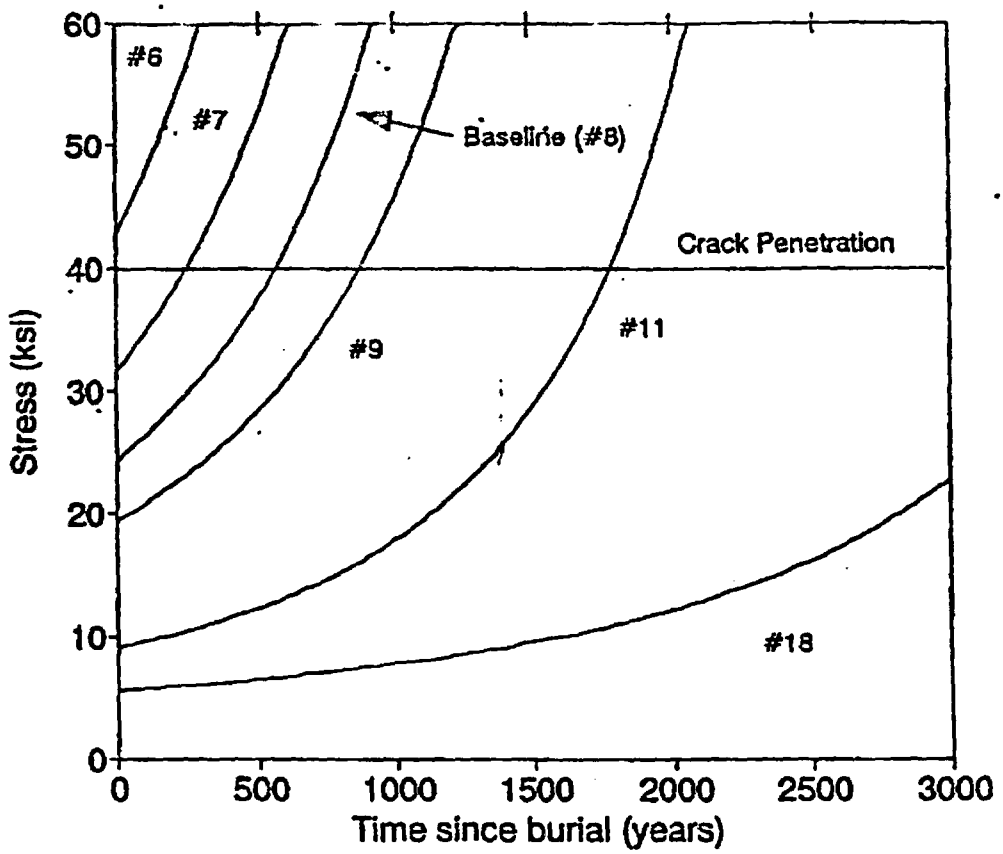

DATE: 9/7/93	ILNT Vault Time to Crack Penetration of Roof; Sensitivity to Rebar Size
REF: #1025-007	
INTERA	Figure 16

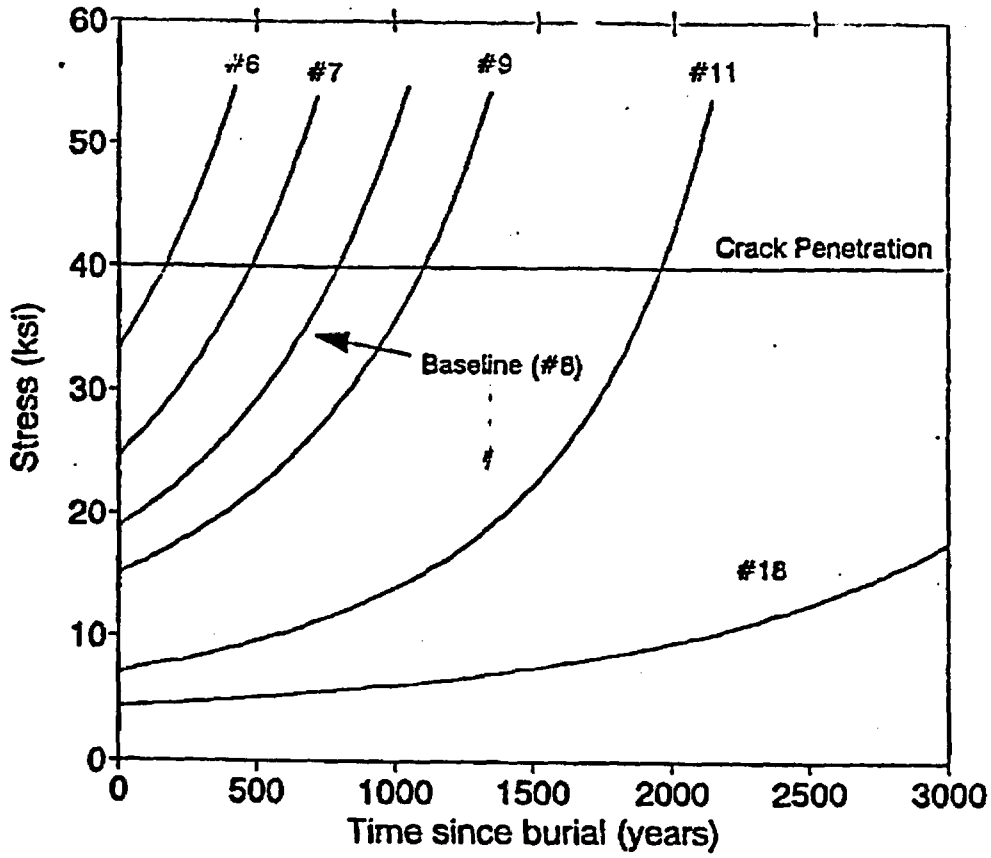

DATE: 9/7/93	ILNT Vault Time to Crack Penetration of Walls; Sensitivity to Rebar Size	
REF: #1025-007		
INTERA		Figure 17

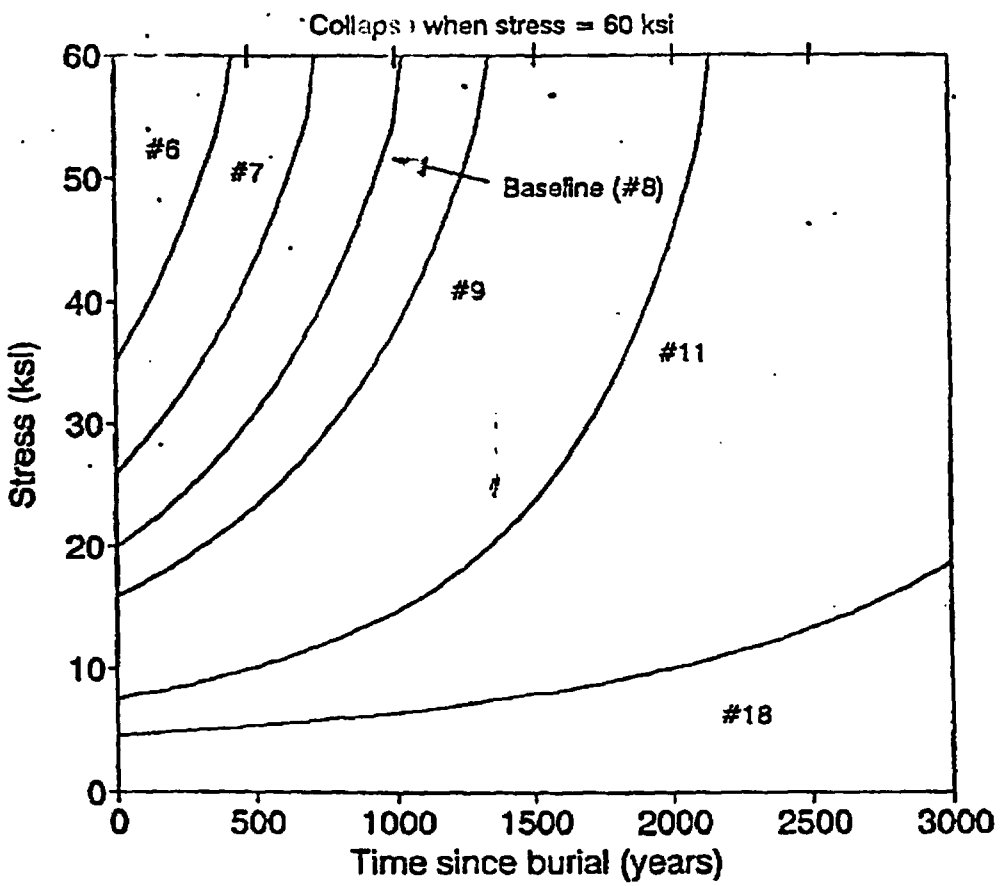

DATE: 9/7/93	ILNT Vault Time to Roof Collapse; Sensitivity to Rebar Size
REF: #1025-007	
INTERA	Figure 18

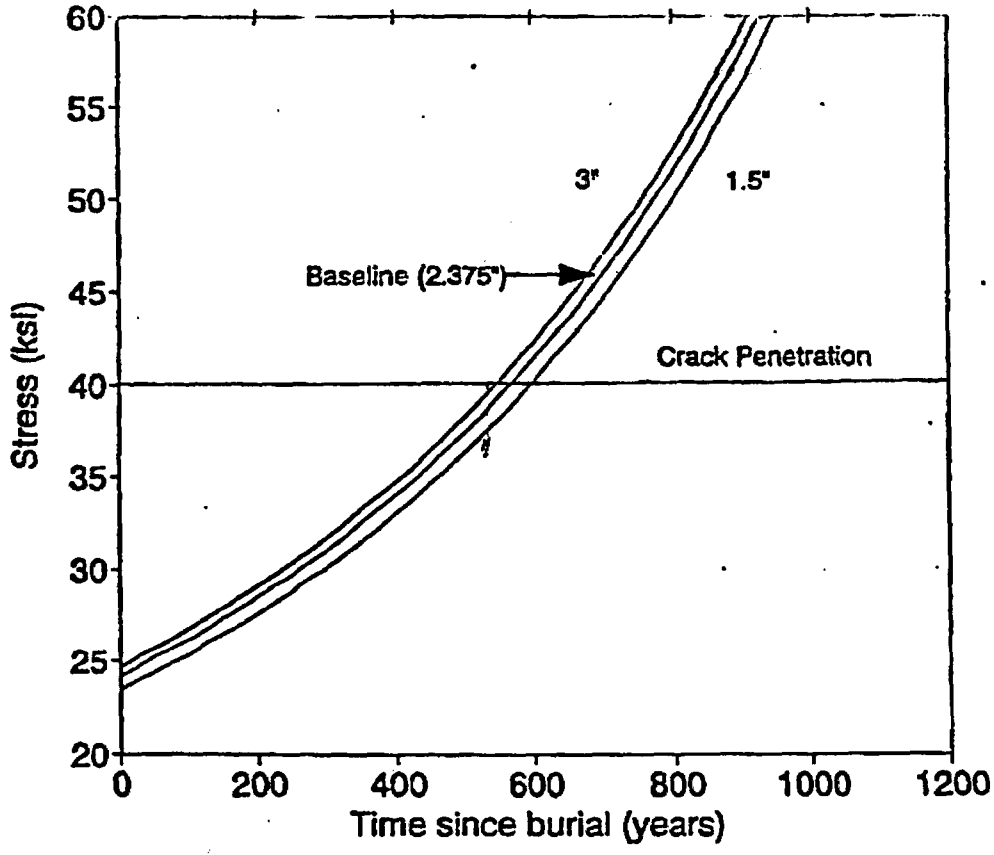

DATE: 9/7/93 REF: #1025-007	ILNT Vault Time to Crack Penetration of Roof; Sensitivity to Depth of Concrete Cover Over Rebar
INTERA	Figure 19

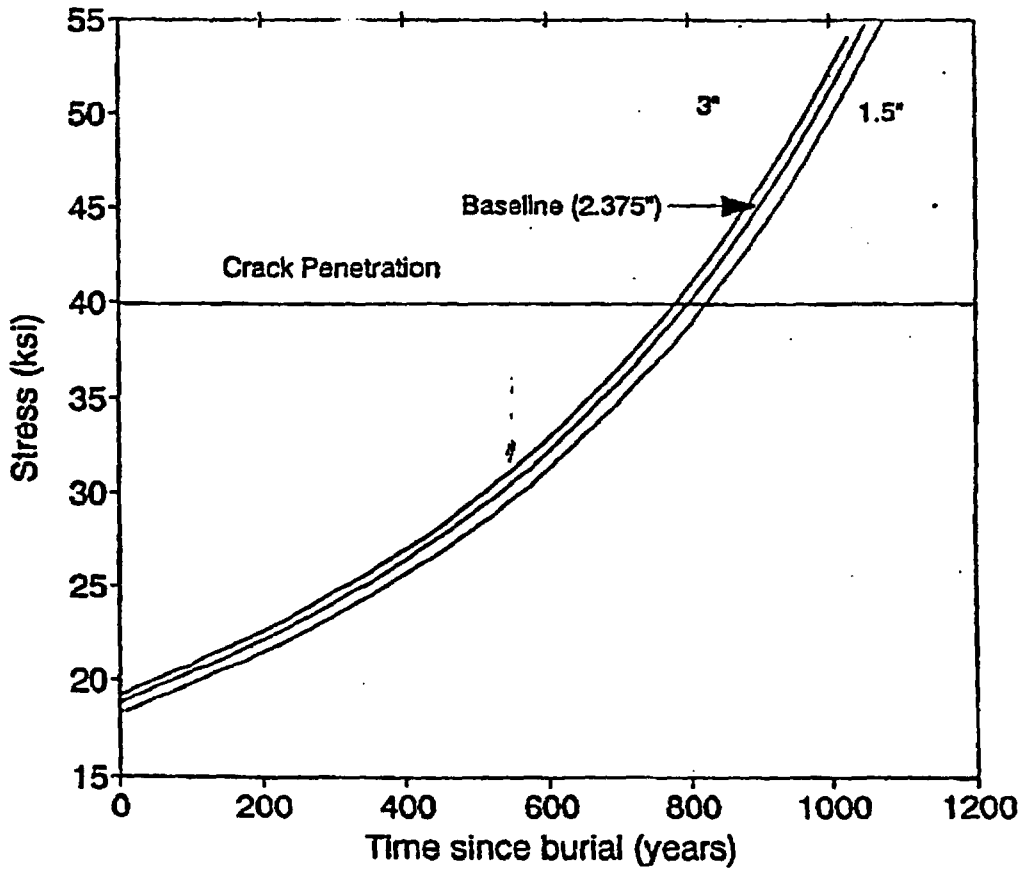

DATE: 9/7/93	ILNT Vault Time to Crack Penetration of Walls; Sensitivity to Depth of Concrete Cover Over Rebar
REF: #1025-007	
INTERA	Figure 20

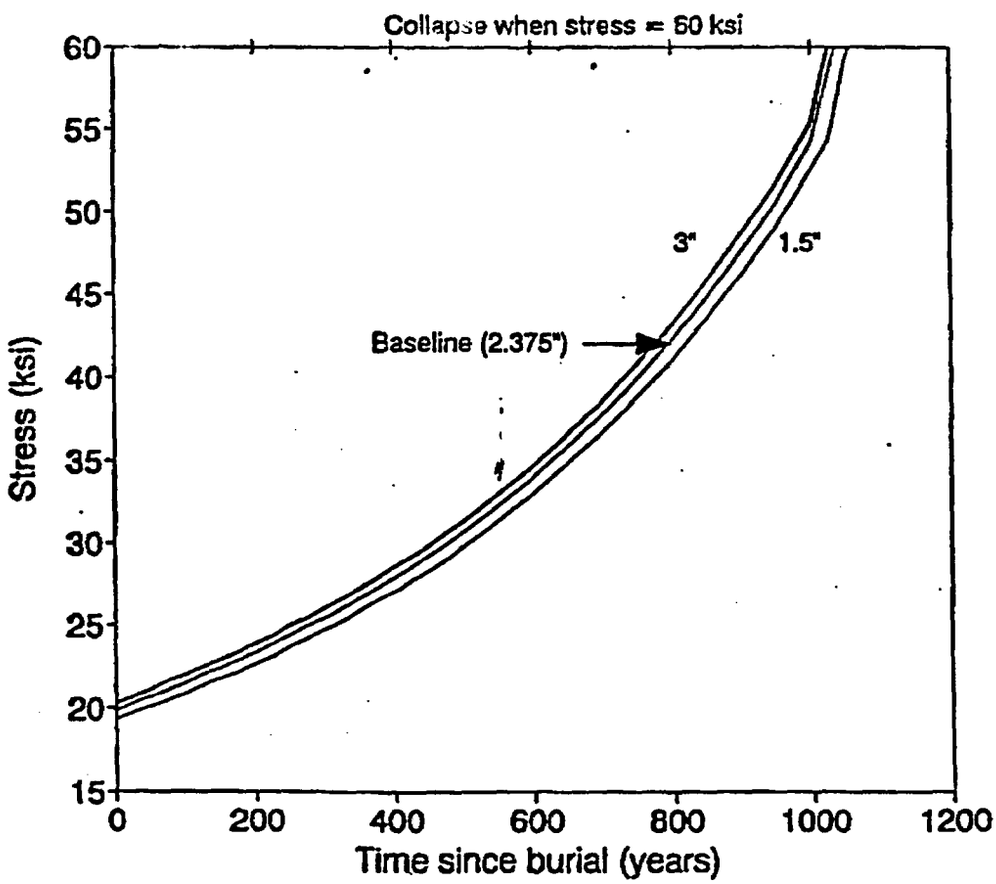

DATE: 9/7/93	ILNT Vault Time to Roof Collapse; Sensitivity to Depth of Concrete Cover Over Rebar
REF: #1025-007	
INTERA	Figure 21

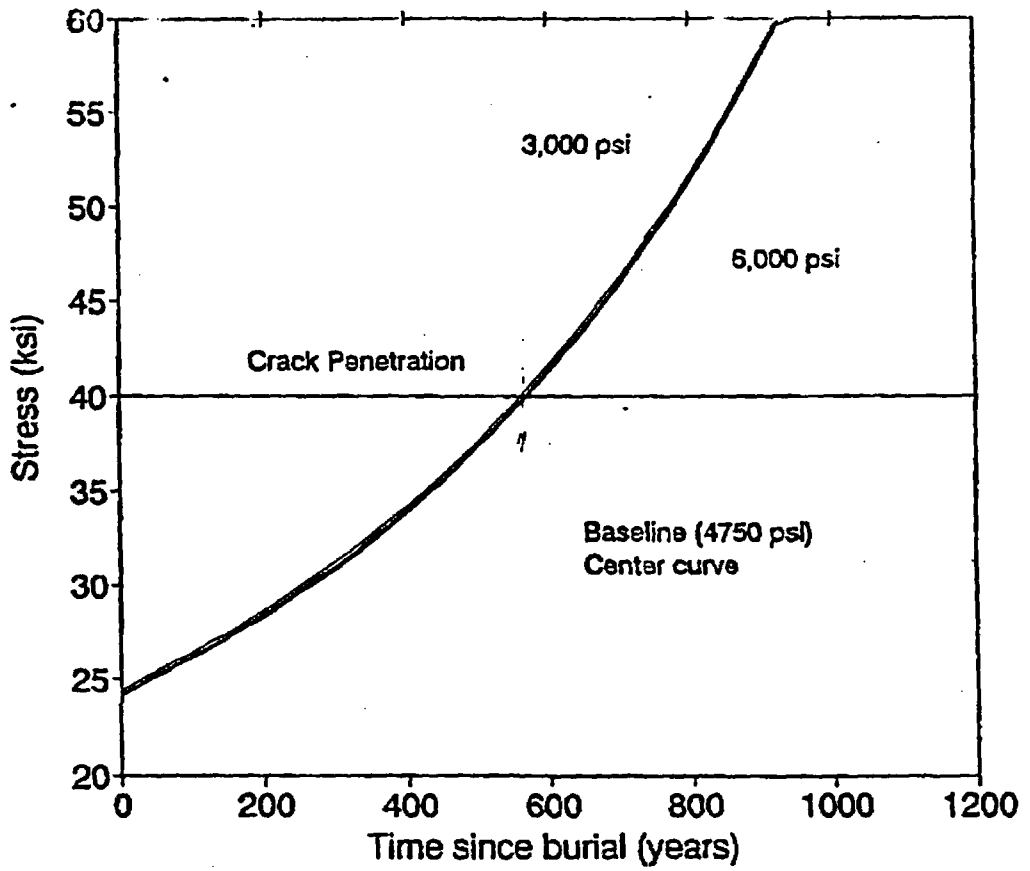

DATE: 9/7/93	ILNT Vault Time to Crack Penetration of Roof; Sensitivity to Concrete Strength
REF: #1025-007	
INTERA	Figure 22

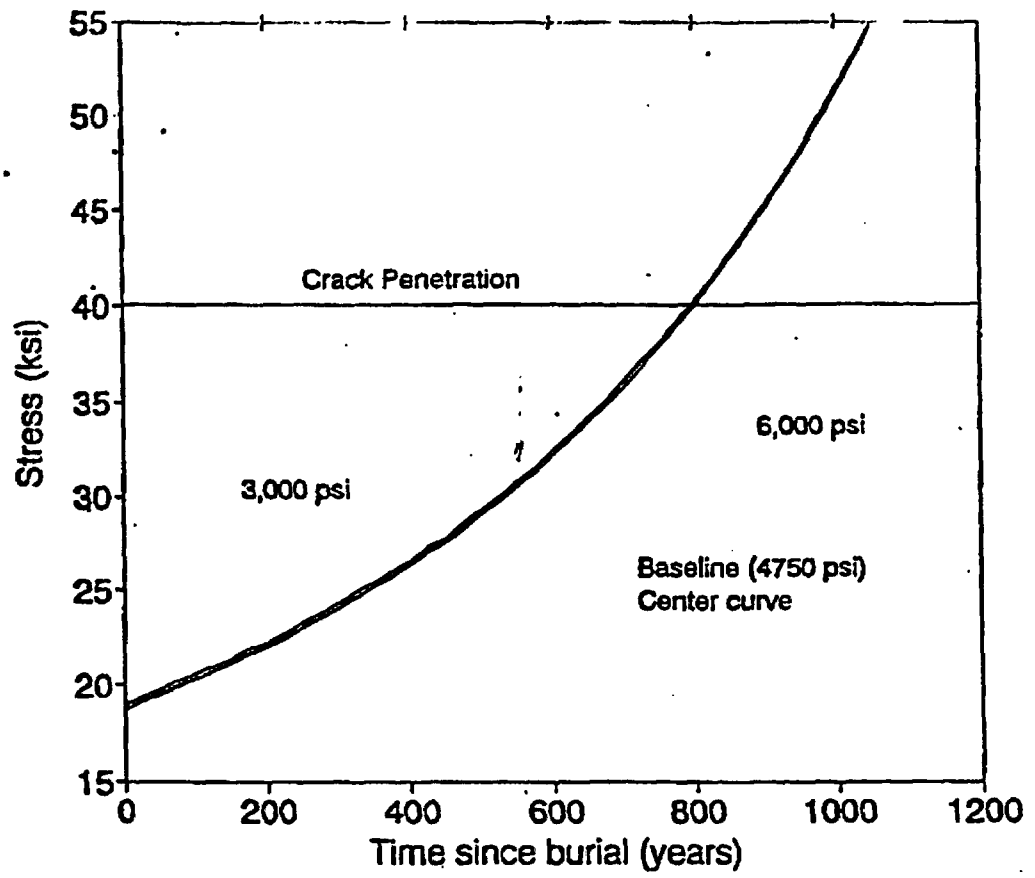

DATE: 9/7/93	ILNT Vault Time to Crack Penetration of Walls; Sensitivity to Concrete Strength	
REF: #1025-007		
INTERA		Figure 23

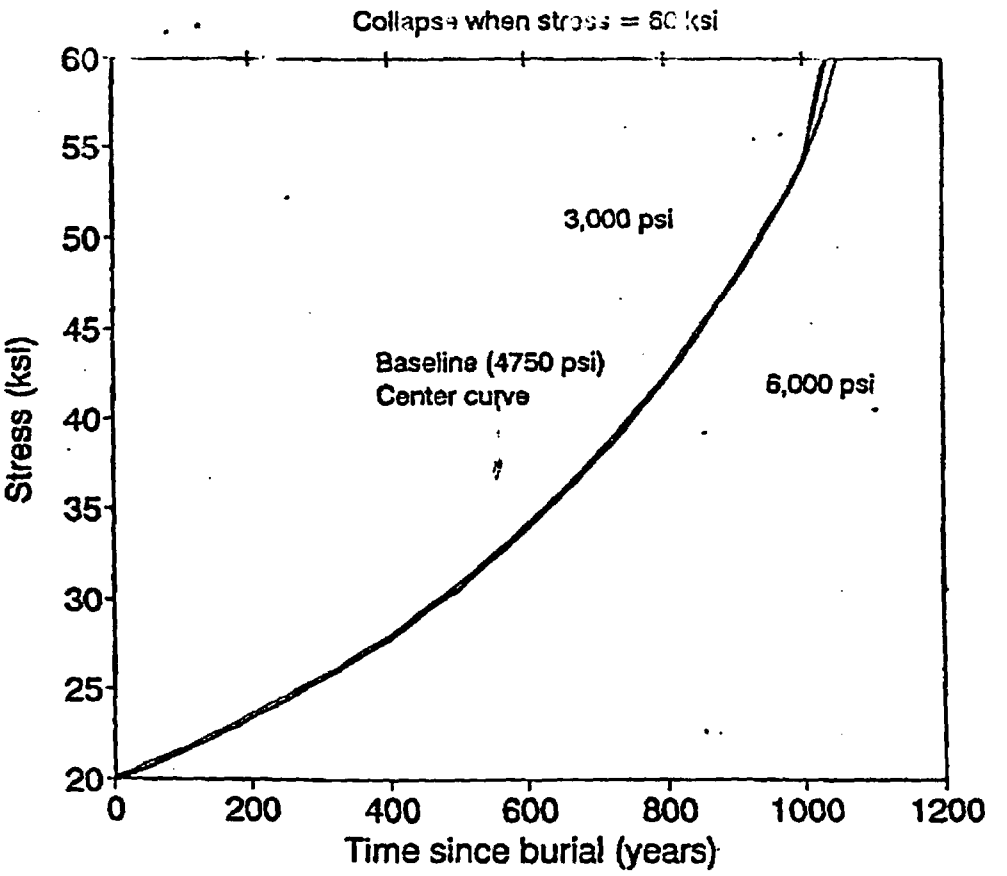

DATE: 9/7/93	ILNT Vault Time to Roof Collapse; Sensitivity to Concrete Strength
REF: #1025-007	
INTERA	Figure 24

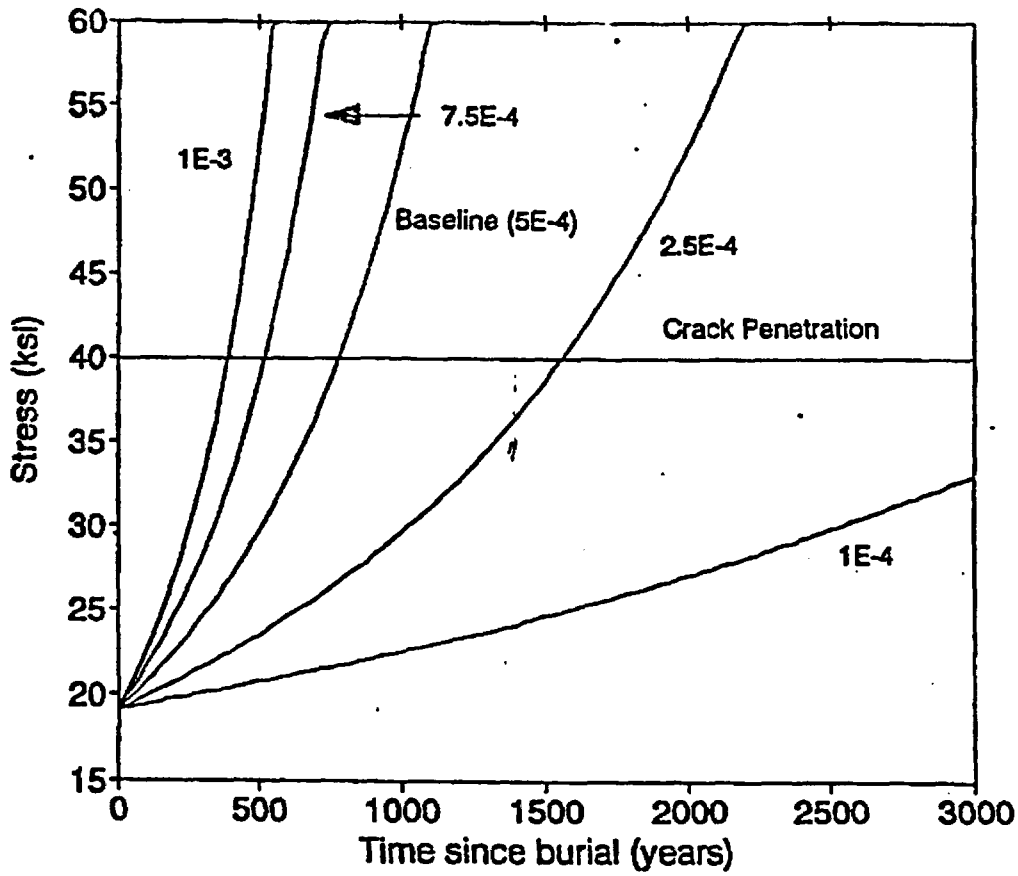

DATE: 9/7/93	ILT Vault Time to Crack Penetration of Roof; Sensitivity to Hydrogen Evolution Corrosion Rate (cm/yr)
REF: #1025-007	
LITERA	Figure 25

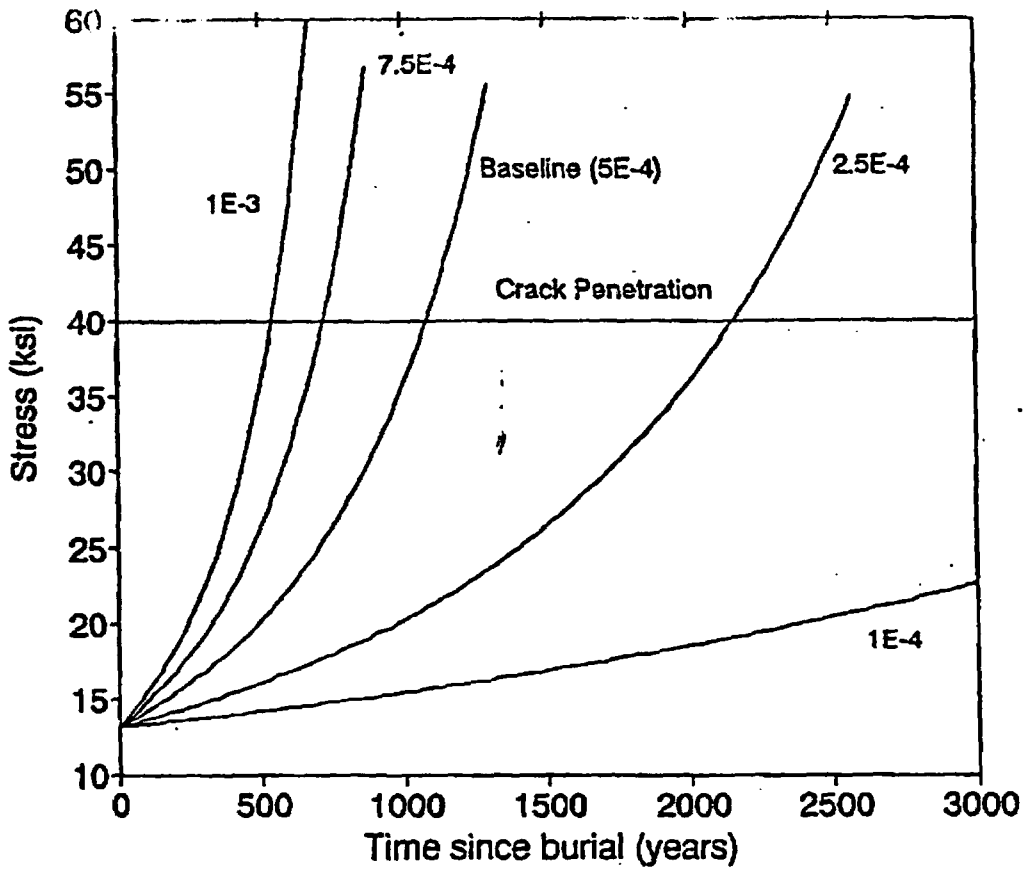

DATE: 9/7/93	ILT Vault Time to Crack Penetration of Walls; Sensitivity to Hydrogen Evolution Corrosion Rate (cm/yr)
REF: #1025-007	
INTERA	Figure 26

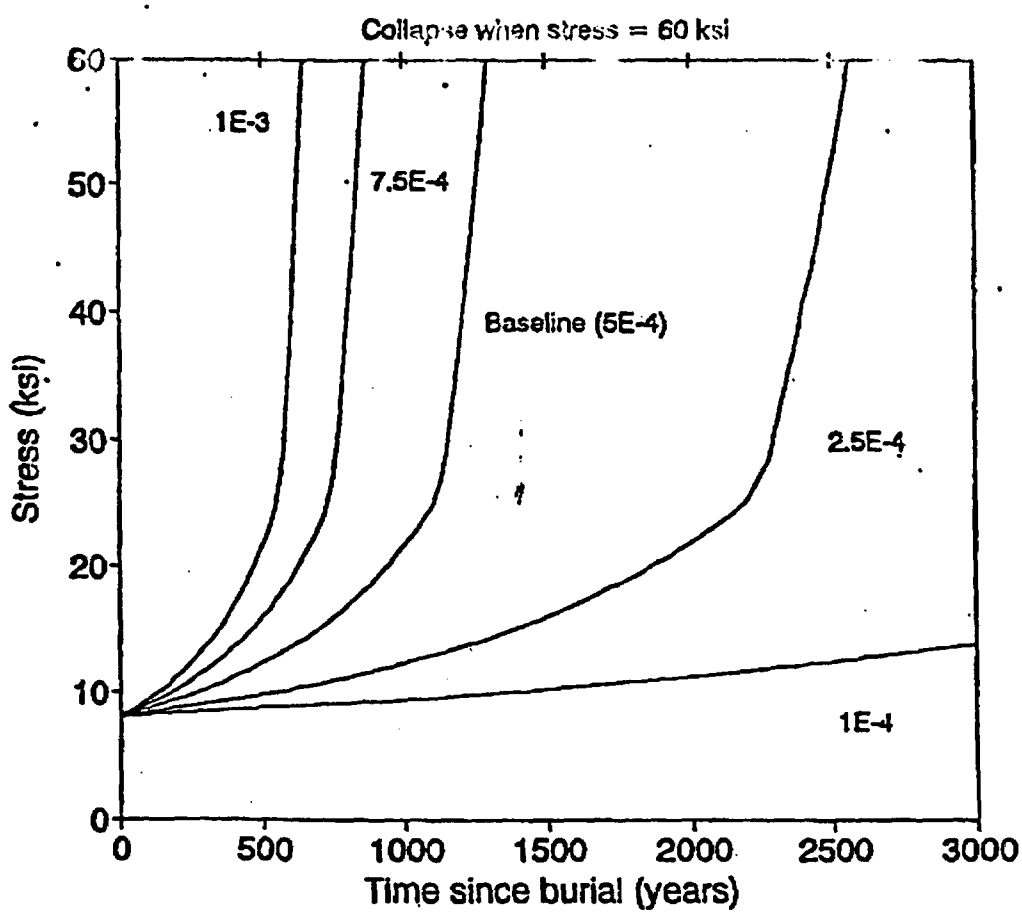

DATE: 9/7/93 REF: #1025-007	ILT Vault Time to Roof Collapse; Sensitivity to Hydrogen Evolution Corrosion Rate (cm/yr)
INTERA	Figure 27

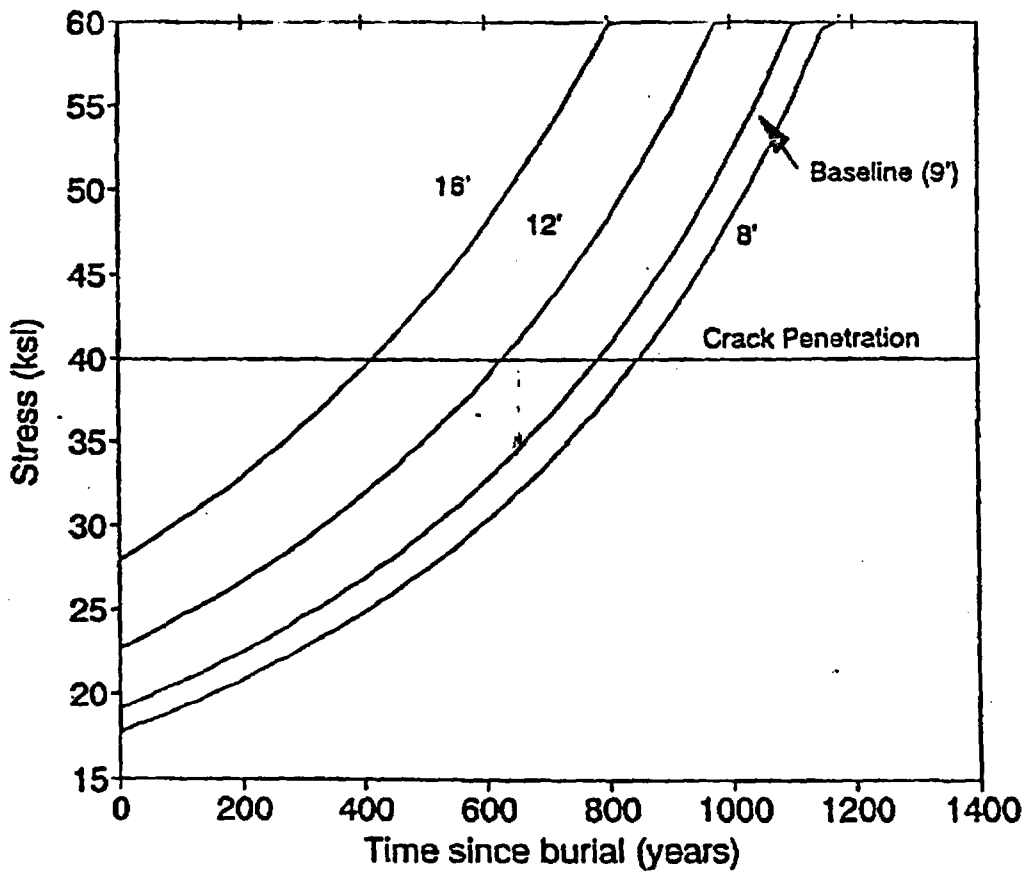

DATE: 9/7/93	ILT Vault Time to Crack Penetration of Roof; Sensitivity to Depth of Soil Cover	
REF: #1025-007		
INTERA		Figure 28

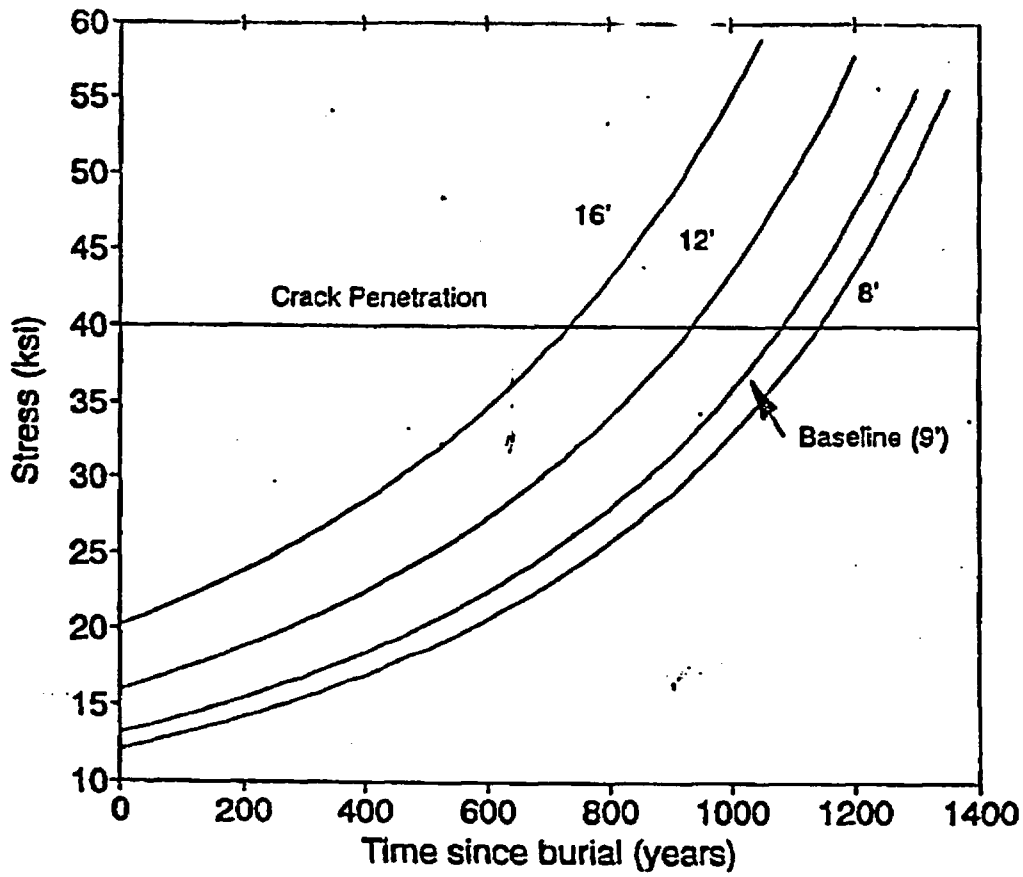

DATE: 9/7/93	ILT Vault Time to Crack Penetration of Walls; Sensitivity to Depth of Soil Cover
REF: #1025-007	
LITERA	Figure 29

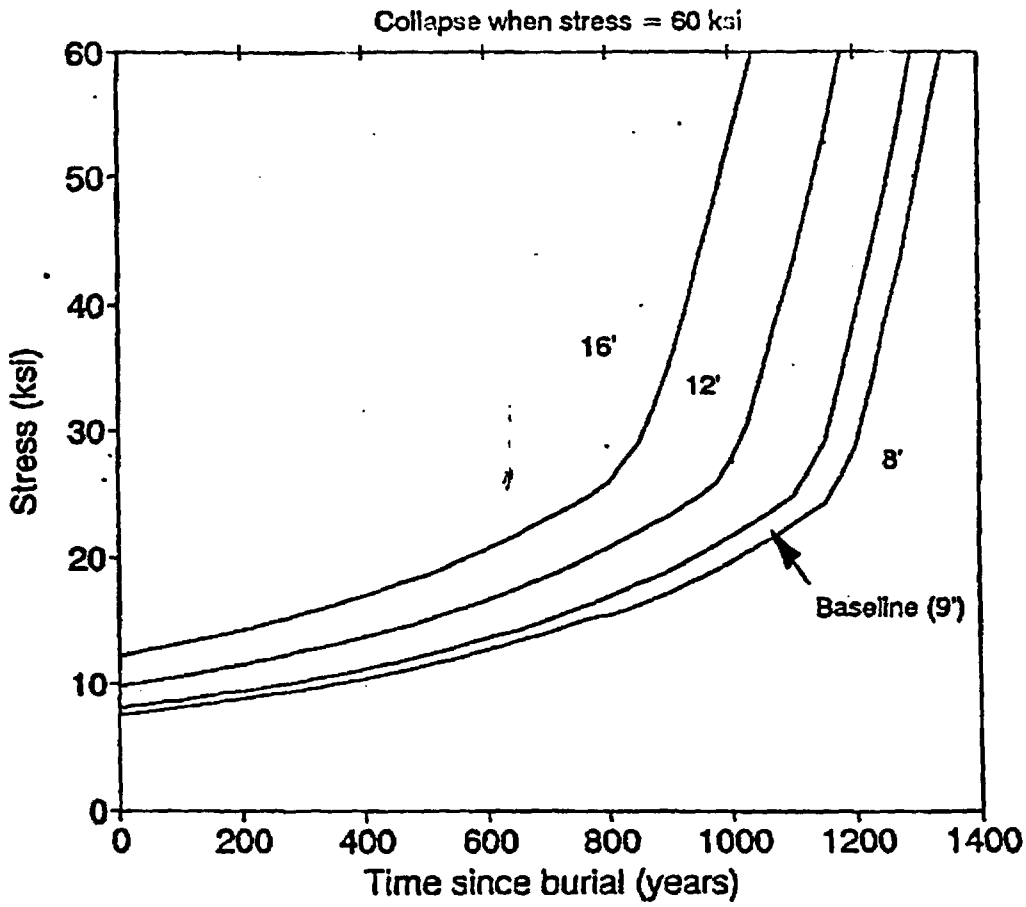

DATE: 9/7/93	ILT Vault Time to Roof Collapse; Sensitivity to Depth of Soil Cover	
REF: #1025-007		
NTERA		Figure 30

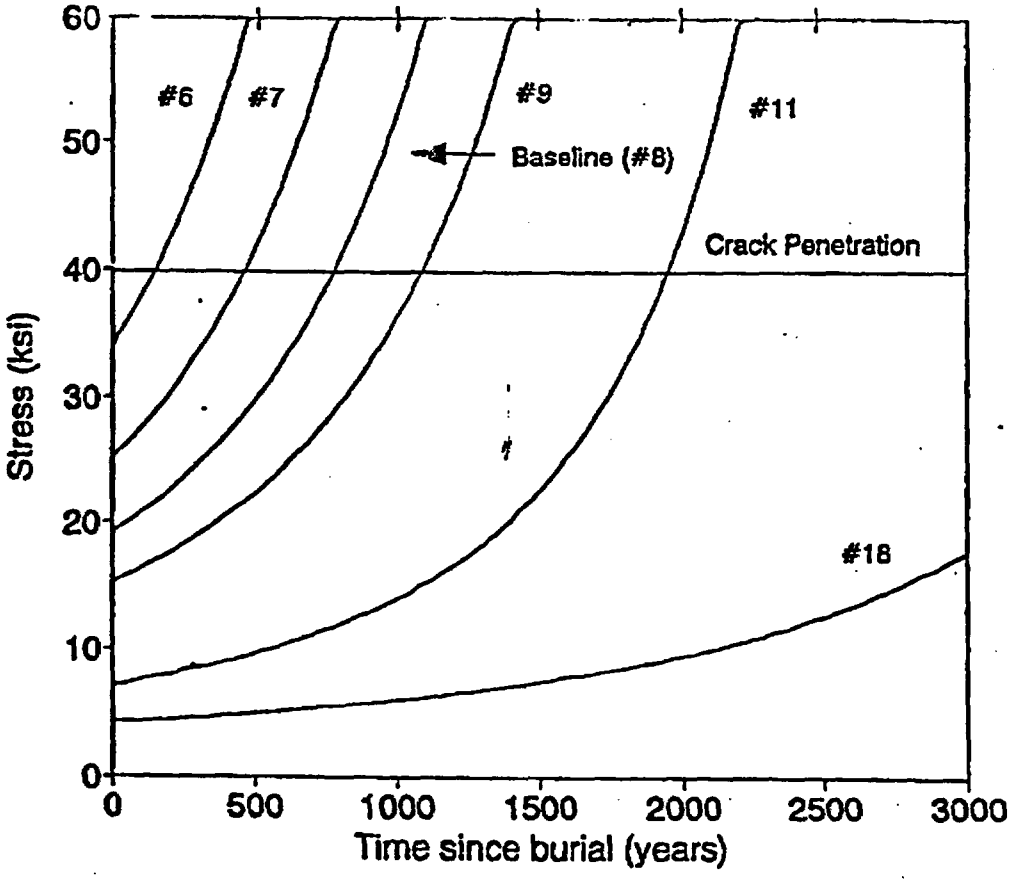

DATE: 9/7/93 REF: #1025-007	ILT Vault Time to Crack Penetration of Roof; Sensitivity to Rebar Size	
MERA		Figure 31

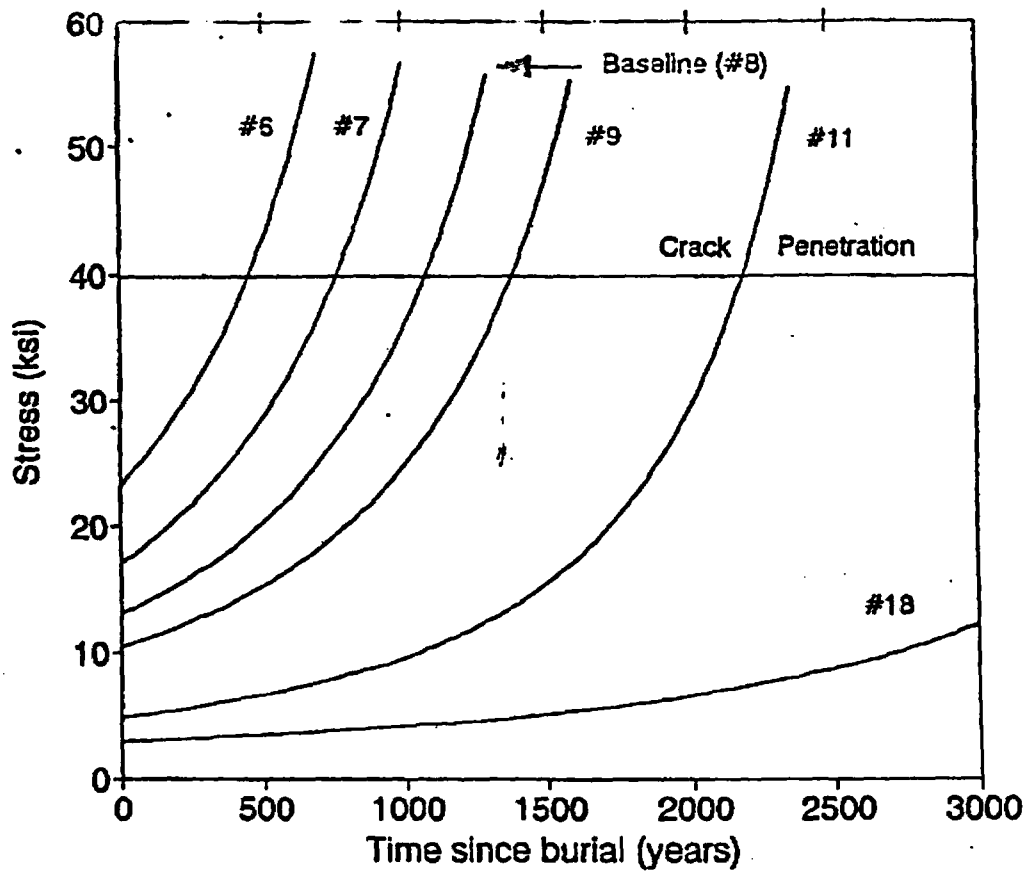

DATE: 9/7/93	ILT Vault Time to Crack Penetration of Walls; Sensitivity to Rebar Size
REF: #1025-007	
INTERA	Figure 32

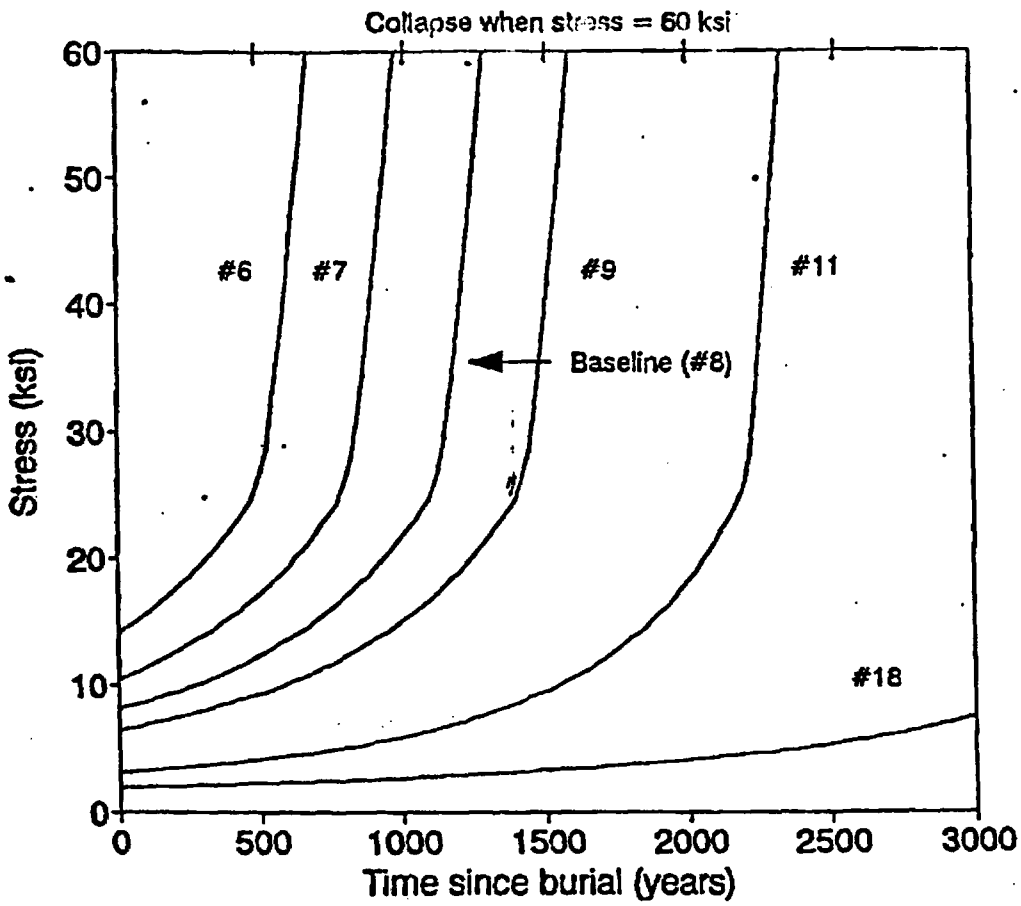

DATE: 9/7/93	ILT Vault Time to Roof Collapse Sensitivity to Rebar Size	
REF: #1025-007		
LITERA		Figure 33

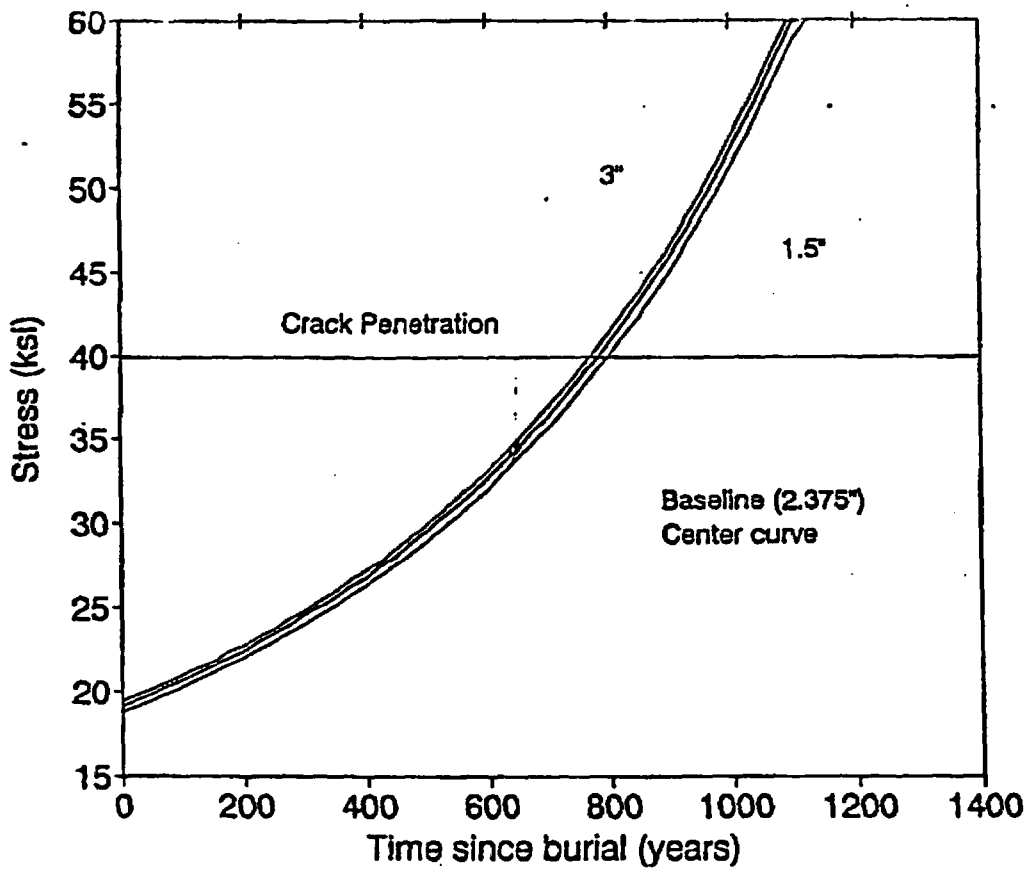

DATE: 9/7/93	ILT Vault Time to Crack Penetration of Roof; Sensitivity to Depth of Concrete Cover Over Rebar
REF: #1025-007	
INTERA	Figure 34

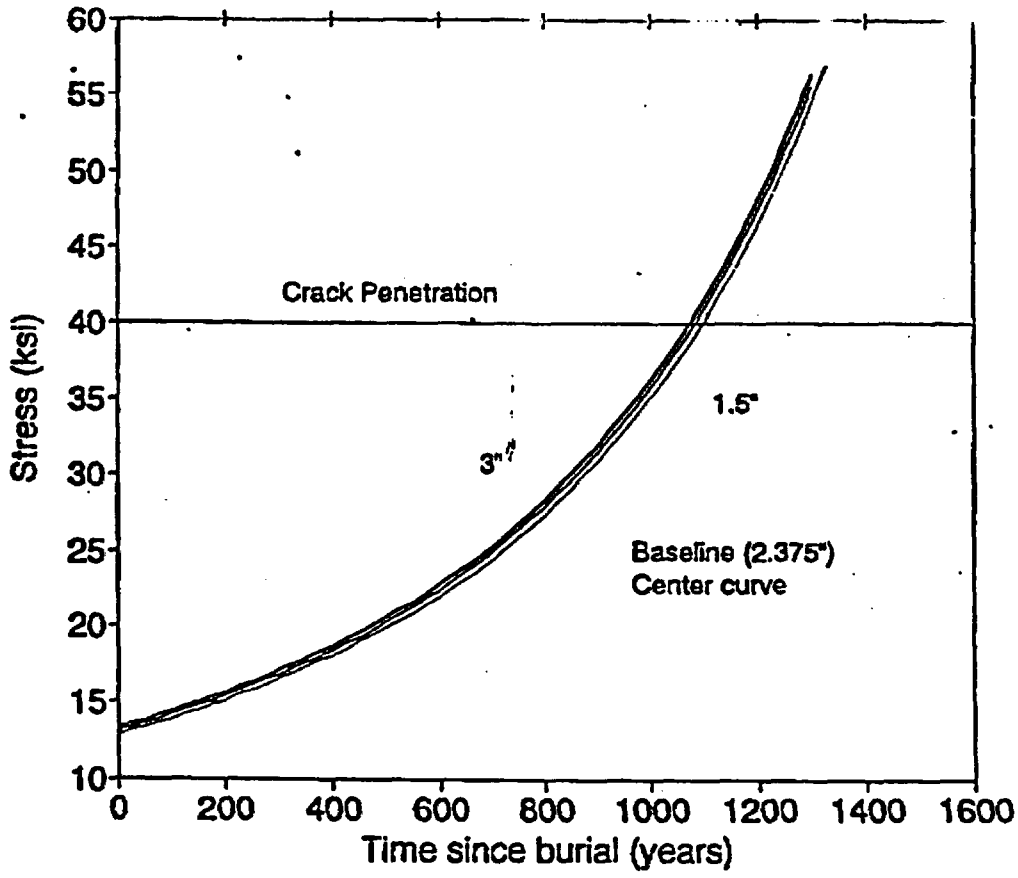

DATE: 9/7/93	ILT Vault Time to Crack Penetration of Walls; Sensitivity to Depth of Concrete Cover over Rebar
REF: #1025-007	
INTERA	Figure 35

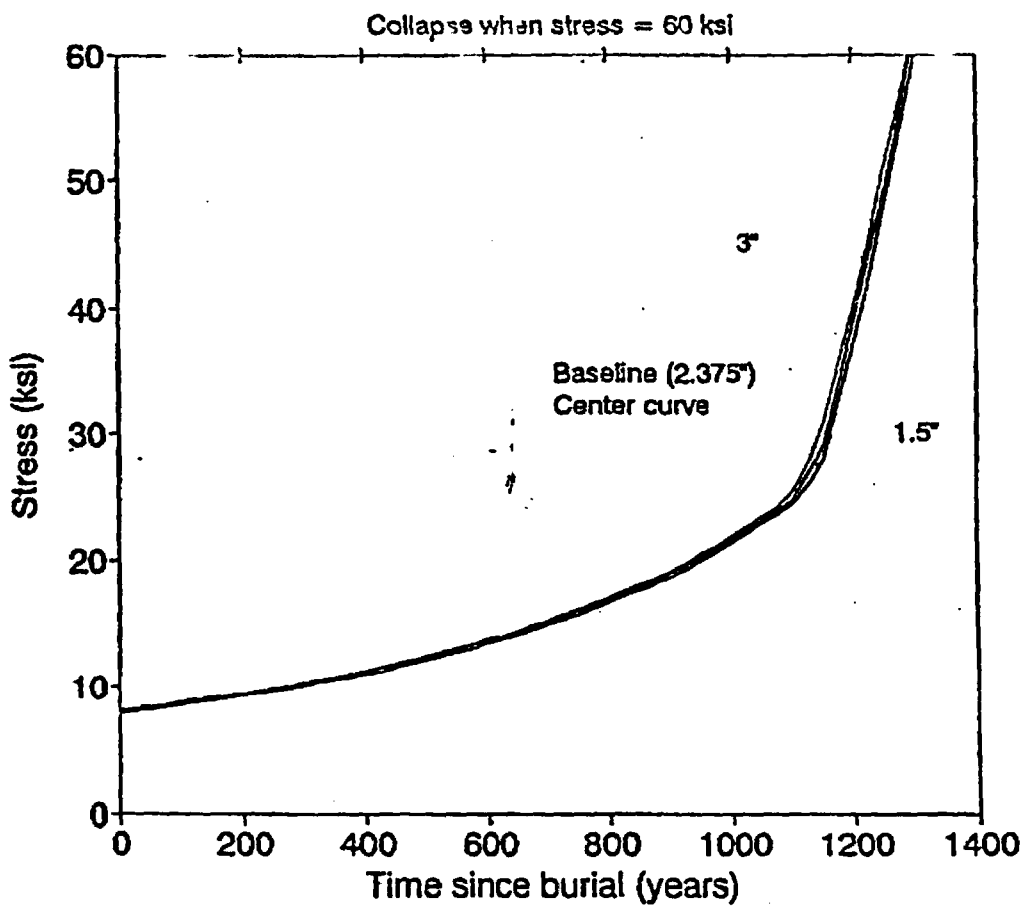

DATE: 9/7/93	ILT Vault Time to Roof Collapse; Sensitivity to Depth of Concrete Cover Over Rebar
REF: #1025-007	
INTERA	Figure 36

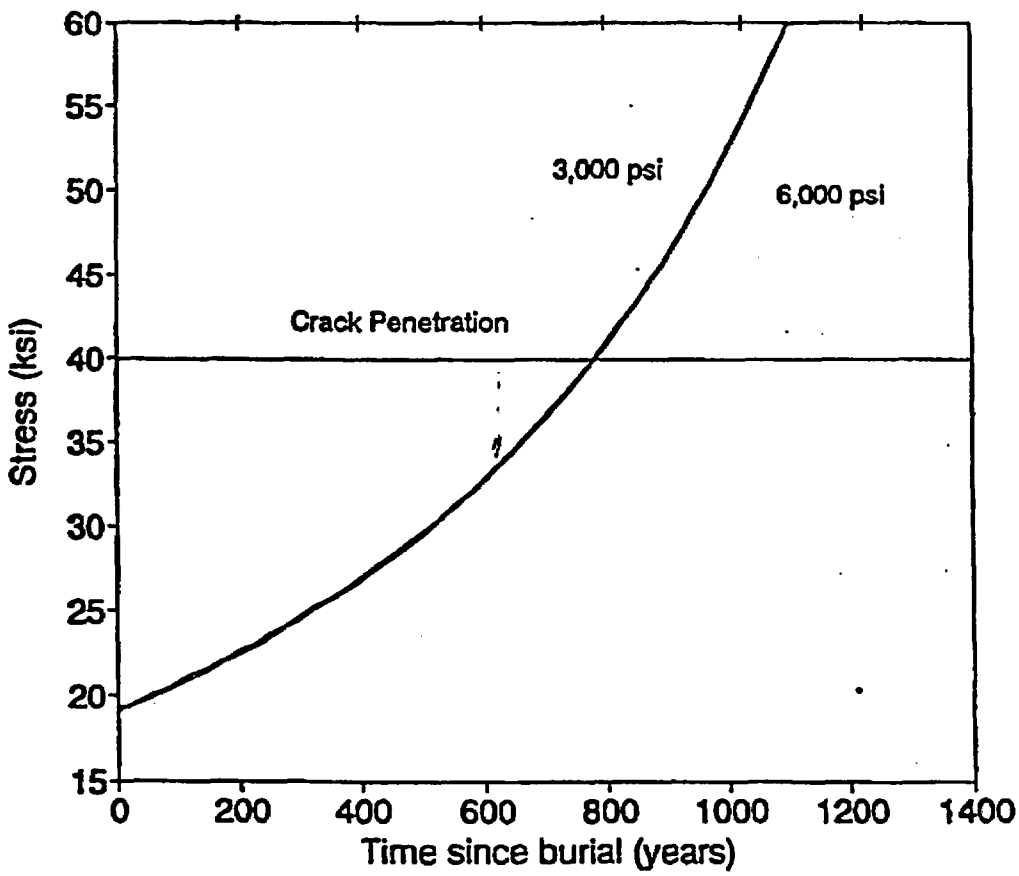

DATE: 9/7/93 REF: #1025-007	ILT Vault Time to Crack Penetration of Roof; Sensitivity to Concrete Strength
LITERA	Figure 37

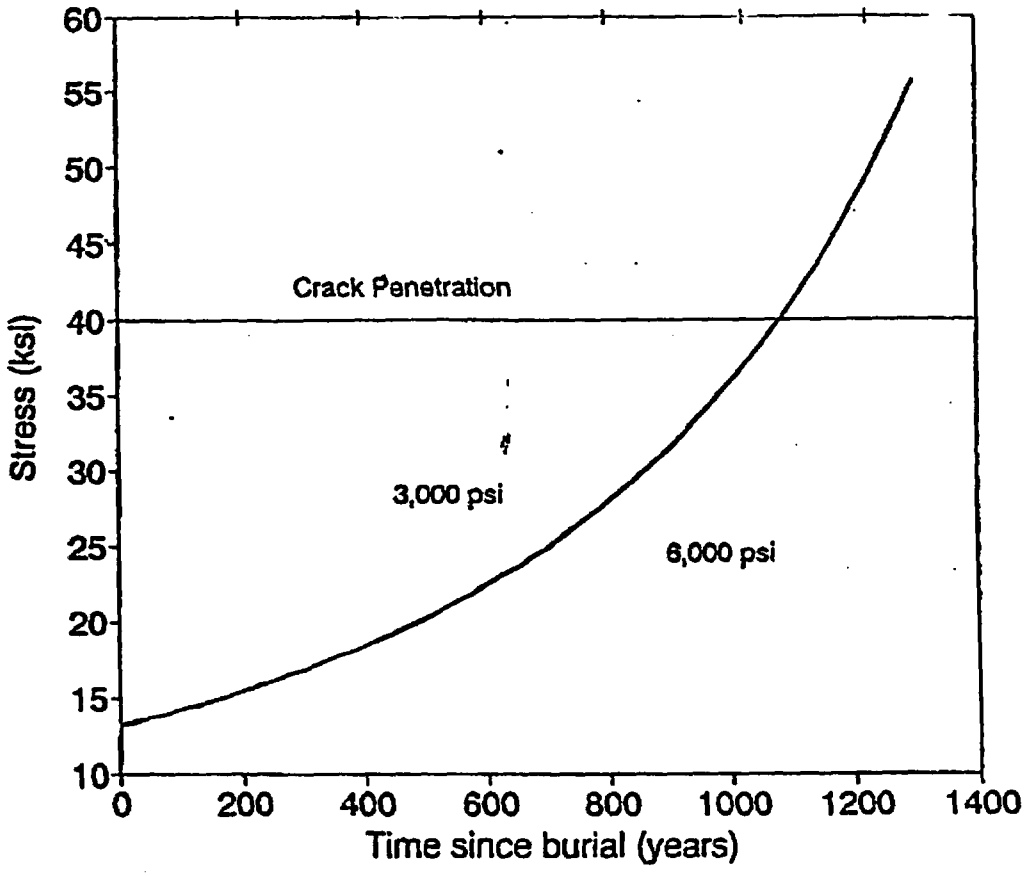

DATE: 9/7/93 REF: #1025-007	ILT Vault Time to Crack Penetration of Walls; Sensitivity to Concrete Strength	
INTERA		Figure 38

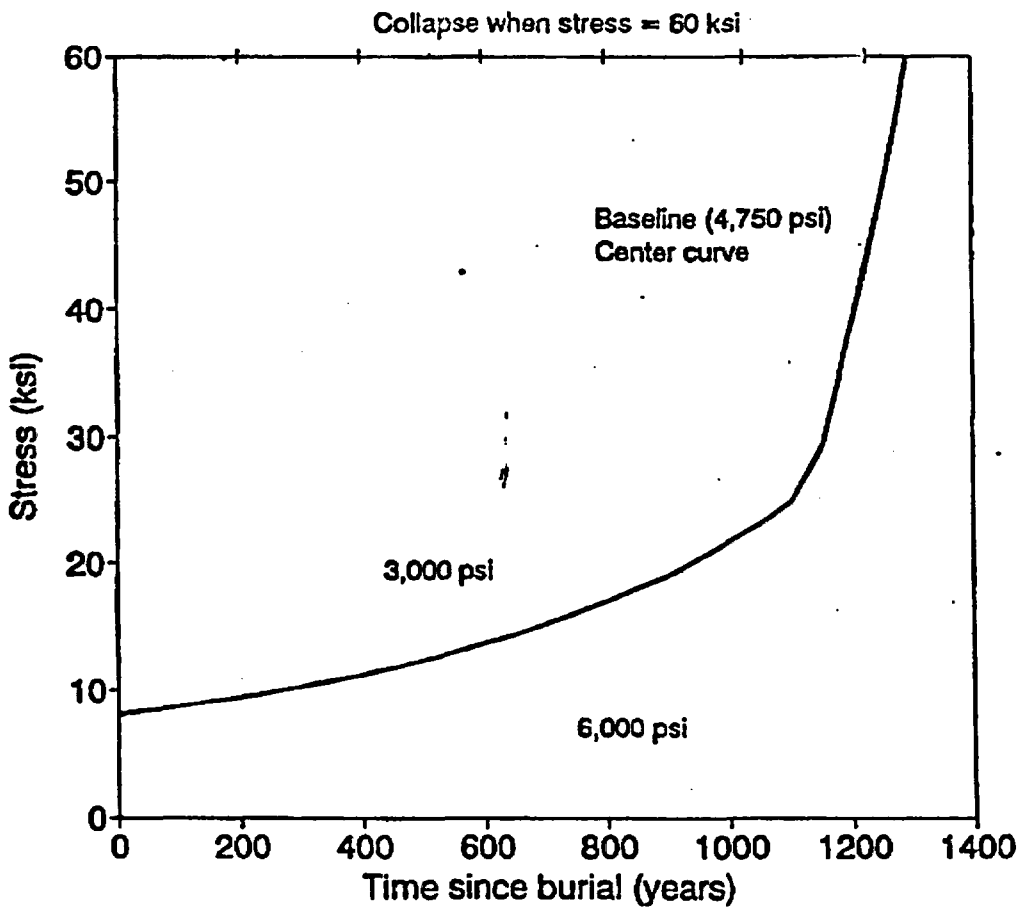

DATE: 9/7/93 REF: #1025-007	ILT Vault Time to Roof Collapse; Sensitivity to Concrete Strength
INTERA	Figure 39

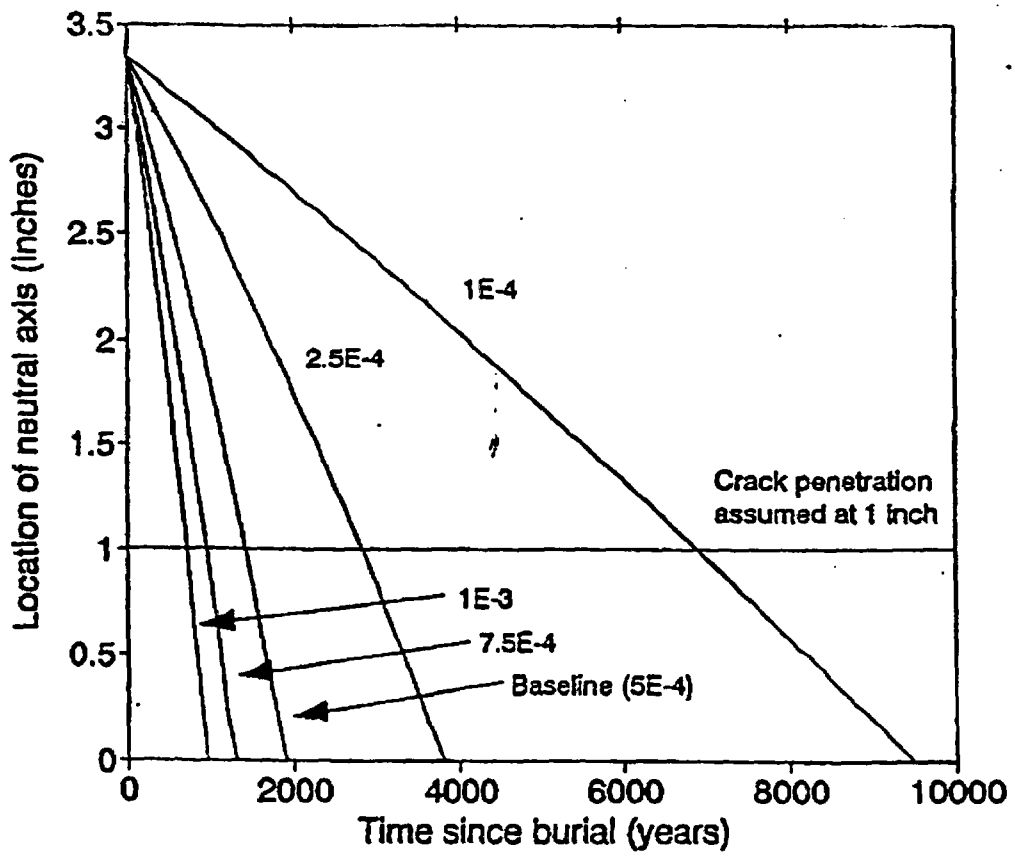

DATE: 9/7/93 REF: #1025-007	LAW Vault Time to Crack Penetration of Roof; Sensitivity to Hydrogen Evolution Corrosion Rate (cm/yr)
LITERA	Figure 40

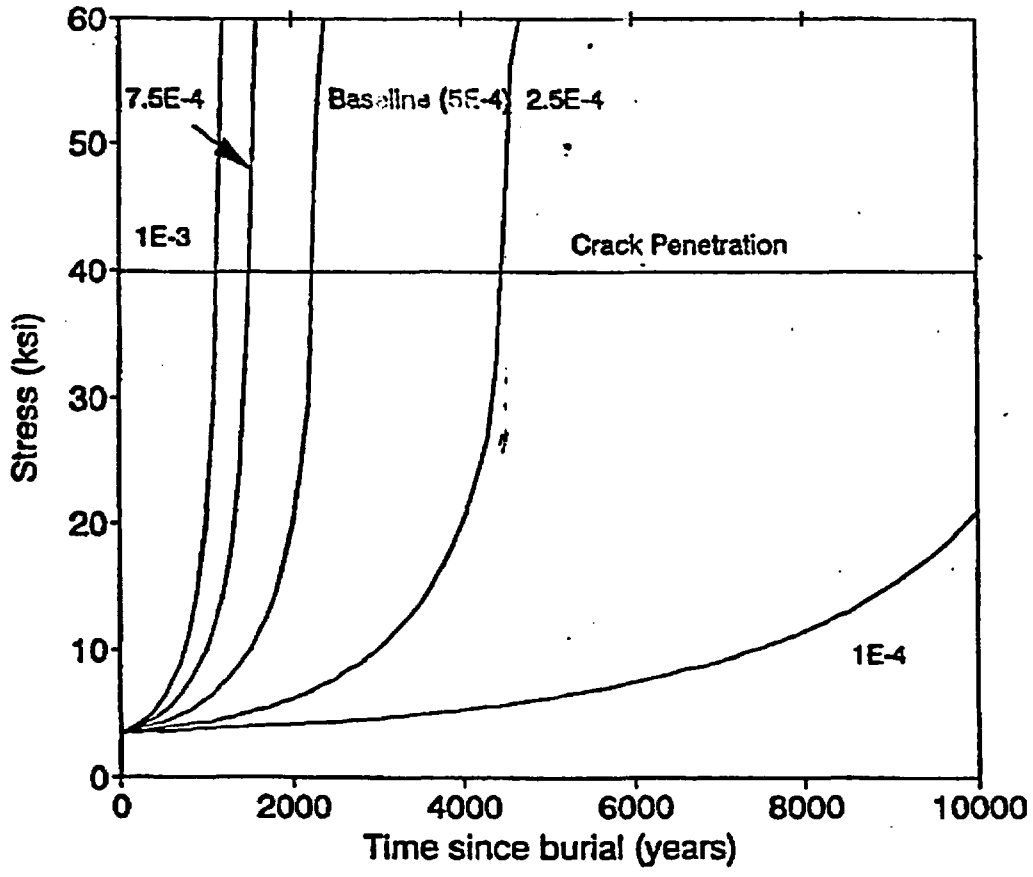

DATE: 9/7/93	LAW Vault Time to Crack Penetration of Walls; Sensitivity to Hydrogen Evolution Corrosion Rate (cm/yr)
REF: #1025-007	
INTERA	Figure 41

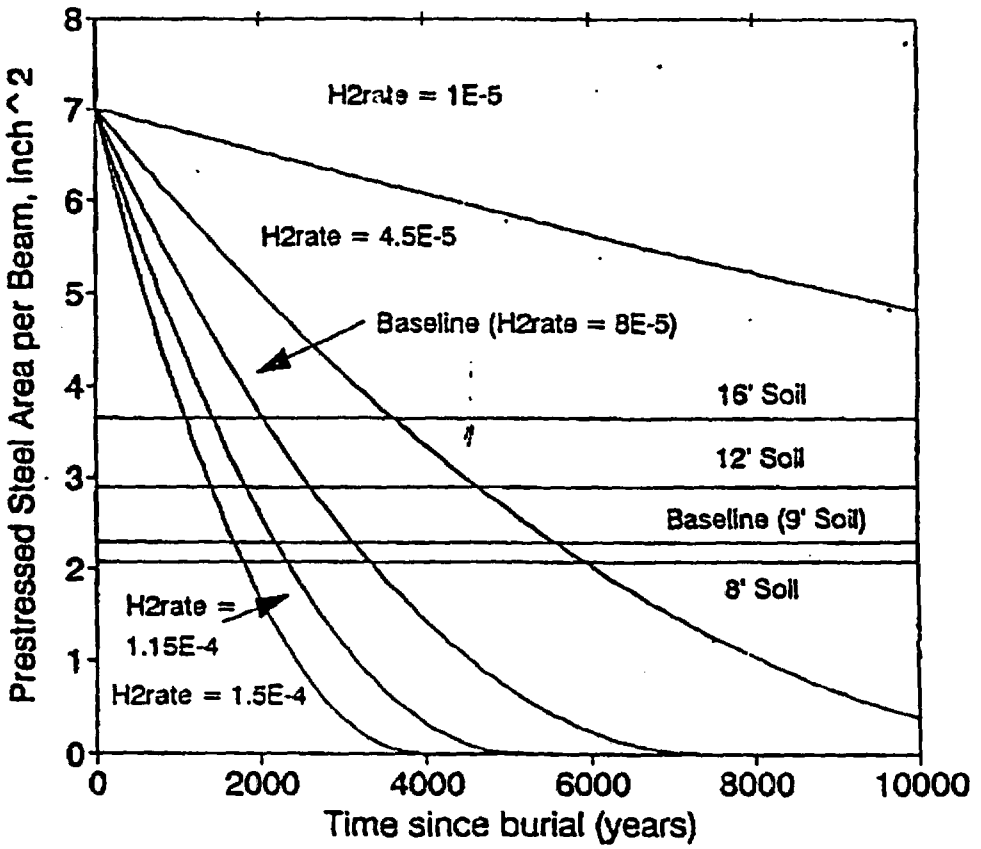

Horizontal lines indicate minimum prestressed steel area required for various depths of soil cover.

DATE: 9/7/93 REF: #1025-007	LAW Vault Time to Roof Collapse; Sensitivity to Hydrogen Evolution Corrosion Rate (H2rate; cm/yr) and Depth of Soil Cover
MITERA	Figure 42

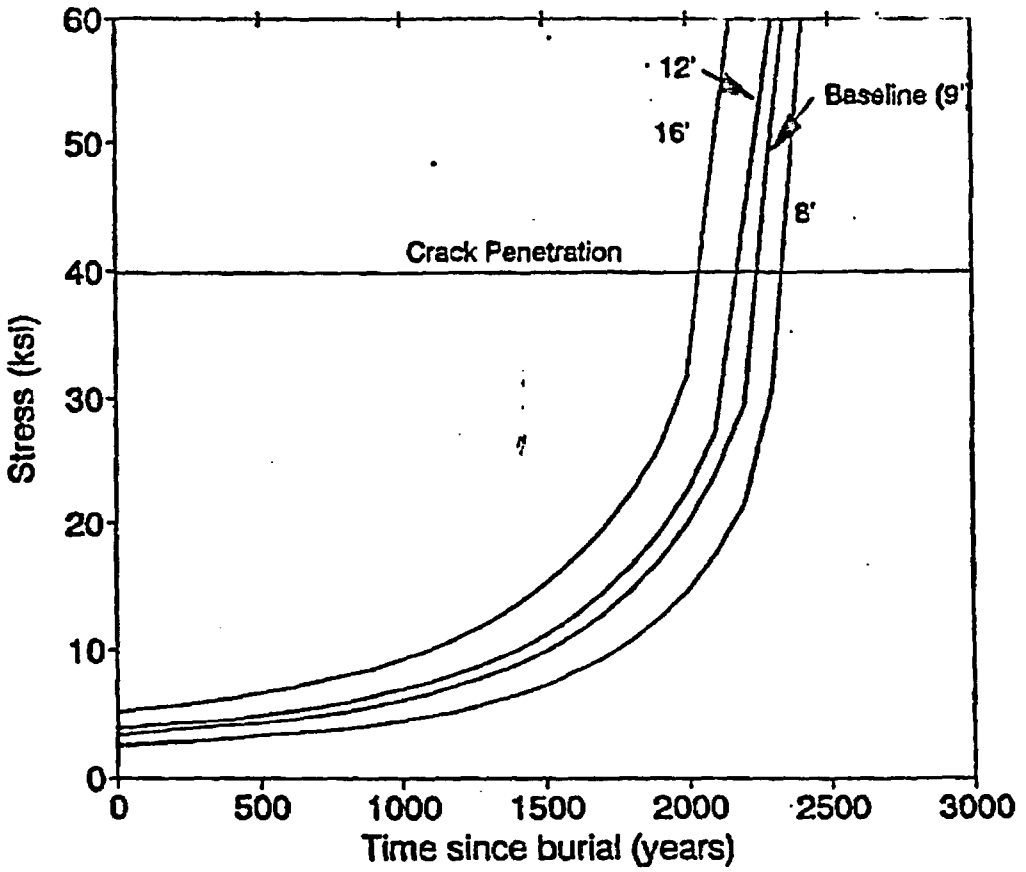

DATE: 9/7/93	LAW Vault Time to Crack Penetration of Walls; Sensitivity to Depth of Soil Cover
REF: #1025-007	
LITERA	Figure 43

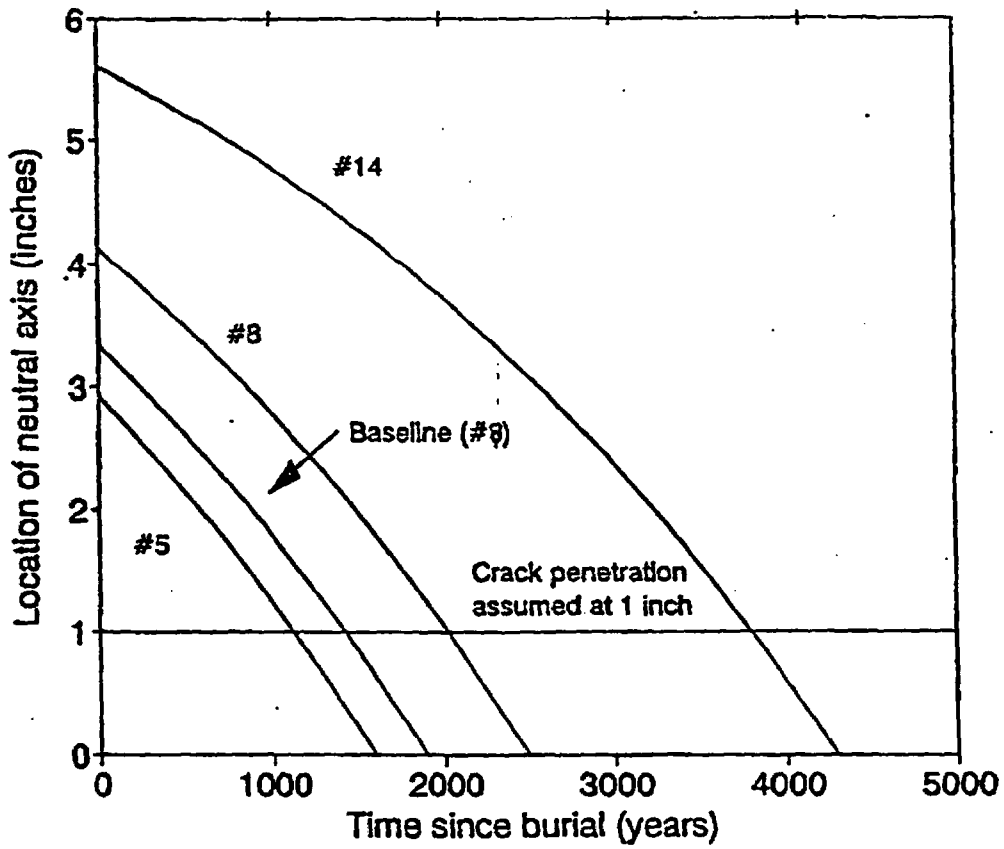

DATE: 9/7/93	LAW Vault Time to Crack Penetration of Roof; Sensitivity to Rebar Size
REF: #1025-007	
INTERA	Figure 44

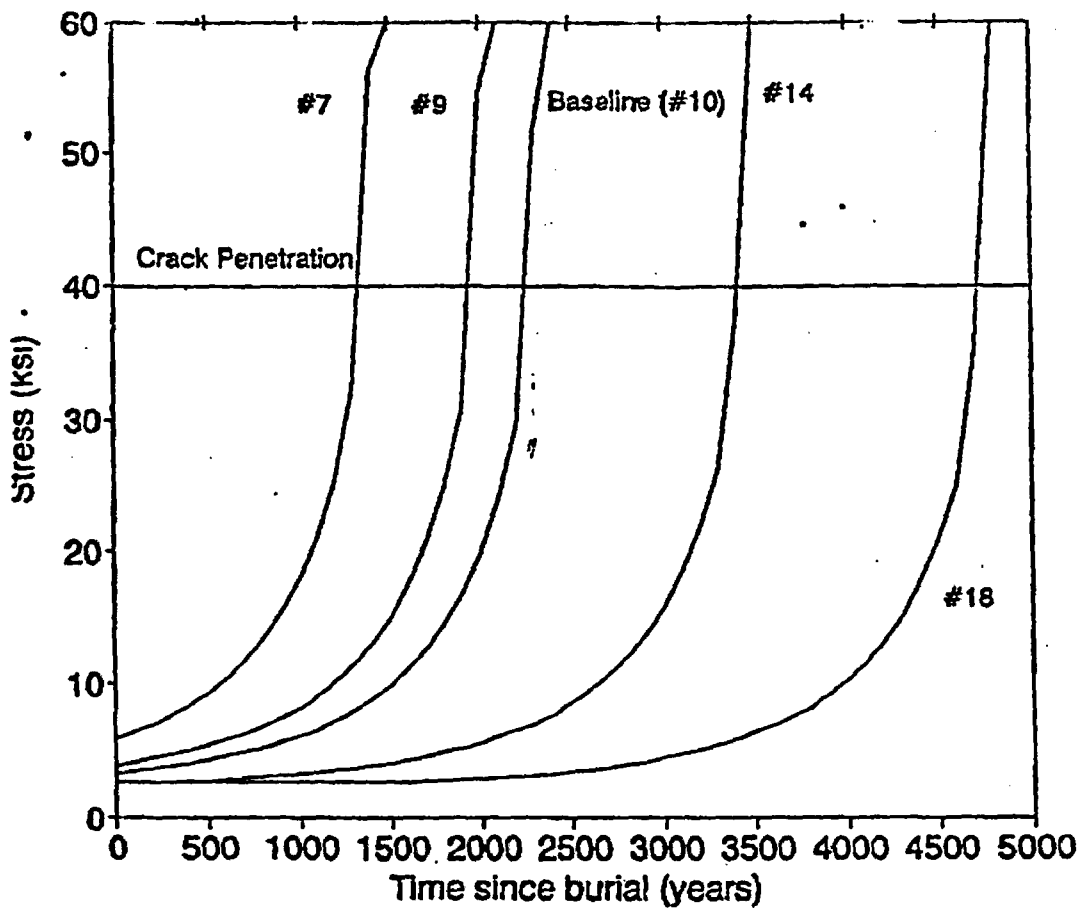

DATE: 9/7/93 REF: #1025-007	LAW Vault Time to Crack Penetration of Walls; Sensitivity to Rebar Size
MTEGRA	Figure 45

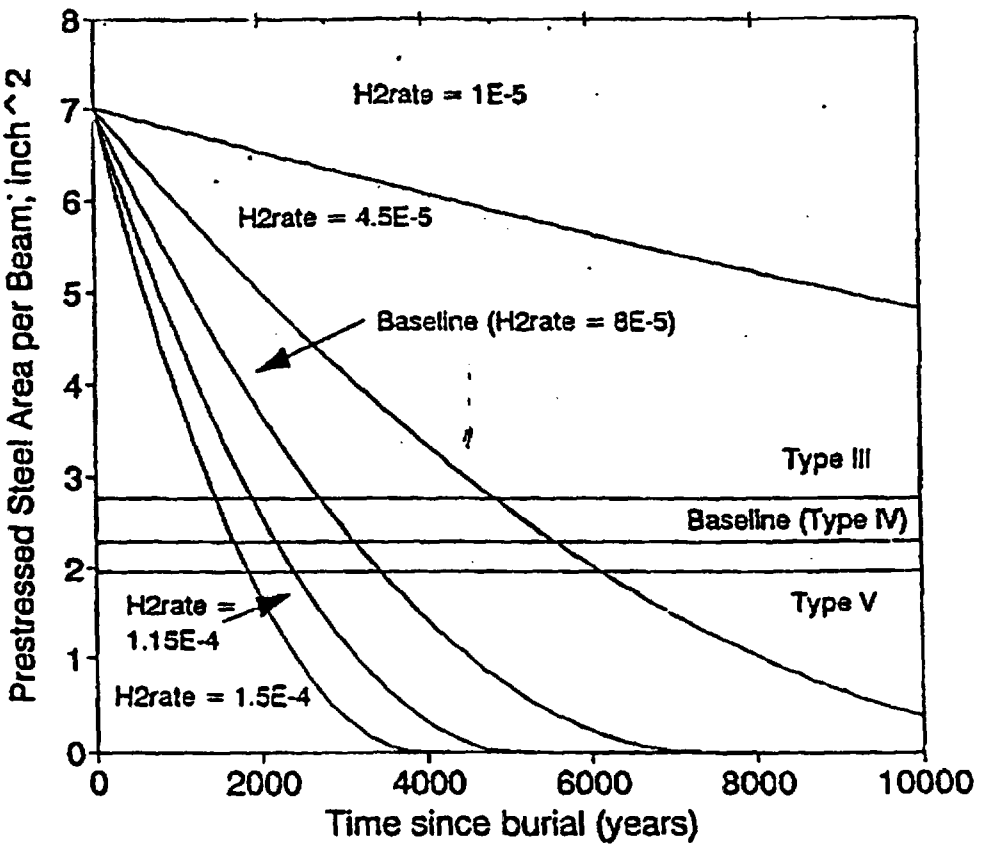

Horizontal lines indicate minimum prestressed steel area required for various sized AASHTO beams.

DATE: 9/7/93	LAW Vault Time to Roof Collapse; Sensitivity to Hydrogen Evolution Corrosion Rate (H2rate; cm/yr) and Beam Type
REF: #1025-007	
LITERA	Figure 48

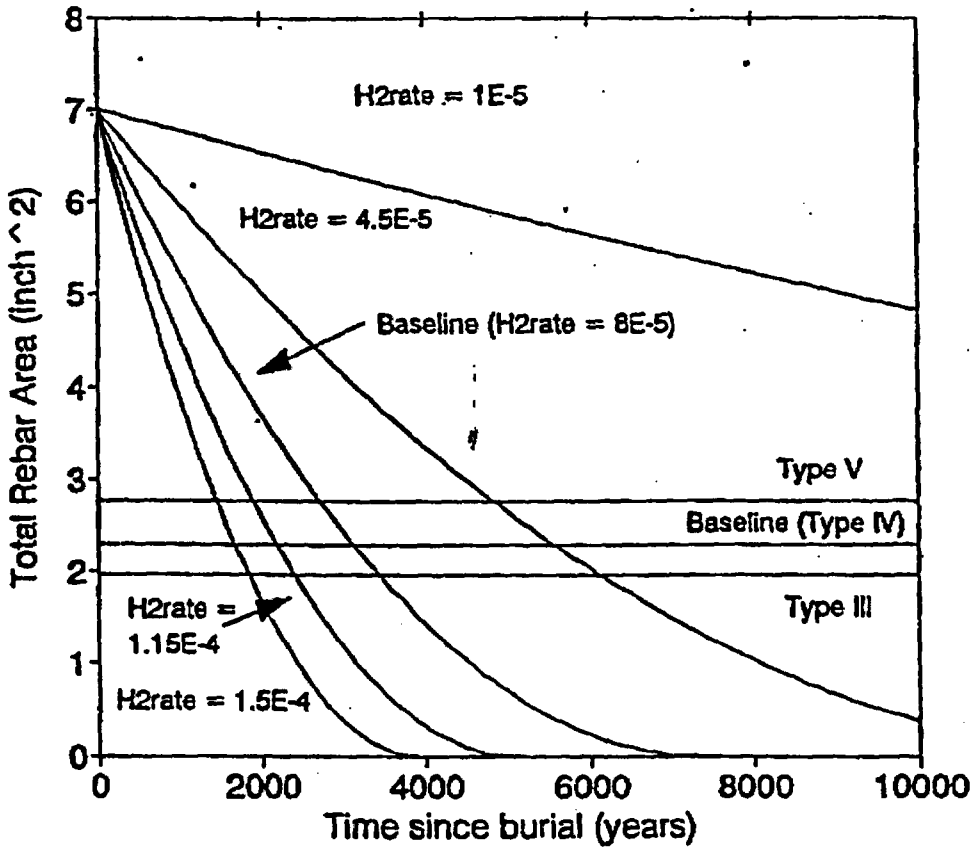

Horizontal lines indicate minimum prestressed steel area required for various sized AASHTO beams.

DATE: 9/7/93	LAW Vault Time to Roof Collapse; Sensitivity to Hydrogen Evolution Corrosion Rate (H2rate; cm/yr) and Beam Type
REF: #1025-007	
INTERA	Figure 46

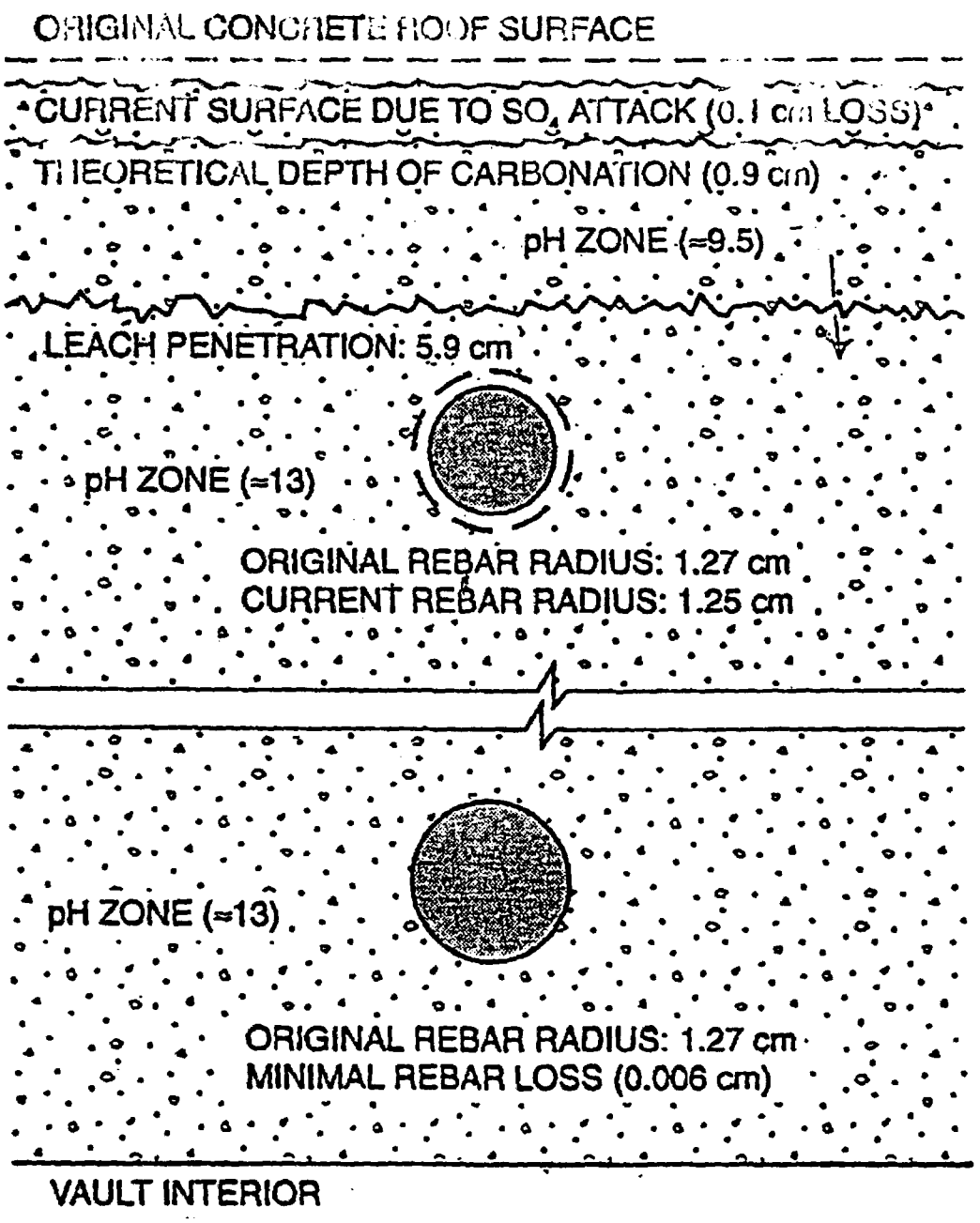

DATE: 9/7/93	Cross-Section of Vault Roof Assuming Use of High-pH Concrete; Degradation at 50 Years	
REF: #1025-007		
INTERA		Figure 47

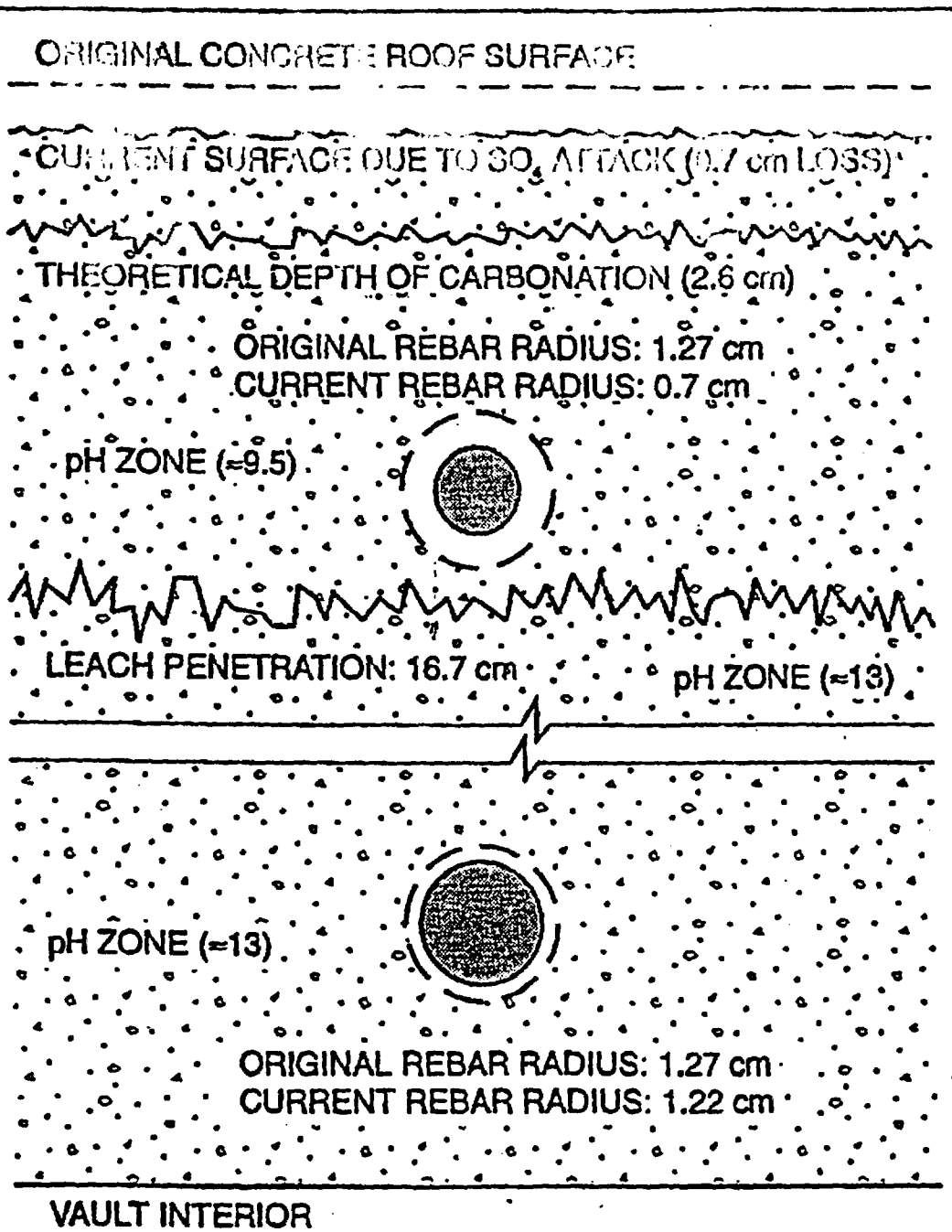

DATE: 9/7/93 REF: #1025-007	Cross-Section of Vault Roof Assuming Use of High-pH Concrete; Degradation at 400 Years	
INTERA		Figure 48

APPENDIX L

DESCRIPTION OF NAVAL REACTOR WASTE DISPOSAL

L.1 DESCRIPTION OF NAVAL REACTOR (NR) WASTE DISPOSAL

Heavily shielded shipping/disposal casks containing NR waste are planned to be disposed of in E-Area. Large quantities of activation products are associated with the metal matrix of the waste forms within the disposal containers. The purpose of this appendix is to assess the performance of the planned method of disposal of the NR waste.

L.1.1 Description of NR Waste Forms

Naval reactor waste consists of a variety of solid activated metal NR components, including core barrels, adapter flanges, closure heads, and other similar equipment. A concise description of the waste forms likely to be present in the disposal containers is not available because of the classified nature of this information. The total volume of the metal waste alone is expected to be about 3.5 m^3 per disposal container. About 3.8×10^{-3} m^3 (1 gal) of water is expected to be present in each disposal cask.

The shipping/disposal containers in which the NR wastes are planned to be disposed are cylindrical in shape, and composed of carbon steel, with 304 stainless steel inner containers. The containers are Type B or Type-B equivalent, and thus, are designed to be impervious to water. A cross-section of a typical disposal container is illustrated in Fig. L.1-1 (WSRC 1992). The inner volume of this typical container is approximately 27 m^3.

L.1.2 Layout and Capacity of NR Waste Disposal Site

In this assessment, it is assumed that 100 disposal casks containing NR waste will be disposed of in E-Area at grade. Given the dimensions provided in Fig. L.1-1, the minimum area for disposal of 100 casks is 1,024 m^2, which corresponds to the area required if 100 casks are placed immediately adjacent to each other in any type of rectangular arrangement. It is likely that there will be a spacing between casks at the time of disposal, and the layout assumed for this assessment is shown in Fig. L.1-2. Here, the spacing between casks is 1 m.

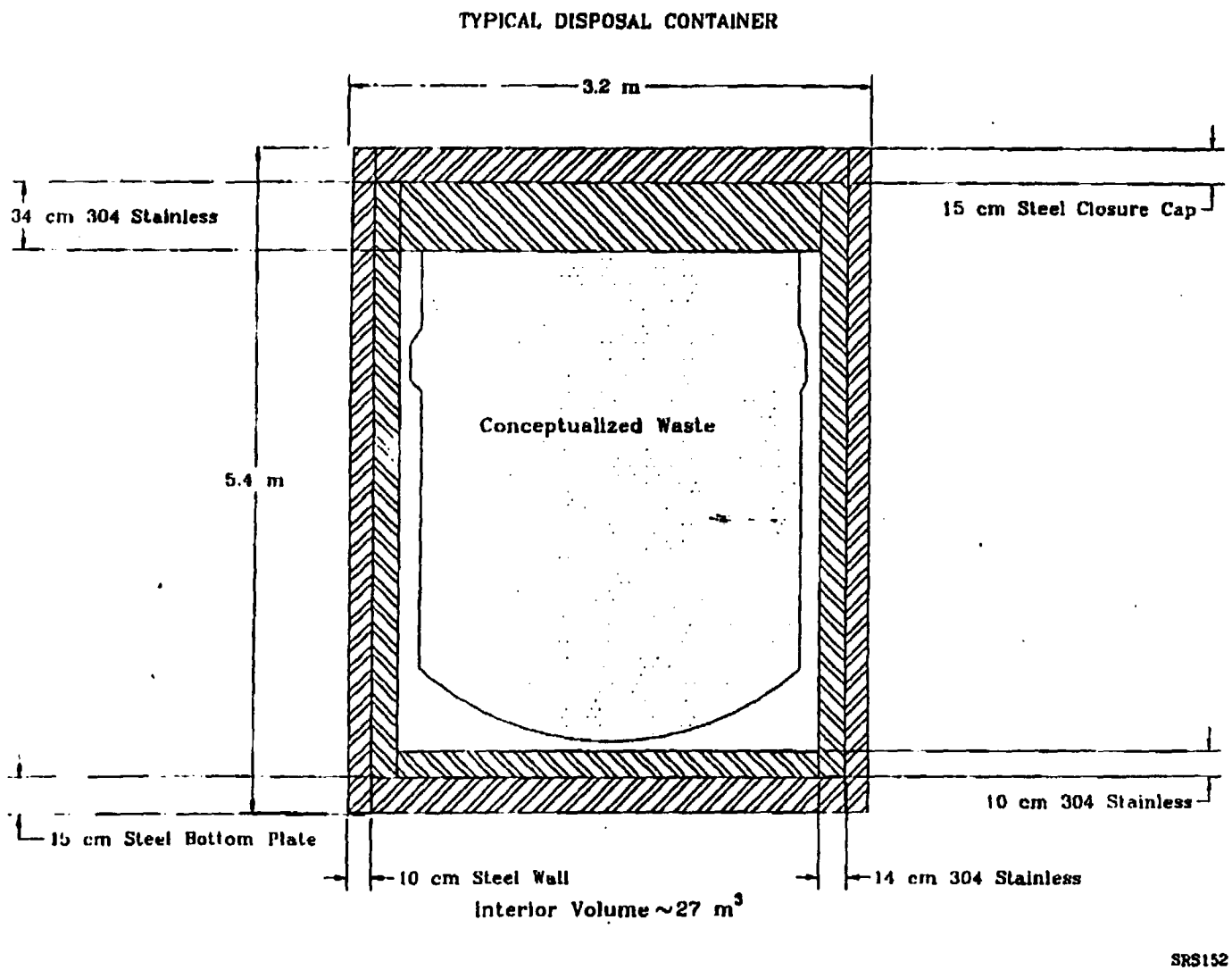

Fig. L.1-1. Naval reactor waste disposal container.

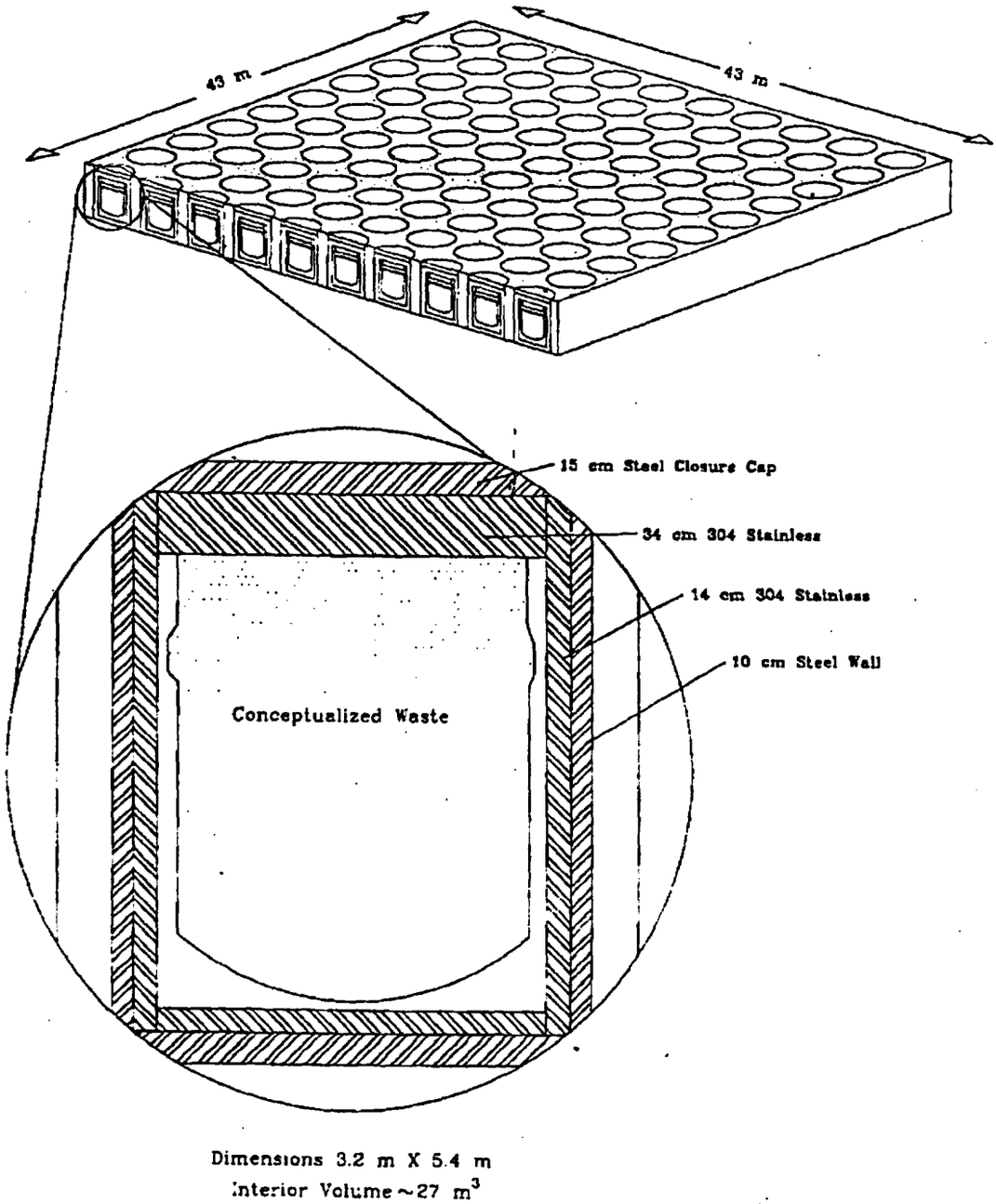

Fig. L.1-2. Proposed layout of Naval Reactor Waste Disposal Area in the EAV facility.

L.1.3 Radioactive Inventory of NR Waste

A radionuclide inventory supplied by the waste generators is presented in Table L.1-1 (WSRC 1992). This inventory applies to 41 casks of five different types that are planned to be delivered to E-Area. The total activity of these casks is estimated to be 5.84×10^6 Ci. This assessment considers, however, that up to 59 more disposal containers will be accepted, with the same general mix of cask types. Allowable inventories for 100 casks will be developed for the radionuclides listed in Table L.1-1.

L.1.4 Closure Concept

Because the NR waste disposal containers will be placed within the EAV facility, final closure will be similar to that for the entire facility. For the purposes of this assessment, the same closure concept as for the EAVs (Sect. 2.9) is assumed. Briefly, backfill of Burma Road sand is assumed to be placed over at-grade casks, above which a laterally extensive moisture barrier is assumed to be placed. The moisture barrier consists of 0.76 m of clay overlain by 0.3 m of gravel and a geotextile fabric. Over this moisture barrier, 0.76 m of backfill is assumed, followed by 0.15 m of topsoil. As a result, a minimum of 2.9 m of cover material is assumed to overlie the NR disposal casks at closure. This requires that the casks be placed in a topographically low spot so as not to project into the cover materials. Revegetation and drainage ditches are assumed to constitute final closure, for the purposes of stabilizing soil, preventing pine tree growth and diverting excess water from the gravel layer.

L.2 ANALYSIS OF PERFORMANCE OF NR WASTE

The methods used to analyze the long-term performance of the NR waste disposal unit within the EAV facility are described in this section. A description of the radionuclide source term posed by the disposal containers is provided in Sect. L.2.1. Pathways to exposure of human receptors are considered in Sect. L.2.2. The conceptual models developed and

Table L.1-1 Radioactive inventory for 11 NR disposal casks to be shipped to E-Area

Number of units: Description:	1 CBOC Hardware	8 Core Barrel	8 Holddown Barrels	16 CSVTS/CH Hardware	8 Adapter Flanges	Total all casks (Ci)
Isotopes:						
H-3	9.6×10^{-3}	1.6	—	5.8×10^{-1}	—	$2.2 \times 10^{+1}$
C-14	3.1×10^{-1}	3.1×10^{-1}	—	$1.1 \times 10^{+1}$	1.6×10^{-3}	$1.8 \times 10^{+2}$
Sc-46	3.3×10^{-3}	—	—	—	—	3.3×10^{-3}
Cr-51	1.8×10^{-1}	$1.5 \times 10^{+1}$	1.6×10^{-1}	$8.1 \times 10^{+3}$	2.8×10^{-5}	$1.3 \times 10^{+5}$
Mn-54	3.1	$2.3 \times 10^{+1}$	1.8×10^{-1}	$5.7 \times 10^{+2}$	8.5×10^{-3}	$9.3 \times 10^{+3}$
Fe-55	$2.1 \times 10^{+2}$	$3.7 \times 10^{+3}$	$2.2 \times 10^{+1}$	$2.1 \times 10^{+4}$	2.6×10^{-1}	$3.7 \times 10^{+5}$
Co-58	$1.5 \times 10^{+1}$	$1.4 \times 10^{+2}$	1.8	$2.1 \times 10^{+4}$	3.8×10^{-2}	$3.4 \times 10^{+5}$
Fe-59	5.1×10^{-2}	7.8×10^{-1}	1.1×10^{-2}	$1.5 \times 10^{+2}$	4.4×10^{-4}	$2.4 \times 10^{+3}$
Ni-59	2.8	$6.3 \times 10^{+1}$	7.8×10^{-1}	$2.1 \times 10^{+2}$	4.8×10^{-4}	$3.9 \times 10^{+3}$
Co-60	$3.0 \times 10^{+2}$	$5.9 \times 10^{+3}$	$5.8 \times 10^{+1}$	$4.5 \times 10^{+4}$	1.5×10^{-1}	$7.7 \times 10^{+5}$
Ni-63	$3.8 \times 10^{+2}$	$6.3 \times 10^{+3}$	$7.8 \times 10^{+1}$	$2.9 \times 10^{+4}$	4.8×10^{-2}	$5.2 \times 10^{+5}$
Zn-65	1.3×10^{-1}	—	—	—	—	1.3×10^{-1}
Sr-90	1.2×10^{-2}	3.2×10^{-4}	2.8×10^{-4}	$2.9 \times 10^{+1}$	6.3×10^{-5}	$4.6 \times 10^{+2}$
Nb-94	6.4×10^{-3}	1.6×10^{-4}	1.4×10^{-1}	3.2×10^{-1}	3.2×10^{-5}	6.2
Nb-95	4.1×10^{-2}	2.4×10^{-3}	2.2×10^{-3}	$1.5 \times 10^{+5}$	4.7×10^{-4}	$2.4 \times 10^{+6}$
Zr-95	—	1.0×10^{-3}	9.4×10^{-4}	—	2.3×10^{-4}	1.7×10^{-2}
Tc-99	3.3×10^{-4}	3.7	—	—	—	$3.0 \times 10^{+1}$
In-113	—	—	—	$4.4 \times 10^{+3}$	—	$7.0 \times 10^{+4}$
Sn-113	—	—	—	$4.4 \times 10^{+3}$	—	$7.0 \times 10^{+4}$
In-114	—	—	—	$5.5 \times 10^{+2}$	—	$8.8 \times 10^{+3}$
Sn-119m	—	—	—	$5.5 \times 10^{+4}$	—	$8.8 \times 10^{+5}$
Sn-123	—	—	—	$1.5 \times 10^{+3}$	—	$2.4 \times 10^{+4}$
Sb-125	—	—	—	$1.2 \times 10^{+4}$	—	$1.9 \times 10^{+5}$
I-129	1.3×10^{-4}	—	—	—	—	1.3×10^{-4}
Cs-137	1.2×10^{-2}	3.2×10^{-4}	2.8×10^{-4}	6.3×10^{-3}	6.3×10^{-5}	1.2×10^{-1}
Hf-181	4.5×10^{-3}	7.0×10^{-4}	6.3×10^{-4}	$2.6 \times 10^{+3}$	1.4×10^{-4}	$4.2 \times 10^{+4}$
Ta-182	2.9	—	—	$1.1 \times 10^{+3}$	—	$1.8 \times 10^{+4}$
Pu-239	2.5×10^{-5}	—	—	—	1.0×10^{-7}	2.6×10^{-5}
Pu-241	8.9×10^{-4}	2.3×10^{-5}	2.1×10^{-5}	4.7×10^{-4}	4.7×10^{-6}	8.8×10^{-3}

computational approach used to assess the performance of the NR waste unit are described in Sect. L.2.3.

L.2.1 Source Term

The NR waste provides a source of radionuclides to the geosphere. To characterize this source it is necessary to consider mechanisms of release. The NR waste is composed of solid activated metal, with less that 1% of the radionuclide inventory in the form of surface contamination (WSRC 1992). Release of radionuclides from the waste form to the interior of the casks will be governed by corrosion of the metal matrix. Corrosion rates are directly proportional to the surface area of the wastes, and are a strong function of the type of metal making up the waste and the chemistry of water contacting the waste. Release to the geosphere requires a breach of the disposal container, such that water contacts the waste *and* requires the presence of corrosion products on the surface of the waste. Upon contact with water, radionuclides present in corrosion products are partitioned between pore water and the iron compounds constituting the corrosion products. The mechanisms relevant to partitioning include: 1) desorption from corrosion products; 2) dissolution of precipitated material within the corrosion product matrix; and/or 3) volatilization into soil gas. Transport in the geosphere occurs as a result of advective and diffusive processes. Advective processes arise as a consequence of the infiltration of water through the disposal unit. Diffusive processes are driven by the concentration gradient that exists between pore fluids of the waste matrix and pore fluids of the surrounding uncontaminated soil.

Corrosion of the steel disposal casks is an important consideration in developing a source term model. The disposal containers prevent release of radionuclides to the environment as a result of leaching until such time that the containers are no longer impervious to water. The outer carbon steel of the disposal casks (Fig. L.1-1) is less resistant to degradation than the inner stainless steel portion.

Degradation of the engineered cover will affect release to the geosphere through the effect on infiltration of water into the trenches. As was described in Sect. 3.1.3.1, a reasonable scenario for degradation of the cover is that the cover may be degraded to the

gravel layer approximately 900 years after closure of the E-Area Facility. Before that time, it is possible that infiltration may increase through the clay layer as a result of head build-up in the gravel layer, if for example the drains fail to divert sufficient water, or as a result of disturbance of the clay layer by roots or burrowing animals.

L.2.2 Pathways and Scenarios

In this section, the pathways to human exposure to potential NR waste constituents are addressed. The time periods of concern for human exposure are identical to those described in Sect. 3.2.1.

L.2.2.1 Transport Pathways

Radionuclides released from the NR wastes to the geosphere have the potential of reaching humans through numerous pathways. Most conceivable pathways for a buried LLW source such as the NR wastes are described in Sect. 3.2.2.1. The same rationale applied in pathway screening for the EAVs applies to the NR wastes, with the result that only pathways related to contaminated air or groundwater are considered to be of potential consequence for off-site exposures. For off-site exposures, pathways considered include leaching of corroded NR wastes, resulting in contamination of groundwater local to E-Area, and volatilization of H-3 and C-14. Intruder exposure scenarios are considered separately in Sect. L.2.2.3.

L.2.2.2 Exposures of Off-Site Members of the Public and Protection of Groundwater

From the discussion in Sect. 3.2.3.3, only the drinking water pathway needs to be considered for off-site releases of radionuclides in groundwater. In cases where the MCL in groundwater corresponds to a dose equivalent less than the performance objective for off-site individuals of 25 mrem per year from all exposure pathways, compliance with the MCL would ensure that the dose to off-site individuals would be substantially less than the performance objective. In cases where the MCL in groundwater corresponds to a dose equivalent greater

than the performance objective for off-site individuals, the dose from all exposure pathways, theoretically, would be considered. However, as discussed in Sect. 3.2.3.3, the dose from pathways other than drinking water would be insignificant compared with the dose from the drinking water pathway.

Other than the groundwater pathway, exposure to atmospheric concentrations of volatile radionuclides must be considered. For atmospheric releases of H-3 and C-14, the calculated dose is compared to the performance objective of 10 mrem per year EDE in this analysis.

L.2.2.3 Exposure Scenarios for Inadvertent Intruders

In Sect. 3.2.4, several exposure scenarios for inadvertent intruders that could be applied to disposal of LLW in concrete vaults were described. Two chronic exposure scenarios (the agriculture and post-drilling scenarios) and two acute exposure scenarios (the construction and drilling scenarios) were based on the assumption that an inadvertent intruder could access disposed waste while excavating or drilling at the disposal site. An additional chronic exposure scenario (the resident scenario) and an additional acute exposure scenario (the discovery scenario), were based on the assumption that an inadvertent intruder was prevented from accessing disposed waste while excavating at the disposal site by the presence of intact engineered barriers, but nonetheless, could receive an external exposure while residing or working at the site.

As described in Sect. L.1.1 and indicated in Fig. L.1-1, the NR wastes will be contained in thick-walled carbon steel and stainless steel casks. These casks presumably will degrade only very slowly by corrosion and, thus, reasonably can be presumed to prevent inadvertent intrusion into the waste for a considerable period of time after disposal. For as long as the casks maintain their integrity, an inadvertent intruder presumably could only receive an external exposure according to scenarios similar to the resident or discovery scenario used in the analysis for waste disposal in concrete vaults.

In the analysis for the NR wastes, three scenarios for exposure of inadvertent intruders are considered. The first is external exposure to waste inside an intact waste cask immediately upon loss of active institutional controls at 100 years after disposal, which is the earliest time

that inadvertent intrusion is assumed to be credible (U.S.DOE 1988a). At this time, a conservative, upper-bound estimate of external dose is obtained on the basis of (1) reported inventories of photon-emitting radionuclides in the waste given in Table L.1-1, (2) the known spectrum of photons in the decay of each radionuclide (Kocher 1981), (3) consideration of the shielding provided by the waste casks for different photon-emitting radionuclides in the waste, and (4) the assumption that the external dose rate at the surface of the waste casks at the present time does not exceed 200 mrem/h, which is an acceptance criterion for the waste casks specified in 49 CFR Part 173.

The second exposure scenario for inadvertent intruders considered in the analysis for the NR wastes is the agriculture scenario, which involves direct excavation into the waste itself. This scenario reasonably can occur only at times long after disposal when the waste casks have been degraded by corrosion. The agriculture scenario assumes that an inadvertent intruder constructs a home directly on top of disposed waste and that some of the waste is exhumed while constructing the foundation for the home. Some of the exhumed waste is mixed with native soil in the intruder's vegetable garden, and the intruder is assumed to receive exposures from ingestion of contaminated vegetables from the garden, direct ingestion of contaminated garden soil, external exposure while working in the garden, residing in the home on top of the waste, and inhalation exposure while working in the garden and residing in the home.

The third scenario considered is a post-drilling scenario which also could occur when the casks have failed. Although, as indicated in Sect. 3.2.4.1 and Appendix A.4, the dose from the post-drilling scenario will always be less than the dose from the agriculture scenario when the two scenarios are presumed to occur at the same time after disposal, the post-drilling scenario is considered because it could occur at an earlier time than the agriculture scenario. In this scenario, waste exhumed by drilling is assumed to be mixed with native soil in the intruder's vegetable garden, and the intruder is assumed to receive exposures from ingestion of contaminated vegetables from the garden, direct ingestion of contaminated garden soil, and external and inhalation exposures while working in the garden.

L.2.3 Models and Assumptions

In Sect. L.2.1 and L.2.2, the potential mechanisms of release of radionuclides from the NR wastes were defined and the relevant human exposure scenarios were described. In this section, the models adopted and assumptions made to carry out the computations necessary to estimate doses are described.

L.2.3.1 Near-Field Model

The near-field model for the NR wastes addresses release of radionuclides from the waste in the containers to the surrounding unsaturated soils of the vadose zone, and subsequent radionuclide transport to the water table. The conceptual models implemented to simulate flow and transport are described below.

Flow of water through the NR waste is limited by the integrity of the disposal container, the amount of infiltration through the overlying cover, and characteristics of the waste and surrounding soil. Using the disposal container design described in Sect. L.1.1, a two-dimensional computational grid was designed to represent a vertical cross-section through the NR waste disposal facility and surrounding soil. The model domain (Fig. L.2-1) forms the basis of the simulations carried out with PORFLOW, Version 2.5 (ACRI 1993), to estimate flow and mass transport through the waste to the water table. The waste is represented within this domain by a zone which is 43 m long and 5.4 m high. The thickness of the slice is assumed to be of unit thickness, or 1 cm in this case.

The amount of infiltration entering the top of the domain shown in Fig. L.2-1 was assumed to be 40 cm/year, which represents the average infiltration without an engineered cover over the waste. Although the cover will likely limit infiltration for hundreds of years if undisturbed, there is considerable uncertainty in the timing and extent of cover degradation. Furthermore, the simulations begin when the disposal containers are assumed to fail, at which time slumping of the cover may occur due to loss of integrity of these containers. Therefore, for this analysis, no credit was taken for reductions in infiltration brought about by the cover.

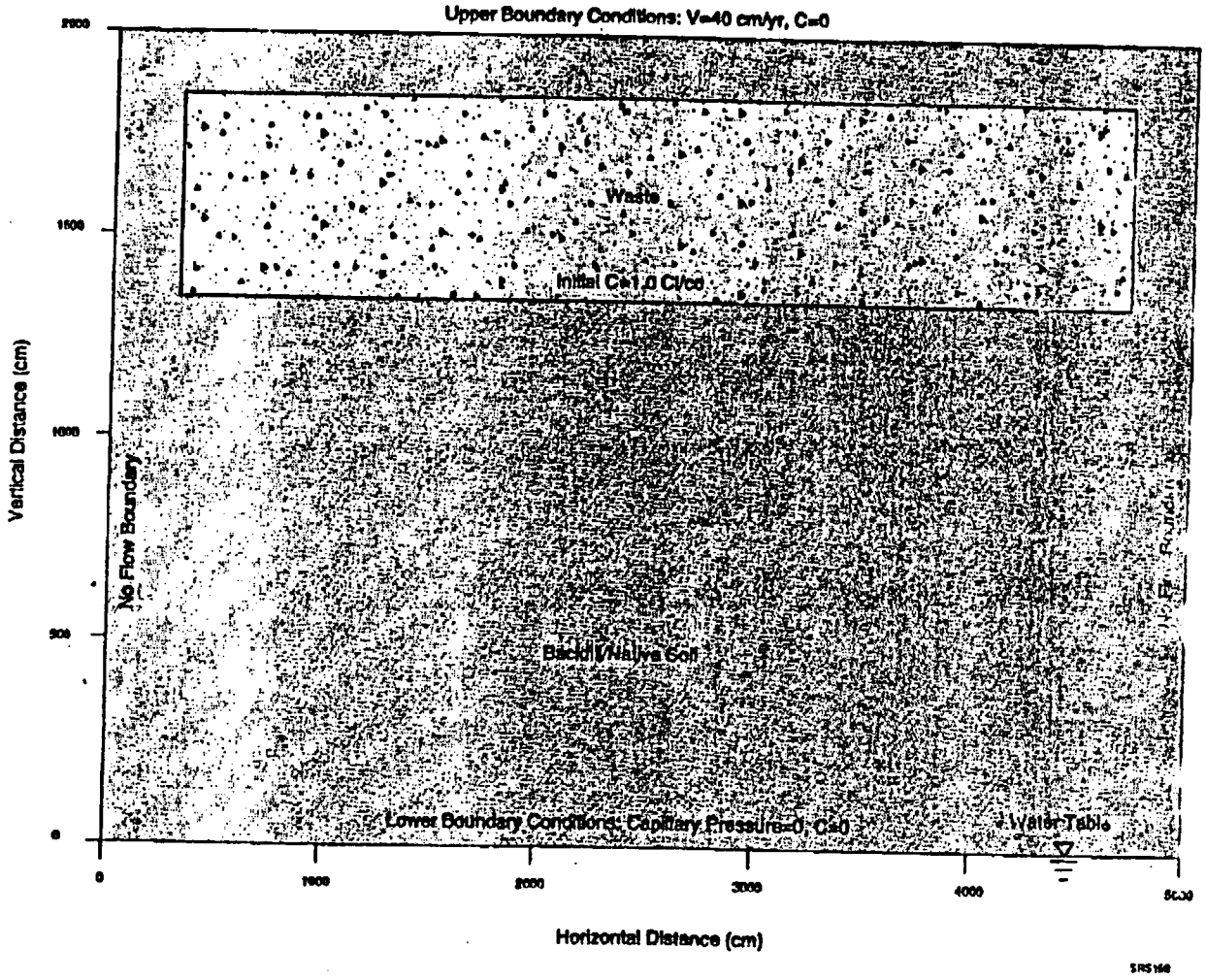

Fig. L.2-1. Near-field simulation domain for NR waste.

Simulation of the path of water through the domain nec
profiles in the NR waste and surrounding soil. For this p
waste inside the disposal casks has achieved hydraulic p
surrounding soil at the time of disposal container failure. I
likely exist in the disposal cask at initial breaching. Howeve
made because of the considerable uncertainty in modeling
over time. The simplified conceptual model might overesti
casks for a relatively short period of time, if water readily
collects in the casks before failure of the bottom portion o
in the casks, the simplified model might briefly underestima
time of failure of the bottom portion. However, this poter
than compensated for by the conservative assumptions inher
include: 1) that water enters the casks as readily as it flo
waste is well-mixed within a porous matrix within the cont
by pore water.

Simulation of radionuclide transport through the near-
the time the disposal containers are considered breached. T
able for transport depends upon the time of breaching of t
the activated metal wasteform. There is considerable unce
processes that affect both of these variables. With respect to
tibility of the welds and any crevices associated with the steel
timing and extent of this event. While the uniform con
extremely slow, and at most 2×10^{-5} cm/year (Sullivan and
corrosion of welds is likely to allow water in and out of the
are predicted with uniform corrosion. However, failure with

is breached before significant radioactive decay has occurred. For the short-lived radionuclides, this assumes that the container breaches immediately (at t = 0). The second scenario assumes that the container breaches at 6,000 years and that the activated metal wasteform is completely in the form of corrosion products. The first scenario is not considered realistic, but rather a means of screening out radionuclides that are insignificant from the standpoint of potential groundwater contamination. The second scenario may be very conservative if the metal wasteform is a corrosion resistant material, like stainless steel.

Hydraulic properties described in Sect. 3.3.1.1 for native soil at the SRS are appropriate for the soil surrounding the NR disposal containers. The moisture characteristic data tabulated by Gruber (1980) were used to define the unsaturated hydraulic conductivity and matrix potential as a function of moisture content. Because the waste and surrounding backfill and native soil are assumed to have identical hydraulic properties, water is assumed to be neither diverted into or out of the NR waste following disposal container failure, but to flow vertically through all materials. Under steady-state hydrologic conditions, the amount of water flowing out of the domain at the water table is equal to the amount of water entering via infiltration; thus, the steady-state flux of water through the NR waste and surrounding soil was 40 cm/year. Flow simulations were carried out with PORFLOW for the two-dimensional domain described above. The PORFLOW input file for these simulations is provided in Fig. L.5-1. The steady-state flow field was subsequently used in mass transport simulations to analyze the advective flux from the casks.

Release of radionuclides from corrosion products of the waste to the geosphere may result from desorption or dissolution processes, as noted in Sect. L.2.1. Advective and diffusive processes act to mobilize the radionuclides in the pore waters of the corroded waste. For the NR waste analysis, radionuclides in the corrosion products are assumed to be completely soluble, and sorption is considered to be a fully-reversible linear process at equilibrium. Equilibrium partitioning between solid (sorbed) and liquid phases is characterized by the distribution coefficients (K_ds) listed in Table L.2-2. The K_d values in this table are average values for sandy soil taken from site-specific literature, when available, and from a review article by Sheppard and Thibault (1990).

Table L.2.2. Distribution coefficients assumed for subsurface transport simulations for radionuclides in NRS waste.

Radionuclide	K_d Value Assumed (mL/g)	Literature Source
H-3	0	
C-14	2	McIntyre 1988
Sc-46	0	not available
Cr-51	70	Sheppard and Thibault 1990
Mn-54	50	Sheppard and Thibault 1990
Fe-55	220	Sheppard and Thibault 1990
Co-58	10	Hoeffner 1985
Fe-59	220	Sheppard and Thibault 1990
Ni-59	400	Sheppard and Thibault 1990
Co-60	10	Hoeffner, 1985
Ni-63	400	Sheppard and Thibault 1990
Zn-65	200	Sheppard and Thibault 1990
Sr-90	10	Hoeffner 1985
Nb-94	160	Sheppard and Thibault 1990
Nb-95	160	Sheppard and Thibault 1990
Zr-95	600	Sheppard and Thibault 1990
Tc-99	0.36	Oblath 1982
In-113	0	not available
Sn-113	130	Sheppard and Thibault 1990
In-114	0	not available
Sn-119m	130	Sheppard and Thibault 1990
Sn-123	130	Sheppard and Thibault 1990
Sn-125	130	Sheppard and Thibault 1990
I-129	0.6	Hoeffner 1994
Cs-137	330	Hoeffner 1985
Hf-181	450	Sheppard and Thibault 1990
Ta-182	220	Sheppard and Thibault 1990
Pu-239	100	Hoeffner 1985
Pu-241	100	Hoeffner 1985

The steady-state flow field from PORFLOW provided flow rates through the waste and to the water table (at the bottom of the domain, Fig. L.2-1), and K_ds, effective diffusion and dispersion coefficients, and radioactive decay constants provided the necessary information for simulating advective-diffusive transport. An example input file is shown in Fig. L.5-2. Effective diffusion (i.e., molecular diffusion corrected for tortuosity of a porous medium) and dispersion coefficients are not radionuclide-specific, and the values used for these parameters in the PORFLOW simulations were: 1) longitudinal dispersivity = 10 m; 2) transverse dispersivity = 2 cm; and 3) effective diffusion coefficient = 158 $cm^2 yr^{-1}$. No data are available for dispersivities in the unconsolidated sediments of the SRS. In the unsaturated zone, where flow velocities are very low, dispersion, which is directly proportional to flow velocity, is likely to be fairly insignificant with respect to plume movement. The values chosen for these simulations are believed to be reasonable based on a discussion of field-scale dispersivity in a reputable groundwater textbook (Freeze and Cherry 1979).

L.2.3.2 Groundwater Transport Model

To simulate transport of radionuclides that are released from the NR component waste to the water table, the conceptual saturated zone transport model described in Sect. 3.3.2 was adopted. The flow field established by PORFLOW simulations, which implemented this conceptual model, was used in the NR waste analysis. Therefore, the groundwater transport model was identical to that described in Sect. 3.3.2 with the exceptions that the source zone was smaller (1 NR waste source node versus 4 nodes for the ILNT vaults and 35 nodes for the LAW vaults), and the K_ds listed in Table L.2-2 were used. The smaller source zone represents the relatively smaller source area presented by the NR waste. An example PORFLOW input file for four radionuclides is shown in Fig. L.5-3.

L.2.3.3 Atmospheric Release Model for Volatile Components

Potential atmospheric release of volatile forms of H-3 and C-14 must be considered in order to consider all potentially significant pathways of exposure to radionuclides from the NR waste. Inadvertent intruders may be exposed to air within residences built on top of the

soil above the waste, and off-site individuals may be exposed to concentrations transported to or beyond the SRS boundary.

To estimate fluxes of potentially volatile radionuclides, H-3 and C-14, from the NR waste, the model developed to conservatively estimate fluxes of these radionuclides arising from the LAW vaults (Sect. A.3.5 and A.3.6) was used. The conservatism of this model lies mainly in the estimates for C-14 flux, because all of the C-14 available for volatilization (i.e., the C-14 in corrosion products of the waste form) is assumed to be in the form of gaseous $^{14}CO_2$. Tritium, on the other hand, is more realistically partitioned into water vapor in air according to the concentration of tritium in water calculated for the casks.

The flux calculations are normalized to a unit of *available* activity (Ci) of each radionuclide per disposal container. The availability of H-3 and C-14 after disposal is a function of the degree of corrosion of the steel waste form, and the amount of radioactive decay, that has occurred when release occurs.

For H-3, the vapor phase concentration in the NR waste is first calculated by assuming that the concentration of H-3 in water vapor in a disposal cask is the same as the H-3 concentration in any water contacting the wasteform. The ideal gas law is used to estimate the ambient concentration of water vapor in air in a disposal container, the results being 9.2 g m^{-3} at 10°C and 100% relative humidity. Converting to activity concentration units (Sect. A.2.3.1), the H-3 concentration in air in the disposal casks, in Ci m^{-3}, is 9.2×10^{-6} times the H-3 concentration in water. As noted above for C-14, all of the C-14 in corrosion products in the disposal casks is conservatively assumed to exist as $^{14}CO_2$ in the air in the disposal casks.

For off-site individuals, diffusion of H-3 and C-14 through soil overlying the NR disposal containers, and subsequent transport to the site boundary were considered. One meter of soil was assumed to cover the casks, although initially approximately 3 m of soil will overly the casks with the engineered cover in place. Per Ci of available H-3 (i.e., undecayed H-3 in corrosion products) in each of the 100 disposal casks, the concentration in the air-filled voids of the casks is calculated from:

$$C_{T,H\text{-}3} = \frac{1\ Ci}{3.8\times10^{-3}\ m^3} \times \frac{9.2\times10^{-6}\ Ci/m^3{}_{(air)}}{1\ Ci/m^3{}_{(H_2O)}}$$

where 3.8×10^{-3} m^3 (approximately one gal) represents the amount of pore fluid in a disposal container. This pore fluid content is based on amount of water expected for an average disposal container (Sect. L.1.1). The resulting air concentration of H-3 in the NR waste containers is 2.4×10^{-3} Ci m^{-3} for every Ci of H-3 in the corrosion products of a container. The flux of H-3 at the soil surface (J_{H-3} in Ci m^{-2} yr^{-1}) is calculated from:

$$J_{H-3} = D_a \left(\frac{C_{TH-3}}{x} \right)$$

where D_a is the molecular diffusion coefficient in air (754 m^2 yr^{-1} for water vapor, CRC 1981) and x is the soil thickness, assumed to be 1 m. The initial flux of H-3 (i.e., at closure) from the overlying soil is calculated to be 1.8 Ci m^{-2} yr^{-1} over an area of 800 m^2 (i.e., 8 m^2 per cask), per Ci of H-3 available for volatilization in each of the 100 NR waste disposal casks. With this flux rate, all of the available H-3 would be released from each disposal container in much less than one year. Therefore, to obtain an average annual flux rate, the total available H-3 in a disposal cask is assumed to be released in one year, and is divided by the individual cask area (8 m^2) to obtain a flux rate of H-3 from the NR waste disposal containers. The flux rate will depend strongly on when and how the disposal container is breached such that gaseous components can escape. If it is assumed that all H-3 is available for volatilization (i.e., corrosion of the waste form is instantaneous at closure), the flux rate from the disposal containers is calculated to be 0.13 Ci m^{-2} yr^{-1}.

Similarly, for inadvertent intruders, H-3 flux from soil above the disposal containers is a function of the time that the gaseous components escape and whether there is a gradual release or instantaneous release. For intruders, however, exposure cannot occur prior to the 100 years of assumed institutional control, and thus, significant decay of H-3 has occurred by that time. Per Ci of total initial H-3 in each NR waste cask, no more than 3.6×10^{-3} Ci would remain at 100 years after closure based on consideration of radioactive decay alone. Leaching is neglected. If it is assumed that all undecayed H-3 is available for volatilization at 100 years, the flux rate of H-3 from the soil overlying the disposal containers is 3.6×10^{-3} times the initial flux rate (0.13 Ci m^{-2} yr^{-1}) calculated above, or 4.7×10^{-4} Ci m^{-2} yr^{-1}. This represents the maximum flux of H-3 assumed to enter the intruder's residence at any time.

For C-14, the concentration in the NR waste containers ($C_{T,C-14}$), in Ci m^{-3} per Ci of available C-14 (i.e., C-14 in corrosion products) in each of the 100 containers, is calculated based on a 100-year Ci content of one; that is, decay has been insignificant and leaching is neglected.. The $^{14}CO_2$ air concentration per Ci available C-14 is calculated for an unwetted void space of 23.5 m^3 (27 m^3 total minus 3.5 m^3 of metal waste) in each cask to be 4.3×10^{-2} Ci m^{-3}. The flux of C-14 at the soil surface, J_{C-14}, is calculated in the same manner was done for H-3, using a diffusion coefficient of CO_2 in air of 440 m^2 yr^{-1} (CRC 1981). The flux of C-14 from the soil overlying the NR waste containers, per Ci of available C-14 in corrosion products, is conservatively estimated to be 1.8×10^1 Ci m^{-2} yr^{-1} over a total cask area of approximately 800 m^2 (8 m^2 per cask). A C-14 flux of 1.8×10^1 Ci m^{-2} yr^{-1} over an area of 800 m^2 corresponds to a loss of the initial 1 Ci per casks available C-14 in much less than one year. Therefore, to obtain an average annual flux rate, the total available C-14 in a disposal cask is assumed to be released in one year, and is divided by the individual cask area (8 m^2) to obtain a flux rate of C-14 from the NR waste disposal containers. The flux rate will depend strongly on when and how the disposal container is breached such that gaseous components can escape. If it is assumed that all C-14 is available for volatilization (i.e., corrosion of the waste form is complete at the time of volatile release), the flux rate from the disposal containers is calculated to be 0.13 Ci m^{-2} yr^{-1} per Ci of C-14 in each disposal cask. This flux rate represents the maximum flux, based on mass balance considerations, that can be assumed for determining off-site exposures and for estimating intruder exposures. Radioactive decay is assumed to be negligible at the time of release.

To more realistically estimate flux rates for H-3 or C-14, corrosion rates of the waste form and mode and time of release need to be considered. The worst case scenario would occur if the majority of the steel waste form corrodes before any release of volatile components, and if the release occurs before radioactive decay significantly diminishes the radionuclide content within the containers.

L.2.3.3 Models for Dose Estimation

Doses to off-site members of the public resulting from use of contaminated groundwater beyond the 100-m buffer zone around all of the projected 100 NR disposal containers were not directly estimated. Rather, comparisons of maximum predicted groundwater concentrations with the more restrictive of either MCLs or allowable concentrations based on 25-mrem per year performance objective were made. The allowable concentrations were calculated by dividing 25 mrem per year by the EDE per unit concentration in drinking water (Table A.4-6, Sect. A.4). These calculations are simple, were performed by hand, and checked several times for accuracy.

Other than contaminated groundwater, the air pathway is the only potentially significant means of exposure that is considered for off-site individuals in the NR waste analysis (Sect. L.2.2.2). Doses to off-site individuals via the air pathway were calculated in the manner described in Sect. A.3.1.3. This methodology utilizes the source term described in Sect. L.2.3.3 above, in Ci yr^{-1} of H-3 or C-14, and the AIRDOS-PC atmospheric dispersion model to estimate the all-pathway dose to an individual residing continuously at the SRS site boundary (5 km from E-Area).

To estimate dose to the intruder from potentially volatile H-3 and C-14 compounds released from the NR waste disposal containers, the same procedure described in Sect. A.3.1.2 was used. Assuming that the intruder's house resides directly on top of soil, 1 m in thickness, overlying the disposal containers, the steady-state air concentration (C_{ss}), in Ci m^{-3}, of H-3 or C-14 to which the intruder is exposed is estimated from:

$$C_{ss} = \frac{J/a}{h}$$

where

J = flux rate of volatile H-3 or C-14 into house, Ci m^{-2} yr^{-1},

a = air exchange rate in house, assumed to be 8760 yr^{-1}, and

h = height of the ceiling in house, 2.4 m.

The method for obtaining conservative estimates of the flux rates were provided in Sect. L.2.3.3 above. The inhalation dose to the intruder (D_{ii}) can be calculated from:

$$D_{ii} = C_{ai} \times B_r \times DCF_i$$

where

B_r = breathing rate (8,000 m^3 yr^{-1}), and
DCF_i = inhalation DCF for H-3 or C-14, (mrem Ci^{-1}).

Doses to inadvertent intruders from the external exposure, agriculture, and post-drilling scenarios were estimated according to the procedures described in Sect. L.3.1.4 below.

L.2.4 Performance Analysis Methodology

The models and assumptions described in Sect. L.2.3 were applied to analyze the performance of the NR waste disposal containers. Doses to off-site individuals and inadvertent intruders and groundwater concentrations at the compliance point for groundwater resource protection per Ci of each radionuclide listed in Table L.2-1 were estimated. The computational results are used to calculate inventory limits for each radionuclide based on performance objectives of the RPA.

Specifically, the near-field model was implemented, using the PORFLOW computer code, to estimate fluxes of radionuclides to the water table over time and to track the inventory in the disposal casks as a function of time. The results of the two-dimensional PORFLOW simulations are expressed in terms of fraction of the inventory in the simulation domain that leaves the bottom boundary of the domain over time, the bottom boundary representing the water table. The simulation domain represents a "slice" through the contents of the breached disposal containers and surrounding soil.

Following estimation of flux to the water table from the NR waste, the groundwater model was implemented, again using PORFLOW, to estimate the time-dependent groundwater concentrations of each radionuclide at the compliance point for groundwater resource

protection. The compliance point was selected from the groundwater simulation results as the node with the highest concentration which is at least 100 m from the edge of the 100 NR waste containers. Inventory limits based on groundwater protection requirements and the 25-mrem performance objective for off-site individuals were calculated from applicable MCLs and allowable inventories derived from dose estimates for the drinking water pathway.

The air pathway was considered by carrying out the calculations described in Sect. L.2.3.3 to calculate fluxes of H-3 and C-14 from the soil overlying the NR waste disposal containers, assuming the approximately 2 m of the engineered moisture barrier had been removed or eroded away. These fluxes were then used to conservatively estimate doses to intruders residing over the casks, or doses to off-site individuals per unit activity in each of the 100 disposal casks. Inventory limits were calculated for the air pathway based on the performance objectives of 10 mrem per year for off-site individuals, and 100 mrem per year for inadvertent intruders.

As described in Sect. L.2.2.3, three scenarios for exposure of inadvertent intruders are considered in the performance analysis for disposal of the NR wastes. The first scenario involves external exposure to intact waste casks at 100 years after disposal when the external dose that could be received would attain its maximum value. For this scenario, a simple model is developed to provide a conservative, upper-bound estimate of dose that might be received at this time, based essentially on the reported activities of photon-emitting radionuclides in the waste and the requirement that the external dose rate at the surface of a waste cask not exceed 200 mrem/h at the time of disposal. The second and third scenarios for inadvertent intrusion considered in this analysis are the agriculture and post-drilling scenarios, described in Sect. 3.2.4.1, which are assumed to occur only at a time long after disposal when the waste casks have been degraded by corrosion and excavation or drilling into the waste could occur. Estimates of potential doses to inadvertent intruders are provided on the basis of (1) the reported inventories of long-lived radionuclides in the waste given in Table L.1-1, (2) the scenario DCFs for the agriculture and post-drilling scenarios given in Tables 4.1-9 and 4.1-11, but modified to take into account those radionuclides that are in the form of activated metals, and (3) the total volume occupied by the waste casks after disposal, as obtained from Fig. L.1-2. However, the primary emphasis of the analysis for the agriculture

and post-drilling scenarios is the very long time after disposal at which the scenarios first would become credible, rather than the doses that might be received at that time.

L.2.5 Quality Assurance

As described in Sect. 3.5, this analysis was conducted under the guidance of the provision of the ANSI/ASME NQA-1 Program Requirements for Nuclear Facilities (U.S.NRC 1989), as required by DOE Order 5820.2A (U.S.DOE 1988a). Pertinent elements of NQA-1 and relevant documentation are cited in that section of the RPA, and apply directly to the NR waste analysis.

L.3 RESULTS OF NR WASTE ANALYSIS

The results of the analysis of performance of the NR waste disposal containers are presented in this section. Predicted releases to the environment (atmospheric releases and releases to the water table), resulting concentrations, results of dose analyses, and allowable inventories in the disposal casks are presented in Sect. L.3.1. The results are interpreted in Sect. L.3.2.

L.3.1 Analysis Results

In this section, results are presented for the near-field model simulations, the groundwater transport simulations, the atmospheric transport calculations, and the intruder dose analysis.

L.3.1.1 Near-Field Model Results

Table L.3-1 lists the PORFLOW simulation results for the near-field model. The fluxes provided represent the peak flux to the water table per Ci inventory of radionuclides (in *available* form; i.e., as corrosion products of activated metal) in all of the 100 shipping casks

Table L.3-1. Peak flux to the water table from NR waste.

Radionuclide	Predicted Fractional Flux (Ci/year/Ci)	Time of Peak Flux (year)
H-3	2.7×10^{-2}	1.4×10^{1}
C-14	2.8×10^{-2}	7.4×10^{1}
Sc-46	1.0×10^{-19}	3.1
Cr-51	—— [a]	——
Mn-54	7.7×10^{-71}	2.2×10^{1}
Fe-55	3.3×10^{-78}	5.0×10^{1}
Co-58	1.9×10^{-68}	4.1
Fe-59	—— [a]	——
Ni-59	1.0×10^{-4}	1.0×10^{4}
Co-60	1.2×10^{-20}	9.3×10^{1}
Ni-63	1.6×10^{-30}	2.1×10^{3}
Zn-65	1.6×10^{-98}	1.8×10^{1}
Sr-90	5.9×10^{-7}	1.6×10^{2}
Nb-94	3.1×10^{-4}	4.7×10^{3}
Nb-95	—— [a]	——
Zr-95	—— [a]	——
Tc-99	8.1×10^{-2}	2.5×10^{1}
In-113	—— [a]	——
Sn-113	—— [a]	——
In-114	—— [a]	——
Sn-119m	2.6×10^{-88}	2.1×10^{1}
Sn-123	—— [a]	——
Sb-125	1.8×10^{-74}	5.0×10^{1}
I-129	6.4×10^{-2}	3.2×10^{1}
Cs-137	7.7×10^{-45}	7.5×10^{2}
Hf-181	—— [a]	——
Ta-182	—— [a]	——
Pu-239	5.9×10^{-4}	2.9×10^{3}
Pu-241	1.4×10^{-37}	3.4×10^{2}

[a] Less than 10^{-99} yr^{-1}.

which potentially will be disposed of in the Area (i.e., peak fractional flux). These [illegible] based on a 40 cm/year infiltration rate through the NR waste, as was noted in Sect. L.2.3.1.

L.3.1.2 Groundwater Concentrations

The results of the groundwater transport simulations are listed in Table L.3-2. The values listed in this table represent peak groundwater concentration per Ci of radionuclide (assuming all of the radionuclide is *available* for leaching) in all of the 100 NR waste disposal casks, at the compliance point for groundwater protection. If the peak occurs at a time greater than 10,000 years after closure, the 10,000 year compliance point concentration is also provided. The compliance point is considered to be the point of maximum groundwater concentration at least 100 m from the edge of the disposal casks.

The groundwater concentrations per Ci inventory in all of the 100 NR disposal casks are compared to MCLs or allowable concentrations derived from the 25-mrem performance objective in Table L.3-3 below, to calculate total inventory limits for all 100 casks. Only the radionuclides in Table L.3-2 with peak groundwater concentrations exceeding 10^{-12} pCi/cc per Ci were considered further in this analysis. Inventory limits for individual casks were not determined because the results depend on the spacing of the casks at disposal, and thus, the limits calculated are only relevant to the spacing assumed (Fig. L.1-2) for this assessment. The MCLs listed in Table L.3-3 are those promulgated under the Safe Drinking Water Act, except where noted. Deviations occur only when current MCLs are not available. Allowable inventories for Pu-239 and Pu-241 (based on Am-241 daughter contributions) are calculated by dividing the 25 mrem per year performance objective by the EDEs per unit groundwater concentration for these isotopes (Table 4.1-7). This alternate to the MCLs is invoked because it results in a more restrictive requirement for groundwater concentration for Pu-239 and Pu-241 daughters.

The groundwater-based inventory limits were determined for the two scenarios assuming different times of breaching of the disposal container (Sect. L.2.3.1) by dividing the MCL or allowable concentration, by the compliance-point groundwater concentration per Ci of available inventory, after converting the concentration to appropriate units. The available

Table 7.3-2. Predicted groundwater compliance concentration for the MR waste.

Radionuclide	Groundwater Concentration at 10,000 years (pCi/cc-Ci)[a]	Peak Groundwater Concentration	
		pCi/cc-Ci	Time of peak (year)
H-3	----	6.7	1.7×10^{1}
C-14	----	2.2	1.1×10^{2}
Sc-46	----	9.0×10^{-13}	7.0
Mn-54	----	1.2×10^{-69}	2.5×10^{1}
Fe-55	----	----[b]	----
Co-58	----	6.0×10^{-61}	1.1×10^{1}
Ni-59	1.2×10^{-3}	8.2×10^{-3}	1.5×10^{4}
Co-60	----	5.4×10^{-15}	1.5×10^{2}
Ni-63	----	5.8×10^{-23}	3.9×10^{3}
Zn-65	----	----[b]	----
Sr-90	----	7.8×10^{-4}	2.4×10^{2}
Nb-94	----	2.4×10^{-2}	7.6×10^{3}
Tc-99	----	8.1	3.5×10^{1}
Sn-119m	----	----[b]	----
Sb-125	----	----[b]	----
I-129	----	5.8	4.7×10^{1}
Cs-137	----	4.8×10^{-37}	1.5×10^{3}
Pu-239	----	4.4×10^{-2}	4.8×10^{3}
Pu-241 Np-237	----	2.4×10^{-29} 1.3×10^{-6} [c]	6.5×10^{2}

[a] If blank, peak occurs before 10,000 years.
[b] Groundwater concentration less than 10^{-99} pCi/cc per Ci inventory in 100 casks.
[c] Concentration reported for Np-237 is per Ci of Pu-241 originally present.

Table L.3-3 Groundwater-based Disposal Limits for the NRC Wastes

Radionuclide	Compliance Point Groundwater Concentration (pCi/cc-Ci)		Allowable Concentration Limit (pCi/L)[a]	Inventory Limit for 100 NRC Waste Disposal Containers (Ci)	
	Container Breach at 0 years	Container Breach at 6,000 years		Container Breach at 0 years	Container Breach at 6,000 years
H-3	6.7	NA[b]	20,000	3.0	NA[b]
C-14	2.2	1.1	6,400	2.9	6.1
Ni-59	1.2×10^{-3}	3.8×10^{-10}	530	4.4×10^{2}	1.4×10^{9}
Sr-90	7.8×10^{-4}	NA[b]	8	[illegible] $\times 10^{1}$	NA[b]
Nb-94	2.4×10^{-2}	7.4×10^{-4}	707[c]	2.9×10^{1}	9.6×10^{2}
Tc-99	8.1	8.0	800	9.9×10^{-2}	1.0×10^{-1}
I-129	5.8	5.8	0.5	8.6×10^{-5}	8.6×10^{-5}
Pu-239	4.4×10^{-2}	2.9×10^{-2}	8.1[d]	1.8×10^{-1}	2.8×10^{-1}
Pu-241 Np-237	2.4×10^{-29} 1.3×10^{-6}	NA[b] 1.3×10^{-6}	530 8.9[d]	6.8×10^{3}	6.8×10^{3}

[a] Allowable concentrations are MCLs promulgated under Safe Drinking Water Act, except where noted.
[b] Radionuclide decays to insignificant levels by 6,000 years.
[c] No MCL given; value used is the new MCL proposed by the EPA in its modifications of DWS.
[d] Value reflects the allowable concentration based on consideration of the 25 mrem per year performance objective, which is more restrictive than the MCL in this case.

NA = not applicable

inventory is considered to be the entire inventory for these calculations, which conservatively assumes that the wasteform is entirely corroded at the time of disposal cask breaching. The first, and most conservative, scenario assumes that breaching occurs instantaneously. The second scenario assumes that water does not enter and leave the cask until the year 6000. As expected, these results indicate that the assumed time of failure of the containers is very important in setting inventory limits for the relatively short-lived radionuclides (H-3 and Sr-90) in the NR waste based on considerations of potential groundwater contamination. For Ni-59 and Nb-94, delayed failure of the casks of at least 6,000 years delays the peak concentration of these more strongly sorbing radionuclides beyond the 10,000 year time at which groundwater concentrations are considered for compliance. For the more mobile radionuclides (C-14, Tc-99, I-129, and Np-237), the results indicate that if the casks fail prior to 10,000 years and if the waste form has entirely corroded by that time of cask failure, the inventory limits will not be significantly affected by the time of failure.

L.3.1.3 Dose Analysis for Off-Site Releases of Radionuclides

As described in Sect. 3.2.3.3, the only performance objective of concern for off-site release of radionuclides is groundwater protection, provided doses from airborne release of radionuclides are insignificant. In order to evaluate the significance of the air pathway for the potentially volatile H-3 and C-14 radionuclides, doses were estimated using the fluxes derived in Sect. L.2.3.3 and the inhalation exposure model described in Sect. L.2.3.4. Flux rates above the soil were calculated assuming the entire waste form had corroded before release occurred, and that the entire inventory of H-3 and C-14 in corrosion products were released over a one year period. The estimated fluxes from the soil per Ci of H-3 and C-14 present in the vaults, the corresponding inhalation doses per unit activity (mrem/Ci), the appropriate performance objectives (mrem/year) and the inventory limits (Ci) based on the air pathway are given in Table L.3-4. The doses are based on 50-year committed dose equivalent factors for inhalation of 6.3×10^4 mrem per Ci for ^3H_2O and 2.4×10^4 mrem per Ci for $^{14}CO_2$ (U.S.DOE 1988b).

Table L.3-1. Disposal limits for NR waste based on the air pathway.

Radionuclide	Flux from Soil ($Ci\ m^{-2}\ yr^{-1}$)	Dose per unit radioactivity (mrem/year-Ci in each cask)	Performance Objective (mrem/year)	Inventory Limit (Ci/cask)
H-3				
Off-Site	1.3×10^{-1}	2.2×10^{-1}	10	4.5×10^{1}
Intruder	4.7×10^{-4}	1.1×10^{1}	100	9.1
C-14				
Off-Site	1.3×10^{-1}	1.2	10	8.3
Intruder	1.3×10^{-1}	1.2×10^{3}	100	8.3×10^{-2}

L.3.1.4 Dose Analysis for Inadvertent Intruders

As described in Sect. L.2.2.3, three exposure scenarios for inadvertent intruders are considered in the PA for disposal of the NR wastes. The first scenario involves external exposure to photon-emitting radionuclides inside an intact waste cask and is assumed to occur at 100 years after disposal when the external dose to an inadvertent intruder would attain its maximum value. The second and third scenarios are the agriculture and post-drilling scenarios involving excavation or drilling into the waste. These scenarios are assumed to occur only at times long after disposal when the waste casks have been degraded by corrosion.

L.3.1.4.1 Analysis of External Exposure of Inadvertent Intruders

This section discusses the analysis of potential external exposures of inadvertent intruders immediately upon loss of active institutional controls at 100 years after disposal. For the reasons described below, a conservative approach is used in estimating external dose at this time.

In principle, given information on the activities of photon-emitting radionuclides in the waste (see Table L.1-1) and the amount of shielding provided by the waste casks (see Fig. L.1-1), estimates of external dose rates near the surface of intact waste packages can be obtained. However, as illustrated by the following example, the available information on the disposed wastes appears to be insufficient to provide the basis for a reasonable estimate of external dose.

Based on the radionuclide inventory data in Table L.1-1 and the known spectrum of photons emitted in the decay of the various radionuclides, the most important photon-emitting radionuclide in the waste appears to be Co-60. That is, for an average waste cask at the present time, a substantial fraction of the external dose rate at the surface of an intact waste package should be due to the inventory of Co-60. From Table L.1-1, the maximum inventory of Co-60 in any waste cask is reported as 4.5×10^4 Ci. If we assume for simplicity that this activity is in the form of a point source at a distance of 1 m from the surface of the waste cask, then the external dose rate at the surface of the cask can be estimated from the known spectrum of photons emitted in the decay of Co-60 and the amount of shielding provided by the walls of the cask. At a distance of 1 m from a point source, the unshielded external dose rate in air per unit activity of Co-60 has been calculated from the decay data of Kocher (1981) as 1.4 rem/h per Ci (Unger and Trubey 1982). From Fig. L.1-1, the minimum thickness of shielding provided by the walls of a waste cask is 24 cm; and, from Fig. 13 of NCRP (1976), a thickness of 24 cm of iron, which is a reasonable approximation for the shielding provided by carbon and stainless steels, reduces the external dose rate from Co-60 by a factor of 6×10^{-4}. Thus, the estimated dose rate for the simplified case considered here is $(4.5 \times 10^4 \text{ Ci}) \times (1.4 \text{ rem/h per Ci}) \times (6 \times 10^{-4}) = 38$ rem/h. This estimate far exceeds an acceptance criterion for the waste casks, specified in 49 CFR Part 173, that the external dose rate at the surface not exceed 0.2 rem/h (200 mrem/h). Indeed, measurements on selected waste casks indicate that the external dose rate is less than 10 mrem/h.

There are two possible explanations for the unreasonably high estimate of external dose given above. The first is that the inventories of photon-emitting radionuclides in the waste could be greatly overestimated. The second, and perhaps more likely, explanation is that the waste is in the form of solid activated metals (see Sect. L.1.1), and the shielding provided by

the waste forms was not taken into account in the simple calculation given below. This shielding undoubtedly is substantial, but there is insufficient information on the waste forms themselves to provide the basis for any reasonable estimate of shielding they provide.

Given the inability to develop a reasonable estimate of external dose based on the available information on the waste forms, waste casks, and reported inventories of radionuclides, a simplified approach is used to obtain a conservative, upper-bound estimate of the external dose that could be received by an inadvertent intruder at 100 years after disposal, which is the earliest time that exposures could occur. This approach is described below.

The expected isotopes in the NR wastes are listed in Table L.1-1. A majority of the isotopes listed are photon-emitters. However, only three radionuclides—i.e., Co-60, Nb-94, and Cs-137 have half-lives sufficiently long that they could occur in substantial quantities in the waste after 100 years of decay. Most of the other radionuclides have half-lives of less than one year and, thus, would decay to minuscule levels within 100 years for any initial activity. The only other radionuclide that possibly could be of concern is Sb-125, which has a half-life of 2.77 years, but the inventory of this radionuclide is reduced by nearly eleven orders of magnitude after 100 years and, thus, would not be of concern for any reasonable levels of initial activity.

Conservative, upper-bound estimates of external doses from Co-60, Nb-94, and Cs-137 at 100 years after disposal are obtained as follows. As stated previously, Co-60 is the most important photon-emitting radionuclide in disposed waste, due to its high average activity in the waste casks (see Table L.1-1) and the high energies and intensities of the emitted photons (Kocher 1981). We first make the conservative assumption that the external dose rate at the surface of a waste cask at the present time is 200 mrem/h, which is the limit for any cask specified in 49 CFR Part 173 but apparently is not approached for any cask. We then assume that all of the dose rate of 200 mrem/h is due to Co-60. This assumption also is conservative (i.e., the dose rate from Co-60 is overestimated), because a substantial fraction of the external dose at the present time is due to other photon-emitting radionuclides in the waste.

Then, if the dose rate from Co-60 at the present time is assumed to be 200 mrem/h, the dose rate at 100 years after disposal would be reduced by a factor of 1.95×10^{-6}, based on the known half-life. Thus, a conservative, upper-bound estimate of the external dose rate from Co-60 at 100 years after disposal would be (200 mrem/h) $\times$ (1.95×10^{-6}) = 3.9×10^{-4} mrem/h.

In order to estimate the contributions to external dose from Nb-94 and Cs-137 at 100 years after disposal, we assume that the activities of Co-60, Nb-94, and Cs-137 in disposed waste are in the same proportions as the total activities of these radionuclides in all casks given in Table L.1-1. That is, the activities of Co-60, Nb-94, and Cs-137 in an average cask are assumed to be in the ratios $(7.7 \times 10^5):(6.2):(0.12)$. Then, taking into account the decay of Co-60 and Cs-137 after 100 years (Nb-94 experiences negligible decay over this time), the activity ratios at 100 years would be (1.5):(6.2):(0.012). We then assume that each radionuclide is a point source, in which case the dose rates per unit activity of each radionuclide calculated by Unger and Trubey (1982) can be used. The values in units of mrem/h per Ci are 1,400 for Co-60, 980 for Nb-94, and 380 for Cs-137. We further assume that the only shielding between the source and receptor locations is the 24 cm of steel at the sides of the casks (see Fig. L.1-1) and use the transmission curves for iron in Fig. 13 of NCRP (1976) to estimate the reduction in dose rate due to shielding for Nb-94 and Cs-137 relative to the reduction for Co-60. The latter assumption provides conservative overestimates of dose rate (i.e., underestimates of shielding) for Nb-94 and Cs-137, because the actual amount of shielding will be greater than 24 cm and the transmission of photons from Nb-94 and Cs-137 relative to the transmission of photons from Co-60 decreases as the amount of shielding increases. The transmission (shielding) factors for Co-60 and Cs-137 for 24 cm of iron are obtained directly from Fig. 13 of NCRP (1976) as 6×10^{-4} and 5×10^{-5}, respectively, and the value for Nb-94 is estimated by interpolation, based on the known photon spectrum for this radionuclide (Kocher 1981), as 1×10^{-4}.

With the information on dose rate per unit activity and transmission through 24 cm of iron given above, a conservative, upper-bound estimate of the external dose rate from Nb-94 can be obtained from the previous upper-bound estimate of the dose rate from Co-60 of 3.9×10^{-4} mrem/h as $(3.9 \times 10^{-4}) \times (6.2/1.5) \times (980/1{,}400) \times (1 \times 10^{-4})/(6 \times 10^{-4}) = 1.9 \times 10^{-4}$ mrem/h. A similar calculation for Cs-137 yields a dose rate of 7.1×10^{-8} mrem/h. Thus, the dose rate from Cs-137 apparently will be negligible relative to the dose rate from Co-60 and Nb-94.

From the calculations described above, we obtain a conservative, upper-bound estimate of external dose rate next to a waste cask at 100 years after disposal of 5.3×10^{-1} mrem/h, which is due essentially to Co-60 and Nb-94. This estimate is conservative because (1) the dose rate from Co-60 alone is overestimated by at least a factor of 20, based on the acceptance criterion on external dose rate for the waste casks of 200 mrem/h and measured dose rates for casks at the present time of less than 10 mrem/h, and (2) the transmission of photons from Nb-94 through all shielding materials relative to the transmission for Co-60 has been overestimated. The analysis would provide an underestimate of the dose rate only if the activity of Nb-94 in the waste relative to the activity of Co-60 has been greatly underestimated.

The conservative, upper-bound estimate of external dose rate obtained above corresponds to a dose from continuous exposure of 5 mrem per year. If an inadvertent intruder were located next to a waste cask continuously throughout the year, with no additional shielding assumed, the conservative, upper-bound estimate of the external dose rate indicates that the dose received from external exposure would be only a small fraction of the dose limit of 100 mrem per year in the performance objective for protection of inadvertent intruders (U.S.DOE 1988a). Thus, although the foregoing analysis is not intended to provide an accurate estimate of external dose at future times, the analysis clearly shows that the external dose to an inadvertent intruder due to exposure to intact waste casks should not be of concern in regard to meeting the performance objectives for disposal of the NR wastes. External dose to an inadvertent intruder could be of concern only if the inventory of Nb-94 in the waste casks relative to the inventory of Co-60 were much larger than reported in Table L.1-1.

L.3.1.4.2 Analysis for Agriculture Scenario

At some distant time in the future, it is conceivable that the carbon steel and stainless steel waste casks will have degraded by corrosion and that the waste could be accessed by excavation, resulting in exposures of inadvertent intruders according to the agriculture scenario described in Sect. 3.2.4.1. This section considers potential doses to inadvertent intruders that could result from this scenario.

O[illegible] corro[illegible] occur, t[illegible] corrosion, a[illegible] Fig. L.1-1 indicates that the thi[illegible] carbon st[illegible] to [illegible] casks is 15 cm [illegible] 34 c[illegible], respectively. In this analysis, corrosion rates of [illegible] 10^{-3} c[illegible]r and 2×10^{-5} cm/year are assumed for carbon steel (Sullivan et al. 1988) and stainless steel (Sullivan and Stout 1989), respectively. Thus, the estimated time for complete corrosion of the carbon steel layer is about 4,000 years, and the estimated corrosion time for the layer of stainless steel is about 2×10^6 years. Unless the corrosion rate for stainless steel has been underestimated by more than two orders of magnitude, which does not appear likely, it seems reasonable to conclude that direct intrusion into the waste by excavation is not a credible occurrence for the first 10,000 years after disposal which, as described in Sect. 1.2.1, is the assumed time period for compliance with the performance objective for protection of inadvertent intruders. Therefore, on the basis of the agriculture scenario, no limits on average concentrations or inventories of radionuclides in waste casks need to be imposed to provide protection of future inadvertent intruders.

Simply for the purpose of providing a perspective on potential doses according to the agriculture scenario, a dose analysis for this scenario can be performed for the radionuclides listed in Table L.1-1. Only the long-lived radionuclides C-14, Ni-59, Nb-94, Tc-99, I-129, and Pu-239 possibly could be of concern at times far in the future. A dose analysis for these radionuclides can be performed taking into account the following factors: 1) the total inventory in all 41 casks reported in Table L.1-1, 2) the total volume of a waste cask, as estimated from Fig. L.1-1, of 43 m^3, 3) the scenario DCFs for the agriculture scenario given in Table 4.1-9, 4) the assumption used in the NRC's 10 CFR Part 61 that the dose per unit concentration of a radionuclide should be reduced by a factor of ten if the radionuclide is in the form of an activated metal, and 5) the assumption based on Fig. L.1-2 that the waste casks will occupy about 40% of the total area of the disposal facility. A scenario DCF for Nb-94 is not given in Table 4.1-9. However, since this radionuclide is a high-energy photon

emitter, the analysis in Appendix A.1 for other such radionuclides indicates that the only important pathway in the agriculture scenario is external exposure while residing in the [illegible]. Using the model for this pathway described in Appendix A.4, the scenario DCF for Nb-94 is estimated to be 2.1×10^{-3} rem/year per $\mu Ci/m^3$.

If the calculations described above are carried out using Eq. (4.1-1), and a reduction in dose by a factor of ten is included for C-14, Ni-59, and Nb-94 in activated metals, as assumed in the NRC's 10 CFR Part 61, the following dose estimates in units of mrem per year are obtained: 60 for C-14, 6 for Ni-59, 290 for Nb-94, and 75 for Tc-99. The estimates for I-129 and Pu-239 are very low, due to the low inventories in the waste.

The dose estimates for the agriculture scenario given above are conservative because they do not take into account reductions in activity by radioactive decay, nor do they take into account any depletion of activity due to transport in infiltrating water. For example, if we assume that the lifetime of the waste casks is 2×10^6 years, as estimated previously, then the dose from the agriculture scenario at that time, taking into account depletion of the radionuclide inventories by radioactive decay only, would be about 0.1 mrem per year for Tc-99 and essentially zero for the other radionuclides listed above. If, as a more pessimistic alternative, we assume that the corrosion rate for the stainless steel on top of the waste casks could be as high as 10% of the assumed corrosion rate for carbon steel, the predicted lifetime of the casks would still be about 90,000 years. If the agriculture scenario could occur at this time and if only radioactive decay were taken into account in estimating depletion of radionuclide inventories over time, the estimated doses in mrem per year would be about 60 for Tc-99, 13 for Nb-94, 3 for Ni-59, and 0.001 for C-14.

The dose estimates for the agriculture scenario for times far beyond 10,000 years after disposal are provided only for the purpose of providing a perspective on the significance of the inventories of long-lived radionuclides in the waste. Because of the considerable thickness of the walls and top of the waste casks and the expected resistance of the casks to corrosion, especially the thick layer of stainless steel, excavation into the waste should not be a credible occurrence for a very long time after disposal, perhaps for as long as one million years or more. Even if the predicted lifetime of the casks is optimistic and excavation into the wastes could occur as soon as about 100,000 years, the estimated dose for the agriculture scenario,

based on the estimated inventories of radionuclides in the waste, would be less than the dose limit in the performance objective for protection of inadvertent intruders. The [illegible] at this time undoubtedly are conservative, because they do not take into account any depletion of radionuclide inventories by mobilization in infiltrating water. This should be a particularly important factor in reducing the inventory of Tc-99 in the waste at times after water could access the waste.

L.3.1.4.3 Analysis for Post-Drilling Scenario

The analysis of exposures of inadvertent intruders according to the agriculture scenario considered in the previous section was based on the assumption that the scenario would not be credible until the top of the waste casks is degraded by corrosion and excavation into the waste could occur. However, it also is possible that, at some time before the casks have completely corroded away, the physical state of the casks would be such that drilling into the waste through a cask that is no longer completely intact could occur. For example, since the sides of the casks are thinner than the top, the top of the casks could collapse after the sides have mostly corroded away, thus providing openings through which drilling could occur.

Based on the thicknesses of carbon steel and stainless steel at the sides of the waste casks shown in Fig. L.1-1 and the estimated corrosion rates of the two materials given previously, we estimate that the lifetime of the sides of the casks should be about 7×10^5 years. Even if this estimate were optimistic and the casks lasted a considerably shorter period of time, the lifetime would be well in excess of 10,000 years even if the corrosion rate for the stainless steel were as high as 10% of the assumed corrosion rate for carbon steel. Therefore, only the long-lived radionuclides considered previously for the agriculture scenario could possibly be of concern for a scenario involving drilling into the waste, i.e., the post-drilling scenario described in Sect. 3.2.4.1.

The analysis of the post-drilling scenario presented in Appendix A.4 and summarized in Table 4.1-11 indicates the following: For radionuclides that do not emit significant intensities of high-energy photons, the dose from the post-drilling scenario would be approximately a factor of ten less than the dose from the agriculture scenario when the two scenarios would

occur at the [illegible] (e.g., see Tables 4.1-9 and 4.1-11). Of the long[illegible] [illegible]nuclides of concern for the NR wastes, this result would apply to C-14, Ni-59, Tc-[illegible], I-129, and Pu-2[illegible]. For photon-emitting radionuclides, the dose from the post drilling scenario is about three orders of magnitude less than the dose from the agriculture scenario, because the pathway involving external exposure during indoor residence, which is by far the most important pathway in the agriculture scenario, does not occur in the post-drilling scenario. Therefore, based on the estimates of dose for the agriculture scenario presented in the previous section, the dose for the post-drilling scenario, based on the inventories of radionuclides listed in Table L.1-1, would always be considerably less than the dose limit of 100 mrem per year in the performance objective for protection of inadvertent intruders (U.S.DOE 1988a), even if the post-drilling scenario could occur well before the agriculture scenario. Again, however, the post-drilling scenario is not expected to be a credible occurrence until well beyond 10,000 years after disposal, due to the expected lifetime of the waste casks.

L.3.1.4.4 Other Considerations Related to Intruder Protection

In addition to the requirement for limiting potential doses to future inadvertent intruders, which the waste casks apparently would have no difficulty in meeting, the DOE requires that the concentrations of radionuclides in individual waste packages not exceed the Class-C limits established in the NRC's 10 CFR Part 61, which also are related to requirements for intruder protection. For the radionuclides listed in Table L.1-1, the NRC's Class-C limits in units of Ci/m^3 are as follows: 80 for C-14 in activated metal, 220 for Ni-59 in activated metal, 7,000 for Ni-63 in activated metal, 0.2 for Nb-94 in activated metal, 3 for Tc-99, 0.08 for I-129, and 4,600 for Cs-137. In addition, the concentration limit for all alpha-emitting transuranic radionuclides with half-lives greater than five years, which would apply to Pu-239 in the NR wastes, is 100 nCi/g, and the limit for Pu-241 is 3,500 nCi/g.

For the radionuclides for which the NRC has specified Class-C limits, the maximum concentration in any waste cask can be estimated from the inventory data in Table L.1-1 and the assumption described in Sect. L.1-1 that the total volume of waste in each cask is 3.5 m^3.

With these assumptions, we obtain the following estimates of maximum concentrations of radionuclides in the waste in units of Ci/m³: 3.1 for C-14, 60 for Ni-59, 3,300 for Ni-63, 0.091 for Nb-94, 1.1 for Tc-99, 3.7×10^{-7} for I-129, 3.4×10^{-3} for Cs-137, 7.1×10^{-6} for Pu-239, and 2.5×10^{-4} for Pu-241. If we assume that the average density of the waste form is approximately the same as the density of iron (7.86 g/cm³), the maximum concentrations of Pu-239 and Pu-241 correspond to 0.06 nCi/g and 2 nCi/g, respectively. Thus, if the inventory data in Table L.1-1 are reasonable, the maximum concentrations of Ni-63 slightly exceed the NRC's Class-C limit, which the DOE applies as a waste acceptance criterion for individual waste packages at its disposal sites (U.S.DOE 1988a), and the reported maximum concentrations of Ni-59, Nb-94, and Tc-99 are within a factor of 3-4 of the NRC's Class-C limits.

L.3.1.4.5 Summary of Dose Analysis for Inadvertent Intruders

The analyses of potential exposures of inadvertent intruders to NR wastes contained in thick-walled steel casks may be summarized as follows.

First, on the basis of the acceptance criterion limiting the external dose rate at the surface of waste casks to 200 mrem/h at the present time and the available data on the inventories of short-lived and longer-lived photon-emitting radionuclides in the waste, external exposures of inadvertent intruders to intact waste casks at any time after loss of active institutional controls at 100 years after disposal could result in doses that are only a small fraction of the dose limits in the performance objective for protection of inadvertent intruders. The external dose to an inadvertent intruder could approach the dose limits only if the average inventory of the long-lived radionuclide Nb-94 in all waste casks were much greater than the maximum inventory reported in any of the waste casks. Furthermore, measurements on selected casks indicate that the dose rate at the present time is at least an order or magnitude less than the acceptance criterion, which provides an additional degree of confidence that the external dose to future inadvertent intruders would be considerably less than the dose limits and that the inventory of Nb-94 and any other long-lived photon-emitting radionuclides would have to be greatly underestimated in order for the external dose at future times to be of concern.

Second, because of the considerable thickness of carbon steel and stainless steel used in constructing the waste casks and the expected low rates of corrosion of these materials, there is a reasonable expectation that the waste casks will maintain their integrity and prevent direct intrusion into the waste, either by excavation or by drilling, for a time far in excess of 10,000 years, which is the assumed time period for compliance with the performance objective for protection of inadvertent intruders. That is, the available data on corrosion rates of steel indicate that the waste casks will be a highly effective barrier to intrusion into the waste for a very long time into the future, perhaps for one million years or more.

If excavation into the waste at some time beyond 10,000 years were a credible occurrence, calculations based on the agriculture scenario indicate that doses to inadvertent intruders could exceed the dose limit in the performance objective, due primarily to the estimated inventories of Nb-94 and Tc-99, but only if the scenario could occur within about 50,000 years. However, the agriculture scenario could occur at this time only if the corrosion rate of stainless steel has been greatly underestimated, which does not appear likely. If the scenario could reasonably occur only at times beyond 100,000 years, then the dose from the agriculture scenario would always be less than the dose limit in the performance objective, unless the inventory of Nb-94 and Tc-99 in the wastes has been underestimated.

Drilling intrusion into the waste also might become credible at some time far into the future. However, the post-drilling scenario could not reasonably occur for thousands of years after disposal, and the dose from this scenario at any such times, based on expected radionuclide inventories in the waste, would only be a small fraction of the dose limit in the performance objective. The post-drilling scenario also could be of concern only if the inventory of Nb-94 and Tc-99 in the wastes has been considerably underestimated.

The analysis of the inventories of long-lived radionuclides in the waste has indicated a concern in addition to the concerns about potential doses to future inadvertent intruders. In particular, the reported maximum concentration of Ni-63 in the waste slightly exceeds the NRC's Class-C limit in 10 CFR Part 61, which has been adopted as a waste acceptance criterion at DOE disposal sites. In addition, the reported maximum concentrations of Ni-59, Nb-94, and Tc-99 are within a factor of 3-4 of the NRC's Class-C limits, so these radionuclides also could be of concern with regard to meeting the DOE's waste acceptance criterion if the maximum concentrations in the waste have been underestimated by these amounts or more.

L.3.2 Interpretation of Results

The results of the analysis of performance of the disposal casks for NR waste indicate that the groundwater pathway is the most limiting pathway for calculation of disposal limits, based on the conservative assumptions made. However, only nine of the 10 radionuclides listed in Table L.1-1 are of any concern with respect to the groundwater pathway. Of these nine, calculated inventory limits are lower than the expected inventory for 100 casks for five radionuclides; H-3, C-14, Ni-59, Sr-90 and Tc-99 (Table L.3-5). The intruder analyses indicated the following: 1) the external exposure to intact casks is not likely to result in doses that are significant with respect to dose limits; 2) the agriculture scenario is not likely to occur before 10,000 years, based on the corrosion resistance of the disposal containers, and thus is not likely to lead to doses exceeding the performance objectives before 10,000 years; 3) the post-drilling scenario would lead to doses that are only a small fraction of the dose limit in the performance objective for inadvertent intruders; and 4) the air pathway results for C-14 indicate a limiting inventory (8.3 Ci), which is less than the expected inventory (44 Ci) for 100 casks.

The derived inventory limits in Table L.3-5 are considered to be very low-end estimates of the allowable inventory in the NR waste, as uncertainties encountered in data or models were addressed by choosing a conservative assumption. In the groundwater pathway calculations, the activated metal waste form is assumed to be completely degraded at the time of disposal cask failure; an assumption necessitated by the lack of information on the composition and configuration of the waste form. Furthermore, no credit was taken for containment afforded by the disposal containers because of the uncertainty in the time that the welds might fail. For the air pathway calculations, all of the C-14 in the NR waste was assumed to be in the form of $^{14}CO_2$, to be released during a one-year period, and to be released at a time when radioactive decay has been insignificant; an obvious overestimate of the source term to the atmosphere.

Table L.3-5 Comparison of Estimated Disposal Limits versus Expected Inventory for the NR Waste

Radionuclide	Estimated NR Waste Inventory Limit[a] (Ci/100 casks)			Expected NR Waste Inventory (Ci/100 Casks)[d]
	Air Pathway[a]	Breach at 0 years[b]	Breach at 6,000 years[c]	
H-3[e]	9.1	3.0	NA[e]	5.4×10^{1}
C-14	8.3×10^{-2}	2.9	6.1	4.4×10^{1}
Ni-59		4.4×10^{2}	1.4×10^{9}	9.5×10^{3}
Sr-90		1.0×10^{1}	NA[e]	1.1×10^{3}
Nb-94		2.9×10^{1}	9.6×10^{2}	1.5×10^{1}
Tc-99		9.9×10^{-2}	1.0×10^{-1}	7.3×10^{1}
I-129		8.6×10^{-5}	8.6×10^{-5}	3.2×10^{-6}
Pu-239		1.8×10^{-1}	2.8×10^{-1}	6.3×10^{-5}
Pu-241 Np-237		6.8×10^{3}	6.8×10^{3}	2.1×10^{-2}

[a] Inventory limit based on the air pathway (Table L.3-4).
[b] Inventory limit based on most conservative scenario, where breaching of disposal casks occurs at time 0 (Table L.3-3).
[c] Inventory limit based on scenario where breaching of disposal casks occurs at 6,000 years (Table L.3-3).
[d] Expected inventory for 100 casks based on Table L.1-1 inventory for 41 casks, scaled to 100 casks by assuming the same general mix of casks.
[e] Radionuclide decays to insignificant levels by 6,000 years.

NA = not applicable.

L.4 PERFORMANCE EVALUATION

L.4.1 Comparison to Performance Objectives

The results of the NR waste analysis are summarized and interpreted in Sect. L.3.2. The results of the intruder analysis suggested that the performance objectives for intruders will be met. The groundwater-based disposal limits, when compared to the expected inventory, suggest that the performance objectives for groundwater protection may not be met for this waste. However, the results in Table L.3-5 do not indicate that the NR disposal casks are unsuitable for disposal in E-Area; rather, they indicate that the analysis must consider the containment provided by the casks *and* the corrosion rate of the waste form. The analysis is severely limited because of the lack of information available on the expected lifetime of welds in the disposal casks, and the composition and physical configuration of the waste form. If the wasteform is composed of stainless steel, the groundwater-based disposal limits would be considerably greater due to the corrosion resistance of stainless steel, and the fact that the uniform corrosion rate of stainless steel would control the source term.

L.4.2 Design Changes Required to Meet Performance Objectives

Unless it can be assumed that no more than 1% of the C-14 in the casks is released as $^{14}CO_2$ in any one year, or that atmospheric releases will not occur before the time that 1% of the C-14 remains in the casks (i.e., about 38,000 years), a means of mitigating potential $^{14}CO_2$ release must be addressed. Venting of the casks would assure a slower release of any $^{14}CO_2$ produced during corrosion of the activated metal wasteform, but would likely contribute to faster breaching of the waste container.

L.4.3 Data and Research Needs

As was noted earlier, this assessment suffers from a lack of information on the composition and physical configuration of the waste form and on the expected lifetime of the welds in the disposal containers. In order to develop a defensible source term, an estimated rate of corrosion, based on composition and size and shape of the waste form is needed. If it is confirmed, as expected, that the waste form is composed of stainless steel, the release of radionuclides from even a breached cask would be significantly less than is estimated here. Other critical types of information needed to improve the assessment of performance of the NR waste are: 1) a means of estimating the chemical behavior of C-14 in air-tight casks, and 2) information pertinent to when the casks might fail with respect to release of volatile compounds in the containers.

The available data on inventories of long-lived radionuclides in the waste casks indicate that the maximum inventories of Ni-59, Ni-63, Nb-94, and Tc-99 in any cask could approach or slightly exceed the NRC's Class-C limits in 10 CFR Part 61, which are applied as WAC at DOE disposal sites (U.S.DOE 1988a). Thus, a re-evaluation of the inventories of these radionuclides in the waste is potentially important in ensuring that the NR wastes meet the DOE's WAC.

L5 PORFLOW INPUT FILES

```
TITLE E-AREA NR Unsaturated Flow Field
/
/ P. S. Lam & A. O. Yu
/ Feb 3, 1994
/
/=================================================================
=====================
GRID 52 by 83
SCALE 1.0000
COORDINATE X
   -25.0    25.0    75.0   125.0   175.0
   225.0   275.0   325.0   375.0   425.0
   475.0   525.0   575.0   625.0   675.0
   725.0   775.0   825.0   875.0   925.0
   975.0  1025.0  1075.0  1125.0  1175.0
  1225.0  1275.0  1325.0  1375.0  1425.0
  1475.0  1525.0  1575.0  1625.0  1675.0
  1725.0  1775.0  1825.0  1875.0  1925.0
  1975.0  2025.0  2075.0  2125.0  2175.0
  2225.0  2275.0  2325.0  2375.0  2425.0
  2475.0  2525.0
SCALE 1.0000
COORDINATE Y
     0.0    19.9    40.7    62.6    85.5
   109.6   134.8   161.3   189.0   218.2
   248.7   280.8   314.4   349.7   386.7
   425.5   466.2   508.9   553.7   600.7
   650.0   699.4   746.5   791.4   834.2
   874.9   913.8   950.8   986.1  1019.7
  1051.8  1082.3  1111.4  1139.1  1165.6
  1190.7  1214.7  1237.6  1259.4  1280.2
  1300.0  1320.0  1340.0  1360.0  1380.0
  1400.0  1420.0  1440.0  1460.0  1480.0
  1500.0  1520.0  1540.0  1560.0  1580.0
  1600.0  1620.0  1640.0  1660.0  1680.0
  1700.0  1720.0  1740.0  1760.0  1780.0
  1800.0  1820.0  1840.0  1860.0  1880.0
  1900.0  1920.0  1940.0  1960.0  1980.0
  2000.0  2020.0  2040.0  2060.0  2080.0
  2100.0  2120.0  2140.0
/
ZONE 1 is from ( 1,  1) to ( 52,  83) $ soil
ZONE 2 is from ( 1,  41) to ( 45,  68) $ waste
/
DATUm = 0. 0.
GRAVity components are: 0.0, -1.
/
```

Fig. L5-1. PORFLOW input file - flow in the vadose zone for NR waste analysis.

```
DENSity of fluid is constant and equal to 1. gm/cc
/
FOR 1 Soil
MATERial PROPerties: rho 1.60 gm/cc, neff = 0.439, ntot = 0.439 , ndif = 0.439
MULT VAN  n = 1.70  alpha = 7.5e-2  sr = 0.088
HYDR  ss = 1.e-3  kx = 315.0  ky = 315.0  kz = 315.0
/
FOR 2  Waste
MATERial PROPerties: rho 1.60 gm/cc, neff = 0.439, ntot = 0.439 , ndif = 0.439
MULT VAN  n = 1.70  alpha = 7.5e-2  sr = 0.088
HYDR  ss = 1.e-3  kx = 315.0  ky = 315.0  kz = 315.0
/
LOCAte subregion (  1,  1) to ( 52,  83) with ID=SOIL
LOCAte subregion (  1, 41) to ( 45,  68) with ID=WAST
/
SET S  = 1.00 in ID=SOIL
/
BOUN P  -1  FLUX =  0.
BOUN P  +1  FLUX =  0.
BOUN P  -2  VALU =  0.
BOUN P  +2  FLUX = -40.
/
/ OPERATIONAL CONTROL
/
PROPerty for P is HARM mean
MATRIX in X and Y directions for P in 3 sweeps using ADI
RELAx P = 0.7
/
DIAGnostic node for V and S at (20,  20) every  5 steps
OUTPut every 900000 steps
/
FLUX BALAnce for P in 'run.flx'  for ID=SOIL  every  50 stps
FLUX BALAnce for P in 'run.flx'  for ID=WAST  every  50 stps
/
TIME=0.
/
CONV for P  REFE; GLOB mode; value = 1.0e-04, max 5 iter, 2 4
SOLV  P 100 init 1.e-7 inc 1.001 max 0.01 min 1.e-9 2.0 900000
/
SAVE      U V P S   in 'run.arc'
END
```

Fig. L.5-1. (cont.)

```
/********** C-11 **********
/
/ E-Area NR Transport (Unsaturated)
/
/ P. S. Lam & A. D. Yu
/ Feb 4, 1994
/
/==================================================================

GRID 52 by 83
SCALE 1.0000
COORDINATE X
   -25.0    25.0    75.0   125.0   175.0
   225.0   275.0   325.0   375.0   425.0
   475.0   525.0   575.0   625.0   675.0
   725.0   775.0   825.0   875.0   925.0
   975.0  1025.0  1075.0  1125.0  1175.0
  1225.0  1275.0  1325.0  1375.0  1425.0
  1475.0  1525.0  1575.0  1625.0  1675.0
  1725.0  1775.0  1825.0  1875.0  1925.0
  1975.0  2025.0  2075.0  2125.0  2175.0
  2225.0  2275.0  2325.0  2375.0  2425.0
  2475.0  2525.0
SCALE 1.0000
COORDINATE Y
     0.0    19.9    40.7    62.6    85.5
   109.6   134.8   161.3   189.0   218.2
   248.7   280.8   314.4   349.7   386.7
   425.5   466.2   508.9   553.7   600.7
   650.0   699.4   746.5   791.4   834.2
   874.9   913.8   950.8   986.1  1019.7
  1051.8  1082.3  1111.4  1139.1  1165.6
  1190.7  1214.7  1237.6  1259.4  1280.2
  1300.0  1320.0  1340.0  1360.0  1380.0
  1400.0  1420.0  1440.0  1460.0  1480.0
  1500.0  1520.0  1540.0  1560.0  1580.0
  1600.0  1620.0  1640.0  1660.0  1680.0
  1700.0  1720.0  1740.0  1760.0  1780.0
  1800.0  1820.0  1840.0  1860.0  1880.0
  1900.0  1920.0  1940.0  1960.0  1980.0
  2000.0  2020.0  2040.0  2060.0  2080.0
  2100.0  2120.0  2140.0
/
ZONE 1 is from (  1,   1) to ( 52,  83) $ soil
ZONE 2 is from (  1,  41) to ( 45,  68) $ waste
```

Fig. L.5-2. Example PORFLOW input file - mass transport of NR waste radionuclides in vadose zone.

```
/
DATUm = 0. 0.
/
READ record 1 'Tomsware'
/
GRAVity components are: 0.0, -1.
/
DENSity of fluid is constant and equal to 1. gm/cc
/
FOR  1  $soil
MATErial PROPerties:  rho 1.60 gm/cc, neff = 0.439, ntot = 0.439 , ndif = 0.439
/MULT  VAN   n = 1.70   alpha = 7.5e-2  sr = 0.088
/HYDR  ss = 1.e-3  kx = 315.0  ky = 315.0  kz = 315.0
TRANsport for C Kd= 2.00E+00  D= 158.  al= 10.  at= 2.
/
FOR  2  $waste
MATErial PROPerties:  rho 1.60 gm/cc, neff = 0.439, ntot = 0.439 , ndif = 0.439
/MULT  VAN   n = 1.70   alpha = 7.5e-2  sr = 0.088
/HYDR  ss = 1.e-3  kx = 315.0  ky = 315.0  kz = 315.0
TRANsport for C Kd= 2.00E+00  D= 158.  al= 10.  at= 2.
/
LOCAte subregion (  1,  1) to ( 52,  83) with ID=SOIL
LOCAte subregion (  1, 41) to ( 45,  68) with ID=WASTE
/
SET C  to 1.0 in ID=WASTe
/
DECAy half life for C is 5.73E+03
/
/BOUN P  -1   FLUX =   0.
/BOUN P  +1   FLUX =   0.
/BOUN P  -2   VALU =   0.
/BOUN P  +2   FLUX = -40.
/

BOUN C  -1   FLUX =   0.
BOUN C  +1   FLUX =   0.
BOUN C  -2   VALU =   0.
BOUN C  +2   VALU =   0.
/
/ OPERATIONAL CONTROL
/
PROPerty for C is HARM mean
MATRIX in X and Y directions for C in 3 sweeps using ADI
RELAx P = 0.7
/
DIAGnostic node for V and C at (20,  5) every  5 steps
/OUTPut every 900000 steps
/
```

Fig. L.5-2. (cont.).

```
FLUX BALAnce for C in 'run.fix' for ID=SOIL every 10 stps
FLUX BALAnce for C in 'run.fix' for ID=WAST every 10 stps
/
TIME=0.
/
CONV for C REFE GLOB mode value = 1.0e-04 max 5 iter 2 4
HISTory for C (25, 50) every 20 in 'run.his'
//////////
DISAble FLOW
//////////
SOLV C     50 ini 1.0E-05 inc 1.05 max 1.0E-01 min 1.E-10 2.0 900000
SOLV C     50 ini 1.0E-05 inc 1.05 max 1.0E-01 min 1.E-10 2.0 900000
SOLV C    900 ini 1.0E-04 inc 1.05 max 1.0E+00 min 1.E-10 2.0 900000
/
OUTPut U V P S C NOW
/
SAVE      U V P S C  in 'run.arc'
END
```

Fig. L.5-2. (cont.).

```
*** C-14 ***
/
/ NAVAL REACTOR TRANSPORT IN THE SATURATED ZONE
/
/ ASSUMING TOTAL NAVAL INVENTORY = 1.E+12
/ PORFLOW version 2.50
/
/ P. S. LAM AND A. D.-YU
/ 2/11/94
/
GRID 38 by 30 by 28
/units are in cm's
COORdinate X    -10000,     0,  45000,  90000, 135000, 145000, 155000,
            165000, 175000, 185000, 195000, 205000, 215000, 225000,
            235000, 245000, 250000, 257500, 265000, 272500, 280000,
            287500, 295000, 302500, 310000, 317500, 325000, 332500,
            340000, 347500, 355000, 362500, 370000, 380000, 390000,
            427500, 465000, 475000,
/
COORdinate Y    -7500,     0,   7500,  15000,  22500,  30000,  37500,
            45000,  52500,  60000,  67500,  75000,  82500,  90000,
            97500, 105000, 115000, 125000, 135000, 145000, 155000,
            165000, 175000, 185000, 195000, 215000, 242500, 292500,
            342500, 352500,
/
COORdinate Z      610,   732,  2073,  3414,  3536,  3658,  3780,
            3901,  4023,  4785,  5547,  5669,  5791,  5913,
            6035,  6157,  6370,  6553,  6751,  6949,  7148,
            7346,  7544,  7742,  7940,  8138,  8336,  8534,
/
/
READ 'eflow40.arc' $40 cm/year through vault regions
/
/identify a no-diffusion zone at top of domain to allow mass conservation
MATErial type  9 from (1,1, 1) to (38,30,28)
MATErial type 10 from (1,1,21) to (38,30,28)
/
FOR 9
ROCK density = 2.65; porosity = .30, .40, .30
TRANsport for C Kd= 2.00E+00  D= 158.  al= 10.  at= 2.
FOR 10:
ROCK density = 2.65; porosity = .30, .40, .30
TRANsport for C Kd= 2.00E+00  D= 0.  al= 0.  at= 0.
/
DECAy half life for C is 5.73E+03
/
INITial C = 0.0 everywhere
```

Fig. L.5-3. Example PORFLOW input file - mass transport of NR waste radionuclides in groundwater.

```
/
BOUNdary C at -1 FLUX =0.0
BOUNdary C at +1 FLUX =0.0
BOUNdary C at -2 FLUX =0.0
BOUNdary C at +2 FLUX =0.0
BOUNdary C at -3 FLUX =0.0
BOUNdary C at +3 FLUX =0.0
/
DISAble FLOW
/
DIAGnostic C, V at (28,14,18)    every 1 step $EXPECTED NAVY PEAK
/
HISTory for C TABLE at 'RUN.HIS'
    (28,14, 6) (28,14, 7) (28,14, 8) (28,14, 9) (28,14,10)
    (28,14,11) (28,14,12) (28,14,13) (28,14,14) (28,14,15)
    (28,14,16) (28,14,17) (28,14,18) (28,14,19) (28,14,20)
    (29,13,16) (29,13,17) (29,13,18) (29,13,19) (29,13,20)
     frequence=5
/
LOCAte subregion (28,13,20) (28,13,20) as ID=NAVY
/
/Source Units in pCi/cc-year per Ci of inventory
/
*** C-14    ***
SOURce C  for ID=NAVY per VOLUme TABLe 50 sets
     0.000E+00     0.000E+00
     3.014E-01     4.410E-67
     2.122E+00     3.479E-35
     6.122E+00     1.094E-21
     1.012E+01     1.372E-15
     1.412E+01     1.037E-11
     2.012E+01     6.833E-08
     2.412E+01     4.017E-06
     2.812E+01     9.338E-05
     3.212E+01     1.095E-03
     3.612E+01     7.593E-03
     4.012E+01     3.490E-02
     4.612E+01     1.893E-01
     5.000E+01     4.185E-01
     5.084E+01     4.840E-01
     5.422E+01     8.039E-01
     5.822E+01     1.266E+00
     6.222E+01     1.747E+00
     6.822E+01     2.316E+00
     7.022E+01     2.431E+00
     7.222E+01     2.500E+00
     7.422E+01     2.519E+00
     7.622E+01     2.491E+00
     7.822E+01     2.417E+00
```

Fig. L.5-3. (cont.).

8.[illegible]E+01	2.20[illegible]E+00
8.[illegible]E+01	2.15[illegible]E+00
8.[illegible]E+01	1.75[illegible]E+00
9.[illegible]E+01	1.38[illegible]E+00
9.[illegible]E+01	9.993E-01
9.8[illegible]E+01	6.75[illegible]E-01
1.005E+02	5.270E-01
1.033E+02	3.736E-01
1.232E+02	1.799E-[illegible]
1.632E+02	4.383E-05
2.032E+02	1.617E-10
2.432E+02	1.895E-15
2.832E+02	1.051E-20
3.032E+02	2.018E-23
3.432E+02	5.509E-29
3.832E+02	1.108E-34
4.232E+02	1.786E-40
4.632E+02	2.448E-46
5.032E+02	2.971E-52
5.432E+02	3.292E-58
5.832E+02	3.405E-64
6.232E+02	3.338E-70
6.632E+02	3.142E-76
7.032E+02	2.863E-82
7.432E+02	2.545E-88
7.832E+02	2.219E-94

```
/
TIME = 0. years
CONVergence for C GLOB REFE 1.e-3, max iterations = 3
/
SOLV C     59 ini 1.2E-03 inc 1.05 max 1.2E-01 min 1.E-10 2.0 90000
SOLV C     29 ini 5.9E-04 inc 1.05 max 5.9E-02 min 1.E-10 2.0 90000
SOLV C    850 ini 1.7E-02 inc 1.05 max 1.7E+00 min 1.E-10 2.0 90000
/
END
```

Fig. L.5-3. (cont.).

APPENDIX I.
REFERENCES

ACRI. 1993. *PORFLOW, A Model for Fluid Flow, Heat and Mass Transport in Multifluid, Multiphase Fractures or Porous Media, Version 2.50.* Draft User's Manual. Analytic & Computational Research, Inc., Bel Air, California.

CRC Press, Inc. 1981. *CRC Handbook of Chemistry and Physics.* Robert C. Weast and Melvin J. Astle, eds. Baca Raton, FL.

Freeze, R. A., and J. A. Cherry. 1979. *Groundwater.* Prentice-Hall, Inc., New Jersey.

Gruber, P. 1980. *A Hydrologic Study of the Unsaturated Zone Adjacent to a Radioactive-Waste Disposal Site at the Savannah River Plant, Aiken, South Carolina.* M. S. Thesis, University of Georgia, Athens, Georgia.

Hoeffner, S. L. 1985. *Radionuclide Sorption on Savannah River Plant Burial Ground Soil: A Summary and Interpretation of Laboratory Data.* DP-1702. E. I. du Pont de Nemours and Company, Savannah River Laboratory, Aiken, SC.

Kocher, D. C. 1981. *Radioactive Decay Data Tables.* DOE/TIC-11026. U. S. Department of Energy.

McIntyre, P. F. 1988. *Sorption Properties of Carbon-14 on Savannah River Plant Soil.* DPST-88-900. E. I. du Pont de Nemours and Company, Savannah River Laboratory, Aiken, SC.

NCRP. 1976. *Structural Shielding Design and Evaluation for Medical Use of X Rays and Gamma Rays of Energies up to 10 MeV.* NCRP Report No. 49. National Council on Radiation Protection and Measurements, Bethesda, MD.

Oblath, S. B. 1982. *Migration of TcO_4^- in SRP Soils.* DPST-82-815. E. I. Du Pont de Nemours and Company, Savannah River Laboratory, Aiken, SC.

Sheppard, M. I., and Thibault, D. H. 1990. Default Soil Solid/Liquid Partition Coefficients, K_ds, for Four Major Soil Types: A Compendium. *Health Phys.*, 59:471-482.

Sullivan, T. M., C. R. Kempf, C. J. Suen, and S. M. Moghaddam. 1993. *Low-Level Radioactive Waste Source Term Model Development and Testing*. NUREG/CR-5[illegible], BNL-NUREG-52160. Brookhaven National Laboratory, Upton, NY.

Sullivan, T. M., and C. J. Suen. 1989. *Low-Level Waste Shallow Land Disposal Source Term Model : Data Input Guides*. NUREG/CR-5387, BNL-NUREG-52206. Brookhaven National Laboratory, Upton, Long Island, NY.

Unger, L. M., and D. K. Trubey. 1982. *Specific Gamma-Ray Dose Constants for Nuclides Important to Dosimetry and Radiological Assessment*. ORNL/RSIC-45/R1, Oak Ridge National Laboratory , Oak Ridge, Tennessee.

U.S.DOE. 1988a. *Radioactive Waste Management, Order 5820.2a*. U. S. Department of Energy, Washington, D.C.

U.S.DOE. 1988b. *Internal Dose Conversion Factors for Calculation of Dose to the Public*. DOE/EH-0071. U. S. Department of Energy, Washington, D.C.

U.S.NRC. 1989. *Quality Assurance Program Requirements for Nuclear Facilities*. ASME NQA-1-1989 Edition. The American Society of Mechanical Engineers.

WSRC. 1992. *Above Ground Storage of Naval Reactor Waste Forms in the SWDF*. Savannah River Site report no. WSRC-TA-92-00005-1. Westinghouse Savannah River Company, Aiken, SC.

APPENDIX M

PORFLOW INPUT FILES

M.1 PORFLOW INPUT FILES - NEAR FIELD

```
TITLE E-AREA ILNT vault post P.A run, 4 cm rate flow run.
/
/ Intact flow run for the ILNT vault.
/
USER CS Cary S. Smith
/
GRID 46 by 72     $ initial grid based on z -area runs
/
SCREen on
COORdinate,X:
/
 -25.0   25.0  100.0  200.0  300.0  400.0  500.0  590.0  650.0  690.0
 720.0  740.0  755.0  $ <— backfill
                765.0  780.0  800.0  830.0  870.0  910.0  950.0
 990.0 1020.0 1040.0 1055.0 $ <— sand
                      1065.0 1078.0 1090.0 1102.0 1115.0 $ wall
                                                  1125.0
1140.0 1160.0 1185.0 1225.0 1275.0 1325.0 1375.0 1425.0 1475.0 1525.0
1575.0 1625.0 1675.0 1725.0 1775.0 1825.0 $<— waste
/
COORdinate Y :
/
 -10.0   10.0   35.0   65.0  105.0  155.0  215.0  295.0  380.0  460.0
 535.0  600.0  655.0  700.0  735.0  760.0  780.0  795.0 $ <–backfill
                                              805.0  820.0
 840.0  855.0  870.0  885.0  $ <–sand
                      895.0  906.0  917.0  928.0  939.0  950.0
 961.0 $ <–concrete
       971.0  985.0 1005.0 1030.0 1065.0 1110.0 1165.0 1230.0 1310.0
1400.0 1490.0 1560.0 1615.0 1660.0 1695.0 1720.0 1740.0 1753.0 $waste
                                                  1763.0
1775.0 1787.0 1800.0 1812.0 1824.0 $ <–concrete
                            1834.0 1844.0 1854.0 1864.0 $<clay
                                                  1874.0
1884.0 1894.0 1904.0 1914.0  $ <–sand
                      1924.0 1939.0 1960.0 1985.0 2005.0 2040.0
2075.0 2125.0 $ <–backfill
/
READ 2 nd record from 'end.2'
/
ZONE 1 is from (  1,   1) to ( 46,  72) $ BACKFILL
ZONE 2 is from ( 14,  19) to ( 46,  64) $ SAND
ZONE 3 is from ( 25,  50) to ( 46,  55) $ CONCRETE (roof)
ZONE 4 is from ( 30,  32) to ( 46,  49) $ WASTE
ZONE 5 is from ( 25,  56) to ( 46,  60) $ CLAY
ZONE 6 is from ( 25,  25) to ( 46,  31) $ CONCRETE (floor)
ZONE 7 is from ( 25,  25) to ( 29,  49) $ CONCRETE (walls)
/
```

Fig. M.1-1. PORFLOW Input File - Flow simulation through intact ILNT vault.

```
DATUm = 0. 0.
GRAVity components are: -0.02, -1.
/
DENSity of fluid is constant and equal to 1. gm/cc
/
FOR 1 $BACKFILL
MATErial PROPerties: rho 1.60 gm/cc, neff = 0.439, ntot = 0.439 , ndif = 0.439
HYDRaulic properties: ss = 1.e-3, Kx = 315.4 Ky = 315.4 cm/yr
MULTiphase flow: VAN, n = 1.7 , alpha = 0.075 /cm, Swr = 0.2000
/
FOR 2 $SAND
MATErial PROPerties: rho 2.60 gm/cc, neff = 0.375, ntot = 0.375 , ndif = 0.375
HYDRaulic prop. ss = 1.e-7, Kx = 3.154e+4 Ky = 3.154e+4
MULTiphase flow: VAN, n = 2.5 , alpha = 0.055 /cm, Swr = 0.2000
/
FOR 3 $CONCRETE roof
MATErial PROPerties: rho 2.60 gm/cc, neff = 0.150, ntot = 0.150 , ndif = 0.150
HYDRaulic prop. ss = 1.e-7, Kx = 3.154e-3 Ky = 3.154e-3
MULTiphase flow: VAN, n = 3.43, alpha = 5.98e-4 /cm, Swr = 0.9800
/
FOR 4 $WASTE
MATErial PROPerties: rho 1.70 gm/cc, neff = 0.50, ntot = 0.50, ndif = 0.50
HYDRaulic properties: ss = 1e-7, Kx = 3.154e-3 Ky = 3.154e-3 cm/yr
MULTiphase flow: VAN, n = 3.43, alpha = 5.98e-4 /cm, Swr = 0.9800
/
FOR 5 $CLAY
MATErial PROPerties: rho 2.60 gm/cc, neff = 0.386, ntot = 0.386 , ndif = 0.386
HYDRaulic properties: ss = 6.e-4, Kx = 3.154 Ky = 3.154
MULTiphase flow: VAN, n = 1.51, alpha = 1.75e-3 /cm, Swr = 0.8800
/
FOR 6 $CONCRETE floor
MATErial PROPerties: rho 2.60 gm/cc, neff = 0.150, ntot = 0.150 , ndif = 0.150
HYDRaulic properties: ss = 1.e-7, Kx = 3.154e-3 Ky = 3.154e-3
MULTiphase flow: VAN, n = 3.43, alpha = 5.98e-4 /cm, Swr = 0.9800
/
FOR 7 $CONCRETE walls
MATErial PROPerties: rho 2.60 gm/cc, neff = 0.150, ntot = 0.150 , ndif = 0.150
HYDRaulic properties: ss = 1.e-7, Kx = 3.154e-3 Ky = 3.154e-3
MULTiphase flow: VAN, n = 3.43, alpha = 5.98e-4 /cm, Swr = 0.9800
/
LOCAte subregion ( 1, 1) to ( 46, 72) with ID=TOTL
LOCAte subregion ( 25, 25) to ( 46, 55) with ID=VALT
LOCAte subregion ( 30, 32) to ( 46, 49) with ID=WAST
LOCAte subregion ( 25, 56) to ( 46, 60) with ID=CLAY
/
/SET S for ID=TOTL to 0.70
/SET S for ID=VALT to 1.00
/SET S for ID=WAST to 1.00
/SET S for ID=CLAY to 1.00
/
```

Fig. M.1-1. (continued).

```
BOUN P -1  FLUX =  0.
BOUN P +1  FLUX =  0.
BOUN P -2  VALU =  0.
BOUN P +2  FLUX =  -4.
/
/ OPERATIONAL CONTROL
/
PROPerty for P  is HARM mean
MATRIX in X and Y directions for P in 2 sweeps using ADI
CONVergence for P; LOCAl mode; value = 1.0e-04, max of  1 iterations
CONVergence for FLOW REFEerence; LOCAl mode; val = 1e-3, max of 5 iterations
/
DIAGnostic node at (30,  40) every 50 steps
OUTPut every 100000 steps
/
FLUX BALAnce for P in 'flux.out' for ID=TOTL every 500 stps
FLUX BALAnce for P              for ID=VALT every 500 stps
/
SOLV for P    500 in AUTO init 1e-4 inc 1.05 max 5 min 1e-9 2.0 900000
SAVE U V P S     NOW in 'end.3'
SAVE       S     NOW in 'end.3'
/
END
```

Fig. M.1-1. (continued).

```
TITLE E-AREA ILNT vault post PA run, 4 cm crack flow run.
/
/ Intact flow run for the ILNT vault.
/
USER CS Cary S. Smith
/
GRID 46 by 72     $ initial grid based on z -area runs
/
SCREen on
COORdinate X:
/
 -25.0   25.0  100.0  200.0  300.0  400.0  500.0  590.0  650.0  690.0
 720.0  740.0  755.0  $ <— backfill
                765.0  780.0  800.0  830.0  870.0  910.0  950.0
 990.0 1020.0 1040.0 1055.0 $ <— sand
                      1065.0 1078.0 1090.0 1102.0 1115.0 $ wall
                                                  1125.0
1140.0 1160.0 1185.0 1225.0 1275.0 1325.0 1375.0 1425.0 1475.0 1525.0
1575.0 1625.0 1675.0 1725.0 1775.0 1825.0 $<— waste
/
COORdinate Y :
/
 -10.0   10.0   35.0   65.0  105.0  155.0  215.0  295.0  380.0  460.0
 535.0  600.0  655.0  700.0  735.0  760.0  780.0  795.0 $ <--backfill
                                              805.0  820.0
 840.0  855.0  870.0  885.0  $ <--sand
                      895.0  906.0  917.0  928.0  939.0  950.0
 961.0 $ <--concrete
      971.0  985.0 1005.0 1030.0 1065.0 1110.0 1165.0 1230.0 1310.0
1400.0 1490.0 1560.0 1615.0 1660.0 1695.0 1720.0 1740.0 1753.0 $waste
                                                  1763.0
1775.0 1787.0 1800.0 1812.0 1824.0 $ <--concrete
                           1834.0 1844.0 1854.0 1864.0 $<clay
                                                  1874.0
1884.0 1894.0 1904.0 1914.0  $ <--sand
                      1924.0 1939.0 1960.0 1985.0 2005.0 2040.0
2075.0 2125.0 $ <--backfill
/
ZONE 1 is from ( 1,  1) to ( 46, 72) $ BACKFILL
ZONE 2 is from ( 14, 19) to ( 46, 64) $ SAND
ZONE 3 is from ( 25, 50) to ( 46, 55) $ CONCRETE (roof)
ZONE 4 is from ( 30, 32) to ( 46, 49) $ WASTE
ZONE 5 is from ( 25, 56) to ( 46, 60) $ CLAY
ZONE 6 is from ( 25, 25) to ( 46, 31) $ CONCRETE (floor)
ZONE 7 is from ( 25, 25) to ( 29, 49) $ CONCRETE (walls)
/
DATUm = 0. 0.
GRAVity components are: -0.02, -1.
/
DENSity of fluid is constant and equal to 1. gm/cc
/
```

Fig. M.1-2. PORFLOW Input File - Flow simulation through cracked ILNT vault.

```
FOR 1 $BACKFILL
MATErial PROPerties: rho 1.50 gm/cc, neff = 0.439, ntot = 0.439 , ndif = 0.439
HYDRaulic properties: ss = 1.e-3, Kx = 315.4 Ky = 315.4 cm/yr
MULTiphase flow: VAN, n = 1.7 , alpha = 0.075 /cm, Swr = 0.2000
/
FOR 2 $SAND
MATErial PROPerties: rho 2.60 gm/cc, neff = 0.375, ntot = 0.375 , ndif = 0.375
HYDRaulic prop. ss = 1.e-7, Kx = 3.154e+4 Ky = 3.154e+4
MULTiphase flow: VAN, n = 2.5 , alpha = 0.055 /cm, Swr = 0.2000
/
FOR 3 $CONCRETE roof
MATErial PROPerties: rho 2.60 gm/cc, neff = 0.150, ntot = 0.150 , ndif = 0.150
HYDRaulic prop. ss = 1.e-7, Kx = 3.154e-0 Ky = 3.154e-0
MULTiphase flow: VAN, n = 1.51, alpha = 1.75e-3 /cm, Swr = 0.8800
/
FOR 4 $WASTE
MATErial PROPerties: rho 1.70 gm/cc, neff = 0.50, ntot = 0.50, ndif = 0.50
HYDRaulic properties: ss = 1e-7, Kx = 315.4 Ky = 315.4 cm/yr
MULTiphase flow: VAN, n = 1.7 , alpha = 0.075 /cm, Swr = 0.2000
/
FOR 5 $CLAY
MATErial PROPerties: rho 2.60 gm/cc, neff = 0.386, ntot = 0.386 , ndif = 0.386
HYDRaulic properties: ss = 6.e-4, Kx = 3.154 Ky = 3.154
MULTiphase flow: VAN, n = 1.51, alpha = 1.75e-3 /cm, Swr = 0.8800
/
FOR 6 $CONCRETE floor
MATErial PROPerties: rho 2.60 gm/cc, neff = 0.150, ntot = 0.150 , ndif = 0.150
HYDRaulic properties: ss = 1.e-7, Kx = 3.154e-3 Ky = 3.154e-3
MULTiphase flow: VAN, n = 3.43, alpha = 5.98e-4 /cm, Swr = 0.9800
/
FOR 7 $CONCRETE walls
MATErial PROPerties: rho 2.60 gm/cc, neff = 0.150, ntot = 0.150 , ndif = 0.150
HYDRaulic prop. ss = 1.e-7, Kx = 3.154e+4 Ky = 3.154e+4
MULTiphase flow: VAN, n = 2.5 , alpha = 0.055 /cm, Swr = 0.2000
/
LOCAte subregion ( 1, 1) to ( 46, 72) with ID=TOTL
LOCAte subregion ( 25, 25) to ( 46, 55) with ID=VALT
LOCAte subregion ( 30, 32) to ( 46, 49) with ID=WAST
LOCAte subregion ( 25, 56) to ( 46, 60) with ID=CLAY
/
SET S for ID=TOTL to 0.70
SET S for ID=VALT to 1.00
SET S for ID=WAST to 0.50
SET S for ID=CLAY to 1.00
/
BOUN P -1 FLUX = 0.
BOUN P +1 FLUX = 0.
BOUN P -2 VALU = 0.
BOUN P +2 FLUX = -4.
/
```

Fig. M.1-2. (continued).

```
/ OPERATIONAL CONTROL
/
PROPerty for P  is HARmonic mean
MATRIX in X and Y directions for P in 2 [illegible] using ADI
CONVergence for P; LOCAl mode; value = 1.E-04, max of 1 iterations
CONVergence for FLOW RESIDuals; LOCAl mode; value = 1e-3, max of 5 iterations
/
DIAGnostic node at (30,  40) every 50 steps
OUTPut every 100000 steps
/
FLUX BALAnce for P in 'flux.out' for ID=TOTL every 500 stps
FLUX BALAnce for P              for ID=VALT every 500 stps
/
SOLV for P    0.1 in init 5e-4 inc 1.00 max 1 min 1e-9 2.0 900000
SOLV for P    0.9 in AUTO init 1e-7 inc 1.05 max 1 min 1e-9 2.0 900000
SAVE U V P S     NOW in 'end.0'
SAVE       S     NOW in 'end.0'
/
SOLV for P      4 in AUTO init 1e-7 inc 1.05 max 1 min 1e-9 2.0 900000
SAVE U V P S     NOW in 'end.0'
SAVE       S     NOW in 'end.0'
/
SOLV for P      5 in AUTO init 1e-6 inc 1.05 max 1 min 1e-9 2.0 900000
SAVE U V P S     NOW in 'end.0'
SAVE       S     NOW in 'end.0'
/
SOLV for P     10 in AUTO init 1e-6 inc 1.05 max 1 min 1e-9 2.0 900000
SAVE U V P S     NOW in 'end.1'
SAVE       S     NOW in 'end.1'
/
SOLV for P     30 in AUTO init 1e-5 inc 1.05 max 1 min 1e-9 2.0 900000
SAVE U V P S     NOW in 'end.1'
SAVE       S     NOW in 'end.1'
/
SOLV for P     50 in AUTO init 1e-5 inc 1.05 max 1 min 1e-9 2.0 900000
SAVE U V P S     NOW in 'end.1'
SAVE       S     NOW in 'end.1'
/
SOLV for P    100 in AUTO init 1e-4 inc 1.05 max 1 min 1e-9 2.0 900000
SAVE U V P S     NOW in 'end.2'
SAVE       S     NOW in 'end.2'
/
SOLV for P    300 in AUTO init 1e-4 inc 1.05 max 3 min 1e-9 2.0 900000
SAVE U V P S     NOW in 'end.2'
SAVE       S     NOW in 'end.2'
/
END
```

Fig. M.1-2. (continued).

```
TITLE E-AREA ILNT vault ; cst PA [illegible], 4 cm [illegible] flow run.
/
/ Intact flow run for the ILNT vault.
/
USER CS Cary S. Smith
/
GRID 46 by 72     $ initial grid based on z -area runs
/
SCREen on
COORdinate X:
/
 -25.0   25.0  100.0  200.0  300.0  400.0  500.0  590.0  650.0  690.0
 720.0  740.0  755,0  $ <-- backfill
                765.0  780.0  800.0  830.0  870.0  910.0  950.0
 990.0 1020.0 1040.0 1055.0 $ <-- sand
                      1065.0 1078.0 1090.0 1102.0 1115.0 $ wall
                                                  1125.0
1140.0 1160.0 1185.0 1225.0 1275.0 1325.0 1375.0 1425.0 1475.0 1525.0
1575.0 1625.0 1675.0 1725.0 1775.0 1825.0 $<-- waste
/
COORdinate Y :
/
 -10.0   10.0   35.0   65.0  105.0  155.0  215.0  295.0  380.0  460.0
 535.0  600.0  655.0  700.0  735.0  760.0  780.0  795.0 $ <--backfill
                                             805.0  820.0
 840.0  855.0  870.0  885.0  $ <--sand
                      895.0  906.0  917.0  928.0  939.0  950.0
 961.0 $ <--concrete
       971.0  985.0 1005.0 1030.0 1065.0 1110.0 1165.0 1230.0 1310.0
1400.0 1490.0 1560.0 1615.0 1660.0 1695.0 1720.0 1740.0 1753.0 $waste
                                                  1763.0
1775.0 1787.0 1800.0 1812.0 1824.0 $ <--concrete
                            1834.0 1844.0 1854.0 1864.0 $<clay
                                                  1874.0
1884.0 1894.0 1904.0 1914.0  $ <--sand
                      1924.0 1939.0 1960.0 1985.0 2005.0 2040.0
2075.0 2125.0 $ <--backfill
/
ZONE 1 is from (  1,   1) to ( 46,  72) $ BACKFILL
ZONE 2 is from ( 14,  19) to ( 46,  64) $ SAND
ZONE 3 is from ( 25,  50) to ( 46,  55) $ CONCRETE (roof)
ZONE 4 is from ( 30,  32) to ( 46,  49) $ WASTE
ZONE 5 is from ( 25,  56) to ( 46,  60) $ CLAY
ZONE 6 is from ( 25,  25) to ( 46,  31) $ CONCRETE (floor)
ZONE 7 is from ( 25,  25) to ( 29,  49) $ CONCRETE (walls)
/
DATUm = 0. 0.
GRAVity components are: -0.02, -1.
/
DENSity of fluid is constant and equal to 1. gm/cc
```

Fig. M.1-3. PORFLOW Input File - Flow simulation through failed ILNT vault.

```
/
FOR 1 $BACKFILL
MATerial PROPerties: rho 1.60 gm/cc, neff = 0.439, ntot = 0.439 , ndif = 0.439
HYDRaulic properties: ss = 1.e-3, Kx = 315.4 Ky = 315.4 cm/yr
MULTiphase flow: VAN, n = 1.7 , alpha = 0.075 /cm, Swr = 0.2000
/
FOR 2 $SAND
MATErial PROPerties: rho 2.60 gm/cc, neff = 0.375, ntot = 0.375 , ndif = 0.375
HYDRaulic prop. ss = 1.e-7, Kx = 3.154e+4 Ky = 3.154e+4
MULTiphase flow: VAN, n = 2.5 , alpha = 0.055 /cm, Swr = 0.2000
/
FOR 3 $CONCRETE roof
MATErial PROPerties: rho 2.60 gm/cc, neff = 0.150, ntot = 0.150 , ndif = 0.150
HYDRaulic properties: ss = 1e-7, Kx = 315.4 Ky = 315.4 cm/yr
MULTiphase flow: VAN, n = 1.7 , alpha = 0.075 /cm, Swr = 0.2000
/
FOR 4 $WASTE
MATErial PROPerties: rho 1.70 gm/cc, neff = 0.50, ntot = 0.50, ndif = 0.50
HYDRaulic properties: ss = 1e-7, Kx = 315.4 Ky = 315.4 cm/yr
MULTiphase flow: VAN, n = 1.7 , alpha = 0.075 /cm, Swr = 0.2000
/
FOR 5 $CLAY.
MATErial PROPerties: rho 2.60 gm/cc, neff = 0.386, ntot = 0.386 , ndif = 0.386
HYDRaulic properties: ss = 1e-7, Kx = 315.4 Ky = 315.4 cm/yr
MULTiphase flow: VAN, n = 1.7 , alpha = 0.075 /cm, Swr = 0.2000
/
FOR 6 $CONCRETE floor
MATErial PROPerties: rho 2.60 gm/cc, neff = 0.150, ntot = 0.150 , ndif = 0.150
HYDRaulic prop. ss = 1.e-7, Kx = 3.154e+4 Ky = 3.154e+4
MULTiphase flow: VAN, n = 2.5 , alpha = 0.055 /cm, Swr = 0.2000
/
FOR 7 $CONCRETE walls
MATErial PROPerties: rho 2.60 gm/cc, neff = 0.150, ntot = 0.150 , ndif = 0.150
HYDRaulic prop. ss = 1.e-7, Kx = 3.154e+4 Ky = 3.154e+4
MULTiphase flow: VAN, n = 2.5 , alpha = 0.055 /cm, Swr = 0.2000
/
LOCAte subregion ( 1, 1) to ( 46, 72) with ID=TOTL
LOCAte subregion ( 25, 25) to ( 46, 55) with ID=VALT
LOCAte subregion ( 30, 32) to ( 46, 49) with ID=WAST
LOCAte subregion ( 25, 56) to ( 46, 60) with ID=CLAY
/
SET S for ID=TOTL to 0.75
SET S for ID=VALT to 0.75
SET S for ID=WAST to 0.75
SET S for ID=CLAY to 0.75
/
BOUN P -1 FLUX = 0.
BOUN P +1 FLUX = 0.
BOUN P -2 VALU = 0.
BOUN P +2 FLUX = -40.
/
```

Fig. M.1-3. (continued).

```
/ OPERATIONAL CONTROL
/
PROPerty for P  is HARM mean
MATRIX in X and Y directions for P in 2 sweeps using ADI
CONVergence for P; LOCAl mode; value = 1.0e-04, max of  1 iterations
COnVergence for FLOW REFEerence; LOCAl mode; val = 1e-3, max of 5 iterations
/
DIAGnostic node at (30,  40) every 50 steps
OUTPut every 100000 steps
/
FLUX BALAnce for P in 'flux.out' for ID=TOTL every 500 stps
FLUX BALAnce for P              for ID=VALT every 500 stps
/
SOLV for P    0.1 in init 5e-4 inc 1.00 max 1 min 1e-9 2.0 900000
SOLV for P    0.9 in AUTO init 1e-7 inc 1.05 max 1 min 1e-9 2.0 900000
SAVE U V P S     NOW in 'end.0'
SAVE       S     NOW in 'end.0'
/
SOLV for P      4 in AUTO init 1e-7 inc 1.05 max 1 min 1e-9 2.0 900000
SAVE U V P S     NOW in 'end.0'
SAVE       S     NOW in 'end.0'
/
SOLV for P      5 in AUTO init 1e-6 inc 1.05 max 1 min 1e-9 2.0 900000
SAVE U V P S     NOW in 'end.0'
SAVE       S     NOW in 'end.0'
/
SOLV for P     10 in AUTO init 1e-6 inc 1.05 max 1 min 1e-9 2.0 900000
SAVE U V P S     NOW in 'end.1'
SAVE       S     NOW in 'end.1'
/
SOLV for P     30 in AUTO init 1e-5 inc 1.05 max 1 min 1e-9 2.0 900000
SAVE U V P S     NOW in 'end.1'
SAVE       S     NOW in 'end.1'
/
SOLV for P     50 in AUTO init 1e-5 inc 1.05 max 1 min 1e-9 2.0 900000
SAVE U V P S     NOW in 'end.1'
SAVE       S     NOW in 'end.1'
/
SOLV for P    100 in AUTO init 1e-4 inc 1.05 max 1 min 1e-9 2.0 900000
SAVE U V P S     NOW in 'end.2'
SAVE       S     NOW in 'end.2'
/
SOLV for P    300 in AUTO init 1e-4 inc 1.05 max 3 min 1e-9 2.0 900000
SAVE U V P S     NOW in 'end.2'
SAVE       S     NOW in 'end.2'
/
END
```

Fig. M.1-3. (continued).

```
TITLE E-AREA ILNT vault post PA run, 4 rad rate flow cut
/
/ Transport run for H3, C14, Ni59, and Tc99
/
USER CS Cary S. Smith
/
GRID 46 by 72
/
SCREen on
COORdinate X:
/
 -25.0   25.0  100.0  200.0  300.0  400.0  500.0  590.0  650.0  690.0
 720.0  740.0  755.0  $ <— backfill
                765.0  780.0  800.0  830.0  870.0  910.0  950.0
 990.0 1020.0 1040.0 1055.0 $ <— sand
                      1065.0 1078.0 1090.0 1102.0 1115.0 $ wall
                                                  1125.0
1140.0 1160.0 1185.0 1225.0 1275.0 1325.0 1375.0 1425.0 1475.0 1525.0
1575.0 1625.0 1675.0 1725.0 1775.0 1825.0 $<— waste
/
COORdinate Y :
/
 -10.0   10.0   35.0   65.0  105.0  155.0  215.0  295.0  380.0  460.0
 535.0  600.0  655.0  700.0  735.0  760.0  780.0  795.0 $ <--backfill
                                              805.0  820.0
 840.0  855.0  870.0  885.0  $ <--sand
                      895.0  906.0  917.0  928.0  939.0  950.0
 961.0 $ <--concrete
       971.0  985.0 1005.0 1030.0 1065.0 1110.0 1165.0 1230.0 1310.0
1400.0 1490.0 1560.0 1615.0 1660.0 1695.0 1720.0 1740.0 1753.0 $waste
                                                  1763.0
1775.0 1787.0 1800.0 1812.0 1824.0 $ <--concrete
                            1834.0 1844.0 1854.0 1864.0 $<clay
                                                  1874.0
1884.0 1894.0 1904.0 1914.0  $ <--sand
                      1924.0 1939.0 1960.0 1985.0 2005.0 2040.0
2075.0 2125.0 $ <--backfill
/
READ 1 st record from 'start'
/
ZONE 1 is from ( 1,  1) to ( 46, 72) $ BACKFILL
ZONE 2 is from ( 14, 19) to ( 46, 64) $ SAND
ZONE 3 is from ( 25, 50) to ( 46, 55) $ CONCRETE (roof)
ZONE 4 is from ( 30, 32) to ( 46, 49) $ WASTE
ZONE 5 is from ( 25, 56) to ( 46, 60) $ CLAY
ZONE 6 is from ( 25, 25) to ( 46, 31) $ CONCRETE (floor)
ZONE 7 is from ( 25, 25) to ( 29, 49) $ CONCRETE (walls)
/
```

Fig. M.1-4. PORFLOW Input File - Mass transport simulation for intact ILNT vault.

```
DATUm = 0. 0.
GRAVity components = -0.0, -1.
/
DENSity of fluid is constant and equal to 1. gm/cc
/
FOR 1  $BACKFILL
MATErial PROPerties:  rho 1.60 gm/cc, neff = 0.439, ntot = 0.439 , ndif = 0.439
TRANsport for C  kd =    0.0, D = 158.0, al = 10.0  at = 2.0 $ C  is H3
TRANsport for C2 kd =    2.40, D = 158.0, al = 10.0, at = 2.0 $ C2 is C14
TRANsport for C3 kd =  300.0, D = 158.0, al = 10.0, at = 2.0 $ C3 is Ni59
TRANsport for C4 kd =    0.36, D = 158.0, al = 10.0, at = 2.0 $ C4 is Tc99
/
FOR 2  $SAND
MATErial PROPerties:  rho 2.60 gm/cc, neff = 0.375, ntot = 0.375 , ndif = 0.375
TRANsport for C  kd =    0.0, D = 158.0, al = 10.0  at = 2.0 $ C  is H3
TRANsport for C2 kd =    5.0, D = 158.0, al = 10.0, at = 2.0 $ C2 is C14
TRANsport for C3 kd =    0.0, D = 158.0, al = 10.0, at = 2.0 $ C3 is Ni59
TRANsport for C4 kd =    0.1, D = 158.0, al = 10.0, at = 2.0 $ C4 is Tc99
/
FOR 3  $CONCRETE roof
MATErial PROPerties:  rho 2.60 gm/cc, neff = 0.150, ntot = 0.150 , ndif = 0.150
TRANsport for C  kd =    0.0, D = 0.315, al =  5.0  at = 2.0 $ C  is H3
TRANsport for C2 kd =  5000.0, D = 0.315, al =  5.0, at = 2.0 $ C2 is C14
TRANsport for C3 kd =  1000.0, D = 0.315, al =  5.0, at = 2.0 $ C3 is Ni59
TRANsport for C4 kd =   700.0, D = 0.315, al =  5.0, at = 2.0 $ C4 is Tc99
/
FOR 4  $WASTE
MATErial PROPerties:  rho 1.70 gm/cc, neff = 0.50, ntot = 0.50, ndif = 0.50
TRANsport for C  kd =    0.0, D = 0.158, al =  5.0  at = 2.0 $ C  is H3
TRANsport for C2 kd =  5000.0, D = 0.158, al =  5.0, at = 2.0 $ C2 is C14
TRANsport for C3 kd =  1000.0, D = 0.158, al =  5.0, at = 2.0 $ C3 is Ni59
TRANsport for C4 kd =    1.0, D = 0.158, al =  5.0, at = 2.0 $ C4 is Tc99
/
FOR 5  $CLAY
MATErial PROPerties:  rho 2.60 gm/cc, neff = 0.386, ntot = 0.386 , ndif = 0.386
TRANsport for C  kd =    0.0, D =  47.0, al =  5.0, at = 1.0 $ C  is H3
TRANsport for C2 kd =    0.0, D =  47.0, al =  5.0, at = 2.0 $ C2 is C14
TRANsport for C3 kd =  650.0, D =  47.0, al =  5.0, at = 1.0 $ C3 is Ni59
TRANsport for C4 kd =    2.2, D =  47.0, al =  5.0, at = 2.0 $ C4 is Tc99
/
FOR 6  $CONCRETE floor
MATErial PROPerties:  rho 2.60 gm/cc, neff = 0.150, ntot = 0.150 , ndif = 0.150
TRANsport for C  kd =    0.0, D = 0.315, al =  5.0  at = 2.0 $ C  is H3
TRANsport for C2 kd =  5000.0, D = 0.315, al =  5.0, at = 2.0 $ C2 is C14
TRANsport for C3 kd =  1000.0, D = 0.315, al =  5.0, at = 2.0 $ C3 is Ni59
TRANsport for C4 kd =   700.0, D = 0.315, al =  5.0, at = 2.0 $ C4 is Tc99
/
```

Fig. M.1-4. (continued).

```
FOR 7 SCONCRETE wells
MATRial PROPerties rho 2.50 gm/cc, ntot = 0.150 , ndlf = 0.150
TRANsport for C kd =    0.0, D = 0.315, al =  5.0  at = 2.0 $ C  is H3
TRANsport for C2 kd =  5000.0, D = 0.315, al =  5.0, at = 2.0 $ C2 is C14
TRANsport for C3 kd =  1000.0, D = 0.315, al =  5.0, at = 2.0 $ C3 is Ni59
TRANsport for C4 kd =   700.0, D = 0.315, al =  5.0, at = 2.0 $ C4 is Tc99
/
LOCAte subregion (  1,  1) to (  46,  72) with ID=TOTL
LOCAte subregion ( 25, 25) to (  46,  55) with ID=VALT
LOCAte subregion ( 30, 32) to (  46,  49) with ID=WAST
LOCAte subregion ( 25, 56) to (  46,  60) with ID=CLAY
/
SET C  to 1.0 in ID=WASTe
SET C2 to 1.0 in ID=WASTe
SET C3 to 1.0 in ID=WASTe
SET C4 to 1.0 in ID=WASTe
/
DECAy half life for C  is 12.3
DECAy half life for C2 is 5730
DECAy half life for C3 is 75000
DECAy half life for C4 is 2.13e+5
/
BOUN C  -1   FLUX =   0.
BOUN C  +1   FLUX =   0.
BOUN C  -2   VALU =   0.
BOUN C  +2   VALU =   0.
/
BOUN C2 -1   FLUX =   0.
BOUN C2 +1   FLUX =   0.
BOUN C2 -2   VALU =   0.
BOUN C2 +2   VALU =   0.
/
BOUN C3 -1   FLUX =   0.
BOUN C3 +1   FLUX =   0.
BOUN C3 -2   VALU =   0.
BOUN C3 +2   VALU =   0.
/
BOUN C4 -1   FLUX =   0.
BOUN C4 +1   FLUX =   0.
BOUN C4 -2   VALU =   0.
BOUN C4 +2   VALU =   0.
/
/ OPERATIONAL CONTROL
/
PROPerty for C C2 C3 C4 is HARM mean
MATRIX in X and Y directions for C C2 C3 C4 in 1 sweeps using ADI
CONVergence for C  REFErence; LOCAl mode; value = 1.0e-04, max of 5 iterations
CONVergence for C2 REFErence; LOCAl mode; value = 1.0e-04, max of 5 iterations
CONVergence for C3 REFErence; LOCAl mode; value = 1.0e-04, max of 5 iterations
CONVergence for C4 REFErence; LOCAl mode; value = 1.0e-04, max of 5 iterations
/
```

Fig. M.1-4. (continued).

```
DIAGnostic node for C2 and C3 at (20, 40) every 4 steps
OOTput every 900000 steps
/
FLUX BALAnce for C in 'flux.out' for ID=TOTL every 20 steps
FLUX BALAnce for C          for ID=VALT every 20 steps
FLUX BALAnce for C2         for ID=TOTL every 20 steps
FLUX BALAnce for C2         for ID=VALT every 20 steps
/
FLUX BALAnce for C3         for ID=TOTL every 20 steps
FLUX BALAnce for C3         for ID=VALT every 20 steps
FLUX BALAnce for C4         for ID=TOTL every 20 steps
FLUX BALAnce for C4         for ID=VALT every 20 steps
/
HISTory for C C2 C3 C4  (31, 33) (40, 33) (45, 33) every 20 in 'hist.out'
DISAble FLOW
/
SOLV for  C C2 C3 C4  100 init 0.050 inc 1.000 max 0.100 mn 1.e-4 1.1 900000
SAVE      C C2 C3 C4  NOW in 'end.0'
/
SOLV for  C C2 C3 C4  100 init 0.100 inc 1.001 max 0.100 mn 1.e-4 1.1 900000
SAVE      C C2 C3 C4  NOW in 'end.0'
/
SOLV for  C C2 C3 C4  100 init 0.200 inc 1.001 max 0.100 mn 1.e-4 1.1 900000
SAVE      C C2 C3 C4  NOW in 'end.0'
/
SOLV for    C2 C3 C4  100 init 0.100 inc 1.001 max 0.100 mn 1.e-4 1.1 900000
SAVE        C2 C3 C4  NOW in 'end.1'
/
SOLV for    C2 C3 C4  100 init 0.100 inc 1.001 max 0.100 mn 1.e-4 1.1 900000
SAVE        C2 C3 C4  NOW in 'end.1'
/
SOLV for    C2 C3 C4   75 init 0.100 inc 1.001 max 0.100 mn 1.e-4 1.1 900000
SAVE        C2 C3 C4  NOW in 'end.1'
/
END
```

Fig. M.1-4. (continued).

```
TITLE E-AREA ILNT vault ; 1st PA run, 4 cm/yr rate flow run.
/
/ Solubility limited run for Pu239, Pu240, Pu242
/
USER CS Cary S. Smith
/
GRID 46 by 72
/
SCREen on
COORdinate X:
/
 -25.0   25.0  100.0  200.0  300.0  400.0  500.0  590.0  650.0  690.0
 720.0  740.0  755.0  $ <-- backfill
                765.0  780.0  800.0  830.0  870.0  910.0  950.0
 990.0 1020.0 1040.0 1055.0  $ <-- sand
                     1065.0 1078.0 1090.0 1102.0 1115.0 $ wall
                                                 1125.0
1140.0 1160.0 1185.0 1225.0 1275.0 1325.0 1375.0 1425.0 1475.0 1525.0
1575.0 1625.0 1675.0 1725.0 1775.0 1825.0 $<-- waste
/
COORdinate Y :
/
 -10.0   10.0   35.0   65.0  105.0  155.0  215.0  295.0  380.0  460.0
 535.0  600.0  655.0  700.0  735.0  760.0  780.0  795.0  $ <--backfill
                                              805.0  820.0
 840.0  855.0  870.0  885.0  $ <--sand
                     895.0  906.0  917.0  928.0  939.0  950.0
 961.0  $ <--concrete
       971.0  985.0 1005.0 1030.0 1065.0 1110.0 1165.0 1230.0 1310.0
1400.0 1490.0 1560.0 1615.0 1660.0 1695.0 1720.0 1740.0 1753.0 $waste
                                                 1763.0
1775.0 1787.0 1800.0 1812.0 1824.0 $ <--concrete
                            1834.0 1844.0 1854.0 1864.0 $<clay
                                                 1874.0
1884.0 1894.0 1904.0 1914.0  $ <--sand
                     1924.0 1939.0 1960.0 1985.0 2005.0 2040.0
2075.0 2125.0 $ <--backfill
/
READ 1 st record from 'start'
/
ZONE 1 is from (  1,  1) to ( 46,  72) $ BACKFILL
ZONE 2 is from ( 14,  19) to ( 46,  64) $ SAND
ZONE 3 is from ( 25,  50) to ( 46,  55) $ CONCRETE (roof)
ZONE 4 is from ( 30,  32) to ( 46,  49) $ WASTE
ZONE 5 is from ( 25,  56) to ( 46,  60) $ CLAY
ZONE 6 is from ( 25,  25) to ( 46,  31) $ CONCRETE (floor)
ZONE 7 is from ( 25,  25) to ( 29,  49) $ CONCRETE (walls)
/
```

Fig. M.1-5. PORFLOW Input File - Mass transport simulation for intact ILNT vault, solubility-limited source.

```
DATUM = 0. 0.
GRAVity components = -0.02, -1.
/
DENSity of fluid is constant and equal to 1. gm/cc
/
FOR 1 $BACKFILL
MATErial PROPerties: rho 1.60 gm/cc, neff = 0.439, ntot = 0.439 , ndif = 0.439
TRANsport for C kd = 100.0, D = 158.0, al = 10.0 at = 2.0 $ C is Pu239
TRANsport for C2 kd = 100.0, D = 158.0, al = 10.0, at = 2.0 $ C2 is Pu240
TRANsport for C3 kd = 100.0, D = 158.0, al = 10.0, at = 2.0 $ C3 is Pu242
/
FOR 2 $SAND
MATErial PROPerties: rho 2.60 gm/cc, neff = 0.375, ntot = 0.375 , ndif = 0.375
TRANsport for C kd = 550.0, D = 158.0, al = 10.0 at = 2.0 $ C is Pu239
TRANsport for C2 kd = 550.0, D = 158.0, al = 10.0, at = 2.0 $ C2 is Pu240
TRANsport for C3 kd = 550.0, D = 158.0, al = 10.0, at = 2.0 $ C3 is Pu242
/
FOR 3 $CONCRETE roof
MATErial PROPerties: rho 2.60 gm/cc, neff = 0.150, ntot = 0.150 , ndif = 0.150
TRANsport for C kd = 5000.0, D = 0.315, al = 5.0 at = 2.0 $ C is Pu239
TRANsport for C2 kd = 5000.0, D = 0.315, al = 5.0, at = 2.0 $ C2 is Pu240
TRANsport for C3 kd = 5000.0, D = 0.315, al = 5.0, at = 2.0 $ C3 is Pu242
/
FOR 4 $WASTE
MATErial PROPerties: rho 1.70 gm/cc, neff = 0.50, ntot = 0.50, ndif = 0.50
TRANsport for C kd = 0.0, D = 0.158, al = 5.0 at = 2.0 $ C is Pu239
TRANsport for C2 kd = 0.0, D = 0.158, al = 5.0, at = 2.0 $ C2 is Pu240
TRANsport for C3 kd = 0.0, D = 0.158, al = 5.0, at = 2.0 $ C3 is Pu242
/
FOR 5 $CLAY
MATErial PROPerties: rho 2.60 gm/cc, neff = 0.386, ntot = 0.386 , ndif = 0.386
TRANsport for C kd = 5100.0, D = 47.0, al = 5.0, at = 1.0 $ C is Pu239
TRANsport for C2 kd = 5100.0, D = 47.0, al = 5.0, at = 2.0 $ C2 is Pu240
TRANsport for C3 kd = 5100.0, D = 47.0, al = 5.0, at = 1.0 $ C3 is Pu242
/
FOR 6 $CONCRETE floor
MATErial PROPerties: rho 2.60 gm/cc, neff = 0.150, ntot = 0.150 , ndif = 0.150
TRANsport for C kd = 5000.0, D = 0.315, al = 5.0 at = 2.0 $ C is Pu239
TRANsport for C2 kd = 5000.0, D = 0.315, al = 5.0, at = 2.0 $ C2 is Pu240
TRANsport for C3 kd = 5000.0, D = 0.315, al = 5.0, at = 2.0 $ C3 is Pu242
/
FOR 7 $CONCRETE walls
MATErial PROPerties: rho 2.60 gm/cc, neff = 0.150, ntot = 0.150 , ndif = 0.150
TRANsport for C kd = 5000.0, D = 0.315, al = 5.0 at = 2.0 $ C is Pu239
TRANsport for C2 kd = 5000.0, D = 0.315, al = 5.0, at = 2.0 $ C2 is Pu240
TRANsport for C3 kd = 5000.0, D = 0.315, al = 5.0, at = 2.0 $ C3 is Pu242
/
```

Fig. M.1-5. (continued).

```
LOCAte subregion (  1,  1) to (  [illegible], 72) with ID=TOTL
LOCAte subregion ( 25, 25) to (  [illegible], 55) with ID=VALT
LOCAte subregion ( 30, 34) to (  46,  49) with ID=WAST
LOCAte subregion ( 25, 56) to (  46,  60) with ID=CLAY
/
SOURce C ; SOLUb. lim CONSt = 1.0e-13 g/cc, s= 4.0214e-1 g, t = 0.0 in ID=WASTe
SOURce C2; SOLUb. lim CONSt = 1.0e-13 g/cc, s= 1.2354e-1 g, t= 0.0 in ID=WASTe
SOURce C3; SOLUb. lim CONSt = 1.0e-13 g/cc, s= 7.1335e-0 g, t= 0.0 in ID=WASTe
/
DECAy half life for C  is 2.41e+4
DECAy half life for C2 is 6.56e+3
DECAy half life for C3 is 3.75e+5
/
BOUN C  -1   FLUX =   0.
BOUN C  +1   FLUX =   0.
BOUN C  -2   VALU =   0.
BOUN C  +2   VALU =   0.
/
BOUN C2 -1   FLUX =   0.
BOUN C2 +1   FLUX =   0.
BOUN C2 -2   VALU =   0.
BOUN C2 +2   VALU =   0.
/
BOUN C3 -1   FLUX =   0.
BOUN C3 +1   FLUX =   0.
BOUN C3 -2   VALU =   0.
BOUN C3 +2   VALU =   0.
/
/
/ OPERATIONAL CONTROL
/
PROPerty for C C2 C3    is HARM mean
MATRIX in X and Y directions for C C2 C3    in 1 sweeps using ADI
CONVergence for C  REFErence; LOCAl mode; value = 1.0e-04, max of 5 iterations
CONVergence for C2 REFErence; LOCAl mode; value = 1.0e-04, max of 5 iterations

CONVergence for C3 REFErence; LOCAl mode; value = 1.0e-04, max of 5 iterations
/
DIAGnostic node for C2 and C3 at (39,  3) every  4 steps
OUTPut every 900000 steps
/
FLUX BALAnce for C in 'fluxout' for ID=TOTL every  20 stps
FLUX BALAnce for C              for ID=VALT every  20 stps
FLUX BALAnce for C2             for ID=TOTL every  20 stps
FLUX BALAnce for C2             for ID=VALT every  20 stps
/
FLUX BALAnce for C3             for ID=TOTL every  20 stps
FLUX BALAnce for C3             for ID=VALT every  20 stps
/
```

Fig. M.1-5. (continued).

```
DISAble FLOW
HISTory for C C2 C3    (39, 29) (39, 21) (39, 3) every 20 in 'hist.out'
/
SOLV for  C C2 C3    100 init 0.050 inc 1.001 max 0.100 mn 1.e-4 1.1 900000
SAVE      C C2 C3    NOW in 'end.0'
/
SOLV for  C C2 C3    100 init 0.100 inc 1.001 max 0.100 mn 1.e-4 1.1 900000
SAVE      C C2 C3    NOW in 'end.0'
/
SOLV for  C C2 C3    100 init 0.200 inc 1.001 max 0.100 mn 1.e-4 1.1 900000
SAVE      C C2 C3    NOW in 'end.0'
/
SOLV for  C C2 C3    100 init 0.100 inc 1.001 max 0.100 mn 1.e-4 1.1 900000
SAVE      C C2 C3    NOW in 'end.1'
/
SOLV for  C C2 C3    100 init 0.100 inc 1.001 max 0.100 mn 1.e-4 1.1 900000
SAVE      C C2 C3    NOW in 'end.1'
/
SOLV for  C C2 C3     75 init 0.100 inc 1.001 max 0.100 mn 1.e-4 1.1 900000
SAVE      C C2 C3    NOW in 'end.1'
/
END
```

Fig. M.1-5. (continued).

M.2 PORFLOW INPUT FILES - GROUNDWATER

```
TITLe Flow Code for Contaminant Transport Modeling
/File Eflow10.dat September 14, 1993
/PORFLOW-3D Version 2.50
/Base flow file for E-Area simulations
/Version for constant heads along internal streams
/Recharge=40cm/yr
GRID 38 by 30 by 28
/
/Note: Length units are in cm, time units are in years
/
COORdinate X   -10000,     0,  45000,  90000, 135000, 145000, 155000,
          165000, 175000, 185000, 195000, 205000, 215000, 225000,
          235000, 245000, 250000, 257500, 265000, 272500, 280000,
          287500, 295000, 302500, 310000, 317500, 325000, 332500,
          340000, 347500, 355000, 362500, 370000, 380000, 390000,
          427500, 465000, 475000,
/
COORdinate Y   -7500,     0,   7500,  15000,  22500,  30000,  37500,
          45000,  52500,  60000,  67500,  75000,  82500,  90000,
          97500, 105000, 115000, 125000, 135000, 145000, 155000,
          165000, 175000, 185000, 195000, 215000, 242500, 292500,
          342500, 352500,
/
COORdinate Z     610,   732,  2073,  3414,  3536,  3658,  3780,
          3901,  4023,  4785,  5547,  5669,  5791,  5913,
          6035,  6157,  6370,  6553,  6751,  6949,  7148,
          7346,  7544,  7742,  7940,  8138,  8336,  8534,
/
/Note: Boundary conditions for Upper Three Runs
LOCAte region (1,1,6) to (1,2,6) ; ID=UT1
LOCAte region (1,3,6) to (1,5,6) ; ID=UT2
LOCATE region (2,5,6) to (2,7,6) ; ID=UT3
LOCAte region (2,8,7) to (2,11,7); ID=UT4
LOCAte region (2,12,7) to (2,15,7); ID=UT5
LOCAte region (2,16,8) to (2,19,8); ID=UT6
LOCAte region (3,19,8) to (3,22,8); ID=UT7
LOCAte region (4,22,8) to (4,23,8); ID=UT8
LOCAte region (5,23,9) to (5,24,9); ID=UT9
LOCAte region (6,24,9) to (6,25,9); ID=UT10
LOCAte region (7,25,9) to (9,25,9); ID=UT11
LOCAte region (10,25,9) to (14,25,9); ID=UT12
LOCAte region (15,25,9) to (16,25,9); ID=UT13
LOCAte region (16,24,9) to (20,24,9); ID=UT14
LOCAte region (21,24,9) to (21,25,9); ID=UT15
LOCAte region (22,25,9) to (24,25,9); ID=UT16
LOCAte region (24,26,9) to (28,26,9); ID=UT17
```

Fig. M.2-1. PORFLOW-3D input files for the groundwater flow field.

```
LOCAte region (29,26,9) to (32,26,9); ID=UT18
LOCAte region (32,27,9) to (33,27,9); ID=UT19
LOCAte region (33,28,9) to (35,28,9); ID=UT20
LOCAte region (35,29,9) to (37,29,9); ID=UT21
LOCAte region (37,30,9) to (38,30,9); ID=UT22
/
//Note: Boundary Conditions for the "Unnamed Branch"
LOCAte region (6,22,9) to (6,23,9); ID=UB1     $Reach 18-19    #2
LOCAte region (7,21,9) to (7,21,9); ID=UB2     $Reach 18-19    #1
LOCAte region (7,20,10) to (8,20,10); ID=UB3   $Reach 18-19    #2
LOCAte region (8,19,10) to (9,19,10); ID=UB4   $Reach 19-20    #2
LOCAte region (9,18,10) to (10,18,10); ID=UB5  $Reach 19-20    #2
LOCAte region (10,17,11) to (11,17,11); ID=UB6 $Reach 19-20    #2
LOCAte region (11,16,16) to (11,16,16); ID=UB7 $Reach 19-20    #1
LOCAte region (11,15,16) to (11,15,16); ID=UB8 $Reach 20-POE   #1
LOCAte region (12,15,17) to (12,15,17); ID=UB9 $Reach 20-POE   #1
LOCAte region (12,14,18) to (12,14,18); ID=UB10 $Reach 20-POE  #1
LOCAte region (13,14,19) to (13,14,19); ID=UB11 $Reach 20-POE  #1
LOCAte region (13,13,20) to (13,13,20); ID=UB12 $Reach 20-POE  #1
LOCAte region (13,12,21) to (13,12,21); ID=UB13 $Reach 20-POE  #1
LOCAte region (14,12,22) to (14,12,22); ID=UB14
/
/Note: Boundary Conditions for Crouch Branch
LOCATe region (24,23,9) to (24,24,9); ID=CB1   $Reach 1-2      #2
LOCAte region (25,22,9) to (26,22,9); ID=CB2   $Reach 2-12     #2
LOCATe region (27,21,9) to (28,21,9); ID=CB3   $Reach 12-13    #2
LOCAte region (28,20,10) to (29,20,10); ID=CB4 $Reach 12-13    #2
LOCAte region (30,19,10) to (32,19,10); ID=CB5 $Reach 13-14    #3
LOCAte region (32,18,10) to (32,18,10); ID=CB6 $Reach 13-14    #1
LOCAte region (33,15,11) to (33,17,11); ID=CB7 $Reach 14-16    #3
LOCAte region (34,15,16) to (34,15,16); ID=CB8 $Reach 14-16    #1
LOCAte region (34,14,16) to (34,14,16); ID=CB9 $Reach 14-16    #1
LOCAte region (34,12,16) to (34,13,16); ID=CB10 $Reach 16-4    #2
LOCAte region (35,12,17) to (35,12,17); ID=CB11 $Reach 16-4    #1
LOCAte region (35,11,18) to (35,11,18); ID=CB12 $Reach 16-4    #1
LOCAte region (35,10,19) to (35,10,19); ID=CB13 $Reach 16-4    #1
/
/Central tributary
LOCAte region (17,22,9) to (17,23,9); ID=CENT  $Reach 17-POE   #2
/
/Regions of initial head conditions for problem domain
/
LOCAte region (2,2,12) to (38,30,28); ID=dom1
LOCAte region (2,2,5) to (38,30,11); ID=dom2
LOCAte region (2,1,1) to (38,30,4); ID=dom3
LOCAte region (1,25,1) to (35,30,28); ID=dom4
LOCAte region (1,1,1) to (2,24,28); ID=dom5
/
```

Fig. M.2-1. (continued).

```
MATErial type 1 from (1,1,1) to (38,30,23) $Barnwell
MATErial type 2 from (1,1,12) to (38,30,15) $Tan Clay
MATErial type 3 from (1,1,9) to (38,30,11) $McBean Formation
MATErial type 4 from (1,1,5) to (38,30,8) $Green Clay
MATErial type 5 from (1,1,1) to (38,30,4) $Congaree Formation
MATErial type 5 from (1,5,1) to (2,30,28) $Congaree Formation
MATErial type 5 from (3,22,1) to (4,30,28) $Congaree Formation
MATErial type 5 from (5,25,1) to (25,30,28) $Congaree Formation
MATErial type 5 from (23,23,1) to (24,24,28) $Congaree Formation
MATErial type 5 from (25,26,1) to (31,30,23) $Congaree Formation
MATErial type 5 from (32,26,1) to (33,30,28) $Congaree Formation
MATErial type 5 from (34,28,1) to (35,30,28) $Congaree Formation
MATErial type 5 from (36,29,1) to (36,30,28) $Congaree Formation
/
/INItial Head conditions for problem domain
/
SET LINEar func P = 7.224e3 -0.01 * Y for ID=dom1
SET LINEar func P = 6.888e3 -0.01 * Y for ID=dom2
SET LINEar func P = 5.090e3 -0.0047 * Y for ID=dom3
SET LINEar func P = 4.115e3 +0.00106 * X for ID=dom4
SET LINEar func P = 3.962e3 +0.00076 * Y for ID=dom5
/
/Note: Boundary conditions for Upper Three Runs
FIXEd P is 3.627e3 for ID=UT1
FIXEd P is 3.657e3 for ID=UT2
FIXEd P is 3.719e3 for ID=UT3
FIXEd P is 3.780e3 for ID=UT4
FIXEd P is 3.840e3 for ID=UT5
FIXEd P is 3.901e3 for ID=UT6
FIXEd P is 3.962e3 for ID=UT7
FIXEd P is 3.993e3 for ID=UT8
FIXEd P is 4.023e3 for ID=UT9
FIXEd P is 4.054e3 for ID=UT10
FIXEd P is 4.084e3 for ID=UT11
FIXEd P is 4.145e3 for ID=UT12
FIXEd P is 4.176e3 for ID=UT13
FIXEd P is 4.206e3 for ID=UT14
FIXEd P is 4.237e3 for ID=UT15
FIXEd P is 4.267e3 for ID=UT16
FIXEd P is 4.328e3 for ID=UT17
FIXEd P is 4.389e3 for ID=UT18
FIXEd P is 4.450e3 for ID=UT19
FIXEd P is 4.511e3 for ID=UT20
FIXEd P is 4.572e3 for ID=UT21
FIXEd P is 4.633e3 for ID=UT22
/
```

Fig. M.2-1. (continued).

```
/Note: Boundary Conditions for the "Unnamed Branch"
FIXED P = 4.267e3 for ID=UB1
FIXED P = 4.572e3 for ID=UB2
FIXED P = 4.876e3 for ID=UB3
FIXED P = 5.182e3 for ID=UB4
FIXED P = 5.486e3 for ID=UB5
FIXED P = 5.791e3 for ID=UB6
FIXED P = 6.096e3 for ID=UB7
FIXED P = 6.248e3 for ID=UB8
FIXED P = 6.401e3 for ID=UB9
/FIXED P = 6.553e3 for ID=UB10
/FIXED P = 6.767e3 for ID=UB11
/FIXED P = 7.010e3 for ID=UB12
/FIXED P = 7.163e3 for ID=UB13
/SET P = 7.346e3 for ID=UB14
/
/Note: Boundary Conditions for Crouch Branch
FIXED P = 4.267e3 for ID=CB1
FIXED P = 4.420e3 for ID=CB2
FIXED P = 4.572e3 for ID=CB3
FIXED P = 4.785e3 for ID=CB4
FIXED P = 5.029e3 for ID=CB5
FIXED P = 5.151e3 for ID=CB6
FIXED P = 5.791e3 for ID=CB7
FIXED P = 6.035e3 for ID=CB8
FIXED P = 6.248e3 for ID=CB9
FIXED P = 6.350e3 for ID=CB10
FIXED P = 6.401e3 for ID=CB11
FIXED P = 6.553e3 for ID=CB12
FIXED P = 6.767e3 for ID=CB13
/
BOUNdary P for -1 FLUX = 0
BOUNdary P for +1 FLUX = 0
BOUNdary P for +2 FLUX = 0
LOCAte region (2,1,5) to (37,1,28); ID=DIV
BOUNdary P for -2 FLUX = 0 for ID=DIV $Drainage divide for the McBean/Barnwell
LOCAte region (2,1,1) to (37,1,4); ID=REG
BOUNdary P for -2 FLUX = 9.0e2 cm/yr for ID=REG $ Regional Congaree flow
BOUNdary P for -3 FLUX = 3.65e-5 cm/yr $ Recharge from the Ellenton
BOUNdary P for +3 FLUX = -4.00e1 cm/yr $ Recharge from precipitation
/
FOR 1:
HYDRaulic ss=0.0001, Kx = 4.0e4, Ky = 4.0e4, Kz = 1.0e4 cm/yr
FOR 2:
HYDRaulic ss=0.0001, Kx = 6.4e1, Ky = 6.4e1, Kz = 4.3e1 cm/yr
FOR 3:     $Barnwell/McBean
HYDRaulic ss=0.0001, Kx = 4.1e4, Ky = 4.1e4, Kz = 3.1e4 cm/yr
FOR 4:
HYDRaulic ss=0.0001, Kx = 3.0, Ky = 3.0, Kz = 2.0 cm/yr
```

Fig. M.2-1. (continued).

```
FOR 5:
HYDRaulic ss=0.0001, Kx = 4.2e5, Ky = 4.2e5, Kz = 4.2e4 cm/yr
/
/Note: Flux Balance for Unnamed Branch
FLUX BALAnce for P for ID=UB1 every 500 steps
FLUX BALAnce for P for ID=UB2 every 500 steps
FLUX BALAnce for P for ID=UB3 every 500 steps
FLUX BALAnce for P for ID=UB4 every 500 steps
FLUX BALAnce for P for ID=UB5 every 500 steps
FLUX BALAnce for P for ID=UB6 every 500 steps
FLUX BALAnce for P for ID=UB7 every 500 steps
FLUX BALAnce for P for ID=UB8 every 500 steps
FLUX BALAnce for P for ID=UB9 every 500 steps
FLUX BALAnce for P for ID=UB10 every 500 steps
FLUX BALAnce for P for ID=UB11 every 500 steps
FLUX BALAnce for P for ID=UB12 every 500 steps
FLUX BALAnce for P for ID=UB13 every 500 steps
/
/Note: Flux Balance for Crouch Branch
FLUX BALAnce for P for ID=CB1 every 500 steps
FLUX BALAnce for P for ID=CB2 every 500 steps
FLUX BALAnce for P for ID=CB3 every 500 steps
FLUX BALAnce for P for ID=CB4 every 500 steps
FLUX BALAnce for P for ID=CB5  every 500 steps
FLUX BALAnce for P for ID=CB6  every 500 steps
FLUX BALAnce for P for ID=CB7 every 500 steps
FLUX BALAnce for P for ID=CB8 every 500 steps
FLUX BALAnce for P for ID=CB8 every 500 steps
FLUX BALAnce for P for ID=CB9 every 500 steps
FLUX BALAnce for P for ID=CB10 every 500 steps
FLUX BALAnce for P for ID=CB11 every 500 steps
FLUX BALAnce for P for ID=CB12 every 500 steps
FLUX BALAnce for P for ID=CB13 every 500 steps
/
/Note:  Flux Balance for entire domain
FLUX BALAnce for P everywhere every 500 steps
/
/Note:  Flux Balance for entire domain
/
CONVergence for P; GLOBal mode; value=1.e-5, 3 iterations
DIAgnostic for P and U at node (33,16,11)
/
MATRix P = 3
/
SOLVe in STEAdy state mode: maximum steps 1000
OUTPut: P,U,V,W
/OUTPUT P, U, V, W in XZ plane
SAVE on file 'eflow40.arc'
END
```

Fig. M.2-1. (continued).

```
TITL: CONTAMINANT TRANSPORT FOR E-AREA
/File Formed: January 14, 1994
/ PORFLOW version 2.50
/
/Contaminant transport including CAW, IC1V, IC2V
/C-14, Tc-99
/
GRID 38 by 30 by 28
/units are in cm's
COORdinate X  -10000,  0, 45000, 90000, 135000, 145000, 155000,
        165000, 175000, 185000, 195000, 205000, 215000, 225000,
        235000, 245000, 250000, 257500, 265000, 272500, 280000,
        287500, 295000, 302500, 310000, 317500, 325000, 332500,
        340000, 347500, 355000, 362500, 370000, 380000, 390000,
        427500, 465000, 475000,
/
COORdinate Y  -7500,  0,  7500, 15000, 22500, 30000, 37500,
        45000, 52500, 60000, 67500, 75000, 82500, 90000,
        97500, 105000, 115000, 125000, 135000, 145000, 155000,
        165000, 175000, 185000, 195000, 215000, 242500, 292500,
        342500, 352500,
/
COORdinate Z  610,  732,  2073,  3414,  3536,  3658,  3780,
        3901,  4023,  4785,  5547,  5669,  5791,  5913,
        6035,  6157,  6370,  6553,  6751,  6949,  7148,
        7346,  7544,  7742,  7940,  8138,  8336,  8534,
/
/
READ 'eflow40.arc' $40 cm/yr through vault regions
/
/identify a no-diffusion zone at top of domain to allow mass conservation
MATErial type 10 from (1,1,21) to (38,30,28)
/
FOR 1:
ROCK density = 2.65; porosity = .30, .40, .30
TRANsport properties for C Kd = 2.0, md = 158., Ld = 300., Td= 30.
TRANsport properties for C3 Kd = 2.0, md = 158., Ld = 300., Td= 30.
TRANsport properties for C2 Kd = 0.36, md = 158., Ld = 300., Td= 30.
TRANsport properties for C4 Kd = 0.36, md = 158., Ld = 300., Td= 30.
FOR 2:
ROCK density = 2.65; porosity = .30, .40, .30
TRANsport properties for C Kd = 2.0, md = 158., Ld = 300., Td= 30.
TRANsport properties for C3 Kd = 2.0, md = 158., Ld = 300., Td= 30.
TRANsport properties for C2 Kd = 1., md = 158., Ld = 300., Td= 30.
TRANsport properties for C4 Kd = 1., md = 158., Ld = 300., Td= 30.
FOR 3:
ROCK density = 2.65; porosity = .30, .40, .30
TRANsport properties for C Kd = 2.0, md = 158., Ld = 300., Td= 30.
TRANsport properties for C3 Kd = 2.0, md = 158., Ld = 300., Td= 30.
TRANsport properties for C2 Kd = 0.36, md = 158., Ld = 300., Td= 30.
TRANsport properties for C4 Kd = 0.36, md = 158., Ld = 300., Td= 30.
```

Fig. M.2-2. PORFLOW-3D input file for the groundwater mass transport of C-14 and Tc-99.

```
FOR 4:
ROCK density = 2.65; porosity = .30, .40, .30
TRANsport properties for C Kd = 2.0, md = 158., Ld = 300., Td= 30.
TRANsport properties for C3 Kd = 2.0, md = 158., Ld = 300., Td = 30.
TRANsport properties for C2 Kd = 1., md = 158., Ld = 300., Td = 30.
TRANsport properties for C4 Kd = 1., md = 158., Ld = 300., Td= 30. .
FOR 5:
ROCK density = 2.65; porosity = .30, .40, .30
TRANsport properties for C Kd = 2.0, md = 158., Ld = 300., Td= 30.
TRANsport properties for C3 Kd = 2.0, md = 158., Ld = 300., Td= 30.
TRANsport properties for C2 Kd = 0.36, md = 158., Ld = 300., Td= 30.
TRANsport properties for C4 Kd = 0.36, md = 158., Ld = 300., Td= 30.
FOR 6:
ROCK density = 2.65; porosity = .30, .40, .30
TRANsport properties for C Kd = 2.0, md = 158., Ld = 300., Td= 30.
TRANsport properties for C3 Kd = 2.0, md = 158., Ld = 300., Td= 30.
TRANsport properties for C2 Kd = 0.36, md = 158., Ld = 300., Td= 30.
TRANsport properties for C4 Kd = 0.36, md = 158., Ld = 300., Td= 30.
FOR 7:
ROCK density = 2.65; porosity = .30, .40, .30
TRANsport properties for C Kd = 2.0, md = 158., Ld = 300., Td= 30.
TRANsport properties for C3 Kd = 2.0, md = 158., Ld = 300., Td= 30.
TRANsport properties for C2 Kd = 0.36, md = 158., Ld = 300., Td= 30.
TRANsport properties for C4 Kd = 0.36, md = 158., Ld = 300., Td= 30.
FOR 10:
ROCK density = 2.65; porosity = .30, .40, .30
TRANsport properties for C Kd = 2.0, md = 0, Ld = 0., Td = 0.
TRANsport properties for C3 Kd = 2.0, md = 0., Ld = 0., Td= 0.
TRANsport properties for C2 Kd = 0.36, md = 0., Ld = 0., Td= 0.
TRANsport properties for C4 Kd = 0.36, md = 0., Ld = 0., Td= 0.
/
/Specification for mass species C; C-14
/
DECAy half life of C is 5730. years
INITial C = 0.0 everywhere
BOUNdary C at -1 FLUX =0.0
BOUNdary C at +1 FLUX =0.0
BOUNdary C at -2 FLUX =0.0
BOUNdary C at +2 FLUX =0.0
BOUNdary C at -3 FLUX =0.0
BOUNdary C at +3 FLUX =0.0
/
/Specifications for mass species C3; C-14
/
DECAy half-life of C3 is 5730. years
INITial C3 = 0.0 everywhere
BOUNdary C3 at -1 FLUX =0.0
BOUNdary C3 at +1 FLUX =0.0
BOUNdary C3 at -2 FLUX =0.0
BOUNdary C3 at +2 FLUX =0.0
BOUNdary C3 at -3 FLUX =0.0
BOUNdary C3 at +3 FLUX =0.0
/
```

Fig. M.2-2. (continued).

```
/Specifications for mass species C2; Tc-99
/
DECAy half-life of C2 is 2.13e5 years
INITial C2 = 0.0 everywhere
BOUNdary C2 at -1 FLUX =0.0
BOUNdary C2 at +1 FLUX =0.0
BOUNdary C2 at -2 FLUX =0.0
BOUNdary C2 at +2 FLUX =0.0
BOUNdary C2 at -3 FLUX =0.0
BOUNdary C2 at +3 FLUX =0.0
/
/Specifications for mass species C4; Tc-99
/
DECAy half-life of C4 is 2.13e5 years
INITial C4 = 0.0 everywhere
BOUNdary C4 at -1 FLUX =0.0
BOUNdary C4 at +1 FLUX =0.0
BOUNdary C4 at -2 FLUX =0.0
BOUNdary C4 at +2 FLUX =0.0
BOUNdary C4 at -3 FLUX =0.0
BOUNdary C4 at +3 FLUX =0.0
/
DISAble FLOW
DIAGnostic U, C at (19,14,20)   $under ILT/ILNT vaults
/DIAGnostic U and C at 26,11,20
/Material type 6 is ILT/ILNT vaults
Material type 6 from (17,14,20) to (17,14,20)
Material type 6 from (19,13,20) to (19,15,20)
LOCAte material type 6 as ID=ILNT
/Material type 7 is LAW vaults
MATErial type 7 from (21,14,20) to (23,14,20)
MATErial type 7 from (21,12,20) to (27,13,20)
MATErial type 7 from (27,9,20) to (27,9,20)
MATErial type 7 from (28,7,20) to (28,10,20)
MATErial type 7 from (29,6,20) to (29,9,20)
MATErial type 7 from (30,4,20) to (30,8,20)
MATErial type 7 from (31,3,20) to (31,6,20)
LOCAte material type 7 as subregion ID=LAWV
/
/MATErial type 8 is Suspect Soil Trenches
/MATErial type 9 is Naval Reactor Components
/
```

Fig. M.2-2. (continued).

*** C-14 ***
SOURce C for ID=ILNT per VOLUme TABLe 30 sets $Ci/cc-yr per pCi inventory

0.0000E+00	0.0000E+00	
3.2400E+02	2.5563E-49	$too low
5.3600E+02	4.5103E-47	$too low
7.4700E+02	6.0532E-32	
9.6100E+02	1.6934E-27	
1.1720E+03	2.8703E-24	
1.3840E+03	3.1624E-23	
1.6610E+03	3.0947E-22	
3.2775E+03	3.2781E-19	
1.2003E+04	3.7479E-17	
1.2739E+04	3.7194E-17	
1.3552E+04	3.6233E-17	
1.4451E+04	3.4615E-17	
1.5444E+04	3.2400E-17	
1.6542E+04	2.9672E-17	
1.7756E+04	2.6593E-17	
1.9096E+04	2.3300E-17	
2.0568E+04	1.9975E-17	
2.2068E+04	1.6954E-17	
2.3568E+04	1.4326E-17	
2.5060E+04	1.2081E-17	
2.6643E+04	1.0051E-17	
2.8393E+04	8.1957E-18	
3.0326E+04	6.5288E-18	
3.2463E+04	5.0716E-18	
3.4824E+04	3.8321E-18	
3.7323E+04	2.8456E-18	
3.9823E+04	2.1102E-18	
4.2323E+04	1.5631E-18	
4.5323E+04	1.0894E-18	

*** TC-99 ***
SOURce C2 for ID=ILNT per VOLUme TABLe 30 sets $pCi/cc-yr per pCi inventory

0.0000E+00	0.0000E+00	
2.4400E+02	4.3160E-40	$too low
4.1600E+02	1.1503E-38	$too low
5.8700E+02	6.4031E-36	$too low
7.5900E+02	8.6662E-20	
9.3100E+02	2.8593E-17	
1.1020E+03	1.6113E-15	
1.2740E+03	6.4433E-15	
1.4460E+03	1.2834E-14	
1.7318E+03	1.7823E-14	
1.8478E+03	1.7147E-14	
1.9949E+03	1.5001E-14	
2.1674E+03	1.1852E-14	
2.4008E+03	8.0364E-15	
2.7158E+03	4.6094E-15	
3.1409E+03	2.3118E-15	

Fig. M.2-2. (continued).

3.7147E+01	1.111[illegible]E-15
4.4891E+03	5.91[illegible]E-16
5.4120E+03	3.831[illegible]E-16
6.6993E+03	2.3791E-16
8.1896E+03	1.2646E-16
9.6896E+03	5.8195E-17
1.1336E+04	2.1068E-17
1.3552E+04	4.2110E-18
1.6542E+04	3.3684E-19
2.0568E+04	7.9463E-21
2.5060E+04	7.4467E-23
3.0326E+04	2.8667E-25
3.7323E+04	9.8763E-28
4.5323E+04	1.2356E-29

*** C-14 ***

SOURce C3 for ID=LAWV per VOLUme TABLe 30 sets $pCi/cc-yr per pCi inventory

0.0000E+00	0.0000E+00
3.0400E+02	5.7979E-34
5.5600E+02	2.0641E-32
8.0800E+02	1.3554E-31
1.0600E+03	4.7169E-31
1.3120E+03	1.1846E-30
1.8788E+03	2.1227E-20
2.6348E+03	8.7186E-19
3.9246E+03	2.5340E-16
4.8129E+03	3.5774E-16
4.9329E+03	3.5656E-16
5.3992E+03	3.3065E-16
6.3208E+03	2.3462E-16
7.5696E+03	1.1693E-16
8.8696E+03	4.8546E-17
1.0065E+04	1.9969E-17
1.1569E+04	6.1735E-18
1.3349E+04	1.5338E-18
1.5827E+04	2.8952E-19
1.9040E+04	8.2027E-20
2.2608E+04	3.5230E-20
2.6577E+04	1.4225E-20
3.1071E+04	4.6617E-20
3.7223E+04	9.0923E-22
4.3723E+04	1.2840E-22
4.9723E+04	1.8533E-23
5.7033E+04	1.5780E-24
6.5716E+04	7.4287E-26
7.7725E+04	9.1264E-28
9.0725E+04	6.4513E-30

*** TC-99 ***

Fig. M.2-2. (continued).

```
SOURce C4 for ID 4LAWV p... VOLU... T... SpCi/cc-yr p... pCi Inventory
   0.0000E+00   0.0000E+00
   2.2700E+02   2.5708E-00
   4.5400E+02   4.[illegible]
   6.7100E+02   2.1523E-23
   8.9400E+02   6.5177E-28
   1.1120E+03   1.5236E-27
   1.3300E+03   3.0497E-27
   1.8368E+03   5.5216E-17
   2.4908E+03   2.9471E-16
   3.2046E+03   4.5871E-15
   3.5106E+03   2.4235E-15
   3.8166E+03   7.1396E-16
   4.0146E+03   2.8688E-16
   4.0609E+03   2.3003E-16
   4.1261E+03   1.6834E-16
   4.2175E+03   1.0851E-16
   4.3460E+03   5.9049E-17
   4.5129E+03   2.8162E-17
   4.6829E+03   1.4811E-17
   4.8529E+03   9.1349E-18
   5.1380E+03   5.6391E-18
   6.4080E+03   1.9519E-18
   8.0696E+03   3.1007E-19
   9.7696E+03   2.6895E-20
   1.1701E+04   1.1990E-21
   1.4413E+04   9.1349E-24
   1.8223E+04   6.2253E-27
   2.3208E+04   2.9453E-31
   2.8689E+04   4.2633E-36   $too low
   3.6723E+04   3.4483E-43   $too low
HISTory for C, C2, C3, C4 TABLE at (17,14,20)(19,17,18)(19,17,16)
  (19,17,20)(30,11,10)(23,16,20)(23,16,18)(22,16,20)
  (22,16,18) frequency=3 on 'ctc.hst'
OUTPUT C, C2, C3, C4
CONVergence for C2 REFE 1.e-3, max iterations = 3
DIAGnostic U, C2 at (19,14,20)   $under ILT/ILNT vaults
SOLVE C, C2, C3, C4 AUTO 1.7e32,DT=1.,fac=2.,mx=100,mn=1.e-8,df=2,nx=100000
SAVE C2, C4 NOW in 'ctc.arc'
SOLVE C, C2, C3, C4 AUTO 1.e2,DT=1.,fac=2.,mx=100,mn=1.e-8,df=2,nx=100000
SAVE C2, C4 NOW in 'ctc.arc'
SOLVE C, C2, C3, C4 AUTO 1.e2,DT=1.,fac=2.,mx=100,mn=1.e-8,df=2,nx=100000
SAVE C2, C4 NOW in 'ctc.arc'
SOLVE C, C2, C3, C4 AUTO 1.1e3,DT=1.,fac=2.,mx=100,mn=1.e-8,df=2,nx=100000
SAVE C2, C4 NOW in 'ctc.arc'
SOLVE C, C2, C3, C4 AUTO 2.0e2,DT=1.,fac=2.,mx=100,mn=1.e-8,df=2,nx=100000
SAVE C2, C4 NOW in 'ctc.arc'
SOLVE C, C2, C3, C4 AUTO 1.0e2,DT=1.,fac=2.,mx=100,mn=1.e-8,df=2,nx=100000
SAVE C2, C4 NOW in 'ctc.arc'
SOLVE C, C2, C3, C4 AUTO 1.0e2,DT=1.,fac=2.,mx=100,mn=1.e-8,df=2,nx=100000
SAVE C2, C4 NOW in 'ctc.arc'   $3.4e3
```

Fig. M.2-2. (continued).

```
CONVergence for C3 RSpR 1.e-3, max iterations = 3
DIAGnostic U, C3 at (19,11,-0)   $under ILT/UNC vaults
SOLVE C, C2, C3, C4 AUTO 1.4e3,DT=1.,fac=2.,mx=100,mn=1.e-8,df=2,nx=100000
SAVE C, C2, C3, C4 NOW in 'ctc.arc'    $4.3e3
SOLVE C, C2, C3, C4 AUTO 1.2e3,DT=1.,fac=2.,mx=100,mn=1.e-8,df=2,nx=100000
SAVE C, C2, C3, C4 NOW in 'ctc.arc'    $6.0e3 years
SOLVE C, C2, C3, C4 AUTO 6.e3,DT=1.,fac=2.,mx=100,mn=1.e-8,df=2,nx=100000
SAVE C, C2, C3, C4 NOW in 'ctc.arc'    $1.2e4 years
SOLVE C, C3 AUTO 1.0e3,DT=1.,fac=2.,mx=100,mn=1.e-8,df=2,nx=100000
SAVE C, C3 NOW in 'ctc.arc'    $1.3e4 years
SOLVE C, C3 AUTO 1.0e4,DT=1.,fac=2.,mx=1000,mn=1.e-8,df=2,nx=100000
SAVE C, C3 NOW in 'ctc.arc'    $2.3e4 years
SOLVE C, C3 AUTO 1.0e4,DT=1.,fac=2.,mx=1000,mn=1.e-8,df=2,nx=100000
SAVE C, C3 NOW in 'ctc.arc'    $3.3e4 years
SOLVE C, C3 AUTO 1.0e4,DT=1.,fac=2.,mx=1000,mn=1.e-8,df=2,nx=100000
SAVE C, C3 NOW in 'ctc.arc'    $4.3e4 years
END
```

Fig. M.2-2. (continued).

OSR 17-84 (Rev 2-8-93)
Stacer: 26-13271.08

687581

Record Indexing

Required with all records submitted to D&RA
Print or type in black ink.

Transmittal No. R 080102

Part A — Transmittal

To: Document and Records Administration	Location	Date	
From: James R. Cook	Location: 773-43A Rm 209	Dept: SRTC/IWT	Phone: 55802

Items in shaded fields are required for all records.

Keywords and other information are also required and shall be supplied as necessary to insure accurate and timely record retrieval.

Part B — Indexing Information (Completed by Originator)

Document ID: WSRC-RP-94-218	Sheet	Revision: 0	Document Type
Alternate ID	Sheet	Revision	

Title: Radiological Performance Assessment for the E-Area Vaults Disposal Facility

Title Classification: u

Author/Originator: James R. Cook

Security Classification of Record: U

Document (or Revision) Date (YYMMDD): 940415

No. of Pages:

Keywords: Low-Level Radioactive Waste; Pathways Analysis; Computer Modeling

Design/Engineering Document Descriptors

Supersedes	Sheet	Revision	Supr-DTD
Reference Document	Sheet	Revision	Supr-DTD
Equipment		Material	
System		Purchase Order Number	
Building	Elevation		Area
Project Number	Project File Number		
Design Function	Category		Design Area
Retention Period (Yrs): Permanent 99 years	Retention Schedule: ~~1963~~ NI-434-89-8-7.b(1)(b)		Paragraph/Item Number: 1960 ~~1963 NI-434-89-8-7.b~~

Part C — For D&RA Use Only

Record Location	
Transmitted By	Date
Received By	Date 6/22/94
Verified By	Date

Distribution: Part 1 - Original, filed with record copy, Part 2 - D&RA use only, Part 3 - Returned to Sender, Part 4 - Retained by user, if needed.